

AD-A175 162

BIOMATERIALS '84 TRANSACTIONS WORLD CONGRESS ON
BIOMATERIALS (2ND) ANNUA (U) SOCIETY FOR BIOMATERIALS
SAN ANTONIO TX S F HULBERT ET AL JUN 84

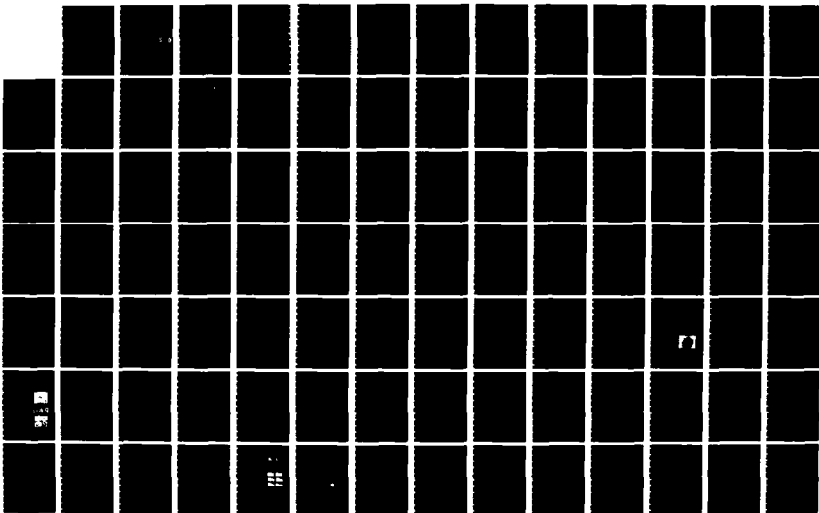
1/3

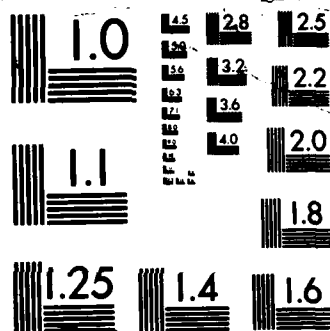
UNCLASSIFIED

DAMD17-84-G-4005

F/G 6/12

NL





PHOTOCOPY RESOLUTION TEST CHART

AD-A175 162

DTIC ACCESSION NUMBER

LEVEL

PHOTOGRAPH THIS SHEET

BIOMATERIALS '84 TRANSACTIONS
SECOND WORLD CONFERENCE ON
BIOMATERIALS
VOLUME VII

INVENTORY

①

APR. 27 - May 1, 1984

DOCUMENT IDENTIFICATION

DISTRIBUTION STATEMENT A

Approved for public release;
Distribution Unlimited

DISTRIBUTION STATEMENT

ACCESSION FOR

NTIS GRA&I ☒

DTIC TAB ☐

UNANNOUNCED ☐

JUSTIFICATION

BY

DISTRIBUTION /

AVAILABILITY CODES

DIST

AVAIL AND/OR SPECIAL

A-1

DISTRIBUTION STAMP



DTIC
ELECTE
DEC 17 1986
S D

DATE ACCESSIONED

DATE RETURNED

DATE RECEIVED IN DTIC

REGISTERED OR CERTIFIED NO.

PHOTOGRAPH THIS SHEET AND RETURN TO DTIC-FDAC

AD-A175 162

BIOMATERIALS '84

TRANSACTIONS



**SECOND WORLD CONGRESS ON
BIOMATERIALS**

**10th Annual Meeting of
The Society for Biomaterials**

Volume VII

April 27-May 1, 1984

Hyatt Regency-Capitol Hill

Washington, D.C., U.S.A.

Approved for public release;
distribution unlimited.

	Saturday, April 28	Sunday, April 29	Monday, April 30	Tuesday, May 1
7:00				
8:00	Session Chairperson's Breakfast C			
9:00	OPENING CEREMONIES T, VF, Y	TECHNOLOGY TRANSFER Panel Presentation and Discussion 19 R-A	KEYNOTE R. Pillar 32 R-A	KEYNOTE M. Jozefowicz 57 R-A
	KEYNOTE T. Yamamuro 1 T, VF, Y		KEYNOTE R. White 33 R-A	KEYNOTE A. Hoffman 58 R-A
10:00	BREAK		Porous Ingrowth 34 R-A	Ligaments & Tendons 59 C
	Biomat. for Trauma Surgery 2 C-A		Corr 35 C-B	Tiss. Interac. Polymers 60 T
	Biointerac. Polymers 3 C-B		Bioresorp. 36 T	Protein Adsorption 61 R-A
	Polymeric Bio-materials 4 T		Infection Biomats. 37 C-A	
11:00		BREAK		
		SOCIETY BUSINESS MEETINGS SFB, USA R-A	Ortho Joint Repl. 38 R-A	Internal Fixation 62 C
			Corr 39 C-B	Bioactive Ceramics 63 T
			New Dev. Biomed. Polym. 40 T	Heparin & Deriv. Surfaces 64 R-A
			Heart Valves 41 C-A	
12:00				
	President Advisory Committee E International Liaison Committee GC LUNCH	LUNCH	LUNCH	SFB, USA New Council Meeting GC LUNCH
1:00				
2:00	KEYNOTE O. Wichterle 5 R-A	KEYNOTE T. Albrektsson 20 R-A	KEYNOTE A. N. Cranin 42 R-A	KEYNOTE A. Callow 65 R-A
3:00	POSTERS 6 Wear & Paric 7 Bone Implant Interface 8 Ophthalmic Mats 9 13 C-B 10 14 R-A 11 15 T 12 BREAK C-C, C-L, BH Bone Repl. & Osteo 16 C-B Bone Implant Interface 17 R-A Tissue Interac 18 T	POSTERS 21 Elec. Aug. Tissues 22 Dental Materials 23 Cell Interac. Polymers 24 26 C-B 25 27 T 28 Y C-C, C-L, BH Ortho Biomech 29 C-B Bioceram 30 T Dental Implants 31 Y	POSTERS 43 Porous Ingrowth 44 Dental Materials 45 PolyUreth. Degrad. & Fatigue 46 51 C-B 47 52 T 48 53 R-A 49 BREAK C-C, C-L, BH Liga. & Tendons 54 C-B Dental Materials 55 T Protein Adsorp 56 R-A	POSTERS 66 Porous Ingrowth 67 Blood Int. Grafts & Shunts 68 Sust. Rel. Diabetes 69 73 C 70 74 R-A 71 75 T 72 BREAK C-C, C-L, BH Bone Cements 76 C Bioceram 77 T Blood Int. Grafts & Shunts 78 R-A
4:00				
5:00	5:15 Busses leave Hyatt Regency Capitol Hill for the 6:00 P.M. Concert by the Boston Symphony at the Kennedy Center		5:30 Busses leave Hyatt Regency Capitol Hill for the Bash - An Old-Fashioned American Barbecue at the Smokey Glen Farm	
6:00		7:00 Cash Bar and Social Hour 8:00 Awards Banquet Regency Ballroom		

Meeting Rooms

R-A Regency A
 T Ticonderoga
 VF Valley Forge
 Y Yorktown
 C-L Concord-Lexington
 BH Bunker Hill

C-A Columbia A
 C-B Columbia B
 C-C Columbia C
 E Everglades
 C Capitol
 Y Yellowstone

Form Approved
OMB No 0704-0188
Exp. Date Jun 30, 1986

Form Approved
OMB No 0704-0188
Exp. Date Jun 30, 1986

BIOMATERIALS '84

**TRANSACTIONS
SECOND WORLD CONGRESS ON BIOMATERIALS**

10th Annual Meeting of The Society for Biomaterials

Sixteenth International Biomaterials Symposium

VOLUME VII

James M. Anderson, Editor and Program Chairman
Departments of Pathology and Macromolecular Science
Case Western Reserve University
Cleveland, Ohio

PROGRAM
SECOND WORLD CONGRESS ON BIOMATERIALS

PARTIALLY SUPPORTED BY

National Institute of Dental Research
Food and Drug Administration, National Center for Devices
and Radiological Health
Office of Naval Research
U.S. Army Institute of Dental Research
National Bureau of Standards

As Host Society, the Society for Biomaterials of the United States of America is pleased to welcome members of the constituent biomaterials societies, other participants, and guests to our nation's Capitol for the Second World Congress on Biomaterials.

CONSTITUENT SOCIETIES

Biomaterials Group of the Biological Engineering
Society of the United Kingdom
Canadian Biomaterials Society
European Society for Biomaterials
Japanese Society for Biomaterials
Society for Biomaterials, U.S.A.

MEETING LOCATION:

The Hyatt Regency Capitol Hill Hotel is located on Capitol Hill, two blocks from the Metro Stop at Union Station (see enclosed map). The hotel is easily accessible from Interstate Route 95, Washington National Airport (15 minutes in normal traffic), and Dulles International Airport (45 minutes, in normal traffic). The hotel is serviced by regular limousine service from both of the Washington area airports.

Numerous airlines serve both Washington National Airport for flights within the United States, and Dulles International Airport for flights within the United States and from abroad. Regular Amtrak passenger train service comes into Union Station, just two blocks from the Hyatt Regency.

HOTEL:

The Hyatt Regency Capitol Hill Hotel is conveniently located near Washington's major sightseeing attractions and Union Station. A special Congress rate of \$75 for a single room, and \$95 for a double room has been arranged at the hotel for Congress attendees. This rate is quite competitive with rates charged at downtown Washington hotels in the Spring. You are encouraged to register *early*, as April is a very busy time in Washington, and hotel rooms fill up quickly. To register, fill out the enclosed hotel reservation form, and return it *directly* to the hotel **No Later Than April 5, 1984**. After that date, all rooms in the Congress block that have not been reserved will be released for general sale at the regular prevailing rates of the hotel.

All Technical sessions of the Congress, as well as the Welcome Reception on Friday evening, and the banquet on Sunday evening will be held at the Hyatt Regency.

REGISTRATION DESK:

Escalator Lobby
Hyatt Regency Capitol Hill Hotel
400 New Jersey Avenue, N.W.
Washington, D.C.

Telephone Number: 202-737-1234, ask for the "Biomaterials Congress Registration"

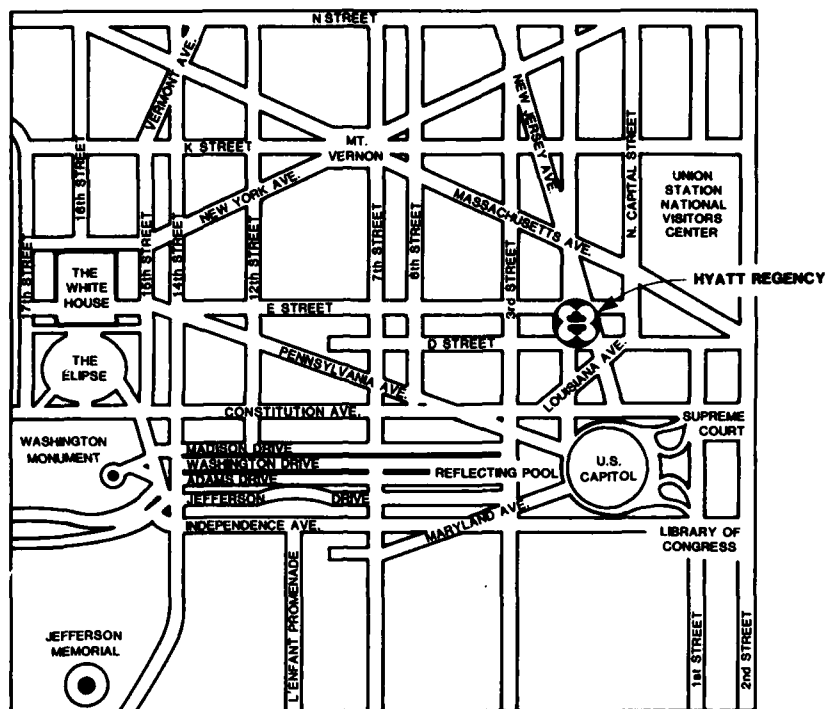
Registration Times: Friday, April 27, 4 p.m. - 8 p.m.
Saturday, April 28, 8 a.m. - 4:30 p.m.
Sunday, April 29, 8 a.m. - 4:30 p.m.
Monday, April 30, 8 a.m. - 4:30 p.m.
Tuesday, May 1, 8 a.m. - 12 noon

REGISTRATION FEES:

Category	Amount Before March 15, 1984	Amount After March 15, 1984
Members of Constituent Societies	\$250.00	\$275.00
Non-Members*	335.00	360.00
Students and Residents	50.00	75.00
Guests	100.00	125.00

Fees for Members and Non-Members include all social functions and Transactions. Fees for Students and Residents include Reception and Transactions. Fees for Guests include all social functions.

*\$85 may be applied toward membership in the Society for Biomaterials, U.S.A.



INFORMATION ON LOCAL ARRANGEMENTS:

Pre-Meeting: Anna C. Fraker, 301-921-2992
Sara R. Torrence, 301-921-2721
Kathy C. Stang, 301-921-3295

Meeting: 202-737-1234, ask for the "Biomaterials Congress Registration"

GUEST PROGRAM:

No formal Guest Program has been planned because of the numerous and wide variety of attractions available in the Washington, D.C. area. Tourist information is available at the Congress Hospitality Desk.

MEETING ROOMS:

Technical sessions will be held on the Convention Level of the hotel except on Tuesday, May 1, when the Capitol Room on the first floor will be used. Keynote Addresses will be held in the Ticonderoga, Valley Forge, Yorktown and Regency A Rooms. Oral Sessions will be held in the Regency A, Columbia A, Columbia B, and Ticonderoga Rooms. The Capitol Room on the first floor will be utilized for Oral Sessions on Tuesday, May 1. Poster Sessions will be held in Columbia C, Concord, Lexington and Bunker Hill Rooms. See Program Outline and Program for details.

CONGRESS OFFICE	Redwood Room
PRESS ROOM	Sequoia Room
SLIDE PREVIEW ROOM	Grand Teton Room

SOCIAL AND MEAL FUNCTIONS:

Friday, April 27.

8:00 p.m. until 10:00 p.m.

– Wine and Cheese Reception, Columbia Room.

Saturday, April 28,

5:15 p.m.,

Buses leave Hyatt Regency Capitol Hill Hotel for Kennedy Center Concert at 6:00 p.m. with the Boston Symphony performing, Seiji Ozawa conducting and Peter Serkin at the piano.

Sunday, April 29,

7:00 p.m.,

Cash Bar and Social Hour – Regency Foyer. 8:00 p.m., Awards Banquet – Regency Ballroom.

Monday, April 30,

5:30 p.m.,

Buses leave Hyatt Regency Capitol Hill Hotel for Smokey Glen Farm in Maryland and an Old Fashioned American Barbecue. This is "The Bash".

BUSINESS FUNCTIONS:

Friday, April 27,

9:00 a.m. – 5:00 p.m.

Annual Meeting of the Board of Directors and the Council of the Society for Biomaterials, U.S.A. – Bryce Room. Officers and Committee Chairpersons are expected to attend.

Saturday, April 28,

7:15 a.m. – 8:15 a.m.

Session Chairpersons Breakfast – Capitol Room. All Session Chairpersons are expected to attend.

12:10 – 1:30 p.m.

Presidents Advisory Committee, Society for Biomaterials, U.S.A. – Everglades Room.

12:10 – 1:30 p.m.

International Liaison Committee – Grand Canyon Room.

Tuesday, May 1,

12:15 p.m. – 1:15 p.m.

New Council for the Society for Biomaterials, U.S.A., Meeting in the Grand Canyon Room.

Officers and Committee Chairpersons are expected to attend.

ASSOCIATED MEETINGS:

The American Academy of Surgical Research will hold its annual meeting during the Biomaterials Congress in the Hyatt Regency on Monday, April 30, 1984, from 12:00 noon to 1:30 p.m. in the Everglades Room. For information contact Dr. Andreas von Recum, Department of Interdisciplinary Studies, Clemson University, Clemson, S.C. 29631.

ASAIO, American Society for Artificial Internal Organs, will hold their Annual Meeting from May 2 through May 4, 1984, at the Sheraton Hotel in Washington, D.C. For information contact the ASAIO National Office, P.O. Box C, Boca Raton, Florida 33429.

AWARDS BANQUET, SUNDAY, APRIL 29, 1984

7:00 PM – Reception

8:00 PM – Awards Banquet Dinner

PROGRAM

Samuel F. Hulbert,
Chairman of the Second World Congress on Biomaterials, Presiding

Dr. John C. Villforth,
Director, National Center for Devices and Radiological Health, FDA
“FDA’s Role in Biomaterials Development and Evaluation”

Presentation of the Clemson Awards for Outstanding Contributions to Biomaterials Research:

Award for Basic Research

Introduction of Professor Otto Wichterle by Martin M. Pollak, President,
International Hydron Corp.

Remarks by Professor Otto Wichterle

Award for Applied Research

Introduction of Dr. Vincent Gott by Dr. Robert Baier,
Calspan Corp., Buffalo, New York

Remarks by Dr. Vincent Gott

Award for Contributions to Literature

Introduction of Professor Allan S. Hoffman by Dr. Robert Leininger,
Battelle, Columbus, Ohio

Remarks by Professor Allan S. Hoffman

Presentation of Special Awards

Presentation of Student Awards

Ph.D. Candidate Category

R.E. Marchant

Intern, Resident or Clinical Fellow Category

Dr. H.B. Kram

Undergraduate, Master’s or Health Sciences Degree

Candidate – M.L. Salgaller

Acknowledgements

Concluding Remarks

1984 CLEMSON AWARDS

Award for Basic Research

Professor Otto Wichterle
Prague, Czechoslovakia

For the development of the soft contact lens and for stimulating the growth and development of hydrogels for medical application.

Award for Applied Research

Dr. Vincent Gott
The Johns Hopkins Hospital
Baltimore, Maryland

For the development of one of the pioneering methods for the assessment of the blood compatibility of materials and for a lifetime involvement in the application of prosthetic materials to cardiovascular problems.

Award for Contributions to the Literature

Professor Allan S. Hoffman
Center for Bioengineering
University of Washington
Seattle, Washington

For key papers published in the scientific literature which have stimulated research and development in the areas of protein adsorption, radiation grafting, biomolecule immobilization and blood-materials interactions.

1984 STUDENT AWARDS FOR OUTSTANDING RESEARCH

Ph. D. Candidate Category

Roger E. Marchant
Department of Macromolecular Science
Case Western Reserve University
Cleveland, Ohio

"In Vivo Leukocyte Interactions with Biomer"

Intern, Resident or Clinical Fellow Category

Dr. Harry B. Kram
Harbor-UCLA Medical Center
Torrance, California

"Use of Fibrin Sealant in Experimental Tracheal Repair"

Undergraduate, Master's or Health Sciences Degree Candidate

Michael L. Salgaller
Children's Hospital
Columbus, Ohio

"Immunogenicity of Glutaraldehyde-treated Bovine Pericardial Tissue Xenografts in Rabbits"

Honorable Mentions

P. Campbell
U.S.C. Dept. of Orthopedics
Los Angeles, California

P. Patka
Free University
Amsterdam, The Netherlands

S. A. Cartledge
University of Keele
Keele, England

K. A. Thomas
Tulane University
New Orleans, Louisiana

ORGANIZING COMMITTEE - SECOND WORLD CONGRESS ON BIOMATERIALS

S.F. Hulbert, Chairman
H. Kawahara
H. Plenk, Jr.

D. C. Smith
D. F. Williams

LOCAL ARRANGEMENTS COMMITTEE

A. C. Fraker, Chairperson
S. R. Torrence, Chief, Special Activities, NBS
K. C. Stang, NBS/NML Conf. Coord.
S. L. Gordon
E. Horowitz

F. A. Pitlick
T. N. Salthouse
R. R. Stromberg
P. Sung
T. M. Valega

PROGRAM COMMITTEE

J. M. Anderson, Chairman
G. Drouin
C. Hassler
G. Hastings
R. Kennedy

B. Ratner
D. C. Smith
P. J. van Mullem
T. Yokobori
S. Barenberg

INTERNATIONAL LIAISON COMMITTEE

G. Drouin - Canada
C. W. Hall - U.S.A.
G. Hastings - United Kingdom
S. F. Hulbert - U.S.A.
H. Kawahara - Japan

H. Plenk, Jr. - Europe
D. C. Smith - Canada
P. J. van Mullem - Europe
D. F. Williams - United Kingdom
T. Yokobori - Japan

AWARDS AND CEREMONIES COMMITTEE

B. Ratner, Chairperson
P. K. Bajpai
M. Gendreau

R. Pilliar
J. P. Park
A. Von Recum

COUNCIL OF THE SOCIETY FOR BIOMATERIALS, U.S.A.

BOARD OF DIRECTORS

President: A. S. Hoffman
President-Elect: J. M. Anderson
Secretary-Treasurer: A. M. Weinstein
Secretary - Treasurer-Elect: J. E. Lemons

Immediate Past-President: J. Black
Immediate Past-President: S. Pollack
Member-at-Large: P. E. Duncan
Editor: A. N. Cranin

Committee Chairpersons:

J. Anderson
S. Barenberg
A. Fraker
L. Gettleman
S. Hulbert
R. James

J. Lemons
S. Pollack
B. Ratner
F. Schoen
M. Spector
T. Valega

BIOLOGICAL ENGINEERING SOCIETY - BIOMATERIALS GROUP - UNITED KINGDOM

Chairman: R. J. Minns
Secretary: G. A. Murray

CANADIAN SOCIETY FOR BIOMATERIALS

President: R. Pilliar
Secretary-Treasurer: J. Brash

Past-President: G. Drouin

EUROPEAN SOCIETY FOR BIOMATERIALS

President: A. J. C. Lee
Vice-President: B. Rahn
Secretary: P. Christel
Assoc. Editor: H. Plenk, Jr.

Treasurer and Membership Secretary: P. J. Van Mullem
Past-President: G. Heimke
Member-at-Large: A. Ravaglioli
Member-at-Large: P. Griss

JAPANESE SOCIETY FOR BIOMATERIALS

President: T. Yokobori
President-Elect: A. Nakajima

Secretary: H. Kawahara

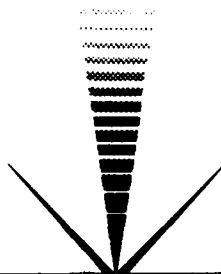
CONTINUING MEDICAL EDUCATION FOR PHYSICIANS

Continuing Medical Education Credit is available for only USA licensed physicians. Participants wishing credit for this activity must sign in at the Registration Desk.

The **Case Western Reserve University School of Medicine** and **Department of Pathology** designates this continuing medical education activity as meeting the criteria for 28 Category 1 credit hours. The **Case Western Reserve University School of Medicine** is accredited by the Accreditation Council for Continuing Medical Education to sponsor continuing medical education for physicians.

CONTRIBUTORS TO THE SECOND WORLD CONGRESS ON BIOMATERIALS

Bard Implants, Inc.
Biomet, Inc.
Calcitek, Inc.
Carbomedics, Inc.
E. I. duPont de Nemours & Co.
DePuy, Inc.
Ethicon, Inc.
Howmedica, Inc.
Impra, Inc.
International Hydron Corporation
Intermedics Orthopedics, Inc.
Johnson & Johnson Products, Inc.,
Orthopedic Division
Kolff Medical, Inc.
3M Company
Medical Device and Diagnostic Industry Magazine –
Canon Communications, Inc.
Medtronic Inc., Energy Technology Division
Richards Medical Company
Shiley, Inc.
St. Jude Medical, Inc.
Toray Industries, Inc.
Ban-tec, Inc.
Zimmer, Inc.



NESAC/BIO

National ESCA and Surface Analysis Center
for Biomedical Problems

NESAC/BIO

National ESCA and Surface Analysis Center for Biomedical Problems

The Division of Research Resources of the National Institutes of Health has established a facility directed to stimulate the application of electron spectroscopy for chemical analysis (ESCA) and other contemporary surface analysis tools to biomedical problems and to provide researchers with access to appropriate instrumentation. The state-of-the-art equipment at NESAC/BIO will be available to qualified researchers at no charge and will permit a detailed analysis of the chemistry and morphology of the uppermost atomic layers of solid surfaces.

Interested researchers are encouraged to contact the Center to discuss the applications of ESCA and other techniques to their particular problems. Please write to:

Dr. B.D. Ratner
NESAC/BIO
Department of Chemical Engineering, BF-10
University of Washington
Seattle, Washington 98195



National Center For Biomedical Infrared Spectroscopy

Sponsored by the National Institutes of Health

NATIONAL CENTER FOR BIOMEDICAL INFRARED SPECTROSCOPY

The National Center for Biomedical Infrared Spectroscopy has been established at Battelle's Columbus Laboratories in Columbus, Ohio, under the support of the Biotechnology Resources Program of the Division of Research Resources of the National Institutes of Health. The overall objective of the Center is to extend the capabilities and applications of Fourier transform infrared spectroscopy (FT-IR) to biomedical research. Work performed at this Center will be directed towards developing methodologies and techniques, and towards making specialized equipment and skills available to the biomedical research community. Other key functions of the Center are to provide training in biomedical FT-IR to graduate students and postdoctoral fellows, and to disseminate information to the biomedical community regarding opportunities and new developments at the Center.

The new National Center will house state-of-the-art Fourier transform infrared spectrometers and dedicated data processing computers. This equipment will be available for Battelle and visiting scientists to use in conducting individual research programs, and to use in conducting collaborative research programs with scientists and universities throughout North America. Research topics will range from the study of proteins such as enzymes and antibodies in solution, to the identification of how synthetic materials interact with blood, to the examination of the structures of RNA and DNA components of cells.

Openings are currently available at the National Center for both graduate students (short-term, 1-year, and 2-year appointments) and postdoctoral fellows (1-year appointments). These positions will provide training in both preparing biological samples for infrared measurements and in operating the FT-IR instruments. Stipends are available for students and graduates interested in learning about biomedical infrared spectroscopy. Those wishing to apply for stipends should submit a vitae to:

Ms. Susan M. Toth
Battelle's Columbus Laboratories
National Center for Biomedical
Infrared Spectroscopy
505 King Avenue
Columbus, Ohio 43201

SCIENTIFIC PROGRAM

Saturday, April 28, 1984

7:15-8:15 Session Chairperson's Breakfast Capitol Room

OPENING CEREMONIES

Ticonderoga,
Valley Forge,
Yorktown Rooms

8:30-9:15 Samuel F. Hulbert, Presiding
Welcome

Dr. James Wyngaarden
Director of the National Institutes of Health
"The Importance of Biomaterials Research to
Improved Health Care"

Representatives of Constituent Societies

- Biomaterials Group of the Biological
Engineering Society of the United Kingdom
- Canadian Biomaterials Society
- European Society for Biomaterials

- Japanese Society for Biomaterials
- Society for Biomaterials, U.S.A.
Sponsor Representatives
Program Chairperson
Local Arrangements Chairperson

SESSION 1

Saturday Morning
April 28, 1984
Ticonderoga, Valley Forge,
Yorktown Rooms

KEYNOTE ADDRESS

Chairperson: L. L. Hench

9:15-9:55 -1 **Establishment of an Interdisciplinary Research System for Biomaterials and Artificial Organs.** *T. Yamamuro*, Research Center for Medical Polymers and Biomaterials, Department of Orthopedic Surgery, Kyoto University, Kyoto, Japan.

9:55-10:10 Break

SESSION 2

Saturday Morning
April 28, 1984
Columbia A Room

BIOMATERIALS FOR TRAUMA SURGERY

Chairpersons: G. Battistone and P. Atkinson

10:10 -2 **A Controlled Release Antibiotic Wound Dressing.** *S. J. Davidson, L. D. Nichols, A. S. Obermayer, and M. B. Allen*, Moleculon Research Corporation, Cambridge, Massachusetts.

- 10:30 -3 **IN VIVO Evaluation of Poroplastic® as a Wound Dressing Material Formulated to Slowly Release Gentamicin Sulfate.** *J. W. Vincent and J. A. Setterstrom*, U. S. Army Institute of Dental Research, Walter Reed Medical Center, Washington, D.C.
- 10:50 -4 **Development of Encapsulated Antibiotics for Topical Administration to Wounds.** *J. A. Setterstrom, T. R. Tice, W. E. Meyers, and J. W. Vincent*, U.S. Army Institute of Dental Research, Walter Reed Medical Center, Washington, D.C.
- 11:10 -5 **The Effects of a Biodegradable Copolymer-Proteolipid (PL) on Osseous Healing in Rats and Dogs.** *J. O. Hollinger*, U.S. Army Institute of Dental Research, Walter Reed Army Medical Center, Washington, D.C.
- 11:30 -6 **Inorganic and Organic Compound Combinations for Bone Replacement.** *J. Lemons, P. Henson, and K. Niemann*, Department of Biomaterials and Division of Orthopedic Surgery, University of Alabama in Birmingham, Birmingham, Alabama.
- 11:50 -7 **Long Term Analysis of Serrated Aluminum Oxide Dental Implants.** *C. R. Hassler, L. G. McCoy, N. E. Arlin, and M. D. Brose*, Battelle-Columbus Laboratories, Columbus, Ohio.

SESSION 3

Saturday Morning
April 28, 1984
Columbia B Room

BIOINTERACTIONS WITH POLYMERS I

Chairpersons: R. Baier and K. Kataoka

- 10:10 -8 **Adsorption and Activation Processes of Contact Phase of Intrinsic Coagulation on Polymer Surfaces.** *T. Matsuda, T. Toyosaki, and H. Iwata*, Research Institute, National Cardiovascular Center, Suita, Osaka 565 Japan.
- 10:30 -9 **Study of the Adhesion and Migration of Endothelial Cells on Pretreated Polyester Prostheses with Various Cross-Linked Protein Matrices in Vitro.** *M. F. Sigot, M. Lanfranchi, S. Ben-Slimane, J. L. Duval, R. Guidoin, and M. Sigot*, Laboratoire de Biologie Cellulaire Expérimentale, Université de Technologie, BP 233, 60206 Compiègne Cedex (France).
- 10:50 -10 **In Vivo Assessment of Blood/Material Interactions of Segmented Polyurethane Used for Blood Pump.** *T. Matsuda, H. Takano, Y. Taenaka, K. Hayashi, M. Umezu, T. Nakamura, T. Nakatani, S. Takatani, T. Tanaka, and T. Akutsu*, National Cardiovascular Center Research Institute, 5-125 Fujishiro-dai, Suita, Osaka 565 Japan.
- 11:10 -11 **Modified Collagen Membrane for Hybrid Organs and Biosimulator.** *T. Akaike, S. Kasai, N. Tominaga, S. Nishizawa, and T. Miyata*, Department of Material Systems Engineering, Tokyo University of Agriculture and Technology, Koganei-shi, Tokyo 184, Japan; Japan Biomedical Material Research Center, Meguro-ku, Tokyo 152.
- 11:30 -12 **The Development of Fluorine-Containing Segmented Polyurethane and Its Application to Artificial Heart Pump.** *K. Imachi, I. Fujimasa, M. Nakajima, S. Tsukagoshi, K. Mabuchi, M. Kato, T. Takakura, M. Yamabe, and K. Atsumi*, Institute for Medical Electronics, Faculty of Medicine, University of Tokyo, Tokyo, Japan; Asahi Glass Co., Ltd., Hazawa-cho, Kanagawa-ku, Yokohama 221, Japan.

- 11:50 -13 **Mitrathrane™ - A New Polyether Urethane Urea for Medical Applications.** *D. K. Gilding, A. M. Reed, I. N. Askill, and S. Briana*, Mitral Medical International, INC., Wheat Ridge, Colorado.

SESSION 4

Saturday Morning
April 28, 1984
Ticonderoga Room

POLYMERIC BIOMATERIALS I

Chairpersons: C. Beatty and M. Vert

- 10:10 -14 **On The Swelling Behavior of 2-Hydroxyethyl Methacrylate (HEMA) Doped with Methacrylic Acid (MAA).** *E. C. Eckstein, L. Pinchuk, M. R. VanDeMark, and E. G. Barroso*, University of Miami, Coral Gables, Florida.
- 10:30 -15 **Polysiloxane Modified Styrene-Ethylene/Butylene-Styrene Block Copolymers: A New Class of Biocompatible Thermo-Plastic Elastomers.** *R. Sterling and E. P. Goldberg*, Concept Polymer Technologies, Inc., 12707 U.S. 19 South Clearwater, Florida; Department of Materials Science & Engineering, University of Florida, Gainesville, Florida.
- 10:50 -16 **Polymerization Kinetics of Cold Curing Acrylic Resins by Quantitative Multiple Internal Reflection Infrared Spectroscopy.** *J. R. de Wijn and P. J. van Kesteren*, Department of Dental Materials, Dental School, University of Nijmegen, Nijmegen, The Netherlands.
- 11:10 -17 **The Synthesis of Organophosphorus Polymers for Biomedical Use.** *R. Smith and D. C. Watts*, University of Liverpool, P.O. Box 147, Liverpool, England; Turner Dental School, The University of Manchester, Manchester, England.
- 11:30 -18 **XPS analysis of Poly(Vinyl Alcohol-CO-N-Vinyl-2-Pyrrolidone).** *D. R. Miller and N. A. Peppas*, School of Chemical Engineering, Purdue University, West Lafayette, Indiana.
- 11:50 -19 **The Effect of Polyether Segment Chemical Structure on the Bulk and Surface Morphologies of Copolyether-Urethane-Ureas.** *K. Knutson and D. J. Lyman*, Department of Materials Science and Engineering, University of Utah, Salt Lake City, Utah.
- 12:10-1:30 Lunch
- 12:10-1:30 Presidents Advisory Committee, Society for Biomaterials, U.S.A. Everglades Room
- 12:10-1:30 International Liaison Committee Yellowstone Room

SESSION 5

Saturday Afternoon
April 28, 1984
Regency A Room

KEYNOTE ADDRESS

Chairperson: B. D. Ratner

- 1:30-2:10 -20 **Highly Swollen Hydrophilic Gels.** *O. Wichterle*, Czechoslovak Academy of Sciences, Prague, Czechoslovakia

2:10-5:00

POSTER PRESENTATIONS

Columbia C, Concord,
Lexington, Bunker Hill

Chairpersons: A. Fraker, P. Sung, R. Connolly, and J. Antonucci

SESSION 6

Saturday Afternoon
April 28, 1984

POLYMERIC BIOMATERIALS II

- 21 **Glass Transition of Polyvinylpyrrolidone (PVP) and Its Copolymers.** *A. Schwartz and D. T. Turner*, Becton Dickinson Research Center, Research Triangle Park, North Carolina; Department of Operative Dentistry and Dental Research Center, University of North Carolina, Chapel Hill, North Carolina.
- 22 **Bion II Elastomers for Biomedical Applications.** *T. R. Pherson, W. J. Stith, and H. Quach*, Lord Corporation, Bioengineering Department, Erie, Pennsylvania.
- 23 **Non-Network Oligomeric Hydrogel Grafted Surfaces, Part 1.** *J. T. Jacob and D. R. Owen*, Department of Chemistry, Tulane University, New Orleans, Louisiana.
- 24 **Surface Fissuring of Polyurethane-Based Pacemaker Leads.** *M. Szycher, D. Dempsey, and V. L. Poirier*, Thermedics, Inc., 74 West Street, P.O. Box 270, Waltham, Massachusetts.
- 25 **In Vitro Degradation of Elastomeric Biomaterial.** *K. Phua, J. M. Anderson, and A. Hiltner*, Department of Macromolecular Science, Case Western Reserve University, Cleveland, Ohio.

SESSION 7

Saturday Afternoon
April 28, 1984

SUTURES

- 26 **Influence of Suture Diameter on the Tensile Strength of Polypropylene Monofilaments.** *R. P. Kusy and J. Q. Whitley*, Dental Research Center, University of North Carolina at Chapel Hill, Chapel Hill, North Carolina.
- 27 **An Evaluation of Carbon Coated Dacron as a Nonabsorbable Suture Material.** *M. A. Kester, S. D. Cook, M. E. Brunet, and H. G. French*, Department of Orthopaedic Surgery, Tulane University School of Medicine and the Veterans Administration Medical Center, New Orleans, Louisiana.
- 28 **Development of the New Absorbable Suture by Chitin.** *M. Nakajima, K. Atsumi, and K. Kifune*, Institute of Medical Electronics, Faculty of Medicine, University of Tokyo, Tokyo, Japan; Unitika Research Laboratory, Unitika Corp., Uji, Kyoto, Japan.

SESSION 8

Saturday Afternoon
April 28, 1984

FIXATION AND MINERALIZATION OF POLYMERS

- 29 **Mineralization of Bovine Pericardium: In Vitro and In Situ Test of Modified Tissues for Potential Inhibition of Mineralization.** *S. T. Li, M. H. Sunwoo, P. Zalesky, and T. S. Freund*, Meadox Medicals, Inc., Oakland, New Jersey; Department of Biochemistry, Fairleigh Dickinson University, School of Dentistry, Hackensack, New Jersey.
- 30 **Mechanism of Tissue Fixation by Glutaraldehyde.** *D. T. Cheung and M. E. Nimni*, Bone & Connective Tissue Research, Orthopaedic Hospital, USC Medical School, Los Angeles, California.
- 31 **Surface Studies of Calculi Deposition on Foley Catheter Materials.** *C. Batich, C. Cheng, C. Johnson, V. Rodriquez, and S. Batich*, Department of Materials Science and Engineering, University of Florida, Gainesville, Florida.

SESSION 9

Saturday Afternoon
April 28, 1984

TISSUE INTERACTIONS I

- 32 **Use of Fibrin Sealant in Experimental Splenic Trauma.** *H. B. Kram, W. C. Shoemaker, and D. P. Harley*, Harbor-UCLA Medical Center, Torrance, California.
- 33 **The Connective Tissue Response to Biomaterials Implantation.** *T. M. Hering, R. E. Marchant, and J. M. Anderson*, Department of Pathology, Case Western Reserve University, Cleveland, Ohio.
- 34
- 35 **Skin Regeneration by Use of a Bioreplaceable Polymeric Template.** *I. V. Yannas, J. F. Burke, D. Orgill, and E. M. Skrabut*, Massachusetts Institute of Technology, Cambridge, Massachusetts; Harvard Medical School and Chief, Trauma Services, Massachusetts General Hospital, Boston, Massachusetts.
- 36 **Comparison of Soft Tissue Ingrowth in Subcutaneous and Percutaneous Dacron Velour Implants.** *S. Hultman and D. Feldman*, Texas A&M University, College Station, Texas.
- 37 **Factors Affecting Soft Tissue Ingrowth into Porous Implants.** *D. Feldman and T. Estridge*, Texas A&M University, College Station, Texas.
- 38

- 39 **Capsule Formation as a Function of Material Texture and Material Compressibility.** *C. D. Enger, G. Picha, and J. DesPrez*, Case Western Reserve University, Cleveland, Ohio.
- 40 **Effect of Surface Microtexture and Implant Orientation on Percutaneous Wound Healing in the Pig.** *J. L. Bence and G. J. Picha*, Department of Biomedical Engineering, Case Western Reserve University, Cleveland, Ohio.

SESSION 10

Saturday Afternoon
April 28, 1984

INVESTIGATION AND IMPROVEMENT OF BONE CEMENTS I

- 41 **Improved Shear Properties of Wire Reinforced Bone Cement.** *S. Saha and M. L. Warman*, Louisiana State University Medical Center, Shreveport, Louisiana.
- 42 **Pathogenesis of Circulatory Reactions During the Implantation of Acrylic Bone Cement - New Animal and Clinical Studies.** *J. Rudigier, K. Wenda, G. Ritter, and D. Theiss*, Division of Accident Surgery, Department of Oral Surgery, University of Mainz, Langenbeckstr. 1, D-6500 Mainz, Federal Republic of Germany.
- 43 **Advancement on Cement Technique: Experimental Study.** *P. Tranquilli-Leali, G. Cerulli, G. C. Paoletti, and F. Pezzoli*, Clinica Ortopedica Università, Cattolica, Roma.
- 44 **Thermal Behavior of Normal and Fiber-Reinforced Bone Cement.** *S. Saha, S. Pal, J. A. Albright*, Biomechanics Laboratory, Department of Orthopaedic Surgery, LSU Medical Center, Shreveport, Louisiana.
- 45 **S-N Curve for Centrifuged and Uncentrifuged PMMA.** *D. O. O'Connor, D. W. Burke, J. P. Davies, and W. H. Harris*, Orthopaedic Research Laboratories, Massachusetts General Hospital and Harvard Medical School, Boston, Massachusetts.
- 46 **Porosity Measurements in Centrifuged and Uncentrifuged Commercial Bone Cement Preparations.** *M. Jasty, N. F. Jensen, and W. H. Harris*, Orthopaedic Research Laboratories, Massachusetts General Hospital and Harvard Medical School, Boston, Massachusetts.
- 47 **Effect of Antibiotic Addition on the Fatigue Life of Centrifuged and Uncentrifuged Bone Cement.** *J. P. Davies, D. O'Connor, and W. H. Harris*, Orthopaedic Research Laboratories, Massachusetts General Hospital and Harvard Medical School, Boston, Massachusetts.
- 48 **Improved Compressive Strength of Bone Cement by Ultrasonic Vibration.** *S. Saha and M. L. Warman*, Department of Orthopaedic Surgery, LSU School of Medicine in Shreveport, Shreveport, Louisiana.
- 49 **Physical Characterization and Histological Response of a Glass Bead Composite Acrylic Bone Cement.** *C. Migliaresi, S. Gatto, G. Guida, and L. Nicolais*, Polymer Engineering Laboratory, University of Naples, Naples, Italy; II Clinica Ortopedica, I Facoltà di Medicina e Chirurgia, University of Naples, Naples, Italy.

SESSION 11

Saturday Afternoon
April 28, 1984

LIGAMENTS AND TENDONS: PROPERTIES AND REPLACEMENT I

- 50 **Clinical Experience of Carbon Fibre Patches.** *R. J. Minns*, Department of Medical Physics, Dryburn Hospital, Durham, England.
- 51 **Shear Creep of Reconstituted Type I Collagen Suspensions.** *B. A. Weiss and D. G. Wallace*, Collagen Corporation, Palo Alto, California.
- 52 **Dielectric and Mechanical Spectroscopy in Collagen and Proteoglycans.** *C. Lacabanne, A. Lamure, N. Hitmi, E. Maurel, M. Th. Pieraggi, and M. F. Harmand*, Laboratoire de Physique des Solides, Universite Paul Sabatier, 31062 Toulouse Cedex, France.

SESSION 12

Saturday Afternoon
April 28, 1984

DENTAL MATERIALS I

- 53 **The Performance of New Composite Restorative Materials in Posterior Teeth.** *D. F. Williams and J. Cunningham*, University of Liverpool, Liverpool, England.
- 54 **Hybridization of Natural tissues with Biocompatible Materials - Adhesion to Tooth Substrates.** *N. Nakabayashi*, Institute for Medical and Dental Engineering, Tokyo Medical and Dental University, Surugadai, Kanda, Tokyo 101 Japan.
- 55 **Comparative Evaluation of Recent Commercial Light Cured Composites.** *S. Waknine, J. Vaidyanathan, and T. K. Vaidyanathan*, New York University Dental Center, Department of Dental Materials Science, New York, New York.
- 56 **Biophysical Studies on the Sm-Co Magnet as a Dental Material.** *M.S. Abd El Baset*, Biochemistry Laboratory, National Research Center, Dokki, Cairo, Egypt.
- 57 **Potential Use of Calcium Phosphates as Fillers in Composite Restorative Biomaterials.** *R. Z. LeGeros and B. Penugonda*, New York University Dental Center, New York, New York.
- 58 **Water Sorption of Polymer Composites with 4-Methacryl-Oxyethyl Trimellitic Anhydride (4-META).** *D. T. Turner and K. Nagata*, Department of Operative Dentistry and Dental Research Center, University of North Carolina, Chapel Hill, North Carolina; Chemistry Department, Tsurumi University, Yokohama, Japan.
- 59 **The Adhesion Mechanism of Dental Cements Containing Polyacrylic Acid - Chemical Analysis by ESCA.** *T. Nasu, K. Nagaoka, F. Ito, and K. Suzuki*, Faculty of Education, Yamagata University, Yamagata, Japan; The Research Institute for Iron, Steel and Other Metals, Tohoku University, Sendai 980 Japan.
- 60 **A Biomechanical Study of Gold and Nickel-Based Dental Bridge Systems Utilizing Distal Abutment Dental Implants.** *M. W. Bidez, J. E. Lemons, and B. P. Isenberg*, University of Alabama in Birmingham, Birmingham, Alabama.

- 61 **The Effect of Methacrylate on the Physical Properties of Poly(Fluoroalkoxy)Phosphazene Elastomer.** *P. H. Gebert, M. R. Capezza, H. R. Rawls, J. K. Smith, and L. Gittleman,* Gulf South Research Institute, New Orleans, Louisiana.
- 62 **A Comparative Study of the Modulus of Rupture of Several Commercial Porcelains.** *M. B. Smyth, N. Sumithra, S. Waknine, and M. Traiger,* New York University Dental Center, Department of Dental Materials Science, New York, New York.
- 63 **Use of Freeze-Dried Dura as a Meniscus Replacement in Temporomandibular Joint Surgery.** *D. E. Stringer, P. J. Boyne, and J. P. Shafqat,* Oral & Maxillofacial Surgery Section, Loma Linda University Medical Center, Loma Linda, California.
- 64 **Replication of the Morphology of Jaw Bones Through High Technology.** *H. P. Truitt and R. A. James,* Loma Linda University, Loma Linda, California.

SESSION 13

Saturday Afternoon
April 28, 1984
Columbia B Room

WEAR AND WEAR PARTICULATE

Chairpersons: J. Parr and P. Christel

- 2:10 -65 **Histological Study of In Vivo Wear of Titanium Alloy Total Hip Prostheses.** *T. A. Gruen, C. W. Smith, C. P. Schwinn, and A. Sarmiento,* Department of Orthopaedics and Pathology, University of Southern California; Bone and Connective Tissue Research Program, Orthopaedic Hospital-U.S.C., Los Angeles, California.
- 2:30 -66 **Particle Size Distribution of Wear Debris from Polyethylene and Carbon Reinforced Acetabular Components.** *L. S. Stern, M. T. Manley, and J. Parr,* State University of New York at Stony Brook, Stony Brook, New York; Zimmer, Warsaw, Indiana.
- 2:50 -67 **In-Vivo Evaluation of Tissue Tolerance to PTFE-Grafted Polyethylene Particles.** *M. Homerin, P. Christel, A. Dryll, and G. Gaussens,* Laboratoire de Recherches Orthopediques, Faculte de Medecine Lariboisiere-Saint-Louis, Paris, France.
- 3:10 -68 **Biodegradation of UHMW Polyethylene in Joint Endoprosthesis.** *P. Eyerer,* Institut fur Kunststoffprüfung und Kunststoffkunde, Universität Stuttgart, Stuttgart, Germany (FRG).

SESSION 14

Saturday Afternoon
April 28, 1984
Regency A Room

BONE/IMPLANT INTERFACE I

Chairpersons: C. Homsy and B. Rahn

- 2:10 -69 **The Effect of Porous-Surfaced Knee Prosthesis Design on Adaptive Bone Modeling.** *J. D. Bobyn, D. Abdulla, R. M. Pilliar, and H. U. Cameron,* Department of Mechanical Engineering, Institute of Biomedical Engineering, Ecole Polytechnique, Montreal, Quebec, Canada.

- 2:30 -70 **Biological Fixation of Porous-Surfaced Hip Prostheses-Clinical Evaluation of Adaptive Femoral Bone Modeling.** C. A. Engh and J. D. Bobyn, Anderson Clinic, National Hospital for Orthopaedics and Rehabilitation, Arlington, Virginia.
- 2:50 -71 **A New Semi-Automatic Micro-Computerized Technique to Quantify Bone Ingrowth into Porous Implants.** P. Dallant, A. Meunier, P. Christel, and L. Sedel, Laboratoire de Recherches Orthopediques, Faculte de Medecine Lariboisiere-Saint-Louis, Paris, France.
- 3:10 -72 **Evaluation of the Tissue Biocompatibility of Carbon-Silicon Carbide Composite Material.** P. Christel, M. Homerin, and A. Dryll, Laboratoire de Recherches Orthopediques, Faculte de Medecine Lariboisiere-Saint-Louis, Paris, France.

SESSION 15

Saturday Afternoon
April 28, 1984
Ticonderoga Room

OPHTHALMOLOGIC BIOMATERIALS

Chairpersons: M. Haffner and A. Yamanaka

- 2:10 -73 **New Polymer Systems for Preparation of Contact Lenses.** J. Vacik, J. Trekoval, O. Wichterle, Institute of Macromolecular Chemistry, Czechoslovak Academy of Sciences, Prague, Czechoslovakia.
- 2:30 -74 **Effect of Silicone Oil on the Cornea.** M. F. Refojo, M. Roldan, and F-L. Leong, Eye Research Institute of Retina Foundation, Boston, Massachusetts.
- 2:50 -75 **Intraocular Lens Loop Materials; Comparison of Mechanical Stress and Photo-Oxidative Properties of Polypropylene and Polymethylmethacrylate Monofilaments.** D. C. Osborn, M. Yalon, J. Stacholy, and E. P. Goldberg, Department of Materials Science and Engineering, University of Florida, Gainesville, Florida.
- 3:10 -76 **Protein Adsorption to Contact Lens Material.** B. D. Ratner and T. A. Horbett, Department of Chemical Engineering and Center for Bioengineering, University of Washington, Seattle, Washington.
- 3:30-3:45 Break

SESSION 16

Saturday Afternoon
April 28, 1984
Columbia A Room

BONE REPLACEMENT AND OSTEOGENESIS I

Chairpersons: A. Weinstein and L. Claes

- 3:45 -77 **Hydroxyapatite Reinforced Polyethylene Composites as Analogous Bone Replacement Materials.** W. Bonfield, J. C. Behiri, C. Doyle, J. Bowman, and J. Abram, Department of Materials, Queen Mary College, London, United Kingdom.

- 4:05 -78 **Strength and Morphology of Different Bone Transplants Following Their Implantation into Diaphyseal Defects.** *Ch. Etter, C. Burri, and L. Claes*, Abteilung für Unfallchirurgie der Universität Ulm Oberer Eselsberg, Ulm, Germany.
- 4:25 -79 **Bimorph PVDF Film: A New Osteogen Material,** *C. Lacabanne, J. J. Ficat, M. J. Francis, F. Micheron, R. Durroux, and P. Ficat*, Université Paul Sabatier, Toulouse Cédex, France.
- 4:45 -80 **Tc₉₉ Scanning and Histological Evaluation of Osteogenesis.** *F. W. Cooke, D. L. Powers, and L. S. Cohn*, Department of Interdisciplinary Studies, Clemson University, Clemson, South Carolina.

SESSION 17

Saturday Afternoon
April 28, 1984
Regency A Room

BONE/IMPLANT INTERFACE II

Chairpersons: J. L. Katz and S. Brown

- 3:45 -81 **A Method for High-Resolution Study of the Tissue Response to Polymerized Bone Cement and Other Polymers.** *L. Linder*, Laboratory of Experimental Biology, Department of Anatomy, University of Göteborg, Sweden.
- 4:05 -82 **Interface and Bone Response to Increased Penetration of Acrylic Cement.** *R. D. Bloebaum, T. A. Gruen, and A. Sarmiento*, Department of Orthopaedics, University of Southern California, Orthopaedic Biomechanics, Bone and Connective Tissue Research Program, Los Angeles, California.
- 4:25 -83 **Bone/Cement Interface of the Carbon Composite THR: Analysis by Thin Section Histology.** *S. Chew, A. McLaren, R. D. Bloebaum, and P. Campbell*, Orthopaedic Biomechanics Laboratory, Bone & Connective Tissue Research Program, Orthopaedic Hospital-USC, Los Angeles, California.
- 4:45 -84 **A Comparative Study of the Interface Zone Between Bone and Various Implant Materials.** *T. Albrektsson, H-A. Hansson, and B. Ivarsson*, Laboratory of Experimental Biology, Department of Anatomy, University of Gothenburg, Sweden.

SESSION 18

Saturday Afternoon
April 28, 1984
Ticonderoga Room

TISSUE INTERACTIONS II

Chairpersons: S. Eskin and C-Y. Tong

- 3:45 -85 **Use of Fibrin Sealant in Experimental Tracheal Repair.** *H. B. Kram, W. C. Shoemaker, and D. P. Harley*, Harbor-UCLA Medical Center, Torrance, California.
- 4:05 -86 **Testing for Biocompatibility of Materials Using the Peritoneal Cavity of the Mouse.** *K. Merritt and S. A. Brown*, Orthopaedic Research Laboratories, University of California, Davis, Davis, California.

4:25 -87 **A Novel A-B-A Block Copolymer Consisting of Poly(γ -Ethyl L-Glutamate) (A) and Polybutadiene (B) as Biomaterial.** *H. Sato, Y. Noishiki, G. Chen, T. Hayashi, and A. Nakajima*, Research Center for Medical Polymers and Biomaterials, Kyoto University, Kyoto 606, Japan.

4:45 -88 **An Electron Microscope Investigation of Blood Vessel Ingrowth into Dacron® Velour.** *D. Feldman, J. Negele, and T. Estridge*, Texas A&M University, College Station, Texas.

SESSION 19

Sunday
April 29, 1984
Regency A Room

8:00-10:15

TECHNOLOGY TRANSFER PANEL PRESENTATION AND DISCUSSION

Chairperson: S. Barenberg

Overview: Industrial Perspective

A. S. Michaels, President, A. S. Michaels, Inc., New York, New York.

How Do You Know You Have a Marketable Product?

C. Hartman, Channing Weinberg, Inc., New York, New York.

Bringing the Discovery Through the Market Place

P. N. Sawyer, Professor of Surgery, Department of Surgery, State University of New York, Downstate Medical Center, Brooklyn, New York.

The Role of the F.D.A.

M. Haffner, Associate Bureau Director for Health Affairs, Food and Drug Administration, Washington, D.C.

Meeting Performance Expectations

E. Muller, Director: Division of Medical Engineering, Office Of Science and Technology, National Center for Devices and Radiological Health, Food and Drug Administration, Washington, D.C.

10:15-10:30

Break

10:30-12:00

Society Business Meetings

Society for Biomaterials, U.S.A., A. Hoffman, Presiding, Regency A Room

12:00-1:30

Lunch

SESSION 20

Sunday Afternoon
April 29, 1984
Regency A Room

KEYNOTE ADDRESS

Chairperson: P. J. Van Mullem

- 1:30-2:10 -89 **Dental Implants: Biological Aspects and Perspectives.** *T. Albrektsson*, Laboratory of Experimental Biology, Department of Anatomy, University of Gothenburg and the Institute for Applied Biotechnology, Gothenburg, Sweden.

2:10-5:00 **POSTER PRESENTATIONS**

Columbia C, Concord,
Lexington and
Bunker Hill Rooms

Chairpersons: E. Duncan, S. Stupp, and C. Hassler

SESSION 21

Sunday Afternoon
April 29, 1984

BLOOD INTERACTIONS: GRAFTS AND SHUNTS I

- 90 **An In Vitro Study of Platelet/Vascular Graft Interactions.** *K. Kottke-Marchant, J. M. Anderson, A. Rabinovitch, and R. Herzig*, Departments of Macromolecular Science and Pathology, Case Western Reserve University, Cleveland, Ohio.
- 91 **Human Umbilical Cord Vein as a Blood Conduit: A Comparative Study of Two Models of Storage of the Raw Material.** *S. T. Li and P. Zalesky*, Meadox Medicals, Inc., Oakland, New Jersey.
- 92 **The Impact of Polyester Arterial Prostheses of Czechoslovakian Origin: An In Vitro and In Vivo Evaluation.** *M. W. King, R. G. Guidoin, K. R. Gunasekera, L. Martin, M. Marois, P. Blais, J. M. Maarek, and C. Gosselin*, Université Laval, Québec, Canada.
- 93 **The Effect of Flow on Platelet Uptake by Vascular Graft Materials in Baboon EX VIVO Shunt Model.** *R. Connolly, E. Keough, W. C. Mackey, K. Ramberg-Laskaris, J. McCullough, T. O'Donnell, Jr., and A. D. Callow*, Tufts University School of Medicine and New England Medical Center, Boston, Massachusetts.
- 94 **Arachidonic Acid Derivative and Platelet Release Reaction Induced by Implant Materials.** *A. Pizzoferrato, M. D'Addato, E. Cenni, T. Curti, D. Cavedagna, and C. Tarabusi*, Center for Biocompatibility Research of Implant Materials, Istituto Ortopedico Rizzoli, Bologna, Italy.
- 95 **Expanded PTFE as a Microvascular Graft: A Study of Four Fibril Lengths.** *D. F. Branson, G. J. Picha, and J. DesPrez*, Division of Plastic Surgery, University Hospitals, Case Western Reserve University, Cleveland, Ohio.
- 96 **Interest of In Vitro Radioisotopic Investigation Techniques to Study Behavior of Coagulation Proteins at the Interface with Biomaterials.** *Ch. Baquey, L. Bordenave, J. Caix, B. Basse-Cathalinat, V. Migonney, and C. Fougnot*, Inserm/Ceemasi-Sc 31, Université Bordeaux II, Bordeaux-Cedex, France; Université de Paris Nord, Villetaneuse, France.

- 97 **Albumin Retention On C₁₈ Alkylated Biomer Vascular Grafts.** *R. C. Eberhart, M. S. Munro, G. O. Bridges, P. V. Kulkarni, and W. J. Fry,* Department of Surgery, University of Texas Health Science Center at Dallas, Dallas, Texas.
- 98 **Properties of Acellular Vascular Matrix.** *R. C. Duhamel, K. Brendel, R. L. Reinert, and J. M. Malone,* University of Arizona, Tucson, Arizona.
- 99 **The Effect of Surface Charge Density and Distribution on Arterial Thrombosis.** *J. A. Goggins and R. D. Jones,* Department of Biomedical Engineering, Case Western Reserve University, Cleveland, Ohio.
- 100 **Polyelectrolyte Grafted Polyurethane Interactions with Blood Proteins and Platelets.** *C. P. Sharma, A. K. Nair,* Biosurface Technology Division, Biomedical Technology Wing, Sree Chitra Tirunal Institute for Medical Science and Technology, Poojapura, Trivandrum, India.
- 101 **Testing of Filled PTFE Vascular Prostheses Using Panel Grafts.** *B. Tenney, W. Catron, D. Goldfarb, and R. Snyder,* Bard Implants Division, A Division of C. R. Bard, Billerica, Massachusetts; Department of Medical Research, St. Luke's Hospital Medical Center, Phoenix, Arizona.
- 102 **Physicochemical Properties of Improved Biosynthetic Grafts for Vascular Reconstruction.** *R. Baier, A. Meyer, M. Fornalik, and K. Kokolus,* Advanced Technology Center, Calspan Corporation, Buffalo, New York.

SESSION 22

Sunday Afternoon
April 29, 1984

SURGICAL PROCEDURES

- 103 **Intralumina Bypass Device for Artificial Aortic Graft Implantation.** *D. Feldman, S. Hale, and J. Hunter,* Texas A&M University, College Station, Texas.
- 104 **Adjustment of an Inflatable Clamp in Vascular Surgery.** *D. de La Faye, J. M. Legendre, C. Lefevre, and R. Guidoin,* Department of Biomaterials and Surgery, Service Lombard, C.H.U. 29279 Brest Cedex, France.

SESSION 23

Sunday Afternoon
April 29, 1984

VASCULAR DEVICES: PHYSICAL CONSIDERATIONS

- 105 **Vascular Hemodynamics and Arterial Wall Transport: An IN VITRO Investigation.** *H. S. Borovetz, A. M. Brant, E. M. Sevick, S. Shah, E. C. Farrell, E. V. Kline, and C. Wall,* School of Medicine, Department of Surgery, University of Pittsburgh, Pittsburgh, Pennsylvania.
- 106 **The Effect of Load Cycling on the Dimensional Stability of Surgical Vascular Fabrics.** *C. C. Chu, B. Pourdeyhimi, S. R. Malkan,* Department of Design and Environmental Analysis, Cornell University, Ithaca, New York.
- 107 **Theoretical Determination of Porosity in Fabrics and Its Application to the Design of Woven Vascular Grafts.** *B. Pourdeyhimi and C. C. Chu,* Department of Design and Environmental Analysis, Cornell University, Ithaca, New York.

POROUS INGROWTH IN ORTHOPAEDICS I

- 108 **Mechanical Property of Synthetic Porous Hydroxyapatite for Bone Graft After Implantation.** S. Niwa, M. Hori, M. Sohmiya, S. Takahashi, H. Tagai, M. Kobayashi, M. Ono, and H. Takeuchi, Department of Orthopaedic Surgery, Aichi Medical University, Aichi, Japan; Chiba Institute of Technology; Mitsubishi Mining and Cement Co., Ltd..
- 109 **Heat Treatments for Porous Coated Ti-6Al-4V Alloy.** E. A. Renz, S. D. Cook, C. L. Collins, and R. J. Haddad, Jr., Department of Orthopaedic Surgery, Tulane Medical School and the Veterans Administration Medical Center, New Orleans, Louisiana.
- 110 **Porosity Determination of a Low Modulus Implant Material.** J. M. Prewitt, III, and C. A. Homsy, The Methodist Hospital, Houston, Texas.
- 111 **The Effect of Porous-Coating Heat Treatments on the Deformation of a Co-Cr-Mo Alloy.** G. C. Weatherly, W. M. Laanemae, R. M. Pilliar, and S. R. MacEwen, Department of Metallurgy and Materials Science, University of Toronto, Toronto, Ontario, Canada.
- 112 **Characterization of Porosity in Porous Polymeric Implant Materials.** R. E. Dehl, Polymer Science and Standards Division, National Bureau of Standards, Washington, D.C..
- 113 **Bone Ingrowth of Porous-Coated Prostheses.** J. P. Collier, M. Mayor, C. Engh, A. Brooker, Thayer School of Engineering, Dartmouth College, Hanover, New Hampshire.
- 114 **The Use of Epifluorescence to Evaluate Bony Ingrowth into Porous Metallic Implants.** R. L. Folger and E. A. Murice, Howmedica Corporate R&D, Groton, Connecticut.
- 115 **A Method for Determining the Bonding Between Inclusions and PMMA.** H. C. Park, Y. K. Liu, and R. S. Lakes, Center for Materials Research, College of Engineering, The University of Iowa, Iowa City, Iowa.
- 116 **Mechanical Durability of Ceramic/UHMWPE Total Hip Systems.** I. C. Clarke, G. Sines, H. Oonishi, and Y. Kitamura, Biomedical Research Institute, Los Angeles; Department of Materials Science, UCLA, California; Department of Orthopaedics, Osaka Minami National Hospital, and Kyocera, Japan.
- 117 **Optimisation of Controlled-Torque Insertions of Monocrystalline Ceramic Screws at Surgery.** I. C. Clarke, E. Ebramzadeh, P. Oette, and Y. Kitamura, Biomedical Research Institute, Los Angeles; Department of Orthopaedics, University of Southern California, Los Angeles; Kyocera, San Diego and Kyoto.
- 118 **Finite Element Analysis of an Uncemented Alumina-Ceramic Total Knee Prosthesis.** H. Oonishi, Y. Kitamura, A. Kawaguchi, and M. Tatsumi, Department of Orthopaedic Surgery and Artificial Joint Section, Osaka Minami National Hospital, Osaka, Japan.
- 119 **Control and Physiological Influence of HAP Ceramic Porosity.** A. Ravaglioli, A. Krajewski, A. Moroni, and B. Olmi, Institute for Technical Research for Ceramic, C.N.R., Faenza, Italy.

- 120 **Development of a New Orthopaedic Material: Screws and Plates Coated with Titanium Nitride (TiN) Ceramic.** *T. Suka, M. Masubuchi, Y. Ooi, and K. Mikanagi*, Department of Orthopaedics, Jichi Medical School, Yakushiju 3311-1, Kawachi-gun, Tochigi-ken, 329-04 Japan.
- 121 **New Porous Zirconium-Titanium Alloys for Implant.** *O. Okuno, I. Miura, H. Kawahara, M. Nakamura, and K. Imai*, Institute for Medical and Dental Engineering, Tokyo Medical and Dental University, Tokyo, Japan; Department of Biomaterials, Osaka Dental University, Osaka, Japan.

SESSION 25

Sunday Afternoon
April 29, 1984

CORROSION I

- 122 **Morphological and Electrochemical Studies of Fatigue and Corrosion Fatigue on Three Orthopedic Implant Materials.** *O. E. M. Pohler*, Fontana Corrosion Center, The Ohio State University, Columbus, Ohio.
- 123 **Effects of Porous Coatings on the Corrosion Behavior of Co-Cr-Mo Material.** *A. C. Van Orden and A. C. Fraker*, National Bureau of Standards, Washington, D. C..
- 124 **Kinetics of the Ni(II) Reaction with Human Blood Serum Albumin.** *G. J. Mattamal and A. C. Fraker*, National Bureau of Standards, Washington, D. C..
- 125 **Stress Corrosion Cracking Susceptibility of 316L and Ti-6Al-4V ELI Implant Alloys.** *V. H. Desai and K. J. Bundy*, Materials Science and Engineering Department, Johns Hopkins University, Baltimore, Maryland.
- 126 **Influence of Chloride Ion Concentration on the Corrosion of Pd-Based Alloys.** *T. K. Vaidyanathan*, New York University Dental Center, Department of Dental Materials Science, New York, New York.
- 127 **The Influence of Stress on the Dissolution Behavior of Surgical Implant Alloys.** *K. J. Bundy, V. H. Desai, and M. A. Vogelbaum*, Biomedical Engineering Department, Tulane University, New Orleans, Louisiana.
- 128 **Serum Concentration Effects on the Biocorrosion of Surgical Stainless Steel.** *H. M. Hsu, R. A. Buchanan*, The University of Alabama in Birmingham, Birmingham, Alabama.
- 129 **Can Performances of Stainless Steel for Implant Application be Improved?** *P. Comte and S. G. Steinemann*, Institut Straumann AG, CH-4437 Waldenburg/Switzerland.
- 130 **Effect of Carbon Coatings on In Vivo Release of Cr, Co & Ni from F-75 Alloy.** *P. H. Oppenheimer, D. M. Morris, A. M. Konowal, C. C. Clark, and J. Black*, McKay Laboratory of Orthopaedic Surgery Research, University of Pennsylvania, Philadelphia, Pennsylvania.
- 131 **Immunological Tolerance After Oral Administration of Nickel and Chromium.** *K. J. J. Vreeburg, K. de Groot, M. von Blomberg, and R. J. Scheper*, Department of Biomaterials, Free University, Amsterdam, The Netherlands.

SESSION 26

Sunday Afternoon
April 29, 1984
Columbia B Room

ELECTRICAL AUGMENTATION OF TISSUES I

Chairpersons: D. Williams and C. Hassler

- 2:10 -132 **The Direct Current Electrical Stimulation of Surgical Repairs of the Rabbit Achilles Tendon.** *M. Zimmerman, J. R. Parsons, T. Poandl, H. Alexander, and A. B. Weiss*, Section of Orthopaedic Surgery, UMDNJ-New Jersey Medical School, Newark, New Jersey.
- 2:30 -133 **Treatment of Congenital and Acquired Pseudoarthrosis with Electromagnetic Fields, Appearance of Strong Periosteal Bone Callus.** *R. Cadossi, G. Fontanesi, F. Giancecchi, R. Rotini, A. Dal Monte, and G. Poli*, University of Modena, Modena, Italy.
- 2:50 -134 **The Role of Cathodic Potential in Electrically Induced Osteogenesis.** *L. Furst, G. Farrington, Z. Davidovitch, and E. Korostoff*, University of Pennsylvania, Philadelphia, Pennsylvania.
- 3:10 -135 **Electro-Active and Biodegradable Composites as Bone Adhesives.** *G. W. Ciegler and S. I. Stupp*, Bioengineering Program and Polymer Group, College of Engineering, University of Illinois at Urbana-Champaign, Urbana, Illinois.

SESSION 27

Sunday Afternoon
April 29, 1984
Ticonderoga Room

DENTAL MATERIALS II

Chairpersons: J. Lemons and A. Hensten-Pettersen

- 2:10 -136 **Compatibility of Various Partial Denture Materials with Gingival Tissues.** *Y. M. Shaker, S. I. Ibrahim, and N. A. Abbas*, Biochemistry Laboratory, National Research Center, Dokki, Cairo, Egypt.
- 2:30 -137 **Energy-Absorbing, Hydrophobic Dental Cements Based on Dimer and Trimer Acids.** *J. M. Antonucci, S. Venz, D. J. Dudderar, M. C. Pham, and J. W. Stansbury*, National Bureau of Standards, Polymer Science and Standards Division, Washington, D. C.
- 2:50 -138 **Correlation Between Hardness and Degree of Conversion During the Setting Reaction of Unfilled Restorative Resins.** *J. L. Ferracane*, Baylor College of Dentistry, Dallas, Texas.
- 3:10 -139 **Environmentally Stable Light-Cured Dental Restorative Composite.** *I. L. Kamel and G. L. Schwartz*, Department of Materials Engineering and the Biomedical Engineering and Science Institute, Drexel University, Philadelphia, Pennsylvania

SESSION 28

Sunday Afternoon
April 29, 1984
Yorktown Room

CELL INTERACTIONS WITH POLYMERS

Chairpersons: T. Horbett and T. Akaike

- 2:10 -140 **IN VIVO Leukocyte Interactions With Biomer®**. *R. E. Marchant, K. M. Miller, and J. M. Anderson*, Departments of Macromolecular Science and Pathology, Case Western Reserve University, Cleveland, Ohio.
- 2:30 -141 **PHEMA/Polyamine Graft Copolymers as new Column Matrix for Chromatographic Sorting of Lymphocyte Subpopulations (B Cells and T Cells)**. *K. Kataoka, T. Okano, Y. Sakurai, A. Maruyama, and T. Tsuruta*, Department of Surgical Science, The Heart Institute of Japan, Tokyo Women's Medical College, Tokyo, Japan; Institute of Medical Engineering, Tokyo Women's Medical College; Department of Industrial Chemistry, Science University of Tokyo, Japan.
- 2:50 -142 **Adhesion of Human Umbilical Vein Endothelial Cells to Mitrathane® ,A Segmented Polyether Urethane, Under Conditions of Shear and Axial Stress (Strain)**. *C. L. Ives, S. G. Eskin, and C. L. Seidel*, Department of Surgery, Baylor College of Medicine, Houston, Texas.
- 3:10 -143 **Adhesive Strength of Cell to Biomaterials by Means of Viscometric Method, In Vitro**. *H. Kawahara and T. Maeda*, Department of Biomaterials, Osaka Dental University, 1-47 Kyobahsi, Higashi-ku, Osaka 540, Japan.
- 3:30-3:45 Break

SESSION 29

Sunday Afternoon
April 29, 1984
Columbia B Room

ORTHOPAEDIC BIOMECHANICS I

Chairperson: R. Treharne and T. Yokobori

- 3:45 -144 **The Development of a New High Strength, Cold Forged 316LVM Stainless Steel**. *D. I. Bardos, I. Baswell, S. Garner, and R. Wigginton*, Richards Medical Company, Memphis, Tennessee.
- 4:05 -145 **Fatigue of Tapered Joints**. *C. Asgian, L. Gilbertson, R. Hori*, Zimmer, Inc., Warsaw, Indiana.
- 4:25 -146 **The Fatigue Resistance of Orthopaedic Wire and Cable Systems**. *F. S. Georgette, T. W. Sander, and I. Oh*, Richards Medical Company, Memphis, Tennessee.
- 4:45 -147 **Influence of Ageing on the Mechanical Behaviour of Carbon-Fibre Reinforced Epoxy**. *U. Soltész and C. Reynvaan*, Fraunhofer-Institut für Werkstoffmechanik, Freiburg i.Br., Germany.
- 5:05 -148 **An IN VITRO Strain Gage Study of Metal Backed Acetabular Cups**. *I. Oh, M. Bushelow, T. W. Sander, and R. W. Treharne*, Huntington Memorial Hospital, Pasadena, California.

- 5:25 -149 **Laboratory Knee Simulation: A Viable Option.** *B. M. Hillberry, J. A. Schaaf, C. D. Cullom, and D. B. Kettelkamp*, School of Mechanical Engineering, Purdue University, West Lafayette, Indiana.

SESSION 30

Sunday Afternoon
April 29, 1984
Ticonderoga Room

BIOCERAMICS I

Chairpersons: H. Kawahara and L. L. Hench

- 3:45 -150 **Soft Tissue Responses to Multifaceted Particles and Discs of Durapatite.** *A. D. Sherer, B. E. Sage, S. S. Rothstein, and P. J. Boyne*, Sterling-Winthrop Research Institute, Rensselaer, New York; Loma Linda University, Department of Surgery, Loma Linda, California.
- 4:05 -151 **Tissue Reactions on Hydroxyapatite in the Infected and Non Infected Middle Ear.** *C. A. van Blitterswijk, J. J. Grote, W. Kuypers, and K. de Groot*, Department of Otorhinolaryngology, University Hospital Leiden, The Netherlands; ENT Department, University Hospital, Leiden, The Netherlands; ENT-Research Laboratory, Nijmegen, The Netherlands; Material Science Department, Amsterdam, The Netherlands.
- 4:25 -152 **Mechanisms for the Bonding of Bone to Dense Hydroxyapatite.** *M. M. Walker and J. L. Katz*, Rensselaer Polytechnic Institute, Troy, New York.
- 4:45 -153 **Experimental Evaluation of 70% Hydroxyapatite as a Bone Substitute in Rabbits.** *S. Ishida, H. Nagura, N. Yamashita, and S. Enomoto*, The 2nd Department of Oral and Maxillofacial Surgery, Faculty of Dentistry, Tokyo Medical and Dental University, 1-5-45 Yushima, Bunkyo-ku, Tokyo 113, Japan.
- 5:05 -154 **Bone Regeneration in Canine Radius Defects Treated by Coralline Implants and Iliac Grafts.** *R. E. Holmes and V. Mooney*, University of Texas Health Sciences Center, Dallas, Texas.
- 5:25 -155 **Clinical Trials Using Durapatite for Alveolar Bridge Augmentation.** *B. E. Sage, S. S. Rothstein, and D. A. Paris*, Sterling-Winthrop Research Institute, Rensselaer, New York

SESSION 31

Sunday Afternoon
April 29, 1984
Yorktown Room

DENTAL IMPLANTS I

Chairpersons: T. Valega and K. de Groot

- 3:45 -156 **Spreading and Growth of Epithelial Cells on Hydrophilic and Hydrophobic Surfaces.** *J. A. Jansen, J. R. de Wijn, J. M. L. Wolters-Lutgerhorst, and P. J. van Mullem*, Department of Dental Materials, University of Nijmegen, Nijmegen, The Netherlands.
- 4:05 -157 **Ultrastructural Study of Epithelial Cell Attachment to Implant Materials.** *J. A. Jansen, J. M. L. Wolters-Lutgerhorst, J. R. de Wijn, P. E. Rijnhart, and P. J. van Mullem*, Department of Dental Materials, University of Nijmegen, Nijmegen, The Netherlands.

- 4:25 -158 **Gingival Attachment of Permucoasal Dental Root Implants of Dense Hydroxylapatite.** *G. L. de Lange, C. de Putter, and K. de Groot*, Free University, Department of Oral Biology, School of Dentistry, Amsterdam, The Netherlands.
- 4:45 -159 **Behaviour of Alveolar Bone Around Permusocal Dental Implants of Dense Hydroxylapatite.** *C. de Putter, G. L. de Lange, K. de Groot, P. A. E. Sillevs Smitt, and A. Kootwijk*, Departments of Prosthetic Dentistry and Biomaterials, Free University, Amsterdam, The Netherlands.
- 5:05 -160 **A Longitudinal Histiometric Evaluation of Micro-Structures Surrounding Semi-Buried Dental Implants.** *R. G. Daniells and R. A. James*, Loma Linda University SD, Loma Linda, California.
- 5:25 -161 **Quantitative Histology of Porous Dental Implants.** *J. C. Keller and F. A. Young*, Department of Materials Science, Medical University of South Carolina, Charleston, South Carolina.

SESSION 32

Monday
April 30, 1984
Regency A Room

KEYNOTE ADDRESS

Chairperson: J. Black

- 8:00-8:40 -162 **Porous Implants: Interfacial Considerations.** *R. M. Pilliar*, Faculty of Dentistry, University of Toronto, Toronto, Ontario, Canada.

SESSION 33

Monday Morning
April 30, 1984
Regency A Room

KEYNOTE ADDRESS

Chairperson: C. W. Hall

- 8:40-9:20 -163 **Porosity and the Blood/Materials Interactions.** *R. A. White*, Harbor/UCLA Medical Center, Torrance, California.

SESSION 34

Monday Morning
April 30, 1984
Regency A Room

POROUS INGROWTH IN ORTHOPAEDICS II

Chairpersons: S. Cook and R. Pilliar

- 9:20 -164 **Adaptive Bone Remodeling with Porous Ingrowth Femoral Surface Replacement.** *D. R. Carter, R. Vasu, and W. H. Harris*, Design Division, Mechanical Engineering Department, Stanford University, Stanford, California; Veterans Administration Medical Center, Palo Alto, California.

- 9:40 -165 **The Effect of Bone Implant Apposition on Bone Ingrowth into Canine Acetabular Porous Metal Implants.** *M. Jasty, N. F. Jensen, E. H. Weinberg, S. P. Rogers, and W. H. Harris*, Orthopaedic Research Laboratory, Massachusetts General Hospital, and Harvard Medical School, Boston, Massachusetts.
- 10:00 -166 **In Vitro Mechanical Testing of Porous-Coated Orthopaedic Implant Support in Bone After 1 Year: Differences Between Fibrous Tissue Support and Bone Ingrowth.** *J. M. Lee, R. M. Pilliar, D. Abdulla, and J. D. Bobyn*, Biomaterials Research, University of Toronto, Toronto, Ontario, Canada.

SESSION 35

Monday Morning
April 30, 1984
Columbia B Room

CORROSION II

Chairpersons: K. Merritt and G. Heimke

- 9:20 -167 **Three Types of Corrosion in 316L C. W. Implantable Stainless Steel.** *E. P. Lautenschlager, M. Tiara, and J. A. Lautenschlager*, Northwestern University, Chicago, Illinois.
- 9:40 -168 **Surface Modifications and Corrosion of Porous Fiber Titanium Alloy Systems.** *J. Lemons, R. Compton, R. Buchanan, and L. Lucas*, The University of Alabama in Birmingham, Birmingham, Alabama.
- 10:00 -169 **Corrosion-Fatigue Behavior of Porous Coated Ti-6Al-4V Implant Materials.** *A. C. Fraker, A. J. Bailey, H. Hahn, and R. H. Rowe, Jr.*, National Bureau of Standards, Washington, D. C. and Artech Corporation, Falls Church, Virginia.

SESSION 36

Monday Morning
April 30, 1984
Ticonderoga Room

BIORESORPTION I

Chairpersons: D. K. Gilding and C. Sharma

- 9:20 -170 **Degradation and Permeability of Biobrane-1 and Glutaraldehyde-Treated or Untreated Bovine Pericardial Tissue.** *J. P. VonderBrink, T. J. Sernka, and P. K. Bajpai*, University of Dayton, Dayton, Ohio.
- 9:40 -171 **Poly(β -Malic Acid), A Functional Polyester of Increasing Pharmacological Importance.** *M. Vert, C. Bunel, C. Braud, and H. Garreau*, Laboratoire des Substances Macromoléculaires, ERA CNRS 471, I.N.S.C.I. Rouen BP 8, 76130 Mont-Saint-Aignan, France.
- 10:00 -172 **Some Characteristics of Chitin (Poly-N-Acetyl-D-Glucosamine) for Orthopaedic Use.** *M. Mayeda, Y. Inoue, H. Iwase, and K. Kifune*, Department of Orthopaedic Surgery, Juntendo University Casualty Center, Shizuoka, Japan.

SESSION 37

Monday Morning
April 30, 1984
Columbia A Room

INFECTION AND BIOMATERIALS

Chairpersons: F. Schoen and D. Absolom

- 9:20 -173 **Preferred Sterilization Techniques for Biomaterials with Diverse Surface Properties.** *R. Baier, J. Natiella, A. Meyer, J. M. Carter, and T. Turnbull*, State University of New York at Buffalo and Advanced Technology Center, Calspan, Buffalo, New York.
- 9:40 -174 **Influence of Skeletal Implant Materials on Infection.** *R. W. Petty, S. S. Spanier, J. J. Shuster, and C. A. Silverthorne*, University of Florida, Gainesville, Florida.
- 10:00 -175 **Bacterial Adherence to Biomaterials: The Clinical Significance of Its' Role in Sepsis.** *A. G. Gristina and J. W. Costerton*, Bowman Gray School of Medicine of Wake Forest University, Winston-Salem, North Carolina.
- 10:20-10:35 Break

SESSION 38

Monday Morning
April 30, 1984
Regency A Room

ORTHOPAEDIC JOINT REPLACEMENT I

Chairpersons: S. Hulbert and T. Yamamuro

- 10:35 -176 **The Design of Canine THR for the Biological Evaluation of Human THR.** *R. R. Tarr and A. McLaren*, Orthopaedic Biomechanics Laboratory, Bone and Connective Tissue Research Program, Orthopaedic Hospital/University of South California, Los Angeles, California.
- 10:55 -177 **Total Hip Arthroplasty in Dogs Using Carbon Fiber Reinforced Polysulfone Implants.** *M. Roffman, D. G. Mendes, Y. Charit, and M. S. Hunt*, Research Center for Implant Surgery, Haifa Medical Center (Rothschild), Faculty for Medicine, Technion, Haifa, Israel.
- 11:15 -178 **Hip Stems Made of Carbon Fiber-Reinforced Carbon Materials - A Mechanical Evaluation.** *P. Christel, P-F. Bernard, and A. Meunier*, Laboratoire des Recherches Orthopediques, Faculte de Medecine Lariboisiere-Saint-Louis, Paris, France.
- 11:35 -179 **Articular Cartilage Response to LTI Carbon and Ti-6Al-4V Alloy Hemiarthroplasties.** *S. D. Cook, R. C. Anderson, and R. J. Haddad, Jr.*, Department of Orthopaedic Surgery, Tulane University School of Medicine, New Orleans, Louisiana.
- 11:55 -180 **Tibial Plateau Coverage in Total Knee Replacement - Arthroplasty.** *J. A. Dupont, A. M. Weinstein, and P. R. Townsend*, Harrington Arthritis Research Center, Phoenix, Arizona.

SESSION 39

Monday Morning
April 30, 1984
Columbia B Room

CORROSION III

Chairpersons: L. Lucas and E. Howard

- 10:35 -181 **Tafel Slopes in Serum and Saline While Static and Fretting.** *R. L. Williams and S. A. Brown*, University of California, Davis, California.
- 10:35 -182 **IN VITRO and IN VIVO Corrosion Analyses of Implant Alloys.** *L. Lucas, P. Dale, R. Buchanan, Y. Gill, D. Griffin, and J. Lemons*, University of Alabama in Birmingham, Birmingham, Alabama.
- 11:15 -183 **Biological Reaction of Ni in TiNi Shape Memory Alloy.** *H. Oonishi, E. Tsuji, M. Miyaga, T. Hamada, Y. Suzuki, T. Nabeshima, T. Hamaguchi, and N. Okabe*, Osaka-Minami National Hospital, Department of Orthopedic Surger, Osaka, Japan; Osaka Prefectural Industrial Research Institute; The Furukawa Electric Co., Ltd..
- 11:35 -184 **Metallic Ion Release and Cell Damage: Experimental Study.** *P. Tranquilli-Leali and S. Bartoli*, Clinica Ortopedica, University of Cattolica, Roma, Italy.
- 11:55 -185 **The Effect of Surface Condition and Environment on the Ti Ion Release.** *P. Ducheyne, W. Colen, M. Martens, and P. Delport*, University of Pennsylvania, Department of Bioengineering, Philadelphia, Pennsylvania.

SESSION 40

Monday Morning
April 30, 1984
Ticonderoga Room

NEW DEVELOPMENTS IN BIOMEDICAL POLYMERS

Chairpersons: S. W. Kim and H. Tanzawa

- 10:35 -186 **Surface Modification of Small Diameter Dacron Vascular Grafts After a Tetrafluoroethylene Glow Discharge Treatment.** *A. S. Hoffman, A. M. Garfinkle, and B. D. Ratner*, University of Washington, Seattle, Washington.
- 10:55 -187 **Evaluation of Materials in Consideration of an Artificial Fallopian Tube.** *S. K. Hunter, D. E. Gregonis, D. L. Coleman, R. L. Urry, and J. R. Scott*, Department of Pharmaceutics and Division of Artificial Organs, University of Utah, Salt Lake City, Utah.
- 11:15 -188 **Phospholipid Polymers - A New Biomaterial.** *J. A. Hayward, M. A. Whittam, D. S. Johnston, and D. Chapman*, Biochemistry and Chemistry Department, Royal Free Hospital School of Medicine, London, United Kingdom.
- 11:35 -189 **RF Plasma-Deposited Films as Model Substrates for Studying Biointeractions.** *B. D. Ratner, Y. Haque, T. A. Horbett, M. B. Schway, and A. S. Hoffman*, Department of Chemical Engineering and Center for Bioengineering, University of Washington, Seattle, Washington.

- 11:55 -190 **Porpoise and Killer Whale Skin as Natural Examples of Low-Drag, Low Adhesion Biomaterial Surfaces.** *R. Baier, M. Meenaghan, J. Wirth, H. Gucinski, and S. Nakeeb*, State University of New York at Buffalo and Advanced Technology Center, Calspan, Buffalo, New York.

SESSION 41

Monday Morning
April 30, 1984
Columbia A Room

HEART VALVES

Chairpersons: M. Helmus and R. Guidoin

- 10:35 -191 **Metallurgical and Thermal-Wave Failure Analysis of Two Bjork-Shiley™ Spherical Disk Valves Used in Jarvik-7™ Total Artificial Hearts.** *P. E. Duncan, R. Rowe, V. Kerlins, and A. Rosencwaig*, Kolff Medical, Inc., Salt Lake City, Utah; McDonnell Douglas Astronautics Company, Huntington Beach, California; Thermo-wave, Inc., Fremont, California.
- 10:55 -192 **Contemporary Explant Analysis of Prosthetic Heart Valves.** *F. J. Schoen and C. E. Hobson*, Cardiac Pathology Laboratory, Brigham and Women's Hospital, Harvard Medical School, Boston, Massachusetts.
- 11:15 -193 **An Animal Model for Testing Prosthetic Heart Valves.** *R. D. Jones, F. S. Cross, and D. M. Dreher*, Division Surgical Research, Saint Luke's Hospital, Cleveland, Ohio.
- 11:35 -194 **Immunogenicity of Glutaraldehyde-Treated Bovine Pericardial Tissue Xenografts in Rabbits.** *M. L. Salgaller and P. K. Bajpai*, Children's Hospital, Columbus, Ohio.
- 11:55 -195 **Prevention of Experimental Bioprosthetic Heart Valve Calcification.** *R. J. Levy, F. J. Schoen, J. T. Levy, M. Hawley, and T. Thomas*, The Children's Hospital and Brigham and Women's Hospital, Boston, Massachusetts, and Wellesley College, Wellesley, Massachusetts.
- 12:15-1:30 Lunch

SESSION 42

Monday Afternoon
April 30, 1984
Regency A Room

KEYNOTE ADDRESS

Chairperson: D. C. Smith

- 1:30-2:10 -196 **The Clinicians Overview on Dental Implants.** *A. N. Cranin*, Brookdale Implant Dental Group, The Brookdale Hospital Medical Center, Brooklyn, New York.

2:10-5:00 POSTER PRESENTATIONS

Columbia C, Concord
Lexington and Bunker
Hill Rooms

Chairpersons: D. Feldman, C. Batich, and S. Hulbert

SESSION 43

SUSTAINED RELEASE: GENERAL

- 197 **The Evaluation as a Potential Drug Carrier of N-(2-Hydroxypropyl)Methacrylamide Copolymers Containing Biodegradable Crosslinks.** *S. A. Cartledge, P. Rejmanová, R. Duncan, J. Kopecek, and J. B. Lloyd*, University of Keele, Staffordshire, England.
- 198 **Sustained Release of Macromolecules from a Subcutaneous Implant.** *V. N. Hasirci and I. L. Kamel*, Department of Materials Engineering and the Biomedical Engineering and Science Institute, Drexel University, Philadelphia, Pennsylvania.
- 199 **Development of Spermicide-Releasing Disposable Barrier Diaphragms.** *R. A. Casper, R. L. Dunn, R. N. Terry, and L. R. Beck*, Southern Research Institute, Alabama.
- 200 **Microencapsulation of Mammalian cells in Synthetic Semi-Permeable Membranes.** *W. T. K. Stevenson, J. W. Blyzniuk, M. Sugamori, and M. V. Sefton*, Department of Chemical Engineering and Applied Chemistry, University of Toronto, Toronto, Ontario, Canada.
- 201 **The Antibiotic Level in Serum and Bone Tissue After Local Application of Antibiotic-TCP-Beads with Delayed Release.** *J. Eitenmüller, G. Peters, K.-H. Schmidt, and R. Weltin*, Department of Traumatology, Surgical University Hospital, Cologne, Germany.
- 202 **Bioadhesive Intraoral Release Systems.** *N. A. Peppas and R. Gurny*, School of Chemical Engineering, Purdue University, West Lafayette, Indiana.
- 203 **Treatment of Osteomyelitis with Resorbable Antibiotic-Coated Drug Delivery Systems - An Experimental Report.** *A. Stemberger, R. Ascherl, W. Erhardt, W. Haller, K. Machka, K. Geissdörfer, H. Langhammer, K. Sorg, and G. Blümel*, Inst. f. Exp. Surg.; Inst. f. Med. Microbiology and Clinic of Nuclear Medicine of the Technical University, Munich, Germany.
- 204 **Strength and Leaching Characteristics of PMMA Beads Containing Antibiotic.** *J. A. von Fraunhofer, P. D. Mangino, and D. Seligson*, Division of Orthopedic Surgery, Department of Surgery, University of Louisville School of Medicine, Louisville, Kentucky.

SESSION 44

Monday Afternoon
April 30, 1984

HEPARIN AND DERIVATIZED SURFACES I

- 205 **Contact Phase Activation Induced with Hydrosoluble Synthetic Dextran and Polystyrene Derivatives.** *J. M. Nigretto, E. Corretge, M. Jozefowicz, and M. Mauzac*, Laboratoire de Recherches sur les Macromolécules, Villetaneuse, France.
- 206 **Anticoagulant Dextran Derivatives.** *J. Jozefowicz, M. Mauzac, A. M. Fischer, J. Tapon-Breaudiere, and S. Beguin*, Laboratoire de Recherches sur les Macromolécules, Villetaneuse, France.
- 207 **Anticoagulant-Surface-Activity of Dicarboxylic Amino Acid Modified Polystyrene Resins: Influence of the Carboxylic Acid Site.** *M. Jozefowicz, D. Labarre, H. Serne, C. Fougnot, C. Douzon, and F. M. Kanmangne*, Université Paris-Nord-Laboratoire de Recherches sur les Macromolécules, Villetaneuse, France.

- 208 **Anticomplementary Activity of Dextran Derivatives.** *F. Maillet, M. Mauzac, J. Jozefonvicz, M. D. Kazatchkine*, Inserum U 28, CNRS ERA 48, Hospital Broussais, Paris, France.

SESSION 45

Monday Afternoon
April 30, 1984

BIORESORPTION II

- 209 **An Alternative Means to Study the Degradation Phenomena of Polyglycolic Acid Absorbable Polymer.** *C-C. Chu and M. C. Louie*, Department of Design & Environmental Analysis, Cornell University, Ithaca, New York.
- 210 **Poly(Ester-Amides): IN VIVO Analysis of Degradation and Metabolism Using Radiolabeled Polymer.** *T. H. Barrows, S. J. Gibson, and J. D. Johnson*, Life Sciences Research Laboratory/3M, St. Paul, Minnesota.
- 211 **IN VITRO Studies on the Degradation of Nylon 6** *J. M. Anderson, S. A. Kline, and P. A. Hiltner*, Departments of Pathology and Macromolecular Science, Case Western Reserve University, Cleveland, Ohio.
- 212 **Synthesis and Properties of a New Biodegradable Polypeptide.** *D. Bichon and W. Borloz*, Battelle Institute, Geneva, Switzerland.
- 213 **New Adsorbents of Bilirubin for Artificial Liver Support.** *K. Teramoto, M. Murakami, H. Tanzawa, T. Sonoda, and Y. Idezuki*, Fiber Research Laboratories, Toray Industries, Otsu, Japan.

SESSION 46

Monday Afternoon
April 30, 1984

BIOCERAMICS II

- 214 **Effect of Alumina on the Reactivity of Bioglass.** *C. S. Kucheria, R. E. Wells, R. S. Matthews, and G. E. Gardiner*, Howmedica Corporate R&D, Groton, Connecticut.
- 215 **Evaluation of Solid Durapatite to Restore Atrophic Alveolar Ridges.** *B. E. Sage, D. R. Mehlich, K. I. Gumaer, and R. L. Salisbury*, Sterling-Winthrop Research Institute, Rensselaer, New York; Biomedical Research Group, Inc., Austin, Texas.
- 216 **Evaluation of Solid Durapatite in Lefort I Osteotomies in Rhesus Monkeys.** *A. D. Sherer, D. Rothschild, S. S. Rothstein, P. J. Boyne, and B. E. Sage*, Sterling-Winthrop Research Institute, Rensselaer, New York; Department of Surgery, Loma Linda University, Loma Linda, California.
- 217 **Use of Resorbable Alumino-Calcium-Phosphorous Oxide Ceramics (Alcap) in Health Care.** *P. K. Bajpai, G. A. Graves, Jr., L. G. Wilcox, and M. J. Freeman*, Physiology Program, School of Medicine, Wright State University, Dayton, Ohio.
- 218 **Results of Biophysical and Biochemical Adaptation of Skeletal Implants.** *A. Engelhardt, G. P. Zoephel, and W. Wagner*, B.a.f.B., 6103 Griesheim, West Germany.

- 219 **Mechanical Properties of Polymer Coated Porous Corraline Hydroxyapatite.** A. F. Tencer, V. Mooney, K. Brown, and P. A. Silva, Biomedical Engineering Program, University of Texas at Arlington, Arlington, Texas.

SESSION 47

Monday Afternoon
April 30, 1984

ELECTRICAL AUGMENTATION OF TISSUES II

- 220 **Streaming Potentials in Osteons: An Anatomical Model.** R. Salzstein, S. R. Pollack, N. Petrov, G. Brankov, and R. Blagoeva. University of Pennsylvania, Department of Bioengineering, Philadelphia, Pennsylvania.
- 221 **Frequency Response of Stress-Generated Potentials (SGPs) in Wet Bone.** S. Singh and S. Saha, Biomechanics Laboratory, Department of Orthopaedic Surgery, LSU Medical Center, Shreveport, Louisiana.
- 222 **Electrical Stimulation of Bone with a Threaded Screw Cathode.** E. Chamoun, J. Lemons, P. Henson, M. McCutcheon, and L. Lucas, University of Alabama at Birmingham, Birmingham, Alabama.

SESSION 48

Monday Afternoon
April 30, 1984

BONE REPLACEMENT AND OSTEOGENESIS II

- 223 **The Influence of Age on the Mechanical and Physical Properties of the Human Femur.** L. Claes and H. Kleiner, Abteilung für Unfallchirurgie der Universität Ulm Oberer Eselsberg, 7900 Ulm, Germany.
- 224 **An Evaluation of Particulate Aluminum Oxide as a Bone Graft Material.** R. E. Luedemann, S. D. Cook, G. Gianoli, R. J. Haddad, and A. Harding, Tulane University School of Medicine, New Orleans, Louisiana.
- 225 **Analysis of Bone Fracture Surface by Scanning Electron Microscopy.** S. Saha, Biomechanics Laboratory, LSU Medical Center, Shreveport, Louisiana.
- 226 **Computer Assisted Microstructural Analysis of Cancellous Bone.** T. P. Harrigan, M. Jasty, W. H. Harris, R. W. Mann, Orthopaedic Research Labs., Massachusetts General Hospital and Harvard Medical School, Boston, Massachusetts, and Department of Mechanical Engineering, Massachusetts Institute of Technology, Cambridge, Massachusetts.
- 227 **Bone Morphogenesis Induced by Perforated Bone Matrix.** E. Gendler, Orthopaedic Hospital, Los Angeles, California.

SESSION 49

Monday Afternoon
April 30, 1984

ORTHOPAEDIC BIOMECHANICS II

- 228 **Pyrolite Carbon - An Alternative Implant Material In Orthopedic Surgery.** *S. L. Kampner and A. M. Weinstein*, University of California Medical Center, San Francisco, California.
- 229 **Finite Element Modeling of Bone-Implant Interactions: Importance of Interface Assumptions.** *J. A. Hipp, J. B. Brunski, M. S. Shephard, and G. V. B. Cochran*, Rensselaer Polytechnic Institute, Troy, New York.
- 230 **Strain Gauge Instrumented Screws and Their Application to Internal Fixation.** *R. J. Pawluk, E. Musso, H. M. Dick, G. I. Tzitzikalakis*, Orthopaedic Biomechanics Laboratory, Orthopaedic Surgery, Columbia University, New York, New York.
- 231 **Surface Oxides on Titanium Implants - Spectroscopic Studies of Their Composition and Thickness, and Implications for the Biocompatibility of Titanium.** *J. Lausmaa and B. Kasemo*, Department of Physics, Chalmers University of Technology, S-412 96 Gothenburg, Sweden.
- 232 **A Biomechanical Investigation of Segmental and Distraction Spinal Instrumentation.** *M. Hollis, J. Lemons, R. Nasca, and R. Casper*, University of Alabama at Birmingham, Birmingham, Alabama.
- 233 **Use of Computerized Tomography and Numerical Control Machining for the Fabrication of Custom Arthroplasty Prosthesis.** *S. Doré, J. D. Bobyn, G. Drouin, R. Dussault, and R. Gariépy*, Department of Mechanical Engineering, Ecole Polytechnique, Montreal, Quebec, Canada.
- 234 **New Methods for Evaluating the Application Characteristics of Polyurethane Resin Orthopaedic Casting Tapes.** *Z. Oser, R. Green, and G. W. Kammerer*, Research Division, Johnson & Johnson Products, Inc., New Brunswick, New Jersey.
- 235 **New Predictive Methods for Evaluating the Stability Characteristics of Polyurethane Resin Orthopaedic Casting Tapes.** *Z. Oser, R. Green, and F. Johnson*, Research Division, Johnson & Johnson Products, Inc., New Brunswick, New Jersey.
- 236 **Notch Sensitivity in Fatigue.** *L. N. Gilbertson*, Zimmer, Inc., Warsaw, Indiana.
- 237 **Fatigue Performance of Cobalt-Based Superalloys and Their Weldments for Implant Devices.** *J. B. Deaton, M. A. Imam, and R. W. Judy, Jr.*, Naval Research Laboratory, Washington, D. C..
- 238 **Inertial Welding of Orthopaedic Alloys.** *L. N. Gilbertson*, Zimmer, Inc., Warsaw, Indiana.

SESSION 50

Monday Afternoon
April 30, 1984

INTERNAL FIXATION MATERIALS AND DEVICES I

- 239 **IN VIVO Study of an Elastomer Coated Bone Fracture Plate.** *J. B. Park, D. Mehta, G. French, H. B. Lee, and W. Stith*, College of Engineering, University of Iowa, Iowa City, Iowa.

- 240 **A Plastic Bone Model for the Evaluation of Femoral Fracture Fixation.** *H. McKellop, R. Glousman, I. Clarke, and A. Sarmiento*, Orthopaedic Biomechanics Laboratory, Bone and Connective Tissue Research Program, Orthopaedic Hospital-USC, Los Angeles, California.
- 241 **The Ulnar Centro-Medullary Locked Nail with Compression or Distraction.** *C. Lefevre, D. Miroux, D. de La Faye, and B. Courtois*, Department of Biomaterials and Surgery, Service d'Orthopédie, C.H.U. 29279 Brest Cedex, France.
- 242 **Carbon Fibre Reinforced Biodegradable and Non-Biodegradable Polymer as Bone Plate Materials.** *J. Kilpikari and P. Törmälä*, Tampere University of Technology, Tampere, Finland.

SESSION 51

Monday Afternoon
April 30, 1984
Columbia B Room

POROUS INGROWTH IN ORTHOPAEDICS III

Chairpersons: M. Spector and J. de Wijn

- 2:10 -243 **Cementless Endoprosthesis Stabilization by a Soft Porous Stem Coating.** *C. A. Hom-
sy, and J. M. Prewitt, III.*, The Methodist Hospital, Houston, Texas.
- 2:30 -244 **A Study of Bone Ingrowth in Some Porous Phosphate Glass-Ceramic Materials.** *F. Pernot, P. Baldet, F. Bonnel, J. M. Saint-André, J. Zarzycki, and P. Rabischong*, Laboratoire des Verres du C.N.R.S., Université Montpellier 2, Place Eugène Bataillon, 34060 Montpellier Cedex, France.
- 2:50 -245 **Segmental Bone Defect Repair with Hydroxyapatite in Weight-Bearing Models.** *P. Patka, A. A. Driessen, K. de Groot, and G. den Otter*, Laboratory of Experimental Surgery, Department of Surgery, Free University, Amsterdam, The Netherlands.
- 3:10 -246 **Effects of Periosteal Activation Agent on Bone Repair and Bone Growth into Porous Implants.** *L. R. Alberts*, Rensselaer Polytechnic Institute, Troy, New York.

SESSION 52

Monday Afternoon
April 30, 1984
Ticonderoga Room

DENTAL IMPLANTS II

Chairpersons: N. Nakabayashi and P. Boyne

- 2:10 -247 **Reconstruction of the Atrophic Alveolar Ridge with Hydroxylapatite: A 5 Year Report.** *J. N. Kent, J. H. Quinn, M. F. Zide, M. S. Block, and M. Jarcho*, LSU Medical Center, Department of Oral and Maxillofacial Surgery, New Orleans, Louisiana.
- 2:30 -248 **Canine Mandibular Ridge Response to Hydroxylapatite Combined with Bone.** *M. S. Block, and J. N. Kent*, Department of Oral and Maxillofacial Surgery, LSU School of Dentistry, New Orleans.

- 2:50 -249 **Comparison of Host Tissue Response to Implants of Synthetic Hydroxylapatite and Ethylene Diamine-Extracted Bone.** *P. J. Boyne, D. E. Stringer, and J. P. Shafqat*, Oral & Maxillofacial Surgery Section, Loma Linda University Medical Center, Loma Linda, California.
- 3:10 -250 **Studies on the Porous Alumina for Free Standing Dental Implant - Animal Experiments and Clinical Observations.** *A. Yamagami, S. Kotera, M. Hirabayashi, and H. Kawahara*, Kyoto Institution of Implantology, Kyoto, Japan.

SESSION 53

Monday Afternoon
April 30, 1984
Regency A Room

POLYURETHANES: DEGRADATION AND FATIGUE

Chairpersons: S. Barenberg and T. Matsuda

- 2:10 -251 **Comparison of Aromatic and Aliphatic Polyetherurethanes for Biomedical Use: By-Products of Thermal/Hydrolytic Degradation.** *R. S. Ward, K. A. White, and J. S. Riffle*, Thoratec Laboratories Corporation, Berkeley, California.
- 2:30 -252 **IN VITRO Aging of Implantable Polyurethanes in Metal Ion Solutions.** *A. J. Coury, P. T. Cahalan, E. L. Schultz, and K. B. Stokes*, Energy Technology Division, Medtronic, Inc., Minneapolis, Minnesota.
- 2:50 -253 **Tensile and Fatigue Properties of Segmented Polyether Polyurethanes and Application to Blood Pump Design.** *K. Hayashi, T. Matsuda, H. Takano, M. Umez, T. Nakamura, Y. Taenaka, and T. Nakatani*, National Cardiovascular Center Research Institute, Suita, Osaka, Japan.
- 3:10 -254 **Environmental Stress Cracking in Implanted Polyurethanes.** *K. B. Stokes, W. A. Frazer, and R. A. Christofferson*, Medtronic, Inc., Minneapolis, Minnesota.
- 3:30 -345 Break

SESSION 54

Monday Afternoon
April 30, 1984
Columbia B Room

LIGAMENTS AND TENDONS: PROPERTIES AND REPLACEMENT II

Chairpersons: B. Sauer and G. Droin

- 3:45 -255 **Mechanical and Histological Evaluation of Ingrowth into Dacron Ligament Implants.** *J. L. Berry, J. S. Skraba, W. S. Berg, J. Shah, J. H. Zoller*, Cleveland Research Institute at Saint Vincent Charity Hospital, Cleveland, Ohio.
- 4:05 -256 **Dynamic Characteristics of Tendon.** *J. Gurtowski, L. Stern, and M. Manley*, Department of Orthopaedics, State University of New York at Stony Brook Health Sciences Center, Stony Brook, New York.

- 4:25 -257 **Comparison of Antigen Extracted, Lyophilized and Glutaraldehyde Fixed Bovine Xenograft: A Preliminary Study.** *J. C. Tauro, J. R. Parsons, J. C. Ricci, H. Alexander, and A. B. Weiss.* Section of Orthopaedic Surgery, UMDNJ-New Jersey Medical School, Newark, New Jersey.
- 4:45 -258 **A Polyester Fiber Reinforced Poly-2-Hydroxyethyl-Methacrylate Artificial Tendon.** *C. Migliaresi, L. Ambrosio, G. Guida, J. Kolarik, L. Nicolais, and D. Ronca,* Polymer Engineering Laboratory, University of Naples, Naples, Italy.

SESSION 55

Monday Afternoon
April 30, 1984
Ticonderoga Room

DENTAL MATERIALS III

Chairpersons: G. Hastings and L. Gettleman

- 3:45 -259 **Studies of the Orthodontic Applications of Crystal Bonding.** *D. C. Smith, R. Maijer, and D. Ruse,* Faculty of Dentistry, University of Toronto, Toronto, Ontario, Canada.
- 4:05 -260 **Metallic Binding to Fractionated Human Saliva Proteins.** *H. J. Mueller and C. Siew,* American Dental Association, Chicago.
- 4:25 -261 **The Adsorption to Calcium-Hydroxylapatite of Biopolymers, Used to Produce an Artificial Saliva.** *A. V. Nieuw Amerongen, P. A. Roukema, J. W. Boerman, M. Valentijn-Benz, C. H. Oderkerk, and K. de Groot,* Departments of Oral Biochemistry and Biomaterials, Vrije Universiteit, Dental School, Amsterdam, The Netherlands.
- 4:45 -262 **Hypersensitivity to Mercury Compounds in Oral Lichen Planus.** *A. Hensten-Pettersen, T. Lyberg, and A. Kullmann,* NIOM, Scandinavian Institute of Dental Materials, Oslo, Norway.

SESSION 56

Monday Afternoon
April 30, 1984
Regency A Room

PROTEIN ADSORPTION I

Chairpersons: L. Vroman and T. Okano

- 3:45 -263 **The Hemoglobin Hypothesis: Hemoglobin and Haptoglobin Surface Properties.** *J. Andrade, J. Chen, J. Pierce, R. Lowe, and D. E. Gregonis,* Department of Bioengineering, University of Utah, Salt Lake City, Utah.
- 4:05 -264 **Interactions of Plasma with Glass: Identification of Adsorbed Proteins.** *J. L. Brash, P. Szota, and J. A. Thibodeau,* Departments of Chemical Engineering and Pathology, McMaster University, Hamilton, Ontario, Canada.
- 4:25 -265 **IgG Interaction with Quartz and Polymer Surfaces Studied by TIRF.** *R. A. Van Wagenen and J. D. Andrade,* Department of Bioengineering, University of Utah, Salt Lake City, Utah.

- 4:45 -266 **Poly(Ethylene Glycol) Surfaces to Minimize Protein Adsorption.** *D. E. Gregonis, D. E. Buerger, R. A. Van Wagenen, S. K. Hunter, and J. D. Andrade*, Department of Materials Science and Engineering, University of Utah, Salt Lake City, Utah.

SESSION 57

Tuesday
May 1, 1984
Regency A Room

KEYNOTE ADDRESS

Chairperson: M. Sefton

- 8:00-8:40 -267 **Heparin-Like Biomaterials.** *M. Jozefowicz and J. Jozefonvicz*. Laboratoire de Recherches sur les Macromolécules, Université Paris-Nord Avenue J. B. Clémont, 93430 Villetaneuse, France.

SESSION 58

Tuesday Morning
May 1, 1984
Regency A Room

KEYNOTE ADDRESS

Chairperson: S. Cooper

- 8:40-9:20 -268 **Polymer Surface Composition and Blood /Materials Interaction.** *A. S. Hoffman*, University of Washington, Seattle, Washington.

SESSION 59

Tuesday Morning
May 1, 1984
Capitol Room

LIGAMENTS AND TENDONS: PROPERTIES AND REPLACEMENT II

Chairpersons: H. Alexander and C. Lacabanne

- 9:20 -269 **Microscopical Characterization of Knee Ligaments: Human and Canine Studies.** *H. Yahia, G. Drouin, and D. Bobyn*, Department of Mechanical Engineering, Ecole Polytechnique of Montreal, Canada.
- 9:40 -270 **Intra-Articular Changes Related Carbon Fiber Reconstruction of Anterior Cruciate Ligament.** *J. Bejui, E. Vignon, D. Hartmann, and F. Bejui-Thivolet*, Faculté Lyon-Nord, Hospital Edouard Herriot, 69373 Lyon Cedex 08, France.
- 10:00 -271 **Connective Tissue Ingrowth in Braided Carbon Tow Compared to Unidirectional Carbon Tow.** *M. Iusim, D. G. Mendes, M. Soudry, M. Silbermann, J. Boss, A. Grishkan, D. Mordejovich, and S. Hamburger*, Research Center for Implant Surgery, Haifa Medical Center (Rothschild), Faculty of Medicine, Technion, Haifa, Israel.

SESSION 60

Tuesday Morning
May 1, 1984
Ticonderoga Room

TISSUE INTERACTIONS WITH POLYMERIC MATERIALS

Chairpersons: J. Andrade and T. Miyata

- 9:20 -272 **Tissue Regeneration Associated with Lactide Containing Implants.** *T. N. Salthouse and B. F. Matlaga*, Clemson University, Clemson, South Carolina.
- 9:40 -273 **Response to Particulate Polysulfone and Polyethylene in an Animal Model for Tumorigenicity Testing.** *M. Spector, N. Reese, and K. Hewan-Lowe*, Emory University School of Medicine, Atlanta, Georgia.
- 10:00 -274 **Evaluation of Porous Acrylic Cement for Application in Reconstruction Surgery. Animal Experiments and Clinical Trials.** *P. J. van Mullem, J. R. de Wijn, J. M. Vaandrager, and M. Ramselaar*, Department of Oral Histology, Dental School, University of Nijmegen, Nijmegen, The Netherlands.

SESSION 61

Tuesday Morning
May 1, 1984
Regency A Room

PROTEIN ADSORPTION II

Chairpersons: J. Brash and K. Hayashi

- 9:20 -275 **Adsorption Control of Proteins on Collagen Derivatives.** *T. Akaike, Y. Itoh, and T. Miyata*, Department Material Systems Engineering, Tokyo University of Agriculture and Technology, Koganei-shi Tokyo 184 Japan; Japan Biomedical Material Research Center, Megure, Tokyo 152 Japan.
- 9:40 -276 **Probing Protein Adsorption: Interfacial Fluorescence and Gamma Photon Detection.** *D. R. Reinecke, R. A. Van Wagenen, J. D. Andrade, and L. M. Smith*, Department of Bioengineering, University of Utah, Salt Lake City, Utah.
- 10:00 -277 **Surface Characterization of Protein-Coated Polymer Surfaces by Means of Sedimentation Volume.** *D. R. Absolom, A. W. Neumann, Z. Policova, and W. Zingg*, Hospital for Sick Children and University of Toronto, Canada.
- 10:20-10:35 Break

SESSION 62

Tuesday Morning
May 1, 1984
Capitol Room

INTERNAL FIXATION MATERIALS AND DEVICES II

Chairpersons: D. Bardos and L. Nicolais

- 10:35 -278 **Totally Biodegradable Fracture-Fixation Plates for Use in Maxillofacial Surgery.** *R. A. Casper, R. L. Dunn, and B. S. Kelley*, Southern Research Institute, Birmingham, Alabama.

- 10:55 -279 **In Vivo Fate of Bioresorbable Bone Plates in Long-Lasting Poly (L-Lactic Acid).** *P. Christel, F. Chabot, and M. Vert*, Laboratoire de Recherches Orthopediques, Faculté de Médecine Lariboisière-Saint-Louis, Paris, France.
- 11:15 -280 **An Isoelastic Fiber Composite Plate for Fracture Fixation.** *L. Nicolais, R. Gimigliano, G. Guida, C. Migliaresi, S. Pagliuso, and V. Renta*, Polymer Engineering Laboratory, University of Naples, Naples, Italy.
- 11:35 -281 **Fracture Fixation Using Polymeric Rods and Transverse Screws.** *N. A. Gillett, S. A. Brown, and N. A. Sharkey*, Department of Pathology, School of Veterinary Medicine, University of California, Davis, Davis, California.
- 11:55 -282 **Biocompatibility Studies of Silver-Coated Fixation Pins.** *J. A. Spadaro, D. A. Webster, J. Kovach, and S. E. Chase*, Department of Orthopedic Surgery, State University of New York (Upstate), Syracuse, New York.

SESSION 63

Tuesday Morning
May 1, 1984
Ticondroga Room

BIOACTIVE CERAMICS

Chairpersons: J. Wilson and U. Gross

- 10:35 -283 **Glass-Ceramic Dental Implants in Rats.** *Th. Kotzur, V. Strunz, and U. Gross*, Institute of Pathology and Department of Maxillo-Facial and Plastic Surgery, Klinikum Steglitz, Freie Universität Berlin, Germany.
- 10:55 -284 **Comparison of Homograft and Bioglass™ Implants in a Mouse Ear Model.** *G. E. Merwin, J. Wilson, and L. L. Hench*, College of Medicine, University of Florida, Gainesville, Florida.
- 11:15 -285 **Bio-Physico Chemical Problems Connected with the Metallic Prostheses Coated with Bioglass.** *A. Ravaglioli and A. Krajewski*, Institute for Technology and Research on Ceramics of C.N.R., Faenza, Italy.
- 11:35 -286 **Bone Bonding Behavior of Some Surface Active Glasses and Sintered Apatite.** *T. Fujiu and M. Ogino*, Glass Division, Nippon Kogaku K. K. Sagami-hara, Kanagawa, Japan.
- 11:55 -287 **IN VIVO and IN VITRO Investigations into Bioglasses™ Which Contain Fluoride.** *D. B. Spilman, J. Wilson, and L. L. Hench*, University of Florida, Gainesville, Florida.

SESSION 64

Tuesday Morning
May 1, 1984
Regency A Room

HEPARIN AND DERIVATIZED SURFACES II

Chairpersons: N. Peppas and T. Komai

- 10:35 -288 **Evaluation of the Antithrombic Activity of Heparin-Like Surfaces Through a New In-Vitro Test Performed Under Circulation.** *V. Migonney, M. Jozefowicz, and C. Fougnot*, Laboratoire de Recherches sur les Macromolécules, Université Paris-Nord, 93430 Villetaneuse, France.

- 10:55 -289 **In Vitro Characterization of Heparinized Polylactide Surface.** *T. C. Lin, J. H. Joist, and R. E. Sparks.* Hexcel Corporation, Dublin, California; Department of Oncology and Hematology, St. Louis University, St. Louis, Missouri; Biological Transport Lab, Washington University, St. Louis, Missouri.
- 11:15 -290 **Adsorption of Antithrombin III.** *S. Winters, D. E. Gregonis, D. Buerger, and J. D. Andrade.* Departments of Pharmaceutics and Materials Science, University of Utah, Salt Lake City, Utah.
- 11:35 -291 **Antithrombic Properties of Polystyrenes Modified by Arginyl Derivatives.** *D. Gulino, C. Boisson, and J. Jozefonvicz.* Université Paris-Nord, Laboratoire de Recherches sur les Macromolécules, Villetaneuse, France.
- 11:55 -292 **A Parallel Flow Arteriovenous Shunt Test System for the Evaluation of Blood Compatible Materials.** *W. F. Ip, M. V. Sefton, and W. Zingg.* Department of Chemical Engineering and Applied Chemistry, University of Toronto, Toronto, Ontario, Canada.
- 12:15-1:15 New Council of the Society for Biomaterials, U.S.A., Meeting in the Grand Canyon Room. Officers and Committee Chairpersons are expected to attend.
- 12:15-1:30 Lunch

SESSION 65

Tuesday Afternoon
May 1, 1984
Regency A Room

KEYNOTE ADDRESS

Chairperson: J. Anderson

- 1:30-2:10 -293 **New Thoughts on Arterial Substitutes: The Biological Period.** *A. D. Callow,* New England Medical Center, Boston, Massachusetts.

2:10-5:00 POSTER PRESENTATIONS

Columbia C, Concord,
Lexington, and
Bunker Hill Rooms

Chairpersons: P. K. Bajpai, S. Hilbert, J. Cunningham, and G. Lautenschlager

SESSION 66

Tuesday Afternoon
May 1, 1984

BIOINTERACTIONS WITH POLYMERS II

- 294 **The Character of the Initial Stages of Blood Interaction with Biomaterials and their Hemocompatibility.** *V. I. Sevastianov, E. A. Tseytina, and A. V. Volkov.* Biomaterials Laboratory, Research Institute of Transplantology and Artificial Organs, Moscow, USSR.
- 295 **Platelet Adhesion and Aggregation Studies with Selected Polyamides.** *J. M. Courtney, M. Travers, G. D. O. Lowe, C. D. Forbes, S. K. Bowry, and H. Wolf.* University of Strathclyde, Bioengineering Unit, Glasgow, United Kingdom.

- 296 **Hemoperfusion with Activated Charcoal Coated by Glow Discharge Technique.** *N. Hasirci and G. Akovali*, Middle East Technical University, Department of Chemistry, Ankara, Turkey.
- 297 **The Effect of Biomaterial-Treated Macrophages on Fibroblast Replication.** *A. Pizzoferrato, S. Stea, and G. Ciapetti*, Istituto Ortopedico Rizzoli, Bologna, Italy.
- 298 **Dynamics of Tendon Cell Growth on Synthetic Fiber Materials In Vitro.** *J. Ricci, H. Alexander, J. R. Parsons, and A. G. Gona*, Section of Orthopaedic Surgery, UMDNJ-New Jersey Medical School, Newark, New Jersey.
- 299 **Auto-Alloplastic Tracheal Replacement Prosthesis, Basic and Experimental Investigations.** *A. Berghaus*, ENT-Clinic, Klinikum Steglitz, Freie Universität Berlin, Berlin, West Germany.
- 300 **The Interactions of Calciumphosphate Crystals and Polymorphonuclear Leukocytes Monitored by Luminol Dependent Chemiluminescence.** *C. P. A. T. Klein, K. de Groot, and F. Namavar*, Departments of Biomaterials and Medical Microbiology, Schools of Dentistry and Medicine, Free University, Amsterdam, The Netherlands.

SESSION 67

Tuesday Afternoon
May 1, 1984

PROTEIN ADSORPTION III

- 301 **Protein Adsorption on Polycarbonate - Changes with L-Ascorbic Acid and Blood Cells.** *C. P. Sharma and T. Chandy*, Biosurface Technology Division, Biomedical Technology Wing, Sree Chitra Tirunal Institute for Medical Sciences and Technology, Poojapura, Trivandrum, India.
- 302 **Plasma Protein Interaction with Biomaterials as Determined by Iso-Dalt Electrophoretic Analysis.** *C. M. Chen and D. R. Owen*, Materials Science and Bioengineering, University of New Orleans, Louisiana.
- 303 **Albumin Uptake on C₁₈ Alkylated Polyurethane Foam.** *L. King-Breeding, M. S. Munro, and R. C. Eberhart*, Department of Surgery, University of Texan Health Science Center at Dallas, Texas.
- 304 **Some Special Features in Protein Adsorption on the Surface of Activated Carbon Fibers.** *V. G. Nikolaev, E. V. Eretskaya, and V. P. Sergeev*, Kavetsky Institute of Oncology Problems, Academy of Sciences of the Ukranian SSR, Kiev, USSR.
- 305 **Effects of Model Polymers on Factor V Activity.** *M.C. Boffa, D. Barbier, N. Aubert, N. Mauzac, C. Fougnot, J. Jozefonvicz, and M. Jozefowicz*, Laboratoire de Recherche en Hémostase et Thrombose C.N.T.S. 6 rue A. Cabanel-75739 Paris Cedex 15 and Université Paris Nord, Av. J. B. Clément Villenaneuse-France.

SESSION 68

Tuesday Afternoon
May 1, 1984

CELL TOXICITY OF BIOMATERIALS

- 306 **Cell Culture Methods for Detecting Immunotoxicity of Synthetic Polymers.** *J. M. Simpson, J. T. Sarley, H. J. Johnson, and S. J. Northrup*, Travenol Laboratories, Inc., Morton Grove, Illinois.
- 307 **In Vitro Myeloid Suspension Cultures for Short-Term Toxicity Studies.** *S. L. Hilbert, F. D. A.*, National Center for Devices and Radiological Health, Rockville, Maryland.
- 308 **An Organ Culture Model for Screening of Bone Implant Materials.** *E. E. Sabelman*, Rehabilitation R&D Center, Palo Alto VA Medical Center, Palo Alto, California.
- 309 **In Vitro Characterization of Silicone Bleed From Breast Prostheses.** *J. R. Dylewski and C. L. Beatty*, Department of Materials Science & Engineering, University of Florida, Gainesville, Florida.
- 310 **Spleen Cell Response to Soluble Polymers.** *P. Y. Wang and J. Ditchfield*, Laboratory of Chemical Biology, Institute of Biomedical Engineering, Faculty of Medicine, University of Toronto, Canada.
- 311 **Chinese Hamster Ovary Cells (CHO) Clonal Growth Assay for the Evaluation of Cytotoxic Effects of Biomaterials.** *R. Sernau, T. Cortina, B. H. Keech, N. E. McCarroll, and M. G. Farrow*, Hazleton Laboratories America, Inc., Vienna, Virginia.
- 312 **Production of LAF (Lymphocyte-Activating-Factor) by Mononuclear Phagocytes Activated with Powdered Biomaterials.** *A. Pizzoferrato, G. Ciapetti, and S. Stea*, Istituto Ortopedico Rizzoli, Bologna, Italy.

SESSION 69

Tuesday Afternoon
May 1, 1984

WEAR AND WEAR PARTICULATE II

- 313 **Polyethylene Wear Against Titanium Alloy Compared to Stainless Steel and Cobalt-Chromium Alloys.** *H. McKellop, A. Hosseinian, K. Burgoyne, and I. Clarke*, Orthopaedic Biomechanics Laboratory, Bone and Connective Tissue Research Program, Orthopaedic Hospital-USC, Los Angeles, California.
- 314 **Improvement of Creep and Wear Properties of Polyethylenes.** *G. Gaussens, J. Berthet, L. Cornet, and M. Nicaise*, Commissariat A L'Energie Atomique, C.E.N., Saclay, Office des Rayonnements Ionisants, L.A.B.R.A.

SESSION 70

Tuesday Afternoon
May 1, 1984

ORTHOPAEDIC JOINT REPLACEMENT II

- 315 **Biomechanics of Pediatric Hip Fixation Following Proximal Femoral Varus Osteotomy.** *G. G. Gleis, S. T. White, and J. A. von Fraunhofer*, Division of Orthopaedic Surgery, Department of Surgery, University of Louisville School of Medicine, Louisville, Kentucky.

- 316 **The Effect of Surface Treatments on the Interface Mechanics of LTI Pyrolytic Carbon Implants.** *K. A. Thomas, S. D. Cook, E. A. Renz, R. C. Anderson, R. J. Haddad, Jr., A. D. Haubold, and R. Yapp,* Tulane University Medical School, Department of Orthopaedic Surgery, New Orleans, Louisiana.
- 317 **Sagittal Plane Strain-Cage Analysis of the Femur Before and After Prosthetic Hip Implantation.** *J. P. Collier, T. Orr, M. Mayor, and F. Kennedy,* Thayer School of Engineering, Dartmouth College, Hanover, New Hampshire.
- 318 **A Multifaceted Approach to the Analysis of the THR Implants in a Canine Model.** *P. Campbell, R. D. Bloebaum, T. A. Gruen, and A. Sarmiento,* Orthopaedic Biomechanics Laboratory, Bone & Connective Tissue Research Program, Orthopaedic Hospital-USC, Los Angeles, California.
- 319 **Load Transmission at the Implant-Bone Interface: A Theoretical, Mechanical and Photoelastic Study.** *J. A. Hobkirk and L. W. Wolfe,* Institute of Dental Surgery, London, England.
- 320 **Stem Modulus in Total Hip Design.** *D. W. Burke, J. P. Davies, D. O. O'Connor, and W. H. Harris,* Orthopaedic Research Laboratories, Massachusetts General Hospital and Harvard Medical School, Boston, Massachusetts.

SESSION 71

Tuesday Afternoon
May 1, 1984

DENTAL IMPLANTS III

- 321 **Examination of the Oral Tissue Interface with the Single Crystal Sapphire Endosteal Dental Implant: Conventional and Alternative Ultrastructure.** *D. E. Steflik, R. V. McKinney, Jr., and D. L. Koth,* School of Dentistry, Medical College of Georgia, Augusta, Georgia.
- 322 **HTR™ (Hard Tissue Replacement) for Edentulous Ridge Augmentation.** *A. Ashman and P. Bruins,* Academy of Implant Dentistry, Northeast District, New York City, New York.
- 323 **An Evaluation of Durapatite Submerged-Root Implants for Alveolar Bone Preservation.** *P. Kanguonkit, V. J. Matukas, and D. J. Castleberry,* Department of Oral & Maxillofacial Surgery, University of Alabama in Birmingham, Alabama.
- 324 **Human Mandibular Alveolar Ridge Augmentation with Hydroxylapatite: Final Report of a Five Year Investigation.** *A. N. Cranin and N. M. Satler,* The Brookdale Implant Group, The Brookdale Hospital Medical Center, Brooklyn, New York.
- 325 **Hydroxylapatite (HA) Cone Implants for Alveolar Ridge Maintenance-One Year Follow-Up** *A. N. Cranin and R. Shpuntoff,* The Brookdale Implant Group, The Brookdale Hospital Medical Center, Brooklyn, New York.
- 326 **Particulate Hydroxylapatite (HA) as an Implantable Device to Salvage Failing Endosteal Implants in Dogs.** *A. N. Cranin, R. Shpuntoff, and N. Satler,* The Brookdale Implant Group, The Brookdale Hospital Medical Center, Brooklyn, New York.

- 327 **Capsules Formed from Fibroblasts Aid Incorporation of Hydroxylapatite Implant Particles in Mandibular Repair.** *J. S. Hanker, J. P. Rausch, B. C. Terry, W. W. Ambrose, S. Li, E. J. Burkes, Jr., and B. L. Giammara,* Dental Research Center, School of Dentistry, University of North Carolina, Chapel Hill, North Carolina.
- 328 **Development of a System for Simultaneous Measurement of Three Force Components on Dental Implants.** *J. B. Brunski, M. El-Wakad, and J. A. Hipp,* Rensselaer Polytechnic Institute, Troy, New York.
- 329 **The Use of Miniature Swine in Dental Implant Research.** *T. R. Hill and J. A. Hobkirk,* Eastman Dental Hospital & Institute of Dental Surgery, London, United Kingdom.

SESSION 72

Tuesday Afternoon
May 1, 1984

BONE/IMPLANT INTERFACE III

- 330 **Studies on Implant-Tissue Interfaces Using a Scanning Ultrasonic Transmission Imaging System (SUTIS).** *A. Meunier, H. S. Yoon, J. L. Katz, P. Das, and L. Biro,* Department of Biomedical Engineering, Rensselaer Polytechnic Institute, Troy, New York.
- 331 **Computerized Axial Tomography as a New Adjunct Method for Evaluation of Post-Mortem Cemented Total Hip Replacements in Situ.** *T. Gruen, B. Orisek, P. Campbell, S. Chew, W. Boswell, D. Hillman, and A. Sarmiento,* Departments of Orthopaedics and Radiology, University of Southern California, Bone and Connective Tissue Research Program, Orthopaedic Hospital-USC, Los Angeles, California.

SESSION 73

Tuesday Afternoon
May 1, 1984
Capitol Room

POROUS INGROWTH IN ORTHOPEDICS IV

Chairpersons: M. Jarcho and H. Oonishi

- 2:10 -332 **The Effect of a Porous Coating on the Fatigue Resistance of Ti-6Al-4V Alloy.** *S. Yue, R. M. Pilliar and G. C. Weatherly,* Department of Metallurgy and Materials Science, University of Toronto, Toronto, Ontario, Canada.
- 2:30 -333 **Load Carrying and Fatigue Properties of the Stem-Cement Interface with Smooth and Porous Coated Femoral Components.** *M. T. Manley, L. S. Stern, R. Averill, and P. Serekian,* State University of New York at Stony Brook, Stony Brook, New York.
- 2:50 -334 **Analysis of Uncemented LTI Carbon and Porous Titanium Hip Hemiarthroplasties.** *R. C. Anderson, S. D. Cook, and R. J. Haddad, Jr.,* Tulane University School of Medicine, New Orleans, Louisiana.
- 3:10 -335 **The In-Vivo Strength of Filler Stabilized Porous Implants.** *S. I. Reger, R. E. McLaughlin, and H. C. Eschenroder, Jr.,* Department of Orthopaedics and Rehabilitation, University of Virginia Medical Center, Charlottesville, Virginia.

SESSION 74

Tuesday Afternoon
May 1, 1984
Regency A Room

BLOOD INTERACTIONS: GRAFTS AND SHUNTS II

Chairpersons: A. Callow and T. Yokobori

- 2:10 -336 **Blood Tolerability of Carbon-Carbon Biomaterials. In Vivo and In Vitro Investigations Using Radiotracers.** *B. Basse-Cathalinat, Ch. Baquey, J. Caix, L. Bordenave, J. Brendel, and D. Ducassou, Inserm/Ceemasi-Sc 31, Université Bordeaux II, 33076 Bordeaux Cedex, France.*
- 2:30 -337 **Improved Patency in Small Diameter Dacron Vascular Grafts After a Tetrafluoroethylene Glow Discharge Treatment.** *A. M. Garfinkle, A. S. Hoffman, B. D. Ratner, and S. R. Hanson, University of Washington, Seattle, Washington and Scripps Institute, San Diego, California.*
- 2:50 -338 **Blood Surface Interaction Investigated with Ultrathin Coatings of Glow Discharge Polymers Applied Onto the Inner Surface of Small Diameter Silastic Tubing.** *H. K. Yasuda, Y. Matsuzawa, S. R. Hanson, and L. A. Harker, Graduate Center for Materials Research, University of Missouri-Rolla, Rolla, Missouri.*
- 3:10 -339 **Thrombogenicity of Small Diameter Vascular Grafts.** *J. M. Malone, R. L. Reinert, K. Brendel, and R. C. Duhamel, University of Arizona, Tucson, Arizona.*

SESSION 75

Tuesday Afternoon
May 1, 1984
Ticonderoga Room

SUSTAINED RELEASE: DIABETES

Chairpersons: H. Gabelnick and E. Hayward

- 2:10 -340 **Magnetically Modulated Release from Implantable Devices.** *J. Kost, E. Edelman, L. Brown, and R. Langer, Massachusetts Institute of Technology, Cambridge, Massachusetts.*
- 2:30 -341 **Glucose Sensitive Membranes: Stability and Biocompatibility Studies.** *T. A. Horbett, J. Kost, D. Coleman, B. D. Ratner, University of Washington, Department of Chemical Engineering, Seattle, Washington; University of Utah, Department of Pharmaceutics, Salt Lake City, Utah.*
- 2:50 -342 **Self-Regulating Insulin Delivery System.** *S. Y. Jeong, S. Sato, J. C. McRea, and S. W. Kim, University of Utah, Department of Pharmaceutics, College of Pharmacy, Salt Lake City, Utah.*
- 3:10 -343 **Polyacrylate Coated Alginate Beads for Microencapsulation of Animal Cells.** *F. V. Lamberti and M. V. Sefton, Department of Chemical Engineering and Applied Chemistry, University of Toronto, Toronto, Ontario, Canada.*
- 3:30-3:45 Break

SESSION 76

Tuesday Afternoon
May 1, 1984
Capitol Room

INVESTIGATION AND IMPROVEMENT OF BONE CEMENTS II

Chairpersons: W. Harris and A. J. C. Lee

- 3:45 -344 **New Semi-Crystalline Bone Cements: Stereochemistry and Properties.** S. I. Stupp, G. B. Portelli, H. L. Yau, and J. S. Moore, Bioengineering Program and Polymer Group, College of Engineering, University of Illinois at Urbana-Champaign, Urbana, Illinois.
- 4:05 -345 **Temperature and Frequency Dependent Ultrasonic Elastic Properties of Bovine Bone Compared with that of PMMA.** R. Maharidge, H. S. Yoon, and J. L. Katz, Rensselaer Polytechnic Institute, Troy, New York.
- 4:25 -346 **Enhancing the Mechanical Properties of Acrylic Bone Cement by Porosity Reduction.** D. W. Burke, E. I. Gates, and W. H. Harris, Orthopaedic Research Laboratories, Massachusetts General Hospital and Harvard Medical School, Boston, Massachusetts.
- 4:45 -347 **Modified Radiopaque Bone Cements with Low Exotherms.** G. M. Brauer, D. R. Steinberger, and J. W. Stansbury, Polymer Science and Standards Division, National Bureau of Standards, Washington, D. C.
- 5:05 -348 **Cement Deformation from Cyclic Loading of the Total Hip Femoral Component.** E. Ebramzadeh, I. C. Clarke, T. Mossessian, H. A. McKellop, T. A. Gruen, and A. Sarmiento, Orthopaedic Biomechanics Laboratory, Bone and Connective Tissue Research Program, Orthopaedic Hospital-USC, Los Angeles, California.
- 5:25 -349 **Fatigue Properties of Current Acrylic Bone Cements.** W. R. Krause and R. S. Mathis, Clemson University, Clemson, South Carolina.

SESSION 77

Tuesday Afternoon
May 1, 1984
Ticonderoga Room

BIOCERAMICS III

Chairpersons: P. Ducheyne and P. Griss

- 3:45 -350 **Physical and Material Properties of Hydroxyapatite Coatings Sintered on Titanium.** P. Ducheyne, W. Van Raemdonck, and P. De Meester, University of Pennsylvania, Department of Bioengineering, Philadelphia, Pennsylvania.
- 4:05 -351 **Biological and Mechanical Properties of a New Type of Apatite-Containing Glass-Ceramics.** T. Kokubo, S. Ito, M. Shigematsu, S. Sakka, T. Shibuya, T. Kitsugi, T. Nakamura, and T. Yamamuro, Institute for Chemical Research, Kyoto University, Uji, Japan.
- 4:25 -352 **Bioglass Coated Alumina: IN VIVO Bone Bonding Studies.** R. L. Folger, C. S. Kucheria, R. E. Wells, and G. E. Gardiner, Howmedica Corporate R&D, Groton, Connecticut.

- 4:45 -353 **Use of Alumino-Calcium-Phosphorous Oxide (ALCAP) Ceramics for Reconstruction of Bone.** *D. R. Maitie, C. J. Ritter, and P. K. Bajpai*, Pathology Branch, Toxic Hazards Division, AFMRL, Wright-Patterson AFB, Ohio.
- 5:05 -354 **Fate of Resorbable Alumino-Calcium-Phosphorous Oxide (ALCAP) Ceramic Implants in Rats.** *F. B. McFall and P. K. Bajpai*, University of Dayton, Dayton, Ohio.
- 5:25 -355 **Histological Examination of Beta-Tricalcium Phosphate Ceramic Implanted in the Canine Calvaria.** *D. S. Metsger and J. W. Ferraro*, Miter, Inc., Columbus, Ohio; Straumann Research Laboratory, School of Veterinary Medicine, Ohio State University, Columbus, Ohio.

SESSION 78

Tuesday Afternoon
May 1, 1984
Regency A Room

BLOOD INTERACTIONS: GRAFTS AND SHUNTS III

Chairpersons: F. Pitlick and Y. Noishiki

- 3:45 -356 **The Interaction of Blood Components with Primary Reference Materials in a Baboon EX VIVO Shunt Model.** *E. M. Keough, R. Connolly, W. C. Mackey, K. Ramberg-Laskaris, T. Foxall, J. McCullough, T. O'Donnell, Jr., and A. D. Callow*, Tufts University School of Medicine and New England Medical Center, Boston, Massachusetts.
- 4:05 -357 **The Relation of Mechanical Properties of the Hetero-Arteriografts for Hemodialysis to their Wall Damage Due to Puncturing with Clinical Needle.** *A. T. Yokobori, Jr., M. Ishizaki, T. Yokobori, H. Takahashi, H. Monma, and H. Sekino*, Department of Mechanical Engineering II, Tohoku University, Sendai, Japan.
- 4:25 -358 **The Effect of Hollow Fiber Dialyzers on Blood Platelets and Plasma Proteins During Extracorporeal Circulation.** *H. Pelzer, R. Michalik, H. Lange, and N. Heimbürger*, Behringwerke AG, D-3550 Marburg, West Germany.
- 4:45 -359 **Experimental Study of Heparinless Temporary Shunt Using Toyobo-TM3-Coated Tube.** *C. Nojiri, S. Aomi, M. Yamagishi, H. Koyanagi, K. Kataoka, and T. Okano*, Department of Surgery, Heart Institute of Japan, Tokyo Women's Medical College, Tokyo, Japan.
- 5:05 -360 **Polyether-Urethane Ionomers: Effect of Surface Properties on Thrombogenicity in a Canine Ex-Vivo Series Shunt.** *M. D. Lelah, J. A. Pierce, T. S. Madsen, L. K. Lambrecht, and S. L. Cooper*, Department of Chemical Engineering, University of Wisconsin-Madison, Madison, Wisconsin.
- 5:25 -361 **Improved Blood Compatibility of Surfaces Pre-Adsorbed with Proteins.** *T. A. Horbett, M. Chopper, and L. O. Reynolds*, University of Washington, Department of Chemical and Nuclear Engineering, Seattle, Washington.

Establishment of an Interdisciplinary Research System for Biomaterials and Artificial Organs

T. Yamamuro

Research Center for Medical Polymers and Biomaterials, Department of Orthopaedic Surgery, Faculty of Medicine, Kyoto University, Sakyo-ku, Kyoto, Japan

One of the results of the advancement in modern science is the capability of replacing pathological lesions or organs in the human body with artificial materials or organs. The practical application of artificial vessels, heart valves, joints and dental materials have certainly had substantial benefits to the improvement on human life and health. Despite this, however, very few researchers can be found over the world who possess comprehensive knowledge and skill enough to meet requirements imposed by this field of medical science and much remains to be done to achieve higher orders of sophistication in performance of artificial tissues and organs. The objectives of the Research Center for Medical Polymers and Biomaterials set up at Kyoto University 3 years ago are to offer training for advanced researchers with interdisciplinary expertise relating to this academic field, and to produce high-performance artificial biomaterials and organs. More specifically, the tasks involved are ; 1) establishing a research system whereby experts on engineering, physics, chemistry, biology, medicine and other related areas of study direct their efforts towards common research goals, especially towards the development and application of biomaterials, artificial tissues and organs, 2) carrying on a series of work on biomaterials at the same institute, including molecular design, synthesis, molding, composite making, construction, animal experiment and clinical application.

To attain these objectives, the following activities are undertaken.

1. Training for Advanced Researchers

Post-doctoral students from the fields of engineering, physics, chemistry, biology and medicine are trained to perform purpose-oriented research and are shown ways to act as interdisciplinary researchers by working together with fellow researchers from various academic disciplines in the same laboratories of this Center. This enables them to have a fuller appreciation of terminology covering engineering, chemistry, biology and medicine, as well as to share relevant information about their respective specialities among themselves. To accomplish the purpose-oriented research, strong demand does exist for the creation of a closely related interdepartmental feedback system by which these researchers can find solutions to their own problems. This Center frequently sponsors interdisciplinary conferences either of domestic or international for improved approaches and results of its activities.

2. Establishment of Research Departments

Following 6 departments have already been set up.

- 1) Department of Synthesis and Chemistry of Biomedical Materials : molecular design-based synthesis of a new generation of biomedical polymers, chemical modification to the existing or natural polymers, synthesis or modification of new hard materials such as metal and ceramics.
- 2) Department for Structure and Property Research on Biomedical Polymers : study of molecular structure, interface, and mechanical properties of

biomaterials, molding and construction of a variety of biomaterials through cooperation with medical electronics experts.

- 3) Department of Functional Polymers : generation of polymers with unique functional characteristics including anti-thrombogenic materials, membranes for dialysis, oxygen-carrying polymers and enzyme-binding polymers.
- 4) Department of Experimental Surgery : in vivo investigations into blood compatibility, histocompatibility and binding property to tissue of biomaterials by implanting them into small animals, in vitro investigations into the biocompatibility of those materials using cultured cells.
- 5) Department of Dental Materials : development of dental casting system for titanium, ceramics, composite resin etc., study on biomechanics of dental prosthetic appliances and dental casting, clinical application of newly produced materials.
- 6) Department of Artificial Organs : investigation into the durability and functions of artificial tissues and organs by implanting them into large- and mid-size animals jointly with surgeons and veterinarians.

To achieve the goal of bringing to completion the biomaterials or artificial organs targeted, these departments interact with one another through repetitious feedback processes. During that course, they may receive technological assistance from other institutions and private research firms. They also offer posts for a visiting professor so as to invite researchers at home or abroad to work at this Center for a few years. The biomaterials and artificial organs thus completed are put to clinical application by surgeons and ME specialists at Kyoto University Hospital, and are then subject to further refinement based on the results obtained.

The biomaterials and artificial organs developed up to the present time at this Center and ready to experimental or clinical use are ;

- 1) anti-thrombogenic arteriole with 0.8 mm of inner diameter made of polyvinyl alcohol or polyurethane with graft copolymerized surface
- 2) adhesion preventive membrane made of polylactic acid which is bioabsorbable
- 3) bioabsorbable drug-polymer composites ; antibiotics, anti-cancer agents, urokinase being bound with polylactic acid
- 4) artificial bone made of apatite-wollastonite containing glass-ceramic which binds chemically to living bone and has strong mechanical property.
- 5) artificial bone filler made of hydroxyapatite-poly-lactic acid composite which is bioabsorbable and bone inducing
- 6) artificial trachea and bronchus made of polypropylene mesh
- 7) artificial chest wall made of polyester and polycaprolactone
- 8) artificial urinary bladder made of polylactic acid
- 9) artificial heart, Utah-Kyoto type, implanted in a sheep which continues to live 200 days now.

A CONTROLLED RELEASE ANTIBIOTIC WOUND DRESSING

S.J. Davidson, L.D. Nichols, A.S. Obermayer, M.B. Allen

Moleculon Research Corporation
Cambridge, Massachusetts

A major focus in controlled release of pharmaceuticals is the development of systems providing sufficiently uniform delivery throughout their operational lifetime. It was once thought that only a rate-controlling barrier or an erodable component could satisfy this need. However, monolithic systems having a dispersed or precipitated drug within a medium of low solvent power can provide virtually constant delivery from an even simpler design. The study described here is an investigation of antibiotic wound dressings prepared by precipitating gentamicin, a broad spectrum topical wound treatment antibiotic, within Poroplastic membranes, an ultramicroporous film of cellulose triacetate capable of hosting a wide range of liquids and suspended solids.

In vitro tests have shown that membranes containing gentamicin sulfate precipitated within a nonsolvent oil phase deliver drug at a rate which roughly approximates zero order for any particular membrane composition. However, the rate itself is strongly dependent on the initial concentration of gentamicin sulfate in the membrane. This provides great flexibility to the system, and has allowed target rates near 50 $\mu\text{g}/\text{cm}^2/\text{hr}$ to be achieved using initial gentamicin loadings between 6% and 7%. Animal tests conducted by the U.S. Army Institute of Dental Research, reported in a separate paper, are highly encouraging and support the selection of this level of loading.

The Moleculon program has involved preparation of concentrated aqueous solutions of gentamicin sulfate by phase separation of dilute drug solutions from isopropanol, dilution of this stock to the desired concentration, impregnation into Poroplastic film, in situ precipitation with isopropanol, diffusive exchange of isopropanol for a nonvolatile oil, and in vitro studies of the resulting films. Gentamicin analyses have been performed using latex agglutination kits and by a spectroscopic primary amine assay based on the nickel complex of a Schiff Base derivative. In vitro drug release tests are conducted in phosphate-buffered pH 7.4 saline at 37°C, using cells which provide single-sided exposure of fully immersed films.

These studies have included variations in such parameters as drug loading, film liquid content, film thickness, and the precise precipitation conditions. Finished films have been exposed to 2 Mrad of sterilizing gamma radiation without impairment of subsequent delivery.

Table 1 shows the relationship between in vitro release rate and drug concentration for films 10 and 20 mils thick; higher load levels require less thickness to achieve an adequate drug payload. Figure 1 displays typical delivery versus time for low, medium and high loading levels.

TABLE 1

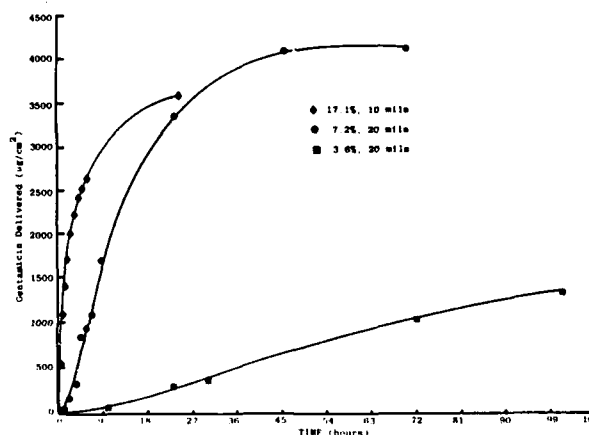
Maximum Delivery Rate vs. Film Parameters

Thickness (mils)	Gentamicin Sulfate (wt-%)	Rate ($\mu\text{g}/\text{cm}^2/\text{hr}$)
20	3.6	15
20	6.9	136
20	7.0*	167
20	7.0	186
20	7.2	144
20	7.3	301
20	7.3*	361
10	9.0	80
10	9.3*	156
10	9.3	236
10	17.7	714
10	17.7*	800

(*) Irradiated Samples

FIGURE 1

In Vitro Delivery into pH 7.4 Saline



This work has been supported under a Phase II Defense Small Business Advanced Technology Program with the U.S. Army Medical Research and Development Command. Dr. Gino Battistone, Dr. Jean Setterstrom and Col. William Carpenter of the U.S. Army Institute of Dental Research have provided technical guidance and in vivo testing vital to the success of this program.

Moleculon Research Corporation
139 Main Street
Cambridge, MA 02142

**IN VIVO EVALUATION OF POROPLASTIC® AS A WOUND DRESSING MATERIAL
FORMULATED TO SLOWLY RELEASE GENTAMICIN SULFATE**

J. W. Vincent and J. A. Setterstrom

U. S. Army Institute of Dental Research, Walter Reed Medical Center,
Washington, DC 20307

An ideal wound dressing is impermeable to bacteria, has a controllable water vapor transmission rate, and is nonadherent to wounds. POROPLASTIC, an ultramicroporous form of cellulose triacetate, possesses these characteristics and can be formulated to serve as a vehicle for the controlled release of antibiotics. In this study, the therapeutic and prophylactic efficacy of gentamicin-sulfate impregnated POROPLASTIC was evaluated for its effectiveness in eliminating *Staphylococcus aureus* (ATCC 12600) from both contaminated and infected wounds. POROPLASTIC films (13-23mil) impregnated with 4.3-8.4% w/w gentamicin sulfate (shown *in vitro* to release drug over a 72-hour period) were tested *in vivo*.

Full-thickness wounds approximately 676mm² were made on the interscapular area of 40 anesthetized guinea pigs. Following removal of the skin to the subcutaneous fat, each wound was inoculated with 4X10⁹ *S. aureus*. Immediately following, POROPLASTIC wound dressings (961mm²) containing 4.3-6.5% (w/w) gentamicin sulfate was applied to 20 of the contaminated wounds. POROPLASTIC dressings containing no antibiotic were applied to the wounds in the remaining 20 animals. On the third day postsurgery, the viable count of *S. aureus*/cm² on the surface of each wound was determined.

The bacterial counts in the inoculum and wash solutions from each wound were determined by a mechanical-bioassay method using a spiral plater and laser bacterial colony counter (Spiral System Instruments, Inc., Bethesda, Md). Bacterial counts per cm² for each wound surface at three days post-treatment with gentamicin-impregnated POROPLASTIC and unloaded POROPLASTIC are shown in Table 1.

TABLE 1. Number of *Staphylococcus aureus*/cm² Remaining on Wound Surfaces at Three Days Following Inoculation With 4 X 10⁹ *S. aureus*/Wound.

Animal	Unloaded POROPLASTIC	Animal	Gentamicin POROPLASTIC	Gentamicin Content %W/W
1	6.29 X 10 ⁶	21	89	5.8
2	3.55 X 10 ⁷	22	0	6.1
3	7.00 X 10 ⁷	23	0	5.7
4	3.55 X 10 ⁷	24	0	5.5
5	9.60 X 10 ⁶	25	0	6.5
6	1.22 X 10 ⁸	26	0	6.4
7	5.02 X 10 ⁶	27	0	6.0
8	2.15 X 10 ⁸	28	1.14 X 10 ⁶	5.7
9	ND	29	1.41 X 10 ⁶	5.7
10	3.93 X 10 ⁷	30	15	4.7
11	5.98 X 10 ⁷	31	4.25 X 10 ⁵	5.1
12	5.98 X 10 ⁷	32	4.25 X 10 ⁶	5.7
13	7.36 X 10 ⁷	33	8.75 X 10 ⁵	5.1
14	1.44 X 10 ⁸	34	12	4.9
15	1.55 X 10 ⁷	35	3.08 X 10 ⁶	4.0
16	9.9 X 10 ⁷	36	4.44 X 10 ⁶	4.5
17	6.02 X 10 ⁷	37	94	4.3
18	2.00 X 10 ⁷	38	23	6.3
19	4.80 X 10 ⁷	39	0	6.2
20	6.02 X 10 ⁷	40	3	5.9

ND: Not Done (anesthesia death)

Although significant reductions in *S. aureus*/cm² were observed on wounds treated with POROPLASTIC

containing 4.0-4.9% w/w gentamicin sulfate, none were sterile. However, sterility was observed in 83% of wounds treated with POROPLASTIC containing 6.0-6.5% w/w gentamicin sulfate.

The 19 surviving guinea pigs which had their wounds overlaid with unloaded POROPLASTIC were used in a sequential experiment. Following a scrub assay at three days post-injury to determine the bacterial count/wound (>10⁵ *S. aureus*/cm²), the animals were divided into two groups. The wounds of all animals in each group were then reinoculated with 2.3x10⁹ *S. aureus*. The wounds of odd-numbered animals were bandaged with POROPLASTIC wound dressings containing 6.0-8.4% (w/w) gentamicin sulfate. The wounds of even-numbered animals were bandaged with unloaded POROPLASTIC. Four days later the wounds were assayed for the quantity of *S. aureus*/cm².

Because these animals had >10⁵ *S. aureus*/cm² of the wound surface at three days, they were considered animals with established infections. Results of treatment of these wounds with POROPLASTIC-gentamicin sulfate containing an antibiotic load of 6.0-8.4% w/w are shown in Table 2.

TABLE 2. Number of *Staphylococcus aureus*/cm² Remaining on Wound Surface* At Four Days Following Treatment of Established Wound Infections.

Animal	Unloaded POROPLASTIC	Animal	Gentamicin POROPLASTIC	Gentamicin Content %W/W
2	1.73 X 10 ⁷	1	0	8.0
4	1.9 X 10 ⁶	3	17	8.4
6	3.8 X 10 ⁷	5	6	6.5
8	4.8 X 10 ⁷	7	6.0 X 10 ¹	7.5
10	2.4 X 10 ⁷	9	ND	6.1
12	2.1 X 10 ⁷	11	0	6.2
14	1.9 X 10 ⁷	13	ND	6.0
16	Contaminant	15	25	6.2
18	1.73 X 10 ⁷	17	Contaminant	6.4
20	6.2 X 10 ⁷	19	0	6.9

*4 X 10⁹ *S. aureus* inoculated on Day 1; 2 X 10⁹ *S. aureus* inoculated on Day 3.

ND: Not Done (anesthesia death)

The difference between the infection rates (>10⁵ organisms/cm²) of the untreated control (100%) and the treated groups (0-15%) were significant (p<.001) for both experiments. The data indicates that POROPLASTIC provides an excellent vehicle for the topical administration of gentamicin sulfate into wounds. Studies are ongoing to provide POROPLASTIC capable of delivering additional drugs and to evaluate the effect of POROPLASTIC on wound healing rates.

ACKNOWLEDGMENTS

The statistical analysis by Dr. Jay D. Shulman and the technical assistance of W. C. Cornett, M. A. Derevanik, and D. R. Frosian is greatly appreciated.

U. S. Army Institute of Dental Research
Walter Reed Army Medical Center
Washington, DC 20307

DEVELOPMENT OF ENCAPSULATED ANTIBIOTICS FOR TOPICAL ADMINISTRATION TO WOUNDS

Jean A. Setterstrom, Thomas R. Tice*, W.E. Meyers*, and Jack W. Vincent

U. S. Army Institute of Dental Research, Walter Reed Medical Center
Washington, DC 20307

An ideal way to deliver antibiotics to wounds is with a single dose having an initial burst of antibiotic at the wound site for immediate tissue perfusion, followed by a prolonged release of antibiotic to maintain an efficacious level at the wound site for up to 14 days. The ability to concentrate the antibiotic within the wound site, rather than medicating systemically ensures an extended period of direct contact between an effective amount of antibiotic and the infecting microorganisms. This method of drug delivery offers advantages in treating wounds with a diminished blood supply, devitalized tissue, and foreign body contaminants.

Such a system of controlled drug release has been developed by coating small particles of ampicillin anhydrate with poly (DL-lactide co-glycolide) (DL-PLG). The DL-PLG copolymer is well suited for *in vivo* drug release because it elicits a minimal inflammatory response, is biologically compatible, and degrades under physiologic conditions to products (lactic acid and glycolic acid) that are nontoxic and readily metabolized. The biodegradation rate of the excipient is controllable because it is related to the mole ratio of the constituent monomers and the surface area of the microcapsules produced.

Due to the unique pharmacokinetic advantages realized with the continuous delivery of ampicillin into tissue from a controlled release vehicle, our studies indicate that a very small dose will obtain an optimal therapeutic effect. Consequently, with a lower dose, undesirable side effects are minimized or eliminated. Microcapsules with diameters $\leq 25\mu\text{m}$ are amenable to direct administration to a wound by a shaker-type dispenser or aerosol spray.

For the preparation of the prototype ampicillin anhydrate microcapsules, DL-PLG was synthesized by a ring-opening, melt polymerization of the cyclic diesters, DL-lactide and glycolide. [^{14}C]ampicillin anhydrate was prepared by the procedure of Valcavi¹. Both labeled and unlabeled ampicillin anhydrate microcapsules were fabricated by an organic phase-separation process. Microcapsules of the desired size (45-106 μm) were isolated from each batch by wet sieving. The radio-labeled microcapsules were used in experiments to determine the microcapsule core load and the release kinetics of the [^{14}C]ampicillin anhydrate.

The rate and duration of release of [^{14}C]ampicillin anhydrate from the microcapsules was determined in rats. Following subcutaneous injection of the microcapsules, urine was collected and analyzed for [^{14}C]-content. The amount of radioactivity excreted daily by each rat was plotted as a function of time.

Experiments were performed to evaluate the efficacy of the prototype microcapsules in artificially induced infections. Wounds 2.5-3.0cm long and 1cm deep were made in the thigh muscle of albino rats. The muscles were traumatized by uniformly pinching with tissue forceps, and inoculated with known quantities of Staphylococcus

aureus and Streptococcus pyogenes. Sterile dirt was placed in each wound to serve as an infection potentiating factor. The wounds were then treated within one hour by sprinkling sterile, preweighed amounts of microencapsulated antibiotic directly in the wound. Control groups consisted of animals with wounds receiving no therapy, unloaded microcapsules, or topically applied, free ampicillin anhydrate. All wounds were sutured closed with 3-0 black silk.

The ampicillin anhydrate microcapsules effectively reduced bacterial counts in the contaminated wounds. Streptococcus pyogenes was present in 90 percent of the untreated wounds at 14 days, but was eliminated from microcapsule treated wounds within 48 hours. Although Staphylococcus aureus remained in all microcapsule treated wounds at 7 days, compared with untreated controls, the bacterial count decreased ($\geq 2 \log_{10}$ /gram of tissue) between day 2 and 7. This reduction was not observed in untreated controls. Wounds treated with unloaded DL-PGL microcapsules, or topically applied free ampicillin anhydrate remained infected at 14 days with $\geq 10^5$ organisms per gram of tissue. Whereas, 60 percent of the wounds treated with microencapsulated ampicillin anhydrate were sterile.

Successful controlled release of bioactive ampicillin anhydrate was achieved *in vitro* and *in vivo*. The system developed provides a successful model that encourages efforts to encapsulate additional antibiotics. Often it may be desirable for broad spectrum control to combine two or more antibiotics in treating wounds. It is anticipated that mixtures of different antibiotic containing microcapsules may be blended and packaged together to increase the versatility of the product.

References:

1. Valcavi, U., Synthesis of 6-(D- α -aminophenyl-acetamido-1- ^{14}C) penicillanic acid, J. Labelled Comp. 8(4):687 (1972).

U.S. Army Institute of Dental Research
Walter Reed Army Medical Center
Washington, D.C. 20307

*Southern Research Institute
Post Office Box 3307-A
Birmingham, Alabama 35255

THE EFFECTS OF A BIODEGRADABLE COPOLYMER-PROTEOLIPID (PL) ON OSSEOUS HEALING IN RATS AND DOGS

Jeffrey O. Hollinger

U. S. Army Institute of Dental Research, Walter Reed Army Medical Center
Washington, DC 20307

INTRODUCTION

Materials such as bone grafts and implants, collagen gels, ceramics, bone derivatives, and biopolymers are some of the many agents which have been employed by orthopedic and maxillofacial surgeons for initiating osseous repair or for replacing bone. Failure to achieve beneficial results with these substances has not been necessarily a consequence of imprudence; but rather, due to deficiencies inherent to the repair or replacement agents. A material was formulated, therefore, that consisted of the biopolymers polylactic acid (PLA) and polyglycolic acid (PGA) combined with a proteolipid (mucopolysaccharide N-acetylmuramoylhydrolase:phosphatidyl inositol 3,4-diphosphate).

MATERIALS AND METHODS

Osseous wounds were prepared in the diaphysis of the tibias of 180 Walter Reed strain rats. The animals were divided equally into three groups: Group A - 50:50 PLA:PGA plus proteolipid (PL); Group B - 50:50 PLA:PGA; and Group C - no treatment. The 50:50 PLA:PGA was prepared in methylene chloride and anhydrous methanol, placed in a teflon mold, and put into a vacuum oven at 50°C, 5 millitorr for 48 hours (Hollinger, 1983). The 50:50 PLA:PGA+PL was made by first combining a lysozyme with phosphatidyl inositol 4,5-diphosphate to produce the PL (Hollinger, 1982). The PL was then added to the solvated PLA:PGA and this mixture was placed into a teflon mold and was treated as previously described. At 3,7,14,21,28, and 42 days post-treatment, ten animals from each group were euthanatized. Recovered tissues were prepared for histomorphometric evaluation using polymethyl methacrylate embedding and a modification of the Goldner-trichrome stain. A Zeiss Image Analysis System[®] was used to quantitate the variables associated with osseous wound repair.

Discontinuity defects were prepared in the mandibles of eight dogs in the following manner: 1.-all teeth distal to the canines were extracted surgically; 2.-after eight weeks a segment of the mandible consisting of dimensions 2cm X 1cm X 1cm was ablated. This resulted in a complete "through and through" mandibular wound. A block of 50:50 PLA:PGA+PL of identical geometry to the defect was fabricated in the same manner described for the rats. Blocks were sterilized with ethylene oxide, aerated, and were inserted into the experimentally created wounds and were stabilized with a stainless steel plate and screws. At monthly intervals the experimental sites were radiographed. The animals were euthanatized with an overdose of sodium pentobarbital and the implants and host tissue were evaluated grossly and by histomorphometric assessment according to the methods described in the rat experiment. A two-way analysis of variance and a sum of squares analysis were performed on the histomorphometric data. Histograms were constructed that allowed for visualization of a comparison of both treatment and temporal groups.

RESULTS

The osseous wounds that were prepared in the rats demonstrated significantly different healing based upon the type of treatment that was rendered. Group A (copolymer and PL) treated wounds demonstrated overall increases in the total volumetric density of bone formation, trabecular diameter, osteoid thickness, and the number of osteoblasts that exceeded the healing response in wounds of Groups B (copolymer) and C (control) ($p < 0.01$). Similarly, Group B results exceeded those of Group C. Overall trends between treatment groups displayed an ascending, predominantly linear difference over time; however, toward the latter stages, a quadratic component of that trend was evident.

The discontinuity defects in the mandibles of dogs that were treated with the copolymer-proteolipid developed an osseous-chondroid type of union after six months. The six-through-eight-month animals had unions that could be manipulated without engendering body movement or fracture. Radiographically, radio-opacity was developing by three months. Histomorphometric quantitation revealed that, with time, there was a linear increase in the bony elements of wound repair.

CONCLUSION

Initial indications suggest that the copolymer-PL material may be useful for stimulating bony repair at either endochondral or intramembranous wound sites.

BENEFITS OF RESEARCH

An osseous union in bony wounds is of paramount importance in assuring stabilization of segments and precluding nonunions. Furthermore, if the compound described can be a successful alternative to autogenous bone, multiple surgical procedures required to harvest such material would be unnecessary.

Division of Research Sciences
U. S. Army Institute of Dental Research
Walter Reed Army Medical Center
Washington, DC 20307

INORGANIC AND ORGANIC COMPOUND COMBINATIONS FOR BONE REPLACEMENT

J. Lemons, P. Henson*, and K. Niemann*

Department of Biomaterials and Division of Orthopaedic Surgery,
University of Alabama in Birmingham
Birmingham, Alabama 35294

A number of synthetic and tissue derived compounds have been proposed, tested and applied for the treatment of bone lesions including non-unions. In general, the synthetic and tissue derived substances, with the exception of autogenous bone, bone morphogenic protein and selected demineralized bone products, have not demonstrated osteogenic characteristics. A number of new substances fabricated as ceramic compounds have become popular within the past five years. These include the hydroxylapatites (trade name Durapatite or Calcitite) and tricalcium phosphates (trade name Synthograft). Many claim osteogenic properties for these compounds or combinations of these compounds with organic substances.

A non-union model using a segmental lesion at the mid-position of the rabbit tibia and external fixation through Steinmann pins has been developed and used in our laboratories to study new substances for bone reconstruction. To date, this model has shown very acceptable results with lesion correction being statistically significant with autogenous bone from the iliac crest. Therefore, the overall objective of this investigation was to evaluate a selected series of the available synthetic ceramic and organic tissue derived products alone and in combination as related to their osteogenic potential for surgical corrections of non-unions.

Non-unions are created at the mid-positions of rabbit tibiae by removing a 12 mm length of bone and the associated periosteum. The bone is stabilized with four Steinmann pins and external splints. After approximately 12 weeks a non-union develops which is evaluated radiographically. The candidate substances are then implanted alone in relative weight ratios, or in combination with autogenous bone with the follow-up extending for 16 weeks. Weekly radiographs and clinical observations are followed by full mechanical and histological studies at necropsy. The histological characterizations include non-decalcified thin sections.

The New Zealand White Rabbit animal model has proven to be very valuable in that only precisely controlled autogenous bone implantations result in healing of these tibial non-unions. Surgical procedures alone and previous procedures including standard metallic, ceramic and polymeric inert biomaterials have not provided a significant number of clinical unions.

The implantations of hydroxylapatite and tricalcium phosphate particulate alone showed clinical unions (bridging by callus across the defect) in zero (0/2) and 25% (2/8) respectively. In contrast, 90% (9/10) of the lesions treated with autogenous bone showed clinical unions. The combination of hydroxylapatite with collagen or a polypentapeptide protein in equal weight ratios

or the collagen alone showed no (0/8) clinical unions. One hydroxylapatite and collagen non-union when subsequently treated with autogenous bone resulted in a clinical union. Mixtures of tricalcium phosphate and autogenous bone in equal weight ratios showed bridging of the defects for 50% (3/6) on the non-unions.

In summary, the only substance showing statistically significant corrections of rabbit tibiae non-unions was fresh iliac crest autogenous bone. Ratios of tricalcium phosphate particulate and autogenous bone showed limited success (50%) while tricalcium phosphate or hydroxylapatite ceramic particulates alone or in combination with collagen or a polypentapeptide protein showed non-osteogenic conditions. All substances showed good biocompatibilities under these implantation conditions.

The support of Omni International and the U.S. Army Medical Research and Development Command are acknowledged.

*Department of Surgery and Division of Orthopaedics, University of Alabama in Birmingham, Birmingham, Alabama 35294.

LONG TERM ANALYSIS OF SERRATED ALUMINUM OXIDE DENTAL IMPLANTS

Craig R. Hassler, Larry G. McCoy, Nancy E. Arlin* and Mark D. Brose*

Battelle-Columbus Laboratories, Columbus, Ohio

Long term implant studies of alumina tooth roots primarily designed for fitting fresh extraction sites are being performed in both humans and baboons. The implants are of single tooth rectangular design with serrations arranged for maximal stress distribution of occlusal loads. A three-piece design is used to minimize stresses upon the root portion during bone ingrowth phase. The serrated root portion is produced from high purity, dense aluminum oxide (Al_2O_3). The upper two parts of the implant (post and core and crown) are conventional dental materials. A series of graded sizes of implants have been produced to provide an interference fit in any size fresh extraction site.

Long term studies in 9 baboons were recently terminated with an average implant residence time of 5.25 years. The longest implant time was 7.71 years. All implants were classified according to their "final" status at time of death or necropsy. Each implant was categorized in according to its least favorable outcome. Forty-three attempts were made to place implants. Thirty-eight, or 88 percent of the implants survived the initial ingrowth phase. All of these ingrowth failures were early implant attempts, suggesting that technique or operator experience may be failure contributing factors. Other suspected failure modes include: fracture of the buccal plate, and placing the root too high relative to the alveolar crest.

Of the 38 implants which were rigidly retained via bone ingrowth, 24 or 63 percent were totally functional and completely functional units at necropsy. The 14 implants not complete at experiment termination included: in service implant fractures, lost crowns and implants never restored. Only one of the 38 implants become loose after initial stabilization via ingrowth. Consequently 37 of 38 (97%) implants which become rigidly fixed in bone could have successfully functioned if extenuating circumstances had not prevented or prematurely shortened the function of these implants.

All fractured roots were uniquely from one batch of implants, used only in baboons. Consequently, poor material quality is suspected. Extreme crown wear was seen on all baboon implants indicated that the animals severely stressed the devices. But, the actual contribution of severe treatment to implant fracture cannot be determined.

Histologic analyses of the bone-implant interfaces has been performed at various time intervals. An increase in bone density appears to be associated with the early functional stage of implant life. Later dense, well organized bone mixed with some connective tissue totally filling the serrations is typically observed. In numerous areas, direct bone apposition between bone and ceramic is observed.

A three dimensional (finite-element) model was used to calculate stresses at three points along the edge of each element as well as in the center of each element.

The moduli used were: ceramic, 54.53×10^6 psi; gold, 11.92×10^6 psi; and bone, 1.98×10^6 psi. Rigid bonding was assumed at the bone-biomaterial interface. Stresses were computed for an axial (occlusal) static load of 25 pounds for the smallest (most critical) implant ($mm \times 4 \text{ mm}$).

The maximum stresses in the bone slightly exceeded the self-imposed 400 psi bone compressive stress limit. Bone stresses at the bone-ceramic interface were consistently lower than those calculated for the centroids. The stresses were fairly uniform at the various positions along each serration. Also fairly uniform stresses were observed at various serration levels despite the differences in serration depth.

To date, human studies have not proven as successful as the baboon studies. Loss of initial stability (poor bone ingrowth) of the implant appears to be the single greatest factor affecting long-term success. Even though all human implants were implanted stable by virtue of an interference fit with the bone, stability in many cases was rapidly lost. In the successful cases, the relative degree of mobility reversed and continually diminished. In implants never completely stable, mobility slowly increased over a period of 1 to 2 years until failure was inevitable. In light of high failure rate due to the loss of initial stability, different stabilization techniques were attempted to improve success. The alternate techniques included: splinting, and deeper initial placement. The latter technique of placing the implant below the alveolar crest has produced a dramatic potential improvement in the results. The extra isolation from mechanical stresses appears to have made a significant difference in maintenance of stability. However, it is premature to claim improvement due to the short residence time of this group of implants. Continued observation of this group is required to validate this statement.

The initial ingrowth phase continues to be the most critical phase of the procedure. If initial stability is maintained throughout the bone ingrowth and reconstruction phase; the long-term prognosis for success appears excellent. The requirement of fitting a fresh extraction site probably negatively affects success, since closer bone apposition, requiring less bone ingrowth is more likely obtainable with devices of simpler cross sections, which are applicable to the edentulous situation.

This research is supported by the United States Army Institute of Dental Research Contract #DAMD 17-82-C-2020.

Battelle-Columbus Laboratories
505 King Avenue
Columbus, Ohio 43201

*The Ohio State University
College of Dentistry

Takehisa Matsuda, Toshiyuki Toyosaki and Hiroo Iwata

Research Institute, National Cardiovascular Center
Suita, Osaka 565 JAPAN

Introduction: The thrombus formation on foreign surfaces is triggered by either activation of adherent platelets or contact phase activation of plasma coagulation pathway. The understanding of molecular events of both initial phases of the thrombus formation process is the essential requirements for evaluation of biomaterials with blood-contacting surfaces and molecular design criteria for an ideal non-thrombogenic polymeric surface. However, there has been few study dealing with the contact phase activation of plasma coagulation on polymeric surfaces. The intrinsic coagulation pathway is initiated by activation of so-called Hageman Factor (FXII), which causes complicated enzymatic cascade reactions at the downstream of coagulation pathway. This eventually leads to the formation of fibrin. This study reports (1) the development of very sensitive and highly quantitative methods for monitoring the adsorption and activation processes in plasma, (2) its application to various types of polymer surfaces and (3) physico-chemical interpretation of adsorption/activation process in conjunction with nature of polymer surfaces.

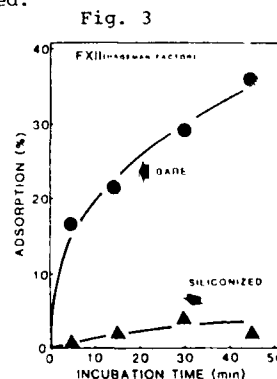
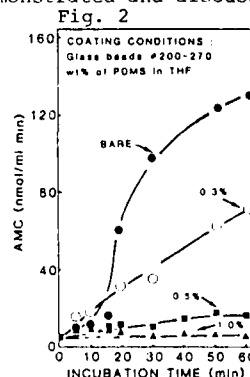
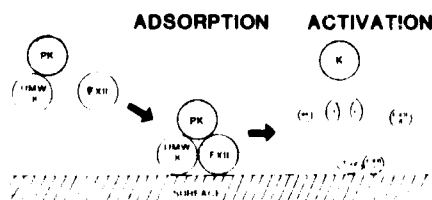
Principle & Experiments: Recent progress of the study on the contact phase of blood coagulation has revealed that the optimal activation requires the presence of three plasma proteins; Factor XII, high molecular weight kininogen (HMW) and prekallikrein (PK). The formation of a trimolecular complex of these participating proteins on a surface is essential for initiation of surface-mediated intrinsic coagulation pathway (Figure 1). The direct assay of activated Hageman Factor (XIIa) is not simple but the assay of kallikrein, which is simultaneously generated at the contact phase reaction and acts as a potent mediator for activation of Factor XII on positive feedback mechanism, can be easily determined by the amidolytic activity toward the fluorogenic oligopeptidyl substrate Z-Phe-Arg-MCA. Thus, the degree of contact phase activation can be determined as the rate of generation of a fluorogenic substance (AMC). The amount of the adsorbed clotting factors, which participate in the contact phase, is measured by newly-developed single radial immunodiffusion technique using an agar-gel containing the antisera to the clotting factor. The combination of both methods developed here allows us to simultaneously monitor the adsorption and activation processes on polymer

surfaces. In order to enhance the surface effect, a high surface-to-volume ratio was applied by using fine glass beads (100-120 mesh). The typical incubation condition was as follows: 0.5 ml of citrated platelet-poor plasma and 250 mg of glass beads coated with polymers in a siliconized tube.

Results & Discussion: Figure 2 shows the typical time-course of the contact activation on glass surface at 0°C, which was measured by the newly-developed fluorogenic synthetic substrate method. No activation was observed in FXII-, PK- and HMW-deficient plasmas. The adsorptional behaviours of FXII on glass, which was determined by the immunodiffusion method developed here, is shown in Figure 3. Similar time-dependent adsorptional behaviors are also observed in other proteins (PK & HMW). Both adsorption and activation are accelerated by elevating the surface-to-volume ratio. Thus, the contact activation observed is ascribed to the surface-mediated initial event of the coagulation system via the formation of the trimolecular complex of FXII, PK and HMW on a surface. No apparent activation is observed for well-coated siliconized surface (Fig.2), whereas the amounts of adsorbed FXII and HMW increase with incubation time, although the amounts are much smaller than those found on glass (Fig.3). This may imply that the activation requires special configuration of the trimolecular complex and/or the favorable conformational change on a surface. In general, fixed negative ion-bearing surfaces significantly enhance the activation, whereas positively-charged surfaces completely inhibit. The surfaces with electron-donor character slightly activate the contact phase, but surfaces with electron-acceptor and nonpolar characters fail to trigger the activation. These would suggest that (1) the electrostatic interaction dominates the adsorption/activation process, (2) the donor-acceptor interaction may also be involved in the contact phase, and (3) the hydrophobic interaction also operates in the adsorption process but fails to induce the activation. The effect of preadsorbed proteins (Alb, Fib, IgG, etc.) will be demonstrated and discussed.

CONTACT ACTIVATION PROCESS ON FOREIGN SURFACES

Fig. 1



This study was fully supported by a Grant-on-Aid for Scientific Research, Ministry of Education & Welfare, Japan (Special Project Research; 57119009).

Study of the adhesion and migration of endothelial cells on pretreated polyester prostheses with various cross-linked proteins matrix in vitro

SIGOT M.F., LANFRANCHI M., BEN-SLIMANE S., DUVAL J.L., GUIDOIN R., SIGOT M.

Laboratoire de Biologie Cellulaire Expérimentale - Université de Technologie - BP 233 - 60206 COMPIEGNE Cedex (France)

Our Aim is to perfect a material able to induce the re-endothelialisation of a prosthesis after implantation. It would not only insure a good healing but also bring forth the properties of the endothelium essential for the integrity of circulation. Previously, we have demonstrated that porous textile, eg. dacron, treated with cross-linked proteins, avoids the preclotting, but shows differences in the biocompatibility, depending on the prosthetic substrate. Albumin added with collagen, a major component of the sub-endothelium and the extracellular matrix, shows good adhesion and migration of the cells when compared with our controls, the preclotted dacron currently used in surgery. However, we were not able to point out a significant difference between collagen and albumin + collagen coatings. This could be due to the fact we were using embryonic cells which evolve too quickly. In the present work, we used adult mammalian cells which show a high stability and we looked into extracellular matrix components able to induce the adhesion and migration of the endothelial cells on our proteinic surfaces. The experimental protocol is as follows : woven, knitted and velour dacron are pretreated with albumin, collagen, albumin + collagen and albumin + collagen + fibronectin, cross-linked with either glutaraldehyde or carbodiimide. Each type of coating is studied as follows :

- Platelet-substrate aggregation in vitro.
- Proteinic surface characterization by titration and radioactive labelling of the proteins.
- Evaluation of the biocompatibility using an organotypic culture technique which allows to obtain the endothelial cells without prior dissociation and to induce the migration of the cells on the surfaces to test. We characterize the endothelial cells by an immunoenzymatic technique. A scanning electron microscopic study gives us an account of the impregnated surface before and after the culture. We observe the cell behavior with a videocinematographic technique during the five days of culture and a counting of the migrated cells on the different coatings quantifies their affinity for the various surfaces. 72 explants are cultivated for each type of coatings.
- Measuring of cell-substrate adhesion after five days of culture with a simple device we have perfected and which allows a dynamic measuring of the phenomenon.

The counting of the migrated cells shows that, whatever the coating is, the velour dacron is the best textile. The collagen is the best coating (table I).

	woven	knitted	velour
Preclotted	5257	7062	7518
Albumin	634	789	1039
Collagen	10.539	10874	12340
Albu+coll	5247	5122	7152
Albu+coll+fib.	5802	6794	8217

Table I - Evaluation of the biocompatibility expresses by the number of migrated cells per explant.

However, the collagen, in spite of being the most favourable surface for the cell migration, does not show the normal cell-substrate adhesion. (Already at low flowing-speed, 46 % of the cells pulled out). It is probably due to a too rapid migration of the cells on the collagen. It seems that the albumin + collagen coating responds best to these criteria, especially with velour dacron. Moreover, the cell morphology is better and when we combine albumin + collagen + fibronectin, we can see that the cells have recovered both, their contact inhibition property and their normal cell morphology (fig. 1).

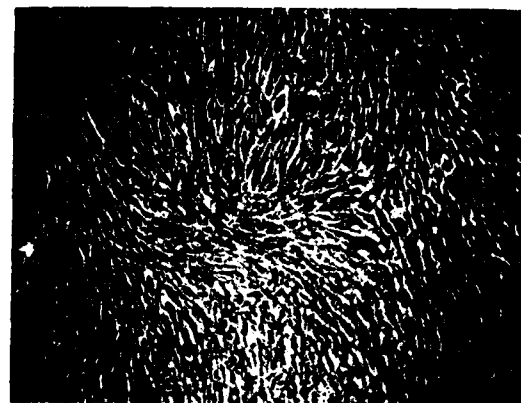


Fig. 1 - Videomicrocinematographic observation of the cell migration after 5 days of culture.

Are these properties preserved after implantation?
The work was supported by the INSEM program (grants CRL n°82 30 16).

IN VIVO ASSESSMENT OF BLOOD/MATERIAL INTERACTIONS OF SEGMENTED POLYURETHANE USED FOR BLOOD PUMP

T. Matsuda, H. Takano, Y. Taenaka, K. Hayashi, M. Umezu, T. Nakamura, T. Nakatani, S. Takatani, T. Tanaka, and T. Akutsu

National Cardiovascular Center Research Institute
5-125 Fujishiro-dai, Suita, Osaka 565 JAPAN

INTRODUCTION

Segmented polyurethanes (SPUs) have been widely used for cardiovascular prostheses such as blood pumps. The well-proven relatively good antithrombogenicity of these multiblock elastomers acceptable for blood pumps has been interpreted by so-called "passivation" mechanism based on the preferential adsorption of albumin. This concept is based on that adsorbed albumin does not induce the activation of the platelet system (adhesion, release & aggregation). However, besides the platelet system, the blood/material interactions encountered in a long-term implantation include coagulation, fibrinolysis, complement and cellular systems (red blood cells, white blood cells & bacteria other than platelets). The entire complicated system contributing to the formation of thrombus shows that these sub-systems are mutually interacting and accelerate or retard the thrombus formation on positive or negative amplification mechanisms (Fig.1). However, there has been few study on in vivo long-term evaluation of antithrombogenicity on SPUs from the point of view of the frame work of multi-interacting blood/material interactions as schematically shown in Fig.1.

This study summarizes our three-year experiences in implantation of assist device made of SPU in goats, emphasizing the long-term blood/material interactions. The methods employed in this study are subdivided into three methodologies; (1)Macroscopic & microscopic observations of thrombus on surfaces, (2)Detection of infarctions at the downstream blood-circulating organs due to (micro)embolization and (3)Monitoring of changes in hematological parameters of circulating blood components, which include the levels and physiological functionalities. Especially, the third one will tell us the information on the dynamic (or time-variant) state of blood/material interactions. This will deepen our understandings of in vivo complicated blood/material interactions.

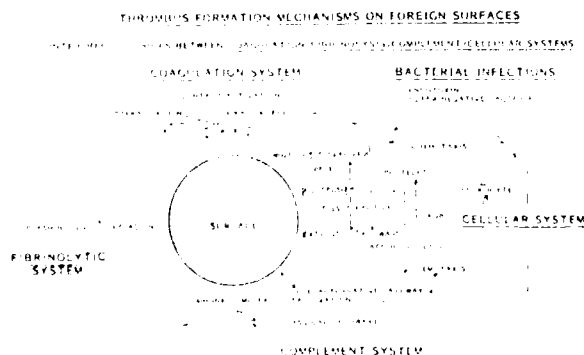
EXPERIMENT

The left ventricular assist devices(LVAD) having SPU(Toyobo Co., Ltd., TM-3) as a blood contacting surface were implanted in goats. Heparinization was performed only during the implantation operation. Hematological parameters monitored were as follows: (1)protein levels of prekallikrein(PK), fibrinogen(Fib), plasma free hemoglobin, antithrom-

bin III, and FDP(fibrinogen-fibrin degradation products), (2)cellular counts of platelet(PL) and white blood cell(WBC), and the aggregability of PL, and (3)coagulation times; prothrombin time(PT), partial thromboplastin time(PTT) and thrombin time(TT). Microscopic observations of implanted surfaces were instrumented by SEM, TEM, EDX and FT-IR-ATR.

RESULTS & DISCUSSION

(1)Coagulation System; The general trend of plasma coagulation times(PTT & PT) shows that both PT and PTT are significantly prolonged in several days after implantation. The level of prekallikrein, which is one of major clotting factors in the contact phase of intrinsic coagulation pathway, was determined by the newly-developed assay method based on using the fluorogenic oligopeptidyl substrate. The PK level was markedly reduced in the first few days but gradually recovered to the preoperative level in one to two weeks. No longer apparent consumption was observed thereafter. The Fb level was also markedly reduced but overshoot much beyond the preoperative level in several days. The FDP level starts to increase in a few days, but no detectable FDP is found after a week. These strongly suggest that the consumption coagulopathy occurs in the early stage of implantation possibly due to the hemostasis resulted from surgical wounds and foreign surface-induced consumption. In order to differentiate these effects, the implanted pump, which is located just outside the body, was exchanged with a new one without any surgical wounds. Upon exchange, both PK and Fb levels were reduced. In addition, both PTT and PT are simultaneously prolonged. This clearly demonstrates that the participation of intrinsic coagulation pathway is evident. All the hematological parameters relating to plasma proteins remains unchanged after about two weeks, suggesting that the passivation would be completed in a relatively short period. (2)Cellular System; The consumption of PL occurs at very early stage, but the PL counts overshoot beyond the preoperative level and then gradually recovered to the preoperative level in a month. The marked change is observed for the ADP-induced aggregability. The reduced aggregability is gradually recovered but remains about 70% of the preoperative level even one month later. At present, it is not clear whether the reduction in aggregability is induced by direct contact with SPU or by mechanical/hydrodynamical stress. Generally, the nature of thrombus formed is characterized as the typical fibrin-PL matrix occasionally entrapping RBCs. However, in the activated states of WBCs such as infections or septic shock, the thrombus is consisted of only WBCs and fibrin. The microscopic observations at the thrombus/SPU interface imply that adhered WBCs trigger the activation of extrinsic coagulation pathway in which tissue factors might be released from adhered WBCs. (3)Implanted Surface Structure; The microscopic analyses showed that implanted surfaces are covered with multilayered proteinaceous deposits of semi-micron order in thickness. The "multilayered passivation" mechanism for long-term antithrombogenicity will be proposed and discussed.



T.Akaike*, S.Kasai*, N.Tominaga*, S.Nishizawa*, T.Miyata**

*Department of Material Systems Engineering, Tokyo University of Agriculture and Technology, Koganei-shi, Tokyo 184, Japan

**Japan Biomedical Material Research Center, Meguro-ku, Tokyo 152

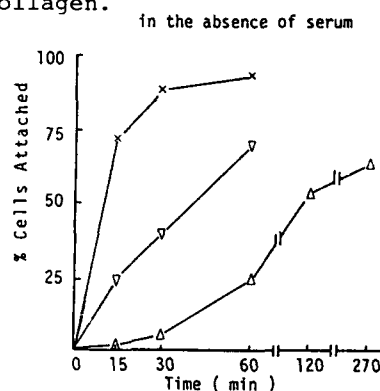
Design of hybrid organs and biosimulator of cellular reaction needs lots of information directed for the control of immobilization of cells and cellular functions. Of recent years much interest has been taken in the role of biological fiber structure, e.g. collagen and fibrin. In this study we analysed the interaction of cells (fibroblast and hepatocyte) with chemically modified collagen fibers and partly fibrin fibers and examined the possibility of regulation of cell attachment and proliferation.

Chemical modification, methylation and succinylation of atelocollagen can alter the net charge of collagen (to plus or minus) without inducing the conformational change of triple-helical backbone. Fig.1 shows that L cell attached more rapidly to methylated AC(MAC) which has positive net charge than to succinylated AC (SAS) with negative net charge in the presence or absence of serum (FCS). However, in the presence of serum (FCS) as the incubation time increased, cell attachment increased to the same extent as MAC. It is interesting that unmodified AC which has substantially neutral in charge attracts fewer L cells with and without serum.

When L cells were cultured on unmodified AC, SAC on MAC in BSA-supplemented, serum-free medium, they proliferated on SAC and MAC surfaces much better than on unmodified AC surface. Adsorption of fibronectin to various collagen surfaces enhanced the proliferation of L cells.

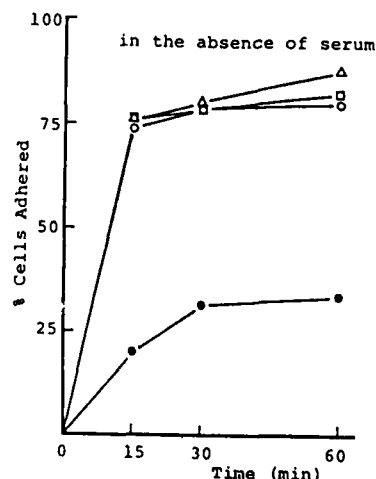
Rat hepatocytes were incubated in chemically modified collagen-coated dishes and non-coated dishes in the presence (Fig. 2) or absence of serum. No difference of hepatocyte adhesion was observed among various collagen surfaces, while fewer

hepatocytes adhered to non-coated surface. It was considered that hepatocytes have high affinity to collagen substrata and are not affected by the net charge of collagen substrata and are not affected by the net charge of collagen. These results show a remarkable contrast to those in L cell adhesion. It is very interesting that there is a significant difference of cellular response to the chemical modification of collagen.



atelocollagen(AC), Δ ; methylated AC, × ; succinylated AC, ▽

Fig. 1 Attachment of L cell to collagen-coated dishes effect of side-chain chemical modification of atelocollagen



AC, ○; MAC, □; SAC, △; non-coating, ●

Fig. 2

Adhesion of hepatocytes to collagen-coated dishes

THE DEVELOPMENT OF FLUORINE-CONTAINING SEGMENTED POLYURETHANE AND ITS APPLICATION TO ARTIFICIAL HEART PUMP

K. Imachi, I. Fujimasa, M. Nakajima, S. Tsukagoshi, K. Mabuchi, M. Kato*, T. Takakura*, M. Yamabe* and K. Atsumi

Institute of Medical Electronics, Faculty of Medicine, University of Tokyo
Tokyo, Japan

Blood compatibility of artificial heart(AH) pump was much improved by using a segmented polyurethane or Avcothane and AH animals had become to survive for more than 8 months without use of any anticoagulants. However, blood compatibility and durability of these AH pump materials are not yet complete and sometimes thrombus formation, pannus formation and calcification were observed inside the pump or at the tissue-materials interface. So, the development of new AH pump material with higher blood compatibility and durability is expected. In this study, the authors have developed a new type segmented polyurethane and tried it to apply to AH pump and evaluated its blood compatibility and durability.

A fluorine-containing segmented polyurethane (FPU) have been synthesized from fluorinated diisocyanate and polytetramethylene glycol(PTMG). FPU has the microphase separated structure which is composed of hydrophilic domains of hydrocarbon chains and hydrophobic domains of fluorocarbon chains. Figure 1 shows the generalized molecular structure of this material. The mechanical properties and microphase structure were changed by the molecular weight of PTMG.

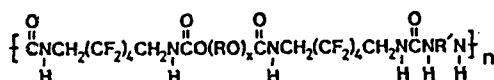


Fig. 1 Generalized molecular structure of FPU

In-vitro and in-vivo blood compatibility and durability of FPU for AH pump were evaluated. In Lee-White test used goat's blood, blood clotting time of this material was 67-91 minutes, which was about same order with Cardiothane. As the result of tensile test, FPU showed superior tensile properties: Tensile strength was 630-700 Kg/cm² and elongation at break was 780 %. FPU was possible to be coated easily on PVC paste or Cardiothane surface. As the initial trial use of this material for in-vivo test, FPU was coated on a part of blood contact surface of AH cannula and atrial cuff of which surface was coated with Cardiothane, and used in goat for several weeks to compare the difference of blood compatibility between these two materials. No thrombus was found on both FPU and Cardiothane surface with visual inspection after 41 days implantation with no anticoagulant. Figure 2 shows a SEM view of the boundary area between FPU and Cardiothane on the atrial cuff of AH. Almost no blood element was attached on both surfaces except boundary line area.

By three times coating of FPU on blood contact surface of AH pump made of PVC paste, about 50 micron thick layer of FPU was formed, which had enough strength to be durable for long term pumping. This pump was used to a goat as the right side pump of total AH for 41 days without anticoagulant and compared its blood compatibility with Cardiothane coated PVC paste pump used as

the left side pump. A visual inspection view of these pumps is shown in Fig. 3. No thrombus was found in both pumps macroscopically. Figure 4 is a SEM view of FPU coated pump, in which almost no blood element observed to attach on the FPU surface. No calcium deposit could be detected by x-ray microanalyzer. FPU layer had never come off from PVC surface and there was no fatigue sign.

These results reveal that FPU has superior blood compatibility and durability, and will be expected as a new artificial heart pump material.

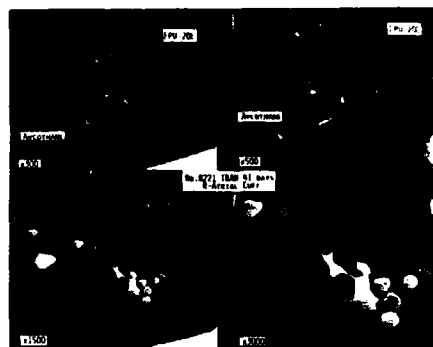


Fig. 2 SEM view of the boundary area between FPU and Cardiothane(Avcothane) of AH atrial cuff



Fig. 3 Macroscopic view of FPU and Cardiothane coated pump used to goat for 41 days with no anticoagulant

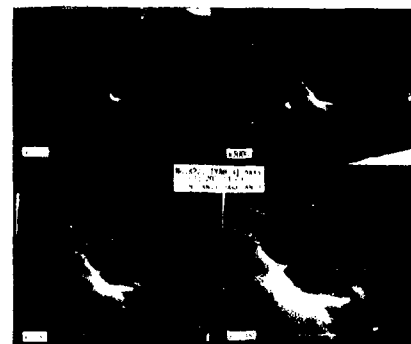


Fig. 4 SEM view of FPU coated pump surface

Institute of Medical Electronics, Faculty of Med.,
University of Tokyo
7-3-1 Hongo, Bunkyo-ku, Tokyo 113 Japan
*Asahi Glass Co., Ltd.
Hazawa-cho, Kanagawa-ku, Yokohama 221, Japan

MITRATHANETM - A NEW POLYETHER URETHANE UREA FOR MEDICAL APPLICATIONS

D.K. Gilding*, A.M. Reed, I.N. Askill, S. Briana

Mitral Medical International, Inc.
Wheat Ridge, Colorado 80033

MitrathaneTM is a new polyether urethane urea developed to exacting specifications for critical medical applications. MitrathaneTM has a similar molecular structure to Biomer^R 1,2 and evolved from systematic studies carried out in the late seventies at the ICI/U. of Liverpool Joint Laboratory.^{3,4}

The structure, synthesis and methods of characterization will be discussed. Solutions in dimethyl acetamide and cast films are crystal clear and both gel and particle free due to rigid quality control procedures.

The mechanical properties that are essentially equivalent to Biomer^R will be compared with currently established materials. Fatigue testing data will be presented for a number of configurations.

In vitro protein adsorption and turnover data will be presented⁴ together with cell adhesion studies.⁵ The results of acute and chronic toxicity studies will also be reviewed.

MitrathaneTM can be fabricated into a variety of porous structures which have potential uses in reconstructive surgery, wound healing, filters and arterial and ureteral prostheses. These structures together with their mechanical and biological properties will be described.

Current data from a limited series of human patients demonstrates that microporous MitrathaneTM patches are ideal for reconstructing congenital heart defects, in that the material most closely simulates the properties of natural tissue.

Animal data with small bore arteries currently demonstrates a high degree of blood compatibility combined with control of compliance matching and excellent suturability.

The MitrathaneTM family of structures represents a systems approach to a new generation of cardiovascular devices.

1. Boretos JW: Past, present and future role of polyurethanes for surgical implant, Pure and Appl Chem, 52:1851, 1980.
2. Gilding DK and Taylor JA. Method for preparing extrudable polytetramethylene ether polyurethane urea resins. US Patent No. 4,062,834, 1977.
3. Gilding DK and Reed AM: Systematic development of polyurethanes for biomedical applications Pt. 1: Synthesis, structure and bulk properties. Trans 11th Int Biomat Symp 3:50, 1979.
4. Reed AM, Gilding DK, Wilson J, Johnson M: Systematic development of polyurethanes biomedical applications Pt. 2: Surface and biological properties. Trans 11th Int Biomat Symp, 3:145, 1979.
5. Ives CL, Eskin SG and Seidel CL, 2nd World Congress Biomaterials, 1984.

*D. Keith Gilding
Mitral Medical International, Inc.
4070 Youngfield
Wheat Ridge, Colorado 80033

ON THE SWELLING BEHAVIOR OF GELS OF 2-HYDROXYETHYL METHACRYLATE (HEMA)
DOPED WITH METHACRYLIC ACID (MAA)

E. C. Eckstein, L. Pinchuk *, M. R. VanDeMark, E. G. Barroso

University of Miami, Coral Gables, FL 33124

While hydrogels based on pure pHEMA have been widely used as implantable biomaterials, they are known to calcify. The deliberate doping of HEMA monomer with MAA to prevent or minimize calcification of the gel has been reported, but a rationale for the use of MAA is lacking. Results below show the swelling behavior of pHEMA/MAA gels in ionic solutions, some of which contain Ca^{++} . The Ca^{++} -induced behavior of pHEMA/MAA differs from that of other ionizable gels exhibiting collapse (1). Combining these new observations, our past work showing the pH dependence of the water content (WC) of pHEMA/MAA gels (2), and the polymer physics related to collapse of gels (3) provides a more complete picture of the macromolecular events relevant to calcification resistance.

Our previous work showed that pHEMA/MAA gels exhibit two distinct levels of WC depending upon the ionization of MAA (2). In isotonic NaCl solution at pH 7.4, gels made of 2.5% MAA, 0.15% TEGDMA (tetraethylene glycol dimethacrylate, a crosslinker) and remainder HEMA have a swollen equilibrium WC of 60%. Even larger WCs occur for solutions of lower ionic strength at pH 7.4. When the solution pH is below 6, the equilibrium WC of the pHEMA/MAA gels equals that of pure pHEMA gels (40%), which exhibit no pH-induced change of volume. The theory of polymer collapse (3) describes the WC of such gels as the balance among three forces, namely polymer-solvent affinity, rubber elasticity and electrostatic interactions of ionized groups. Ionization of the MAA in the pHEMA/MAA gels induces the larger WC observed at pH 7.4. The reduction of WC from the higher values observed in solutions of low ionic strength is primarily due to shielding of the ionized groups.

Methods. Gel disks (2.5 mole% MAA, 0.15 mole% TEGDMA, remainder HEMA) were made with methods reported in (2); these methods stress analysis and purity of the HEMA and reliable, reproducible production of homogeneous gel. A stock solution of 0.1 M Na-based pH 7.4 buffer was used to establish a convenient, initial swollen condition of gel disks and to make solutions of various molarities in Ca^{++} , Mg^{++} , Na^{+} and K^{+} . The presence of low molarity buffer ensures that results are due to ionic effects and not to pH-induced shrinkage. Regular monitoring of the solution pH assured the buffer was not exhausted. Using traditional techniques, values of WC were calculated from the wet and dry weights. Accuracy of the WC measurements is better than 5%. Gel equilibrium was judged as no change of WC over a one-month period.

Results and Discussion. Figure 1 shows the water content of the gels in ionic solutions of various strengths. Notice that effects due to Na^{+} and K^{+} are nearly equal. However, the Ca^{++} does not have the same capacity as Mg^{++} to drive the gel to a lower water content. This behavior distinctly contrasts with that reported for p(acrylamide/MAA) gels, for which divalent ions induce shrinkage in an equivalent fashion at low concentrations (1).

The level of WC in these gels can be modelled as a form of "critical point" behavior (3). In

solvents of suitable theta temperature, these gels show a discontinuous change of swollen volume (SV) for a small change of an environmental parameter, such as pH or ion concentration (i.e. the gel "collapses" as it goes from a maximum to a minimum SV). At other theta temperatures there are smoother, but still large changes of SV for small changes of the environmental parameter. The intermediate states of equilibrium SV are described by the thermodynamic methods of Maxwell, wherein the intermediate SV exists as a two phase mixture of the maximum and minimum SV states (3). For the pHEMA/MAA gels, domains of collapsed polymer form one phase and domains of expanded, ionized polymer, the other. The difference of ionization makes this situation similar to having distinct components. Thermal motions allow individual polymer strands to change the domains with which they are associated within the restriction that the average state of the gel follows the Maxwell description. This reassociation of strands between domains is not found in pure pHEMA gels since they do not exhibit the collapse behavior that is prerequisite for the two phase description.

Further, data for the p(acrylamide/MAA) gels suggests that reassociation of strands may not occur in all implanted collapsible gels since low levels of divalent ions, in conjunction with physiological levels of monovalent ions, may keep such gels at minimal SV. The lack of ability of Ca^{++} to collapse the MAA-doped pHEMA gels thus allows extra macromolecular events that may be critical to calcification resistance.

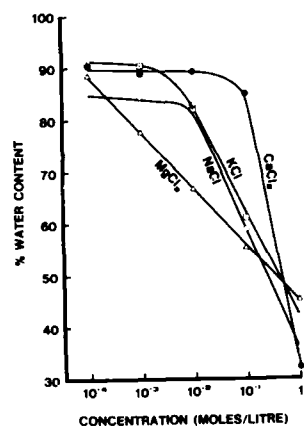


Figure 1. Water Content vs. Ion Concentration

(1) Ohmine, I. & Tanaka, T. Salt Effects on the Phase Transition of Ionic Gels, *J. Chem. Phys.* 77:5725, 1982

(2) Pinchuk, L. et al. Effects of Low Levels of MAA on the Swelling Behavior of pHEMA, *J. Appl. Polymer Sci.*, In press; Eckstein, EC. et al. A Responsive Hydrogel Surface..., submitted for Amer. Chem. Soc. Sympos. Vol. on Hydrogels, ACS Meeting, Seattle, Mar., 1983.

(3) Tanaka, T., Gels, *Scientific Amer.* 244 1981 (See also other references cited in 1.)

* Current Address: Cordis Research Corp., P.O. Box 025700, Miami, FL 33102

This work sponsored by NIH Grant AM-26630.

POLYSILOXANE MODIFIED STYRENE-ETHYLENE/BUTYLENE-STYRENE BLOCK
COPOLYMERS: A NEW CLASS OF BIOCOMPATIBLE THERMOPLASTIC ELASTOMERS

R. Sterling¹ and E. P. Goldberg²

Concept Polymer Technologies, Inc.¹, 12707 U.S. 19 South, Clearwater, FL.
33546, and Dept. Materials Science & Engineering,² University of Florida
MAE 217, Gainesville, Florida 32611

The development of new semi-rigid and elastomeric polymers combining improved biocompatibility, good physical properties, versatile processability and moderate cost is an area of growing research attention. The need for increasing the safety of polymeric medical devices and implants is underscored by such continuing problems as (a) tissue damage due to contact with device surfaces, e.g. endotracheal tubes and vascular catheters (b) hard fibrous tissue encapsulation of implants (c) blood clotting in small diameter vascular prostheses (d) uncertainties regarding the potential adverse effects of leachable plasticizers, e.g. DOP in vinyl polymers and (e) encrustation and infection associated with ureteral catheters.

We report here for the first time, the preparation and properties of a new family of semi-rigid to elastomeric thermoplastics with superior properties for medical device applications. These thermoplastic elastomers (C-Flex®) were prepared by polydimethylsiloxane (PSi) modification of styrene-ethylene/butylene-styrene (S-EB-S) block copolymers.

Styrene-butadiene-styrene block copolymers (e.g. Kraton®) have become commercially important thermoplastic elastomers but exhibit some processing and thermal/oxidative property deficiencies. Hydrogenation of the butadiene segments produces a more stable fully saturated ethylene/butylene central block. Such S-EB-S compositions were therefore used for further modification in this study. Polysiloxanes were found to exhibit surprising compatibility in blends with S-EB-S. Incorporation of 4-5 wt.% PSi was readily achieved resulting in significant improvement in surface properties and processing characteristics (especially for extrusion of thin sections). Polypropylenes (PP) also showed good compatibility when added to PSi modified block copolymers. Polymer modulus and hardness increased and were readily controlled by varying the PP concentration. The resulting PSi/PP/S-EB-S compositions were shown to possess a uniquely favorable balance of properties for biomedical use. In particular, they contain no phthalate plasticizers and exhibit silicone-like surface qualities coupled with thermoplastic processability and improved elastomer strength properties. Good blood and soft tissue compatibility have been demonstrated and numerous medical device applications identified. This paper will present physical and biological property data and briefly summarize results showing significant advantages in a few important device applications (blood pump and dialysis tubing, ureteral catheters, endotracheal tubes, enteral feeding tubes, and myringotomy tubes).

PSi/PP/S-EB-S compositions containing 1-8 wt% PSi and 5-25 wt% PP were prepared by plasticizing polyblends in Banbury or twin-screw compounders at 350-400°F with mineral oil as the rubber extender. Resulting compositions were readily extruded or injection molded and exhibited excellent flow, mold release and surface smoothness. The physical properties for 15-20 mil extruded films of 3 representative compositions containing 4% PSi with varying PP content are given below:

Wt.% PP	5	13	24
Hardness (Shore A)	30	50	70
Tensile Strength (PSi)	1700	1650	1900
% Tensile Elongation	1100	850	790

These compositions also exhibited excellent low temperature properties (brittle point of -100°F) and good stability to thermal aging at 125°C for one week. All conventional sterilization methods produced little change in properties (ethylene oxide, steam/autoclave, gamma at 2.5 Mrad). Radio-opaque fillers were also readily incorporated (barium and bismuth compounds) at high loadings with retention of useful properties.

An extensive investigation of toxicology and biocompatibility has to date indicated no significant adverse effects due to chemical or physical surface properties or leachable material. Soft tissue implants (one year) show good bioacceptance and no evidence for migration of polymer constituents into surrounding tissue. Blood compatibility (hemolysis and platelet adhesion tests) has been shown to be at least as good as that of polysiloxanes.

Tubing for blood pumping in open heart surgery and blood dialysis has surpassed other polymers (silicone, vinyl, urethane) in tests at the Baylor Medical Center comparing mechanical strength, pump life and blood damage. For endotracheal tube cuffs, low durometer compositions have shown lower sealing pressures and less tracheal tissue damage in clinical tests as compared with vinyl, latex or silicone. Ureteral catheters have demonstrated minimal mineral encrustation in the urinary tract and bladder. Overall, the unusual combination of physical, chemical, surface and biological properties exhibited by these siloxane modified thermoplastic elastomer polyblends make them most interesting for a wide range of medical applications.

POLYMERIZATION KINETICS OF COLD CURING ACRYLIC RESINS BY QUANTITATIVE
MULTIPLE INTERNAL REFLECTION INFRA RED SPECTROSCOPY

J.R. de Wijn and P.J. van Kesteren

Dept. of Dental Materials, Dental School, University of Nijmegen, Nijmegen,
The Netherlands.

Based on Multiple Internal Reflection Infra Red Spectroscopy a method has been developed which enables the continuous recording of polymerization in self curing acrylic resins. This method can be applied to the quantitative study of polymerization kinetics and the influence thereupon of initiating systems, comonomers etc. This study concerns the polymerization rate and ultimate conversion in methylmethacrylate/polymethylmethacrylate mixtures as determined by: benzoylperoxide and dimethyltoluidine concentrations, the powder to liquid ratio and the presence of crosslinking and retarding comonomers.

A standard MIR-accessory was modified to provide a space of 25x12x3 mm on each side of a KRS-5 crystal. This cell could readily be filled with fresh mixtures of powder and monomer. During the polymerization the transmittance at 1648 cm^{-1} (double bond) was measured as a function of time, thus enabling monitoring the polymerization of the material in contact with the sides of the crystal. Calibration was accomplished using mixtures of monomer and the corresponding ester of iso-butanolic acid, the latter serving as a fluid "stand-in" for the saturated polymer. The obtained conversion-time curves were corrected for the dissolution of pre-polymer into monomer.

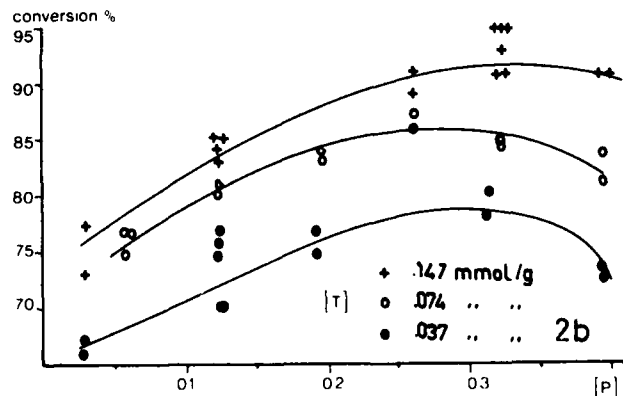
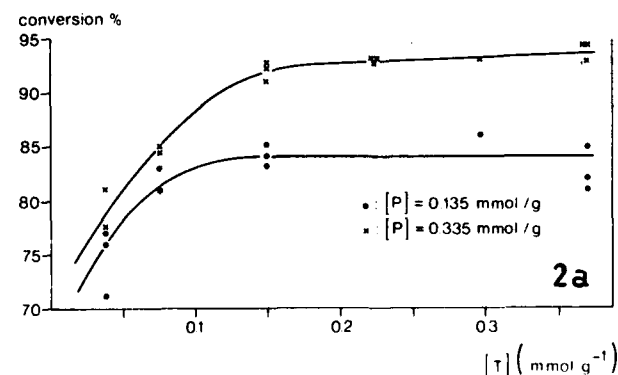
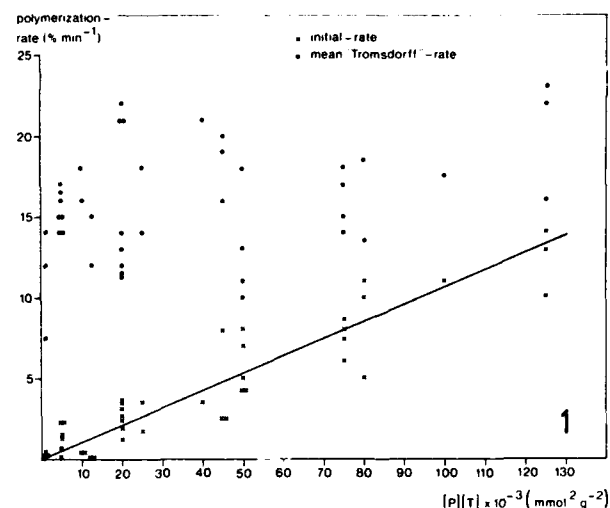
The peroxide and toluidine concentrations were varied over a range of 0.03 to 0.42 mmol per gram of monomer in various ratio's. It appeared that the initial polymerization rate correlates linearly with the concentration product, whereas the rate during the autoaccelerated stage seems to be hardly affected by the initiator concentration (Fig. 1).

The ultimate conversion (or residual monomer content) appeared to be related in a more complex way: up to about 0.15 mmol/g toluidine the conversion is correlating with the 0.6th power of the concentration product. Higher values of toluidine concentrations are not effective in improving the conversion in contrast to the peroxide concentration which is effective up to 0.33 mmol/g (Figs. 2a, b). No correlation between polymerization rate and ultimate conversion could be established.

The results for polymerization rates and conversion were not affected by the powder to liquid ratio of the resin mixture nor by the addition of crosslinking ethyleneglycoldimethacrylate up to concentrations of 10%. Butylmethacrylate is effective in reducing both initial and autoaccelerated polymerization rates but does not affect the relations between ultimate conversion and concentrations of the initiating system. Separate experiments showed that the addition of butylmethacrylate will indeed significantly reduce the maximum temperature at a (simulated) bone-resin interface.

It is concluded and will be shown that the properties of cold curing acrylic resins can be optimized by higher peroxide concentrations (better

conversion) and the addition of retarding comonomers as butylmethacrylate (lower maximum temperature). Addition of crosslinking agents compensates for loss of strength which to some extent may be caused by the lower molecular weight material that is formed at higher peroxide concentrations.



R. Smith, D. C. Watts*

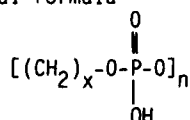
University of Liverpool, P.O. Box 147, Liverpool, England.

Research into the use of organophosphorus compounds in the biomedical field has been particularly intense over recent years, one of the main areas of interest being concerned with bonding to hard mineralised tissue.

This paper reports on research performed into the synthesis and use of organophosphorus polymers as the liquid component of dental cement formulations and indicates other areas of potential usage in the biomedical field.

In the early 1970s the work of Anbar *et al*¹⁻⁴ demonstrated the use of phosphonates as adhesives in the restoration of teeth and as potential preventive agents of dental caries. Phosphonates were considered superior to phosphates due to the latter's relative ease of hydrolysis. However, Penczek *et al*⁵ showed that certain polyorganophosphates were hydrolytically stable. The polymers synthesised in this study are those first described by Penczek.

Several water soluble poly (alkylenephosphates) of general formula



were synthesised via a ring opening polymerisation mechanism. These polymers are interesting in that they are similar to the backbone of nucleic and teichoic acids and as such, may show favourable biocompatibility. The synthesised polymers were characterised by techniques including NMR, rheology and GPC. Each polymer was found by NMR to be linear and GPC showed the molecular mass to be in the region of $2 \times 10^4 - 1 \times 10^5$. Potentiometric titration of aqueous solutions of poly (alkylenephosphates) gave similar profiles to strong acids.

The cement forming capability of aqueous solutions of poly (alkylenephosphates) was assessed by mixing with zinc oxide and ion leachable glasses. In all cases reaction was too rapid to be considered useful, a probable consequence of the polymers high acidity. The incorporation of the polymers into commercial cement formulations was also studied. Deterioration in cement properties was observed, particularly stability to water, samples disintegrating after a few hours storage. The mechanical properties were similar to the unadulterated cement when stored dry.

In an attempt to reduce the high reactivity of poly (alkylenephosphate) solutions, various metal ion additives were incorporated, eg. Al^{3+} , Zn^{2+} , Sn^{2+} . It was found that the addition of tin II fluoride at 10% w/w gave a workable cement paste when the solution was mixed with zinc oxide; however, due to adverse stability to water, mechanical strengths were considerably reduced when compared to a control. It is, thus, apparent that the hydrophilicity of poly (alkylenephosphates) needs to be reduced in an attempt to confer water stability on cements.

References

1. Anbar, M. and St. John, G. A. J. Dent. Res. 50(3) 778 (1971).
2. Anbar, M., St. John, G. A. and Scott, A. C. J. Dent. Res. 53(4) 867-78 (1974).
3. Anbar, M. and Farley, E. P. J. Dent. Res. 53(4) 879-88 (1974).
4. Farley, E. P., Jones, R. L. and Anbar, M. J. Dent. Res. 56(8) 943-52 (1977).
5. Penczek, S. Pure and Appl. Chem. 48 363-71 (1976).

This research was supported by a grant from the Science and Engineering Research Council ref. GRA 56186.

Department of Dental Sciences, School of Dental Surgery, University of Liverpool, P. O. Box 147, Liverpool L69 3BX, England.

*Turner Dental School, The University of Manchester Manchester, England.

D. R. Miller and N.A. Peppas

School of Chemical Engineering, Purdue University,
West Lafayette, Indiana 47907

Surface analysis of poly(vinyl alcohol-co-N-vinyl-2-pyrrolidone) (PVA/PNVP) is presented here to form the basis for future work on protein adsorption. Various aspects of membrane manufacture and analysis methods are investigated in this work.

Experimental Methods

Copolymers of vinyl acetate and N-vinyl-2-pyrrolidone (VAc/NVP) were prepared by γ -irradiation which removes the possibility of residual initiator contamination. The composition of the copolymer was controlled by varying the ratio of monomers before irradiation. The PVA/PNVP material was synthesized by a procedure involving alkaline methanolysis in 0.1N NaOH at ambient temperature; by-products of the methanolysis were removed by dialysis over several days. The bulk composition of the copolymers and structural verification were obtained by elemental analysis, H-NMR and IR spectroscopy.

XPS analysis was performed on dry samples except for one swollen sample. The copolymers were dried by cutting 1 cm² specimens, and freeze-drying them. Surface labeling of polymers employed a modified reaction scheme of Pennings *et al.* (1980), using heptafluorobutyric acid chloride. The XPS instrument employed a Mg target with a double pass, cylindrical-mirror type analyzer with a retarding grid input stage.

Results and Discussion

The copolymer membranes produced by this procedure are amorphous, transparent, highly hydrated materials. Table 1 gives the bulk and surface composition of the materials produced, where f_1 is the mole fraction of VAc in the monomer mixture and F_1 is the mole fraction of VA incorporated in the copolymer. Quantitative XPS was obtained by using pure homopolymers of PVA and PNVP as standards.

Table 1
Copolymer Bulk and Surface Composition of a
Function of Feed Composition

f_1	$(F_1)_{\text{bulk}}$	$(F_1)_{\text{XPS}}$
0.00	0.00	0.02
0.20	0.12	0.20
0.40	0.20	0.28
0.60	0.41	0.30
0.80	0.60	0.58
1.00	1.00	1.00

The XPS analysis was normally done with the C_{1s}, N_{1s}, and O_{1s} photopeaks. The Table 1 F_1 XPS values correspond to the face of the copolymer gel that formed against the glass petri dish. The values of F_1 given are the average compositions calculated. These results calculated by either ratio were a verification of the copolymer structure.

Comparison of surface composition values and bulk values from Table 1 show that at low values of f_1 , VA is preferentially incorporated in the surface region. A non-dried swollen sample was also examined on a cold probe for comparison to the equivalent dried sample. The results showed carbon contamination at the low temperature (77K)

and a water layer on the sample surface. Modeling of XPS analysis of a swollen sample indicated that sublimation of the water may have occurred even with use of a cold probe.

Surface labeling of the hydroxyl groups was also employed to investigate the polymer conformational changes that occur when a swollen membrane is freeze dried. Table 2 presents the labeling results, where the symbol I_{ij} represents the XPS intensity ratio of I_i/I_j . Sputtering results were also obtained. If no chain rearrangement occurs upon freeze drying, the fluorine intensity should drop off drastically with penetration depth since the labeling reaction is very surface specific.

Table 2
XPS Data of Labeled Copolymers

f_1	I_{CO}	I_{NO}	I_{FO}
1.0	0.838	0.000	0.723
0.6	1.456	0.307	0.502
0.4	1.688	0.231	0.440
0.2	1.861	0.394	0.053

The results indicate that the fluorine is localized near the sample surface (the first 200 Å). If polymer chain rearrangement occurs with freeze drying, the rearrangement must be limited to approximately the first 100 Å.

Peak shape analysis was used to explain the asymmetry of pure PVA membrane C_{1s} XPS spectrum. The two carbon states in linear PVA should give approximately equivalent photopeaks. With crosslinking and branching, two new carbon states were produced which could produce peak asymmetries. Modeling indicated that the effect of branching and crosslinking was to produce primarily tertiary alcohol units in the XPS sampling region. Similarly, the copolymers must also have had new carbon states created by crosslinking and branching but due to structure complexities they could not be studied by peak analysis.

D. R. Miller and N.A. Peppas, School of Chemical Engineering, Purdue University, West Lafayette, Indiana 47907. USA.

The Effect of Polyether Segment Chemical Structure on the Bulk and Surface Morphologies of Copolyether-urethane-ureas

K. Knutson and D. J. Lyman

Department of Materials Science and Engineering
University of Utah, Salt Lake City, Utah 84112

Block copolyurethanes form domain-matrix morphologies due to the chemical and steric incompatibilities of the chemically different blocks or segments. The unusual range of physical and chemical properties associated with copolyurethanes results from the morphological separation. In addition, blood compatibility properties of copolyurethanes are also often associated with morphology. (1-3) Surface and bulk morphologies of a series of copolyether-urethane-ureas having polyether segments of different chemical structures, tacticities and molecular weights have been studied by Fourier transform infrared spectroscopy. Six model polymers were used to characterize the individual polyether matrix, urea domains and urethane interfacial regions.

The block copolyurethanes were synthesized from 1:2:1 molar ratios of the polyol, methylene bis(4-phenylisocyanate) and ethylene diamine using a two-step polymerization process. (3) The polyols included atactic polypropylene glycols (3000, 2000, 1000, 700 and 400 MW), isotactic polypropylene glycols (1900, 1370 and 1000 MW) and polytetramethylene glycols (2000 and 1000 MW). The model polymers included isotactic and atactic polypropylene oxide to model the influence of tacticity on the polyether matrix. A polyurea synthesized from a 1:1 molar ratio of methylene bis(4-phenylisocyanate) and ethylene diamine was used to model the urea domains. The urethane interfacial region broadened by mixing between the urethane segments and the polyether matrix was modeled with two copolyether-urethanes. The copolymers were synthesized from a 1:1 molar ratio of polypropylene glycol (2000 and 1000 MW) and methylene bis(4-phenylisocyanate). Broadening of the urethane interfacial region due to mixing between the urethane segments and urea domains was modeled with a copolyurethane-urea synthesized from a 1:2:1 molar ratio of propylene glycol, methylene bis(4-phenylisocyanate) and ethylene diamine.

Spectra (1 cm^{-1} , 256 scans) were obtained using a Digilab 14 B/D FTS. Transmission studies of the solution cast polymer films also included the use of parallel and perpendicular polarization to obtain dichroic ratios. Internal reflection spectra were obtained using the Harrick 4X beam condensor with Ge internal reflection elements at 60° incident angles.

Urea domains were not mixing within the polyether matrix as evidenced by the presence of the single N-H stretching bands near 3300 cm^{-1} and the urea carbonyl stretching Amide I bands near 1640 cm^{-1} indicating complete hydrogen bonding of the urea domains. However, urethane interfa-

cial regions were broadened due to mixing of urethane segments with primarily polyether segments. Urethane N-H groups were essentially completely hydrogen bonded. However, 50-65% of the urethane carbonyls were not hydrogen bonded according to the Absorbance percentages of the urethane Amide I forming the nonhydrogen bonded shoulder (absorbing near 1730 cm^{-1}) of the total Absorbance of the band. The carbonyls were freed from hydrogen bonding due to interactions between the urethane N-H groups and primarily polyether oxygens. The extent of mixing within the urethane interfacial regions was a function of the chemical structure, tacticity and molecular weight of the polyether segment. Copolyurethanes based on polytetramethylene glycols had narrower interfaces as compared to copolyurethanes based on polypropylene glycols of similar molecular weight. The influence of tacticity of polypropylene glycols on the degree of mixing within the interfacial region was minor. However, the molecular weight of the polyether segment within a series of copolyurethanes based on the same chemical structure and tacticity of the polyether segment influenced the hydrogen bonding of the urethane carbonyls from 1-5% as determined from the Absorbance percentages. In addition, the influence of molecular weight on mixing within the urethane region was a function of the particular chemical structure of the polyether segment. Therefore, the morphologies of the copolyurethanes studied were characterized by the urea domains being well-separated from the polyether matrices, although the narrowness of the urethane interfacial regions were varied. The narrowness of the interfacial regions was primarily determined by the chemical structure of the polyether segment and to a lower degree by the molecular weight of the particular chemical structure.

1. K. Knutson and D.J. Lyman, Advances in Chemistry Series No. 199 Biomaterials: Interfacial Phenomena and Applications, S.L. Cooper and N.S. Peppas, eds., ACS, Washington, D.C., (1981) 109.
2. D.J. Lyman, IUPAC Macromolecular Symposium, C.F. Ciardelli and P. Giusti, eds., Pergamon Press, Oxford, 1980, 205.
3. D.J. Lyman, L.C. Metcalf, D. Albo, Jr., K.F. Richards and J. Lamb, Trans. Am. Soc. Artif. Intern. Organs, **20**, 474, 1974.

This work was supported by the National Science Foundation, Grant DMR 83-03594, Polymer Program and National Institute of Health, General Medical Sciences, Grant GM 24487-06.

HIGHLY SWOLLEN HYDROPHILIC GELS

O. Wichterle

Czechoslovak Academy of Sciences,
Prague, Czechoslovakia

The equilibrium swelling of gels in water or in the physiological surrounding can be adjusted to any degree by a proper choice of structural units. Highly swollen gels, approaching in permeability that of pure water, can be obtained in many ways, but their usefulness for medical applications is mostly limited by their rather poor mechanical properties. Either their modulus of elasticity is too low because of low cross-linking, or their strength is too low because of excessive cross-linking.

The cross-linking by chemical bonds can be supported by intermolecular links of various nature and more stiff materials can be obtained without inducing brittleness. In contrast to chemical cross-links, the physical ones can be loosened in a reversible way. Under extreme deformations chemical bonds in the overloaded segments of the network are broken and destruction is induced. On the other hand physical intermolecular bonds under the same extreme conditions are loosened in a more or less reversible way. After relaxation the initial state of minimal energy is resumed, especially if some slight chemical cross-linking provides for the shape stability.

The physical cross-linking in hydrophilic networks can be achieved in two ways:

- (1) Joining parts of segments in crystalline domains or
- (2) Formation of microphases by cohesion of hydrophobic portions of the network.

Ordering of network segments into crystalline bundles occurs only in rare instances. The exceptional mechanical properties of collagen tissues or gels obtained by cross-linking of collagen solutions belong to this type. Among synthetic polymers, gels containing sequences of acrylonitrile units alternating with blocks of acrylamide units represent another unique example of this type.

Discrete hydrophobic portions in hydrophilic structures can be obtained in particular cases by copolymerization of monomers having different nature and tending to form sequences of the same kind instead of chains with statistical distribution of both units.

A more consequent method consists in the incorporation of prefabricated hydrophobic oligomers in a hydrophilic network. Although polymers of different nature are usually non-compatible, the macroscopic phase separation can be prevented by strong fixation of hydrophobic blocks in the cross-linked network just at the beginning of polymerization. The phase separation occurs then only in finely divided areas, small enough to make the resulting gel even optically homogeneous.

The mechanical properties of highly swollen gels depend strongly on the degree of dilution of the system at the moment of formation of the three-dimensional network. Large subsequent dilatation of the network formed in the condensed state introduces internal tensions which raise the probability of mechanical destruction. In extreme cases the

mechanical strength of the specimen drops to zero and spontaneous destruction occurs. Therefore, the popular method of production of shaped gel articles by mechanical machining of dry hydrophilic xerogels and subsequent high swelling of shaped miniature replicas is not to be recommended. Casting techniques starting with highly diluted monomer mixture give much more chance of obtaining the best mechanical properties.

Institute of Macromolecular Chemistry
Czechoslovak Academy of Sciences
Heyrovský Square
162 06 Prague 6
Czechoslovakia

A. Schwartz and D. T. Turner[†]Becton Dickinson Research Center
Research Triangle Park, North Carolina

Since its successful use as a blood plasma extender, polyvinylpyrrolidone (PVP) and its copolymers have been considered for a number of biomedical applications. This interest has resulted in a closer examination of the way in which various conditions of polymerization affect structure and properties. One property of basic importance is the glass transition temperature (T_g) which can be measured conveniently on small samples (several mg) by differential scanning calorimetry (DSC). Previously, extremely varied values of T_g have been reported for samples of PVP ranging from 54° to 175°C. Tan and Challa have shown how the value of T_g is depressed by water content and suggested that the wide variation in literature values is caused by the hygroscopic nature of PVP (Polymer 17, 739 (1976)).

Our DSC studies of commercial samples of PVP (GAF, Inc., New York) have shown retention of a few percent water even after prolonged storage in a vacuum desiccator. Most of this residual water is driven off during the first run (to 200°C) giving an endotherm with a peak between 100-120°C (Fig. 1). A minor, and unexplained, endothermal peak was observed near 62°C. A second run clearly reveals inflections typical of a glass transition near 162°C. This value is confirmed in subsequent runs (Fig. 2) but eventually the value of T_g gradually increases, presumably because of crosslinking caused by thermal degradation.

One interesting aspect of the above observations is in relation to the problem of the "state of water" in polymers which previously had been studied in polypeptides and in other complex proteinaceous systems (Berlin, et al., J. Coll. Int. Sci. 34, 488 (1970)).

Additional samples of PVP were prepared from purified monomer either by γ -irradiation or by heating with azo-bis-isobutyronitrile, under nitrogen. DSC runs on these polymers differed from ones on the commercial materials in two respects. First, the endothermal peak at 62°C was not observed and so presumably this is not an inherent property of PVP. Second, values of T_g ranging from 130-180°C were found to depend on the method of polymerization. As these samples had been rigorously dried by repeated runs to 200°C, moisture is not a factor. Instead, it appears that the value of T_g is influenced by variations in the structure of the polymer molecules such as molecular weight, branching, crosslinking, and tacticity. Such an influence would have important implications concerning variations in other physical properties and is under investigation.

Copolymers of vinyl pyrrolidone have been made by including monomers such as methyl methacrylate along with a few percent of a dimethacrylate as a crosslinker. Free radical polymerization should yield a random copolymer with a single value of T_g intermediate between values of PVP (up to about 175°C) and polymethyl methacrylate (about 105°C). Actually, when these monomers are first mixed with water and subsequently irradiated to yield a hydrogel, the dried polymeric product (a xerogel)

exhibits more complex behaviour (Fig. 3). The high value for a T_g , 179°C, suggests the presence of long blocks of PVP as distinct from a random copolymer. This observation has important implications concerning the influence of the method of preparation of hydrogel copolymers on physical properties.

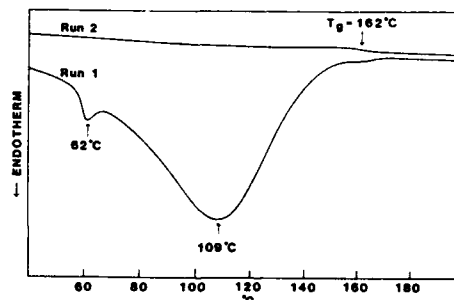


Figure 1. Thermograms of a commercial sample of PVP (K-30, GAF Corporation, New York).

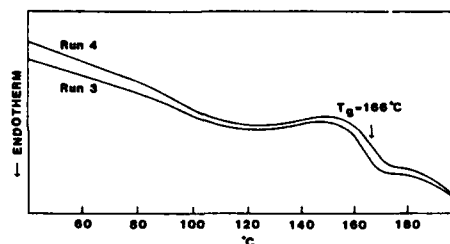


Figure 2. Further runs on K-30 at maximum sensitivity.

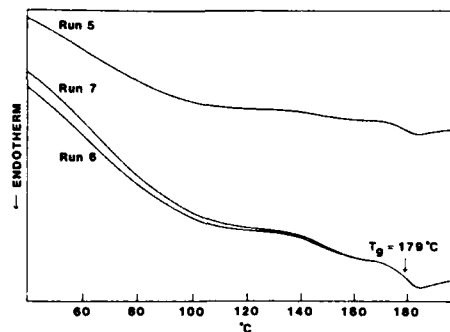


Figure 3. Thermograms of a copolymer xerogel.

Becton Dickinson Research Center, Materials Research Department, PO Box 12016, Research Triangle Park, North Carolina 27709.

[†] Department of Operative Dentistry and Dental Research Center, University of North Carolina, Chapel Hill, North Carolina 27514.

BION[®] II ELASTOMERS FOR BIOMEDICAL APPLICATIONS

T. R. Pherson, W. J. Stith, and H. Quach

Lord Corporation - Bioengineering Dept.
Erie, Pennsylvania

The musculoskeletal system relies on materials with elastic and viscoelastic properties to obtain movement simultaneously in several planes, motion compliance, and shock damping. Elastomeric compounds have been commonly used in industrial applications to address similar motion problems. However, the in vivo uses of elastomers have been limited because of low strength or poor bondability of most biocompatible elastomers.

BION[®], a reinforced polyhexene elastomer, was developed by Goodyear under the name Hexsyn[®] to fill this void. This thermoset elastomer, now licensed to Lord Corporation, has a five-year implant history as the flexing element of the Biomer[™] finger joint. BION was shown to have exceptional fatigue resistance and good bondability to various metal substrates.¹ Hexsyn has also undergone exhaustive testing for use in circulatory assist devices.² The material did require post-vulcanization solvent extraction prior to use to remove vulcanization by-products.

Recently, an improved family of BION-type compounds, tentatively named BION II, has been developed. These materials have been compounded in a range of different moduli and thus can be custom-tailored to specific applications. Although the base polymer is the same, changes made in the curative system have resulted in elastomers that are non-cytotoxic in both cured and uncured forms without the necessity for solvent extraction. The carbon black used to reinforce BION II is extracted prior to mixing to remove polynuclear aromatic hydrocarbons. Table 1 shows the results of biocompatibility testing of BION II performed by North American Science Associates (Northwood, Ohio).

Physical property testing of BION II elastomers (Table 2) showed enhanced tear strength and tensile properties. The material can be compounded with moduli from 75 to over 250 psi which enhances its versatility. Figure 1 shows typical stress/strain curves for low (100 psi) and medium (150 psi) moduli compounds. Exposure to 2.5 and 5.0 Mrads of radiation sterilization dose had negligible effects on the physical properties of the elastomers.

Of great interest in prostheses applications is the excellent bondability of BION II elastomers. The bonding of a low modulus elastomer to a high modulus substrate can make possible complex motion compliance and control not attainable by either material alone. Shock attenuation can be accomplished by loading the material in a combination of compression and shear modes. In tests using 316 LVM stainless steel, 6Al4V titanium, and P-1700 polysulfone substrates, it was found that the interfacial bond strength between BION II and the substrate was greater than the strength of the elastomer (test method ASTM D429). This was true even after four weeks in 90°C pseudo extracellular fluid. Extensive long-term environmental and fatigue testing is currently in progress. Results will be reported as they are obtained.

TABLE 1
BIOCOMPATIBILITY TESTING

In Vitro

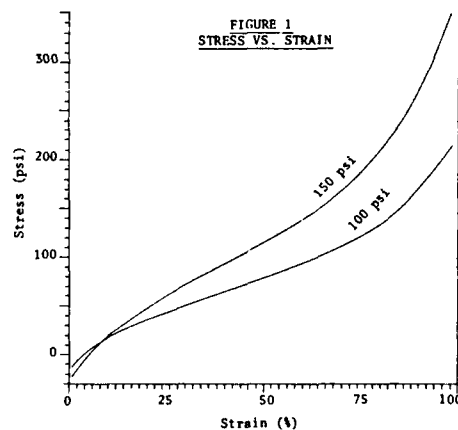
72-hr. MEM Elution (Cured)	Non-Toxic
72-hr. MEM Elution (Uncured)	Non-Toxic
Ames Mutagenicity Test	Non-Mutagenic

In Vivo

Acute Systemic Injection (T18)	Passes
(Saline & Cottonseed Extracts)	
Intracutaneous Injection (T17)	Passes
(Saline & Cottonseed Extracts)	
IM Implantation Test (T10)	Macro: No Reaction
	Micro: No Reaction
	(Non-Irritant)

TABLE 2
PHYSICAL PROPERTIES OF BION II ELASTOMERS

Tensile Strength	ASTM D412	12.4 - 14.5 MPa
Elongation	ASTM D412	700 - 200%
Tear Strength	ASTM D426	1787 - 2150 kg/m
Hardness	ASTM D2240	40 - 90 Shore A
Flex Life	ASTM D430	50 X 10 ⁶ + Cycles



REFERENCES

1. Lee, H. B., Quach, H., Berry, D. B., and Stith, W. J., "Characteristics of Implantable BION Elastomer - Effect of Filler and Cross-linker Content", ACS Org. Coating and Appl. Poly. Sci. Proceed., Vol. 48, March, 1983.
2. McMillin, C. R. and Tucholski, D., "Physical Testing of Polymers for Use in Circulatory Assist Devices", Eleventh Quarterly Progress Report, N01 HV 02909, Monsanto Research Corporation, Dayton, Ohio, 1983.

Lord Corporation
Bioengineering Dept.
P.O. Box 10039
Erie, PA 16514-0039

Jacob, Jean T. and Owen, Donald R..

TULANE UNIVERSITY, NEW ORLEANS, LA DEPT. OF CHEMISTRY

Over the past 20 years a significant research effort has been undertaken to develop hydrogels as blood and tissue interfacial biomaterials. While the initial data as blood contacting surfaces for these hydrogel systems looked very promising, hydrogels have not realized their foreseen potential. The deposition of protein onto these gels appears to be demonstrably less when compared to other more hydrophobic surfaces; however, they are still thrombogenic.

The failure of hydrogels, such as HEMA, HEA, and GMA, may be a result of the lack of homogeneity at the sub-micron level as well as the absence of anionicity. Sub-micron homogeneity requires a degree of freedom of the polymer backbone that allows orientation to the least energetic state. The crosslinking required in hydrogels holds the polymer chains essentially frozen in space. The frozen polymer carbon-carbon backbone no longer has the ability to orientate itself to the most favorable energy state. This results in regions where "exposed" carbon-carbon backbone is directed outward toward the contact media rather than the more hydrophilic polymer components. The low hydroxyl group to carbon atom ratio of most hydrogels makes this orientation critical. The lack of ionicity of a hydrogel may also reduce the size of its hydration sphere and thereby influence the total hydrophilicity. Single pendant hydroxyl groups result in a much smaller hydration sphere than that of a polyhydroxy, a carboxylic acid or the sulfonic pendant groups found in the mucopolysaccharides that line the natural human intima.

To support this postulate the first phase of experimentation was undertaken to produce polyhydroxy non-network hydrogel surfaces consisting of hydrophilic chains attached at one end to a substrate and protruding out from that substrate in "finger-like" extensions. These "finger-like" chains have the ability to be fully hydrated by the contact media and form a non-oblative homogeneous surface. Specifically,

polyhydroxymethylene moieties were chemically grafted via one end group functionality to a hydrophobic substrate. This produced a non-crosslinked surface of free-ended polyhydroxy chains which were capable of independent movement. Grafted surfaces were characterized in terms of surface structure, percent water imbibement, contact angle and albumin adsorption. The characterization results were then compared to similar data generated from a series of typical hydrogel network gels. Calculations the hydroxyl to carbon ratio for the grafted surfaces and its relation to increased hydrophilicity were also made.

Surface Fissuring of Polyurethane-based Pacemaker Leads

M. Szycher, Ph.D., D. Dempsey, V.L. Poirier

Thermedics Inc., 74 West St., P.O. Box 270, Waltham, MA
02254

The advent of linear segmented polyurethanes has provided pacemaker manufacturers a hemocompatible polymer with low coefficient of friction, outstanding flexure endurance and good mechanical strength. This unusual combination of properties has allowed the clinical introduction of polyurethane pacing leads that are thinner and stronger than conventional silicone leads; these thinner-wall polyurethane leads can be used in smaller vessels, or allow multiple leads to be introduced into a single vein for sequential pacing.

Recent reports have shown that pacing leads made with Pellethane 2363-80A exhibit shallow surface fissuring; some pacemaker or lead constructions have failed, particularly at areas of chronic mechanical stress. Several mechanisms have been proposed as the cause of surface fissuring: protein absorption with associated swelling, leaching of low molecular weight substances to the surface, or lipid absorption. However, there is little evidence supporting any of these mechanisms.

Our studies suggest that polyether-based polyurethanes are susceptible to in vivo oxidation of the polyether chain. In this chain, the most susceptible group is the $-CH_2$ group in the alpha position to the ether oxygen, which undergoes peroxidation, free radical dissociation and, eventually, chain cleavage, leading to significant reductions in molecular weight averages. Attenuated Total Reflectance Infrared (ATR-IR) studies at the surface of the fissured polyurethanes have shown the presence of oxidative byproducts such as hydroxyl end groups ($-OH$).

Based on these preliminary results, we hypothesize that progressive surface degradation is caused, in part, by stress-induced oxidation of the polyether macroglycol used in the synthesis of polyurethane elastomers. Our hypothesis has been reinforced by experimental evidence that surface cracking can be significantly reduced, if not eliminated, by using higher-durometer polyurethanes because these polymers contain fewer polyether macroglycol chains in the molecular backbone.

References

- Szycher, M., McArthur, W.A. "Surface Fissuring of Polyurethanes Following In Vivo Exposure" ASTM Symposium on Corrosion and Degradation of Implant Materials, Louisville, KY 1983 (In Press).
- Parins, D.J., McCoy, K.D., and Horvath, N.J., "In Vivo Degradation of a Polyurethane, "Cardiac Pacemakers, Inc., St. Paul, MN 1981.
- Guerrand, K., "Biostability of a Polyurethane, "Intermedics, Inc., Freeport, TX, 1981.
- McArthur, W.A., "Long-Term Implant Effects on Three Polyurethane Leads in Humans, "Pacesetter Systems, Inc., Sylmar, CA, April 1982.
- Ulrich, H. and Bonk, H.W., "Emerging Biomedical Applications of Polyurethane Elastomers, "Proceedings, 27th Annual Conference, SPI, Bal Harbor, FL, p. 143, 1982.
- Szycher, M., Poirier, V.L., Dempsey, D.J., and Robinson, W.R., "Second Generation Biomedical-Grade Thermoplastic Polyurethane Elastomers, "Society of Plastic Engineers, Vol. XXXIX, 4, 1983.
- Pande, G.S., "Polyurethane Insulation for Cordis Permanent Pacing Leads, "Technical Memorandum 35, April 1982.

In Vitro Degradation of An Elastomeric Biomaterial

K. Phua, J.M. Anderson and A. Hiltner

Department of Macromolecular Science, Case Western Reserve University
Cleveland, Ohio 44106

The extent and mechanism of enzymic degradation of elastomeric materials and the evaluation of the effect on performance properties have been examined under in vivo and in vitro conditions. Our initial studies (1,2) involved a model elastomer, poly(2-hydroxyethyl-L-glutamine) (PHEG), which is known to be degraded in vitro by nonspecific proteolytic enzymes (2). Implantation of crosslinked PHEG subcutaneously in rats and in the peritoneal cavity of mice resulted in degradation of the polymer as determined by changes in swelling ratio (1). Histological examination of the implant site led to the hypothesis that enzymes released during the acute inflammatory response were involved.

The cellular and enzymic activity at the implant site were subsequently quantified with a cage implant system (3). Initially PHEG and then Biomer® (4) were enclosed in a stainless steel cage and implanted subcutaneously in rats. Analysis of the exudates demonstrated cellular activation and enhanced enzyme exocytosis by the inflammatory cells as a result of cell-polymer interactions. Correlation with cellular events occurring on the polymer surface suggests a preferential adherence of macrophages over polymorphonuclear leukocytes. Removal of the cellular components revealed extensive pitting of the Biomer® surface.

Recently, the effect of in vitro exposure to enzymes on the performance properties of Biomer® has been examined. The action of two proteolytic enzymes with broad specificities, papain and urease, has been studied. The Biomer was treated in the form of ultrathin films, about 35 μ m thick, cast from DMF solution. Exposure to active enzymes for up to one month resulted in significant loss of fatigue resistance compared to control treatments which included the papain activating solution, the urease buffer and distilled water. Films cycled between 0 and 250 percent elongation failed on an average 90 percent sooner after exposure to papain and 60 percent sooner after exposure to urease. Premature initiation of the crack accounted for the low fatigue lifetime since propagation of the crack occurred over 15-20 cycles prior to fracture in all specimens.

The damage could not be detected in stress-strain or modulus measurements which are known to be less sensitive to such effects than fatigue or cyclic measurements. The damage was not associated with specific features of the surface although all treatments including the controls produced some surface pitting which was detectable in SEM micrographs.

To date, the study has clearly shown that in vitro exposure to proteolytic enzymes

similar to those present during the inflammatory response shortens the fatigue lifetime of a polyurethane elastomer. This performance characteristic, in addition to being closely related to end-use applications of the material, is more sensitive to material damage than other mechanical parameters such as modulus and failure strain in tension. Future work will address the relationship of chemical bond rupture to the solid state structure and the mechanism of fatigue crack initiation.

References

1. Dickinson, H.R., Hiltner, A., Gibbons, D.F. and Anderson, J.M., Biodegradation of a Poly(α -Amino Acid) Hydrogel. I. In Vivo, J. Biomed. Mater. Res., 15, 577-589 (1981).
2. Dickinson, H.R., Hiltner, A., Biodegradation of a Poly(α -Amino Acid) Hydrogel. II. In Vitro, J. Biomed. Mater. Res., 15, 591-603 (1981).
3. Marchant, R., Hiltner, A., Hamlin, C., Rabinovitch, A., Slobodkin, R. and Anderson, J.M., In Vivo Biocompatibility Studies. I. The Cage Implant System and a Biodegradable hydrogel, J. Biomed. Mater. Res., 17, 301-325 (1983).
4. Anderson, J.M., Marchant, R., Suzuki, S., Phua, K., Hamlin, C., Rabinovitch, A., and Hiltner, A., In Vivo Biocompatibility Studies. IV. "Biomer" and the Acute Inflammatory Response, to be published in Polyurethanes in Medicine, H. Plank, editor.

INFLUENCE OF SUTURE DIAMETER ON THE TENSILE STRENGTH OF POLYPROPYLENE MONOFILAMENTS

Robert P. Kusy and John Q. Whitley

Dental Research Center, University of North Carolina at Chapel Hill,
Chapel Hill, NC 27514

Recently the creep rupture and tensile strength of polypropylene (PP) sutures has been reported as a function of diameter (d) and radiation exposure. In the course of this experimental work, the ultimate tensile strength (σ_f) of the unmodified sutures was considered. Since ongoing studies concentrated on only the 4-0 to 7-0 suture sizes, two manufacturers were requested to provide additional data for their PP product. A detailed analysis of those results suggests that the σ_f of both knotted and straight pulled PP sutures is dependent upon d in two ways: $\log \sigma_f$ vs. $\log d$ and $1/\sigma_f$ vs. $d^{1/2}$. Moreover, the analysis implies that some fundamental changes of the USP specification may be warranted, if other Class I type sutures obey the same functional relationship.

Unirradiated PP monofilaments, designated Prolene® (Ethicon, Inc.▲) and Surgilene® (Davis + Geck Co.▼), were tested in the "knot pull" configuration according to the USP specification. In addition these same sizes, 10-0 to 2 and 7-0 to 2 for each respective product, were tested in the unknotted or "straight pull" configuration. Unlike most sutures, these Class I materials were sterilized by ethylene oxide gas. Consequently, the specifications for knotted sutures were increased by a factor of 1.25. This is proper because the use of ethylene oxide gas has no known effect on the tensile properties of PP.

In the first phase of the analysis, σ_f vs. d , σ_f vs. $1/d$, and breaking force ($F_b = \sigma_f A$) vs. cross sectional area ($A = \pi d^2/4$) plots were made in order to adduce a working relationship. While σ_f vs. d oftentimes shows that fibers increase in strength with diameter and σ_f vs. $1/d$ has been generally used to explain the strength of metallic whiskers, neither of these plots yielded a straight line relationship (significance $p > 0.1$). Moreover, although a linear relationship has been suggested between F and A for not only PP but also other materials, the selection of only three suture sizes and the inherent problems associated with scaling such a plot proved unsatisfactory. Nevertheless, one positive aspect of this method was that the σ_f could be determined directly from a linear regression of the figure.

When plots of $\log \sigma_f$ vs. $\log d$ (Figure 1) and $1/\sigma_f$ vs. $d^{1/2}$ (Figure 2) were plotted for knotted and straight pulled data, a common linear relationship was observed for both manufacturers' products. This first proportionality was consistent with the empirical relationship reported by Batchelder, Galiotis, Read, and Young who then extended the work of Kelly and Marsh to include organic fibers. Thus, the second expression is derived from a fracture theory which states that surface defects, such as steps, create stress concentrations which ultimately lead to failure via the nucleation of cracks. By superposing the minimum USP XX specification for Class I knotted sutures in both the sterilized and either the non-sterilized or chemically sterilized state, a different linear relationship was obtained over the suture sizes ranging from 10 to 8-0. For the remaining four smallest suture

sizes, a markedly more conservative relationship was observed: When $1/\sigma_f$ vs. $d^{1/2}$ was plotted, a parabolic-like functional relationship appeared, the vertex of which was at the 8-0 size (cf Figure 2). Fortunately, this vertex corresponded to the least conservative element of the current specification. Using this suture size as the basis for a rational specification, $0.60 \sigma_f$ and an $0.75 \sigma_f$ (i.e., $1.25 \times 0.60 \sigma_f$) lines were constructed for both knotted and straight pulled data. This analysis shows that the PP monofilament specification could be established on a more fundamental basis using $0.60 \sigma_f$ as the generalized criterion, and suggests that other sutures composed of silk or synthetic fibers of monofilament, twisted, or braided construction should be evaluated similarly.

Supported by NIH Research Grant DE-02668.
Thanks to Ethicon and Davis + Geck for their cooperation.

Dental Research Center, University of North Carolina, Chapel Hill, NC 27514.

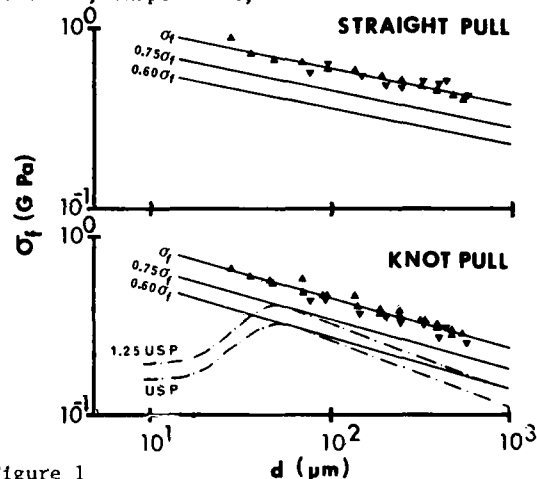


Figure 1

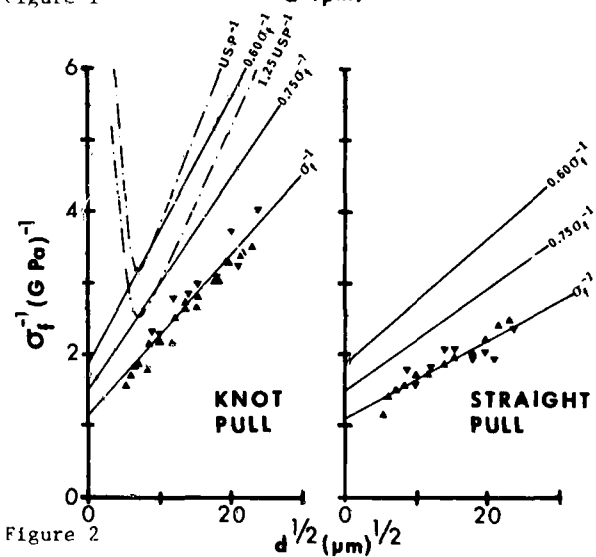


Figure 2

An Evaluation of Carbon Coated Dacron As A
Nonabsorbable Suture Material

M.A. Kester, S.D. Cook, M.E. Brunet and H.G. French

Department of Orthopaedic Surgery, Tulane University School of Medicine and
the Veterans Administration Medical Center, New Orleans Louisiana 70112

Ultra low temperature isotropic (ULTI) carbon (Biolite) is a surfacing biomaterial [1,2] whose potential use as a suture coating merits investigation. Biolite can be applied to many materials including metal, ceramics and polymers, as a thin coating ($\leq 0.5 \mu\text{m}$) such that it does not alter the substrate mechanical properties or gross dimensions. Currently, an area of concentrated research is in the utilization of flexible carbon fiber in knee ligament prosthetics.[3] By redirecting the use of the carbon as a coating material and coupling it with a material with acceptable biocompatibility and superior mechanical characteristics, enhanced performance may be expected. The present investigation evaluated histologically and biomechanically the use of Biolite coated nonabsorbable (Dacron) suture used to repair the surgically incised canine medial collateral ligament and superficial tissues.

Suture material (size 1) of either uncoated Dacron (Mersilene), Biolite coated Mersilene, or polybutylate coated Dacron (Ethibond) was used to repair a surgically incised medial collateral ligament in adult mongrel dogs. The ligament was repaired using a standard weave stitch followed by anchoring the incised distal portion of the ligament to the apposed bone by passing the suture through a prepared tunnel in the tibia. Additionally, as the surgical approach required the incision of the canine pes anserine tendon and the medial rectinacular fascia, these tissues were repaired using the same suture type of size 0 and 00, respectively. The surgical procedure was performed bilaterally with no animals receiving the same type sutures bilaterally. The animals were allowed unlimited activity until sacrifice at periods of 1,3,6,9,12,24,36 and 48 weeks.

At sacrifice, the superficial and deep suture material and surrounding tissue were removed and paraffin embedded histologic sections were made from both repair sites. Decalcified sections were prepared from the tibial anchor site to allow an examination of the bone - suture interface. All sections were stained with Hematoxylin and Eosin. Histologic grading was performed based upon morphology, the quantity of the cellular reaction and the presence of tissue growth into the suture material. The standardized grading scheme devised incorporated numerical values one through five. A grade of one represented a suture section with excellent fibrous tissue ingrowth and a minimum of inflammatory response. An assignment of five was indicative of the presence of tissue necrosis, PMN's, and granulomas with no fibrous ingrowth.

Lengths of suture material were also placed subcutaneously in the left and right groin region. These sutures (sizes 1, 0 and 00) were implanted unstressed in tunnels created by blunt dissection. Upon sacrifice, this suture material was tested in tension to failure on a MTS closed

loop hydraulic test machine operated in stroke control at a constant displacement rate of 50mm/min. Data collected from test specimens that broke from grip induced failure were disregarded in subsequent calculations. The suture was kept moist with a normal saline solution until tested. Baseline mechanical properties were determined from freshly opened packages of suture as received from the manufacturers.

Mechanical test results at baseline, six and twelve weeks showed excellent strength retention for all suture types. Generally, Ethibond broke at lower force magnitudes than did comparable sizes of Mersilene or Biolite coated Mersilene for the same aging interval. With regard to size 1 suture, the size used to repair the medial collateral ligament, the ULTI carbon coated Dacron exhibited the best strength retention with time. This could have resulted as a consequence of enhanced tissue ingrowth afforded by the bioinert ULTI carbon coating.

The short term results (12 weeks) of the histological evaluation of tissue response revealed comparable reactions to the three suture materials. Generally, the responses observed in the superficial tissue were more cellular than the reaction noted in the corresponding medial collateral ligament. The tissue response to the three materials was minimal, in the 1.5 - 2.5 range. All material types had extensive fibrous tissue ingrowth by 12 weeks; however, the ULTI carbon coated Dacron displayed some tissue ingrowth by three weeks. There were no clinical infections or predominant PMN reactions to suggest infection or acute toxicity even in the one week specimens. All sutures exhibited comparable responses in the superficial tissue. In the medial collateral ligament tissue, the reaction to the ULTI carbon coated Dacron was equal to or better than either Mersilene or Ethibond. Longer term histologic and mechanical data is currently being collected and evaluated.

REFERENCES

1. Shim, H.S. and Meyer, C.H., Jr., J. Bioeng., 99, 1977.
2. Haubold, A.D., et. al., Biocompatibility of Clinical Implant Retrievals, Williams, D.F. Ed., CRC Press, 1981.
3. Jenkins, D.H.R., et.al., J. Bone Joint Surg. 59-B:53-57, 1977.

Department of Orthopaedic Surgery
Tulane University Medical School
1430 Tulane Avenue
New Orleans, Louisiana 70112

DEVELOPMENT OF THE NEW ABSORBABLE SUTURE BY CHITIN

M. Nakajima*, K. Atsumi* and K. Kifune**

Inst. of Med. Electr., Faculty of Med., Univ. of Tokyo, Tokyo, Japan

The characteristics of an ideal surgical suture are; 1. Maintain tissue adaptation until healing occurs. 2. Suture disappears when healed 3. Suture does not disturb healing. The currently available absorbable surgical sutures are very limited and not always satisfiable from aforementioned points of views in various biological conditions such as acid, alkali or enzymatic effects. On the other hand, N-acetyl D-glucosamine (NADG) is the component of chitin which is derived from shells of Crustacea. This material is known as a possible wound healing accelerator.¹⁾ Recently we succeeded in producing the surgical absorbable suture from NADG. In this report, the production method of the suture and mechanical and biological evaluation of the suture are discussed in comparison with other absorbable sutures.

Production of the chitin suture: The calcium carbonate and protein of Japanese pink crab shells were almost completely removed. The chitin powder was then solved in amide solvent to make dope after the chemical structure was modified a little. Fine filaments of about 5 μ m in diameter were spun from the spinneret of 0.05 mm diameter using butyl alcohol as coagulant. The multifilaments after the complete coagulation were transparent and flexible fibers with tensile strength of about 50 kg/mm². Then 16 or 20 bundles of the filaments were braided, rinsed, coated with a surfactant, attached needle and sterilized. The sutures obtained were 3-0 and 4-0 about USP standard suture size.

Materials and methods: In order to evaluate the physical and biological properties of the chitin suture, the following studies were performed with the suture in comparison with polyglycolic acid suture (PGA) and catgut. 1. Dry and wet tensile strength in straight and surgical knot. 2. Time course of tensile strength of the sutures in bile, urine, pancreatic and gastric juice. 3. Tissue reaction of the implanted sutures. 4. Toxicity tests of the chitin suture.

Results:

1. In dry and wet condition, both straight and knot tensile strength of the chitin suture was less than PGA but almost the same as catgut and elongation of it was less than the other sutures. (table 1)
2. The strength of the chitin suture was maintained longer than the other sutures in dog and human bile, human infected urine, bovine serum and human pancreatic juice but in dog gastric juice, weakening occurred earlier than PGA.
3. Tissue reaction of the sutures implanted in back muscle of the rabbit was essentially almost the same as that of PGA. Inflammatory cell infiltration was slightly stronger but appearance of foreign body macrophage and phagocytosis was less and fibrosis or the collagen synthesis around the suture was rather accelerated with the chitin suture.

Table 1: MECHANICAL PROPERTIES (N=10)

USP SIZE			CHITIN	PGA	CATGUT
			4-0	4-0	4-0
STRAIGHT	DRY	STRENGTH(Kg)	1.86 \pm 0.05	2.56 \pm 0.06	1.73 \pm 0.28
		ELONGATION(%)	8.9 \pm 0.6	17.2 \pm 1.5	15.8 \pm 3.6
	WET	STRENGTH	1.71 \pm 0.07	2.42 \pm 0.08	1.63 \pm 0.25
		ELONGATION	11.6 \pm 0.8	16.8 \pm 1.4	17.2 \pm 4.3
KNOT PULL	DRY	STRENGTH	0.92 \pm 0.04	1.46 \pm 0.09	1.03 \pm 0.21
		ELONGATION	9.2 \pm 0.8	17.3 \pm 1.5	16.1 \pm 2.5
	WET	STRENGTH	1.05 \pm 0.09	1.46 \pm 0.08	0.89 \pm 0.19
		ELONGATION	13.8 \pm 1.2	17.0 \pm 1.8	17.8 \pm 2.8

4. The toxicity tests of the chitin suture including mutagenicity, acute toxicity, pyrogenicity, hemolysis and skin reaction were negative in all respects.

Discussion: The chitin suture is composed of NADG which is degraded to fructose by lysosomal enzymes. Thus the material is discharged in respiratory gas as carbon dioxide or in bile from liver. Other possible way of metabolism is the utilization of the degraded products as a source of connective tissue to repair wound. The results of almost negative toxicity and good histocompatibility are well explained by these metabolic pathways of the chitin suture. From the view point of surgical usefulness as an absorbable suture, it has the advantage of more resistance to alkali, digestive enzymes and infected urine than PGA or catgut. This property is very beneficial to apply for most of the digestive tract surgery and urological surgery. Further more the softness and knot reliability are other advantages of the chitin suture. Beside the possibility of the wound healing acceleration which is in current investigation, this suture can be a clinically applicable new absorbable suture.

Reference: 1. Prudden, J. F. et al. The discovery of a potent pure chemical wound healing accelerator. Amer. J. Surg. 119:560, 1970.

* Inst. of Med. Electr., Faculty of Med., Univ. of Tokyo, 7-3-1 Hongo, Bunkyo-ku, Tokyo, 113, Japan
 ** Unitika Research Lab., Unitika Corp., Uji, Kyoto, Japan

MINERALIZATION OF BOVINE PERICARDIUM: IN VITRO AND IN SITU TEST OF MODIFIED TISSUES FOR POTENTIAL INHIBITION OF MINERALIZATION.

S.T. LI, M.H. SUNWOO, P. ZALESKY, and T.S. FREUND*

MEADOX MEDICALS, INC. OAKLAND, NEW JERSEY

Pericardial tissues of animal origin have been utilized, in recent years, for the construction of bioprosthetic heart valves. The tissues have been pre-treated to reduce antigenicity and simultaneously increase *in vivo* stability with a fixative such as glutaraldehyde. Although encouraging results have been observed in adult patients, their acceptability for long term implantation in humans is still under investigation. Due to early mineralization of the valves, for instance, it is not recommended, at this time, to implant tissue valves in children or young adults. Currently, for those groups, diseased valves are replaced with mechanical valves requiring extensive anti-coagulant therapy.

As a result of its mechanical strength and *in vivo* acceptability, the pericardium continues to look promising for bio-prosthetic valve construction. Consequently, considerable efforts have been devoted toward reducing the potential for tissue mineralization. This paper reports on a number of chemical modification techniques which we have employed in an effort to decrease the pericardial tissue's mineralization potential. The modified tissues were examined in two systems: *in vitro* using the measurement of calcium uptake and *in situ* by means of implanting treated tissue pieces subcutaneously in rats.

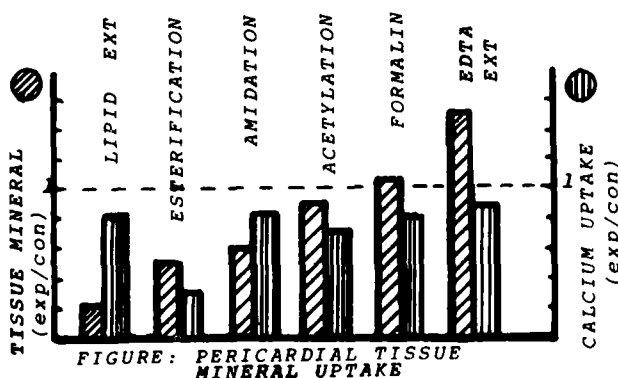
Fresh bovine pericardial tissues were collected from an abattoir and scraped clean to remove surface lipids and loose connective tissues. Prior to fixation (1% glutaraldehyde, pH 7.4 for 24 hours at 4°C), the tissues were rinsed several times in saline. The fixed pericardium was cut into seven pieces, pooled and divided into subgroups for chemical modification. For the *in vitro* studies, the tissues were shaken in 1mM calcium and 1mM phosphate solution (pH 7.4 at room temperature) in the presence of radiocalcium as a tracer. At the end of 16 days, the tissues were sampled for calcium analysis by means of liquid scintillimetry. The net calcium uptake was determined according to a previously established method (Li, S.T. and E.P. Katz, Biopolymers, 15, 1439 (1976)). The *in situ* studies, on the other hand, were conducted with 1cm² pieces of tissue, implanted subcutaneously into peritoneal sites of adult rats. Control and modified tissues were implanted in the same rats in order to eliminate animal related variations. After 16-21 days, the animals were sacrificed and the tissues removed for initial analysis and histology (von Kossa stain). The calcium (atomic absorption) and phosphorus (colorimetric) analyses were accomplished utilizing wet ashed samples.

The Figure below shows the *in vitro* calcium uptake from various treated tissues. The only modification that has effectively suppressed this measure of mineralization potential is esterification. This finding is consistent with the results reported for the purified, reconstituted

steer skin collagen (Li and Katz, Biopolymers, 15, 1439 (1976)). Apparently, the alteration in the net charge characteristics towards greater repulsion of calcium has inhibited its tissue uptake. Treatment of glutaraldehyde fixed tissue with reagents that abolish the amino groups in the tissue had minimal effect. This finding is again consistent with the view that glutaraldehyde has already reacted with most of the amino groups in the tissue. Lipid and glycoprotein extraction had a minimal effect on the calcium uptake suggesting that the total charge moieties associated with these components in the intact tissue are negligible.

The *in situ* animal data shown in the same Figure, indicate that two modified tissues are of particular interest: the esterification has suppressed the total calcium and phosphorus content by more than 70% while lipid extracted tissue contains only 15% of the total as compared to the controls. The histological staining for calcium paralleled the chemical analysis and indicated that the calcium was located within the tissue rather than at the surface, suggesting the intrinsic mineral accumulating nature of the tissues.

The pericardial tissue contains all the potential sites that have been proposed for the initiation of mineralization. The purposes of the present study were two fold: (1) finding a means for reducing or inhibiting mineralization of pericardial tissue in human implantation and (2) searching for relevant test methods that can provide such information. This combined physicochemical and *in situ* rat study can be applied concurrently toward a resolution of problems inherent in soft tissue mineralization. A further investigation of the fabricated tissue devices in the proper sites of animals is required to provide direct information as to the blood and biocompatibility of pericardial tissues as a biomaterial.



*Department of Biochemistry, Fairleigh Dickinson University, School of Dentistry, Hackensack, NJ

MECHANISM OF TISSUE FIXATION BY GLUTARALDEHYDE

David T. Cheung and Marcel E. Nimni

Bone & Connective Tissue Research, Orthopaedic Hospital, USC
Medical School, Los Angeles, CA 90007

INTRODUCTION: Glutaraldehyde is a slow penetrating fixative and it is uncertain how its degree of reactivity with tissue proteins varies as the distance from the surface increases. This may present problems when fixing tissues for electron microscopy or for use as xenograft derived bioprosthesis. Incomplete crosslinking of the structural collagenous network in tissues can allow biodegradation, antigenicity and loss of mechanical function. We have explored the use of chemical and enzymatic methods to assess the degree of crosslinking of collagen by glutaraldehyde in bovine pericardium.

MATERIALS AND METHODS: Pieces of pericardium (5 mm diameter) were fixed in various concentrations of glutaraldehyde for different lengths of time. The fixed tissues were either treated with CNBr, or digested with pronase after borohydride reduction and heat denaturation. The solubilized material was then separated from the residue by centrifugation and the hydroxyproline content in each fraction was measured after acid hydrolysis.

RESULTS: At low concentration of glutaraldehyde (0.05%), 50% of the collagen is solubilized after 1.5 to 2 h or fixation. As the concentration of glutaraldehyde increased, the amounts of collagen solubilized decreased rapidly after only short fixation times. At concentrations of glutaraldehyde higher than 1.0%, CNBr became an ineffective solubilizer (fig. 1). After 30 min. in 1% glutaraldehyde, no soluble hydroxyproline could be detected.

Pronase was ineffective in solubilizing fixed tissues unless they were first denatured by boiling. At low concentrations of glutaraldehyde (0.05%), 90% of the collagen can be solubilized from specimens fixed for 48 h. At the highest concentration tested (2%), approximately 40% of the collagen was extracted from specimens fixed for 48 h (fig. 2).

DISCUSSION: We described previously various aspects of the mechanism of the reaction of glutaraldehyde with amines, soluble collagen and reconstituted collagen fibers (1,2). The current study confirms our earlier finding that glutaraldehyde rapidly forms polymers at the surface of the fibers while the interstitium of the fibers is not readily accessible for crosslinking. We have also identified a slower fixation process which continues to operate over a long period of time beyond that of actual penetration of glutaraldehyde. The nature of this process is unknown.

References:

- Cheung, D.T. and Nimni, E., Conn. Tiss. Res. **10**: 187-199, (1982)
- Cheung, D.T. and Nimni, E., Conn. Tiss. Res. **10**: 201-216, (1982)

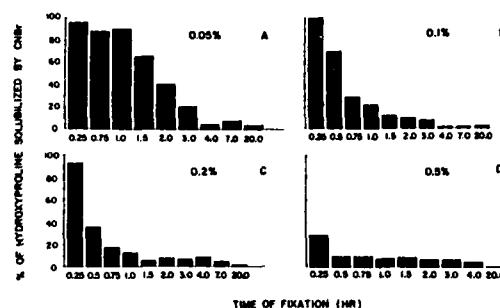


Fig. 1. Percentage of collagen solubilized by CNBr after tissues were fixed in different concentrations of glutaraldehyde for various lengths of time. A. 0.05%, B. 0.1%, and C. 0.5% glutaraldehyde.

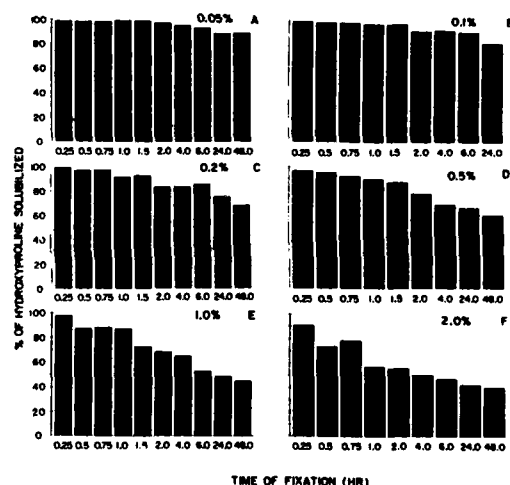


Fig. 2. Percentage of collagen solubilized by pronase digestion after tissues were fixed in different concentrations of glutaraldehyde for various lengths of time. A. 0.05%, B. 0.1%, C. 0.2%, D. 0.5%, E. 1.0% and F. 2.0% glutaraldehyde.

Supported by NIH grant AM 10358

David T. Cheung, Ph.D.
Orthopaedic Hospital, D & T 5th Floor
2400 South Flower Street
Los Angeles, CA 90007

Surface Studies of Calculi Deposition on Foley Catheter Materials

C. Batich, C. Cheng, C. Johnson, V. Rodriguez and S. Batich*

Dept. Materials Science and Engineering
University of Florida, RHN 246
Gainesville, Florida 32611

Indwelling bladder-catheters are used to a large extent in the U.S. (more than 7.5×10^6 /year) and have significant problems. A recent study has associated about 50,000 deaths per year with nosocomial infections resulting from such catheter use⁽¹⁾. Additionally, devices must be changed regularly to prevent infection or obstruction due to deposition of calculi in the lumen⁽²⁾. We have examined catheters retrieved at autopsy to understand the deposition process and have measured the amount of calcium oxalate (CaOx) forming on various polymeric surfaces in a precipitation cell in order to exert some control over this deposition. Certain surface modifications of existing materials were shown by XPS (x-ray photoelectron spectroscopy) and SEM (scanning electron microscopy) to inhibit CaOx deposition in our laboratory (in vitro) cell. A deposition of elastomeric fluorocarbon (Viton-A®)⁽³⁾ was particularly effective. It is expected that such reduced surface deposits will decrease the rate of infection as well as discomfort and damage involved in removing an encrusted device.

Foley catheters are locked into position by inflation of a balloon in the patient's bladder. Materials used for their construction are currently natural rubber and silicone with a variety of combinations and surface treatments available. CaOx crystals were slowly grown in solution from a mixing of 0.1M CaCl₂ and 0.1M Na₂Ox aqueous solutions as shown in figure 1. Several polymeric films were exposed at one time to avoid reproducibility problems and various additives could easily be added to the solution to measure their effect on deposition.

The exposed polymer films were removed after about 12 hours and then examined by SEM after drying. Large differences in CaOx crystal size and number were noted. Surlyn 1601⁽³⁾, cellulose acetate and cast Viton A films showed lower levels of CaOx deposition than E/MAA or PET films although the levels deposited on PET depended upon the degree of surface crystallinity. Varying degrees of surface crystallinity were obtained by annealing amorphous film and measured using an XPS labeling technique⁽⁴⁾.

Natural rubber surfaces were treated and exposed to various coating solution. The effect of washing upon these films was followed by XPS and also by contact angle measurement. Many coatings, including those on some commercial catheters, were shown to be quite easily removed during conditions similar to long-term use. Ratios of hydrocarbon to fluorocarbon surface signals increased rapidly with washing unless some pretreatment to form acid sites was first undertaken (see table and Figure 2). An electric arc oxidation of the surface provided

such a more strongly binding site. Although washing removed most of the fluorocarbon coating, significant residue remains and may be sufficient to retard CaOx precipitation nuclei from reaching critical sizes.

Sample		Surface Atomic Ratios (XPS)	
		O/C	F/C
A.	Natural rubber	.16	<.002
B.	Arc oxidized	.22	<.002
C.	Viton coated A	.05	1.1
D.	Viton coated B	.03	1.2
E.	C washed*	.16	.029
F.	D washed*	.13	.050

* aqueous creatine, pH - 8.0

1. R. Platt et al, New. Eng. J. Med. 307, 637 (1982).
2. B. Priefer et al, Urology, 20, 141 (1982).
3. DuPont Co.
4. C. Batich and T. Saitta, unpublished.

We thank Dr. H. Baer of the Shands Teaching Hospital for providing samples of used catheter materials.

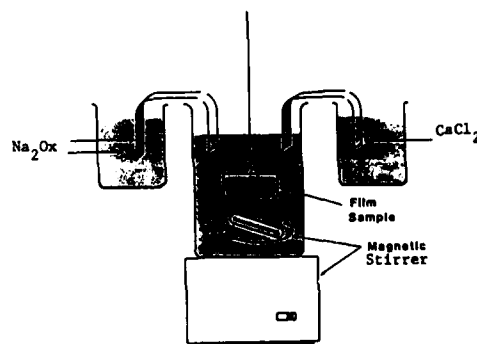


Figure 1. Slow precipitation cell using filter paper siphon.

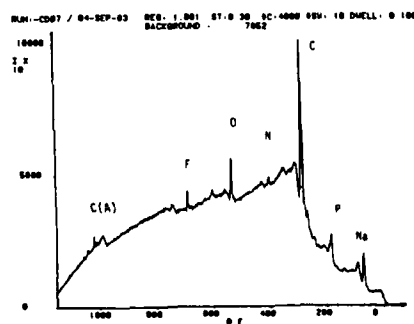


Figure 2. X-ray photoelectron spectrum of Sample D.

USE OF FIBRIN SEALANT IN EXPERIMENTAL SPLENIC TRAUMA

Kram, H.B., Shoemaker, W.C., Harley, D.P.

Harbor-UCLA Medical Center
Torrance, California

Splenic sacrifice may result in catastrophic post-splenectomy sepsis. Suture splenorrhaphy and partial splenectomy, although sometimes effective, have limitations in splenic preservation after trauma. The efficacy of Fibrin Sealant (FS)*, a two component biological adhesive that is effective in face-to-face sealing of tissues, wound healing and establishing hemostasis, was evaluated in controlling experimentally produced splenic injuries. Twenty-six splenic injuries were created in five adult mongrel dogs. There were ten small superficial lacerations (less than 2.0 cm in length), six large superficial lacerations (greater than 2.0 cm in length), three small wedge resections, and eight stab wounds extending to the splenic hilum. These defects were effectively repaired using FS without needing suture splenorrhaphy or temporary splenic hilar occlusion. At the termination of the procedure, FS was firmly adherent to the created injuries. Complete hemostasis was achieved in all animals prior to skin closure. Dogs were re-explored postoperatively at varying intervals ranging from 4 hours to 6 weeks (mean = 21 ± 20 days). At sacrifice there was no gross evidence of splenic disruption or recurrent bleeding, and the spleens had contiguous capsules. Light microscopic examination demonstrated a regenerated fibrous capsule extending over the superficial injuries as well as into the deep injuries. We conclude that FS is effective in 1) establishing hemostatic control of superficial and deep splenic injuries, 2) promoting splenic wound healing, and 3) is an effective technique for splenic preservation after trauma.

* Immuno; Vienna, Austria

THE CONNECTIVE TISSUE RESPONSE TO BIOMATERIALS IMPLANTATION

Thomas M. Hering, Roger E. Marchant, and James M. Anderson

Dept. of Pathology
Case Western Reserve University, Cleveland, Ohio 44106

Following surgical implantation of a prosthetic device into a human or animal recipient there occurs a host response to heal the tissues surrounding the implant. This process involves mechanisms common to normal wound healing processes. The response to implantation of a prosthetic device generally involves an acute inflammation during which there occurs an influx of leukocytes into the tissues surrounding the foreign object, and an increase in vascular permeability resulting in exudation of plasma, with subsequent encapsulation of the device in fibrin. Following this acute response, there follows a process to remove the fibrin by phagocytosis and fibrinolytic mechanisms, and to replace it with connective tissue, laid down by fibroblasts migrating into the fibrin layer. Blood vessels surrounding the implant will respond to chemically transmitted stimuli by sending capillary offshoots into the organizing tissue. Over the course of weeks to months the tissue matures, a process involving condensation of collagen bundles, a decrease in tissue cellularity, and a loss of capillaries to form what will remain a mature connective tissue capsule.

In the case of wound healing around and within a prosthetic device, however, there may be characteristics of the implant which could modify the normal course of events. The nature of the material used, characteristics of its surface, porosity, etc., as well as the anatomical location of the implant could influence the healing process. In order to understand the influence of material characteristics on the healing process, it is necessary to better understand the basic biochemical mechanisms involved in this tissue response to materials implantation, and for this purpose we devised a model system to examine connective tissue ingrowth. The implant device that we chose to use is a stainless steel mesh cylinder implanted subcutaneously in rats. During time intervals from 4 to 90 days the implants were recovered, and the connective tissue capsules in different stages of development were removed. These tissues were analyzed using histological and histochemical techniques, and biochemical methods to examine the rate of collagen deposition, collagen maturation, and to determine the ratio of collagen types I, III, and V over time.

Histology showed a rapid replacement of fibrin within the interstices of the mesh by collagenous connective tissue, followed by a condensation of the collagen fibrils into progressively more dense arrays. In addition, there also occurred a progressive increase in cellularity and vascularity in the earlier samples, and a significant decrease in the older capsules. Hydroxyproline analysis showed a progressive increase in collagen over 90 days that was most rapid during the first 21 days. This earlier rapidly accumulating collagen was found to be more resistant to extraction than that which was deposited later, suggesting more extensive or stable crosslinking during this time.

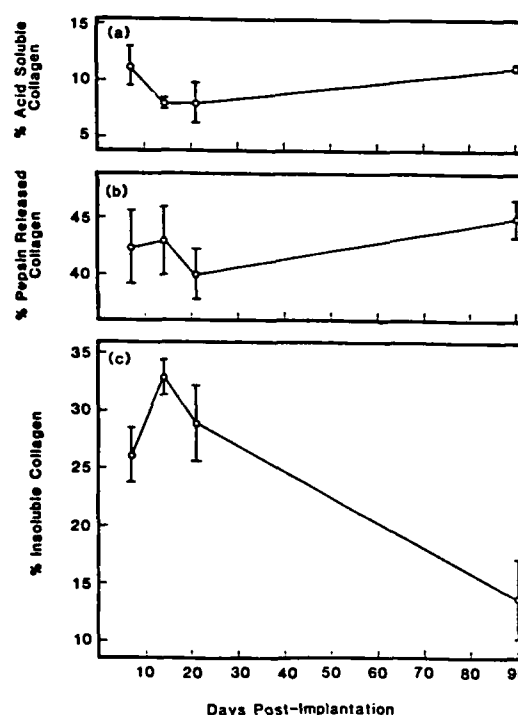


Figure 1. Changes with time in percent of capsule collagen sequentially extracted with 0.5N acetic acid (a), 0.5N acetic acid with pepsin digestion (b), and that which remained insoluble (c).

Over all time points considered, type I collagen averaged 75.7%, type III averaged 22.6%, and type V collagen averaged 1.8%, as determined by SDS-polyacrylamide gel electrophoresis. The ratio of type I to type III remained constant, while type V increased and decreased in parallel with the changing vascularity of the tissue. Type V collagen is thought to play a role in cell migration and movement, thus explaining its variable expression, while types I and III are thought to be primarily structural components.

Connective tissue deposition surrounding implants may either enhance or interfere with the intended function of the device. A better understanding of the dynamics of connective tissue ingrowth may provide a means of controlling this process.

I.V. Yannas¹, J.F. Burke², D. Orgill¹ and E.M. Skrabut¹

Massachusetts Institute of Technology, Cambridge, MA 02139

Previously we have described a biodegradable polymeric template which can induce wound tissue to synthesize new skin [1,2]. This template, a highly porous, crosslinked collagen-glycosaminoglycan (CG) network, is currently used to treat excised skin wounds in patients who have suffered extensive burns [3,4].

We now report certain structural and functional properties of the newly synthesized tissue. This preliminary characterization of the regrown organ suggests its close similarity to, as well as certain distinct differences from, the intact skin adjacent to it.

The polymeric template was a bilayer membrane consisting of a 0.5-mm-thick top layer of poly-(dimethylsiloxane) and a 1.5-mm-thick layer of a highly porous crosslinked collagen-chondroitin 6-sulfate (CG) network. The method of preparation has been described elsewhere in detail [2].

Prior to grafting the polymeric template was seeded with autologous basal cells, implanted into the CG layer using a centrifugation procedure which has been described [2].

A full-thickness skin wound, measuring 3 x 1.5 cm or 4 x 4 cm, was prepared under aseptic conditions by excising the skin down to, but not including the panniculus carnosus of the guinea pig. The surgical procedure for preparing a skin deficit has been described.

Immediately following excision of the skin, a graft which had been cut to fit within the wound perimeter was placed on the wound bed and was sutured on immediately adjacent skin as described. After careful bandaging of the grafted area, the animals were placed in cages and were fed Charles River Guinea Pig Formula.

One week following grafting the wounds were unbandaged and photographed. When the wound had just been covered by a confluent neoepidermis, usually between 10 and 14 days, the sutures were cut off and the silicone layer was removed at virtually zero peel strength. The moisture flux rate was determined with an Evaporimeter (Servo Med, Stockholm) after the silicone layer has been removed. The probe was placed alternately on the wounded area and on intact skin, previously shaven, about 5 cm away from the wound perimeter. A simple neurological test (pin prick) was occasionally administered to the area of the wound and to an intact skin area. Vascularization of the grafted area was confirmed by observing blanching following application of hand pressure.

At various time intervals, animals were sacrificed and specimens of the wound contents as well as of an intact skin area about 5 cm from the wound perimeter were either removed for mechanical testing, or were fixed prior to processing for histological staining. Tensile specimens were stored in physiological saline at 4°C and were stretched in an Instron Universal Tester Model TM at 100% min⁻¹ at room temperature within 24 h of sacrifice. Specimens for histological study were stained with hematoxylin and eosin and viewed in a light microscope.

Not later than 7 days after grafting, islands of new epidermis had formed between the silicone layer and the CG layer of the graft, while the host epidermis was invading the area just below the silicone layer at the site of the wound perimeter. Between 10 and 14 days, the neoepidermis had become fully confluent over the entire wound area. The neoepidermis which formed by proliferation of the seeded basal cells to the silicone-CG interface became distinctly keratinized, as viewed histologically, by days 12 to 14. The collagen-chondroitin-6 sulfate layer was invaded by a variety of mesodermal cells and synthesis of new collagen fibers became histologically evident between days 14 and 18. By day 28 the morphology of the newly synthesized collagen fibers had become well established in the layer of neodermis. The neodermis showed histological and clinical evidence of being richly vascularized by day 14, or earlier. Simple neurological testing gave positive results before day 21.

A preliminary comparison of properties of newly synthesized (regenerated) skin and intact (normal) skin shows several close similarities. However, differences are also apparent, striking among them being the absence of skin accessory organs, including hair (the guinea pig has no sweat glands).

Preliminary characterization shows that newly synthesized skin is strikingly similar, though not identical, to intact skin. Ongoing studies are directed towards biochemical characterization of macromolecular components in new skin, detailed morphological analysis and elucidation of the kinetics of synthesis of the new organ.

These preliminary results suggest that the polymeric template used in this work stimulates the wounded mammalian tissue in a novel way. The result of such stimulation is not scar, as is the case when this template is not used. Future work will address the question of the extent to which such an unexpected outcome results from repetition of certain late stages of the ontogenetic development of skin.

References

1. I.V. Yannas and J.F. Burke, J. Biomed. Mater. Res. 14, 65-81 (1980).
2. I.V. Yannas, J.F. Burke, D.P. Orgill and E.M. Skrabut, Science, 215, 174 (1982).
3. J.F. Burke, I.V. Yannas, W.C. Quinby, C.C. Bondoc and W.K. Jung. Ann. Surg., 194, 413 (1981).
4. I.V. Yannas, J.F. Burke, M. Warpehoski, P. Stasikelis, E.M. Skrabut, D. Orgill and D.J. Giard Trans. Am. Soc. Artif. Org. 27, 19 (1981).

This research was partly supported by National Institute of Health Grants HL 14322, GM 23946 and GM 21700; by the Department of Mechanical Engineering, MIT; and by the Provost's Office, MIT.

¹Fibers and Polymers Laboratories, Massachusetts Institute of Technology, Cambridge, MA 02139.

²Harvard Medical School and Chief, Trauma Services, Massachusetts General Hospital, Boston, MA 02114.

COMPARISON OF SOFT TISSUE INGROWTH IN SUBCUTANEOUS AND PERCUTANEOUS DACRON® VELOUR IMPLANTS

Hultman, S. and Feldman, D.

Texas A&M University
College Station, TX 77843

Clinical failure of percutaneous devices (PDs) is most often attributed to infection and/or mechanical trauma (1). Concurrent appearance of epidermally induced failure modes have also been noted (2). These include: epidermal downgrowth and extrusion due to basal cell maturation (within porous materials). Prevention of epidermal failure modes, however, does not preclude PD failure (1). Additionally, some failures involving porous materials have been explained by the "wick" theory, which suggests microbial agents travel through the material into percutaneous tissues (1,3). Despite this, use of materials with interconnecting pores such as Dacron® velour, have been advocated for skin and/or dermal interfaces. Ideally, a porous material should stop epidermally induced failure modes by connective tissue ingrowth and lessen mechanical trauma through better stress distribution (2).

The object of this study was to observe variations in the tissue ingrowth of percutaneously and subcutaneously implanted Dacron® velour patches. And to test whether this difference could, in part, explain the etiology of failure seen within percutaneously implanted Dacron® velour.

Mechanical factors including stress distribution, associated with implant shape, and mechanical trauma, resulting from implant movement and tissue/biomaterial compliance disparity, can not be eliminated. While measurement of these factors at specific foci remain elusive, mechanical factors will be greater in a percutaneous situation. Placement of the implant perpendicular to the plane of the tissue produces a large moment. And the integument itself contains a system of natural stress lines. Additionally, PDs encounter a continuous microbial bombardment due to lack of an epidermal seal. Thus, if subcutaneous implants exhibit a low level pathogenicity, it is not surprising that PDs, which incur greater mechanical trauma and microbial assault become pathogenic to the point of total functional loss and eventual rejection.

A simple implant design of USCI Dacron® velour sheets, glued back to back with Type A Silastic® Medical Adhesive, and cut into small rectangles was chosen. These Dacron® patches were implanted subcutaneously and percutaneously along the dorsum of a canine. After implantation periods of 1 week, 1 month and 2 months, implants were retrieved and prepared for light and electron microscopy.

Tissue sections were then evaluated by the following criteria:

- 1) over all cellularity
- 2) differentiation of specific cell types and their population density
- 3) phagocytic/fibroblastic cell density ratio
- 4) density and type of fibers
- 5) capsule thickness

Additionally, local porosity, tissue vascularity and evidence of microbleeding were noted. Also, in a concurrent study of subcutaneous ingrowth in rats, enzyme histochemistry was done.

In this study, the subcutaneous case was considered the "least" stressed situation. In these implants, mature collagen ingrowth was observed in

the more porous outer region of the Dacron®. A moderate polymorphonuclear (PMN) cell population, however, was observed even after 2 months of implantation. And perhaps more importantly, heavy giant cell populations persisted, with giant cells seen around almost every fiber.

Close to 30% of the percutaneous implants had been avulsed before harvesting. Of the remainder, 30% appeared grossly infected as evidenced by extremely dense populations of PMNs. Those that appeared uninfamed and well attached at the time of harvesting, exhibited epidermal downgrowth and/or permigration (a type of extrusion due to epidermal basal cell maturation).

It appears that all failures are linked to the immaturity of connective tissue ingrowth into the velour. This is caused by implant configuration and its related foreign body response as well as by mechanical trauma (1,2,3).

Inferences between subcutaneous and percutaneous applications of the same material are complicated by unknown but certainly unequal variables. While the ingrowth of subcutaneous Dacron® implants grossly appear healthy, microscopically a chronic foreign body reaction persists. If tissue ingrowth of this least stressed situation can be improved by material parameter modifications, such as average porosity and/or fiber size, perhaps the more stressed percutaneous tissue ingrowth will likewise be improved (3).

Future studies should reduce the number of variables examined at one time, i.e. elimination of epidermal failure modes (2) and/or elimination of mechanical trauma.

References

1. Feldman, D.S., and von Recum, A.F., The Pathophysiology of Avulsion as a Failure Mode of Percutaneous Implants, Presented at the 2nd Southern Biomedical Engineering Conference, 1983.
2. Feldman, D.S., Colaizzo, R.S., and von Recum, A.F., Epidermal Contact Inhibition Around Percutaneous Implants, Presented at the 9th Annual Meeting of the Society for Biomaterials, 1983.
3. Feldman, D.S., Hultman, S.M., Colaizzo, R.S., and von Recum, A.F., Electron Microscope Investigation of Soft Tissue Ingrowth into Dacron® Velour With Dogs, Biomaterials, 4, 105, 1983.

This research was supported by NSF Grant #ECS-8204597.

Bioengineering Program
Industrial Engineering Department
Texas A&M University
College Station, TX 77843

FACTORS AFFECTING SOFT TISSUE INGROWTH INTO POROUS IMPLANTS

Feldman, D. and Estridge, T.

Texas A&M University
College Station, TX 77843

Porous implants have been used for many different applications. Due to the pioneering work of Hulbert and Klawitter (1), the requirements for hard tissue ingrowth into porous implants has been well characterized. There still, however, is little consensus or cooperation among researchers in the requirements for soft tissue ingrowth into porous implants.

Therefore, the objective of a review of previous studies is to determine unifying concepts for soft tissue porous implants.

Porous soft tissue implants have usages including:

- 1) Fixation or stabilization for electrodes, artificial heart valves, artificial larynx, artificial bladder, artificial skin, artificial tendons and ligaments.
- 2) Tissue ingrowth to create a blood compatible surface such as for artificial vessel replacement.
- 3) Scaffolding to help the body repair or regenerate (possibly using a resorbable system--e.g. artificial tendons and ligaments).
- 4) Prevention of epidermal downgrowth by mature connective tissue ingrowth as in percutaneous implants.

There are many different materials and manufacturing techniques for porous implants. These include:

1. Use of a fabric material which varies weaves or knitting patterns to alter porosity and pore size.
2. The sintering of carefully controlled sizes of metallic and ceramic beads in order to achieve a specific pore size.
3. A partially resorbable implant that resorbs, *in vivo*, to leave a porous surface.
4. Manufacturing a polymeric implant, with salt crystals on the surface, and then dissolving away the salt.
5. A replaineform material made from a positive or negative cast of coral to achieve interconnecting porosity.
6. Any number of surface texturing techniques such as sand blasting and ion beam etching.
7. Using a foaming agent during processing. This causes bubbles to form and leaves pores on the surface of a ceramic as it hardens.

One of the more difficult tasks is measurement of pore size and porosity. Many techniques assume a spherically or symmetrically shaped pore. This is not usually the case--especially in fabric implants. Techniques employed in the past include mercury porosimeter, the flow rate of H₂O through one square centimeter of material at 120 mm Hg, and measurement from 2-D micrographs using principles of stereology.

Although porous soft-tissue implants are very common, there is a dearth of data relating to the effect of implant porosity on tissue response. There is also little cooperation or consensus among investigators. These discrepancies are mostly due

to differences in location of the implant, type of implant and implant material, application of the implant, duration of study, measurement of pore size and porosity, and type of animal model used. There are, however, some unifying concepts:

1. Tissue vascularity is the key to long-term ingrowth. Thus, pores need to be at least 40 μ m in diameter (some select 100 μ m as the minimum acceptable pore size). Cells die due to lack of nutrition, if removed by more than 100 μ m from their blood supply (2).
2. Large pores or interconnecting pores do not fill completely with tissue and can lead to infection.
3. Tissue ingrowth in humans is slower than in most of the animal models currently being used.
4. Good initial stabilization is important to prevent breakage of tissue bridges before maturation is complete.
5. Certain conditions appear to stimulate ingrowth including some resorbable systems and certain growth factors.
6. Pores over 600 μ m can decrease the rate of ingrowth.

In summary, although some strides have been made in understanding soft tissue ingrowth into porous implants, much is left to be examined. One can not overemphasize the importance in attaining a detailed understanding of the rate of tissue ingrowth into porous materials as a function of implant configuration, implantation time, implant location, implant application, and implant material. This requires the cooperation of investigators who will study one variable at a time. Also, a concentrated effort is necessary to determine the differences in animal model responses and in turn, compare these responses to human clinical data.

References

1. Klawitter, J., "A Basic Investigation of Bone Growth Into a Porous Ceramic Material, Ph.D. Dissertation, Clemson University, 1970.
2. Daly, B.T., Tufts University, Personal Communications, June 1981.

Bioengineering Program
Industrial Engineering Department
Texas A&M University
College Station, TX 77843

CAPSULE FORMATION AS A FUNCTION OF MATERIAL TEXTURE AND MATERIAL COMPRESSIBILITY.

Christine Dale Enger, G. Picha, and J. DesPrez

Case Western Reserve University
Cleveland, Ohio

The underlying principle being studied here is the fibrous capsule contracture found clinically in the post augmentation mammoplasty patient. One factor thought to be responsible for the capsule formation and contracture is the myofibroblast cell, an altered fibroblast cell form. In order to study myofibroblasts in the developing fibrous capsule, the sprague dawley rat was chosen as the animal model since contracture has been observed. In addition, we have observed myofibroblasts in wound contracture sites in the rat.

The implant design was a cylindrical sac, chosen for ease of fabrication. A round pillow shaped implant was attempted, but failed because the polymer used was not strong enough to withstand the stresses involved when the implant were removed from the mandril. The cylindrical implants were prepared by dipcasting, using brass mandrils and Dow Corning Q7-2213 silastic dispersion (poly dimethyl silicate). The thickness of the implants were 15 mils. After being removed from the mandrils, the cylindrical implants were sealed with a silastic patch and filled with 4 cc of saline. The saline was injected with a hypodermic needle and the hole was sealed with silastic and cured. Three different surface textures were chosen to mimic clinically used prostheses. First, the smooth silastic implant was fabricated as described above, ultrasonically cleaned, equilibrated with sterile saline overnight, and implanted subcutaneously on the anterior segment of the dorsal spine. Second, a silastic implant was fabricated as above, except that a 100 1:4 aspect ratio pillar textured (1) strip made of Dow Corning MDX4-4210 was wrapped around the cylinder, just after dipping the third time, and then the two part system was cured. Third, a polyurethane foam strip was wrapped onto the cylinder after the third dip and then cured. This implant is similar to the "Natural Y" prosthesis in clinical use. The implantation procedure was as follows. First, the rat was anesthetized with ether, shaved, and prepped. A dorsal lateral incision was made perpendicular to the spine just anterior to the thoracic region using a bovie. The wound was then cleaned with saline and the tissue was spread open with a hemostat. A subdermal cavity was created with the hemostat that ran from the incision to the tail. Next, a foley catheter was inserted anteriorly into the cavity and 10cc of water was used to inflate the balloon, acting as a tissue expander. The purpose was to create an adequate subcutaneous volume for the implant to be inserted, without it being under tension. The implant was then placed into the cavity and the wound stapled.

Deflection of the implant under various increasing loads was investigated. The implant compressibility was measured by a durometer through a Gaertner scope. The deflection was measured with 0,3,6,9,12, and 15 gram loads. By measuring the deflection before implantation, and then in vivo on a weekly basis, the tightening or loosening of the fibrous capsule was observed. Weekly deflection measurements were taken out to 8 weeks implantation, and one long term rat was measured at 6 months.

Another important aspect of this experiment was the variable presence of myofibroblasts. The myofibroblast is the muscle-like cell that is the

suspected cause for contracture. In order to identify these cells, an immunoperoxidase technique using an antiactin antibody was used. Through rabbit antiactin, goat antirabbit, and peroxidase anti-peroxidase, the myofibroblast cell was selectively stained and could be identified in the histologic sections of the implant sites. Other actin containing cells were stained too, but only the myofibroblast had the morphologic spindle shape with a large nucleus and granulated cytoplasm. With this method of quantifying the presence of the myofibroblast, correlation with the compressibility of the fibrous capsule could be obtained. Histological specimens were analyzed for smooth, textured, and foam implants at times of 1,2,4,6, and 8 weeks in an effort to classify the response of the myofibroblasts with time and material.

Certain trends were noted in the analysis of the results from the polyurethane and silastic implants. The polyurethane foam implants showed a decrease in compressibility which correlated with an increased amount of collagen fibers in the capsule. The polyurethane clusters interrupted the long range order that was seen in the capsule, which resulted in short range or segmented collagen bundles intertwined in the foam. The capsule showed longitudinal long range order of the collagen that was fairly thick. Numerous blood vessels were seen and the myofibroblasts did not seem ordered within the capsule. At late time periods (6-8 weeks), the foam was showing signs of degradation, due to the presence of surrounding multi-nucleated giant cells. The foam also contained a significant amount of exudate, which was not as prevalent in the smooth implants. The smooth silastic implants tended to increase in compressibility at early time periods (2-3 weeks), which corresponded to the thin capsules that had uniformly distributed myofibroblasts. The collagen was more ordered and cells seemed quiescent. However, the second and third weeks seemed critical in determining the course of the future capsule formation. As a result, two different groups of smooth implants were identified; those that showed an increase in compressibility, and those that decreased in compressibility. This leads to the possible remodeling which could be explained by a change in mucopolysaccharides, a loss of extracellular fluid, a difference in myofibroblast population, and an increased crosslinking of collagen fibers. The textured silastic implants showed an increase in compressibility with implant time.

In conclusion, a correlation between capsule compressibility and capsule cellularity was observed, and the difference between foam and smooth implants was noted. The animal model appeared suitable since myofibroblasts did appear, but contracture was not observed to date. Long term experiments examining variations in the histological components of the fibrous capsule, thickness of the fibrous capsule, surface texture of the implant, and fibrous capsule compressibility with time are currently underway.

This work was funded by NASA, and in part by the Division of Plastic Surgery.

(1)Banks, B.A., "Ion Beam Applications Research - 1981 Summary of Lewis Research Programs". NASA Technical Memorandum 81721. (1982).

EFFECT OF SURFACE MICROTEXTURE AND IMPLANT ORIENTATION ON PERCUTANEOUS WOUND HEALING IN THE PIG

J.L. Bence and G.J. Picha

Department of Biomedical Engineering, Case Western Reserve University
Cleveland, Ohio 44106

Surface texture has been shown to alter epidermal downgrowth in the percutaneous environment (1,2). Previous studies have not addressed the question of surface texture in a well controlled or well characterized manner. This study makes use of ion beam thruster technology to produce Silastic and Biomer implants with regular arrays of dimensionally precise pillars of 50 and 100 microns in diameter and aspect ratios ranging from 1-3. The clinical and histological response of these implants were evaluated and compared against smooth controls.

EXPERIMENTAL: The animal model used was the dorsal surface of the young female Large White pig, which is similar to the human with respect to cutaneous anatomy, follicular density, cutaneous blood supply, and lack of a panniculus carnosus. Much of our effort over the past several years has been dedicated to developing a surgical procedure that is as atraumatic and reproducible as possible in order that material and device related variables could be studied (2,3). Some highlights of the technique are as follows: 1) intradermal and subcutaneous injection of epinephrine at an optimal concentration to provide hemostasis while avoiding prolonged vascular shutdown with subsequent epidermal sloughing; 2) avoidance of wound pre-strain by use of a specially modified Keves skin punch for wound formation and use of Wullstein forceps to bring the implant into position; 3) use of an implant:incision radius ratio of 1.5 to achieve an initial compressive stress at the tissue/implant interface; and 4) a total procedure of 55 minutes for 20 implants per animal. Implants were fabricated by successive transfer casting from ion-etched PTFE Teflon negatives. Cylindrical devices made of Silastic (MDX4-4210, Dow-Corning) and Biomer (Ethicon) were fabricated, implanted, and evaluated. Implants were oriented either perpendicular to the surface of the skin, or at an angle of 45 degrees with respect to the anterior of the animal. A total of 14 pigs were implanted with 20-24 implants each for a period of two weeks.

RESULTS: The first several experiments resulted in retention of only 37% of the implants at two weeks post-operative. The subcutaneous bases of the implants were enlarged and fenestrations added to provide additional stabilization via soft tissue ingrowth. Subsequently, implant retention was 96%. Implants were evaluated by a semi-quantitative scheme that assigned numerical scores to post-operative and pre-sacrifice comments on the quality of the implant/tissue interface, and to the degree of epidermal downgrowth, sulcus, and cellular reaction (2). Post-operative observations were uniformly optimal. Pre-sacrifice observations could generally be grouped into two categories at the extreme ends of the quantitative scale. The implants were either clean, with perhaps small traces of dry, crustaceous exudate, surrounded by normal skin, or the implant interface was highly inflamed, broken, and characterized by the presence of purulent exudate. Intermediate responses were rarely seen. Histologically, evaluation was con-

founded by the large number of implants that could not be scored, due to the observation that the epidermis had never contacted the implant morphology. This resulted in a high degree of data variability. The strongest trend that could be extracted from the data was the more optimal response observed for angled Silastic implants compared with Silastic implants oriented normal to the skin surface, as shown in Table 1.

DISCUSSION: The noted effect of enlarging the bases and adding fenestrations confirms previous studies and underlines the necessity for mechanical stability for percutaneous devices. While there may be a direct textural effect in the dimensional range tested here, it is small in magnitude compared with other (probably surgical) variables that we were unable to identify or control, and thus was not detectable. Whether the more optimal response of the tilted implants was due to purely mechanical effects or to some more directly physiological parameter remains to be determined.

Table 1.
Effect of Implant Orientation for Silastic Implants

Morphology	Orientation	Post-op	Sacrifice	Histology
Smooth	normal	3.2±0.6	4.1±1.9	8.2±4.5
	angled	2.0±0.0	2.8±0.5	7.5
50 1:1	normal	2.1±0.4	3.8±2.1	12.0
	angled	2.0±0.0	2.0±0.0	2.0
50 2:1	normal	2.2±0.4	3.7±1.9	9.3±5.0
	angled	2.0±0.0	2.3±0.6	6.5
100 1:1	normal	2.2±0.4	3.9±2.0	13.2
	angled	2.0±0.0	2.3±0.6	11.0
100 2:1	normal	2.0±0.0	3.3±1.4	9.7±2.3
	angled	2.0±0.0	2.8±0.4	7.5±4.2
100 3:1	normal	2.6±1.3	3.4±2.0	9.8±5.3
	angled	2.0±0.0	2.3±0.6	-----

A lower number indicates a more optimal response.
Values are mean ± 1 standard deviation.

REFERENCES:

1. Winter, G.D., Transcutaneous Implants: Reactions of the Skin-Implant Interface. J Biomed Mater Res, 8(3):99-113, 1974.
2. Picha, G.J., and S.R. Taylor, First Annual Report on Percutaneous Connectors. Annual Report, NASA Grant NAS-3-22654, 1981.
3. Taylor, S.R., G.J. Picha, and D.F. Gibbons, The Development of a Surgical Model for the Study of the Percutaneous Interface. Final Report, NASA Contract #NAS-3022443, 1981.

This work was supported by NASA Contract Number NAS-3-22654 and Applied Medical Technology, Inc., Brecksville, Ohio

Current mailing address:
McKay Laboratories of Orthopaedic Surgery Research
School of Medicine, University of Pennsylvania
Philadelphia, Pennsylvania 19104

Subrata Saha and M.L. Warman

Louisiana State University Medical Center - Shreveport, Louisiana

The use of acrylic bone cement (PMMA) in orthopaedic surgery has increased markedly in the last decade. However, its brittle character has restricted its use to areas mainly subjected to compressive forces. This limitation could be overcome by reinforcing PMMA with metal wires, similar to the use of metal reinforcement in reinforced concrete. Metal wire reinforced PMMA has been used clinically in stabilizing spinal fractures [1]. We have shown previously that the tensile and bending strength of bone cement could be increased significantly by metal reinforcement [2,3]. The objective of this study was to determine if the resistance of PMMA to shear forces could also be significantly improved by reinforcing it with metal wires.

Standardized rectangular specimens (30 mm long, 12 mm wide and 4 mm thick) of acrylic bone cement (Simplex P, radiopaque) were fabricated using teflon molds. Surgical grade 316 stainless steel wire was used for reinforcement. The specimens were stored in Ringer's solution for 48 hours and then tested in shear in the wet condition using an Instron testing machine at a cross head speed of 2.54 mm/min.

Shear tests were performed on control specimens of cement alone and on test specimens of cement reinforced with 2, 3, 4, and 5 strands of 0.5 mm diameter stainless-steel wires. Ten specimens were tested in each group. For all specimens, the load increased continuously with increasing strain till the initiation of first crack at which point there was a sudden drop in the load. For reinforced specimens, the failure was in several steps and even after complete failure of the cement, the reinforcing wires still supported a considerable fraction of the maximum load (Fig. 1).

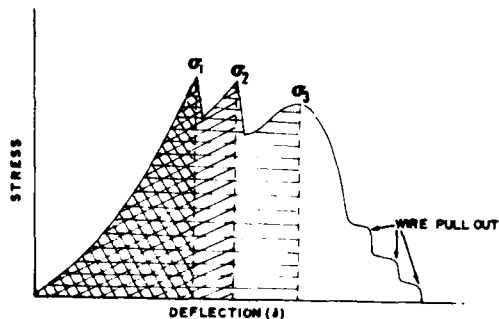


Fig. 1. Typical stress vs. deformation curve obtained during shear testing of wire-reinforced PMMA showing stresses at initial crack (σ_1) and subsequent cracks (σ_2 and σ_3).

The stress at the point of first crack initiation was considered the failure stress and this is compared for different specimen groups in Fig. 2. The energy absorption capacity was 12.9 ± 2.3 KJ/m² for control unreinforced specimens, and 16.1 ± 3.1 , 18.2 ± 3.9 , 16.5 ± 2.4 and 16.3 ± 4.4 KJ/m² for

specimens reinforced with 2, 3, 4, and 5 wires respectively. It is evident that the addition of metal reinforcement produced significant improvement in both the maximum stress and the energy absorption capacity of bone cement specimens. However, increasing the number of 0.5 mm diameter reinforcing wires from three to four and five produced a decrease in the failure load which is similar to our finding in bending tests [3]. Compaction of bone cement in these specimens was difficult due to the large number of reinforcing wires and this may be the reason for the decreased strength.

The result of this study shows that the load carrying capacity of acrylic bone cement in shear can be improved considerably by addition of reinforcing metal wires. Moreover, for reinforced bone cement, following fracture of cement, the reinforcing wires continue to support a significant amount of load. This is a distinct advantage of using reinforced bone cement in clinical situations.

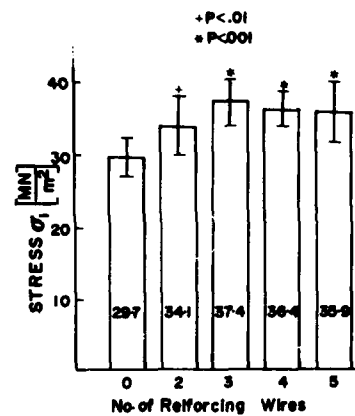


Fig. 2. Comparison of the maximum shear stress of control (0) and reinforced PMMA specimens. The significance level with respect to the unreinforced control group is indicated by * and +.

REFERENCES

1. Dunn, E.J. (1977) Spine, 2: 15-24.
2. Taitzman, J.P., and Saha, S. (1977) J. Bone and Jnt. Surg. 59-A: 419-425.
3. Saha, S. and Kraay, M.J. (1979) J. Biomed. Mater. Res. 13: 443-457.

Department of Orthopaedic Surgery
Louisiana State University Medical Center
Post Office Box 33932
Shreveport, LA 71130-3932

AD-A175 162

BIOMATERIALS '84: TRANSACTIONS WORLD CONGRESS ON
BIOMATERIALS (2ND) ANNUAL (U) SOCIETY FOR BIOMATERIALS
SAN ANTONIO TX S F HULBERT ET AL JUN 84

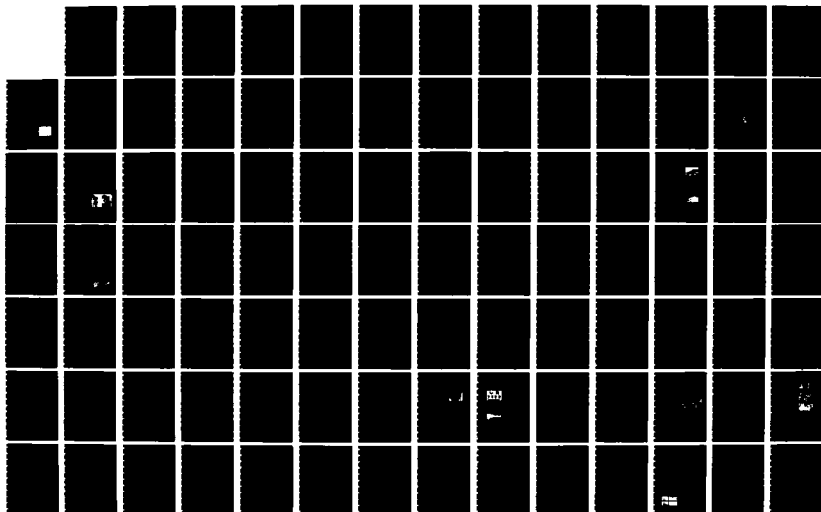
2/8

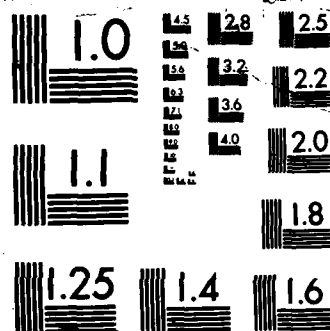
UNCLASSIFIED

DAMD17-84-G-4005

F/G 6/12

NL





XERO COPY RESOLUTION TEST CHART

PATHOGENESIS OF CIRCULATORY REACTIONS DURING THE IMPLANTATION OF ACRYLIC BONE CEMENT - NEW ANIMAL AND CLINICAL STUDIES -

J. Rudigier, K. Wenda, G. Ritter, D. Theiss

Division of Accident Surgery, Dept. of Surgery, University of Mainz
Langenbeckstr. 1, D-6500 Mainz, Federal Republic of Germany

Circulatory and respiratory reactions have been observed during or immediately after the implantation of acrylic bone cements used for anchoring endoprosthetic joint replacements in the medullary cavity of a long bone. Most of these reactions take the form of a temporary and spontaneously reversible reduction of the arterial blood pressure fluctuations, and a lowering of the arterial oxygen tension in the postoperative phase have been described. The liquid component of bone cements (methylmethacrylate monomer) or the outpour of bone marrow substances from the affected bone marrow cavity in the circulation caused by a pressure increase during the cement implantation are thought to be chiefly responsible for these effects. As third mechanism a direct neural reflex process may be involved.

The aim of our investigations was to clarify the question of the relative importance of these most discussed theories and to gain further information on the pathophysiology of the circulatory reactions. For the experiments were used rabbits and dogs. Our arrangement in experiments was able to investigate the possible factors separately. The following types of experiments were compared:

1. Experiments with application of intramedullary overpressure (without using bone cement)
 - a) without influence on the vegetative reflex pathways
 - b) with influence on the vegetative reflex pathways (cut-off the parasympathicus system, ganglion blockade)
2. Experiments with liquid bone cements.

For the animal experiments the tibial medullary canal was selected as the object of experimentation since it permits more selective cut-off the vascular supply or of the nerves than the femur (the cut-off the vascular supply as prevention of an invasion of bone marrow substances in the blood circulation and the cut-off the nerves for prevent neural reflexes). A similar reaction of all long bones was assumed. After anesthetizing of the animals with urethane (the spontaneous respiration was preserved) the following parameters were recorded on a polygraph during the experiments: the central venous pressure, the aortic pressure, the respiratory rate and ECG. Blood samples were taken for blood gas analysis. The lungs and the diencephalon were histologically examined.

In the experimental groups with application of bone cement were made gaschromatographic analyses of monomer in blood samples taken of the vena cava inferior. 5 - 10 animals were tested in every group. Because quantitative questions are not important for the results and clear, qualitatively consistent reactions were found for the individual animal experiments, an additional statistical evaluation was not deemed necessary.

The results of the animal experiments presented in this report shows:

1. The transient and reversible circulatory reactions (Fig.1), as a rule misinterpreted as reactions to cement monomer, are largely based on direct nerve reflex processes.

2. The reactions could not be prevented neither by administration of atropine nor by a bilateral cervical vagotomy as a reliable way of interrupting the parasympathicus (Fig.2). This was only possible under the influence of a ganglion blocker.

3. The longer-lasting circulatory and respiratory depression that may extend to lethal complications may be attributed primarily to massive embolic release of bone-marrow substance during the operation. The effects of the two pathomechanisms being completely superimposed on one another or perhaps even potentiating one another. Both mechanisms are triggered by the increase of pressure in the medullary canal.

Clinical observations during implantations of hip endoprostheses by using three different methods of anesthesia (general a., spinal a., peridural a.) confirmed the results obtained from the animal experiments.

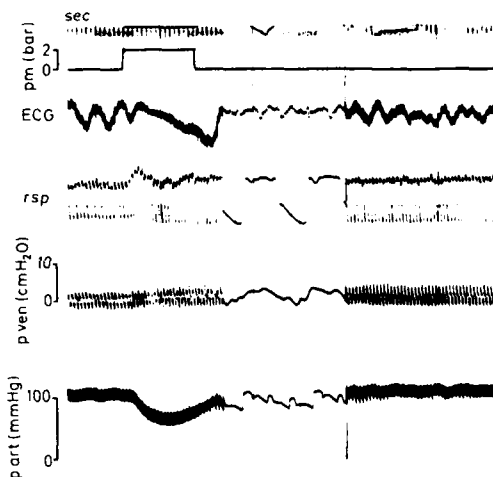


Fig.1: Curves recorded in a rabbit after induction of intramedullary overpressure (pm) immediately after interruption of the vascular supply.

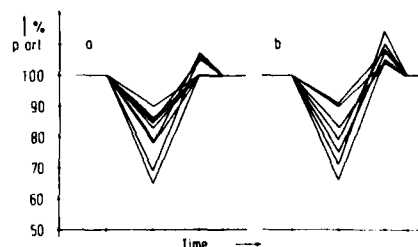


Fig.2: Graphic of the bloodpressure reductions in each animal a) without vagotomy b) vagotomized

Address: Prof. Dr. Jürgen Rudigier
Oberarzt an der Abteilung für Unfall-
chirurgie der chirurgischen Universitäts-
klinik Mainz
Langenbeckstr. 1
D - 6500 Mainz West Germany

ADVANCEMENT ON CEMENT TECHNIQUE : EXPERIMENTAL STUDY

TRANQUILLI-LEALI P., CERULLI G., PAOLETTI G.C., PEZZOLI F.

CLINICA ORTOPEDICA UNIVERSITA' CATTOLICA ROMA

THE LOOSENING IS THE MAIN REASON FOR CEMENTED THR FAILURES. TO DECREASE THE FAILURE RATE IT'S POSSIBLE TO MODIFY THE COMPOSITION OF PMMA OR TO IMPROVE THE CEMENT TECHNIQUE. THE AIM OF THIS RESEARCH IS TO ANALYZE COMPARATIVELY THE DIFFERENT TECHNIQUES OF INSERTION AND MANUAL VS MECHANICAL MIXING.

SERIES I : SIX SPECIMENS OF SIMPLEX R.O. CEMENT WERE PREPARED INTO PLASTIC MOULDS USING 4 DIFFERENT METHODS OF INSERTION :

- MANUAL (M)
- HOMMEDICA CEMENT GUN (P)
- HARRIS CEMENT GUN (H)
- COMPRESSED AIR GUN (A)

THE COMPRESSED AIR GUN IS AN ORIGINAL DEVICE REALIZED AT THE PERUGIA UNIVERSITY. ALL THE TRIALS WERE CARRIED OUT AT THE SAME ENVIRONMENTAL AND TECHNICAL CONDITIONS.

SERIES II : THREE DIFFERENT OPERATORS EXECUTED THE MANUAL MIXING AT THE SAME ENVIRONMENT, DOING EACH ONE THREE SPECIMENS, ALL INSERTED BY USING COMPRESSED AIR GUN. WE ALSO PREPARED TWELVE SAMPLES BY USING A MECHANICAL MIXER WITH A CONSTANT PITCH HELIX TWO DIFFERENT MIXING TIMES (1.5 AND 2 MINUTES) AND TWO INSERTION DEVICES (HOMMEDICA AND COMPRESSED AIR CEMENT GUNS) WERE USED (A= 2'+A; B= 2'+P; C= 1.5'+A; D= 1.5'+P).

ALL THE SPECIMENS WERE ANALYZED BY :

- XRAVS
- SCANNING ELECTRON MICROSCOPE
- IMAGE ANALYZER
- UNIVERSAL TESTING MACHINE (INSTRON)

THE IMAGE ANALYSIS WAS CARRIED OUT TO MEASURE THE AREA AND THE NUMBER OF VOIDS (BUBBLES) INTO THE SAMPLE AND TO ASSESS THE % POROSITY INDEX.

WE FURTHERLY EVALUATED SEMIQUANTITATIVELY THE PARIETAL PRESSURES ON PLASTIC MOULDS AND THE INCIDENCE RATE OF LUNG EMBOLISM ON RABBITS BY LUNG SCAN.

THE COMPRESSED AIR GUN TECHNIQUE PROVED TO BE BETTER THAN THE OTHERS FROM X-RAY, MORPHOMETRIC (TAB.I) AND MECHANICAL (TAB.II) EVALUATIONS.

TABLE I :	A	H	P	M
n.bubbles	145	269	292	266
mean area bubbles $10^3 \mu^2$	58	186	138	235
porosity index 2.5 %	14.3	7.2	17.9	

TABLE II :

Ultimate Compressive strength	Ultimate Bending strength
A 9.96	Kg/mm ² 6.98
H 9.30	" " 5.47
P 9.25	" " 5.76
M 7.91	" " 4.70

THERE ARE SIGNIFICANT DIFFERENCES BETWEEN THE SAMPLES PREPARED MANUALLY BY THE THREE OPERATORS. THE MOST EXPERIENCED OBTAINED THE BEST RESULTS MORPHOLOGICALLY (TAB.III) AND MECHANICALLY (TAB.IV).

TABLE III :	02	01	03
n.bubbles	120	180	173
mean area bubbles $10^3 \mu^2$	63	80	71
porosity index	3.1 %	6.3	5.4

TABLE IV :

Ultimate compressive strength	Ultimate bending strength
02 9.64	Kg/mm ² 6.90
01 9.60	" " 6.88
03 9.50	" " 6.70

THE MECHANICALLY MIXED SPECIMENS (TIME 1.5'+ COMPRESSED AIR GUN) WERE MORE HOMOGENOUS (TAB.V) AND RESISTANT (TAB.VI).

TABLE V :

	A	B	C	D
n.bubbles	49	34	19	32
mean area bubbles $10^3 \mu^2$	72	77	33	74
porosity index 4.1 %	6.3	3.1	7.4	

TABLE VI :

Ultimate compressive strength	Ultimate bending strength
A 12.50	Kg/mm ² 8.30
B 10.25	" " 7.11
C 13.31	" " 8.64
D 9.85	" " 7.09

FINALLY THE SEMIQUANTITATIVE ANALYSIS SHOWED THAT THE PARIETAL PRESSURE USING COMPRESSED AIR GUN IS NOT TO HIGH COMPARED TO THE OTHER METHODS AND NO LUNG EMBOLISM WAS DETECTED IN RABBIT SERIES.

IN CONCLUSION THE MECHANICAL INSERTION OF CEMENT USING COMPRESSED AIR DEVICE SEEMS TO BE BETTER THAN OTHERS BECAUSE IT IMPROVES PHISICAL AND MECHANICAL PROPERTIES OF PMMA WITHOUT INCREASING THE RISK OF BIOLOGICAL DAMAGE. THE MECHANICAL MIXING IS BETTER THAN MANUAL ONE BECAUSE REDUCES THE INTERINDIVIDUAL SCATTERING AND ALLOWS A MORE HOMOGENOUS AND REPETITIVE DOUGH PREPARATION.

- 1) CERULLI G., TRANQUILLI-LEALI P., MORICONI F., PAOLETTI G.C., EXPERIMENTAL STUDY OF THE THR CEMENT TECHNIQUES, FOURTH EUROP.CONF.ON BIOMATERIALS, LOUVAIN, BELGIUM, 1983
- 2) TRANQUILLI-LEALI P., CERULLI G., CONSIDERAZIONI SULLE CARATTERISTICHE DEL METILMETACRILATO IN RELAZIONE A DIFFERENTI TECNICHE DI CEMENTAZIONE, MIN.ORTOP., 33, 821-824, 1982.

THERMAL BEHAVIOR OF NORMAL AND FIBER-REINFORCED BONE CEMENT

S. Saha, S. Pal and J. A. Albright

Biomechanics Laboratory, Dept. of Orthopaedic Surgery
LSU Medical Centre, Shreveport, LA 71130

Surgical bone cement or PMMA is used extensively in orthopaedic surgery for fixation of total joint replacements. However, when the liquid monomer component of PMMA is mixed with methylmethacrylate powder, it polymerizes with the evolution of heat of 2600 calorie per one commercial unit. Many authors measured the temperature during polymerization and obtained peak values ranging from 80° to 124°C (1,2). Experimentally it has been observed that the bone-cement interface temperature varied between 48°C and 58°C and duration was several seconds (3). This suggests that although the use of bone cement has greatly facilitated the success of artificial joint replacements, a high rise in temperature during setting of bone cement may cause tissue necrosis (4) and thus reduction of peak temperature is highly desirable in the clinical use of bone cement. Previously we have shown that carbon and aramid fiber reinforcement could significantly improve the mechanical properties of bone cement (2,5). The objective of this study was to determine if such fiber reinforcement could also be used to decrease the peak temperature rise during polymerization of bone cement.

PMMA mix, after reaching the dough stage during hand mixing, was introduced in a cylindrical teflon mold (size: 56 mm dia x 52 mm height with 18 mm inner bore). A needle microprobe (Type ICT-4, Bailey Inst.) thermo couple was introduced at the center of the polymerizing bone cement mass. The terminals of the thermo couple were connected to a Digital thermometer (BAT-12, Bailey Inst.) and the analogue output of this was fed to a strip chart recorder. The temperature rose slowly at the beginning and then rose sharply during rapid polymerization and subsequently came down to room temperature slowly.

Similar standardized test specimens were prepared from low viscosity normal and commercially available low viscosity carbon reinforced bone cement (Zimmer, USA, Inc.) and from hand mixed aramid fiber (DuPont, Inc.) reinforced bone cement specimens, using teflon molds (2). Temperature profiles during polymerization of these samples were then recorded, similar to the normal PMMA specimens.

The maximum temperature developed during the polymerization was observed to be 91.5°C with 2% aramid and it was only 71.4°C when 4% of aramid was used. The temperature record is shown in Fig. 1.

Figure 2 shows the record of the temperature developed during polymerization of normal PMMA and CFR-PMMA (2 w/o) while setting in a teflon mold. The size of the samples were the same (18 mm diameter x 32 mm long). Figures 1 and 2 show that both aramid and carbon fiber reinforcements produced a significant decrease in the peak temperature during setting, which is of great clinical advantage.

4. Jefferies, C.D., Lee, A.J.C. and Ling, R.M.S. (1975) J.Bone & Joint.Surg., 57B:511-518.
5. Saha, S., Pal, S. and Albright, J.A. (1981) Trans. 7th Ann.Mtg. Soc.Biomater. 4:21.

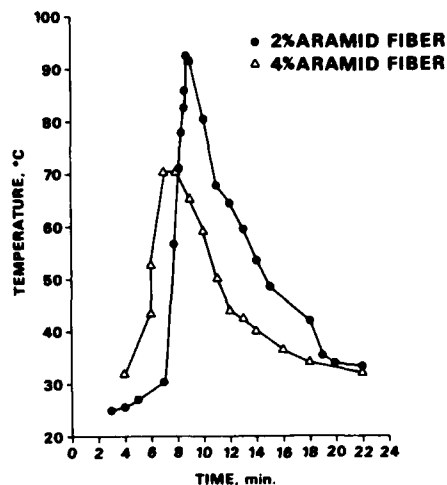


Fig. 1. Temperature record during rapid polymerization of PMMA samples (18 mm dia. x 32 mm long) reinforced with 2% and 4% aramid fibers.

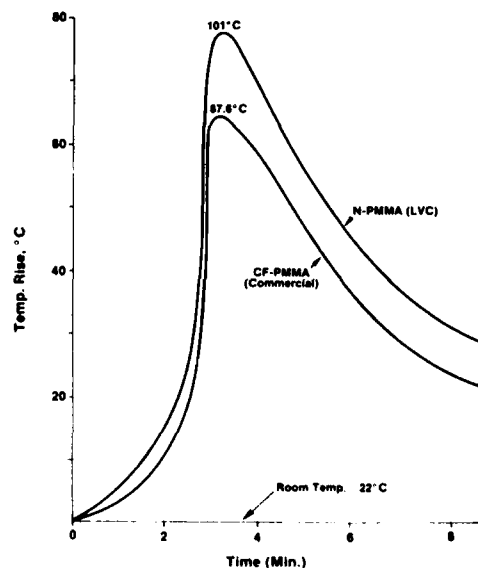


Fig. 2. Temperature profile during polymerization of normal and carbon fiber reinforced PMMA samples.

1. Kusy, R.P. (1976) J.Biomed.Mater.Res., 12:271-305.
2. Saha, S. and Pal, S. (1983) J.Biomechanics (in press)
3. Weinstein, A.M., et al. (1976) Clin.Orthop. 171:67-73.

D.O. O'Connor, D.W. Burke, J.P. Davies and W.H. Harris

Orthopaedic Research Laboratories, Massachusetts General Hospital and
Harvard Medical School, Boston, MA 02114.

In cemented total joint replacement today, the longevity of the rigidly fixed implant depends primarily on the weakest link in the reconstruction. In the cemented total joint composite the material with the least strength is PMMA. This observation has led us to study extensively the fatigue properties of PMMA and specifically in terms of an S-N curve. An S-N curve for centrifuged PMMA bone cement has not been derived before.

Burke et al.¹ have measured cement strains *in vitro* in cadaver femurs in conditions simulating gait and found peak cement strains to be in the order of 1000 microstrain. With this information, we felt it was of special importance to study the fatigue properties of bone cement at strain levels as low as 1000 microstrain.

Methods: In generating our S-N curves we studied two different preparations of Simplex-P bone cement. The first was bone cement prepared in a standard fashion, which we called control cement. The second was the identical material which had been mixed in a similar fashion but was then centrifuged at 4000 rpm for 30 seconds as proposed by Burke et al.² All test specimens were prepared in identical conditions of temperature (21°C) and humidity (50%). The cement prepared in the two fashions mentioned were then injected into cylindrical molds and allowed to cure in the water bath at 37°C. They were then machined into identical waisted test specimens for fatigue testing. They were then tested on an MTS test system in load control set at initial strains with fully reversed tension-compression cyclic fatigue, and at 37°C, 100% humidity at a frequency of 2Hz except for the 2000 microstrain level, where specimens were tested at 2Hz and 20Hz, and also for the 1000 microstrain level where all specimens were tested at 20Hz because of time constraints. Strain levels for testing ranged from .015 to .001 microstrain.

Results: In all tests, the centrifuged cement lasted significantly longer in fatigue life than control cement at all strain levels (Fig. 1). Cipolletti and Cooke³ found similar fatigue results at low stress levels with a different test specimen with control cement. In the more physiologic tests, i.e., those done at low strain levels, none of the centrifuged cement specimens broke when tested to 10 million cycles. In contrast 70% of control specimens failed prior to 10 million cycles. This is a statistically significant difference. It is interesting to note that at the 2000 microstrain level both centrifuged and control specimens lasted significantly longer in fatigue at 20Hz compared to 2Hz.

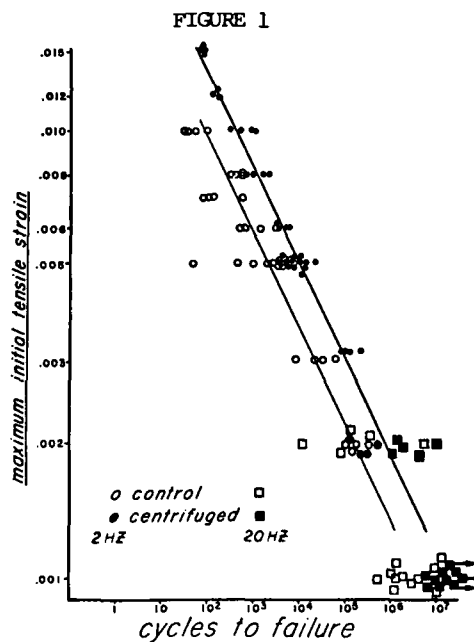
Conclusion: An S-N curve is presented for surgical Simplex-P bone cement prepared in the ordinary way. At strain values which can be expected to occur in gait, the majority of samples failed prior to 10 million cycles. Thus, late failure of bone cement, particularly in heavy or young patients is not surprising. An S-N curve is presented for the same bone cement that has been

improved by centrifugation, which reduces the porosity of the material. At all strain levels tested the centrifuged material was significantly better in fatigue than the standard preparation.

The centrifuged material did not fail at 10^7 cycles when tested at strain levels of 1000 microstrain, which are the highest strain levels found *in vitro* in simulated gait conditions in total hip replacements in cadaver femurs.

References

1. Burke, D.W.; Davies, J.P.; O'Connor, D.O.; and Harris, W.H.: Acrylic Cement Strain in the Femoral Shaft. (in preparation).
2. Burke, D.W.; Gates, E.I.; and Harris, W.H.: Improvement of Tensile and Fatigue Properties of PMMA by Centrifugation. J. Bone and Joint Surg., in press.
3. Cipolletti, G.B.; and Cooke, F.W.: Fatigue of Bone Cement in Physiological Saline at One Hz. Transactions of the Fourth Annual Meeting, Society of Biomaterials, 2: 134-135, 1978.



POROSITY MEASUREMENTS IN CENTRIFUGED AND UNCENTRIFUGED COMMERCIAL BONE CEMENT PREPARATIONS.

M. Jasty, N.F. Jensen and W.H. Harris

Orthopaedic Research Laboratories, Massachusetts General Hospital and Harvard Medical School, Boston, MA 02114.

Failure of total joint arthroplasty is often attributed to primary disruption of the cement mantle surrounding the implant. Specifically, the high porosity of the PMMA bone cement has been shown to be the key feature in the low fatigue strength of this material. Recently developed centrifugation techniques have substantially increased the mechanical properties of bone cement by reducing its porosity. Recognizing the role of porosity, we systematically investigated porosities of several commercial bone cement preparations and the reduction in porosity with centrifugation.

Methods and Materials: We studied Simplex-P, AKZ, and Palacos R. The control specimens were mixed in recommended proportions, at 21°C, 50% humidity, at approximately 2Hz, for 45 seconds. Specimens were poured into cement syringes and allowed to cure. Control specimens were also prepared by chilling the monomer to 0°C and mixing for 75 seconds, to allow for complete wetting and mixing. Additional Simplex-P controls were prepared by prolonging the mixing time to 1.5 minutes and 5 minutes before inserting into cement syringes. Centrifuged specimens were prepared under identical environmental conditions. The unchilled specimens were mixed for 45 seconds and the chilled specimens for 75 seconds. The syringes were then placed into an IEC model CL centrifuge and spun at 4,000 rpm. To assess the effect of centrifugation time, one set of specimens were spun for 30 seconds and the other set for 2 minutes. After curing the syringe, the prepared cylindrical specimens were cut into six 5mm discs. The discs were ground flat on a Bheuler grinding wheel, polished with a .3u alumina powder to a mirror finish, and spray painted with a flat black spray paint. The dried paint was then wiped clean on the surface, leaving the pores stained black.

The areal fraction measurements were done using an image analyzing system consisting of a video camera, and a video digitizer interfaced to a PDP 11/23 computer. To increase the resolution, the specimens were magnified under the microscope X12. The discs were divided into nine pie shaped quadrants and rotated by the computer. The areal fraction measurements were taken for each quadrant and averaged to yield a total fractional areal porosity of the disc. Each disc was counted two times.

Results: The areal porosity of Simplex-P control specimens ranged from 8.2% to 15%. This represented more variability than that obtained for centrifuged specimens. Porosity values for specimens centrifuged for 30 seconds ranged from 3.1% to 5.1%. After two minutes of centrifugation these porosity values fell to a range of 2.4% to 3.5%. These results indicated that the areal porosity of Simplex-P bone cement is substantially decreased by centrifugation. The almost threefold reduction in porosity applied both to cement prepared with chilled and to the cement prepared with unchilled monomer. In both cases, centrifugation for 2 minutes proved slightly better

in decreasing porosity than centrifugation for 30 seconds.

Porosity in AKZ control specimens ranged from 10.2% to 12.2%. Centrifugation for 30 seconds reduced the porosity to 7.8% for non-iced monomer and to 4.8% for iced monomer. Two minute centrifugation reduced the porosity to 6% for non-iced monomer and to 5.8% for iced monomer. The reduction in the mean porosity for centrifuged AKZ was less than that obtained for centrifuged Simplex-P specimens at both centrifugation times.

Areal porosity in Palacos R control specimens ranged from 10% to 12%. Differences in total areal porosity were not obtained either with Palacos R or with Palacos R with gentamicin, when centrifuged for 30 seconds or 2 minutes. This held true for specimens prepared both by the monomer at 21°C and at 0°C.

Conclusions: Although many different commercial preparations of bone cement are available, they all appear to suffer from gross structural defects in the form of voids. Our prior studies have shown that such voids substantially decrease the strength of the material. In this study, centrifugation considerably reduced the overall porosity of Simplex-P bone cement. Less reduction in porosity was achieved with AKZ and only minimal reduction in porosity with Palacos after centrifugation.

Specimens centrifuged for 2 minutes showed slightly more reduction in porosity than those centrifuged for 30 seconds.

EFFECT OF ANTIBIOTIC ADDITION ON THE FATIGUE LIFE OF CENTRIFUGED AND UNCENTRIFUGED BONE CEMENT

J.P. Davies, D.O. O'Connor and W.H. Harris

Orthopaedic Research Laboratory, Massachusetts General Hospital and
Harvard Medical School, Boston, MA 02114

The addition of antibiotics to bone cement for the treatment and/or prevention of deep wound infection in total joint replacements has generated concern over reduced mechanical properties, particularly the fatigue behavior of these antibiotic impregnated cements. For example, a previous report found that the addition of one gram of gentamicin to Palacos R significantly reduced the fatigue life of the cement.¹ In a recent study in our lab, the fatigue life of Simplex-P was shown to be significantly improved by centrifuging the cement immediately after mixing.² The present study was undertaken to investigate the effect of antibiotic addition on the fatigue strength of bone cement and also to assess whether the fatigue lives of these antibiotic impregnated cements could be improved by centrifugation.

To conduct this investigation, fifteen specimens each of Palacos R, Simplex-P and their commercially available antibiotic impregnated counterparts Palacos R with gentamicin and AKZ bone cements were prepared in the standard fashion according to manufacturers instructions. Fifteen specimens of each cement type were also prepared with the addition of centrifugation immediately after mixing. All Simplex-P based cements were centrifuged for thirty seconds. The Palacos R based cements, because of their inherent higher viscosity, were centrifuged for one minute. The mixed cements prepared by both techniques were injected into a cylindrical mold, cured in a water bath at 37°C and then machined into waisted specimens with a central diameter of 5mm. Fully reversed tension-compression fatigue tests were carried out with an initial strain of 0.005mm/mm at a frequency of 2Hz at 37°C and 100% humidity. The number of cycles to failure were recorded and compared on the basis of the students t-test and Weibull analysis.

The fatigue test results are shown in Table 1. There was no significant difference in the fatigue lives of Palacos R and Palacos R with gentamicin when both cements were prepared in the standard fashion. Centrifugation did not significantly improve the fatigue lives of either the Palacos R or the Palacos R with gentamicin.

Likewise, when the Simplex P and AKZ cements were prepared in the standard fashion, there was no significant difference in the fatigue lives of the two cements. However, centrifugation significantly improved the fatigue life of both the Simplex-P and AKZ bone cements. Furthermore, the fatigue life of the centrifuged Simplex-P was significantly greater than the fatigue life of the centrifuged AKZ cement. It is also important to note that the fatigue life of centrifuged AKZ is significantly greater than the fatigue life of uncentrifuged Simplex-P.

In summary, no significant reduction in fatigue life was evident between the uncentrifuged Palacos R and uncentrifuged Palacos R with gentamicin nor was there a significant difference in the fatigue lives of uncentrifuged Simplex P and uncentrifuged AKZ. In addition, centrifugation significantly

improved the fatigue lives of both Simplex-P and AKZ bone cements. Centrifugation did not improve the fatigue lives of Palacos R or Palacos R with gentamicin.

References

1. Schurman, D.J. et al: In The Hip C.V. Mosby Co., St. Louis: pp.87, 1978.
2. Burke D.W., Gates, E.I., and Harris, W.H. Centrifugation as a Method of Improving Tensile and Fatigue Properties of Acrylic Bone Cement. JBJS (in press) 1983.

Table 1
Fatigue Test Results

Cement Tested	Method of Preparation	Log Cycles to Failure	(t-test)
		Mean \pm std. dev.	p < 0.05
Palacos R	Standard*	3.62 \pm .50	NS
Palacos R with gentamicin	Standard	3.59 \pm .24	
Palacos R	Centrifuged	3.65 \pm .15	S
Palacos R with gentamicin	Centrifuged	3.49 \pm .24	
Simplex P	Standard	3.38 \pm .61	NS
AKZ	Standard	3.21 \pm .43	
Simplex P	Centrifuged	3.94 \pm .22	S
AKZ	Centrifuged	3.71 \pm .17	

*Prepared according to manufacturer's suggestions.

S=Significant Difference

NS=No Significant Difference

IMPROVED COMPRESSIVE STRENGTH OF BONE CEMENT BY ULTRASONIC VIBRATION

Subrata Saha and M. L. Warman

Department of Orthopaedic Surgery, LSU School of Medicine in Shreveport,
1501 Kings Highway, P.O. Box 33932, Shreveport, La. 71130-3932

Self-curing polymethylmethacrylate (PMMA) or acrylic bone cement is used extensively in total joint replacements, in the repair of bony defects, in the fixation of highly comminuted and pathological fractures, and in obtaining immediate stabilization of spinal fusions. For surgical use, the methylmethacrylate polymer and the liquid monomer are hand mixed. This hand mixing entraps air bubbles making the cement porous. Presence of these bubbles adversely affects the mechanical properties of bone cement, making it much weaker under load (1). This phenomenon is similar to the mixing of concrete which also absorbs air bubbles during the mixing process (2). During concrete construction, vibration is often used to eliminate the entrapped air and thus obtain increased density and consequently improved mechanical strength characteristics (2). The objective of this study was: 1) to determine if a similar technique could also be used to reduce the porosity in bone cement, and 2) to evaluate the resulting improvement in its mechanical behavior.

Radiopaque acrylic bone cement powder (Surgical Simplex P, Howmedica Inc.) was mixed with the liquid monomer by hand, in stainless steel bowls, following the manufacturer's directions. To increase the dough time, the powder and the monomer were refrigerated before mixing. When the mixture reached a liquid state, the bowls were placed on the tray of an ultrasonic cleaner (Cole Parmer, model 8845-3). As the ultrasonic vibration caused the air bubbles to rise to the top, they were removed by a spatula. The cement, in a dough state, was then poured into cylindrical teflon molds to prepare compression specimens which were 30 mm in length and 17 mm in diameter. A second batch of bone cement, not subjected to the ultrasonic vibration, was used to prepare a similar group of compression specimens, to be tested as the control. The specimens were stored in water for at least 24 hours before testing them mechanically in compression using a floor model Instron testing machine.

As shown in Figs. 1 and 2, both the ultimate compressive stress and the energy absorption capacity increased significantly ($p < .05$) when vibrated ultrasonically. Fig. 1 also shows that the improvement in strength was equivalent to an increase in strain rate by an order of magnitude (3). This study indicates that ultrasonic vibration may be a practical way of reducing porosity and thus improving strength of surgical grade PMMA.

References:

1. deWign, J.R., Slooff, I.J.J.H., and Driessens, F.C.M. (1975) Characterization of bone cements. *Acta Orthop. Scand.*, 46:38-51.
2. Billing, K. (1960) *Structural Concrete*. Macmillan & Co., Ltd., London, pp. 92-98.

3. Saha, S. and Pal, S. (1983) Strain-rate dependence of the compressive properties of normal and carbon-fiber-reinforced bone cement. *J. Biomed. Mater. Res.* (in press).

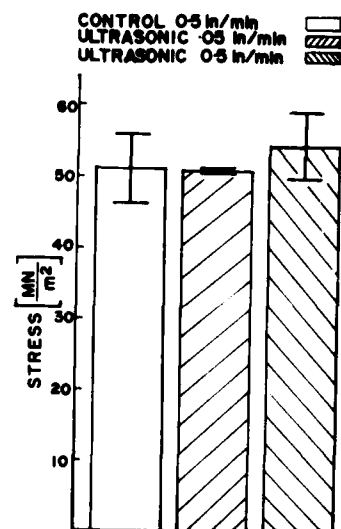


Fig. 1 Increased compressive strength of bone cement when subjected to ultrasonic vibration in the dough state. This increase of strength was equivalent to an increase of deformation rate from 0.05 to 0.5 in/min.

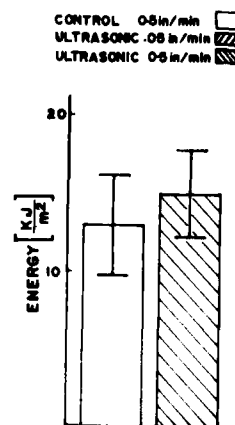


Fig. 2 Improved energy absorption capacity of vibrated bone cement compared to normal.

PHYSICAL CHARACTERIZATION AND HISTOLOGICAL RESPONSE OF A GLASS BEAD COMPOSITE ACRYLIC BONE CEMENT

C. Migliaresi, S. Gatto^o, G. Guida^o, L. Nicolais, V. Riccio

Polymer Engineering Laboratory, University of Naples, Naples, Italy

Acrylic bone cements introduced by Charnley in 1960 are today widely used in orthopedics for bone prosthesis fixation. Nevertheless, high temperatures reached during the "in vivo" polymerization, shrinkage and low dimensional stability of commercial cements are unacceptable faults which often cause necrosis of tissues surrounding the cements and loosening of the prosthesis.

Although in the past many solutions have been proposed in order to reduce these inconvenients, such as addition of heat sinks or different formulations, no practical results have been obtained due to the decreased mechanical properties of the cements.

However it is well assessed in polymer and composite technology that the use of crosslinking agents and reinforcing fillers can successfully improve both short and long term mechanical properties and dimensional stability provided that opportune amounts of crosslinking agent are used and adhesion between fillers and matrix is achieved.

The physical characterization of a new glass bead composite crosslinked cement of composition reported in Table 1, indicates an appreciable decrease of the reaction temperature with respect to that of a commercial cement (see Figure 1), and a corresponding improvement of mechanical properties and dimensional stability. Moreover crosslinked glass bead composite cements with different compositions and formulations have been prepared and characterized. The results will be presented and discussed in terms of their intrusion properties, doughing and setting times, temperatures of reaction and mechanical properties.

Clinical evaluation of cements polymerized in vivo in the iliac bones of rabbits and histological response at different implantation times demonstrate that the composite cements is well tolerated and better adheres to bone than commercial cements.

Results obtained with cements of different compositions will be presented and related to the cement characteristics.

Table 1. Composition of the glass bead composite crosslinked bone cement

Phase 1(40% by wt.):

- 30% wt. solution of poly-methylmethacrylate in methylmethacrylate
- Ethylenedimethacrylate(2% by wt. referred to methylmethacrylate content)
- Dimethylparatoluidine(2% by wt. referred to methylmethacrylate content)

Phase 2(60% by wt.):

- Glass beads
- Benzoyl peroxide(1% by wt. referred to the methylmethacrylate content in phase 1).

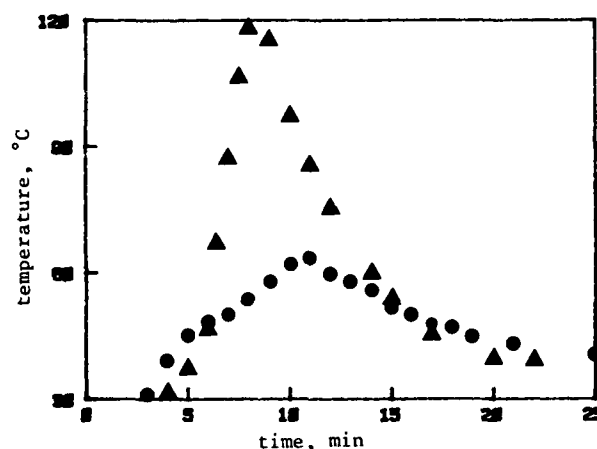


Fig. 1. Reaction temperature versus the time for the glass bead composite cement (circles) and a commercial (Sulfix) cement (triangles). The reactions have taken place in a 20cm³ reactor immersed in water at 37°C.

Polymer Engineering Laboratory, University of Naples
Piazzale Tecchio, 80125 Naples, Italy
^oII Clinica Ortopedica, I Facoltà di Medicina e Chirurgia, University of Naples, Naples, Italy

CLINICAL EXPERIENCE OF CARBON FIBRE PATCHES

R.J. MINNS

Department Medical Physics, Dryburn Hospital,
Durham, England.

Thirdly, clinical trials have commenced using large woven carbon fibre patches in the inducement of fibrosis associated with inguinal and incisional hernias.

The Department has been involved with the biocompatibility and clinical use of carbon fibre in three major surgical applications. Firstly, the regeneration of concave articular surfaces in degenerative joint disease using loosely woven carbon fibre patches implanted into defects within the articular surfaces. Pure filamentous carbon fibre patches of 3mm thickness and several diameters (8-22mm) in defects made in the concave articular surface of osteoarthritic joints to produce a biological resurfacing. No metallic fixation methods were necessary and no alignment instrumentation was required. In rabbit knees using the same material, but 4mm in diameter, a new fibrocartilage was quickly formed (in less than 4 weeks) giving good wearing characteristics with fixation through supportive bone intertwined within the base of the carbon fibre patch. Thirty patients were treated for hallux rigidus with a follow-up of 6-30 months. Clinical assessments were made as 25 excellent and 5 good. The operation was simple, quick, required little training with the material and no loss of toe length. Degenerate areas in the patella, wrist, head of radius and femoral condyles have also been treated successfully by these pads and (follow-up period 3-12 months) early clinical observations show good results.

Secondly, much larger carbon fibre loosely woven patches have been used in the inducement of fibrosis over bony protuberances in patients who are at risk to extensive pressure sores in these regions. This employs the properties of a particular type of carbon fibre pad implanted surgically over the bony prominence. The response of the pad to loading has been examined. The host tissue response to the presence of the pad involves penetration of the interstices of the pad and in nine paraplegics, the host tissue - carbon fibre pad complex has been found to be highly vascular. Clinical trials show promising results and surgeons are encouraged by the following features particularly:

The satisfactory reduction in pressure under the ischial tuberosities when the patient is sitting post-operatively as measured on an 'Ischiobarograph'. (A seating pressure measuring device)

If it should be necessary for any reason the carbon fibre pad can be removed or replaced without difficulty. All procedures required can be accomplished without a general anaesthetic. Bearing in mind the difficulties of treating pressure sores and their relatively frequent occurrence, our experience so far justifies continued careful development of the technique.

Shear Creep of Reconstituted Type I Collagen Suspensions

Weiss, B.A. and Wallace, D.G.

Collagen Corporation, Palo Alto, CA, USA

Shear creep experiments are of fundamental interest in characterizing material rheology¹ and have been previously applied to fibrillar protein suspensions, such as fibrin clots.^{2,3,4} These experiments were undertaken to determine the behavior of reconstituted bovine type I fibrillar collagen in shear creep.

Purified, reconstituted, bovine type I collagen (ZYDERM^R Collagen Implant, Collagen Corporation, Palo Alto, CA) was used in these experiments. The material is an aqueous fiber suspension containing 3-4% protein per ml.

Plots of $\log J(t)$ versus $\log(t)$ are shown in Figure 1. Shear stresses are shown in Table 1. Shear rates varied between 10^{-7} and 10^{-6} sec⁻¹. The traces are as expected for a lightly crosslinked, but highly entangled structure.¹

The strain versus time responses for three experiments are shown in Figure 2. The results may be modeled by applying a modified superposition principle to obtain a reduced non-linear constitutive equation

$$\epsilon(\sigma, t) = k_0 \sigma_0 + (k_1 \sigma_0 + k_2 \sigma_0 + \dots) t/t' + t'$$

where ϵ is strain, σ_0 is applied stress, t is time, k_0 , k_1 , and k_2 are coefficients of kernel functions and t' is a characteristic time. The kernel functions may be approximated as follows:

$$K_1 = k_0 + k_1 (t/t' + t')$$

$$K_2 = k_2 (t/t' + t')$$

$$K_n = k_n (t/t' + t')$$

In the figure, the points (x) are experimental; the curves are predicted by the model using the parameters shown in the second part of Table 1.

This model is a good fit (sum of squared residuals 1×10^{-5} - 1×10^{-4}) for shear creep in the stress range tested, although ultimate strain is shown to be independent of applied stress, a surprising result. It is possible that fibril population variability between samples is the cause or that strain response does not vary predictably within the stress range possible with this material and device.

Some preliminary experiments on collagen suspensions prepared similarly but cross-linked with glutaraldehyde have been conducted also. The results obtained so far indicate behavior similar to the uncrosslinked materials, but with terminal creep compliance approximately one order of magnitude lower and t' one order of magnitude higher.

Two main conclusions may be drawn from this work:

1. Collagen suspensions behave in shear creep conditions as expected for a lightly cross-linked, highly entangled structure.
2. Shear creep behavior may be successfully modeled by a reduced, non-linear constitutive equation based on a modified superposition principle.

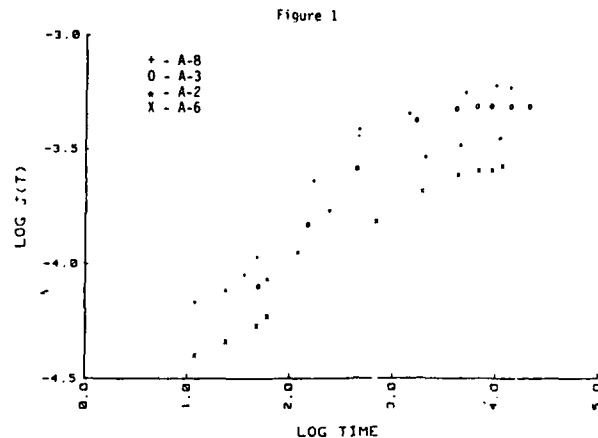
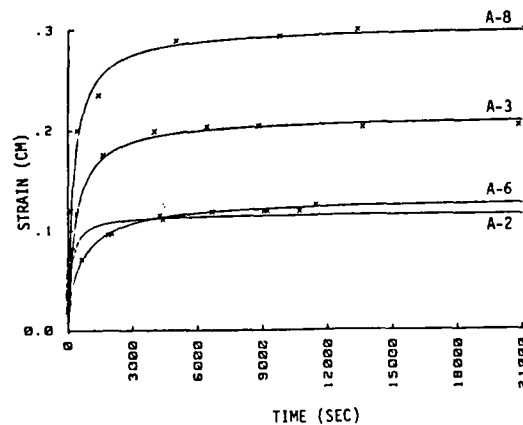


Table 1.

Experiment	A-2	A-3	A-6	A-8
Stress (dynes/cm ²)	340	425	473	521
Parameters:				
k_0	-5.0×10^{-5}	1.6×10^{-5}	3.9×10^{-5}	3.8×10^{-5}
k_1	2.3×10^{-4}	3.1×10^{-6}	2.0×10^{-4}	2.9×10^{-4}
k_2	4.8×10^{-7}	4.1×10^{-7}	8.3×10^{-8}	4.8×10^{-7}
t'	127	375	789	308

Figure 2



References:

1. Ferry, J.D., Viscoelastic Properties of Polymers, John Wiley and Sons, NY, 1980.
2. Roberts, W.W., Kramer, O., Rosser, R.W., Nestler, F.H.M., Ferry, J.D., Biophys. Chem. 1 (1974) 152.
3. Gerth, C., Roberts, W.W., Ferry, J.D., Biophys. Chem. 2, (1974) p 208-217.
4. Nelb, G.W., Gerth, Ferry, J.D., Biophys. Chem. 5 (1976) pp 377-387.
5. Vakili, J., J. Rheology, 27(3), 1983, p 211-222.

Lacabanne C., Lamure A., Hitmi N., Maurel E.[†], Pieraggi M.Th.[†] and Harmand M.F.^{††}Laboratoire de Physique des Solides, Université Paul Sabatier
31062 Toulouse Cédex, France

Physical properties of connective tissues such as piezoelectricity have an important biological role. In order to give some light on their molecular origin, we have investigated the molecular movements responsible for the electric polarization of collagen and the deformation of proteoglycans (PG). Because of their high resolving power, the thermostimulated current (TSCu) and thermostimulated creep (TSCr) techniques are particularly well suited to this work.

Principle of thermostimulated current/creep

An electric/mechanical field is applied to the sample at the temperature T_a for a given time. The temperature is decreased to $T_c \ll T_a$ where the molecular movements that we want to observe are frozen and the field is cut off. Then, the return to equilibrium of the sample is induced by a controlled temperature rise while the conductivity σ /reciprocal of the viscosity η is recorded versus temperature.

Thermostimulated creep of proteoglycans

The anelastic properties of connective tissues are strongly dependent on PG. So, we have undertaken the TSCr study of PG subunits extracted from calf cartilage.

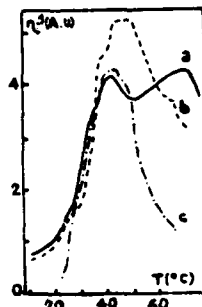


Figure 1 : Thermostimulated creep spectra of proteoglycans. a, b, c correspond to increasing dehydration levels.

The TSCr peak situated around 70°C (spectrum a of figure 1) is shifted towards lower temperature (spectrum b) before disappearing (spectrum c) during dehydration. This behavior that has been found to be reversible, implies an increasing of the potential barriers during hydration. This antiplasticizing effect has been attributed to a stiffening of the PG chains by hydrogen bonded water molecules.

Thermostimulated current of collagen

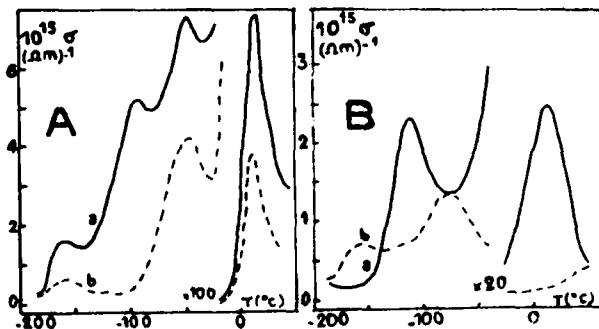


Figure 2 : Thermostimulated current spectra of collagen. a and b correspond to increasing hydration levels. A and B are respectively for immature (three weeks) and mature (twelve weeks) collagen.

The electric polarization of connective tissues is essentially due to collagen. So, we have performed a TSCu study of male rat skin of three and twelve weeks. In immature collagen (figure 2A), the TSCu peak observed at -100°C disappears after dehydration while in mature collagen (figure 2B), both TSCu peaks at -115°C and +10°C are missing in the dehydrated sample.

TSCu relaxation mode in the tropocollagen units

The mode observed at the lowest temperature only in hydrated collagens, is located at -100°C in immature collagen and at -115°C in mature collagen. It corresponds to the β_2 relaxation investigated by S. Nomura et al. from dynamic mechanical experiments (1). It has been attributed to the double hydrogen bonded water located within the triple helix which has been previously observed from energy changes in the absorption of water by M. Pineri et al. (2). The plasticization of this mode during maturation might be due to a stabilization of the tropocollagen units.

Relaxation mode in the interhelical regions

The TSCu relaxation mode observed in immature collagens at -50°C corresponds to the β_1 mechanical relaxation (1). It is important to note here that water in excess of two molecules per peptide alters the X-ray pattern which is accommodated by lateral expansion of the collagen equatorial spacing has suggested to S. Nomura et al. (1) that this water is located in the interhelical regions. The ionic side chains involved in this mode might be cross-linked during maturation (3,4).

Relaxation mode in the interfibrillar regions

The TSCu relaxation mode observed around +10°C in immature collagen independently of the hydration level has been assigned to free and bound water located in the interfibrillar regions. In mature collagen this mode exists only in the hydrated samples showing the determinant effect of maturation at this stage of structural hierarchy.

REFERENCES

- (1) Nomura S., Hiltner A., Lando J.B. & Baer E. Biopolymers **16**, 231-46, (1977).
- (2) Pineri M., Escoubes M. & Roche G. Biopolymers **17**, 2799-2815, (1978)
- (3) Diamant J., Keller A., Baer E., Litt M. & Arridge B. Proc. Roy. Soc. London, **B180**, 293-315, (1972)
- (4) Betsch D.F. & Baer E. Biorheology, **17**, 83-94, (1980)

ACKNOWLEDGEMENT

This work was generously supported by the Centre National de la Recherche Scientifique (Sciences de la Vie).

[†] Laboratoire d'Anatomie Pathologie, Université Paul Sabatier, 31062 Toulouse Cédex, France

^{††} Centre d'Elaboration et d'Expérimentation de Matériaux et de Systèmes Implantables, INSERM 8031 Université de Bordeaux II, 33076 Bordeaux Cédex, France.

THE PERFORMANCE OF NEW COMPOSITE RESTORATIVE MATERIALS IN POSTERIOR TEETH

D. F. Williams and J. Cunningham

University of Liverpool
Liverpool, England.

Composite materials, typically a quartz-filled aromatic dimethacrylate, have gained universal acceptance as restorative materials for anterior teeth. They possess good aesthetic properties, can be manipulated and inserted into cavities fairly readily and are stable in the oral environment. Their use has, however, been largely restricted to the anterior part of the mouth since their mechanical properties, and especially abrasion resistance, have not been commensurate with the higher stresses associated with posterior teeth. There are many reasons for considering the use of composites in posterior teeth as alternatives to amalgam, including potentially much improved aesthetics and elimination of the dental mercury hazard, and the development of improved performance composites has been a priority in dental materials for a number of years (1).

One of the impediments to progress in this area has been the lack of acceptable techniques for the assessment of the performance of posterior restorative materials and the correlation between clinical performance and results of laboratory investigations.

The principle objectives of this programme of work have, therefore, been to develop a rigorous protocol for the assessment of posterior composite restorations and to use this protocol to evaluate a new type of composite material developed specifically for this purpose.

The composite used in this study was based on a urethane dimethacrylate that is command set by visible light. This material has been developed by Imperial Chemical Industries P.L.C. Two specific formulations were used, one which was radiopaque (A) and one radiolucent (B). Complete restorations were made with A whilst with B, a layering technique was employed in which A was placed in the cavity first and B used for the occlusal surface. The materials have been used to restore occlusal and proximo-occlusal cavities. Conventional amalgam cavities were cut and the enamel walls acid-etched and coated with a urethane dimethacrylate bonding agent. This and the composite resins were cured with visible light. To date 35 cavities have been filled with A and 17 using the layering technique. A further 15 cavities have been filled with non-gamma-two amalgam as controls.

Assessment has been by a combination of clinical and technical parameters. Using modified Ryge criteria, 18% of marginal sites with over one years service with A showed some deterioration compared to 12% for compound restorations and 20% for amalgams. No abrasive wear has been detected clinically in any restorations. Objective measurements of wear, using the laser dual source contouring methods previously reported (2) are currently being undertaken. The loss of excess marginal material was detected in 22% of the restorations of A but in none of the compound or amalgam fillings. No marked deterioration in gingival condition was observed in any group. Difficulty in achieving contact with the adjacent tooth occurred in 28% of cases with A, in 39% with compound restorations,

and 11% with amalgam. Radiopacity of A was less than that of amalgam, but very satisfactory for diagnostic purposes.

At patient recall, impressions have been taken of the restored teeth and their near neighbours and epoxy models made. These are being used for the laser dual source contouring to determine amounts of wear and for the observation of surface morphology in the scanning electron microscope. The limited data so far obtained with the early time periods has revealed little of clinical significance except for interesting observations on the accumulation of bacterial plaque on the surfaces. These more objective methods of assessment are expected to be most useful as restorations enter their second year of use.

It can be concluded at 12 months that the radiopaque composite (A) can be compared favourably to amalgam at 1 year. The composite B demonstrated superior clinical behaviour, although the lack of radiopacity is a limitation.

This study was supported by Imperial Chemical Industries P.L.C.

References

1. Williams, D. F. British Dental Journal. 1980. 150, 215-6.
2. Atkinson, J., Groves, D., Lalor, M., Cunningham, J. and Williams, D. F.. Wear. 1982. 76. 91-104.

Department of Dental Sciences
University of Liverpool
P. O. Box 147
Liverpool L69 3BX.

HYBRIDIZATION OF NATURAL TISSUES WITH BIOCOMPATIBLE
MATERIALS --- ADHESION TO TOOTH SUBSTRATES ---

N. Nakabayashi

Institute for Medical and Dental Engineering, Tokyo Medical
and Dental University, Surugadai, Kanda, Tokyo 101 Japan

Bonding of natural tissues with artificial materials is always important to connect artificial organs and dental prostheses. Generally, tissues would not accept foreign materials. Regeneration of tissues could be expected in soft tissues and bones. But it could not in teeth and we have to use artificial materials such as plastics, metals and/or ceramics to repair the defects. Metabolism of tissues is another important factor in the connection. Differences of physical properties between two components are also big problem to get good joint.

We could select plastics which have nearly the same Young's modulus as hard tissues. Then stress concentration at the interface could be minimized. On the other hand, stress concentration in the tissue side juncture is very severe in soft tissues and mechanical failure is often misunderstood as a lack of the biocompatibility.

I have been working on adhesives to hard tissues on the assumption that some of adhesive materials have something common with hard tissue compatible polymer and this information could also expand to the development of new biocompatible materials. Connection to decalcified dentin, adhesion to dentin pretreated, has been found to be the bonding of collagen with polymers.

Several new monomers which are effective to get adhesion to tooth substrates have been prepared based on the concept that monomers with hydrophobic and hydrophilic groups have biocompatibility with the tissues and promote the infiltration of monomers into the tissues. The bond between the tissues and polymers is taken place by the polymerization of the infiltrated monomers in situ.

Prepared monomers were 2-hydroxy-3- β -naphthoxypropyl methacrylate (HNPM), 2-methacryloxyethyl phenyl hydrogen phosphate (Phenyl-P) and 4-methacryloxyethyl trimellitate anhydride (4-META). The studied adhesives were MMA polymerized by TBB-O (MMA-TBB), and HNPM, Phenyl-P or 4-META added in MMA-TBB. The bond strength to etched enamel was controlled by the monomer composition and the etchant. The strength of HNPM/MMA-TBB was lower than MMA-TBB but the former gave better clinical data. SEM analyses suggested that HNPM promoted the monomer penetration and longer tags were observed. The penetration improved the stability. Average tag length of four adhesives was 11 μ in MMA-TBB, 16 μ in HNPM, 18 μ in Phenyl-P, and 23 μ in 4-META/MMA-TBB on phosphoric acid etched enamel. It decreased to 12 μ on 30% citric acid etched enamel in 4-META/MMA-TBB and was comparable to pure MMA on the phosphoric etched. It was

concluded that the prepared monomers in MMA promoted the penetration and good joints were obtained. Phosphoric acid etching of enamel which has been necessary can be deleted or we can use milder acids as citric acid in the adhesion to enamel with the application of amphipathic monomers.

Adhesion to dentin is much more complicated and interesting. Dentin consists of collagen, apatite and water. There are peritubular and intertubular dentin and tubules. Both chemical and solid structures play important role in the adhesion. Tag formation to tubules was main interest before. But the infiltration of monomers into dentin itself has changed the situation very much. Tags are not necessary to get adhesion to dentin. Structure of collagen is important to the bonding. Acid etching decreased the strength to 6 MPa and it was attributed to mechanical interlocking of tags in tubules. When we could minimize the denaturation of collagen during pretreatment of dentin for adhesion, high strength as 18 MPa was obtained. Ferric chloride prevented the denaturation. Modification of collagen in dentin with glutaraldehyde also suppressed the denaturation by acid. Monomers penetrated in peritubular and intertubular dentin polymerized in situ unified the dentin and the cured adhesive, and good adhesion was obtained.

The monomers infiltrated into dentin and polymerized was confirmed by SEM observation on partially demineralized specimen of adhered dentin (Fig. 1). There is a HCl insoluble resinous dentin band in the subsurface of dentin. The band is a resin reinforced dentin and has good resistance against decalcification. The band is a hybride of natural tissue with biocompatible artificial material.



Fig. 1 A partially demineralized fracture surface orthogonal to the joint surface (X2000). Tags (1) are seen in the hybrid (2) which is a porous band. Cured resin is 3 and demineralized dentin is 4.

Ref. J.Biomed.Mater.Res., 16,265,1982.

Comparative Evaluation of Recent Commercial Light Cured Composites

Samuel Waknine, J. Vaidyanathan and T.K. Vaidyanathan

New York University Dental Center, Dept. of Dental Materials
Science, 345 E. 24th St., New York, New York 10010

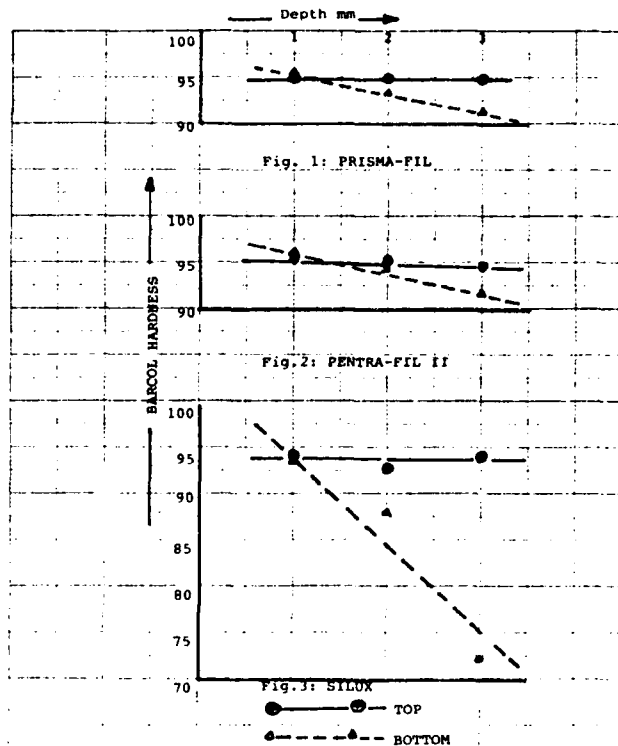
Recently, a large number of visible light cured composites have been introduced as dental restorative pastes. These contain three separate groups of filler particle size ranges which include the relatively coarse conventional particles, the more recent finer/hybrid particle types and the microfill system. There is a need to characterize and compare these different composite systems as to their physical and mechanical properties, water sorption, particle size, optical properties, etc. The objective of this investigation was to study different commercial composite systems with respect to their properties.

Eight different commercial composites covering the three groups of particle size ranges including different weight fractions and method of filler incorporation were studied. These included Heliolit, Durafill, VisioDisperse, Prisma, Silux, Command, Ultrafine, Visarfil and Pentrafil II. The filler fraction was extracted using methanol and/or dichloromethane solvents and subsequent gravity filtration. The average particle size of the filler was determined using a Fisher Sub Sieve Sizer Model #95. The properties of the composites were determined as per the ADA specification #27 for direct filling resins. These properties included the Diametral tensile strength (DTS), Barcol hardness (BH), depth of cure and water sorption. In addition compressive strength was also determined.

Particle size analysis revealed that the average particle size ranged from less than 1μ to a high of 20μ . The range of DTS values in psi shown by different composites are: Heliolit 4867 ± 270 ; Silux 5043 ± 130 ; Durafill 5374 ± 579 ; Visio Disperse 5803 ± 628 ; Visar-fil 6861 ± 176 ; Command Ultrafine 7213 ± 898 ; Prisma 7931 ± 943 ; Pentra-Fil II 7663 ± 294 . Compressive strength values ranged from 35,000 to 52,000 psi. Top and bottom BH values ranged from a low of 70 (Visio Disperse-bottom) to a high of 96 (Visar-fil-Top). Comparison of depth of cure characteristics is seen in figures 1, 2 and (3) indicating two extreme cases. The water sorption values of the different products ranged from a low of 0.31 mg/cm^2 to a high of 1.15 mg/cm^2 .

DTS, compressive strength, top and bottom Barcol hardness together with the depth of cure characteristics indicate that there is a significant correlation between the average particle size and the composite properties. In addition, the amount of filler fraction is also of significant effect on the DTS and compressive strength values. Analysis of the data also indicates that there is a particle size range of the filler that tends to optimize

the composite properties tested in this study.



BIOPHYSICAL STUDIES ON THE Sm-Co MAGNET AS A DENTAL MATERIAL.

M.S. ABD EL BASET.

Biochemistry Lab., National Research Centre, Dokki, Cairo, Egypt.

Recently it was established that the samarium - cobalt magnet possesses an excellent magnetic properties. Besides a very small Sm-Co magnets in the range of mm. gives forces similar to those obtained from Cm of another magnetic alloys. As known that the dental material must have high corrosion resistance. Thus the corrosion resistance of the magnet is tested in human saliva pH 7.8, 2% NaCl pH 5.3, 1% KCl pH 5.1, 0.1% HCl pH 2.2, 0.05% H_2SO_4 pH 2.1, 1% Lactic acid pH 2.3, 1% citric acid pH 2.35, 1% urea pH 6.2 and 0.5% guanidine hydrochloride pH 3.2. The effect of magnetic field on oxyhemoglobin was also studied.

The test piece was a rectangular prism of 25x15x3mm with a hole of 2mm in diameter. The pieces were washed by water and alcohol 96% and then suspended in the corrosive solutions at $37 \pm 1^\circ C$ for 7 days. Weight changes due to corrosion were measured periodically every day. The cleaned pieces were suspended also in Hb (2.8×10^{-5} M) at $4^\circ C$ for 12, 24, 36 and 48 hours and the absorption spectrum of Hb was recorded using automatic spectrophotometer Shimadzu. uv- 240 .

The obtained data revealed that, weight loss occurred rapidly in the beginning and reached to steady state after 4 days in the case of saliva, NaCl, and KCl. The average weight changes in these solutions were in the range 0.04-0.09 mg/cm² . Thus the corrosion resistance is considered high, when compared with the allowance in dental alloys.

Regarding to the other solutions it was found that, the weight loss increased gradually with increasing immersed time. The weight loss were in the order, $H_2SO_4 > HCl > Guanidine - HCl > citric acid > lactic acid > urea$.

As the magnetic force is 200 gw and HbO₂ contain iron in porphyrin, it is convenient to study the effect of magnetic field on the spin state of heme-iron. Thus the absorption spectrum was the way of this study. Also the constant of spin state and thermodynamic parameters were calculated. It was found that heme-heme interaction was affected slightly in the first two periods and significantly changed in the last exposure period. This result indicated that the spin state of heme iron (λ max. 578) may be converted to new position. When the magnet had been removed the spin state gradually returned to its normal state especially in the case of low time exposure. Whereas in the case of long time

exposure, the spin state returned to its normal state after 12 hrs. According to this result , it is safely to suggest that there are a reversible conformation states

Concerning the globin- heme interaction slight changes were obtained. It is due to the fact that the changes in heme parts lead to a consequent effect in globin. Attention should be drawn to the gradual decrease in Soret band (λ max. 410 nm). This decrement did not return to its original intensity after transferring the magnet. It was also found that the $\lambda_{578}/\lambda_{542}$ ratio was decreased gradually as compared with non exposure HbO₂ . This decrement was concomitant with the appearance of growing new band at 630 nm. These finding proved that HbO₂ was converted to Methemoglobin . The degree of conversion appeared as a function of exposure time. Thus the effect of magnetic force changes the oxidation reduction potential of the hemoprotein . This effect may be negligible in vivo if methemoglobin reductase system is normal .

Spin state constant decreased with a corresponding increase of free energy due to magnet effect . This result represents another prove of existing a different reversible conformation states. Regarding to ΔH and ΔS a negative values were detected as well as control .

The possibility of using Sm-Co magnet as a dental material is still needed a further studies in vitro and vivo. It needs a distribution map of cations and anions , besides the study of chronic exposure effect .

Biochemistry Lab., National Research Centre, Dokki , Cairo , Egypt.

POTENTIAL USE OF CALCIUM PHOSPHATES AS FILLERS IN COMPOSITE RESTORATIVE BIOMATERIALS.

R. Z. LeGeros and B. Penugonda

New York University Dental Center, New York, New York 10010.

Commercial composite restorative materials (e.g., Adaptic, Concise, Silar) consist principally of polymers (e.g., bis-GMA) and inorganic fillers (e.g., fused silica, crystalline quartz, lithium-aluminum silicate and borosilicate glass). The biological composites (e.g., bone, dentine, enamel, pathological calcifications), on the other hand, are composed mainly of a biopolymer and a calcium phosphate filler (collagen and calcium-hydroxy apatite, respectively, in the cases of bone, dentine, and cementum).

The purpose of this study was to explore the possibility of using calcium phosphates [apatites and related calcium phosphates such as tricalcium phosphate (TCP), dibasic calcium phosphate (DCP), etc] as fillers in new composite restorative biomaterials. Unfilled resin (Delton from Johnson & Johnson) was used in most of the experiments. Other self-curing polymers (Aurafil, Command) and light-cured resins were also tried. The polymer/calcium phosphate (CP) composites were prepared using a paste-to-paste system in the case of self-curing resins. The polymer/CP ratio ranged from 50/50 to 20/80 by weight. The resulting composite was tested for working/setting time, hardness, diametral tensile strength, compressive strength and water sorption (37°C, 24h).

Preliminary observations: (a) setting time = 8 min.; (b) minimum working time = 1.5 min; (c) hardness - up to 93 (on Barcol instrument); (d) diametral tensile strength - up to 3992 psi after 1h, 3864 psi after 24h; (e) polymer/CP ratio (by weight) up to 25/75; (f) stability in distilled water (absence of leaching out); (g) aesthetically pleasing; (h) opaque to x-rays; (i) SEM shows smooth surface.

A distinct advantage of using calcium phosphate as the inorganic filler over those used in commercial composites is the elimination of the costly process of syllination with a coupling agent. Other obvious advantages besides those observed in this study are biocompatibility and similarity in properties with the inorganic phases of calcified tissues (teeth and bones) which should allow intergrowth with the bone and tooth structures.

These very preliminary results indicate that calcium phosphates (apatite, B-TCP, DCP) as fillers for composite have good potential for success and warrants further investigation. Such composites should have properties best approximating the biological composites and would be useful as restorative and as tooth implant biomaterials.

Ref.: Lambrechts, P.: Basic Properties of Dental Composites and their Impacts on Clinical Performance. Ph.D. Thesis, Katholieke Universiteit, Leuven, 1983.

LeGeros, RZ: Apatites in Biological Systems. Prog. Crystal Growth & Character. 4:1-45, 1981

Professional collaboration: Drs. A. Chohayeb, S. Wakin, TK Vaidyanathan, A. Schulman; discussions with Drs. R. Norman (USI), HR Rawles (LSU), H. Horn (NYU); tech. asst: DJ LeGeros. Supported by BSRG and Departmental funds (NYU).

WATER SORPTION OF POLYMER COMPOSITES WITH 4-METHACRYLOXYETHYL
TRIMELLITIC ANHYDRIDE (4-META)

D.T. Turner and K. Nagata *

Department of Operative Dentistry, and Dental Research Center,
University of North Carolina, Chapel Hill, NC

Composites of ceramics in a polymer matrix are used to restore teeth and as implants. In order to improve mechanical properties, it is important to get good coupling between the two components. Currently, this is done by prior treatment of the ceramic with various silanes but this method has limitations and so the search for coupling agents continues. Recently it has been reported that inclusion in the monomer of 4-META increases the mechanical strength of certain composites and it was suggested that this was due to coupling (Atsuta et al., J. Biomed. Mater. Res. 16 (1982) 619 et seq.). The purpose of the present work is to evaluate this suggestion using water as a penetrant.

Benzoyl peroxide (2 wt-%) was dissolved in triethylene glycol dimethacrylate (TGDM). In some cases the TGDM included 4-META (5%) as comonomer. Powders were added by spatulation to give smooth pastes containing a hydroxyapatite (HA, 50%) and a silanated lithium aluminum silicate (SS, 75%). Specimens of thickness ca 0.1 cm were immersed in water and weighed periodically to allow estimation of a diffusion coefficient (D) and a limiting value of sorption (c.f. Turner, Polymer 23 (1982) 197). Analysis of early runs was complicated by loss of extractibles and the results in Table 1 were obtained from a fifth run, made after two cycles of wetting and drying.

Table 1 Values of Diffusion Coefficient and Water Sorption (37°C)

Additive	No 4-META		5% 4-META	
	D(cm ² S ⁻¹) x10 ⁸	Sorption (%)	D(cm ² S ⁻¹) x10 ⁸	Sorption (%)
None	2.8	7.15	2.8	7.45
HA (50%)	2.7	4.20	1.8	3.90
SS (75%)	0.8	1.75	0.6	1.90

The value of D is expected to be significantly smaller in a composite if there is effective interfacial coupling, on account of the greater tortuosity factor. This is found to be the case for the SS-composite but not for the HA-composite (column 2). The finding that inclusion of 4-META in the HA-composite reduces D is consistent with the suggestion that it acts as a coupling agent. A similar inference can be made by comparison of experimental values of sorption with ones calculated on the assumption that only the polymer takes up water. Agreement with this assumption is found for the SS-composite but not for the HA-composite which, presumably, can accommodate additional water at the interface (Table 2; column 4). This additional water accommodation is reduced by use of 4-META (column 7).

Table 2 Comparison of Experimental and Calculated Values of Water Sorption (%)

Additive	No 4-META			5% 4-META		
	exp.	calc.	excess over exp. (%)	exp.	calc.	excess over exp. (%)
None	7.15	--	--	7.45	--	--
HA (50%)	4.20	3.58	17	3.90	3.73	5
SS (75%)	1.75	1.79	-2	1.90	1.86	2

In conclusion, both the kinetics and equilibrium uptake of water are consistent with the suggestion that 4-META can act as a coupling agent between hydroxyapatite and a network made from a dimethacrylate monomer. Experiments continue in order to test the long term performance of 4-META.

More generally, this information is important because of the increasing use of 4-META in dental adhesives.

This work was supported by NIH grants DE-02668 and RR-05333 (DTT) and by Tsurumi University (KN).

Department of Operative Dentistry and Dental Research Center, University of North Carolina, Chapel Hill, NC 27514 USA.

*Chemistry Department, Tsurumi University, 2-1-3 Tsurumi, Tsurumi-Ku, Yokohama, Japan 230.

THE ADHESION MECHANISM OF DENTAL CEMENTS CONTAINING POLYACRYLIC ACID -CHEMICAL ANALYSIS BY ESCA-

T.Nasu, K.Nagaoka, F.Ito* and K.Suzuki*

Faculty of Education, Yamagata University
Yamagata, Japan

1. Introduction

The adhesive force to human tooth and metallic restoration of dental cements which contain polyacrylic acid (to be clipped P.A.A.) are stronger than that of the former cements. D.C.Smith proposed the model of the adhesion mechanism of these cements to tooth surface and metals. But few experiment have been performed concerning the chemical interaction between the carboxylate groups of P.A.A. and metals. We studied the chemical interaction between metals and the carboxylate groups of P.A.A. at the interface by ESCA combined with Ar^+ ion sputtering method to examine the mechanism of adhesion.

2. Experimental

The samples for the ESCA method were as follows. Liquid was a 2.5% aqueous solution of polyacrylic acid. Metal plates of Au, Pt, Ag, Cu, Co, Cr, Sn and In which were the elements of dental alloy were shaped $6 \times 15 \times 0.5 \text{ mm}$. Ar^+ ion sputtering was performed to the metal plate coated with P.A.A. to scrape the P.A.A. very slowly in the sample chamber of the ESCA equipment. After a few minutes of sputtering, ESCA spectra were measured. The sputtering and ESCA measurement were repeated alternately. When P.A.A. vanished from the metal surface by the sputtering, the ESCA measurement was concluded. Thus chemical states of metal near the interface between P.A.A. and metal were analyzed.

3. Results and discussion

The ESCA spectra of Au coated with P.A.A. is illustrated in Fig.1.

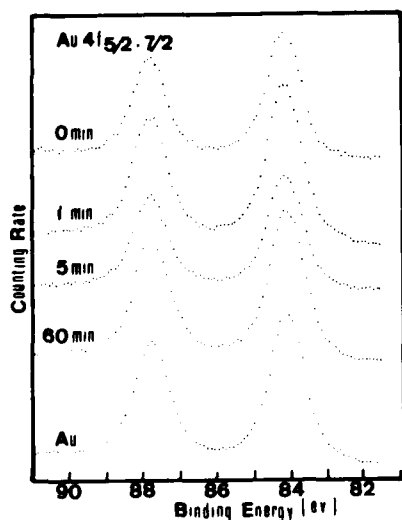


Fig.1 ESCA spectra of Au $4f_{5/2}$, $4f_{7/2}$ levels of Au coated with P.A.A. and sputtered with Ar^+ ions 0 min, 1 min, 5 min, and 60 min.

Profile of the spectrum and binding energy of $4f_{5/2}$ and $4f_{7/2}$ of the Au coated with P.A.A. did not change by the Ar^+ ion sputtering, and was same as no coated one. The change of ESCA spectra of Pt coated with P.A.A. by sputtering was same manner as Au. These aspects of spectra corresponded to the McLean's results which showed that these cements had very small adhesive strength to Au and Pt, but strong adhesive force to tinned Au and Pt. The ESCA spectra of Sn coated with P.A.A. is illustrated in Fig.2.

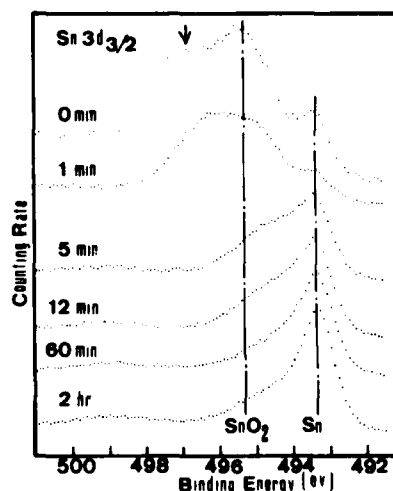


Fig.2 ESCA spectra of Sn $3d_{3/2}$ level of Sn coated with P.A.A. and sputtered with Ar^+ ion 0 min, 1 min, 5 min, 12 min, 60 min and 2 hr.

There were three chemical states on it. The lowest binding energy peak was assigned to pure Sn. The middle one was assigned to SnO_2 . The highest one (arrow marked in Fig.2) was assigned to Sn combined with carboxylate groups of P.A.A. The chemical reaction corresponding to the highest binding energy peak seems to contribute to the strong adhesive force of these cements to Sn.

ACKNOWLEDGEMENT The authors acknowledge that Faculty of Education, Yamagata University supported this contribution.

Section of Technology, Faculty of Education, Yamagata University, Koshirakawa Yamagata 990 Japan

*The Research Institute for Iron, Steel and Other Metals, Tohoku University, Sendai 980 Japan

A BIOMECHANICAL STUDY OF GOLD AND NICKEL-BASED DENTAL BRIDGE SYSTEMS UTILIZING DISTAL ABUTMENT DENTAL IMPLANTS

M. W. Bidez, J. E. Lemons*, B. P. Isenberg**

University of Alabama in Birmingham
Birmingham, Alabama 35294

Dental implant design and material composition, as well as the degree of relative motion of the implant, have been cited as causative factors in determining the clinical success or failure of a dental implant. Differences in loading patterns for free-standing vs. multiply abutting implants have also been reported, but without respect to the possible role of varying the bridge material. To date, there have been no published studies investigating the effect of varying implant design and bridge material in the same experimental series in order to gain insight into the relative motion exhibited by the entire system as a function of both parameters.

The primary purpose of this investigation was to obtain quantitative data regarding the relative displacements exhibited by the distal (2nd molar) and mesial (canine) abutments in a five unit fixed dental bridge under controlled force application as a function of bridge material and implant design utilized in the distal abutment site.

Six systems were tested:

1. Au (modified type III; ORY gold, Jeneric Gold Co.) bridge utilizing a natural 2nd molar as the distal abutment.
2. NiCr base (Rexillum, Jeneric Gold Co.) bridge utilizing a natural 2nd molar as the distal abutment.
3. Au bridge utilizing a blade implant (L4S model, Ora-tronics, Inc.) as the distal abutment.
4. NiCr bridge utilizing a blade implant as the distal abutment.
5. Au bridge utilizing a Hollow-Basket implant (Colmed, Inc.) as the distal abutment.
6. NiCr bridge utilizing a Hollow-Basket implant as the distal abutment.

A completely dentulous, dry human mandible was used as the experimental model, and a pseudo-periodontal ligament (PDL) was constructed from a precisely formulated polyurethane ($E = 976.4$ psi) within the mandible's abutment sites. The 2nd bicuspid, 1st molar, and 3rd molar were extracted bilaterally, and their extraction sites filled with degassed PMMA ($E = 3 \times 10^5$ psi) to simulate trabecular bone. A force transfer system was constructed from Epon 828 resin on the occlusal surface of the distal abutment bilaterally to achieve a relatively even force distribution. Bridges were constructed of Au and NiCr to precisely fit the prepared mandible, and stabilization was achieved with IRM temporary dental cement to allow for easy removal of the bridges as the experimental protocol dictated. The basket implant was placed into the mandible with a simulated direct bone interface (degassed PMMA) and the blade implant with a pseudo-fibrous tissue encapsulation constructed of Silastic 382 ($E = 327$ psi).

An Instron machine was used as a controlled force application device, and a specially designed base platform to house the experimental model was constructed to fit on the compression load cell. Three dial gauges (precise to 0.001 in.) were positioned in orthogonal directions around each abutment site bilaterally to provide displacement data in the x (mesial/distal), y (buccal/lingual), and z (occlu-

sal/gingival) directions. Compression loads of 40# and 80# were applied to the distal abutments of each bridge system under bilateral (simulated bruxism) and right and left unilateral loading (simulated mastication) conditions as well as a 10# bilateral tensile (simulated bruxism) load. Each experimental series was repeated 10 times to ensure reproducibility.

A rectangular beam model provided a simplistic and valid means of characterizing the displacement of a five unit fixed dental bridge under compression loading in the z (occlusal/gingival) directions at both the distal and mesial abutment sites with reactant forces, R_1 and R_2 , at the distal and mesial abutment sites, respectively. The reactant force R_1 may be considered to be a function of the interfacial morphologies characteristic of a given implant which affects the relative z displacement exhibited by the system at the mesial abutment sites. As predicted by the beam model and substantiated by experimental results, a more flexible material (Au) will exhibit displacement in the +z direction mesially under a high load applied distally as compared to a less flexible material (NiCr) which tends to induce -z displacement at the mesial abutment.

The results of a two-way classification analysis of variance indicated statistically significant differences existed in the occlusal/gingival (z) displacements exhibited at all abutment sites with respect to abutment type and at all mesial abutment sites with respect to bridge material. Significant differences existed in the buccal/lingual (y) displacements exhibited at all abutment sites for abutment type. The NiCr bridges showed a consistent trend of greater displacements at the mesial abutment sites compared with the Au bridges for all abutment types. The Au bridges showed a consistent trend of displacements at the distal abutment sites greater than or equal to the NiCr bridges for all abutment types. The magnitudes of result displacements showed the blade implant systems to consistently exhibit the greatest displacements at the distal abutment sites, while the basket implant systems exhibited the greatest displacements at the mesial abutment sites. Due to the simulated fibrous tissue interface characterizing the blade implant bridge systems, the mesial abutment tends to extrude for both bridge materials tested.

This work was supported by a grant from the Alabama Dental Implant Study Group.

Department of Biomedical Engineering

* Department of Biomaterials, University of Alabama in Birmingham, Birmingham, Alabama 35294

** Department of Operative Dentistry, University of Alabama in Birmingham, Birmingham, Alabama 35294

THE EFFECT OF METHACRYLATE ON THE PHYSICAL PROPERTIES OF POLY(FLUOROALKOXY)PHOSPHAZINE ELASTOMER

P.H. Gebert, M.R. Capezza, H.R. Rawls, J.K. Smith, and L. Gettleman

Gulf South Research Institute,
P.O. Box 26518
New Orleans, LA 70186-6518 USA

The utility of poly(fluoroalkoxy)phosphazine elastomer (PNF-200, Firestone) as a permanent soft denture liner has previously been demonstrated (1-4). In an attempt to optimize the physical parameters of PNF elastomer formulations, the effects of methyl methacrylate (MMA) and butyl methacrylate (BMA) monomer concentration on hardness, tensile strength, elongation, tensile stress at 100% elongation (100% modulus), peel strength, and water sorption were investigated. Incorporation of methacrylates has been used in the past to improve the bonding to poly(methyl methacrylate) (PMMA) baseplates of removable dentures.

Uncured PNF/methacrylate samples were blended and analyzed for MMA or BMA by gas chromatography immediately prior to test specimen preparation. For this study, test samples were prepared using a rectangular PMMA (Lucitone-199) baseplate to which were bonded PNF/methacrylate elastomer test strips approximately 3.5 mm X 7.5 mm X 75 mm. Baseplate and elastomer test strips were cured simultaneously in a dental flask under standard conditions (1.5 hours at 74°C and then 0.5 hours at 100°C).

The resultant PMMA-backed elastomer test strips routinely reached peel strengths of 3000-4000 newtons/meter (N/m) using ASTM D 903 which proved sufficiently strong for the intended end use (5). Tensile strength, elongation, and 100% modulus data were also derived from an Instron test machine at a crosshead speed of 10 cm/min. Most notable was a dramatic improvement in tensile strength and elongation as a result of increasing MMA concentration. Cured unblended PNF itself is unsuitable as a denture liner material because it is too soft and exhibits very low peel strength. Durometer A hardness measurements (ASTM D 2240) showed rapidly increasing values with increasing MMA concentrations. A hardness of 40-50 is a desirable range for a soft denture liner, combining adequate cushioning of biting forces with the ability to grind and polish the liner. Unmodified PNF has a hardness of 15 when cured under dental conditions.

Butyl methacrylate additions did not markedly improve the test parameters although hardness paralleled that of MMA with increasing additions of monomer. The texture and appearance of tested PNF/BMA samples were not acceptable.

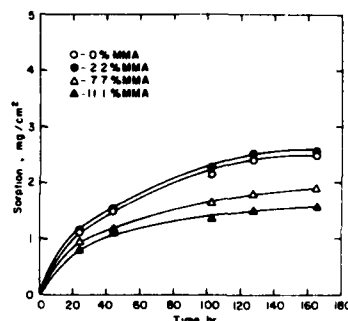
Initial data on sorption (ADA 12) as expressed in mg/cm² indicate that uptake of water decreases with increasing monomer content, with relatively small differences seen between MMA or BMA. Long term water sorption tests are currently in progress as are sorption and dimensional stability at an elevated temperature (60°C). Initial results indicate acceptable sorption values for a soft liner material (1-2 mg/cm²) and good dimensional stability.

In summary, the suitability of PNF elastomer as a permanent soft denture liner material is greatly improved by the addition of MMA monomer resulting in physical properties substantially improved over the original elastomer.

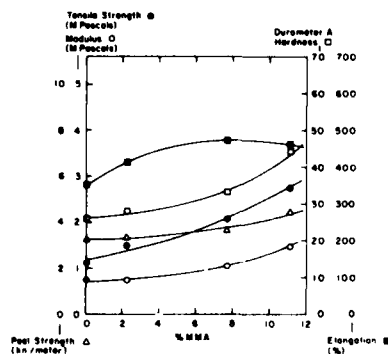
Supported by research grant No. DE04814 from the National Institute of Dental Research, Bethesda, Maryland.

References

1. May, P.D., Farris, C.L., Gettleman, L., Holland, F.F., and Cabasso, I. IADR Abstracts, No. 507, 1981.
2. Gettleman, L., LeBoeuf, R.J., Jr., and Rawls, H.R., AADR Abstracts, No. 725, 1983.
3. Gettleman, L., LeBoeuf, R.J., Jr., and Rawls, H.R., Soc. for Biomat. Transactions, No. 71, 1983.
4. May, P., and Guerra, L.R.: Phosphonitrilic Fluoroelastomer Lined Denture. U.S. Patent No. 4,251,215, Feb. 17, 1981.
5. Wright, P.S.: J. Dent., 9:3:210-223, 1981



The effect of MMA on water sorption of PNF elastomer.



The effect of MMA on the physical properties of PNF elastomer.

A Comparative Study of the Modulus of Rupture of Several Commercial Porcelains

M.B. Smyth, N. Sumithra, S. Waknine, M. Traiger

New York University Dental Center, Dept. of Dental Materials
Science, 345 East 24th Street, New York, New York 10010

Very limited research has been done on dental porcelain in general and on its strength in particular. This paper is a preliminary study of the strength of dental porcelains by measuring the modulus of rupture of several commercially available body porcelains. These measurements will be the bases for future development of stronger porcelains.

Six commercial porcelains; Vita, Ceramco, Biobond, Micro-bond, Pencraft and Will-Ceram were used in this study.

The specimens were prepared by pressing 6.0 gms of powder into rectangular bars in a stainless steel mold using a hydraulic press. The specimens were fired in a dental furnace following manufacturer's recommendations. Ten samples were made of each porcelain.

The Modulus of Rupture tests were carried out according to ASTM designation #C674-71. This is the fastest and most precise measurement. An Instron machine was used with a three point load assembly as shown in Fig. 1. The cross-head speed used was 0.002"/min. The formula used for calculating the results is

$$MOR = \frac{3PL}{2bd^2} \text{ in lbs/sq in}$$

where P = load in lbs.
L = distance between supports
in inches
b = width in inches
d = depth in inches

The results range from about 8000 to a little over 9,000 psi

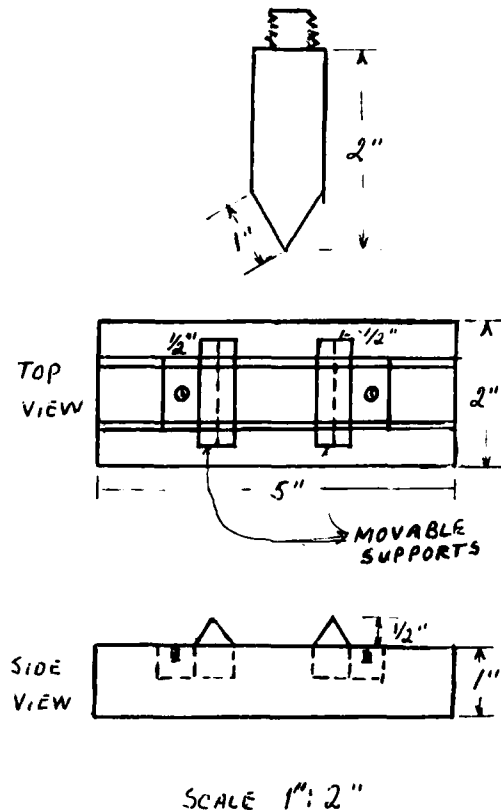


Fig. 1 Three point Load Assembly for Testing Modulus of Rupture of Dental Porcelain Using an Instron Machine.

USE OF FREEZE-DRIED DURA AS A MENISCUS REPLACEMENT IN TEMPOROMANDIBULAR
JOINT SURGERY.

Stringer, D. E., D.D.S., Boyne, P. J., D.M.D., Shafqat, J. P., D.D.S.

Oral & Maxillofacial Surgery Section, Loma Linda University Medical Center,
Loma Linda, California

Freeze-dried allogeneic dura has been used in various types of reconstructive oral and maxillofacial surgical procedures as a soft tissue replacement. In the treatment of temporomandibular joint bony ankylosis by gap and interpositional arthroplasty, freeze-dried dura has been used by Boyne as a substitute for alloplastic materials such as silastic. In order to evaluate the use of freeze-dried dura as a replacement for the meniscus removed for internal derangements of temporomandibular joints presenting with non-ankylosed and functioning condyle heads, a series of 22 cases were operated presenting with preoperative signs of temporomandibular joint meniscus abnormalities and or perforations. The patients at surgery were found to have perforations of the meniscus consistent with the preoperative arthrograms and the clinical evaluation. The meniscus was removed in each case and replaced by a cap of freeze-dried dura placed over the end of the condyle and secured by a purse-string suture and by a wire ligature placed around and through the condylar neck. The patients were allowed to function and to move the mandible on the first postoperative day, functioning on a soft diet for two weeks time and being gradually advanced to a regular diet. Eighty percent of the patients following the LLUMC pain scale were found to be pain free. The remaining 20% had varying degrees of postoperative pain return of which approximately two cases had no improvement in overall comfort and function.

Clinically, there was no slipping of the dura, no increased popping or grating of the joint, and no evidence of loss of the dura or return to bone surface to bone surface joint abrasion. Radiographically, the joints appear to be functioning in a normal manner.

This clinical use of the freeze-dried dura parallels studies of the use of dura in animals in temporomandibular joint surgery and in oral-antral closures in which it was found histologically that the dura was replaced by normal, heavy connective tissue of the host at the recipient site. It is believed that the same situation occurs in these clinical patients. Initial preliminary evaluation of the patient over a two year period has indicated that more extensive use of the material should be undertaken on a long-term basis to determine the effectiveness of the dura as the biological replacement material for the pathologically destroyed meniscus.

Dale E. Stringer, D.D.S.
Oral & Maxillofacial Surgery Section
Department of Surgery, Room 2585
Loma Linda University Medical Center
Loma Linda, California 92350

REPLICATION OF THE MORPHOLOGY OF JAW BONES THROUGH HIGH TECHNOLOGY

H.P. Truitt and R. A. James

Loma Linda University
Loma Linda, CA

Many dentists have provided patients with subperiosteal dental implants over the past 30 years in order to enable those patients to function with their mouths more comfortably and more securely. Gershkoff and Goldberg in 1949, were the first in this country to report on the use of these devices. They utilized an altered cast technique in order to fabricate an implant which would approximate the contour of the bone. Most early attempts following their technique were unsuccessful due to the poor fit of the implant to the bone, and by 1952 direct bony impressions of the mandible had become the accepted technique being followed by the early pioneers in this field. This involved extensive oral surgery which basically has changed very little up to the present time. This work has been initiated in an effort to eliminate the need for the extensive surgery necessary to obtain a direct bone impression.

Computerized Axial Tomography (CAT) has been employed in an attempt to achieve this goal. The steps have involved, (1) developing programs to match the CAT scan images to exact one-to-one dimensions, (2) developing programs to interface with a mill to develop plates which correspond with each scan, (3) developing programs to key each plate and the construction of a model of the jaw bone by assembling all of the plates.

Initial work was done on cadaver heads and attempts made to replicate the morphology of the mandible. Models were made, implants constructed, the mandibles dissected from the cadavers and the fit of the implants to the bone was evaluated. Results have shown the method to be sufficiently accurate to proceed to human studies.

These authors see this as the most significant advance in the field of subperiosteal implantology since the development of the techniques by Gershkoff and Goldberg.

H.P. Truitt
Loma Linda University
School of Dentistry
Loma Linda, CA 92350

HISTOLOGICAL STUDY OF IN VIVO WEAR OF TITANIUM ALLOY TOTAL HIP PROSTHESES

T.A. Gruen, C.W. Smith, C.P. Schwinn, and A. Sarmiento

Department of Orthopaedics and Pathology
University of Southern California
Bone and Connective Tissue Research Program
Orthopaedic Hospital-U.S.C.

Introduction:

In vivo wear of total hip replacements remains to be seen as a major complication with respect to the implant's longevity. In-vitro wear testing, particularly for titanium alloy (Ti-6Al-4V) articulating with UHMW polyethylene, has been paradoxical, which may be due to the variations in the test methodology and differences in wear measurements (1). Some studies done with intentional contamination by acrylic cement debris have indicated that titanium alloy may not be a satisfactory bearing surface (2). These results have convinced some implant manufacturers to improve surface treatments or to use other materials for the femoral head. So far as is known, there is no published data on histological evaluation of periarticular tissues from any clinical series of total hip replacements with Ti-6Al-4V femoral components articulating with polyethylene acetabular components. The purpose of this study is to assess the presence of any particulate debris, metallic or polymeric, and their histological reactions in view of the concern of in vivo wear.

Materials and Method

Nine STH total hip replacements (Ti-6Al-4V on polyethylene) were reoperated for various reasons between December 1975 and September 1983. Periarticular tissue specimens were obtained for eight of the nine cases and submitted for routine pathology. The hematoxylin and eosin stained sections were examined with transmitted and polarized light microscopy for the presence of debris (metallic, polyethylene, or acrylic cement) and presence of histological reactions (acute and/or chronic inflammation, foreign body giant cells, and debris-laden histiocytes). These were graded in a semi-quantitative manner as described by Mirra et al. (1976). Clinical, radiographic, and intraoperative findings were also obtained for these eight cases.

Results:

The reasons for reoperation were: femoral component loosening (n=6), trochanteric advancement for recurrent subluxation (n=1), and plate removal following healed fracture of the femoral shaft (n=1). The average time from

surgery to reoperation was 32.3 months (range 12-57).

Intraoperative visual examination revealed neither grey discoloration of the soft tissues or joint fluid nor any obvious wear of the femoral head bearing surfaces.

The histological findings in these eight cases for particulate debris were: metallic (0 of 8), polyethylene (4 of 8), and acrylic (7 of 8). The tissue reactions were: acute inflammation (0 of 8), chronic inflammation (2 of 8), debris-laden histiocytes (6 of 8), and foreign body giant cells (5 of 8). No metallic particles were seen in any of the sections, acrylic cement debris was noticed in almost all of the cases. This appears to indicate a lack of obvious abrasive wear of the titanium alloy bearing surfaces over the time period examined.

Comparing the data with those by Mirra et al. (3), who evaluated eight non-infected Co-Cr-Mo alloy on polyethylene THRs, the results were similar with respect to polymeric debris and tissue reaction. The most noticeable difference was the absence of metallic debris in this titanium alloy series, whereas metal debris was seen in all eight Co-Cr-Mo/polyethylene THRs.

The difference between the laboratory and clinical wear resistance of titanium alloy may be due to biochemical and/or physiological loading conditions. The less severe in-vivo conditions may favor maintaining the mechanical integrity of the titanium alloy bearing surface passive layer.

(1) Clarke, et al., Titanium Alloys in Surgical Implants, ASTM STP 796, p. 136, 1983.

(2) McKellop, et al., Trans. Orthop. Res. Soc., 5: 96, 1980.

(3) Mirra et al., Clin. Orthop., 117: 221, 1976.

Address: Orthopaedic Biomechanics
Orthopaedic Hospital-USC
2400 S. Flower Street
Los Angeles, CA 90007

Particle Size Distribution of Wear Debris from Polyethylene and
Carbon Reinforced Acetabular Components

Stern, L.S., Manley, M.T., Parr, J. *

State University of New York at Stony Brook, Stony Brook, N.Y. 11794

Studies on component wear in total joint replacement have tended to concentrate on measurements of wear rate, surface damage and creep (1,2). Comparisons of wear rates and creep in polyethylene and carbon reinforced polyethylene (Poly 2) components have shown differences in their performance in vitro (2,3). However, particulate size distribution profiles which would more adequately characterize the comparative wear performance of these components have not been reported.

The objective of this study was thus to quantitate and compare the size distribution of particulate wear debris collected from polyethylene and poly-2 acetabular components after extended wear testing in a hip joint simulator.

MATERIALS

Wear tests were conducted on 6 poly-2 acetabular components and 6 UHMWPE components. Both types of acetabuli were moulded components with a 32mm diameter socket. Mating femoral components were Cr/Co or titanium alloy. Bovine serum or ds.H2O was used as the lubricant. Each acetabular component was subjected to a minimum of 1.5M wear cycles. The serum lubricant and debris were collected and frozen; the ds. H2O samples were passed through 0.8 micron acetate filters to collect the particulate matter.

METHODS

Serum samples were first acid treated, centrifuged and resuspended in ds. H2O. Filtered debris was resuspended by dissolving the filter paper in acetone. Samples were allowed to stand overnight before final separation of the ppt and solute by decanting.

The larger wear particles contained in the ppt were placed on aluminum stubs and analyzed by SEM. Polyethylene particles were identified by illumination with polarized light. A 1mm x 1mm area of debris was imaged and compared to micrographs of latex beads of known size on a digitizing pad. The maximum diameter and the area of the imaged wear particles were quantitated.

The solutes were diluted 50:1 with appropriate solvent and analyzed by particle counter (HIAC PA-720) while magnetically stirred.

RESULTS

SEM: Comparison of micrographs showed that the UHMWPE debris contained large sheet-like flakes of polymer with particle dimensions as large as 300 microns (Fig. 1A). Poly-2 debris clearly showed carbon fiber particles of various lengths (Fig. 1B). The lengths of these free fibers were generally in the 60 - 200 micron range. Large sheets of poly-

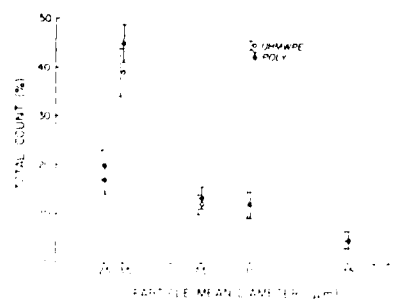
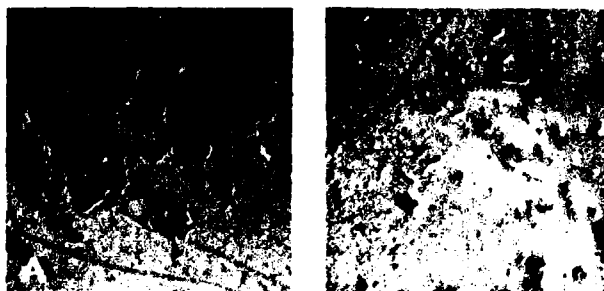
ethylene debris were not present in the Poly-2 samples.

PARTICLE ANALYZER: In order to resolve data in the lower particle size range, (less than 50um) the smaller particles remaining in the solute were analyzed by particle counter. The comparative distribution of Poly 2 and UHMWPE debris is shown in the Fig. 2. While there was some variation in size distribution among individual samples, the pooled distributions for Poly-2 and UHMWPE debris showed that the majority of particles in the solutes were in the 3-10 micron size range.

DISCUSSION

These data indicate that the size distribution of wear particles recovered from UHMWPE components is dissimilar in the larger size ranges (greater than 50um) than that seen in the Poly-2 samples. The debris from the UHMWPE cups imaged by SEM, appeared to have been peeled as sheets from the surface of the polymeric component. Sheet type debris was not seen in the Poly-2 specimens. This is presumably because the carbon fibers in the composite cups acted as "rip-stops", during the wear/abrasion process, thereby reducing the potential size of polymeric particles.

- 1) McKellop, H., Clarke, I., Markolf, K., Amstutz, H. J. Biomed. Mat. Res. V 15:619-653:1981
 - 2) Rose, R, et al. JBJS V 62-A:537-549:1980
 - 3) Farling G., Bardos D. Proc. 3rd Conf. Materials, Keele, U.K. 1978
- *Zimmer, Warsaw, Indiana



IN-VIVO EVALUATION OF TISSUE TOLERANCE TO PTFE-GRAFTED POLYETHYLENE PARTICLES

HOMERIN M., CHRISTEL P., DRYLL A., GAUSSENS G.

LABORATOIRE DE RECHERCHES ORTHOPEDIQUES - Faculté de Médecine Lariboisière-Saint-Louis, Paris - FRANCE.

INTRODUCTION : In an attempt to enhance the mechanical properties of prosthetic replacement devices, investigation concerns two neighbouring fields : on the one hand, discovery and development of new materials and on the other hand, improvement of those currently used. Considering the latter, any amelioration of a well known material should only arise without affecting its other qualities, particularly biological.

In this work are compared the tissue reactions to the particles of such a modified material, i.e. polytetrafluoroethylene-grafted (PTFE) and reticulated polyethylene, with the particles of a reference material U.H.M.W. polyethylene.

MATERIALS AND METHODS : The PTFE-grafted and reticulated polyethylene was developed by means of ionizing beam energy. The wear debris were obtained by grinding a hip socket with several files of different grain size and pounding the chips collected in a Multifix ball-mill for 17 hours. The particles were then placed in a sieve with ethanol medium and split into two grain size distributions, i.e. 5 to 20 μ m and less than 5 μ m. The control particles of UHMW polyethylene were prepared through exactly the same procedure from a standard non irradiated commercial cup. These different powders exhibited characteristics appearing hereunder :

	Particles 5-20 μ m		Particles <5 μ m	
	PTFE-PE	PE	PTFE-PE	PE
Shape	round/square 100 %	round long	78% 15%	round 100%
Size	10-20 μ m 20% 5-10 μ m 40% <5 μ m 40%	10-20 μ m 20% 5-10 μ m 40% <5 μ m 40%	2-5 μ m 50% <2 μ m 50%	2-5 μ m 75% <2 μ m 25%
Weight	20 mg	20 mg	8 mg	8 mg

The powders were eventually divided in flasks under inert atmosphere (nitrogen) and sterilized by gamma-irradiation (2.5 Mrad).

24 male New-Zealand rabbits were implanted with the powders suspended in 1 cc of saline. The identification of the flasks was randomized, in such a manner that the injections performed intra articularly (knee) and intra muscularly would both be of the PTFE-grafted polyethylene of one grain size distribution on one side, and of the control polyethylene of the same grain size distribution on the other. The animals were killed at 1, 4, 16 and 26 weeks. After in vivo glutaraldehyde fixation, several synovial villousities were excised for transmission electron microscopy examination. The synovial membranes were then removed, as also the implanted muscles, and processed for histological evaluation by means of methylmethacrylate embedding. The tissue reaction was estimated through different criteria, each invested with a specific mark : thickness of synovial mesothelium, turn-over of synoviocytes, lymphoplasmocytic and histiocytic infiltrates,

vascularization and fibrous stiffening. Each synovium was eventually reported on one mark, mean of all sections examined. These marks were then analyzed after the code clue had been given. Muscular findings evaluation was simplified.

RESULTS : Optical microscope examination of the synovium one week after implantation showed a much stronger reaction towards the bigger particles, but no evidence of any behaviour discrepancy between the two polyethylenes. The tissue reaction in both cases was remarkably located in patches throughout the synovium : diffuse inflammatory thickening of the border up to 15 layers of cells with slight lymphoplasmocytic infiltrates, intense giant cell formation and trapping of the particles in granulomas.

The four-week response showed a clear drop of the size-related reactivity, as also for those of the further terms. The local reaction was mainly granulomatous with evidence of migration of the smaller particles and fibrous infiltration.

The 16 and 26 week responses exhibited the remarkable continuance of local acute reaction, the increase of collagenous stiffening and the tendency of granulomas to become encysted.

However, no significative difference was ever noticed in the tissue reactions to the two types of particles. No necrosis was ever found in any preparation.

Additional observations by transmission electron microscopy, particularly the blood vessel alterations, were similar for both polyethylenes.

Intramuscular implantation findings were quite compatible with the intra-articular implantations conclusions, i.e. PTFE-polyethylene grafted copolymer particles did not give rise to different or stronger tissue reactions than UHMW polyethylene. The short-term responses were in inflammatory ; there was some noticeable muscular cell degeneration. The much more concentrated particles induced intense foreign body reactions with granulomas, enormous giant cells with degenerating nuclei patches, but no evidence of necrosis. The further terms responses evolved towards particle migration, fibrous parcelling and insulation of the implantation site, after invasion by enlarged vessels and connective tissue.

CONCLUSION : The implantations performed up to six months of particles of two different grain size distributions of a PTFE-grafted and reticulated polyethylene, compared to a standard UHMW polyethylene, exhibited in the short term response a stronger incidence of grain size distribution ; at every interval, no evidence was found of any enhancement of tissue reaction towards the modified material, in comparison with the original one. Thus, PTFE-grafting of polyethylene did not noticeably alter the tissue behaviour with regard to its wear particles.

Acknowledgements : Thanks to Mrs HOTT and Mrs LANSAMAN for their technical assistance and grants from C.E.A. - O.R.I.S.
Laboratoire de Recherches Orthopédiques,
10, avenue de Verdun - 75010 Paris, France.

P. Eyerer

Institut für Kunststoffprüfung und Kunststoffkunde Universität
Stuttgart, Stuttgart, Germany (FRG)

The combined chemical and mechanical influences of the body environment cause property changes of ultra high molecular weight polyethylene (UHMWPE).

This results from an analysis of 76 retrieved hip cups (69) and parts of knee prosthesis (7) of UHMWPE. 9 different types of joint endoprosthesis were analysed with implantation periods ranging from 3 weeks to 16 years. Reasons for reoperations were infections (5), loosening (69), death (not loosened, 2) and other (5).

Property changes of retrieved UHMWPE prosthesis were determined by density, infrared absorption, DSC, extraction, molecular weight, hardness and SEM.

Gibbons et al. /1/, Haas et al. /2/ and Grood et al. /3/ published similar investigations. Due to the lower number of their tested implants and to the shorter implantation times the differentiation and the conclusions were restricted.

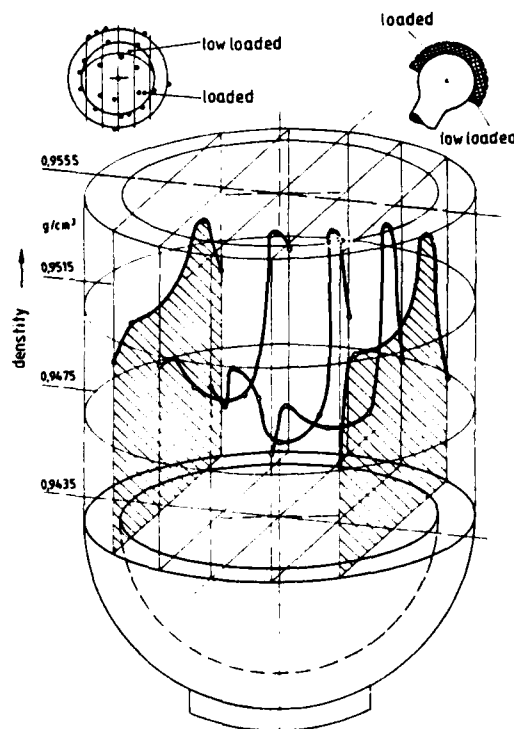
The density of the UHMWPE increases strongly especially in the low loaded and/or loosened areas of the hip cup, Fig. 1. This can be explained by post crystallization. This is due to oxidative chain scission of the macromolecules mainly caused by the influence of the neo synovial body liquid. Chain scissions in turn increase the molecular mobility which causes post crystallization. Consistent to this interpretation is the increase of the low molecular parts of the UHMWPE implants depending on implantation time and on local stresses /4/. Brittle fracture is the consequence. Within 10 years of implantation the young's modulus near the surface increases by 100 percent.

Measurements of properties as a function of hip cup wall thickness show the time dependent effect of degradation. The analysis of the wall cross-section also shows a damaging influence of sterilization by irradiation. The degree of damage corresponds to an in vivo implantation time of about 3 or 4 years. SEM pictures of the wall cross-section (cold broken at minus 196°C) of retrieved hip cups confirm these results /5/. At the inner surface of a 9 year implanted hip cup which is opposite to the femoral head, fracture lines follow the boundaries of the sinter particles. In the middle of the wall and in new UHMWPE samples the boundaries remain stable with the cracks running through the sinter particles.

Mainly two improvements are based on these results: first they help to begin with improving the properties of UHMWPE and second they allow to improve the in vitro simulation methods and lower therefore the risks with new biomaterials. Improving steps concern

synthesis, processing and clinical application.

- /1/ Gibbons, D.F.; Anderson, J.M.; Martin, R.L.; Nelson, T; in: Syrett/Acharya (ed) Corrosion and degradation of implant materials. Philadelphia: ASTM STP 684, 20, 1979,
- /2/ Haas, T.W.; Rostoker, W.; Galante, J.; Proc. 25th Orthop. Res.Soc. Trans. 1979, 262,
- /3/ Grood, E.S.; Shastri, R.; Hopson, C.N.; J. Biomed. Mater.Res. 16, 399, 1982.
- /4/ Eyerer, P.; Ke, Y.C.; J. Biomed. Mater.Res., in print,
- /5/ Eyerer, P.; Z. Werkstofftechnik, in print.



Figur 1: Density distribution at the inner surface of a 7 year implanted hip cup.

The author wish to acknowledge Prof.Dr. F.Lechner and Drs. R.Ascherl, K.-D.Dittel, U. Holz and U. Weber for providing the retrieved implants for these studies and for many important discussions.

Prof. Dr.-Ing. P. Eyerer
Institut für Kunststoffprüfung und Kunststoffkunde, Universität Stuttgart
Pfaffenwaldring 32, D-7000 Stuttgart 80,
Tel.: 0711/685-2667.

THE EFFECT OF POROUS-SURFACED KNEE PROSTHESIS DESIGN
ON ADAPTIVE BONE MODELING

J.D. BOBYN, D. ABDULLA*, R.M. PILLIAR*, H.U. CAMERON*

Department of Mechanical Engineering, Institute of Biomedical
Engineering, Ecole Polytechnique, Montreal, Quebec, CANADA, H3C 3A7

Porous-surfaced knee prostheses designed for cementless implantation and «biological fixation» by tissue ingrowth are in current clinical use despite a lack of thorough understanding of the relationship between implant design and long-term reactive or adaptive bone modeling¹. A previous experimental study in dogs with an unconstrained total knee prosthesis demonstrated detrimental femoral bone modeling (both formative and resorptive) due to rigid bone ingrowth fixation of a long intramedullary stem in the femoral component². The purpose of this study was to further elucidate the effect of porous-surfaced knee prosthesis design on adaptive bone modeling in a series of canine experiments.

The basic unconstrained knee prosthesis design utilized in the previous study was retained². The femoral component was fabricated from cast cobalt-base alloy. The tibial component was manufactured from medical grade high density ultra high molecular weight polyethylene. The central stem of this component was machined with circumferential grooves for immediate fixation by mechanical interlock and potential fixation by tissue ingrowth. Powder-made porous surfaces on both components were formed by sintering a multiple layer of cobalt-base alloy spherical particles into a network of fully interconnecting voids³. The porous surface had an average pore size of approximately 200 micrometers, a depth of approximately 800 micrometers, and a surface and volume porosity of about 35 per cent.

Three different femoral component designs and two different tibial component designs were studied. A femoral component with a porous-surfaced U-channel and a long smooth-surfaced central stem was utilized in conjunction with a polyethylene tibial component. Two animals were implanted with this prosthesis for a period of 12 months. A femoral component with a porous-surfaced U-channel and no central stem was utilized in conjunction with a tibial component that included a porous-surfaced metallic base or support plate (Figure 1). Four animals were implanted with this prosthesis, two for a period of 8 months, and one each for 21 and 24 months. Finally, a femoral component with a partially porous-surfaced U-channel was utilized in conjunction with the tibial component that had a porous-surfaced metallic plate (Figure 2). Two animals were implanted with this prosthesis, one for 10 months and the other for 12 months. Adaptive bone modeling was studied by examining series of lateral radiographs during the course of the implant period. Upon elective animal sacrifice each knee was removed and processed for histology.

Bone modeling around the femoral component with the smooth-surfaced stem was less severe or marked compared with the same design with a porous-surfaced intramedullary stem². Preservation of the normal appearance of the anterior and posterior aspects of the femoral cortex and of the cancellous bone within the U-channel improved. As in the previous experiment, each tibial component became surrounded by a thin radiopaque shell of bone that served to grossly immobilize the implant without

preventing small movement upon loading.

The femoral components with the fully porous-surfaced U-channel (no stem) resulted in the most acceptable long-term appearance of the bone-implant interfacial regions (Figure 1). There was excellent maintenance of both cortical and cancellous bone structure. Histology confirmed rigid fixation of all four components by bone ingrowth. The femoral components with the partially porous-surfaced U-channel resulted in an «hourglass» modeling of the distal femur that is considered to be detrimental (Figure 2).

The six tibial components with the porous-surfaced support plate were all sufficiently stable to permit load bearing and relatively normal activity. Histology revealed, however, that three were fixed by osseous tissue ingrowth and three were fixed by fibrous tissue ingrowth. The components fixed by bone ingrowth radiographically showed little or no evidence of bone densification under the metallic support plate or around the central polymeric stem (Figure 1). The components fixed by fibrous ingrowth showed radiolucency under the metallic support plate and pronounced radiodensity around the central polymeric stem (Figure 2).

In conclusion, subtle changes in femoral component design can have a profound effect on the biological response to or adaptive bone modeling around porous-surfaced implants. A tibial component with a polymeric central stem and porous-surfaced metallic support plate that becomes ingrown with bone causes the least alteration of normal bone structure. Cases of fibrous tissue fixation were attributed to poor initial implant stability achieved at surgery. Regions of pronounced radiodensity or change in bone structure are indicative of non-uniform or non-physiological stress transfer due to either implant design or type of fixation.



Figure 1

Figure 2

1. Hungerford, D.S. et al., Clin. Orth. 176:95, 1983
2. Bobyn, J.D. et al., Clin Orthop. 166:301, 1982
3. Pilliar, R.M. et al., J. Biomed. Eng. 10:126, 1975

Supported by the Medical Research Council and the IMASCO-CDC Research Foundation (CANADA).

* Department of Metallurgy and Materials Science, University of Toronto, Ontario, CANADA.

BIOLOGICAL FIXATION OF POROUS-SURFACED HIP PROSTHESES-
CLINICAL EVALUATION OF ADAPTIVE FEMORAL BONE MODELING

Charles A. ENGH and J. Dennis BOBYN*

Anderson Clinic, National Hospital for Orthopaedics and Rehabilitation
Arlington, Virginia 22206

INTRODUCTION

A variety of porous-surfaced femoral hip prostheses designed for cementless implantation and «biological fixation» by tissue ingrowth are currently being employed clinically¹. One issue or concern that has been repeatedly raised in connection with their use is the potential for detrimental bone modeling (resorption) that might result from stress shielding of the femur due to excellent bonding of a high modulus prosthesis. These fears are well-founded since porous-surfaced metallic stems that become ingrown with bone have been shown experimentally in dogs to cause bone resorption by disuse atrophy in a femoral segmental replacement model by Miller et al.², a femoral head surface replacement model by Hedley et al.³, and a femoral condylar replacement model by Bobyn et al.⁴ The purpose of this study was to clinically examine and identify the adaptive bone modeling that develops as a result of the altered stress distribution within the femur.

MATERIALS AND METHODS

The prosthesis under study is a cast cobalt-based alloy (ASTM F-75) long, straight-stemmed modified Moore prosthesis. The porous surface is the cobalt-based alloy powder-made sintered system that has frequently been described in the literature over the past decade⁵. The average pore size of the porous surface is approximately 100 micrometers, the thickness of the porous surface is approximately 600 micrometers, and the surface and volume porosity are both approximately 35%. Anteroposterior (AP) and lateral radiographs were obtained on each patient postoperatively, at three month intervals during the first year after surgery, and annually thereafter. Extreme care was taken to obtain radiographs of equivalent orientation and density. The radiographs were closely examined for evidence of both resorption and formation of bone in the bone-implant interfacial regions. A total of seventy-seven femurs with a minimum implantation period of two years (average of 3 years) was evaluated for this study.

RESULTS

The patients were grouped into three main categories based on the postoperative position of the implant within the femur as viewed on an AP radiograph. Patterns of adaptive bone modeling were also divided according to these categories. Patients were observed to have either excellent (category 1), good (category 2), or poor (category 3) contact of the prosthetic stem with cortical bone in the diaphysis. Also, the proximal medial aspect of the implant was observed to have either contacted (sub-category A) or not contacted (sub-category B) the cortical bone of the calcar.

New endosteal bone was frequently observed to develop between six months and two years postoperatively in regions of close contact of the porous surface with cortical bone, particularly near the distal tip of the prosthesis on an AP projection

and along the concave posterior femoral cortex on the lateral projection. This bone generally developed more quickly and to a greater extent in category 1 compared with the other categories. Between six months and two years postoperatively, progressive cancellous bone hypertrophy was observed adjacent to the proximal portion of the implant, particularly with patients in sub-category B.

Resorption or loss of bone as a result of hypophysiological stress transfer appears to be primarily confined to the periosteal aspect of the proximal medial cortical bone (calcar). Slight but distinct modeling in this region is typically visible from six months to two years after surgery. A similar bone loss occurs at the anterior aspect of the femoral neck, an area also subjected to decreased stress. A general resorption of femoral bone as a result of stress shielding by the high modulus implant has not been observed in any instances. This includes twelve patients in whom the prosthesis has been implanted for six years. In about one-half of the patients there develops at some point in time either faint or distinct densification of bone in the form of a thin radiopaque line that can be visualized adjacent and parallel to the prosthesis but separated from it by a small space of about one millimeter or less. The radiopaque line is an asymptomatic feature that has been postulated to form at some point in time as an osteoblastic response to slight but cyclic implant motion.

DISCUSSION AND CONCLUSIONS

The biological fixation of this particular hip prosthesis design does not lead to gross femoral resorption by stress shielding to an extent that can be detected radiographically. This is possibly due to the implant geometry and loading configuration that result in adequate proximal stress transfer. The majority of the adaptive bone modeling that develops is, in fact, formative or osteoblastic as opposed to destructive or osteolytic. Based on results to date, this system appears to represent a viable alternative to implant fixation by bone cement. Clinical trials with this prosthesis are continuing with cautious enthusiasm.

1. Galante, J.O. (ed): Clin. Orthop. 176:2, 1983
2. Miller, J.E. et al: Orthop. Trans. 5:380, 1981
3. Hedley, A.K. et al: Clin. Orthop. 163:300, 1982
4. Bobyn, J.D. et al: Clin. Orthop. 166:301, 1982
5. Pilliar, R.M. et al: J. Biomed. Eng. 10:126, 1975

Supported in part by Natural Sciences and Engineering Research Council, CANADA.

* Dept of Mechanical Engineering, Institute of Biomedical Engineering, Ecole Polytechnique, Montreal, Quebec, CANADA, H3C 3A7.

"A NEW SEMI-AUTOMATIC MICRO-COMPUTERIZED TECHNIQUE TO QUANTIFY BONE
INGROWTH INTO POROUS IMPLANTS"

DALLANT P., MEUNIER A., CHRISTEL P., SEDEL L.

LABORATOIRE DE RECHERCHES ORTHOPEDIQUES - Faculté de Médecine Lariboisière-
Saint-Louis, Paris - FRANCE.

INTRODUCTION : Orthopaedic prostheses may be conceived with or without bone cement. In this last case, porous materials can be used with the hope of improving mechanical properties of the interface by bone ingrowth into the implant. During the development of such porous implants, quantification of bone ingrowth may be a real technical difficulty. Quantification by computer methods would be of benefit in simplifying operator's part and increasing the accuracy of calculations.

Our purpose is to present a new technique for bone ingrowth quantification, using a common laboratory microcomputer.

MATERIAL : Samples are embedded in polymethylmethacrylate and polished according to usual metallographic techniques. Analysis is then performed on photographic enlargements (21 x 30 cm) obtained by either microradiography or transmitted or reflected light microphotography.

The hardware consists of :

- a microcomputer HP 85 (with integrated graphic display of 192 x 256 points and total core memory of 32 Kbytes capacity)
- a double flexible disk drive (HP 82901 M)
- a X Y graphic plotter (HP 7225 A)
- a graphic tablet (HP 9111 A) with an interactive pen (digitization area : 22 x 30 cm ; resolution : 100 points/mm²)
- a printer (HP 82905 A)

METHOD : Software package "CONTOUR PI" (Porous Implants) has been developed in HP BASIC language. Its core part consists of an algorithm of digitization and an algorithm of calculation.

The operator first selects and names the structures to be digitized : implant structure, calcified areas and fibrous areas inside the porous implant. Using the interactive graphic tablet pen, each boundary is digitized indifferently clockwise or counter clockwise. When pen is switched on, the digitizing algorithm continuously generates pen tip coordinates at a constant rate of 3.25 points/second. Each digitized point is sent to the HP 85 and displayed on the microcomputer video monitor. After digitization, a loop gives to the operator the choice of continuing the program or again digitizing the contour-line.

Coordinates are then stored on a flexible disk for latter calculations and drawing.

Calculating algorithm shifts in a step-wise manner along the digitized contour-line, dividing the cross sectionnal surface into a series of triangles. The three summits of all the triangles are the lower left corner of the graphic tablet and 2 consecutive perimeter points. For each triangle, area and centroid's coordinates are calculated, then added to obtain area and centroid of the whole structure. Bone ingrowth features are inferred from all the structures' basic characteristics : bone ingrowth, fibrous tissue, and empty area surface densities.

Plotting of digitization is obtained (Fig. 1) and final results are printed out

APPLICATION : This technique was developed to quantify bone ingrowth into porous implants. These implants have a cylindric shape (O.D. = 4.8 mm ;

l = 10 mm) and are made of titanium spheres (diameter : 600 μ m). The cylinders are implanted in sheep metatarsi. An example of this application is presented in figure 1.

DISCUSSION : There are two different sorts of techniques for area evaluation : "grid based" techniques and "contour based" techniques.

"Grid based" techniques, which are non computerized ones, are more time consuming and less accurate than "CONTOUR PI".

"Contour based" techniques allow an exact evaluation of areas and densities. Among them, "Paper weight" method (1) still remains the only usable technique in such studies. Due to fully automatic calculations of a large points number, software "CONTOUR PI" provides an interesting alternative to this method.

CONCLUSIONS : Software package "CONTOUR PI" allows computerized quantification of bone ingrowth into porous implants, joining efficiency of human analysis to comfort of automatic calculations. All the studied parameters are evaluated from digitization of contour-lines alone. Results obtained with this technique can be usefully correlated with mechanical testing results.

REFERENCE : 1. EVANS F.G., Relations between the microscopic structure and tensile strength of human bone. Acta Anat., 1958, 35, 285 301.

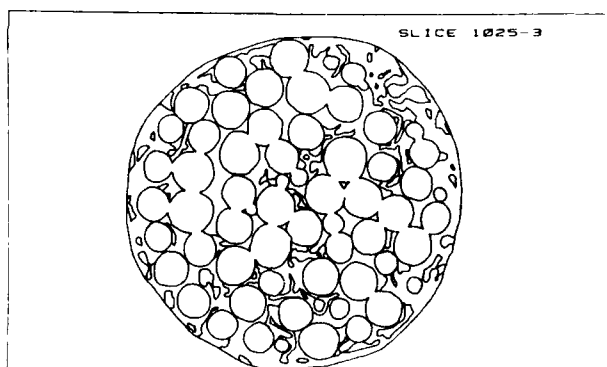


Fig.1: Plotting of digitization

Supported by a medical research grant from C.R.A.M.I.F. (French Social Security).
Laboratoire de Recherches Orthopédiques
10, avenue de Verdun - 75010 Paris, France.

CHRISTEL P., HOMERIN M., DRYLL A.

LABORATOIRE DE RECHERCHES ORTHOPEDIQUES - Faculté de Médecine Lariboisière-
Saint-Louis - Paris, FRANCE.

INTRODUCTION

Biocompatibility of carbon materials has been well documented and their mechanical properties led to consider them as potential biomaterials for orthopaedic applications. However since wear resistance of such materials is low, and impregnation with ceramics has been proposed to improve this problem. Among the various carbon ceramic composites candidates, carbon silicon carbide combination (C-SiC) seems to be promising but few data are available on SiC tissue biocompatibility. The purpose of the current study was to investigate tissue biocompatibility of implants and powders made of C-SiC material with reference to pure carbon and alumina ceramic.

MATERIAL AND METHOD

IMPLANTS EXPERIMENT: Two materials were compared : a) carbon fibers impregnated with pyrolytic carbon by CVI and coated with pyrolytic carbon, b) carbon fibers impregnated both with pyrolytic carbon and SiC by CVI and coated with SiC. Each implant was a cylinder measuring 2 mm in diameter and 6 mm in length. The specimens were degreased and cleaned with ultrasounds in alcohol and rinsed in distilled water prior to implantation. The cylinders were implanted intramuscularly on each side of the spine in Sprague Dawley rats according to ASTM F 361 protocol. Animals were sacrificed at 1, 3, 9, 16 and 26 weeks. After metacrylate embedding, histology was performed either on thick slices ground to 40 μ m preserving tissue implants interface and on thin slices (5 μ m), the implant being removed. Fibrous encapsulation thickness was measured with an image analyzer.

POWDER IMPLANTATION : The tissue tolerance to the wear particles of a carbon-SiC composite was compared with these of a well tolerated material, surgical grade sintered alumina. The particles were prepared by grinding the articular surfaces of a prosthesis with a diamond tool, milling the debris in a Bangauman ball-mill, and collecting the particles after a dry sieve processing.

Since any discrimination between C and SiC components was impossible, it was thought that the composition of every particle was of both materials, in a 3/2 proportion respectively.

At examination, the particles consisted of polyedric grains of 15-20 μ m and dust of less than 1 μ m in size. The alumina control particles were spherical with a mean diameter of 24 μ m. Particle amount in terms of volume was similar.

16 male New-Zealand rabbits were implanted intra-articularly (knee) and intra-muscularly with the C/SiC and the alumina powders, on the right and on the left side, respectively. The animals were killed at 1, 4, 16 and 26 weeks. After in-vivo glutaraldehyde fixation, several synovial villousities were excised for transmission electron microscopy examination. Synovial membranes and muscles were then processed for histology through methyImethacrylate embedding. Inguinal lymph nodes were retrieved for histological evaluation.

RESULTS

IMPLANTS EXPERIMENT : Except at 1 week, where the membrane thickness was quite larger with C-SiC when

compared to pure carbon, the fibrous reaction was not statistically different between the 2 materials for the remaining observation period (Table I). Histological observation showed that at 1 week particles migrated from both type of implant with a stronger inflammatory reaction around C-SiC certainly related to a greater particle release from this material. At week 3, plasmocytes and fibroblasts were present without neutrophils. There was an increase of collagen fibers density with the C-SiC capsule slightly more hemorrhagic and inflammatory when compared to carbon. At 9, 16 and 26 weeks no difference was observable in the tissue reaction around both type of implants.

Table I	Time (weeks)	mean membrane thickness (C - SiC)	(μ m)
	1	296	67
	3	59	49
	9	58	58
	16	42	46
	26	52	36

POWDER IMPLANTATION : Synovium implanted with C-SiC particles exhibited in the short term response no noticeable alteration, but with evidence of early particle migration. In contrast, alumina particles induced an acute inflammatory and foreign body reaction, with hypervascularization and increased fibrogenesis. In further terms, the synovial border lost its C-SiC black staining by migration, while the larger particle collections became encysted. The alumina implanted synovium recovered its normal aspect within 4 weeks, despite of residual hypervascularization and fibrous stiffening.

Additional observations by transmission electron microscopy revealed some damage to the blood vessels of C-SiC implanted synovium, i.e. vesiculation and vacuolisation of the cytoplasm of endothelial cells and pericytes, which seemed to be specific for this material.

Acute reaction with alumina did not occur after intra-muscular implantation ; however, the implantation site and surroundings were remarkably more infiltrated with fibrous tissue, whereas a thin sheath isolated the C-SiC particles ; no particles were ever found in the inguinal lymph-nodes.

CONCLUSIONS : Comparison of the tissue reaction to pure carbon and carbon silicon carbide implants demonstrated a similar fibrous and histological responses, except at the initial period of observation (1 week). The stronger reaction to C-SiC material could be related to a higher particle release from this material. However, the evaluation of the tissue reactions towards such particles showed acceptable results : the synovium displayed minimal changes, but particle migration and ultrastructural vascular alterations would be questions of concern. The alumina particles enhanced reactivity might be related to their higher mean size.

Acknowledgement : Supported by INSERM (P.R.C. - Biomateriaux Carbonés n° 81/1780). Materials were provided by S.E.P. and CERAVER Companies. Laboratoire de Recherches Orthopédiques 10, avenue de Verdun - 75010 PARIS, France.

NEW POLYMER SYSTEMS FOR PREPARATION OF CONTACT LENSES

J. Vacík, J. Trekoval, O. Wichterle

Institute of Macromolecular Chemistry, Czechoslovak Academy of Sciences,
162 06 Prague 6, Czechoslovakia

In the last 5-10 years, there has been an increasing need for new materials among ophthalmologists, which would make possible their long-term application, and would also add users of advanced age to regular customers. The two factors that are to be satisfied in such case are high diffusivity of oxygen and an excellent compatibility of the chosen material with human eye. The factor of high diffusivity of oxygen in new materials with respect to continuous supply of oxygen to the human eye tissue is of particular importance in the long-term application of contact lense.

Our study was concerned with copolymers of 2-hydroxyethyl methacrylate, diethyleneglycol monomethacrylate, methacrylic acid, N-vinylpyrrolidone and of many other vinyl monomers with oligomers possessing in their structure groups capable of being incorporated in the arising structures during radical polymerization.

Domains of formation of phase separation were investigated for the individual polymerization systems as a function of the length of these oligomers and of the character of the solvent or of the system of solvents.

Concentration dependences of oligomeric sequences on the mechanical properties of the forming copolymers were examined, using both bulk and solution crosslinking radical polymerization.

Soluble fractions in the tridimensional structures thus obtained were determined for the individual systems under study.

Equilibrium swelling ratios of the polymers were evaluated, and domains of their applicability in the preparation of contact lenses were defined.

EFFECT OF SILICONE OIL ON THE CORNEA

Miguel F. Refojo, Manuela Roldan and Fee-Lai Leong

Eye Research Institute of Retina Foundation
Boston, Massachusetts

Perfluorocarbon compounds and silicone oil have a particularly large capacity for dissolving oxygen and are chemically and biologically inert; thus they can be used to deliver oxygen to hypoxic tissues. In ophthalmology, they might be used with fluid scleral lenses. If the fluid filling the lens had enough oxygen reservoir to satisfy corneal needs for an entire day, the fluid lens could benefit many patients who are difficult to manage at this time: (a) to protect the cornea and maintain vision in severe dry-eye patients, (b) to prevent exposure keratitis in patients with impaired blinking (neuroparalytic keratitis, and (c) in difficult keratoconus patients. Silicone oil offers some advantages because of its easy availability and low cost. We have tested the tolerance of silicone oil of different viscosities (500, 1000, and 12,500 centistokes; Petrarch Systems, Inc., and 1000 cs; 360 Medical Fluid, Dow Corning) on the rabbit eye. When drops of silicone oil were applied repeatedly to the rabbit cornea, the cornea developed a persistent but mild punctate staining. When the oil was allowed to remain for several hours on the eyes of anesthetized rabbits, within a cup formed by the lids and hanging sutures, the immediate reaction was mild. After 3 to 6 days, however, the epithelium thickness increased (Table). Histological examination demon-

strated an increase both in the number of epithelial layers and in the volume of the epithelial cells. The latter feature was more marked in the basal layer, where some atypical mitosis was observed. The only reference that we were able to find about the ocular surface tolerance of silicone oil is from Dow Corning literature, which states, "When applied to the eye, produces a transitory, mild irritation that subsides in a few hours."

Our findings could be interpreted as having been caused by the interaction of the silicone oil and the epithelium lipids. The corneal epithelium contains phospholipids, triglycerides, cholesterol, and cholesterol esters.

As indicated in the Table, the variance of epithelial thickness was higher when a commercial type of silicone oil was used than when a medical grade was used. Although we still don't have enough data, we suspect that the greater variability may be due to some impurity in the commercial grade. We are currently investigating further (with EM and scanning) the tolerance of medical-grade silicone on the rabbit ocular surface.

Supported by grant EY00327 from NIH.

M. F. Refojo, D.Sc., Eye Research Institute, 20 Staniford Street, Boston, MA 02114

Treatment		Enucleation after treatment, days	Epithelium thickness \bar{X} , μm	Variance σ^2
Material	Time, hr			
Control	0	0	23.27	1.06
BSS*	6	0	22.05	0.74
PDMS** (500 cs)	3	0	31.54	4.68
	3	3	29.76	56.87
	3	4	32.63	22.20
	3	8	25.39	13.43
PDMS** (1,000 cs)	3	3	28.01	18.43
PDMS*** (1,000 cs)	4	3	26.28	3.02
	4 1/2	7	25.18	0.87
PDMS** (12,500 cs)	6	3	31.17	10.64
	3 1/2	7	34.43	3.29
Poly(methyl-3,3,3-trifluoropropylsiloxane (300 cs)	3	0	35.51	3.64
	3	5	37.57	4.30
	3	7	31.48	7.82

*Balanced salt solution, Alcon®

**Poly(dimethylsiloxane), Petrarch Systems, Inc.

*** 360 Medical Fluid, Dow Corning®

INTRAOCULAR LENS LOOP MATERIALS: COMPARISON OF MECHANICAL STRESS AND
PHOTO-OXIDATIVE PROPERTIES OF POLYPROPYLENE AND
POLYMETHYLMETHACRYLATE MONOFILAMENTS

D. C. Osborn, M. Yalon, J. Stacholy and E. P. Goldberg

Department of Materials Science and Engineering
University of Florida, MAE 217
Gainesville, Florida 32611

Because of excellent optical properties and biocompatibility in the eye, polymethylmethacrylate (PMMA) has been used for several decades as the optical material of choice for intraocular lens (IOL) implants. Polypropylene (PP) has been used with great success as a suture material (e.g. in cardiovascular surgery) since the 1960s and for IOL loops since the mid-70s. However, there has been an interest in recent years in PMMA itself as the IOL haptic material. The long-term mechanical stability of a rigid polymer such as PMMA for a flexible stress-bearing implant device is of concern as is the possible photo-oxidation of PP in the eye. The study reported here was therefore conducted to evaluate the relative photo-oxidative and mechanical stress stability of PMMA and PP. Data for PP biocompatibility in the anterior chamber were also obtained for one year rabbit implants.

Photo-Oxidative Stability

PP possesses a uniquely favorable combination of chemical and mechanical properties for use as an IOL loop material. It is stable to hydrolysis and displays good strength and flexibility. However, because of the molecular structure, i.e. the repeating tertiary carbon-hydrogen bond in the polymer chain, theoretical questions have been raised regarding the possibility that photo-oxidative degradation might affect implant life. Accelerated UV aging tests were conducted on clear PP, blue PP and PMMA IOL loop monofilaments immersed in physiological saline. Following UV irradiation (at $>300\text{nm}$, using a Xenon arc) at different dose levels, polymer properties were measured (tensile strength and elongation, flex cracking, molecular weight). Very conservative estimates from data for clear PP suggest adequate long-term photo-stability for IOL implants. Blue PP was more stable than clear PP. The blue colorant appears to act as a photo-oxidation stabilizer.

The influence of various environmental parameters on long-term stability have been considered in detail (UV intensity, temperature, oxygen concentration, intermittent irradiation, sample thickness). Assumptions regarding "normal" human UV exposure and radiation that actually enters the eye are especially important. Exposure levels of about 1.0 mW/cm^2 for 300-400nm irradiance have been assumed by several investigators and used to estimate stability of 30-75 years for clear PP. However, since retinal exposure to a 50 times lower dose ($20 \mu\text{W/cm}^2$) for 1000 seconds can cause severe retinal damage in primates, all estimates of useful PP haptic life to date, including our own, may in fact be conservative by as much as 50-100X. The difference between atmospheric

irradiance and UV at 300-400 nm which actually enters the eye is evidently quite large.

Mechanical Stress Stability

The growing use of PMMA for IOL haptics places mechanical property demands upon PMMA not previously required. Since PMMA is notch-sensitive and susceptible to stress fatigue cracking, it is important to insure that potential mechanical stress failures be avoided through safe IOL design and extensive testing. Flexural and tensile stress properties of currently used blue PP and PMMA loop monofilaments were studied. A cyclic flexural test using a special fiber jig was devised to test flexural stress cracking under severe accelerated conditions. Notch sensitivity for a scratched or damaged surface was tested both in tension and in flexure by introducing a 0.001" razor cut in fiber sample surfaces. Data are summarized below:

	Tensile Strength (psi)	Elong- ation (%)	Flexural Failure No. Cycles At:		
			180°	135°	90°
PP	59,100	126	>1000	>1000	>1000
PMMA	11,300	63	3	16	164
PP/Notch	41,000	44			>1000
PMMA/Notch	9,500	4			9

PP monofilament has exceptional strength in tension or repeated flexural stress. PMMA is much weaker and, most important, is very sensitive to flexural stress cracking and surface damage. PP, even notched, did not break or crack to the 1000 cycle limit of even the most severe flexural stress test.

Biocompatibility

IOLs with clear PP loops were implanted in the anterior chamber of rabbit eyes. The eyes were quiet and normal during the one year implant period with no evidence of adverse tissue reactions. Tissue and loop surfaces were examined by optical and electron microscopy.

Conclusions

In the absence of significant clinical data to date indicating photo-oxidation or biodegradation failure of 4/0 and 5/0 PP implants, PP monofilament appears to be a satisfactory IOL loop material. Blue PP exhibits superior photo-oxidative stability and thereby affords a significant additional margin of safety. PMMA exhibits markedly inferior mechanical properties, especially if surface-damaged, compared with PP. The potential for long-term stress-fatigue failure of PMMA requires much further investigation to insure the safety of flexible PMMA haptic lens designs.

PROTEIN ADSORPTION TO CONTACT LENS MATERIAL

B.D. Ratner and T.A. Horbett,

Department of Chemical Engineering and Center for Bioengineering,
University of Washington, Seattle, WA. 98195

Of all clinical devices which incorporate biomaterials, contact lenses are probably the most common. Although contact lenses are often viewed as simple "cosmetic" devices, there is evidence that serious biological reaction to them can occur. Little is known about the differences in the biological reaction to the many polymers placed in the eye for contact lens applications. In this study, large differences in protein adsorption behavior from artificial tear solution were noted between a number of different contact lens polymers. Since the nature of the protein film which forms on a biomaterial is believed to strongly influence the biological reaction to that material, this result would suggest that different contact lenses will have differing degrees of biocompatibility.

Two series of materials were examined in separate experiments. In the first series, a number of commercial contact lenses packaged by the manufacturers were studied and compared to poly(methyl methacrylate) (PMMA) and a poly(HEMA-methyl methacrylate) (p-HEMA-MMA) copolymer prepared in our laboratory. The exact compositional description of most of the commercial lenses was not revealed by the manufacturers. Therefore, the second experiment utilized cross-linked hydrogel materials prepared in our laboratory which were made with monomers common to the manufacture many commercial contact lenses (lens analogues).

The contact lenses and lens analogues were exposed to an artificial tear solution using a procedure which avoided passing the polymer surfaces through an air-solution interface during the protein adsorption step. The artificial tear solution consisted of a mixture of the three primary tear proteins in approximately their physiologic ratio in a buffered saline solution. Each adsorption experiment was performed three times with each one of the three proteins individually tagged by I¹²⁵. The gamma emission from each specimen was counted and converted back to $\mu\text{g}/\text{cm}^2$ of protein on the specimen. By summing the amount of IgG, albumin and lysozyme on the specimens from each set of experiments, the total amount of protein on each specimen can be estimated.

Table 1 presents the data obtained with commercial lenses. The most interesting finding from this experiment was that some lenses now used in humans pick up over 200 times more protein than other lenses. In addition, the composition of the protein in the adsorbed layer differs widely with some materials picking up 99% lysozyme and others adsorbing 92% albumin.

Data on the lens analogue materials are presented in Table 2. It is observed that methacrylic acid (MAAc)-containing lenses pick up substantially more protein than hydrogel compositions free of this component. Also, the MAAc polymers strongly fractionate lysozyme from the protein mixture. Poly(N-vinyl pyrrolidone) (pNVP) incorporation or poly(acrylamide) (pAAM) incorpor-

ation also affects the ratio of the three proteins and the total amount of protein on the polymers, though to a lesser extent than observed after MAAc incorporation.

The large differences in protein pickup by various hydrogel polymers have not been previously reported. The implications of these observations for contact lens clouding, and the more serious problem, contact lens-induced reaction should be investigated. This work has additional implications for all biomaterials studies. It illustrates how the nature of a surface can selectively fractionate a complex protein mixture and generate new protein-mediated interfaces with widely differing compositions. The reaction of a biological system to these new interfaces can also be expected to be different.

Table 1
Protein Adsorption to Commercial Contact Lenses¹

Lens code	Total Protein ²	%Alb.	%IgG	%Lyzo.
1	0.13	92	3	5
2	0.14	78	13	9
3	8.28	0.9	0.1	99
4	15.63	0.7	0.1	99
5	0.60	77	5	18
PMMA	0.52	53	19	28
p(HEMA/MMA)	0.22	62	27	11

1- Measured after an initial rinse and a 24 hr. soak-rinse.

2- $\mu\text{g}/\text{cm}^2$

Table 2
Protein Adsorption to Contact Lens Analogues²

Polymer	Total Protein ²	%Alb	%IgG	%Lyzo.
p-HEMA	0.07	43	43	14
p(80HEMA/20NVP)	0.07	43	29	29
p(60HEMA/40NVP)	0.15	20	13	67
p(40HEMA/60NVP)	0.28	11	7	82
p(90HEMA/10MAAc)	390.37	0.01	0.01	99.98
0(70HEMA/30MAAc)	374.12	0.01	0.03	99.96
p(80HEMA/20AAM)	0.18	11	6	83

1- after initial rinse and 24 hr. soak-rinse

2- $\mu\text{g}/\text{cm}^2$

These experiments were supported by Cooper-Vision, Inc.

HYDROXYAPATITE REINFORCED POLYETHYLENE COMPOSITES AS ANALOGOUS BONE REPLACEMENT MATERIALS

W. Bonfield, J.C. Behiri, C. Doyle, J. Bowman, J. Abram

Department of Materials, Queen Mary College, London, E1 4NS, U.K.

As precise mechanical property data for cortical bone, particularly of elastic moduli and fracture mechanics parameters, have become increasingly available (e.g. 1, 2), it has become possible to consider the development of a synthetic equivalent for bone, in composite form, which has comparable mechanical properties as well as being biocompatible. If, in addition, hydroxyapatite is utilised as the reinforcing phase, then the composite is also potentially bio active, i.e. significant bone ingrowth into the composite becomes possible, which is not dependent on surface porosity alone. This approach has been investigated by injection moulding hydroxyapatite particles (either from calcined bone ash or in synthetic form) with high molecular weight polyethylene to form a series of composites (3) with a hydroxyapatite volume fraction in the range from 0.1 to 0.6, with corresponding Young's modulus values from 4 to 12 GPa (4). In all, about 50 different composites have been prepared, moulded and examined, the different composites arising from controlled variations in the molecular weight and density of the matrix and the composition, volume fraction and particle size distribution of the reinforcement. The initial compounding of such materials is critical and has been optimised by a novel co-rotating twin screw technique. In this paper, the results obtained for the elastic moduli, stress-strain behaviour and fracture mechanics parameter of K_{IC} (the critical stress intensity factor) of the hydroxyapatite-polyethylene composite system are reported in comparison with those of cortical bone. A cytotoxicity evaluation and some six months "in vivo" tests of a prosthetic device are also described.

The authors gratefully acknowledge the generous financial support of the Science and Engineering Research Council, through its Specially Promoted Programme in Medical Engineering, of the British Technology Group and of Johnson and Johnson Ltd.

REFERENCES

- 1 J.C. Behiri and W. Bonfield, Crack velocity dependence of longitudinal fracture in bone, *J. Mater. Sci.*, 15, 1841, 1980.
- 2 W. Bonfield and A.E. Tully, Ultrasonic analysis of the Young's modulus of cortical bone, *J. Biomedical Eng.*, 4, 23, 1982.
- 3 W. Bonfield, J. Bowman and M.D. Grynpas, Composite material for use in orthopaedics, U.K. Patent Application 8032647, 1980.
- 4 W. Bonfield, M.D. Grynpas, A.E. Tully, J. Bowman and J. Abram, Hydroxyapatite reinforced polyethylene - a mechanically compatible implant material for bone replacement, *Biomaterials*, 2, 185, 1981.

ABRAM, J.

STRENGTH AND MORPHOLOGY OF DIFFERENT BONE TRANSPLANTS FOLLOWING THEIR IMPLANTATION INTO DIAPHYSEAL DEFECTS

Ch. Etter, C. Burri and L. Claes

Abteilung für Unfallchirurgie der Universität Ulm
Oberer Eselsberg, 7900 Ulm, Germany

The superiority of the autologous cancellous bone graft for the filling of large bone defects is indisputable (1-4). The effectiveness of the available substitutes is controversial. However, various preserved homologous bone transplant tissues still offer an alternative.

Contradictory data are noted about the desirability of freeze-dried and frozen homologous cancellous bone (2,3). Little is known about orthotopic implantations of osteoinductive bone relative into diaphyseal defects (4).

The present study is an attempt to evaluate under controlled conditions the value of this clinically relevant homologous bone grafts compared with autologous cancellous bone. We were not only interested in the histomorphological course, but also in the strength of the transplant.

From the diaphyses of sheep metaphyseal sections of 1.5 cm in length and half in diameter were removed. These defects were filled with 1.5 g of the following transplant materials:

- (I) Fresh autologous cancellous bone
- (II) Homologous frozen cancellous bone
- (III) Freeze-dried homologous cancellous bone
- (IV) Osteogenin containing gelatine.

As control two defects were left unfilled. The freezing procedure was performed at -20°C. For lyophilisation the sections were rapidly frozen to -80°C and then subjected to vacuum for 24 hours. The osteogenin containing gelatine was prepared from sheep cortical matrix by a sequential extraction procedure.

Eight weeks after the operation, 28 defined bone samples were prepared. The strength (N/mm²) of longitudinal sections with the transplant area in the middle was examined by a tensile test on a materials testing machine. The same samples, 2 mm thick, were x-rayed and the bone density as % of the whole area was evaluated using a Delux-Microvideomat. The rate of new bone formation was quantitatively determined on 10 µm thick nondecalcified longitudinal sections from the middle of the transplant using microphotographs. The same specimens were stained with Janus Green for histological examination.

Table 1:

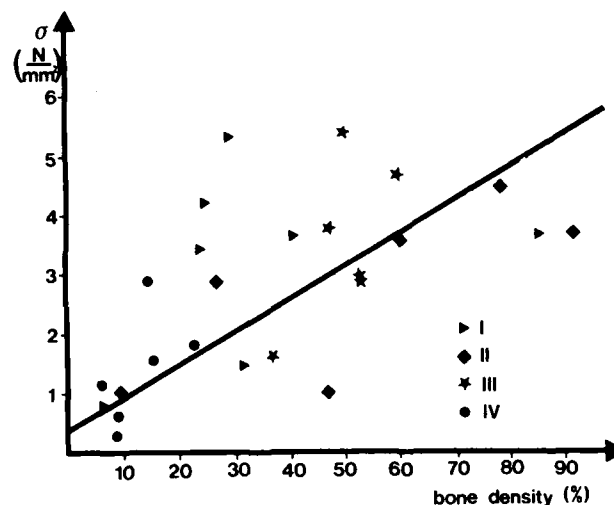
GROUP	STRENGTH (N/mm ²)	DENSITY (%)	NEW BONE (%)
I	18.7 ± 3.3	54.2 ± 3.3	17.7 ± 3.3
II	18.7 ± 3.3	54.2 ± 3.3	17.7 ± 3.3
III	18.7 ± 3.3	54.2 ± 3.3	17.7 ± 3.3
IV	18.7 ± 3.3	54.2 ± 3.3	17.7 ± 3.3

The quantitative results after a test period of eight weeks are shown in table 1.

Osteogenin containing gelatine came off badly (p<0.05) to homologous and autologous cancellous bone in all our tests. There was no difference between frozen and freeze-dried homologous bone grafts.

The lower values for autologous cancellous bone compared with homologous can be explained by the more advanced recanalisation of the marrow cavity as shown by histological examination. Only slight regrowth of bone could be observed in the controls.

The strength test gave valuable additional information to morphological criteria. The correlation between strength and bone density is demonstrated in the following figure (r=0.65).



To summarize, frozen and freeze-dried homologous cancellous bone offer an alternative to the autologous cancellous bone. However, from practical clinical view, the more complicated lyophilisation procedure does not prove to be more advantageous.

1. Ham, A.W., Harris, W.R.: In Bourne G.R. (ed): The biochemistry and physiology of bone. Academic Press, New York, San Francisco, London, 3, 337, 1974
2. Heiple, K.G. et al.: J. Bone Joint Surg., 45A, 1593, 1963
3. Veithmann, D.: Akt. Traumatol. 4, 61, 1974
4. Thielemann, F.W.: Langenbecks Arch. Chir. Forum, 151, 1974

Dr. med. Ch. Etter, Abteilung für Unfallchirurgie, Hand-, Plastische- und Wiederherstellungschirurgie der Universität Ulm Oberer Eselsberg, D-7900 Ulm.

Lacabanne C., Ficat J.J., Francis M.J.[†], Micheron F.^{††}, Durroux R. and Ficat P.

Université Paul Sabatier
31062 Toulouse Cédex, France

The power of monomorph piezoelectric PVDF film (film which generates an electric current in response to normal and shear stresses) to stimulate osteogenesis has previously been reported (1). We have performed further studies using bimorph PVDF films sensitive only to bending stresses. The osteogenic power of this second generation material appears greatly increased.

Materials and methods

Two experimental series were performed on 15 white New-Zealand rabbits and 10 Wistar rats. All these animals were adult males. The implants were placed around the femoral diaphysis of both legs under general anaesthesia.

In the first series, on rabbits, a bimorph PVDF film of one of three thicknesses (175 μ , 250 μ and 450 μ) was compared for its osteogenic effect with a monomorph film of the same thickness implanted on the contralateral side. New bone formation was studied radiographically at two weeks intervals. The animals were sacrificed after two months and the implant sites subjected to histological examination.

A precise quantitative study of the osteogenic response was not found to be possible because of the variability of the morphology and location of the callus. The amount of callus was therefore assessed blindly by two examiners on several microscopic sections and categorized grossly into three stages.

In the second series, on rats, bimorph PVDF films (thickness 450 μ) were compared with inert PVDF films of the same thickness. Histological examination of the callus was performed four months post operatively.

Results and discussion

The results of the first experimental study show that the thickest bimorph PVDF film have the greatest power to stimulate osteogenesis and are able to induce extensive remodelling of the cortical bone adjacent to the film (figures 1 and 2).

The new osteons so induced appear to orient themselves at 90° to normal cortical osteons (figure 3).

The results of the second series show that PVDF films are capable of stimulating osteogenesis in rats as well as rabbits. However after four months the orientation of the new osteons remains disorganized probably because the growing callus progressively immobilizes, and therefore inactivates, the piezoelectric films.

The mechanism of action of piezoelectric films has been discussed a few years ago by E. Fukada (2). One of the most plausible hypothesis is the existence of a rectifying element: the unidirectional crossing of ions through a membrane might induce an ionic concentration. The destabilization of the cell at a given level would be the origine of the cell activity.

In conclusion, the promising behavior of bimorph PVDF films might herald a new generation of osteogenic materials.

References

- (1) Ficat J.J., Durroux R., Fauran M.J., Escourrou J., Ficat P., F. Micheron, C. Lacabanne, "Current advances in skeletogenesis, M. Silbermann & M. C. Flavin

Excerpta Medica, ICS 589, 38, (1982)

- (2) Fukada E., "Mechanism of growth control", O.R. Becker Ed, CCT (1981)



Figure 1 : Callus induced by bimorph film of 450 μ at two months.



Figure 2 : Histological view of the callus shown on figure 1.



Figure 3 : Orientation of new osteons in the callus shown on figure 1.

[†] Nuffield Department of Orthopaedic Surgery
Nuffield Orthopaedic Centre
Oxford, OX3 7LD, England

^{††} L.C.R. Thomson CEF
Orsay, 91 401 France

F. W. Cooke, D. L. Powers, and L. S. Cohn

Dept. of Interdisciplinary Studies, Clemson University, Clemson, SC 29631

The healing of all bone fractures and the success of every surgical procedure that involves osteotomy depends on the body's ability to repair these defects by the growth of new bone. This process has been called reparative osteogenesis. Although the physiology of reparative osteogenesis has been studied in great depth and the mechanics of healing bone have also been examined, no objective method has ever been developed to measure quantitatively the rate of osteogenic repair. Lacking such a measure there is no quantitative method for studying such fundamental questions as the influence of disease states (e.g. osteoporosis) on healing rate or the difference in healing rate between human patients and experimental animals used in orthopaedic research.

Our goal in this study was to develop a simple method to assess reparative osteogenic activity quantitatively in canines. It was also our intention to develop this method so that it could be subsequently applied to humans. This would then provide a rational basis for extrapolating the results of animal studies to human clinical practice.

The experimental procedure consisted of surgically creating a minor but standard bone defect by using a 5.0mm dia. trephine (bone biopsy "needle") to acquire a full thickness biopsy from the iliac crest of the dog. These defects were allowed to heal for time periods of 2, 4, 6 and 8 weeks. Periodically during the course of healing, the osteogenic activity at the biopsy site was monitored by technetium scanning. For each scan an 8 to 10 m Ci dose of technetium 99 labeled MDP was administered to the anesthetized animal. Scans were performed approximately 2 $\frac{1}{2}$ hours after injection with the animal in ventral recumbency. The intensity of the emitted radiation as a function of location was recorded digitally and stored for later evaluation. The intensity of all radiation released from the area of the biopsied crest was recorded and expressed as a ratio to the background intensity recorded at the same time.

At sacrifice, the total amount of new bone formed within and around the biopsy site was determined by quantitative histomorphometry from diametral (through thickness) histologic and micro-radiographic sections of the iliac crest.

The iliac crest biopsy was chosen as the standard defect because this is a diagnostic procedure that is coming into relatively common use in the management of a variety of human orthopedic and metabolic conditions. It therefore provides an opportunity when coupled with Tc scanning, to monitor directly the time course of healing in humans and to compare this on an entirely comparable basis to healing rates in various experimental animals.

Results: The Tc scans indicated that there was much less activity at the biopsy site than had been expected (Figure 1). On the day of biopsy, the activity ratio was only 5 and increased only slightly after 8 days. In some animals, this increase was not significant and even in the most extreme case was less than twice the activity of the first day. By the 20th post biopsy day, all

activity had dropped to the same level as the first day. Systematic histomorphological analysis of 12 dogs revealed that infilling of the defect proceeds by appositional growth from the edges of the hole accompanied by some degree of cortical over growth. These growth patterns were extremely variable between animals, however. At one extreme were a few animals whose defects appeared to fill progressively, while in others the hole was filled with soft tissue and essentially no bone ingrowth had occurred after 8 weeks (Table 1).

Conclusions: It is concluded that the iliac crest biopsy is not a suitable procedure on which to base quantitative monitoring of reparative osteogenesis rates because of the great variability in the dynamics of bone healing at the site. This conclusion is reached with considerable reluctance because iliac crest biopsy is currently the only clinically acceptable method of creating a standard bony defect suitable for the direct measurement of these rates in humans. This observation may also have implications relative to the nuclear imaging of other lesions involving reparative osteogenesis, e.g. hip arthroplasty.

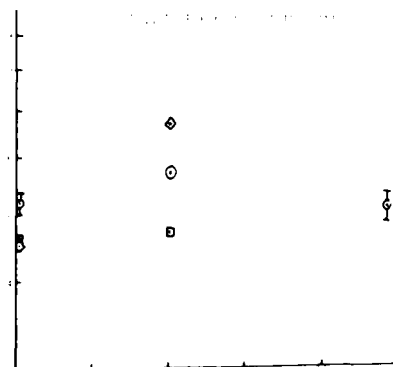


Table 1

Healing Time (Weeks)	Volume % New Bone in Defect		
	Ingrowth (V/o)	S.D.	N.
2	15.6	5.6	17
4	42.0	15.1	15
6	33.2	15.3	15
8	26.7	8.6	18

Acknowledgements: The collaborative assistance of Drs. W.J. Fajman and M. Spector and Mr. G. Malveaux of Emory Univ. Med. School and the financial support of the NSF is gratefully acknowledged.

F.W. Cooke, Ph.D., Dept. of Interdisciplinary Studies, 301 Rhodes Engineering Research Building, Clemson University, Clemson, SC 29631.

A METHOD FOR HIGH-RESOLUTION STUDY OF THE TISSUE
RESPONSE TO POLYMERIZED BONE CEMENT AND OTHER POLYMERS

Lars Linder

Laboratory of Experimental Biology, Department of Anatomy,
University of Göteborg, Sweden

Bone cement is usually found to be surrounded by a thin fibrous membrane when implanted into bone. There have been many speculations as to the origin of this membrane, such as polymerization heat, monomer leakage, surgical trauma, loading conditions, interface micromovements, to name a few.

Charnley has shown that in the perfectly stable condition the cement may lie in direct contact with bone. This has lately been documented in electron micrographs (1), but the findings of the latter study also indicate that an extremely mild, long-term reaction is present at the same time.

Such data would suggest that several factors, alone or together, may contribute to the tissue reaction seen in clinical biopsies. Obviously, to study the reaction to bone cement as such, all such factors as are unrelated to the cement must be excluded. This is fundamental to the understanding of bone reactions to implants in general, and also to future improvements of implant characteristics.

The method to be described here is designed to evaluate the tissue response to polymerized bone cement in an experimental model, where interface micromovements are eliminated and the surgical trauma minimal.

DESCRIPTION OF THE METHOD

Plugs of bone cement are produced by polymerization in titanium moulds. The plugs are then coated with pure titanium, 100-200 nm in thickness (2). The titanium is then carefully removed in small areas over the surface so that a mosaic implant surface is obtained (Fig. 1). The plugs are implanted into the rabbit tibia (2). After animal sacrifice the plugs and surrounding bone are removed with a trephine en bloc, fixed in glutaraldehyde and osmium, and embedded in epoxy resin with or without prior decalcification in EDTA.

During embedding in epoxy resin the cement is dissolved out by the propylene oxide, leaving the titanium film on the surface of the bone (Fig. 2). After the epoxy is polymerized the bone can be sectioned with an intact bone/titanium interface and an undisturbed bone/cement interface as well. One-micron sections can be made for light microscopy (Fig. 3), and ultrathin ones (70 nm) for electron microscopy, if desired.

Fig. 1. Appearance of the plug. The white area is titanium, evaporated onto the bone cement (black). The narrow part of the plug is inserted into a hole in the rabbit tibia, the wider part serving as an extra-osseous stabilizer.



DISCUSSION

In this model titanium implants are reliably healed into bone with a direct bone/titanium contact, provided interface micromovements are absent. The ultrastructure of such an interface is well known (2).

Here, each plug serves as its own control with

titanium as a reference to rule out micromovements or any factor disturbing bony healing.

Any deviation from this interface situation at the bone/cement interface would indicate that bone cement has an inherent negative influence on the tissue.

This model can be used not only for the study of the biocompatibility of bone cement but also for comparative, high-resolution studies of different brands of bone cement. In fact, any polymer can be studied, provided it can be cut on the ultratome.



Fig. 1



Fig. 2

Fig. 1. Surface of the bone specimen, embedded in epoxy. The cement has been dissolved out. The titanium film is now on the surface of the bone. The black areas represent the bone/cement interface.

Fig. 2. One micron section, showing bone with the titanium film (black) on the surface. (x 260).

REFERENCES

- (1) Linder, L., Hansson, H.-A.: Ultrastructural aspects of the interface between bone and cement in man. *J. Bone Joint Surg.* 56-B, No. 4, 1983.
- (2) Linder, L., Albrektsson, T., Brånemark, P.-I., Hansson, H.-A., Ivarsson, B., Jönsson, U., Lundström, I.: Electron microscopic analysis of the bone-titanium interface. *Acta orthop. Scand.*, 54, 45-52, 1983.

This work was supported by the Swedish Medical Society, Asker's Stiftelse, Hjalmar Svenssons Forskningsfond, Trygg-Hansas Forskningsfonder and Gustaf V 80-årsfond.

Laboratory of Experimental Biology
Department of Anatomy
University of Göteborg
Box 33031
S-400 33 Göteborg
SWEDEN

INTERFACE AND BONE RESPONSE TO INCREASED
PENETRATION OF ACRYLIC CEMENT

R.D. Bloebaum, T.A. Gruen, and A. Sarmiento

Department of Orthopaedics/University of Southern California
Orthopaedic Biomechanics/Bone and Connective Tissue Research Program

Long-term results of implants fixed with acrylic cement have demonstrated that a major cause of loosening is at the cement-bone interface. This problem has been addressed by endeavors to improve initial, and hopefully, long-term fixation by a variety of techniques including pulsatile lavage, intramedullary brushing, syringe injection, use of cement in its low viscosity stage, and pressurization. In vitro tests have shown that these measures have individually or in combinations resulted in improved cement-bone interface strengths due to deeper intrusion of the cement into cancellous bone. However, there is concern on the biological responses of the cancellous bone in the face of deeper cement penetration which may lead to thermal necrosis (1) and/or adverse bone remodeling. The purpose of this study was to examine the biological effect of increased penetration of acrylic cement on cancellous bone in a canine model.

MATERIALS AND METHODS:

Under general anesthesia the greater trochanteric and lateral condylar regions of the femur and the lateral tibial plateau were exposed. A hole (1/4" inch) in diameter was drilled through the cortex only. Acrylic cement in its low viscosity stage was then injected into the cancellous bone. The cement was allowed to polymerize in situ under pressure with no subsequent implant insertion into the cement.

Eight animals were sacrificed with two each for time intervals of 3, 6, and 12 weeks and one animal each for 6 and 12 months after acrylic cement implantation. The femora and proximal tibia were dissected and processed for microangiography, microradiography, ground hard plastic section histology, paraffin and epon-araldite histology.

RESULTS:

The cement was noted to penetrate at least ten millimeters through the marrow contents of the intramedullary canal. The short-term response at the cement interface consisted of a soft tissue layer containing numerous immature fibroblasts and proliferating blood vessels. The increase in vascularity at the interface was observed on both sides of the interface, i.e. in the cancellous bone adjacent to the cement as well as within the cement-bone composite! One interpretation for the blood vessels penetrating the cement is the apparent "burrowing" of the blood vessels following active resorption and thinning of pre-existing traumatized trabeculae.

In the longer term animals the trabeculae within the cement-bone composite were observed to be both viable and necrotic with continuing evidences of resorption. The surrounding cancellous bone near and at the interface appeared to undergo hypertrophy. At some parts of the interface around the cement bolus the fibrous soft tissue layer became wider with an appreciable number of foreign body giant cells containing particulate acrylic cement.

SUMMARY

The histological and vascular responses were intense with active remodeling of the trabecular bone in all specimens. A fibrous tissue layer was found often at the cement-bone interface of the cement bolus, while the trabeculae within the cement mass were being thinned by osteoclasts. The trabeculae adjacent to the periphery of the cement mass appeared to hypertrophy.

The extensive biological responses observed in this study raise concern about the long-term clinical performance with the excessive penetration of acrylic bone cement in the presence of mechanical stresses at the interfaces of cemented prosthetic components.

- (1) Huiskes, R. and Slooff, T.J., Trans. Orthop. Res. Soc., 6: 134, 1981.

Address: Orthopaedic Biomechanics
Orthopaedic Hospital-USC
2400 S. Flower Street
Los Angeles, CA 90007

S. Chew, A. McLaren, R.D. Bloebaum, P. Campbell

Orthopaedic Biomechanics Laboratory, Bone & Connective Tissue Research
Program, Orthopaedic Hospital-USC, 2400 S. Flower St., Los Angeles, CA

INTRODUCTION:

New materials with different mechanical characteristics are being introduced to make total hip prostheses with different structural characteristics. Many studies have been conducted on these new implants. Interface studies are felt to be the most reliable for prognostication of the implant fixation. Many studies are still being conducted solely by paraffin histology and/or ground histological methods.

The limiting factor in ground histology is the extreme section thickness. The dense overlapping of acrylic cement and bone obscures direct observation of cellular details at the interface. If the interface holds the key to determining implant performance and potential for longevity, understanding the cell types and their response at the implant-bone interface is essential.

While it is recognized that thin resin sections offer great cellular detail, the application of this method to the study of interface histology has not been fully utilized. This has been due to the technical difficulties associated with processing and sectioning large hard bone specimens. Paraffin wax sections of the interface are frequently folded and yield poorly defined cellular structure. Thick celloidin sections being many cells thick show poor definition of cellular details.

A simple method has been developed for the cutting of large fold-free 2.0 um Epon-Araldite (EA) sections of bone to clearly show intercellular relationships and microstructural detail of the cement/bone interface.

MATERIALS AND METHODS

Total hip arthroplasties were performed in 6 dogs using a carbon fiber polysulfone femoral component and a polyethylene acetabular component. At 12, 24 and 52 weeks post-operatively, the dogs were sacrificed and perfused with Karnovsky's fixative. Both femurs and acetabulae were harvested, photographed and radiographed.

Transverse sections, were taken at 1 cm increments from the collar to 1 cm beyond the distal tip of the implant. A specimen 0.5 cm X 0.2 cm was trimmed from this 2 mm piece to include the cement and bone interface. This specimen was decalcified in 10% formic acid for 48 hours with constant agitation and processed for EA sections(1).

Two micron EA sections were cut on the Sorvall JB-4 Microtome using standard one inch Ralph Knives. The sections were dried in an 80°C slide oven for 80 minutes. They were deplasticized by using potassium ethoxide and stained by a modified H&E method (2).

RESULTS:

Macroscopically, the sections were free of

preparatory artefacts.

At low magnification, good preservation of soft cellular marrow components and trabecular and cortical bone was noted. The relationships between these tissue components showed little, if any distortion and displacement. The interface area could be easily distinguished. Where the cement intruded into the cancellous spaces, marrowless pockets some containing remnants of necrotic bone spicules were observed. Adherent to the cancellous bone surrounding these pockets is a thin discontinuous fibrous tissue layer (5-20 um in width). The cancellous spaces in the immediate vicinity of this layer are relatively more cellular and contain many blood vessels.

Under higher magnification, the fibrous layer was seen to contain active fibroblasts. These cells appear to merge with cuboidal shaped osteoblasts lining the underlying trabecular bone. Multinucleated osteoclasts, some with phagocytic vacuoles, are observed near and at the interface of the 12-week animals (Fig. 1).

DISCUSSION:

Cellular detail was clearly observed from these EA sections and identification of cell types are easy to distinguish. There is a marked histological and vascular response to the implanted acrylic bone cement. The variation in regional histology around the interface indicated a continuous active remodelling in the early stages of implantation and apparent stabilization by one year.

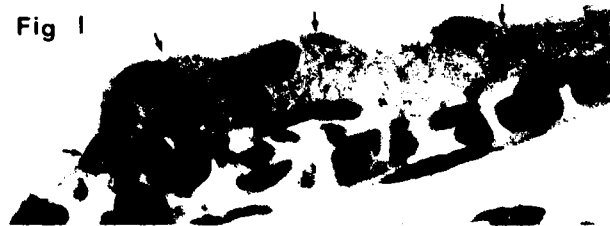
The following are observations made from the histology of the fibrous tissue layer seen in EA sections additional to those previously observed in paraffin sections:-

1. Its cellularity and vascularity suggest that it plays a more dynamic than a physical role in response to the acrylic.
2. The evidence of active mesenchyme-like cells and stellate fibroblasts in the layer adjacent to the osteoblasts of the underlying bone suggest that this tissue layer may be osteogenic in character.
3. The layer abutting the acrylic cement possess quiescent but viable fibrocytes.

REFERENCES:

1. Anderson, W.A. and Andre, J.: J. Micros. (Fr) 7: 343-354. (1968).
2. Chew, S.: Aust. J. Med Technol., 5: 103 (1974).

Fig 1



A COMPARATIVE STUDY OF THE INTERFACE ZONE BETWEEN BONE AND VARIOUS IMPLANT MATERIALS

T. Albrektsson, H-A Hansson and B. Ivarsson

Laboratory of Experimental Biology, Dept of Anatomy, Box 33031, University of Gothenburg, Sweden.

The exact nature of the interface zone between metallic implants and bone is difficult to investigate. Attempts to perform sectioning through undecalcified bone and bulk metal generally fail due to accidental split up of the interface and/or breakage of the sectioning knife. However, Albrektsson et al (1982) showed that in situ sectioning of the intact bone to metal interface was possible if a thin layer of metal was evaporated onto a plastic implant. Calcified tissue was demonstrated to directly border the titanium implant whereas gold implants invariably were separated from the bone by a discontinuous layer of cells. The purpose of the present paper is to compare the bone to metal interface of plastic implants coated with either titanium (reference), zirconium or stainless steel 316 L.

Cylindrical polycarbon plastic plugs of a diameter of 4 mm were manufactured.

Group A Either titanium (99.75% pure) or zirconium was evaporated under high temperature in argon atmosphere onto the surface of ten plastic plugs. The thickness of the metal coat was around 1000 Å. Group B Either titanium (99.75% pure) or stainless steel (316 L) was sputtered at +4°C in argon atmosphere onto the surface of another ten plastic plugs. The reasons for using sputtering was two-fold: 1. To avoid high temperature melting of the stainless steel alloy which would cause physical changes of the alloy 2. To provide for a qualitative comparison between the bone-to-titanium interface of evaporated and sputtered titanium implants, respectively.

Each implant was inserted in the proximal metaphysis of the tibia of adult rabbits and were left in situ for 6 months. A zirconium implant was inserted in one tibia and an evaporated titanium implant in the other tibia of the same animal (Group A). A stainless steel implant was inserted in one tibia where a sputtered titanium implant served as a control in the other tibia of the same animal (Group B).

After 6 months of implantation a trephine was used to remove the implant and surrounding bone en bloc. Fixation was performed in glutaraldehyde to which in some cases ruthenium red had been added. Further methodological details are found in Albrektsson et al (1982).

RESULTS

Group A The titanium-evaporated implants were in an intimate contact with the bone without any interposed fibrous tissue. The collagen was arranged in bundles that became replaced by filaments at a distance of about 2000-4000 Å from the metal border. The last 200-400 Å from the titanium lacked collagen filaments. This narrow zone without collagen consisted of a partly calcified ground substance layer as indicated by the staining reactions proteoglycans and glucosaminoglycans.

Zirconium-evaporated implants from the contralateral extremity of the same animals were directly bordered with bone without any interposed fibrous tissue. However, the zone with collagen-free proteoglycans was much wider than around titanium implants. On average, there was a zone of about 5000 Å proteoglycans close to the metal which lacked collagen and was poorly calcified. A few macrophages were seen in the interface.

Group B The characteristics of the interface between bone and sputtered titanium was not discernible from the interface between bone and evaporated titanium. In both cases there was a proteoglycan layer of around 200 (at places up to 400) Å which separated the bone from the metal surface.

The stainless steel sputtered implants were slightly unstable and could, in contrast to the titanium controls, be manually removed from the implantation site. There was a coat of fibrous tissue consisting of 1-2 cell layers separating the bone from the implant. There were scattered inflammatory cells in the interface zone.

DISCUSSION

Implants inserted under the conditions described in the present paper are "semi-loaded". The actual compressive load on the implant is dependent on the ratio between the modulus of elasticity of the bone and that of the implant.

The technique of coating an implant by evaporation or sputtering produces an implant surface which in both cases differs from that of a machine produced implant surface. What has been demonstrated in this paper is that titanium may be anchored in bone without any interposed fibrous tissue. The very interface between bone and titanium consisted of a partly calcified ground substance layer of a width of mostly around 200 Å, i.e. similar to the thickness of the ground substance layer seen between individual collagen filaments in the case where no implant has been inserted. Zirconium implants demonstrated a fibrous tissue-free interface but a proteoglycan coat of around 5000 Å width. In another study where bone cement covered the plastic plug, a proteoglycan layer of 20,000 Å was observed (Linder et al 1983). We propose that a bone interface with a thin proteoglycan layer of around 200 Å is "nature-like" and thereby indicate a better biocompatibility of titanium in comparison to zirconium, bone cement, stainless steel or gold - the latter metal tested by Albrektsson et al (1982).

REFERENCES

Albrektsson, T. et al Advances in Biomaterials vol 4
Linder, L. et al, J Bone Jt Surg (Br) in press.

Dept of Histology, University of Gothenburg, Sweden
Dept of Physics and Measurement Technology, University of Technology, Linköping, Sweden.

USE OF FIBRIN SEALANT IN EXPERIMENTAL TRACHEAL REPAIR

Kram, H.B., Shoemaker, W.C., Harley, D.P.

Harbor-UCLA Medical Center
Torrance, California

Tracheal stenosis is a devastating complication of tracheal resection and is related to improper suture selection and technique, as well as extensive surgical devascularization. This study evaluated Fibrin Sealant (FS)*, a two component biological adhesive, as a method of reducing and possibly eliminating the need for sutures in tracheal surgery. This adhesive has been found to be effective in face-to-face sealing of tissues, wound healing, and in establishing hemostasis. Five adult mongrel dogs underwent tracheal repair with FS. Three had tracheal hemitranssections (1/2 to 3/4 of the circumference) and were repaired using one absorbable suture and FS. Two had complete transections (one had two tracheal rings removed) repaired using five absorbable sutures and FS. Postoperatively there were 1) no air leaks, 2) the tracheal wounds were stable in cervical flexion and extension, and 3) ventilation was unimpaired in the intubated and extubated states. The animals were sacrificed at intervals ranging from six hours to six weeks (mean = 20 ± 14 days). No animal had gross evidence of significant tracheal stenosis and the endotracheal mucosa appeared nearly normal. We conclude that the use of FS in tracheal reconstruction results in a stable, leakless trachea, and that it significantly reduces the number of sutures needed, thereby decreasing the potential for anastomotic granulomas and late tracheal stenosis.

* Immuno; Vienna, Austria

TESTING FOR BIOCOMPATIBILITY OF MATERIALS USING THE PERITONEAL CAVITY OF THE MOUSE

Merritt, K., and S.A. Brown

Orthopaedic Research Laboratories, University of California, Davis
Davis, California

When a foreign material is inserted into the host, an inflammatory response usually results. The intensity, duration, and type of inflammatory response will in part determine the fate of the implant. A major component of the inflammatory response is phagocytic cells. These may be polymorphonuclear leukocytes, monocytes, and/or macrophages. If the inflammatory response is intense and chronic, foreign body giant cells may be formed. It is often assumed that the foreign body giant cells are formed from fusion of macrophages and engulfment of dead cells and that once they form they may be nonfunctional. It has been difficult to study the foreign body giant cells since methods to obtain them are unpredictable. An inexpensive method that would screen various biomaterials for the ability of inflammatory cells to stick to them and for stimulation of the inflammatory response and formation of foreign body giant cells would be advantageous. Available *in vivo* methods include using a caged implant system or using the peritoneal cavity of rodents.

We chose the mouse peritoneal cavity as an *in vivo* culture chamber to test for adherence of inflammatory cells to the biomaterials. Mice were prestimulated with saline as a control, with casein, with thioglycollate, or with glycogen to increase the number of inflammatory cells in the peritoneal cavity. Implants of candidate materials 5mm x 2mm were inserted into the peritoneal cavity with a 14 gauge needle and trocar. The mice were sacrificed at 3,5,7,14, and 21 days. The implants were stained with Diff-Quik stain and the implants observed for amount of cell coverage and types of cells. Polymers that were translucent were chosen for this experiment for observation with transmitted light microscopy.

Candidate materials included polyethylene, nylon 12, silicone, polychlorotrifluoroethylene (PCTFE), ethylene-chlorotrifluoroethylene copolymer (ECTFE), a polyethylene-silicone blend, and blends of copper and polyethylene and copper and nylon 12.

Differences in cell adherence to the implants and differences in types of cells were evident. Stimulation with thioglycollate or glycogen had the most effect although cell adherence was evident even in the saline controls. Polymorphonuclear leukocytes (PMNS) were not present in large numbers on these implants. In general the cells that were present were monocytes, macrophages, and giant cells. Giant cells were most evident on polyethylene and PCTFE. They were rare on silicone and nylon. Giant cells were evident as early as 5 days after implantation with increasing numbers apparent during 2 weeks of implantation. The giant cells seemed to form from a coalescence of PMNS and of monocytes and macrophages.

There were many cells adherent to the polymers containing copper. The cells appeared to have inclusions of copper in their cytoplasm and were attempting to phagocytize the material. The macrophages and monocytes that were present appeared necrotic and undergoing various morphological changes indicating toxicity of the implant material. The number of giant cells was not as great as that seen on the PCTFE. It would appear that cell viability is necessary for formation of giant cells and these unhealthy cells grown on copper did not coalesce.

It is unknown as to whether or not foreign body giant cells function as phagocytic cells or release substances associated with inflammation. If these giant cells could be obtained in large numbers, then the function could be assessed. Implants were removed from the peritoneal cavity after 5-7 days and placed in culture in chamber slides. They were allowed to grow for 7 days and then the implant and the slide were stained with Diff-Quik and the cells observed. It was apparent that the foreign body giant cells were viable and were spreading on the implant. The rounded form associated with surface of implants and tissue sections had become a flattened cell with numerous pseudopods. There were vacuoles in the cytoplasm indicating that the cells had mechanisms for internalizing foreign substances. Studies on the ability of these cells to phagocytize sheep red blood cells are currently underway. These studies will be extended to observe other functions and measure release of substances such as chemotactic factor by these cells.

The peritoneal cavity of rodents can be used to advantage to screen for biocompatibility of implants. This will allow simple screening for methods of modification of biomaterials to increase their biocompatibility. The role of surface roughness, various surface treatments, surface free energy, blends, and perhaps shape in the tissue reaction to implants can be investigated easily. In addition since these cells can be maintained in culture, their function can be studied and methods to enhance or decrease their activities investigated.

Orthopaedic Research Laboratories
TB 139
University of California, Davis
Davis, California 95616

A NOVEL A-B-A BLOCK COPOLYMER CONSISTING OF POLY(γ -ETHYL L-GLUTAMATE) (A)
AND POLYBUTADIENE (B) AS BIOMATERIAL

Sato, H., Noishiki, Y.,* Chen, G.,** Hayashi, T., and Nakajima, A.

Research Center for Medical Polymers and Biomaterials, Kyoto University,
Kyoto 606, Japan

Synthetic polyamino acids, e. g., poly(L-glutamic acid) (1), seem accessible to biodegradation according to the in vivo pathway of metabolism. Taking into consideration many reports that polymer membranes in occurrence of microheterophase structures showed good antithrombogenicity, we synthesized A-B-A block copolymers consisting of poly(γ -ethyl L-glutamate) as the A component and polybutadiene as the B component, designated EBE. The biocompatibility of EBE membranes will be discussed in comparison with A-B-A block copolymers, MBM, consisting poly(γ -methyl L-glutamate) as the A component and polybutadiene as the B component.

Synthesis of EBE block copolymers:

A homopolymer, poly(γ -ethyl L-glutamate), designated as PELG, and A-B-A type block copolymers, EBE, were synthesized (2) according to the method reported in the previous paper (3). The N-carboxy anhydride of γ -ethyl L-glutamate (γ -ELG) was prepared from L-glutamic acid as a starting material. A cycloaliphatic secondary amine terminated polybutadiene (ATPB), (MW, 3600), was used as the middle block for all the EBE block copolymers reported in this study. The EBE block copolymers were prepared by the polymerization of various amounts of NCA of γ -ELG onto ATPB in a mixture of dioxane and methylene dichloride (1:2 v/v) at 20°C for 72 h. The molar percentage of γ -ELG in EBE block copolymers was estimated from the results of elemental analysis and of IR spectra.

Results and Discussion:

Membrane structure of EBE block copolymers containing 5.5, 10.5, 19.4, 39.5, and 68.5 mole % polybutadiene, abbreviated by EBE-05, EBE-10, EBE-20, EBE-40, EBE-70, respectively, were observed under an electron microscope after staining the polybutadiene portion in the membranes, cast from a mixture of chloroform and trifluoroethanol, by osmium tetroxide. The structure of PELG in block copolymer membranes is regarded as α -helical structure. Depending on the content of polybutadiene, various microheterophase structures were observed as follows: spherical structure of the polybutadiene block domains in the matrix of the PELG component in the EBE-05 block copolymer membrane; an intermediate structure of B between sphere and cylinder in the matrix of E (EBE-10); cylindrical structure of B in the matrix of E (EBE-20); lamella-like structure of B in the matrix of E (EBE-40); and lamella-like structure of E in the matrix of B (EBE-70). Observed micelle dimensions of those structures were from 350 to 480 Å.

With respect to the water permeability of EBE and MBM block copolymer membranes, the permeability coefficients of those membranes were influenced by membrane structures. The permeability coefficients were considered as the contribution of regions such as α -helical polypeptide domain, hydrophobic polybutadiene domain, and the hydrophilic interface domain between polypeptide and polybutadiene chain domain. In result, the permeability coefficients of the interfacial domain in EBE

block copolymer membranes were clarified to be higher values than those of MBM block copolymer membranes.

The tissue compatibility of EBE block copolymers was examined by implanting in mongrel dogs subcutaneously for 4 weeks, while MBM samples coated on the mesh cloth of polyester fiber were implanted subcutaneously in rabbits for 4 weeks (4). The results are listed in Table I, where the levels to evaluate the biocompatibility of materials are as follows: (-), cells do not recognize as foreign body; (\pm), inbetween recognition of (-) and (+); (+), cells recognize as foreign body, giant cells and fibroblasts gather close to the test materials, and cell layers less than 10 surround the foreign body, which corresponds light foreign body reaction; (++) , inbetween reaction of (+) and (+++); (+++), multiple layers of cells like a lump gather close to the test material, which is remarkable foreign body reaction; (++++), the test material works as poison to cells, which causes necrosis.

The degree of absorbance by living body is evaluated according to the following 5 bases; (-), no absorbance or scarcely low absorbance is observed; (+), about 25% of test material is absorbed; (++) , about 50% of test material is absorbed; (+++), about 75% of test material is absorbed; (++++), more than about 95% of test material is absorbed.

Table 1. Tissue Compatibility of EBE and MBM Materials

Samples	Foreign body reaction	Absorbance by living body
PELG	(+)	-
EBE-05	(\pm)	- or +
EBE-10	(+)	- or +
EBE-20	(\pm)	-
EBE-40	(+)	-
PMLG	(\pm)	+ or ++
MBM-20	(+++)	\pm
MBM-43	(\pm)	-

In conclusion, the EBE block copolymers were found out to have good biocompatibility.

References:

- Anderson, J. M., Gibbons, D. F., Martin, R. L., Hiltner, A., and Woods, R., J. Biomed. Mater. Res. Symp. 5, 197 (1974).
- Nakajima, A., Hayashi, T., Kugo, K., and Shinoda, K., Macromolecules, 12, 840 (1979).
- Chen, G., Hayashi, T., and Nakajima, A., Polym. J., 13, 433 (1981).
- Noishiki, Y., Nakahara, Y., Sato, H., and Nakajima, A., Artif. Organs, 9, 678 (1980).

Research Center for Medical Polymers and Biomaterials, Kyoto University, Kawaracho 53, Shogoin, Sakyo-ku, Kyoto 606, Japan

* Institute for Thermal Spring Research, Okayama University

** Dept. of Polymer Chemistry, Kyoto University

AN ELECTRON MICROSCOPE INVESTIGATION OF BLOOD VESSEL INGROWTH INTO DACRON®
VELOUR

Feldman, D., Negele, J., and Estridge, T.

Texas A&M University
College Station, TX 77843

Porous materials have been used extensively in biomaterials applications. There is controversy, however, among investigators on the pore diameter needed for optimum tissue ingrowth, in soft tissue applications. Some discrepancy is expected due to differences in location of the implant, implantation time, and type of animal model used. There has been a lack of systematic studies to determine optimum pore size, since most materials have only been made with a limited range of porosity or pore size. This is especially true of fabric materials, which do not have discrete pores. Since they have a wide range of pore sizes, however, they are amenable to response vs. pore size studies.

Investigators, however, agree that there are at least two categories of pore sizes, in relationship to tissue ingrowth. Small pores, which allow little ingrowth or non-vascularized ingrowth, lead to only temporary ingrowth. Cells more than approximately 100 μ m from their blood supply will eventually die. Large pores, however, allow vascularized ingrowth and, thus, a more permanent ingrowth. Although investigators have suggested limiting pore sizes--throughout the 40-100 μ m range--the onset of vascularization is cited as the common factor necessary for permanent ingrowth.

The objectives of this study, therefore, were to

- 1) Develop a technique to observe the vascular response to porous implants
- 2) Use this technique to measure the vascular response to a specific Dacron® velour.

Two Dacron® velour specimens (1 cm x 3 cm) were glued back to back (knitted side to knitted side) with a Silastic® adhesive and implanted subcutaneously in the dorsum of a dog. Two dogs had four implants each--one each at 1 week, 2 weeks, 3 weeks, and 4 weeks. For each animal there were four separate implantations to allow harvesting of all the implants simultaneously.

At the time of harvesting, the thoracic aorta and inferior vena cava of the anesthetized and ventilated animal were catheterized. The aorta was catheterized cranially to the implants and clamped caudally to the implants. The blood was flushed from the aorta and the intercostals, supplying the area surrounding the implant, by a saline drip. Once the venous return became fairly clear, a polymer solution (Batson's #17 anatomical corrosion compound--Polyscience, Inc.) was injected at approximately 7 ml/min. After polymerization (20-30 minutes) the implants, with the surrounding tissue, were harvested and placed in potassium hydroxide at 60°C for 4-6 days. Specimens were then critical point dried and sputter coated in preparation for scanning electron microscopy.

Although this technique is not perfected, it has much promise in enabling quantification of the

vascular response to porous implants. The results obtained corroborated previous light microscope (1,2) and transmission electron microscope (TEM) (3,4) studies--indicating that blood vessels did not grow into this type of velour, in the subcutaneous dorsum of dogs, until about a 100 μ m pore diameter. Pore diameter was measured as the distance between fibers in cross-section (3,4).

This technique is more versatile than either light microscope or TEM studies of vascularity because it allows a three-dimensional view of the vessel ingrowth. It also permits a larger area to be examined in a shorter period of time and in an easier fashion than TEM, and it permits accurate identification of small vessels (as small as 6 μ m) which is difficult with light microscope. In addition, other parameters can be explored more easily such as vessel size, vasculature structuring, and vascular growth patterns. The ultimate goal being that the effect of implant configuration (pore size, porosity, etc.) implant location, implantation time, and animal model on vascular ingrowth--and thus, tissue ingrowth--can begin to be characterized.

References

1. Feldman, D., "Percutaneous Implants: Histological Interface Study," Dissertation, Clemson University, 1982.
2. Feldman, D., Colaizzo, R.S., and von Recum, A.F., "The Use of Biological Spacers Around Percutaneous Implants," Presented at the 8th Annual Meeting of the Society of Biomaterials, 1982.
3. Feldman, D., Colaizzo, R., Hultman, S., and von Recum, A., "Electron Microscope Investigation of Soft Tissue Ingrowth Into Dacron® Velour with Dogs," *Biomaterials*, 4(2): 105-111, April 1983.
4. Feldman, D., Colaizzo, R., Hultman, S., and von Recum, A., "Electron Microscope Analysis of Tissue Ingrowth Into Dacron® Velour," Presented at the 8th Annual Meeting of the Society of Biomaterials, 1982.

This research was supported by the Industrial Engineering Department of Texas A&M University.

Bioengineering Program
Industrial Engineering Department
Texas A&M University
College Station, TX 77843

DENTAL IMPLANTS: BIOLOGICAL ASPECTS AND PERSPECTIVES

Tomas Albrektsson

Laboratory of Experimental Biology, Dept of Anatomy, University of Gothenburg and the Institute for Applied Biotechnology, Gothenburg, Sweden.

In theory, a dental implant may be anchored in the host tissues with a true periodontal ligament(1) an interface of fibrous tissue(2) or a direct bone attachment(3). So far, no-one has been able to establish and maintain a proper periodontal ligament around a dental implant. Dental implants anchored in fibrous tissue have been extensively used, but there are no reports known to the present author, where a consecutive patient material of adequate size has been analysed and demonstrated acceptable long-term results as defined by the Harvard consensus meeting of 1979. In contrast, directly bone-anchored dental implants as the osseointegrated titanium screw introduced by Brånemark(1969, 1977, 1983) have been inserted in a large series of patients with results clearly exceeding(Adeil et al 1981) the demands put up by the Harvards conference(Schnitman & Shulman 1979). However, bone anchorage of a dental implant is difficult to achieve, while it is easy to insert the same implant and have it anchored in fibrous tissue. A proper bone integration is a multifaceted problem dependent on the biocompatibility(a), the macrostructure(b) and microstructure(c) of the implant, the status of the implant bed(d), the surgical technique(e) and the loading conditions(f). In the following the osseointegrated titanium screw will be analysed with respect to these parameters.

a. Implant biocompatibility Analyses of the interface between bone and titanium of clinical dental implants which were removed in spite of an undisturbed bone anchorage after up to 7 years of function revealed a fibrous tissue-free interface around the titanium screw. Interfacial analyses of experimental titanium implants using the plastic plug technique have revealed a direct contact between calcified tissues and bone at a resolution level of 30-50 Å.

b. Implant macrostructure An advantage with screw-shaped implants is the initial good resistance to shear stress, in comparison to a smooth or porous implant. Once properly osseointegrated, the screw is able to transmit an axial tensile or compressive load to the surrounding bone primarily by compression on the inclined faces of the screw(Skalak 1983).

c. Implant microstructure Surface roughness and porosity of an osseointegrated implant have a beneficial interlocking effect similar to that of screw threads at a microscopic scale (Skalak 1983).

d. Status of the implant bed Experimental investigations with the Bone Growth Chamber and the Harvest Chamber(Jacobsson & Albrektsson 1983) have indicated that previous irradiation is not a contraindication for implant insertion. A single dose of 5 Gy(= 500 rads) produces a significant reduction in bone incorporation of a titanium implant immediately after the irradiation while the negative osteogenic effects of doses up to 15-20 Gy seem to be compensated for, if a delay of at least half a year is allowed before implant insertion. Clinically, osseointegrated implants have been inserted in previously irradiated beds after a delay of at least 1 year(Brånemark 1983). Another important bed factor is the necessity of a healthy bone without infection while alveolar ridge resorption, on the other hand, is no contraindication for osseointegrated dental implants. In an unselected

consecutive material of 500 treated jaws there have been no indications for bone grafting in the mandible while 10 % of the treated maxillas had to be grafted before implant insertion(Brånemark 1983). e. Surgical technique Experimental studies(Eriksson & Albrektsson 1983) with theoptical bone chamber indicate that the critical temperature for bone necrosis is as low as 47°C applied for one minute. In contrast, drilling under routine clinical conditions at a rotatory speed of 20.000 rpm with profuse saline cooling produces a considerable heat impact, for instance in the case of inserting screws for Richard plates in the live human femur averaging 89°C(Eriksson, Albrektsson 1983). A graded series of well sharpened drills, low rotatory speeds and adequate cooling appear to be important measures for the establishment of a direct bone contact with the implant (Albrektsson 1983).

f. Loading conditions Too early loading of an implant causes micromovements, and increases the risks for fibrous tissue anchorage. Clinically, a minimal unloading period of 3 months is essential for the establishment of a reliable osseointegration(Brånemark 1983).

To date, the complete material of the osseointegrated screw comprises more than 7000 dental implants inserted into totally or partially edentulous jaws of around 1500 patients. The outcome of each and every inserted implant has been registered and all patients have been subjected to at least annual controls. The 5- and 10-year positive results of mandibular implants have been 91%(Adeil et al 1981, Brånemark & Albrektsson 1983). All implants which unintentionally have become anchored in fibrous tissue have been removed as failures within one year after implantation, even if these soft-tissue-anchored implants seemingly caused no harm. With control of the failures observed during the first year after mandibular implantation, 10 year success rates of more than 99 % has been reported(Brånemark & Albrektsson 1983). Average annual bone height loss after the first postoperative year has been 0,05mm and the inflammation score according to Tagge et al(1975) has been 0 in 58% and 1 in 37% of randomly selected 125 implants with an average insertion time of 7,5 years (Lekholm et al 1983).

The literature on oral implantology has long been dominated by anecdotal reports that have misled some dentists into thinking that implantology is a clinical treatment method to be rapidly incorporated into their practices(Zarb 1983). The insertion of dental implants is, however, a complicated procedure which for the achievement of clinically reliable results calls for simultaneous control of several parameters. The work of Brånemark has demonstrated that a strictly controlled technique of implant insertion leads to predictable clinical results over decades or more of follow-up, and there seems to be little doubt that the 1980ies will become the clinical and academic breakthrough time for dental implants.

Laboratory of Experimental Biology, Dept of Anatomy, Box 33031, S-400 33 Gothenburg, Sweden.

AN IN VITRO STUDY OF PLATELET/VASCULAR GRAFT INTERACTIONS

Kandice Kottke-Marchant, James M. Anderson, A. Rabinovitch, and R. Herzig

Depts. of Macromolecular Science and Pathology, Case Western Reserve University, Cleveland, Ohio 44106

An *in vitro* perfusion system has been developed to study the interaction of blood with vascular graft materials. Fresh human donor blood (500ml), anticoagulated with either citrate (10mM) or heparin (3 U/ml), was recirculated at 450 ml/min by a peristaltic pump in a circuit comprised of a reservoir connected to a loop (1.0 m) of medical grade silicone rubber (SR) tubing (3/8 in ID) into which various vascular graft materials were inserted in a sleeve-like fashion. The blood was divided into two equal fractions and used to fill two simultaneous circuits, one of which was a control with only SR tubing, the other a test circuit containing a test material (either expanded polytetrafluoroethylene (ePTFE), crimped Dacron Bioknit (DB), or preclotted Dacron Bioknit (DB/PC)). Blood samples were taken prior to starting the pump and at 15, 60 and 180 min. during recirculation.

Platelet counts were stable for both the SR and ePTFE throughout the circulation time using both citrate and heparin. With DB and DB/PC, the platelet count was significantly ($p < 0.05$) lower than SR at 15 min., possibly signalling platelet adhesion to the test surface. As seen in Figure 1, the DB platelet count remained at this level, while the platelet count continued to decrease for DB/PC.

Platelet α -granule release, as measured by plasma levels of Platelet Factor 4 and β -thromboglobulin showed dramatic increases over baseline ($p < 0.05$) for both DB and DB/PC by 15 minutes, while there was little platelet release seen for SR or ePTFE. In addition, there was greater release observed using heparin than citrate for the same material. Ordering the materials by the observed extent of platelet release gave: DB/PC-hep, DB-hep>DB/PC-cit>DB-cit>ePTFE-hep>ePTFE-cit>SR-hep>SR-cit.

PF3 activity, measured by a clotting assay, remained constant for both SR and ePTFE throughout the recirculation, while there was a progressive increase in PF3 activity for both DB and DB/PC, which became statistically different from SR by 180 minutes. Platelet retention, measured by the glass bead column method, was increased over baseline for all materials at 15 min. when citrate was used, and then steadily decreased to below baseline by 180 minutes. Platelet retention behavior was variable using heparin, although generally decreased from baseline during the recirculation. In ADP-induced platelet aggregation, there was an increased sensitivity to ADP over baseline at 15 min. for all materials, which decreased progressively with recirculation time, although aggregability was greater with heparin than citrate.

Prothrombin times and partial thromboplastin times remained near control levels for all materials at all recirculation times. Fibrinogen levels decreased slightly for all materials by 15 min., then stabilized for SR and ePTFE, but continued to decrease for DB. In correlation with this (Figure 2), fibrinopeptide A levels (in citrate) remained constant for SR and ePTFE, rose 3X for DB and rose 150X for DB/PC, suggesting this system as a method for studying blood interaction with various preclotting techniques.

These studies show this *in vitro* system to be valuable for discriminating platelet-activating effects of materials, with Dacron and especially preclotted Dacron to be more platelet and coagulation activating than either the ePTFE or Silicone Rubber, the latter two being quite similar.

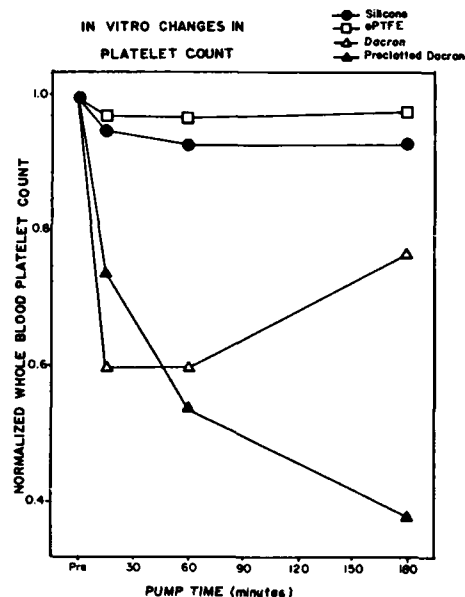


Figure 1.

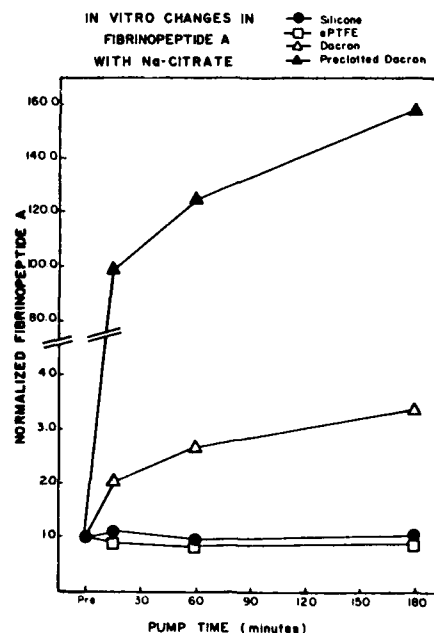


Figure 2.

HUMAN UMBILICAL CORD VEIN AS A BLOOD CONDUIT: A Comparative Study of Two Modes of Storage of the Raw Material

S.T. Li and P. Zalesky

Meadox Medicals, Inc. Oakland, N.J.

Implantable medical devices that are derived either wholly or partly from biological tissues, such as the processed human umbilical vein graft (Dardik Biograft) or tissue heart valves, depend critically upon the initial state of the tissues that are subsequently processed for device fabrication. The condition of tissue procurement and storage could affect the quality and thus, the safety of the product as a long term implant. Processed human umbilical vein has been successfully applied as a peripheral arterial substitute for the past five years. One of the factors contributing to the success of the product is the tight control of the raw material procurement. An immediate washing with physiological saline after delivery and limited duration storage in a hospital refrigerator before shipping to the manufacturing plant have been enforced. Even so, batch to batch variations in tissue quality have often been observed. Consequently, an alternative mode of cord storage has been sought in an effort to minimize the possibility of tissue degradation due to bacteria and endogenous enzymes. In this report, we compare the results of morphological, physico-chemical and mechanical characterization studies of the fresh and frozen human umbilical veins as well as their respective processed final products and conclude that immediate freezing is an effective mode of cord storage.

Fresh cords were collected according to a recommended procedure. The identical number of cords were collected simultaneously from the same hospitals and were immediately frozen (for up to 7 + 1 days) after proper flush of the lumen with physiological saline. The frozen cords were thawed overnight in a refrigerator and then subjected to the same initial inspection procedure as the fresh cords. Aliquots of the respective cords were sampled for histological evaluation. The cords were then processed according to the manufacturing specifications. Samples were collected during the process and in the final product form for characterization studies. The morphological properties were examined by light microscopy employing standard H&E and trichrome staining techniques. Lumen surface energetics and composition were characterized by critical surface tension (CST) and internal reflection infrared (IR) spectroscopic measurements respectively. The tissue stability was determined by a thermal shrinkage temperature measurement. The mechanical properties

were characterized by a suture pull out strength test as well as by leak rate and compliance measurements under physiological pressure conditions.

The light microscopy of stained thin cross-sections of raw human umbilical cords showed one vein and two arteries. In the vein region a thick uniform smooth muscle was surrounded by a homogeneous appearing Wharton's jelly. The elastic lamina appeared intact and continuous throughout. The frozen cords, in addition, exhibited numerous prominent vacuolizations in the smooth muscle and the Wharton's jelly layer. The glutaraldehyde fixed cords appeared distorted as compared to the raw material, showing a compact and morphologically identical structure for both the fresh and frozen cords. The subsequent chemical processing did not alter the morphology of the respective fixed cords to any significant extent. In addition, the lumen surface energetics, lumen surface chemical composition, thermal stability and mechanical properties were all identical in both products (results shown in the table). These results suggest that the grafts made from fresh or frozen cords will function equally well in vivo. The general applicability of frozen technique to other biological tissues such as bovine pericardium, a major material for bioprosthetic heart valve construction, is under investigation.

	FRESH PRODUCTS (S.D.)	NO. OF MEASURE- MENTS	FROZEN PRODUCTS (S.D.)	NO. OF MEASURE- MENTS
SHRINKAGE TEMP (°C)	78(1)	6	78(1)	6
CST (dynes/cm)	32(0.6)	37	32(0.6)	23
SUTURE PULL (g/mm)	207(53)	73	199(51)	67
LEAK RATE (ml/cm ² /min)	0.003(0.002)	38	0.004(0.002)	26
COMPLIANCE (mmHg ⁻¹)	0.12(0.02)	37	0.11(0.01)	28

ACKNOWLEDGEMENTS: We thank Ms. Cathie Squatrito for technical assistance.

MEADOX MEDICALS, INC.
103 Bauer Drive
Oakland, N.J. 07436

THE IMPACT OF POLYESTER ARTERIAL PROSTHESES OF CZECHOSLOVAKIAN ORIGIN:
AN IN VITRO AND IN VIVO EVALUATION

M.W. King, R.G. Guidoin, K.R. Gunasekera*, L. Martin, M. Marois, P. Blais**,
J.M. Maarek and C. Gosselin.

Université Laval,
Québec, Canada.

Introduction:

For over 25 years U.S. scientists, clinicians and manufacturers have been the pioneers in the design and production of arterial prostheses. More recently researchers in other countries have also been making contributions to this field. One such group emanating from the collaborative efforts of the Surgical and Knitting Research Institutes of Czechoslovakia has developed a series of new polyester prostheses for the bypass and replacement of large and medium caliber arteries. This paper assesses the significance of this development by evaluating the Czechoslovakian prostheses by "in vitro" tests and by an "in vivo" study using a thoraco-abdominal bypass in dogs. A comparison is made with models of current U.S. manufacture (1).

Methodology:

The study included 4 different designs:

- DK1n : Knitted, without crimp,
- DK1 : Knitted and crimped,
- DK2 : Knitted, crimped and externally supported,
- DK3 : Knitted with a taper, without crimp.

The virgin prostheses were exposed to a series of standard textile tests (2) to define their fabric and yarn structures and to measure certain physical properties such as crimp extension, bursting strength, water permeability and dilatation under static internal pressure. A total of 24 dogs were involved in the thoracoabdominal bypass protocol (3), each design being implanted for one of six predetermined periods ranging from 4 hours to 6 months "in situ". Following the sacrifice, routine pathological and histological examinations of the explanted grafts and kidneys were undertaken to determine the extent of healing and the presence of infarcts caused by embolization. In addition, further textile tests were completed on the cleaned proximal, central and distal sections to assess "in vivo" changes in the strength and dimensional stability of the prostheses.

Results and Discussion:

The "in vitro" tests indicated that all four models have the same weft knitted construction, and contain thicker, heavier yarns than are found in U.S. devices. Consequently they have higher bursting strengths than their American counterparts. Also, all four models exhibit less than 5% dilatation at 120 mm Hg pressure, which is within the acceptable limit defined by the proposed ISO standard (4). We believe, however, that greater dimensional stability could be achieved in the long term with the use of a warp knitted, rather than a weft knitted, construction.

The animal study demonstrated that all four models heal satisfactorily with good encapsulation, a low incidence of embolization, fair dimensional stability and adequate strength retention. The two crimped models, DK1 and DK2, gave similar "in vivo" performances to weft knitted prostheses of U.S. origin, except that DK2, the externally supported design, lost some strength and contained laminar fibers on its external surface apparently caused by abrasion of the loosely weaved supporting

monofilament. Both uncrimped models, DK1n and DK3, lost tension distally during the first month of implantation. This resulted in fiber swelling, fabric shrinkage and the formation of creases and folds in the wall of the prosthesis, together with a high incidence of mural thrombi. Such evidence suggests that determining the correct tension is more critical and difficult to achieve when inserting long segments of uncrimped prostheses. Furthermore, it appears that in addition to preventing occlusion caused by collapsing or kinking, the crimped configuration has a heretofore unrecognized role, particularly for long segments, namely in ensuring that the graft maintains adequate longitudinal tension throughout its residency, in spite of graft stretching, and relaxation and relocation of the attached vessels.

Conclusion:

We believe that the thoraco-abdominal bypass procedure is a valuable and versatile experimental instrument for two main reasons. Firstly longer segments provide a more sensitive measure of the extent of healing and they reflect more closely the experience in humans. Secondly, by using larger specimens, additional tests can be included, for example, to evaluate the mechanical and dimensional changes to the graft, as well as completing pathology, histology and biochemical studies.

While we recommend that the two crimped designs of Czechoslovakian prostheses, DK1 and DK2, merit further clinical evaluation, we do not foresee them having a significant impact on the choice of North American surgeons.

References:

1. Guidoin R., Gosselin C., Martin L. et al, Polyester prostheses as substitutes in the thoracic aorta of dogs, *J. Biomed. Mater. Res.*, (In press)
2. King M.W., Blais P., Guidoin R. et al, Polyethylene terephthalate (Dacron) vascular prostheses: material and fabric construction aspects, *Biocompatibility of Clinical Implant Materials*, Vol. 2, D.F. Williams, CRC Press, Boca Raton, Fla., 1981, pp. 177-207.
3. Gosselin C., Guidoin R., Marois M. et al, Thoraco-abdominal bypass as a method of evaluating vascular grafts in dogs, *Biomat. Med. Dev. Art. Org.* 9: 196-212, 1973.
4. ISO DP 7192, Draft standard for synthetic tubular vascular prostheses, *AAMI*, Washington, DC., March 1982.

This work was supported in part by the Departments of Family and Community Health, and Health and Welfare Canada.

Laboratoire de chirurgie expérimentale,
Bâtiment André-Armand-Lavoie,
Université Laval,
Québec, Québec, L3C 3G1, Canada.

*University of Manitoba, Winnipeg, Canada.

**Health and Welfare Canada, Ottawa, Canada.

THE EFFECT OF FLOW ON PLATELET UPTAKE BY VASCULAR GRAFT MATERIALS IN A BABOON EX VIVO SHUNT MODEL

R. Connolly, E. Keough, W.C. Mackey, K. Ramberg-Laskaris, J. McCullough, T. O'Donnell, Jr., and A.D. Callow

Tufts University School of Medicine and New England Medical Center
Boston, Massachusetts

The patency of small caliber vascular grafts may be determined by the early interactions of blood components with their luminal surface. In order to investigate the interaction of ¹¹¹Indium labeled platelets with a variety of graft biomaterials, an *ex vivo* percutaneously placed arteriovenous shunt was developed in the baboon.

Mature male baboons were anesthetized with sodium pentobarbital, blood was withdrawn, platelets isolated and labeled with ¹¹¹In oxine. The shunt circuit consisted of intravascular catheters, short segments of medical grade Silastic tubing, 4mm id test material, 4mm id preclotted knitted Dacron, an in-line flowmeter, and an adjustable downstream resistance. Platelets were injected, flow initiated in the shunt circuit, and platelet accumulation over a 2.5 hour period monitored using dynamic gamma camera scanning. Data were analyzed by counts per minute normalized to injected dose and corrected for isotope decay and background activity. Dacron(D), PTFE, and glutaraldehyde stabilized human umbilical vein (HUV) were studied at low (25cc/min) and high (200cc/min) flow rates.

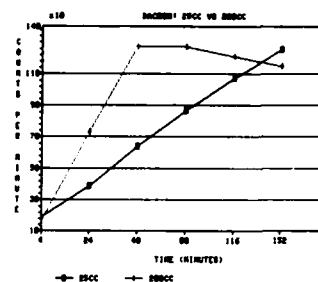
D accumulated platelets rapidly at both high and low flow; however maximum accumulation was delayed with low flow (graph 1). PTFE accumulated few platelets at high flow; however with low flow, platelet accumulation approached that of D (graph 2). HUV was moderately platelet reactive at both flow rates (graph 3).

Low flow simulates the clinical situation and controlled low flow studies are necessary to evaluate a biomaterial for use in small caliber grafts. Results suggest that the flow effect on platelet accumulation differs with different biomaterials.

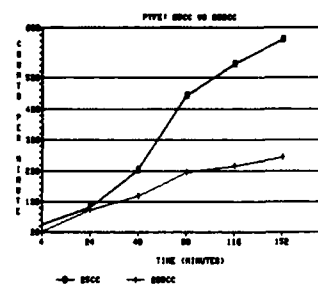
The similarity of the results obtained with D and PTFE in high flow shunt circuits to those obtained in previous *in vivo* studies using carotid interposition grafts supports the shunt as a reasonable model for studies of blood interactions with biomaterials.

The increase in platelet uptake on PTFE at low flow when compared to that at high flow offers an explanation for the clinical observation that current synthetics perform poorly in small caliber low-flow circuits.

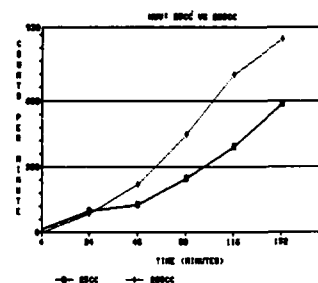
Graph 1



Graph 2



Graph 3



Supported by NIH RHL24447-4 and New England Medical Center Ziskind, Posner and General Research Support Funds.
Raymond Connolly, Ph.D.
New England Medical Center
171 Harrison Avenue
Boston, MA 02111

ARACHIDONIC ACID DERIVATIVE AND PLATELET RELEASE REACTION
INDUCED BY IMPLANT MATERIALS.

A. Pizzoferrato, M. D'Addato*, E. Cenni, T. Curti*,
D. Cavedagna, C. Tarabusi.

Center for Biocompatibility Research of Implant Materials -
Istituto Ortopedico Rizzoli - Bologna (Italy).

The use of foreign materials in a living organism may induce platelet adhesion and aggregation with synthesis of thromboxane and release of beta-thromboglobulin and platelet factor 4 (1,2).

The thrombogenicity of the following materials was tested: Woven Dacron, Knitted Dacron, Straight Knitted Velour Dacron, Double Velour Dacron, polytetrafluoroethylene or PTFE, Dacron-Urethane, Dacron-Urethane coated with isotropic carbon, Alumina and Copper.

These materials were brought into contact with citrate platelet rich plasma (PRP), for a fixed time. As control, normal PRP without material was tested.

Platelet counts and radioimmunoassays of thromboxane B_2 , beta-thromboglobulin and platelet factor 4 were performed both on PRP that had been in contact with the foreign surfaces and on the control.

A highly significant decrease of platelet number was observed after contact of PRP with Woven Dacron, Knitted Dacron, Straight Knitted Velour Dacron, Double Velour Dacron, Alumina and Copper.

Dacron-Urethane coated with isotropic carbon, PTFE and Dacron-Urethane induced only small changes of platelet number.

Copper, Alumina and Dacron caused also remarkable increases of thromboxane B_2 ; Dacron-Urethane coated with isotropic carbon caused only a modest increase; PTFE and Dacron-Urethane induced only small changes in thromboxane B_2 levels.

All test materials, except Dacron-Urethane, caused a highly significant release of beta-thromboglobulin. PTFE and Straight Knitted Velour Dacron did not cause any significant change in the plasmatic level of platelet factor 4. Significant changes were induced by other materials tested.

The increase of thromboxane B_2 , beta-thromboglobulin and platelet factor 4 was correlated with the decrease of platelet number.

The release of these substances is associated with morphological changes. At microscopic evaluation, it was possible to see platelet aggregates, which were more numerous after contact with Alumina, Copper and the kinds of Dacron used in Vascular Surgery. We employed a technique based on the use of a cyto-centrifuge and Giemsa staining.

Using transmission electron microscope, the loss of alpha granules and dense bodies content could be observed.

Platelet counting permits to evaluate bio material thrombogenicity by quantifying platelet adhesion, but it does not offer any information on release reaction induced by the contact with foreign surfaces. Only thromboxane B_2 , beta-thromboglobulin and platelet factor 4 assays permit to evaluate platelet release reaction induced by the contact with foreign surfaces.

Microscopic evaluation allows to correlate biochemical changes with morphological aspects of platelet activation.

Among the materials tested, Dacron-Urethane, PTFE and Dacron-Urethane coated with isotropic carbon were the most thromboresistant.

Knitted Dacron, Woven Dacron, Straight Knitted Velour Dacron and Double Velour Dacron showed different degrees of thrombogenicity.

Double Velour Dacron and Woven Dacron caused the most remarkable changes in all the tests performed, comparable with the changes induced by Alumina and Copper.

The assays of thromboxane B_2 , beta-thromboglobulin and platelet factor 4, especially if associated, may be very useful in evaluating the grade of thrombogenicity of biomaterials and in investigating the mechanism of thrombus formation on foreign surfaces.

- 1 - J. Lindon, R. Rodvien, D. Brier, G. Greengard, I.W. Merrill, and E.W. Salzman: J. Lab. Clin. Med., 92, 904-915, 1978.
- 2 - D. L. Coleman, A. I. Atwood and J. D. Andrade; J. Bioeng. 1, 33-44, 1976.

This work is supported by National Research Council (C.N.R.).

A. Pizzoferrato

Center for Biocompatibility Research of
Implant Materials.

Istituto Ortopedico Rizzoli
40136 - BOLOGNA (Italy)

*Chirurgia Vascolare, Policlinico Gemelli

Expanded PTFE as a Microvascular Graft: A Study of Four Fibril Lengths

Branson, D.F.; Picha, G.J.; DesPrez, J.

Div. of Plastic Surgery, University Hospitals, CWRU, Cleveland, OH.

Advances in clinical microsurgery have demonstrated the utility of a 1mm microvascular graft. To date only autologous vein has been found to be acceptable in clinical practice. Qualities of a microvascular prosthesis include 1. acceptable patency rates, 2. ease of handling, 3. availability, and 4. resistance to infection. This study evaluates four fibril lengths of expanded PTFE with a 1mm diameter to determine 1. utility of PTFE as a microvascular graft, and 2. characteristics of this graft.

163 grafts were implanted in the descending aorta of Sprague Dawley rats weighing 350-500gr.

All grafts were implanted by one surgeon using 8 sutures proximally and distally. The proximal anastomosis was accomplished with the aid of a mandril (20ga. intracath). No systemic anticoagulant or antiplatelet drugs were used. All grafts were observed in situ for 30 min. before closing the rat. Grafts implanted had fibril lengths of 30u, 60u, 90u, and 120u. Production batch numbers were recorded for all implants. Grafts were harvested at 10min., 30 min., 24 hrs., 4 days, 7 days, 1 month and 3 months. Patency was evaluated by standard clinical methods. Implants were evaluated by standard histology and SEM.

All grafts were patents initially. No transmural (transgraft) bleeding was noted. The 90u and 120u grafts were noted to dilate during the first 10 min. of flow. The 90u graft dilated approximately 10% over baseline, while the 120u graft dilated approximately 25-30% over baseline. This dilatation did not appear to clinically proceed for the duration of the study. All grafts that failed had thrombus present at the distal anastomosis. At 3 months, all grafts had a smooth intimal lining to macroscopic examination. The 60u graft was stenotic at the distal anastomosis, which macroscopically appeared similar to pseudointimal hyperplasia.

Patency data at 3 months is as follows: 60u=46.3% (19/41); 90u=97.7% (42/43); 120u=88.6% (31/35). All 30u grafts clotted by 45 minutes after blood flow was established.

During the course of the study, a second production batch of 90u material was tested with a patency rate of 33% (2/6) at one month. This material did not display the similar distensible character with blood flow noted with the "good" material. Significant differences were found in the nature of the fibril composition between the two materials. The fibril structure noted in the "good" batch of material displayed a more random, less organized pattern.

SEM examination was grouped according to time period of harvest. At early time periods (30 minutes or less), the blood graft interface displayed a dynamic interaction occurring, as might be expected. The specimens varied from homogeneously exposed graft to a laminated matrix

of fibrin and formed blood components. Each individual specimen was uniform in its appearance (i.e. exposed graft vs. fibrin & formed elements). A minor increase in the presence of fibrin was noted from proximal to distal. The density of formed blood elements, as well as the type of blood elements found was consistently variable between materials. The 60u material had a combination of fibrin, platelets, and red cells. The 90u material displayed only fibrin and platelets, with occasional deposits of red cells. The 120u material showed fibrin, platelets, red cells, and white cells. The 60u material displayed the thickest deposits of fibrin, etc. This relative presence/absence of formed components remained constant throughout the time periods tested, with decreasing density of formed elements occurring with time. By one month, all grafts displayed a relatively smooth pseudo-intima. The nodes of the graft material remained exposed. Sutures at the proximal anastomosis remained exposed, while those at the distal anastomosis were covered by pseudo-intima. By three months, the entire graft surface was covered by pseudo-endothelial cells arranged in the direction of flow. The relative prominence of these cells by SEM is as follows 90u>120u>60u. The pseudo-intimal hyperplasia noted with the 60u graft at three months appeared to involve the full thickness of the graft, with the majority of the fibrosis present extrinsic to the graft.

Of the 163 grafts implanted, 35 specimens were excluded from the data for the following reasons: 17/35 died before scheduled harvest, with the graft clinically patent at autopsy; 6/35 rats expired intra-operatively; and 14/35 died prior to scheduled harvest without autopsy.

It is clear from this study that expanded PTFE has significant potential as a microvascular graft. It also appears clear that fibril length alone does not contribute to patency, but that fibril characteristics become critical at the 1mm graft size. To date, a duplicate of the "good" batch of material has not been produced. It would appear that quality control will be a critical factor to widespread clinical use of an expanded PTFE microvascular graft.

(This project was supported by W.L. Gore & Assoc., Flagstaff, AZ)

Denis F. Branson, M.D.
Div. of Plastic Surgery
University Hospitals of Cleveland
2074 Abington Road
Cleveland, Ohio 44106

INTEREST OF IN VITRO RADIOISOTOPIC INVESTIGATION TECHNIQUES TO STUDY BEHAVIOR OF COAGULATION PROTEINS AT THE INTERFACE WITH BIOMATERIALS.

Ch. BAQUEY, L. BORDENAVE, J. CAIX, B. BASSE-CATHALINAT, V. MIGONNEY*, C. FOUGNOT*.

INSERM/CEEMASI-SC 31 - Université Bordeaux II, 33076 BORDEAUX-CEDEX

*L.R.M., Université de Paris Nord, 93430 VILLETANEUSE (France).

INTRODUCTION

We have described elsewhere (1) (2) biomaterials demonstrating anticoagulant properties, these latter coming from the ability of the biomaterial surface to catalyse the Thrombin-Antithrombin III (T - AT III) reaction. A possible mechanism for such an activity could come from a specific affinity of the surface for AT III leading in vivo to the adsorption of the antiprotease and the activation of its inhibitory effect against T action. Thus it was important to design experiments able either to evidence or to reject this mechanism and particularly the ability of the surface to adsorb AT III. Moreover such experiments could be used as a tool for quality control of modified materials.

MATERIALS AND METHODS

Results reported here deal with medical grade polyethylene tubing ($\emptyset = 2.85$ mm), the inner surface of which has been radiation grafted with styrene (2 mg/cm²) grafted polystyrene being chlorosulfonated and then reacted with the dimethyl ester derivative of a dicarboxylic amino-acid, according to procedures previously described (3). The chemical treatment is followed by extensive conditioning through repeated washings with various buffers, saline and distilled water.

To study the adsorption of proteins onto the modified surfaces exposed to protein solution ¹²⁵I or ¹²⁵I labelled proteins were prepared according classical methods. AT III and T were provided by the Centres Français de Transfusion Sanguine.

Radioactive measurements were made using a Ge-diode detector according a sequential procedure already described (4). The distribution of the adsorbed protein along the tubing could also be obtained using a gamma camera (CGR..) fitted with a specially designed collimator.

40 cm long segments of modified polyethylene tubings are tested under dynamic conditions, i.e. proteins solutions are circulated at a given flow rate and for a chosen period of time through the tubing previously primed with Michaelis buffer so as to avoid any contact with air at the protein solution material interface. Fig. 1 shows the set up used for this study. The two three ways valves allow complete filling of the loop with buffer, elimination of any air bubbles, replacement of the buffer by the labelled protein solution, rinsing of the circuit by saline, and desorption of the eventually adsorbed protein by a concentrated sodium chloride solution. Two procedures have been run comprising several steps :

PROCEDURE A : Step 1 : incubation for 30 mn of the tube to be tested under flowing conditions at room temperature with a labelled protein solution,

Step 2 : rinsing of the circuit by NaCl 0.15M,

Step 3 : desorption of the adsorbed protein by NaCl 3M.

PROCEDURE B : Steps 1 and 2 : as in Proc. A,

Step 3 : exchange of the adsorbed protein by a cold protein solution at the same concentration under flowing conditions.

Step 4 : rinsing of the circuit by

NaCl 0.15M

RESULTS. Fig. 2 shows the presence of an adsorbed amount of AT III on the tested surface and that more than 60 % of this amount is still remaining after rinsing with NaCl 3M.

A tentative of exchange of the adsorbed hot protein by circulating, through the tubing, a solution of cold AT III at various concentrations, revealed that about 75 % of the protein could not be replaced, probably because irreversibly adsorbed.

Fig. 3 shows that the adsorbed protein is distributed almost homogeneously on the exposed surface and the amount appears much more important on the modified surface than on the virgin material.

CONCLUSION : A method allowing a better knowledge of the dynamic behavior of coagulation proteins when they meet an artificial surface designed to demonstrate anticoagulant properties, is proposed. The experimental set up allows study of various factors : flow velocity through the tubing, flowing solution composition, protein concentration. With such a tool, exchange rate of adsorbed protein with protein in solution can also be assessed.

As tubings are to be tested also in vivo the method can also be used to check the homogeneity of the treatment of their inner surface, and the reproducibility of the treatment.

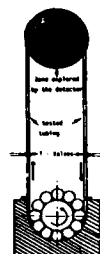


Fig. 1 - Set-up used for studying protein adsorption and desorption under flowing conditions



Fig. 3 - Gamma camera imaging of two tubings (modified PE on the left, unmodified PE on the right) filled with AT III solution (a) and rinsed with NaCl 0.15M (b). The unmodified PE cannot be visualized after rinsing.

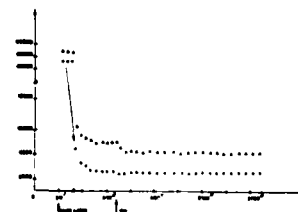


Fig. 2 Adsorption and desorption by NaCl solutions of AT III on modified Polyethylene (PE) (▲) and on virgin PE (●).

ACKNOWLEDGEMENTS This work has been partly supported by the Centre National de la Recherche Scientifique (GRECO n° 130048).
1-FOUGNOT C, & al. Ann. Biomed. Eng., 7 : 429, 1979.
2-FOUGNOT C, & al. Ann. Biomed. Eng., 7 : 441, 1979.
3-LAUTIER A, BAQUEY C, & al. Int. J. Art. Org., 5 : 199, 1982.
4-BASSE CATHALINAT B, & al. Int. J. Appl. Rad. Isot., 31 : 747, 1980.

R. C. Eberhart, M. S. Munro, G. O. Bridges, P. V. Kulkarni and W. J. Fry

Department of Surgery, University of Texas Health Science Center at Dallas
Dallas, Texas 75235

One of the most demanding tests of thromboresistance occurs in studies of implanted small vessel grafts. In such applications microthrombi form and embolize, even when most stringent protective measures are employed. A method which may improve the thromboresistance of such grafts is to provide a dynamically renewable, endogenous albumin coat between the surface of the device and the blood. The albumin layer serves to mask the substrate from blood-borne host defense activation mechanisms. We have developed an alkylation process which takes advantage of the high affinity of serum albumin for 16 and 18 carbon aliphatic chains. C₁₈ or C₁₆ alkyl groups are covalently bound to the polymer of interest. In theory, serum albumin is continuously adsorbed and desorbed at these sites by hydrophobic interactions. We report experiments testing the ability of alkylated polyurethane to bind and retain albumin in vivo, and to improve thromboresistance of small vessel vascular grafts. Five mm I.D., 5 cm wire reinforced vascular grafts of solution grade Biomer® were C₁₈ alkylated in our laboratory. The reaction involves an alkyl isocyanate and proceeds at a urethane secondary amide group. Control and C₁₈ alkylated Biomer® grafts were placed at femoral arterial sites in the dog, using a sleeving technique. Systemic heparinization was necessary to inhibit albumin-binding clot formation on control grafts. Cannulae were placed proximally and distally to each graft, via branch vessels. ¹²⁵I labeled, pooled canine albumin (15 mg/dl) was preadsorbed on the grafts for 30 min, followed by 2 hrs of blood exposure. The grafts were then flushed with saline, reexposed to the albumin solution and the incubation/blood exposure protocol was then repeated in its entirety. Measurements of ¹²⁵I albumin uptake were carried out with a manual scanning, gamma counting system. Albumin uptake on C₁₈ alkylated grafts, prior to blood exposure, was significantly greater than on the corresponding control grafts (Fig. 1). Albumin desorption was characterized by an immediate fast phase and a following slow phase. Approximately 80% of the preadsorbed albumin was rapidly desorbed from both alkylated and control grafts upon blood exposure. However, albumin retention on the alkylated grafts during the 2 hr blood exposure period was always greater than on the corresponding controls. Following the fast desorption phase, the remaining albumin was slowly desorbed from both alkylated and control grafts. The slow phase desorption rate from alkylated grafts was significantly lower than it was from controls (Fig. 2). Albumin uptake during (30 min) reincubation with albumin solution was again significantly greater on alkylated grafts than on the corresponding controls. However, more albumin bound to controls during this second exposure period than in the first period. This suggests that an intermediate protein, bound during the first blood exposure, may subsequently complex with albumin. Eighty percent of preadsorbed albumin was again rapidly desorbed from both

alkylated and control grafts upon exposure to blood. Following the fast desorption phase, similar to that observed in the first exposure period, the slow phase desorption rate tended to be lower for alkylated grafts than for controls. Thrombus was frequently observed at sacrifice on control grafts; significantly less thrombus was seen on the alkylated grafts. Our results suggest a higher albumin affinity exists in vivo for C₁₈ alkylated Biomer® grafts than for controls. The results also support the concept that preferentially bound albumin promotes thromboresistance in vivo, even in the presence of systemic heparinization.

Supported by USPHS Grant HL28690-01.

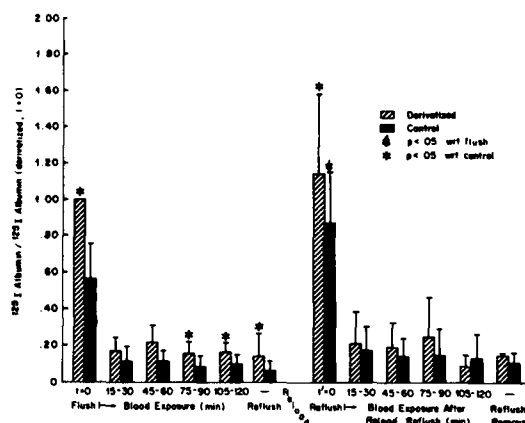


Fig. 1. Albumin retention on alkylated and control grafts for two sequential blood exposure periods, with reincubation with albumin following blood flush at 2 hrs. Values are compared with adsorbed ¹²⁵I albumin on derivatized graft, following 30 min incubation and flush, at t = 0.

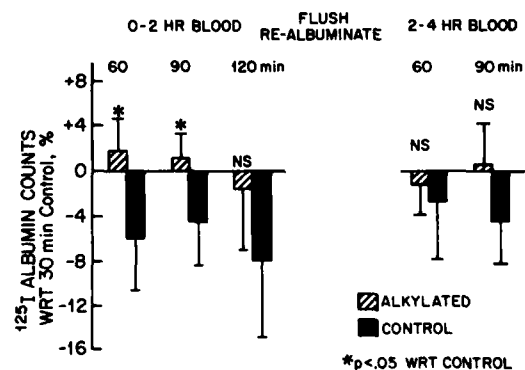


Fig. 2. Desorption rate of preexposed ¹²⁵I albumin on alkylated and control grafts.

Robert C. Eberhart, Ph.D., Department of Surgery, University of Texas Health Science Center at Dallas, 5323 Harry Hines Blvd., Dallas, TX 75235

PROPERTIES OF ACELLULAR VASCULAR MATRIX

R.C. Duhamel, Ph.D., K. Brendel, Ph.D., R.L. Reinert, B.S.*
and J.M. Malone, M.D.*

University of Arizona, Tucson, Arizona

We have developed a novel procedure for the preparation of vascular grafts from biological materials. The procedure consists of extensive extraction of biological tissues with detergents in order to produce extracellular matrix that is denuded of cytoplasmic and nuclear cellular components. To produce acellular vascular matrix (AVM) suitable for use as a small diameter vascular graft, native dog carotid arteries were sequentially extracted with the detergents, Triton X-100 and sodium dodecyl sulfate for 4-16 and 96 hours, respectively, at ambient temperature. During the Triton X-100 extraction, cytoplasmic membranes disintegrate and endogenous nucleases are activated which hydrolyze nuclear DNA even though nuclear membranes remain morphologically intact. Nuclear membranes disintegrate during the subsequent extraction with dodecyl sulfate. Protease inhibitors and frequent exchanges of solution are used during the extractions to prevent proteolysis.

The objectives behind the preparation of AVM are: (1) the removal of cells, nuclei and cellular antigens, (2) the avoidance of proteolytic damage, and (3) the maintenance of compatible surfaces for recellularization by host cells after implantation or reseeding with endothelial cells prior to implantation.

Detergent-treated AVM is free of nuclei, nucleic acids, cellular membranes, and lipids, as indicated by histological staining and direct biochemical analysis. Amino acid analysis indicates that collagen and elastin are the primary components of AVM.

Amino Acid Compositions

	Native Vessel	AVM	Elastin Fraction
	residues/1000		
3-Hydroxyproline	0.0	0.00	0.0
4-Hydroxyproline	48.13	78.41	10.1
Aspartic acid	53.75	39.98	3.8
Threonine	34.19	23.01	14.4
Serine	42.27	33.91	88.5
Glutamic acid	74.06	60.25	26.8
Proline	98.45	111.96	14.1
Glycine	244.70	307.35	347.2
Alanine	117.21	129.90	234.7
Half-cystine	12.79	0.00	0.0
Valine	52.13	45.70	103.2
Methionine	11.42	8.52	1.2
Isoleucine	26.25	18.93	26.6
Leucine	51.73	35.80	44.0
Tyrosine	23.85	16.11	27.2
Phenylalanine	26.64	19.30	23.2
Hydroxylysine	4.02	6.75	0.0
Lysine	29.74	17.57	2.6
Histidine	10.25	8.02	7.5
Arginine	38.41	38.55	6.1

Several extracellular matrix proteins are detectable by immunohistology in addition to interstitial collagen and elastin: these include the non-collagenous proteins, fibronectin and laminin, and type IV or basement membrane collagen. The two latter proteins are restricted to the luminal surface of the inner elastic membrane. Proteoglycans are also detectable histologically. As seen by scanning electron microscopy, the sub-endothelial basement membrane is fully intact.

The tensile strength, compliance, and suturability of non-crosslinked AVM approach that of the native vessel. Of course, AVM can be crosslinked with glutaraldehyde or other crosslinking agents as desired. We have observed, however, that non-crosslinked AVM may be more rapidly recellularized upon implantation than crosslinked AVM, indicating that non-crosslinked AVM may be a better substratum for recellularization. The absence of nuclei from AVM prior to implantation facilitates study of the recellularization process. For example, host nuclei are readily detectable by fluorescence microscopy in frozen sections stained with propidium iodide.

Upon implantation of non-crosslinked 4 mm I.D. x 4-6 cm segments in the carotid position in greyhound dogs, AVM exhibits extensive recellularization at 90 days. A monolayer of cells is found on the luminal basement membrane which, by scanning electron microscopy, has the cobblestone appearance of a sheet of endothelial cells. Host cells also invade the adventitial layer and the extreme antiluminal layers of the media of the AVM graft, indicating substantial healing of the graft.

ACKNOWLEDGEMENTS: This work was supported in part by NIH Grant HL29164 to K.B., V.A. Merit Review Grant #008 to J.M.M., and a grant from Bard Implants Division, C.R. Bard, Inc.

Department of Pharmacology, College of Medicine
University of Arizona, Tucson, AZ 85724
and

*Department of Surgery, College of Medicine
University of Arizona, Tucson, AZ 85724

J.A. Goggins, R.D. Jones*

Department of Biomedical Engineering, Case Western Reserve University,
Cleveland, OH

Many factors influence blood response to polymeric materials. Surface charge generated on the material surface in flowing blood and its influence on the thrombogenic and cellular response have been reported. The exact nature of this relationship is not yet clear. Blood response to polymeric surface charge can be characterized using a copolymer of methacrylic acid and polyethylene, known commercially as Surlyn[®]. The presence of methacrylic acid permits negative charge manipulation by neutralization of the acid, with some cation, to a salt form. Additionally, the salt may be changed by the choice of the cation. The copolymer, also referred to as an ionomer, forms three phases and the ratio of these phases in a given sample is affected by thermal history. There is a crystalline polyethylene phase, an amorphous phase of non-crystalline polyethylene and ionic groups (methacrylic acid or its neutral salts) and a third phase composed solely of methacrylic acid or its salt, known as the ionic domain. This domain consists of ion pairs, multiplets or clusters(1). The size of this third region also appears to vary with thermal treatment(2). Samples of the copolymer Surlyn[®] in acid and neutralized Na and NH₄ salt forms were prepared to obtain different surface charge densities. After annealing treatments which alter surface charge distribution and degree of crystallinity, these materials were tested in an *in vivo* model, previously described(3). Cellular and thrombogenic response was recorded and the resulting data was evaluated by analysis of variance for significant differences due to surface charge density and distribution.

Samples of Surlyn[®] containing approximately 3.5 mole % methacrylic acid were prepared as 100% acid (0% salt), 50% Na salt, 100% Na salt and 100% NH₄ salt, by refluxing in tetrahydrofuran and either HCl or an appropriate hydroxide solution. Confirmation of these alterations was obtained for the bulk polymer by Fourier Transform Infrared Spectroscopy. The samples were then heated to 190°C and quenched in liquid nitrogen. This quenching treatment also generated a free surface. All samples had one of three thermal histories, the quench already described, a 14 day anneal at 25°C, or a two day anneal at 80°C. It has been suggested that these conditions yield the greatest differences in the degree of crystallinity and ionic domain size(2). Medical grade polyethylene served as a control and was treated in the same manner as the ionomer. Rectangular patches, 2 mm x 5 mm x 0.1 mm were implanted in the femoral and carotid arteries (diameter-approximately 4 mm) of mongrel dogs. Each implant was prewetted before implantation in an appropriate solution for example, dilute acid, dilute base, neutral H₂O or neutral isotonic saline. This was done to avoid air-blood interactions and the solutions were selected to prevent material equilibration in wetting agent rather than in the blood. Similar prewetting of the polyethylene controls did not significantly alter the cell response to that polymer. Hematocrit and activated clotting time were measured for

each animal and the ranges permitted were 35% to 50% for the former and 50 to 120 seconds for the latter. Initial implantation intervals were 15 minutes, after which samples were rinsed, fixed and prepared for evaluation by scanning electron microscopy.

The percent of implant covered by non-aggregated platelets, white blood cells, fibrin, exposed polymer, and thrombus (aggregates of platelets and/or white blood cells) was recorded. Analysis of variance by thermal treatment showed no significant differences among the samples for this short time interval. However, analysis of variance by salt treatment indicated a significant difference (>95%) for platelets, exposed polymer and fibrin. 100% Na salt and 100% NH₄ salt implants had the largest percentage of exposed polymer and platelets, while fibrin covered a larger amount of the 0% salt surface. Means and standard deviations of the sample groups were calculated. Increasing salt concentration favored platelet deposition and exposed polymer, while fibrin percentage diminished. Polyethylene controls appeared similar to the 0% salt samples. Fig. 1 is a 4 x 3 matrix grouped by salt concentration and thermal treatment of the means and standard deviations of the percent fibrin covering the implant surface after 15 minutes exposure to blood. Note the inverse relationship between the percent fibrin and the salt concentration.

The polymer surface has been altered by charge manipulation and annealing. Charge density appears to influence both formed elements and proteins (fibrin). Longer implantation experiments are underway in order to observe further developments in the blood response to the materials.

	0%	50% Na	100% Na	100% NH ₄
0°C	28.8±27.5	9.2±15.9	9.6±9.7	11.7±12.9
25°C	57.7±32.0	34.6±42.4	20.1±18.9	6.2±6.6
80°C	39.8±18.9	38.0±26.9	6.3±6.1	2.5±3.4

Fig. 1 Percent of surface covered by fibrin at minute implantation.

*Division of Surgical Research, St. Luke's Hospital, Cleveland, OH

**E.I. DuPont DeNemours, Wilmington, DE

References

1. MacKnight, W.J., Earnest Jr., T.R. J. Polym. Sci.: Macromol. Rev. **16**:41-122 (1981)
 2. Painter, P.C. et al J. Polym. Sci. Polym. Phys. Ed. **20**:1069-1080 (1982)
 3. Van Kampen, C.L. et al Biomat. Med. Dev. Art. Org. **6**(1):37-56 (1978)
- Supported by the St. Luke's Hospital Association and the Timken Fellowship for J.A.G.

POLYELECTROLYTE GRAFTED POLYURETHANES INTERACTIONS WITH BLOOD PROTEINS & PLATELETS

CHANDRA P. SHARMA AND AJANTA K. NAIR

BIOSURFACE TECHNOLOGY DIVISION, BIOMEDICAL TECHNOLOGY WING
SREE CHITRA TIRUNAL INSTITUTE FOR MEDICAL SCIENCES & TECHNO-
LOGY, POOJAPURA, TRIVANDRUM - 12, INDIA.

SUMMARY

The outstanding anticoagulation activity of Heparin, a natural mucopolysaccharide is attributed to the presence of sulphate sulfamides and carboxylic groups. Synthetic heparinoid PE have also been found to possess anticoagulant activity¹, and have been used for surface modification by grafting them on silicon rubber².

Polyelectrolyte from natural poly Cis-1,4 isoprene (source *Hevea Brasiliensis* "Para Rubber") has been synthesized in our lab as discussed elsewhere¹. We have attempted to graft this product on PEUU precipitated on clean glass rods in the form of vascular grafts <5mm in diameter. Using γ -irradiation to produce an anti-thrombogenic surface.

Invitro studies were performed on these modified surfaces using platelet rich plasma (calf) to assess the platelet adhesion and with labelled proteins to study the protein surface interactions. Table I lists the platelet count on various surfaces with different exposure time to 50 mgm% polyelectrolyte solution and irradiated with a dose rate of 0.275 M Rad. For comparison heparinised surfaces were used. (Precipitated PEUU grafts were dipped in TDMAC Heparin Complex for 15 mts & later vacuum dried).

T A B L E - I
Platelet Adhesion

Time of exposure to PE & Irradiated	Platelet count in 0.4mm ² \pm s.d (n=20)
15'	1.80 \pm 0.77
1 hr.	1.70 \pm 0.73
2 1/2 hr.	1.05 \pm 0.84
4 hr.	1.0 \pm 0.73
5 hr.	1.0 \pm 0.73
24 hr.	0.55 \pm 0.60
Bare	1.85 \pm 0.75
Bare (non irradiated)	2.50 \pm 0.83
Heparin (non-irradiated)	1.47 \pm 0.92

Table II & III indicate the protein adsorption desorption study from the protein mixture with blood concentration ratio (Albumin 50 mgm%, Fib. 2.5 mgm% & γ -Globulin 18.75 mgm%) using trace labeling methods. 24 hrs. polyelectrolyte adsorbed and subsequently irradiated samples were used. Adsorption desorption after 3 hrs. are indicated. However the Kinetics of adsorption and desorption are also studied.

T A B L E - II
Adsorption Desorption Studies

Surfaces	Albumin μ gm/cm ²		Fibn μ gm/cm ²	
	Adsorp- tion 3 hrs.	Desorp- tion 3 hrs.	Adsorp- tion 3 hrs.	Desorp- tion 3 hrs.
Bare	0.28	0.16	0.24	0.10
Polyelec- trolyte	0.29	0.15	0.25	0.07
Heparin	10.01	6.55	2.46	1.87

T A B L E - III
Adsorption Desorption Ratio

Surfaces	Ratio of Alb Ads/Des	Ratio of Fib Ads/Des	Ratio of Fib/ Alb Ad- sorbed	Molar Ratio of Fib/Alb
Bare	1.75	2.40	0.86	0.17
Polyelec- trolyte	1.93	3.57	0.86	0.17
Heparin	1.53	1.32	0.25	0.05

The results indicate that the presence of heparinoid polyelectrolytes on the surface has a marked effect in decreasing the platelet count. Also its interactions with proteins is minimal compared to Heparinised surface. Thus polyelectrolyte on the surface can act as a passive layer and help the surface in being blood compatible. Ratio of Albumin Ads/Des appears to be comparable in all the three cases, however in case of Fib. this ratio is relatively higher in case of polyelectrolyte samples. This indicate that the amount remained after desorption is less on these surfaces, i.e less stability of Fibrinogen molecules.

Although from Molar ratio of Fib/Alb it seems that fibrinogen molecules are only 5% on the Heparinised surfaces compared to 17% of polyelectrolyte grafted & Bare surfaces, but taking the number of adhere platelets into account it seems polyelectrolytes grafted surfaces may also be one of the very good candidates to enhance blood compatibility.

References:

1. Van Der Does et al J. Poly. Sym. 66, 337, 1979.
2. Sederel et al, Comac Workshop on: New Aspects in Anticoagulant Therapy During Extracorporeal Circulation, Lyndhurst (UK) December 1979.

ACKNOWLEDGEMENT

This work was funded by DST, India.

Testing of Filled PTFE Vascular Prostheses Using Panel Grafts

B. Tenney¹; W. Catron²; D. Goldfarb, M.D.²; R. Snyder, Ph.D.¹

1. Bard Implants Division, A Division of C. R. Bard, Billerica, MA.

2. Dept. of Medical Research, St. Luke's Hospital Med. Ctr., Phoenix, AZ.

In 1977, D. Goldfarb [1] described the effect of including a graphite powder into the Expanded Polytetrafluoroethylene (e-G/PTFE). The canine data indicated an improvement in the patency rates. Additional data by Goldfarb [2, 3] confirmed these early observations. However, it was difficult to compare surfaces using typical paired graft tests due to the variability from dog to dog and from side to side. Thus, a paneled graft containing both filled and unfilled PTFE on the same luminal surface was developed. This prosthesis was then implanted in 4 sites in the canine and the results compared at several different implant times.

MATERIAL PROPERTIES

Manufacturing parameters were adjusted to yield similar physical dimensions in both the e-PTFE and the e-G/PTFE. Some post-processing shrinkage was noted in the filled material, but had an insignificant effect on the final dimensions.

Zero to 25% filler was investigated. The depth of filled material varied from 30 to 100% of the thickness. A review of the strength and elongation properties indicated that up to 15% filler had only minimal impact on these parameters. In addition, the depth of the filler had little impact on preliminary compatibility results. In-vitro labeled platelet studies (Tenney [4]) showed little impact of the depth parameter. Thus it was decided to concentrate on the 0 to 15% graphite in 30% of the wall thickness (from the luminal surface).

A study of the effect of the presence of graphite on the final crystalline/amorphous structure of the e-G/PTFE was undertaken using a Differential Scanning Calorimeter (DSC). A concern existed that the presence of the graphite might effect the heat transfer properties of the PTFE and, thus, modify this ratio. The effect was shown to be minimal. These grafts were then subjected to cyclic testing (Tenney [4]). The presence of the graphite did not appear to enhance the notch sensitivity of the PTFE.

CANINE STUDY

Prostheses were fabricated with 33% of the circumference e-PTFE, 33% of the circumference 10% e-G/PTFE, and 33% of the circumference 15% e-G/PTFE. Both filled sections were 30% of the thickness. Six centimeter lengths of 5mm diameter grafts were then implanted in 4 locations in the canine model. Two grafts were implanted in the right and left carotids and 2 were implanted in the right and left femoral arteries. All prostheses were implanted interpositionally.

These grafts were then harvested at 1 week, 2 weeks, 1 month, 3 months, and 6 months. The grafts were photographed and then sectioned and examined histologically.

RESULTS

Results of this test demonstrated an overall improvement in thrombus formation of e-G/PTFE sections over unfilled e-PTFE. Furthermore, in the majority of surfaces there is a distinct demarcation between the thrombus covered unfilled e-PTFE and the thrombus free filled e-G/PTFE panels. These samples will be further examined via a Thrombus Free Surface Analysis [5].

DISCUSSION

For several years, canine studies using synthetic vascular prostheses have been performed by implanting prostheses in 4 positions; i.e., left and right carotid and femoral arteries. Control prostheses are usually implanted contralaterally. One problem with this type of testing is the limited information available per canine. Another potential problem is the difference in blood parameters between implant positions. There have been indications that any event that occurs in one carotid artery may occur in the other. This is due to a redundant blood supply; i.e., the carotids are connected in the Circle of Willis located at the base of the brain. In addition, there is an anatomical size difference between the left and right femoral arteries.

An attempt was made by Botzko, et al to minimize these effects by performing sequential graft tests. That is, suturing together end to end controls and test prostheses. However, there is still the possibility of having the proximal prosthesis influence the distal prosthesis and that the surgical anastomosis may influence only the proximal prosthesis. For the first time, a unique method of manufacture results in a prosthesis that is capable of minimizing the effects described above.

BIBLIOGRAPHY

1. Goldfarb, D.; Houk, J. A.; Moore, J. L., Sr.; and Gain, D. L.: Graphite-Expanded Polytetrafluoroethylene: An Improved Small Artery Prosthesis. *Trans. Am. Soc. Artif. Intern. Organs*, 23:268, 1977.
2. Goldfarb, D.; Houk, J.; Moore, J., Sr.; Catron, W.: Modified Graphite-Expanded PTFE (G-PTFE) For Use as a Superior Vena Cava (SCV) Substitute. *Trans. Am. Soc. Artif. Intern. Organs* 24:201, 1978.
3. Catron, W.; Goldfarb, D.; Moore, J., Sr.; Houk, J.; Jeffrey, K.; Expanded PTFE: Long Term Follow-Up. *Trans. Am. Soc. Artif. Intern. Organs*, 28:190, 1982.
4. Tenney, B.; Gelfand, J.; Snyder, R.: In-Vitro Testing of Expanded Graphite PTFE Grafts. To be published, 1984.
5. Sauvage, L. R.; Walker, M. W.; Berger, K.; et al: "Current Arterial Prostheses: Experimental Evaluation by Implantation in the Carotid and Circumflex Coronary Arteries of the Dog", *Arch of Surg*; Vol. 114, pp 687-691; 1979.

PHYSICOCHEMICAL PROPERTIES OF IMPROVED BIOSYNTHETIC GRAFTS FOR VASCULAR RECONSTRUCTION

R. Baier, A. Meyer, M. Fornalik, K. Kokolus

Advanced Technology Center, Calspan Corporation, P. O. Box 400,
Buffalo, NY 14225

New mesh-reinforced tissue grafts show significantly improved surface and bulk properties over previous attempts at producing biological tubes for vascular substitution or repair. Mandril-grown tissue tubes, usually known as Sparks Mandril Grafts, have had a checkered history and have been generally abandoned in arterial reconstructive surgery in humans, perhaps prematurely.

The improved grafts characterized here overcome previously noted problems by specific control of growth periods in subdermal ovine locations prior to harvesting, and by preservation with precisely mixed, glutaraldehyde-based tanning fluids prior to storage in aqueous ethanol solutions for indefinite periods. The result is the production of tissue tubes with fully incorporated reinforcing meshes, displaying high mechanical integrity and luminal wall properties associated with biocompatible performance in contact with flowing blood.

Major problems to be overcome were these: The original autologous tissue grafts were so weak that failure by aneurysm was both early and frequent. Attempts to use reinforcing meshes courted the difficulties of mesh show-through, triggering thrombogenesis, without developing adequate wall integrity. When it was shown that chemical tanning procedures could significantly strengthen the tissue tubes as well as suppress immunogenic sites, both homologous and heterologous tissues were open to use. A common problem among all such mandril-grown grafts, however, was their propensity for high contents of lipoidal materials in both surface and bulk depots. Excess lipid near or at the interface led to compromise or loss of desirable flow surface properties, risking both early and later thrombogenic sequelae.

Analytical Criteria of Graft Quality. Multiple attenuated internal reflection infrared spectroscopy of the luminal wall surfaces of the biosynthetic grafts allowed determination of the relative proportions of protein, lipid, carbohydrate, tanning reagents, and other species in the interfacial zone.

Critical surface tension determination, together with calculation of the relative polar and dispersive force contributions to the composite surface free energy function of the flow surface, was based on careful contact angle measurements with a large series of purified, calibrated test liquids.

Scanning electron microscopy of critical-point-dried specimens allowed determination of the luminal wall morphology, presence or absence of deposits or particulate debris, and evidence of mesh extrusion. Energy-dispersive x-ray analysis of the same specimens provided data on the elemental abundances of all components with atomic number greater than eleven.

Wall integrity and resistance to either mechanical or biological deterioration were assessed in a circulatory loop wherein physiologic saline (with Evans Blue dye) was continuously pumped under accelerated arterial conditions until over 1,000,000 pulses had been sustained by each test vessel. The room temperature bath in which the grafts were supported during measurements of ultrafiltration volume were deliberately kept nonsterile to challenge the grafts with infective microorganisms during mechanical stressing. Each mechanical pumping trial was terminated by incrementally increasing the intraluminal pressure of the graft, still pulsing at about 90 beats/minute, until failure occurred by either wall rupture or a multiplicity of small leaks.

Results. Internal reflection infrared spectra reveal, almost uniquely for these tissues raised against implanted foreign materials in carefully controlled settings, luminal wall compositions dominated by proteinaceous components and remarkably diminished lipid contents over prior-art specimens. Critical surface tensions of the internal flow boundaries are in the range between 20 and 30 dynes/cm, characteristic of fully endothelialized natural vessels and of prosthetic surfaces exhibiting long-term thromboresistant qualities. Polar/dispersion force ratios of the components of surface energy are about equal to those for natural and tanned blood vessels. Scanning electron microscopy confirms that mesh show-through is reduced generally below 5% of the luminal wall area, and in some specimens to zero. Energy-dispersive x-ray analyses reveal freedom from adventitious contaminants and from elements predisposing to early mineralization. Mechanical pumping trials certify these biosynthetic grafts as being of excellent physical integrity, sustaining continuous simulated arterial pumping with low transluminal ultrafiltration rates despite mechanical and bacterial challenge. Ultimate burst strengths are in excess of 25 pounds per square inch.

Based on comparative data obtained with variously preserved bovine heterograft and human umbilical cord vessels also prepared for use as arterial prostheses, these new biosynthetic grafts are now ready for final clearance in animal/clinical trials.

INTRALUMINAL BYPASS DEVICE FOR ARTIFICIAL AORTIC GRAFT IMPLANTATION

Feldman, D., Hale, S., Hunter, J.

Texas A&M University
College Station, TX 77843

Artificial vascular grafts are in very common usage today. There are 50,000-150,000 grafts implanted every year (1). The most common reasons for graft implantation are aneurysms and arteriosclerosis (atherosclerosis). There are many different types of vascular grafts with the most common made of Dacron® or Teflon® fabric--similar to the design first suggested by DeBakey when he sutured a piece of polyester into a tube over 20 years ago.

There are various surgical procedures to implant an artificial aortic graft. These require either bypass of the area to be replaced or clamping off of the area to be replaced. The major concerns are: prevention of a sudden increase in peripheal resistance and left ventricular overload, which can lead to ventricular fibrillation or cardiac arrest; and prevention of permanent ischemic changes to distal organs - particularly the spinal cord and kidney - which can lead to death or paraplegia (2). Based on the published work of nine authors during the past 10 years, bypass and shunting procedures led to a 1-11% incidence of paraplegia and a 11-21% death rate (2). A cross-clamping technique used in 112 patients between 1962 and 1980 led to a 0.9% incidence of paraplegia and a 9% death rate (2). Careful pharmacological control of cardiac and circulatory hemodynamics, as well as, speed during the surgical procedure, however, are necessary to obtain these success rates. Although the time limits of cross-clamping in humans is unknown, in one study, problems did not arise until 15 minutes of cross-clamping and were insignificant even after 90 minutes of cross-clamping (the longest time during that study) (2). The reason for success of that technique was its simplicity, in contrast to shunts and bypasses, as well as careful monitoring and control of hemodynamics and proper fluid replacement (2).

Therefore, the objective of this study was to develop a simple surgical procedure for replacement of the aorta without the need for bypasses, shunts, or the careful monitoring and speed necessary for successful cross-clamping. This technique could be used by researchers without sophisticated equipment or technical expertise, as well as, by many surgeons who could not otherwise do this type of vascular surgery.

The intraluminal bypass device was a Silastic® tube, 4.5 cm long; with polyethylene nozzles on either end - attached in such a way to leave grooves to facilitate bypass clamp attachment (figure 1).

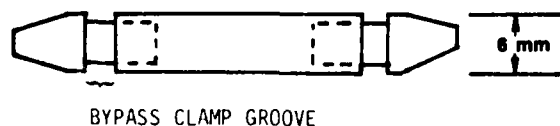


Figure 1. Intraluminal bypass device

For implantation, a thoracotomy was performed, on dogs placed on their right side--between the fifth and sixth rib--and the thoracic aorta was exposed. A pair of clamps (umbilical tape and rubber tubing) were placed on each side of the section of aorta to be removed and were secured by Kelly hemostats. The outside clamps were closed, the aorta was cut and the heparinized intraluminal bypass device, with the graft around it, was clamped into place by the two inside bypass clamps. The two outside clamps were then released to allow blood flow through the bypass device to the distal thoracic aorta. Blood flow was maintained during suturing of the graft. When all but the last two sutures on the proximal side of the anastomosis were complete the outside clamps were closed, the inside clamps were released, and the intraluminal bypass device was removed. Then the final sutures were placed, air was removed from the inside of the graft, and then the outer clamps were removed.

The procedure worked very well in the three dogs used in this study. The implant was designed so the length of the device could be shortened easily during the surgical procedure, if necessary. Which was important since it took practice to determine the optimum size of the bypass device necessary for each situation. Since no human clinical trials have been performed, the incidence of paraplegia and the death rate are unknown. The procedure, however, has similar advantages as the cross-clamping procedure; in addition it does not require the careful monitoring necessary for the cross-clamping procedure and blood flow is stopped for only a few minutes. Therefore, the paraplegia rate and death rate should be at least as good as the cross-clamping procedure.

A similar technique was developed by Dr. Sundt (3) to allow cerebral circulation during carotid endarterectomy procedures. This device presently is manufactured by American Heyer-Schulte Corporation and is performing well.

References

1. Beall, A., Baylor College of Medicine, Personal Data, 1980.
2. Crawford, E., Walker, H., Saleh, S., and Normann, N., "Graft Replacement of Aneurysm in Descending Thoracic Aorta: Results Without Bypass or Shunting," *Surgery*, January 1981, 73-85.
3. Peipgras, D., and Sundt, T., "Clinical and Laboratory Experience with Heparin-Impregnated Silicone Shunts for Carotid Endarterectomy," *Annals of Surgery*, 184:5, November 1976, 637-641.

This research was supported by the Office of University Research and the Industrial Engineering Department of Texas A&M University.

Bioengineering Program, Industrial Engineering Department, Texas A&M University, College Station, TX 77843.

ADJUSTMENT OF AN INFLATABLE CLAMP IN VASCULAR SURGERY

DE LA FAYE D., LEGENDRE J.M., LEFEVRE C., GUIDOIN R.,

DEPARTMENT OF BIOMATERIALS AND SURGERY

Service Lombard
C.H.U. 29279 BREST CEDEX (FR)

ry and for the clamping of delicate transplants such as the Biograft Dardik, Solco-graft, Johnson and Johnson whose vulnerability to clamping devices is well known.

The classical vascular occluder cause intimal and medial lesions on arteries and veins walls. The frequency of the traumatism observed in an analytic study of the animal lead us to propose a clamping mechanism through an inflatable device.

Material and method

1st phase : 320 clampings have been realized on the aortas of 2,5 kg. New-Zealand albinorabbits and on the aortas of 17 kg Mongrel dogs.

Five types of instruments have been used in homogenous series : schwartz clip, micro-coronary Bull Dog, Bull Dog, Satinsky and De Bakey aorta clamp.

In the qualitative analysis the optical microscopy (x 30 to x 500) and the scanning electron microscopy (X 1 000 to X 10 000) were used. In the radioisotopic quantitative analysis platelets labelled with the indium 111 and fibrinogen labelled with iodine 125 were used.

Results

Clamping lesions have been noted in 100 % of the cases.

The microscopic analysis specified the degree of anatomical effect ; the radioisotopic study measured the importance of the wall thrombus.

The seriousness of the lesions lead up to adjust a less traumatizing, inflatable clamp.

2nd phase

The prototypes of our instruments have been tested according to the above said protocol.

The clamp is flexible and fitted with one or more air pumps. The progressive inflating stops when necessary and is sufficient to stop the flow of blood (A microprocessor linked with the monitoring can govern the automatism of the inflating. This device is being studied).

Results

The endothelial lesions come down to a limited endothelial desquamation. The intima is spared in 97 % of the cases and its lesion, when there, is no thicker than 3 %.

Conclusion

These qualitative and quantitative methodologies have allowed us to adjust a little traumatizing instrument. Its use proves to be efficient both in arterial and venous surge-

I.N.S.E.R.M n° 825014 DGRST n° 82M0917

D. de LA FAYE - CHU Morvan - 29279 BREST CEDEX
FRANCE

R. GUIDOIN - LAVAL UNIVERSITY - QUEBEC -
CANADA G1K7P4.

VASCULAR HEMODYNAMICS AND ARTERIAL WALL TRANSPORT: AN IN VITRO INVESTIGATION

H.S. Borovetz, A.M. Brant, E.M. Seveck, S. Shah, E.C. Farrell, E.V. Kline, and C. Wall

School of Medicine, Department of Surgery, University of Pittsburgh
Pittsburgh, Pennsylvania 15261

In order to study those hemodynamic and biologic transport parameters which are involved in the pathogenesis of arterial disease, including the failure of small diameter vascular prostheses, a pulse duplicator apparatus (PDA) has been designed for simulation in vitro of vascular hemodynamics. The PDA is characterized by the realistic pulsatile flow of radiolabelled (^{14}C -4) serum cholesterol through either excised canine carotids or carotid-prosthetic junctions. A unique feature of its design is that such variables as mean pressure, transmural pressure, pulse pressure, heart rate, and arterial flow rate may be independently varied (i.e. on a one by one basis) and the hemodynamic response of the carotid artery or the anastomotic interface to these flow processes studied in detail. The PDA, which was developed originally for evaluation of the hemodynamic behavior of prosthetic heart valves, is comprised of a pumping unit, prosthetic valve testing chamber, tissue housing compartment, and appropriate instrumentation. The valve testing chamber is interfaced with a model cast of the human aorta. The rigid aortic section is attached to a small compliance chamber (which represents some compliance effects of the natural aorta by varying the volume of air contained within this chamber). The left atrial compartment of the valve testing chamber is connected to a serum reservoir for maintenance of diastolic pressure. This reservoir also serves as a sampling site for serum during a perfusion experiment.

Upon exiting the valve chamber and model aorta, the flow of serum is led to the tissue housing compartment (Figure 1), a precisely machined lexan block in which the carotid artery or carotid-prosthesis to be perfused is housed. The tissue housing chamber has been so designed to ensure a fully developed, pulsatile velocity profile in the vessel (prosthesis) and to accommodate conduits of various lengths (7-14 cm) and inner diameters (2-4 mm). The flow then passes through an electromagnetic flow probe and is returned to the serum reservoir, thereby connecting the entire system in a closed loop.

Instrumentation for the PDA permits the continuous and simultaneous dynamic measurements of vascular pressure drop (Millar Corp. Micro-Tip pressure catheters), volumetric arterial flow rate (Carolina Medical Products 501-D flowmeter), instantaneous axisymmetric radial motion of the carotid artery or anastomotic junction (Kaman Measuring Systems inductive displacement transducers), and temperature of the serum perfusate (Omega Engineering Inc.). The viscosity and density of the serum perfusate are measured using a capillary viscometer (Schott America) and pycnometer (Fisher Scientific).

Sixteen perfusion studies of two hour duration have been conducted using freshly excised canine carotids in the PDA. The hemodynamic simulation corresponded to the "normal" vascular case with mean pressure = 100 mm Hg, transmural pressure = 100 mm Hg, pulse pressure = 20 mm Hg, flow rate = 150 cc/min, pulse frequency = 1/sec and $T = 37^\circ\text{C}$. As such this data will serve as a con-

trol for the simulations using prosthetic materials. Samples of labelled serum were taken hourly from the reservoir of the PDA for analysis of their activity ($\sim 1 \mu\text{Ci/cc}$) and electrophoretic profile.

At the termination of each study the artery was removed from the PDA, emptied of serum, and gently rinsed with saline for several minutes both internally and externally. The vessel was then restretched to its in vivo or perfusion length and rapidly cut by a linear array of razor blades spaced 0.5 or 1 cm apart. The position of each section was noted with respect to the in vivo orientation of the artery. The two end sections (i.e. those secured by suture material to the ports of the tissue housing compartment of Figure 1) were discarded. The remaining individual sections were either submerged in liquid nitrogen and mounted on pre-frozen specimen blocks for radial sectioning, fixed in formalin and submitted along with a non-perfused control segment of artery for histomorphologic examination, or counted en bloc for determination of the overall arterial uptake of ^{14}C -4 cholesterol.

Among the interesting findings from this set of experiments are: 1) no trauma to the endothelial cells was evident upon histomorphologic examination; 2) the reservoir concentration and the carriage form (by lipoproteins) of ^{14}C -4 cholesterol remain essentially constant during each study; 3) radial dilatation of the vessel wall reaches an average peak distension of ~ 0.005 inches (range 0.002-0.008 inches); and 4) the overall uptake of ^{14}C -4 cholesterol by the artery is not controlled by boundary layer phenomena. These data offer a novel perspective into the interaction between vessel wall transport and arterial vascular hemodynamics and are directly applicable to consideration of arterial prostheses in the PDA.

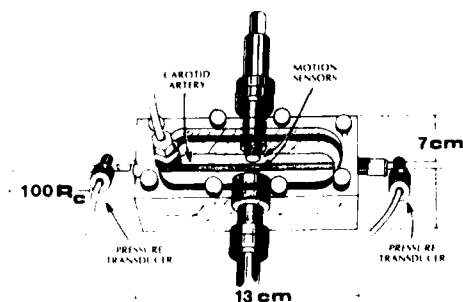


Figure 1 Tissue housing chamber and associated instrumentation. The entrance and exit lengths for establishment of serum flow equal $100 \times$ the radius of the vessel (R_c).

THE EFFECT OF LOAD CYCLING ON THE DIMENSIONAL STABILITY OF SURGICAL VASCULAR FABRICS

C. C. Chu, B. Pourdeyhimi, and S. R. Malkan

Department of Design and Environmental Analysis,
Cornell University, Ithaca, New York, USA 14853-0218

Introduction

Immediately after implantation, vascular grafts are subjected to pulsatile stress. This stress would undoubtedly result in an increase in the diameter of the synthetic vascular grafts. This diameter growth would eventually lead to a decrease in tensile strength and possible false aneurysm. In addition, once the graft stretches in one direction, it would contract in the direction perpendicular to the stretched one. In vascular grafts, the pulsatile pressure is basically experienced in the radial (weft or course) direction. Thus, a growth in diameter (i.e., a decrease in warp or wale/cm) and a contraction in the length (i.e., an increase in weft or course/cm) would be evident.

In this report, the dimensional growth of 6 commercially available vascular fabrics was studied in vitro condition

Experimental Procedure

The fabrics used were obtained from USCI and Meadox Medicals: Cooley Woven, DeBaKey Woven, Cooley Knitted, Weavenit, Cooley Double Velour, and DeBaKey Elastic. The mechanical testing was done under the standard atmospheric conditions ($21 \pm 1^\circ\text{C}$, and $65 \pm 2\% \text{ RH}$).

The deformation and residual deformation (recovery) tests were performed on Instron tensile tester. Three specimens of 4×1 inch each were cut in the weft or course direction from each fabric. The specimens were conditioned in the standard atmosphere for 24 hours before testing. The cross-head speed was 1 in/min, the chart speed was 10 in/min. The gauge length was 3 inches.

After loading the specimen to the full-scale deflection of 1 lb, the cycle was immediately reversed until the crosshead unit reached the original gauge length. The process of loading and unloading the specimens was repeated for 50 cycles. The deformation at a load of 1 lb was measured for the first cycle. The residual deformation at each cycle was determined by measuring from the origin to the point where the load/extension curve departed from the extension axis. The average values of the deformation were calculated for each fabric from the results of three repeated tests. The ease of deformation was determined from the initial portion of the load/elongation curve. The average breaking load for each fabric was calculated both before and after cycling.

Results

First, a wide range of breaking load was observed among the 6 commercially available surgical vascular fabrics. Cooley Woven was the strongest (104 lbs), while the DeBaKey Elastic Dacron was the weakest (42 lbs). Second, after cycling, Cooley Knitted and Weavenit exhibited the least decrease in strength. Third, the DeBaKey Elastic Dacron would require the lowest amount of force to be deformed as shown in Figure 1. DeBaKey Double Velour ranked the second and behaved very similar to the DeBaKey Elastic Dacron. Weavenit and Cooley

Knitted would require much greater force to exhibit the same degree of deformation, whilst the woven grafts would require a considerable amount of force to exhibit any deformation. Furthermore, they broke at about 50% extension. Figure 2 shows the percentage growth of these 6 surgical fabrics as a function of the number of cycles. It can be immediately recognized that the growth was inversely proportional to the ease of stretch. In other words, when a fabric requires a greater amount of force to be stretched to a given extent, it would grow or deform less for a given force. In this respect, the woven surgical fabrics are better than knitted fabrics, except the Cooley Knitted and Weavenit which were not significantly different from the woven fabrics. DeBaKey Elastic and DeBaKey Double Velour, however, exhibited a very significant growth. Fourth, the dimensional growth occurred most significantly during the first 10 cycles. This may indicate that the period immediately after implantation is relatively important. Of course, preclotting could modify their growth behavior.

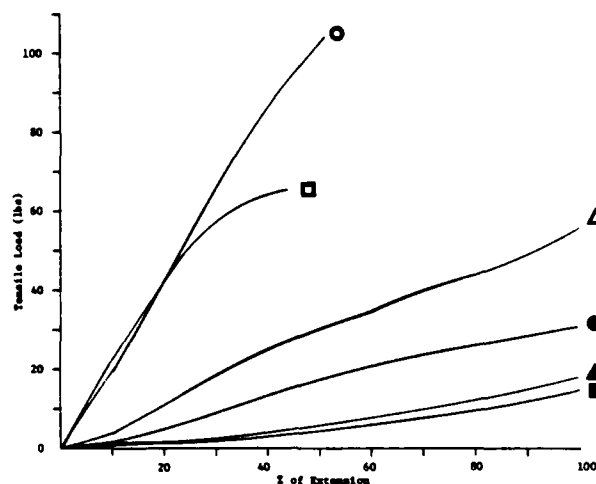


Figure 1. ● DeBaKey Woven; ■ Cooley Woven; ▲ Cooley Knitted; ○ Weavenit; △ DeBaKey Double Velour; □ DeBaKey Elastic Dacron.

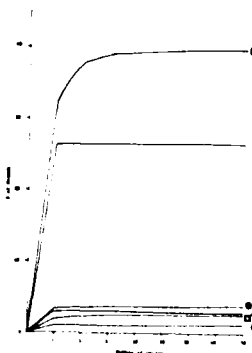


Figure 2. Dimensional growth of surgical vascular fabrics. Same symbols as Figure 1.

Theoretical Determination of Porosity in Fabrics and Its Application to the Design of Woven Vascular Grafts

Benham Pourdeyehimi & Chih-Chang Chu

New York, 14853, USA

Department of Design & Environmental Analysis, Cornell University, Ithaca,

Introduction

Porous prostheses designed for attachment to the body by tissue ingrowth have found applications in many areas of biomedical materials. One of their important applications is in the reconstruction of injured blood vessels in which the porosity was shown by Weslowski to be probably one of the most critical factors in the healing process of the arterial grafts.

Although the importance of controlling the porosity of synthetic vascular grafts has been well established, all existing porosity data of these grafts are experimentally determined by the so called water flow-through method developed by Weslowski.¹ No theoretical means to determine the porosity of vascular grafts has been reported in the literature. Therefore, it is the purpose of this study to provide a theoretical approach to the determination of porosity in woven vascular grafts.

Theoretical Design of Porous Woven Vascular Grafts

All woven vascular grafts today in use employ a plain weave (taffeta) structure.

In a woven fabric, two sets of yarns the warp and the weft (filling) interlace at right angles to each other in the plane of the fabric. In a given weave, the thread spacing and the relative closeness of the set of yarn depend primarily upon the yarn diameter, its density as well as the spaces between the yarns. Thread spacing, T , is the sum total of the yarn diameter, d , and the opening between the two adjacent yarns, P , (porosity). T can be simply ascertained by counting number of threads per cm (n).

$$nT = 1 \text{ cm} \\ \text{where } n = \text{threads per cm} \\ \text{thus } T = 1/n$$

$$\text{However, since } \text{Porosity } P = T - d \quad (1) \\ \text{Then } P = 1/n - d \quad (2)$$

The area of the pore can be calculated as shown below:

$$\text{If for the warp direction; equation 2 becomes:} \\ P_1(\text{warp}) = \frac{1}{n_1(\text{warp threads/cm})} - d_1(\text{dia. of warp threads}) \quad (3)$$

$$\text{and for the weft direction:} \\ P_2(\text{weft}) = \frac{1}{n_2(\text{weft threads/cm})} - d_2(\text{dia. of weft threads}) \quad (4)$$

Then the area of one single pore A_p (in cm^2) would be:

$$A_p = P_1 \times P_2 = (1/n_1 - d_1)(1/n_2 - d_2) \quad (5)$$

Percentage porosity may be defined as the total porous area to the total area covered by the fabric. Total area covered by the fabric = $T_1 \times T_2 = 1/n_1 \times 1/n_2$ and the percentage porosity (% P) would be:

$$\% P = (1 - n_2 d_2 - n_1 d_1 + n_1 n_2 d_1 d_2) \times 100 \quad (6)$$

It will be far more convenient to be able to readily calculate the porosity without having to measure the yarn diameter using a theoretical approximation of yarn diameter. Considering the yarn to be an incompressible cylinder, the diameter may be calculated using the following equation:

$$d = 0.00357 \frac{N}{D(\text{yarn})} \quad (7)$$

where N = Tex value of the yarn; and $D(\text{yarn})$ = yarn density (g/cm^3)

It would be more convenient to relate the density of the yarn to that of fiber. Packing coefficient is an indication of the degree of the packing density of the fibers within a yarn. It has been recently determined experimentally that the packing coefficient of yarns varies between a lower limit of 0.55 to an upper limit of 0.75. Because woven vascular graft

fabrics have a tight structure and constitute low twist multi-filament yarns, thus the value of 0.75 should be used. Thus, the diameter (in cm) of the yarn would, from equation 7 becomes:

$$d = 0.0041223 \frac{N}{D(\text{fiber})} \quad (8)$$

By substituting equation 8 in equations 3 and 4, the porosity can be calculated using equations 9 and 10 below, once the density of fibers and the number of warp and weft threads per cm are known.

$$P_1 = \frac{1}{n_1} - \frac{0.0041020 N_1}{D_1(\text{fiber})} \quad (9)$$

$$P_2 = \frac{1}{n_2} - \frac{0.0041020 N_2}{D_2(\text{fiber})} \quad (10)$$

Where N_1 = Tex value of warp threads
 D_1 = fiber density of warp threads
 N_2 = Tex value of weft threads
 D_2 = fiber density of weft threads

Table 1 has been constructed using the formulas described above for maximum weavable constructions.

In conclusion, the porosity of the woven graft can thus be designed to vary from zero to whatever size that may be desired. Such a theoretical calculation could act as a tool to control the porosity of woven vascular grafts. It has also been shown that the existing woven vascular grafts do not permit complete healing due to their low degree of porosity.

TABLE 1

PORE SIZES IN MAXIMUM WEAVABLE CONSTRUCTIONS
WHEN $N = 18$

n_1	T_1	n_2	T_2	P_1	P_2	$P_1 P_2$	P_d	%P
67	0.0149	34	0.0294	0.375	145.239	54.46	8.3	0.12
66	0.0151	34	0.0294	2.636	145.239	382.85	22.1	0.86
64	0.0156	34	0.0294	7.371	145.239	1070.56	36.9	2.33
*60	0.0167	34	0.0294	17.788	145.239	2583.51	57.3	5.27
59	0.0169	34	0.0294	20.613	145.239	2993.81	61.7	6.00
**56	0.0178	34	0.0294	29.692	145.239	4312.50	83.6	8.21
54	0.0185	34	0.0294	36.306	145.239	5273.05	81.9	9.68
52	0.0192	35	0.0286	43.429	136.835	5942.61	86.9	10.82
49	0.0204	35	0.0286	55.203	136.835	7553.70	98.1	12.95
48	0.0208	35	0.0286	59.454	136.835	8135.54	101.7	13.67
45	0.0222	36	0.0278	73.343	128.899	9453.84	109.7	15.31
42	0.0238	36	0.0278	89.216	128.899	11499.85	121.0	17.39
40	0.0250	38	0.0263	101.121	114.279	11556.01	121.3	17.56
38	0.0263	40	0.0250	114.279	101.121	11556.01	121.3	17.56
35	0.0286	46	0.0217	136.835	68.512	9374.84	109.2	15.09

N = Tex value of warp and weft threads

n_1 = Warp threads per cm

T_1 = Thread spacing in the warp direction (in cm)

n_2 = Weft threads per cm

T_2 = Thread spacing in the weft direction (in cm)

P_1 = Pore size in the warp direction (in m)

P_2 = Pore size in the weft direction (in m)

$P_1 P_2$ = Pore area (in m^2)

P_d = Equivalent Pore diameter (in m)

%P = Percentage porosity

* This corresponds to Woven Cooley Verisort® vascular graft manufactured by Meadox Medicals

** This corresponds to Woven DeBaKey® vascular graft manufactured by USC1

Acknowledgement: We are grateful for the financial support of the Whitaker Foundation.

MECHANICAL PROPERTY OF SYNTHETIC POROUS HYDROXYAPATITE FOR BONE GRAFT AFTER IMPLANTATION

S. Niwa, M. Hori, M. Sohmiya, S. Takahashi, H. Tagai*, M. Kobayashi*, M. Ono** and H. Takeuchi**

Department of Orthopedic Surgery, Aichi Medical University
Aichi, JAPAN

INTRODUCTION

Synthetic hydroxyapatite has an excellent osteoconductive activity which is dependent upon heating temperature and the diameter of pore of hydroxyapatite in porous material by our previous fundamental research work since 1978. This paper reports the mechanical strength of porous hydroxyapatite on 4, 8 and 12 weeks after implantation in the femoral condyl of rabbit. These results will support the possibility of clinical application of these materials.

MATERIALS AND METHODS

Porous hydroxyapatite which has 70% porosity, pore-size 90 μ and a cylinder shape (diameter 4 mm, length 7 mm) were inserted in the small hole making by drilling in the femoral condyl of adult rabbit. By 4, 8 and 12 weeks after implantation the mechanical strength of porous hydroxyapatite and cancellous bone of the femoral condyl as a control were measured by indenter (speed 1 mm/min, diameter 3 mm ϕ), and also the histological observation of same materials were carried out by the microradiogram.

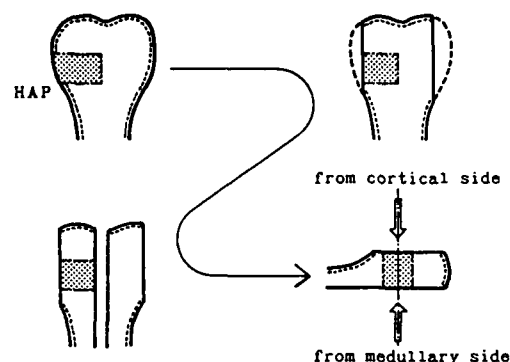
RESULTS

1) Porous hydroxyapatite (70% porosity, pore size 90 μ and heated at 900°C) in vitro showed the mechanical strength 25.5 \pm 8.8 kg/cm (max. 43.4 kg and min. 15.7 kg/cm).

2) By 4 weeks after implantation porous hydroxyapatite were investigated its mechanical strength from cortical side and medullary side. The strength from cortical side was 165.6 \pm 124.7 kg/cm and from medullary side was 86.2 \pm 66.2 kg/cm. Newly formed cancellous bone 4 weeks after drilling as a control, showed 233.8 \pm 89.1 kg/cm from cortical side and 119.6 \pm 96.5 kg/cm from medullary side. The mechanical strength of porous hydroxyapatite in vitro was 6 times stronger than in vivo 4 weeks after implantation. These strength was almost same value of cancellous bone.

3) Also by 8 and 12 weeks after implantation, the strength of these material will be presented further investigation, and be discussed the relation between the histological finding and these materials.

METHOD



Mechanical strength (by indenter)

	Hydroxyapatite	Control
from cortical side	165.6 \pm 124.7 kg/cm	233.8 \pm 89.1 kg/cm
max.	441.8	336.8
min.	43.4	106.5
from medullary side	86.2 \pm 66.0	119.6 \pm 96.5
max.	218.4	249.8
min.	14.8	29.6

(4 weeks after implantation)

Department of Orthopedic Surgery
Aichi Medical University
21 Karimata Yazako, Nagakute-cho
Aichi-gun, Aichi-ken
480-11, JAPAN

* Chiba Institute of Technology

**Mitsubishi Mining and Cement Co., Ltd.

Heat Treatments for Porous Coated Ti-6Al-4V Alloy

E.A. Renz, S.D. Cook, C.L. Collins, R.J. Haddad, Jr.

Department of Orthopaedic Surgery, Tulane Medical School and
the Veterans Administration Medical Center, New Orleans,
Louisiana 70112

The development of porous coated orthopaedic implant devices for attachment by bone ingrowth has been the subject of much research. A porous metal coating applied to a solid substrate has been shown, *in vivo*, to offer advantages over current methods of fixation. These include a higher interface shear strength between implant and bone and a more uniform distribution of stresses. These devices however require a sintering heat treatment to apply the porous coating. Sintering heat treatments have been shown to have a detrimental effect on the material mechanical properties of some orthopaedic alloys.

One of the materials of choice for porous coated systems is Ti-6Al-4V alloy. This is based upon its high corrosion resistance, low toxicity and favorable mechanical properties. However, the fatigue strength, the most important mechanical property when considering the design of a load bearing orthopaedic device, has been found to decrease due to both the sintering heat treatment and the porous coating.

In previous studies[1] uncoated Ti-6Al-4V orthopaedic alloy was found to have an endurance limit of 605 MN/m². The application of a porous Ti-6Al-4V coating decreased the endurance limit of the system by approximately 77%, and when the uncoated substrate material was only heat treated to the same temperature as the porous coated samples (1250°C for 2 hours) a degradation of approximately 34% in fatigue strength was observed. The great difference between the porous coated samples and the only heat treated samples was theorized to be due to the porous coating acting as a notch since the introduction of a machined notch was found to decrease the endurance limit of the material by 65%.

The reduction of fatigue properties by the heat treatment is due to the transition from the as-received equiaxed microstructure to the lamellar structure upon sintering. This lamellar structure has been shown to have inferior fatigue properties relative to the equiaxed structure. Thus, the need for a heat treatment to improve the fatigue properties after sintering seems apparent.

In the present study, microstructural analysis was performed on six different post sintering (1250°C for 2 hours) heat treatments of Ti-6Al-4V in an attempt to improve the fatigue properties. The heat treatments were:

- #1-Argon quench;
- #2-Argon quench, followed by a 4 hour anneal at a temperature low in the α and β region with a subsequent Argon quench;
- #3-Cool to just above β -transus, slowly cooled through β -transus, and furnace cooled;
- #4-Argon quench followed by a 15 minute anneal slightly above β -transus, slowly cooled through β -transus, and furnace cooled;
- #5-Argon quench preceding an anneal at just below β -transus for 4 hours followed by an Argon quench;

#6-Argon quench, then anneal at slightly below

β -transus, cooled very slowly to a temperature low in the α and β region, then Argon quenched.

The six heat treatments produced alternative microstructures from the lamellar structure obtained in the sintering heat treatment where slow cooling from the sintering temperature took place. Quenching from sintering temperature (heat treatment #1) resulted in shorter, fine interwoven α plates with localized areas of equiaxed α and fewer colony boundaries. Annealing this structure in the low α and β region for 4 hours (heat treatment #2) produced a microstructure with large α plates of varying dimensions and orientation differing from a lamellar structure. Annealing at a temperature just below the β -transus (heat treatment #5) resulted in large α plates which became more globular and equiaxed, and the retained β more dispersed. The outside of the sample exhibited a 0.12mm layer of an acicular α in a β or finely transformed β matrix with a few small globular α particles dispersed in the layer.

Slow cooling through the β -transus (heat treatments #3 and #4) produced a transient structure which showed some areas of an equiaxed structure. The differences between the two heat treatments were minimal and thus the Argon quench before the β annealing and slow cooling through the β -transus makes little difference. The recrystallization annealing (heat treatment #6) resulted in a structure of coarse α plates in an abundant and very fine martensitic matrix. This structure was uniform throughout, free of any type of colony boundary.

In previous studies where the sintering heat treatment was followed by a slow furnace cool to room temperature, a lamellar structure consisting of large colonies of α plates in the same crystallographic orientation with retained β between them was obtained. It has been shown that crack propagation can occur easily in both parallel and perpendicular directions to the long axis of the alpha grains. The heat treatments described above provide microstructures somewhat different from the original sintering heat treatment, with some exhibiting considerably different microstructures. Thus, these heat treatments may help in resistance to crack initiation and propagation during the cyclic loading of porous Ti-6Al-4V orthopaedic devices and thus result in improved fatigue properties. To date, limited fatigue testing has shown an improved endurance limit for some cases. However, more tests must be performed to determine statistical significance.

- [1] Cook, S.D. et al.: The Fatigue Properties of Porous Coated and Carbon Coated Ti-6Al-4V Implants, Transactions of the 29 O.R.S., March 1983.

Department of Orthopaedic Surgery
Tulane Medical School
New Orleans, Louisiana 70112

POROSITY DETERMINATION OF A LOW MODULUS IMPLANT MATERIAL

J.M. Prewitt, III, C.A. Homsy

The Methodist Hospital
Houston, Texas

There are several techniques that may be used to measure either the pore size distribution and/or void volume of a porous material. Interpretation of results using these techniques may depend on the specific porous system under investigation.⁽¹⁾

Such interpretive difficulties were observed in experiments conducted to quantify the pore structure of a low modulus porous composite of PTFE and vitreous carbon fiber. The pore structure of this material is complex and anisotropic.

Three techniques were used to study the void volume of this material. A compression technique expresses the void volume as a ratio of the post to the pre-pressurization dimension of a known shape of the material. A second and simpler way to measure the percent void volume uses apparent density and ingredient densities. A third technique was mercury intrusion porosimetry. The results using all three techniques agreed on void volume in the range of 70-85%.

Two techniques were used to study pore size distribution of this porous material. The technique of optical microscopy met with only limited success. The main problem with this technique was the fact that the view of a pore was in two instead of three dimensions. It was quite difficult to determine how a particular pore changed its size and shape below the surface under examination. This technique did inform that the material had pores as large as 400 microns and as small as 5-10 microns.

The technique of mercury intrusion porosimetry was also used to study the pore structure. This technique was found to be limited in that only interpore connection size range could be inferred, but not the volume percentages of discrete pore sizes. The results of using this technique suggested that a majority of the pore interconnections for the material were in the 30-50 micron range. However, due to the anisotropic nature of the material, and the so called "ink bottles" effect, the technique tends to distort the computed pore interconnection size to lower values.⁽²⁾

References

1. Rootare, H.M.: "A Short Literature Review Of Mercury Porosimetry As A Method Of Measuring Pore-Size Distributions In Porous Materials, And A Discussion Of Possible Sources Of Errors In This Method". Aminco Laboratory News Vol.24(3):4A-4H, Fall 1968.

2. Ibid.

The Prosthesis Research Laboratory, The Methodist Hospital, Houston, Texas.

John M. Prewitt, III, Prosthesis Research Laboratory, The Methodist Hospital, 6560 Fannin Suite 2080, Houston, Texas 77030.

THE EFFECT OF POROUS-COATING HEAT TREATMENTS ON THE DEFORMATION OF A CO-CR-MO ALLOY

G.C. Weatherly; W.M. Laanemäe[†]; R.M. Pilliar; S.R. MacEwen*.

Department of Metallurgy and Materials Science
University of Toronto, Toronto, ON, Canada M5S 1A4

Our recent studies of porous-coated implant alloys [1,2] have prompted us to reconsider the microstructure-mechanical property relationships in the ASTM F75 Co-Cr-Mo alloy to ensure that the as-sintered/heat-treated parts meet the F75 standard and that the composition of the alloy is optimized for this application. The composition limits for the F75 alloy are 27-30% Cr, 5-7% Mo, 0-2.5% Ni, 0-0.75% Fe, 0-1% Si, 0-1% Mn and 0-0.35% C (by weight). Cr, Mo and Fe are carbide formers. All of the alloying elements (including C) could contribute to solid solution strengthening depending on the heat treatment. In addition, as the alloy is metastable at room temperature, a strain induced transformation from f.c.c. to h.c.p. Co could contribute to the strength [3].

This paper reports the results of a detailed study of the tensile deformation of as-cast as well as heat treated specimens of F75. The variation of the strain-rate sensitivity with flow stress and the initial rate of work-hardening are used to determine the role of solute atoms and precipitate particles in the deformation behaviour of F75, using the method of Mulford [4].

As-cast F75 alloy specimens containing 27% Cr, 6.5% Mo and 0.25% C by weight were examined in four conditions: a) as cast, b) solution annealed at 1220 °C/1 hour and water quenched, c) sinter annealed at 1300 °C/1 hr and He quenched, and d) sinter annealed at 1300 °C/1 hr, cooled at 1 °C/min to 1200 °C, held for ½ hr and He quenched. Treatment (d) has been shown to remove most of the eutectic liquid phase that forms at 1300 °C [2].

The samples were machined into tensile specimens with a 25 mm gauge length and a 6 mm gauge diameter. Mechanical tests were performed in air at room temperature using an MTS Alpha testing system. A high rate of data acquisition was used for all tests, the base strain-rate was set to 10⁻³ sec⁻¹. Relaxations were performed at increments of about 50 MPa. The total strain in the specimen was held constant throughout the 15-30 min relaxation.

The mechanical properties of the four conditions are summarized in Table I. With the exception of the as-cast samples, the proportional limit of the three heat-treated samples was the same, about 300 MPa. However, the 0.2% yield stresses differed and when the data for the as-cast specimens is included it is clear that the initial rate of work-hardening increases as the volume fraction of second phase increases (we do not distinguish between the different carbide, σ or eutectic phases [2] in arriving at the volume fractions shown in Table I, since they will all behave as non-deformable obstacles to plastic flow). At strains greater than 1-2%, the flow curves are similar with a low rate of work-hardening up to final fracture.

The stress relaxation tests were done in the low work-hardening range of the stress-strain curve. From these tests one obtains a measure of $\partial\sigma/\partial\ln\dot{\epsilon}$ as a function of flow stress [4] (here σ and $\dot{\epsilon}$ are the true stress and true strain rate). The results of all the tests are summarized in Fig. 1. Too few tests were done to determine if there were statistically significant differences among the different heat-treatments. All gave positive intercepts on the $\partial\sigma/\partial\ln\dot{\epsilon}$ axis (see Fig. 1, where a least squares line has been drawn through all the data points). This positive intercept, together with the low values measured for $\partial\sigma/\partial\ln\dot{\epsilon}$, 5-10 MPa, indicate that the flow stress is controlled by solid solution strengthening after the first 1-2% plastic strain [4,5].

More detailed examination of the stress-strain curves shows that they may be divided into four distinct regions (Fig. 2): a) the elastic region, b) a region at strains just beyond the proportional limit where the curves for all heat treatments coincide, c) a region from just before the 0.2% yield stress up to 1-2% strain, and d) the region of low work-hardening at strains greater than 1-2%. In regions (b) and (c), the second phase has a major role in deformation. In region (b), some grains in the

grains begin to undergo plastic deformation while others remain elastic. Both the grain orientation and the second phase are important in this region. In region (c) all grains undergo plastic deformation but the second phase remains elastic and reinforces the matrix to produce a variation in work-hardening rate and thus in the 0.2% yield stress. In region (d), a plastic relaxation mechanism combining carbide cracking and slip of the matrix around the second phase reduces the contribution of the particles to the flow stress and further deformation is controlled by the solute atoms.

Our detailed deformation study of the F75 alloy shows that many strengthening mechanisms act during deformation. In order to produce porous-coated implants with acceptable mechanical properties, these results must be incorporated in the design of heat treatments to maintain the mechanical property requirements of the ASTM F75 standard.

In conclusion, the deformation of the F75 alloy is controlled mainly by the amount of second phase at strains less than 2% and by solute atoms at higher strains. The amount of second phase does not affect the proportional limit, but does affect the initial work-hardening and thus affects the 0.2% yield stress.

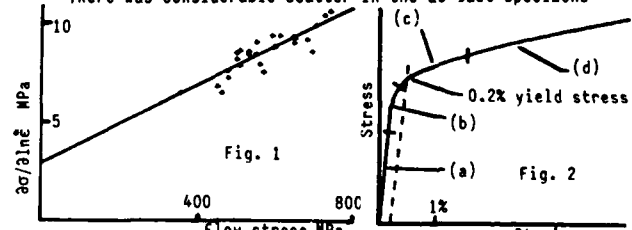
References

1. Elve, M.A., Kilner, T., Pilliar, R.M. and Weatherly, G.C., Trans. 7 Am. Soc. Biom. Meeting, p. 75 (1981).
2. Kilner, T., Pilliar, R.M., Weatherly, G.C. and Allibert, C., J. Biom. Mater. Res. 16, 63 (1982).
3. Rajan, K. and Vander Sande, J.B., J. Mat. Sci. 17, 769 (1982).
4. Mulford, R.A., Acta Met. 27, 1115 (1979).
5. MacEwen, S.R., Acta Met. 30, 1431 (1982).

Table I

Selected Properties of the Heat Treated Conditions				
Property	As-cast	Solution ann.	Sinter ann.	Sinter ann./cooled
Prop. lim. MPa	80,196*	285	305	320
0.2% y.s. MPa	416,448*	550	500	460
Fracture str. MPa	680	766	648	587
Elongation	6%	15%	5%	20%
Volume fraction of 2nd phase	0.21	0.06	0.05	0.01

* There was considerable scatter in the as-cast specimens



Acknowledgements: Mr. J.F. Mecke assisted with the experimental work. Financial assistance by the Natural Sciences and Engineering Research Council of Canada and Canadian Oxygen Ltd.

Department of Metallurgy and Materials Science,
University of Toronto, Toronto, ON, Canada M5S 1A4

*Atomic Energy of Canada Ltd., Chalk River Nuclear Laboratories,
Chalk River, ON, Canada K0J 1J0

[†]Now at: Max-Planck-Inst. für Metallforschung, Inst. für Werkstoffwissenschaften, Seestraße 92, 7000 Stuttgart 1, W. Germany

CHARACTERIZATION OF POROSITY IN POROUS POLYMERIC IMPLANT MATERIALS

R. E. Dehl

Polymer Science and Standards Division, National Bureau of Standards,
Room A143, Building 224, Washington, DC 20234

Further studies have been conducted on the characterization of porosity in porous implant materials, which are designed for use as tissue-ingrowth media. Earlier work at this laboratory has previously been reported (Transactions of the Eighth Annual Meeting of the Society for Biomaterials, Vol. V, 1982, p. 51). These studies are intended to provide a critical review and intercomparison of the currently available methods for determining pore volume and pore size in implant materials. To date, the studies have been confined to two commercially available polymeric materials, a porous polyethylene (PPE) and a porous composite of polytetrafluoroethylene and carbon (PTFE-C).

The results of three pore volume fraction measurements for the two materials have been reported, as well as the determination of pore size parameters by the well established technique of mercury porosimetry. Another method of estimating pore size was reported, in which the average "diameter" of the pores is proportional to the ratio of the specific pore volume to the specific surface area. In order to obtain numerical values for the pore "size" by either of the above methods, it was necessary to assume that the pores have a certain regular geometrical shape, which is hardly a true representation of the irregularly shaped pores in either material. Such assumptions necessarily lead to poor agreement between different pore size determinations, and one must remember that "size" is only a parameter specific to a given type of measurement.

At least one type of pore size measurement is free from geometrical assumptions of the above techniques. It is based upon analysis of cross-sections of the materials by quantitative optical microscopy. If the various phases in the material can be clearly differentiated under the microscope, a number of measurements may be made which define an average "diameter" of the desired phase, which in this case is the pore fraction. A method was selected for this study which can be performed easily by manual techniques. It permits the measurement of both the pore volume fraction and the "mean intercept length", which is defined as the average length of all possible chords intersecting the pore regions, for all possible lines drawn through the sample.

In order to produce smooth, flat cross-sections of the materials for optical analysis, it was necessary to fill the pores with a thermosetting resin which could be ground and polished to a mirror finish. Thirty photomicrographs were taken at random sites on each material. A 6x4 line transparent grid was laid on each photograph, and two parameters were determined by a simple counting procedure, which together yielded both the pore volume fraction and the mean intercept length. The results for both materials are shown in Table I. It is apparent from the

Table I
Porosity Parameters from Quantitative Microscopy

	Pore Volume Fraction		
	Mean (of 30)	SD	SD/Mean
PPE	0.48	0.09	0.19
PTFE-C	0.69	0.10	0.14
	Mean Intercept Length (μ m)		
	Mean (of 30)	SD	SD/Mean
PPE	76	17	0.22
PTFE-C	67	14	0.21

standard deviations that a great number of measurements is required to obtain accurate estimates of the true mean parameters. This is in contrast to mercury porosimetry, for example, where a single pressure-volume curve, obtained in a few minutes, yields much information about interconnecting pore "diameters" as well as an estimate of the size distribution.

Further recent advances include a method for plotting mercury porosimetry data which yields a finely detailed histogram of pore "diameter" frequency vs pore size. The curve has the general appearance of a log-normal distribution, a type which is often found when there is a lower limit to the size (in this case 0) but no definite upper limit. In addition, compressive stress-strain measurements were performed on both materials to estimate the effect of applied pressures as they might occur, for example, during a mercury intrusion experiment.

This work was supported in part by the Office of Medical Devices (FDA).

Polymer Science and Standards Division, National Bureau of Standards, Room A143, Building 224, Washington, DC 20234

Bone Ingrowth of Porous-Coated Moore Prostheses

J.P. Collier, M. Mayor*, C. Engh**, A. Brooker***

Thayer School of Engineering, Dartmouth College, Hanover, NH 03755

INTRODUCTION

The porous-coated Moore prosthesis has been available for limited clinical use since 1976. In the past year we have received six retrieved prostheses bringing our total to eleven. The patient age has ranged from 25 to 87 years and the duration of implantation from 10 days to nine months. The series includes prostheses with a fine pore size of 50 to 100 microns as well as more recently manufactured stems with a pore size of 150-350 microns. Both fully-porous coated and partially-coated stems are represented. Two of the prostheses were retrieved intact in the excise¹ femurs.

METHODS

All prostheses were stabilized in formalin and then dried in alcohol and acetone. Each was photographed and sections were cut for SEM analysis where applicable. The stems were then embedded in acrylic, cut on a diamond saw and hand ground and polished to 50-80 microns in thickness. Each section was then stained with H & E for histological examination.

RESULTS

Retrieved prostheses with the fine pore size showed good fibrous ingrowth of all pores with no apparent sequestration of the prosthesis by a fibrous band as is sometimes seen with cemented prostheses. No bone ingrowth of the pores was seen although bony adaption to the coating was common.

The fully-porous coated and partially-coated prostheses with the larger pore size showed ingrowth by bone as well as fibrous tissue. The greatest amount of bone ingrowth was found on the lateral side of the prosthetic stems approximately 10 to 13 cm from the tip of the stem. The prosthesis retrieved 10 days postoperatively showed fibrous tissue adherence but no ingrowth. Prostheses retrieved three weeks to four months postoperatively all showed healthy fibrous tissue ingrowth with varying amounts of bone ingrowth. The greatest amount of bone ingrowth was present

in the prosthesis with the longest postoperative period before retrieval.

CONCLUSIONS

Femoral prostheses of the Moore-type geometry with a porous coating providing pores of 150 to 350 microns are ingrown with bone and/or fibrous tissue within 4 weeks postoperatively. By four months post-operatively, one 25 year old patient demonstrated significant amounts of bone remodelling and ingrowth. In all cases to date, the greatest amount of tissue adherence and bone ingrowth has been found on the lateral side of the prostheses in the region adjacent to a line drawn through the head of the prosthesis at about 20° to the vertical which represents the line of load application.

Ingrowth by fibrous tissue appears to precede bony ingrowth. The amount of bony ingrowth is greater with longer periods between implantation and retrieval. At four months, 10 to 20% of the stem is ingrown by bone. It is too early to determine what the maximum ingrowth amount may be but the active remodelling of the bone at four months indicates that it could take considerably longer than four months to reach equilibrium.

This research was supported by DePuy of Warsaw, Indiana.

* Dartmouth-Hitchcock Medical Center,
Hanover, NH

** Anderson Clinic, National Hospital for
Orthopedics and Rehabilitation,
Arlington, VA

*** Department of Orthopedics, John Hopkins
University, Baltimore, MD

THE USE OF EPIFLUORESCENCE TO EVALUATE BONY INGROWTH INTO POROUS METALLIC IMPLANTS

Folger, R. L., Murice, E. A.

Howmedica Corporate R&D, Groton, Connecticut

Preparations of thin sections of bone are difficult. When bone is coupled with a metallic implant, the prospects of good, consistent thin sections become even more unfavorable. An unstressed porous implant model in white New Zealand rabbits was used to develop a technique for the assessment of bony ingrowth into a porous metal implant. Tetracycline labels¹ and Villanueva's bone stain² were found to be useful in identifying bone in thick around sections of bone and metallic implants. The use of epifluorescence made it possible to see the bony ingrowth and its close association with the porous implant. Further work with this model should permit the three dimensional visualizations of the association between the bone and the implant.

White New Zealand rabbits (3kg+) received porous implants (Fig.1) in the distal end of the femoral medullary canal. Under anesthesia, the rabbits' knees were opened and a 6mm hole was formed between the anterior region of the femoral condylar groove in direct line with the medullary canal. The 6mm diameter by 11mm long Vitallium® implant was inserted into the medullary canal via this hole.

During the implant period, which lasted either 21 or 42 days, the animals were pulsed several times with tetracycline. At sacrifice, the femurs were placed in 70% ethanol and then sectioned through the implant with a diamond saw. The implant-bone sections (5mm thick) were embedded in Spurr's low viscosity embedding medium and then ground to a 600 fine surface on a Leco Autopolisher. The embedded ground sections were then stained with Villanueva's bone stain for 90 minutes. This was followed by a final 600 fine polishing for 1-2 minutes.

The Villanueva's bone stain is composed of fast green FCR, orange G, basic fuchsin and azure II. After 90 minutes staining time the sections are differentiated in 0.01% acetic acid in 95% methanol. The Osteoid seams stain either green to jade green or red to dark red. Partially mineralized bone stains red or yellow orange depending upon the density and the zone of demarcation light green.

Inspection under an epifluorescence microscope showed that trabeculae from both the cortical and trabecular bone had grown up to the implant surface where they not only completely surrounded heads on the surface but also grew into the innermost pores of the implant making direct contact with the core of the porous implants. Areas of fibrous interface and direct contact

between the implant and mineral matrix were observed. The three dimensional orientation of growth patterns in the bony ingrowth reduced the effectiveness of the tetracycline labels for establishing a time frame for ingrowth. The tetracycline did aid in demonstrating direct contact between the bone and the metal implant.

¹Frost, H.M., Calc. Tiss. Res., 3:211-237, 1969.

²Villanueva, A.R., Stain Tech., 49:1-8, 1974.

Howmedica Corporate R&D, Groton, CT 06340

H.C. Park, Y.K. Liu and R.S. Lakes

Center for Materials Research, College of Engineering, The University of Iowa, Iowa City, Iowa 52242

One of the current methods for improving prosthesis fixation and life is to modify the bone cement polymethylmethacrylate (PMMA) by adding various substances, e.g., glass and carbon spheres, carbon fibers, sugar, tricalcium phosphate, and inorganic bone, to it. These additions seek to ameliorate the cement's material properties and/or facilitate tissue ingrowth. Utilizing elastic composite theory with inclusions, the degree of bonding between inorganic bone particles and PMMA was estimated from experiments on bone-particle impregnated PMMA.

Materials and Method: All PMMA used were surgical grade radiopaque Zimmer Bone Cement in packets containing 40 g of prepolymerized powder and 20 ml of monomer. To obtain the necessary inorganic bone particles, fresh human cadaveric sacra and vertebrae were cut into small pieces and soaked in sodium hydroxide (0.4N) from 4 to 8 days to remove all soft tissues. The dried inorganic bone was brittle and was ground with a mortar and pestle. After grinding, the resultant particles were passed through calibrated screens to yield only particles between 150 and 300 μ m in size.

The bone particle were mixed with the powder phase on a percent by weight basis. For instance, to obtain a specimen containing 10% bone particles by weight, add 1 g of bone particles to 6 g of powder and then mixed with 3 g of monomer, i.e., the powder to monomer ratio is constant at 2 to 1. The specimens were cast in a circular cylinder aluminum mold, and machined to its final cylindrical shape of approximately 6.35 mm in diameter and 43 mm long.

One end of the specimen was fixed to rigid frame while the other end was attached to a permanent magnet-cum-mirror assembly. Cyclic torque was applied by the magnetic field of a Helmholtz coil acting on the permanent magnet. A laser beam was directed at the mirror through a 300 lines/inch grating. The grating generated interference fringes which passed through a second 300 lines/inch grating to a light detector. Each fringe is proportional to a known angular displacement of the mirror.

Young's modulus and shear modulus of elasticity were found via the bending and torsion formulae for a cantilever beam. Maximum strains did not exceed 10^{-3} ; thus insuring both material and geometrical linear behavior.

Results: To date, we have completed tests on six as-received (0%), six 10%, five 15%, five 25% and two 35% specimens. For all bone-particle impregnated PMMA specimens, there were linear increases in both E and G of the composite as a function of bone concentration. The linear regression equations are:

$$E_c = 2.84 + 0.19 C \quad (1)$$

$$G_c = 1.06 + 0.50 C \quad (2)$$

where E_c and E_o are the Young's moduli for bone-particle-impregnated and as-received PMMA respectively, G_c and G_o are the corresponding shear values and C is the bone-particle

concentration by weight.

Analysis of Results: To examine whether or not bonding exists between the inorganic bone particles and the PMMA matrix, we appeal to the isotropic two-phase elastic composite theory due to Hlavacek [1-2]. If the bone particles are considered voids then the effective moduli should decrease as the percentage of voids increases. However, our experiments show linear increases in the effective moduli with the percentage of bone concentration, which is predicted by a two-phase elastic composite. Thus, by inference, some bonding took place between the bone particles and the PMMA. A possible index of bonding is outlined in the following schema: 1) Measure the moduli of elasticity of the elastic composite and the (PMMA) matrix separately; 2) Predict the moduli of the inclusion (bone) using the appropriate equations for the effective moduli given in [2]; and 3) The ratio of the predicted moduli of the inclusion (bone) with its experimentally determined values is the index of bonding. The index varies from zero for a void to one for a perfect bond.

A light microscopic examination of the inorganic bone particles showed mostly ellipsoidal elements with an average length to diameter ratio of 3. A parametric study showed that the Young's moduli of the bone particles stayed in the range between 5.4-5.6 GPa for a Poisson's ratio of 0.3. Mack [3] found the value of E to be 17.1 GPa for inorganic bone in tension. Thus, the inferred index of bonding is approximately 0.3.

Conclusions: 1. The Young's shear modulus of bone-particle-impregnated PMMA increased linearly as a function of bone concentration by weight.

2. The above behavior is in good agreement with the prediction of Hlavacek's theory for isotropic elastic composite with ellipsoidal inclusions.

3. The index of bonding between the 150-300 μ m ellipsoidal bone particles is about 0.3.

4. The index of bonding appear to be stable with respect to variations (up to 40%) in bone content.

5. The present procedure appears to be applicable in principle to other inclusions.

References:

- [1] M. Hlavacek, "A Continuum Theory for Isotropic Two-Phase Elastic Composites," *Int. J. Solids Structures* Vol. 11, 1975.
- [2] M. Hlavacek, "On the Effective Moduli of Elastic Composite Materials," *Int. J. Solids Structures* Vol. 12, 1976.
- [3] R.W. Mack, "Bone - A Natural Two-Phase Material," Technical Memorandum, Biomechanics Laboratory, Univ. of California, Berkeley.

Mechanical Durability of Ceramic/UHMWPE Total Hip Systems.

I.C. Clarke¹, G. Sines², H. Oonishi³ and Y. Kitamura⁴

Biomedical Research Institute¹, Los Angeles,
Dept. of Materials Science, UCLA², and
Dept of Orthop, Osaka Minami National Hospital³, and Kyocera⁴, Japan

Al₂O₃ ceramic has been used extensively for the femoral heads and acetabular sockets of hip prostheses in France, Germany, Switzerland and Japan. The stems generally have a ceramic ball which press-fits onto a precision-tapered metallic trunnion. However, until the advent of the Mittelmeier hip in the last year, there had been no prior clinical experience in the USA.

Ceramics are considered ideal for total-joint applications because of their inertness, excellent biocompatibility and optimal wear characteristics. They are exceedingly strong in compression (UTC=4900 MPa) but an order of magnitude weaker in tensile strength (UTS=274 MPa). It is therefore very important that such material technologies incorporating ceramic ball/metal-stem combinations be strong enough to withstand the cyclic loading in the typical active American patient. The objective of this study was to determine the performance of ceramic balls (in combination with UHMWPE cups) at and above the normal patient hip loadings.

Stainless steel femoral stems were used, typically with a trunnion diameter of 10mm and included angle 20° 51'. The ceramic balls (Bioceram[®], Kyocera) had diameters from 28 to 44mm and came pre-mounted on the stems. The tests were conducted on a direct-stress fatigue system and a drop-tower rig. In this study, we used 0 to 20° range as representative of in-vivo loading axis. (Published studies have used both 0° and 45° femoral neck/load-axis angles). Fatigue tests were conducted in saline environment (frequency 10 to 30Hz, for 1 to 10 million cycles). The first set of tests were designed to include static load and shock-load tests to failure and fatigue tests under normal conditions. The second series was designed to study the survivorship data for the same designs with particulate contaminants inserted between the ceramic ball and the metal trunnion.

Load studies of varied trunnion dimensions demonstrated that 10 mm trunnions were optimal (Table 1) with minimum static load levels exceeding 30,000 for 28mm dia. ceramic balls. This is 10 times higher than that expected in an active patient.

IAPER	N	LOAD (N)	AVERAGE (N)
8mm	4	30,400-33,110	31,390
10mm	4	30,660-37,280	33,990
12mm	4	19,130-20,601	19,870

The 28 and 42mm balls tested in fatigue under standard conditions or with contaminants (Table 2, B-C: 3mm dia drops of blood) survived three tests of 30 million cycles total, at loads of 3,000 to over 11,000 N. However, when bone was introduced between ball and trunnion (1mm cubes), given a 3,900N proof load-test and then cycled, the ball fractured at as little as 85,000 cycles.

Table 2

BALL DIA (mm)	PEAK LOAD (N)	FATIGUE TESTS	RESULT	NOTES
42	2840-6380	3	intact	std
28	6380-11770	3	intact	B-C
28	2940-4900	2	intact	B-C
28	2940-6380	3	intact	std
28	2940	85,530c	FX	Bone

The impact studies used 28mm ceramic balls in UHMWPE sockets. After each test, the only observable damage was the depression in each socket, 2mm deep and 8mm in diameter (Table 3, A-D). However when the tests were repeated with particulate bone-fragments intentionally introduced between ball and trunnion, the cups both fractured on the 4th test of increasing load magnitude (E and F).

TABLE 3

TEST	WEIGHT (N)	HEIGHT (m)	ENERGY (Nm)	RESULTS
A	29.8	1.0	29.8	intact
B	112.8			intact
C	21.9	1.39	30.4	intact
D	29.8	1.0	29.8	intact
E	2-30(4)	1.39	41.7	FX
F	2-30(4)	1.39	41.7	FX

With careful design and manufacturing, it is apparent that ceramic heads can withstand in excess of 30,000N static loading (10 times hip load) and fatigue loads of 3,000-11,000N. However any contaminants introduced at surgery could drop the strength considerably. It may be desirable for such devices to come preassembled and sterile from the manufacture for optimal clinical performance.

Acknowledgements: This work was supported by the Biomedical Research Institute, Los Angeles. Thanks are due to Kyocera, Japan, for the components.

Biomedical Research Institute
344 Mira Loma Avenue,
Glendale, CA 91204.

Optimization of Controlled-torque Insertions of Monocrystalline Ceramic Screws at Surgery

I.C. Clarke¹, E.Ebrazadeh², P.Oette³ and Y.Kitamura³

Biomedical Research Institute¹, Los Angeles,
Dept. Orthop²., University of Southern California, Los Angeles,
and Kyocera³, San Diego and Kyoto.

Mono-crystalline ceramic screws are being used increasingly for dental and orthopaedic applications in Japan because of their inertness and excellent biocompatibility characteristics. The screws (Bioceram[®]) are made from a single crystal of Al₂O₃ ceramic (monocrystalline) which is much stronger than the polycrystalline material. Their use in bone grafting, trochanteric osteotomy, avulsion fractures and as cement-spacers in total joint procedures etc., prompted this study of their mechanical properties relevant to the surgical insertion techniques. The clinical performance of cortical or cancellous bone screws is dependent on the quality of the bone, the torque applied by the surgeon at insertion and in particular, the resulting bone clamping force exerted by the screw, i.e. the tensile axial screw-load. The objective of this study was to measure the insertion torques and axial screw-loads on stainless steel and ceramic screws.

A custom screwdriver design was fabricated and instrumented with strain gauges to measure accurately the insertion torques produced by the surgeon. A jig was fabricated for installation of human cortical and cancellous bone samples and then instrumented to measure the axial loads generated in the screws. The cancellous screws had ID = 4.85, OD = 6.5mm and length 50 - 75mm. The cortical screws had ID = 3.6, OD = 4.75mm and length 30 - 38mm.

Test #	Screw Type	Torque Nm	Notes
1	Cancellous	0.96	Bone strip
2	Cancellous	3.28	Bone strip
3	Cancellous	0.60	Bone strip
4	Cancellous	0.63	Bone strip
5	Cancellous	2.08	Bone strip
6	Cancellous	3.63	Ultimate test
7	Cortical	2.08	Bending fx
8	Cortical	3.63	Head fx
9	Cortical	3.58	Head fx

These studies demonstrated that driving screws into the cancellous bone of human femoral condyles required torques of 0.6 to 3.3 Nm to strip the bone threads. Thus the failure criteria in cancellous bone was the bone itself.

The insertion torques to drive the Sapphire screws through the 1st cortex (C1), 1st and 2nd cortices (C2) and then tighten down until ultimately fracture occurred (C3) are illustrated in the figure.

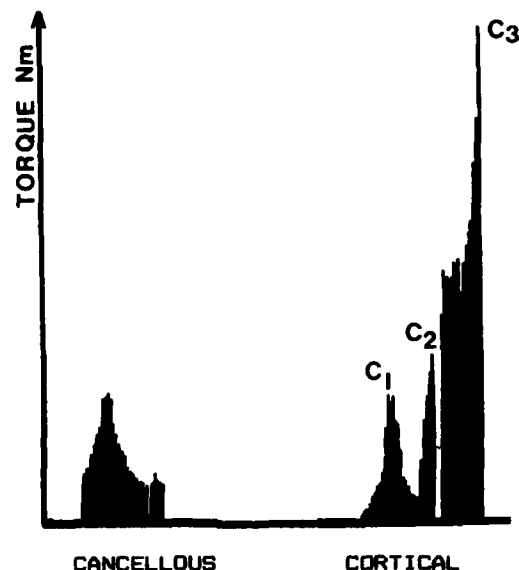


FIG. 1. Torque profiles for screw insertions in human cadaveric femoral bone.

To drive cortical screws through two human cortices required torques of 1 - 2 Nm. Applying further torques until fracture required 3.6 Nm on average for the ceramic screws (Fig. 1b).

While this monocrystalline screw material is much stronger (230%) than the polycrystalline material, these screws are not intended for major load-carrying roles and must be handled accordingly. This study of the interaction between insertion torques and ultimate fracture demonstrated that the limiting surgical torques should be in the 2 to 2.5 Nm range. The resulting clamping force in these various applications is under investigation. Current studies are considering the role of a torque-limiting instrument (2 - 2.5 Nm) to allow the surgeon to further extend with confidence the applications for Sapphire bone screws.

Acknowledgements: This study was supported by the Biomedical Research Institute. Thanks are due to Kyocera, Japan for supply of the Sapphire screws.

Biomedical Research Institute,
344 Mira Loma Avenue,
Glendale,
California 91204.

Finite Element Analysis of An Uncemented Alumina-Ceramic Total Knee Prosthesis

Hironobu OONISHI, Yasuhiro KITAMURA, Akio KAWAGUCHI and
Masanori TATSUMI

Department of Orthopedic Surgery and Artificial Joint Section, Osaka
Minami National Hospital, Osaka, JAPAN

Since November 1981, we have performed 300 total knee procedures using press-fit knee replacements where both the tibial tray and femoral condyles were made totally of alumina ceramic (Figure 1). The tibial component was conceived with wide fixation posts and was designed to achieve load transfer by anterior cortical bone, the posterior sloping shelf of cortical bone, and then, where possible, by cancellous bone.



Figure 1

To better understand the role of load transmission in this clinically successful procedure, a finite element analysis was conducted of the tibial bone and ceramic tray using special non-constrained ceramic-bone boundary conditions. There were 1,188 isoparametric solid elements with 6 to 8 nodal points and 30 shell elements for a total of 4,100 degrees of freedom (Figure 2).

The moduli assumed were as follows: ceramic = 377,000 MPa, Cortical bones = 50,000 MPa, dense cancellous bones 1,000 MPa, and poor cancellous bones 100 MPa. The model was run with inhomogeneous isotropic linear material characteristics. Loads of 490 and 980 Newtons were applied at varied axes to different positions of the tibial prosthesis.

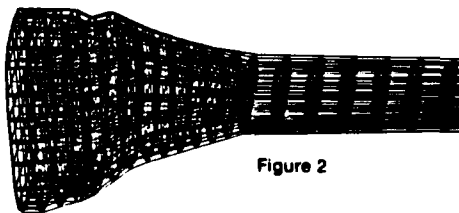


Figure 2

The assumed kinetic conditions permitted no shear or tensile loads, but allowed transmission of all compressive forces (Figure 3).

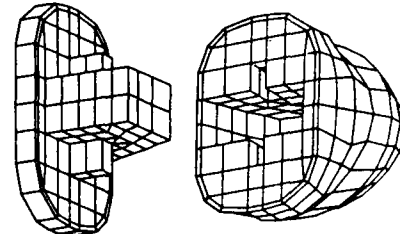


Figure 3

To investigate the clinical relevance of bone pathology, the model was run under the following assumptions: a) OA, cancellous bone = 1,000 MPa and preferential subchondral bone presence in medial and lateral plateaus, and b) R.A., cancellous bone = 100 MPa, again with and without the subchondral bone plate. Two examples of unilateral loading conditions are shown on Figure 4.

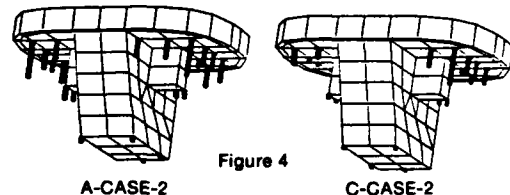


Figure 4

These clearly show the nodal sites and magnitudes of the load transfer to bone.

In the OA model, there was mixed loading between cortical bone and cancellous bone whereas in the RA model, it was predominantly cortical transfer, particularly on the sloping posterior shelf. The large flanges appeared effective in reducing the bone stress and maintaining equilibrium.

Even loading of tibial plateau on the side without cortical bone support provided only a slight increase in the observed stresses, due no doubt to the large contact areas presented by the ceramic tibial tray. We believe that these features and the excellent biocompatibility of this ceramic were contributory to the clinical success of this procedure.

ADDRESS: Dr. Hironobu OONISHI, Osaka Minami
National Hospital 677-6, Kido-Cho,
Kawachinagano-Shi, Osaka, 586, JAPAN.

Kyocera Company
Century Research Co.

A. RAVAGLIOLI, A. KRAJEWSKI, A. MORONI, B. OLMÍ

INST. TECH. RESEARCH FOR CERAMICS - C.N.R. FAENZA (ITALY)

INTRODUCTION

The use of HAP as a prothetic material is well known. Some problems arise from the workability when aiming at obtaining such ceramic product, or from its histological behaviour. The Authors take in consideration some of the results on the two aspects of the problem.

POROSITY CONTROL

Some compact samples were obtained a long time ago; later on, tape casting HAP product were proposed too. More recently the casting technique was developed. One must remember, however, that the HAP product obtained by firing, after a traditional pressing (about 300 kg/cm²) show a high shrinkage coefficient also up to 25% with a slope variation of the curve in correspondence of 1200°C. To obtain a product without any fault one must evaluate accurately the nature and the quantity of the binders and of the pertinent solvents.

To have porous samples a dense suspension in H₂O (with binders and solvents) was prepared within a suitable mold. Such mold can be constituted by hollow dies, or by soaking natural or synthetic sponges. The use of polymeric sponges gives rise to products at a regular porous plot, however sufficiently brittle for the very thin connections. Since we are interested, however, in a lower porosimetric class in respect to those obtained with polymeric sponges, investigations on samples obtained by hollow dies were carried out. A great importance is ascribed to the absorption rate by the mold. The chalk, e. g., proved too much absorbent, while other refractory materials resulted still less suitable. Some cement-based compositions will prove very useful. Different molds were prepared with different kinds of cement mixed, in different ratios, with pore forming substances and H₂O. The materials prefired at 1170°C, shaped on the lathe in order to obtain a central hole having the size requested by the plug utilized for the osteosynthesis, were fired in a laboratory kiln for 6 h at 1240°C ± 10°C. Some samples were then examined with the mercury porosimeter in view of a classification.

RESULTS OF THE GRAFT ON RABBITS

The obtained cylinders, having a diameter of 10 mm, were grafted for 9 months, trying to ascertain the role of every porosimetric class in the samples (a porosimetric class 15 micron) to demonstrate, with a different experimental test, what was previously observed (1) with regard to the Ca²⁺ enrichment at the edge of the implanted bulk. The histological and microradiographic tests carried out after 9 months of implantation, put in evidence a complete interlinking between HAP ceramic and skeletal tissue, not verified in analogous tests made after two months. Furthermore, the grafted samples were examined as weight changes between the weight before the graft into the rabbits and that one obtained after the heating at 700°C for over three hours of the samples themselves after taking them out of the rabbits. The difference showed an increase in weight that can be ascribed neither to H₂O nor to any residual organic material. Table 1 reports the pore size distribution with the diameter of the different porosimetric classes.

TAB. 1		% pore size distribution until 15 µm of pores diameters (microns)				Overall volume until 15 µm for 1 g of sample cm ³ g
Sample	ΔP/P ₀	<0.8	0.8→1.0	1.0→1.2	1.2→1.5	
1	0.02718	16	17	53	14	0.1022
2	0.03315	5	25	60	10	0.0774
3	0.06415	0	100	0	0	0.0968
4	0.06810	12	88	0	0	0.1108

The changes in the weight of every sample in respect to the initial weight are reported. Such increase is likely to be ascribed to a deep mineralization brought about by the physiological liquids, confirming what the Authors asserted previously (4). The ascertained difference lets one think of the influence connected with the different porosimetric textures.

REFERENCE

(1) R. MONGIORGI, A. ROMAGNOLI, A. KRAJEWSKI, A. RAVAGLIOLI, A. MORONI, R. OLMÍ; "Mineralization and Ca²⁺ Fixation within a porous apatitic ceramic, implanted in rabbit femurs" in print.

Development of a new orthopaedic material-screws and plated coated with titanium nitride (TiN) ceramic.

Suka, T., Masubuchi, M., Ooi, Y. and Mikanagi, K.

Dept. of Orthopaedics, Jichi Medical School, Yakushiji 3311-1,
Kawachi-gun, Tochigi-ken, 329-04 JAPAN

Purpose : Ceramic have excellent properties such as non-corrosiveness, non-soluble, non-toxicity and non-stimulant, although the largest problem, the brittleness is not resolved completely yet. We have been thinking to utilize the excellent biocompatibility of ceramic to the orthopaedic materials, therefore TiN ceramic was used to coat stainless steel. And so, the stainless steel coated with TiN ceramics should have the excellent biocompatibility in addition to the strength. Screws and plates made with it have been studied on the strength, the reaction to acid and alkaline and the influence on the around tissues.

Material and Method :

1. Bending test

Test piece (40X20X15mm) coated with TiN ceramic, 1.5micrometer, 3.0 micrometer, 4.5 micro meter thick were bent and the co-relation between strain and crack formation was studied.

Result : The least strain to make crack was 30×10^{-6} with mean that stainless steel coated with TiN ceramic in these thickness has some elasticity and doesn't crack before stainless steel drops into permanent flexion.

2. Wear of the TiN ceramic

A0 screw coated with TiN ceramic in 3.0 micro meter thick was screwed in the aluminum plate after tap and the surface was investigated with S.E.M.

Result : Stainless steel appeared after 10 - 15 times screwing, although the surface was roughened by 5 times screwing in non-coated screw. This observation shows the offensiveness of the TiN ceramic.

3. Corrosiveness

Experimental pieces coated with 5 micrometer thick TiN ceramic were soaked in 50 % hydrochloric acid and 23 % saline. Decrease of weight of the pieces was weighed in 50 hours.

Result : Test pieces decreased 8.52 mg/dm^2 in hydrochloric acid and 0 mg/dm^2 in saline, although stainless steel which was not coated lost 14600 mg/dm^2 in hydrochloric acid, 7.80 mg/dm^2 in saline.

4. Influence of TiN ceramic on around tissue

stainless steel screws coated with TiN ceramic were inserted into femur of adult rabbit and the new bone

Okuno, O., Miura, I., Kawahara, H.^{*}, Nakamura, M.^{*} and Imai, K.^{*}

Institute for Medical and Dental Engineering, Tokyo Medical and Dental University, Tokyo, Japan

Introduction

Various porous metals by powder metallurgy process have been investigated for the fixation of implants to bone. One of the problems in porous metals is that of poor strength. Open pore should be needed as large as about 150 μm in order to ingrowth the greatest amount of bone into porous metals. But, strength of porous metals with such a large and open pore were usually as low as human cortical bone. Porous metals should have higher static strength, considering fatigue stress.

The object of the present study was to develop high strength porous zirconium-titanium alloys for implant by sintering mixture of titanium and zirconium spherical particles. Both titanium and zirconium possess good mechanical properties, excellent corrosion resistance and biocompatibility. Titanium and zirconium form complete solid solution. The mixture of these particles would be sintered easily and quickly. The best Titanium/zirconium ratio as implant materials was investigated from the points of mechanical properties and pore structure.

Materials and Methods

Titanium and zirconium spherical particles used were made by REP (Rotating electrode process). 420-500 μm spherical particles were sieved. These spherical particles were mixed enough by V-type mixer. The mixture ratios were varied from 10-70 wt% zirconium. These spherical particles were filled gravitationally in alumina mold and pre-sintered in a high vacuum at 1000°C. The specimens that were taken out of the alumina mold were re-sintered in a high vacuum for 3-24 hr at 1400°C. Compression test was performed on a Instron machine using crosshead speed of 0.5 mm/min. Size of testpiece was 4x8 mm. Surface and cross-section of porous zirconium-titanium alloys were observed and analyzed with SEM and EPMA. Porosity and pore size were measured by image analyzer.

Results

Compressive strength as a function of zirconium wt% is presented in Fig.1. The compressive strength of porous zirconium-titanium alloys increased rapidly with increasing zirconium wt% and exhibited peak at 50-60 wt% zirconium. The compressive strength at these compositions were 4-8 times as large as porous pure titanium or zirconium and about 2 times as large as human cortical bone. Young's modulus of the porous zirconium-titanium alloys at these compositions were 4.6-7.4 GPa from compression testing. The strain at ultimate compressive stress were more than 7 %.

Phot.1 shows surface and cross-section of the porous zirconium-titanium alloys at 50 wt% zirconium. Titanium spherical particles and zirconium spherical particles bonded tightly. Therefore, compressive strength of porous zirconium-titanium alloys at 50-60 wt% zirconium showed the highest strength. On the other hand bonding between titanium-titanium or zirconium-zirconium were loose. Image analysis of cross-sections of porous zirconium-titanium alloys at 50 wt% zirconium revealed porosity of 28-38 % and average pore size of 167-204 μm . It would be expected that bone would

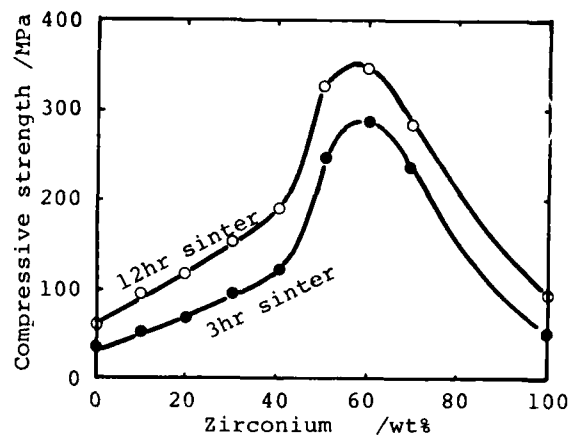
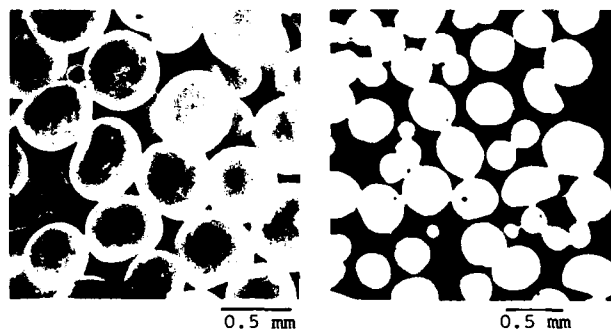


Fig.1. Compressive strength of porous zirconium-titanium alloys.



Phot.1. Porous zirconium-titanium alloy.
50 wt% zirconium, 12 hr sinter

ingrowth into these pore.

The results of this study indicate that porous zirconium-titanium alloys at 50-60 wt% zirconium would be suitable for the fixation of implant to bone, considering mechanical properties and pore structure. We are examining fatigue and biological compatibility in detail.

Institute for Medical and Dental Engineering,
Tokyo Medical and Dental University
2-3-10, Surugadai, Kanda, Chiyoda-ku, Tokyo, 101
Japan

^{*}Department of Biomaterials, Osaka Dental University
1-47, Kyobashi, Higashi-ku, Osaka, 540 Japan

MORPHOLOGICAL AND ELECTROCHEMICAL STUDIES OF FATIGUE AND CORROSION FATIGUE
ON THREE ORTHOPEDIC IMPLANT MATERIALS

Ortrun E.M. Pohler

Fontana Corrosion Center, The Ohio State University
Columbus, Ohio

In a long term study, cases of broken orthopedic implants were analyzed metallurgically and clinically. With few exceptions, the implants failed through material fatigue caused by dynamic loading under unstable mechanical conditions which was confirmed by radiographic and weight-bearing histories of these cases.

Although primary corrosion signs are not usually found on broken implants, the question arises if the fatigue processes are enhanced by the biological environment. Therefore, fully reversed fatigue bending tests were performed in Ringer's solution, in Ringer's solution + fibrinogen, and in air on 316LR stainless steel, on a wrought cobalt-alloy, and commercially pure titanium. The materials were tested in soft and cold worked condition at different loads.

The implant performance depends more on the fatigue initiation stage than on the crack propagation stage, but less systematic research has been done on fatigue crack initiation than on crack propagation in metals. Thus, the fatigue initiation mechanism was studied qualitatively and quantitatively by microscopic and electrochemical means on all three materials in the various environments. In addition, the fracture surfaces were analyzed by scanning electron microscopy to detect possible environmental damage and to compare the fracture modes of the different materials.

S-N fatigue curves were generated from the fatigue endurance data. These curves show that the fatigue resistance of all three materials improves through the cold working process, which corresponds to the increase of the tensile strength. In general, the cobalt-alloy has the highest fatigue resistance under comparable conditions. This is particularly pronounced at high stress levels. However, the soft titanium has a higher fatigue endurance limit than the cobalt-alloy or the stainless steel in soft condition. At higher stresses, the latter two materials are superior to titanium. This behavior is explained by the different slopes of the fatigue curves.

The fatigue resistance of all three materials is reduced in Ringer's solution. This effect is less noticeable in soft material conditions, and the reduction is less for the titanium than for the other two alloys. With the addition of fibrinogen, the negative effect of the Ringer's solution is reduced. Since even at high magnifications no sign of corrosion was detected on any of the materials, it is assumed that the reduction of the fatigue life in Ringer's solution is caused through damage to the passive film that forms on the material surface. This is supported by the findings of the microscopic and electrochemical investigations.

During fatigue testing, crack development on the specimen surface was studied "in situ" in all environments by a replica technique. It was shown that fatigue damage occurs as an accumulative process. On the stainless steel and the cobalt-alloy, which have cubic face centered structures, the crack initiation is governed by glide processes. First, persistent glide bands, from which precracks emerge, are formed on the surface.

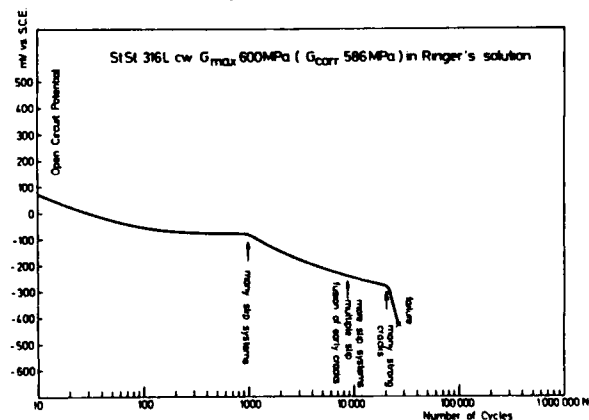
Through crack growth and coalescence, larger cracks and a main crack develop. The crack initiation process on the hexagonal titanium is more complex since in addition to intracrystalline glide, grain boundary glide and twin formation also contribute to the surface damage.

On all materials, the damaging processes are more intense and occur more rapidly under higher loads. On soft materials, these processes are shifted to lower loads compared to the cold worked materials. In Ringer's solution, the fatigue initiation mechanism does not seem to be altered, but the individual damaging structures occur earlier, thus shortening the fatigue life time.

On the broken specimens, the extension of the fatigue surface damage at the fracture edges was measured at 100x and 400x magnification. The size of the damaged areas changes consistently as a function of the applied stress, the material strength, and the environment in the same sense as described above for the observations made on the surface replicas.

During fatigue testing in the liquid environments, the open circuit potentials were recorded. The tested materials tend to passivate in Ringer's solution, but under cyclic loading, the potentials decline as the surface damage structures develop. This indicates the destruction of the passive film. The possible effect on the fatigue life can be explained by various models. The diagram below gives an example of the relation between potential decay and surface damage.

The morphologic observations of this study are consistent with those made on broken implants and confirm that the implants fail through a fatigue mechanism. The acquired knowledge of the fracture morphology and the fatigue initiation structures as a function of the load will aid in the failure analysis of broken implants.



Open Circuit Potential for Cold Worked 316LR SS
Recorded During Fatigue Testing at $\sigma = 600$ MPa

The author wishes to thank Professor D.D. Macdonald, Director of the Fontana Corrosion Center at the Ohio State University, and Dr.h.c. F. Straumann, Director of the Straumann Institute, for their support and encouragement in this work.

Effects of Porous Coatings on the Corrosion Behavior of Co-Cr-Mo Material

A. C. Van Orden and A. C. Fraker

National Bureau of Standards, Washington, DC 20234

Porous metal coatings are being used on metal prostheses in an effort to improve fixation of the device. Limited metal ion release and high corrosion resistance are important requirements for implant metals. Porous coated surfaces have increased surface area which can result in increased metal ion release. Also, the surface morphology is different, and this can result in a different type of corrosion from that found on smoother surfaces. This study deals with the corrosion behavior of Co-Cr-Mo sintered spheres on a Co-Cr-Mo substrate. The objective of this research is to characterize the corrosion behavior of porous coated Co-Cr-Mo alloys when exposed to Hanks' and other physiological saline solutions. The electrochemical data will be related to the pore size, the effects of sintering and the alloy composition.

Specimens of sintered Co-Cr-Mo spheres on a Co-Cr-Mo substrate were obtained for investigation. The sphere size was in the range of -18 to +30 mesh. Anodic polarization measurements were made on porous coated specimens in the non-passivated and passivated conditions, and results were compared with data from tests on smooth surfaced Co-Cr-Mo. Specimens were ultrasonically cleaned in water and rinsed in ethanol prior to corrosion testing. Specimens were exposed in Hanks' physiological saline solution which was held at a temperature of 37°C and had a pH of 7.4. Specimens were polarized potentiostatically at a rate of 0.006V/min. until breakdown occurred. The ASTM F-746 standard test method for pitting and crevice corrosion was applied to the porous material and no pitting was observed.

The smooth Co-Cr-Mo and the unpassivated porous coated material showed a breakdown potential at 0.47 volts vs. Saturated Calomel Electrode while the passivated specimens broke down at a more noble potential of 0.80 V. Corrosion current for the porous materials was higher but the current density for these porous specimens was the same. Second phases can be present at the necks of the sintered spheres as is indicated in Figure 1 (arrow). The material used in these studies was processed to eliminate some of this second phase at the neck.

Scanning electron microscopy and energy dispersive x-ray analysis were used to analyze the surface films. Figure 2 is an electron micrograph of the corroded spheres and Figures 3 is a higher magnification micrograph of the surface film. Data from this film in Figure 4 shows the film to be enriched in Cr, Mo and Fe. Films within the interstices are thicker than films on the top surface. These films within the interstices of the pores and at necking locations are being analyzed to determine the mode of corrosion in these areas. Electron Spectroscopy for Chemical Analysis (ESCA) is being applied in the surface studies to determine the oxidation state of the elements present in the film. Effects of pore size on the corrosion resistance and the nature of the corrosion film within the interstices will be determined.



Figure 1. Light micrograph of Co-Cr-Mo.

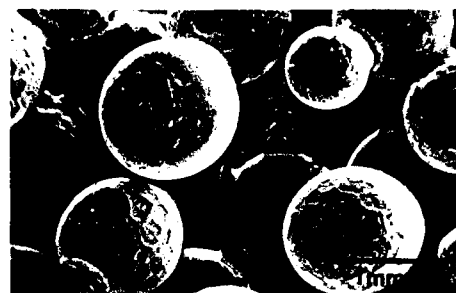


Figure 2. SEM micrograph of corroded Co-Cr-Mo.



Figure 3. SEM micrograph of oxide film on Co-Cr-Mo.

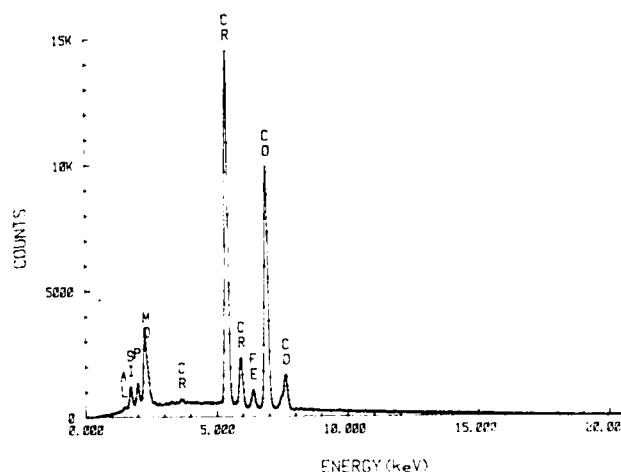


Figure 4. EDS data: Oxide film comp. on Co-Cr-Mo.

Metallurgy Division, National Bureau of Standards
Washington, DC 20234

Kinetics of the Ni(II) Reaction with Human Blood Serum Albumin

G. J. Mattamal and A. C. Fraker

National Bureau of Standards, Washington, DC 20234

Metal ion interactions with body fluids are important when considering long term effects of metal implants. These interactions will become more significant with the use of porous implants which have more surface area exposed to the body. This study provides a better understanding of mechanisms involved in metal ion transport or reactions with body fluids. This investigation is of interactions of nickel and/or chromium ions with human blood serum albumin and addresses the thermodynamics and kinetics of metal ion/protein interactions. Both chromium and nickel ions are being studied individually and in combination as can be the case when these metal ions are released from metal prostheses.

Electrochemical techniques are used to release ions into the human blood serum albumin (HSA) solution. Implant metal specimens and pure metals are exposed to HSA solutions (0.1% to 1%) and potentiostatically polarized. Metal ions also are added to the HSA solution in the form of chloride salts. Reactions in the solutions are determined by separating the protein with the bound metal from the solution with the free metal. This separation is carried out using ultrafiltration techniques and a 10 PM membrane. Solutions are analyzed for metal ion content using atomic absorption spectroscopy methods and the amount of the bound metal ion is determined from these data.

One example of this work is a set of three experiments which involved Ni(II) interactions with HSA. Reactions were carried out in a vessel which was held at a temperature of 37°C, and nitrogen gas was bubbled through the HSA and metal ion solution. Specimens were taken at 1 hour intervals over a 3 hour period for ultrafiltration, atomic absorption and ultraviolet spectroscopy analysis. The first experiment had a constant concentration of 1% HSA with the Ni concentration varying from 10 ppm to 650 ppm in an unbuffered 0.15M NaCl solution. The second experiment was conducted under the same conditions but was in a solution buffered at a pH of 7.4. The third experiment involved holding the Ni(II) at a constant concentration of 60 ppm and varying the serum albumin in the range of 0.1% to 2%.

The results show the following:

1. The extent of binding of Ni(II) ion by HSA increases with increasing pH in the pH range studied. This is illustrated in curves 1 and 2 of Figure 1.

2. HSA has approximately 15 identical and negligibly interacting binding sites for Ni(II) ion in the pH range of 5.6 to 6.3 in unbuffered solution and has an affinity constant, K , of 0.567×10^3 .

3. The standard free energy for binding involved in this Ni(II) ion/HSA interaction will be -5.6 Kcal/mole .

Additional data will be presented regarding chromium interactions with HSA. Interactions of nickel ions and chromium ions in a given HSA solution will be discussed.

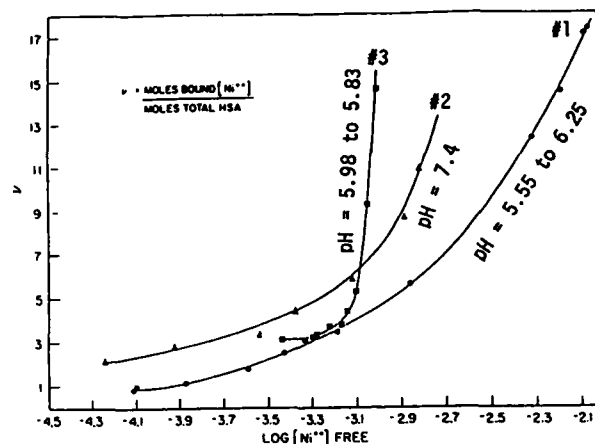


Figure 1. Binding of Ni(II) by HSA at 37°C.

Metallurgy Division, National Bureau of Standards
Washington, DC 20234

STRESS CORROSION CRACKING SUSCEPTIBILITY OF 316L AND Ti-6Al-4V ELI IMPLANT ALLOYS

V.H. Desai and K.J. Bundy*

Materials Science and Engineering Dept.
Johns Hopkins University, Baltimore, MD. 21218

INTRODUCTION: It has been suggested that the environmental conditions to which implants are subjected in the body are not severe enough to cause stress-corrosion cracking (SCC)¹. On the other hand, there have been at least nine reports of implants which have seemed to fail by SCC after *in vivo* service². This apparent discrepancy is perhaps a result of the failure to duplicate important aspects of the body environment in laboratory studies. It is possible that organic components present in body fluids and *in vivo* bioelectric effects may be influencing SCC behavior of implants³. There is thus a need for laboratory studies under conditions which attempt to simulate relevant physiological conditions and to identify the conditions for SCC susceptibility of implant alloys. It is also important to determine quantitative parameters such as the threshold stress intensity K_{ISCC} , crack propagation velocity V_{II} , and incubation time for crack initiation t_i in order to be able to rate present implant alloys and alloys of the future with regard to their susceptibility to SCC.

MATERIALS AND METHODS: A fracture mechanics approach was used for assessing the SCC susceptibility of 316L and Ti-6Al-4V ELI alloys. Double cantilever beam type specimens were wedge-loaded to different stress intensity levels. The stress intensity at the crack tip was determined using the compliance calibration technique of Irwin and Kies⁴. The loaded specimens were exposed to three chloride containing environments: boiling $MgCl_2$ at 154°C to relatively quickly ascertain the SCC susceptibility in chloride media, 5% HCl at 37°C to determine susceptibility in chloride media at body temperature, and Ringer's solution at 37°C for closer simulation of *in vivo* conditions.

Both polarized and unpolarized specimens were tested in order to determine the effect of applied potentials on SCC behavior. In Ringer's solution four different patterns of polarization were imposed in order to create and ascertain electrochemical conditions which are suitable for SCC in this environment. These were 1) maintaining an anodic overpotential which did not allow repassivation after initially damaging the passive film, 2) maintaining an anodic overpotential 100mV above the corrosion potential, 3) galvanostatically controlling the anodic current density to $10\mu A/cm^2$, and 4) superimposing an AC potential on an applied DC potential to cycle the resultant potential above the limit for breakdown of passivity.

RESULTS AND DISCUSSION: Both 316L and Ti-6Al-4V ELI alloys exhibited SCC in $MgCl_2$ and 5% HCl environments. In Ringer's solution so far, only condition 1 has produced SCC crack propagation in 316L. Although in this work the passive film was initially disrupted by a high anodic overpotential, it may also be destroyed mechanically in actual *in vivo* service (for example by fretting). Fretting has been proposed as a possible mechanism for SCC crack initiation⁵. Table 1 shows SCC

parameters for these alloys for various test conditions.

Material/ Environment	Table 1		
	Polar- ization Condition	Average V_{II} (m/s)	Average K_{ISCC} ($MNm^{-3/2}$)
316L/ $MgCl_2$ 154°C	none	8.5×10^{-8}	9.5
	50mV anodic	9×10^{-8}	13
	150mV cathodic	6.3×10^{-8}	19
316L/HCl 37°C	none	4.5×10^{-10}	70
316L/Ringer's 37°C	1	2.4×10^{-10}	--
Ti-6-4/ $MgCl_2$ 154°C	none	8.5×10^{-5}	22.6
Ti-6-4/HCl 37°C	none	2.4×10^{-9}	53.9

Another important finding was that t_i was dependent upon the stress level, with low stress levels requiring high t_i and vice versa according to the functional relationship: $t_i = C \exp(-AK)$ where A and C are constants. Also, polarization seemed to reduce t_i significantly. This may be very important in accelerating SCC studies employing implant materials.

This is perhaps the first time that SCC has been demonstrated in the laboratory at body temperature. SCC studies of implant materials are hindered because of the long time period required in such studies. Even slow strain rate testing, a relatively quick screening test, may have to be performed at very low strain rates to adequately test these alloys. Testing in harsher environments like the ones used here could serve as screening tests for SCC susceptibility of implant alloys.

References

1. Taussig, L.M., in Implant Retrieval: Material and Biological Analysis, NBS Special Publication 601, Weinstein, A., et al, eds., 1981, 201-222.
2. Bundy, K.J. and Desai, V.H., "Studies of Stress Corrosion Cracking Behavior of Surgical Implant Materials Using a Fracture Mechanics Approach," paper presented at 2nd Int. Surg. Implant Corrosion Symposium, Louisville, May 9-10, 1983.
3. Bundy, K.J., Marek, M., and Hochman, R.F., J. Biomed. Mater. Res., **17**, 467-87 (1983).
4. Irwin, G.I. and Kies, J.A., Welding J. Res. Suppl., **33**, 193-8 (1954).
5. Jones, R.L., Wing, S.S., and Syrett, B.C., Corrosion, **34**, 226-35 (1978).

This research was supported in part by a National Association of Corrosion Engineers Seed Grant for Corrosion Research.

*Associate Professor
Biomedical Engineering Dept.
Tulane University
New Orleans, La. 70118

Influence of Chloride Ion Concentration on the Corrosion of Pd-Based Alloys.

T.K. Vaidyanathan

New York University Dental Center, Dept. of Dental Materials
Science, 345 E. 24th St., New York, New York 10010

The effect of Pd alloying on the chloride corrosion behavior of binary alloy systems (1 to 4) of Ag-Pd, Cu-Pd, Co-Pd and Ni-Pd is to introduce: (1) a significant ennobling effect as revealed by an active to noble shifting of the active regions of the anodic polarization curves representing Ag/AgCl, Cu/CuCl, Co/Co⁺⁺ and Ni/Ni⁺⁺ oxidation reactions. (2) a sharp active-passive polarization profile, as revealed by the anodic loop associated with the orders of magnitude current density decrease at higher anodic potential regions.

The objective of this investigation was to study the effect of chloride ion concentration on the anodic polarization behavior of the Pd based binary alloys.

Binary alloys were prepared by vacuum induction melting. The alloys studied included the Ag-Pd, Cu-Pd, Co-Pd and Ni-Pd systems. Compositions studied included pure Pd, Pd-20%X, Pd-40%X, X-40%Pd, X-20% Pd and pure X where X is Ag, Cu, Co or Ni. Chloride corrosion behavior was studied by potentiodynamic polarization using a PARC potentiostat, Universal potential programmer, XY recorder, Electrometer Probe and Corrosion cell. All the alloys were cast into 1sq cm section discs, mounted metallographically and polished through 600 grit emery paper. Potentiodynamic Scanning was carried out in the active to noble direction. Chloride media covering a range of chloride ion concentration (0.1% to 10% sodium chloride solutions) were used for the study.

Figures (1) and (2) show typical polarization profiles showing the effect of chloride ion concentration. In general, the chloride ions shifted the polarization curves in the active direction.

The following parameters were analyzed to study the effect of chloride ion concentration (1) The potential value of the intercept of the tafel region of active anodic oxidation process extrapolated to the potential axis at 0.001 mA/cm² (hereafter designated as E_a) (2) The corrosion potential value E_{corr}. (3) The primary passivation potential E_{pp}. (4) The critical current density (i_{cr}) prior to passivation. (5) Passive current density (i_p).

The results indicate that chloride ion concentration increase generally shifts E_{corr}, E_a, i_{cr} and i_p values in the active direction and E_{pp} value in the noble direction. These results confirm that chloride ions tend to destabilize passivity as well as to accelerate the oxidation processes. Destabilization of passivity appears to be enhanced where the primary anodic oxidation reactions lead to soluble ionic species rather than insoluble corrosion films. The electron donor acceptor theory of passivity

also appears to be confirmed where the oxidation leads to insoluble corrosion products whereas significant deviation effects are observed in systems which lead to soluble products. This indicates that chloride ions can effectively compete to destabilize passivity probably in the absence of insoluble corrosion products.

FIG-1 Anodic Polarization Scans on 80Pd-20Ni

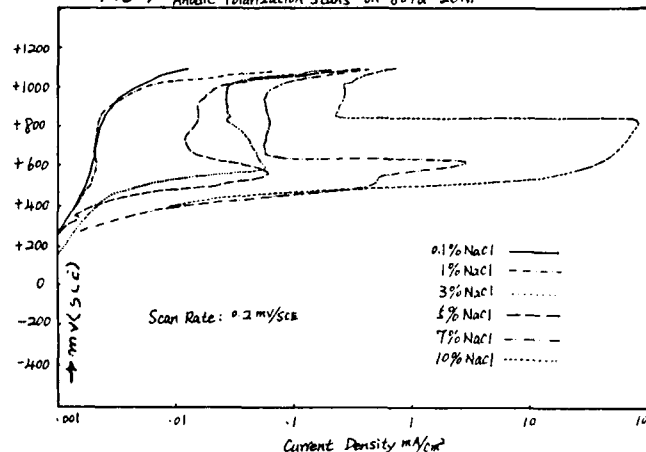
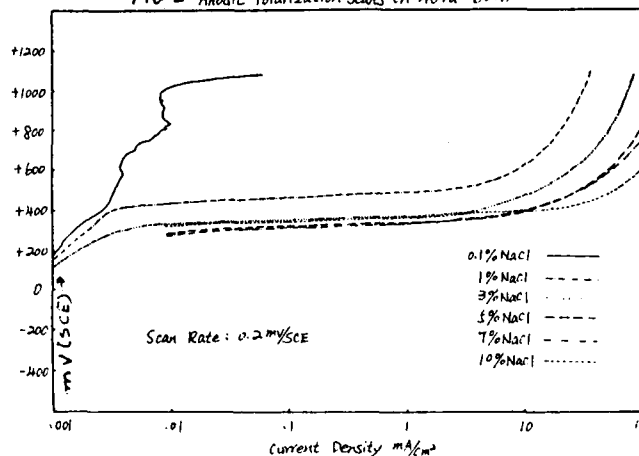


FIG-2 Anodic Polarization Scans on 40Pd-60Ni



1. S. Sastri, T.K. Vaidyanathan and Mukherjee, K. Metallurgical Transactions, 13A, 313-317 (1982).
2. T.K. Vaidyanathan, IADR Program & Abstracts (1981).
3. B. Penugonda, T.K. Vaidyanathan and Prasad, A., IADR Programs & Abstracts, 1982.
4. Khan, Shan Shih, T.K. Vaidyanathan and J. Vaidyanathan, IADR Programs & Abstracts 1983.

THE INFLUENCE OF STRESS ON THE DISSOLUTION BEHAVIOR OF SURGICAL IMPLANT ALLOYS

K. J. Bundy, V. H. Desai*, and M. A. Vogelbaum*

Biomedical Engineering Department
Tulane University, New Orleans, LA 70118

INTRODUCTION: In recent years increased attention has been directed to the biological consequences of release of ions into the *in vivo* environment due to the corrosion of metallic surgical implants. Improvements in the biocompatibility of devices have been achieved by decreasing the dissolution rate, but much research still needs to be done to clarify the actions that released ions have on biological functioning and to understand the factors which promote increased corrosion rates *in vivo*. Since most alloys used in orthopedic and dental applications are subjected to mechanical stresses, it is important to determine whether or not applied stress can accelerate dissolution of these materials.

METHODS: Two separate approaches were used to investigate this question. Polished 316L stainless steel test specimens were employed in each case in a 37°C physiological saline solution. In one series of experiments $\frac{1}{2}$ " x 3" rods were loaded by a fixture which stressed them in 3 point bending. The fixture, the loading points, and most of the specimen surface were covered with insulating materials. A small area of the specimen directly under the loading bolt on the tension side was not covered and was exposed to the electrolyte. This arrangement allowed the dissolution behavior of specimens stressed to different levels to be determined. A 100 mV anodic potential was applied, and the resultant current was integrated with a digital coulometer (EG & G PAR Model 379). The time averaged current density \bar{i} for different stress levels could be obtained in this manner. In these potentiostatic tests, the potentials of the samples were below the breakdown potential for pitting E_{bd} which was observed in polarization tests with unstressed material.

In another series of tests, the anodic polarization behavior of wedge-loaded double cantilever beam type fracture mechanics samples, as influenced by immersion time and stress intensity level, was investigated. Polarization curves were obtained after 1 hour of immersion at levels of 0 and 79 MNm^{-3/2} and after 1 week of immersion at 0, 47, and 94 MNm^{-3/2}. Corrosion potential E_c versus immersion time data was also acquired.

RESULTS: Table 1 shows \bar{i} for three stress levels: a zero stress control, the yield stress σ_y , and the ultimate tensile strength σ_{uts} . There appears to be no significant difference in the rate of ion release as long as there is only limited plastic deformation in the material. In fact \bar{i} for the σ_y level is about 50% of that for the zero stress control. On the other hand, when there was extensive plastic deformation (at σ_{uts}), although there was considerable scatter in the data, the mean \bar{i} value was 23.5 times that of the zero stress control and 46.5 times that of the σ_y samples. The inference is that application of plastic deformation to 316L stainless steel causes a disruption in the passive film which allows a greater current to pass through it.

This effect of stress in disrupting the passive film could be seen more clearly in the

anodic polarization tests. The results of these experiments are summarized in Table 2 which shows the corrosion potential and breakdown potential for the different immersion times and stress intensity levels examined. The E_{bd} values were substantially lower for stressed samples as compared to the controls even after 1 week of immersion. No passive region at all was observed for the stressed specimen 1 hour after immersion. All of the stressed samples seemed to give evidence of damaged passive films. This is probably because all of them were stressed into the plastic region. The unstressed condition showed a much more pronounced increase in E_c with time than did the stressed condition. This effect has been associated with a thickening of the passive layer (1). **DISCUSSION AND CONCLUSIONS:** Application of stress which causes plastic deformation in 316L stainless steel weakens its passive film in physiological saline solution. This makes the alloy more prone to ion release and more susceptible to damage by pitting corrosion. The disruption of the passive film persists for at least 1 week after the application of stress.

TABLE 1
Time-Averaged Current Density for Different Stress Levels

\bar{i} ($\mu A/cm^2$)	Stress Level
0.166 ± 0.084	0
0.084 ± 0.055	σ_y
3.90 ± 3.68	σ_{uts}

TABLE 2
Corrosion Potential & Breakdown Potential for Different Immersion Times & Stress Intensity Levels

Stress Intensity (MNm ^{-3/2})	Immersion Time	E_c (mVvsSCE)	E_{bd} (mVvsSCE)
0	1 hour	-160	+255
79	1 hour	-155	specimen was in active region
0	1 week	+174	+380
47	1 week	-105	+260
94	1 week	-77	+280

REFERENCE: 1. Hoar, T. P., Mears, D. C., Proc. R. Soc. Lond. Ser. A, vol. 294, p. 486 (1966).

*Mr. V. H. Desai and Mr. M. A. Vogelbaum are, respectively, a Ph.D. candidate and an undergraduate student in the Materials Science and Engineering Department of Johns Hopkins University. Dr. Bundy was formerly an assistant professor in this department.

H. M. Hsu and R. A. Buchanan

The University of Alabama in Birmingham
Birmingham, Alabama

Studies have indicated that serum proteins influence the biocorrosion properties of surgical alloys, where the influence is material-dependent and may result in acceleration or deceleration of corrosion. Consequently, it is recommended that laboratory electrochemical evaluations utilize a proteinaceous saline electrolyte. However, it has also been suggested that interactions at the protein-molecule/metallic-surface interface can lead to corrosion processes that are undetected by standard electrochemical polarization methods. This is a serious challenge, for it places the results of such studies, as well as the analytical methods themselves, in positions of questionable worth. In order to address these issues, the present study sought to answer the following two questions with regard to surgical stainless steel (ASTM F138): (1) Are electrochemical polarization experiments valid in measuring corrosion characteristics when serum proteins are involved?, and (2) How does the serum concentration influence the corrosion properties under *in vitro* conditions?

The electrolytes employed were isotonic saline (0.9 w/o NaCl) and isotonic saline plus 10, 25 and 50 volume percent calf serum (Gibco, Cat.200-6170). The solutions were oxygenated for 30 minutes and adjusted to a pH of 7.00 ± 0.05 prior to testing, then heated to and maintained at $37 \pm 1^\circ\text{C}$ throughout testing. The cylindrical corrosion samples were abraded through 600 grit SiC paper, polished with $1.0 \mu\text{m Al}_2\text{O}_3$, then cleaned in boiling benzene (no passivation/sterilization treatments). The samples were placed in the electrolytes and allowed to stabilize for one hour. The testing methods included cyclic anodic polarization, predicted vs. actual weight losses at constant anodic potential, cathodic polarization, and polarization resistance.

The cyclic anodic polarization curves produced by surgical stainless steel in saline and saline/10%-serum are shown in Figure 1. To test the validity of electrochemical corrosion predictions, current densities were measured as a function of time at selected potentials in both electrolytes, then integrated to predict weight losses by corrosion. The samples were then weighed to evaluate agreement or disagreement with the predicted values. The results were:

Electrolyte	Potential mv vs. SCE	Predicted Weight Loss (mg)	Measured Weight Loss (mg)
Saline	700	61.7	61.0
Saline	550	20.2	21.0
Saline/Serum	550	38.2	36.0
Saline/Serum	400	2.9	4.0

The agreement was excellent. The hysteresis behavior in the cyclic anodic curves indicated susceptibility to pitting corrosion in both electrolytes. The pitting or breakdown potentials differed: 425 mv in saline as compared to 275 mv in saline/serum, indicating a detrimental serum effect. Tafel extrapolation of cathodic polarization curves was utilized to evaluate the following corrosion rates: $36 \times 10^{-3} \mu\text{A}/\text{cm}^2$ in saline and 47×10^{-3}

$\mu\text{A}/\text{cm}^2$ in saline/10%-serum -- a small increase in the serum electrolyte.

Polarization resistance methods were employed to evaluate the corrosion-rate dependence on serum concentration. This method should probably be preferred over the Tafel extrapolation method since it involves very small deviations from the corrosion (open-circuit) potential, and consequently would minimize the electrophoretic mobility of serum proteins. The results are presented in Figure 2. The corrosion rate increased with increasing serum concentration, but the effect was relatively small.

For surgical stainless steel, the results of this *in vitro* corrosion study indicated that: (1) electrochemical polarization analyses produce valid results in proteinaceous electrolytes, and (2) corrosion rates increase by small amounts with increasing serum concentration.

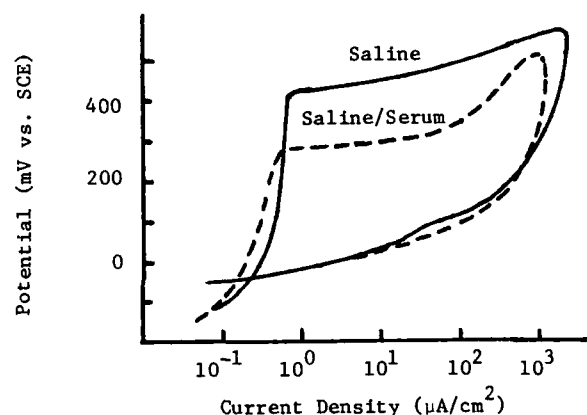


Figure 1

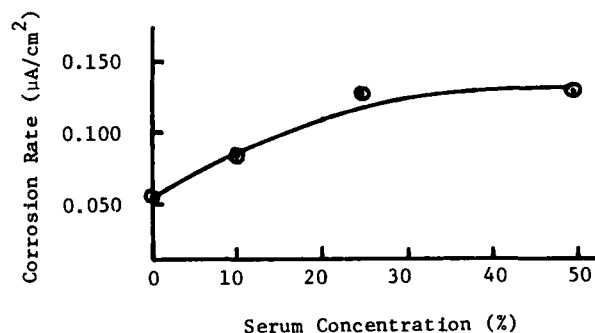


Figure 2

Department of Materials Engineering, The
University of Alabama in Birmingham, University
Station, Birmingham, Alabama 35294

CAN PERFORMANCES OF STAINLESS STEEL FOR IMPLANT APPLICATION BE IMPROVED

P. Comte, S.G. Steinemann*

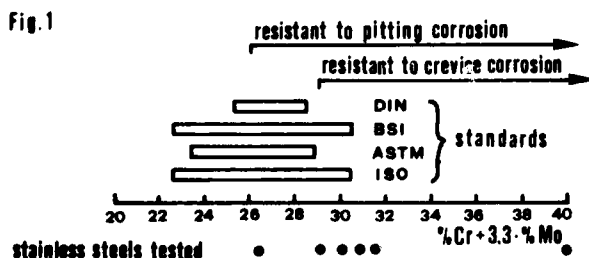
Institut Straumann AG
CH-4437 Waldenburg/Switzerland

High strength and ductility combined with its low cost and ease of fabrication have made austenitic stainless steel a widely used material for surgical implant application. Although stainless steel 316L has so far demonstrated excellent clinical record, its sensitivity to pitting and crevice corrosion is still of some concern. The present standards of steel 316L still allow ranges of composition that can lead to localized attack, e.g. crevice corrosion accompanying conditions of fretting. Since relatively new stainless steel developed for sea water applications have demonstrated a good immunity to pitting and crevice corrosion, their use as potential implant material is now considered. New criterias for pitting and crevice corrosion are given based on electrochemical polarization measurements and immersion tests.

The resistance to pitting and crevice corrosion of stainless steel is particularly important in applications where several components are assembled and where cavities and microgaps cannot be avoided. Internal fixation devices, such as bone plates and hip screws, are such examples.

The corrosion resistance of stainless steel is related to its composition, structural cleanliness and the degree cold-working. Lorenz et al. (1) suggest the use of the sum $\%Cr + 3.3 \%Mo$ as corrosion index, and the work of Crolet et al. (2) and Steinemann (3) shows how this index depends on crevice conditions, cleanliness of structure and cold-work. Based on potentiostatic and immersion tests, limits have been suggested for surgical application (4):
-remelted, cold-worked stainless steel resists pitting corrosion if $Cr+3.3 Mo \geq 26$ and crevice corrosion if $Cr+3.3 Mo \geq 29$.

On figure 1 a corrosion index scale



is represented with the position occupied by the composition limits given in the national standards.

Corrosion has kinetic and statistical aspects. Thus, the result of potentiodynamic polarization tests depends on rate, sample size, etc. Immersion tests in electrolytes imposing a redox reaction at sufficiently high potential enable to simulate more closely in-service conditions (5). A new definition for pitting and crevice attack can be found by measuring the pitting corrosion temperature and crevice corrosion temperature in electrolytes such as $FeCl_3$, $NaCl+H_2O_2$, etc.

We have performed immersion tests in 0.8 % $FeCl_3$ solutions with a redox potential of about 0.6 V SCE on different steel qualities whose corrosion index varies from 27 to 40. Finished products such as plates and screws have been used and the critical corrosion temperature for crevice corrosion established for plates mounted with screws. From these results it appears that resistance to crevice corrosion cannot be achieved within the ranges of the present standards and that the use of high Mo steels developed for sea water environments could be considered for surgical implant applications.

References

1. K.Lorenz, H.Fabritius and G.Médawar, *Mém. scient. Rev. Met.* 66, 779-93(1969)
2. J.L. Crolet, J.M. Defranoux, L.Seraphin and R. Tricot, *Mém. Scient. Rev. Met.* 71, 797-805(1974)
3. S.G.Steinemann, *Rev.Met.* 65, 651-58(1968)
4. S.G. Steinemann, In *Evaluation of Biomaterials*, ed. G.D. Winter, H.L. Leary, K. de Groot John Wiley & Sons Ltd (1980)
5. A. Garner, *Corrosion-Nace*, 37, no. 3, March (1981)

Institut Straumann AG
CH-4437 Waldenburg

*Université de Lausanne
CH-1015 Lausanne-Dorigny

EFFECT OF CARBON COATINGS ON IN VIVO RELEASE OF Cr, Co & Ni FROM F-75 ALLOY

P.H.Oppenheimer, D.M.Morris, A.M.Konowal,
C.C.Clark, & J. Black

McKay Laboratory of Orthopaedic Surgery Research
University of Pennsylvania, Phila.PA 19104

INTRODUCTION: Release of metal ions occurs to some degree in all alloys implanted in biological systems [1]. In particular Co-Cr alloys have been shown to release Cr, Co, and Ni in both humans and animals resulting in elevated concentrations of these metals in the serum, urine, and internal organs [2,3]. Little is known about the way in which the body handles the increased burden of metal ions produced as a result of implants, but much effort has been devoted to limiting release of these ions which may produce carcinogenic, mutagenic, and immunologic effects in humans and animals with long-term exposure [4].

Research in this laboratory has been centered around determining the dose response relationship between surface area/body weight ratios (SA/BW) and the elevation of metal concentration in serum and urine in rats. Wapner [5] and Koegel [6] observed a dose related peak in Cr concentration 3 days post operatively which rapidly decayed toward pre-op levels. It has been proposed that a carbon coating on the surface of a metal implant might retard the release of ions and therefore reduce the total body burden of these metals. This study is designed to observe the release of metal from such coated spheres in direct comparison with these previous studies.

METHODS AND MATERIALS: Fifty 350 g male Sprague-Dawley rats were caged in groups of 10 and allowed to acclimate for 2 weeks. 2 ml blood samples were drawn by retro-orbital stick with acid washed Pasteur pipettes 7 days preop from all animals before 2 animals weighing the least were removed from each group. Three groups of 8 received fluidized bed carbon coated F-75 microspheres, and one group received UHMW polyethylene granules of approximately the same mesh value as the bare spheres. The bare spheres had a mean diameter of 54.4 μ m and a specific area of 131 cm²/g. Implantation was at the 100X SA/BW acceleration factor (5) to the posterior hind thigh. A small incision was made exposing the muscle and a pocket was created using blunt dissection. Absorbable tag sutures were used to open the pocket while the powders were introduced from glass Pasteur pipettes. The four tag sutures were tied together and the skin was closed with silk. Blood samples drawn on days 3, 10, and 30 post-operatively were separated into clot and serum and analyzed for Cr, Co, and Ni by electrothermal atomic absorption spectrophotometry. Serum samples were analyzed for protein content by the Lowry assay [7] and metal concentrations were normalized by serum protein content. One animal from each group was sacrificed by cardiac puncture on days 10 and 30. Full autopsies and dissection of the implant site were performed.

RESULTS Serum concentrations (mean group value \pm 95% C.I.)(ng/g protein)

	Cr	Pre Op	Day 2	Day 10	Day 30
PE	9.1 \pm 3.5	15 \pm 4	13 \pm 6	7.3 \pm 18	
F-75	4.8 \pm 1.1	69 \pm 19**	35 \pm 7**	15 \pm 12	
"+.3C*	6.7 \pm 1.8	279 \pm 63**	183 \pm 35**	69 \pm 12**	
"+.5C*	7.6 \pm 2.1	166 \pm 22**	119 \pm 35**	77 \pm 37**	
"+1C*	9.2 \pm 1.5	187 \pm 38**	90 \pm 14**	39 \pm 7**	
Co					
PE	9.4 \pm 3	5.5 \pm 2	17 \pm 10	7.2 \pm 4	
F-75	7.5 \pm 2	266 \pm 69**	42 \pm 6**	19 \pm 11	
"+.3C	15 \pm 6	2326 \pm 520**	1117 \pm 276**	689 \pm 260**	
"+.5C	11 \pm 2	4890 \pm 2560**	7771 \pm 4025**	4505 \pm 1142**	
"+1C	5.9 \pm 3	916 \pm 161**	289 \pm 140**	266 \pm 32**	
Ni					
PE	85 \pm 22	203 \pm 72**	79 \pm 48	3.0 \pm 4**	
F-75	55 \pm 15	132 \pm 55**	191 \pm 82**	11.7 \pm 29	
"+.3C	81 \pm 28	154 \pm 26**	260 \pm 85**	59.2 \pm 33	
"+.5C	58 \pm 17	242 \pm 111**	190 \pm 63**	104 \pm 72	
"+1C	54 \pm 17	139 \pm 56**	128 \pm 98	38.7 \pm 44	

*Nominal coating thickness (μ m)

**Significant Difference from pre-op (p<0.05)

DISCUSSION: The results of this experiment suggest two major conclusions: serum Cr and Co levels at 100X exposure for bare F-75 are in agreement with two previous studies [5],[6]; and carbon-coated F-75 significantly raises the serum levels of Cr and Co above PE and bare F-75 control levels. The F-75 Cr and Co levels correlate well with Wapner's and Koegel's data for 10X, 30X, 100X, and 300X exposure, while the Ni data show peaks and fluctuations not present in Koegel's data. The coated F-75 groups produced Cr and Co levels significantly (p<.05) greater than bare F-75 throughout and they remained significantly elevated above pre-op levels at day 30. At day 30 bare F-75 serum Cr and Co were not significantly different from pre-op. It is probable that carbon coating produced alloy segregation and may have induced crevice corrosion due to coating.

This work was supported by NIH Grant AM25272 and a grant in aid from Johnson & Johnson Products.

REFERENCES:

- [1] Ferguson, A. et al., JBJS 42A:77, 1960.
- [2] Coleman, R.F. et al., Brit. Med. J., 1:527, 1973.
- [3] Dobbs, H.S., et al., Biomaterials 1:193, 1980.
- [4] IARC Monograph on the Evolution of Carcinogenic Risk of Chemicals to Man, Vol. 23, WHO 1980.
- [5] Wapner, K.L. et al., Trans ORS, 8:240, 1983.
- [6] Koegel, A. et al., Trans SFB; 6:44, 1983.
- [7] Lowry, O.H. et al., Bioch. Biophys. Acta. 63:403, 1962

University of Pennsylvania
Department of Orthopaedic Surgery
424 Medical Education Building
Philadelphia, PA 19104

IMMUNOLOGICAL TOLERANCE AFTER ORAL ADMINISTRATION OF NICKEL AND CHROMIUM

K.J.J.Vreeburg*, K.de Groot*, M.von Blomberg**, R.J.Scheper**

Dept.Biomaterials, Free University, De Boelelaan 1115, 1081 HV Amsterdam, The Netherlands

The induction of delayed hypersensitivity to nickel, chromium and other metals through skin contact is well known. In dental literature it has been suggested that contact sensitivity can be induced through the oral cavity.

However only few cases have been described. In immunologic literature suppression of immune reactivity after oral exposure with non-metallic sensitizing agents has been described.

In our experiments we exposed guinea pigs to both nickel and chromium orally. In a first experiment with a cast occlusal Ni-Cr splint fixed to the upper jaw for a period of 1 month. In a second experiment we fed guinea pigs different amounts of nickel and chromium powder during six weeks. A subsequent attempt to immunize both groups of pretreated guinea pigs failed in most animals whereas non pretreated guinea pigs became clearly hypersensitive. (Fig. 1 and 2).

These results show that oral administration of nickel and chromium induces a state of (partial) tolerance to both metals.

Tolerance as shown in our experiments could contribute to the low incidence of allergologic problems in orthodontic and prosthodontic dentistry. From patient studies we obtained evidence, suggesting that the incidence of hypersensitivity among individuals who in the past underwent orthodontic treatment, is smaller than in other individuals. Our present experiment suggests that non-presentation individuals may become tolerant to metal sensitizers as a result of presenting metals through the oral cavity. The use of such a preventive protocol in individuals at high risk deserves further attention.

This research is partially funded by Prevention Funds, Netherlands.

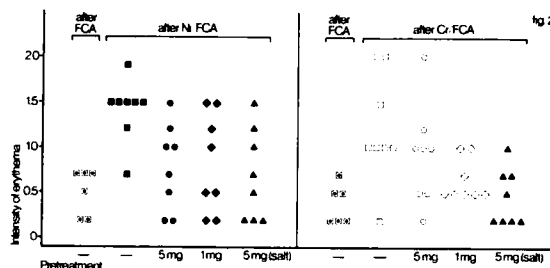


Fig. 2. 24 hours skin reactivity to nickel and chromium as measured by epicutaneous testing after immunization with FCA either or not containing Ni-Cr. Guinea pigs had been pretreated by feeding Ni-Cr in metallic or salt form, or normal food as indicated in the figure. Each point represents one animal. Comparison of pretreated groups with positive controls (Wilcoxon): nickel p 0.01, chromium 0.05 p

1. Blanco-Dalman, L.: The nickel problem. J.Prosth.Dent. 1982, 48: 99-101.
2. Mowat, A., McI., Strobel, S., Drummond, H.E. and Ferguson, A.: Immunological responses to fed protein antigens in mice. I Reversal of tolerance to ovalbumin by cyclophosphamide. Immunology Vol.nr. 45: 105-113, 1982.
3. Parker, D. and Turk, J.L.: Delay in the development of the allergic response to metals following intratracheal installation. Int.Archs Allergy appl.Immun. Vol. nr. 57: 289-293, 1978.

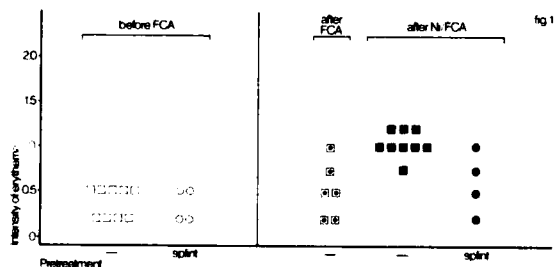


Fig. 1. 24 hours skin reactivity to nickel as measured by intradermal testing before (left part) and after (right part) immunization with FCA either or not containing NiSO₄. Former splint wearing guinea pigs: circles, non-pretreated control groups: squares. Each point represents one animal.

THE DIRECT CURRENT ELECTRICAL STIMULATION OF SURGICAL REPAIRS OF THE
RABBIT ACHILLES TENDON

M. Zimmerman, J.R. Parsons, T. Poandl, H. Alexander and A.B. Weiss

Section of Orthopaedic Surgery, UMDNJ-New Jersey Medical School,
100 Bergen Street, Newark, NJ 07103.

INTRODUCTION - Researchers have investigated the possibility of enhancing soft tissue repair, using electrical stimulation systems^{1,2}. Electrical stimulation of soft tissue could be useful in treating a number of serious medical problems, including repair of damaged tendons and ligaments.

In our laboratories, carbon fiber and carbon fiber composites have been used successfully to repair large soft tissue defects in tendons and ligaments in a variety of animal models^{3,4}. In this capacity, carbon fiber initially secures the repair and later acts as a scaffold for regrowth of new collagenous tissue.

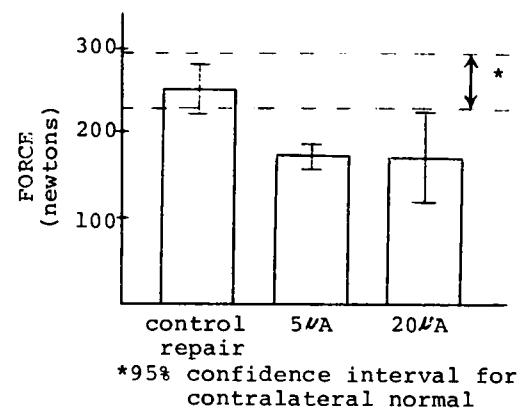
In a preliminary study, we demonstrated that carbon fiber could also be used as an electrode to stimulate bone growth in a rabbit medullary canal model⁵. In addition to stimulation of bone, we observed a significant stimulation of fibrous tissue within the canal. Given this observation, we wished to investigate the possibility of enhancing tendon and ligament repair using carbon fiber not only as a repair medium, but also as an electrode.

MATERIALS AND METHODS - The central third of the right Achilles tendon of 12 male, white, New Zealand rabbits was excised. The deficit was spanned by a bundle of 10 carbon fibers woven into the tendon remnants distally and proximally. In 4 animals, this repair served as a control repair. In the remaining animals, fully implantable battery packs supplied a constant cathodic current to the carbon fiber utilized in the repair. A stainless steel anode, distant from the repair, completed the circuit. In 4 animals, the packs supplied a constant current of 5 A. In 4 animals, the packs supplied 20 A.

After 3 weeks, the animals were sacrificed. The repaired and contralateral normal Achilles tendons and gastrocnemius muscles and their respective bony attachments were resected. The muscle/tendon units were mechanically tested to failure in tension in a hydraulically actuated mechanical test machine (MTS) at an extension rate of 0.025 M/S. Mean failure strengths and 95% confidence intervals for the different experimental groups and contralateral normals were calculated.

RESULTS - A comparison of normal contralateral control tendons and control carbon fiber repairs demonstrated that the repaired tendons were approaching the full strength. This supports the earlier findings of Aragona et al³. Tendon repairs receiving electrical stimulation were significantly weaker than the non-stimulated control carbon fiber repair (Student's t-test, p 0.05). All values are displayed graphically in Figure 1.

FIGURE 1



DISCUSSION - Repairs receiving 5 A and 20 A of constant direct current were statistically weaker than non-stimulated control repairs. Ricci et al⁶ recently reported on in-vitro tissue culture of mammalian tendon fibroblasts on carbon fiber electrically stimulated with direct currents of 1 A and 5 A. In these experiments, no stimulation occurred on cathodic fibers as measured by cell migration and mitosis. Depression of mitosis occurred on anodic fibers. This work would support a finding of no enhancement of repair but cannot explain the negative effects we observed. Grossly, the tissue about control carbon fiber and stimulated fiber appeared similar. It is reasonable to assume that the added trauma of battery-pack implantation may have resulted in delayed healing of the stimulated repairs.

Histologic evaluation of stimulated repairs in additional rabbits is now underway in our laboratory and may provide information regarding these preliminary observations.

REFERENCES

1. Frank, C et al: 1st Ann. Brags, 24, 1981.
2. Konikoff, J: Annals of Biomed. Eng., 4:1-5, 1976.
3. Aragona, J et al: Clin. Orthop. Rel. Res., 160:268-278, 1981.
4. Aragona, J et al: Am. J. Sports Med., 11:228-233, 1983.
5. Zimmerman, M et al: 8th Mtg. Biomaterials, 31, 1982.
6. Ricci, J et al: 3rd Ann. Brags, 1983. Section of Orthopaedic Surgery, UMDNJ-New Jersey Medical School, 100 Bergen Street, Newark, New Jersey 07103

TREATMENT OF CONGENITAL AND ACQUIRED PSEUDOARTHROSIS WITH ELECTROMAGNETIC FIELDS. APPEARANCE OF STRONG PERIOSTEAL BONE CALLUS.

Cadossi R., Fontanesi G., Gianceschi F., Rotini R., Dal Monte A., Poli G.

University of Modena
Modena, Italy

The main techniques to electrically stimulate the osteogenesis are: (I) the use of low intensity electrical currents with electrodes inserted in the non-union site and (II) the use of low energy Low Frequency Pulsing Electromagnetic Fields (LFPEF) generated outside the organism. Recently Luben and coworkers (1982) showed that the cellular response to low energy LFPEF is obtained through some specific effect at the membrane level; Emilia and coworkers (1983) demonstrated that at least one of the effects of the signal we employ is on the closed calcium channels of the cellular membrane, the signal promotes Ca^{++} influx into the cell and cell activation. This study, performed in Italy during the last 5 years in a cooperative clinical trial in 8 orthopaedic departments, shows that the pseudoarthrosis healing is accompanied by the appearance of a strong periosteal bone callus. This particular effect was never obtained by other authors (Bassett, 1977; Sharrard, 1982) using analogous non-invasive techniques, but different signals, so suggesting that signals employed may act on different biological targets.

105 patients suffering from acquired pseudoarthrosis and 7 from congenital pseudoarthrosis (6 of the tibia and 1 of the ulna) were treated.

The unit (Biostim-Igea) that we utilized has the following characteristics: (1) powered by 220V mains current; (2) output: single rectangular pulse with rising edge 400 usec. (in operative conditions), selected frequency 75Hz, impulse width 1.3msec. and voltage presettable between 160 and 220V. The generated single pulses supply a couple of Helmholtz coils made by 1400 turns of copper wire (0.25 mm \varnothing). The electrical resistance of each coil is 300 Ohm. The voltage supplying the Helmholtz coils is established each time to obtain an induced voltage between 3 and 5mV in an Helmholtz coil probe made of 50 turns (0.5 cm i.d.) of copper wire (0.20 mm \varnothing). The Fourier serie of the signal induced in the probe shows that the low frequencies are mainly represented.

All the 7 congenital pseudoarthrosis were treated with a double approach: endomedullary nail fixation of the pseudoarthrosis site followed by stimulation with LFPEF. In 6 cases (5 congenital pseudoarthrosis of the tibia and 1 of the ulna) radiological image of bone union was observed. All cases were treated for 12 months, 12 hours/day and controlled after the end of the treatment every 6 months. No delayed bone resorption was observed. The imbalance of the leg length did not increase after the start of the treatment. It is important to underline that all the patients were very young, aged less than 7.

89 out of 105 patients suffering from acquired pseudoarthrosis healed. The patients performed the treatment at home for 10-12 hours every day until consolidation was obtained. The average stimulation time was 5 months. 3 patients who reached the consolidation after more than 12 months stimulation were considered unsuccessful treatments. As 12 months in our protocol was considered the end time for a successful treatment. In the vast majority of cases (74%) we observed the appearance of a strong periosteal bone callus which linked the pseudoarthrosis stumps: this is the first time that the activation of the periosteum is described with non invasive techniques. Only the cases subjected to autologous bone graft because of large bone loss (15 cases), did not show a periosteal reaction, as expected on the basis of serious damage of the periosteum. Our experience allows us to identify the most significant period leading to consolidation during the first 45-60 days of stimulation: just at the end of this period we observe fracture stumps "sclerolysis" accompanied by periosteum activation which will promote the consolidation. We suggest that the LFPEF possibly trigger a mechanism which previously failed to start; once the healing process starts the stimulation does not appear to be so significant in hastening the healing process. However in all the cases the treatment was maintained until we were certain that the consolidation had been achieved. No stress fracture or delayed bone resorption was observed. The treatment appears useful, safe and economical as regards the cost of a hospital stay or of a surgical procedure. No side effects were detected during the treatment.

It is worthwhile emphasizing that a successful treatment is strictly bound to a correct conventional orthopaedic procedure.

The observations concerning the appearance of periosteal bone callus encouraged us to test the efficacy of our signal in the treatment of a fresh fracture through a double blind trial: the initial results seem to confirm the possibility of shortening the disability time.

Supported by: National Council for Research

Cadossi R., Center for Experimental Haematology,
Policlinico, Via del Pozzo 71,
41100 Modena, Italy

* Arcispedale S. Maria Nuova, Reggio Emilia
Department of Orthopaedic Surgery

* Istituti Ortopedici Rizzoli, Bologna
Department of Infantile Orthopaedics
and Traumatology.

THE ROLE OF CATHODIC POTENTIAL IN ELECTRICALLY INDUCED OSTEOGENESIS

Furst, L., Farrington, G. C., Davidovitch, Z., and Korostoff, E.

University of Pennsylvania
Philadelphia, Pennsylvania

Electrically induced osteogenesis has found clinical application in a variety of areas (1): healing of non-unions, arresting osteoporosis, and remodeling of the dental alveolar ridge. Yet only the sketchiest information is known about the mechanism of stimulation. The purpose of this work is to establish whether electrically induced osteogenesis is current or potential dependent.

This experiment measured the response of osteoblasts of the feline alveolar ridge to a range of constant currents over a range of cathodic potentials. The latter were achieved by using three different cathode materials: platinum, stainless steel, and mercury amalgamated on gold. Each of these have distinctively separate hydrogen overpotentials in the in vivo system. Constant currents of 1, 5, 20, and 50 micro amperes (μ a) were obtained using a potentiostat/galvanostat for short stimulation periods of 15 minutes (2). The degree of stimulation was measured by differences in the level of adenosine 3'-5' monophosphate (cAMP) in osteoblasts. These differences were marked by the intensity of immunohistochemical staining (2), in the osteoblasts as measured with a Zeiss microscope/photometer.

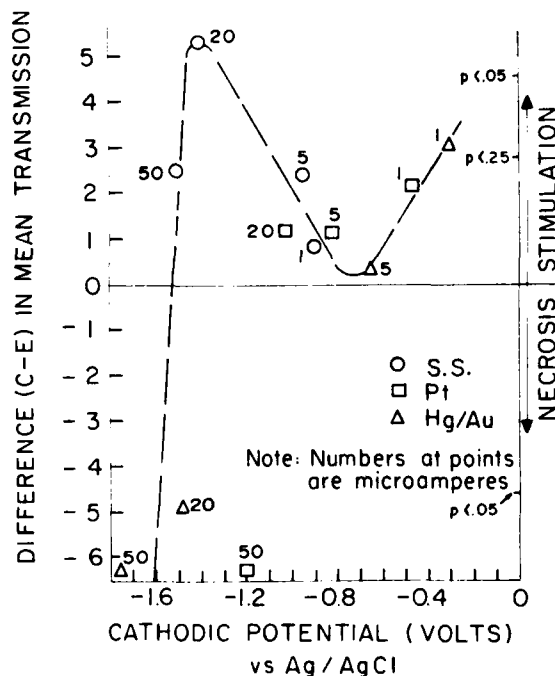
The young adult female cat was selected for experiment on the basis of its use in prior studies (2), in which it had been shown that remodeling of the underlying alveolar bone takes place when the stimulating electrodes are placed topically on the gingiva. Thirty six, one year old female domestic cats were divided into four levels of electric current of three cats each, repeated for each of the three cathode materials. The appliances consisted of single stranded pure gold anodes (24g) and cathodes, which were adapted for each cat to the tissue around the maxillary canine. The electrodes were insulated, except at the gingival surface, and were bonded to the canine. They were connected to the potentiostat with shielded cables.

One maxillary canine served as control (no current) and its opposite was the experimental (with current). The cathodic potential was continuously recorded during the 15 minute stimulation, after which the cat was decapitated with immediate freezing in liquid nitrogen. Sectioning, staining, and quantitation of staining were as previously described (2). The data were examined by analysis of variance with repeated measures, and a computer program (BMDP.2V).

A summary of the results is given in Figure 1. It is evident from this figure that electrical stimulation of the osteoblasts is strongly potential dependent and shows significant peaks at -1.4 volt and at

>-0.3 volt. The figure also provides clear evidence that electrical stimulation is not dependent on current level, e.g., at the level of 20 microamperes we find all of the following: significant ($p < 0.05$) stimulation with stainless steel; no significant ($p > 0.05$) stimulation with platinum; and significant ($p < 0.05$) necrosis with Hg/Au. While Pt at 50 microamperes shows significant ($p < 0.05$) necrosis at only -1.2 volt, it is above the H-overvoltage and results in a large evolution of hydrogen gas.

The results of this research support the hypothesis that electrically induced osteogenesis is potential-dependent (3). This might then suggest that stimulation of osteoblasts occur via charge transfer or an electron exchange in electroactive couples.



(1) Spadaro, J.A., Clin. Ortho. Rel. Res. 122:325, 1977. (2) Davidovitch, Z., et al, J. Dent. Res. (Submitted). (3) Similar conclusion suggested from uncontrolled data by Baranowsky, T. and Black, J., Trans. 29th Ann. ORS Mtg., March, 1983, p. 352.

THIS WORK SUPPORTED BY NSF GRANT NO. PFR-8006137 AND PARTLY BY NIH GRANT DE-05412. Address replies to Dr. Laura Furst (c/o Dr. E. Korostoff), University of Pennsylvania 3231 Walnut Street, Philadelphia, PA 19104.

*Presently at Ohio State University

G. W. Ciegler and S. I. Stupp

Bioengineering Program and Polymer Group, College of Engineering,
University of Illinois at Urbana-Champaign, Urbana, IL 61801

INTRODUCTION

Our research is aimed at the development of biodegradable and osteoinductive bone adhesives or coatings for *in situ* surgical placement on endoprostheses. Such biodegradable templates for bone growth could accelerate or improve the quality of device fixation; they could also replace in some cases the need for conventional fracture stabilization implants. An aspect of interest in this work is the possibility of accelerating bone growth through electrostatic potentials at interfaces within the microstructure of biodegradable composite materials. Experimental composites were formulated in our laboratories using glycogen as a biopolymeric matrix and pulverized calcium phosphate (TCP) as the reinforcing phase ($\text{Ca}_{10}(\text{PO}_4)_6\text{OH}_2$). TCP particles were the carriers of electrical activity, induced by electric fields in the form of surface polarization.

EXPERIMENTAL

The experimental implants are pliable materials produced by gelation of the glycogen matrix in a slightly basic aqueous solution (pH=8.5-9.0). Polarization of TCP particles is induced in oxygen-free atmospheres under field intensities in the order of $10,000 \text{ Vcm}^{-1}$ at 200°C . *In vivo* testing of the composite implants was carried out with white laboratory rats. The proximal end of the femur was exposed via an incision after shaving the surgical site. A dental drill was then used to bore a 1 mm-diameter cavity into the lateral side of the femur just distal to the greater trochanter. Prior to implantation, the composite is mixed with distilled water to form the final gel and then packed into the cavity. The animals were serially sacrificed over an 8-week span and the excised femurs were prepared for scanning electron or light microscopy. Sections for electron microscopy were freeze dried, while optical microscopy sections were fixed, decalcified, sectioned and stained with H&E.

RESULTS AND DISCUSSION

Scanning Electron Microscopy (SEM) of retrieved specimens reveal a honeycomb-like network as a predominant feature in the 3-week electro-active implant. Control implants, on the other hand, still remain relatively solid after this period of time (figures 1a and 1b). After 4 weeks, Energy Dispersive Analysis with X-rays (EDAX) shows a significant increase in the amount of S, P, and Cl (relative to a fixed number of Ca counts) for electro-active implants (see Table).

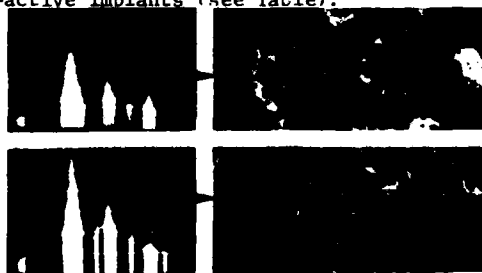


Fig. 1. SEM micrographs of retrieved implants (3 weeks) and their corresponding EDAX spectra.

TABLE
ELEMENTAL COUNTS FROM THE RETRIEVED IMPLANT
RELATIVE TO 58 COUNTS OF CALCIUM

Implant	Phosphorous Counts	Sulfur Counts	Chlorine Counts
Control (3 weeks)	149	8	69
Electro-active (3 weeks)	175	30	86
Control (4 weeks)	130	8	74
Electro-active (4 weeks)	210	42	105

The data can be interpreted as an enhanced biodegradation rate and greater cellular activity in electro-active implants. Sulfur peaks are indicative of collagen fiber infiltration and, in fact, 4-week electro-active implants appear quite fibrous in SEM micrographs.

A second series of surgeries was performed for optical microscopy evaluation. Stained sections reveal the presence of macrophages and multinucleated giant cells in the vicinity of the implant. This is observed in all sections up to the third week. It is clear that implant removal is occurring after 2 weeks as evidenced by the presence of TCP particles within macrophages. Fibroblastic activity is seen shortly after macrophage infiltration. The electro-active implants apparently lead to an increased density of freshly laid down matrix within the implant's cavity. Prior to the fourth week, sections from electro-active implants show higher levels of basophilic staining of osteoblasts relative to controls. This observation suggests a more intense cellular activity.

Our current model for the electro-active composite is a microstructure in which space charges on TCP particles are neutralized by adsorbed glycogen and electrolytes. As glycogen degrades, finite and short-lived zeta potentials appear. The implant can then become an electro-active sponge as a result of streaming potentials when the limb is used. Our observations of enhanced cellular activity could therefore involve implant-induced bio-electric phenomena.

The authors acknowledge the Center for Electron Microscopy at UIUC and M. R. Simon of Veterinary Biosciences for surgical advice and facilities.

COMPATIBILITY OF VARIOUS PARTIAL DENTURE MATERIALS WITH
GINGIVAL TISSUES .

Y.M.Shaker*, S.I.Ibrahim**, N.A.Abbas**

Biochemistry Laboratory , National Research Centre , Dokki ,
Cairo , Egypt.

Metallic and non-metallic denture base materials are used in partial denture construction. Many clinicians prefer metallic denture base over non-metallic, since the metallic denture base materials possess a higher thermal conductivity, more rigid, highly polished and fit more accurately than acrylic resin.

Some authors concluded that the periodontium is traumatized following partial denture use. The tissue responses for partial denture vary according to its type. Among tissue changes described are gingival inflammation, retraction of gingival margin and mobility of the abutment teeth which may be the end result of inflammatory reaction of traumatic origin. The pressure or trauma over the soft tissues from partial denture causes expulsion of tissue fluid. This fluid is derived from the intracellular sources in the inflamed tissue and from disintegrating shed cells in the pocket area. An increase in the tissue fluid occurs when mechanical stimulation is applied externally to the pocket. The amount of fluid flow increases also with the severity of the inflammation.

In a previous study Bayers et al.(1975) applied the protein immunoelectrophoresis technique in the analysis of gingival fluid and found a marked increase in the levels of IgG, IgA and IgM in inflamed gingival tissues as compared to that of the levels present in healthy gingivae . Thus this method can be used to reveal the compatibility of various partial denture materials with gingival tissues. The purpose of the present study is to determine the amount of gingival inflammation in relation to various partial denture materials by means of protein immunoelectrophoresis technique.

Twenty patient were selected to be including in this study, their ages ranged between 20-42 years. All patients needed bounded partial denture appliances. The patients were grouped into three groups according to the material used, each group was composed of five patients. In the first group gold was used, in the second group cobalt chrome was used , in the third group acrylic resin was used, while the remaining five patients were left without construction of partial denture to serve as controls. The gingival exudate samples were collected after one year from fitting the appliances to ensure the settlement of all reactions. Glass capillary tubes of 0.02 ml capacity and 8 cm long were selected for collection. Only the clear fluid was considered. The samples

were stored at - 20°C until analysis. Protein fractions of the gingival exudate were separated by agar-gel immunoelectrophoresis, polyvalent antihuman serum (horse antibodies against human proteins) was used.

Our findings showed that both albumin and IgG fractions were the prevalent components which demonstrated in most cases of the different groups. These findings are supported by previous studies which suggested that the presence of albumin in gingival exudate is due to its high concentration in serum, besides its high speed of migration in comparison to the other protein fractions. The appearance of IgG in the gingival fluid is attributed to two factors, the first is its high concentration in serum, the second is its local secretion in the gingival tissues.

Our results showed close protein immunoelectrophoresis patterns of the gingival exudate between the gold and cobalt-chrome groups , detecting in most cases albumin and IgG arcs . On the other hand most cases of the acrylic group showed more dense arcs of albumin and IgG besides the appearance of other protein fractions namely transferrin, α_2 , B lipoproteins.

These results indicated that the use of metal partial dentures caused less inflammation of the gingival tissues than the acrylic one, and hence the use of the metal partial dentures is recommended not only for that reason but also for the previously mentioned advantages.

* Biochemistry Laboratory, National Research Centre, Dokki, Cairo, Egypt.

** Prosthetic Dentistry Department, Faculty of Oral & Dental Medicine, Cairo University, Cairo , Egypt.

ENERGY-ABSORBING, HYDROPHOBIC DENTAL CEMENTS
BASED ON DIMER AND TRIMER ACIDS

J. M. Antonucci, S. Venz*, D. J. Dudderar,
M. C. Pham and J. W. Stansbury

National Bureau of Standards, Polymer Science and Standards Division,
Building 224, Room A143, Washington, DC 20234.

In spite of their relatively poor durability, dental cements are extensively used in a variety of dental applications. Cements in current use lack toughness (i.e., they have a propensity to brittle failure) and hydrolytic stability (i.e., they exhibit excessive erosion in the oral environment). In addition, most cements lack adequate adhesive qualities, especially to tooth structure. Noteworthy exceptions are the polycarboxylate type cements, formed by the reaction of concentrated aqueous solutions of poly(alkenoic acids), e.g., 40% poly(acrylic acid), with basic inorganic powders, e.g., zinc oxide, which are adhesive to enamel, dentin and stainless steel (1,2). These cements have highly carboxylated binders that are stiff hydrogels (i.e., rigid and hydrophilic matrices) formed primarily by ionic crosslinking reactions.

The aim of this study was to examine the feasibility of forming cements having polymeric matrices that are less carboxylated and much less rigid and hydrophilic by acid-base, chain extension reactions of dimer (DA) or trimer (TA) acids with a variety of basic powders. DA and TA are moderately viscous liquid polyacids with a unique chemical structure consisting of a bulky, flexible, hydrophobic hydrocarbon core which terminates in 2 or 3 COOH groups, respectively. Using fusion or metathesis, Cowan and Teeter prepared several divalent metal dimerates which exhibited polymeric properties (3). Because of their dual salt-like and polymeric nature, such metal dicarboxylates have been termed halatopolymers (4). The feature which distinguishes divalent metal dicarboxylates from other ionic polymers is the presence of ionic metal bonds in the polymer backbone.

The reactivity of DA or TA with metal oxides, hydroxides or other basic reactants is dependent on a number of factors: the inherent basicity of the reactant, its state of subdivision and its degree of surface activation. Calcium hydroxide, Ca(OH)_2 , is more reactive than calcium oxide, CaO , as is micronized zinc oxide (ZnO) compared to the usual reagent grade oxide. Sluggishly reactive metal oxides can be activated by treatment with diluents containing small amounts of carboxylic acids, e.g., propionic acids (5), or by admixture with more reactive bases, e.g., Ca(OH)_2 . For example, DA mixed with micronized or activated ZnO in a powder/liquid ratio (P/L) of 7 set to a tough, hydrophobic cement in 7 minutes at 37°C. Specimens had the following properties after 24 hours: compressive

strength (CS) = 50 MPa, diametral tensile strength (DTS) = 7 MPa, water solubility (WS) = 0.1%, and solubility in aqueous lactic acid (pH = 4) of 0.2%. DA and Ca(OH)_2 , P/L = 1.5, yielded a nonbrittle cement having a setting time of 3 min., CS = 25 MPa, DTS = 4 MPa and WS = 1.5%. Under compressive stress (crosshead speed = 1 mm/min.) specimens of this cement resisted fracture but showed marked deformation. The addition of reinforcing fillers such as tricalcium phosphate, aluminum oxide, titanium oxide, and polymers enhanced both the mechanical properties and dimensional stability of the DA- Ca(OH)_2 cement while reducing its WS and maintaining its resistance to brittle fracture.

Stronger but more brittle cements resulted from DA and MgO , P/L = 1, CS = 34 MPa, DTS = 4 MPa; for P/L = 2, CS = 50 MPa, DTS = 4 MPa. With equal parts of Ca(OH)_2 , MgO and tricalcium phosphate in the powder component, DA gave a nonbrittle cement (P/L = 2, CS = 41 MPa, DTS = 6 MPa). With the same powder, TA yielded a somewhat stronger cement (P/L = 2, CS = 48 MPa, DTS = 6 MPa). DA with 1 part MgO and 2 parts titanium oxide yielded a tough cement (P/L = 3, CS = 57 MPa, DTS = 5 MPa). A similar TA cement again was somewhat stronger, (CS = 60 MPa).

DA and TA cements do not inhibit the polymerization of resin-based dental materials and may be used to formulate hybrid composite-cements. Their relatively low COOH content coupled with their bulky nature should yield low-shrinking, biocompatible cements. The versatile nature of these new types of polycarboxylate cements suggests many potential dental applications.

REFERENCES

1. Smith, D.C.: Brit Dent J 125:381, (1968).
2. Phillips, R.W.; Swartz, M.L.; and Rhodes, G.: J Am Dent Assoc 81:1353, (1970).
3. Cowan, J.D. and Teeter, H.M.: Ind Eng Chem 36:148, (1944).
4. Economy, J.; Mason, J.H.; and Wohrer, L.C.: J Polym Sci A18:2231, (1970).
5. Dougherty, E.M.: U.S. Patent 3,509,089, (1970).

This study was supported by NIDR/NBS Interagency Agreement Y01-DE-30001.

National Bureau of Standards, Polymer Science and Standards Division, Building 224, Room A143, Washington, DC 20234.

*Klinik fuer Zahn-Mund und Kieferheilkunde, Freie Universitaet Berlin, Assmannshausen Str. 4-6, D 1000 Berlin 33, West Germany.

AD-A175 162

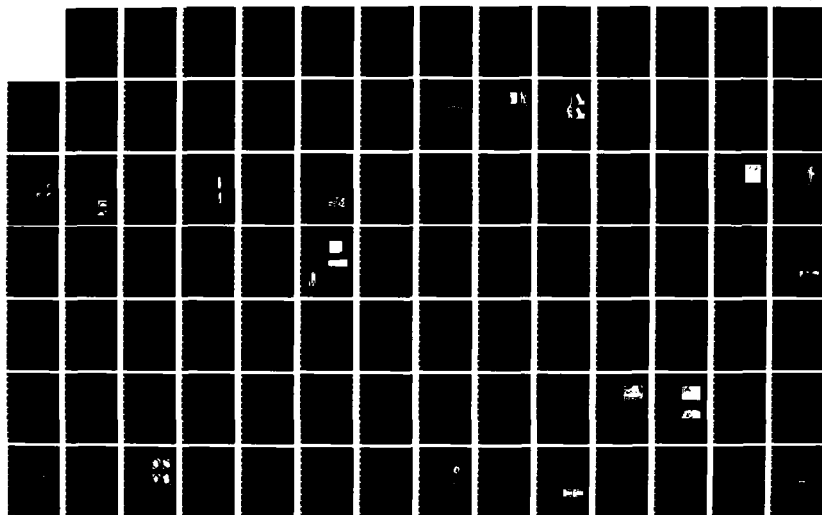
BIOMATERIALS '84 TRANSACTIONS WORLD CONGRESS ON
BIOMATERIALS (2ND) ANNUAL (U) SOCIETY FOR BIOMATERIALS
SAN ANTONIO TX S F HULBERT ET AL JUN 84
DAMD17-84-G-4005

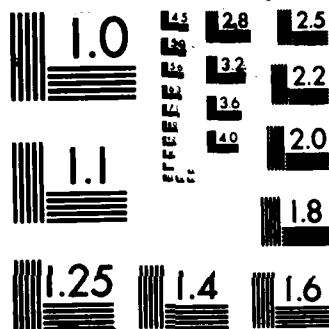
3/5

UNCLASSIFIED

F/G 6/12

ML





XERO COPY RESOLUTION TEST CHART

Correlation Between Hardness and Degree of Conversion During the Setting Reaction of Unfilled Restorative Resins

Jack L. Ferracane

Baylor College of Dentistry Dallas, Texas

The physical and mechanical properties of most polymeric materials are dependent upon the extent of the reaction which converts monomer to polymer. This premise has led to the use of mechanical properties tests, such as hardness¹⁻³, transverse¹ and tensile strength³⁻⁴, as indirect methods for determining the degree of conversion in dental restorative resins. However, the correlation between properties and the conversion reaction becomes somewhat clouded when considering the cross-linked, network-forming polymers used in these dental resins. The properties of these systems are very likely dependent upon the quality of the network formed, as well as the concentration of residual unreacted species.

The purpose of this study was to determine the nature of the correlation between the degree of conversion and the micro-hardness of unfilled dental restorative resins. An attempt was also made to compare the time frames between conversion and the acquisition of maximum hardness in these quick-setting resins. Hardness testing was chosen since it has been most often used as the indirect method for degree of conversion determination.

Three commercially available, chemically-cured Bis-GMA-based resins were used in this study. They were: Delton Pit and Fissure Sealant (Johnson and Johnson), Profile bonding agent (S.S. White-Penwalt) and Concise Enamel Bond (3M). These unfilled resins were chosen on the basis of differences in monomer compositions⁵ and viscosities. This was expected to produce polymers with varying degrees of conversion, as has been previously reported⁴.

The degree of conversion was analyzed with a Fourier Transform Infrared (FTIR) spectrometer in a transmission mode. The carbon-carbon double bond peak at 1640 cm⁻¹ was monitored in reference to the peak at 1610 cm⁻¹ which corresponds to the aromatic ring in the Bis-GMA monomer, using a baseline technique. The conversion during the first 1.5 through 30 minutes was obtained by curing the resins between IR transparent AgCl windows in the path of the IR radiation. The temperature started at 34°C and rose to 40°C by the end of the 30 minutes. The conversion between 30 minutes and 24 hours was determined by transmitting the IR through thin resin films (20-40 micrometers) which had been cured between glass slides at 37°C.

Knoop hardness (KHN) was determined for the resins after curing between 5 minutes and 24 hours at 37°C in steel disk molds (6mm x 3mm). The testing was performed under a 100 gram load.

Early determinations of conversion showed that clinical setting (approximately 1.25-1.5 minutes) was achieved when fewer than 40% of the available reactive groups had converted. This is consistent with views of polymer gelation and a previous study⁶. After 5 minutes, approximately 80% of the maximum conversion had taken place, yet the resins had attained only 36-53% of their 24 hour hardness values (see Table). After 6 hours at 37°C, hardness and conversion were essentially maximized. No further changes were noted with additional curing

beyond 24 hours, as has been shown for light-cured composites².

There was a significant (p=.05) correlation between hardness and degree of conversion for each resin with respect to time. However, a specific hardness value could not be directly correlated to a specific degree of conversion. For example, Delton had a KHN of 9.8 at 62% conversion, while Profile had a hardness of 18.9 at the same conversion, but at a much later time.

The degree of conversion for Delton and Concise were equivalent (77%) at 24 hours. Profile, however, had a significantly lower conversion (62%). This can be explained by the differences in composition between the resins. Profile contains a higher concentration of Bis-GMA⁵, thereby making it more viscous and reducing the conversion.

The hardness of the three resins was essentially equivalent at 24 hours, despite the fact that the degree of conversion for Profile was lower. This suggests that the ultimate hardness of these cross-linked systems is very much dependent upon the quality of the network which forms during the setting reaction, rather than solely upon the degree of conversion. Such indirect tests may be valid for determining the relative degree of cure for a given resin at different time periods or under variable conditions. However, it does not appear to be valid to relate degree of cure between different materials by such tests. Since the degree of conversion may also have an effect on dimensional stability, color change and other properties, the use of hardness tests to indirectly determine degree of cure in dental restorative resins appears to be somewhat limited.

TIME	DELTON		PROFILE		CONCISE	
	DC*	KHN**	DC	KHN	DC	KHN
5m	62%	9.8	45%	8.1	57%	6.4
10m	67	10.0	47	9.4	61	7.6
20m	68	10.9	49	10.6	63	9.1
30m	69	12.0	53	11.2	64	9.7
60m	70	13.3	56	13.1	68	11.2
120m	71	14.9	57	15.3	70	12.7
6h	75	19.0	59	18.2	72	17.5
24h	77	18.6	62	18.9	77	17.6

*S.D.=2% or less (n=3) **S.D.=10% or less (n=5)

1. Tirtha, R.; Fan, P.L.; Dennison, J.B. and Powers, J.M., J Dent Res, 61(10):1184-1187, 1982.
2. Leung, R.L.; Fan, P.L. and Johnston, W.M., J Dent Res, 62(3):363-365, 1983.
3. Asmussen, E., Scand. J Dent Res, 90:484-489, 1982.
4. Ferracane, J.L.; Newman, S. and Greener, E.H., J Dent Res, 61:271, No. 832, 1982.
5. Ruyter, I.E. and Sjøvik, I.J., Acta Odontol Scand, 39:133-146, 1981.
6. Cook, W.D. and Standish, P.M., JBMR, 17(2): 275-282, 1983.

Acknowledgements

The author would like to thank Analect Instruments of Irvine, CA for the use of the FX6250 FTIR spectrometer for this study.
BCD Dental Materials Science, 3302 Gaston, Dallas, TX

Environmentally Stable Light-Cured Dental Restorative Composite

I.L. Kamel and G.L. Schwartz

Dept. of Materials Eng. and the Biomed. Eng. and Sci. Inst., Drexel University, Philadelphia, PA 19104

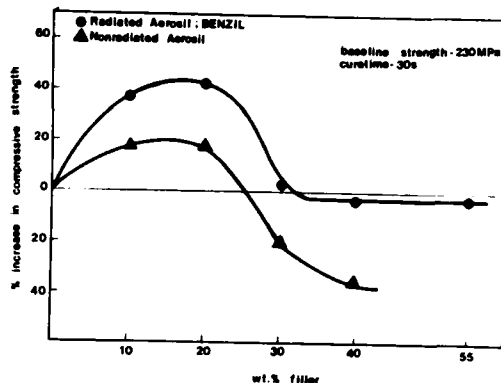
Several different variables can affect the performance of a light-cured dental restorative composite. These variables include the chemical nature of the polymeric matrix, the initiation mechanism, the size, shape and loading of the hard filler, and most importantly the interfacial bond between the filler and matrix. Generally, it is the weak interface which is usually credited with the deterioration of the composite in vivo. The combination of high mastication stresses and the diffusion of fluids from the oral cavity causes debonding of particles from the polymeric matrix and the creation of porosity at the interface. This condition leads to faster and more pronounced erosion of the restoration.

A new approach is presented in this work where an organic polymer is chemically bonded to the surface of inorganic microfiller particles using γ -radiation induced grafting. When the modified filler is then incorporated into the restorative composite, the presence of the organic material on its surface helped improve the physical affinity and the intermolecular bonding at the interface. Wetting of the particles by the resin was significantly better resulting in improved curing of the composite due to increased light transmission. In addition, substantial enhancement in the composite's mechanical properties was realized and can be related to higher filler loading and lower porosity at the interface.

The grafting technique utilized in this work involves the exposure of the fine filler particles ($\sim 0.04 \mu\text{m}$ diameter) to gamma radiation in the presence of acrylic acid vapor. After a dose of one Mrad, the filler particles were dried under vacuum to remove excess monomer and stored until used in making the composite samples. Compressive strength, depth of cure and hardness were measured as a function of exposure time to a commercial light source for curing. Summary of the comparison between untreated and grafted fillers show the following advantages of the grafted material:

- Increased maximum filler loading by about 40%.
- Significant improvement of composite compressive strength, (Fig. 1).
- Improved mixing of filler and matrix.
- Stability of composite samples when aged in aqueous solution for up to 3 months.

Although the composite processing variables were not optimized in this study, the mechanical properties of samples with untreated filler particles were in the range obtained from commercially available products.



IN VIVO LEUKOCYTE INTERACTIONS WITH BIOMER®

Roger E. Marchant, Kathleen M. Miller and James M. Anderson

Depts. of Macromolecular Science and Pathology, Case Western Reserve University, Cleveland, Ohio 44106

A cage implant system was utilized to quantitatively and qualitatively characterize *in vivo* leukocyte interactions with cast Biomer®. Scanning electron microscopy (SEM) in conjunction with cytochemical staining procedures was used to investigate the cellular events at the leukocyte/Biomer® interface as well as in the inflammatory exudate at 4, 7 and 21 days postimplantation time.

Stainless steel mesh cages, 3.5 cm in length and 1 cm in diameter, each containing a Biomer® film specimen (1.6 cm x 0.5 cm x 0.14 cm) were subcutaneously implanted in 3-month-old Sprague-Dawley rats. Following the withdrawal of the inflammatory exudate, the animals were sacrificed and the Biomer® samples retrieved. The concentration of leukocytes in the exudate was determined, and Wright's and non-specific esterase stains were used to identify and differentially count the various leukocytes. The possibility of intracellular enzyme activity was demonstrated cytochemically by staining slide preparations with either an alkaline phosphatase stain for neutrophils, or an acid phosphatase stain, for all leukocytes. Portions of the retrieved Biomer® film were stained with either Wright's stain or the alkaline or acid phosphatase stains or fixed in glutaraldehyde solution for SEM analysis. The Wright stained polymer specimens were initially characterized qualitatively and then every cell attached to the surface was counted differentially. Differential counts were also made from the alkaline phosphatase stained specimens. Adherent leukocytes were characterized with SEM on the basis of their surface morphology and spreading behavior.

In the exudate, the acute phase of the inflammatory response was still prevalent at 4 days, since the characteristic cell type, the polymorphonuclear leukocyte (PMN) remained predominant. At 7 and 21 days, however, mononuclear leukocytes were predominant and this reflected a change in the inflammatory response from acute to mildly chronic. The concentration of all leukocytes in the exudate diminished with implantation time.

The population density of leukocytes adhered to the Biomer® surface diminished with implantation time. The population density of foreign body giant cells (FBGC) on the surface remained constant, while the number of nuclei per giant cell increased with time. In contrast to the cellular events that occurred in the exudate, the predominant cell type on the Biomer® surface at all time points was the macrophage. The results showed that there was preferential adherence of macrophages to the Biomer® surface relative to other leukocytes in the exudate. It appeared, from the SEM analysis, that with time of adherence the macrophages go through several morphological phases; secured attachment (phase I), cytoplasmic spreading (phase II), whole cell spreading (phase III) and cellular disintegration (phase IV). At 4 days, the adherent leukocytes were roughly divided between those in phase I and phase II. By 7 days, most of the macrophages

were either in phase II or phase III, and by 21 days there were only a small number of adherent macrophages, virtually all of which showed phase II or III morphology. FBGCs were observed on all implants at each time point. The number of nuclei per giant cell ranged from 2 to greater than 50 for some of the giant cells at 21 days. In addition, single leukocytes were often observed to be in the process of merging or fusing into an existing giant cell.

The intracellular acid phosphatase staining of the adherent macrophages appeared to correspond to the morphological events. As the macrophages spread out over the Biomer® surface and passed through morphologic phases I, II and III, degranulation and loss of lysosomal enzymes occurred such that many of the adherent macrophages on day 7 and particularly day 21 demonstrated little or no remaining phagocytic capability. The occurrence of non-staining macrophages on the Biomer® surface was in contrast to the observed exudate macrophages which always stained. The phagocytic capability of FBGCs also tended to parallel the events occurring to the single leukocytes with time. FBGCs showed diminished acid phosphatase activity with time and with increasing number of nuclei.

In conclusion, leukocyte adhesion and spreading along with the presence and growth of multinucleated foreign body giant cells were observed on cast Biomer® surfaces *in vivo*. The preferential adherence of macrophages compared to other leukocytes in the inflammatory exudate was shown and the phagocytic capability of all adherent leukocytes, including FBGCs, decreased with time and this corresponded to changes in cellular morphology observed with SEM.

PHEMA/POLYAMINE GRAFT COPOLYMERS AS NEW COLUMN MATRIX FOR CHROMATOGRAPHIC SORTING OF LYMPHOCYTE SUBPOPULATIONS (B CELLS AND T CELLS)

K. Kataoka, T. Okano*, Y. Sakurai*, A. Maruyama**, and T. Tsuruta**

Dept. of Surgical Sci., The Heart Inst. of Japan, Tokyo Women's Med. Coll.
Tokyo, Japan

There is a wide demand in the field of biomedical science for the development of effective method of isolating vital lymphocyte subpopulations (B cells and T cells) with high yield and purity. Adhesion chromatography, one of the promising cell sorting techniques, is a method which utilizes differences in the adhesive properties of the cells with solid matrices as a basis for their separation. The aim of our research project is to develop effective column matrices which have ability to distinguish the physical and chemical properties of plasma membrane of each lymphocyte subpopulation. Through our series of studies on the interaction of blood cells with synthetic polymers having microphase separated structure on their surfaces, we have found that albuminated surface of polystyrene/polyamine graft copolymers (SA copolymers) have successfully worked as a column matrix used for chromatographic separation of B and T cells (1). Albumin coating, however, was required for SA copolymer column to be capable of separating B and T cells.

Important facets of this study are to establish the efficient separation of B and T cells without existence of any adjuvant protein, including albumin, and to indicate that the formation of microphase separated structure on matrix surface is the most important factor which decides the separability of lymphocyte subpopulations. For these purposes, PHEMA/polyamine graft copolymers (HA copolymers), which have more hydrophilic nature than SA copolymers, were newly prepared, and separation of T cells from B cells by HA copolymer columns were carried out. This is the first report of the successful separation of B and T cells by adhesion chromatography without any adjuvant proteins in the medium or on the matrix surface.

Materials and Methods: PHEMA/polyamine graft copolymer (HAX: x represents the wt-% of polyamine portion in copolymer) was prepared by the radical copolymerization of 2-hydroxyethyl methacrylate and polyamine macromer. Poly(2-hydroxyethyl methacrylate) (PHEMA) and poly(p-diethylaminoethylstyrene) (PEAS) were prepared by the radical polymerization of the corresponding monomers. PHEMA and PEAS can be regarded as models for trunks and branches of HA copolymer, respectively. Each polymer was coated on glass beads (48-60 mesh) by solvent evaporation technique.

Selectivity for lymphocyte subpopulations was evaluated by passing lymphocyte suspensions through the column packed with polymer-coated glass beads. lymphocytes were obtained from mesenteric lymph node of Wister male rat aged 5 weeks, and suspended in Hanks' balanced salt solution (HBSS) in a concentration of $(1.0 \pm 0.3) \times 10^7$ cells/ml. Lymphocyte suspension was passed through the column by the use of infusion pump for a definite period of time at a flow rate of 0.4 ml/min. Spectrophotometric detector was equipped at the column outflow to monitor the elution pattern of lymphocytes. Lymphocyte counts in the effluent were performed with Coulter Counter to determine the lymphocyte retention in the column. The percentage of B cells, which ex-

press immunoglobulins(Ig) on their membrane surface, was determined by immunofluorescence staining of Ig molecules, using FITC-labeled rabbit anti-rat IgG.

Results and Discussion: The logarithm of the reciprocal of B and T cell effusion from the column was found to be proportional to the column bed volume. The proportional constants for B and T cells were abbreviated as A_B and A_T , respectively. Then, separability can be estimated by the ratio of A_B/A_T , such that the higher the value of this ratio, higher is the selectivity for B cells. Values of A_B/A_T ratio were determined from the slopes of straight lines obtained by plotting the reciprocal of the logarithm of B cell effusion against that of T cell effusion.

HA copolymer columns were found to have remarkably high value of the A_B/A_T ratios, that is as high as 5.1, indicating that the preferential retention of B cells over T cells took place in these columns. By using HAI3 column, T cell population with 95% purity was obtained in 60% yield. None of the homopolymer columns (PHEMA and PEAS) showed the value higher than 1.9, and T cell populations with 95% purity was obtained in less than 10% yield by the homopolymer columns. Surprisingly, HA copolymer columns maintained their high efficacy of separating T cells from B cells even in the absence of adsorbed albumin on matrix surfaces. This forms sharp contrast with the necessity of albumin coating for SA copolymer (polystyrene/polyamine graft copolymer) columns to be capable of separating T cells from B cells. Reduction of hydrophobic interaction between matrix and lymphocyte is considered to be most plausible reason for HA copolymers to successfully work as a column matrix in protein-free environment.

In conclusion, our results demonstrated that B cells were selectively retained on the surfaces of the polyamine graft copolymer even though there exists no serum protein, suggesting an essential role of microphase separated structure of the column matrix in separating lymphocyte subpopulations. As a possible mechanism, we have considered that the microphase separated structure of the graft copolymers may suppress the activation of attached lymphocytes through its effect on a redistribution of proteins and/or lipids present at the plasma membrane of lymphocytes, and stabilize their own membrane-structures which are different enough to be recognized by the multi-phase matrices. This proposed mechanism is consistent with the results of SEM observation that lymphocytes attached on HA copolymer surfaces scarcely suffered any shape changes.

(1) K. Kataoka, et al, Eur. Polym. J., in press.

Dept. of Surgical Science, The Heart Institute of Japan, Tokyo Women's Medical College, 10 Kawada-cho, Shinjuku-ku, Tokyo 162, Japan

* Inst. of Medical Eng., Tokyo Women's Med. Coll.

**Dept. of Industrial Chem., Science Univ. of Tokyo

ADHESION OF HUMAN UMBILICAL VEIN ENDOTHELIAL CELLS TO MITRATHANE^R A SEGMENTED POLYETHER URETHANE, UNDER CONDITIONS OF SHEAR AND AXIAL STRESS (STRAIN)

C.L. Ives, S.G. Eskin, C.L. Seidel*

Department of Surgery, Baylor College of Medicine
Houston, Texas

Animal studies have shown that endothelial growth (either by prior seeding or neointimal formation) on the surface of devices implanted in the cardiovascular system improves their blood compatibility. In man, to date, little endothelialization of such implants has been found to occur.

Endothelial cells lining the cardiovascular system are subjected to fluid mechanical forces; the fluid movement at the blood/vessel wall interface produces a shearing stress; and the fluid pressure on the compliant wall produces an axial stress/strain. The fluid mechanical forces in artificial devices may be higher than physiological because of poor fluid dynamics or because of the mechanical properties of the material e.g. compliance. The inability of human endothelial cells to withstand higher than normal levels of these fluid mechanical forces may be a contributing factor in the failure of surfaces to endothelialize in man. This failure might also be due to different adhesive interactions with different substrates or differences in endothelial regenerative ability.

At present the *in vitro* testing of materials for implantation usually only involves study of cell growth under static conditions, and the materials used for prostheses are hydrophobic i.e. polytetrafluoroethylene and polyethyleneterephthalate.

The aim of this study was to investigate the growth of human umbilical vein endothelial cells (HUVEC) on a segmented polyether urethane urea, Mitrathane^R, a relatively hydrophilic, elastomeric polymer (similar to Biomer^R) under static, shear stress and axial stress/strain conditions that simulate the normal physiological range.

HUVEC were harvested by collagenase treatment of human umbilical cord veins. The cell pellet was seeded directly onto the material and either grown to a monolayer under static conditions and then subjected to fluid mechanical forces, or transferred to an experimental chamber and grown under these conditions initially. Mitrathane^R surfaces were prepared by film casting techniques and used either attached to glass 2½" x 3½" (as a rigid support) or as a thin sheet 2" x 2."

The Mitrathane^R coated glass surfaces seeded with cells were either used to form the floor of a parallel plate flow chamber in which by altering the flow rate the cells could be subjected to controlled constant levels of shear stress or kept in petri dishes under static conditions.

The thin sheets of Mitrathane^R were mounted individually in a specially designed chamber so that the surface was flat and in a fixed geometry. HUVECs were seeded onto the membrane and either grown under stationary conditions or the membrane was stretched sinusoidally by measured amounts (up to 10%) and at specific frequencies (1-2 Hz), conditions within the physiological range. During the experiments, the surfaces were monitored at frequent intervals by videomicroscopy and 35 mm camera.

The results show the HUVECs grow well on Mitrathane^R under stationary conditions. The cells

also remain attached and grew when subjected to shear stresses of 50 dynes cm⁻² or the axial stress/strain produced by the sinusoidally applied 10% stretch at 1 Hz, for three days.

Comparison of the morphology of the cells grown under these various conditions shows interesting differences. Under static conditions, cells had a characteristic polygonal/endothelial appearance. Under flow conditions, the cells became progressively more elongated with their long axes aligned with flow. When subjected to axial stress/strain the cells became elongated but more rapidly than in response to shear stress and with their long axes perpendicular to the axis of stress. These results suggest that the endothelial cell/Mitrathane^R interaction is strong enough to withstand these simulated *in vivo* fluid mechanical forces; although it is possible that the combined effect of shear and strain produced by pulsatile flow *in vivo* may be more rigorous.

Other workers using different materials e.g. silicon rubber and latex, and different cell types e.g. fibroblasts and smooth muscle cells have observed cell detachment during stretching. These substrates are relatively hydrophobic compared with Mitrathane^R and it may be that the more hydrophilic nature of the polyurethanes results in a better cell/substrate adhesive interaction. The morphological changes undergone by the cells in response to the fluid mechanical forces described here may well be important in determining the spindle shape and flow oriented appearance of the endothelial cells *in vivo*. We have previously reported that bovine aortic endothelial cells align faster in response to a given level of shear stress than HUVEC which indicates that there is interspecies variation in cell sensitivity to these fluid mechanical forces. The results reported here also suggest that endothelial cells may be more sensitive to one component of the fluid mechanical forces than another i.e. to axial stress/strain more than shear stress. This sensitivity to fluid mechanical forces may be a feature of both substrate and cell origin and is possibly a significant factor in causing the interspecies variation of graft/device endothelialization.

Funded by HL23016 and HL23815 from the NIH.

Dr. C.L. Ives
Department of Surgery
Baylor College of Medicine
Texas Medical Center
Houston, Texas 77030

*Dr. C.L. Seidel
Department of Medicine
Baylor College of Medicine
Houston, Texas 77030

ADHESIVE STRENGTH OF CELL TO BIOMATERIALS BY MEANS OF VISCOMETRIC METHOD, IN VITRO

KAWAHARA, H. and MAEDA, T.

Department of Biomaterials, Osaka Dental University
1-47 Kyobashi, Higashi-ku, Osaka 540, JAPAN

Adhesive strength of cell to biomedical materials was measured by attempting to separate the adhered cells from the materials' surface with supersonic vibration (Imai, Kawahara and Nakamura, 1979). It is, however, difficult to numerize correctly the adhesive strength of the energy sufficient to separate the cell-material adhesion, due to the cytoplasmic degeneration and damages caused by cavitation, heating and interface disturbance of supersonic vibration.

In this work, the strength of cell adhesion to various types of biomedical materials were measured by viscometric method, which was able to measure the adhesive strength of cultivated cells contacting with the substratum in cell culture, applying the shear stress of 3.7 dyne/cm² generated by streaming of the culturing medium (Kawahara, Maeda and Nakamura, 1981).

In order to investigate the mechanism of cell adhesion to biomaterials, adhesive strength of HeLa S3 cells to test plate of glass, single crystal alumina (Al₂O₃), polycrystal alumina (Al₂O₃), titanium (Ti), titanium nitride (TiN), polymethyl methacrylate (PMMA) and polyvinylchloride (PVC) were measured by the viscometric method.

The adhesive strength of cells to PVC plate showed the same degree as that to glass plate in the 4 days cultivation, but after the 7 days cultivation, the strength decreased remarkably. While the adhesive strength of cells to polycrystal alumina plate was smaller degree than that to the single crystal alumina plate and other plates in the 4 days cultivation, the adhesive strength became to be increased with cultivation time and showed the almost same degree as that to glass plate and other plates after the 7 days cultivation. On the other hand, in the plate of single crystal alumina, pure titanium, titanium nitride and PMMA, the adhesive strengths were almost same degree to that of glass plate through the cultivation time (Fig. 1).

In order to analyze the difference between the both cell adhesive strengths to polycrystal alumina and single crystal, the surface roughness of the plates was measured (Fig. 2). The adhesive strength depends upon the surface roughness in the 4 days cultivation, but no dependence was observed in the 7 days cultivation (Fig. 1).

Morphological observations on the HeLa S3 cells adhered to PVC plate showed fibroblastic like in spite of epithelial like cell of HeLa S3, while to other plates of PMMA, Al₂O₃ (polycrystal, single crystal), Ti, TiN, the cells manifested the epithelial like of normal form in the case of glass plate. These morphological observations were consistent with results in the experiment of adhesive strength.

From these findings, it is revealed that, the adhesive strength of cell to biomaterials may depend upon the chemical activity, physical activity and molecular structure of materials' surface rather than their surface roughness.

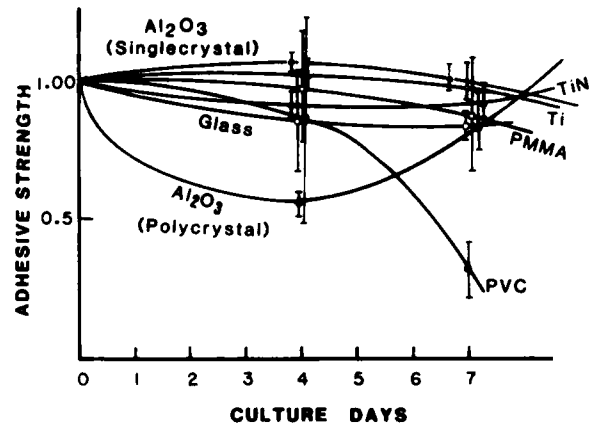


Fig. 1 Adhesive strength of HeLa S3 cells to materials.

$$\text{Adhesive Strength} = \frac{\text{Adhered cell number after shear stress}}{\text{Adhered cell number before shear stress}}$$

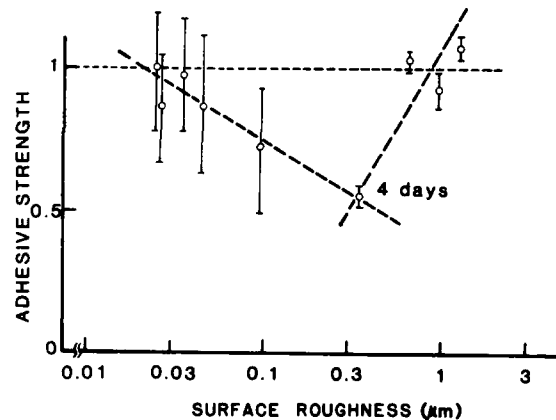


Fig. 2 Adhesive strength of HeLa S3 cells and surface roughness of the materials.

References

1. Imai, K., Kawahara, H. and Nakamura, M.: Medico-dental use of Titanium and Zirconium alloys, Transactions of the 1st Meeting of Japanese Society for Biomaterials, Sendai, 1979.
2. Kawahara, H., Maeda, T. and Nakamura, M.: Adhesive strength of cell to biomaterials by using viscometric method, in vitro, Transactions of the 13th Inter. Biomat. Sympo., Troy, NY, 1981.

Granted by Special Project Research, Design of Multiphase Biomedical Materials, VB57119009, Ministry of Education, 1982 and 1983.

THE DEVELOPMENT OF A NEW HIGH STRENGTH, COLD FORGED 316LVM STAINLESS STEEL

BARDOS, D.I., BASWELL, I., GARNER, S., WIGGINTON, R.

RICHARDS MEDICAL COMPANY

INTRODUCTION

Orthopaedic surgical implants have greatly benefited from advances in materials technology. This paper describes the development and improvements of the metallurgical processing of surgical grade 316LVM (F-138) stainless steel.

Small, stainless steel orthopaedic fracture fixation devices with axial symmetry such as intramedullary rods, bone screws, pins and wires are strengthened by cold rolling and drawing. Larger and more complex shapes such as Compression Hip Screw plates are hot forged. Hot forging austenitic stainless steel results in a material that is equivalent to soft, annealed stainless steel that has lower mechanical properties than cold worked stainless steel.

MATERIAL AND METHODS

A metallurgical processing technology has been developed and improved upon to increase the mechanical properties of large stainless steel implants. Two types of cold forged material were studied. The first one was a relatively simple cold forging process. The second was a more complex, high strength, cold forging process. Both processes consist of a rapid cold reduction of stainless steel bars and cold dynamic pressing at pressures exceeding the yield strength of the material. Radial and axial plastic deformation of the material allow the fabrication of complex, nonsymmetrical shapes with considerable cold working throughout the part.

The strengthening mechanism involves the production of slip bands within the fine-grained material. Plastic deformation in excess of 66% reduction of area has been achieved in the high strength, cold forged material. This degree of reduction has never before existed in large stainless steel implants.

Compression Hip Screw devices were fabricated using both cold forging processes from stainless steel conforming to ASTM standard F-138, Grade 2 chemical composition. Control samples were taken from commercially available products of similar design and geometry that were produced by conventional hot forging. These control samples met the ASTM

F-621 specification for forged stainless steel. Standard tensile specimens were fabricated from the plate portion of both cold forged processes and hot forged conventional devices to determine comparative mechanical properties. Yield strength and ultimate tensile strength values were measured.

RESULTS

Microhardness tests were conducted on several cross sections of the high strength cold forged device and compared to the hot forged products. Average values as high as 40 on the Rockwell C scale were obtained on the high strength cold forged process material while the control, hot forged group averaged 82 on the B scale.

The static average mechanical properties of the cold forged materials are reported below and compared to conventional hot forged stainless steel.

	Yield Strength (KSI)	Ultimate Strength (KSI)
Hot Forged	48	85
Cold Forged	106	135
High Strength, Cold Forged	176	196

CONCLUSIONS

The new metallurgical processing technology for producing high strength orthopaedic surgical implants resulted in a three fold increase in mechanical properties. This high strength, cold forging technology will make it possible to design and fabricate orthopaedic implants with greatly improved mechanical characteristics. This new biomaterials development should reduce fatigue fracture and/or mechanical deformation of devices. It will also allow engineers the opportunity to design parts with thinner sections, yet with comparable strength.

Denes I. Bardos
Research and Development Div.
Richards Medical Company
1450 Brooks Road
Memphis, Tennessee 38116

ASGIAN, C., GILBERTSON, L., HORI, R.

ZIMMER, INC., WARSAW, IN 46580

INTRODUCTION: The use of tapered joints in orthopaedic devices is increasing. They have been used in segmental replacements and total hip replacements. They offer a modular design approach that can provide good design versatility with a minimal number of parts. Such joints, commonly referred to as "Morse tapers," are widely used in the tooling industry to machine parts.

When the taper angle is small, less than 8° included, socket and taper joints are self-locking (Chao and Kasman¹, 1982). The efficacy of these taper joints depends, to a great extent, on machining both the taper and the socket within small tolerances. The advent of numerically controlled machining has done much to alleviate these difficulties.

The tapered joint must carry large cyclic loads in a permanent prosthetic application. When cyclic loads are transmitted across mechanical joints, there is the possibility that: 1. the joint will debond and separate, and, 2. that micromovement in the joint will decrease the fatigue load-carrying ability of the joint. This micromovement is usually referred to as fretting. The damage due to fretting can vary with joint geometry, materials, and load regime. Chao and Kasman¹, 1982, reported on the results of fatigue tests performed on a socket and taper joint with a 4° included angle and a taper root diameter of 15.88 mm. They showed that the taper joint could withstand cyclic loads at physiological levels to 10 million cycles and maintain the integrity of the joint. However, the test apparatus consisted of a rotating beam with a fixed axial compressive load and was not a close simulation of the *in vivo* condition. These experiments were undertaken to further examine taper joints under conditions that might be experienced in total hip replacement systems.

METHODS: Two types of samples, each with different load regimes, were used in this series of tests. The socket of the Type-I sample was rigidly held with its axis vertical and the taper was pressed vertically downward into the socket. Fatigue loading was then applied to the taper in line with the axis of the taper but offset from the central axis to apply a substantial bending moment. The Type-I samples were made of Ti-6Al-4V, and the taper angle was 8° included. The Type-II sample was held such that the axis of the taper was inclined at 45° from the vertical. The socket was placed on the taper and loading was applied vertically to the socket. Two material combinations were used for the Type-II samples: a) with both components of chrome-cobalt alloy, and b) with the taper made of Ti-6Al-4V and the socket made of chrome-cobalt alloy. The taper angle on the Type-II samples was 6° included.

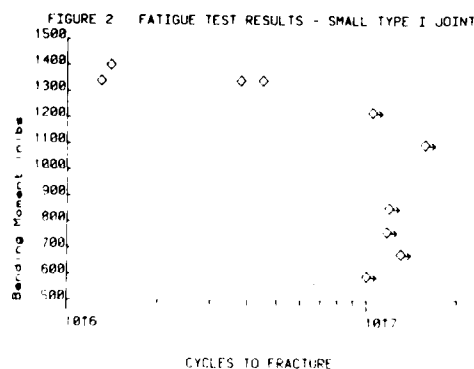
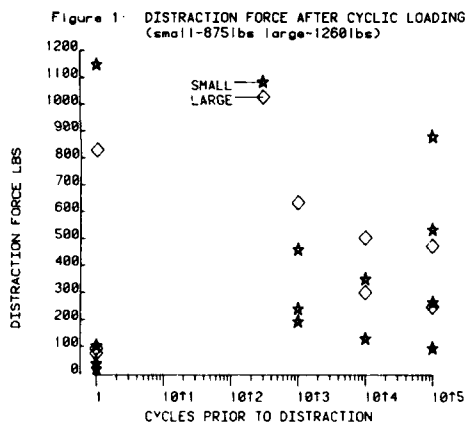
Both types of joints were loaded with constant

amplitude fatigue loads. At several different preset numbers of cycles, testing was stopped and the force required to separate the joint along its central axis was measured. Testing was continued to 10^7 cycles or to fracture.

RESULTS: Figure 1 shows the results of the distraction tests. The tests show that the force required to pull the joint apart was substantial, proving the self-locking nature of these taper joints. Results of the fatigue testing of the Type-I taper joint are given in Figure 2. Preliminary fatigue results of the cobalt-chrome Type-IIa taper joint indicate that it can withstand bending moments in excess of 1000 in-lb. The test results are very close to those obtained from beam theory, indicating that fretting does not seriously compromise the fatigue strength of this joint.

REFERENCE:

1. Chao, E. Y. and R. A. Kasman "Conical Press-Fit in Tumor Prosthesis Design." Trans. 29th ORS, 8(1983), 107.



Zimmer, Inc.
P. O. Box 708
Warsaw, IN 46580

The Fatigue Resistance of Orthopaedic Wire and Cable Systems

Georgette, F.S., Sander, T.W., Oh, I.

Richards Medical Co., Memphis, TN

The use of wire in various orthopaedic surgical techniques has become commonplace. Applications such as fracture fixation, spinal fusion, reconstruction of tendons and ligaments, and reattachment of the greater trochanter in total hip arthroplasty, rely heavily on effective stabilization by wires. A recent review of the literature revealed, however, that wire breakage in trochanteric reattachment occurs approximately 24 percent of the time. Wires not breaking by tensile overload in the operating theater, were found to break predominantly by fatigue mechanisms. In order to better understand this mode of breakage, a study was conducted which evaluated the fatigue properties of various wire systems (1). It was found that by stranding fine monofilament wires into a multifilament cable, a drastic increase in fatigue strength could be achieved. These results promoted the present investigation into potential candidate materials for a cable system.

MATERIALS AND METHODS

The fatigue properties of both monofilament and multifilament wires were evaluated using a previously reported fatigue testing fixture (1). Testing was performed 'in air' at 0.6 Hz with an applied load cycling between 9 and 90 N. Stainless steel wire was evaluated in both monofilament and multifilament forms. Four additional candidate materials commonly used in orthopaedic surgery were evaluated in the multifilament cable form. Samples of each material were examined using a scanning electron microscope subsequent to testing.

Table 1 - Stainless Steel Wires and Cable

Condition	Size (mm OD)	Tensile Strength (MPa)	Cycles To Fracture
Monofilament Wire	1.0	607	535 ± 61
Monofilament Wire	1.2	556	819 ± 104
Multifilament Cable	1.2	579	5351 ± 397

Results

All wires were found to break by fatigue mechanisms. The improvement in fatigue resistance as a result of modifying the cross-section of wire is demonstrated for stainless steel by examining Table 1. It was found that the cable system exhibited greater than 6½ times the fatigue resistance of the monofilament wire of the same diameter. Among the other cables tested, it was found that both the MP35N® and Ti-6Al-4V alloys exhibited the highest fatigue resistance (Table 2).

Table 2 - Multifilament Cable

Cable Material	Size (mm OD)	Tensile Strength (MPa)	Cycles To Fracture
F138 (316L SS)	1.2	579	5351 ± 397
F67 (C.P.Ti)	1.2	696	12,003 ± 1538
F90 (Co-Cr-W-Ni)	1.2	979	13,744 ± 721
F136 (Ti-6Al-4V)	1.2	1165	50,914 ± 5769
F562 (MP35N®)	1.2	688	64,420 ± 8660

Discussion

Orthopaedic wires are likely to be subjected to both tensile and bending loads *in vivo* due to the forces imposed by both the musculature and by weight bearing. The design of the wire fatigue tester simulated these conditions. The substantial increase in fatigue resistance of multifilament cables indicated their excellent potential for use in fracture fixation. Although stainless steel is the most common material employed for wire fixation, other candidate materials in both monofilament and multifilament forms might prove more suitable. When compared to the stainless steel cable, the wrought Co-Cr-W-Ni and C.P. titanium alloys had 2-2½ times the fatigue resistance, the Ti-6Al-4V material had 10 times the fatigue resistance, and the MP35N material had 12 times the fatigue resistance.

In an attempt to further improve fatigue resistance, the MP35N® cable was coated with an elastomeric material. Initial testing showed that this coating could increase the fatigue resistance 3½ times (230,000 cycles to failure) that of an uncoated cable.

The results of these fatigue tests have shown that the development of both coated and uncoated multifilament cables may lead to a significant reduction in the incidence of orthopaedic wire failures.

(1) Sander, et al, J.B.M.R., 17:587-596 (1983).

®MP35N is a registered trademark of SPS Technologies, Inc.

Richards Medical Company
1450 Brooks Road
Memphis, Tennessee 38116

INFLUENCE OF AGEING ON THE MECHANICAL BEHAVIOUR OF CARBON-FIBRE REINFORCED EPOXY

U. Soltész, C. Reynvaan

Fraunhofer-Institut für Werkstoffmechanik
Freiburg i.Br., Germany

Carbon-fibre reinforced composites are regarded to be candidate materials for different types of implants. It is anticipated that devices with optimum biomechanical properties may eventually be developed. The mechanical properties measured under quasistatic and laboratory conditions for new composites are often comparable with those of common biomaterials and therefore seem to be sufficient. However, problems could arise from the mostly unknown long term behaviour under physiological conditions.

In this investigation the hygrothermal behaviour of a carbon-fibre reinforced epoxy was studied. This material was reinforced unidirectionally by HT-fibres (Rigilor AXT, 60 vol.%). For the mechanical testing bar-shaped specimens ($100 \times 10 \times 5 \text{ mm}^3$) were prepared. One series was tested non-aged, two more sets of specimens were stored for ageing in Ringer's solution at 40 and 60°C between three months and more than half a year until a specific moisture concentration of at least 95% was achieved.

The mechanical behaviour was characterized by 3-point-bending tests. Young's or bending moduli and flexural strengths were determined by using a support distance of 80 mm and a constant loading rate of 14,4 MPa/s. Fatigue behaviour was investigated in the same arrangement by applying sinusoidal cyclic loads at a frequency of 10 Hz and by measuring the number of cycles until fracture at different amplitudes (maximum stress in Fig.2) for the same minimum stress level (10% of the quasistatic strengths). Creep tests were performed by using a shorter support distance of 40 mm in order to increase the shearing stress of the matrix under a constant load of 760 N ($\approx 180 \text{ MPa}$) which generates stresses expected in a femoral stem component under physiological conditions [1]. All tests were conducted at 37°C in Ringer's solution to simulate the physiological environment.

Except for the bending modulus (Fig. 1) all other properties considered show significant changes due to ageing. The quasistatic strength decreases by 25 to 35% depending on the ageing temperature (Fig.1). An even more pronounced reduction is observed under cyclic loading (Fig.2). The fatigue

strength for 10^7 cycles is reduced by about 45 to 55% compared with the corresponding quasistatic value. Altogether the strength decreases under physiological long term conditions by about 70% compared with the quasistatic value of the new material. Finally, also the creep behaviour is strongly influenced by ageing (Fig.3). A remarkable increase in creep with increasing ageing temperature is observed if one considers e.g. the deflection with time which is depicted in Fig. 3 in normalized form equal to the reciprocal bending modulus.

These results demonstrate the necessity of evaluating the long term behaviour of composite materials under physiological conditions if they are to be used for biomedical applications. Comparison of the different ageing conditions shows that higher temperatures for accelerating the ageing process lead to additional changes in the material behaviour and do not simulate the physiological conditions sufficiently.

/1/ Soltész, U., Richter, H., Biomaterials 1980, Wiley and Sons, 1982, 33.

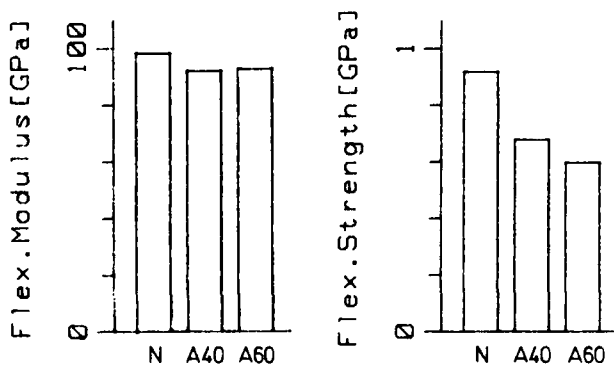


Fig. 1. Bending moduli and flexural strengths for the non-aged material (N) and after ageing at 40°C (A40) and 60°C (A60)

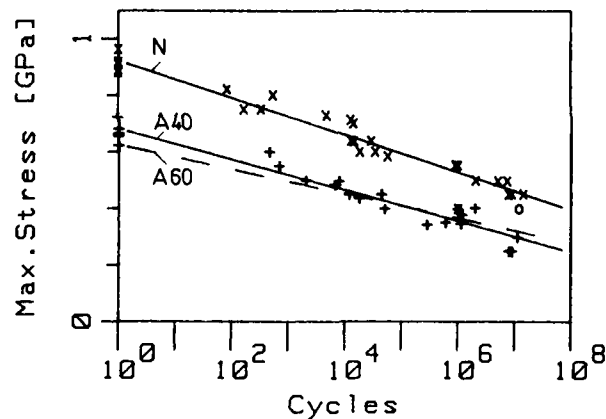


Fig. 2. Fatigue behaviour, data with linear fit (x N, + A40, -- A60 data not included)

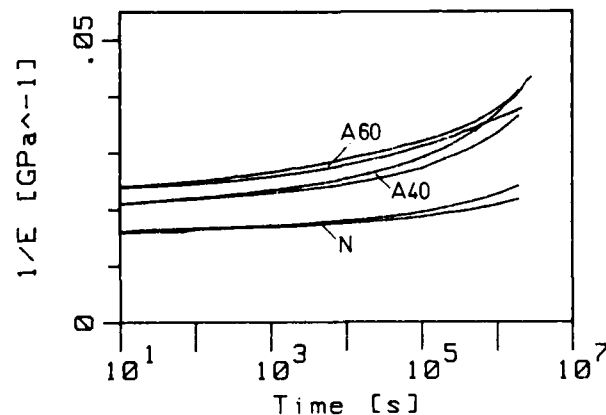


Fig. 3. Creep behaviour

"An In Vitro Strain Gage Study of Metal Backed Acetabular Cups"

Oh, I., Bushelow, M., Sander, T. W., Treharne, R. W.

Huntington Memorial Hospital
Pasadena, California

Late loosening of the cemented acetabular cup in total hip arthroplasties has proven to be an increasingly frequent complication. Experience has shown that the component usually loosens at the bone/cement interface and/or by fracture of the cement mantle around the cup. Previous studies have shown cement mantle shape and thickness to be a significant factor in the distribution of strains within the cement surrounding an all-plastic cup.¹ In this study, the effect of bone cement shape and thickness on the cement strain around a metal backed cup was evaluated.

MATERIALS AND METHODS: Hemispherically reamed hardwood blocks were used to simulate the acetabulum and act as cement molds. Six metal backed cups, OD - 49 mm, were each coated with a 1 mm thick layer of cement. Two rectangular rosette strain gages were bonded to the cups: one at the base and one along the side of the cup. Three different cement mantle configurations were tested.

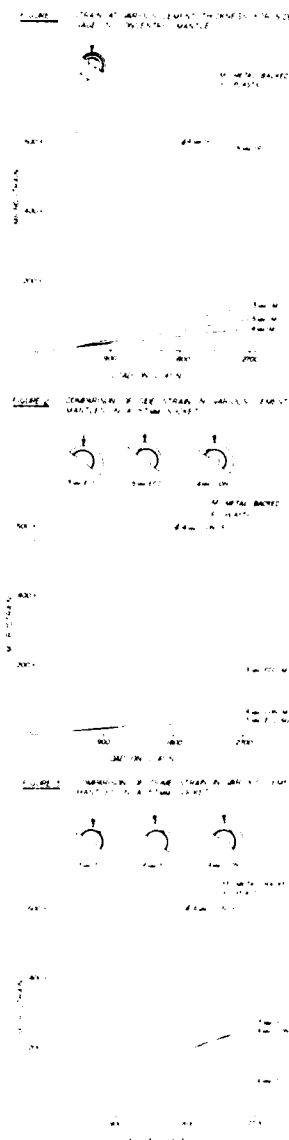
Effect of Concentric Cement Mantle: 1) A basic specimen was consecutively coated with 1 mm thick layers of cement. Tests were performed with 3, 4 and 5 mm concentric cement mantles. **Effect of Eccentric Cement Mantle:** 2) A basic specimen was offset sideways in a 57 mm socket such that one side had a 5 mm total cement thickness and the opposite side had a 3 mm total cement thickness. 3) A basic specimen was placed too deep in a 57 mm socket such that a 3 mm total cement thickness was created at the base of the cup. All cups, seated in hardwood blocks, were tested on an MTS testing machine at a 45° angle. A vertical load was applied to the cups via a 32 mm femoral head. Strains were recorded at 450 N increments up to 2700 N. Metal backed cups with a 1.5 mm metal thickness and 7.4 mm UHMWPE thickness, were compared to a previous study on plastic cups with a 8.4 mm UHMWPE thickness.¹

RESULTS AND DISCUSSION: 1) For a concentric cement mantle, metal backed cup base gages showed significantly higher strains than their corresponding side gages. This result is opposite to that found with the all plastic cups. No significant difference was seen between corresponding (3 and 4 mm) plastic and metal backed cup base gages at higher loads. A significant reduction in strain at the side gage location was seen when comparing metal backed versus all plastic acetabular cups (Figure 1). 2) The 5 mm eccentric side gage showed significantly lower strains than the 3 mm eccentric side gage. No significant difference was seen between the 4 mm concentric side gage and the 5 mm eccentric side gage (Figure 2). 3) The 4 mm eccentric base gage showed significantly less strain than the 3 mm eccentric base gage at loads above 1350 N. No statistically significant difference was seen between the 3 mm eccentric base gage and the 4 mm concentric base gage (Figure 3).

This study indicates that a metal backed acetabular cup minimizes the strains and distributes the strains more evenly in both concentric and eccentric cement mantles when compared to an

all-plastic acetabular cup.

Also, this study agrees with the findings of the previous all-plastic cup study: it is desirable to ream the acetabulum concentrically and use a cup with design features that provide even cement thickness and concentric seating within the cement mantle.



¹Oh, I, Trans 9th SFB, 6:95, 1983

Indong Oh, MD
10 Congress Street, Suite 103
Pasadena, California 91105

LABORATORY KNEE SIMULATION: A VIABLE OPTION

B. M. HILLBERRY, J. A. SCHAAF, C. D. CULLOM AND D. B. KETTELKAMP

School of Mechanical Engineering, Purdue University, W. Lafayette, IN

Simulation Testing

The design and development of total knee prostheses has become an evolutionary process. Much of the preliminary prosthesis development could readily be evaluated in the laboratory through simulation testing prior to implantation. This would significantly reduce development costs as well as possible revisions. For laboratory testing to provide an acceptable evaluation, the simulator must provide an adequate representation of the loading and environmental conditions that the prosthesis would see in a clinical implantation.

The simulator used in this study was developed specifically to test knee prostheses. The loading conditions for the prosthesis are generated in the simulator using hydraulic cylinders operated in closed-loop control. The prosthesis is mounted with bone cement in aluminum fixtures. Data from normal subjects walking across a force plate with simultaneous measurement of the position of the lower limb segments are used to derive the input to the simulator.

A vertical load is applied at the "hip" using the load versus time load profile from the above data. This vertical load is balanced by a hydraulic cylinder acting as a "quadracep" muscle. Attached to this cylinder are two cables which pass over a patella prosthesis and attach to the "tibia". This cylinder moves to give the flexion versus time profile as measured experimentally. In addition an ad/ab force and a tibial torque are applied at the equivalent "ankle". All of the input load profiles and the flexion profiles are synchronized in time to simulate the activity (walking, ascending or descending stairs, etc.) from which the data were collected.

One limitation of the simulator is the lack of the "hamstring" muscle force. However, for evaluating total joints this may not be a serious limitation since during the weight bearing portion of the walk cycle, the hamstrings are only active just prior to toe off [1]. A second limitation is the lack of an achilles tendon which changes the moment generated at the knee. This has been accounted for by modifying vertical load profile to generate forces across the knee that are the same as seen anatomically. An environmental chamber surrounds the knee and either can be filled with serum or have filtered water circulated through it.

Prosthesis Evaluation

A major advantage to laboratory prosthesis testing in a simulator is the ability to measure the changes that occur due to the simulation. Contact area measurements are made at the beginning and end of the test using pressure sensitive film. At the beginning and at regular intervals throughout the test, a series of stability tests are run to evaluate changes to the prosthesis that have occurred due to the cyclic loading. In each of these tests a 32kg vertical load is applied and the knee slowly flexed, slowly rotated and slowly forced in ad/ab. The response or motion is measured from which the stiffness and energy are determined. These periodic

measurements provides a method for quantifying the changes that occur due to the cyclic loading. Microscopic examination of the components and wear debris analysis following the test provide a direct observation of wear and deformation.

Test Results

Eleven prostheses of seven different designs have been tested. Each of the designs either is or has been commercially available. The tests were run under simulated walking conditions for an 82kg subject with water at 37°C circulate through the environmental chamber. Two tests were run for 500,000 cycles, eight tests for 100,000 cycles and one test was stopped after 111,000 cycles.

Included in the objectives of the test program were 1) to demonstrate that the simulator reproduced conditions similar to that which is observed clinically and 2) to establish a suitable test duration for future testing.

The one test was terminated because the prosthesis failed catastrophically due to a fatigue crack which developed in the femoral component. This prosthesis, an Herbert, failed in the same manner as had been observed clinically in 1 to 2 years of service. The other prostheses of current design, all performed very satisfactorily throughout the testing. There were significant changes in the energy absorbed and stiffness behavior during the first 100,000 cycles but appeared to remain stationary for the remaining duration of the testing. Significant changes in contact area were observed indicating a "wearing in" or "seating" behavior in those prostheses with point or line contact.

A retrieval analysis of each of the prostheses [2] was made to provide a direct comparison with clinically retrieved prostheses. The wear and/or deformation of the polyethylene occurred in the same locations and was very similar to that observed clinically in about two years of service. The pitting type wear observed clinically was not observed in these tests.

The results indicate that the laboratory simulator provides a direct means for identifying what may result in early catastrophic failure and also detect when excessive wear may occur. In addition, the simulator provides a good duplication of loading conditions and provides a means for evaluation performance changes that occur during the cyclic loading.

Acknowledgements

The retrieval analysis was performed by Dr. T. M. Wright, Hospital for Special Surgery, and the work sponsored in part by Zimmer, USA.

References

1. Morrison, J.B., Ph.D. Thesis, University of Strathclyde, Glasgow, Scotland, 1967.
2. Hood, R.W., Wright, T.M. and Burstein, A.H., J. Bio. Mat. Res., Vol. 17, 1983.

SOFT TISSUE RESPONSES TO MULTIFACETED PARTICLES AND
DISCS OF DURAPATITE

A.D. Sherer,*B.E. Sage,*S.S. Rothstein,* and P.J. Boyne**

Sterling-Winthrop Research Institute
Rensselaer, New York 12144

Durapatite, a nonresorbable, highly dense, ceramic bone-grafting implant material, has been demonstrated to be clinically effective when implanted subperiosteally for alveolar ridge augmentation. Because unintentional placement or migration into soft tissue may occur, several studies were therefore conducted to determine the soft tissue response to multifaceted particles and contoured discs. This report summarizes the histopathologic findings from implantation of the material subcutaneously into laboratory rats and subcutaneously and subperiosteally into beagle dogs for time periods varying from 7 days to 6 years.

In rats, after 1 week and 1, 6 and 12 months of subcutaneous implantation, neither multifaceted particles nor discs resulted in any microscopically remarkable inflammation. After subcutaneous implantation of multifaceted particles and discs in beagle dogs for 7 and 24 days, 9 months, and 2 and 6 years, no implant migration was observed. Collagen encapsulation of particles and discs, increasing in thickness with time, was seen throughout the 6 years of observation. Except for a few isolated macrophages seen within the connective tissue stroma at 7 and 24 days, no other evidence of inflammation was found. In tissue sections taken at 6 months from beagle dogs in which multifaceted particles were placed subperiosteally beneath the gingiva, dense connective tissue was observed adjacent to and surrounding the individual particles. These results show that durapatite implanted subcutaneously in rats and dogs produces little or no inflammatory response and is tissue compatible irrespective of shape of implant or contour.

*Sterling-Winthrop Research Institute
81 Columbia Turnpike
Rensselaer, New York 12144

**Loma Linda University
Dept. of Surgery
Loma Linda, California 92354

TISSUE REACTIONS ON HYDROXYAPATITE IN THE INFECTED AND NON INFECTED MIDDLE EAR.

C.A.van Blitterswijk^x, J.J.Grote^x, W.Kuypers^{xx}, K.de Groot^{xxx}.

Department of Otorhinolaryngology
University Hospital Leiden, the Netherlands

At present the use of biomaterials in otologic surgery is rapidly gaining ground. Early applications of materials with an autogenous, homogenous or allogeneous origin did not often result in success. However some of the recently developed allogeneous biomaterials, as for example calciumphosphate ceramics, glass-ceramics and several composite polymeric materials, seem to justify the expectation for better results.

This contribution will evaluate one of the calciumphosphate ceramics, sintered hydroxyapatite, in order to test its suitability for middle ear implantation. Two different kinds were used, a dense (microporosity (+ 3 μ m) <5%) and a macroporous form (microporosity <5%, macroporosity (+ 100 μ m) +26%). The ceramic was used for implantation in the rat middle ear as obliterative and occlusive material. Survival periods extended from one week to one year. Since infection will often be encountered in middle ear surgery, part of the middle ears was infected by means of an intratympanic injection of *Staphylococcus aureus* suspension. The material thus achieved was prepared for routine histology, autoradiography, bone fluorochromes, transmission, scanning and analytical electron microscopy. In this way a total of 376 implants was studied (table 1).

table 1.

SUR	1	2	4	13	26	52	TOT
	N I	N I	N I	N I	N I	N I	N I
His D	12	12	12	10	12	10	10
mp	12	12	12	10	12	10	12
TEM D	4	4	4	4	4	4	4
mp	4	4	4	4	4	4	4
SEM D	4	4	4	4	4	4	2
mp	4	4	4	4	4	4	2
TOT D	20	20	20	18	20	18	16
mp	20	20	20	18	20	18	16

SUR = survival time in weeks

His = implants destined for histology

TEM = implants destined for transmission electron microscopy

SEM = implants destined for scanning electron microscopy

TOT = total number of implants

mp = macroporous D = dense N = non infected

I = infected

In order to obtain a trustworthy interpretation of the results, control studies were performed concerning the infected and non infected middle ear of the rat without the presence of an implant (ref. 1).

The surface of the implant directed towards the lumen side of the middle ear will be covered by a tissue highly similar to the mucosa normally present on the middle ear wall, which therefore consists of a flat polygonal epithelium separated from the implant by a lamina propria. Occasionally ciliar and goblet-like cells may be encountered. Proliferation of the mucosal cells is most prominent in the first weeks after implantation.

The occurrence of infection may induce the proliferation of fibroblasts in the mucosa.

When in contact with the middle ear wall bone will be deposited on the implant surface. Bone deposition originates both from the implant as from the middle ear bulla as was demonstrated by the use of bone fluorochromes. The bond of the bone to the implant is direct and even the micropores will become filled. The presence of muscle tissue in the direct vicinity of the implant gives rise to the presence of mononuclear phagocytes and multinuclear cells, some of which apparently demonstrate phagocytic activity. Both in infectious as in non infectious surroundings these cells show a relatively high tritiated thymidine uptake. The presence of these cells may be due to mechanical irritation caused by the bordering muscle tissue.

Morphometric analysis showed the macropore lumen to be initially filled with mucus and fibrous tissue gradually replaced by bone. Although autoradiography demonstrated the proliferative activity of the cells in the pores to decrease one month following upon implantation, the application of bone fluorochromes revealed osteogenic activity up to six months after implantation. In infected circumstances the biomaterial appears to take part in the middle ear events without indication of major resorption (limited to the ultrastructural level) or infiltration of pores by exudative fluid, pores in contact with the lumen however may show exudative cells.

These results together with data derived from earlier experiments (ref. 2) and human biopsies suggest the suitability of hydroxyapatite for bone substitution and for application as part of the total alloplastic middle ear prosthesis (ref. 3) even when reoccurrence of infection may be expected.

1. J.J.Grote, C.A. van Blitterswijk, 1983. Acute otitis media: An animal experimental study. *Acta otolaryngol.* (accepted).
2. J.J.Grote, W.Kuypers, 1983. The use of biomaterials in reconstructive middle ear surgery, in: *Biomaterials in reconstructive surgery*. Ed. Ruben, R.J.: 987.
3. J.J.Grote, W.Kuypers, 1980. Total alloplastic middle ear implant. *Arch. Otolaryngol.*, 106: 560

x ENT Dept. University Hospital, 2333 AA Leiden, the Netherlands

xx ENT-research laboratory, Nijmegen, the Netherlands

xxx Material Science Dept., Amsterdam, the Netherlands

MECHANISMS FOR THE BONDING OF BONE TO DENSE HYDROXYAPATITE

Michael M. Walker and J. Lawrence Katz

Rensselaer Polytechnic Institute Troy, New York 12181

A mechanism is proposed for the observed adhesion of bone to dense polycrystalline hydroxyapatite surfaces (1). This model is based on:

(a) Empirical observations of surface chemical interactions of various chemical species onto hydroxyapatite and other minerals in comparison to their with conventional metallic, polymeric and ceramic implant materials.

(b) Correlations between the ability of bone to adhere to various implant materials with the abilities of the latter to chemisorb oxyacids.

(c) In vivo testing of materials predicted by the bonding model to meet the requirements for bony adhesion.

The strong adhesion observed between bone and dense hydroxyapatite is especially interesting when compared to the lack of such bonding between bone and conventional implant materials such as aluminum oxide ceramics, polyethylene, and titanium. Since adhesion is a surface phenomenon, it follows that the surface of dense hydroxyapatite is able to react with one or more of the components of regenerating bone to form strong chemical bonds. Similarly, the surfaces of the nonbonding materials apparently do not allow the formation of such bonds.

Calcium phosphate minerals have long been known to react with surface active agents used in ore flotation. In this process surfactants containing carboxylic acid or sulfate groups chemisorb onto exposed calcium sites on the hydroxyapatite surface forming stable salt like surface compounds.

The components of healing bone are rich in materials containing carboxylate and sulfate side groups. Chondroitin sulfate, a major component of the glycoprotein fraction of bone, is especially rich in both of these acidic groups. Thus, it would be expected that chondroitin sulfate as well as other biological polyanions containing sulfate and/or carboxylate groups should adsorb onto the surface of hydroxyapatite in vivo as they are known to do in vitro.

Light and electron microscopic examinations of the interface of dense hydroxyapatite and bone have consistently revealed the presence of mineralized ground substance which is

rich in chondroitin sulfate (2). Thus, since chondroitin sulfate is demonstratable at the interface of bone and dense hydroxyapatite and since this material is richly endowed with carboxylate and sulfate groups which are known to adsorb to the apatite surface, it is reasonable that the adhesion of bone to the surface of hydroxyapatite is at least in part resultant from a strong chemisorption of chondroitin sulfate onto the implant surface.

If the proposed theory is valid then bone should also adhere to other materials which also chemisorb carboxylate as it adheres to hydroxyapatite. To test this theory samples of calcite and dolomite were implanted into osseous defects. As reported earlier, bone strongly adheres to both calcite and dolomite implants (3). Since both of these materials strongly chemisorb carboxylate in vitro, the predictions of the model are supported. Furthermore, all materials so far tested which do not chemisorb carboxylate fail to bond with bone. Thus, the ability of a material to chemisorb carboxylate from aqueous solution seems to be a required but not necessarily fulfilling prerequisite for bony adhesion.

REFERENCES

1. Jarcho, M. et al., J. Bioeng. vol. 1: 79-92, 1976.
2. Jarcho, M. et al., Trans. 4 th. Ann. Soc. Biomat. No. 71, 1978.
3. Walker, M.M. and Katz, J.L., Trans. 1 st. World Biomaterials Congress, No. 4.1.3, 1980.

This work was sponsored by NIH through NIDR Training grant # 5 T32 DE0 7054-5

Department of Biomedical Engineering
Rensselaer Polytechnic Institute
Troy, New York 12181

Experimental evaluation of 70% hydroxyapatite as a bone substitute in rabbits.

Satoshi Ishida, Hideaki Nagura, Naoya Yamashita, and Shoji Enomoto

The 2nd Department of Oral and Maxillofacial Surgery, Faculty of Dentistry, Tokyo Medical and Dental University, 1-5-45 Yushima, Bunkyo-ku, Tokyo 113, JAPAN

Hydroxyapatite (HA) has been considered as one of the best materials for the reconstruction of bone defect or tooth implant because of the excellent biocompatibility up to date.

It, however, has some disadvantages such as brittleness and difficulty to handle. We have developed a new material, HA containing 3G resin.

This investigation was aimed to evaluate the biocompatibility of the new composite material for bone and soft tissues.

Material and Methods

Material

The material used in this investigation composed of 70% weight of fine HA powder in 30% weight of triethylene glycol dimethacrylate resin (3G-resin). It has following physical properties: Young's modulus; 9.4 GPa, compressive strength; 274MPa, flexural strength; 60MPa.

Methods

1) Cytotoxicity test: Human cell line (Ca-9-22) which was established in our laboratory was used to examine the cytotoxicity effect upon this material.

The cells (5×10^4 cells/ml) were cultivated in Eagle's minimal essential medium supplemented with 10% fetal bovine serum in minivial and the test samples (13mm in diameter \times 1mm in thickness) were added to the test vials with concentration of $1 \mu\text{Ci/ml}$ of tritiumated thymidine on one, three, five, and seven days. Each sample after culture was counted by the liquid scintillation counter.

Thermanox sample was used for the culture as control.

2) Microradiographic examination and histological findings: Male albino rabbits were used to examine the histocompatibility in their bone or soft-tissues.

Inferior borders of the mandibles were precisely osteotomized in size of $2 \times 1 \times 2$ mm, and 70% OH.AP material ($2 \times 1 \times 30$ mm) were implanted between both osteotomized sites like bridge through the soft tissue under m. mylohyoideus. Animals were sacrificed for the histological examination on 2 weeks, 1, 3, 6 and 9 months after operation.

After roentgenographic examination, the grafted portion including 70% OH.AP was resected.

After the specimens were fixed in 10% Formalin solution, the undecalcified thin sections of approximately 50 μm in thickness were prepared.

These sections were examined with micro-radiogram, and were stained with 0.5% toluidine blue (pH 7.4 in phosphate buffer) to observe by light microscopy.

Results

1) Cytotoxicity test: The cells which were cultivated with test samples showed incorporation of tritiumated thymidine as fig.1.

Each point is the average of three replicate cultures, standard deviation being about 12%.

There was no significant difference between the new material and control.

No morphological changes were observed in each cultured cells.

2) Microradiographic findings: After a month, microradiographic findings showed thin new bone formation on the surface of implant at both sites of osteotomized mandible, but there was no sign of bone formation at it's surface of in the soft-tissue.

After three months, bony union between both sites was observed at the surface of the material, and the width of bone surrounding material increased with months.

3) Histological findings: After two weeks, no inflammation was observed, and osteoblasts around trabeculae and newly formed blood vessels were observed in the spaces between material and osteotomized surface of mandible. On the other hand implant was surrounded with fibrous tissue in the region of soft tissue.

After two months, new bone formation began at the mid-area of grafted material. But cartilaginous tissues were also observed at some part. After three months, implants were surrounded by bone, and after six months the material were covered by a thick bone tissue with bone marrow.

Conclusion

1) The results of cell culture indicated, there was no cytotoxicity effect upon the cell proliferation when compared with controls.

2) Histologically, bone formations were observed adjacent to the implants, after three months.

3) Above the results, demonstration of this material can be utilized as substitute for bone or tooth.

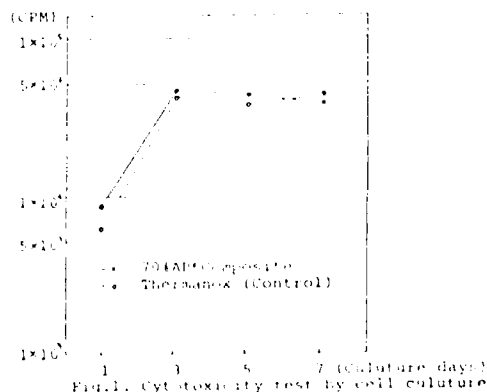


Fig.1. Cytotoxicity test by cell culture

Bone Regeneration in Canine Radius Defects
Treated by Coralline Implants and Iliac Grafts

Holmes, R.E. and Mooney, V.

University of Texas Health Science Center
Dallas TX

Intro: A previous study supported the concept that compact bone regeneration within a cortical bone graft is limited by the resorption of its osteons. Coralline hydroxyapatite porites (CHAP) implants, with microarchitectural similarities to osteon evacuated cortical bone, were found to become filled throughout with mature osteons. This per primum regeneration of compact bone within an implant suggested a potential benefit over cancellous autografts which depend on physiologic remodelling of the regenerated trabecular bone into compact bone to achieve adequate skeletal strength.

Hypothesis: In a diaphyseal defect the quantity of CHAP implant and its regenerated bone (CHAP+RB) will exceed the quantity of cancellous graft and its regenerated bone (GRAFT+RB) until physiologic remodelling is completed.

Implant: The aragonite exoskeleton of the colonial reef building (scleractinian) coral *P. porites* contains channel spaces averaging 230 microns in diameter. The channel walls (scleroseptae), averaging 95 microns in thickness, are highly fenestrated with channel inter communications averaging 190 microns in diameter. The dissepiments and thecae of the corallites are also highly fenestrated. For use as a bone graft substitute the coral is converted to hydroxyapatite in a hydrothermal exchange reaction with diammonium hydrogen phosphate.

Method: Mature dogs of 20-40 kg weight had bilateral radial diaphyseal windows created measuring 8 mm in width and 20 mm in length. One side received a CHAP implant and the other an iliac crest autograft. Four dogs were sacrificed at each of 3, 6 and 12 months. The radii were perfused with Karnovsky's fixative. The specimens were then infiltrated and embedded in PMMA and sectioned with a diamond saw. Approximately 20 sections from each specimen were stained with Alizarin Red S / Methylene Blue, Fast Green / Chromotrope 2R, or Hematoxylin / Eosin to permit easy identification of histological elements. The test side histoelements measured were implant (CHAP), regenerated bone (RB) and void space (VS). In the control side the graft and regenerated bone were measured together (GRAFT+RB). The measurement utilized a 25 element ocular grid, camera lucida attachment, and digitizing pad with multibutton cursor. For each sector the 25 histoelements sampled by the grid were identified and stored in a dedicated microcomputer. The descriptive statistics were prepared by time(3), segment(4) and sector(4). The 4 segments each represented a contiguous quarter of the stained sections in a specimen. The 4 sectors each represented a position within the stained sections.

Results:

Time	CHAP	RB	CHAP+RB	GRAFT+RB
3 mos	44.2	41.7	85.9	64.0
6 mos	43.6	46.3	89.9	63.1
12 mos	42.4	51.2	93.6	78.4

Table 1. Volume fraction (%) of histoelements at 3, 6 and 12 months.

Segment	CHAP	RB	CHAP+RB	GRAFT+RB
1	45.1	44.0	89.1	70.2
2	42.2	47.6	89.8	69.6
3	43.4	47.7	91.1	63.9
4	42.8	46.3	89.1	70.4

Table 2. Volume fraction (%) of histoelements in proximal to distal segments.

Sector	CHAP	RB	CHAP+RB	GRAFT+RB
1	43.4	46.7	90.1	73.6
2	44.6	45.0	89.6	60.8
3	43.4	46.2	89.6	64.3
4	42.1	47.6	89.7	75.4

Table 3. Volume fraction (%) of histoelements in medial to lateral sectors.

The implant was occupied by compact bone at 3 months with the small subsequent increases due in part to implant biodegradation. Corticalization of the graft did not begin until after 6 months and remained incomplete at 12 months. The quantity of CHAP+RB exceeded the quantity of GRAFT+RB ($p=.0002$). The segment and sector distributions of CHAP+RB and GRAFT+RB did not differ ($p=.264$; $p=.480$).

Discussion: The implant and graft differ in the morphology and quantity of regenerated bone. The implant and graft did not differ in their affect on the signals (mechanical? humoral?) responsible for the distribution by sector or segment of bone regeneration. The mechanical benefits of a composite material (CHAP+RB) with less void space suggest that the implant strength might equal or exceed the graft strength.

Supported by the Veterans Administration and the University of Texas Health Science Center, Dallas, TX.

Division of Orthopedic Surgery, University of Texas Health Science Center, 5323 Harry Hines Blvd, Dallas TX 75235.

CLINICAL TRIALS USING DURAPATITE FOR ALVEOLAR RIDGE AUGMENTATION

B.E. Sage*, S. S. Rothstein*, and D. A. Paris*

Sterling-Winthrop Research Institute
Rensselaer, New York

Following the extraction of teeth, the alveolar ridge resorbs. Since there are estimated to be over 20 million completely edentulous Americans with deficient alveolar bone, resorption of the alveolar ridge constitutes a major socio-economic problem. Methods to compensate for the loss of alveolar bone using different types of extensive surgical procedures with autogenous and homogenous transplantation of tissues have been no more retentive than the bone the patient has already lost through resorption. Alloplastic materials have been used with limited success.

Alveograf™, durapatite (18-40 mesh) has been successfully used to augment deficient alveolar bone in clinical trials. Durapatite is a non-resorbable, highly dense, particulate hydroxylapatite ceramic bone-grafting implant material. It has been shown to elicit essentially no inflammatory or foreign body response and no systemic or cytotoxic effects have been observed preclinically. New bone deposits directly on the surface of the particles thus providing a permanent supporting matrix for the deposition and maintenance of normal bone.

In this study, one hundred ninety eight patients had 207 ridge augmentations at six university-affiliated centers. Patients were examined by a prosthodontist and an oral surgeon to assess inadequacies in their removable dentures and in alveolar ridge support. In 69% of the cases durapatite alone was implanted while 31% used durapatite combined with autogenous bone marrow. Of these 207 augmentations, 24 (11.6%) used either durapatite alone or durapatite combined with bone marrow in conjunction with onlay and interpositional bone grafts, osteotomies or staples. After a healing period of 4 to 6 weeks, new dentures were constructed and delivered to the patients.

The augmented alveolar ridges were evaluated over a 24-month period by measuring panoramic radiographs for height increases and dental casts for width increases. The ability of the augmented ridge to support a denture was determined by evaluation of denture stability, retention, comfort and aesthetics. The patient also evaluated denture satisfaction using the modified Cornell Medical Index. Global evaluations by the oral surgeon

and the prosthodontist were also recorded. Safety of durapatite was assessed clinically and by laboratory tests.

Results show that durapatite reduces morbidity, does not resorb and provides a matrix for new bone growth. Negligible amounts of height reduction from the immediate postoperative period to follow up periods were observed with durapatite alone or durapatite with marrow. Practical advantages of durapatite are to provide a base for denture stability and retention by increasing alveolar ridge height and/or width without resorption.

*Sterling-Winthrop Research Institute
Columbia Turnpike
Rensselaer, New York 12144

SPREADING AND GROWTH OF EPITHELIAL CELLS ON HYDROPHILIC AND HYDROPHOBIC SURFACES

J.A. Jansen, J.R. de Wijn, J.M.L. Wolters-Lutgerhorst and P.J. van Mullem.

Depts. of Dental Materials, University of Nijmegen, Nijmegen, The Netherlands.

One of the parameters considered of interest for cellular interaction with alien materials but which is not yet fully understood is the surface free energy. One of the complicating factors is that the surface characteristics of a solid are changed in biological environments by the adsorption of proteins and/or lipids.

As a part of our research for permucosal aspects of dental implants we perform in vitro experiments with cultures of epithelial cells on various substrates. The purpose of this study is to determine:

1. the change of the wettability of solid materials after immersion in protein solutions.
2. the correlation between the wettability and cellular attachment.
3. the correlation between wettability and cellular spreading.
4. the relevance of wettability for the growth-rate of the cultures.

1 and 2. We reported on these items earlier (Jansen 1983). The investigated test substrates were: Teflon, PMMA, Tissue Culturing Polystyrene (TCPS, Falcon(R)), Carbon, Titanium, Gold (the last three vapour deposited on TCPS), synthetic apatite and glass. The wettability was determined by a pendant air-bubble method in bidistilled water and expressed in contact angle. The results showed that the wettability of the more hydrophobic surfaces (teflon, PMMA, carbon) was increased significantly after immersion in foetal calf serum to the level of the more hydrophilic surfaces (TCPS, apatite, carbon, glass, gold, titanium) the wettability of which did not appear to be altered by contact with serum. No significant relation was found between the percentage of attached cells (approximately 90% for all substrates) and the original wettability.

3. On the inner surfaces of TCPS-dishes, as received or after coating (vacuum evaporation) with titanium and carbon films and on teflon and glass discs, guinea pig epidermal cell suspensions derived from cultures prepared in our laboratory were seeded and incubated for 16 hrs. at 37°C and in 5% CO₂-atmosphere. Then, the non-attached cells were removed by rinsing with phosphate buffered saline and the attached cells were fixed and phluorescein stained with the aid of quantitative incident light microscopy the fixed cells were counted and the surface that was occupied measured. Thus, cell spreading could be determined and expressed in terms of average occupied surface per cell (S). Table 1 shows these results as well as the contact angles for and after immersion in serum (θ_0 and θ_1) that were determined in the earlier studies.

TABLE 1. Cell spreading (S) and contact angles θ

SUBSTRATE	$S(\text{mm}^2 \times 10^{-3})$	θ_0	θ_1
Glass	3.36	15.6°	16.8°
Titanium	5.04	19.3	19.9
TCPS	4.12	20.5	21.1
Carbon	4.33	43.3	21.4
Teflon	3.94	93.5	23.4

Although it seems that the cells had spread somewhat better on titanium surfaces, the standard deviation are so large (an estimated 50% of the mean value S) that the differences in S are not statistically significant. A correlation between the contact angles and cell spreading could not be determined.

4. Guinea pig epidermal cell suspensions of known cell concentration were seeded and incubated on the same substrates as used in the cell spreading experiment. The number of cells attached to the various substrates was determined with a Coulter counter after 6, 16, 24 hrs. and 3, 7 and 14 days. Three successive complete experiments were performed. The growth-rate of the cultures was determined in terms of percentage increase over 0-3 days, 3-7 days and 7-14 days and related to the corresponding rates of the cultures on TCPS. The results are compiled in Table 2.

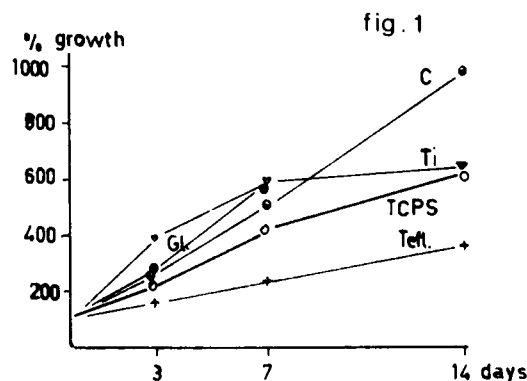
TABLE 2. Mean relative growth-rate on substrates

Incubation period	TCPS	Titanium	Carbon	Teflon	Glass
0 - 3 days	1	2.0	1.2	0.9	1
3 - 7 days	1	0.8	1.1	0.8	0.9
7 - 14 days	1	0.7	1.3	0.8	-

* values of one experiment only.

The growth curves are schematically given in Fig. 1. The general picture is that cells initially appear to grow faster on titanium and slower on teflon. However, eventually the numbers of attached cells are similar for all substrates except for carbon. From transmission electron micrographs it became evident that a multilayer growth pattern on this last substrate was responsible for the continuing growth of the culture, while on the other substrates only monolayer cultures were formed. The results of Table 2 and Fig. 1 do not indicate the existence of a correlation between growth-rate and wettability.

References: Jansen, J.A. and others, "In vitro studies on epithelial attachment to hydrophobic and hydrophilic substrates", 4th European Conference on Biomaterials, Leuven (Belgium) 1983, paper No. 48.



ULTRASTRUCTURAL STUDY OF EPITHELIAL CELL ATTACHMENT TO IMPLANT MATERIALS

J.A. Jansen, J.M.L. Wolters-Lutgerhorst, J.R. de Wijn, P.E. Rijnhart and P.J. van Mullem.

Depts. of Dental Materials, University of Nijmegen, Nijmegen, The Netherlands.

According to statistical evaluation (Cranin, 1977), the clinical success of endosteal dental implants is probably determined by the quality of the attachment of the gingival mucosa in the transitional area. Similar to the natural situation, hemidesmosomes are believed to play a mediating role in epithelial cell attachment to the protruding implant. This morphologically relevant cell structures are only discernable on the electron microscopical level. In in vitro culture of guinea pig epidermal cells hemidesmosomes have indeed been observed in the membranes of the cells adhering to the polystyrene dishes (Cristophers, 1975).

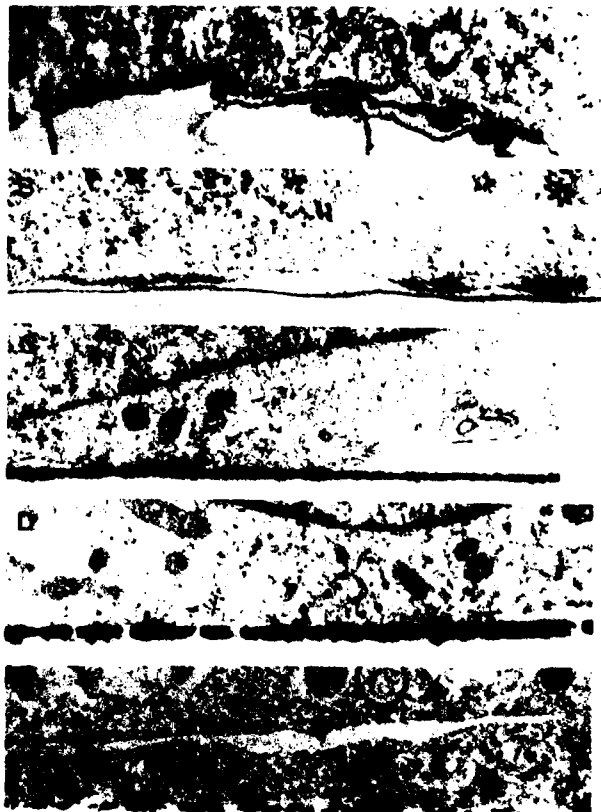
In vivo studies on the interface between oral epithelium and actual implants are hampered by the technical impossibility of obtaining implant material and adhering tissue in one and the same ultra thin section. Preceding disruption of the bond between implant and tissue may destroy the relevant information. To partially overcome this problem we developed a technique that allows for the preparation of ultra thin sections of metal/cultured cells interfaces (Jansen, 1982). The objective of this study is, by means of in vitro experimentation, to obtain more information on the morphology of tissue-implant interfaces and on the influence thereupon of the nature of the implant material.

On the inner surface of tissue culture polystyrene dishes (TCPS, Falcon^(R)), as received or after vapour coating with thin layers of titanium, gold and carbon, guinea pig epidermal cell suspensions, derived from cultures prepared in our laboratory, were seeded and incubated for 8, 11 and 14 days. Similar cultures were prepared on substrates consisting of sintered hydroxyapatite and carbonate apatite. At the end of the incubation period non-attached cells were removed by phosphate buffered saline rinses. The attached cells were fixed with 2.5% glutaraldehyde, OsO_4 postfixed and, together with the substrates, embedded in liquid epoxy resin. Ultra thin sections containing the metal, carbon or TCPS substrates as well as the cells attached to them were prepared. The apatite substrates, after unilateral embedding, were removed by "decalcification" in 5% nitric acid prior to counter-embedding and sectioning.

As shown in Figs. A and B hemidesmosome-like structures are observed in the membranes of cells cultured on the apatites and on TCPS. In these pictures the substrates are seen to be covered by a thin electron-dense layer presumably consisting of proteins. The cells seem to contact the substrate surface seldomly, being separated from it by a distinct layer of unidentified extracellular material. In contrast, the cells cultured on the metal and carbon surfaces (Figs. C, D, E) do not display any attachment structures in the interface although zonulae occludentes are present between adjacent cells. The presence of a protein layer cannot be confirmed in these images because of the electron density of the substrates.

Striking, however, is that intimate contact, between cells and substrate-surface occur much more frequently than in case of the non-metallic substrates.

In studies presented elsewhere (Jansen, 1983, 1984), attachment, growth rates and spreading behaviour of epithelial cells on similar surfaces were studied. The potential of the cells to attach was not found to differ for the various substrates although cells on titanium were observed to grow faster and spread somewhat better than for instance on TCPS and carbon. Comparing those results with the morphology revealed here leads to the conclusion that such differences in culture behaviour cannot be related to the presence or absence of attachment structures in the cell membranes and vice versa.



Micrographs of epithelial cell interfaces with:
A: apatite, magnification 38,700x. B: TCPS, 66,500x. C: titanium, 24,500x. D: gold, 24,500x. E: carbon, 24,500x.

References.

- Cranin, A.M. et al., JADA: 94, 315-329, 1977
- Cristophers, E. et al., Nature, 256, 209-210, 1975
- Jansen, J.A. et al., Advances in Biomaterials, Vol. 4, pg. 271, John Wiley, 1982
- Jansen, J.A. et al., 4th Eur.Conf. Biomat., Leuven, 1983, abstr. 48.
- Jansen, J.A. et al., 2nd World Cong. Biomat., Washington, 1984, submitted.

GINGIVAL ATTACHMENT AT PERIMUCOSAL DENTAL ROOT IMPLANTS OF DENSE HYDROXYL APATITE

DE LANGE, G.L., DE PUTTER, C., DE GROOT, K.

Free University, Dept. of Oral Biology, School of Dentistry, P.O.Box 7161, 1007 MC Amsterdam, The Netherlands

One of the most important factors for success of a perimucosal implant is acquiring an effective biological seal around the cervical part of the implant. In healthy natural dentition teeth are surrounded by an epithelial attachment of junctional epithelium and by a network of supra alveolar collagen fibers firmly connected to bone and teeth. Both epithelium and connective tissue are maintained by continuous renewing of tissues, thus forming an effective biological seal (1,2). Inadequate sealing of mucosa is always accompanied by disruption and breakdown of this gingival attachment apparatus, leading to bone resorption and excess tooth mobility, finally resulting in loss of teeth (3). If this failure is mainly caused by lack of gingival attachment - as it does in natural dentition - much attention must be paid to the nature of gingival attachment at dental root implants.

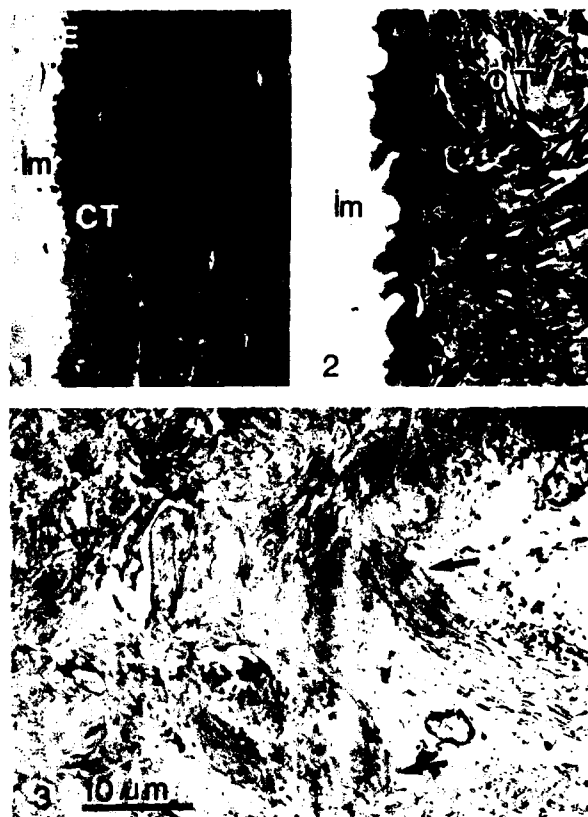
Root implants of sintered calciumphosphate were placed in predrilled holes in edentulous parts of the lower jaw of premedicated dogs. The implants were loaded and left in situ for one to two years and inspected weekly (4). Thereafter the dogs were sacrificed and their jaws fixed. Histological sections were made for light and electron-microscopy. The interfaces between implant and soft tissues were compared with neighbouring natural teeth. The following results were obtained:

Implants with a healthy gingiva were lined on the oral side with a thin limited layer of flat and non-keratinized epithelial cells (Fig. 1). These cells showed the same characteristics as a normal junctional epithelium surrounding natural teeth. It was followed by a small zone of connective tissue of about 0,2 mm length, which was free of inflammation. On lower level, still far above alveolar bone, the implant surface was covered by a calcified tissue (Fig. 2) which was continuously connected with alveolar bone (6). Thick gingival fiber bundles were embedded in this layer, just as in natural root cementum (Fig. 3). From this study several conclusions could be drawn.

1. Gingiva was fixed at implant surface.
2. Fixation of gingiva was of biological nature.
3. Attachment of gingival fibers was comparable with fixation around natural teeth.

References:

1. M.A.Listgarten (1966) Am. J. Anat. 119: 147.
2. R.M.Frank et al. (1972) J. Periodontol. 43: 597.
3. S.Schlager et al. (1977) Periodontal disease: Lea and Febiger, Philadelphia.
4. C.de Putter et al. (1983) J.Prosth. Dent. 49:87.
5. C.de Putter et al. (1984) Abstract 10th Ann. Meeting Soc. Biomat.).



Figs 1 and 2. Light micrographs of gingiva bordering implants of dense hydroxylapatite. Implants (Im) removed by decalcification.

1. Gingiva shows a well limited seal of non-keratinized epithelium (E) and a small zone of connective tissue (CT). Both tissues had a close adaptation to the implant surface which was rough in texture.
2. Tip of growing calcified tissue layer covering the implant (I) has a few cells and contains embedded gingival fibers (arrow).
3. Electron micrograph of connective tissue of gingiva surrounding the hydroxylapatite implant. Collagen fibers of gingiva (arrow) are embedded in the calcified tissue which covers the implant surface.

Behaviour of alveolar bone around permucosal dental implants of dense hydroxylapatite.

C. de Putter, G.L. de Lange, K. de Groot,
P.A.E. Sillevs Smitt, A. Kootwijk.

Depts. of Prosthetic Dentistry and Biomaterials
Free University, Amsterdam, The Netherlands.

Permucosal dental implants of dense hydroxylapatite are, like ankylotic natural teeth, in contact with three different tissues: epithelium, underlying connective tissue and bone. For clinical permucosal application of these implants these three interfaces have to be studied, as well as the mechanical behaviour of the hydroxylapatite itself. About the bio-mechanical properties of the implants, the fatigue failure and the prevention of fractures due to fatigue, by prestressing of the implants was reported earlier (ref. 1,2), as well as about clinical aspects and histological findings of implantations in animal experimental studies (ref. 3.)

In this report we describe more in detail the attachment of the implants in alveolar bone, where the most interesting point is the point of the transition to the mucosal tissues: being the supra-bony connective tissues. (The results with regard to epithelium and connective tissue are presented in the paper of Dr. De Lange). There is a strong cohesion between the behaviour of the soft mucosal tissues and bone: only by a good attachment of the epithelium and connective tissue the ankylotic attachment of the alveolar bone to the implant can come to existence and be protected.

Materials and methods.

The nature and the level of the attachment of the alveolar bone to the implant is studied for this report in two ways:

A. Histology: 56 solid implants of dense hydroxylapatite were implanted in 7 Beagle and 5 Mongrel dogs (ref. 2). After implantation periods of 6-24 months the implants were studied by light and electron microscopy both in undecalcified and decalcified state.

B. Roentgenology: 28 prestressed implants were placed in 4 Beagle and 2 Mongrels dogs (ref. 1,2). Every week standardised X-ray photographs were taken for a period of 26 weeks. The distance from the lower-side of the upper cap of each prestressed implant until the bone-level on the mesial and distal side was measured after a standardised 5x magnification of the X-ray photographs.

Results.

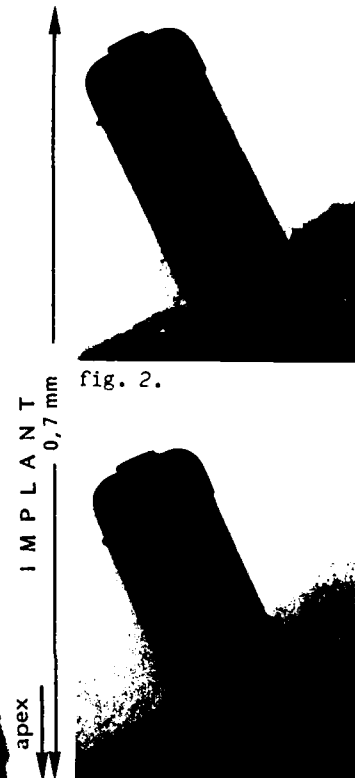
A. Histology: A direct ankylotic bonding of bone to the hydroxylapatite is shown. A thin layer of newly formed bone is growing up along the implant surface. In this same calcified layer are, higher on the level of the supra-bony gingival tissues, collagen fibers attached. (fig. 1)

B. Roentgenology: This upgrowth of bone is confirmed and quantified on the photographs. In most of the cases the level of attachment decreased the first few weeks after implantation (fig. 2), whereafter repair and upgrowth followed (fig. 3). The highest level was reached after about 16-20 weeks, whereafter stabilisation or decrease of the level followed. It appeared that in 69.3% of the measured sites absolute upgrowth had taken place 26 weeks after implantation, on a distance of 0.5

till 1.78 mm. In 30.7% of the cases a lower level of attachment was found: 0.06 until 2.38 mm.



fig. 1.



Discussion and conclusion.

Loaded permucosal dental implants of dense hydroxylapatite showed the ability to stimulate new bone formation. Formation of new bone was completed as measured on X-rays in about 16-20 weeks. It is stated that this favourable situation of alveolar bone, as also shown histologically, can only be reached by connection of supra-alveolar soft tissues to the implant, protecting the ankylotic attachment of the bone.

References.

1. C. de Putter et al. in: Ceramics in Surgery, p. 395, Elsevier Publ. Comp., Amsterdam, 1983.
2. C. de Putter et al. Book of Abstr. 9th Ann. Meeting. Soc. for Biomat. no. 27, 1983.
3. C. de Putter et al. J. of Prosth. Dent. 49:87, 1983.

Address: C. de Putter, Departments of Prosthetic Dentistry and Biomaterials, Free University, P.O. Box 2161, 1007 MC Amsterdam, Holland.

A LONGITUDINAL HISTIOMETRIC EVALUATION OF MICROSTRUCTURES SURROUNDING
SEMI-BURIED DENTAL IMPLANTS

R.G. Daniells and R. A. James

Loma Linda University SD
Loma Linda, CA

Dental implants are being used clinically in ever-increasing numbers, but little is known about the development of the microstructures around these devices. Some claim connective tissue lies at this interface while others claim epithelium lies at this interface; structures noted in the early stages of the healing and alleged to be epithelium may in fact be endothelium involved in the microvasculature. This study seeks to clarify this matter along with changes seen in the developing bone, microvasculature, and peri-implant ligament.

Semi-buried endosteal implants of surgical Vitallium[®] were randomly placed in monkey jaws at specific time intervals (14, 30, 60 and 90 days). The monkeys were perfused with india ink and calf serum and the peri-implant tissues were recovered and examined for histopathologic response and microvasculature in sagittal and transverse planes in four different zones.

(Illustrations to be inserted here later.)

Findings - Fourteen Days:

The end of the epithelium was easily defined and appeared to be well differentiated, extending apically along the implant post approximately 1.21 mm from the gingival crest and was confined to zone 1. The osteotomy showed an early framework of osteoid material developing between implant and the original cut bone. There was also an area of osteoclastic activity showing evidence of remodeling in zone 3. The width of the ligament between bone and implant was 0.086 mm in zone 2, 0.076 mm in zone 3, and 0.356 mm in zone 4; wider than in later specimens, especially in the area of the blade. Blood vessels were well differentiated and a vascularity index found the 14 day microvasculature to be fewer in number and larger in size than in later specimens. Index figures for the 14 day specimens were 28% for zone 1, 40% for zone 2, 47% for zone 3, and 45% for zone 4.

Thirty Days: The epithelium had extended further apically along the post to an average distance of 1.35 mm from the gingival crest but was still confined to zone 1. The osteotomy had a more advanced development of new bones along the implant than previous specimens. The ligament space between bone and the implant was on the average narrower than the 14 day specimens, particularly in the area of the blade. The width of the ligament measured 0.054 mm in zone 2, 0.076 mm in zone 3, and 0.043 mm in zone 4. Vascularity was increased from the amount of the 14 day specimens with an average index of 48% in zone 1, 40% in zone 2, 59% in zone 3, and 55% in zone 4.

Sixty Days: The epithelium had extended further apically along the post to an average distance of 1.56 mm from the gingival crest to the end of the epithelium and was still confined to zone 1. The osteotomy was sparsely filled with well differentiated new bone, a definite layer of which lay very close to the implant with some

areas showing no evidence of a connective tissue layer interposed. Average ligament width for the sixty day specimens was 0.32 mm in zone 2, 0.022 mm in zone 3, and 0.010 mm in zone 4. Vascularity again was increased in number from previous specimens and the index was 57% in zone 1, 63% in zone 2, 63% in zone 3, and 63% in zone 4.

Ninety Days: The epithelium had advanced to an average length of 2.73 mm and still was confined to zone 1. The osteotomy contained well differentiated new bone, and as seen in the sixty day specimens, a definite layer in some areas had no evidence of a connective tissue layer interposed. The average ligament width was 0.021 mm in zone 2, 0.032 mm in zone 3, and 0.010 mm in zone 4. The microvasculature showed increased numbers from previous specimens but smaller lumen size than any previous specimens. The microvasculature index for zone 1 was 69%, zone 2 was 75%, zone 3 was 75% and zone 4 was 70%.

Discussion:

There was a general decrease in ligament width with time and with distance from the gingival crest. The microvasculature decreased in lumen size and increased in number with time. There was a slight increase with time in the distance from the gingival crest to the end of the epithelium as measured along the implant surface. This distance increased 1/2 mm during the last seventy-six days of the study. No epithelium strands were noted in the developing tissue as others have reported.

R.G. Daniells
Loma Linda University
School of Dentistry
Loma Linda, CA 92350

John C. Keller and Franklin A. Young

Department of Materials Science, Medical University of South Carolina,
Charleston, South Carolina 29425

INTRODUCTION

Previous work by the authors and others has established that bone ingrowth into porous surfaces is a suitable method of fixation of dental implants. The success of porous implants is also dependent in part, on the prevention of apical migration of soft tissue into the implant site. Descriptions of the changes that occur in hard and soft tissues surrounding dental implants have remained largely qualitative in nature. Few quantitative descriptions of such alterations in tissue structure with time due to the presence of implants have been made.

The purpose of this work was to study the long term histological effects of the presence of porous rooted Ti alloy implants using histomorphometric analyses of ground sections. Tissue sections of implant sites prepared by conventional LM techniques (decalcified and paraffin embedded) were also studied for the effects of the implants on the surrounding soft tissues.

MATERIALS AND METHODS

In this work, a two stage dental implant consisting of a porous surface endosseous root and a smooth pergingival abutment were fabricated from Ti-6Al-4V. The porous roots were implanted into the mandibles of 14 previously edentulous Rhesus monkeys. After an initial healing period of 4-6 weeks which allowed for bone ingrowth and gingival healing to occur, the smooth surfaced abutment was placed into the pre-threaded root.

The implants were in function for periods of 0.5-60 months, at which time the animals were sacrificed and the mandibles were fixed in formalin. Ground sections were prepared by embedding blocks of tissue containing implants into low viscosity plastic embedding media. Multiple sections were cut, polished to 30µm and were stained with alizarin Red S and toluidine blue for the study of calcified tissues adjacent to and within the pores of the implant. Microradiography of the ground sections was performed for further qualitative evaluations of bone ingrowth.

Histomorphometric analyses of the ground sections were used to quantitatively describe various parameters of bone ingrowth into the porous implant roots for short term (< 2 years) and long term (2-5 years) implants. Parameters that were investigated were the percentage of bone in the surface and internal pores (see Table).

Thusfar 10 implant sites have been prepared to study the short term effects, while 13 implant sites have been prepared to study long term effects of implantation.

Eight additional long term implant sites were prepared using conventional LM techniques in order to more fully evaluate the interface between the tissue and the implant. After

decalcification, the implants were dissected from the tissues, which were then embedded in paraffin, cut in 6-8µm sections and stained in order to study the responses of the soft tissues to the long term presence of the implants.

RESULTS AND DISCUSSION

Initial histomorphometric analysis of the ground sections (Table) revealed an apparent increase in the percentage of bone occupying the entire porous surface of the implants as a function of time after implantation. The enhanced bone ingrowth that occurred with long term implants apparently took place in the portions of the implant originally placed into cancellous bone which included the base. Due to the stresses of long term function, the trabecular bone pattern became closed along the length of the implant and was oriented horizontally to the long axis of the implants. Deposition of dense, mature bone, occurred in the margins of the implants placed into cortical bone, but this process apparently was not significantly affected by increased implantation time.

Tissue sections prepared by conventional LM revealed areas of fibrous connective tissue adjacent to the abutments of the implants. Areas of slight to moderate inflammation were present within the connective tissue, but did not extend beyond the height of the crestal bone. There was no apparent migration of epithelium or inflammation in the implant crypt.

CONCLUSIONS

The responses of the tissues surrounding long term porous rooted implants assisted in the support of masticatory loads. Bone remodeling occurred around the implant and showed little sign of deterioration. Soft tissue responses did not interfere with the long term success of the implant.

Initial Histomorphometric Analyses
of Percent Bone Ingrowth in Porous Areas (%)

	Entire Implant Surface	Cortical Areas	Base	Cancellous Areas
Short Term	56.3+ 17.1	57.8+ 25.6	68.8+ 4.0	43.0+ 23.3
Long Term	64.7+ 10.0	64.2+ 21.5	75.6+ 17.1	54.5+ 10.1

Supported by NIH-NIDR DE03497.

Porous Implants: Interfacial Considerations

R.M. Pilliar

Faculty of Dentistry, University of Toronto
Toronto, Ontario CANADA

The past three decades have witnessed extensive experimentation with surgical implants designed to permit integral tissue-implant bonding by direct tissue ingrowth into porous structured implants. As a result, implants so designed are presently being used in cardiovascular, orthopaedic and dental applications. The rationale for such a design approach relates to the achievement of effective implant-tissue bonding to satisfy various performance criteria for the implant dependent on its exact application. Thus, load-bearing orthopaedic or dental implants will be designed to allow strong interface bonding by suitable connective tissue ingrowth. A blood-interfacing component with a porous region for attachment of a pseudoendothelial layer would utilize quite different structures with different pore sizes and materials, for example, being required.

This paper will attempt to review the wide variety of applications in which porous structured implants appear to have been successfully utilized. A complete understanding of the process of tissue ingrowth in the different areas is not presently available and this has resulted in implant designs that probably are not optimal. The problem of acquiring a better basic understanding of the processes involved during intra and inter porous tissue development will require sophisticated studies both for characterizing the porous regions (including characterization of the surfaces within the pores) and the nature of the enveloping tissue from early post-implantation periods to times at which mature tissue has finally formed.

Although our present state of knowledge of the ingrowth phenomenon is limited, porous implants (either partially or fully porous) are being used with at least an acceptable degree of success for the time periods experienced to date. It is generally recognized that these porous implants introduce new variables such as increased implant surface area, altered stress states in tissue adjacent to the implant (because of good interfacial bonding) and changing elastic properties as the tissue ingrowth and maturation process continues. The consequences of these new design variables are only now being studied by a relatively small number of investigators.

It appears that porous implants offer a potentially useful approach to solving some of the more perplexing problems associated with materials used in implant applications including loosening of orthopaedic and dental bone-interfacing implants and thrombosis of blood-interfacing cardiovascular implants. However, a continued effort toward a better understanding of the phenomena operative both locally (within and next to the porous structures) and more

globally (near to the implant and systemically) is essential to avoid misuse of this approach.

Faculty of Dentistry, University of Toronto
124 Edward Street, Toronto, Ontario M5G 1G6

R.A. White

Harbor/UCLA Medical Center
Torrance, California

Porosity improves the long-term blood compatibility of many synthetic cardiovascular implants. Impervious materials are successful only in high-flow, high-shear applications or when thromboresistant collagen tubes or autogenous tissue are used. Although the importance of porosity in synthetic vascular prostheses remains controversial, nonporous materials do not remain patent when used as small internal diameter arterial substitutes.

Porosity is a parameter which is difficult to describe quantitatively. Wesolowski described the permeability of fabric prostheses as the volumetric water flow through the fabric at a pressure differential of 120mm Hg. An alternative definition of porosity is the ratio of open space to solid (by volume, area or weight) of a material. Overall, it is important to characterize and describe as extensively as possible the pore size and shape, the dimensions of interporous connections and the permeability of prosthetic materials.

Porous synthetic materials have been used clinically and experimentally in several applications. Fabric materials, in particular Dacron[®], have been used extensively for vascular replacement, cardiovascular patches, and cardiac valve ring and strut coverings. More recently, expanded polytetrafluorethylene (PTFE) which has a rented 30-40 μ m porous node and fibril configuration has provided improved thromboresistance and is being used in more challenging clinical situations such as small internal diameter arterial and venous replacements. Currently other synthetic polymers including polyurethane and silicone rubber are being evaluated as small internal diameter vascular prostheses, flow surfaces for circulatory assist devices and as components of artificial hearts.

There are several generalized statements which can be made regarding porous cardiovascular implant materials. Materials with pore sizes less than 15 μ m are minimally incorporated with tissue. Pores less than 5 μ m prevent ingrowth. Materials with pore sizes from 20-45 μ m become infiltrated with well-vascularized fibrohistiocytic cellular elements. Materials with pores greater than 50 μ m become rapidly infiltrated with fibrous tissue. Recent work has demonstrated that implants with a 20-45 μ m pore size have a higher Type III collagen content than those greater than 50 μ m which consist predominantly of Type I collagen. Preliminary experiments suggest that these differential biochemical responses have an influence on the long-term mechanical characteristics of the implant such as compliance and predisposition to calcification. Pore size also has an affect on the rate and quantity of tissue ingrowth which is related to material, particularly in the 20-45 μ m pore size implants. For example, silicone rubber prostheses are more slowly and minimally infiltrated with cellular elements while polyurethane implants become more rapidly and completely ingrown.

The degree of tissue ingrowth required for adequate function of a cardiovascular prosthetic is related to the site of implantation. In high-flow cardiac or large internal diameter central vascular

implants larger pore sizes permit rapid tissue incorporation and stabilization of a nonthrombogenic flow surface. Rapid incorporation of highly porous prosthetic materials has been shown to decrease the susceptibility to infection in systemic sepsis, to improve the anchoring of the prosthesis to surrounding tissues preventing seromas and perigraft hematomas, and to improve flow surface endothelialization. Clinically, however, porous vascular conduits with greater than 5000cc/min/cm² have excessive transmural bleeding at the time of implantation and require preclotting. Small internal diameter vascular replacements or applications requiring immediate thromboresistant surfaces such as linings for an artificial heart require small pores or smooth surfaces.

Pore size also has an affect on the thrombogenicity of the luminal surface. Polymeric prostheses with pore sizes of 20-45 μ m are less thrombogenic than prostheses with pore size of 100-300 μ m. This principal is illustrated clinically by the more thromboresistant nature of the 20-40 μ m PTFE prostheses and of Dacron velour grafts. The effect of porosity of thrombogenicity is, in part, attributed to the roughness of the surface. In high-flow cardiovascular applications smooth, polished, nonporous surfaces are functional by preventing accumulation of cellular debris. Surface defects of 1-2 μ m stimulate thrombus formation. In low-flow, small internal diameter vascular prostheses, smooth nonporous surfaces initially provide thromboresistance but they do not maintain long-term patency. Recent studies have resolved this dilemma by suggesting that smoother, porous coatings with thromboresistant materials enhance the thromboresistance yet maintain the advantages of porous prostheses.

In light of these observations, it has been proposed that there are two alternatives for designing improved cardiovascular flow surfaces: 1) development of a material that is completely nonthrombogenic and blood compatible, and 2) a porous prostheses with a smooth flow surface which accumulates a minimal protein and cellular layer which eventually becomes thromboresistant or endothelializes. Fundamental to resolving this question is determining whether prosthetic permeability is required only for transmission of fluid and ions or if tissue ingrowth is required. It also remains to be determined whether a thromboresistant porous coating will remain patent indefinitely or if endothelialization is required. Recent advances in cell seeding techniques may offer an interim solution. For example, initial studies of endothelial seeding concluded that Dacron arterial prostheses with water porosities of 1,400-1,600ml/min/cm² and limited amounts of fabric in a luminal weft-knit are optimum for seeding techniques.

Division of Vascular Surgery, Harbor/UCLA Medical Center, 1000 West Carson Street, Box 304, Torrance, CA 90509.

ADAPTIVE BONE REMODELLING WITH POROUS INGROWTH FEMORAL SURFACE REPLACEMENT

D.R. Carter, R. Vasu, and W.H. Harris+
Design Divison, Mechanical Engineering Dept.,
Stanford University,
Stanford, CA 94305 and VA Medical Center, Palo Alto, CA 94304

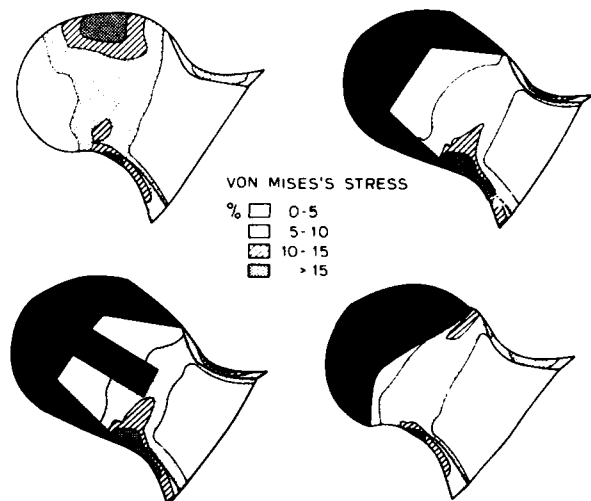
It was hoped that surface replacement arthroplasty would be a reconstruction procedure that is especially suitable for younger patients. The failure rates of many types of cemented surface replacement components, however, are disappointing. Numerical and experimental stress analyses of these devices have offered some mechanical explanations for the clinical failures (1,2). Porous ingrowth (uncemented) surface replacement designs in dogs have shown promise (3). A major problem with these components, however, is the adaptive bone remodelling which results in response to alter stress fields. In particular, the use of metal pegs for initial fixation was found to have a pernicious influence; causing extreme remodelling, loss of proximal bone support, and eventual implant failure. Implants without pegs were much more successful (3).

In this study, finite element stress analyses were conducted of the canine femoral head before and after implantation of surface replacement-type components. Four implant geometries were investigated; a) shell, b) shell with peg, c) shell with rod, and d) a new, epiphyseal replacement design. All implants were modelled to simulate bony ingrowth along the underside of the shell and along the surfaces of the peg and rod. The influences of implant material (co-chrome vs. polyacetyl) and adaptive bone remodelling on the stress fields were examined.

The computer models were constructed using the right and left femoral head and neck of an adult dog. One femur served as the normal model and the other was prepared with a surface replacement shell/rod design. The femoral heads were sectioned to obtain geometry and bone porosity distributions. The generated models used 2-D elements (constant strain triangles and quadrilaterals) of varying thickness. The thickness of each element was established by the principal of equivalent thickness composite models. Each element was thus considered to be a possible combination of cortical bone, cancellous bone, and metal as required by their presence and amount within the element region. Each model consisted of about 300 elements. The loading simulated the joint reaction force during gait.

The results indicated that in the normal femur the stresses are

transferred from articular surface through the femoral head cancellous bone to the inferior cortical shell of the femoral neck. After shell-type surface replacement, stresses were transferred more distally at the rim of the shell and at the end of the peg or rod, thereby reducing the stresses in the proximal head cancellous bone (Fig.). The stress distributions of the shell/peg design were strikingly similar to the bone remodelling changes previously reported (3). Computer simulation of bone remodelling due to proximal bone stress reduction was shown to accentuate the abnormality of the stress fields, suggesting a vicious cycle of remodelling and eventual failure. Surface replacement with a lower modulus material created a less abnormal redistribution of bone stresses.



The new epiphyseal replacement design resulted stress distributions similar to those in the normal femoral head and minimal shear stresses at the implant/bone interface (Fig.). These findings suggest that the epiphyseal replacement concept may provide better initial mechanical integrity and create a more benign milieu for adaptive bone remodelling than conventional, shell-type surface replacement components.

(1) Shybut, et al. (1980) Proc. 8th Mtg. Hip Soc., pp. 192-224.

(2) Huiskes, R. and Heck, J. van (1981) Proc. ORS 6:174.

(3) Hedley, A.K. (1980) Proc. 8th Mtg. Hip Soc., pp. 329-337.

+Ortho. Res. Labs., Mass. General Hosp., Boston, MA 02114

*Supported by NIH Grants AM32378 and AM01163 and Howmedica, Inc.

THE EFFECT OF BONE IMPLANT APPPOSITION ON BONE INGROWTH INTO CANINE ACETABULAR POROUS METAL IMPLANTS.

M. Jasty, N.F. Jensen, E.H. Weinberg, S.P. Rogers and W.H. Harris

Orthopaedic Research Laboratory, Massachusetts General Hospital, and Harvard Medical School, Boston, MA 02114.

The magnitude of the problem of long-term mechanical loosening of cemented total joint implants has created interest in biologic fixation using porous metallic implants. Although many studies have been done to show that bone does grow into pores of these implants, few have been done on weight bearing joint implants, and most are done under variable experimental techniques which have not determined bone ingrowth in a quantitative manner. We approached the problem of quantification of bone ingrowth by developing an image analyzer. With this we then studied a key parameter on bone ingrowth: apposition of the implant to the bone bed in canine total hip replacement.

Methods: The implant design was hemispherical with three flanges from the rim, through which three screws are inserted into the pubis, ischium and ilium. Chrome cobalt spheres of two different sizes, mean 450 μ and 850 μ , were sintered into the chrome cobalt implant 3 layers thick obtaining a mean pore size of 187 μ and 450 μ . The acetabulum contained a polyethylene liner designed to fit a femoral resurfacing arthroplasty.

The surgery was carried out on 10 fully mature mongrel dogs (either sex) weighing at least 25kg. In four dogs the acetabulum was reamed without particular attention to obtaining intimate, and uniform contact between the implant and the bone bed. Postoperative radiographs showed radiolucencies ranging from .5mm to 1mm covering 40 to 80% of the implant surface in all dogs. Precise surgical techniques were employed in the remaining 6 dogs to ensure intimate contact of the implant to the bone bed. The acetabulum was carefully reamed at 1/2mm increments. A pressure sensitive film (Fugi Prescale) was placed in the acetabulum and the implant was lightly tapped over it. This film shows a color pattern, the density of which corresponds to the pressure applied. On inspection if there is uniformly good contact between the implant and the bone bed the component is fixed in that position. If the contact is not uniform, further reaming is carried out till there is uniformly excellent apposition. All of the six dogs achieved intimate apposition and did not show radiolucencies of postoperative x-rays.

Sacrifice was carried out at 12 weeks. The entire acetabulum including the implant was removed, fixed and dehydrated. Whole acetabulae were embedded in methyl methacrylate and serially sectioned, ground to 300 μ and microradiographed. The specimens were then attached to glass slides and ground further to 50 μ using a lapping apparatus, and were stained with hemotoxylin, eosin, and paragon stains for histologic examination.

The amount of bone ingrowth into the implant was assessed by using computer assisted image analysis. A TV camera was attached to the microscope and the signal was digitized by a high speed frame buffer, and processed by a PDP 11/23 computer. The area fraction of the implant beads and the area fraction occupied by the bone within the porous part of the

implant as a percent of the total area available for bony ingrowth were determined.

Results: Computer assisted areal fraction measurements showed that for the acetabulae which did not achieve intimate contact, bone occupied $6.7\% \pm 2.3\%$ of the total area present within the porous layer of the implant. For the acetabulae with intimate contact throughout the implant, a mean of $12.5\% \pm 1.47\%$ of bone was present within the porous layer. The beads themselves occupied 50% - 70% of the total area from the solid substrate to the top of the porous layer.

Histologic examination of sections of acetabulae with intimate apposition showed fully mature bone trabeculae uniformly within the pores of the implant. There were only occasional areas of fibrous tissue ingrowth.

In the sections from the acetabulae without intimate apposition the bone ingrowth was only noted at the periphery of the implant. The remaining area only achieved fibrous ingrowth. Many islands of fibrocartilage were noted around the implants. In some areas there was calcification of the cartilage and metaplasia into bone. In other areas the bone had formed a new subchondral plate and there was no evidence of osteogenesis adjacent to the implant.

Conclusions: The controversial point about the importance of implant apposition to the bone bed in generating bone ingrowth has been addressed. In our experimental study using loaded acetabular bone ingrowth implants in mature dogs, we could compare the amount of apposition achieved at surgery, to the amount of resulting bone ingrowth into the implants. Significantly more bone ingrowth took place into the implants when intimate contact was achieved between the implant and the prepared bone bed at surgery. In the implants where intimate apposition was not achieved, the bone ingrowth was inferior both quantitatively and qualitatively.

Figure 1-A. Microradiograph of an implant with excellent apposition and bone ingrowth.



Figure 1-B. Inferior ingrowth into an implant which did not have intimate apposition at surgery.



In Vitro Mechanical Testing of Porous-coated Orthopedic Implant Support in Bone After 1 Year: Differences Between Fibrous Tissue Support and Bone Ingrowth

J. Michael Lee, Robert M. Pilliar, David Abdulla, and J. Dennis Bobyn*

Biomaterials Research, University of Toronto, CANADA

INTRODUCTION

If bone ingrowth is to occur with porous-coated orthopedic implants, relative movement between the device and the surrounding bone must be limited. Otherwise, calcification does not occur, and the device is supported (if at all) by soft fibrous tissue. Using a canine segmental replacement model, Pilliar et al.¹ demonstrated that early loading of intramedullary rods can lead to the appearance of a radiopaque line (or halo) surrounding the implant. A similar radiographic feature has been observed in some human cases. They showed that this line corresponds histologically to a region of dense bone surrounding the implant but not contacting it. The gap is filled with fibrous tissue aligned in the direction of stress. We have used this model system to produce intramedullary rods supported by: (1) bone ingrowth, and (2) fibrous tissue. An in vitro testing jig has been developed for direct testing of the viscoelastic properties of the tissue support under physiological conditions.

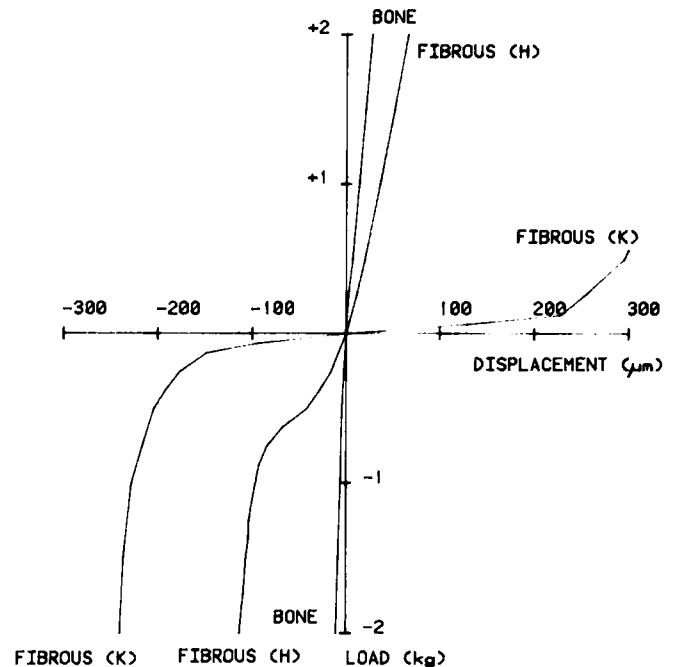
METHOD

Segmental replacements were constructed from 316L stainless steel, with each intramedullary rod partially porous-coated with sintered Co-Cr-Mo powder. Bone segments from the right femurs of 10 adult beagles were replaced with the devices. The intramedullary rods extended well into the cancellous bone at each end of the femur, and the animals loaded the limbs 2-3 days after surgery. Nine implants were harvested after 1 year. While some implants showed plastic deformation of the stainless steel rods, and some ends were loose due to excessive rotation, two relatively "pure" cases did develop: (1) one femur showed a uniform radiographic halo at each end, indicating fibrous tissue attachment; (2) one femur showed radiographic evidence of bone ingrowth.

Mechanical tests were conducted in a tissue bath containing circulating Hanks solution at 37°C. The explanted femur was separated into two halves using its central male-female screw connector and 1 cm of bone was removed from the base of each intramedullary rod with a Dremel tool. This exposed uncoated rod and left a ledge of cortical bone. Each half was connected to a tension-compression cell and embedded in Vel-Mix gypsum dental stone for compressive support. The bone was set wet for ½ hr and lowered into the tissue bath where stainless steel cantilevers were placed under the coupler and against the cortical ledge for tensile support. Each implant was subjected to cyclic loading between 2 kg tension and compression and examined for stress relaxation at ± 1 and ± 2 kg. After testing, the sample was fixed, embedded in PMMA, and examined using ground sections and polarized light.

RESULTS

The two samples (4 femoral ends) tested showed distinct mechanical differences between the bone-implant interface and the fibrous tissue-implant interface. The bone-ingrown sample showed linear load-deformation curves with different slopes in the tensile and compressive directions.



Stress relaxation results were symmetric about zero load. Little strain rate dependence was observed. The fibrous tissue supported sample displayed non-linear load deflection curves. Greater stress relaxation and strain rate dependence were seen than in the bone-supported sample. Stress relaxation results were no longer symmetric about zero; greatest relaxation occurred in the compressive direction. Histological study confirmed the radiological findings. However, in the case of fibrous tissue support, quarter-wave polarization revealed collagen oriented both normal and parallel to the implant surface. Helical orientation of fibers was found in the distal (knee) half of the implant. This was due to greater rotational freedom which contributed to the compliance of this segment in load-deflection tests (Figure). Our results confirm that early loading can lead to implant support by fibrous tissue alone, with a greater viscoelastic "shock-absorbing" character. The clinical adequacy of this support remains to be assessed.

REFERENCE

Pilliar RM, Cameron HU, Welsh RP, Binnington AG (1981) Clin Orthop 156: 249-257

ACKNOWLEDGEMENTS

This work was supported by a grant from the Medical Research Council of Canada. Dr. Lee is an MRC post-doctoral fellow.

ADDRESS

Dr. J. Michael Lee, Biomaterials Research
Faculty of Dentistry, University of Toronto
Rm. 405, 123 Edward St., Toronto, Ont.
CANADA, M5G 1G6

*Ecole Polytechnique, Montreal, CANADA

Three Types of Corrosion in 316L C.W. Implantable Stainless Steel

Lautenschlager, E. P., Taira, M. and Lautenschlager, J. A.

Northwestern University, Chicago, IL.

The basic goals were to evaluate the corrosion resistance and fatigue life of implantable stainless steel. After hundreds of tests, such a wide variation of results has been found that, unless the surface finish is completely and thoroughly characterized, a definitive statement of corrosion resistance or fatigue life is not possible. In particular, depending on the surface preparation, incidences of pitting and crevice corrosion can occur during anodic polarization along with an additional interface corrosion. While all three of these types are symptomatic of corrosion activity, the latter type can be highly localized and particularly detrimental to fatigue life.

Fig. 1 shows the corroded surface of a non-passivated (NP) specimen which had a Teflon crevice ring while tested according to ASTM G5-78 standard method for making potentiostatic anodic polarization measurements. In this case a 25 mV increase from open circuit potential was made every 5 minutes up to a 3000 $\mu\text{A}/\text{cm}^2$ critical current density. It should be noted that all three types of corrosion are encountered. The majority of the metal depletion was apparently caused by crevices near the central region which had been masked by the Teflon ring. Numerous small pits occur over all the surface exposed to the 0.9% sodium chloride electrolyte. A minor amount of interface corrosion can be observed at what had been the air/electrolyte interface. As reported last year in paper #108, the NP specimens were extremely sensitive to surface finish with breakdown potentials varying by some 300 mV depending on the goodness of finish. It has now been established that the best corrosion resistance and fatigue life of NP samples is apparently obtained with alternating direction mechanical polishing down to 600 grit sand paper, followed by electropolishing. Coarser finishes, unidirectional polishing, applied stress fields and crevice rings all contribute to lowering the corrosion resistance. Interface corrosion problems have been solved for the NP specimens by placing finger nail polish at the electrolyte line.

For specimens passivated (P) in heated 30% nitric acid, the results are quite different. In general, as tested with ASTM G5-78, the breakdown potentials, where current begins to increase rapidly with increasing voltage, were significantly higher for P versus NP specimens. Also, with ASTM F746-81, wherein corrosion was stimulated in a short burst at 800 mV vs. SCE, the potentials at which specimens can recover their passivity were greater for P than NP specimens. Thus, it would appear that passivation is very good for this implantable stainless steel. However, Fig. 2 indicates a disturbing laboratory phenomenon, namely, interface corrosion. This highly localized third type of corrosion occurs in P specimens at the electrolyte/air interface. When attempts were made to shield this interface, in about 70% of the cases corrosion initiated under the finger nail polish. The fatigue specimens fail along the nail polish or electrolyte line rather than in the

reduced cross-section region machined in the central portion of the specimen. They also fractured in a relatively short time.

Fortunately, interface corrosion defects did not appear in P samples until approximately 300 mV vs. SCE was applied following 800 mV stimulation. This means interface corrosion will definitely appear in ASTM F746-81 testing of P specimens but may require too large an overvoltage to be of clinical consequence.

Figure 1

Non-passivated



Interface

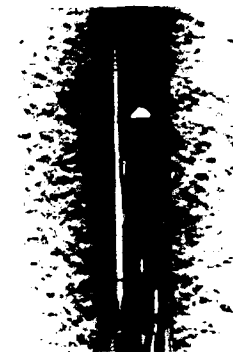
Pits

Crevice

Pits

Figure 2

Passivated



Interface

Pit

Pit

This research was supported in part by NIHR Grant #G008300070.

Northwestern University Dental School
Department of Biological Materials
311 E. Chicago Ave.
Chicago, IL. 60611

J. Lemons⁺, R. Compton⁺, R. Buchanan^{*}, and L. Lucas^{**}The University of Alabama in Birmingham
Birmingham, Alabama

Studies have demonstrated the ability of fiber titanium alloy systems to provide biologic fixation of several types of orthopaedic and dental prostheses^{1,2}. Some of these studies have now been extended to human clinical trials and the opportunities for long term anchorage of functioning devices appears to be good. One question concerning the use of porous metallic systems involves the long term biocompatibility of the structures. The increased surface area of the porous systems provides a possibility for accelerated corrosion magnitudes. Long term laboratory animal studies have demonstrated the presence of metallic constituents within both local tissues and major organs after several years of implantation for selected devices. These studies raise a number of questions with respect to the possible influences of these metallic constituents over the long term. At this time, these questions remain unanswered for the human population.

One method proposed to reduce the biocorrosion of fiber titanium alloy systems is to selectively surface treat the alloy, e.g. electrochemical anodizing by one of several techniques. The objective of the current study was to evaluate the corrosion characteristics of fiber titanium alloy specimens (9.7 diameter X 18.5 mm length) whose surface had been passivated (ASTM F86-76) and electrochemically anodized. The corrosion behavior for these fiber alloys was compared with fiber alloys whose surfaces were passivated (ASTM) but unanodized. To determine the corrosion rates, anodic and cathodic polarization curves were generated in 0.9% sodium chloride solution at pH 7.0 and 37 ± 1 C.

The porous fiber titanium alloy specimens were made following current manufacturing technology for human prostheses³ and consisted of a Ti-6Al-4V alloy core and non-alloyed crimped wire sintered to the alloy substrate. The anodizing treatment was an exposure to a 110 ml glycerin, 60 ml ethanol, 35 ml water, 10 ml lactic acid, 5 ml phosphoric acid, 5 gm citric acid and 5 gm oxalic acid solution at 75 volts direct current. This resulted in a relatively uniform surface interference color at all locations which indicated a uniform thickness of oxidation.

True surface areas were determined for the fiber specimens by quantitative optical microscopy techniques. Two independent methods were employed, and the results showed the true surface area for the fiber specimens to be 6.03 times higher than the nominal surface area (i.e. the area based on nominal specimen dimensions).

Figure 1 presents the potentiostatic polarization curves for unanodized and anodized fiber titanium. The anodic and cathodic currents were normalized to 1 cm^2 of nominal surface area, so that conversions to full-scale implant-device sizes could be easily made (i.e. simply by multiplying by the total nominal surface area). The anodic curves indicated that the anodizing treatment produced substantial reductions in dissolution currents, e.g. at +0.200 volt vs. SCE, the current was reduced from 24.0×10^{-2} to $3.1 \times 10^{-2} \mu\text{A}$.

The corrosion rates at the open-circuit potentials were evaluated by Tafel extrapolation of the cathodic curves. The results were 4.4×10^{-2} and $1.7 \times 10^{-2} \mu\text{A}/(1 \text{ cm}^2 \text{ nominal area})$ for the unanodized and anodized conditions respectively. Therefore, at the open-circuit or corrosion potential, the anodizing treatment reduced the corrosion rate by a factor of 2.6 times.

By reducing the corrosion rate, the quantity of ionic constituents released to the surrounding tissues is reduced. Since the surface area of the fiber alloy was 6.03 times the surface area of a solid form of the alloy, the fiber alloy has the potential of a six-fold increase in quantity of material released to the tissues. By reducing this overall increase by a factor of 2.6 times, it was shown that anodizing can significantly decrease the ionic release to the tissues. Until the systemic effects of titanium are totally understood, all methods for reducing ionic release should be investigated.

These limited *in-vitro* investigations indicate that anodizing and/or other surface modifications of fiber titanium alloy systems may provide an opportunity to decrease *in-vivo* corrosion phenomena. Additional studies are strongly recommended.

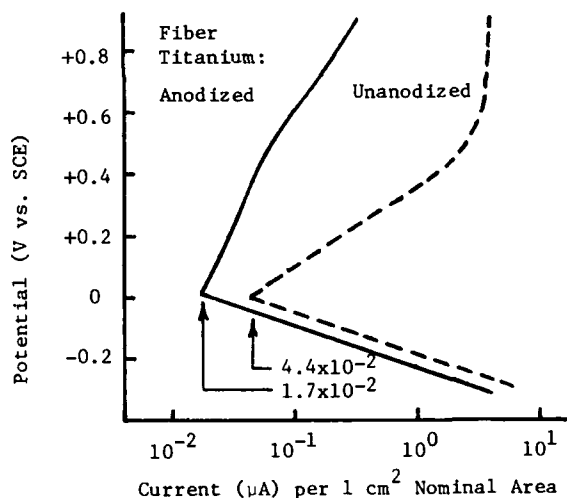


Figure 1

⁺Specimens and support provided by Zimmer, Inc. Warsaw, Indiana

- Galante, J., NIH and AAOS Workshop on Implant Interfaces, Chicago, September, 1983.
- Weiss, M. B., Rostaker, W., and Blackburn, J., Five Year Evaluation of Endosseous Fiber Metal Implant, J. Dent. Res., 60, 418, 1981.

^{*}Dept. of Biomaterials, School of Dentistry; ^{*}Dept. of Materials Engineering, ^{**}Dept. of Biomedical Engineering; The University of Alabama in Birmingham, University Station, Birmingham, AL 35294

Corrosion-Fatigue Behavior of Porous Coated Ti-6Al-4V Implant Materials

A. C. Fraker*, A. J. Bailey*, H. Hahn** and R. H. Rowe, Jr.**

*National Bureau of Standards, Washington, DC 20234

**Artech Corporation, 2901 Telestar Court, Falls Church, VA 22042

Surgical implant prosthesis fixation in the bone has been a subject of concern and study for many years. Improvements in fixation can be attained by means of bony ingrowth or cement attachment to porous coated prostheses. This paper deals with an investigation of arc plasma sprayed porous coated Ti-6Al-4V implant material and shows the effects of the application of the porous coating and subsequent heat treating on the microstructure, hardness and fatigue life of the material. Other methods for applying metal porous coatings include sintered metal fibers and sintered metal spheres. Production techniques involved in the application of these porous coatings can cause alloy phase changes, microstructural variations and surface effects which will influence the performance of the metal prosthesis in terms of mechanical and electrochemical behavior.

Experimental procedure involved the preparation of corrosion-fatigue test specimens from ELI grade Ti-6Al-4V. Specimens were 6.5 mm in diameter, 76 mm long and the center section of 12.7 mm was decreased in diameter to 5.0 mm. The center section was grit blasted and then arc plasma coated with either sponge titanium or -20 +40 mesh Ti-6Al-4V. The application of the plasma coating has been described in detail previously¹. Corrosion-fatigue tests were conducted in fully reversible torsion with an applied shear strain amplitude of ± 0.010 and at a frequency of 1 Hz. During the fatigue testing, specimens were exposed to flowing Hanks' solution which was held at a temperature of 37°C and had a pH of 7.1. Prior to the corrosion-fatigue testing, some specimens were sintered at temperatures indicated in Table 1.

Table 1 shows corrosion-fatigue data for a polished control specimen and for effects of the grit blasting step, the application of the porous coat and the sintering of the porous coat. These data show that grit blasting and application of the porous coat do not shorten the fatigue life of the material. Sintering at the temperatures indicated causes some reduction in the fatigue life. Sintering above the beta titanium transus temperature, 980°C (1796°F), as a final step should always be avoided.

Application of the porous coat can result in some additional oxygen in the porous coat. Some surface oxygen can be removed by sintering in vacuum but in the specimen interior, some oxygen can be driven into the specimen, and this will affect the mechanical properties. Figure 1 shows a micrograph of a porous coated Ti-6Al-4V substrate. Arrows indicate the locations of hardness measurements. These hardness data from two specimens are shown in Table 2. The bond of the coating is strong with a lap shear strength of 7 MPa (1000 psi) and a tensile strength of 14 MPa (2000 psi). Fracture occurred within the coating and not at the interface. Some separation of coating and substrate was observed after corrosion fatigue testing in the low cycle region. These studies indicate that arc plasma sprayed porous coatings can be applied

to Ti-6Al-4V prosthetic materials without negatively affecting the mechanical strength. Further studies are needed to optimize the processing conditions.

1. Hahn, H., Lare, P. J., Rowe, R. H., Jr., Fraker, A. C., and Ordway, F., ASTM STP, Corrosion and Degradation of Implant Materials, Vol. 2, 1983.

Table 1. Cor.-Fat. Results; Sh. Strain Amp., ± 0.010

Ti-6Al-4V Specimen	No., Cycles to Failure
Polished, control	$> 10^6$
Grit blasted, unsintered	$> 10^6$
Grit Blasted, unsintered	$> 10^6$
Ti-6Al-4V coat, unsintered	$> 10^6$
Ti-6Al-4V coat, sintered, 900°C	9.3×10^5
Ti-6Al-4V coat, sintered, 900°C	9.4×10^5
Ti top coat, unsintered	$> 10^6$
Ti top coat, sintered, 871°C	2.2×10^5

Table 2. Knoop Hardness (mean) Values for Ti-6Al-4V Coat on Ti-6Al-4V for A, Sintered and B, Unsintered. () denotes standard deviation.

Specimen	Coating	Interface	Substrate
A	523.7 (49.3)	569.1 (86.9)	379.5 (22.1)
B	936.3 (166.2)	530.8 (116.2)	348.7 (8.5)



Figure 1. Light micrograph of Ti-6Al-4V coating on Ti-6Al-4V substrate.

Metallurgy Division, National Bureau of Standards, Washington, DC 20234
Artech Corporation, Falls Church, VA 22042

DEGRADATION AND PERMEABILITY OF BIOBRANE-1 AND GLUTARALDEHYDE-TREATED OR UNTREATED BOVINE PERICARDIAL TISSUE

J.P. VonderBrink*, T.J. Sernka** and P.K. Bajpai*

University of Dayton
Dayton, Ohio 45469

Both Biobrane and glutaraldehyde-treated bovine pericardial tissues (GTBPT) have been used successfully as bioprostheses. This investigation was conducted to assess the feasibility of using Biobrane and/or GTBPT for repairing and/or replacing diseased gastrointestinal tissue.

Biobrane-1 obtained from Woodroof Labs, Inc., was stored at 25°C. Both untreated bovine pericardial tissue (UTBPT) and GTBPT were prepared by 0.5% glutaraldehyde tanning procedures. UTBPT was stored in chilled phosphate-buffered (pH 7.4) saline (PBS) at -20°C. GTBPT was stored in 4% formaldehyde at 4°C.

DEGRADATION STUDIES

Degradation characteristics were studied by incubating Biobrane-1, GTBPT and UTBPT in separate Erhlemeyer flasks (125 ml) containing an acid enzyme solution (80 ml). Each 4 cm² piece of pericardial tissue or Biobrane-1 was incubated for two six-hour periods at 37°C in a Dubnoff Metabolic Shaker oscillating at 21 RPM. Biobrane-1 and pericardial tissues were washed for one hour in PBS at 37°C following each six-hour incubation period. Hydroxyproline content of each acid-enzyme solution was analyzed after each six-hour incubation by a colorimetric procedure. The first and second incubations were conducted in acid-saline (pH 1) containing 0.96 Kilounits of pepsin to simulate gastric juice. The two final incubations were conducted in acid-saline solution (pH 3.5) containing 0.96 Kilounits of trypsin to simulate duodenal chyme.

The amount of hydroxyproline liberated by GTBPT in acid-saline-enzyme solutions was significantly lower than the amounts of hydroxyproline liberated from UTBPT in acid-saline-enzyme environments (Figure 1). Amounts of hydroxyproline liberated from UTBPT and Biobrane-1 in acid-saline-enzyme solutions did not differ significantly. Variation of saline pH, enzymes and time of incubation did not alter the amounts of hydroxyproline liberated by UTBPT, GTBPT and Biobrane-1. The data indicate that 0.5% glutaraldehyde treatment of bovine pericardial tissue and subsequent storage in 4% formaldehyde slow down the degradation of pericardial tissues in acid-saline-enzyme environments.

PERMEABILITY STUDIES

Permeability of Biobrane-1 and pericardial tissues were determined by measuring the ²²Na flux through each piece of Biobrane-1 or pericardial tissue in an ion flux chamber. Rat gastric mucosal tissues were used as controls for ion flux studies. Ion flux was measured from the mucosal (m) side containing Ringer's solution (pH 3.4) to the submucosal (s) side containing Ringer's solution (pH 7.4). After isotopic equilibration, ion flux measurements were determined at 15 and 30 minutes. Permeability studies were conducted on unincubated Biobrane-1, GTBPT and UTBPT as well as Biobrane-1 and GTBPT incubated for 12 hours in saline-pepsin solution (pH 1). Incubated UTBPT was too severely damaged to be used in permeability studies.

Permeability of all pericardial tissues to Na⁺ ions was significantly higher (11 to 17X) than the permeability of rat gastric mucosa to Na⁺ ions

(Figure 2). Incubation of GTBPT in acid-saline-enzyme solution did not significantly decrease the permeability of tanned pericardial tissue. Ion flux data showed that both unincubated Biobrane-1 and Biobrane-1 incubated in acid-saline-enzyme solution were totally impermeable to Na⁺ ions. Since Biobrane-1 incubated in acid-saline-enzyme solution is impermeable to cations like Na⁺, it seems reasonable that Biobrane-1 would also prevent the transfer of H⁺ ions across gastric mucosa. Movement of H⁺ ions across the repaired and/or replaced gastrointestinal lining would break down the gastric mucosal barrier leading to ulceration. In this respect, the high permeability of GTBPT to ions may limit its application for gastric repair.

On the basis of the *in vitro* data obtained in this investigation and the success of Biobrane as a burn dressing, it seems that Biobrane-1 could be used effectively to repair and/or replace damaged gastric and intestinal tissues.

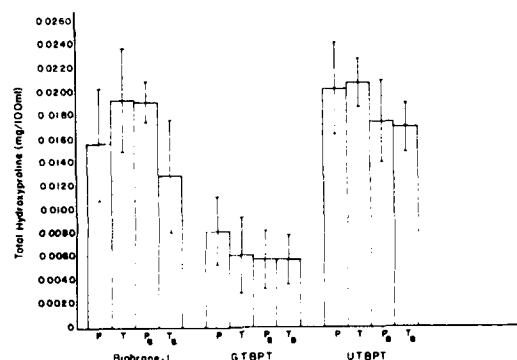


Figure 1 Total hydroxyproline liberated from biomaterials upon incubation (P=pH 1 saline, pepsin, hour 0-6; T=pH 3.5 saline, trypsin, hour 0-6; P=pH 1 saline, pepsin, hour 7-13; T=pH 3.5 saline, trypsin, hour 7-13)

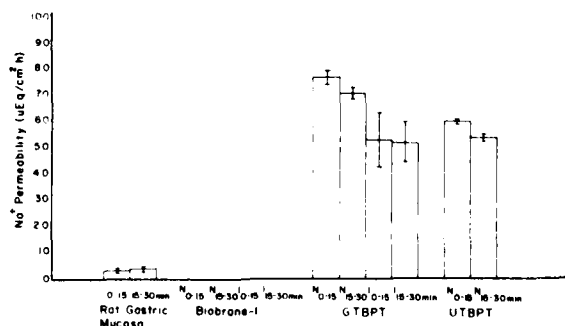


Figure 2 Relative permeabilities of rat gastric mucosa and non-incubated (N) or incubated (I) biomaterials.

Acknowledgements are due to Dr. A. E. Woodroof for donating Biobrane-1.

* University of Dayton, Dayton, Ohio 45469

**Wright State University, Dayton, Ohio 45435

POLY(β -MALIC ACID), A FUNCTIONAL POLYESTER OF INCREASING PHARMACOLOGICAL IMPORTANCE

M. VERT, C. BUNEL, C. BRAUD and H. GARREAU

Laboratoire des Substances Macromoléculaires, ERA CNRS 471, I.N.S.C.I. Rouen
BP 8, 76130 Mont-Saint-Aignan, France.

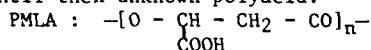
Uses of synthetic polymers injected in body fluids for therapeutic purposes have been considered for many years (1).

Beside microencapsulation in solid micro- or nano- particles, pharmacologically active polymers have received increasing attention either as polymeric drugs, i.e. as macromolecules active by themselves, or as macromolecular prodrugs, where the polymer acts as a drug-carrier.

In the field of macromolecular prodrugs, a great number of polymer-drug systems have been studied. Problems were investigated such as drug fixation on functional polymers, drug availability, kinetics of drug-release *in vivo* and *in vitro*, importance of the nature of cleavable bonds, effects of spacer arms and, in a much smaller extent, the role of conformational structures on biological properties.

Many data have been collected which allowed one to distinguish prerequisites for effective therapeutical uses in humans (2). However, it is noteworthy that most of the work has been done in disorder in the sense that no chemical structure-conformational behavior- biological property relationship is available for given systems so far.

It is to investigate such relationships for well-defined and polyvalent polymeric carriers of non-biological origin that we initiated, a few years ago (3), research work on poly(β -malic acid) an until then unknown polyacid.



PMLA was selected on the basis of various factors : - potential biodegradability because of its polyester backbone of the poly (β -hydroxy-acid) type derived from malic acid, - presence of acid pendent groups for water-solubilization and drug-attachment, and-presence of a chiral center in the main chain to modify the configurational structure.

After the finding of a route to synthesize PMLA (4), a fast screening of the various prerequisites related to the particular field we wanted to deal with has been undertaken stepwise to show whether this compound is really suitable for drug transportation, for structure-property investigations and for pharmaceutical applications eventually.

PMLA is a weak polyacid ($\text{pK}_{1/2} = 4.4$, for $c = 5 \times 10^{-2}$ N in water). It is a very hygroscopic material soluble in water whatever the pH and soluble in many organic solvents in the presence of trace of water. So far, PMLA with molecular weight in the range of $M_w \sim 10,000$ shows very good biological characteristics, especially low acute toxicity ($\text{LD}_{50} = 3.3 \text{ g.kg}^{-1}$ in mice) and no induced immune-response after repeated injections in rabbits. Furthermore, we have recently shown that distribution of hydrophobic substituents attached to the polymer through carboxylic groups can be a significant factor not only for water-solubility but also for acute toxicity (5).

In this paper, we wish to show that PMLA degrades in water at neutral as expected and that

complex macromolecules based on malic acid units, can be easily tailor-made by combining simple chemical reactions.

Degradation of PMLA in non-sterile water at neutral was monitored by GPC using 1M NaNO_3 as the mobile phase and TSK columns. Initially, M_{GPC} was 29,000 in regard to dextran standards. After 13 days, the GPC peak shifted to larger elution volumes with a maximum corresponding to $M_{\text{GPC}} = 16,500$. After 60 days, the peak was very close to total volume and appeared as a shoulder on the peak due to the solvent and the degradation products. Therefore it is concluded that PMLA does degrade in water at neutral and thus should be biodegradable *in vivo*.

That PMLA is synthesized through ring-opening polymerization of benzyl malolactonate, a β -substituted β -lactone monomer, with further hydrogenolysis of benzyl ester protecting groups of the resulting polymer provide worthwhile means to tailor-make complex macromolecules, especially if these two reactions are combined with copolymerization reactions involving other β -lactones or other heterocyclic monomers and with coupling reactions using classical coupling reagent. As an example to demonstrate the feasibility of the tailor-making of macromolecular prodrugs from PMLA, a ter-polymer containing 50 % methyl ester, 25 % benzyl-ester and 25 % carboxylic side-chains respectively has been prepared as follows

1. homopolymerization of benzyl malolactonate in bulk with triethylamine as initiator.
2. deprotection of 50 % of the protected carboxylic groups by catalytic hydrogenation using Pd/C as the catalyst.
3. methylation of the deprotected COOH by diazo-methane.
4. deprotection of 50 % of the remaining protected COOH to yield the desired ter-polymer whose composition was checked by ^1H NMR. The various resonance lines and their respective weights well agree with the theoretical composition. As we have already shown that chemical coupling of compounds with activated H atoms is easily achieved with DCC (6), one can conclude that tailor-making of rather complex macromolecules is absolutely feasible in the series of PMLA derivatives.

In conclusion, the degradation of PMLA chains and the possibility to tailor-make complex macromolecules through simple reactions reinforce the potential of PMLA in regard to effective use as polyvalent drug-carrier.

REFERENCES

- 1) L.G. DONARUMA and O. VOGL Eds, "Polymeric drugs" Acad. Press, New-York (1978).
- 2) H. RINGSDORF, J. Polym. Sci., Polym. Symp., 51 135 (1975).
- 3) M. VERT and R.W. LENZ, ACS Polymer Preprints, 20, 608 (1979).
- 4) R.W. LENZ and M. VERT, US pat. n° 4,265,247 (1981).
- 5) C. BRAUD and M. VERT, ACS Polymer Preprints, 24, 71 (1983).
- 6) C. BRAUD, C. BUNEL, H. GARREAU and M. VERT, Polym. Bull., 2, 198 (1983).

Some Characteristics of Chitin (poly-N-acetyl-D-glucosamine) for Orthopaedic Use.

Mutsuhiro MAYEDA Yukio INOUE Hideaki IWASE Kouji KIFUNE

Department of Orthopaedic Surgery, Juntendo University Casualty Center, Shizuoka, Japan.

INTRODUCTION

Chitin is a substance that sustains and protects the body of crabs and fungi.

We obtained the purified chitin from crab shells. Little work has been done on chitin, especially on properties of the solid or molded compounds, it is necessary to carry out extensive studies on mechanical properties and behaviour in dry and wet states and in vivo. Therefore, we examined the biocompatibility of molded chitin with a view towards medical application.

EXPERIMENTAL

We obtained molded chitin after decalcification and deproteinization from Japanese pink crab shells.

(Product process) crab shells=1st. decalcification
=1st. deproteinization=grinding=2nd. decalcification
=2nd. deproteinization=molecular weight arrangement
=purified CHITIN POWDER=chitin dope=wet molding
=washing=dry stretching=CHITIN ROD.

(Materials used for experiments)

- 1) white purified chitin powder (ϕ 50-100 μ m)
- 2) weaved monofilaments (60 Denier)
- 3) chitin rod (ϕ 2-5mm)

Experiment 1. Measurements of Mechanical Properties. Rods and filaments were prepared. Tensile and bending strength were measured. Those in the wet state were measured immediately after removing the samples that had been soaked to the equilibrium absorption in Ringer's solution. And water uptake rate was measured.

Experiment 2. Observation of Molded Chitin in the Process of Absorption and Degradation. Chitin rods were imbedded in canine back muscles. Periodically, the dogs were sacrificed, the surface of the samples was observed macroscopically and microscopically, especially with scanning electron microscope. Variation in the specific gravity and bending strength in vivo were measured and compared with those in Ringer's solution (37 degrees centigrade) after 90 days.

Experiment 3. Degradation of the Molecular Chain in vivo. Molded chitin filaments were imbedded into rabbit back muscles, periodically taken out, and the average molecular weight (M_w) was measured. Controls were preserved in Ringer's solution.

Experiment 4. Evaluation of Biocompatibility in vitro and in vivo. Chitin purified powder and monofilaments were prepared. The experiments in vivo were 1) the powder was injected into the abdominal cavity of mice, 2) the filaments were imbedded in rabbit subcutaneous tissue and in vitro with tissue culture method according to Rice, R.M. with L-929 mouse fibroblast.

Experiment 5. Wound Healing Study. Applying the powder into rat back skin wound in which size and depth had been determined, sutured with silk blade in the same operative technique, ultimate breaking strength to separation was measured on the 5th. and 8th. day. Chitin purified powder, non-absorbable polymer (polyacetal copolymer) and untreated groups were prepared.

RESULTS AND DISCUSSION

1. Bending strength and elastic modulus were 19.5 kg/mm², 638.9 kg/mm² (mean) in the dry state for the chitin rods. In the wet state, the strength

decreased to about one fiftieth. Water uptake rate was more than 100%. On the other hand, for weaved chitin filaments more than half tensile strength in the dry state was retained in the wet state. Increasing rate of volume was at the most 18.5%. Mono-filaments are highly crystalline, the high retainment of the strength in the wet state was attributed to increased crystallization. Molded chitin rods were not formed at this point.

2. A decrease in bending strength and elastic modulus in vivo was noted. Observation of the chitin rod surface showed the loss of smoothness in vivo in comparison with the samples soaked in Ringer's solution. The specific gravity in vivo was decreased.

3. Average molecular weight varied from 10^5 to 10^4 with time. Chitin was insoluble in most solvent. The high decrease in molecular weight and the other results indicate the probable absorption of molded chitin in vivo.

4. In the tissue culture method, chitin powder showed good cell increase rate and morphological findings. In vivo, chitin filaments imbedded in rabbit back muscles had about the same inflammatory reaction with giant cells and histiocytes as absorbable polymer (dextran). Chitin powder had almost the same tendency except with the same granulation.

5. The ultimate breaking strength to separation was significantly higher than the other polymer (polyacetal copolymer) and the untreated control at both 5th. and 8th. day.

CONCLUSIONS

Natural polymers are attracting much attention recently. Chitin is the most interesting biomaterials for the reasons that the product process to the molded compounds is accomplished except for some small problems, and it is absorbed and degradable in vivo. Wound healing activation has been reported by Prudden et al., and the same effect was recognized. As the polymerizing and crystallization process is improved, stronger compounds and composite materials will be obtained. We would like to introduce them to the orthopaedic fields; such as for strings, artificial ligaments for the knee joint, and the materials for less rigid fixation, which is still in the process of experiments.

Mutsuhiro MAYEDA Yukio INOUE

Dept. of Orthopaedic Surgery, Juntendo Univ. Casualty Center,
Hideaki IWASE

Dept. of Bioengineering, Juntendo Univ. Casualty Center, 1129 Nagaoka, Izunagaoka-cho, Tagata-gun, Shizuoka, Japan. #410-22

Kouji KIFUNE

UNITIKA Research and Development Center, 23 Kozakura, Uji, Kyoto, Japan. #611

PREFERRED STERILIZATION TECHNIQUES FOR BIOMATERIALS WITH DIVERSE SURFACE PROPERTIES

R.Baier, J.Natiella, A.Meyer, J.M.Carter, T.Turnbull

State University of New York at Buffalo and Advanced Technology Center,
Calspan, P. O. Box 400, Buffalo, NY 14225

An important task in implant evaluation trials is selection of appropriate sterilization methods that will not compromise the surface quality of the otherwise carefully prepared test materials. Yet, the differential surface properties selected for screening almost guarantee that no single sterilization protocol will be suitable for all test specimens, even if their bulk properties are identical.

This problem has now been addressed and resolved by a series of experimental measurements of surface changes on metallic and organic-coated metallic specimens subjected to sterilization by standard steam autoclaving, ethylene oxide gas exposure, glutaraldehyde immersion, alcohol swabbing, and radio-frequency glow-discharge-treatment (RFGDT). Complete surface characterization of the metallic specimens was first accomplished with specimens prepared in manners typical for implants of dental and orthopaedic devices; polishing to smoothness with common abrasives (carried in stearate-rich organics); passivation by ASTM-recommended procedures; scrupulous cleaning of all organic residues; and deliberate final coating with inert organic films. Sterilization protocols were then followed according to standard clinical procedures, prior to re-inspection of the test plates for evidence of surface contamination or other changes in quality important to implant/host response evaluation.

Surface characterization methods employed included scanning electron microscopy and energy-dispersive x-ray analysis for judgment of surface topographic and compositional changes. Multiple attenuated internal reflection infrared spectroscopy was used to record the unique signatures of superficial contaminant layers, and ellipsometry was used to estimate the thickness of these layers. The base test materials were flat plates of cobalt-chromium (Vitalium), typical of dental and orthopaedic implants, and germanium (optically polished to allow use of both internal reflection and ellipsometric techniques on the specimen). Dimensions were closely held to 10 mm x 5 mm x 1 mm (thick). Implantation of similar specimens into the oral mucosa of Rhesus monkeys, as part of an ongoing investigation of primate healing around dental implants, is in progress (NIDR Grant No.DE-04226).

RESULTS. Control Vitalium specimens, brought to a smooth, shiny surface state by conventional polishing, exhibited little surface contamination aside from the stearate coating resulting from the polishing step. Contact angle analysis allowed graphical determination of the critical surface tension at 21 dynes/cm.

Sterilization by ethylene oxide left insignificant residues, determined by ellipsometry to be less than 10 Å, with no compromise of the surface spectral quality or wettability. Sterilization by glutaraldehyde immersion left the surfaces coated with substantial residues that could be almost completely rinsed away in fresh tapwater (thus compromising the sterility). Nevertheless, the specimen critical surface tension remained 10 dynes/cm

higher than the control value, as a result of substantial increases in both the polar and dispersive components contributing to the surface energy state.

Sterilization by steam autoclaving was exceptionally unsuitable for the low energy specimens. Deposits of about 100 Å average thickness remained from hygroscopic salts and organic contaminants within the condensed steam droplets. Only modest increases in the surface energy values were measured however, due to the intrinsic hydrophobicity of the stearate (or silicone, on germanium) which kept the steam droplets isolated in discrete patches. Sterilization with alcohol left significant residues and permanently modified the surface energy to a higher and significantly more polar state. This latter change is attributed to uptake of the alcohol contaminants by the soft organic coatings, and would be expected to be much more troublesome with polymeric materials than with these coated metallic test plates.

Sterilization by RFGDT, followed by storage in boiled distilled water, was accompanied by both removal and oxidation of the organic surface layers, as indicated by all the characterization techniques. This is clearly undesirable if a low-energy coating is to be evaluated in the implant environment.

ASTM-recommended passivation of the Vitalium did not remove or substantially oxidize the stearate surface layer, but did render the subjacent metal more susceptible to erosion and loss when subjected to any of the sterilization protocols. For example, steam sterilization of the passivated Vitalium produced a final implant surface typical of "clean" metals, neither of high nor low surface energy. Evaluation of "intermediate" energy surfaces showed RFGDT to be unsuitable specifically because it scrupulously cleaned and activated the material to a high energy state that, without further precautions in storage, adsorbed adventitious contaminants (18 Å average thickness). Ethylene oxide sterilization left residues of 73 Å average thickness and imparted an extreme contaminant-related hydrophilicity to what was a badly compromised surface state. Glutaraldehyde soaking of intermediate-energy specimens, followed by copious rinsing, resulted in average residue thicknesses of about 34 Å, imparting wettability aberrations not consistent with the goals of implantation trials. Steam autoclaving left hygroscopic salt and organic residues as previously described by these authors, averaging 70 Å in thickness and imparting significant surface heterogeneity to the specimens. Alcohol soaking or swabbing left residues in excess of 100 Å in many cases, seriously compromising the surface state.

CONCLUSIONS. Based on the results of this project to date, the following recommendations for implant sterilization can be made. In order to maintain the cleanliness of high-energy metal implants, RFGDT should be applied and followed by storage in boiled distilled water. Steam autoclaving, although not ideal, is the method of choice for sterilization of medium energy and passivated metal implants. Implants having thin low energy coatings should be sterilized by routine ethylene oxide gas procedures.

INFLUENCE OF SKELETAL IMPLANT MATERIALS ON INFECTION

R.W. Petty, M.D., S.S. Spanier, M.D., J.J. Shuster, Ph.D., and
C.A. Silverthorne, M.S.

University of Florida
Gainesville, Florida 32610

A large amount of research has centered on the development of implant materials that are compatible with the internal environment of mammalian tissues. There has been little investigation of the effect of modern implants on the incidence of infection. We have determined that many commonly used skeletal implant materials make infection more likely in operative wounds contaminated with Staphylococcus aureus. Only polymethylmethacrylate that polymerized in vivo was associated with an increased incidence of infection in wounds contaminated with Staphylococcus epidermidis or Escherichia coli. Systemic antibiotics, wound irrigation with antibiotic solution and antibiotics in bone cement reduced the incidence of infection associated with implantation of bone cement.

METHODS

Experiments were performed in 246 dogs ranging in weight from 10 to 15 kilograms. Three bacterial strains, Staphylococcus epidermidis, Staphylococcus aureus, and Escherichia coli were used in the experiments. Twelve animals had both proximal femoral canals prepared surgically, but no bacteria and no foreign materials were placed in the femoral canal. Eighteen animals had bacterial contamination with serial ten-fold dilutions of one of the three organisms in one or both femoral canals. Remaining animals had implants of stainless steel, chrome cobalt, polyethylene, pre-polymerized polymethylmethacrylate, or dough polymethylmethacrylate implanted in addition to bacterial inoculation. Additional animals had bacterial contamination of the operative wounds followed by implantation of polymethylmethacrylate in the dough stage but were, in addition, treated with intravenous cefazolin 25 mg./kg., wound irrigation with saline or 0.5 percent neomycin solution, or with gentamicin added to bone cement (0.5 gm. gentamicin sulfate per 40 gm. powder). All animals were sacrificed 15 days following surgery, and the femurs were examined histologically and bacteriologically. The effect of the different implant materials (and no implant) and different treatments on the incidence of infection was compared by determining the infectious dose 50. For some organisms and implants, an ID-50 could not be determined because there was not enough of a dose-related response. When this occurred, exact chi-square analysis was used.

RESULTS

All implants were significantly more likely to be associated with infection with Staphylococcus aureus. Polymethylmethacrylate that polymerized in vivo was found to be significantly more likely than all other implants and the control to be associated with infection with Escherichia coli and Staphylococcus epidermidis.

When thorough histological evaluation was performed, infection was found to be correlated with an increased inflammatory response histologically

for all three bacteria at a high level of significance ($p < .001$). However, even with this highly statistically significant correlation, the correlation was not absolute. If only limited portions of randomly selected tissue specimens were examined, there was low correlation of inflammatory reaction and infection.

For all three organisms, polymethylmethacrylate that polymerized in vivo was associated with a significantly ($p < 0.01$) lower ID-50 (higher infection rate) when compared to no implant. For Staphylococcus aureus and Escherichia coli, this adverse effect was significantly reversed by treatment with neomycin irrigation, systemic cefazolin, and polymethylmethacrylate-gentamicin, but not by saline irrigation. For Staphylococcus epidermidis, the adverse effect was significantly reversed by treatment with systemic cefazolin and polymethylmethacrylate-gentamicin, but not by saline or neomycin solution irrigation. There were fewer infections in animals treated with polymethylmethacrylate-gentamicin than in animals with no implant.

DISCUSSION

These results confirm that for contamination with some bacteria (Staphylococcus aureus), many commonly used skeletal implant materials make infection more likely. The results also confirm that for some bacteria, the type of implant material and, perhaps more important, the method of implantation (i.e., in vivo polymerization) strongly influences infection incidence. The studies reported here add additional evidence from controlled laboratory experiments that systemic antibiotics and wound irrigation with antibiotic solutions are both effective in preventing infection in operative wounds associated with skeletal implants when those wounds become contaminated with bacteria. In these experiments, bone cement containing gentamicin was very effective in lowering infection incidence in wounds contaminated with bacteria. Its use was the most effective of all treatment methods evaluated; the incidence of infection in contaminated wounds in which polymethylmethacrylate was implanted was lower when antibiotic was added to the cement than when no implant was used.

This research was supported in part by NIH Grant No. 5 R01 AM 24007-04 AFY.

Department of Orthopaedics, J-246, JHMC,
University of Florida, Gainesville, Florida,
32610.

BACTERIAL ADHERENCE TO BIOMATERIALS: THE CLINICAL SIGNIFICANCE OF ITS ROLE IN SEPSIS

Anthony G. Gristina, M.D., J. William Costerton, Ph.D.

Bowman Gray School of Medicine of Wake Forest University
Winston-Salem, North Carolina

In the past decade, the use of implanted biomaterials has increased exponentially, but the presence of a biomaterial makes the adjacent tissues susceptible to both immediate and delayed infections. Those infections are notoriously resistant to antibiotic therapy and are seldom cured unless the biomaterial is removed.

Once it was known that microcolonization within adherent biofilms is a common mode of bacterial growth in natural ecosystems, in industrial aquatic systems, and on both normal and diseased mucosal and epithelial surfaces, it seemed logical that bacteria might also grow in an adherent mode on a biomaterial. And, it seemed probable that adherence might account for the resistance of biomaterial-related infections to antibiotics and host immune systems, just as adherence of bacteria in industrial systems protects them from chemical biocides and antiseptics, and adherence of autochthonous bacteria to epithelium protects them from surfactants and other host defenses.

Adherence as a growth mode of bacteria on clinically implanted biomaterials has been proved over the last three years, but the mechanism by which the bacteria adhere remains controversial, as does the mechanism by which the adherent bacteria are protected from host response and antibiotic therapy. An ongoing clinical study at Bowman Gray School of Medicine was begun to evaluate three hypotheses: 1) that resistant infections are caused by bacterial adherence to biomaterials, that adherence being effected by a polysaccharide mucoid film (the glycocalyx) produced by the bacteria themselves; 2) that the impenetrable biofilm might explain, in part, the resistance of biomaterial-related infections to antibiotic therapy and host defenses; and 3) that identification of the true pathogens in such infections is different because adherent forms are difficult to detect and free-floating, nonrepresentative organisms are more frequently sampled. Thus, culturing and sensitivity tests lead to incorrect antibiotic therapy.

In this study, when acute or chronic infection is identified adjacent to a biomaterial and antibiotic therapy is not adequate, that biomaterial and surrounding tissues are removed, stained with ruthenium red (a cationic stain specific for polyanionic structures such as polysaccharides), and studied with scanning and electron microscopy. Pathogens thus seen are compared with cultures of pathogens from the same patient processed by both the hospital clinical laboratory and our research laboratory.

To date, for these clinical (*in vivo*) infections, we have 1) identified heterogeneous and homogeneous bacterial colonies adhering to the surfaces of polytetrafluoroethylene grafts, Foley catheters, Vitallium and stainless steel endoprostheses and devices, nylon sutures, stainless steel skin staples, T-tubes, methylmethacrylate, high-density polyethylene, and tissues adjacent to the biomaterials; 2) demonstrated on biomaterials and on periprosthetic tissues, adherent pathogens organized into microcolonies surrounded by a bio-

film (the polysaccharide glycocalyx); and 3) shown that bacterial colonies cultured routinely are not always the same as those stained and identified as above by scanning and electron microscopy.

Detailed examination of the bacteria within the adherent biofilms shows that the complex multispecies consortia appear to be site- and tissue-specific as well as surface-specific (e.g., biomaterial-specific). Forming adherent glycocalyx-enclosed microcolonies appears to be a protective, inherent mode of growth even in the presence of potent host and exogenous antibacterial forces allowing these infections, which we call "cryptic," to persist until the biomaterial is removed and can no longer serve as an infective nidus.

For the clinician, microbiologic sampling and culturing methods currently in use are adequate for the recovery and taxonomic identification of bacterial pathogens causing acute systemic disease and for the determination of their antibiotic susceptibility. Our studies show that careful and complete sampling and staining are needed to detect the subtle panorama of adherent infections, so that extrapolation from *in vitro* data on antibiotic sensitivity to the effective *in vivo* dose for antibacterial therapy is accurate. Complicating the problem are the facts that some bacteria have both a "slime"-coated and a noncoated strain; the adhering glycocalyxes of some bacteria are progressively lost in *in vitro* subculture; and that growth in the free-floating mode radically increases the sensitivity of bacteria to chemical bactericides.

The significance of these findings is far-reaching, and the therapy of biomaterial-related infections must be approached with these problems in mind. In addition to considering massive doses of antibiotics to overcome the infections (as has been done in cystitis and cystic fibrosis) and to studying further the microstructure and chemical structure of the adherent mechanisms to determine the effectiveness of blocking analogs (as has been tried in endocarditis), we believe that if the surface or substance of a biomaterial could be made resistant to adherence, the number of biomaterial-related infections could be decreased.

In summary, we believe that microbial adherence effected by the glycocalyx is a fundamental and pivotal factor in sepsis involving biomaterials, and that it may explain the basic susceptibility of patients with implants to infections and the resistance of such infections to host defense mechanisms and to antimicrobial therapy. In effect, bacterial adherence is the reason why foreign bodies become infected.

Section on Orthopedic Surgery, Bowman Gray School of Medicine, Winston-Salem, NC 27103; and University of Calgary, Calgary, Alberta, Canada.

THE DESIGN OF CANINE THR FOR THE BIOLOGICAL
EVALUATION OF HUMAN THR

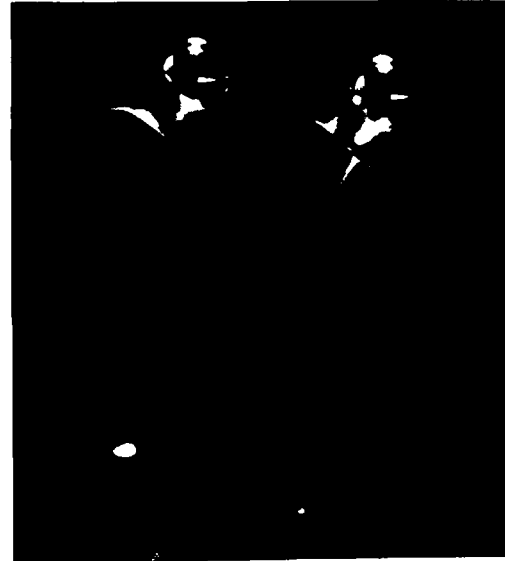
R.R. Tarr and A. McLaren

Orthopaedic Biomechanics Laboratory
Bone and Connective Tissue Research Program
Orthopaedic Hospital/University of Southern California

Although total hip replacement (THR) is a successful, widely accepted procedure, long term failures of the early designs are being reported with greater frequency. These failures are mainly mechanical from loss of fixation. As a result many new prosthetic designs have been introduced. Materials of differing modulus of elasticity, more accurate anatomical relationships and non-cemented fixation have been proposed in an attempt to overcome fixation failures. In order to adequately test new design features before humans are subjected to these empirical and theoretical improvements, investigations delineating the mechanical and biological responses are required.

The canine model has been used to examine the biological response of bone to orthopaedic implants and procedures and is believed to be acceptable for investigating total hip prostheses. The problems experienced in the past with dislocation of canine THR are correctable with close attention to operative technique and with proper prosthetic design. If the results of canine investigations are to be extrapolated to the human situation, canine prostheses must be designed using the same principles employed in the design of the human prostheses they are simulating, i.e. offset, neck-shaft angle, neck length, stem-bone proportion, cement mantle thickness, collar, as well as surgical and fixation techniques. However, the details of the anatomy and biomechanics of the canine hip joint are significantly different than the human hip (Arnockzky and Torzilli, 1981). Therefore, details of the design of canine prostheses need to be specific to the canine anatomy and hip joint forces in order that proposed design features may be accurately incorporated. Scaling down the human femoral prosthesis often leads to unacceptable discrepancies between the prosthesis and the canine proximal femur.

In order to investigate the biological response to identical femoral components of differing material characteristics, a cemented femoral component and a "total contact" press fit femoral component have been designed specific to the details of canine hip anatomy and biomechanics. The stems were characterized with regard to their size and shape, cross-sectional area and axial, flexural and torsional moments of inertia. Mechanical tests including



cantilevered bending of strain gaged stems anchored at the head and stems implanted in strain gaged proximal femurs allowed measurement of yield and ultimate strength parameters as well as strain distribution in the stems and proximal femur. Biological response data including thin section, ground section and microangiograms from a series of 18 dogs with implant periods from 3 months to 1 year have also been analyzed and compared for the various stem designs and materials.

The results of mechanical testing have been correlated with similar experiments using human prostheses and human cadaver femurs. In addition, the results of the biological investigations can cautiously be projected to the expected clinical response of an analogous human prosthesis design.

Reference

Arnockzky, S.P. and Torzilli, P.A.: Biomechanical Analysis of Forces Acting About the Canine Hip. *Am. J. Vet. Res.* 42: 1581-1585, 1981.

Acknowledgement:

Research was supported by Hexcel Corporation, Medical Division.

Address:

Orthopaedic Hospital
2400 South Flower Street
Los Angeles, CA 90007

TOTAL HIP ARTHROPLASTY IN DOGS USING CARBON FIBERS REINFORCED POLYSULFONE IMPLANTS

Moshe Roffman M.D., David G. Mendes M.D., Yehuda Charit Ph.D.,
M.S. Hunt Ph.D.

Research Center for Implant Surgery, Haifa Medical Center (Rothschild)
Faculty of Medicine, Technion, Haifa, Israel.

Arthritis is a progressive disorder which occurs in two stages. To date no method for complete cure or way of arresting the progress of this degenerative disease had been found. At the final stage the treatment of choice is a surgical one namely reconstruction of the destroyed joint. The most widely used method today for hip arthroplasty is by resurfacing or total joint replacement with an artificial implant. The main problem with these artificial joint implants is that in the long run they tend to fail and the results for long-term follow-up are less promising than those which were achieved on short term basis. It is now over 20 years since the mechanical method had gained wide use in practical orthopaedic surgery, namely the use of new materials, prosthetic designs and perfection of surgical techniques. In spite of all this we are facing problems. Recently more and more articles dealing with complications and revision of total hip replacement have been published as an indication of the clinical problems with this method. The two main causes of failure of total hip replacement are infection and aseptic loosening of the implants and both are connected with the design and the material of the implant as well as the use of the methylmethacrylate bone cement.

In attempt to overcome the problem of different modulus elasticity between the implant and the femoral bone and in order to avoid the use of the bone cement recently a few centers started to use the isoelastic cementless hip prosthesis which made of porotic con-polyacetal. The use of metal implant coated with porous carbon-polysulfone in dogs was described recently with good results. As an alternative method, we offer the use of porotic implant made of carbon reinforced with polysulfone. The modulus elasticity of this implant almost resembles that of the cortical bone and the porotic areas allow an ingrowth of tissue and bone into the implant which will produce a biological fixation. As far as the design is concerned this special hip implant is colorless with straight figure to allow an absolute fit with the femoral cortex. A set of special tools was designed for use with this implant.

In 10 dogs, 20 total hip replacement were performed using these implants. The femoral implants were inserted and absolute fixation was achieved without use of bone cement. The H.M.H.D. Polyethylene acetabular cups were secured in place with methylmethacrylate bone cement. P.O.P. spica cast was applied for 3 weeks and then the dogs were allowed to walk and jump free.

At one year, the dogs were sacrificed and mechanical studies to assess the nature of fixation of the implant to the femoral bone as well as histological studies for assessing the type of tissue ingrowth into the porotic areas were done. The early results are promising and the findings will be discussed.

We believe that the use of porotic implant with modulus elasticity which resembles that of the bone and in such a design which will allow an absolute fitting between the implant and its bed will decrease to minimum the mechanical problems and will improve our experience with an artificial implant.

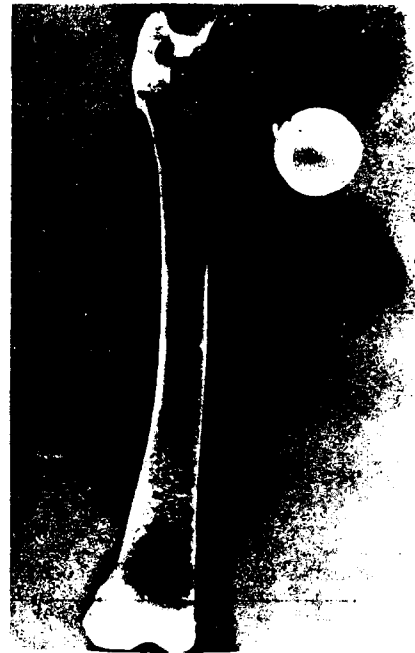


Fig. I The Implant

HIP STEMS MADE OF CARBON FIBER-REINFORCED CARBON MATERIALS - A MECHANICAL EVALUATION

CHRISTEL P., BERNARD P-F., MEUNIER A.

LABORATOIRE DE RECHERCHES ORTHOPEDIQUES - FACULTE DE MEDECINE LARIBOISIERE-
SAINT-LOUIS, PARIS, France.

INTRODUCTION : Stress protection of the upper femoral extremities with total hip replacement (THR) has been already demonstrated by many investigations and related to implant rigidity. Because of their low Young's modulus composite materials have been proposed as candidates for THR. When only made of pure carbon, these materials are not sensitive to stress corrosion, they are stable in time and do not release any soluble compounds. The mechanical strength of these implants can be modulated according to design and material structure and need critical evaluations. The purpose of current experiment was to investigate the mechanical behavior of carbon carbon hip stems of identical design, but having different material structure, both in static and fatigue conditions in comparison with a hip stem of the same design but made of MP 35 N alloy.

MATERIAL AND METHODS : 3 femoral components having the Müller straight stem's shape were examined. 2 were made of carbon fiber carbon material with an alumina ceramic head and one made of MP 35 N. The composite stem materials were made of two different bidirectional carbon fibers embedded in an anisotropic pyrolytic carbon matrix obtained using a Carbon Vapor Impregnation process. Static materials properties are listed in Table 1.

Material	CFRC	CFRC	MP 35 N
(MPa)	550	640	1200
(GPa)	58	48	200

TABLE I

Each prosthesis was instrumented with a total of 14 foiled strain gauges along medial and lateral stem aspects. In order to allow comparison of stem mechanical properties without influence of external parameters such as cement thickness or bone characteristics, the prostheses were first tested in a 3-point-loading configuration (1).

Strain gauge's outputs were recorded after load increments of 50 daN up to 300 daN. Thereafter the instrumented prostheses were cemented into fresh human femurs with PMMA and radiographed. The femoral condyles were embedded into methyl-metacrylate. Femoral loading was applied according to the Pauwel's resultant load orientation from 0 to 300 daN in 50 daN increments. Only linear strain gauges' outputs were saved. The area moment of inertia and the implant sectional rigidity were computed for each stem.

3-point-bending fatigue test was performed on carbon-carbon cylindric bars in air, at a 3 Hz frequency. The samples were first tested during 10^6 cycles using a cyclic load which maximum was equivalent to 80 % of the material static strength. Unbroken samples were then tested on the same equipment with a maximal load equivalent to 95 % of the static bending strength.

RESULTS : The prostheses, either in the 3 point loading apparatus or implanted within femurs, exhibited a bell shape curve of tensile stresses distribution on their lateral aspect and compressive stresses on their medial aspect. Composite stems exhibited both higher tensile stress and stress concentration factor ($\frac{\Delta\sigma}{\sigma}$) and a lower security factor ($\frac{\text{fatigue strength}}{\text{max. tens. stress}}$) than

MP 35 N stem (Table II).

Stem materials	Maximum tensile stress MPa	Stress concentration factor MPa/mm	Security factor
CFRC type 1	120	3.0	2.9
CFRC type 2	116	2.6	2.4
MP 35 N	107	1.6	5.6

TABLE II

However carbon prostheses which present a larger cross section when compared to the metal stem have quite lower sectional rigidities allowing better stress transfer to bone.

Fatigue did not led to any carbon specimen fracture after 10^6 cycles using 80 % of the static strength. With a 95 % stress level, fractures occurred between 3,000 and 27,000 cycles according to materials structure.

CONCLUSION

The comparison of these results with the literature (1,2) shows that the carbon carbon prostheses exhibit a mechanical strength similar to 316 L stainless steel THR stems and a Young's modulus four time lower.

REFERENCES :

1. P.S. CHRISTEL et al. - 8th Annual Meeting of the Society for Biomaterials, Orlando, 1982, p. 136.
2. J.D. REUBEN et al., Clinical Orthopaedics, 1979, 141, 55-65.

Acknowledgement : This work was supported by a grant from S.E.P. Company.

Laboratoire de Recherches Orthopédiques,
10, avenue de Verdun - 75010 PARIS, France.

Articular Cartilage Response to LTI Carbon and Ti-6Al-4V Alloy Hemiarthroplasties

S.D. Cook, R.C. Anderson and R.J. Haddad, Jr.

Department of Orthopaedic Surgery, Tulane University School
of Medicine, New Orleans, Louisiana 70112

The remodelling of proximal femoral bone in cemented and non-cemented hip replacement has been studied in numerous experimental and finite element investigations. Calcar resorption has been related to the differences in material elastic properties of the implant and surrounding bone. LTI carbon implants, with a material elastic modulus similar to cortical bone, have been shown to result in better maintenance of proximal femoral bone when compared to Ti-6Al-4V alloy implants of the same design [1]. However, little information exists on the effect of implant modulus on the articular surface. The objective of this study was to evaluate the short and long term histologic characteristics of articular cartilage when wearing against Ti-6Al-4V alloy and LTI carbon hip hemiarthroplasties in dogs.

An implant design having a hemispherical head with a straight stabilizing stem was utilized. One implant system was fabricated by depositing a 0.5 mm thick LTI pyrolytic carbon (elastic modulus 20GPa) coating on a graphite substrate. The stem and cap regions of the implant in contact with bone had the 5-10 μ m surface porosity associated with the as-deposited process while the articulating surface was highly polished. The second implant system consisted of a Ti-6Al-4V alloy substrate (elastic modulus \sim 110GPa) with a sintered 0.5 mm thick porous coating of commercially pure titanium on the stem and cap regions for implant retention by tissue ingrowth (pore size 200 μ m, pore volume 50%). The porous titanium portion of the implant was coated with a 0.5 μ m layer of vapor deposited carbon. The articulating surface was highly polished.

Adult mongrel dogs were screened for femoral head size and roundness to avoid undue contact stress due to a non-conforming acetabulum. The unilateral devices were placed in a neutral or slightly valgus position using a lateral approach with trochanteric osteotomy. The nonoperated hip served as a control. The animals were allowed immediate unrestricted weight bearing. The animals were sacrificed at periods of 2,4,5,9,12, and 18 months.

Clinical observation, monthly radiographs and periodic gait analyses using force plates were used to evaluate the functional post-operative activity of each animal. In all cases gait analysis confirmed that the animals were loading the operated hip from 85% to 100% of that of the non-operated side. No differences in gait were noted between animals with LTI carbon and those with porous titanium devices. Radiographically, the titanium implants were associated with hypertrophy and densification of cancellous bone in the load bearing dome. This phenomenon was not observed with the LTI carbon implants.

At sacrifice, a thick fibrous capsule was found holding the prostheses of both types tightly in the acetabulum. The synovial fluid was colorless in all cases. Red-brown areas in the central cartilaginous area were observed in most titanium implant animals but was not present or was present

to a much lesser degree in the LTI carbon animals. Marked differences were also noted in the amount of articular cartilage present. The titanium implants were associated with a progressive loss of articular cartilage with time particularly in the load bearing regions. At 18 months less than 25% of the articular cartilage present in the control (nonoperated) side was present in the implanted side. The LTI carbon implants were also associated with some loss of articular cartilage, however, at 18 months approximately 75% of the cartilage was still present.

The acetabulum of both the operated and non-operated sides were fixed in formalin, dehydrated in alcohol solutions and embedded in PMMA. Each acetabulum was split at the area of the greatest diameter. Undecalcified ground histologic and corresponding microradiographic sections were then prepared from one half of each acetabulum. The approximately 50 μ m sections were stained with toluidine blue and basic fuchsin. The other half of each acetabulum was used to prepare 3-5 μ m thick sections using a Jung K sledge microtome. A variety of histologic stains including Goldner's trichrome, Kruttsay's von Kassa stain, Giemsa, PAS and toluidine blue were utilized.

Histologically, the titanium implants were associated with a significant progressive reduction in cartilage thickness particularly in load bearing regions. A significant loss was observed as early as 2 months post-operative. In longer term animals, cartilage erosion to the underlying bone was present in some areas. The cartilage layer was found to be less cellular than the control side and in some areas there was a transition to fibrocartilage. The LTI carbon implants were also associated with some loss of cartilage thickness but to a much lesser extent than the titanium implants. The cartilage appeared remarkably normal with respect to cell size and number. There were only minimal areas of transition to fibrocartilage and no areas of complete cartilage erosion to the underlying bone.

In summary, the wear characteristics of Ti-6Al-4V alloy and LTI carbon against articular cartilage were studied in the dog. Titanium implants were found to greatly reduce with time the amount, thickness, and quality of articular cartilage. LTI carbon implants resulted in significantly better cartilage maintenance compared to the titanium implants. Thus the LTI carbon implants appear to have the potential for better long term maintenance of the articular cartilage and possibly longer term successful performance.

1. Cook, S.D., et al.: Evaluation of Direct Skeletal Attachment Mechanisms For Hip Prostheses, Transactions of the O.R.S., p.158, 1983.

Biomaterials Laboratory, Department of Orthopaedic Surgery, Tulane University Medical School
1430 Tulane Avenue
New Orleans, Louisiana 70112

TIBIAL PLATEAU COVERAGE IN TOTAL KNEE REPLACEMENT - ARTHROPLASTY

Joseph A. Dupont, Allan M. Weinstein, Paul R. Townsend *

HARRINGTON ARTHRITIS RESEARCH CENTER, Phoenix, Arizona

Prosthetic sizes of initial condylar type total knee replacements were developed utilizing measurements on cadaver material and on radiographs from a normal population rather than from an arthritic population requiring total knee arthroplasty (TKA). In addition, the surgical technique for insertion of this type of device reduces the femoral dimensions leading to a reduction in the size of the tibial component width which is proportionately sized to match these reduced femoral dimensions. Mid- to long-term clinical results with these designs have indicated that mechanical failure nearly always occurs on the tibial side. Stress analysis techniques have clearly shown the importance of the cortical tibial shell in load transmission, thus reducing the stresses on the subchondral cancellous bone. The less the cortical support, the greater the tendency for mechanical failure. Current tibial plateau designs, which do not utilize the cortical support mechanism can therefore overload the supporting cancellous bone structure, particularly in the diseased knee.

The purpose of this study was to determine the adequacy of existing designs in providing tibial plateau coverage of arthritic knees requiring total knee replacement and to determine the anatomical measurements of these diseased knees.

Measurements were made retrospectively of the AP and ML dimensions on 200 roentgenograms of the post-operative tibia in consecutive TKA and prospectively intraoperatively during 50 consecutive TKA. Additional data which was obtained for each patient included weight, height, sex and disease. The intraoperative data was obtained using nine graduated templates and measuring the excess bone or excess template once the best fit template was selected. The manufacturer's dimensions of the tibial plateaus of the following devices were obtained: (a) Posterior Stabilized; (b) Robert--Brent- Brigham; (c) Total Condylar I; (d) Total Condylar III; (e) Duo Patellar. The above designs provided a total of 17 tibial plateau sizes to be compared with the measured anatomical data.

The sizes (in mm) of the surgically prepared tibial plateaus measured from the radiographs are shown below.

		Min.	Avg.	St.Dev.	Max.
Male	M/L	67.6	80.9	5.5	95.9
	A/P	47.7	55.6	3.4	65.8
Female	M/P	58.0	69.8	5.4	87.0
	A/P	43.4	49.1	3.4	61.4

This data can be compared to the measurements of normal knees reported by Walker (1); M/L Males = 74.4, M/L Females = 66.3, and Krug, et al. (2); range of M/L 60 to 80; range of A/P 30 to 60. Both of these studies clearly indicate the skewing of data in favor of smaller sizes for normal knees.

With the 17 tibial plateau sizes utilized for comparison, 53 of the 200 surgically prepared tibial plateaus would not have been covered within two millimeters in the ML dimension (nine of 114 females and 44 of 86 males). Only 8 of the 17 sizes were found to provide coverage of the tibial plateau and of these 8, 4 covered only the 5 smallest tibial plateaus measured. Thus, only 4 of 17 available sizes were useful in covering a substantial number of tibial plateaus. An analysis of the AP dimensions showed a similar lack of coverage.

With regard to the intraoperative measurements, 35 of 50 (25 of 40 females, 10 of 10 males), would not have been covered in the ML dimension with any of the existing 17 sizes. The largest size prosthesis of the 17 sizes used for comparison was 10mm smaller than the smallest size male tibial plateau measured. Again, similar findings were obtained for the AP dimension.

In addition, it was interesting to note that a linear relationship was found between the ML dimension and AP dimension of the surgically prepared tibial plateau.

The use of the templates indicated that substantial tibial coverage could be obtained with a reasonable number of components. All of the 50 tibial plateaus measured intraoperatively could be covered using 7 of the 9 templates. Based on the measurements from the radiographs, approximately 95% of the female patient population and 85% of the male population could receive total coverage with 9 tibial plateau sizes.

It was concluded from this study that current tibial designs do not provide adequate tibial coverage for the arthritic knee to insure a more appropriate load distribution in the proximal tibia. The small size of available tibial plateau components in comparison to the size of the actual plateau in the arthritic knee may thus be a contributing factor to the incidence of mechanical failure being observed on the tibial side with total knee replacement.

1. Walker, P.S., Human Joints and Their Artificial Replacements, 1977 Thomas.
2. Krug, W.H., et al., Trans. Society for Biomaterials, Vol. VI, 1983, p.114.

*Johnson & Johnson Products, Inc., Orthopedic Division

TAFEL SLOPES IN SERUM AND SALINE WHILE STATIC AND FRETTING

Williams, R. L. and S. A. Brown

University of California, Davis
Davis, California

Electrochemical techniques have been used in an attempt to further understand the mechanism by which proteins effect the corrosion rates of implant materials. Previous investigators using weight loss and chemical analysis techniques have shown that the presence of proteins increases static dissolution but decreases the fretting corrosion rate. The objectives of the present study were to use polarization resistance and Tafel constant measurements to learn more about the interactions between proteins and the anodic and cathodic reactions.

The corrosion behavior of 316L stainless steel was studied in static and fretting conditions in 0.9% saline and 10% calf serum. Two hole DCP plates, cut from longer plates, with spherical headed screws were used. The plates were screwed onto the posts of a fretting device (1). They were then ultrasonically cleaned in acetone, rinsed in distilled water and dried. The posts were attached to the fretting machine with one held stationary and the other attached to a plunger such that fretting caused pivoting of the screw head in the countersink of the plate. Rod specimens as specified in ASTM F-746 were also used. Some of the specimens did not receive the final 600 grit sanding, and some did not have the teflon collar.

Polarization resistance was measured using the two hole plates in the static and fretting condition. They were placed in the electrolyte and allowed to reach an equilibrium potential. The specimen was polarized galvanodynamically using a 363 Princeton Applied Research potentiostat. The potentiostat was externally driven using a variable power supply and a clock motor was used to produce a constant scan rate. The current was initially stepped to cause a potential change of +20mV from equilibrium. A single sweep was then made to cause a total change in potential of -40mV, and the potential versus current recorded on an X-Y plotter.

Tafel slopes were measured using the same initial preparation until equilibrium potential was reached. The cathodic Tafel slope was measured first by polarizing the specimen galvanodynamically to cause a potential change of -300mV. A plot of the potential versus log current was simultaneously recorded. When the specimen had returned to equilibrium the anodic Tafel slope was measured by polarizing the specimen to +300mV. This procedure was followed for the two hole plates and the rod specimens.

Polarization resistance data (table 1) indicated that the presence of proteins was associated with an increase in static corrosion rate by a factor of three and a decrease in the fretting corrosion rate by a factor of seven. These results correlate well with weight loss data.

The Tafel constants in serum and saline were shown to be similar at a pH of approximately 7. Further studies are planned to measure Tafel slopes at different pHs in serum and saline.

However significant differences were observed in the cathodic Tafel slopes between the static and fretting condition. In the static condition the cathodic Tafel slope showed a two component curve as shown in fig.1. whereas when fretting the curve had only one component with the gradient similar to that of the second component in the static condition. The cathodic Tafel slope for the rod specimens when the final 600 grit sanding was not done also showed a two component curve. However when sanded with 600 grit a one component curve was again observed. The results for the rod specimens were independent of the presence of the teflon collar.

From these results we can see that the specimens with the more noble equilibrium potential exhibit the two component cathodic Tafel slopes, and the specimens with the more active equilibrium potential only show a one component curve. The more active equilibrium potential in the case of the sanded rod specimen is due to the more stable passive layer, whereas in the case of fretting the passive layer is mechanically removed. This would suggest that there are two different mechanisms occurring. The two component curve in the case of the static plate or the unsanded rod could be indicative of two levels of passivity due to surface damage.

Reference:

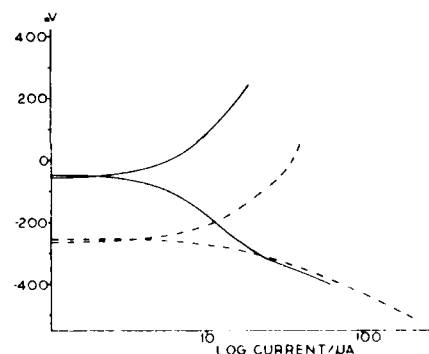
1. Brown S.A. and Merritt K. "Fretting Corrosion in Saline and Serum." J. Biomed. Mater. Res. 15, 479-488 (1981).

This work was funded in part by NIH grant AM32138.

Table 1. Corrosion rate expressed as the reciprocal of the polarization resistance.

	Static	Fretting
Saline	.0024	.1300
10% serum	.0070	.0190

Fig.1. Tafel slopes of a two hole plate in static (solid line) and fretting (broken line) conditions.



Orthopaedic Research Laboratories, TB 139
University of California, Davis
Davis, California 95616

IN VITRO AND IN VIVO CORROSION ANALYSES OF IMPLANT ALLOYS

L. Lucas*, P. Dale*, R. Buchanan†, Y. Gill*, D. Griffin†, and J. Lemons^o

University of Alabama in Birmingham, Birmingham, Alabama, USA

The corrosion characteristics of surgical alloys are often investigated utilizing electrochemical corrosion analyses. Most of the published corrosion studies have utilized an isotonic saline solution for these analyses. Current studies have shown that proteinaceous fluids added to the saline electrolytes may influence the corrosion characteristics of the tested alloys. Since biological fluids contain proteins, the electrochemical corrosion tests conducted in saline and serum should be more representative of *in vivo* corrosion rates. The objective of this study was to evaluate the corrosion characteristics of two implant alloys with (1) *in vitro* corrosion tests conducted in 0.9% sodium chloride electrolyte, (2) *in vitro* tests conducted in 0.9% sodium chloride solution plus 10% calf serum, and (3) *in vivo* tests conducted in the back muscles of rabbits. The materials evaluated were the cobalt base alloy, Co-Cr-Mo (ASTM F75) and a nickel base alloy* (55% Ni, 31% Cr, 10% Mo and 2% W).

The *in vitro* and *in vivo* corrosion characteristics for both alloys were evaluated by conducting standard anodic and cathodic polarization curves. For the *in vitro* tests, the alloy surfaces were cleaned and passivated according to ASTM F86-76. Duplicate anodic and cathodic curves were generated in both electrolytes. For the *in vivo* corrosion tests, cylindrically shaped alloy specimens (length = 1.0 cm, dia = 0.5 cm, same surface treatment used for the *in vitro* tests) were implanted in the back muscles of rabbits. The implanted alloys contained an insulated wire lead spot welded to one end of the cylindrical implant. The wire lead extended from the muscle layers into the subcutaneous area of the neck region. The wire leads were exposed by a surgical incision for connection with the corrosion apparatus. The only difference in the equipment utilized for the *in vivo* experiment was that Ag/AgCl skin electrodes were used as the counter and reference electrodes as compared with the platinum (counter) and calomel (reference) electrodes utilized for the *in vitro* investigations. Replicate curves were generated for each alloy.

The cathodic polarization curves predicted a corrosion rate for the nickel base alloy of $5.2 \times 10^{-4} \text{ A/cm}^2$ (*in vitro*-saline), $4.5 \times 10^{-4} \text{ A/cm}^2$ (*in vitro*-saline+serum) and $5.2 \times 10^{-3} \text{ A/cm}^2$ (*in vivo*). No significant differences were observed between the *in vitro* and *in vivo* tests. The cathodic polarization curves predicted a corrosion rate for the cobalt base alloy of $4.9 \times 10^{-3} \text{ A/cm}^2$ (*in vitro*-saline), $0.56 \times 10^{-3} \text{ A/cm}^2$ (*in vitro*-saline+serum) and $19.0 \times 10^{-3} \text{ A/cm}^2$ (*in vivo*). A small increase was demonstrated for the *in vivo* corrosion rate as compared with the rates predicted from the *in vitro* curves.

Figures 1 and 2 show the *in vitro* and *in vivo* anodic polarization curves for the nickel base and cobalt base alloys, respectively. Some differences between the *in vitro* and *in vivo* curves were observed. The *in vivo* corrosion potentials for both alloys were more active than the *in vitro*

potentials. At potentials greater than 600 mV, the *in vivo* polarization curves demonstrated greater slopes than did the *in vitro* curves. Some features of the curves were not significantly different. For example, no significant differences were observed for the breakdown potentials under the three test conditions for either alloy.

In conclusion, the *in vitro* and *in vivo* corrosion evaluations for the nickel base alloy revealed similar corrosion rates and anodic behavior. For the cobalt base alloy, the anodic behavior was similar; however, the *in vivo* cathodic curves predicted a higher corrosion rate than did the *in vitro* curves. The results of this study indicated that *in vitro* polarization curves conducted in saline adequately predicted the *in vivo* corrosion behavior of nickel and cobalt base alloys. From a biocompatibility point of view, the quantity of specific ions released and the possible accumulation sites of these ions are also very important. These questions are currently being addressed through further *in vivo* corrosion experiments.

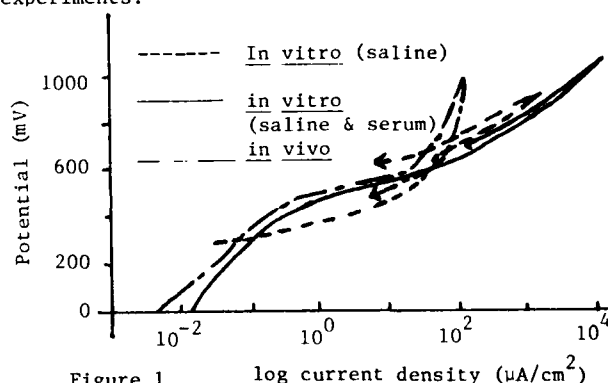


Figure 1

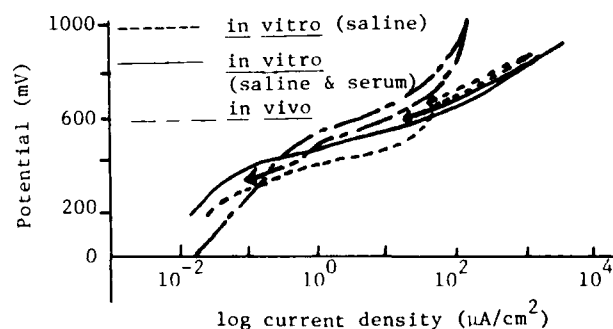


Figure 2

*Biomedical Engineering, The University of Alabama in Birmingham, Birmingham, AL 35294

†Materials Engineering, UAB

^oDepartment of Biomaterials, School of Dentistry, UAB

*Allcorr manufactured by Teledyne-Allvac

H. Oonishi*, E. Tsuji**, M. Miyaga**, T. Hamada**, Y. Suzuki***,
T. Nabeshima*, T. Hamaguchi*, and N. Okabe*

Osaka-Minami National Hospital, Dept. of Orthop. Surg.
Osaka, Japan

It is well known that NiTi shape memory alloy has a good corrosion-resistance and a good biocompatibility. We observed biological reaction of NiTi alloy in the bone and soft tissue around the NiTi alloy implanted.

1. Methods :

Two kinds of NiTi plates, those with a rough surface and those with micro-finished surface, were implanted on the tibia of mature rabbits. The rabbits were sacrificed 2, 3, 4 and 6 weeks after implantations. Histological observations were made by using an optical microscope, a section of the plate-bone interface and the surface of the plate contacting the bone were observed by a scanning electron microscope and an elementary analysis in the bone and soft tissue around the NiTi alloy was made by using an X-ray microanalyzer. Similarly, the stems having Ms point of 15°C were implanted in tibia of two living sheep. The stems have a lot of nails which are spread in body temperature and fixed in the bone canal. These sheep were sacrificed six months after the implantation. Histological observations were made and an elementary analysis in the bone and soft tissue around the NiTi stems was made by using an X-ray microanalyzer.

2. Results :

In the connective tissue membrane and the bone contacting the NiTi plates no pathological inflammations were observed, and osteoid-like structure was seen after two weeks, and new bone formations were markedly seen after four weeks. A small amount of Ti and Ni elements were observed in the circumferential tissue of the NiTi plate in the all cases. The amount of Ni elements were found much more than Ti elements. There were no difference between rough surfaces and micro-finished surfaces. Similarly, new bones invaded into spaces of the nails on the NiTi stems and cortical bone formations were seen on weightbearing areas coming in contact with stems in all cases (Fig. 1).



Fig. 1

The stem implanted in tibia of a living sheep for 6 months.

Ni elements were observed here and there in the bone and the soft tissue coming in contact with the NiTi stems (Fig. 2), while Ti elements were scarcely observed on the same areas.

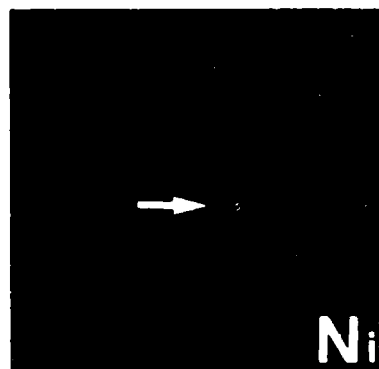


Fig. 2

The electron microanalysis.

A large amount of Fe, Ca and P also were observed on the same areas (Fig. 3). However, the same areas could not be observed histologically. On the whole, no pathological inflammations were seen histologically.

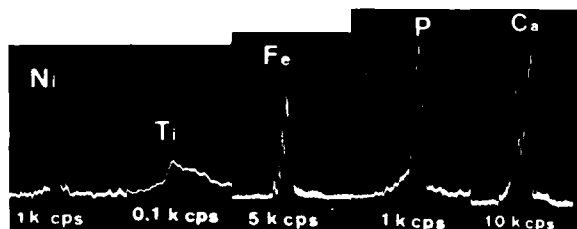


Fig. 3

The electron microanalysis on the same area.

3. Conclusion and discussion

In conclusion, as Ni elements alone were separated from NiTi alloy and a large amount of Fe, Ca and P were observed on the same areas, Ni elements were supposed to activate blood supplies and biological reactions, and as the results bone formations were accelerated. Therefore, for clinical use, NiTi alloy has to be coated by some biocompatible materials as Ti, TiN or Al₂O₃.

* 677-2, Kido-Cho, Kawachinagano-Shi, 586 Osaka JAPAN

** Osaka Prefectural Industrial Research Institute

*** The Furukawa Electric Co., Ltd.

P. TRANQUILLI-LEALI M.D. , S. BARTOLI Ph.D.

CLINICA ORTOPEDICA, UNIV. CATTOLICA, ROMA, ITALY

IT IS COMMONLY KNOWN THAT A METALLIC DEVICE IMPLANTED IN THE BODY NORMALLY RELEASES IONS IN THE ENVIRONMENT. IN OUR BIOMATERIALS LABORATORY THE CELL/ METAL INTERACTIONS ARE EVALUATED BY USING FIBROBLAST MONOLAYER CULTURES TESTED WITH DIFFERENT METAL SALTS AND GROWING ON DIFFERENT SUBSTRATA. METAL SALTS ARE ALSO TESTED ON PHA INDUCED PROLIFERATION OF HUMAN LYMPHOCYTES. THE CELL REACTION IS EVALUATED AS :

- CELL COUNT
- DNA, PROTEIN, MALONILALDEHYDE (MDA) ASSAYS
- 3H-THYMIDINE INCORPORATION OF FIBROBLASTS AND LYMPHOCYTES
- S.E.M. MORPHOLOGY

THE EFFECTS ON FIBROBLAST GROWTH ARE SUMMARIZED AS % CELL NUMBER INHIBITION IN TABLE I.

TABLE I : % INHIBITION (Mean +/- S.E.)-72 HRS
OF FIBROBLAST GROWTH WITH 12 mcg/ml OF METAL SALTS.

CoCl ₂	49.30	+/- 1.47
NiCl ₂	27.16	.62
CrCl ₃	14.31	.87
FeCl ₂	4.68	.79
TiCl ₃	-8.00	7.22

A BETTER UNDERSTANDING OF THIS PHENOMENON IS POSSIBLE ANALYZING THE RESULTS REPORTED IN TAB.II.

TABLE II : % INHIBITION (Mean +/- S.E.)-72 HRS					
3H-THYMIDINE INCORPORATION			DNA SYNTHESIS		
FeCl ₂	-1.14	+/- .23	15.58	+/- 4.26	
CoCl ₂	44.4	5.01	61.90	7.23	
TiCl ₃	.5	3.43	11.26	4.65	

FROM THIS EXPERIMENTAL SERIES IS EVIDENT THAT SOME METALS, OVERALL COBALT, MARKEDLY REDUCE THE CELL DUPLICATION VIA A SPECIFIC BLOCK OF THYMIDINE INCORPORATION AND CONSEQUENTLY OF DNA SYNTHESIS.

THIS INHIBITING EFFECT IS ALSO PRESENT ON CELL GROWING ON METALLIC DISHES. BY S.E.M. WITH AN ORIGINAL FIMATION TECHNIQUE THE CELL DENSITY AND DISTRIBUTION OF FIBROBLASTS GROWING ON DIFFERENT SUBSTRATA IS REPORTED. THE EXPERIMENTAL DATA SHOWED THAT ON TITANIUM AND Ti AL6 V4 ALLOY THERE IS AN HOMOGENEOUS AND NORMAL MONOLAYER, WHILE ON AISI 316 THE DENSITY OF CELLS IS REDUCED AND ON CO-CR ALLOY IS ALMOST COMPLETELY INHIBITED.

FOR ANALYZING SOME MINOR ASPECIFIC EFFECTS OF METAL IONS, CELL MEMBRANE LIPOPEROXIDATION -AS M.D.A. PRODUCTION- WAS TESTED. EXCEPT COBALT ALL METAL IONS EXAMINED INDUCE, WITH A DIFFERENT EXTENT, A M.D.A. PRODUCTION. THE MOST EFFECTIVE ION IS TITANIUM (30 % MORE THAN CONTROL SYSTEM). NICKEL HAS A LOWER EFFECT AND TRIVALENT CHROMIUM A SCARCE ONE. THESE DATA INDICATE THAT SOME METAL IONS CAN BE INDIRECTLY TOXIC THROUGH A MECHANISM OF CELL MEMBRANE PEROXIDATION.

THE METAL ION CAN BE ALSO TOXIC FOR HUMAN LYMPHOCYTES. IN FACT LYMPHOCYTES PROLIFERATION INDUCED BY P.H.A. (.6 mcg/ml) IS STRONGLY INHIBITED FROM 50 µM METAL SOLUTIONS (TAB.III)

TAB.III : % LYMPHOCYTE PROLIFERATION INHIBITION
(Mean +/- S.D.)

CoCl ₂	87.5	+/- 1.9
MnCl ₂	43.1	5.7
NiCl ₂	17.9	2.3
CrCl ₃	n.d.	

IN CONCLUSION METAL IONS CAN BE TOXIC FOR CELLS EITHER SPECIFICALLY BY BLOCKING DNA SYNTHESIS PATHWAYS, AS COBALT, EITHER ASPECIFICALLY BY DAMAGING THE CELL MEMBRANES VIA REDOX REACTIONS AS TITANIUM. FOR THESE REASONS COULD BE BETTER TO REDUCE THE IMPLANTATION OF CO-CR ALLOYS AND DO NOT USE TITANIUM IN ARTICULATING SURFACES BECAUSE MANY IMPLANT FAILURES AND ALSO LATE INFECTIONS COULD BE EXPLAINED BY THE OVERMENTIONED MECHANISMS.

- 1) MEARS, D.C., ELECTRON-PROBE MICROANALYSIS OF TISSUE AND CELLS FROM IMPLANT AREAS, J.B.J.S. 48-B, 3:567-576, 1966
- 2) RAE, J., A STUDY ON THE EFFECTS OF PARTICULATE METALS OF ORTHOPAEDIC INTEREST ON MURINE MACROPHAGES IN VITRO, J.B.J.S., 57-B, 4:444-450, 1975
- 3) TRANQUILLI-LEALI P., BIOCOMPATIBILITY OF IMPLANT MATERIALS, ATT.ORT.TRAUM., 1-18, 1982.

P. Ducheyne*, M. Martens, W. Colen, P. Delpont

Departments of Materials Science and Orthopaedics
University of Leuven, Belgium

Most metals currently in use for implant devices derive their excellent corrosion resistance from a thin but adherent oxide layer which forms spontaneously at their surface. These metals such as stainless steel type AISI 316L, cobalt-chromium base alloys or titanium and titanium alloys are in the so-called passive condition when placed in a physiological environment. There is no perceptible degradation except when, for whatever reason, the passivity would be disturbed. Although these metals, and especially titanium and its alloys, are very corrosion resistant they release metal ions or compounds into the surrounding tissues. The objective of the present paper in threefold: i) the identification of the release of Ti from porous Ti under various conditions of simulated physiological environment and surface state; ii) the *in vitro* determination of the relationship between the previously reported (1,2) increase of Ti oxide thickness and the amount of Ti release, if any, and iii) the *in vivo* determination of Ti ion release from porous titanium for the surface condition with lowest *in vitro* release.

Methods and Materials

Porous fiber materials with Ti fibers of 50 μ m diameter were fabricated using conventional pressing techniques and subsequent sintering at 925°C for 30 minutes. Cylindrical specimens 3 mm in height and 15 mm in diameter were immersed in Hank's solution (H) as such or to which either 2% citrate buffer (C) or EDTA (E) was added in an effort to simulate the complexation action of the physiological environment. The specimens came both in the passivated and the non-passivated condition. Passivation was by the use of a 40 vol. % nitric acid solution at 55°C.

Dense specimens, with polished surfaces were used for the A.E.S. analyses. Parameters of the study were similarly passivation or not and the composition of the simulated physiological solution.

Porous specimens were implanted intramedullary in the femur of sheep for periods ranging up to 4 months. The Ti ion concentration in serum and urine for various periods of time up to sacrifice were determined using GFAAS (graphite furnace atomic absorption spectroscopy).

Results and Discussion

Table 1 shows the results of the *in vitro* metal ion release from the porous Ti. It follows from the data that there is an effect from the complexation action of the citrate and the EDTA. Since citrates are present in bone tissue and the complexation action of EDTA depends, similar to the one of proteins, on the amino and carboxyl groups,

these data substantiate the interaction between the outer Ti oxide layers and complexing agents contacting it. When the surface is passivated, the net effect is much smaller. This is probably due to the formation of a Ti oxide structure of near ideal structure and composition.

TABLE 1

passivation	solution	time of immersion (wks.)	concentr. (ppb)
/	H	1	5
		2	/
		4	5
x	H	1	7
		2	11
		4	10
/	H + 2%C	1	27
		2	47
		4	44
x	H + 2%C	1	22
		2	21
		4	42
/	H + 2%E	1	415
		2	996
		4	2,353
x	H + 2%E	1	35
		2	36
		4	40

It is also found that when Ti is passivated there is no noticeable *in vitro* increase of the Ti oxide thickness. This is unlike for non-passivated Ti where the oxide film thickness doubled after a 6 month immersion in Hank's. The *in vivo* experiments were carried out with passivated Ti fiber material. Prior to implantation no Ti could be detected in any of the five animals of the study. However, as soon as one week after implantation, measureable contents of Ti appeared in the serum and in the urine. There was no noticeable increase with time in the serum, but probably one in the urine.

References

- McQueen, D. et al. Auger Electron Spectroscopic studies of Ti implants in "Clinical Application of Biomaterials" Eds. AJC Lee, T. Albertson, P.I. Branemark, J. Wiley, 1982, p. 179-185.
- Ducheyne, P. et al. The *in vivo* changes of the surface of Ti and Ti alloys: A hypothesis for the Titanium Ion Release J. Biomed. Mater. Res., Submitted

Acknowledgements

Financial support for part of the present work was obtained from the Foundation for Medical Research, Belgium and Zimmer Inc., Warsaw, USA.

* Present Address:

Dr. Paul Ducheyne, Associate Professor of Biomedical Engineering University of Pennsylvania Philadelphia, PA 19104

SURFACE MODIFICATION OF SMALL DIAMETER DACRON VASCULAR GRAFTS AFTER A TETRAFLUOROETHYLENE GLOW DISCHARGE TREATMENT

A.S. Hoffman, A.M. Garfinkle, and B.D. Ratner

University of Washington
Seattle, WA 98195 USA

Glow discharge treatment to modify biomaterial surface compositions remains a relatively untapped resource for clinical applications today. This technique has certain advantages, which include an ability to change surface chemical composition of a substrate without altering texture, porosity, surface area, or desirable bulk properties such as compliance. In plasma or glow discharge polymerization an organic compound (monomer) in the gas phase is introduced into a vacuum system containing the substrate material to be treated. The monomer gas is then subjected to some form of electric discharge, in the case here an inductively coupled electrodeless discharge. Active species are generated in the gas due to absorbed energy, and these species may react with and covalently bond to the substrate.¹ To obtain adequate surface coverage, flowing gas is commonly used. Important process parameters include monomer flow rate, initial system pressure, radio-frequency discharge power, geometrical design of the reactor and the location of the substrate within the reactor.

We have used a glow discharge of TFE gas to treat the luminal surface of 4-5mm ID Dacron vascular grafts of varying porosities. The Dacron samples were pre-cleaned by sonication in trichloroethylene, followed by methanol and then deionized water. ESCA spectra showed C/O and C/H ratios to be constant for all Dacron grafts after this cleaning procedure. Cleaned Mylar film (also composed of polyethylene terephthalate) was used as a model substrate for the Dacron fibers. Glow discharge system variables were then investigated using Mylar films and Dacron grafts treated together in the reactor. Specific conditions were determined which would reproducibly generate a mechanically strong, covalently bound, uniform, ultrathin fluoropolymer film on the substrate material.

ESCA spectra of PTFE, Dacron, and TFE-treated Dacron are compared in Fig. 1. These data show the TFE-treated Dacron to have a highly fluorinated surface that is distinctly different from both polyethylene terephthalate and PTFE. ESCA studies of the Dacron grafts indicated that the TFE glow discharge treatment was uniform along the graft (Table I).

When the untreated and TFE-treated Dacron grafts were soaked in methylene blue solutions, the untreated Dacron picked up dye and exhibited an even blue color while the treated Dacron showed no dye pickup at all. This also indicates that the TFE glow discharge treatment was evenly deposited along the Dacron fibers. Scanning electron microscopy showed no observable change in treated Dacron graft surface morphology at 7000X. Graft porosity was remeasured and did not change.

Critical surface tension measurements using the Zisman technique on treated Mylar surfaces yielded a γ_c of approximately 13 dynes/cm. This is lower than the value measured for PTFE, which was ca. 20. The difference may result from the significant concentration of $-CF_2$ groups on the treated surfaces as compared to PTFE Teflon (Table I). The stability of the films generated on Mylar was examined by remeasuring the critical

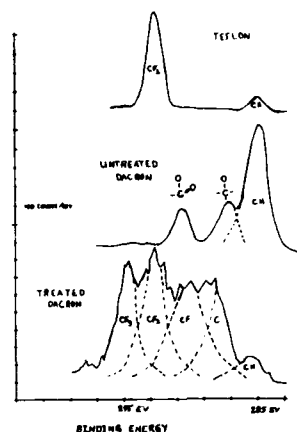


Figure 1. ESCA spectra of PTFE Teflon, untreated Dacron, and TFE glow discharge-treated Dacron.

TABLE I: HOMOGENEITY OF SURFACE FLUOROPOLYMER COATING ON A MEDIUM POROSITY DACRON KNIT VASCULAR GRAFT

ESCA Sample Location (cm)*	C/F	C1s Peak Areas (% of total)				
		CH	C	CF	CF ₂	CF ₃
Inside downstream (+1.)	0.70	1	26	18	34	21
Inside upstream (-1.)	0.67	1	22	22	36	19
Outside downstream (+1.)	0.70	0	26	18	34	22
Outside upstream (-1.)	0.71	1	21	22	33	23
PTFE (theoretical)	0.5	--	--	--	100	--

* 0 = center of sample

surface tension after exposure to either acetone, methanol or phosphate buffer at 20°C for two-hour periods. These experiments showed small rises in γ_c , the extent of the increase being dependent on the particular solvent treatment. All surfaces remained very low in energy, similar to PTFE.

The TFE glow discharge treated grafts have been tested in an *ex vivo* femoral baboon shunt and have been found to remain patent for periods up to three weeks, while untreated Dacron grafts rapidly occlude with thrombus.³ This treatment may, therefore, enhance the performance of Dacron vascular grafts in general, and in particular, those used for small diameter graft applications.

Acknowledgment: The authors would like to acknowledge the support of the NHLBI, Devices and Technology Branch, Grant #HL-22163-03 to -05. We also thank Stacy Yamasaki for carrying out the critical surface tension studies.

References

1. Yasuda, H. and T. Hsu, Surface Sci., 76, 232 (1978).
2. Yamasaki, S., unpublished data, Center for Bioeng., Univ. of Wash., Seattle (1983).
3. Garfinkle, A.M., A.S. Hoffman and B.D. Ratner, Trans. Soc. for Biomats., Wash. DC, April 1984

Center for Bioengineering and
Department of Chemical Engineering
University of Washington FL-20
Seattle, WA 98195 USA

EVALUATION OF MATERIALS IN CONSIDERATION OF AN ARTIFICIAL FALLOPIAN TUBE

S. K. Hunter, D. E. Gregonis, D. L. Coleman, R. L. Urry, and J. R. Scott

Department of Pharmaceutics and Division of Artificial Organs, University of Utah, Salt Lake City, Utah

In the U.S.A., 15 to 20% of married couples are unable to conceive, primarily due to obstruction of the fallopian tubes. Successful treatment of nonpatent tubes is limited to a small percentage of patients with this problem. New microsurgical techniques used for tubal repair and in-vitro fertilization have been only moderately successful in achieving intrauterine pregnancies. A prototype artificial fallopian tube has been designed and constructed from Silastic for implantation in the rabbit. Other materials are being tested in vitro to determine their biocompatibility with sperm and ovum. Table 1 lists 8 polymers which have been selected for in-vitro studies based on their surface tensions (α).

Table 1

Material	α (Dynes/cm)
1. Fluorinated ethylene-propylene	16
2. Poly(dimethyl siloxane)	23
3. Polyethylene	30
4. Segmented poly(ether urethane)	34
5. Poly(ethylene glycol)	42
6. Poly(ethylene glycol)urethane	42
7. Nylon 6,6	42-46
8. Poly(hydroxyethyl methacrylate) (hydrated)	70

All materials are characterized by 1) optical microscopy, 2) SEM and x-ray microanalysis, 3) dynamic and receding contact angles 4) ESCA, 5) ATR-IR and 6) inhibition of cell growth toxicity tests.

METHODS

Materials 1 through 4 and 7 are obtained commercially as small-diameter tubing. Polymers 5, 6, and 8 are coated on the inner surface of glass tubes similar in diameter to the polymer tubes.

Material 5 is a water-soluble polyether with terminal hydroxyl groups, and has been shown to be nontoxic both orally and intravenously. We have covalently bound PEG to the amino groups of aminopropyl silanized glass. This was accomplished by phosgene derivatization of PEG to form PEG bis-chloroformate and results in a PEG-urethane linkage at the silica surface. In aqueous environments the unreacted PEG chloroformate is immediately hydrolyzed to regenerate the terminal hydroxyl group. We have demonstrated that PEG functionalized glass does not adhere protein when exposed to whole serum.

The PEG urethane, material 6, is prepared in 2 steps: 1) end capping PEG, MW 600, with 2 moles of methyl bis(phenyl isocyanate); and 2) chain extending this prepolymer with ethylene diamine.

The poly(hydroxyethyl methacrylate) (PHEMA), Material 8, is the hydrogel commonly used in soft contact lens formulations. This hydrogel is not water soluble and remains in place on the glass substrate for in-vitro testing.

In-Vitro Gamete Materials Compatibility Studies

Sperm mobility and viability. Sperm is collected, washed, and mixed with a nutrient media. This solution is then injected into tubes comprised of the materials discussed above. The tubes

containing the sperm and nutrient media solution are placed in a triple-gas incubator (5% CO₂, 5% O₂, 90% N₂) at 37°C. At various time intervals small increments of the solution are removed and submitted for microscopic evaluation to determine mobility, viability, and morphology.

Sperm penetration studies. Eggs from super-ovulated hamsters are collected, made zona-free with trypsin, and introduced into tubes containing human sperm in nutrient media. After 4 to 6 hours the tubes are flushed and the effect the various materials have had on the percent of penetration are noted.

Mouse embryo growth and division. Two-cell mouse embryos are collected and injected into the different tubes with a nutrient media. At predetermined times the tubes are flushed, the embryos isolated, and the effects the different materials have had on the degree of embryo growth is noted.

Table 2 lists data on sperm mobility and viability for polyurethane and Silastic tubing.

Table 2

Group and Incubation Time	Progressive Motility	Motility Score
<u>Polyurethane</u>		
Initial	46.2 ± 4.3*	188.5 ± 10.3
1 hour	43.5 ± 3.7	172.7 ± 11.1
2 hours	37.3 ± 3.6	146.9 ± 12.8
3 hours	36.0 ± 3.9	128.9 ± 11.9
<u>Silastic</u>		
Initial	43.1 ± 5.3	195.6 ± 23.9
1/2 hour (control)	52.5 ± 2.1	181.9 ± 6.9
1/2 hour (tube)	40.6 ± 3.6	164.4 ± 9.3
1 hour (control)	45.6 ± 2.7	174.4 ± 10.5
1 hour (tube)	28.1 ± 5.9	118.8 ± 17.9
2 hours (control)	36.4 ± 6.2	139.3 ± 18.4
2 hours (tube)	15.0 ± 5.0	72.1 ± 12.6

*mean ± SEM ($n = 8$)

The percent progressive motility is a semi-quantitative measure of sperm activity and is based on the total number of sperm moving in a reasonably straight line with normal speed. Sperm are graded from 0 to 4 based on their activity and unidirectional mobility. The percent of sperm in each category is determined, multiplied by the respective grade, and summed to give a motility score. Table 3 illustrates the effects of these materials on sperm penetration in zona-free hamster eggs.

Table 3

Group	(%) Eggs Penetrated
Control	70.0 ± 7.5*
Silastic tube	47.2 ± 8.1
Polyurethane	66.1 ± 5.3

*mean ± SEM ($n = 12$)

Work was funded by a biomedical research support grant through the Col. of Pharmacy and the Depart. of Obstetrics and Gynecology.

Col. of Pharmacy, 301 Skaggs Hall, University of Utah, Salt Lake City, Utah 84112, U.S.A.

J.A. Hayward, M.A. Whittam, D.S. Johnston, and D. Chapman

Biochemistry and Chemistry Dept., Royal Free Hospital School of Medicine
Rowland Hill Street, London NW3 2PF

Many studies have been made of the structure and dynamics of biological membranes and it is now generally accepted that a lipid bilayer provides the matrix in or upon which proteins and glycoproteins are located. Compositional asymmetry is characteristic of biological membranes. It has been suggested that in the case of blood cells the observed asymmetric polar lipid distributions may serve a biological purpose in the maintenance of the delicate balance between haemostasis and thrombosis. The cytoplasmic leaflets (comprised largely of negatively charged phospholipids) of the plasma membrane of erythrocytes and quiescent platelets, or liposomes of similar lipid composition, exhibit high procoagulant activities. In contrast, the outer surfaces of both cell types (comprised largely of neutral phospholipids), or neutral phospholipid vesicles, are inactive in coagulation tests. Our aim has been to develop a stable polymer with a hydrophilic surface that mimics the interfacial characteristics of non-reactive cell surfaces. The simplest common factor among these cellular surfaces is the high content of neutral phospholipid. We have, therefore, pursued the development and application of polymerisable phospholipids.

We have synthesized phosphatidylcholine molecules that contain diacetylene groups in the acyl chains (Figure 1). These lipids form cross-linked polymers upon exposure to ultraviolet light or X-ray irradiation. The polymer chain, which is composed of conjugated multiple bonds, absorbs in the visible region of the spectrum and the polymers are strongly coloured. The colour arises from the conjugated double and triple bonds that make up the polymer backbone. Formation of the polymer can be induced when the lipids are arranged in monolayers, multilayers, or bilayers.

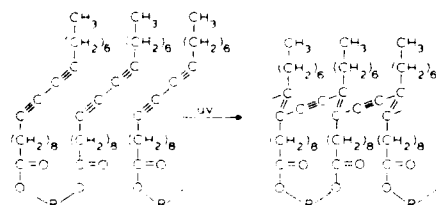


Figure 1. Schematic of the formation of the conjugated polymer.

The dynamic properties of the monomeric, diacetylenic phospholipid were studied by optical and magnetic resonance spectroscopy, and by calorimetric and monolayer techniques, and appear to resemble the properties of naturally occurring lipids. We have shown that it is possible to grow cells in media containing diacetylenic fatty acids. Large amounts of the fatty acids are bio-synthetically incorporated into the membrane phosphatides which, upon irradiation with ultra-

violet light, polymerise. In this manner, a stable polymeric membrane is obtained that entraps membrane and cellular components.

We have described the procedures used to prepare Langmuir-Blodgett type multilayers of polymerisable phospholipids. Varied materials (glass, quartz, perspex, teflon and mica) were coated with ordered layers of diacetylenic phosphatidylcholines in which the polar groups of the lipid form the outer coated surface. The layers after polymerisation were quite stable in aggressive media and, with some precautions, could be handled without damage. The ability to coat an artificial surface with a stable polymeric phospholipid should render the surface biocompatible, especially when the polymer mimics the surface of host cells.

Finally, we have examined the properties of liposomes prepared from diacetylenic phosphatidylcholines. Polymerisation markedly enhances the stability of liposomes to precipitation, and polymerisation reduces their permeability to glycerol. Polymeric liposomes may have important applications as pharmacological capsules for drug delivery. The haemocompatibility of liposomal preparations was estimated by comparing the recalcification clotting times of citrated pooled normal plasma in the presence of assorted lipid dispersions (Figure 2). A brain lipid extract (containing large amounts of negatively charged phospholipids) markedly accelerated the rate of clot formation in a concentration-dependent manner. In contrast, and in agreement with results obtained by previous authors, liposomes prepared from dimyristoyl phosphatidylcholine, did not reduce the blank clotting times. Similarly, clot formation was not affected by diacetylenic phosphatidylcholine when present in either monomeric or polymeric form. These preliminary results support our concept for biocompatible surfaces, and suggest that the polymeric phosphatidylcholines may find extensive applications in vivo.

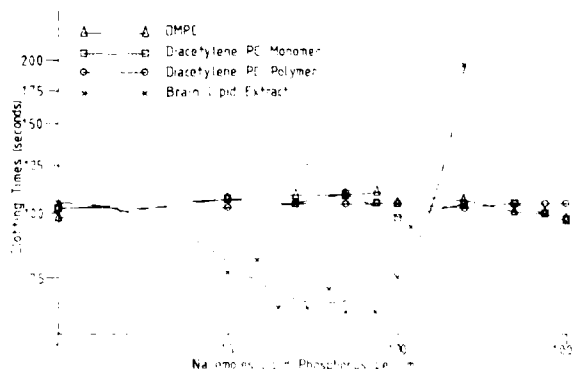


Figure 2. The effect of diacetylenic phospholipids on clotting time.

Supported by the Muscular Dystrophy Association, the S.E.R.C., and Shell Research, Ltd.

B.D. Ratner[†], Y. Haque^{*}, T.A. Horbett[†], M.B. Schway^{*} and A.S. Hoffman[†],^{*}Dept. of Chemical Engineering and [†]Center for Bioengineering, University of Washington, Seattle, WA. 98195

A reliable set of rules does not yet exist to predict the way biological systems (proteins, cells, blood, tissue, etc.) will interact with synthetic materials. Such a set of rules would be valuable for understanding responses to implanted devices and for designing new biomaterials and devices. It has been our goal over the last few years to synthesize model sets of surfaces which can be used to explore biological reactions with synthetic materials, and to develop an understanding of the factors controlling such reactions so that generalizations which can be used in prediction or design might be made.

RF-plasma deposition of thin films is an attractive method for preparing surfaces which might be useful to explore bioreactions. A variety of supports can be coated and the coatings are transparent, ultrasmooth, durable, pinhole-free and can be generated with a wide range of surface energies. In this study, surface energy was of particular interest. A series of RF plasma-deposited surfaces varying in surface energy over a wide range has been prepared and used to study the influence of surface energy on fibronectin (FN) adsorption.

A reactor, constructed in our laboratory, concentrates a plasma produced using a 13.56 MHz RF generator within a low pressure chamber into which gases and gas mixture can be introduced through a mass flow-controlled gas blending system (Linde FM4590). The gases used in this work were perfluoropropane (C_3F_8) and ethylene oxide (C_2H_4O). Films were deposited on glass or Lux (Mylar) cover slips which were first etched in the reactor in an oxygen or argon plasma to clean their surfaces.

Critical surface tension (γ_c) values of films prepared using C_3F_8 , and C_2H_4O , are listed in Table 1. A wide range of γ_c values was observed. By varying the gas ratio, a graded series of surfaces throughout the entire range is possible. The extremely low γ_c values obtained for the C_3F_8 films may reflect inherent limitations in the γ_c method attributable to the use of liquids exhibiting substantial polar character on extremely non-polar surfaces. However, since PTFE sheet, under the same test conditions, gave γ_c values of 18-19 ergs/cm², we speculate that these surfaces have energies lower than that of Teflon. Blending of additional oxygen with the C_2H_4O or pre-etching with oxygen can result in films with higher γ_c 's than those obtained with the pure C_2H_4O gas.

The chemistry of the surface region is readily examined by ESCA. The absence of any oxygen detectable by ESCA in the surface region of these films indicates that the C_3F_8 polymer forms a contiguous overlayer on the glass or Lux which is at least 100Å thick. The chemistry of the surfaces of the graded series ranges from one dominated by CF_3 - and $-CF_2$ - moieties (top spectrum, Figure 1) to a composition rich in hydrocarbon material and containing a variety of carbon-oxygen functional groups (bottom spectrum, Figure 1).

At a 50:50 ratio of C_3F_8 to C_2H_4O , hardly any fluorine can be detected in the film - C_2H_4O shows a much greater tendency towards incorporation than C_3F_8 .

The surfaces shown in Figure 1 are being studied with respect to their ability to adsorb ¹²⁵I-labelled fibronectin from serum. By diluting the serum, the competition between FN and other serum proteins for surface sites is reduced. A maximum in FN adsorption has been observed as a function of serum dilution on glass surfaces. This maximum may be related to the inherent affinity of the surface for the protein. Analogous experiments with fibrinogen in plasma have shown that the peak adsorption occurred at different dilutions on glass, Teflon and polyethylene. Using this series of RF-plasma polymer films, we hope to establish whether the FN adsorption maxima also varies with surface energy.

Table 1 γ_c for RF Plasma Films

C_3F_8	C_2H_4O	O_2	γ_c (ergs/cm ²)
100	-	-	1
50	50	-	22 ¹
-	100	-	40 ¹
-	100	-	43 ²
-	80 ³	20 ³	45

- 1 - Glass pre-etched with argon plasma
2 - Glass pre-etched with oxygen plasma
3 - approximate values

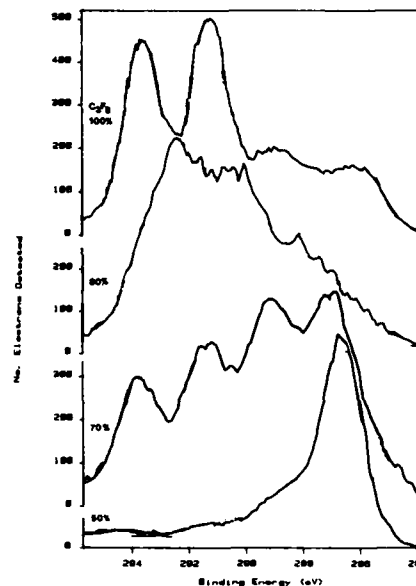


Figure 1 - C1s ESCA spectra of RF Plasma films

This work was supported by NHLBI grant HL19419.

PORPOISE AND KILLER WHALE SKIN AS NATURAL EXAMPLES OF LOW-DRAG, LOW ADHESION BIOMATERIAL SURFACES

R. Baier, M. Meenaghan, J. Wirth, H. Gucinski, S. Nakeeb

State University of New York at Buffalo and Advanced Technology Center,
Calspan, P. O. Box 400, Buffalo, NY 14225

Histopathologic analyses of full thickness skin specimens from trained porpoises and killer whales illustrate remarkable similarities to oral mucosa. Particularly prominent is the parakeratotic nature of the epidermal cells, nucleated up to and including the superficial squamous layer, and the interdigitating rete pegs of the epidermis and connective tissue papillae of the dermis. Numerous intriguing details of the dermal vascularization, innervation, and collagenous fiber arrays have been assessed as they might relate specifically to the reputed drag reducing properties of the surface structures of these marine mammals. Of special interest is a uniform, amorphous protein layer observed in transmission electron micrographs to be the true interfacial material in contact with the seawater environment. Occasional oil droplets noted to be resting on this surface (as an artifact of sample retrieval and storage) exhibit surprisingly large contact angles, even when viewed at high magnifications in TEM sections, suggesting the interfacial layer to be of low surface energy.

Concurrent investigations of the surface properties of the living animals in aquarium and open ocean environments have confirmed the low-energy, fouling-resistant character of these natural biomaterials. Immediately after full or partial removal from their seawater milieu, porpoises and killer whales have been subjected to these mild examinations of their surface chemistry, surface energy, and surface texture (as first calibrated on the skin of the investigators): (1) optically smooth, clean plates of germanium, in geometries suitable for multiple attenuated internal reflection infrared spectroscopy, have been gently stroked along various body surfaces of the marine mammals to acquire thin layers of the most superficial substances; (2) tiny droplets of a series of highly purified test fluids of known, calibrated surface tensions have been placed onto the still-hydrated (but not grossly wet) skin surfaces of many porpoises and 3 killer whales to assess wetting/spreading behavior and determine "critical surface tensions;" and (3) replicas of the surface textures of various skin areas have been obtained with a fast-curing polysulfide material originally developed for producing high-resolution replicas of the surface detail in the human oral cavity. Total time consumed by a well-trained investigative team in acquiring these data and specimens has ranged from 12 to 20 minutes per animal, assuring safe and rapid return of the animals to their aqueous environments without obvious distress.

RESULTS. Living porpoises and killer whales are surfaced with thin, glycoproteinaceous layers that cover fully-nucleated, relatively easily shed epidermal cells, the entire structures displaying shallow parallel surface striations of about 0.3 mm wavelength and oriented transverse to the body length. The surface-localized substance is substantially free of lipoidal or saccharide components, although these ingredients are present in the subjacent epidermal and dermal layers. Yet, significantly, the measured critical surface tension for

living porpoise and killer whale skin is between 20 and 30 dynes/cm, a characteristic shared with the oral mucosa and the endothelial lining of blood vessels.

Thus, the skin of marine mammals historically known to exhibit excellent long-term freedom from drag-enhancing surface accretions (biofouling deposits, etc.) in a saline milieu may be taken as a large-surface-area, externalized model of similar low-drag, low-adhesion interfaces in the oral cavity, vascular tree, or elsewhere in the human body.

Although it has also been speculated that certain marine species especially porpoises and killer whales, might have active or passive drag-reducing properties, there is no evidence from this work that such properties can be attributed to the interfacial structures or components. Interestingly, the fine "grooved" surface texture is oriented at nearly right-angles to the flow direction, 90° out of phase with flow-smoothing elements sometimes suggested to delay onset of turbulence, over streamlined objects. No obvious oil depots or regular morphological features are present to suggest sufficient compliance of the surface layers to damp turbulent eddies. The sloughing and/or exudation rate of the superficial protein-rich coating and squamous cells is too small to account for significant drag reduction by mechanisms described for high-molecular-weight polymers (e.g., polyethyleneoxide, polyacrylamide) or suspended asymmetric particles.

Using a novel stagnation-point flow cell to determine relative drag-reducing characteristics of various solution additives and surface coatings, it has been possible to observe (at much lower Reynolds Numbers than for standard pipeline or flat plate parallel flow) true drag-reducing, drag-enhancing, and net neutral effects of surface coatings on test plates. Transferred surface material from porpoises, like saliva, neither augments nor reduces the drag of seawater flowing through this laboratory test device. Conversely, biological slime films such as the thin microfouling layers that form spontaneously on all manmade materials in the sea, and even some fish slimes, actually increase the drag. It seems likely, therefore, that the operating advantage of marine mammals like porpoises and killer whales in the sea results from their freedom from the penalties of adherent biofouling films rather than from some positive drag-reducing function. Again, the analogy to the performance of the oral mucosa and the vascular endothelium as biofouling-resistant natural surfaces is obvious.

CONCLUSION. It has been learned from the application of multiple attenuated internal reflection infrared spectroscopy, contact angle measurements, and surface replicas of living porpoise and killer whale skin, supported by scanning electron microscopy/energy-dispersive x-ray analysis, and histopathology at both light and electron microscope levels of full thickness biopsies, that these marine mammals reputed to display extraordinary fouling-resistant flow surfaces in nature are covered with tissue most similar to the "modified skin" of oral mucosa.

METALLURGICAL AND THERMAL-WAVE FAILURE ANALYSIS OF TWO BJORK-SHILEYTM
SPHERICAL DISK VALVES USED IN JARVIK-7TM TOTAL ARTIFICIAL HEARTS

P. E. Duncan, R. Rowe,^{**} V. Kerlins,^{**} A. Rosencwaig^{***}

Kolff Medical, Inc., Salt Lake City, Utah

Failure of a Bjork-Shiley spherical disk valve in the JARVIK-7TM total artificial heart after 13 days in Dr. Barney Clark was cause for reassessment of the choice of valve. The failure mechanism was examined for the valve from Barney Clark and for another Bjork-Shiley spherical disk valve which failed coincidentally after 162 days in a calf. The failure analysis was conducted using a new non-destructive thermal-wave imaging technique, as well as traditional metallurgical methods.

METHODS: Failure analysis included a review of an earlier study following reported clinical failures.⁽¹⁾ Operating parameters of both the HERCULES and Barney Clark left ventricles were also reviewed to ascertain any contributing effects to valve failure.

Both broken valves were examined by a method⁽²⁾ new to biomaterial analysis, thermal-wave imaging. Weld regions on an intact, "experimental-quality" Bjork-Shiley spherical disk 27mm valve were examined by thermal-wave imaging to determine how well strut weld characteristics could be revealed. Subsurface microstructural transitions are visible with thermal-wave because these regional variations result in detectable thermal features when an electron beam scans across the sample and is absorbed. Periodic heating results at the beam modulation frequency and can be imaged by the employment of an acoustical carrier wave.⁽³⁾ Thermal-wave images were produced of both the HERCULES and the Barney Clark 29mm valves and of alternative single-pieced machined valves from Medtronic, Inc. and Shiley, Inc.

The Materials & Processes Laboratory of McDonnell Douglas Astronautics Company conducted the metallurgical failure analysis. It was determined that the Bjork-Shiley (clinical quality) valve which failed in the left ventricle of Barney Clark should be analyzed, in so far as possible, with non-destructive techniques. The McDonnell Douglas team was thus limited to fractography for that valve. The "experimental-quality" valve which failed in the calf HERCULES, could be analyzed by fractography, metallography and hardness testing which required sectioning of the valve.

RESULTS: Fractographic and metallographic results were compared to the findings from the thermal-wave study to determine the value of thermal-wave imaging in understanding causes of fracture failure.

Thermal-wave imaging of the unused "experimental-quality" Bjork-Shiley valve weld regions revealed a pattern of bisecting, large columnar grains running circumferentially through the central section of the weld where the strut is joined to the ring; the point of maximum stress concentration in this valve design. Thermal-wave imaging of the broken Bjork-Shiley valve from Barney Clark did not reveal the specific cause of failure, due in part to acoustical "ringing" from the free strut member. The images which were obtained showed that although the pattern of bisecting, large columnar grains was visible, the fracture was not limited to this region, suggestive of another cause of failure. In the SEM-mode, while examining the broken section, the surface flaws later determined to be the stress concentrators, were observed and noted. The thermal-wave images of the HERCULES valve likewise revealed

the large columnar grain transitions, but also work hardening of the opposite strut.

Visual and SEM examination of the Bjork-Shiley valve from Barney Clark revealed the presence of a flattened area cut or ground during manufacturing into the weld fillet of the failed strut. SEM examination at magnifications up to 3000X of various features of the fracture surface of the strut indicated that a high-cycle fatigue crack initiated at tool or grinding marks left in the flattened surface. The reduced cross-section of the strut together with the presence of tool or grinding marks, resulting from the manufacturing process, caused a stress concentration which led to early fatigue fracture.

A detailed examination of the cracked strut from the HERCULES heart valve indicated that it failed by high-cycle fatigue which initiated and propagated at essentially the same location on the strut as the fracture in Barney Clark's valve. The fracture initiated adjacent to the weld in material which had been softened as a result of heating during welding. There were no flaws, such as tool marks, where the fracture initiated, and the microstructure and hardness were normal for an as-welded Haynes 25 alloy. **CONCLUSIONS:** Thermal-wave imaging is a useful, non-destructive technique for biomaterial analysis. The failures of the Bjork-Shiley valves from both Barney Clark and HERCULES occurred by high-cycle fatigue at the same location at the strut weld. The shorter life of the Barney Clark valve is attributed to the presence of a stress concentration in the strut weld produced during manufacture of the valve. The potential for Bjork-Shiley valve failure was predicted in the 1976 UBTL Report to the FDA and may have occurred in these valves due to insufficient quality control. Although the closing pressures on the mitral valve in the JARVIK-7 left ventricle are higher than those in the human natural heart, the operating parameters of the artificial hearts at the time of valve failure were within typical range.

THERMAL-WAVE IMAGE



REFERENCES: (1) Yates, W.G. et al. UBTL Report, Feb. 1976, TR 168-002. (2) Thermal-wave imaging system is manufactured by THERMA-WAVE, INC. (3) Rosencwaig, A. Science, V.218, No. 4569, Oct.15, 1982.

TM: JARVIK-7 is a trademark of Kolff Medical, Inc.

ACKNOWLEDGEMENT: Dr. A.U. Daniels, University of Utah
ADDRESS 1st AUTHOR: 825 North 300 West, SLC, UT 84103

****McDonnell Douglas Astronautics Company, H'ing B. CA**
*****Therma-wave, Inc. Fremont, CA**

CONTEMPORARY EXPLANT ANALYSIS OF PROSTHETIC HEART VALVES

Frederick J. Schoen and Charles E. Hobson

Cardiac Pathology Laboratory, Brigham and Women's Hospital,
Harvard Medical School, Boston, MA

Prosthesis-associated problems are commonly either the cause of death or the indication for re-operation after valve replacement. The purpose of this study was to determine the presently encountered causes of failure of valve prostheses.

METHODS

Sixty-five patients had reoperation for, and 8 other pts died of, valve-related complications during the period July, 1980 to June, 1983, at our hospital. These 73 pts (mean age 50 yrs, range 18 to 76), many of whom had initial operation elsewhere, were 1-264 (mean 67 months) postoperative. There were 32 mitral (M), 36 aortic (A), 4 M + A and 1 M + tricuspid replacements, by 30 mechanical prostheses (MP) and 48 bioprostheses (BP). All specimens were examined grossly and photographed; cultures were taken where endocarditis was suspected. Histologic sections were made where appropriate. Bioprostheses were radiographed in axial projection (40 KV X 0.8 min). Clinical records were reviewed.

RESULTS

Failure etiologies are tabulated in Table 1 as a function of valve type. Thrombotic occlusion occurred with five aortic replacements by Bjork-Shiley tilting disc valves with pyrolytic carbon occluders. Tissue overgrowth occurred on several prostheses in either the mitral or the tricuspid location. Most BP were removed for degenerative processes, particularly those related to calcification (CALC). Thrombosis occurred on one aortic BP. Paravalvular leaks and endocarditis occurred independently of valve design.

The postoperative interval at failure is indicated in Table 2. Paravalvular leaks, thrombosis and endocarditis presented as early as one month and as late as 17, 9 and 22 yrs, respectively. In contrast, tissue overgrowth and biomaterials degeneration became important generally only after long intervals. Durability failures of MP occurred only after 120-156 mos. Intrinsic BP CALC with leaflet tears was seen earliest after 44 mos; in contrast, several BP encountered after very long implantation times (6-10 yrs) had no detectable calcific deposits. Tears unrelated to CALC were seen as early as 12 mos. Endocarditis potentiated extrinsic BP CALC.

Table 1 - CAUSES OF VALVE FAILURE

	Number (%) of Patients with Failure Mode		
	MECHANICAL	BIOPROSTHETIC	TOTAL
Paravalvular Leak	6(21)	7(16)	13(18)
Thrombosis	5(18)	1 (2)	6 (8)
Tissue Overgrowth	6(21)	0 (0)	6 (8)
Degeneration	3(11)	25(56)	28(38)
Endocarditis	5(18)	10(22)	15(20)
Other	3(11)	2 (4)	5 (7)
TOTAL	28(100)	45(100)	73(100)

Table 2 - POST-OPERATIVE INTERVAL AT FAILURE

	No. Cases with Failure Mode at Interval (mos)				
	1-24	25-60	60-120	120+	mean (range)
Paravalvular Leak	10	0	1	2	46(1-204)
Thrombosis	3	2	1	0	37(1-108)
Tissue Overgrowth	0	1	4	1	80(47-120)
Mechan Degeneration	0	0	1	2	140(120-156)
Biopros Degeneration					
With CALC	0	5	14	0	77(44-108)
W/o CALC	1	2	2	1	58(12-122)
Endocarditis	4	6	3	2	58(24-264)
Other	1	2	0	1	87(24-216)
TOTAL (73 pts)	19	18	27	9	67 (1-264)

DISCUSSION

Explant Analysis The objectives of explant analysis are: 1) Enhanced valve selection criteria and patient/prosthesis matching, 2) Enhanced patient management and recognition of complications, 3) Elimination of complications by progressive prosthesis development, 4) Identification of sub-clinical patient/prosthesis interactions, 5) Elucidation of mechanisms of patient/prosthesis and tissue/biomaterials interactions. Complete analysis includes gross examination and photography, radiography, dissection, histology, and indicated special procedures, such as functional testing, microbiologic cultures, dimensional analysis, profilometry, biochemical procedures or scanning electron microscopy.

Causes of Failure This study emphasizes the risk of thrombotic occlusion of tilting disk valves. In most cases, alteration of anticoagulation regimen closely preceded thrombosis. BP failures were dominated by valve cuspal degeneration with or without CALC. Nevertheless, CALC occurs at widely different rates among individuals. Considerable progress has occurred in the last two decades in biomaterials and design development of heart valve substitutes and in post-operative management. Recent clinical studies utilizing actuarial methods have demonstrated a decreased incidence of prosthesis-related pathology. Nevertheless, such complications continue to be important in the long-term prognosis of many patients. Deficiencies in biomaterials are often contributory. Focused future engineering research and development efforts as well as attempted improvements in clinical management are justified to prevent and provide evaluation of late problems, especially thrombotic complications, endocarditis and degradative phenomena. Explant analysis is an important adjunct guiding potential improvements.

Acknowledgements: The authors are grateful to Drs. L.H. Cohn, J.J. Collins, Jr., and R.A. Shemin of the Division of Thoracic and Cardiac Surgery, Brigham and Women's Hospital, for their kind assistance and encouragement.

Address: Frederick J. Schoen, MD, PhD, Department of Pathology, Brigham and Women's Hospital, 75 Francis Street, Boston, MA 02115

AN ANIMAL MODEL FOR TESTING PROSTHETIC HEART VALVES

R. D. Jones, Ph.D., F. S. Cross, M.D., Ph.D., D. M. Dreher, B. S.

Division Surgical Research, Saint Luke's Hospital, Cleveland, Ohio

There is a need for an animal model in which to test prosthetic heart valves with a reasonable survival rate and sufficient survival time to permit evaluation of valve function and potential design faults. A recent publication reported 20% survival at 4 weeks following implantation of prosthetic heart valves in dogs.¹ We have developed a pre- and post-operative treatment protocol and cardiopulmonary bypass techniques which have provided a 76% survival rate to death or elective sacrifice for periods of 1 to 7 months following implantation of a variety of pericardial and mechanical mitral valve prostheses in dogs.

Because we previously demonstrated that intestinal bacteria were released into the circulation during cardiopulmonary bypass in this species,² we instituted a regimen of pre-operative protein free diet and bowel sterilization (Vibramycin) which essentially eliminated this source of bacteremia. Prophylactic cephalosporin* antibiotic treatment, 1 gm 3 times daily, was initiated on the morning of operation and continued for 10 days post-operatively. Meticulous aseptic techniques, skin preparation with betadine solution, self-adhesive plastic drapes, and skin towels were used to reduce iatrogenic infection.

Cardiopulmonary bypass was carried out under sodium pentobarbital anesthesia using a variety of pediatric bubble oxygenators or a reduced prime, rotating disc oxygenator developed in this laboratory.³ A marked reduction in post-operative hemorrhage as a cause of death was achieved by reducing the heparin dose to 1.5 mg/Kg given just prior to cannulation. No other heparin was administered during the bypass procedure which required 45 to 55 minutes. Venous cannulae in the superior and inferior vena cava were placed through right atrial appendage purse-string sutures. Arterial return was through a cannula in the right femoral artery.

Bypass was initiated with an oxygenator priming volume of 100 ml of Ringer's Lactate solution, sufficient operating volume being maintained by emptying the dog's venous system into the oxygenator. Additional electrolyte was rarely required during the procedure and donor blood was never used to replace the 200 to 400 ml blood loss which occurred during surgery and immediately post-operatively. Flow rates sufficient to maintain an arterial pressure of 60 to 80 mmHg ranged from 1500 to 2500 ml/min.

The left atrium was exposed by dissection through the interatrial septum, cardiopulmonary bypass was initiated and the heart was fibrillated electrically. The left atrium was opened and the mitral leaflets excised leaving a 1-2 mm remnant of leaflet around the annulus. The valve was inserted using 14 to 16 interrupted 4-0 sutures. The ventricle and atrium were allowed to fill during closure of the atriotomy, the heart defibrillated and cardiopulmonary bypass was discontinued. Blood remaining in the

oxygenator was returned immediately following cessation of bypass and systolic arterial pressure was kept below 120 mmHg by intravenous administration of nitroglycerine solution as required. Protamine was not used to neutralize the heparin which was metabolized in the next 3 to 4 hours.

Sixty-six consecutive prosthetic mitral valve replacement experiments were carried out using these techniques. Of the 66 valves implanted, 13 were mechanical disc valves, 3 were canine pericardium leaflet valves, 2 were Surlyn^(TM) leaflet valves and 48 were bovine pericardium leaflet valves, 6 which were known to have defective leaflet function. The animals were assigned survival periods but were sacrificed upon appearance of clinical signs of valve failure (sacrificed - sick).

Survival data obtained are as follows:

Category	Average Time of Survival	Number of Dogs
Operative Death	10 hours	10 (15%)
Died or Sacrificed-Sick, <1 month	15 days	6 (9%)
Died or Sacrificed-Sick, >1 month	3.3 months	16 (24%)
Elective scheduled Sacrifice	2.6 months	28 (42%)
Alive and Well	3.8 months	6 (9%)
Total		66

Thus, of 56 animals surviving surgery, 50 lived 1 month or more, a long term survival rate of 89% for an average of 2.9 months.

Bacteremia and prosthetic valve infection appears to be the primary cause of valve thrombosis and dehiscence following mitral valve replacement in the dog. We feel that the techniques described produce a convenient animal model with a good survival rate for testing prosthetic heart valves from which valid information on valve function and failure modes may be obtained.

*Generously supplied by Eli Lilly and Co., Indianapolis, IN
(TM) Registered Trade Mark, DuPont, Wilmington, DE

References

1. J. Dale, et al., Eur. Surg. Res. 15:248, 1983
 2. R. Jones, et al., Circulation, Supp I, 39 & 40:1235, 1969
 3. R. Jones, et al., Acta MedicoTechnica 22:272, 1974
- Supported by the Saint Luke's Hospital Association, Cleveland, OH

IMMUNOGENICITY OF GLUTARALDEHYDE-TREATED BOVINE PERICARDIAL TISSUE
XENOGRAFTS IN RABBITS

SALGALLER, M.L. AND BAJPAI, P.K.

CHILDREN'S HOSPITAL, 700 CHILDREN'S DR., COLUMBUS, OHIO 43205

Xenograft heart valves composed of glutaraldehyde-treated bovine pericardium show superior transvalvular gradients and hemodynamic parameters without anticoagulant therapy. According to some investigators the cross-linkage of tissue proteins by glutaraldehyde not only increases stability and insolubility, but also confers immunological inertness (1). However, there is considerable evidence to suggest that glutaraldehyde-treated proteinaceous materials retain some measure of altered immunogenic potential (2). This investigation was conducted to demonstrate whether or not whole pieces of glutaraldehyde-treated bovine pericardial tissue (GTBPT) retain the capacity to induce humoral and cellular immune responses.

Pericardial tissue pieces were stabilized by placing xenografts in 0.5% glutaraldehyde for two weeks. The xenografts were sutured to the abdominal musculature of mature male rabbits. Three groups of eight animals were implanted with three 1 x 2 cm. sections of sterile dialysis tubing, untreated bovine pericardial tissue (UTBPT), or GTBPT. Ninety days following initial implantation of tissues, all tissues were removed for histopathological study. Eight new non-immunized controls were then obtained and operated on in a similar manner. Four animals in each experimental group were subsequently implanted with identical secondary xenografts. The other four received non-corresponding secondary xenografts. Ninety days after secondary graft implantation, all tissue sections were removed for morphological examination. Indirect hemagglutination, leukocyte migration inhibition factor (LIF), and skin tests were performed at thirty-day intervals during the 180 day duration of the study.

There was no demonstrable anti-UTBPT or anti-GTBPT antibody titers in the sera obtained from sham-operated animals. At 90 days, the majority of tissue implanted rabbits exhibited antibodies to both UTBPT and GTBPT. Implantation of secondary UTBPT grafts did not increase corresponding serum anti-UTBPT titers to any great extent. Sera obtained from these animals showed sustained levels of anti-GTBPT antibodies. Similar results were obtained with rabbits implanted initially with UTBPT and subsequently with GTBPT grafts. Anti-UTBPT or anti-GTBPT antibody titers reacting with GTBPT homogenate never exceeded four units. However, all eight rabbits implanted with primary GTBPT grafts exhibited a higher range of anti-UTBPT antibody titers throughout the second 90-day period of the investigation.

The implantation of secondary GTBPT grafts in some GTBPT-grafted animals resulted in as much as a four-fold increase in antibody titers against

homologous antigen. Serum samples obtained from four rabbits initially implanted with GTBPT-grafts exhibited maximal reaction to both heterologous and homologous antigen after 30 days of implantation of either secondary xenograft. All rabbits showed maximal responses 90 days following secondary implantation.

The capacity of grafts to induce cellular immune responses were assayed by LIF and skin tests. Ninety days after initial GTBPT insertion, migration of leukocytes obtained from the rabbits was significantly inhibited in the presence of either antigen. Migration of leukocytes obtained from rabbits with initial GTBPT grafts and secondary UTBPT or GTBPT xenografts demonstrated a 25% increase in percent migration inhibition during the second 90 days of study. Migration data of leukocytes obtained from rabbits with initial UTBPT grafts and secondary UTBPT or GTBPT xenografts indicated a similar, though less significant, increase in cellular immune response during the second phase of study. Ninety days after primary tissue implantation, nearly all tissue-implanted rabbits exhibited a positive skin response (greater than 5 mm) 48 hours after homologous antigen challenge. After the second 90 days of study, most rabbits with UTBPT secondary grafts did not give a positive skin response to UTBPT or GTBPT antigen. However, secondary GTBPT implants increased delayed hypersensitivity response regardless of the initial xenograft type.

Results obtained in this study indicate that 0.5% glutaraldehyde treatment of bovine pericardial tissue xenografts does not confer immune inertness to the tissue. Continued immune responses to heterologous antigens suggest that glutaraldehyde alters, but does not abolish, antigenic determinant sites. Secondary GTBPT xenograft implantation, especially in rabbits given primary GTBPT grafts, aggravated both humoral and cell-mediated immune reactivity. The immunological fate of this type of heart valve should be monitored to assess the full impact of immunological alteration on replacement of primary bovine pericardial tissue valve bioprosthesis.

1. Carpentier, A.; Lemaigre, G.; Robert, L.; Carpentier, S.; and Dubost, C., J. Thorac. Cardiovasc. Surg. 58, 467-483, 1969.
2. Bajpai, P.K. Antigenicity of glutaraldehyde stabilized biologic materials in Biomaterials in Reconstructive Surgery, L.R. Rubin (ed.), C.V. Mosby Co., St. Louis, MO, pp. 243-251. 1983

M.L. Salgaller
Dept. Hem./Onc.
Children's Hospital
700 Children's Drive
Columbus, Ohio 43205

P.K. Bajpai
Dept. of Biology
University of Dayton
Dayton, OH 45469

PREVENTION OF EXPERIMENTAL BIOPROSTHETIC HEART VALVE CALCIFICATION

Robert J. Levy*, Frederick J. Schoen, Judith T. Levy, Marguerite Hawley, Theresa Thomas

The Children's Hospital and Brigham and Women's Hospital, Boston, MA, and Wellesley College, Wellesley, MA.

Introduction

Clinical failure of glutaraldehyde-preserved porcine aortic valve bioprostheses is most often due to calcific degeneration of the cusps (1). This process is conveniently studied with subcutaneous implants of bioprosthetic cusps (BC) in rats. The subsequent calcification, morphologically and biochemically comparable to clinical bioprosthetic valve calcification, occurs over an accelerated time course, with mineral deposits noted as early as 3 days and calcium content reaching levels seen clinically by 21 days (2). In the present study, two distinct strategies were examined for the prevention of bioprosthetic valve calcification: pretreatment of the cusps with the detergent sodium dodecylsulfate (SDS); and post-implantation therapy with ethanehydroxydiphosphonate (EHDP).

Methods

Specimens (BC) were prepared from porcine aortic valves which were pretreated with glutaraldehyde according to established procedures (2). Some BC were also subsequently incubated in a 5% SDS solution (pH 7.40, 0.05M HEPES) for 24 hours at room temperature prior to implantation. Organic phosphorous content was quantitated on BC before and after SDS pretreatment, as an index of changes in phospholipid content. BC, both SDS treated and non-SDS treated, were implanted subcutaneously in 3 week old male rats for the durations indicated (Table I). Several populations of rats (Table I.) received either parenteral EHDP therapy (25 mg/kg/24 hours), or local EHDP administration by osmotic minipump (ALZA, Palo Alto, CA). Calcium and inorganic phosphorous were determined on retrieved BC and serum. Representative cusps were fixed with buffered 2.5% glutaraldehyde/2% paraformaldehyde, pH 7.2 for 24 hours followed by immediate dehydration in graded alcohols, and examined by light and electron microscopy.

Results and Discussion

Each experimental approach, SDS-pretreatment and EHDP therapy, resulted in diminished BC calcification (Table I.). SDS pretreatment, removing 89.1% of the total phospholipid content, proportionately reduced the extent of calcification. No differences were noted in total protein content and amino acid composition between unimplanted BC and SDS pretreated BC. Furthermore, the histologic appearance of SDS pretreated BC prior to implantation did not differ from routinely prepared BC. After implantation, SDS pretreated BC demonstrated no calcific deposits by either light or electron microscopy.

Parenteral therapy with EHDP (30mg/kg/24 hours) prevented BC calcification (Table I), but resulted in marked growth retardation with EHDP treated animals weighing 28.6% less than controls after 21 days. In contrast, local administration of EHDP (5mg/kg/24 hours) was equally effective in preventing BC calcification (Table I) and had no deleterious effects on growth. Light microscopy of valves removed from animals with either systemic or local EHDP confirmed near-complete inhibition of calcification by both therapeutic approaches.

We conclude that BC calcification can be effectively prevented by either pretreatment of the cusps with SDS, or EHDP therapy. SDS pretreatment appears to achieve its effect through the extraction of phospholipid. EHDP was effective either systemically or locally; however, growth retardation occurred with parenteral administration, but not with local therapy. Either of these approaches to the prevention of BC calcification is potentially applicable to the clinical setting.

TABLE I

Bioprosthetic Valve Cusp Calcification

Implant	N	Duration(days)	Ca++(ug/mg)*
Unimplanted	7	--	2.8±0.7
Control	19	21	154.9±4.1
SDS pretreated	10	21	18.9±4.3
EHDP, parenteral	19	21	4.2±4.2
EHDP, MINIPUMP	8	14	4.3±0.7
Control	12	14	135.4±6.2

*Mean ±Standard Error of the Mean

References

1. Schoen FJ, Collins JJ, Cohn LH. Am J Cardiol 1983, 51: 957-964.

2. Levy RJ, Schoen FJ, Levy JT, Nelson AC, Howard SL, Oshry LJ. Am J Path 1983, In Press.

Grant Support: American Heart Association Grant-in-Aid 81760, and NHLBI Grant 24463.

*Department of Cardiology
The Children's Hospital
300 Longwood Ave.
Boston, Massachusetts 02115

THE CLINICIANS OVERVIEW ON DENTAL IMPLANTS

Cranin, N.

Brookdale Implant Dental Group. The Brookdale Hospital Medical Center
Brooklyn, New York 11212

INTRODUCTION: Man has sought to replace teeth with simple, non-removable, life-like replicas, but his efforts have been thwarted due to the unique anatomic, physiologic, microbiologic problems and immune responses of the host. One of the most attractive, romantic and compelling methods attempted has been the surgical implantation of tooth-like devices into the jaws. Several factors will be considered:

a) Research. b) Criteria for success. c) Acceptability and limitations of host and operative sites. d) Methods of evaluation.

A. Research - Unlike many disciplines in surgery in which basic research modalities were used prior to the introduction of the technique into clinical practice, dental implants have evolved essentially on a pragmatic basis. Using animals for untried procedures has obvious advantages. One has the opportunity of experimenting without the dangers inherent in using human subjects. These dangers might be overt--such as the introduction of infection or the loss of tissue or organs or life--or covert, such as induced toxicity not readily or immediately recognized or manifested. At best when a human study apparently terminates in success one can make only the simplest of clinical observations. Some of the observations that have occupied us in the research laboratory have been concerned with materials, others with design and still others with prosthetic implementation.

B. Criteria for Success: Many implants have been adjudged successful, despite radiographic or clinical evidence of failure, simply because they continue to remain symptom-free in-situ. With reasonable agreement, however, the following criteria must be met in order for an implant to be considered satisfactory:

1. In place for 60 months or more.
2. Lack of significant evidence of cervical saucerization on radiographs.
3. Freedom from hemorrhage.
4. Lack of mobility.
5. Absence of pain.
6. No pericervical hyperplasia.
7. No evidence of a widening peri-implant space on radiography.

C. Acceptability and Limitations of Host and Operative Sites: Though not established officially, certain physical problems contraindicate implant surgery. They are well known and include endocrinopathies, granulomatoses, collagen diseases, metabolic bone problems, alcoholism and drug dependencies. Local problems contraindicating implant surgery include: insufficient ridge width and

height, affective muscle attachments, mucositis, poor oral hygiene and unacceptable natural abutment teeth. Of all the essentials, ridge thickness is the most significant factor related to endosteal implant success. The wider and more generous the buttressing spongiosa, the greater the chance for sound initial healing.

D. Methods of Evaluation: In many instances even judicious probing may prove to be invasive. Too, probing measurements are dependent on the passivity of the prober, the fineness of the probe, and the sharpness of its tip. Since many implants are splinted, it is not always possible to test for mobility. Radiographs, despite their well-known shortcomings, continue to serve as the most reliable single source of implant status.

Retrospective Evaluation - Several statistical studies have been presented in the past few years. Despite superficial differences among them, analytical evaluations revealed general agreement that metal blade and blade-variant implants presented a five year success rate from 50-65% depending on the criteria used by the reviewers. The Harvard School of Dental Medicine in June, 1978 conducted an NIDR sponsored Consensus Development Conference focusing on dental implants. All of the data were presented in uniform statistical tables and were highly structured in terms of time periods for analysis, success criteria, insertion technique, patient-follow-up and implant risk-benefit. Although imaginative interpretation was required to translate the statistics, the final result indicated about a 65% success rate after 5 years. The universal denominator is the host site response. Epithelial adhesion has been investigated by the presence of hemidesmosomes and positive PAS staining. Surface texture and porosity are responsible for creating responses which lend themselves more favorably to infrastructural support. Significant design changes have included shoulder elimination, the highly polished cervix and the sintered implant. The role of the biomaterials scientist has added additional dimensions and values to the levels of basic research.

The Brookdale Hospital Medical Center
Linden Blvd. at Brookdale Plaza
Brooklyn, New York 11212

THE EVALUATION AS A POTENTIAL DRUG CARRIER OF N-(2-HYDROXYPROPYL)METHACRYLAMIDE COPOLYMERS CONTAINING BIODEGRADABLE CROSSLINKS.

S.A. Cartlidge, P. Rejmanová, R. Duncan, J. Kopeček, and J.B. Lloyd.

University of Keele
Staffordshire, England.

The attachment of chemotherapeutic agents to soluble macromolecules restricts cellular uptake to the mechanism known as pinocytosis, thus preventing indiscriminate penetration into cells. Conjugate formation also ensures retention within the bloodstream, if the molecular weight of the macromolecule is sufficiently high to prevent glomerular filtration. Soluble synthetic polymers have been designed to which drugs can be attached by linkages stable in blood but susceptible to intralysosomal enzymic cleavage following pinocytosis. (1). The incorporation of suitable residues into the structure enables the conjugate to be targeted to particular cells (2).

As an approach to the problem of polymer accumulation within the body following administration of such conjugates, short polymer chains connected by potentially biodegradable crosslinks have been evaluated as a drug delivery system. Low molecular weight N-(2-hydroxypropyl)methacrylamide copolymers were crosslinked with di(oligopeptide)hexamethylenediamine sequences below the gel point and fractionated using Sepharose 6B GPC to produce five samples of different mean molecular weights (M_w 34,000-400,000). The preparations were radiolabelled with ^{125}I iodide.

We have investigated the effect of molecular weight on the rate of pinocytic uptake and intracellular degradation of these crosslinked copolymers by rat visceral yolk sac and adult rat intestine cultured in vitro. The accumulation of copolymer was size-dependent in each tissue. In the rat yolk sac the rate of accumulation of copolymer increased with decreasing molecular weight, whereas in everted intestinal sacs the accumulation of copolymer increased with increasing molecular weight.

Low molecular weight degradation products deriving from the oligopeptide moieties were observed in culture medium after a 5h incubation period with yolk sacs. The extent of intracellular hydrolysis was independent of the mean molecular weight of the copolymer preparation. Degradation products were not observed in the medium after incubation for 1.5h with intestinal sacs, but transport of intact macromolecules and of degradation products across the gut into the serosal space was observed.

Between 40 and 64% of the total radioactivity transported was in macromolecular form irrespective of the molecular weight of the copolymer.

In vivo studies demonstrated that a substantial proportion of the radiolabelled copolymer is retained in the circulation after 1h and that there is very little accumulation of copolymer in the liver, lung, kidney and spleen. Targeting to liver was achieved by making use of the hepatocyte receptor for galactose-terminating glycoproteins. The incorporation of diglycyl-D-galactose amine into an unfractionated crosslinked copolymer showed rapid blood clearance and a marked increase of uptake by the liver.

These experiments show that it is possible to target crosslinked polymers in vivo and that following uptake by cells, the crosslinks are degraded to yield polymer chains small enough to be excreted by the kidney.

We thank the University of Keele for a research studentship (S.A.C.) and the Cancer Research Campaign, British Council and Royal Society for financial support of this research.

References

1. R. Duncan *et al* (1981). *Biochim. Biophys. Acta* **678**, 143.
2. R. Duncan *et al* (1983). *Biochim. Biophys. Acta* **755**, 518.

S.A. Cartlidge, R. Duncan and J.B. Lloyd
Biochemistry Research Laboratory
Department of Biological Sciences
University of Keele
Staffordshire ST5 5BG,
England.

P. Rejmanová and J. Kopeček
Institute of Macromolecular Chemistry
Czechoslovak Academy of Sciences
16206 Prague 6
Czechoslovakia.

Sustained Release of Macromolecules from a Subcutaneous Implant

V.N. Hasirci and I.L. Kamel

Dept. of Materials Eng. and the Biomed. Eng. and Sci. Inst., Drexel University, Philadelphia, PA 19104

Sustained drug release has become an important research area particularly for the applications of drugs where dose variation or frequent administration of the drug is not desirable because of the safety index (e.g. anticancer drugs), therapeutic effectiveness (e.g. antibiotics, contraceptive hormones) or patient convenience (e.g. pilocarpine in glaucoma treatment) [1,2]. Most of the current applications, however, deal with the packaging and release of small molecules via diffusion through permeable membranes, porous media or devices [2]. A major effort in drug release has recently concentrated in the area of macromolecules such as enzymes. Release of insulin [3] and heparin are good examples where an attempt is made for the release of a macromolecule continuously and at a desired rate for a long time period.

The problem of macromolecular release, however, is a difficult and involved one. The slow mobility, molecular entanglements and low diffusion coefficients makes the design of a packaging medium or device complicated and it often must be tailored to fit the specific macromolecule under study.

In this investigation a novel implantable package has been developed for the adaptation to the slow release of macromolecular substances. Spectrum Orange was chosen as the model release compound for this study because of its similarity in structure and size to heparin in addition to its ease of detection spectrophotometrically.

In this study a porous implant core was developed which holds the macromolecule to be released along with a soluble calcium sulfate hemihydrate as the matrix material. This core was surrounded by a specially designed membrane based on polyvinyl pyridine (PVP). In this design, calcium sulfate slowly dissolves out leaving a porous implant core and helps the release of the desired Spectrum Orange. The key to the zero order release and the rate of that release is the partly hydrophilic membrane surrounding the implant. PVP is a hydrophobic polymer but upon oxidation it becomes water soluble [4] allowing swelling of the oxidized regions. By this technique, it is possible to control the size and rate of the diffusing substance through controlling the size and extent of the diffusing substance through controlling the size and extent of the oxidized region of the packaging membrane.

Oxidation was determined by IR and Auger analyses and the results indicated that varying certain processing steps can be sufficient to change the membrane oxidation levels. Rates of release of Spectrum Orange will be shown and correlated with the processing of the

membrane. Generally, the results demonstrate the feasibility of the release of this macromolecule by this novel approach at wide rate values. The current values for Spectrum Orange release are to be compared with those for heparin release both in the laboratory and in experimental animals. These experiments are in the preparation stage.

References

1. T.J. Roseman, in "Controlled Release of Biologically Active Agents", Eds. A.C. Tanquary and R.E. Lacey, Plenum Press, N.Y. 1974, p. 99.
2. Sustained Release Medications, Ed. J.C. Johnson, Noyes Data Corporation, Park Ridge, N.J., 1980.
3. B.K. Davis, *Experientia*, **28**, 348 (1972).
4. V.N. Hasirci, Ph.D. Thesis, Reading University, U.K. 1976.

DEVELOPMENT OF SPERMICIDE-RELEASING DISPOSABLE BARRIER DIAPHRAGMS

R. A. Casper, R. L. Dunn, R. N. Terry, L. R. Beck*

Southern Research Institute
Birmingham, Alabama 35255-5305

Introduction:

Concerns with the safety of IUDs and oral contraceptives are prompting many women to reconsider the use of the barrier diaphragm as a contraceptive method. There are, however, a number of factors which continue to prevent wide-spread acceptance of the diaphragm method. These problems include: (1) the messiness associated with diaphragm used in conjunction with spermicidal creams or jellies, (2) the increased expense of replenishing the spermicide when the diaphragm is used frequently, (3) the need for a ready source of water for cleaning, and (4) the care in handling required to prevent tearing or deterioration of the diaphragm during frequent use.

A disposable, vaginal diaphragm has been developed which eliminates these problems. The diaphragm releases spermicidal agents in a controlled fashion and does not require application of creams or jellies. The system has been found effective in preventing pregnancy in baboons and is now scheduled for Phase I clinical trials in women.

Materials and Methods:

The diaphragms were fabricated from Estane 5714F-1, a biocompatible polyether/polyurethane developed by B. F. Goodrich. Nonoxynol-9 (NN9) was selected as the spermicide and polyethylene glycol (PEG) was incorporated into the formulation to provide surface lubricity for ease of diaphragm insertion.

Films were prepared for evaluation by centrifugal spin casting. The release of NN9 from Estane films and Estane films containing PEG was then determined in vitro. Duplicate circular samples of each film were immersed in 50 mL of normal saline maintained at 37 °C. Aliquots of this receiving fluid were removed at periodic intervals and the NN9 concentration was determined by ultraviolet spectrophotometry. Results of these studies were used to determine the NN9 and PEG loading necessary for fabricating diaphragms which would release an efficacious amount of NN9 over a 24 h period. Prototype diaphragms were then fabricated for use in baboons by solution dip coating. The in vitro release of NN9 by these diaphragms was then determined in the same fashion as for film specimens.

Diaphragms of this type were then evaluated in baboons for up to 48 h. Diaphragms containing no NN9 were used as controls. An embryo recovery procedure was then used to determine the presence of fertilized eggs.

Results and Discussion:

NN9 release from Estane followed first order kinetics. The rate and amount of NN9 release increased with higher NN9 loadings. PEG was added to the NN9-loaded Estane in an effort to increase the initial burst of NN9 from Estane to the level of our target release profile. Because it is water-soluble, the release of PEG from Estane provides additional diffusion path-

ways for NN9, and increases both the burst and overall release of NN9. PEG incorporation had the additional advantage of providing a lubricating surface on the Estane, which should ease insertion of the diaphragm into the vagina.

Based on the results of the in vitro release of NN9 from film samples, prototype diaphragms sized for baboons were fabricated containing 7-10% NN9 and 10-15% PEG and evaluated for in vitro release. Using the ratio of average-female-baboon weight to average-female-human weight, we determined from these results that Estane diaphragms loaded with 9 wt % NN9 and 15% polymer wt of PEG (9N/15P/E) would release the desired amount of Nonoxynol-9 over a 24 h period. The NN9 release from a prototype baboon diaphragm comprised of this material is shown in the figure.

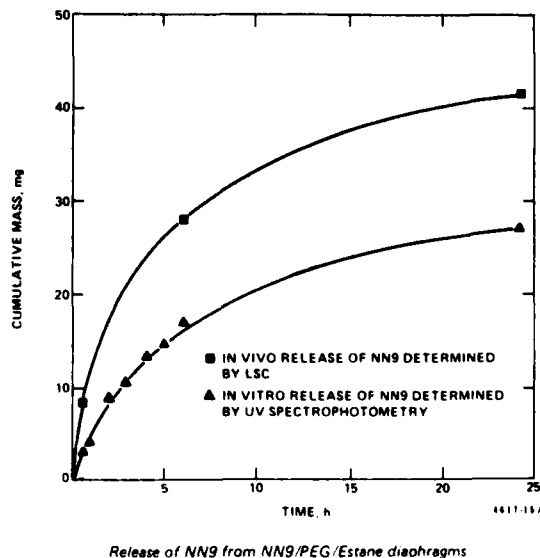
The spermicide releasing diaphragms were found to be effective in preventing pregnancy in the baboons and were more successful than control diaphragms not containing spermicide.

Acknowledgment:

This work was supported by the National Institute of Child Health and Human Development under contract N01-HD-0-2854.

SOUTHERN RESEARCH INSTITUTE
2000 9th Ave., South
P. O. Box 55305
Birmingham, AL 35255-5305

*Laboratory of Reproductive Biology
Department of Obstetrics & Gynecology
University of Alabama in Birmingham
University Station
Birmingham, AL 35294



MICROENCAPSULATION OF MAMMALIAN CELLS IN SYNTHETIC
SEMI-PERMEABLE MEMBRANES

W.T.K. Stevenson, J.W. Blysiuk, M. Sugamori and M.V. Sefton

Department of Chemical Engineering and Applied Chemistry
University of Toronto, Toronto, Ontario, M5S 1A4

Live mammalian cells have been microencapsulated in water insoluble polyacrylates without apparent loss of viability. Microencapsulated pancreatic islets, for example, are potentially useful as a means of restoring normoglycemia in insulin dependent diabetics, to avoid the associated degenerative complications. The biocompatible capsule wall, by being permeable to insulin and glucose yet impermeable to antibodies is able to prevent the immune rejection of the transplanted cells, while the cells continue to respond to elevated glucose levels with additional insulin.

Towards this objective, three systems have been devised to microencapsulate live animal cells, using water insoluble hydrophilic polyacrylates rather than alginate and/or polylysine (1) as the capsule wall forming material. Hydrophilic polyacrylates have the potential to be sufficiently biocompatible to meet the requirements of this application. However, encapsulation is substantially more difficult than for water soluble polymers, because of the need to use non-aqueous solvents.

A. EUDRAGIT RL/diethyl phthalate

Rat pancreatic islets has been microencapsulated in a commercial acrylic acid/methacrylic acid copolymer (Eudragit RL100) using an interfacial precipitation procedure previously used with erythrocytes (2). Microcapsules were formed by extruding the cell suspension through the inner barrel, and the polymer in diethyl phthalate (DEP) solution through the outer barrel, of a double barrelled needle assembly. Droplets were blown by compressed air from the needle tip into a corn oil solution to remove DEP and precipitate the polymer around the islet. Microcapsules were examined by light and UV microscopy and shown to contain islets which appeared viable by the fluorescein diacetate test (3). The microencapsulated islets secreted insulin in response to a 300 mM/dL glucose challenge.

B. HEMA/MMA copolymer/polyethylene glycol

Erythrocytes have been microencapsulated in a 75 hydroxyethyl methacrylate/25 methyl methacrylate (HEMA/MMA mole ratio) copolymer. The cell suspension was extruded through the inner barrel, and the polymer in polyethylene glycol (PEG200) solution was extruded through the outer barrel of a coaxial needle assembly. Droplets were blown into an aqueous dextran solution to remove PEG and deposit a membrane around the cells. The dextran was used to keep the polyacrylate solution immiscible in the aqueous phase. A high molecular weight polysaccharide (Ficoll 400) was used to increase the density of the droplet and a commercial surfactant (Pluronic F68) was used to reduce the surface tension of the receiving solution, both to aid droplet penetration. Red blood cells appeared intact after encapsulation on

the basis of microscopy and the absence of significant lysis.

C. HEMA/MMA copolymer/sodium alginate

Aqueous sodium alginate (NaA) solutions were found to form unstable gels when mixed with PEG 200. A suspension of red blood cells in dilute NaA, and a solution of polymer in PEG 200, were pumped into a pre-mix chamber and extruded into a buffered solution of CaCl_2 . The high viscosity of the droplets and the formation of a calcium alginate shell on contact with the receiving solution allowed the capsule to survive the mechanical shock of penetration, and reduced the rate of diffusion of PEG from the droplet, to produce microcapsules under controlled conditions. Red blood cells appeared intact after encapsulation on the basis of microscopy.

The latter two processes are being refined and extended to encapsulate pancreatic islets.

References:

1. F. Lim and A.M. Sun, *Science*, **210**, 908 (1980).
2. M.V. Sefton and R.L. Broughton, *Biochimica et Biophysica Acta*, **717**, 473 (1982).
3. B. Rotman and B.W. Papermaster, *Proc. Nat. Acad. Sci. (U.S.A.)*, **55**, 134 (1966).

The authors acknowledge the financial support of the Natural Sciences and Engineering Research Council.

THE ANTIBIOTIC LEVEL IN SERUM AND BONE TISSUE AFTER LOCAL
APPLICATION OF ANTIBIOTIC-TCP-BEADS WITH DELAYED RELEASE

J.Eitenmüller, G.Peters, K.-H.Schmidt, R.Weltin

Department of Traumatology (Leader: Prof. Dr. Reichmann)
Surgical University Hospital-Cologne (Dir.: Prof. Dr. Dr. Pichlmaier)

The signs of infection decrease rapidly in animal experiment after filling up an osteomyelitic bone cave with biodegradable porous antibiotic tricalciumphosphate beads. To increase the safety of treatment a high and sufficiently long acting antibiotic time level is to be demanded. This can be achieved in delaying the release of the antibiotics from the beads utilising coatings of different thickness with reabsorbable materials.

Animal experiments: On six mongrel dogs each six holes were drilled at the long bones and each was filled up with 1g coated or for comparison non coated Flucloxacillin-TCP-beads, on further six dogs we used coated and non coated Fosfomycin-TCP-beads. As coating-material we used Ethocel, Dynason 118, Zein and Copolymer. For one week we took a serum sample daily, the animals were sacrificed respectively on the 1st, 3rd and 6th day and after 2, 4 and 6 weeks. The sampling of spongoid bone and cortex bone was done separately in defined distances of the pharmacon depot.

Results: The serum values of both antibiotics did not exceed a level of 5 µg/ml. There was non antibiotic level detectable in the bone directly beneath the TCP-beads after 24 hours if no coating was used. In contrast to the above, under the adequate local and time conditions there were tissue levels of 30-250 µg/g fresh bone tissue.

After 72 hours the tissue levels of both antibiotics exceeded a value of 4 µg/g fresh bone tissue in the bone next to the TCP-beads. This is valid for the treatment value of the most relevant bacteria. Only with a coating consisting of Ethocel and Copolymer an effective bone tissue level of Fosfomycin could be kept up for several weeks. With increasing distances from the pharmacon depot the antibiotic bone tissue level rapidly decreased, the levels in the spongoid bone were much higher than in the cortex.

High bone tissue levels of antibiotics could be kept up on long term with the completely biodegradable pharmacon depot; by changing the thickness of the coating the velocity of antibiotic release can be varied. The substance Copolymer has been well established as surgical suture mate-

The TCP-beads acts as much as a bone substitute as a carrier substance.

From a grant of the Government
of the German Federal Republic

Chirurgische Universitätsklinik
Josef-Stelzmann-Str. 9
5000 KÖLN 41

x) Hygiene-Institut der Universität Köln
Goldeneffsstr., 5000 KÖLN 41

N. A. Peppas and R. Gurny *

School of Chemical Engineering, Purdue University, West Lafayette,
Indiana 47907

Treatment of oral mucus in cases of paradontoses, aphthae and lesions by trauma requires development of bioadhesive, controlled release formulations which can adhere to the mucus for several hours. We have designed and tested new formulations for release of aluminum lactate or febuverine hydrochloride.

Experimental Part

The bioadhesive polymer systems were prepared from polyethylene gel (a dispersion of 5 wt% polyethylene FP with $M_w = 147,000$ in petrolatum) to which there were added different amounts of the hydrocolloids sodium carboxymethylcellulose ($M_n = 90,000$), sodium alginate ($M_w = 50,000$), hydroxyethylcellulose, tragacanth gum or hydrolyzed gelatin ($M_n = 10,000$). Febuverine hydrochloride and/or aluminum lactate (Sepos S.A., Switzerland) were added at 2% or 5% respectively.

Adhesion studies were performed using a tensile tester equipped with a custom-made cell for measurement of the adhesive bond strength. In a typical experiment, a specific bioadhesive preparation was placed between the two parallel disks held at an initial distance of 2 mm and the disks were pulled at 0.1 mm/min. The stress-strain curves were recorded and the modulus and visco-elastic behavior of the systems were related to the bioadhesive strength.

Release experiments of the bioactive agents were performed at $37 \pm 0.5^\circ\text{C}$ under perfect sink conditions. The released drug concentration was measured by UV spectrophotometry.

Results and Discussion

From the stress-strain curves for different formulations it was determined that there is an increase in the stress as a function of strain up to a yield point. This phenomenon is associated with slippage of the macromolecular chains of the bioadhesive paste, leading eventually to separation of the biomedical paste between the two plates.

As a function of the content of NaCMC, the main bioadhesive component of the formulations, the bioadhesive strength increases up to a maximum value. Beyond this value, either because of shielding of active groups in the coiled molecules or because of macromolecular slippage, the chains of NaCMC are not effective in the bioadhesive process. The elastic modulus passes also through a maximum at 20 wt% NaCMC.

Typical plots of the release of febuverine-HCl as a function of time show $t^{1/2}$ dependence which is characteristic of Fickian controlled release.

These results were used to design the optimal release formulation for this specific application.

Prof. N.A. Peppas, School of Chemical Engineering,
Purdue University, West Lafayette, IN 47907, USA

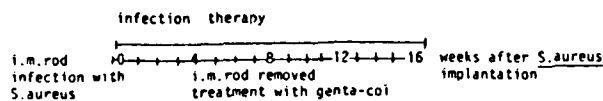
*Dr. R. Gurny, Department of Pharmaceutics,
University of Geneva, 1211 Geneva 4, Switzerland

Treatment of osteomyelitis with resorbable antibiotic-coated drug delivery systems - an experimental report *

Stemberger, A.; Ascherl, R.; Erhardt, W.; Haller, W.; Machka, K.*; Geißbörfer, K.; Langhammer, H.***; Sora, K.**; Blümel, G.

Inst.f.Exp.Surg.; *Inst.f. Med. Microbiology and ***Clinic of Nuclear Medicine of the Technical University Munich; **Fa. Dr. Rüchland Nachf. GmbH, Neustadt/Donau, F.R.G.

The various forms of osteomyelitis still pose surgical problems and have stimulated the development of resorbable antibiotic-coated drug delivery systems. In vitro studies revealed that gentamicin-coated collagen sheets (gentacol) are suitable devices. The gentamicin release was investigated by chromatography and analysis of the effluent with the IDX-genta-assay (Abbott, sensitivity 0.16 µg/ml). The gentamicin liberation kinetics in vivo were studied following implantation of sterile gentacol in the femur of 12 rabbits (gentamicin dose: 5 or 10 mg/kg bw). The animals were kept in metabolism cages. Gentamicin levels in serum and urine were determined by the IDX-assay and in bone by bioassay. Gentamicin levels of up to 1.5 µg/ml were found in serum within the first 24 h and the drug was still detectable after 72 h. Elimination rates in urine were 24 % after the first day and 40 % after the ninth day. Gentamicin was detectable in bone specimens, in some instance levels of 8 µg/g bone being found after 28 days.



In a further series of experiments an intermedullary rod was implanted in the femur of 31 rabbits. Eight days later the drilled cavity in the bone marrow was infected with 10^7 Staphylococcus aureus ATTC 6538. Osteomyelitis was evident clinically and radiologically after 4 weeks. Sixteen animals were then treated with gentacol without debridement; 15 animals remained untreated. Two weeks after gentacol application bone fragments of treated and non-treated infected animals were examined microbiologically and histologically and compared to the femur of non-infected animals. Specimens from 15 of 16 treated animals were negative during the therapy period of 12 weeks; S.aureus could be detected in one animal in very small numbers. From all 15 specimens of the infected, non-treated animals S.aureus could be isolated. The advanced bone infection was visible macroscopically and resulted in osteolysis.

In the light of these results, the favourable antimicrobial activity of gentamicin and the positive effect of collagen on bone regeneration clinical trials with gentacol has been started. In these patients, gentacol (pathogens gentamicin sensitive) was applied following good surgical nettoyage including sequestrectomy. The data from 15 patients confirm the experimental results. Further indication and application of this treatment have to be investigated in longterm clinical trials, to compare this new developed material with established techniques such as suction drainage or gentamicin-pmma.

*support was received from fund of the Wilhelm-Sander-Stiftung Neustadt/Donau

Dr.rer.nat. Axel STEMBERGER
Institute for Experimental Surgery of the
Technical University Munich
Ismaninger Str.22, D-8000 München 80, F.R.G.

STRENGTH AND LEACHING CHARACTERISTICS OF PMMA BEADS CONTAINING ANTIBIOTIC

J.A. von FRAUNHOFER, P.D. MANGINO and D. SELIGSON

DIVISION OF ORTHOPEDIC SURGERY, DEPARTMENT OF SURGERY, UNIVERSITY OF LOUISVILLE SCHOOL OF MEDICINE, LOUISVILLE, KENTUCKY 40292

Acrylic (PMMA) resin bone cement beads impregnated with antibiotic may be useful for the prevention and treatment of bone and soft tissue infections. The requirements of the implants are that they be stable, non-toxic, and of sufficient strength for easy insertion and removal from the surgical site.

Since bead strength, surface rugosity and antibiotic leaching characteristics are essential to the clinical application of the system, the following studies were undertaken: i. scanning electron microscopy (SEM) of the bead surfaces; ii. compressive strength of beads with and without antibiotic addition; iii. compressive strength of beads after *in vivo* insertion and water immersion; iv. water sorption behavior of the PMMA beads; v. antibiotic leaching rate from the beads; vi. inhibition zone measurements for filter paper discs soaked in bead eluents for 6 species of micro-organisms.

PMMA beads containing tobramycin, admixed during preparation of the resin, were fabricated from three brands of bone cement, using a teflon-coated mold, the beads being formed around stainless steel wire as a carrier. The antibiotic addition levels were 1.2g/40g of powder (single strength, SS) and 2.4g/40g of powder (double strength, DS). The antibiotic and PMMA powders were thoroughly mixed before monomer addition and bead fabrication.

The three brands of bone cement were Surgical Simplex, Palacos, and Zimmer, all mixed at a powder-monomer ratio of 40g/20ml. The bead diameter was 6mm, formed around multistrand stainless steel wire, 1.2mm in dia. Compressive strength studies were performed with a Unite-O-Matic universal test machine at a cross-head speed of 5mm/min. Water sorption specimens were weighed on a Sartorius 5-figure balance over a period of 340 hr, when equilibrium was attained.

SEM studies showed that there were distinct differences in surface texture and in the pore density for the three different PMMA bead types. Water immersion and *in vivo* placement of the beads resulted in a small increase in surface rugosity and pore density but no evidence of breakdown. Differences in water sorption and leaching behavior would appear to be due to the surface characteristics and pore size and density on the bead surface.

Compressive strength studies indicate that there are no statistically significant differences between the three bone cements when mixed at the 2:1 powder/monomer ratio. At lower P:L ratios, however, compressive strength is significantly affected. Two cements, Palacos and Zimmer, did not appear to be affected by long-term soaking, but the compressive strength of Surgical Simplex was affected to some degree, although this would not appear to be clinically significant.

Water sorption studies on the beads showed a parabolic relationship between (weight gain)² and time: (weight gain)² = a + b · (time, h). a = appr. 0.4 for Palacos and Simplex, but the value of b was 0.01 for Palacos and 0.06 for Simplex, viz. Simplex showed a greater and faster uptake of

water. The correlation between weight gain squared and immersion time was 98% for both systems.

The *in vitro* study of leached antibiotic from beads against two strains of *S.aur.*, *P.aerug.* and *E.cloacea*, showed differences in organism effectiveness for the different cements and tobramycin addition levels. At the SS level, activity against *S.aur.* and *S.aur.502A* had ceased after 10 days for the Zimmer and Palacos beads, but effectiveness was maintained for 21 days at the DS level and for both addition levels for Simplex beads. Poor activity against *E.cloacea* was found for Simplex SS and DS and Palacos SS, but Palacos DS showed reasonably good activity for up to 21 days. Activity against *P.aerug.* had virtually disappeared for all beads at both the SS and DS addition levels after 5 days.

The relationship between the diameter of the zone of inhibition on agar plates and the time in days was found to follow a curvilinear relationship of the type $xy = ax + by$: or, zone diameter = constant, a + constant, b · (zone diameter / time in days). Plots of zone diameter against zone diameter were straight lines of slope = constant, b and intercept = constant, a on the zone diameter axis. The values of a and b differed for the 3 beads and the micro-organism. It was found that where there was poor bacteriostatic activity, a < 10 and b > 0.5. When good activity was found against micro-organisms, the values were a > 10 and b < 0.5.

Leaching studies on tobramycin from the beads showed a similar curvilinear relationship between the leached amount and time:

leached tobramycin = $\frac{A \cdot (\text{time in days})}{(\text{time in days}) - B}$, and this relationship gave straight lines of slope = B and intercept on the Y-axis (leached tobramycin) = A. The value of constant B was appr. 0.95 for all three beads at both the SS and DS addition level. The values of constant, A differed significantly for the three beads at the two addition levels. There was high correlation between the value of the constant, A found in the leaching studies and the value of constant, a obtained from the agar plate inhibition zone study.

This study indicates that mechanically solid antibiotic impregnated PMMA beads can be fabricated by admixing tobramycin powder with the PMMA powder component. These beads release antibiotic *in vitro* at a diffusion limited rate dependant upon the surface characteristics of the beads. It is to be anticipated that the clinical efficacy of these implants will depend upon the sensitivity of the target organisms to the selected antibiotic.

This study was funded in part by a grant from Eli Lilly and Company, Indianapolis Indiana.

CONTACT PHASE ACTIVATION INDUCED WITH HYDROSOLUBLE SYNTHETIC
DEXTRAN AND POLYSTYRENE DERIVATIVES

J.M.NIGRETTO, E.CORRETGE, M.JOZEFOWICZ and M.MAUZAC.

Laboratoire de Recherches sur les Macromolécules. VILLETANEUSE (FRANCE)

Research is aimed at evaluating the biocompatibility of polymers and, in a more precise manner, at investigating the influence of the net electric charge and of the functionality, expressed in terms of chemical nature and statistical composition of various substituents, on the activation of Factor XII. Indeed, much should be gained in the knowledge of the sterical site and in the conditions prevailing for kallikrein generation.

The following hydrosoluble biomaterials have been synthesized and chemically characterized (1):

- dextran derivatives :
 - . carboxymethyl (CMD)
 - . carboxymethylbenzylamine (CMDB)
 - . carboxymethylbenzylamine sulfonate (CMDBS)
- polystyrene derivative :
 - . polystyrene sulfonate (PSS).

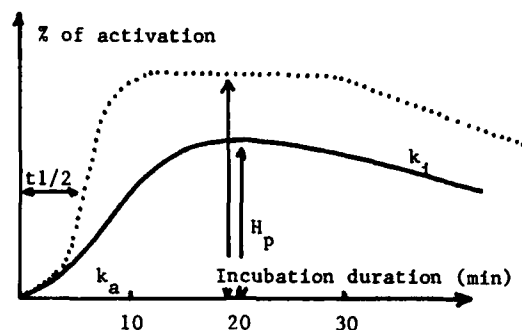
The statistical distribution of the chemical substitution of these compounds (percentages refer to the rate of dextran substitution) is given in the Table below:

POLYMER	%CM	%B	%SO ₃	%D
D				100
CMD	91			9
CMDB	37	21		42
CMDBS	47	1	3	49
	76	0	3	21
	47.5	0	6	46.5
	37	11	9	43
	71.5	0	5	23.5
	44.5	0	4.6	50.9

The behavior of two additional classes of materials, Heparin (Hep) and pentosan polysulfate (PPS) as natural compounds on the one hand, dextran (D) and dextran sulfate (DS) on the other, was also tested for the sake of comparison. The latter polysaccharides are known to exert respectively high and no activity on the contact phase and will therefore be used as references.

The extent of the in-vitro activation of plas-matic contact phase is followed according to the method developed by C.Kluft (2). The activity of kallikrein generation is measured with the availability of kallikrein specific synthetic substrates, spectrophotometrically with H-D-Pro-Phe-Arg-pnitro anilide and electrochemically with H-D-Pro-Phe-Arg-paminodiphenylamide. Both procedures agree as shown in assays involving purified kallikrein. The latter procedure has been used in cases where precipitation occurred, promoted by the peptide substrate in the presence of plasma and some polymers.

The shape of a typical activation curve relating the kallikrein generation induced upon incubation of plasma with the polymers as a function of the incubation duration is represented in the figure below. The dashed curve indicates the profile obtained through classical dextran sulfate activation.



Results show that the shape of the activation curve is strongly influenced by the chemical nature, the statistical composition and obviously by the concentration of the substituents linked to the polymeric system. In order to draw correlations between these variables and the experimental results, the parameters describing the kinetic activation curve, namely :

- . the height of the limiting plateau (H_p),
 - . the lag-time corresponding to 50% activation ($t_{1/2}$)
 - . the rate constants of the exponential equations fitting the initial increase (k_a) and decrease (due to the action of the inhibitors for long incubation durations of the plasma) (k_d),
- will tentatively be taken into account for quantifying the polymer/contact phase interaction in plasma.

In first approximation, the studied polymers can be divided into four classes according to their activating potency:

DS > CMDBS > Hep > PSS > PSS > D

The most striking fact observed in this study is that the existence of a negatively charged material (the term "surface" should be used cautiously) is not a sufficient prerequisite for inducing Factor XII activation. This could be assessed with the experiment conducted with CMDB carrying 91% of carboxylic groups substituting dextran as a model for such a highly negatively charged polymer (noted ** in the Table). The other effect is related to the observation that sulfonate groups cooperate to promote the activity of carboxylic groups, the latter beginning to exert activity only beyond a threshold composition in sulfonate groups.

Analytical evaluations translating quantitatively the kinetics of the activation phase as a function of the chemical and electrical characteristics of the polymeric materials will be presented.

1. J.JOZEFOWICZ, M.MAUZAC, A.M.FISCHER, J.TAPON-BRETAUDIERE and S.BEGUIN. This meeting.
2. C.KLUFT. Determination of prekallikrein in human plasma. J.Lab.Clin.Med., 91, 83-95, 1978.

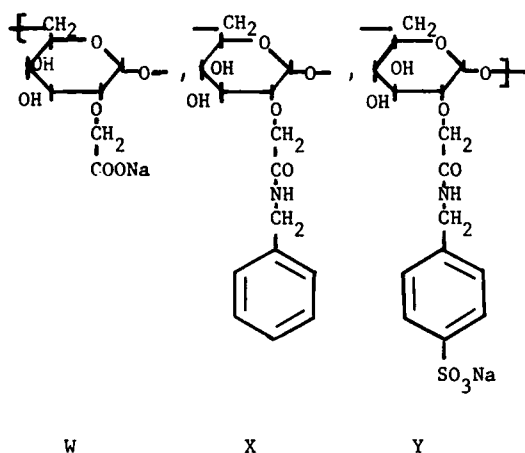
ANTICOAGULANT DEXTRAN DERIVATIVES

J. JOZEFONVICZ*, M. MAUZAC*
A.M. FISCHER**, J. TAPON-BRETAUDIERE**, S. BEGUIN**

Laboratoire de Recherches sur les Macromolécules - VILLETANEUSE - FRANCE -

Heparin is a well known natural anticoagulant polysaccharide ; however the precise relationship between structure and anticoagulant activity has not yet been demonstrated. Our approach is first to synthesize compounds possessing well defined chemical groups, similar to those of heparin and, secondly to examine their anticoagulant properties.

Dextran being used as a plasma volume expander, it provides an attractive support. Previous works (1) have shown that the binding of benzylsulphonate and carboxylic groups to insoluble crosslinked dextrans endows this material with significant anticoagulant activity. We report here anticoagulant potency of similar but soluble modified dextrans :

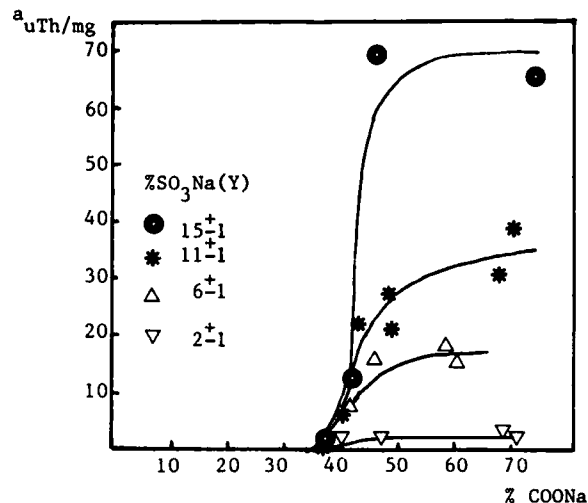


The antithrombic activity, a , has been determined by measuring thrombin clotting times of platelet-poor plasma in the presence of various amounts of polymer. The coefficient " a " will be expressed as the number of thrombin units inactivated by one milligram of polymer. In these conditions, commercial heparin "Choay lot n° H 108" (Specific activity of 173 IU/mg) exhibits an activity of 3800 u Th/mg.

The antithrombic activity of dextran derivatives was correlated with the ratio of each substituent methylcarboxylic and benzylsulphonate (see figure).

This activity appears to be maximum when the compound contains more than fifty per cent of carboxylic acid groups and simultaneously about fifteen per cent of benzylsulfonate functions. This observation agrees well with the fact the carboxylic and O or N sulphate groups are involved in highly active heparin (2) (3).

Experiments carried out with fibrinogen prove that the anticoagulant properties of dextran derivatives are connected with the presence of antithrombin (AT_{III}).



A comparison of the effect of some dextran derivatives and heparin has been made by different clotting assays : APTT, calcium thrombin time, reptilase clotting time, thrombin generation test in the presence and in the absence of AT_{III}. Heparin-like activity was measured by anti IIa assay using chromogenic substrate.

The dextran derivatives exert their effects on the coagulation cascade by the same mechanism than heparin but are less effective (about 50 times). It would be interesting to go further in this way, to obtain the same kind of materials with a higher potency, to be useful in therapy.

- (1) M. MAUZAC, N. AUBERT and J. JOZEFONVICZ, Antithrombic activity of some polysaccharide resins, *Biomaterials*, 1982, **3**, 221-224.
- (2) R.D. ROSENBERG, G. ARMAND and L. LAM, Structure-function relationships of heparin species, *Proc. Natl. Acad. Sci. U.S.A.*, 1978, **75**, 3065-3069.
- (3) U. LINDAHL, G. BÄCKSTROM, M. HÖÖK, L. THUNBERG, L.A. FRANSSON and A. LINKER, Structure of the antithrombin-binding site in heparin, *Proc. Natl. Acad. Sci. U.S.A.*, 1979, **76**, 3198-3202.

*Université PARIS-NORD
Laboratoire de Recherches sur les Macromolécules
Avenue J.B. Clément - 93430 VILLETANEUSE - FRANCE

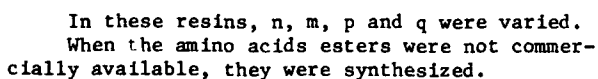
**Department of Haematology, Hospital Necker
PARIS - FRANCE

M. JOZEFOWICZ, D. LABARRE, H. SERNE, C. FOUGNOT, C. DOUZON and F.M. KANMANGNE

In previous papers, we described the preparation and the heparin-like properties of insoluble modified polystyrene resins. Then we demonstrated that the antithrombic activity of insoluble poly(styrene sulfonate) resins (PSS) was linearly related to the surface density of sulfonate groups, taking into account the variable hydrophilicity of the resins. We consider now the influence of the geometry of the site on the heparin-like properties of the resins: so we have bonded various dicarboxylic amino acids by reacting them with chlorosulfonated polystyrene.

The copolymer styrene-divinylbenzene was chlorosulfonated as previously described. The amino acids esters were either purchased or prepared following a procedure described elsewhere. After binding and purifications, the resulting resins were characterized chemically and physically and their anticoagulant potency determined by quantitating the weight of resin able to neutralize one unit of thrombin in presence of plasma.

Chlorosulfonated polystyrene beads were reacted in an anhydrous medium with esters of the amino acids and the resulting resins were saponified and isolated so that the following resins were obtained :



The anticoagulant activity of the resins was quantified by measuring the clotting time of resin-plasma suspensions to which thrombin (T) has been added. So, it was possible to calculate the amount of resin required to inactivate one unit of T. By introducing different parameters - i.e. density, swelling ratio, average grain size, anticoagulant activity- we were able to calculate the average surface \bar{S}_D of resin able to neutralize one unit of T and we defined A, Antithrombic-Surface-Activity, as the inverse of \bar{S}_D . Taking into account the chemical composition of the resins, we were able to compare A for each type of substituent, other parameters being constant (Figure).

no significant difference could be evidenced between the different types of substituents. Moreover, the resulting effect was additive between amino acid sulfamide and sulfonate groups.



- * = Aspartic Acid
- ▲ = Glutamic Acid
- = 2 Amino Adipic Acid
- ◇ = Amino Malonic Acid
- △ = Amino Methyl Succinic Acid
- = Amino Ethyl Succinic Acid
- ⊕ = Amino Methyl Glutaric Acid

A : Units of Thrombin/cm²
C_{SO₃} and C_{AA} : mmol/g

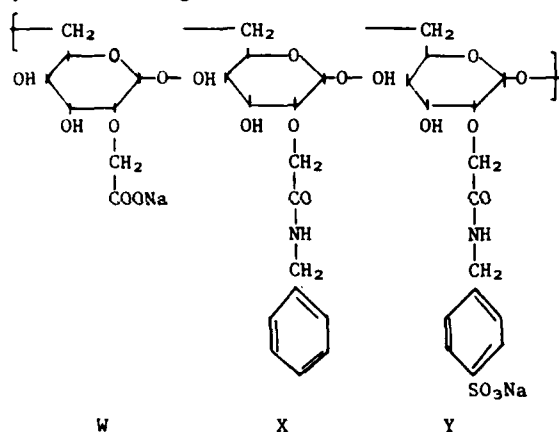
ANTICOMPLEMENTARY ACTIVITY OF DEXTRAN DERIVATIVES

F. MAILLET*, M. MAUZAC**, J. JOZEFONVICZ** and M.D. KAZATCHKINE*

INSERM U 28, CNRS ERA 48, Hopital Broussais, Paris, France

Heparin glycosaminoglycan is a natural polyanionic polysaccharide that is composed of alternating O-sulfated uronic acids and O- and N-sulfated N-acetylglucosamine. Heparin inhibits activation of the human complement system by interfering with formation and regulation of the classical and alternative pathway C3 convertases and with function of late components of the system. The inhibitory activity of heparin on formation of the amplification C3 convertase C3b,Bb,P *in vitro* is observed at concentrations similar to those necessary for its antithrombin III cofactor activity, and requires O-sulfation and N-substitution of the molecule (1). In this study, the anticomplementary activity of several synthetic dextran derivatives was assessed, the chemical requirements for this effect were determined and compared with those necessary for antithrombic activity (2).

Hydrosoluble dextran derivatives containing carboxylic groups (W) and/or benzylamine groups alone (X) or substituted with sulfonates (Y) were synthesized (Fig. 1).



Antithrombic activity (a) of the substituted derivatives was assessed by measuring thrombin clotting times of platelet-poor plasma in the presence of incremental amounts of polymers and expressed as the calculated number of thrombin units that would be inactivated by 1 mg of polymer (3). Inhibition of C3b,Bb,P formation was determined by assembling the amplification convertase on C3b bearing sheep erythrocytes (EAC43b) using purified human alternative pathway proteins (1) in the presence or in the absence of increasing amounts of test polymers. Convertase sites were developed by addition of complement components C5-C9 in EDTA. The anticomplementary activity of the derivatives was calculated as the input of polymer that would inhibit 50 % convertase formation on 10⁷ EAC43b.

The relative anticomplementary and antithrombic activities of polymers bearing various amounts of W, X and/or Y units are shown in the Table.

Chemical composition of test polymer (% substituted units)			Anticomplementary activity $\mu\text{g}/10^7 \text{ EAC43bBbP}$	Antithrombic activity aTh/mg
W	X	Y		
40.0	12	3.0	60.0	3
45.0	0	4.0	13.0	15
64.0	0	5.0	11.0	18
71.0	7	2.0	21.5	1
37.0	15	4.5	60.0	1
47.5	0	5.0	9.0	25
60.0	14	5.0	10.0	16
37.0	11	9.0	45.0	1
43.0	4	11.0	7.5	23
50.0	3	10.0	4.0	22
68.0	0	12.0	4.0	31
71.5	0	9.5	3.0	40
Reference porcine heparin (159 u/mg)			1.0	3500

Above a threshold of 40 % W units, increasing substitution with carboxylic groups was associated with increasing anticomplementary activity until a plateau was reached. For a given content of carboxylic groups, the anticomplementary activity increased with increasing substitution with SO₃Na. Increasing substitution with COOH and/or SO₃Na enhanced anticomplementary and antithrombic activities in a similar fashion. On a weight basis, the relative ratio of anticomplementary to antithrombic activity of the polymers was much higher than that of heparin. These studies demonstrate that dextran derivatives bearing carboxylic and sulfonated groups modulate the complement and coagulation systems and suggest that uronic acid and N-acetylglucosamine in the heparin molecule are important, besides carboxylic and sulfate groups, in conferring high anticoagulant activity to anticomplementary polyanionic polysaccharides.

- (1) KAZATCHKINE M.D., D.T. FEARON, D.D. METCALFE, R.D. ROSENBERG and K.F. AUSTEN. 1981. Structural determinants of the capacity of heparin to inhibit formation of the human amplification C3 convertase. *J. Clin. Invest.*, 67 : 223.
- (2) JOZEFONVICZ J., M. MAUZAC, A.M. FISCHER, J. TAPON-BRETAUDIERE and S. BEGUIN. 1983. Anticoagulant dextran derivatives. 2nd world congress on biomaterials. Submitted.
- (3) MAUZAC M., N. AUBERT and J. JOZEFONVICZ. 1982. Antithrombic activity of some polysaccharide resins. *Biomaterials*, 3 : 221.

Supported by ATP "biomatériaux" from CNRS, France.

* INSERM U 28, CNRS ERA 48, Hopital Broussais, 96 rue Didot, 75014 Paris, France

** Laboratoire des macromolécules. Université Paris Nord, Villetaneuse, France.

AN ALTERNATIVE MEANS TO STUDY THE DEGRADATION PHENOMENA OF POLYGLYCOLIC ACID ABSORBABLE POLYMER

Chih-Chang Chu & May C. Louie

Department of Design & Environmental Analysis, Martha Van Rensselaer Hall, Cornell University, Ithaca, New York, USA 14853-0218

INTRODUCTION

One of the major concerns of using polymeric materials in surgery is their stability or inertness in the presence of the hostile biological environment. The degree of degradation is not only a function of time and site of implantation but also a function of the structure of the polymers and the mechanical force the implant experiences.

An important application of biodegradable polymers is in the wound closure, such as sutures. All existing methods used to study the degradation phenomena of synthetic absorbable sutures are largely based on the loss of mechanical strength of the suture as a function of time. The problem with this approach, however, is that an overall picture of the degradation profile is difficult to obtain, particularly during the very early interval and beyond the period of measurable strength.

In this study, an alternative means to evaluate the degradation phenomena of synthetic absorbable polymers is reported. The method is based on the monitoring the appearance of color and its intensity resulting from the chemical reaction of glycolic acid, the degradation product of polyglycolic acid, with chromotropic acid.

EXPERIMENTAL PROCEDURE

1) Preparation of a calibration curve

One ml of each of the six different concentrations of pure glycolic acid obtained from duPont, (2.00×10^{-3} , 1.00×10^{-3} , 6.67×10^{-4} , 5.00×10^{-4} , 3.33×10^{-4} , 1.60×10^{-4} M) was mixed with 3 ml of analytical grade chromotropic acid obtained from Fisher Scientific. The resulting absorbance of the most concentrated solution was determined by scanning the solution through the wavelength ranging from 200 to 900 nm in a Cary 219 uv/visible spectrophotometer. The wavelength at which the maximal absorbance was observed were taken for the determination of the subsequent absorbance of the six sample solutions. The calibration curve was constructed by plotting the observed maximal absorbance vs. the corresponding solution concentration.

2) Application to PGA degradation

Dexon 2-0 suture obtained from Davis & Geck were irradiated at 0, 5, 10, and 20 Mrads in the absence of oxygen. A fixed amount of the above suture materials was then immersed in 5 ml of phosphate buffer of pH = 7.4. The solution was kept at 37°C for a predetermined period of time. One ml of each of the immersion solution was withdrawn after the predetermined period of immersion and mixed with 3 ml of the analytic grade chromotropic acid. One ml of the corresponding buffer mixed with 3 ml of the analytic grade chromotropic acid served as the control. The absorbance maximum of each solution was determined in the same manner described above. The corresponding glycolic acid concentration at the absorbance maximum was determined by the use of the calibration curve constructed previously.

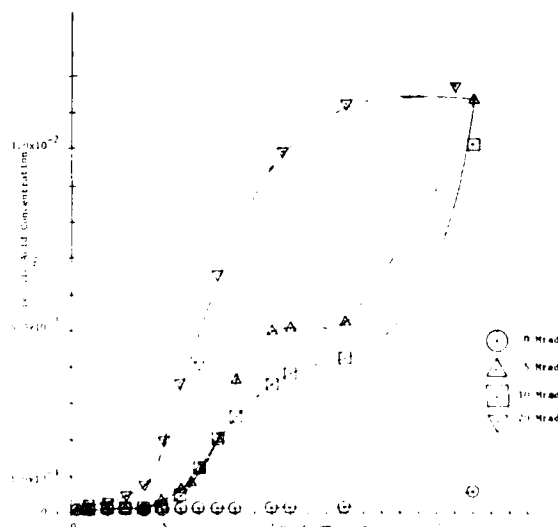
RESULTS

When the glycolic acid solution reacted with the chromotropic acid, colors ranging from pink to violet developed depending on the concentration of glycolic acid. The wavelength of the maximal absorbance was found to be at 568 nm.

The calibration curve showed a reproducible straight line correlation between glycolic acid concentration and absorbance with the slope equal to 296.6.

The degradation profiles of PGA sutures in terms of the change of glycolic acid concentration with time are shown in Figure 1.

The data indicate clearly the advantages of the proposed method over the conventional tensile strength study in evaluating the detailed degradation mechanism of PGA. First, the method can detect the degradation of PGA as early as 4.5 hours after immersion. The initial increase in the concentration of glycolic acid demonstrates that the hydrolytic degradation could occur right after immersion. Second, additional information about the degradation of PGA can be obtained even beyond the period of measurable strength, particularly in the irradiated specimens. Third, the major difference in the degradation between the unirradiated and irradiated PGA specimens was the time period required to observe the sharp increase in the concentration of the degradation product. The required time periods were 15, 5, 4, and 3 days for 0, 5, 10, and 20 Mrad PGA specimens, respectively. Fourth, the degradation profiles of the irradiated PGA specimens were, in general, similar to each other during the early stage of immersion, but they differed from each other at a later period of degradation. Fifth, the concentration of the degradation product started to increase significantly during or after the tensile strength became unmeasurable.

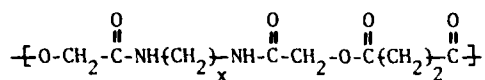


POLY(ESTER-AMIDES): IN VIVO ANALYSIS OF DEGRADATION AND METABOLISM
USING RADIOLABELED POLYMER.

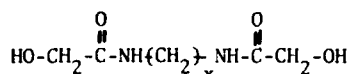
T. H. Barrows, S. J. Gibson*, and J. D. Johnson*

Life Sciences Research Laboratory/3M
St. Paul, Minnesota 55144

A new class of fiber-forming, thermoplastic polymers designed for the absorbable suture application has recently been reported. (1,2) A subset of this class of poly(ester-amides) being studied further is described by the formula shown below where $x = 6, 8, 10$, and 12 .



These polymers, in turn, are made from the corresponding amidediol monomers, shown below, by polymerization with succinyl chloride.



The *in vivo* absorption times for amidediol monomers and low molecular weight polymers were obtained for comparison by subcutaneous implantation of uniform pellets in mice. These results suggested that monomer solubility influences the rate of polymer absorption and that the amide bond is relatively stable to *in vivo* hydrolysis.

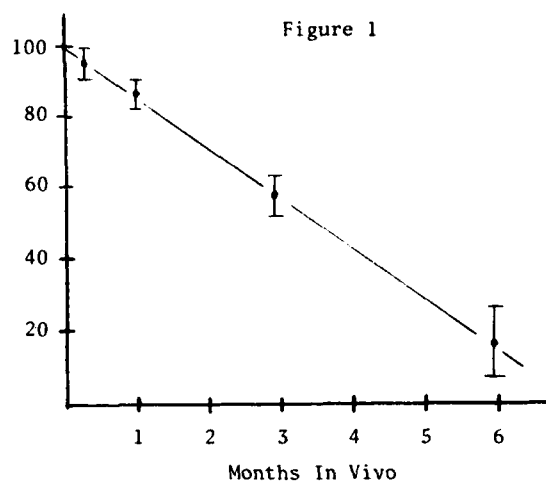
In order to study the mechanism of *in vivo* polymer degradation further and to examine the metabolic fate of degradation products, an experiment was conducted using radiolabeled polymer. Poly(ester-amide), $x=6$, was synthesized from amidediol labeled with carbon-14 in the hydroxyacetamide moiety to give radiochemically pure polymer with a specific activity of 6.89 $\mu\text{Ci}/\text{mg}$. The carbon-14 polymer was melted and drawn to form thin filaments which were cut to 1.0 cm. lengths. One piece of polymer was implanted in each of thirty-five rats by means of an 18-gauge needle inserted into the crural muscles of the right leg.

The rats were sacrificed in groups of five at 7 days, 1,3,6, and 9 months postimplantation. An additional group of ten rats was sacrificed at 10 months postimplantation. At the time of necropsy, blood, liver, heart, spleen, kidneys, crural muscles (contralateral implant control site), the implant site, lymph node, and abdominal fat were collected and analyzed radiometrically. In the group of ten rats sacrificed at 10 months, all urine and feces were collected and monitored for carbon-14 content for individual rats. In addition, urine was analyzed chromatographically and rats selected randomly were placed individually in a sealed system for measurement of $^{14}\text{CO}_2$ elimination.

As shown in Figure 1, loss of radioactivity from the implant site is virtually linear. No accumulation of radioactivity was detected in any of the peripheral tissues. Although some loss of radioactivity was due to excretion via feces and respiration, the primary route of elimination was urinary excretion.

Moreover, the major radiochemical compound in the urine was found to be unchanged amidediol monomer.

% Radioactivity Remaining
at Implant Site



Thus polymer degradation probably results from hydrolysis of the poly(ester-amide) to succinic acid and amidediol followed by excretion of the latter in the urine.

In a separate experiment, the acute toxicity of amidediol monomer ($x=6$) was tested in ten rats by intraperitoneal injection of 5,000 mg/Kg. Under these conditions there was no evidence of toxic effects for two weeks post-dose nor were any visible lesions detected during necropsy.

In conclusion, the *in vivo* degradation and metabolism of this polymer occurs at a potentially useful rate and yields relatively nontoxic breakdown products. Poly(ester-amides), therefore, continue to show promise as a new class of synthetic absorbable polymers.

1. T. H. Barrows, U.S. Patent No. 4,343,931 (1982).
2. T. H. Barrows, D. M. Grussing, D. W. Hegdahl, 9th Annual Meeting of the Society for Biomaterials, Birmingham, Alabama, 1983.

Life Sciences Research Laboratory/3M
3M Center - Bldg. 201-2W 17
St. Paul, Minnesota 55144

*Riker Laboratories/3M

IN VITRO STUDIES ON THE DEGRADATION OF NYLON 6

James M. Anderson, Sally A. Kline, and P. Anne Hiltner

Depts. of Pathology and Macromolecular Science, Case Western Reserve Univ.
Cleveland, Ohio 44106

Condensation polymers are susceptible to *in vivo* degradation through cleavage of labile bonds in the main chain of the macromolecule. As a condensation polymer, Nylon 6 (polycaprolactam) is vulnerable to acid or base catalyzed hydrolysis of the amide bond. The qualitative characterization of the degradation and resorption of Nylon 6 in both animals and humans has been well documented (1,2). Quantitatively however, less is understood concerning the rate of degradation and the physico-chemical and morphological factors controlling the rate of degradation. The rate is dependent upon the local environment at the polymer-tissue interface. In turn, the *in vivo* environment is determined by the magnitude of the inflammatory and foreign body reactions. The goals of this study therefore, were to quantitatively determine the rates at which a Nylon 6 polymer would degrade in several different environments, to investigate the significance that the geometric form of the material plays in altering the rate and the type of degradation (surface vs. bulk) and to follow the change in the polymer properties that accompany degradation.

The medical grade polymers used in this study were all Nylon 6 derived from ϵ -caprolactam and marketed by S. Jackson, Inc., Alexandria, VA. Two of the four geometric forms investigated were smooth films (0.1 mm and 0.4 mm thickness) utilized mainly for reconstructive surgery. The remaining forms were suture materials consisting of either a monofilament or polyfilament construction.

Controllable and reproducible degradation was obtained using an *in vitro* accelerated testing system. The system was designed to allow the temperature, the pH of the solution, the form of the material and the time of degradation to be independently varied. This approach permitted the quantitative determination of kinetic rate constants, and the continuous monitoring of degradation parameters such as weight loss, water absorption, percent crystallinity and mechanical properties.

The rate constants were determined from a pseudo-first order equation expressed as:

$$\bar{M}_v(t) = \bar{M}_v(o) \exp(-kt)$$

where \bar{M}_v is the viscosity average molecular weight. The rate constants obtained at the elevated temperatures of 90°C and 70°C were related to a rate constant for hydrolysis at the *in vivo* temperature of 37°C using the classical Arrhenius equation. The values calculated for the rate constants are shown in Table 1. For a given geometric form, an increase in acidity from pH 7.4 to pH 6.0 increased the rate constant for chain cleavage by at least 34% in every case.

The trends in the variations of the polymer properties help to address the more fundamental uncertainties accompanying the degradation process. The percent water in the bulk of each polymer increased slightly over the first few days and reached its equilibrium water content relatively quickly. The percent water absorbed in the 0.4 mm and 0.1 mm thick films was essentially equivalent suggesting that the hydrolysis is not surface

reaction limited, but rather occurs within the bulk of the material. This is also supported by the fact that similar rate constants for degradation of the two films were obtained.

The percent crystallinity of the polymer, as measured by x-ray diffraction, increased as a function of time. Calculations suggest that the increase in crystallinity may be due to mass loss from the amorphous regions and crystallization of chain segments in the remaining portions of the amorphous regions. The crystallinity of the polymer and the average chain length in the amorphous region both contribute to the overall mechanical properties of the material. For the period of time tested, neither the crystallinity change nor the decreased amorphous chain length produced significant changes in the stress-strain curve. The percent elongation at break, the load to break and the modulus showed only slight changes as a function of degradation time.

Thus, the Nylon 6 monofilament, polyfilament and films are shown to undergo environmental dependent bulk degradation, with the suture materials demonstrating a slightly greater resistance to hydrolytic chain cleavage than the film materials.

The hydrolytic degradation of Nylon 6 was marked by distinct trends in the variation of polymer properties. For each geometric form, the largest percent change was seen in the percent decrease in molecular weight. The changes in the molecular weights yielded decreases that were at least an order of magnitude greater than other measured variations. The load to break demonstrated the second largest percent change from the control material. The next parameter, the water absorbed in the polymer matrix, was approximately eight percent by weight for each of the forms measured. The smallest percentage change was seen in the crystallinity increases and the weight losses. None of the values measured for these parameters exceeded 7.5%.

References:

1. Kronenthal, R., *Ophthalmology*, **88**(9), 965 (1981).
2. Stinson, N., *Brit. J. Exp. Path.*, **XLVI**(2), 135 (1964).

Table 1. Calculated First-Order Rate Constants at 37°C Based on Viscosity Changes at pH 7.4

Sample	pH	k_1 , day ⁻¹
Film (0.1mm)	7.4	1.63×10^{-4}
Film (0.4mm)	7.4	1.53×10^{-4}
Polyfilament	7.4	6.19×10^{-5}
Monofilament	7.4	6.12×10^{-5}

SYNTHESIS AND PROPERTIES OF A NEW BIODEGRADABLE POLYPEPTIDE

D. Bichon and W. Borloz

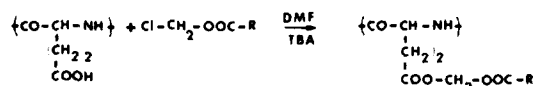
Battelle Institute, Geneva, Switzerland

Introduction

Synthetic polypeptides represent a class of polymers which have been investigated as biomaterials in a number of domains [1]. Apart from their general high biocompatibility they are often biodegradable. The biodegradation of polymers of glutamic acid esters [2] and of copolymers of aspartic acid esters and leucine [3] has been studied in detail *in vivo*: the time required for the biodegradation of poly[Glu(OMe)/Glu(OH)] for example varied considerably, from ten days to two months, by increasing the degree of esterification from 60% to 64% [4]. This large variability led us to search for new esters of polyglutamic acid which would be degraded in a more controlled manner.

Materials and Methods

As labile acyloxymethylesters have been used with success for the synthesis of diverse prodrugs, we have attempted to synthesize similar esters of polyglutamic acid. Poly(acyloxymethylglutamates) were prepared by the following reaction:



In a typical reaction polyglutamic acid (PGA) was dissolved in DMF and two equivalents of tributylamine added. Two equivalents of chloromethylpivalate (R = *tert*iobutyl) were added dropwise and the reaction was allowed to proceed for two days. The polymer obtained was then precipitated in water, redissolved in acetone, precipitated in petroleum ether, and dried. NMR analysis showed an 80% esterification and GPC analysis showed no change in molecular weight from the initial PGA. The poly(pivaloyloxymethylglutamate) or poly(POMEG) is soluble in acetone, methylethylacetone, THF, DMF, dioxane, polyethyleneglycol, but insoluble in chlorinated solvents and benzene, this behaviour being unusual for polyglutamic acid esters.

Other acyloxymethyl esters of PGA as well as copolymers with leucine can be obtained using the same method. These copolymers are all soluble in acetone.

Biodegradation studies

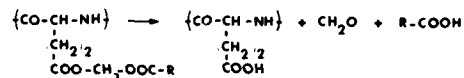
In vitro biodegradation studies on poly(POMEG) were carried out using: 1) a polymer labelled on the pivaloyloxymethyl group; 2) a polymer labelled on the peptidic backbone by incorporation of a small amount of ¹⁴C-leucine.

Thin films of these materials were incubated in either leucine aminopeptidase (LAP) from hog kidney in Tris-HCl 0.1 M buffer, pH 8.5, 37°C, or esterase from hog liver in Tris-HCl 0.1 M buffer, pH 7.5, 37°C and the radioactivity

released in the medium was measured as a function of time. In the LAP containing medium poly(POMEG) was entirely degraded in 16 days.

The results obtained showed that biodegradation occurred in two steps:

- hydrolysis of the pivaloyloxymethyl ester which is pH-dependent and catalysed by esterase and LAP by the following mechanism:



- main chain degradation/dissolution, mainly promoted by LAP.

These results also showed that the solvent used for casting the film had a major influence on the biodegradation rate. Enzymatic degradation was roughly doubled from an acetone-casted (helix forming solvent) to a trifluoroacetic acid-casted sample (in which the polymer has a random coiled structure in solution).

Subcutaneous implantation of thin films of poly(POMEG) in rats revealed that the polymer disappeared from the implantation site within two weeks. Histological examination revealed no acute inflammation at the site of the implant. In addition no lethal effect was observed in mice even after implantation of 2 g/kg of poly(POMEG).

Conclusions

The physico-chemical and biological characteristics of poly(acyloxymethylglutamates) show that these products could be of great interest as biodegradable carriers for drug delivery systems. In addition, these polymers can be thermoformed at low temperature in a plasticized form with polyethylene glycol for galenic purposes. They could also find other applications as implants or materials for surgical dressings.

References

- (1) Anderson J.M. *et al.*, J. Biomed. Mater. Res. 5(1), 197 (1974)
- (2) Sidman K.R., J. Membrane Science 7, 277 (1980)
- (3) Marck K.W. *et al.*, J. Biomed. Mater. Res. 11, 405 (1977)
- (4) Sidman K.R. *et al.*, NICHD/CPR/CDB/81-1 (1981)

BATTELLE INSTITUTE
Centre for Toxicology & Biosciences
7, route de Drize
1227 Carouge-Geneva
Switzerland

NEW ADSORBENTS OF BILIRUBIN FOR ARTIFICIAL LIVER SUPPORT

K. Teramoto, M. Murakami, H. Tanzawa, T. Sonoda, Y. Idezuki

Fiber Research Laboratories, Toray Industries, Otsu, Japan

An anion exchange resin fiber (IONEX) is able to adsorb bilirubin. Direct hemo-perfusion or plasmapheresis with IONEX has proved effective in reducing bilirubin in the blood of jaundiced dogs. But its adsorptive capacity seems to be insufficient to use it clinically in jaundiced patient with severe hepatic failure. Therefore 30 sorts of IONEX derivatives whose ligands differ from one another were newly prepared to be evaluated their adsorptive capacity to bilirubin and heparin. Consequently two of them were found out to have about 3-fold capacity of former IONEX to bilirubin but one-third capacity of it to heparin.

An island-sea-type conjugated polystyrene fiber reinforced polypropylene was reacted with N-methylol- α -chlor-acetamide to be converted α -chlor-acetamidomethylated polystyrene fiber (F-1). Former IONEX had been prepared by hydrolyzing F-1 with conc. hydrochloric acid and by methylating it with HCHO/HCOOH. New IONEX derivatives were prepared by reacting F-1 with various amino compounds comprising twelve secondary amines and eighteen tertiary amines. New IONEX derivatives were prepared by reacting F-1 with various amino compounds. They were evaluated by their adsorption isotherm of bilirubin at the temperature of 37°C. Bilirubin solutions were prepared by diluting a 200 mg/dl aqueous solution of bilirubin sodium with a bovine serum or a 5 % aqueous solution of bovine serum albumin so that the concentration of bilirubin became 20 mg/dl. Their adsorptive property of heparin were estimated by the amount of heparin adsorbed in a 0.1 mg/ml aqueous solution of heparin sodium.

Their adsorptive capacity of bilirubin was found out to correlated closely with the chemical structure of their ligand.

Fibers whose ligands are quarternary ammonium groups show a larger adsorptive capacity than those whose ligands are primary, secondary or tertiary amino groups. As well as the chemical structure, the swelling-ability of the fiber affects the adsorptive capacity. The larger the swelling-ability of the fiber is, the larger the adsorptive capacity of it is, as far as their ligand are the same.

When the capacity of each adsorbent is represented by the number of milligram of bilirubin which one gram of the fiber adsorbs in the concentration of 10 mg/dl bovine serum, the capacity of triethyl-, tri-n-propyl-, tri-n-butyl- and tri-n-amy ammonium acetamidomethylated poly-styrene fiber (F-2, F-3, F-4 and F-5, respectively) are 35, 50, 60 and 4.5, respectively, whereas that of dimethylaminomethylated one (former IONEX) is 17 and that of dimethyl-aminoacetamidomethylated one (F-6) is 2.1. The amount of heparin which one gram of F-2, F-3, F-4, F-5, former IONEX and F-6 adsorb are 25, 11, 5, 4, 15 and 70 mg, respectively. And further, F-3 and F-4 were checked to eliminate no poisonous substance on condition of the steam-sterilization.

From these data, the best adsorbent of bilirubin is F-4 and the second best is F-3.

EFFECT OF ALUMINA ON THE REACTIVITY OF BIOGLASS

C. S. Kucheria, R. E. Wells, R. S. Matthews, G. E. Gardiner

Howmedica Corporate R&D, Groton, Connecticut 06340

Bio glass compositions are known to form a strong bond to bone. However, Bio glass by itself is a structurally weak material and cannot withstand loading as a bulk implant. Therefore, Bio glass coated alumina composites, which combine the good mechanical properties of alumina and ability of Bio glass to form chemical bond with bone, have been proposed as implant materials (1-2). Two major problems have been encountered in Bio glass coated alumina implants: (i) microcracking in Bio glass coating and (ii) loss of Bio glass reactivity.

Two grades of alumina, Alsiman 614 containing 96% Al_2O_3 and an in-house slip-cast body containing 99% Al_2O_3 , were used in this study. Bio glass 45S (SiO_2 -45%, CaO -24.5%, Na_2O -24.5% and P_2O_5 -6.0%) was prepared and ground using an alumina ball mill. Alumina samples were coated with Bio glass and fired upto 1350°C for 15 minutes.

Microcracking: The Bio glass coating on alumina always contained microcracks. The width of the microcracks ranged between 0.4 and 0.9 μm and dimensions of uncracked islands ranged between 40 and 110 μm . These microcracks arise because the thermal expansion coefficients of Bio glass and alumina are not matched. The coefficients of expansion of 45S Bio glass and 99% polycrystalline alumina in 25-550°C range are $15.69 \times 10^{-6}/^\circ C$ and $7.78 \times 10^{-6}/^\circ C$ respectively. The difference in the thermal expansion creates tensile stresses in the Bio glass resulting in microcracking when the coating is cooled.

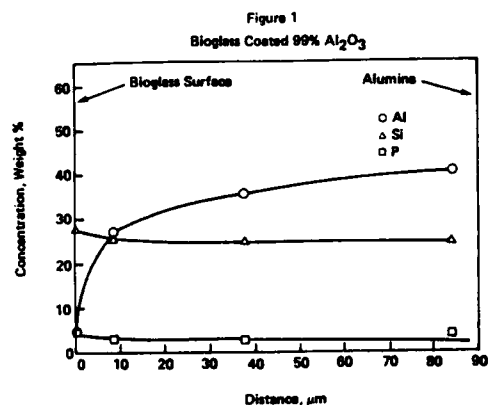
Loss of Bio glass Reactivity: The EDXA concentration profiles of Al, Si and P at the Bio glass coated alumina cross section, shown in Figure 1, indicate 5 wt.% Al at the surface of glass coating, 27% Al at 10 μm inside the surface and 34% Al at 20 μm inside the surface. There are two sources of Al contamination in the glass coating; about 1-1.5% Al is due to grinding of the glass frit in an alumina ball mill and the balance is introduced by thermal diffusion of Al_2O_3 from the alumina substrate. The presence of alumina in the glass reduces its corrosion rate, thereby, impairing its ability to form a bond with bone.

Five compositions of 45S Bio glass containing 0.3, 1.8, 5.0, 10.0 and 15.0 wt.% Al_2O_3 were prepared. Cylindrical samples of these glasses were allowed to corrode in tris buffer at 37°C. The diluents from the reactivity study analyzed for leaching of Na^+ and Ca^{2+} , are shown in Figure 2 and 3. These results clearly indicate that the reactivity of 45S Bio glass decreases drastically as

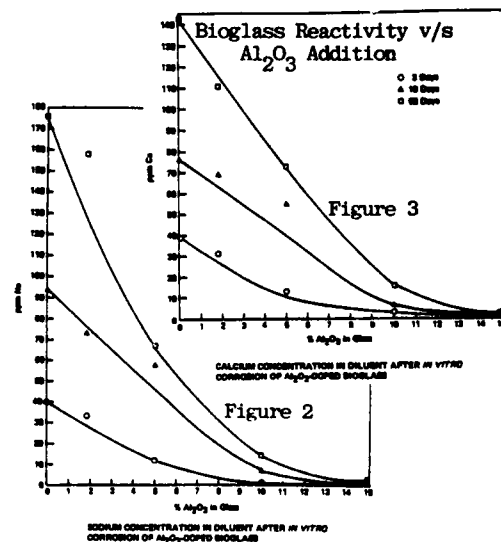
Al_2O_3 is added to the glass. Therefore, Bio glass coated alumina implants which may contain up to 35% Al in the glass coating should be expected to exhibit poor reactivity.

¹ Greenspan, D.C., Ph.D. Dissertation, University of Florida, Gainesville, Florida (1977).

² Hench, L.L. and Greenspan, D.C., U.S. 4,103,002, (July 25, 1978).



CONCENTRATION PROFILES OF AL, SI, P IN BIOGLASS COATING



Howmedica Corporate R&D
Eastern Point Road
Groton, CT 06340

EVALUATION OF SOLID DURAPATITE TO RESTORE ATROPHIC
ALVEOLAR RIDGES

B. E. Sage,* D. R. Mehlich**, K. I. Gumaer,* and
R. L. Salisbury*

Sterling-Winthrop Research Institute
Rensselaer, New York

The atrophic alveolar ridge can be a difficult problem for the patient, the oral surgeon and the prosthodontist. Restoration by autogenous bone graft, vestibuloplasty with or without skin grafting or use of alloplastic materials all have had limited rates of success. The use of some autogenous bone is usually necessary for severe cases of atrophic alveolar ridges. This can have a significant degree of morbidity regardless of the site from which the bone is taken (iliac crest or rib).

Durapatite is a nonresorbable, highly dense, hydroxylapatite ceramic material. Studies with durapatite have demonstrated its biocompatibility, bioactivity and nonbiodegradability that induces neither an inflammatory nor immune response. In vivo studies have demonstrated that durapatite acts as a scaffolding for new bone growth.

Eleven Rhesus monkeys (*Mucaca mulatta*) underwent odontectomy procedures to remove their posterior teeth including impacted third molars. Radical alveolectomy was performed to simulate the natural resorptive process and create atrophic maxillary and mandibular ridges. Three months later after healing was complete, solid half-round shaped durapatite cylinders measuring 5 mm wide, 5 mm high and 15 mm long were implanted through vestibular mucoperiosteal flap approach onto the crest of either the right or left maxillary and mandibular ridges chosen by random assignment. Two monkeys were sacrificed at six months and three monkeys each at 12, 19 and 24 months post-implantation. Results were assessed clinically, radiographically, histologically and with tetracycline labelling.

Radiographically bone deposition was evident at the mesial and distal ends of the implants and increased over the 24 month experimentation period. Bone encroachment over the occlusal surface of the implant was not observed radiographically in any of the monkeys. In general, radiographs revealed that the implanted alveolar ridges maintained their height and width as compared to the unimplanted ridges in which atrophy was observed. Gross examination, confirmed these findings. In addition, alveolar ridges, both implanted and control, demonstrated grossly a normal overlying gingiva. Serial cross

sections of the implanted and unimplanted maxillae and mandibles were prepared and stained with hematoxylin and eosin. The implants interfaced with new and dense trabecular bone and/or dense fibrous connective tissue interspersed with parallelly arranged, elongated flattened fibrocytic nuclei. The new bone, seen primarily at the mesial and distal ends of the implants, was characterized as a thin layer composed of trabecular plates with active osteocytes on their surfaces. No inflammatory response was evident and the gingiva and subgingival tissue were normal throughout.

It is the conclusion of this study that durapatite can be used as a scaffold to restore atrophic alveolar ridges and that it can be used in a denture bearing area.

*Sterling-Winthrop Research Institute
Columbia Turnpike
Rensselaer, N.Y. 12144

**Biomedical Research Group, Inc.
1500 West 38th Street
Suite 51
Austin, Texas 78731

EVALUATION OF SOLID DURAPATITE IN LEFORT I OSTEOTOMIES IN RHESUS MONKEYS

A. D. Sherer,* D. Rothschild,** S. S. Rothstein,*
P.J. Boyne*** and B. E. Sage*

Sterling-Winthrop Research Institute
Rensselaer, New York

INTRODUCTION

Surgical correction of dento-facial deformities sometimes creates osseous defects that require bone grafting to maintain stability. Various bone grafting techniques have been employed using synthetic and bone materials, particularly autogenous bone. The major drawbacks to the use of these materials are: 1) the need for a second operation when autogenous bone is used and 2), the resorption of the implant with consequent failure of the surgical correction. Durapatite, a dense nonresorbable, highly biocompatible hydroxylapatite, may be a viable alternative as a bone grafting material in these surgical procedures.

METHOD

A modified LeFort I osteotomy procedure was performed on six Rhesus monkeys under general anesthesia. A curvilinear mucoperiosteal flap was developed high in the lip from first molar to first molar. The posterior maxilla was then approached via a mucoperiosteal tunnel. An osteotomy was performed on the maxilla in which a step was created just superior and distal to the first premolar. The osteotomy was continued along the lateral maxillary wall to the tuberosity. A curved osteotome was used to cleave the pterygoid plate from the tuberosity. The vomer and lateral nasal wall attachments were transected with an osteotome and the maxilla was down fractured with digital pressure. The down fractured maxillary segment was advanced to create a space at the step portion of the osteotomy. This space was implanted with a durapatite block, approximately 4 x 4 x 6 mm. The down fractured maxillary segment, along with the implant, were fixed to the base of the maxilla with 26 gauge stainless steel wire. Advancements of the maxillary segment were approximately 6 mm. The mucoperiosteal flap was closed with resorbable sutures.

Photographs and radiographs were taken throughout the course of the study. See figure.

Monkeys were sacrificed at 8, 12 and 20 weeks post implantation. Tetracycline labeling was carried out and tissue sections were processed for fluorescent and light microscopic evaluation.



Durapatite block in place following step osteotomy of the maxilla.

*Sterling-Winthrop Research Institute
Columbia Turnpike
Rensselaer, N.Y. 12144

**Doctors Building
Hospital Ave.
North Adams, MA 01247

***Loma Linda University
Dept. of Surgery
Loma Linda, CA 92354

USE OF RESORBABLE ALUMINO-CALCIUM-PHOSPHOROUS OXIDE CERAMICS (ALCAP)
IN HEALTH CARE

P. K. Bajpai†, G. A. Graves, Jr.*, L. G. Wilcox**, and
M. J. Freeman***

Physiology Program, School of Medicine, Wright State University,
Dayton, Ohio 45435.

Over a decade of research has culminated in the development of porous resorbable alumino-calcium-phosphorous oxide ceramics (ALCAP) for use in health care.

ALCAP ceramics are fabricated by calcining mixtures of aluminum, calcium, and phosphorus oxide powders and sintering the compressed blocks of desired size calcined particles.[1] By varying the dimensions of the die, particle size and sintering time and temperature ALCAP ceramics of various densities, porosities, strength, and resorption rates have been manufactured for repairing a wide variety of bone defects[2] and delivering substances of varying molecular weights.[3] The fate of ALCAP ceramics in both in-vitro and in-vivo environments has been studied by means of an array of procedures including chemical analysis of tissues, chemical and enzyme analysis of implants, radiography, radioactive isotope uptake, scanning electron microscopy, energy dispersive X-ray analysis, and histology. ALCAP ceramics are biocompatible and not toxic, cytotoxic, hemolytic, or mutagenic.[4]

In-vitro delivery of gamma globulin, bovine serum albumin, human chorionic gonadotropin, chymotrypsin, insulin, gonadotrophic releasing hormone (GnRH) and testosterone has been accomplished by means of ALCAP ceramic reservoirs. ALCAP ceramics have also been used for sustained delivery of GnRH and insulin in rats.

Experimentally induced defects in long bones of rats, iliac crest and long bones of monkeys and mandibles of rabbits have been corrected by means of ALCAP ceramics. In humans ALCAP ceramics have been used for posterior fusion of spine (Figure 1) and bridging of cleft palate (Figure 2).

The purpose of this presentation is to display and discuss on a one to one basis the uses and potential of ALCAP ceramics in health care.

REFERENCES

1. P. K. Bajpai, S. N. Khot, G. A. Graves, Jr., and D. E. McCullum, IRCS Med. Sci., 9, 696 (1981).
2. P. K. Bajpai, "Biodegradable Scaffolds in Orthopedic, Oral and Maxillofacial Surgery," in Biomaterials in Reconstructive Surgery, L. R. Rubin, Ed., C. V. Mosby & Co., St. Louis, MO, pp. 324-326, 1983.
3. A. Al-Arabi and P. K. Bajpai, Clin. Res., 30, 204A (1982).
4. D. R. Mattie, "Biocompatibility and Toxicity of Alumino-Calcium-Phosphorous Oxide (ALCAP) Ceramics," Ph.D. Dissertation, University of Dayton, Dayton, Ohio (1983).

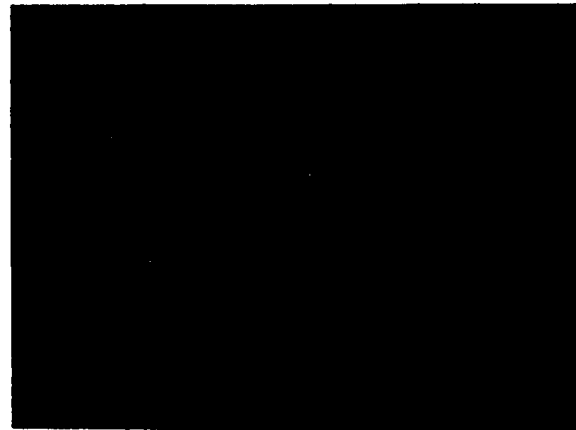


Figure 1. Radiograph Showing Placement of ALCAP Ceramic Between L-4 and S-1 Vertebrae (Lateral View).



Figure 2. Radiograph Showing Bridging of Cleft-Palate by Means of an ALCAP Ceramic.

†Physiology Program, School of Medicine, Wright State University, Dayton, Ohio 45435.

*University of Dayton, Dayton, Ohio 45469.

**833 South Beckham, Tyler, Texas 75701.

***2661 Salem Avenue, Dayton, Ohio 45406.

RESULTS OF BIOPHYSICAL AND BIOCHEMICAL ADAPTATION OF SKELETAL IMPLANTS

A. Engelhardt, G.P. Zoepfel, W. Wagner

B.a.f.B., 6103 Griesheim, West Germany

The new implant system with physiological force transmission and ceramic-coated metal cores has proved to be successful in clinical trials. Results obtained with tumor implants, extending over a period of more than 10 years post operationem, and 5 years of total endoprostheses, show a tight fitting osseous integration of the implants. These results are based on the elimination of interfering biophysical impulses, which occur in conventional endoprostheses.

By the new implant concept it is possible to reach an optimal formfit between implant and tissue. However, the aim was to obtain a chemical bonding to supplement the biomechanical adaptation. The chemical bonding is thought to restore the required pattern of impulses for the control of tissue dynamics as far as possible.

Roux, Wolff, Frost, Pauwels, Kummer et al. have shown that cell differentiation as well as material distribution within the bone depend, as to direction and density, on the mechanical loading.

Differentiation processes and formation of skeletal structures are cellular performances, which are regulated mainly on a biochemical basis.

Today, the assumption that these processes are controlled by direct mechanical influence can be considered as not appropriate with respect to the current findings.

Fucada, Yassuda, Basset et al. have proved bioelectrical phenomena occurring in bone and their influence on osteocellular functions.

Piezoelectric potentials, for example, of collagenous matrix structures contribute to the development of electro(-chemical) impulse patterns. The collagenous matrix is the basic shaping element of the osteon. The organic fiber structure offers the essential sites for apposition of inorganic apatite crystals.

It is questionable, whether one can speak of a chemical bond at all in case of tissue contacts with bioactive glass ceramics. (Hench et al.)

In addition, it is doubtful, whether and how far structural, material continuity at the interface can be obtained by this method in vivo.

The chemical bond of shaping matrix structures and preoperative provision of organic coupling sites to the implant surface give the possibility to organize the synthetic courses of reparative processes in a more physiological manner.

For this reason a biological (organic) coating of implant surfaces has been developed.

It renders the possibility to reinstall interrupted biological impulse patterns by way of a structurally adapted chemical bonding. Accordingly, orthopaedic and dental implants could be directed towards a safer long-term fixation by way of shorter reparative, postoperative processes.

Sponsored by: Federal Ministry of Research and Technology, Bonn

Author's address:

Dr. Achim Engelhardt
B.a.f.B.
Ostend 29
6103 Griesheim
West Germany

A.F.Tencer*, V.Mooney,†, K.Brown‡, P.A.Silva*

Biomedical Engineering Program, University of Texas at Arlington,
Arlington, Texas

INTRODUCTION: Autogenous cancellous bone has shown to be an effective material for bone grafting (1), however the supply is limited and the procedure creates additional surgical trauma. Xenogenic grafts (2) made from processed animal bone appear to remain weakly autogenic, thus efforts have been focused on the development of synthetic ceramics (3,4). A coralline hydroxyapatite porous material formed through hydrothermal conversion of the calcium carbonate exostructure of the sea coral, genus *Goniopora* (CHAG), has been reported to allow bone ingrowth in both animal models (5,6) and in clinical use (7). While the mechanical properties of CHAG with bone ingrowth have been found to be equivalent to those of autogenous cancellous graft with bone ingrowth at 6 months (8), the material, which is pure hydroxyapatite, is brittle at the time of implantation. Thus, clinical use is presently limited to non-load bearing applications. The objective of this study was to determine whether improvements could be made in the mechanical properties of CHAG with out significantly altering its porous structure.

METHODS: Preliminary studies defined a number of variables affecting the mechanical properties of CHAG. In order to standardize these effects, 1 cm cubes of CHAG, cut with a dimensional accuracy of ± 0.5 mm on all sides using a three axis Bronwill diamond saw, were distributed to four groups such that the average properties of the samples for the four groups were within 1.44%, Table 1. Both polymethyl methacrylate (PMMA, LVC, Zimmer, Warsaw, IN) and polylactic acid (PLA) were considered as coating agents. External coatings were produced on three sides of the cube by placing the CHAG in an oversize mold and pouring in the viscous polymer. Nominal coating thickness was 1.25 mm. Internal coatings were produced by wetting the internal surfaces with a fixed volume of low viscosity polymer and measuring the change in porous crosssectional area. After coating, all specimens were reweighed and the dimensions of the externally coated specimens remeasured. Mechanical properties were evaluated by testing specimens to failure in compression at a constant displacement rate of 12.7 mm/min using an Instron type 1120, mechanical tester.

RESULTS: Table 1 shows that the increases in specimen density were more significant with PLA coatings than PMMA coatings. Mechanical properties are shown, Fig. 1, for uncoated CHAG, cancellous graft from canine tibial metaphyses (8) and coated specimens. Externally coated PMMA CHAG specimens showed the largest increases in properties, however the uncoated hydroxyapatite core failed at low loads due to its higher stiffness compared with the PMMA shell. Internally microcoated PMMA specimens were nearly equal to cancellous graft, except for energy absorption. Internally and externally coated PLA specimens were nearly equal in properties, and while 3.27 times as strong as uncoated CHAG, were only 0.36 times as strong as cancellous graft. It should be noted that both CHAG and cancellous graft properties are sensitive to orientation and that properties of

CHAG coated specimens are reported for the orientation of least strength, while those of cancellous graft are for the orientation of maximum strength.

CONCLUSIONS: Internal microcoatings of PLA and PMMA increased the strength of CHAG 3.27 and 10.36 times respectively. External coatings resulted in failure of the internal uncoated CHAG core at low loads, although the polymer shell remained intact.

COATING TYPE	AVERAGE GROUP PROPERTIES			
	CHANNEL/LOAD AXIS ANGLE (deg)	LOADED SURFACE AREA, (cm ²)	UNCOATED DENSITY (gm/cm ³)	COATED DENSITY (gm/cm ³)
PMMA, external, 3 sides, 1.25mm	74.56	1.0255	0.7922	0.9445
PLA, external, 3 sides, 1.25mm	75.25	1.0234	0.7921	1.3377
PMMA, internal	75.00	1.0167	0.7903	0.9957
PLA, internal	73.50	1.0186	0.7911	1.1440

TABLE 1. GROUP MEAN PROPERTIES OF CHAG SPECIMENS USED IN COATING STUDIES

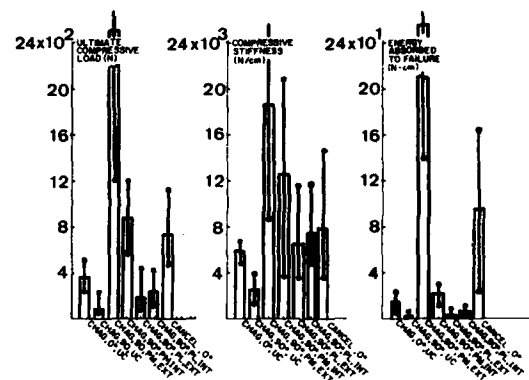


Fig. 1 MECHANICAL PROPERTIES OF COATED CHAG, UNCOATED CHAG, AND CANCELLOUS GRAFT SPECIMENS. Legend: UC-uncoated, 0°-specimen channel axis parallel to load axis, 90°-specimen channel axis perpendicular to load axis, PM-polymethylmethacrylate, PL-polylactic acid, EXT-3sided external coating, 1.25mm thick, INT-internal microcoating.

- (1) Heiple, KG, Chase, SW, Herndon, CH, JBJS, 45A:1593-62, 1963. (2) Salama, R, Clin. Orthop., 174:113-121, 1983. (3) Graves, GA, Hentrich, RL, Stein, HG, Bajpai, PK, J. Biomed. Res. Symp., 2:92, 1971. (4) Webber, JN, White, EW, Mat. Sci. Eng., 5:151, 1973. (5) Chiroff, RT, White, EW, Webber, JN, Roy, DM, J. Biomed. Mat. Res. Symp., 6:29-45, 1975. (6) Holmes, RE, Plast. Recon. Surg., 63:626-633, 1979. (7) Mooney, V, Holmes, RE, Bucholz, RW, Tencer, AF, Clin. Orthop., submitted. (8) Holmes, RE, Tencer, AF, Carmichael, TW, Mooney, V, Trans. 29th ORS, 147, 1983.

Supported by Interpore International, Irvine, CA., and the Instron Corp., Canton, MA.

*Biomedical Engineering Program, University of Texas at Arlington, P.O. Box 19138, Arlington, TX, 76019.

†Division of Orthopedics, University of Texas Health Science Center at Dallas, Dallas, TX.

‡Department of Chemistry, University of Texas at Arlington, Arlington, TX.

STREAMING POTENTIALS IN OSTEONS: AN ANATOMICAL MODEL

R. Salzstein*, S.R. Pollack*, N. Petrov**, G. Brankov** and R. Blagoeva**

University of Pennsylvania, Department of Bioengineering
Philadelphia, Pennsylvania 19104

An anatomical mathematical model for streaming potentials within an osteon is developed to characterize the electromechanical effect in fluid filled bone. This model is based upon first principles from the fields of electrochemistry, electrokinetics, continuum mechanics, and fluid dynamics. The model is based on parameters that allow full numerical analysis. Many of the previously reported experimental results on a micro-scale (within a single osteon) and on a macro-scale (spanning tens of osteons) are explained for the first time in terms of an electrokinetic model. The cusp-like intra-osteonal potential profile is explained, the dependence of the potentials on solution viscosity and conductivity is demonstrated, and much insight is gained relative to the time dependence of stress generated potentials (SGPs).

Cortical bone contains approximately 20% fluid by weight. The fluid fills various channels in bone which include the Haversian canals, Volkmann's canals, lacunae, canaliculi, and the porous matrix.

The osteon is modelled as a cylinder with spherical lacunae axisymmetrically located at various radii (u). The initial lacunar volume (V_0) is pressurized (relative to the Haversian canal of radius \bar{u} which remains near atmospheric or arterial pressure) due to macroscopic deformation of the sample resulting from uniaxial step loading. The model considers Poiseuille flow in n_l rigid fluid channels of length L_l and radius R_l which connect the lacuna and the Haversian canal. The equilibrium charge distribution in these channels is determined (prior to any fluid flow) and the convective streaming current is obtained as a result of laminar flow. The convective current results in a radially dependent potential difference between the Haversian canal and the cement line of the osteon. This potential causes a reverse conduction current and steady state is obtained when the conduction current equals the convective current. The electrical potential that results at this steady state condition is called the intra-osteonal streaming potential, ϕ , which has the following form:

$$\phi(u, t) = \frac{Z \epsilon}{4 \pi \sigma \eta} P_{eff}(u, t/\tau) \ln(u/\bar{u})$$

$$\tau = \frac{2 \eta L_l V_0}{n_l \pi R_l^4} \left[\frac{4 \mu_l + 3 K_w}{\mu_l K_w} \right]$$

Z is the zeta potential; ϵ and η are the dielectric permittivity and viscosity of the fluid; σ is the conductivity of the bone-fluid system; τ is the relaxation time; μ_l is the shear modulus of bone; K_w is the bulk modulus of the fluid; P_{eff} is a function of the distribution of the lacunae, the fluid channels, μ_l , K_w , and the mechanical loading. P_{eff} has been determined for a continuous axisymmetric distribution of lacunae within the osteon.

All of the parameters in the expressions for

ϕ , P_{eff} , and τ have been numerically evaluated. Figure 1 shows the predicted results for ϕ and this is in excellent agreement with previously reported results. The cusp-shape shown satisfies the $\ln(u/\bar{u})$ dependence near the Haversian canal reported by Starkebaum et al. (1979).¹ The inverse relationship between ϕ and σ and between ϕ and η found experimentally is predicted by this expression for ϕ .

The expression for τ is applicable to intra-osteonal potentials but the same functional dependence on η ought to hold for macroscopic potentials. This predicted proportionality between τ and η and the independence of τ on σ have been found experimentally. The model also predicts multiple relaxation times, dependent on the location of the lacunae within the osteon and this may account for similar results found in the macroscopic case.

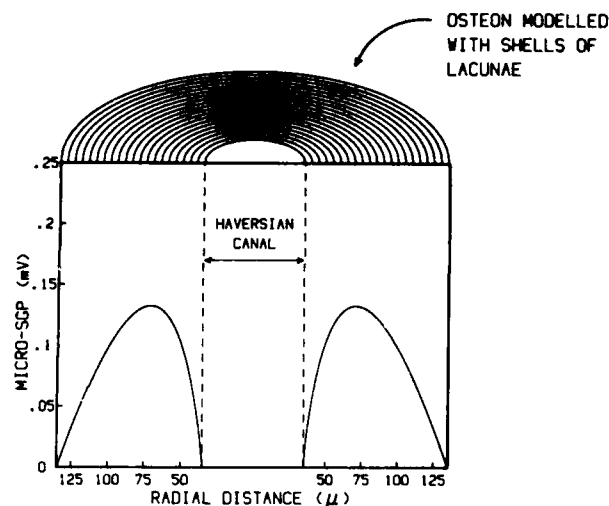


Figure 1

¹ Starkebaum, W.S., Pollack, S.R. and Korostoff, E. (1979) J. Biomed. Mater. Res. 13, 729-751.

The authors acknowledge with great appreciation the support of the National Science Foundation (Grants INT 81-8481 and ECS 80-17856) and the Bulgarian Academy of Sciences for their continued support throughout this collaborative study.

* Department of Bioengineering
University of Pennsylvania
Philadelphia, Pennsylvania 19104

** Institute of Mechanics and Biomechanics
Bulgarian Academy of Sciences
Sofia, Bulgaria

FREQUENCY RESPONSE OF STRESS-GENERATED POTENTIALS (SGPs) IN WET BONE

S. Singh and S. Saha

Biomechanics Laboratory, Department of Orthopaedic Surgery
LSU Medical Center, S'Port, LA 71130

INTRODUCTION:

Since the first discovery of piezoelectricity in bone in mid-fifties(1), many authors have examined various aspects of stress-generated potentials (SGPs) in bone, due to its possible biological and physiological significance in bone-growth, repair, and remodelling(2,3). Recent observations show that SGPs in fluid-saturated bone can be explained in terms of piezoelectricity and streaming-potentials(4-6). As little information is available on the frequency response of SGPs in bone, we have investigated the electromechanical behavior of wet bone as a function of frequency.

MATERIALS AND METHODS:

Rectangular compact bone specimens were machined from the diaphysis of mature bovine femurs, using a low speed saw. The bone specimens, when not being used for measurements, were stored by wrapping with cotton soaked in 0.9% NaCl solution. Experimental set-up used in this study was similar to the one reported by Bur (7), except the sample cell and balancing circuitry. Essentially it consisted of a PZT driver, a dynamic load cell (PCB model 208A02), a static load cell and electrode. Chlorided metal electrodes were used (8). Measurements were carried out in the frequency range of 100 Hz to 100 kHz. To reduce the relative noise level, measurements were taken only at resonance. This limited the measurements to frequencies of resonances. The SGPs signal and dynamic load cell output were noted with the help of dual beam oscilloscope (Tektronix 5A26) and gain phase meter (HP model 3575 A).

RESULTS:

The results are presented in terms of the voltage constant 'g' for different frequencies in the range of 300 Hz to 15 kHz, as shown in Table 1. The voltage constant was calculated by finding the ratio of the electric field across the specimen to the stress applied to it. Table 1 represents the average values for five bovine specimens. It is clear from Table. 1 that the maximum value of 'g' was found around 3 and 7 kHz. As the sample was allowed to dry, the amplitude of SGPs decreased. Thus the bone sample should be tested as soon as possible after sacrifice of the animal, for determining the in vivo properties of bone.

The percentage of the change in the value of both the SGPs and the voltage constant decreased beyond 10 kHz. This suggests that the upper cut off frequency limit, for the electrokinetic phenomena i.e. streaming-potentials, may fall somewhere in the neighborhood of 10 kHz.

TABLE 1.

Average values of stress-generated potentials (SGPs) for wet bone ($\mu\text{V-cm/N}$) for different frequencies at temperature and R.H. of 29°C and 70% respectively (n=5).

Freq. (kHz)	voltage constant 'g' for wet bone		
	after 5 mts.	after 16 hrs.	after 36 hrs.
0.29	58.35	19.11	8.3
0.74	12.96	8.4	2.71
1.06	19.42	5.16	2.13
3.36	67.46	57.47	53.50
7.2	79.43	58.40	49.65
8.5	30.89	28.40	22.60
15.2	42.31	44.64	39.32

REFERENCE:

1. Fukada E, Yasuda I: On the piezoelectric effect of bone. J. Phys. Soc. Japan 12:1158, 1957.
2. Bassett CAL: Biological significance of piezoelectricity. Calc. Tiss. Res. 1:252-272, 1968.
3. Gjelsvik A: Bone remodelling and piezoelectricity:I. J. Biomechanics 6:69, 1973.
4. Anderson J, Eriksson C: Piezoelectric properties of dry and wet bone. Nature 227:491, 1970.
5. Gross D, Williams WS: Streaming potentials and the electromechanical response of physiologically moist bone. J. Biomechanics 15(4): 277, 1982.
6. Pienkowaski D, Pollack, SR: The origin of stress-generated potentials in fluid saturated bone. J. Orthop. Res. 1: 30-42, 1983.
7. Bur AJ: Measurements of the dynamic piezoelectric properties of bone as a function of temperature and humidity. J. Biomechanics 9:495, 1976.
8. Singh S, Saha S: The effect of different electrodes on the measurement of electrical properties of bone. In: (ed. by C.W. Hall) Biomed. Eng. II. Recent Developments, Pergamon Press, N.Y., 1983., p179-182.

ELECTRICAL STIMULATION OF BONE WITH A THREADED SCREW CATHODE

E. Chamoun*, J. Lemons^o, P. Henson⁺, M. McCutcheon*, L. Lucas*

University of Alabama in Birmingham, Birmingham, Alabama, U.S.A.

Clinical and research studies have shown that electrical stimulation of bone induces osteogenesis. A variety of electrical parameters, electrode geometries and materials have been investigated. The objective of this investigation was to evaluate the osteogenic potential of a new threaded screw cathode geometry. To evaluate the osteogenicity of this electrode configuration, the electrode was stimulated with current magnitudes of 80 micro A and 20 micro A. The cathode was a Kirschner stainless steel wire, 28 gauge, 5 cms in length, and 1.4 mm in diameter. The pitch was 3 threads/mm resulting in a surface area of approximately 930 mm² for the cathode.

Adult male New Zealand white rabbits, weighing 3 to 4 kgs each were anesthetized using Inno-var-Vet and placed on inhalation anesthesia (Halothane). The medial surface of one tibia, 3.0 cm distal to the tibial plateau was exposed and a 4 to 5 mm hole drilled through the medial cortex under sterile conditions. A similar surgical procedure was performed on the contralateral tibia in each rabbit. The cathode was inserted in both tibiae, while the anode pad (positive electrode) was placed on the thigh. Roentgenograms were taken every 3 days. Current and lead wires were adjusted and checked every day until sacrifice on day 21. There were two groups, each consisting of 4 rabbits. Rabbits of Group I had the threaded screw electrode inserted intramedullary in each tibia. One cathode was connected to a power supply which delivered a constant 80 micro A current. The contralateral tibia acted as a control without stimulation. Group II also employed the threaded screw electrode. The experimental cathode was connected to a power supply which delivered a constant 20 micro A current. The control electrode was not stimulated.

The initial results of Group I (threaded electrode, 80 micro A) showed a thicker cylindrical shell of bone surrounding the stimulated cathode (Figure 1) than did the control (Figure 2). This was an interesting finding since other investigators have observed extensive cellular necrosis after stimulating bone with a current of 80 micro A (1). Rabbits of Group II (threaded electrode, 20 micro A) showed an extensive growth of new bone in the medullary cavity (Figure 3). Also, the volume of calcified callus in the marrow cavity around the stimulated cathode was noticeably larger than for the nonstimulated control shown in Figure 4.

The following conclusions were made:

1. The threaded screw electrode configuration of this study induced bone formation.
2. Both current magnitudes, 80 micro A and 20 micro A, stimulated bone formation. However, more new bone growth was observed for the rabbits stimulated with 20 micro A.

Currently, studies are being expanded to compare the osteogenic behavior of the threaded screw electrode geometry with the distributive electrode geometry utilized by Brighten, et.al.(1) Both current magnitudes are being evaluated.



Figure 1



Figure 2



Figure 3



Figure 4

(1) Brighten, C.T., Friedenber, Z.B., Electrically induced osteogenesis: relationship between charge, current density, and the amount of bone formed, *Clinical Orthopaedics and Related Research*, Number 161, November-December, 1981.

- * Biomedical Engineering, The University of Alabama in Birmingham, Birmingham, AL, 35294
- ^o Department of Biomaterials and Division of Orthopedics, The University of Alabama in Birmingham, Birmingham, AL, 35294
- ⁺ Department of Surgery and Division of Orthopedics, The University of Alabama in Birmingham Birmingham, AL, 35294

THE INFLUENCE OF AGE ON THE MECHANICAL AND PHYSICAL PROPERTIES OF THE HUMAN FEMUR

L. Claes and H. Kleiner

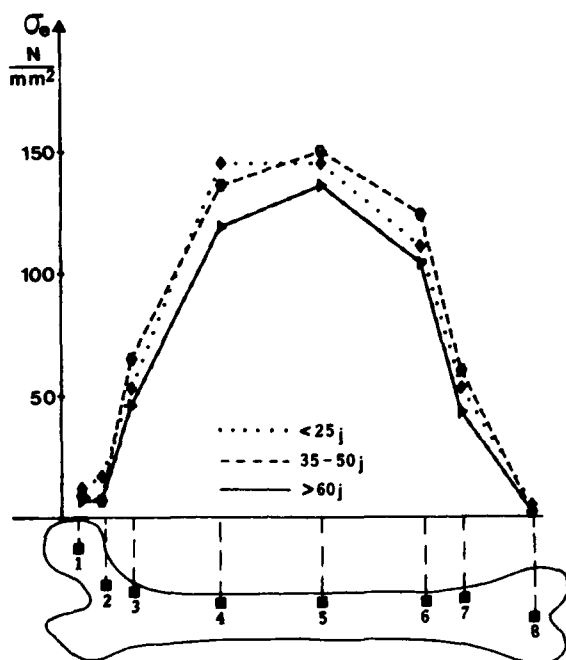
Abteilung für Unfallchirurgie der Universität Ulm
Oberer Eselsberg, 7900 Ulm, Germany

The correlation between strength and mineral content, measured by the ash weight is known (1). From a clinical point of view it is advantageous to know, the relationship between the x-ray density and the strength of the bone. Therefore the sensitivity of this parameter to determine bone strength was investigated.

The investigation was carried out on 24 fresh human cadaver femora which were divided into 3 groups. Group I (age < 20 years), group II (35 - 50 years) and group III (age > 60 years). From each femur 8 specimens of 5x5x5 mm were taken along the longitudinal axis of the bone (fig.1). The following experiments were performed on the 192 samples.

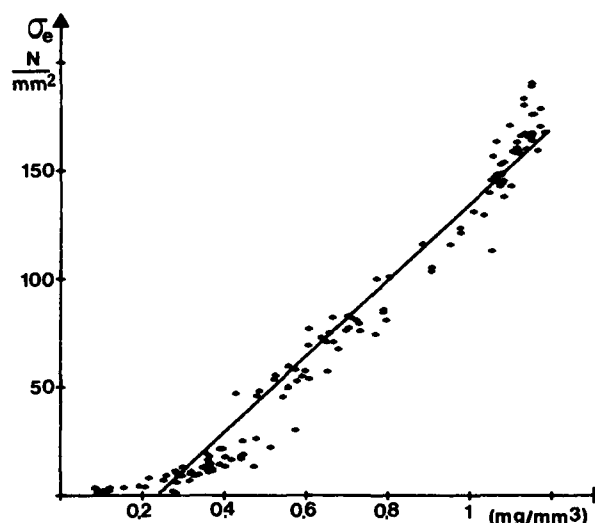
1. X-rays and measurement of their density. Calculation of the equivalent apatite concentration (2).
2. Compression tests and determination of the ultimate strength, stress at the linear limit and the modulus of elasticity.
3. Determination of the specific ash weight.

As described in the literature (1) large variations of mechanical properties were noted along the longitudinal axis of the femur (fig.1). The cancellous bone in the femur neck showed a greater strength than that of the knee condylus. In the same group we found a small standard-deviation in the mechanical properties of the cortical bone, but a large s.d. for the cancellous bone specimen. Whereas the ultimate compression strength did not show significant differences between the 3 groups, the stress at the linear limit (fig.1) and the



modulus of elasticity decrease with increasing age. The analyses of the different positions demonstrate that the decrease of these mechanical properties started at the area of cancellous bone (position 1,2,8, fig.1) within the range of 35 - 50 years and was followed by a change of the cortical bone for ages greater than 60 years. In difference to the mechanical data the x-ray density and the specific ash weight could not be related significantly to age.

Nevertheless there was a correlation between the mechanical and physical data. The correlation between the stress at the linear limit and the apatite concentration determined by the x-ray density (2) is significant ($k = 0.98$).



The results indicate that age has an influence on the mechanical properties of bone. Though a strong correlation between the mechanical properties and the x-ray density was found, this clinical parameter for the examination of the bone mineral content cannot be considered sensitive enough to describe the variations in mechanical properties.

1. Evans, F.E.: Mechanical properties of bone, C. Thomas Publisher, Springfield 1973
2. Meema, H.E., C.K. Harris, R.W. Porret: A method of determination of bone-salt content of cortical bone, Radiology 82, 986, 1964

Privatdozent Dr. L. Claes, Abteilung für Unfallchirurgie, Hand-, Plastische- und Wiederherstellungschirurgie der Universität Ulm, Oberer Eselsberg, D-7900 Ulm.

An Evaluation of Particulate Aluminum Oxide as a Bone Graft Material

R.E. Luedemann, S.D. Cook, G. Gianoli, R.J. Haddad, A. Harding

Tulane University School of Medicine
New Orleans, Louisiana 70112

Autogenous bone and the calcium phosphate ceramic hydroxylapatite (HA), $[\text{Ca}_{10}(\text{PO}_4)_6(\text{OH})_2]$ have both demonstrated an ability to be used as a bone graft. HA has been demonstrated to be locally and systemically non-toxic, non-inflammatory and associated with a direct bone-implant interface. Aluminum oxide ceramics have also demonstrated this type of biocompatibility. The objective of this study was to evaluate the potential use of particulate Al_2O_3 as a bone graft material.

The implant systems studied were autogenous bone, HA alone and mixed with autogenous bone, Al_2O_3 alone and mixed with autogenous bone. Autogenous bone was mixed with the HA and Al_2O_3 in order to study their effect as a graft extender. The HA consisted of rounded particles 425 to 850 μ m in diameter. The spray dried Al_2O_3 particles were high purity, with a diameter of 212 to 300 μ m. The implant materials were surgically inserted into three adult mongrel dogs. A Trephine burr was used to create defects in the medial aspect of the tibia and femur in the metaphyseal regions. The cancellous bone removed by the burr was used as the control autogenous graft and was also used with the implant materials. The implants were placed bilaterally and their location was varied to eliminate bias for side. Mixtures of HA and Al_2O_3 with autogenous bone were also placed on opposite sides of the median sacral crest as bone grafts in a spinal fusion of the L2 to L4 region. The animals were sacrificed at 4, 8 and 12 weeks. Fluorescent labels (oxytetracycline, tetracycline and alizarin red S) were administered at 4 week intervals.

The retrieved specimens were fixed in Millonig's solution, dehydrated in alcohol solutions and embedded in PMMA. Undecalcified ground histologic and corresponding microradiographic sections, perpendicular to the long axis of the host bone and transverse to the vertebral column, were produced and stained with toluidine blue and basic fuchsin. The sections were evaluated in fluorescence, polarized light and transmitted light. The parameters studied were the amount of bone growth into the graft material, time dependent bone activity, implant-bone interface behavior and general tissue response.

At four weeks, a greater degree of viable bone was associated with the autogenous graft compared to the other systems. Active mineralization and bridging between the graft and the surrounding bone was observed. A significant amount of bone growth with direct implant-bone contact was also observed with the HA-bone mixture. A bone-implant interface with no apparent interposing fibrous tissue layer was observed. Fluorescent labels indicated active bone formation adjacent to and around the particles. Although the tissue response was similar with the HA alone, the amount of bone formation, implant-bone contact and active labels were slightly reduced.

Some bone growth around the particulate Al_2O_3 with autogenous bone was also observed at 4 weeks. The amount of bone formation was less than that observed around the HA systems. There was only a small amount of direct implant-bone contact found. The particulate Al_2O_3 alone was almost completely infiltrated with fibrous tissue at 4 weeks post-operative. At 8 weeks, the greatest amount of bone growth was still observed within the autogenous bone graft. The tissue response to the other implant materials was similar to that observed at 4 weeks except that the amount of ingrowth, direct implant-bone contact and active mineralization were slightly increased. Again, the most extensive bone ingrowth, direct implant-bone contact and active mineralization among the non-autogenous materials was associated with the HA. The Al_2O_3 alone was associated with some bone ingrowth but the amount was less than with the Al_2O_3 with autogenous bone.

There was no significant bone present around either the particulate Al_2O_3 or HA spinal bone grafts at 4 weeks. Both materials were infiltrated with fibrous tissue. By 8 weeks, the HA material was surrounded by osteoid tissue. Ultra-violet fluorescent labels indicated active bone formation within the graft material. At this time period the Al_2O_3 graft material was infiltrated by a relatively dense and cellular fibrous tissue. No fluorescent labeling was observed among the Al_2O_3 particles. The results at 4 and 8 weeks would appear to indicate that although the Al_2O_3 was not associated with as much early bone ingrowth, it is a potentially successful bone graft material. Possibly, a larger Al_2O_3 particle size would have made a better graft material. The rate of ingrowth was enhanced in all cases by mixing the material with autogenous bone. At 8 weeks; however, the majority of the defect was still infiltrated with non-osseous tissue in all cases except the autogenous bone graft.

Department of Orthopaedic Surgery
Tulane University Medical School
1430 Tulane Avenue
New Orleans, Louisiana 70112

Analysis of Bone Fracture Surface by
Scanning Electron Microscopy

Subrata Saha

Biomechanics Laboratory, LSU Medical Center
Shreveport, Louisiana 71130

Although there exists a considerable amount of literature on the mechanical and fracture properties of bone (1), our understanding of the micromechanics of bone fracture is still in its infancy (2). Fractographic analysis of the bone fracture surface can be a useful tool in bridging this gap between the micro and macro aspects of bone fracture, similar to its application in metals (3). In this investigation, bone fracture surfaces obtained by controlled laboratory experiments were examined fractographically by scanning electron microscope (SEM) with the objective of correlating the fracture surface topography with its mechanical properties and microstructure.

Standardized compact and cancellous bone specimens were prepared from beef and human femurs (both embalmed and fresh) and were tested in wet condition in bending, dynamic tension and longitudinal shear. Stress-strain history during failure were recorded on an x-y blotter or on a storage oscilloscope for each specimen. The fracture surfaces of the tested samples were first examined in an optical microscope. The samples were then defatted in ethyl Alcohol and the fracture surfaces were coated with a thin gold platinum coating and examined in an AMR 900 or an ETEC scanning electron microscope. The microstructure of the specimens were subsequently studied in a reflected light Leitz microscope using metallographic polishing techniques.

Macroscopically most beef and human compact bone specimens fractured in a brittle fashion. Macroscopic appearances of most fracture surfaces exhibited a fairly rough texture, indicating a quasi-cleavage type of failure. Where signs of large plastic deformation were present, it was verified from the stress-strain record. Fracture surfaces sometimes passed through a natural bone fault, such as a Volkmann's canal, showing that the fracture might have originated there. On the other hand, when an advancing crack met a natural bone cavity, the crack front was either stopped or deviated, indicating that existing natural voids in bone, like Haversian canal, Volkmann's canal, resorption cavity, etc., might also be helpful in containing the growth of the crack front.

Most bone specimens failed without any signs of complete osteon pull-outs, unlike the fiber pull-outs in the failure of composites. The results indicated that, in case of catastrophic failures, secondary microcracking and not osteon pull-out was

the main mechanism of plastic deformation in bone fracture. For notched specimens, a pull-out at the notch root was common, showing this to be a fracture initiating mechanism. Once the crack was initiated, subsequently it absorbed little energy to propagate.

Cracks sometimes propagated along the interfaces between the lamellae of the osteons, indicating the weakness of the interface due to the passage of very few collagen fibers across this interface. This was particularly true for the fracture surfaces created by longitudinal shear (4).

Several cancellous bone specimens were subjected to a dynamic compression inside a scanning electron microscope, thus allowing fracture of single bony trabeculae to be examined and photographed. It was evident that even a simple compression produced bending and tension of the trabeculae due to their complex interconnected structure. Secondary microcracks also often accompanied the main fracture surface.

Fractographic examination at higher magnification showed that, at an ultrastructural level, even the smallest fragments of bone showed the characteristic fibrous appearance of a pull-out fracture. It appeared that bone fracture surface was not affected by submicroscopic cavities like lacunae and canaliculi.

The results of this study showed that fractographic analysis of bone fracture surfaces can be very helpful in increasing our understanding of the micromechanics of bone fracture. The results also indicated that scanning electron microscopy can be utilized as a convenient means for studying bone microstructure and its relation to fracture properties.

REFERENCES:

1. Evans, F.G. (1973) Mechanical Properties of Bone, Charles C. Thomas, Springfield, Illinois.
2. Saha, S. (1975) Scanning Electron Microscopy 1975, IIT Res. Inst., pp. 425-432.
3. Beachem, C.D. and Warke, W.R. (1976) Fractography, ASTM STP 600.
4. Saha, S. (1977) J. Mater. Sci., 12, pp. 1798-1906.

T.P. Harrigan†, M. Jasty, W.H. Harris, and R.W. Mann*

Orthopaedic Research Labs, Mass. General Hospital and Harvard Medical School, Boston, MA 02114 and *Dept. of Mech. Engineering, Mass. Institute of Technology, Cambridge, MA 02139

Attempts to provide detailed microstructural analysis of cancellous bone thus far have been hampered due to the difficulty in measuring and characterizing anisotropy of this porous material.

A recently described mean intercept length tensor, based on measurements made in any three mutually perpendicular planes, allows fully three dimensional quantifications of microstructural anisotropy of trabecular bone. This tensorial representation provides especially facile incorporation of material anisotropy into stress-strain relations, since both stress and strain are also second rank tensors. This tensor should thus prove useful in quantitatively studying bone remodelling in pathologic states and in reaction to joint arthroplasty.

To avoid the tedium of manual quantification of trabecular orientation levels, we have developed an automated system which enables accurate, routine measurements of the mean intercept length tensor in cancellous bone, and which also generates routine microstructural measurements such as volumetric density, and trabecular widths.

Methods: The technique of measurements involves superimposing an array of straight parallel lines on a polished specimen face, and measuring the intersections between this grid and microstructurally important features such as the trabecular boundaries. The intersections per unit line length are counted at many different grid orientations and are inverted to arrive at mean intercept lengths. These lengths are found to obey the relation $1/L^2 = \bar{n} \bar{n}^T$; \bar{n} is the mean intercept length tensor and \bar{n} is a unit vector in the measurement direction. Measurements made on three of the specimens determine the components of this tensor, if orthotropic symmetry is assumed.

The measurement system employs a T.V. camera attached to a dissecting stereomicroscope. A high speed A-D converter converts each frame into 768 by 512 pixel, 8 bit digital signals at 30Hz. The data are stored in a frame buffer with internal memory of 3 million bits. Twenty six control and data registers occupy directly accessible memory positions within the PDP11 architecture. This makes possible very high speed analysis of the digitized information without the necessity of off loading the data into memory or disk. The analysis is carried out by a PDP11/23 computer (Fig. 1).

Software is comprised of several assembly language subroutines driven from a fortran main. One of the 3 colors in digitized frames is interactively thresholded using grey scales in real time by the operator. The computer computes the number of intercepts formed by the parallel T.V. scan lines with the trabeculae. The specimen stage is rotated at 5° increments by a computer driven stepper motor and the whole sequence is repeated until a full 180° rotation of the specimen is completed. Thus, the intercept lengths as a function of specimen angle relative to the camera are obtained.

The intercept length measurements were obtained from each face of 15 cancellous bone blocks

measuring .5 by .5 by 1cm, which were cut from the cadaveric proximal femur. The specimens were defatted with ether. Each face of the block was polished on a grinding wheel and stained black with silver stain. Fine alumina powder wiped over the block gave good black and white contrast.

Results: The analysis of the specimens proceeded rapidly; in less than two minutes per specimen. The maximum and minimum orientation levels measured by the system could be correlated to those noted by careful visual inspection of the specimens, although the latter method is much more subjective and arbitrary.

Data obtained from the experimental cancellous bone specimens were normalized to fit a unit amplitude sine function as shown in Figure 2. The pattern clearly fits a sine with minimal experimental noise. The poorer fitting points are traceable to the more isotropic specimens. Table I shows components of a typical mean intercept length tensor measured from a sample of cancellous bone from the proximal femur.

Conclusions: The anisotropy of microstructure in orthotropic materials is represented in terms of a second rank tensor that can be measured via planar methods applied to any three mutually perpendicular planes in the material. A computer assisted image analysis system enabled accurate, rapid measurements of the mean intercept length tensor in cancellous bone. Experimental data obtained from 15 cancellous bone specimens validated the methodology. Applications such as the study of relationships between mechanical stress applied to bone tissue and the degree of tissue anisotropy is easily accomplished using this representation of its microstructure.

Table 1

0.24500	-0.05844	-0.00372
-0.05844	0.27348	-0.00372
-0.00372	-0.02196	0.48153

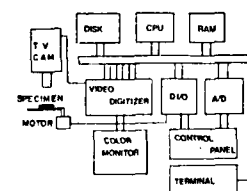


Figure 1

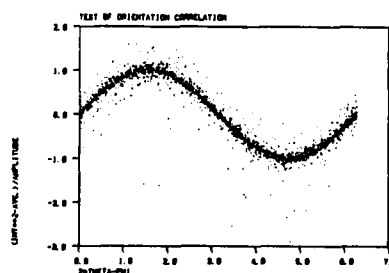


Figure 2

BONE MORPHOGENESIS INDUCED BY PERFORATED BONE MATRIX

E. GENDLER

Orthopaedic Hospital, Los Angeles, CA 90007

INTRODUCTION: It has been shown by numerous researchers that bone matrix possesses the ability to induce osteogenesis after implantation into animals. The purpose of this study was to develop a material with high osteogenic potential that can be used for stimulation of bone regeneration in orthopaedic surgery. It was able to show that creation of multiple artificial perforations in bone matrix significantly increased its ability to induce osteogenesis.

METHODS: Bone matrix was prepared from the long bones of rats in which multiple perforations with a diameter of 0.25 - 2.0 mm were created with a drill. Subsequently, perforated bone was demineralized in 0.6 M HCl, cut into rectangular plates and implanted subcutaneously to young rats. Animals were sacrificed at different intervals and implants were examined histologically.

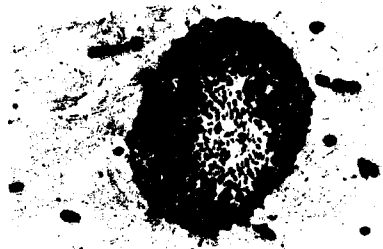
RESULTS AND DISCUSSION: Four days after the implantation there was an accumulation of large numbers of young undifferentiated cells which demonstrate high activity of alkaline phosphatase.

Seven days after implantation considerable numbers of mature chondroid cells were seen among the undifferentiated cells filling the perforations. Alkaline phosphatase activity in the cells is increased compared to previous observations using decalcified bone powder or non-perforated matrix.

Two weeks after the implantation there was a resorption process around the edges of the perforations with replacement of matrix material by chondroid cells and newly formed trabecular bone. The perforations were filled with newly formed trabecular bone covered by osteoblasts with very high activity of alkaline phosphatase. Three to four weeks after the implantation, a part of the perforated bone matrix underwent resorption and were replaced by newly formed bone interspaced with occasional islands of chondroid tissue.

Samples of perforated bone matrix with different sizes of perforations were compared for ability to induce osteogenesis after subcutaneous implantation. It was shown that osteogenesis was most active when perforations had diameters of 0.25 to 0.5mm. Osteogenesis was less active when perforations had diameters of 0.75-1.0mm, and samples having perforations with diameters of 1.25 - 2.0 mm had the lowest osteogenic activity. The creation of multiple artificial

perforations in bone matrix stimulates osteogenesis which occurs at a significantly higher rate than in intact matrix. Multiple perforations create channels that facilitate ingrowth of blood vessels and cambial cells, and so enhance bone morphogenesis.



1 week after implantation
C. cartilage



2 weeks after implantation
B. Bone

E. Gendler, M.D., Ph.D.
Orthopaedic Hospital
2400 S. Flower
Los Angeles, CA 90007

PYROLITE CARBON-AN ALTERNATIVE IMPLANT
MATERIAL IN ORTHOPEDIC SURGERY

S. L. Kampner, M.D. and A.M. Weinstein, Ph.D.

University of California Medical Center
San Francisco, California

Pyrolite carbon has the material property characteristics that appear to be ideally suited as an implant material for selected orthopedic joint prostheses, offering great advantages over previously used implant materials. Two areas where adequate performance of metal/polymer articulating implants with or without cement fixation has been limited, has been the hand and foot. It was for these reasons that a different, more ideal implant material was sought, and it was felt that pyrolite carbon met these criteria.

The carbon crystalline spectrum ranges through a series of partially ordered graphite-like structures to a state in which the layers have no stacking order at all, with the disorders being totally random such as is seen with pyrolite carbon. It is this disordered arrangement, termed turbostratic, along with its strong interplanar covalent bonds which contributes to pyrolite carbon's material characteristics. Similarly contributing to its property characteristics, is that there is no preferred orientation of its crystallite layers as they are deposited to form an aggregate structure, thus being isotropic.

Pyrolite carbon is formed by the pyrolysis of a gaseous hydrocarbon depositing the resultant carbon particles as a layer of approximately 1 to 2 mm. thickness onto a preformed substrate (usually graphite) which is levitated in a fluidized bed.

It has a fracture stress of approximately 500 MPa or 4-5 times the strength of the cortical bone it is implanted into. When stressed under slow crack propagation conditions, the energy to cause fractures is of the same order as cortical bone. Under catastrophic crack propagation conditions or high stress rate, pyrolite carbon is approximately sixty times tougher than cortical bone.

It has a modulus of elasticity of 2×10^4 MPa being similar to cortical bone, allowing both materials to deform together when a stress was applied, resulting in negligible stress being transferred to the implant/bone interface.

The strong covalent bonding and small crystallite structure of the carbon atoms combined with the ultra smooth surface finish makes implant wear virtually negligible. The coefficient of friction whether articulating against itself in a total joint arthroplasty or articulating against cartilage or bone in a hemiprosthetic arthroplasty situation is no higher than that of ceramics, polymers or metal alloys.

It has a microscopic pore surface on the stem allowing direct tissue ongrowth for fixation of the stem to bone. The pores are approximately 10 microns in diameter with a depth of approximately 20 microns. Implants placed into dog femurs and into baboon jaws showed mature bone directly against the implant surface within a period of 6 months without any intervening fibrous interface.

Its biocompatibility has been well documented in numerous animal studies as well as in human clinical application.

Clinical experience with this implant material thus far has been primarily with arthroplasty of the basal joints of the thumb and the metatarsophalangeal joint of the great toe. The implants were designed to essentially resurface the respective destroyed arthritic joints.

When confronted with arthritic changes primarily at the trapezio-metacarpal joint, the base of the metacarpal is resected and a Metacarpal Resurface Implant is utilized as a hemiprosthetic arthroplasty. If it is decided to perform a total joint replacement, the trapezium has been resurfaced to articulate with the Metacarpal Resurface Implant and, similarly, the scaphoid has been resurfaced to articulate with the Trapezial Body Implant.

With respect to the great toe, the implants were similarly designed as a system to resurface either the destroyed base of the proximal phalanx or the head of the 1st metatarsal as a hemiarthroplasty or alternatively, to combine the two implants to articulate against each other as an unconstrained total joint replacement.

There have been 18 MTP Toe Implants and 10 MTS Thumb Implants followed for a minimum of 18 months. These arthroplasties were all performed for a painful osteoarthritis or failed previously performed silicone prosthetic replacement of the effected joint.

Of the 10 MTS Thumb Prostheses implanted, 6 were hemiprosthetic replacements and 4 were total joint replacements. All replaced basal thumb joints functioned well with great improvement in the patients clinical status in spite of some technical complications. There were 3 cases for revisions of failed silicone elastomer trapezium replacements which required bone grafting to fill the enlarged canal. This precluded a good interference fit with the implant stem and all of these cases showed a 1 mm. radiolucent zone adjacent to the implant on X-ray immediately post operatively. Since this did not increase over the next 18 months, it was felt that this zone of radiolucency represented a firm fixation of the implant, though with fibrous tissue rather than bone.

Of the 18 MTP Toe Prostheses implanted, all were total joint replacements resurfacing the base of the proximal phalanx and metatarsal head.

All patient's did well, showing marked improvement from their preoperative clinical state. Only 1 had slight occasional pain. Roentograms showed direct bone apposition against the implant stem without any evidence of loosening or interfacial motion occurring over the followup period in all cases except for 1 which was a revision of a failed silicone implant.

The short term results appear to be similar to those results utilizing previously existing implants. On the basis of what appears to be vastly superior mechanical properties of the implant material, along with a design allowing for a more judicious replacement of the effected joints, it is felt that the great benefit will be the improved results seen with the long term followup when compared with other types of existing implant arthroplasties.

S.L. Kampner, M.D.
2320 Sutter Street
San Francisco, CA 94115

FINITE ELEMENT MODELING OF BONE-IMPLANT INTERACTIONS: IMPORTANCE OF INTERFACE ASSUMPTIONS

J.A. Hipp*, J.B. Brunski*, M.S. Shephard†, G.V.B. Cochran**

Rensselaer Polytechnic Institute, Troy, New York

INTRODUCTION: Since the biomechanical conditions at the tissue-implant interface are thought to have an important role in the "loosening problem" with both orthopedic and dental implants, many workers have attempted stress analyses of these implants in bone. Finite element (FE) modeling has been frequently used for such analysis. While the FE method can provide meaningful results, the results depend almost entirely on the fidelity with which the model portrays the problem geometry, mechanical properties, and especially, the conditions at the implant-tissue interface.

Though the interface conditions are of particular concern, little experimental data exist on interface mechanics. With a few exceptions, nearly all FE models assume perfect bonding at this interface. To demonstrate the extent to which interface assumptions affect the results of FE models, we have solved several problems relating to orthopedic and dental implants in bone, using two limiting interface assumptions: 1) perfect interface bonding (i.e. infinite friction) and 2) interfacial slippage (i.e. frictionless contact).

PROCEDURE: Models solved as part of this study include: 1) Axisymmetric models of two different bone screw threads, 2) Plane stress models of several different cross sections of an experimental dental implant in a dog mandible and 3) Plane stress models of a longitudinal representation of the dental implant in a dog mandible. Each problem was solved several times using graded mesh densities, in order to test for convergence. Isoparametric elements with quadratic shape functions were used in the plane stress and axisymmetric models. Problems were solved using interactive computer graphics software developed at RPI. Frictionless contact was simulated with an algorithm based on lagrange multipliers.

RESULTS: Figures 1-3 demonstrate the main points of this paper, using axisymmetric models of a screw being pulled, with a uniform load in the positive Z-direction, out of bone. The structure being modeled would be obtained by rotating the figures about an axis parallel to the Z-axis. Figure 1 shows the displacements, magnified 20 times, of a model assuming frictionless contact between bone and screw. Note the relative displacements at the interface. Also note that the area of contact between the loaded implant and bone is less than the "resting" contact surface. Figures 2 and 3 show R-Z shear stress contours in the bone around the screw for the infinite friction (left) and frictionless (right) cases respectively. For clarity, the implant is not shown in these figures. The models were identical except for the interface assumption, and the grey levels represent the same stresses in Figures 2 and 3.

Generally, a much greater range of stresses, and much higher maximum stress magnitudes are found

with the frictionless contact models. For instance, the R-Z shear stresses in the bone (figures 2 and 3) ranged from -52 to 8 MPa in the perfect bond case, and -210 to 50 MPa in the frictionless case.

CONCLUSIONS: The assumptions made regarding interface mechanics can have a strong influence on the results of FE models of implant-bone interactions. Therefore, correlations between mechanics and tissue physiology will be unrealistic if the interface is not properly represented. The frictionless contact model allows parametric comparisons of relative displacements, contact forces and contact areas. Unfortunately, there is not yet sufficient experimental data to determine the detailed mechanics at the interface between bone and inert implants. Experimental data on interface mechanics is desperately needed to facilitate more meaningful FE studies.

FIGURE 1

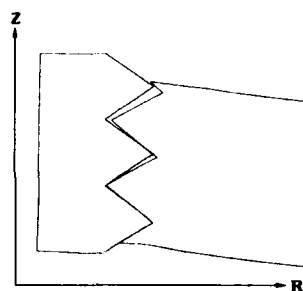
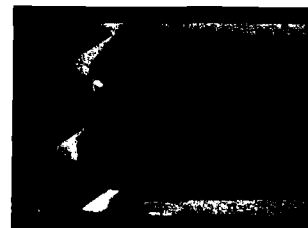


FIGURE 2



FIGURE 3



ACKNOWLEDGEMENTS: Contract #V533P887 from the Veterans Administration

* Department of Biomedical Engineering

† Department of Civil Engineering
Rensselaer Polytechnic Institute
Troy, N.Y.

** Orthopedic Engineering and Research Center
Helen Hayes Hospital,
West Haverstraw, New York.

STRAIN GAUGE INSTRUMENTED SCREWS AND THEIR APPLICATION TO INTERNAL FIXATION

R. J. Pawluk, E. Musso, H. M. Dick, and G. I. Tzitzikalakis

Orthopedic Biomechanics Laboratory, Orthopedic Surgery
Columbia University

Introduction: Although screws are extensively employed for fracture fixation, the effect of screw loading on the strain profile of individual screws has not been widely studied. Strain gauge instrumented screws have been fabricated, therefore, to investigate alterations in screw strain distribution in an anatomic model.

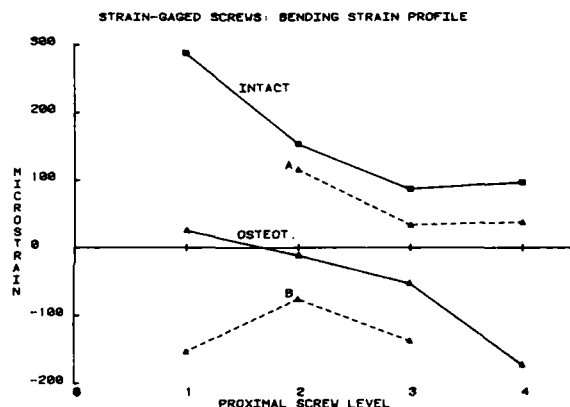
Methods: Synthes 4.5mm malleolar screws were modified and instrumented with dual uniaxial strain gauges. Malleolar screws were chosen because the existing shank is devoid of threads, thus offering a suitable surface for strain gauge placement in association with a machined nut which substituted for the standard screw head. Each 70mm malleolar screw was first modified by removing the head while retaining 29mm of the original shank, 25mm of which were then threaded. The newly threaded section was designed to receive a substitute screw head in the form of an elongated steel nut whose underside geometry duplicated the standard screw head shoulder. The remaining 4mm of shank, between the standard cortical screw threads and the portion containing the screw head nut, provide a preselected region for instrumenting two uniaxial gauges. These gauges were aligned with the screw long-axis and separated by 180°. This modification of a malleolar screw provided a means to measure both bending and axial strains at a level coinciding with the plate-cortical bone junction. In addition, a broad eight-hole plate instrumented with dual rectangular triaxial gauges, at midlength, was employed.

Results: Each eight-hole plate was fixed either to intact or osteotomized femora and a composite joint reaction force (spinal load plus abductor muscle force) of 50 ± 2.5 kg was employed. Plate bending strains ranged from $34 \pm 8 \mu\epsilon$ for the intact condition to $2,279 \pm 227 \mu\epsilon$ when employing a 2mm wide osteotomy. In addition, torsional plate strain altered from -10 ± 4 to $-223 \pm 2 \mu\epsilon$ for these two conditions. The screw bending strain distribution for the intact mode ranged from 86 to $287 \mu\epsilon$ and from 24 to $-173 \mu\epsilon$ with the osteotomy. Of specific note was the reversal in screw bending strain distribution between the two above experimental conditions (see curves INTACT and OSTEOT. in diagram). For the intact mode the most proximal screw (number one) exhibited the highest bending strains ($287 \mu\epsilon$) with successively lower values for the remaining three proximal screws. With a 2mm wide osteotomy, it was the number four screw position (immediately adjacent to the osteotomy site) which exhibited the highest strain ($-173 \mu\epsilon$). In general, the central number two and three screws generated lower average strains ($152 \mu\epsilon$) as compared to the peripheral proximal screws, one and four, whose average strain was $266 \mu\epsilon$. This strain pattern between central and peripheral proximal screws was also repeated when investigating the effects of screw loosening when employing an unreduced osteotomy.

Simulated clinical screw loosening was accomplished by unloading each of four proximal screws independently, thus always maintaining "normal" plate-bone fixation through the remaining three proximal screws. In all cases, three of the proximal

mal and all of the distal screws were maintained at a standard torque of 1 N-m.

Independent loosening of any proximal screw always resulted in a substantial alteration of the screw strain distribution. Individual screw strains range from 11 to $209 \mu\epsilon$ and averaged $162 \mu\epsilon$. These differences, however, were most noticeable when either of the instrumented peripheral screws (one or four) was loosened. In this case, their most distant counterpart, four or one respectively, now produced the greatest change in bending strain (curves A and B). The average increase in strain for the peripheral screws was $194 \mu\epsilon$, whereas the two central screws averaged only $91 \mu\epsilon$. Loosening either of the central screws (two or three) resulted in a less substantial change in screw strain distribution, with the number four screw experiencing an average reduction of $94 \mu\epsilon$ and the number one screw an average increase of $59 \mu\epsilon$.



Discussion: For the given model under test, all screw strain distributions exhibited a non-linear profile indicating the four proximal screws are not under uniform bending or axial strain. In addition, a reversal in the strain magnitude profile, between the intact and osteotomy conditions, suggests a possible redistribution of load transfer for individual plate screws which may occur during the normal fracture healing process. Further studies employing bone to bone contact vs. large resection gaps should clarify this effect as well as the associated role of increased plate torsion.

Pilot experiments involving individually loosened screws indicated a preferential screw strain distribution sensitivity to peripheral rather than centrally located, proximal screws and thus the potential importance of screw positions one, four, five and eight in fracture plate fixation. Although these data are derived from preliminary *in vitro* investigations, utilizing prototype strain gauge instrumented plate screws, the initial studies do provide a basis for observing alterations in load transfer between screws and plates under a variety of conditions.

Orthopedic Surgery, Columbia University
630 West 168th Street, New York, New York 10032

SURFACE OXIDES ON TITANIUM IMPLANTS - SPECTROSCOPIC STUDIES OF THEIR COMPOSITION AND THICKNESS, AND IMPLICATIONS FOR THE BIOCOMPATIBILITY OF TITANIUM.

Jukka Lausmaa and Bengt Kasemo

Department of Physics, Chalmers University of Technology, S-412 96
Gothenburg, Sweden.

The chemical properties and thus the biocompatibility of almost all metallic implant materials are determined by their surface oxides and not by the metal itself (1). The reason is that the primary interactions between the biomolecules of the host tissue and the inorganic implant take place over a distance ≤ 1 nm, while most metals (with possible exceptions for Au, Pt and Pd) have surface oxides of thickness > 1 nm.

In this work the surface oxides of titanium dental implant materials have been investigated by several surface spectroscopic techniques, e.g. X-ray photoemission spectroscopy (XPS or ESCA), secondary ion mass spectroscopy (SIMS), Auger electron spectroscopy (AES) and nuclear micro analysis.

The titanium dental implants used by the Gothenburg team (2) have an oxide thickness of 3-5 nm and a chemical composition very close to TiO_2 . The latter is concluded by comparing fig. 1.a and 1.b, which show XPS spectra from an autoclaved titanium implant with a 3.5 nm thick oxide and from a bulk TiO_2 sample, respectively. Dry sterilized implants show only minor changes in the oxide when compared to autoclaved ones.

The influence of the various implant preparation steps (machining, cleaning and sterilizing) on the surface (bio)chemical properties is discussed. An example is given where trace amounts of fluorine in the preparation procedure can dramatically change the surface oxide properties of the implants. The fluorine has the effect of accelerating the oxide growth on titanium during the autoclaving procedure, resulting in surface oxides more than ten times thicker than on normal implants.

An alternative implant preparation method to the one presently used is anodic oxidation, by which the thickness and to some extent the structure and composition of the surface oxides can be controlled. The oxide thickness can easily be varied in the range 5-200 nm. The composition of these oxides is mainly TiO_2 .

Two important conclusions from the work presented above are

- (i) Small changes in the implant preparation procedures can influence the implant surface composition and thereby maybe also the biocompatibility. Surface sensitive spectroscopies give the possibility to control the reproducibility of implant surfaces.
- (ii) It is, in principle, possible to tailor-make implant surface oxides by a combination of surface preparation techniques (e.g. electro-

polishing and anodic oxidation) and surface spectroscopic investigations of surface composition.

REFERENCES

1. Kasemo, B. Biocompatibility of titanium implants: Surface science aspects. *J. Prosthet. Dent.* **49**, 832 (1983)
2. Brånemark, P-I. et al. A 15-year study of osseointegrated implants in the treatment of the edentulous jaw. *Int. J. Oral Surg.* **10**, 387 (1983)

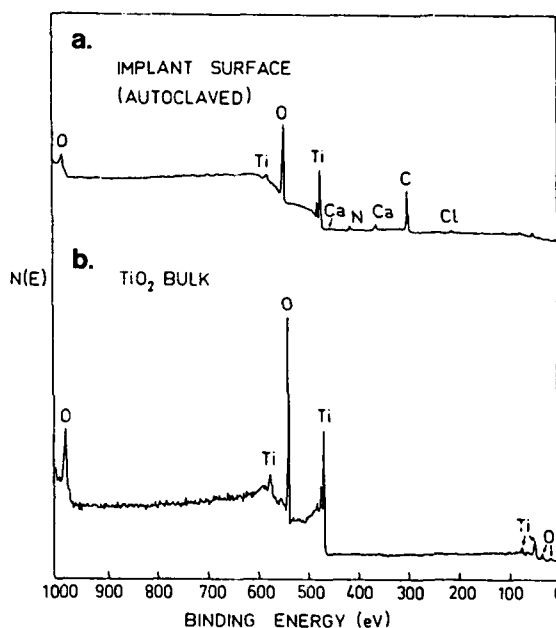


Fig. 1. XPS spectra from surface of an autoclaved titanium implant (a) and from a bulk TiO_2 sample (b). The similarity between the two spectra, regarding the Ti and O signals, shows that the implant surface oxide has a composition very close to TiO_2 .

A BIOMECHANICAL INVESTIGATION OF SEGMENTAL AND
DISTRACTION SPINAL INSTRUMENTATIONS

M. Hollis,^Δ J. Lemons,^{*} R. Nasca,⁺ and R. Casper[°]

University of Alabama in Birmingham, Birmingham, Alabama

The most commonly used operative technique for the correction of the lateral curve of a scoliotic spine is the Harrington rod instrumentation with Spinal Fusion. Another method of spinal instrumentation has been developed by E. R. Luque. The Harrington rod instrumentation provides correction of the lateral curve by a distraction force on the concave side of the curve applied at a point on the spine at both ends of the curve. The Luque rod, a segmental spinal instrumentation, provides correction of the lateral curve by wiring two stainless steel rods to each individual vertebra in the curve. Both of these methods of instrumentation when combined with spinal fusion have been successful in effecting some degree of correction. The objective of this study was to compare some of the mechanical and kinematical properties of spines instrumented using these two methods.

The study consisted of two different series of tests. The first series was designed to determine the deflections of the instrumented spines under axial loading and how these deflections changed with increasing numbers of loading cycles. Four swine spines were used, two were instrumented with Harrington distraction rods, and two instrumented with Luque rods. The testing device used was a pneumatically driven machine with a selectable displacement and cycle rate. Markers were placed on the upper, lower, and middle instrumented vertebrae. The position and orientation of these markers were determined from two photographs taken from two different locations with a reference system fixed on the machine. The position measurements were made for each of the spines with the spine at its neutral length before cycling. Measurements were then made with the spine in the compressed position after 0, 100, 1000, and 10,000 cycles.

The second series of tests were performed using four swine spines which were tested in an Instron machine fitted with a load cell. The displacement of the loading head was a constant 2.54 cm. Each of the spines was tested with no instrumentation, with Harrington distraction instrumentation, and with Luque segmental instrumentation. The displacements of the upper, lower, and middle instrumented vertebrae were measured using the photographic system and markers. Force-displacement curves were obtained in each of the twelve tests for loading and unloading.

The results of the first series of tests showed that the Harrington instrumented spines shortened an average of 0.3 cm. in the instrumented section while the Luque instrumented spines shortened an average of 1.8 cm. The Harrington instrumented spines tended to rotate and displace more in the sagittal plane than did the spines with Luque instrumentation. The horizontal displacement in this plane was an average of 1.4 cm., 4.8 cm., and 3.1 cm. at the upper, middle and lower vertebrae for the Harrington instrumented spines while the horizontal displacement in the Sagittal plane for the Luque instrumented spines

was an average of 0.9 cm., 1.5 cm., and 0.7 cm. The cyclic loading did not produce any significant changes in the deflection properties of the spines with increasing numbers of cycles for either the Harrington or the Luque instrumentation. Neither the Harrington nor Luque rods displayed any plastic deformation after the 10,000 compression cycles. It was observed that the Luque rods moved with respect to the retaining wires upon compression of the spine which produced wear products.

The load-displacement curves produced in the second series of tests were very non-linear. This non-linearity was due to the spines becoming more stiff with increased shortening. The loads required to produce the 2.54 cm. shortening of the spines varied greatly between the spines. The lowest value for the spines uninstrumented was 80 lbs. (36.3 kg.) and the largest load was 160 lbs. (72.6 kg.) with an average load of 120 lbs. (54.4 kg.). The Harrington instrumented spines required from 160 lbs to 220 lbs (72.6 kg.-99.8 kg.) and an average of 193 lbs. (87.5 kg.). The load produced by the Luque instrumented spines was an average of 220 lbs. (99.8 kg.) with a range of 165 lbs. to 280 lbs. (74.8 kg. - 127 kg.).

In conclusion, the displacement trends observed visually during testing were in agreement with the values calculated from the experimental protocol. The results of these experiments show distinctive trends for each method of instrumentation. However, the studies did not demonstrate a superiority of one instrumentation system over the other. Clearly, further investigations of current instrumentation for scoliotic spines needs to be conducted.

^ΔDepartment of Biomedical Engineering
University of Alabama in Birmingham
School of Engineering
University Station
Birmingham, Alabama 35294

^{*}Department of Dental Biomaterials
UAB School of Dentistry

⁺Department of Orthopaedic Surgery
UAB Medical Center

[°]Southern Research Institute
Birmingham, Alabama

USE OF COMPUTERIZED TOMOGRAPHY AND NUMERICAL CONTROL MACHINING FOR THE FABRICATION OF CUSTOM ARTHROPLASTY PROSTHESES

S. DORÉ, J.D. BOBYN, G. DROUIN, R. DUSSAULT*, R. GARIÉPY*

Department of Mechanical Engineering, Ecole Polytechnique,
Montreal, Quebec, CANADA H3C 3A7

Joint arthroplasty prostheses are currently manufactured in a pre-selected variety of shapes and sizes. They are surgically made to fit the implant site in a standard manner regardless of patient to patient variations in anatomic configuration of the diseased joint that is being replaced. With some joints, the knee joint for example, the articulating surfaces of prosthetic replacements seldom resemble the shape of the natural femoral condyles and tibial plateaus. Even «anatomic» knee prostheses are designed on the basis of «average» representations of human joints and so in any given application cannot accurately reproduce individual knee kinematics. As a result, problems can arise with joint function and stability or implant loosening due to improper stress distribution at the bone-implant interfaces¹. Further problems with implant design and fabrication materialize when custom implants need to be manufactured based solely on plane radiographs of the joint in question.

The purpose of this study is to examine the feasibility of combining well-established computerized tomography (CT) and numerical control machining technology into a new non-invasive technique for the fabrication of custom arthroplasty prostheses. The knee was chosen for initial study because of current problems with implant loosening and recognition of the benefits of anatomic implant design. Also, successful application of the technique to a complex geometry such as the knee would mean that it could be applied to other articulations as well.

Three basic steps are involved in the manufacturing of a custom fit prosthesis. The first is to visualize and obtain an accurate representation of the joint to be resurfaced. Secondly, information about the contours or surface of the joint must be expressed mathematically or in a form suitable for programming a computer assisted machining device. The final step involves either machining the final prosthesis or a mold from which a prosthesis may be cast.

Initial studies were performed using dry, clean cadaveric femurs. Each femur was suspended in a container of water during tomography in order to avoid artifacts caused by air. CT scans were taken transverse to the long axis of the femur at 4 millimeter intervals beginning at the distal condyles and ending proximal to the patellar groove. The contour of each CT scan provides the required information about the shape of the femur at the various locations (Figure 1). Contour information was obtained by manually digitizing the outline described by the CT scan with a series of points. Periodic cubic spline functions were used to approximate the contour between the digitized points. Figure 2 illustrates the digitized approximation of the contour of the CT Scan in Figure 1. A computer program is being written to automatically extract contour information by utilizing raw data (values of X-ray attenuation or density of each pixel composing the tomogram) and edge finding algorithms².

Once the contour of each slice was extracted,

it was put to scale and aligned, forming a good approximation of the surface (Figure 3). Interpolation with cubic spline functions in planes perpendicular to the initial contour resulted in further refinement of the surface. In this manner, the surface of the distal femur was completely described three-dimensionally in mathematical terms.

Numerical control machining is very well suited for manufacturing complex shapes on the basis of mathematically-defined surfaces³. The contour information obtained from tomography was used to produce a numerical control tape which programs the machining of a replica of the distal femur.

We are currently in the stage of evaluating the accuracy of this new technique by comparing the shapes of the femur and the machined replica. Preliminary results are encouraging. Parameters that affect precision of the final product include resolution of the CT scans, thickness of the tomographic slices (i.e. number of slices used to build a picture of the femur), and sophistication of the computer programs that extrapolate between points to establish each contour and between contours to establish the entire three-dimensional representation. The technique could be used for the fabrication of either total or hemi knee prostheses, particularly surface replacement prostheses that require little or no bone resection prior to implantation. It could also be extended to the manufacture of custom arthroplasty prostheses for other articulations.



Figure 1

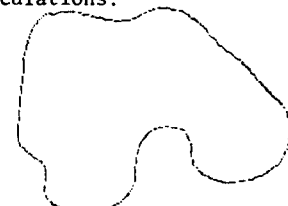


Figure 2

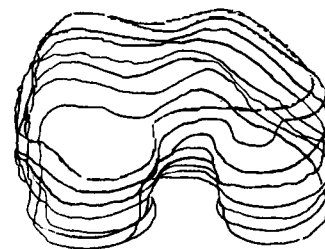


Figure 3

1. Rand, J.A. et al; J. Bone Joint Surg. 62-A:226, 1980
 2. Liu, H.K.; Comp. Graph. Image Proc. 6:123, 1977
 3. Childs, J.C.; Principles of Numerical Control. Industrial Press Inc., New York, p. 294, 1965
- * Hôtel-Dieu Hospital, Montreal, Quebec, CANADA.
Supported by Fondation des Diplômés de l'Ecole Polytechnique and Natural Sciences and Engineering Research Council (CANADA).

AD-A175 162

BIOMATERIALS '84: TRANSACTIONS WORLD CONGRESS ON
BIOMATERIALS (2ND) ANNUAL (U) SOCIETY FOR BIOMATERIALS
SAN ANTONIO TX S F HULBERT ET AL JUN 84

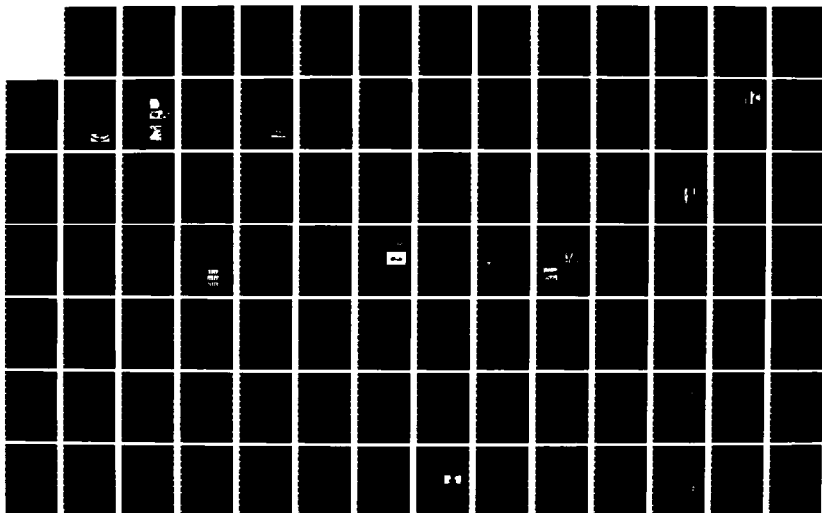
4/5

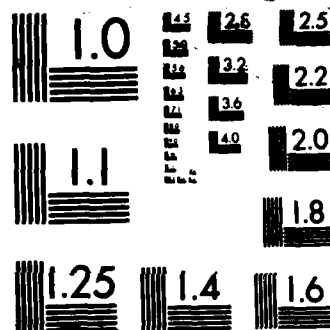
UNCLASSIFIED

DAND17-84-G-4805

F/G 6/12

NL





MICROCOPY RESOLUTION TEST CHART

NEW METHODS FOR EVALUATING THE APPLICATION CHARACTERISTICS OF POLYURETHANE RESIN ORTHOPAEDIC CASTING TAPES

Z. Oser R. Green G. W. Kammerer

Research Division - Johnson & Johnson Products Inc
New Brunswick, New Jersey 08903

Introduction

Polyurethane resin composite casts, also known as synthetic casts, are light weight, strong and porous while plaster of Paris casts are heavy and brittle; however plaster bandages are generally recognized as being more conformable than polyurethane casting tapes during application. Efforts therefore have been placed on evaluating the behavior of these newer types of materials during their application and subsequent transformation from casting tape to cast.

Also included in this evaluation is the identification of the several stages of setting unique to the polyurethane casting tapes.

An operational definition of "conformability" has been developed. It includes values of 13 properties, each of which has a measureable characteristic. These can be sequentially evaluated during the application of a standardized short arm cast, allowing an overall quantitative evaluation of any casting tape in terms of conformability as well as setting behavior.

Setting Behavior

The setting of polyurethane resin casting tapes, during cast formation, has been observed to proceed through several clearly discernible stages as a function of time, once the process has been initiated by dipping in water. These stages occur sequentially and have been called (1) tack time (2) working time (3) molding time (4) set time and (5) rigidity time.

Optimum values for each, from a user perspective, have been defined by conducting detailed interviews with 25-30 orthopaedic surgeons and cast technicians from whom these data were distilled. These values therefore define an "ideal" product. These are: Tack time: 30 seconds (onset); Working time: 2.5 minutes (minimum); Molding time: 3.0 to 4.5 minutes; Set time: 4.5 minutes; and Rigidity time: 7.0 minutes. Time is measured from the moment when the casting tape is dipped into water.

In determining the timing of each of these stages as well as to permit reproducible conformability determinations a standard short arm cast (forearm) has also been developed.

Conformability

The conformability of either plaster bandage or polyurethane resin casting tape has been defined as that property which describes the ability of the bandage or tape to adapt to or intimately lay down against the compound curves and protrusions of a body member.

Thirteen constituent properties have been identified which collectively make-up the property of conformability. These were ascertained from the same interviews described above together with the information which permitted the weighted values for each property to be assigned based on importance to the professional user of casting tapes working in

the clinical setting. Examples of data generated in this way are shown below. These were tabulated in a format so that during the application of a standardized short arm cast a number assignment can be made for each property, sequentially, as the casting tape under evaluation is applied.

Table 1		
Observation Point	Property	Weighted Score
Upper Forearm	Drape	10
Mid Forearm	Tuck	10
Mid Forearm	Tack	6
Lower Forearm	Neck Down	10
Heel of Palm	Drape	10
Back of Hand	Neck Down	8
Inside of Hand	Twist	2
Front to Back of Hand	Fold	7
Front to Back of Hand	Tack	7
Front to Back of Hand	Cross Direction	10
Lower Forearm	Stretch	10
Top of Forearm	Stretch	10
Wrist	Fold	5
	Mould*	5

Conformability Rating 100

*Example of rating: Tape lays down against bony prominence of wrist and intimately hugs bone = score of 5; does not lay down at all, i.e., stands away from bone = score of 0

Table 2			
Tape #	Sum of 13 Individual Ratings**		Conformability Rating
	Fiberglass	Fabric	
1	+		100
2		+	90
3	+		87
4		+	100
5	+		93

*Average of 2 samples per determination of C.R.

**Reproducibility of C.R. has been found to be + 2 units within a single trained tester and also between different trained testers.

These methods have been found to be useful in comparing experimental casting tape materials during development as well as in evaluating commercially available products.

Z. Oser, Research Division, Johnson & Johnson Products Inc., New Brunswick, N.J. 08903

NEW PREDICTIVE METHODS FOR EVALUATING THE STABILITY CHARACTERISTICS OF POLYURETHANE RESIN ORTHOPAEDIC CASTING TAPES

Z. Oser R. Green F. Johnson

Research Division - Johnson & Johnson Products Inc
New Brunswick, New Jersey 08903

Introduction

Shelf stability has become one of the more important characteristics of polyurethane resin casting tapes, because, when compared to plaster of Paris bandages, synthetic casting tapes have been found to exhibit relatively short functional life times. For example, most of these materials have useful shelf lives of between 6 months and 24 months, depending on the formulation utilized, when stored at or near room temperature. However, in the development and characterization of these newer materials it is obviously difficult to efficiently evaluate the extent of ambient temperature shelf life other than to wait these lengths of time. With this in mind two methods have been developed for predicting ambient temperature stability based on elevated temperature degradation rate observations.

Method 1 - Rate of Loss of Isocyanate

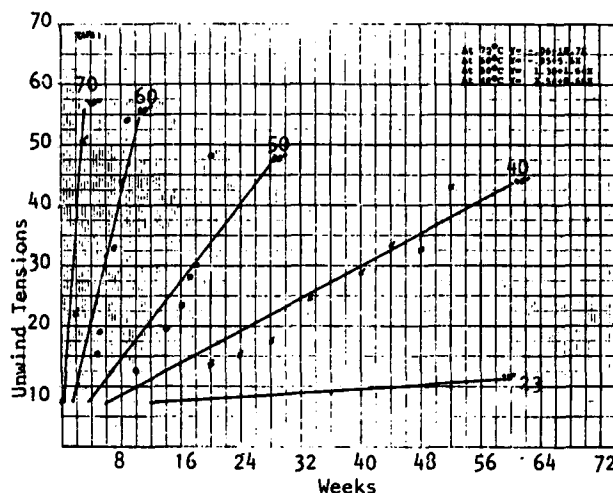
This method is based on the observation that the reactive prepolymers present in polyurethane casting tapes follow Arrhenius type kinetics in their thermal (non-water) degradation reaction at temperatures up to 70°C. By following the isocyanate content of a series of casting tapes as a function of time, degradation rates at a series of elevated temperatures have been obtained. A log plot of these rate constants vs. reciprocal absolute temperatures yields a straight line. The end point in such testing is the isocyanate content of the resin when gelation occurs and a concomitant loss of functionality of the tape is observed. Correlation of these data with actual 23°C shelf life testing data has shown that one can predict the degradation rate at ambient (23°C) storage temperature.

Since chemical analysis for isocyanate* is based on back titration of excess amine added during the testing procedure a correction must be made for the tertiary amine catalyst content of the prepolymer under evaluation.

*ASTM D1638-59T

Method 2 - Rate of Change in "Unwind" Tensions

This method involves measuring the force necessary to unwind a roll of casting tape and is based on the observation that "unwind" tensions are measurable and increase with tape age. Ambient temperature shelf life predictions can be made by analysis of tension data obtained for tapes exposed to a series of elevated temperatures. These tensions can be conveniently measured by use of an instrument such as the MSI Unwind Tension Tester* which is normally used to measure the unwind tensions of adhesive tapes. The accuracy of the instrument is 1% of scale (400 oz.). A plot of unwind tensions vs. time at a series of temperatures is shown.



Results

	<u>Predicted Mean</u>		<u>Actual</u>
<u>Casting</u>	<u>Shelf Life @ 23°C(Yrs)</u>		<u>Shelf Life</u>
<u>Tape #</u>	<u>(Range @95% Confidence Limit)</u>		<u>@23°C</u>
	<u>Method 1</u>	<u>Method 2</u>	
1 Fab.	5.1(3.6-7.2)	4.9(3.6-7.1)	2(ongoing)
2 Fab.	NA	1.8(1.0-3.3)	1.8
3 Fibg.	NA	0.8(0.5-2.0)	0.9

(NA: Found to be Not Applicable because of inability to correct for catalyst in prepolymer in these tests; i.e., data too scattered to draw regression line.)

Discussion

Method 1, which is based on chemical analysis for decrease in isocyanate content, was found to agree reasonably well with Method 2 where the same casting tape could be evaluated by both methods. Unfortunately attempts to use Method 1 with the other two casting tapes led to spurious results because both the type and amount of tertiary amine catalyst were unknown and could not be readily determined in these tapes. Where possible, comparisons were made with observations actually made at 23°C. Again these indicated that there was reasonable agreement.

Conclusions

Two novel methods have been developed for predicting the functional life or shelf life of polyurethane casting tapes at ambient temperatures. These methods are based on exposing the tapes to a series of elevated temperatures. Subsequently these observations, made at elevated temperatures, are extrapolated to obtain the time for loss of functionality at ambient temperature. Based on limited data these methods agree reasonably well with each other and with actual observations made at ambient temperature.

*Model 800099 manufactured by Kershaw Instrumentation, Inc., Sewell, N.J. 08080
Z. Oser, Research Division, Johnson & Johnson Products, Inc., New Brunswick, N.J. 08903

NOTCH SENSITIVITY IN FATIGUE

GILBERTSON, L. N.

ZIMMER, INC., WARSAW, IN 46580

In a tensile sample, engineering stress is the force divided by the unit area. It is assumed that the stress is constant over the entire loaded area. Such an assumption, even in tensile loaded samples, is valid only in a few cases in the real world. In almost all devices, there are local anomalies in the stress distribution. The stress distribution can change due to geometric factors related to the design or manufacture of a device. The local stress will increase or concentrate around things such as holes, changes in section, or even tool marks.

There are many handbooks available that have used analytical and/or experimental techniques to come up with theoretical stress concentration factors (K_t) for various geometric configurations and loading modes. In determining fatigue properties of an actual device, these stress concentration factors may be combined with material fatigue strength data to provide a first estimate of the fatigue strength of the device. However, different materials respond differently to different levels of stress concentration. One of the ways to quantify this response is to test standard test samples with known stress concentration factors. These tests will result in a fatigue notch factor (K_f):

$$K_f = \frac{\text{unnotched fatigue strength}}{\text{notched fatigue strength}}$$

The fatigue strength is that value of stress at which a fatigue fracture will occur after a given number of stress cycles. Usually, the fatigue notch factor is less than the stress concentration factor and the difference increases with a decrease in the notch radius and/or a decrease in material tensile strength.¹ Another way of quantifying the difference is the notch sensitivity index (q) proposed by Thum.² $q = (K_f - 1)/(K_t - 1)$. Index values greater than one indicate extreme notch sensitivity in fatigue and those less than one a lowered notch sensitivity.

Test Description

In order to access the notch sensitivity of 316 LVM stainless steel, small rotating beam samples (.188 inch diameter gauge section) were fabricated with an unnotched hour glass configuration, and notches of .030 inch, .060 inch, and .090 inch radii. The samples were polished and tested in laboratory air at approximately 70 cycles per second. A subjective median 10 million cycle fatigue strength was selected for each group.

Material

Two different lots of 316 LVM with different amounts of cold reduction, and thus different mechanical strengths, were used in the tests. The first group had an ultimate strength of 143 ksi, and a yield strength of 117 ksi. The second group had an ultimate strength of 180 ksi, and a yield strength of 140 ksi.

Results

The results of the fatigue tests are presented in Table I. The theoretical stress concentrations were calculated using Peterson's³ values for bending of a round bar with a U-groove. The notch factors and sensitivity index were calculated and presented in Table II.

Discussion

Even in reverse bending, the fatigue strengths of the higher strength materials was much higher. The ratio of the unnotched specimen fatigue strength is roughly the same as the ratio of either the yield or ultimate strengths. The fact that the notched sensitivity indexes go above one for the low stress concentration (.090 inch radius) is probably due to the fact that the K_t value for that radius had to be extrapolated. For both materials, the notch sensitivity does increase with increasing K_t , but it does not follow the general material trend on strength. The higher strength material appears to have lower notch sensitivity index than the lower strength material.

Conclusions

316 LVM stainless steel is not a very notch sensitive material, and the notch sensitivity does not increase with increasing cold work.

References

1. Reemsnyder, H. S., "Stress Analysis", Proceedings of the SAE Fatigue Conference, P-109, April 14-16, 1982, pp. 75-84.
2. Heywood, R. D., "Designing Against Fatigue of Metals", Reinhold Publisher, New York, 1962.
3. Pederson, R. E., Stress Concentration Factors, John Wiley & Sons, 1974.

Table I. 10 Million Cycle Median Fatigue Strength

Specimen	180 ksi Material	140 ksi Material
Unnotched	75.8 ksi	60.1 ksi
.090" radius	60.8 ksi	49.5 ksi
.060" radius	55.5 ksi	42.0 ksi
.030" radius	55.6 ksi	39.0 ksi

Table II. Notch Factors

Radius	K_t	180 ksi Material		140 ksi Material	
		K_f	q	K_f	q
.090"	1.2	1.25	1.23	1.21	1.05
.060"	1.42	1.37	.87	1.43	1.03
.030"	1.75	1.36	.49	1.54	.72

Zimmer, Inc.
P.O. Box 708
Warsaw, IN 46580

Fatigue Performance of Cobalt-Based Superalloys and Their Weldments for
Implant Devices

J.B. Deaton, M.A. Imam, and R.W. Judy, Jr.

Naval Research Laboratory, Washington, D.C. 20375

It has long been recognized that the mechanical properties of orthopedic implant materials, in particular fatigue performance, must be improved to increase the *in-vivo* performance of these devices. Haynes Alloy 25 is used in some implanted devices; the present investigation deals with the fatigue behavior of this alloy in both base metal and in weldments. Test specimens machined from 1.22 mm diameter wire had a reduced cross-section in the central region. Experimental evaluations of fatigue properties were performed in a device where ten cantilever-loaded samples were tested simultaneously. *In-vitro* conditions were simulated by the use of aerated Ringer's solution, which is kept at a pH of 6.5 and a temperature of 37°C. To isolate the effect of simulated physiological conditions, tests were also conducted in laboratory air. Finally, metallographic and fractographic examinations were carried out to evaluate the microstructural characteristics and fracture modes as a function of different welding techniques and test environments. Evaluations of the relative suitability of various welding techniques in cobalt-based Haynes Alloy 25 for use as an implant material were based on the metallurgical observations and fatigue tests.

INERTIAL WELDING OF ORTHOPAEDIC ALLOYS

L. N. GILBERTSON

ZIMMER, INC., WARSAW, IN 46580

INTRODUCTION: Inertial welding is a process developed by Caterpillar Tractor Company for joining parts with rotational symmetry. It is a form of friction welding where a fly wheel is used to store all the energy required for the welding process. A fly wheel of specific mass is rotated to a calculated speed to provide a predetermined kinetic energy input. When the fly wheel reaches the desired speed, the two pieces to be welded are pushed together. The kinetic energy of the rotating fly wheel is converted to heat at the weld interface. The weld occurs with a final axial thrust when most of the energy of the fly wheel is converted into heat. Although inertial welding is called welding, it is actually a form of forge-bonding in that no material should actually be melted during the process. Because no materials are melted, inertial welds are much stronger than conventional welds. Also, it can be used to weld dissimilar materials.

MATERIALS AND METHODS: Several material pairs, as shown in Table I, were joined using inertial welding. Samples of each set were submitted for metallographic examination, and others were machined into tensile specimens. A third, larger group, consisting of ASTM F-75 alloy forge bar bonded to forged ASTM F-75 alloy, was made into rotating beam fatigue specimens. Care was taken to position the weld zone at the minimum cross section of the fatigue specimen.

METALLOGRAPHY: The inertial weld of 17-4PH to itself appeared to be sound metallographically with the weld extending completely across the cross section. The welding of 17-4PH stainless steel to 304 stainless steel was also very successful with the weld zone extending beyond the rod cross section. Despite the rough appearance of the flash on the high strength Co-Cr-Mo alloy (ASTM F-799) welded to itself, the weld was sound and extended completely across the entire cross section. The grain boundaries were delineated, probably by small carbides, and the grain size was refined. Despite the ragged appearance of the cast F-75 welded to ASTM F-799, the weld was sound and extended across most of the cross section. There was no noticeable microstructural change within the ASTM F-799, but the cast F-75 had a swirled appearance directly adjacent to the weld zone. At the weld interface, there was the same delineated, refined grain structure found in all the ASTM F-799 sample. Despite the lack of flash on the attempt to weld cast F-75 to itself, there was a sound weld that covered most of the rod cross section. In addition to the obviously swirled cast structure adjacent the immediate weld site, there was the same central zone of highly refined grains at the weld site. In the Ti-6Al-4V to Ti-6Al-4V welds, there was

still an obvious weld zone. The structure was not equiaxed. There was a transition to a more acicular structure in the weld zone which probably comes from the quick heating and rapid cooling of the small weld zone. On cobalt/Ti-6Al-4V welds, most of the deformation appears to occur in the Ti-6Al-4V. The weld zones were very narrow and there appeared to be a third-phase structure in the weld zone. Most of the welds appears to be sound although there was evidence on some that they may not have penetrated the full diameter of the rods.

TENSILE TESTING: All of the samples, except those where Ti-6Al-4V was welded to a cobalt alloy, fractured away from the weld zone indicating that the weld was stronger than at least one of the base materials. All of the tensile samples, again with the exception of the titanium to cobalt samples, gave tensile strength values equal to the weaker of the base materials (Table I). Despite the fact that the fracture of the titanium-to-cobalt weld samples occurred at the weld site, the ultimate strengths involved were extremely high.

FATIGUE TESTING: The effective fatigue strength of the inertial welded samples was better than 90 ksi. I call this the effective fatigue strength because it reflects that some of the samples did not fail at the weld zone but were forced to fail away from the minimum diameter section in the weaker parent material. There is still a minimum 30 ksi improvement between the cobalt forging bar and the inertial welded sample.

SUMMARY: Inertial welding appears to be a viable means of forming high-strength parts from high-strength components. The potential application of this process to orthopaedic products is exciting. It portends a new era of design versatility coupled with lower manufacturing costs.

TABLE I Tensile Test Results

Material	Ultimate Strength ksi	Elongation %
17-4PH/17-4PH	111.4	N.A.
17-4PH/304S.S.	173.7	N.A.
F-799/F-799	152.0	14.7
F-75/F-799	107.6	4.7
Ti-6Al-4V/Ti-6Al-4V	136.9	17
Ti-6Al-4V/F-75	86.4	1
Ti-6Al-4V/F-799	109.6	1
F-799 Forged Bar/ Forged F-799	163.3	10

Zimmer, Inc.
P.O. Box 708
Warsaw, IN 46580

In Vivo Study of an Elastomer Coated Bone Fracture Plates.

J.B. Park, D. Mehta, G. French, H.B. Lee, and W. Stith

College of Engineering, University of Iowa,
Iowa City, Iowa 52242

The conventional 316L stainless steel bone fracture plates have some drawbacks including 1) high modulus (200 GPa) relative to cortical bone (18GPa), 2) prone to corrosion, and 3) can induce metal sensitivity [1,2]. In order to alleviate some of the problems an elastomer (Bion®, Lord Corp.) coated fracture plates have been studied for a preliminary evaluation.

A thin (0.01 mm) and thick (1.0 mm) layer of the elastomer was coated on the entire surface of fracture plates except the holes (Richards Mfg. Co. 12-7459) using a template. A metal shim was placed on each hole before coating in order to prevent tearing of the elastomer during insertion of screws. As received bone plates were used for controls.

After a routine aseptic surgical preparations of the experimental dog, the femur was exposed along the border of the biceps femoris muscles, and four 1/16 inch holes were drilled in the midsection for attachment of the plate using screws (Richard Mfg. Co. 12-8293 and 4). One femur received the elastomer coated plate and the contralateral femur received the control plate. No osteotomy was attempted and a routine closure of the wound including the periosteum membrane over the plates were made. The tightness of the screw was controlled by one orthopedic surgeon who performed all the surgeries. Total 8 animals were used but one died after surgery hence excluded.

After predetermined period (4 and 8 weeks) the femurs were harvested and sectioned into AM, AL, PL and PM quadrant mechanical test samples (1/8x1/8x2" long) similar to Woo's [3] by using a diamond saw. After 3-point bend tests the broken pieces were cut into 1/4" long pieces again for density and mineral content measurements.

Table 1 shows the results of the mechanical tests. The only statistically (student t-test) significant difference ($p < 0.05$) between control and experimental is the ultimate yield strengths for the 8 week implants for both thin and thick coating. Other properties (modulus toughness) did not change significantly by the elastomer coating. This tends to indicate that significant changes of ultimate tensile strength may occur after at least 4 weeks and can be influenced by the changes in plate material properties.

The other properties (density and percent mineral content) did not change significantly at all. The soft tissue histology around the plate showed thin layer of collagenous membrane coverage for both implants. The lymph nodes (groin and popliteal) histology showed no particulates of implants or unusual tissue reactions. SEM-EDAX analysis also showed no significant concentration of metal ions released by both implants. This may be due to the fact that the bones are not osteotomized.

Table 1. Summary of Mechanical Tests

Period	Thick- ness	Prop- erties	Con- trol	Experi- mental	t-test
4 wk	thin	E^a	1.91	2.19	NS
		σ^b	25.7	26.1	NS
		A^c	1.49	1.39	NS
4 wk	thick	E	1.85	1.17	NS
		σ	21.6	21.7	NS
		A	1.40	1.40	NS
8 wk	thin	E	1.67	1.97	NS
		σ	23.8	25.1	<0.05
		A	1.24	1.38	NS
8 wk	thick	E	1.59	1.92	NS
		σ	24.0	26.5	<0.05
		A	1.06	1.14	NS

- a. E (modulus of elasticity) $\times 10^6$ psi
b. σ (ultimate tensile strength) $\times 10^3$ psi
c. A (fracture energy or toughness) in-lb.

In conclusion, the preliminary in vivo study indicates that the coating of bone fracture plates with an elastomer can be beneficial to decrease the stiffness of the overall bone plate rigidity, [indeed, if we made the control plates as large as the elastomer coated ones we could have obtained more definite results] rate of corrosion (in vitro corrosion tests showed a much higher corrosion rate for the uncoated control plates) although no corrosion could be noted for both plates in this study. It was also evident that the increased surface contact area between bone and plates due to more deformable elastomer resulted in the thinner collagenous membranes underneath the elastomer-coated plates.

[1] J.B. Park, Biomaterials Science and Engineering, Chap. 8 and 12, in print, Plenum Pub., 1983.

[2] H.K. Uhthoff (ed.), Current Concepts of Internal Fixation of Fractures, Springer-Verlag, Berlin, 1980.

[3] S.L.Y. Woo, "The relationships of changes in stress levels on long bone remodelling," in Mechanical Properties of Bone, S.C. Cowin (ed.), ASME, AMD-vol. 45, 107, 1981.

Acknowledgement: The financial support of Lord Corp. and assistance given by Dr. S.D. Cook (Tulane Univ.) are gratefully acknowledged.

A Plastic Bone Model for the Evaluation of Femoral Fracture Fixation

H. McKellop, R. Glousman, I. Clarke, A. Sarmiento

Orthopaedic Biomechanics Laboratory,
Bone and Connective Tissue Research Program,
Orthopaedic Hospital-U.S.C., Los Angeles, CA 90007

Laboratory studies of femoral fracture fixation have often involved mechanical tests of as many as 50 to 100 cadaver specimens. However, such studies invariably encounter a large amount of scatter in the data due to the great variation in specimen age, size, shape and bone quality. Consequently, the experiments are limited to a few variables, and even these can only be evaluated on a rough statistical basis. To alleviate this problem, we have developed a composite plastic bone analog (PBA). This report compares fixation of transverse femoral neck osteotomies fixed either with four Knowles pins or a compression screw and side plate, using cadaveric and PBA specimens.

Silastic (Type E) was used to copy both the external (cortical) and internal (cancellous) bone geometries of a human femur. A positive replica of the cancellous bone structure was then moulded using urethane foam (Foamex, polyol isocyanate GSD-104-8). The urethane core was aligned in the Silastic cortical mould, which was then filled with epoxy reinforced with fiberglass powder (Ciba Geigy: 6010 resin with 956 hardener). This produced a replica of the original cadaver femur with an epoxy cortex and urethane foam cancellous core. The mechanical properties of specimens of the epoxy and urethane were measured by conventional mechanical tests. The silastic moulds could be re-used numerous times to produce replicate plastic bones.

For the fracture fixation model, cadaver femurs were stripped of soft tissues and stored frozen until needed. A strain rosette was placed on the medial cortex just below the intended osteotomy line. The intact bones were loaded in an MTS machine to 1000N, with the load at 35° to the osteotomy line, while calcar strain and downward deflection of the head were recorded. The bones were then sectioned through the neck and fixed either with four Knowles pins (rights) or a compression screw (lefts). Load was re-applied to failure. This experiment was repeated using four plastic bones fixed with Knowles pins and three with compression screws.

Calcar strain (compared to intact) was measured as an indication of the portion of the load being transmitted through the bone. Femoral head displacement (relative to intact) was a measure of the rigidity of the fixation. The intact calcar strain for the plastic bones was mid-range of the cadaver values but much more reproducible (Table). This also applied to the osteotomized femurs fixed with Knowles pins. The calcar strains with compression screws tended to be higher for the PBA femurs than the cadavers. Similarly, the deflection of the PBA and cadaver specimens was more comparable for the Knowles pins specimens than with compression screws.

BONE TYPE	FIXATION DEVICE	CALCAR STRAIN (AT 1000N)		DEFLECTION (mm/1000N)			MAX LOAD ESTIMATED (N)
		INTACT	%/SWITCHING RATIO	INTACT	%/OSTEOTOMY RATIO		
CADAVER (N=5)	KNOWLES PINS	1200 (±300)	1620 (±1600)	1.5 (+0.1)	0.4 (+0.3)	2.3 (+0.3)	2560 (±1300)
PLASTIC (N=4)	KNOWLES PINS	1275 (±95)	1700 (±174)	1.4 (+0.05)	0.7 (+0.3)	1.9 (+0.3)	2875 (±411)
CADAVER (N=5)	COMPRESSION SCREW	1090 (±540)	1060 (±640)	1.0 (+0.3)	0.8 (+0.1)	0.9 (+0.3)	2930 (±300)
PLASTIC (N=3)	COMPRESSION SCREW	1700 (+0)	3370 (±1300)	2.4 (+0.2)	1.3 (+0.4)	2.2 (+0.4)	3600 (±408)

The mode of failure was very similar with PBA and cadaver specimens for both types of devices. Knowles pins cut through the cancellous bone, applying progressively more load to the calcar. At failure the anterior cortex of the calcar suddenly fractured, and the pins were bent sharply over the cortex. With compression screws, the calcar strain initially increased until 2000-3000 N were applied. Above this level the additional load was carried primarily by the fixation device. Failure was taken as the point where a large (3mm) superior gap had opened at the osteotomy. On unloading this gap closed but the proximal fragment was permanently displaced several millimeters distally. Neither the Knowles pins nor the compression screws cut through the cancellous bone of the femoral head (cadaver or plastic).

The elastic moduli were about 3500 to 5200 MPa for the epoxy and 75 to 100 MPa for the urethane, somewhat lower than typical values for cortical and cancellous bone, i.e., 18,000 MPa and 500 MPa, respectively. We are evaluating other epoxy and urethane formulations to obtain moduli closer to those of bone, to improve the accuracy of the plastic bone model.

Follow-up experiments will include instrumentation to compare the longitudinal and shear motions at the osteotomy, which strongly influence initial fracture healing. The elimination of the problem of variation among cadaver specimens from such experiments is a major step toward obtaining a method for improving fracture fixation techniques, especially with more complicated unstable femoral neck and intertrochanteric fractures.

This project is supported by the Doctor's Education and Research Fund of Orthopaedic Hospital.

Biomechanics Research Laboratory
Orthopaedic Hospital-USC
2400 S. Flower, Los Angeles, CA 90007

THE ULNAR CENTRO-MEDULLARY LOCKED NAIL WITH COMPRESSION OR DISTRACTION

LEFEVRE C., MIRoux D., de LA FAYE D., COURTOIS B..

DEPARTMENT OF BIOMATERIALS AND SURGERY

Service d'Orthopédie
C.H.U. 29279 BREST CEDEX (FR)

2) Setting in distraction : ulna lengthening on traumatic after-effects, or Kienbock disease.

The traumatic and orthopaedic pathology of the ulna among the adults requires orthopaedic (10 %) and mainly surgical (90 %) methods.

The surgical treatment of an isolated or not fracture of the ulna calls on two methods:

- open seat treatment (screwed-on plate) : good interfragmentary compression, anatomical reduction but traumatism of the muscles and of the periosteum, emptying of the initial haematoma, risks of infection and of radio-ulnar synostosis.

- closed seat treatment (centro-medullary nailing down) : this method prevents the above said risks but is unable to keep the compression of the fracture seat which is essential to the healing of the bone (from which risks of non-union).

No ulnar nail proposed until now has allowed the simultaneous control of the rotation and of the putting into compression of the bone fragments.

The here proposed programme aims at adjustment of a new centro-medullary nail of the ulna whose mechanical conception allows :

- a closed-seat surgery thanks to the instrumental device specially studied for the setting of the implant.

- a continuous checking of the rotation of each fragment thanks to a double mechanism of proximal and distal closing.

- a checking of the lengthening of the set nail allowing a setting either in compression or distraction.

For simplicity sake, a single example of the nail allows the osteosynthesis of a right or left ulna, whatever its length.

The indications of the proposed implant could be as follows :

1) Setting in compression

- traumatology : isolated fracture of the ulna, Monteggia fracture, fracture of both bones of the forearm (the radius can be fixed in a classical way), oblique fracture of the olecranon, aseptic non-union.

- orthopaedics : shortening osteotomy, osteotomy on angular or rotatory vicious callus.

Society BENOIST GIRARD & Cie (HOWMEDICA)

C. LEFEVRE - CHU Morvan - 5, avenue Foch -
29279 BREST CEDEX - FRANCE.

CARBON FIBRE REINFORCED BIODEGRADABLE AND NON-BIODEGRADABLE POLYMERS AS BONE PLATE MATERIALS

Kilpikari, Jyrki and Törmälä, Pertti

Tampere University of Technology
Tampere Finland

Bone plates are usually made of metallic materials (stainless steel, titanium, vitallium). Metals are very stiff materials and when metal plates are used the fixation of fracture is rigid. Rigid fixation of fracture causes growth of porous bone under the plate and this porosity decreases the strength of the bone (1,2). Metals also corrode in body and corrosion products may cause severe tissue reactions. Two surgical operations are also required when metal plates are used.

Polymeric materials are less stiffer than metals and many polymers have very good biocompatibility. Biodegradable polymers also degrade slowly in body and only one surgical operation is needed. Many studies about bone plates made of polymeric materials have been made. Most common materials in these studies have been epoxy resins (EP), polymethylmethacrylate (PMMA), polylactide (PLA) and polyglycolide (PGA). PGA and PLA are biodegradable materials and EP and PMMA are non-biodegradable materials. These materials can be reinforced with carbon fibres to obtain sufficient mechanical properties (3,4).

In this study we have measured some mechanical properties of carbon fibre reinforced PGA/PLA (90/10) copolymer, carbon fibre reinforced PMMA and carbon fibre reinforced EP (table 1). The decrease of the tensile strength of carbon fibre reinforced PGA/PLA copolymer during eight weeks storage in water was also measured (figure 1).

Table 1. Mechanical properties of carbon fibre reinforced polymers.

material	flexural strength	modulus
	MPa	GPa
PMMA+carbon fibre	200	15
EP+carbon fibre	1000	500
PGA/PLA+carbon fibre	290	

Carbon fibre reinforced EP had best mechanical properties but mechanical properties of carbon fibre reinforced PGA/PLA copolymer was also very good. Very interesting result was that 12 % of carbon fibres increases the strength of this copolymer from 40MPa to 290 MPa. The decrease of tensile strength of PGA/PLA copolymers was slow during first four weeks but the decrease was quite rapid during second four weeks.

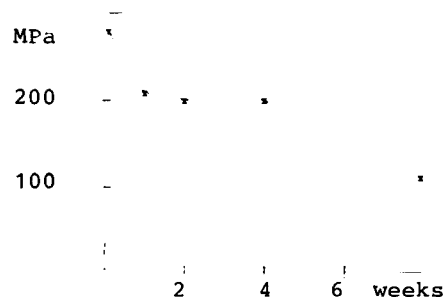


Figure 1. The decrease of tensile strength of PGA/PLA copolymer during water storage.

It is possible to coat the biodegradable with some kind of hydrophobic coating to bring forward the start of the degradation of polymers.

References

1. S.L.-Y. Woo, W.H. Ikeson, B. Levenetz, R.D. Coutts, J.V. Matthews and D. Amiel, J. Biomed. Mat. Res., 8 (1974)
2. P. Paavolainen, E. Karaharju and P. Slätis, Clin. Orthop., 136 (1978)
3. H. Alexander, Bioengineering-9th., Elmsford, N.Y. (1981)
4. M. Vert, F. Chabot, Macromol. Chem., Suppl. 5, 30-41 (1981).

CEMENTLESS ENDOPROSTHESIS STABILIZATION BY A SOFT, POROUS STEM COATING

C.A. Homsy, J.M. Prewitt, III

The Methodist Hospital
Houston, Texas

Fifteen years of laboratory, animal and clinical studies have informed the scientific and surgical principles for successful endoprosthetic stabilization using a soft, porous, tissue ingrowth stem coating (Proplast®). These efforts were impelled by inadequacies of acrylic cement stabilization especially in younger, more active patients.

The coating is 70-80% void volume and formed with PTFE polymer and vitreous carbon for biocompatibility and tissue ingrowth efficacy. It exhibits mechanical properties close to that of fibrous tissue in order to minimize early and later motion trauma between invading tissue and the porous matrix of the implant material.⁽¹⁾ The tensile modulus of the composite approximates that of loose connective tissue (8 MPa).

The modulus increases to values reported for collagen as the porosity becomes filled with highly collagenated fibrous tissue. The coating with in situ tissue becomes a resilient interface which is mechanically coupled both to the endoprosthesis and to surrounding tissue. Animal studies confirmed retention strength of 6 Kg/cm² from tissue ingrowth into the coating which could sustain physiological loads for stems exhibiting areas of 80 to 100 cm².⁽²⁾

Between 1972 and 1977, 111 F-Thompson endoprostheses, with coated stems, were implanted in patients with acute femoral neck fractures. Recovered implants confirmed tissue ingrowth fixation analogous to that seen in previous and concurrent animal studies. However, the use of the coating in and of itself using conventional implantation techniques did not significantly improve the overall clinical performance of the implant. The results taught that operative technique must provide an initial press fit of the implant in the medullary canal.

In 1979, '80, and '81, 86 Au-Franc Turner type femoral components with 2 mm composite stem coatings were used in total hip arthroplasties with instruments and protocol intended to produce initial press fit stabilization. Sixty-four hips were available for review in July of 1983. These were between 3 mos. and 51 mos. postoperation (avg. 34 months); 6 (9%) were unsatisfactory (criteria of Ref. 4) of which 4 (6%) have been revised to conventionally cemented components. Three were removed easily without evidence of tissue ingrowth. The fourth required multiple mallet blows on a distraction punch and the coating material retained on the implant and recovered from the medullary canal showed ingrowth of fibrous connective tissue. This implant and one of the three others demonstrated posterior rotational movement within surrounding cancellous bone. Inadequate press fit at the time of surgery was implicated in these failures, but more significantly, in all of these cases, radiographs showed relatively large proximal femoral canals in comparison to the corresponding cross sectional area of the implant.

Subsidence of the component was also remarkable in the failed cases.

The failed implants taught that endoprosthetic cross sections needed to be larger to insure tissue ingrowth fixation and stable load transmission to cortical bone or to dense cancellous bone. This was accomplished by adopting a modified Austin Moore stem geometry with a 2 mm composite coating (Anaform®) after December, 1981. Sixty-four of these implants have been followed between 3 months and 19 months (avg. 1 year); 1 (2%) is unsatisfactory.

The 138 patients who received 152 soft porous coated total hip endoprostheses were 19-81 years of age (avg. 40 years). Average followup time is 25 months (3 months - 4 years 3 months). There were 3 (2%) early infections, 7 (6%) were unsatisfactory and of these 4 (3%) were revised. Reports on cemented components in comparable younger patients indicate that 21%⁽³⁾ and 22%⁽⁴⁾ were unsatisfactory (avg. followup 67 months and 54 months, respectively). Since soft porous coated implants generally fail early in contrast to cemented implants, their advantage is indicated. Postoperative rehabilitation follows conventional post total hip arthroplasty protocols.

The implant may be placed by conventional surgical approaches with or without trochanteric release. Intramedullary reamers and precision rasps are used to develop an intramedullary cavity slightly undersized the implant such that uniform press fitting is achieved through slight compression of the coating without risk of cortical fracture.

Our experience shows that successful cementless endoprosthetic stabilization requires precise attention to the mechanical specifications for a soft, porous stem coating; the shape relationship between cortical architecture and implant; and the interference fit safely achievable between implant and surrounding tissue.

References

1. Homsy, C.A., et.al.: "Porous Implant Systems for Prosthesis Stabilization", C.O.R.R., 89, 220-235, November-December, 1972.
2. Rhinelander, F.W., et.al.: "Growth of Tissue into a Porous, Low Modulus Coating on Intramedullary Nails: an experimental study", C.O.R.R., 164, 293-296, April, 1982.
3. Chandler, H.P., et.al.: "Total Hip Replacement in Patients Younger than Thirty Years Old". J.B.J.S., 63-A, 1426-1434, December, 1981.
4. Dorr, L.D., et.al.: "Total Hip Arthroplasties in Patients Less than Forty-five Years Old". J.B.J.S., 65-A, 474-479, April, 1983.

The Prosthesis Research Laboratory, The Methodist Hospital, Houston, Texas.

Charles A. Homsy, Sc.D., Prosthesis Research Laboratory, The Methodist Hospital, 6560 Fannin Suite 2080, Houston, Texas 77030.

A STUDY OF BONE INGROWTH IN SOME POROUS PHOSPHATE GLASS-CERAMIC MATERIALS

Pernot F., Baldet P., Bonnel F., Saint-André J.M.,
Zarzycki J., Rabischong P.

Laboratoire des Verres du C.N.R.S, Université Montpellier 2,
Place Eugène Bataillon - 34060 Montpellier Cedex - FRANCE

SUMMARY

Porous glass-ceramics were prepared by the controlled crystallization of various phosphate "foam glasses". They were implanted inside the bones of rabbits or sheeps and the resulting bone ingrowth was investigated. It is shown that the ingrowth depends rather on the texture than on the composition of the materials.

INTRODUCTION

In orthopaedic and bone surgery, ceramic or glass-ceramic materials are more and more used. These products are well accepted by the living organism and may be easily tailored to promote a direct bond between the bone tissue and the implants. To obtain such a result, one solution is the use of porous glass-ceramics, such materials with optimal textural properties permit tissue ingrowth and thus a perfect anchoring with the surrounding bone. The aim of this paper is to relate the texture and the composition of these materials with the quality of bone ingrowth.

MATERIALS and METHODS

Samples of various porosity and interconnection pore size distribution were prepared by the ceramization of various phosphate foam glasses.

TABLE 1. Composition of "foam glasses" studied

glasses	molar proportions		
	CAP	CKAP	CASPS
Constituents			
$\text{Ca}(\text{PO}_3)_2$	83.38	78.38	83.38
AlPO_4	33.24	33.24	31.24
K PO_3	-	10.00	-
SiO_2	-	-	4.00

They were implanted under the tibial plate or within the cortical bone of rabbits or sheeps. The animals were killed after periods ranging from 1 to 18 months and after sacrifice operated bones were fixed, dehydrated and finally embedded in hard plastics. Sections of 1 mm thick were cut and then ground down to about 50 μ m thickness. The samples were then stained for histological examination in conventional or polarized light to identify the nature of the bone formed in and around the implants. To determine the degree of calcification, the samples were also observed by microradiography. The growth process was also studied by scanning electron microscopy and reflection optical microscopy. Quantitative studies were made from histological as well as microradiographic observations. Measurements of the bond strength between the bone and the implants were realized by a push out test on cylindrical samples implanted within the cortical bone.

RESULTS

In rabbit for the most porous materials, the growth process was as follows.

After one month, a woven bone tissue began to embed the implants, while the pores were invaded by a highly vascularized fibroblastic tissue. The deposition of calcium salt was relatively minor.

After two months, the implants were totally embedded by bone tissue. Inside the implants, fibrous tissue condensed close to the periphery of the pores and began to transform into primary woven bone. A beginning of mineralization was clearly apparent.

After 3 months, bone ingrowth was nearly complete while adipose tissue appeared in the pores. Calcification continued to increase.

After 6 months, differentiation of lamellar bone was almost complete and the first hematopoietic cells were observed in adipose tissue. Calcification appeared to be very important.

From 9 th to 18 th month, histological aspect did not show any significant variation and the bone inside the implants seemed totally calcified after 9 months.

The degree of bone ingrowth defined as the ratio between the respective volume fraction of bone and pores increased from the 1 st to the 9 th month, when it reached more than 50%.

In sheep, the growth process followed the same mechanism but it took place at a lower rate than in rabbit.

CONCLUSION

This bone ingrowth presented general characteristics of intramembraneous ossification and seemed to depend only on the textural properties of the materials. No significant differences were observed in the growth process as a function of the composition of the materials.

The shear strength measured from push out test was estimated to be about 4 MPa after 18 months in rabbit. In sheep, it was 2.5 MPa after 4 months and reached 7 MPa after 6 months.

Patka, P., Driessen, A.A., Groot de, K., Otter den, G.

Laboratory of Experimental Surgery, Department of Surgery, Free University
Van der Boechorststraat 7, 1081 BT Amsterdam, The Netherlands.

From the review of the literature of segmental bone defect repair, it is apparent that there is a common need for suitable material for temporary or permanent bone replacement. Generally, transplants of autogenic, allogeneic or xenogenic bone tissue are limited in quantity and/or offer a poor quality of tissue for segmental bone replacement. Therefore, the research into artificial materials (xenotransplants) suitable for the repair of bone defects has become an important issue. Biocompatible ceramics such as hydroxyapatite have been proved to be suitable materials for small quantity implantations with no, or only compressive, physiological loads. The excellent biocompatibility of hydroxyapatite is related to the similarity between natural bone tissue and the composition of this material.

The aim of the present study is to evaluate the bone-defect-repairing capacity of relatively large implants of hydroxyapatite under weight-bearing conditions. The 40 percent macroporous hydroxyapatite implants were compared with dense implants. Pentacalciumhydroxide-triphosphate $\text{Ca}_5(\text{PO}_4)_3\text{OH}$ was used for the preparation both of dense, and of porous, apatite implants. Pores had an average diameter of 100-200 μm , because of expected rapid bone tissue ingrowth. Dense implants had better physical (mechanical) properties. The experiment consisted of the production of a relatively large (15mmx10mmx10mm) mid-diaphysary defect in the left femur of 18 mongrel dogs. Six cylindrical, and twelve semi-cylindrical, hydroxyapatite implants were placed in these bone defects in order to restore continuity. The proximal and distal osteotomy ends were stabilized by internal fixation. The implanted materials were exposed to full loadbearing, similar to that of the original bone tissue. The semicylindrical implants were internally supported for six months. The cylindrical ones were supported for one and a half years. After these periods the internal fixation material was removed. The whole study lasted two years. The following problems were points of interest:

- the suitability of hydroxyapatite in porous or compact form for large segmental bone defect repair in animals;
- the progress of bone tissue ingrowth into pores in hydroxyapatite under weight-bearing conditions;
- the implant-tissue surface reactions in solid implants under weight-bearing conditions.
- the possibility, regarding the results of this study, of predicting the clinical application of hydroxyapatite in bone-defect repair.

The biocompatibility of implanted material has been studied physiologically, radiographically, scintigraphically and histologically for up to two years after implantation.

The hydroxyapatite implants are radiodense, and easily located and observed by standard radiographic methods. Radiographic exposures of the implant areas were obtained directly, one month and a half, one, and two years after surgery. The porous and dense hydroxyapatite implants showed no change in radiodensity on the radiographs. Radio-

graphically, no evidence was found of degradation of porous and dense hydroxyapatite specimens up to two years after their implantation. The microradiographic analysis of the surface structure of dense hydroxyapatite samples showed no obvious changes up to two years after implantation. The implant surface was in narrow contact with the new bone in half year implants. The radionuclide bone imaging technique was used to determine osseous changes in the sites of the hydroxyapatite implants, and to investigate differences in osseous changes in the sites of the porous implants compared with the dense hydroxyapatite implants. Bone images were obtained from one to twenty-four months after implantation of hydroxyapatite. The dense implants showed decreasing uptake of technetium compared with porous ones at later performed recordings. This suggests continuing remodelling of bone tissue inside the porous implant.

Macroscopic and histological observations were performed at six months, one, and two years. All hydroxyapatite implants adhered so strongly to the bone tissue that it was impossible to separate the implants from the bone tissue of the femur. The strong binding was present in porous and non-porous implants, while no resorption of the material was seen macroscopically. Undecalcified sections were available for light and fluorescence microscopy. There was direct bone-implant contact with no signs of fibrous tissue encapsulation. The pores in parts of the implant which were in contact with the cortex were completely filled with bone in the half year period, in contrast to pores of the central part of the sample. These central pores contained varying amounts of bone, bone marrow tissue, macrophages and multinuclear cells. The bone was seen to proliferate from the endosteal side to the medullar surface of the implant, and from the periosteal site along the outer implant surface. After one year, the pores of the central part of the implants were almost completely filled with bone. There has been no sign of an inflammatory reaction in the two years experimental period. Although no degradation or loosening of the implant surface has appeared, there have been two mechanical failures of two dense implants after removing supporting material.

Histologically, radiologically and scintigraphically the hydroxyapatite implants demonstrated biocompatibility with bone tissue. However, it has to be stressed that the mechanical (physical) properties are still inferior, as the need of additional implant support and two implants failures illustrates. Hydroxyapatite is a serious candidate for bone tissue replacement because of its biocompatibility and its bonelike composition. The mechanical properties, however, have to be improved.

EFFECTS OF A PERIOSTEAL ACTIVATION AGENT ON BONE REPAIR AND BONE GROWTH INTO POROUS IMPLANTS.

L.R. Alberts

Rensselaer Polytechnic Institute
Troy, NY 12181

In the 1950's and 1960's, Squibb laboratories developed a procedure to extract an osteogenic material from the cancellous bones of growing mammals. This osteogenic material has a pronounced effect on the periosteum. By activating the cells of the cambium or deep cellular level of the periosteum, it elicits what Tornberg and Bassett (1) described as an "explosive" growth of new bone, nearly doubling the diameter of some rat bones in just seven days. Here we describe some of the effects of this periosteal activation agent (PAA) on healing of a circular defect and bone ingrowth into a porous implant in the femora of male rabbits.

Circular defects, 4 mm in diameter, were drilled through the lateral cortex of the femurs of 2 kg, male rabbits. Two defects, 20 mm apart, were drilled in each femur. Two series of experiments were performed. In the empty defect series (ED), the defects were left open. In the implant series (I), the defects were filled with porous high density polyethylene implants (2) that abutted against the opposite cortex. The implants had an average pore diameter of 127 μ m and a porosity of 46.8%.

In both series, the PAA (periosteal activation agent) was applied seven days after surgery. Thus, in this model, the agent is being applied to a site that is already undergoing tissue repair. A dosage of 400 mg of PAA per kg of body weight was applied over the periosteal surface of each experimental femur. The contralateral control femur received an application of an identical volume of pyrogen-free saline. The application in both the experimental and control femurs was made while stroking the bevel edge of an 18-gauge needle over the periosteal surface. In both series, rabbits were killed at time periods of 1, 3, 5, 7, 10, and 14 days after application of PAA. There were three rabbits in each time period. The I series had a long-term group of 56 days.

The results were characterized by uptake of strontium-85, histological examination of hematoxylin and eosin slides, and image analysis of H and E and Lillies silver impregnation technique slides using a MOP-III electronic planimeter and a Quantimet® image analysis computer.

One day before each rabbit was killed, it was given an intrathoracic injection of 0.2 μ Curies of strontium-85. After the rabbits were killed, the diaphysis of each femur were sectioned into three segments.

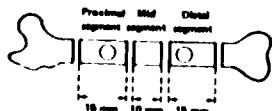


Fig. 1 Proximal, medial and distal segments of each femur.

The radioactivity of each segment was counted in a Picker deep well counter, and a strontium tracer ratio (STR) was calculated for each segment.

$$STR = \frac{E - b}{C - b}$$

where E = activity of the experimental segment, C = activity of its contralateral control segment, and b = background radiation. Thus, an STR greater than 1.0 indicates enhanced uptake of strontium in the experimental segment.

The average activation ratios for the defect segments are shown in Tables 1 and 2.

Table 1. r-45 ratios, D series, defect segments.

Days	Ave.	S.D.	Str.
1	1.14	.11	.01
3	1.13	.20	.05
5	1.08	.30	.01
7	1.11	.53	NS
10	1.13	.17	NS
14	1.07	.52	.05

Table 2. r-45 ratios, I series, defect segments.

Days	Ave.	S.D.	Str.
1	1.12	.24	.05
3	1.06	.22	NS
5	.89	.18	NS
7	1.18	.45	NS
10	1.18	.36	NS
14	1.14	.36	NS
56	.99	.28	NS

The STR average of the defect segments for all time periods in the ED series was $1.28 \pm .39$ ($p < .0005$) and the average for the I series, days 1 through 14, was $1.14 \pm .32$ ($p < .025$).

Hematoxylin and eosin stained microscope thin sections taken from the proximal segments appeared to show an enhanced periosteal bony callus formation. An attempt was made to quantify this with a MOP-III electronic planimeter. Three areas of new bone growth were identified in the I series and two areas in the ED series. Ratios of the areas of new bone in the experimental segment divided by the area in the control segment (analogous-to-strontium tracer ratios) were calculated for each area of bone growth. After excluding four area ratios where the denominator was zero or less than 10% of the numerator, the correlation between the STR's and the area ratios was found to be 0.915.

Image analysis of silver impregnated segments indicated that PAA, as applied here, had no effect on bone ingrowth into the porous implant. The PAA did not appear to change the types of tissue observed or the sequence of events in the healing response. It did not appear to enhance healing of the circular defect. It did enhance uptake of strontium-85, most probably by enhancing periosteal callus formation. The enhancement of strontium uptake occurred as early as one day after application ($p < .01$, ED series; $p < .05$, I series) and as late as 14 days after application ($p < .05$, ED series).

1. Tornberg, D.W. and C.A.L. Bassett, 1977. Activation of the resting periosteum. Clin. Orthop. Relat. Res. 129:305-312.
2. Glasrock, 7380 Bohannon Rd., Fairburn, GA.

Support from the Engineering Research Institute at Iowa State University is gratefully acknowledged.

RECONSTRUCTION OF THE ATROPHIC ALVEOLAR RIDGE WITH HYDROXYLAPATITE: A 5 YEAR REPORT

John N. Kent, DDS, James H. Quinn, DDS, Michael F. Zide, DDS,
Michael S. Block, DMD, and Michael Jarcho, PhD

LSU Medical Center, Dept. of Oral & Max. Surgery
New Orleans, LA 70119

MATERIALS AND METHODS

HA, a highly biocompatible, osteoconductive calcium phosphate material provides a permanent support matrix for deposition of fibrous tissue and bone by direct chemical bonding mechanisms. In 1978 our institution initiated prospective clinical trials for ridge reconstruction with dense particulate HA. Atrophic maxillary and mandibular ridges were classified according to the degree of deficiency and were augmented with approximately 4-16 gms of 18-40 mesh irregular shaped particles (1978-81) or 20-40 mesh rounded particles (1981-83). In some of the class III and IV ridge deficiency patients 12-20 grams of HA mixed with finely crushed autogenous cancellous iliac bone (1 gm. to 1 cc) was used to provide increased strength and stability. Surgical technique involved subperiosteal pocket tunneling injection of HA with modified plastic syringes. Maxillary and mandibular splints used infrequently from 1978 to 1981 were more commonly used thereafter.

RESULTS

228 ridges on 208 patients have been followed 5 years. 55 ridges were augmented with irregular shaped HA and 173 ridges were augmented with rounded particulate HA. Tables 1-4 demonstrate the ridges reconstructed, demographic data, mandibular and maxillary augmentation with respect to the ridge deficiency classification. In nearly all cases mental nerve dyesthesias improved with normal sensation returning to the lower lip by the sixth postoperative month. No permanent lip anesthesias were observed. Vestibuloplasties were necessary in most class IV patients because of displacement of the sulcus mucosa toward the ridge crest. Incision dehiscence and erosion of mucosa which occurred within the first few postoperative weeks healed by secondary intention without loss of particles distant to the incision area. Displacement of material was related to the severity of the atrophic ridge (Class IV), deficiencies in surgical technique, and absence of splints. Aspiration of hematoma and seromas were common in Class III and IV ridge deficiencies prior to use of splints. (Table V)

Radiographic studies by Kent⁴ and Block⁵ in patients followed up to 48 months showed ridge height maintenance to be in excess of 90% of the original augmentation height. There was no apparent statistical significant difference between HA alone and HA with bone augmentation, less than 5% and 10% loss of ridge height respectively. The known decrease in ridge height following onlay autogenous bone grafts alone is approximately 60% through two years of follow up with increasing resorption through longer term follow-up. Denture construction began as early as 3 to 4 weeks post augmentation. Skin and mucosal graft vestibuloplasties were possible 2 months post augmentation compared to 4 to 6 months post augmentation following autogenous bone grafts alone. Augmentation of alveolar deficient ridges with HA has resulted in a permanent improved ridge

height with non mobile mucosa convex contour.

*Durapatite, Sterling Winthrop Lab, Albany, N.Y.
**Calcite, Calcitek, Inc., San Diego, CA

1. Jarcho, M. *Clin Orthop*-157(6): 259-278, 1981.
2. Kent, J.N.; et al: *JADA* 105: 993-1001, Dec. 1982.
3. Kent, J.N. et al: *JOMS*, Oct. 1981
4. Kent, J.N., et al: First World Biom. Cong., Baden, Austria, Apr. 8-12, 1980.
5. Block, M.S. & Kent, J.N. Submitted to J.O.M.S. Sept. 1983
6. Baker, et al: *J Oral Surg* 37(4): 429-434., 1974.

TABLE I

RIDGES RECONSTRUCTED		
Durapatite	55	
Calcite	173	
Class I-II	40%	
Class III-IV	60%	

	Mand	Max
HA Alone	133	43
HA Bone	40	12
TOTAL	173	55
	(76%)	(74%)

TABLE II

DEMOGRAPHIC DATA

PATIENTS	Male	Female
208	64	144(70%)
AGE - 27-75 yr.,	AV-58	
# of Denture 1-10,	AV-3	
Years Edentulous 1-40,	AV-18	

TABLE III

MANDIBLE

	Class I	II	III	IV
HA Alone 115	20	34	47	14
HA Bone 33		3	17	13
Staple 13			8	5
Other Dental Implant 6		2	2	2
Visor 6		2	2	2
TOTAL	20	41	76	36

TABLE IV

MAXILLA

	Class I	II	III	IV
HA Alone 43	5	23	13	2
HA Bone 12		1	5	6
TOTAL 55	5	24	18	8

TABLE V

COMPLICATIONS

Mental N	37
Vestibuloplasty	32
Mucosa Breakdown	20
Displacement	17
Hematoma	10



CANINE MANDIBULAR RIDGE RESPONSE TO HYDROXYLAPATITE
COMBINED WITH BONE

Block, Michael S., and Kent, John N.

Department of Oral and Maxillofacial Surgery, LSU School of
Dentistry, New Orleans, Louisiana

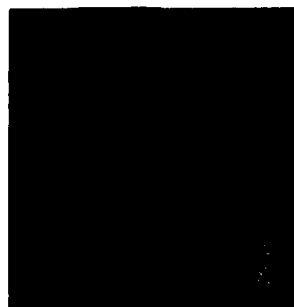
This study describes in detail the healing response of mandibular alveolar ridge augmentation with hydroxylapatite (HA)* with and without the addition of autogenous bone. Nine mongrel dogs were edentulated in the right and left maxillary and mandibular body regions and a complete alvelectomy was performed. After eight weeks of healing, the dogs were augmented with either 12 cc's of hydroxylapatite (Group I) or 12 cc's of hydroxylapatite combined (1 gm HA:1 cc bone) with autogenous iliac cancellous bone (Group II). The bone graft was harvested and placed in a bone mill to create small bony particles. The HA was then added to the bone and stirred thoroughly to create a homogenous mixture. The material was then placed over the mandibular ridge through a subperiosteal tunnel. The dogs were allowed to heal for periods of 4, 8, and 16 weeks. Ten days prior to sacrifice the dogs received oxytetracycline (25 mg./kg.) intravenously to label bone turnover. The mandibles were sectioned and processed for routine decalcification and ground sections. The ground sections were fluoresced to demonstrate the oxytetracycline bone label. Microradiographs were obtained from the ground sections.

RESULTS

The augmented ridge at four weeks showed no bony infiltration in either of the two groups. In both groups, hydroxylapatite particles were "cemented" by a thin, fibrous connective tissue with a mild inflammatory response. In Group 2 specimens, small pieces of the non-viable bone graft were seen with osteoclasts at their periphery. New osteoid was not found in the 4 week specimens. The 8 week and 16-week specimens contrasted the 4-week specimens in that Group II dogs augmented with HA combined with bone demonstrated a definitive osteogenic ingrowth with bone interspersed between the hydroxylapatite particles throughout the ridge. Group I dogs did not demonstrate bone ingrowth into the augmented ridge. Particles were held together with only dense fibrous tissue. The 8 week specimens in Group II demonstrated new osteoid being formed as well as early bone formation. Osteoclasts were not seen nor was there evidence of bone formation by "creeping substitution." The bony trabecula interspersed between the particles in the group 2 dogs were found to mature and the 16-week specimens demonstrated a homogenous mixture of bone and HA within the augmented ridge. The bone in the HA ridge in the 16 week specimens was lamella in character, with Haversian systems and growth lines demonstrating maturation. (See Figures) This animal

experiment demonstrated that bony ingrowth could be induced into the hydroxylapatite ridge by the use of autogenous bone grafts. Future studies are underway to examine this osteogenic inductive phenomena more completely.

*Calcitite, 2040 Mesh, Calcitek, Inc., San Diego, California.



HA Ridge without the addition of bone. Note lack of bony ingrowth into the HA ridge (2x)



40x

2x

Microradiograph of trabecular bone within the HA Ridge. Note Haversian systems. (16 weeks, HA + Bone)



Trabecular bone between HA Particles (16 weeks, HA plus Bone, 40x)

COMPARISON OF HOST TISSUE RESPONSE TO IMPLANTS OF SYNTHETIC
HYDROXYLAPATITE AND ETHYLENE DIAMINE-EXTRACTED BONE

Boyne, P.J., D.M.D., Stringer, D.E., D.D.S., Shafqat, J.P., D.D.S.

Oral & Maxillofacial Surgery Section, Loma Linda University Medical Center,
Loma Linda, California

The tissue response to implantation of hydroxylapatite placed in a subperiosteal tunnel along edentulous alveolar ridges in animals and man would appear to be one of eliciting a loose connective tissue encapsulation of the particles with only those particles adjacent to the host bony surface exhibiting apposition of new bone along the implant surfaces. The similarity between this type of response and the use of ethylenediamine-extracted xenogeneic cortical calf bone, which was developed 25 years ago, but found generally to be clinically unacceptable, is thought to be remarkably similar. In order to compare the relative host responses, a study was undertaken in adult Macaca Mulatta monkeys in which 20-40 particles of ethylenediamine extracted cortical calf anorganic bone (AN) were placed by a tunnel procedure utilizing the tuberculin syringe-technique on the lateral surface of the alveolar ridge on one side of the animal with the contralateral side being implanted with the commonly used clinical form of solid-nonporous hydroxylapatite particles (CHA). The animals were labeled appropriately with Tetracycline at three to four week intervals and sacrifice one-half of each specimen was decalcified and stained with hematoxylin and eosin. The companion-half specimen in each case was treated as a ground-section and photographed under ultraviolet light to determine the degree if any, of host-bone tissue response around the implanted particles. The results of these studies in a total of 12 test sites in Macaca Mulatta monkeys would indicate that ethylenediamine extracted xenogeneic cortical bone particles elicit essentially the same response as hydroxylapatite particles, except for the apparent heightened osteophytic response of the hydroxylapatite particles when they were found adjacent to the host alveolar ridge. The AN bone implants were found to have the same type of connective tissue surrounding each particle as the (CHA) implants. The observations of this study appear to indicate the remarkable similarity of responses of host tissues to these two materials. Additionally, there is an implication that clinical acceptance criteria for a bone substitution implant material may have changed in the last 30 years. Further, the cost factor for extracting and preparing anorganic bone was minimal. This may indicate a product source which would be less expensive than the commercially prepared hydroxylapatite which is now being utilized clinically.

Oral & Maxillofacial Surgery Section
Loma Linda University Medical Center
Loma Linda, CA 92350

Studies on the porous alumina for free standing dental implant
- Animal experiments and clinical observations -

A.YAMAGAMI, S.KOTERA, M.HIRABAYASHI and H.KAWAHARA*

Kyoto Institution of Implantology, Kyoto JAPAN

Many reserchers have reported on the basic reserch of metals, polymers and ceramics. But porous materials has short comings in mechanical strength and hazard of bacterial contamination. H.Kawahara, A. Yamagami and M.Hirabayashi have designed a porous alumina implant with a core made of single crystal alumina to prevent the mechanical breaking and bacterial contamination. This porous material is designed of alumina ceramic with pore sizes average 50 μ and 100-300 μ . Experimental studies on the porous alumina implant were presented at the 2nd Biosimp in Italy(1982) and 61st I.A.D.R. at Sydney(1983).

At the present work, the porous alumina implants were implanted into mandible of rhesus monkeys at the premolor portion to observe biting stress on super structure of the implants. After 4, 6 and 8 months, histological examinations were carried out. To analyse new bone ingrowth into the pore, a light polarizing microscope, SEM, EPA(electron probe analyzer) and histological observation were used. The success rate after 6 years of clinical observation proved to be quite high in free standing implant(Fig), intermediate abutment of long span bridge and free end bridge cases. Out of 16 clinical cases, 3 were failures. 2 of them were failed possibly, due to invasions by microbe into the pore during the operation performance. One which was self-standing failed due to separation of the single crystal core from the porous portion after the 3 years period. After that, sintering technique for porous to single crystal core was improved. In the present time, high successful rate was achieved by immersing the implant into the tissue culture medium of 199 before the insertion.

Contrasting the single crystal alumi-

na with porous implants, 3 months after implantation over biting tests in the single crystal alumina cases, x-rays showed slightly radiolucent space around the surrounding tissue of the implnat, where as in porous implants new bone growth adhered to their surface. However satisfactory biting strength was observed with the single crystal alumina, as well as healthy bone growth. On the other hand in the case of the alumina porous implant showed that the thickness of compact bone was much wider than that of the single crystal alumina.

Furthermore, 1.5 months after the implantation, the porous implants torque was greater than that of the single crystal alumina.

The surrounding tissue showed strong adhesion between gingival tissue and the single crystal post. In the pore, new bone growth was originated from the ceramic surface. In clinical application, this porous ceramic implants have been performed under clinical condition over the 6 years. This alumina porous ceramic implants are potential materials for artificial tooth roots in free standing implants.



Fig. 1 year after operation 6

*Dept. of Biomaterials, Osaka Dental Univ.

COMPARISON OF AROMATIC AND ALIPHATIC POLYETHERURETHANES FOR BIOMEDICAL USE:
BY-PRODUCTS OF THERMAL/HYDROLYTIC DEGRADATION.

R.S. Ward, K.A. White & J.S. Riffle

Thoratec Laboratories Corporation
Berkeley, California

Segmented polyurethanes and polyurethaneureas are the materials of choice for a broad range of implantable and extracorporeal biomedical devices. They are the reaction products of hydroxy-terminated polyether oligomers, chain-extending, low molecular weight diols or diamines and diisocyanates. The latter may be aliphatic, cycloaliphatic or aromatic.

The majority of "biomedical" polyurethanes and polyurethaneureas are synthesized from the aromatic diisocyanate diphenylmethane-4,4'-diisocyanate (MDI). Of all the commercially available diisocyanates, MDI gives the best combination of physical/mechanical properties in thermoplastic formulations and in the spandex elastomers such as Biomer^R and Lycra^R. In the latter the thermodynamic incompatibility of the MDI/ethylene diamine hard segment with the polyether soft segment is thought to be responsible for the extremely low hysteresis behavior and excellent flex life of this class of elastomers relative to aliphatic and cycloaliphatic polyurethanes.

Long flex life is a first order requirement for candidate elastomers in applications like circulatory assist devices, vascular grafts, pacemaker leads and similar biomedical applications. Material failure in these devices can result in immediate and potentially fatal consequences to the device user. Recently there has been increased concern regarding the release of potentially carcinogenic degradation by-products from MDI-based polyurethanes. The formation of urethane from an isocyanate and a hydroxyl is an equilibrium reaction. As temperature is raised urethane groups dissociate back to the hydroxyl and the isocyanate. This process occurs in all polyurethanes during extrusion and molding. Urethane bond reformation is partially responsible for the time-dependence of physical properties seen following melt processing.

If water is present when urethane groups dissociate, it can react with free (di)isocyanate to form the corresponding amine. In the case of the aromatic isocyanates, the hydrolysis product is an aromatic amine or aniline compound, several of which give positive results in the Ames test. The mutagenicity of the corresponding cycloaliphatic diamines is unknown at this time.

Practical considerations require that the polyurethane thermoplastics be processed in the absence of water. Extrusion or molding polyurethanes in the presence of water generates CO₂ in the same reaction which forms free amines. Even a small amount of CO₂ generation produces obvious bubbles and surface defects in the configured product and is easily detectable. Most biomedical devices are used below 40°C. In this temperature range there is no evidence that urethane dissociation occurs at any detectable rate. The only other set of conditions which might be encountered by a device that could result in amine formation are those used in steam sterilization. Manufacturers of biomedical urethanes recommend against steam sterilization for this reason. The 120°C temperature used in the typical autoclave

cycle is sufficient to dissociate urethane bonds and the abundance of ambient water definitely can lead to amine formation. However, for thermoplastic polyurethanes these same conditions produce gross and permanent distortion in the configured part, leaving no doubt about its thermal history. Proper handling and processing of aromatic thermoplastic polyurethanes can effectively prevent the formation of aromatic amines. In reproducing the work of Ulrich and Bonk in our laboratory we could detect no methylene dianiline (MDA) in MDI-based urethanes extruded at standard processing conditions. We do, however, see the need to standardize a sensitive and rapid analytical method capable of detecting MDA in the ppb range. Of the several methods we have evaluated to date, an LC method involving derivatization and a thin layer chromatographic technique appear to be the most sensitive. A procedure used by Szycher et. al. begins with a chloroform extraction step of the solid polymer. The extraction, done at reflux temperatures, is itself capable of inducing degradation in some polyurethanes. When subjected to this process the aliphatic polyetherurethane, Tecoflex^R, was completely solubilized and badly discolored.

Reliable test methods for polyurethane degradation products can supplement molecular weight measurements by GPC in the development of polyurethanes with increased thermal/hydrolytic stability. Because autoclaving is such a severe test for this property, we use it as an accelerated test method to evaluate structure/thermal stability relationships in polyurethaneureas. We have found that the most thermally unstable portion of the polyurethanes based on poly(tetrahydrofuran) glycols is this polyether soft segment, not the hard segment containing the diisocyanate residue. Degradation causes molecular weight reduction with little effect on the polydispersity of the molecular weight distribution. Multiple autoclave cycles causes reduction in tensile strength and an increase in ultimate elongation. With changes in structure and stabilization we have prepared polyurethaneureas which actually increase in molecular weight and strength through several autoclave cycles. The evolution of (toxic) decomposition products such as tetrahydrofuran monomer in these modified materials is reduced concomitantly.

Tecoflex^R, Pellethane^R, Biomer^R, Cardiothane^R and the majority of polyurethanes of interest biomedically, are synthesized from poly(tetrahydrofuran) glycols. Before any subset of this useful class of materials is condemned for its tendency to produce toxic decomposition products, we should better understand the similarities and real differences which exist among them.

Thoratec Laboratories Corporation
2023 Eighth Street
Berkeley, California 94710

IN VITRO AGING OF IMPLANTABLE POLYURETHANES IN METAL ION SOLUTIONS

A. J. Coury, P. T. Cahalan, E. L. Schultz, and K. B. Stokes

Energy Technology, Division, Medtronic, Inc.
Minneapolis, MN 55430

Implantable thermoplastic polyurethane elastomers have provided several advantages over silicones in medical devices such as pacing leads.¹ The lubricity of polyurethanes in aqueous environments is exceptionally high. The toughness of these elastomers allows thin wall insulation and small overall diameters. Inherent blood compatibility reduces the danger of thrombosis and embolization. Under certain forcing conditions of mechanical stress or chemical attack,²⁻⁴ irreversible changes can occur in physical properties or chemical structure.

This study focuses on the effects of certain metallic ion solutions on the properties of thermoplastic polyurethane elastomers and provides evidence for mechanisms and sites of degradation. Such metal ions may be present in the environment of polyurethane components of devices following a primary breach in the device's insulation and may secondarily act as oxidizing agents on the polymer.

Microtensile test specimens of polyurethane elastomers were immersed in solutions of metal ion salts for various periods. Degradation of mechanical properties was approximately directly proportional to: Oxidation potential of the metal ion (Table 1), time, temperature, and salt concentration (Table 2).

The cause of degradation appeared to be primarily oxidative rather than hydrolytic as evidenced by immersion studies using nitric acid (HNO₃), hydrochloric acid (HCl), and sodium hydroxide (NaOH) solutions. Degradation was much more severe in the oxidizing acid, HNO₃, than in the reducing acid, HCl, or the strong base, NaOH.

Oxidative degradation occurred primarily in the polyether "soft segments" of the thermoplastic polyurethanes (Table 3). For example, Pellethane 2363-80A (Upjohn Corporation) showed a greater susceptibility to oxidative changes than Pellethane 2363-55D. The latter contains a smaller percentage of polyether "soft segments." It is, however, a stiffer material and may be inappropriate for certain device designs. A model segmented polyurethane containing short-chain and long-chain diols without polyether was virtually unaffected by strongly oxidizing metal ion solutions or HNO₃.

Oxidation products of the aged polyurethanes were detectable by infrared spectroscopy. Scanning electron microscopy and energy dispersive analysis by X-rays of test specimen cross-sections showed high levels of metal penetration.

A mechanism for the oxidation of polyurethanes is proposed. Via primary insulation breaches in pacing leads, polyurethane elastomers may secondarily be exposed to soluble metal ions (e.g., Ag⁺, Fe³⁺) generated by an electric potential and a conductive pathway (electrolyte) between free metal conductors. The metals become oxidized and enter the electrolyte as soluble salts which participate in the oxidation of the polyurethane.

Table 1
Effect of Oxidation Potential on
Tensile Properties of Polyurethane

Salt	Potential M ¹⁺ +ne ⁻ →M ⁰	Δ Tensile Str. (%)	Δ Elongation (%)
PtCl ₂	ca+1.2	-87	-77
AgNO ₃	+0.799	-54	-42
FeCl ₃	+0.771	-79	-10
Cu ₂ Cl ₂	+ .521	- 6	+11
Cu(OAc) ₂	+0.153	-11	+22
Ni(OAc) ₂	-0.250	- 5	+13
Co(OAc) ₂	-0.277	+ 1	+13

Conditions: Pellethane 2363-80A, .1M salt, 90°C, 5 weeks

*Versus controls aged for 7 days at 90°C in deionized water

Table 2
Aging of Pellethane 2363-80A in AgNO₃ Solution
Under Various Conditions

Salt Concen- tration(M)	Time (Days)	Tempera- ture(°C)	Tensile Str.(psi)	% Elongation
.3	7	37	5200	625
.3	7	90	3750	550
.3	35	37	5500	650
.3	35	90	0	0
.7	7	37	6300	630
.7	7	90	1225	305
.7	35	37	5825	635
.7	35	90	0	0

Table 3
Effect of Ag⁺ on
Polyurethanes of Different Structures

Polyurethane	Comments	Δ Tensile Strength(%)	Δ Elongation (%)
Pellethane 2363-80A	High Polyether	-54	-42
Pellethane 2363-55D	Low Polyether	-23	-10
Model Segmented Polyurethane	No Polyether	0	0

Conditions: 0.1M AgNO₃, 90°C, 35 days

References:

1. Stokes, K. and Cobian, K., "Polyether Polyurethanes for Implantable Pacemaker Leads," *Biomaterials*, Vol. 3, 1982, pp. 225-231.
2. Stokes, K., "The Long Term Biostability of Polyurethane Leads, Stimucor, Vol. 10, 1982, pp. 205-212.
3. Szycher, M., Thermo Electron Corp., ASTM Symposium, "Corrosion and Degradation of Implant Materials," May 9-10, 1983.
4. Pande, G.S., "Thermoplastic Polyurethanes as Insulating Materials for Long Life Cardiac Pacing Leads," *Pace*, Vol. 6, No. 5, Part 1, 1983, pp. 858-867.

Energy Technology, Division, Medtronic, Inc., 6700
Shingle Creek Parkway, Minneapolis, MN 55430

TENSILE AND FATIGUE PROPERTIES OF SEGMENTED POLYETHER POLYURETHANES AND APPLICATION TO BLOOD PUMP DESIGN

K. Hayashi, T. Matsuda, H. Takano, M. Umezu, T. Nakamura, Y. Taenaka and T. Nakatani

National Cardiovascular Center Research Institute
Suita, Osaka, Japan

Besides blood-compatibility, mechanical flexibility and strength are most important requirements of elastomeric polymers used for the diaphragms of artificial heart pumps. Segmented polyether polyurethanes like Biomer® (Ethicon) and Avcothane® 51 (Avco) have been rather widely used in blood pumps in recent years owing to the current favorable experience with these materials. Just recently, Toyobo Co., Osaka, has developed a series of segmented polyurethanes with different molecular weight of soft segment component in collaboration with our research group. The designated Toyobo TM5 polyurethane is being used in our left ventricular assist devices (LVADs).

Mechanical characteristics required of the diaphragm material are flexibility, high strength and long-term durability. Stability of mechanical properties for the duration of applications is also very important for the long-term guarantee of the performance of implant devices. Although we have a lot of blood compatibility test data and tensile test data on many kinds of elastomeric candidates, almost no basic information is available on their fatigue properties.

In selecting a diaphragm material for our LVAD pumps, we have carried out a series of integrated studies on the tensile and fatigue properties of several elastomeric polymers like Biomer®, Avcothane® 51, Toyobo TM5, Texin® MD85A (Mobay) and Hexsyn® (Goodyear). Preliminary experiments by the tensile and fatigue tests in air at room temperature indicated that Biomer® and Toyobo TM5 have more favorable characteristics for our LVAD pump diaphragm than the other polymers. Then, we have studied further the mechanical properties of these two materials by testing them in a saline solution of 37°C to know the moisture effect and in a cholesterol-lipid solution (CL-solution) to study the influence of plasma constituents. Avcothane® 51 has also been studied in these experiments since this material has been used rather widely in cardiac prostheses.

These in vitro mechanical tests have shown that Avcothane® 51 has a few handicaps in terms of mechanical stability, that is, it has fairly unstable mechanical properties under dynamic loading condition. It exhibits a remarkably large stress relaxation in the very early stage of fatigue test in the moist environment possibly due to the plasticizing effect of absorbed water. Soak in a CL-solution of 37°C for 1 month increases the elastic modulus and decreases the tensile strength and ultimate elongation: these change in the tensile properties are enhanced by cyclic deformation. On the other hand, Biomer® showed the most stable behavior under cyclic deformation. There is little influence of the immersion in the CL-solution on the static and dynamic mechanical properties of Biomer®: humidity, temperature and cyclic deformation have some effects.

Toyobo TM5 polyurethane has almost the same tensile strength (4.29kg/mm²) and ultimate elongation (1263%) as Biomer® (4.40kg/mm² and 1231%, respectively), although its flexibility is slightly

worse and less stable. The dynamic elastic modulus of Toyobo TM5 decreases from the original 0.56 kg/mm² to 0.43kg/mm² by the cyclic deformation applied for 1 month in the CL-solution of 37°C under conditions of 50% of mean strain, 10% of strain amplitude and 2Hz of cyclic rate, while that of Biomer® remains unchanged (0.42kg/mm²) during the cyclic deformation. Both water and lipids absorption might occur in Toyobo TM5 and change the mechanical properties.

Although there are a few drawbacks in Toyobo TM5 in terms of mechanical stability compared with Biomer®, we decided to use it for our LVAD pump diaphragms because it has still good mechanical properties and also because a series of polyurethanes with different molecular weight of soft segment component are obtained from the manufacturer. A pusher-plate type of LVAD pump was designed so as to minimize the net stress developed in the diaphragm by the bending and blood pressure forces, taking the mechanical properties of material into consideration.

These pumps were implanted in goats, and used to bypass around 3l/min of blood flow from the left atrium to descending aorta. After pumping for variable periods of time, animals were sacrificed and specimens were cut out from the diaphragms for tensile tests.

It was demonstrated that the implantation in animals remarkably decreased the strength and elongation of the diaphragm. The tensile strength dropped to 60% of that of the non-implanted, virgin material within 1 week after implantation and remained unchanged thereafter for over 2 months. Its elongation decreased gradually and reached 70% of the virgin material 2 months after implantation. The elastic modulus increased very slightly: it became 106% of the virgin material by 2 months implantation. These remarkable change in the tensile properties were primarily ascribed to the contact of material with blood rather than to the cyclic deformation. Comparison with the in vitro test results indicated that the lipid absorption as well as the elution of low molecular weight monomers play important roles in the weakening and embrittlement of the material. Mechanical stability was greatly improved by introducing a refined grade of the same material which contains minimal amount of oligomers.

Acknowledgement: The authors wish to thank Messrs. K. Murayama and M. Tanaka of Toyobo Co. and Dr. T. Tsunetsugu of Sumitomo Bakelite Co. for providing materials used in this study.

Address correspondence to:
Kozaburo Hayashi, Ph. D.
Department of Biomedical Engineering
National Cardiovascular Center Research Institute
Fujishirodai 5, Suita, Osaka 565
Japan

ENVIRONMENTAL STRESS CRACKING IN IMPLANTED POLYURETHANES

Kenneth B. Stokes, Warner A. Frazer and Roger A. Christofferson

Medtronic, Inc., 3055 Old Highway Eight, Minneapolis, MN 55418

Animal implants over several years proved that injection molded Pellethanes (P) 2363-80A and 55D polyether polyurethanes are both biocompatible and biostable¹. Permanent polyurethane (P80A) cardiac pacing leads first used in humans in 1977 now exceed 300,000 implants. Certain models have demonstrated excellent biocompatibility and biostability. Others, however, have experienced varying degrees of failure in their extruded insulation of up to 0.4% verified in one model (0.05% overall)². The principal failure mechanism has been identified as environmental stress cracking (ESC).

The objective of our research is to develop a reasonably rapid method to evaluate the resistance of implanted polymers to ESC. Small pieces of stainless-steel wire were bent into .5" long staple, or figure 8 shapes. These were then inserted in extruded tubing, strained to various elongations (%E), up to 500%, ligated at the ends, tied in strips of three or four, and implanted subcutaneously in rabbits. Explants were made weekly for 12 weeks. Materials tested so far include: P80A, and 55D; Tecoflex (T) EG80A and 60D; and Cardiothane (C)-51 coatings (on P80A). Explants were analyzed by techniques including optical and scanning electron microscopy and surface infrared spectroscopy (IR).

Different results were obtained with P80A depending upon how the tubing was extruded. Specimens extruded with a relatively hot melt temperature and a hot takeoff tank began to fail (2 out of 20 specimens) after four weeks implant at fixed elongations of $\geq 214\%$. From Week 6 through Week 12, all but four out of 50 specimens with $\geq 330\%$ E cracked through (N = 35), suffered ligature cut-through (N = 5) or were severely cracked almost through (N = 6). Only 3 out of 32 specimens with 214% E failed over the 12-week experiment. No failures or surface cracking of any kind was observed on specimens fixed at $\leq 114\%$ E. Thus, a strain threshold (ST) appears to exist between 200 and 330% E, requiring an induction period (I) of about four weeks implant to induce failure. When strained specimens were heated to accelerate stress relaxation, they no longer exhibited ESC failure on implant. Tubing quenched in a cold tank during extrusion began to fail after only one week's implant at elongations $> 200\%$. By Week 6, all quenched specimens with $\geq 100\%$ elongation were failing and surface cracking was beginning to appear on unstrained specimens.

P55D has not cracked at any elongations up to 400% in 12-week experiments. The other polymers tested, however, all exhibited failures with different strain thresholds and induction times as shown in the table.

ESC is defined as the generation of cracks or crazing caused by exposure of articles to certain chemicals and stresses³. Stresses arise from three sources; material processing, device assembly and implant. Some body material (so far

not identified but not water or saline) is absorbed to plasticize the surface, decreasing its tensile strength. If residual skin-core stresses formed during extrusion are high enough, a craze forms, quickly followed by a crack. Extrusion processes that minimizing skin-core effects give results superior to those which maximize residual stresses. Strains generated during device assembly and at implant can accentuate residual stresses. A strain threshold can be reached where neutral axes disappear and cracks can propagate to failure.

EFFECTS OF STRAIN ON IMPLANTED POLYMERS

Pellethane 2363-80	Variable, depending on process. With optimum processing, ST = $> 200\%$ E, I = 3-4 weeks, no evidence of chemical change.
Pellethane 2363-80AE	Variable, depending on lot of raw material. Ranges from 80A to very poor.
Pellethane 2363-55D	Excellent, no cracking of any kind seen, no evidence of chemical change.
Tecoflex EG 80A	ST $< 200\%$, I = 2-3 weeks. Mud-cracked surfaces with IR evidence of oxidation.
Tecoflex EG 60D	ST about 400% E, I = 9-10 weeks, with IR evidence of slight loss of amide ether.
Cardiothane 51	No failure at 300% E up to one year, but occasional shallow surface cracks.

Various polymers are more or less susceptible to the generation of residual stresses, depending upon how easy they are to process. In addition, the absorption of stress-cracking chemicals is dependent upon both the molecular configuration and conformation. Some polymers are susceptible to reactions which can act as ESC initiators, or chemical degradation, per se. Thus, different polymers behave differently, but even the same material processed by various methods can have varying degrees of biostability.

In conclusion, P-55D has the best resistance to strain-induced failure of those polymers tested, followed by T-60D. But these are relatively stiff polymers. Of the softer materials, P80A and C51 coatings have performed the best so far. These conclusions are only valid when the materials have been properly processed.

1. Stokes, K. and Cobian, K.: Polyether polyurethanes for implantable pacemaker leads. *Biomaterials*, 3, 225-231, 1982.
2. Stokes, K.: The long-term biostability of polyurethane leads. *Stimucor*, 10, 205-212, 1982.
3. Whittington, L.R.: Whittington's Dictionary of Plastics. Technomic, Stamford, 1st Edition, 90, 1968.

MECHANICAL AND HISTOLOGICAL EVALUATION
OF INGROWTH INTO DACRON LIGAMENT IMPLANTS

J.L. Berry, J.S. Skraba, W.S. Berg, J. Shah* and J.H. Zoller

CLEVELAND RESEARCH INSTITUTE
at Saint Vincent Charity Hospital
Cleveland, Ohio

INTRODUCTION. Increased participation in recreational activities and in athletics by the general public has been accompanied by an increase in the incidence of various ligamentous injuries. These tissues have poor regenerative capabilities and frequently chronic instability results. Without adequate reconstruction degenerative changes in synovial joints are likely to ensue (1). However, such ligamentous injuries are often difficult to repair or reconstruct. This has led to the current interest in the development of a suitable artificial ligament.

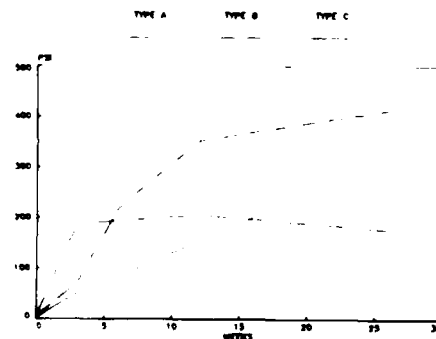
Among the various biomaterials that have been used for this purpose is Dacron mesh fabric. This material has been studied in chickens and monkeys (2). The present study was designed to evaluate the static mechanical and histologic properties of Dacron fabric ligament substitutes of three different weaves.

PROCEDURE. The left and right tibiae of twelve radiographically confirmed adult canines were used as the model. Three types of Dacron material were analyzed: Type A - plain weave; Type B - twill weave; and Type C - weft knit velour. Under aseptic conditions, the medial surface of the proximal half of the tibia was exposed. Two pairs of 5/32" diameter holes were made through both cortices in the proximal and midshaft tibia. The implants were looped through a pair of holes and secured. Sacrifice of the animals occurred at time intervals of 3, 6, 12 and 26 weeks. The implants from the left tibiae provided two pull-out specimens per implant. They were mechanically tested in an Instron Materials Testing system at an extraction rate of 0.5 inches/minute. The interface shear strength was calculated and plotted as a function of time. At each time period there were four data points for each type and type. Implants from right tibiae were examined by microangiography and by light, fluorescence and polarized light microscopy for evidence of tissue reaction and ingrowth.

RESULTS. The data show that fabric B exhibits the greatest strength of attachment to surrounding bone. At 3 weeks Type A and Type B at three weeks show strength less than Type C. However, after 6 weeks Type C has no strength after this time. After 12 weeks Type B appeared to be the strongest, while Type A is apparently the weakest. Similar results are obtained when the data is plotted as a function of time (metaphyseal) versus time (diaphyseal) attachments. With a few exceptions the ligaments implanted into the metaphyseal regions were more strongly attached to bone than the diaphysis. There was no evidence of adverse tissue reaction, grossly or histologically.

DISCUSSION. Our data indicate all three types of Dacron fabric are capable of attachment to bone. It is significant that the fixation made into the metaphyseal region results in a much greater strength than that of the diaphyseal regions. The twill weave (Type B) may be a better choice for eventual strength, but weft knit velour (Type C) offers an extremely rapid early gain in strength prior to three weeks. However, from that point on that fabric virtually exhibits no change in strength. This may be due to the fact that the knit fabric ligament was often damaged in specimen preparation because the free ends of the implant tended to attach to the bone surface. Failure often occurred in the ligament substance rather than at the interface. The choice of fabric type would depend upon the site of implantation and the need for rapid versus eventual interface strength.

INTERFACE SHEAR STRENGTH OF DACRON LIGAMENTS



REFERENCES:

1. Clancy WC, et al.: *JBJS* 63A(8):1270-84, 1981.
2. Kessler S, et al.: *Plastic Recons Surg* 39: 307-10, 1967.

CLEVELAND RESEARCH INSTITUTE
at St. Vincent Charity Hospital
2351 East 22 Street
Cleveland, Ohio 44115

*Elyria Memorial Hospital
Elyria, Ohio 44035

DYNAMIC CHARACTERISTICS OF TENDON

Gurtowski, J., Stern, L., Manley, M.

Department of Orthopaedics, State University of New York at Stony Brook,
Health Sciences Center, Stony Brook, New York 11794

Autogenic, xenographic and artificial materials are currently undergoing clinical trials for tendon and ligament reconstruction. Little attempt has been made to match the properties of the replacements to that of normal ligament and tendon, other than by retrospective comparisons of elastic and structural behaviour (1,2). Data describing the elastic properties of tendon have been published (3,4) but measurements of rheologic or fatigue properties are scant. Our experiments were designed to evaluate the viscoelastic and dynamic characteristics of fresh tendon so that the behaviour of the material can be described more adequately.

Methods In order to improve the accuracy of tendon characterization, specific testing methods for the measurement of specimen cross section, specimen strain and specimen gripping under load were developed.

Precise measurements of tendon cross section were achieved using a laser-optic shadow casting technique during tendon rotation. Calibration showed an accuracy of better than 2% for measured values of tendon cross section. Strain measurements were achieved with a low cost minimally contacting optical strain sensor specially developed for the study. The sensor consists of a bar code scanning and binary counting system which utilizes two high resolution optical reflective sensors which scan gold markers bonded to the tendon. The sensor does not mechanically load the tendon specimen and can be used in a 100% humidity environment.

Tendon grips were custom fabricated from cylinders of PMMA which were split longitudinally, and then individually machined for each tendon sample. After tendon insertion the grips were closed with cyanoacrylate adhesive and radial clamps. The method allowed tendon slippage to be avoided with failure occurring between and not at the grips.

Increasing load was applied to specimens at a strain rate of 7.5mm. per minute in a small tensile testing machine. Modulus, yield and maximum strength were determined. Creep and stress relaxation were measured under static and no load conditions. Fatigue tests were run at a frequency of 0.25hz at constant displacement with an initial applied stress of 20 - 120% of yield for the tendon under study.

RESULTS Creep and stress relaxation results from 12 fresh avian flexor tendons showed time constants of 0.2

± 0.04 secs and 0.14 ± 0.03 secs respectively. The natural frequency of the same tendons calculated from impact test data was 16.1 ± 2.3 Hz with a damping ratio of 0.106 ± 0.05 .

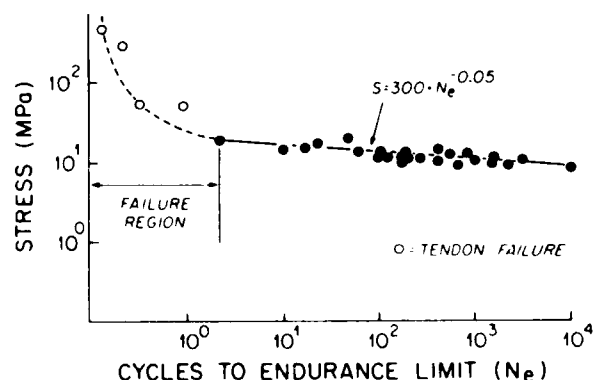
The figure summarizes fatigue data recovered from 30 fresh avian tendons. The curve is a statistical best fit of all fatigue data and shows the correlation between initial stress applied to the tendon and the number of fatigue cycles required to reach tendon endurance or tendon failure. It is noticeable that at levels of applied stress below 1MPa tendon failure did not occur.

Conclusion Testing data from avian and xenographic tendons indicate that the static and dynamic mechanical properties of tendon can be sufficiently described to facilitate development of tendon replacement. The fatigue testing data shows that repetitive loading of specimens does not cause failure as long as the polymer chains are intact and loads do not approach yield. It was found that virtually no reduction in tendon cross section (less than 3%) occurred in those tendons which reached an endurance limit.

References

1. Berg, W. et al Trans. 29 Orthop. Res. Soc. 8: 87, 1983.
2. McMaster, W. et al: J. Biomed. Matl. Res. 10: 259-271, 1976
3. Woo, S.L. et al: J. Orthop. Res. 1, 22-29, 1983.
4. Butler, D. et al: Trans 25 Orthop. Res. Soc. 4: 81, 1979

Address: Orthopaedic Research Laboratories, Health Sciences Center, SUNY at Stony Brook, Stony Brook, N.Y. 11794



COMPARISON OF ANTIGEN EXTRACTED, LYOPHYLIZED AND GLUTARALDEHYDE FIXED
BOVINE XENOGRFT: A PRELIMINARY STUDY

J.C. Tauro, J.R. Parsons, J.C. Ricci, H. Alexander and A.B. Weiss

Section of Orthopaedic Surgery, UMDNJ-New Jersey Medical School,
100 Bergen Street, Newark, NJ 07103

INTRODUCTION - The availability of bovine tendon material makes it potentially desirable for use in the repair of damaged tendons and ligaments in man. The use of bovine tendon, however, is limited by the immune response evoked by any xenograft and the problems of handling, sterility, and the initial and eventual mechanical strength of the graft. In addition, the ideal xenograft should not be inert, but act as a scaffold for host fibroblast proliferation and eventual total remodeling by the host.

The primary antigenic component of mammalian tendon is not found in the collagen fibers themselves, but in the cells and ground substance dispersed within the collagen fiber matrix. This paper describes the development of a bovine tendon xenograft which has been subjected to a chemical extraction procedure. This procedure selectively fractionates and removes cellular material and ground substance while leaving the collagen fibers of the graft relatively intact.

Other investigators have used or are using techniques such as lyophilization or glutaraldehyde fixation of bovine tendon to diminish antigenicity and provide a graft with the necessary mechanical and handling properties^{2,3,4}. In this preliminary animal study, we compared the initial strength and time-dependent in-vivo response of antigen extracted (AE) tendon with glutaraldehyde fixed (GF) and lyophilized (LY) bovine tendon.

MATERIALS AND METHODS - Extensor tendons from the feet of freshly killed steer were removed under sterile conditions and placed immediately in either: 1) Chloroform methanol solution at 25 degrees C. (AE tendons), 2) phosphate buffered pH 7.4 0.2% glutaraldehyde solution (GF tendons), 3) Hanks's Balanced Salt Solution (lyophilized within 2 hours).

The AE tendons remained in chloroform methanol for 18 hours and then were transferred to a pH 7.4 phosphate buffer containing 100 m molar iodoacetic azide at 25 degrees C for 24 hours. The AE tendons were then placed in normal saline with 2% penicillin-streptomycin until implantation. GF tendons remained in 0.2% glutaraldehyde solution for at least 10 days and were rinsed in 1000 cc normal saline for at least 1/2 hour before implantation. LY tendons were rehydrated in sterile normal saline overnight prior to implantation. Similarly sized samples of each type of xenograft were mechanically tested.

The middle 2/3 of the right Achilles tendon of 15 white New Zealand rabbits was removed. Groups of 5 animals received AE grafts, GF grafts, and LY grafts. The xenografts were trimmed to the length and diameter of the excised tendon and then attached end to end using a Bunnel stitch and non-absorbable suture material. One animal from each group was sacrificed at 1, 2, and 12

weeks post-operatively for histological study. Two animals from each group were sacrificed at 12 weeks and the repaired and contralateral normal Achilles-gastroc mechanism mechanically tested to failure.

RESULTS - Examinations of 1 and 2 week specimens revealed an acute inflammatory response to all three graft types. The response to GF graft was judged most severe. At 12 weeks, the GF graft remained encapsulated, acellular, and distinct from host tissue. A chronic inflammatory response was evident. The AE graft and LY graft were incorporated in host tissue and repopulated with fibroblast-like cells. Inflammatory response was much less evident than with GF material.

Mean pre-implantation strengths of similar sized grafts, as well as 12 week post-implantation strengths of the Achilles' repairs are tabulated below:

Graft Group	Strength	Post-Op Strength
Glutaraldehyde	550N	123N, 130N
Lyophilized	445N	246N, 322N
Antigen Extracted	95N	235N, 154N*

*Failure At Grip

DISCUSSION - Glutaraldehyde-fixed grafts have the greatest initial mechanical strength but are poorly incorporated into the host tissue within the time frame of this experiment. This lack of integration and remodeling of the GF tendon ultimately resulted in inferior mechanical strength of the repair. Lyophilized tendon has good initial strength and apparently the best 12 week mechanical strength of repair. Grossly, lyophilized tendon seems to be less well incorporated by the host with less remodeling than the AE tendon. AE tendon has the lowest initial mechanical strength but is well incorporated by the host. The mechanical strength of the AE tendon was noted to decrease with time due to apparent overhydration in the storage solution. Immediate lyophilization after extraction in addition to refinements in the extraction procedure may result in increased initial and eventual repair strength while maintaining the desirable in-vivo host-graft response.

REFERENCES

1. Minami, A et al: The Hand, 14(2):111-119, 1982.
 2. McMaster, WC et al: J. Biomed. Mater. Res., 10: 259-271, 1976.
 3. Cameron, RR et al: Plastic and Reconstructive Surg., 37(1):39-36, 1971.
 4. Flynn, JE et al: JBJS(A), 42(1):91-110, 1960.
 5. Aragona, J et al: Clin. Orthop. Rel. Res., 160:268-278, 1981.
- Orthopaedic Surgery, UMDNJ-New Jersey Medical School, 100 Bergen Street, Newark, NJ 07103

A POLYESTER FIBER REINFORCED POLY-2-HYDROXYETHYLMETHACRYLATE ARTIFICIAL TENDON

C. Migliaresi, L. Ambrosio, G. Guida^o, J. Kolarik⁺, L. Nicolais, D. Ronca^o

Polymer Engineering Laboratory, University of Naples, Naples, Italy

Tendons and ligaments, as most part of biological tissues, are composite structures where the overall properties are a well balanced compromise of the single component properties. In fact they consist of collagen fibers and a matrix which contains gel-like acid mucopolysaccharides and fibroblast cells. The structure and morphology of collagen fibers are rather complicate and not completely elucidated. However their waved shape and the elastic properties of the matrix are responsible for the characteristic tensile properties of ligaments which show low initial elastic modulus up to deformations of 4-6%, followed by a sudden increase in stiffness caused by the alignment of collagen fibers which further resist deformation.

While often tendon or ligament prostheses have been proposed without taking into account the relationships between morphology, properties and functionality, in the design of such biocompatible prostheses these conditions cannot be neglected.

In a previous paper¹ it has been shown that by using the composite mechanics concepts it has been possible to construct a polyethyleneterephthalate fiber/poly-2-hydroxyethylmethacrylate (PET/PHEMA) composite (see Figure 1) for use as tendon or ligament prostheses, where the amount of fibers and their disposition inside the hydrophilic matrix control both mechanical and viscoelastic properties.

In Figure 2 the tensile properties of such composite structure well compare with those of a natural tendon and reported in reference 2.

In this paper a further physical characterization of such prostheses has been performed by means of long term creep experiments on samples immersed in water at 37°C. Moreover clinical response has been studied in rabbits through implants of the prostheses in muscles, for biocompatibility evaluations, and substitutions of tendons and ligaments.

The implants in the tibialis muscle reveal the absence of any inflammatory response and fiber degradation, up to more than one year, and the results obtained on tendon and ligament repair appear to be very promising.

The design parameters, the physical characterization and the clinical performance of the prostheses will be presented.



Fig. 1. Longitudinal and cross views of the PET/PHEMA artificial tendon

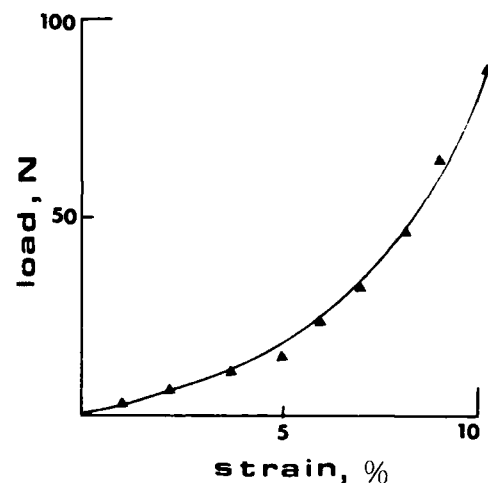


Fig. 2. Load-deformation curve of the PET/PHEMA artificial tendon (full line) and of a natural tendon (triangles, from ref. 2)

1. J. Kolarik, C. Migliaresi, M. Stol, L. Nicolais J. Biomed. Mater. Res., **15**, 147 (1981)
2. R.M. Kenedi, T. Gibson, J.H. Evans, J.C. Barbenel, Phys. Med. Biol., **20**, 699 (1975)

Polymer Engineering Laboratory, University of Naples Piazzale Tecchio, 80125 Naples, Italy

^oII Clinica Ortopedica, I Facoltà di Medicina e Chirurgia, University of Naples, Naples, Italy

⁺Institute of Macromolecular Chemistry, Czechoslovak Academy of Sciences, Prague, Czechoslovakia

D.C. Smith, R. Maijer and D. Ruse

Faculty of Dentistry, University of Toronto
Toronto, Ontario CANADA

In previous work (Maijer, R. and Smith, D.C., J. Biomed. Mater. Res. Vol. 13, pp. 975-85, 1979) it was demonstrated that a solution of polyacrylic acid (PAA) containing sulphate ion would interact with the surface of tooth enamel to produce a needle-shaped spherulitic growth of gypsum crystals nucleated in the surface. This strongly-bonded crystal growth acted to provide a micromechanical interlock with polymerisable monomer compositions used to bond to teeth which had similar bond strength but important practical advantages over the currently used technique of phosphoric acid etching of enamel for bonding. Further studies showed that by suitable adjustment of the PAA molecular weight, concentration, and sulphate concentration the crystal growth could be induced rapidly (60s.) and controlled to provide a bonding interface. More detailed investigation of the crystal growth parameters has now shown that several types of bonded crystals can be grown on enamel in various media but that appropriate conditions allow gypsum crystals to be used as a bonding interface especially suitable for the direct bonding of orthodontic attachments to teeth. The effect of reaction conditions on crystal growth was determined to produce a practically useful treatment technique which yielded acceptable bond strength and resistance to dye penetration in vitro. A clinical trial using this treatment solution was then initiated.

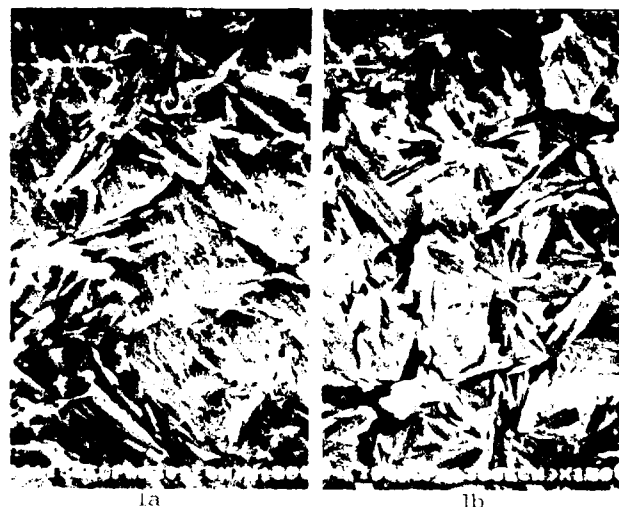
Polyacrylic acid and solutions of various molecular weights were produced by aqueous polymerisation of polyacrylic acid. Concentration and sulphate concentration were varied. PAA solutions containing other anions and similar anionic solutions based on methyl cellulose were also prepared. Bovine enamel from teeth stored at 0-5°C was wet ground on silicon carbide papers up to 600 grit to provide a flat surface for bonding. The prepared surfaces were treated with the appropriate solution washed and dried and a mesh backed stainless steel lingual orthodontic button bonded to the prepared tooth surface using one of several orthodontic bonding resins. After setting the bonds were stored in water and fractured in tension and a bond strength calculated. Leakage was evaluated by immersion in a one per cent Procion Red solution for 30 min. before bond fracture. Crystal growth on the bovine enamel was followed for various treatment times using SEM. The results showed that calcium sulphate crystals could be grown using sulphate solutions in various media such as methyl cellulose. Such growths could yield high bond strengths (7-10 MPa) but some enamel etching occurred than with PAA. Oxalate solutions gave rise to calcium oxalate crystals which could also be made to yield significant bond strengths (4MPa). Polyacrylic acid-sulphate solutions gave bond strength in the range 8-10 MPa which showed only slight fall on water storage or lactic and minimal dye leakage. A suitable solution for practical use contained 35% PAA with a molecular weight of 12×10^3 and was used to

study crystal growth parameters. It was observed that crystal growth on the enamel surface began after 5s and continued for 120s. Too dense a crystal growth inhibited penetration of the bonding resin. It was extremely important to wash away the polyacrylic acid before bonding and drying time was critical. The table shows representative results for tensile bond strength showing the effect of varying contact time, washing time and type of bonding resin. The data shows that a 15-30s contact time with 30-60s washing time gives bond strengths equivalent to those obtained in the phosphoric acid etch technique. The figures show the bond fracture surfaces on the enamel (Fig. 1a) and on the bracket (Fig. 1b). Resin and crystals can be seen adhering to each surface. The tensile bond strength of this specimen was 9.4 MPa. In the clinical trial a cross-over half mouth trial was undertaken on patients. Brackets were bonded using the same resin but with phosphoric acid etch on one side and the crystal bond on the other. A total of 30 patients were treated. After 18 months there was a loss of 10% brackets for the acid etch with 4 white spot lesions versus comparable figures of 9% and 0 for crystal bonding. Debonding and clean up were significantly easier for the latter.

Tensile Bond Strength of Crystal Bonded Orthodontic Buttons to Bovine Enamel

Application Time s.	Washing Time s.	Bonding Resin	Bond Strength 24 hr. MPa
15	15	ST	8.2 ± 0.9
15	30	ST	9.4 ± 1.1
15	60	ST	10.4 ± 1.1
30	60	ST	9.5 ± 1.0
30	60	De-Dy	10.1 ± 1.5
30	60	ST	11.4 ± 1.1
30	60	ST	11.6 ± 1.6*

ST=Solotach D=Delton Dy=Dynabond *30 days storage



1a

1b

H. J. Mueller and C. Siew

American Dental Association, Chicago

INTRODUCTION

Human saliva contains a variety of different types of proteins. Some of these include a high molecular weight mucous glycoprotein and lower molecular weight proline-rich proteins, tyrosine-rich proteins, histidine-rich proteins, and a calcium precipitable protein. The isoelectric points range from strongly acidic to neutral and basic. Previous studies concerned with the corrosion of bioalloys in protein containing solutions have, for the most part, not elucidated upon the effect of protein type on the corrosion process. This consideration may be important in rationalizing the diversity in the corrosion results reported. Some of these have shown inhibition, while others have shown acceleration, and still others no change. Besides the differences in the protein composition and conformation, an additional factor shown to be important in regard to corrosion is the pH of the protein-containing solutions compared to the pI of the proteins. The discrepancy occurring between the laboratory test evaluations of alloys which are usually conducted in salt solutions to their in-service performances may likewise be clarified by the considerations contained herein.

The overall theme contained in this report is to relate the different proteins fractionated from human saliva to their interactional behavior with metallic materials. The particular metallic-protein interactional property chosen to be studied was the binding ability of these proteins to various ions corroded from dental alloys.

MATERIALS AND METHODS

Chilled beakers surrounded by crushed ice were used to collect whole mixed human saliva samples. After collecting about 50 ml, the saliva was centrifuged at 3000 rpm for 15 minutes. The supernatant was decanted into separate vials for further preparative procedures while the residue pellets were discarded. Dialysis membranes of 1000 MWCO were then filled with the saliva supernatant and dialyzed against a 40% solution of polyethylene glycol (M.W. 15,000-20,000) until about 80-90% of the saliva supernatant was reduced in volume. This dehydration process was carried out in a refrigerator and took 4-6 hours. By these procedures 250 ml of supernatant was reduced in volume to about 30 ml which was subsequently stored in smaller sample sizes in a freezer prior to use. Gel filtration chromatography was then carried out with sephacryl S-200 in a 26 mm dia by 60 mm long column contained in a cold chamber and at a flow rate of 1 ml/min which utilized a Tris buffer maintained at a pH = 7 by HCl. The 3 ml eluted fractions were analyzed for absorbance at 280 nm wavelength with a Beckman dual beam grating spectrometer. The void volume of about 150 ml of the column was determined by eluting blue dextrane (M.W. 2×10^6). Calibration for mol-

ecular weight determinations of the unknown saliva fractions was done by eluting standards of ribonuclease A, chymotrypsinogen A, beta-lactoglobulin, bovine serum albumin, and catalase.

Following fractionation, the desired saliva protein fractions were then placed into dialysis membranes and dialyzed using tris buffer at pH = 7 by HCl which had priorly been exposed to Progold (Birdsall Enterprises, Ballwin, Mo.) during a constant current corrosion experiment of 100 microamps for 4 days and appropriately diluted to the desired concentrations. Following filtration, these concentrations of zinc and copper, as well as those inside the membranes were analyzed by atomic absorption spectrophotometry.

RESULTS AND DISCUSSION

The absorbance vs elution fraction number of a 4 ml concentrated saliva supernatant sample shows one strong main band of absorbance of 0.7 towards the end of the elution which corresponds to low molecular weight of around 10,000. Several broad much smaller intensity bands (0.12) also occurred prior to this main band as well as still other similarly smaller intensity bands but of a sharper profile. Combining the fractions which were included by the main band is denoted by F₁₀₇ and used as-is in the binding experiments. A saliva concentrate sample and a corroded Tris buffer pH = 7 which was used as the control, denoted respectively as F_S and F_C, were run at the same time for binding ability. The Table below indicates the concentrations for Cu and Zn for the Tris buffer corroded solution as well as the concentrations of the solutions enclosed inside the dialysis membranes.

Sample	Zinc (ppm)	Copper (ppm)
Corroded buffer	11.1	5.3
F _C	11.4	5.3
F ₁₀₇	12.4	5.5
F _S	34.9	12.5

As can be seen, F₁₀₇ exhibits a small amount of binding to both Zn and Cu, whereas the concentrated saliva sample, F_S exhibits a 2.2 x greater binding for Zn and a 1.4 x greater binding for copper. Not knowing the concentration of the proteins in these fractions makes generalizations and further conclusions unwise to be made at this time. These evaluations have started. NIH DE 05761 support.

American Dental Association Health Foundation
211 E. Chicago Ave.
Chicago, Illinois 60611

THE ADSORPTION TO CALCIUM-HYDROXYLAPATITE OF BIOPOLYMERS, USED TO PRODUCE AN ARTIFICIAL SALIVA

Nieuw Amerongen, A.V., Roukema, P.A., Boerman, J.W., Valentijn-Benz, M., Oderkerk, C.H. and De Groot, K.

Depts of Oral Biochemistry and Biomaterials, Vrije Universiteit, Dental School, 1007 MC Amsterdam, The Netherlands

In saliva several proteins and glycoproteins are present, which can be adsorbed rapidly and strongly to apatite surfaces of natural tooth. To these biopolymers belong both low molecular weight proteins and high molecular weight mucins. The latter compounds consist of a long polypeptide backbone, densely packed with covalently bound oligosaccharide chains. These substances have a high contribution to the viscosity of saliva.

Moreno et al. (1979) reported that small salivary proteins can bind Ca^{2+} strongly, and that saliva can be supersaturated in relation to hydroxylapatite, without precipitation of mineral. On the other hand, adsorbed proteins may be involved in the protection of apatite surfaces against demineralization.

Particularly the latter function is important for the development of appropriate artificial salivas, to relieve xerostomia patients, whose teeth are subjected to a strong demineralization process. Xerostomia patients have a dry, painful mouth. This can be caused by irradiation of the salivary glands in tumor therapy, but also by the use of tranquilizers, especially those which block the autonomic nervous tissue, thereby blocking, among others, the salivary secretion process.

We are interested in studying appropriate artificial salivas, which might have a protecting effect on the oral cavity in general, and particularly:

- on the oral mucosa against infection and inflammation
 - on the apatite surface against demineralization.
- For these reasons artificial saliva should contain biopolymers, such as mucins, which have viscous properties. Mucins are characterized by their terminal carbohydrate on the oligosaccharide chains, and by the presence of sulphate to their amino-sugars.

As starting material Saliva Orthana^R was used, which contains pig gastric mucin (PGM) as a biopolymer ('s Gravenmade and Panders, 1981). This mucin is composed of sialic acid for 3%, which is a negatively charged terminal sugar, and of sulphate for 3%.

For comparison two other mucins were studied, namely human submandibular mucin (HSM), containing 4% sialic acid and 1% sulphate, and ovine submandibular mucin (OSM), containing 25% sialic acid and no sulphate (Roukema and Nieuw Amerongen, 1979).

The adsorption of these mucins was studied with hydroxylapatite (HAP) from Biorad (Biogel-HTP). Portions of 20 mg were washed three times with distilled water and equilibrated with 2 ml of 2 mM phosphate buffer. The adsorbates (200-2000 µg/ml) were then added and the closed tubes rotated end over end at room temperature for 4 to 24 h. After centrifugation the adsorption of the mucins was measured by the determination of sialic acid, sulphate or aminosugar.

The results indicate that the sulphomucin in PGM shows a strong adsorption to HAP, with a maximum binding capacity (in µg/m² HAP) of at least 10-fold higher than that of the sialomucin OSM. The dependence of the adsorption on the pH is compar-

able for PGM and HSM. Both sulpho-sialomucins have still a strong adsorption to HAP at pH 7.0, whereas OSM displays a very low adsorption at this pH. Moreover, the adsorption of OSM at pH lower than 7 is very sensitive to the removal of sialic acid. Even at pH 5.0 hardly any desialo-OSM can be adsorbed. Removal of sialic acid may occur in the oral cavity by the presence of the enzyme sialidase as secreted by oral bacteria, and may have an influence on the adsorption of sialocompounds. In contrast, the adsorption of the sulphate-containing mucins PGM and HSM was influenced only slightly by removal of sialic acid. It is assumed that this is due to the presence of sulphate residues.

From this study it can be concluded that:

- sulphate-containing sialomucins, such as PGM and HSM, adsorb relatively strong to HAP and their adsorption is much less susceptible to the removal of sialic acid, than that of mucins containing only sialic acid, e.g. OSM
- in this respect the sulphomucin PGM in artificial saliva should therefore be preferred to sialomucins derived from ovine and bovine submandibular glands
- it seems that PGM has no direct protecting effect on the demineralization of synthetic HAP at pH 4.6 and 5.0. In that respect phosphocompounds e.g. phytate (myo-inositol hexaphosphate) are much more effective.

REFERENCES

1. Moreno, E.C., Varughese, K. and Hay, D.I. *Calcif. Tissue Int.* 28: 7-16 (1979).
2. 's Gravenmade, E.J. and Panders, A.K. *Front. Oral Physiol.* 3: 154-161 (1981).
3. Roukema, P.A. and Nieuw Amerongen, A.V. In: *Saliva and Dental Caries*, pp 67-80 (1979).

HYPERSENSITIVITY TO MERCURY COMPOUNDS IN ORAL LICHEN PLANUS

A.Hensten-Pettersen*, T.Lyberg** and A.Kullmann*

NIOM, Scandinavian Institute of Dental Materials, Oslo, Norway

INTRODUCTION - Lichen planus is a relatively common inflammatory disease of the skin and mucosa. Lichen planus is an old and familiar disease entity, still little is known about its etiology and pathogenesis. Oral lichen planus has a typical histopathological picture which is characterized by subepithelial band-like infiltrate of mononuclear cells, mainly dominated by lymphocytes. The mucosal infiltrate is composed primarily of T cells, which is strongly suggestive of a cell-mediated immune reaction similar to that seen in delayed type hypersensitivity reactions. One possibility is that small molecular weight substances liberated from dental restorative materials can serve as haptens, which on adsorption and binding to epithelial elements can form complete antigens capable of eliciting delayed hypersensitivity reactions.

MATERIALS AND METHODS - 20 patients with oral lichen planus, 3 men and 17 women, mean age 57 years (range 36-76 years) were studied. The diagnosis was based on clinical and histopathological criteria. In addition, biopsies from 11 patients were also subjected to direct immunofluorescence staining with commercially obtained labelled goat antisera to human IgG, IgM, IgA, C3 and fibrin according to standard techniques. All patients had amalgam restorations. One patient had a chromium-cobalt prosthesis in the upper jaw. All clinical variants of oral lichen planus were represented. The control group included 14 individuals, 1 man and 13 women, mean age 43 years (range 20-69) referred for patch testing to dental materials for other reasons (diverse oral and general symptoms). None of these had signs of lichenoid eruptions on their oral mucous membranes. Patch testing was performed using Finn^R chambers attached to the lateral aspects of upper arm with surgical tape. The patch tests were removed after 48 h and reading was performed after 48 and 96 or 120 h. The test reaction was considered positive if erythema and infiltration, papules or vesiculopapules occurred. The following test substances were routinely employed:

1. Mercury 0.5 % in petrolatum
2. Mercuric nitrate 0.05 % in aq.dest.
3. Mercuric chloride 0.1 % in aq.dest.
4. Phenylmercuric acetate 0.1 % in spir.fort.
5. Merthiolate (as is)
6. Merthiolate 0.1 % in petrolatum
7. Silver nitrate 2 % in aq.dest.
8. Copper sulphate 5 % in aq.dest.
9. Stannous chloride 5 % in spir.fort.

In the one patient wearing a chromium-cobalt prosthesis, nickel sulphate (5 % in petrolatum), potassium dichromate (0.5 % in petrolatum) and cobalt chloride (1 % in petrolatum) were also included.

The patients' responses to mercury compounds were further evaluated by a modified lymphocyte transformation test (LTT). Isolated lymphocytes were incubated for 7 d with the

mercury compounds and DNA synthesis assessed by adding ³H-thymidine 16 h before harvesting the cultures. The IgA, IgG, IgM and C3c levels in plasma were determined with commercial tripartigen immuno diffusion plates.

RESULTS - The present study demonstrated a high frequency of hypersensitivity to mercury compounds in patients with oral lichen planus.

Positive patch test with	Lichen planus patients (n = 20)	Controls (n = 14)
--------------------------	---------------------------------	-------------------

≥ 1 Compound	18	6
≥ 2 Compounds	11	1
≥ 3 Compounds	4	0
≥ 4 Compounds	2	0
≥ 5 Compounds	1	0

80 % of the patients developed skin reactions to merthiolate (as is) which is an irritant. 55 % of the patients had positive patch test to two or more mercury compounds. This high frequency is in accordance with the observations of Finne et al (1982). In contrast, the frequency of positive patch test reactions to mercury in the control group was 7 %. The immunopathologic findings were in good agreement with earlier published results, the presence of a broad band of fibrin at the basement membrane zone being highly characteristic of lichen planus. There were no statistically significant differences between the oral lichen planus and control patients as regards LTT results, IgA, IgG, IgM and C3c levels.

DISCUSSION - Dental amalgam is probably the most common source of contact with mercury in human beings. Although the amounts of mercury liberated from amalgam fillings and further absorbed to the oral mucosa, perhaps is too small to sensitize an individual, the amounts can nevertheless be sufficient to initiate and maintain a local hypersensitivity reaction in otherwise sensitized persons. Similar considerations may also be extended to oral lichen planus in patients wearing dental prosthetic appliances of either chromium-cobalt or acrylic type.

CONCLUSIONS - It is tempting to suggest an etiologic role for mercury (and possibly other haptens derived from dental restorations) in oral lichen planus. Supporting this conclusion is the fact that in 5 of our patients, removal of amalgam fillings and replacing them with composites or precious metals, complete healing of the lichenoid lesions occurred. The present results suggest that replacement of amalgam fillings lying in close contact with oral lichen planus lesions is justified and advisable, and may have important bearings on the therapy of this disease.

REFERENCE - Finne et al., Int. J. Oral. Surg. 1982, 11, 226-239.

* NIOM, Forskningsveien 1, Oslo 3, Norway.

** Department of maxillo-facial surgery, Ullevål Hospital, Oslo, Norway.

THE HEMOGLOBIN HYPOTHESIS: HEMOGLOBIN AND HAPTOGLOBIN SURFACE PROPERTIES

J. Andrade, J. Chen, J. Pierce, R. Lowe, D. E. Gregonis

Department of Bioengineering, University of Utah, Salt Lake City, Utah 84112

INTRODUCTION: The hemoglobin (Hb) hypothesis is based on five somewhat circumstantial pieces of evidence:

1. Horbett has reported [1] that Hb readily adsorbs on apolar surfaces, totally out of proportion to its solution concentration. Surface enhancements range 10 to 100 fold that of other plasma proteins.
2. The Battelle biological infrared spectroscopy group commonly observe IR bands in *in vivo* adsorption experiments which may be related to Hb.
3. Pierce and Andrade [3] have studied the adsorption of various ligand forms of Hb on partially hydrophobic alkyl agarose substrates and found that the adsorption of Hb is dependent on the ligand state of the molecule.
4. Coleman and others in the Artificial Heart Group at Utah observed significant surface discoloration in retrieved artificial heart implants which appeared to correlate with regions of turbulence and perhaps local hemolysis and with actual pumping diaphragm abrasion resulting in local hemolysis [4]. They suggest that the coloration may be due to heme byproducts.
5. It is generally accepted that implants in the arterial and venous systems behave differently perhaps due to pO₂, pH, pressure, and/or flow differences, but perhaps also due to different ligand forms of the Hb which may be present.

It is clear that blood contact with foreign surfaces, even under mild flow conditions results in local hemolysis, in large part dependent on specific surface interactions [5]. Thus Hb may be present in sufficient concentration at local regions where sublethal hemolysis occurs, even though the systemic concentration of the protein may be very low.

Figure 1 summarizes the various forms of hemoglobin. OxyHb when released into the plasma, is rapidly and irreversibly bound by haptoglobin (Hp), a plasma-glycoprotein [6].

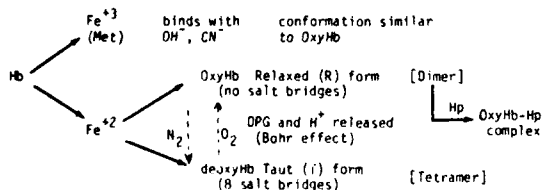


Figure. Different forms and characteristics of Hb. Oxy and deoxy Fe²⁺ are the forms of major clinical interest.

The hemoglobin hypothesis is formulated as follows: If there exists regions of local turbulence or other trauma which can result in local Hb release, that released Hb can adsorb onto foreign surfaces in concentrations orders of magnitude greater than one would expect based on the solution concentration. Hb released on the venous side (in the deoxy form) may adsorb significantly differently than Hb released on the arterial side (in the oxy form and complexed with Hp). This behavior, if it occurs *in vivo*, may be in part responsible for the different blood

compatibility of implants in the venous and arterial system.

If surfaces containing Oxy or deoxyHb, Hp or the Oxy Hb-Hp complex prove to show different blood interactions, then surfaces designed for arterial compatibility may require different properties than those destined for venous application. It may also be that in a complex cardiovascular device where there are regions of local blood turbulence, the surface properties in local regions of blood trauma may even need to be different than the surface properties in other regions of the device.

Results: To date we have only studied the adsorption of pure human Oxy and deoxyHb and, in a preliminary day, human Hp (type 2-2). Details on protein and surface preparation and experimental methods are available (7).

The 60 minute static adsorption data for 0.25 mg/ml pure Hb solutions are given in the table, together with the receding water contact angles as determined by the Wilhelmy plate technique (8), for 5 different surfaces. Note that the adsorbed amounts range from ~ 0.1 to 0.6 Mg/cm² for Oxy Hb and from 0.3 to 0.8 Mg/cm² for deoxy Hb. There is a strong correlation between the adsorbed amounts and the receding water contact angle. The advancing angle does not correlate very well. This is expected as the receding angle is more representative of the interfacial state in aqueous solutions.

Preliminary studies of human Hp adsorption by the total internal reflection intrinsic fluorescence (TIRF) method (9) on both clean (hydrophilic) and silanized (hydrophobic) quartz indicate substantial adsorption which is largely irreversible upon solution dilution. Although Hb adsorption has not been detected by intrinsic UV TIRF due to its very low quantum efficiency (10), Hp is readily detected.

Discussion/Conclusions: Although this work is ongoing, the following preliminary conclusions can be drawn (7):

1. DeoxyHb adsorbs more than Oxy Hb on all surfaces examined (Table). The deoxyHb surface is more hydrophobic than the Oxy form, due to the conformational change upon oxygenation. The increased adsorption of deoxyHb on hydrophobic surfaces may be due to a surface-induced

Table: Hb Adsorbed (μg/cm²) at 60 minutes of exposure to a 0.25 mg/ml H¹⁵-Hb in PBS, pH 7.4, 20°C. (std. dev. ~ 0.1 μg/cm²). θ_{rec} is the receding water contact angle. θ_{adv} is the advancing water contact angle.

Material	Glass	Polyether Urethane	NPS Glass	Poly-styrene	PDM SO
θ _{rec}	2 ± 5°	30 ± 10°	62 ± 10°	70 ± 5°	75 ± 5°
θ _{adv}	15 ± 5°	75 ± 10°	75 ± 10°	88 ± 5°	110 ± 5°
OxyHb	0.21	0.14	0.36	0.56	0.58
deOxyHb	0.37	0.31	0.47	0.72	0.80

dimerization (7), which would make the Oxy Hb dimer more hydrophobic than the deoxy tetramer.

2. The more hydrophobic the surface, the more adsorption of both Hb forms.

References available from senior author.

INTERACTIONS OF PLASMA WITH GLASS: IDENTIFICATION OF ADSORBED PROTEINS

J.L. Brash, P. Szota and J.A. Thibodeau

Depts. of Chemical Engineering and Pathology
McMaster University, Hamilton, Ontario, Canada

Although it is widely recognized that blood-material interactions leading to thrombosis are initiated by protein adsorption there is little or no information regarding the identity of the proteins in the adsorbed layer. Most studies have emphasized the more abundant proteins and adsorption data have been obtained by trace-labelling techniques. However it has been shown (1,2) that the most abundant proteins, e.g. albumin, fibrinogen and IgG, are adsorbed only to a limited extent, suggesting that less abundant proteins may be important components of adsorbed layers. The present paper describes an attempt to identify proteins adsorbed from plasma to glass using a chromatographic column approach. Plasma is first incubated on the column and then washed out. Adsorbed proteins are then eluted and identified by gel electrophoresis and immunoassay.

Exptl: Glass bead columns were prepared using beads of average diameter 50 μ m in columns 30 x 1.5 cm diameter. After equilibration of the column with isotonic Tris buffer pH 7.4, human plasma prepared from blood collected into ACD anticoagulant was loaded on. After a suitable equilibration time, the column was washed extensively with isotonic Tris and then eluted sequentially with 1M Tris pH 7.4 followed by 2% SDS in isotonic Tris. Eluted fractions were concentrated by ultrafiltration and subjected to SDS polyacrylamide gel electrophoresis (SDS-PAGE). Ouchterlony double diffusion immunoassays of eluted fractions were run against various antibodies to human proteins.

Results: Experiments were done using three different types of plasma: (a) normal plasma, (b) plasma diluted by a factor of 200:1 with isotonic Tris, and (c) plasma that had been defibrinated by treatment with the snake venom clotting enzyme Arvin.

With normal plasma incubated on the column for either 3h or 0.5h, the fractions eluted by 1M Tris showed moderately complex SDS-PAGE patterns. Albumin and IgG were shown to be present. Most notably, considerable quantities of plasmin-induced fibrinogen degradation products (FDP) were found and initially eluted fractions contained more FDP than those eluted later. FDP were reported previously on elution of purified fibrinogen (containing a trace of plasminogen) from glass (3). The SDS-eluted fractions contained some undegraded fibrinogen and a major component of MW about 25,000. This species is as yet unidentified; it appears to be a whole protein as opposed to a component polypeptide chain. Several other unidentified components were present in both the 1M Tris and SDS eluates. Ouchterlony analysis showed that the following proteins were probably not present: α_2 -macroglobulin, complement C3, LDL, VLDL, haptoglobin, fibronectin and antithrombin III.

Experiments with diluted (0.5%) plasma showed the following: (a) 1M Tris eluates contained mainly IgG along with a number of high MW

proteins. There was no evidence of FDP. (b) SDS eluates contained undegraded fibrinogen and the unknown major component of MW 25,000.

With defibrinated plasma the proteins eluted by 1M Tris gave gels of considerably increased complexity relative to normal plasma. Major components having MW's of 80,000, 72,000, 69,000, 50,000, 31,000 and 14,000 were observed but no positive identifications have as yet been made. SDS eluates also showed altered gel patterns compared to normal plasma but the 25,000 MW species was again a major component.

Conclusions: (a) Plasma deposits complex, multicomponent protein layers on glass. (b) Adsorbed fibrinogen appears to be degraded by plasmin thus implying that glass surface can activate plasminogen. With diluted plasma adsorbed fibrinogen is not degraded and this may result from the reduced availability of plasminogen for fibrinogen digestion. The same effect may explain previous data using radiolabelled fibrinogen (4) which showed a marked increase in adsorption from diluted plasma. (c) Removal of fibrinogen from plasma leads to much more complex protein adsorption patterns suggesting that in the absence of fibrinogen other proteins are able to compete for surface sites. It may be inferred, in agreement with conclusions drawn by others (5), that fibrinogen plays a key role in blood-material interactions.

References:

- (1) S. Uniyal and J.L. Brash, *Thromb. Haemostas.* 47, 285 (1982).
- (2) W. Breemhaar et al., *Proc. Eur. Soc. Artif. Organs*, p. 295 (1982).
- (3) J.L. Brash and B.M.C. Chan, *Trans. Soc. Biomat.*, 5, 85 (1982).
- (4) J.L. Brash and P. ten Hove, submitted for publication.
- (5) L. Vroman et al., *Blood*, 55, 156 (1980).

Department of Chemical Engineering, McMaster University, Hamilton, Ontario, Canada L8S 4L7.

Supported by the Medical Research Council of Canada and the Ontario Heart Foundation.

R.A. Van Wagenen and J.D. Andrade

Department of Bioengineering, University of Utah, Salt Lake City, Utah 84112

Total internal reflection fluorescence (TIRF) is a versatile method for studying interfacial protein adsorption. The technique utilizes the evanescent, interfacial wave created by total internal reflection to excite fluorescence of proteins both adsorbed to and close to a transparent solid-liquid interface. The fluorescence may be extrinsic if an external fluor is covalently linked to the protein or intrinsic if tryptophan or tyrosine moieties are caused to fluoresce via UV excitation. The TIRF technique permits continuous, real time (1 sec. resolution), *in situ* sensing of protein adsorption and desorption. It is applicable to flat, low surface area polymer films. Intrinsic TIRF [1] has the added advantage of providing fluorescence emission spectra of tryptophan moieties which are sensitive to local microenvironmental conformational changes experienced by adsorbing proteins. Extrinsic TIRF [2] can be utilized to study competitive protein adsorption via the use of different labels. Both approaches must rely upon an independent method (such as isotope label) of quantitating bound fraction, however, modelling studies [3] using internal fluorescence calibration have been reasonably successful in quantitating adsorption.

The IgG adsorption isotherms (25°C) for hydrophilic (h)-quartz and polystyrene (PS) are shown in Figure 1. Intrinsic TIRF detectability limits (10 sec. resolution) were 1 µg/ml C_{bulk} and 2 ng/cm² adsorbed protein. IgG adsorbs more readily to hydrophobic PS at C_b < 0.1 mg/ml. At higher C_b IgG may bind more to (h)-quartz. Indirect quantitation of IgG bound on (h)-quartz indicates about 0.15 µg/cm² at C_b of 1 mg/ml. Both isotherms plateau at C_b ~ 2 mg/ml. Analysis of protein adsorption-desorption rates requires an understanding of both flow cell and interfacial diffusional kinetics. This was empirically determined using 64,000 D fluorescein-Dextran having the same diffusion coefficient as IgG. With high injection and flush shear rates (210 sec⁻¹) 50 seconds were required to attain equilibrium boundary conditions.

Desorption of IgG from (h)-quartz was a linear function of (time)^{1/2}. Moreover, this desorption behavior and rate are statistically identical for IgG surface residence times of 1, 10, 100, and 1000 minutes suggesting that IgG-quartz affinity (and possibly IgG conformation) does not change over a 16 hour period. The IgG desorption behavior on hydrophobic n-pentyl silane (nPS) and PS surfaces is very different in that there are two distinct rates with a break point of about four minutes. See Figure 2. During the first desorption phase from nPS, increasing surface residence time (1, 10, and 100 min.) seemed to enhance the rate. The 100 minute IgG desorbed at a significantly lower rate from nPS in the second phase suggesting conformational changes which enhanced bonding. The first phase IgG desorption rate from PS (10 minute residence) was comparable to nPS (same residence time), however, the second phase rate was much

slower - virtually zero - indicating high irreversibility. Radiofrequency glow discharge (10 sec., 200 µ Hg, 35 watts, O₂ gas) of the PS surface rendered it hydrophilic (θ < 10° and no hysteresis) and the single IgG desorption rate was identical to that of (h)-quartz.

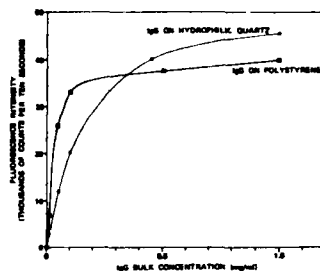


Figure 1. Adsorption isotherms for IgG on PS and (h)-quartz.

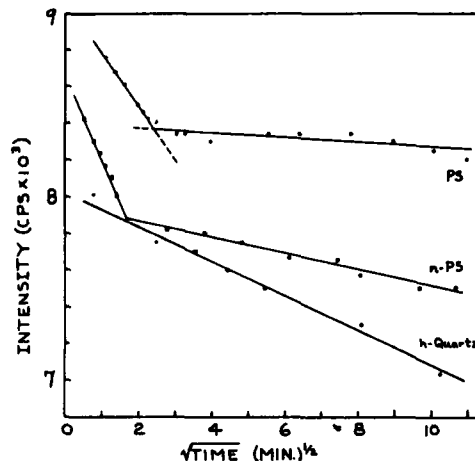


Figure 2. IgG desorption on (h)-quartz, nPS and PS as a function of (time)^{1/2} for surface residence times of 100,000 and 10 min., respectively.

1. R.A. Van Wagenen, S. Rockhold, J.D. Andrade, "Probing Protein Adsorption: Total Internal Reflection Intrinsic Fluorescence," in *Biomaterials: Interfacial Phenomena and Applications*, ACS Series, 199, 351 (1982).
2. B. Lok, Y. Cheng, and C.R. Robertson, *J. Colloid Interface Sci.*, 91, 87 and 104 (1983).
3. S.A. Rockhold, R.D. Quinn, R.A. Van Wagenen, J.D. Andrade, and M. Reichert, *J. Electroanal. Chem.*, 150, 261 (1983).

This work was supported by NIH grant HL18519, University of Utah Biomedical Sciences Support Grant RR07092, and a gift from the Becton-Dickinson Corp.

POLY(ETHYLENE GLYCOL) SURFACES TO MINIMIZE PROTEIN ADSORPTION

D.E. Gregonis, D.E. Buerger, R.A. Van Wagenen, S.K. Hunter, and J.D. Andrade

Department of Materials Science and Engineering, University of Utah, Salt Lake City, Utah 84112

Proteins adsorb to almost all surfaces during the first few minutes of blood exposure, and the amount, type, conformation, and orientation of these bound proteins primarily determines the overall blood compatibility response of the material. To attempt to clarify these protein interactions, it was felt necessary to learn how to minimize or eliminate this irreversible protein adsorption process. Surfaces which minimize protein adsorption are not only of interest for blood-materials interactions but other applications as gel permeation chromatography, contact lens polymers, coatings to minimize biofouling, separation membranes, and surfaces for immunoassay detection methods.

In this work, protein adsorption is measured using total internal reflectance intrinsinc fluorescence (TIRIF) techniques [2] using the inherent fluorescence of tryptophan containing proteins. This method eliminates artifacts sometimes found when using various labelling procedures. Excitation light at 280 nm is totally reflected to a quartz-aqueous buffer interface. Due to the nature of the total reflectance process, the photoenergy exponentially decays into the aqueous buffer. The 280 nm energy is adsorbed by tryptophan in solution and re-emits the light at 330-350 nm. This signal intensity provides a measure of protein concentration at or near the interface. The aqueous buffer is in a thermostated flow cell in which the surface can be challenged with various protein and buffer rinse regimes.

We have found that covalent binding of poly(ethylene glycol) (PEG) molecules to the quartz interface essentially eliminates irreversible protein binding in physiological buffer solutions. To accomplish this bonding, the quartz is treated with vapors of γ -aminopropyl triethoxysilane (APS) to introduce amino groups at the surface. The terminal hydroxyl groups of PEG are reacted with phosgene to form bis- α,ω -chloroformate PEG derivatives. This intermediate reacts with the amino functionalized glass to covalently bond the PEG via a urethane linkage. All these surface reactions are characterized by advancing-receding aqueous contact angles and X-ray photoelectron spectroscopy (ESCA).

The protocol for protein adsorption-desorption at the quartz and modified quartz surfaces use the following solutions: 1) Human immunoglobulin (IgG) (100 mg/100 ml) followed by phosphate buffered saline (PBS), pH 7.4 rinse; 2) Human albumin (4 g/100 ml) followed by PBS rinse; 3) Human serum followed by PBS rinse. The fluorescent counts are normalized to a zero background intensity of the PBS solution and a 10,000 counts fluorescence intensity of 0.10 mg/ml tryptophan monomer calibration solution. The fluorescence counts are now measured after the protein are allowed to adsorb to the surface followed by a thorough rinse of PBS in low shear, laminar flow conditions. These fluorescence signal intensities are shown in the table

below.

Surface	Adsorbed IgG Fluorescence	Adsorbed Albumin Fluorescence	Adsorbed Serum Protein Fluorescence
Clean quartz	25,330 \pm 1,400	--	36,900 \pm 360
APS-quartz	31,840	30,090	128,110
PEG-Mw 750	5,390	5,430	12,500
PEG-Mw 1,900	580 \pm 820	410 \pm 700	9,730 \pm 1,210
PEG-Mw 3,400	590	790	3,630
PEG-Mw 5,000	440 \pm 500	320 \pm 480	2,050 \pm 260
PEG-Mw 14,000	390	390	1,610

From this table, it is shown that PEG effectively minimizes irreversible protein adsorption, and the higher the molecular weight of the bound PEG, the more effective it is for this purpose. Studies are in progress to optimize this PEG binding reaction at surfaces and to determine its hydrolytic stability. Preliminary blood studies of these surfaces have also been performed.

1. This work is funded in part by NIH Grants HL 26469 and HL18519.
2. R.A. Van Wagenen, S. Rockhold, and J.D. Andrade, "Probing Protein Adsorption: Total Internal Reflection Intrinsinc Fluorescence," in S.L. Cooper and N.A. Peppas, (eds.), Advances in Chemistry Series, 199, 353-370 (1982).

Laboratoire de Recherches sur les Macromolécules - GRECO 130048 -
Université PARIS-NORD Avenue J.B.Clément-93430 VILLETANEUSE - FRANCE.

As it is well known from studies of coagulation, heparin is a natural catalyst of the inhibition reaction of thrombin and, therefore, a very anticoagulant drug.

There is a wide variety of heparin-like biomaterials which are used in contact with blood. They include ionic binding of heparin on a solid matrix and numerous attempts where devoted to get blood compatible anticoagulant materials.

On one side, as for instance did R.I. LEININGER (1), ionic bonding of heparin onto suitably polymers have been largely developed. This procedure to immobilize heparin permits the mucopolysaccharide to be gradually released into the blood. Thus, the concentration of mucopolysaccharide near the surface is sufficient for brief periods to avoid the development of thrombin but is gradually diminished over prolonged intervals. Such materials could provide an answer to the problem of temporary prostheses, extracorporeal circulation, catheterism... Thrombogenicity is actually tested with some of such catheters in ex-vivo test in dogs.

On the other side, covalent attachment of the mucopolysaccharide to an appropriate polymer was achieved by specific modification of surfaces with binding of heparin via chemical or radiation-processing treatments. Another approach has been explored for preparing the nonthrombogenic surfaces in which the mucopolysaccharide is treated with cerium IV salt or irradiated with X-rays in order to produce free radicals utilized to induce the polymerization of vinyl monomers. However, these heparin-like biomaterials, i.e. biomaterials which, when placed in suspension in blood plasma, have anticoagulant heparin-like properties, were not suitable for the make of long-term cardiovascular prosthetic devices.

Heparin has also been entrapped in cross-linked gels by chemical or radiation treatments involving polycationic monomers. While the gels were very promising, with regard to their biological activities, the anticoagulant properties of covalently bonded heparin solid surfaces are not very high, generally attributed to a lack of mobility of the heparin chain.

Another variety of heparin-like biomaterials have been achieved either by reaction of N-chlorosulfonyl isocyanate with an unsaturated polymer (for instance 1-4 cis polyisoprene) or by binding sulfonate or amino acid sulfamide groups onto crosslinked polystyrenes or cross-linked polysaccharides. These materials have been proved to be heparin-like.

For instance, the modified polystyrenes or polysaccharides can be assumed to catalyse the antithrombin III-thrombin inhibition reaction. By direct kinetic studies performed on suspensions of the polymer in aqueous solution of

antithrombin III and thrombin, these materials have antithrombic heparin-like activity. In contrast with heparin releasing polymers, the use of such materials for the make of cardiovascular permanent implant appears to be promising.

Ex vivo animal experiments were performed on surface-treated small diameter tubing made of polystyrene-polyethylene copolymers. They showed that no significant platelet adhesion could be observed on the wall of the tubing despite their poor mechanical properties.

Moreover, based on the same principle, heparin-like soluble and biodegradable polysaccharides have been recently developed. The antithrombic heparin-like activity of these materials is strongly dependent upon the percentage of the monomer units bearing the carboxylic and sulfonate groups. They may be used as heparin substitutes of plasma expanders.

- (1) R.I. LEININGER, R.D. FALB and G.A. GRODE
"Blood compatible plastics". Ann. N.Y. Acad. Sci., 146 (1), 11-20 (1968).

A.S. Hoffman

University of Washington
Seattle, Washington, USA

There are a wide number and great variety of clinically important cardiovascular implants and devices. Some may only contact the blood once, and for a relatively short time; others may be exposed to blood for hours, while implants will hopefully last for years, or the lifetime of the patient. All of these implants and devices contain materials which are recognized by blood as foreign; the result is a process of thrombogenesis and thrombosis, sometimes followed by formation of thromboemboli. This process is generally agreed to involve a sequence of protein adsorption steps followed by blood cell interactions (especially involving platelets).

Indeed, one may delineate three possible routes to the formation of blood thrombi: (1) the intrinsic blood coagulation system, involving a series of enzymatic activation steps presumed to begin with the surface activation of prekallikrein to kallikrein, which then activates Factor XII (Hageman Factor), and continues to the formation of fibrin on this surface; (2) the extrinsic blood coagulation system, initiated by the release of a tissue factor (thromboplastin) which can trigger a cascade of enzyme reactions (in a similar sequence to part of the intrinsic system), again leading to fibrin deposition; and (3) the adhesion and aggregation of platelets at the foreign interface, leading to the formation of a platelet thrombus on that surface (Figure 1).

High shear rate (arterial) flow conditions promote thrombi composed largely of platelets; such deposits are called "white thrombi." Low shear rate (venous) flow conditions promote thrombi composed of red cells and platelets entrapped in a fibrin mesh, referred to as "red thrombi." Sometimes, a smooth layer of fibrin may also be deposited. Embolization of the white or red thrombi may produce ischemia and infarction in distal circulatory beds.

The causative mechanisms and prevention of thrombosis and embolization at foreign surfaces continue to be elusive goals of a significant number of researchers world-wide. Most researchers in this field will agree that there are three key system components which can interact in varying ways and to varying degrees, leading to the process of thrombosis and embolization at foreign interfaces. They are: (1) the biomaterial, (2) the nature of the blood flow (or hemodynamics), and (3) the biologic environment. Some of the most important biomaterial surface parameters are listed in Table I.

This presentation will critically review various hypotheses which have been proposed to relate blood-biomaterial responses with the biomaterial surface properties.

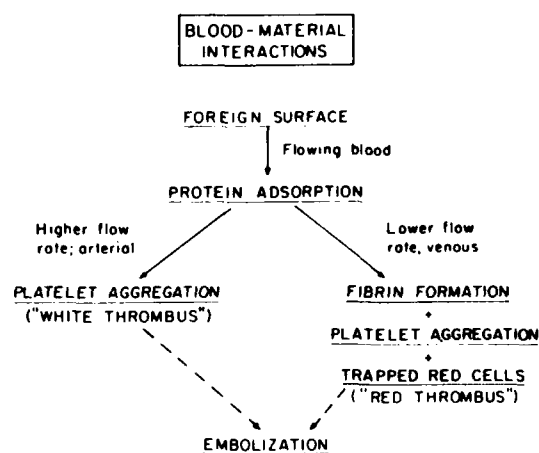


Figure 1. Blood-Foreign Surface Interactions.

Table I. Some Important Biomaterial Interface Parameters which may Influence Blood-Material Responses

1. Surface composition
 - a. polar vs. apolar groups
 - b. acidic vs. basic groups
 - c. H-bonding groups
 - d. immobilized biomolecules, drugs
 - e. double layer effects
 - f. surface energetics (γ_s ; $\gamma^d + \gamma^p + \gamma^h$)
 - g. presence of impurities, particles
2. Water sorption
(surface water structure)
3. Surface crystalline/amorphous structure
4. Surface smoothness, roughness, and porosity
5. Mechanical compliance of surface, bulk
6. Regular or irregular distribution of surface "domains" of the above
7. Bulk leachables (including biomolecules, drugs), degradation products

Allan S. Hoffman
Center for Bioengineering and
Department of Chemical Engineering
University of Washington FL-20
Seattle, WA 98195 U.S.A.

MICROSCOPICAL CHARACTERIZATION OF KNEE LIGAMENTS:
HUMAN AND CANINE STUDIES

H. YAHIA, G. DROUIN AND D. BOBYN

Department of Mechanical Engineering,
Ecole Polytechnique of Montreal, CANADA H3C 3A7

INTRODUCTION

Among the main approaches undertaken for modelling the ligaments, the structural approach which seeks to develop constitutive relations based on the tissue's structure has considerable merits. The parameters of the structural models are physical quantities (1). However, due to a lack of microstructural knowledge of human tissue, various assumptions have been made (2, 3) and structural parameters extrapolated from animal studies (1, 4).

The objectives of this investigation are to obtain the pertinent structural parameters of the human ligaments, and to provide information on the collagen waviness and the collagen-elastin arrangement.

METHODS AND MATERIALS

Samples of human patellar and anterior cruciate ligaments (ACL) were obtained during autopsy performed no later than four hours post-mortem. Canine ligaments were excised immediately after sacrifice. The specimens were prepared by using standard methods for scanning electron microscopy (SEM) and transmission electron microscopy (TEM). Elastin was labelled by using an enzyme-gold technique based on the interaction between an enzyme (elastase) and its substrate (5). Measurements of the structural parameters were made directly on scanning and transmission electron micrographs.

RESULTS

In both human and canine ligaments, it was determined that collagen was assembled in a hierarchical structure. For human ligamentous tissue, the dimensions of the structural units, i.e. fibril, fibre, subfascicle, and fascicle, ranged respectively from 50 to 500 nanometers, 0.7 to 20 micrometers (μm), 50 to 250 μm , and 225 to 1200 μm . These values are larger than those previously reported for canine ligaments (6). It was also observed that the cross-sectional shape of the human ligament fascicle was very irregular. This is in contrast to canine tissue where the shape is roughly triangular.

Two kinds of collagen waviness have been observed in longitudinal sections: periodic and sporadic waviness. Periodic waviness, observed mainly at the subfascicular level, was regular and uniform along the subfascicle. Sporadic waviness occurred randomly at both fibril and fibre levels and was uneven throughout the microscopic sections. Our results also revealed that not all the collagen subfascicles were undulated. Often, only those not densely packed in a fascicle demonstrated undulation.

Within any given species (e.g., human) differences in the periodic waviness parameters (period, amplitude) existed for anterior cruciate and patellar ligaments. In addition, for each ligament type (e.g. anterior cruciate), differences were observed in the periodic waviness parameters for human and canine tissues (Table 1).

Transverse sections revealed that the collagen fibers of the epitenon (loose connective tissue surrounding the fascicules) were perpendicular to

the ligament axis. Those of the paratenon (sheath covering the entire ligament) were arranged in a helical morphology.

Elastin could only be studied ultrastructurally in canine ligaments because the enzyme-gold technique requires specimens fixed immediately post-mortem. The elastin (located on the micrographs by presence of bound enzyme-gold complexes) was found to be localized in the ground substance lying between collagen fibres. Very few gold particles labelling the elastin were observed between the collagen fibrils.

DISCUSSION AND CONCLUSIONS

The present microscopic investigation has shown that the human fascicular shape can no longer be modelled as circular in cross-section.

Also, it is believed that the sporadic waviness observed in the fibrils and fibres is probably an artifact related to the preparation technique of the specimens. It is not likely to be an intrinsic anatomical feature.

Further development of structural models for ligaments should take into account the periodic waviness, the epitenon fibres, and the collagen-elastin arrangements. In addition to collagen and elastin, the remaining component of ligament tissue, proteoglycans, is currently being characterized in order that a complete understanding of the ligament's microstructure and the interactions between its components may be achieved.

	HUMAN		CANINE	
	Period	Amplitude	Period	Amplitude
ACL Ligament	10-30	2-7	7-16	1-4
Patellar Ligament	20-65	4-12	12-45	3-9

Table 1 - Period + amplitude values for human and canine ACL and patellar ligaments (values in micrometers).

1. Thiry, P.S. and al.; ASME Biomech. Symp. 43:271, 1981
2. Lanir, Y.; J. Bioeng. 2:119, 1978
3. Decarmer, W.F. and al.; J. Biomech. 13:463, 1980
4. Kastelic, J. and al.; J. Biomech. 13:887, 1980
5. Bendayan, M.; J. Histochem. Cytochem. 29:531, 1981
6. Yahia, H. and al.; 3rd Int. Conf. on Mech. in Med. and Biol., Compiègne, France, 1982

The authors are grateful to Dr P. Ranger for providing the human specimens and to Dr M. Bendayan for providing the enzyme-gold complexes.

This work was supported by the Natural Sciences and Engineering Research Council of CANADA.

INTRA-ARTICULAR CHANGES RELATED CARBON FIBER RECONSTRUCTION OF ANTERIOR CRUCIATE LIGAMENT

J. Bejui, E. Vignon, D. Hartmann, F. Bejui-Thivolet

Faculté Lyon-Nord - Hôpital Edouard Herriot
69373 Lyon Cedex 08 France

Carbon fibers have been recommended as a suitable material for the replacement of ligaments including the anterior cruciate ligament (A.C.L.) (1,3). In previous works (2), we were not able to create a "new ligament" through an augmentation of the carbon-fibre tow which was due to a foreign body reaction. The present study was conducted to answer the following questions: will the ingrowth of connective tissue around the carbon fibre be improved by the shape of the implant? What is the behavior of the implant in the absence of mechanical stress? Are carbon particles able to disturb the cartilage?

METHODS - 14 adult male Beagle dogs were used. Two groups were studied. First (7 dogs), the A.C.L. was completely excised and replaced by a pyrocarbon coated 3 braids 48 000 filament carbon fiber tow to simulate the 3 bundles of the A.C.L. In the second group (7 dogs), a 16 000 filament carbon fiber braids was implanted crossing the joint on the preserved A.C.L. without tension. The left knees were used as controls. Additionally filaments were coated with vapour phase deposited pyrocarbon to prevent fragmentation without fusing the fibers together and to increase the fiber resistance to shearing forces. Seven months after, the animals were sacrificed. Implants were submitted to mechanical testing in an INSTRON 1026 testing machine. For histological studies, paraffin sections stained with hemalum-phloxine safran were made. Specimens were fixed in formaldehyde for electron microscopy. Gross pathology study of cartilage was conducted according to the method of MEACHIM with Indian ink. A biochemical analysis was performed using the Fixed Charge Density (F.C.D.) method to measure the total glycosaminoglycans (4).

RESULTS - All the animals but one were found to have clinically stable joints with no positive jerk test. On exposure of the operated side, we found the carbon fiber implant covered by whitish fibrous tissue filling the intercondylar notch. In all cases (two groups) the implant was broken in its middle intra-articular portion. The synovium was colored black in all cases. In group 2, no significant difference in the mechanical performance was found with 600 newtons between implanted knees and controlateral A.C.L. In group 1, tissue had grown much better than in previous experiments (2) conducted with only one plaited bundle of 48 000 filaments. Tissue growth occurred in both tensioned and non-tensioned implants. In both groups, individual fibers were surrounded by macrophages and foreign body giant cells were always present between the broken filaments but microstructural organization was less fibrillar and dense as compared with the arrangement of a normal A.C.L. The inguinal and aortic lymph nodes contained carbon particles in three cases. In every operated joint, the trochlea and the patella cartilage showed fibrillations demonstrable by Indian ink staining with occasional small prominent osteophytes at the femoral trochlea margins.

In group 1, a minimal fibrillation was found in the tibial plateaus and femoral condyles in contrast with the gross changes noted in a knee the A.C.L. of which had been cut 7 months before. Osteophytosis and synovitis were less marked after replacement of the A.C.L. However in group 2, small patches of minimal fibrillation and osteophytes were observed on cartilage surfaces. Cartilages from group 1 operated joints had a higher water content than controls and a decrease in the F.C.D. was found. A slight difference was noted between the operated and control joints in group 2.

DISCUSSION - In group 2, carbon fiber implant breakage could be observed without mechanical stress, despite increasing resistance with pyrolytic carbon coating. Thus, failure of the implant is not only likely due to repetitive stresses with low tensile strength. The autogenous tissue cannot take over the mechanical stresses normally associated with a normal A.C.L. A foreign body giant cell reaction to the carbon ligaments was a constant finding but the microscopical observations were different from those found in an organized ligament-like tissue. The direction of collagen fibers appeared to be due only to the long axis of the filaments. The existence of a good clinical evolution may be due to the filling up of the notch by reactive tissue. However it is unlikely that such fibrous tissue can duplicate the subtle working of a normal cruciate (group 1). The incidence of fissurations correlates well with the degree of anterior drawer sign while Indian ink staining shows dissociated arthritis lesions. The degree of osteophytosis is less pronounced than the percentage of fissuration. The reason for a lack of osteophytes remains unclear but the lesions were much less important than after the simple section of the ligament. However in group 2, A.C.L. preserved, cartilage gross changes developed. The decrease in glycosaminoglycan contents and the higher water content rather suggested that the cartilage degenerative alterations occurred with the degradation of carbon materials. Further investigations will be necessary to study the responsibility of carbon fibers coating with pyrolytic carbon in such cartilage degenerative lesions and in the migration of carbon particles.

REFERENCES

- 1 H. Alexander, J.R. Parsons, G. Smith, R. Fong, A. Mylod and A.B. Weiss, Proceedings of the 28 th Annual ORS, Louisiana, New-Orleans, 1982, pp. 45
- 2 J. Bejui, J. Tabutin and F. Perot, in G.D. Winter, D.F. Gibbons and H. Plenk, Jr (Eds), Biomaterials 1980, England, 1982, pp. 295-301
- 3 D.H.R. Jenkins, J. Bone Joint Surg., 6013 (1978) 520-522
- 4 A. Maroudas and H. Thomas, Biochim. Biophys. Acta, 215 (1970), 214-221

Supported by a grant from INSERM PRC 125010, the AICOV Grant and SEP Industry

Faculté Lyon-Nord - Hôpital Edouard Herriot
69374 Lyon Cedex 08 France

Institut Pasteur, radioanalyse 69007 Lyon France

CONNECTIVE TISSUE INGROWTH IN BRAIDED CARBON TOW COMPARED TO UNIDIRECTIONAL CARBON TOW.

Moshe Iusim M.D., David G. Yendes M.D., Y. Soudry M.D., Y. Silbermann Ph.D.
J. Boss M.D., A. Grishkan M.D., D. Mordejovich Dr.V.M., S. Hamburger M.D.

Research Center for Implant Surgery, Haifa Medical Center (Rothschild)
Faculty of Medicine, Technion, Haifa Israel.

Carbon fibers tows have been used as an augmented implant for ligaments and tendons replacement due to mechanical properties. The high tensile strength and flexibility of this material made it attractive for that purpose. However, to provide the biomechanical function of a natural system it should include restoration of its elasticity. Experimental studies by Claes (1) showed that braiding the fibers provided elasticity of the carbon tow which increased with the number of strands in 43° angle. However morphological data on the biological response to the braided tow are not available. The present study was initiated to compare the connective tissue ingrowth in commercially available braided carbon tow (LAFIL) with a longitudinally oriented tow (FLASTAFIL) qualitatively and quantitatively. The carbon implants were used to augment tendons, and this to assuring a continuous load on the new composite system.

MATERIAL AND METHODS

Ten adult mongrel dogs, 15-20 kg. each were used. Under thiopental anesthesia, surgery was performed in all four limbs of each dog in two different sessions, using the quadriceps and triceps tendons. Each tendon was completely cut, distally to the musculotendinous junction and sutured end to end with one tow of carbon fibers. The distal ends of the tow were passed through and through into the muscle and tendon. Eight dogs were reconstructed with unidirectional tows in one side and with braided tows on the other side. Special care was given to achieve a good tension of the carbon fibers at the end of surgery. Two dogs served as control where a sham operation was performed by the tendon division without suture. Two limbs were operated in the same session: a fore limb and the contralateral hind limb. Post operatively the limbs were immobilised in a Plaster of Paris cast which was removed one week later. At that time the dogs were encouraged to be mobile. Sacrifice of the animals was performed at 3 weeks, 6 weeks, 12 weeks and one year postoperatively. From each time interval group eight limbs were available for the following studies: Histological, Histochemical, Biochemical and Biomechanical.

Histologically, half of the specimens were stained with hematoxylin and eosin. Histochemically the same number of cases was stained with toluidine blue, masson and fuchsin. The other half of the material was examined for collagen typing. The hydroxyproline content was examined according to the method of Woessner and the hydroxylisine according to the method of Blumenkrantz and Ashoe-Hansen. The biomechanical properties of the augmented tendons were tested using Instron and compared to the normal and to the control tendons. These last two investigations are currently under process.

RESULTS

Healing of the surgical procedures was

completed in all dogs within two weeks and they could climb stairs and eventually jump on their rear limbs. The gross appearance of the augmented tendons was striking in that the unidirectional tows caused a bulkier neotendon as compared to the braided one and to the control. Histological and histochemical studies showed an extensive and intensive infiltration of connective tissue between the carbon fibers. During the first 3-6 weeks this was dominated by granulation tissue with large number of macrophages, giant cells and capillaries having the same orientation as the carbon fibers. Indeed the fibroblasts, macrophages and the laid down collagen fibers had an intimate cohesive relation with the carbon fibers. The inflammatory response was heavier in the unidirectional augmented tendons at the 3 weeks period as compared to the braided tow augmented tendons. There were more blood vessels and more histiocytic reaction. At the 6 and 12 weeks period, no difference was noted between the two tows where both were massively infiltrated with fibroblasts and collagen well oriented parallel to the carbon fibers. At autopsy, carbon particles were noted in all the regional lymph nodes and in the paraortic nodes in two of the dogs.



Figure 1. On the left: Bundle with unidirectional carbon fibers (FLASTAFIL) consisting of 40,000 fibers. On the right: Braided carbon fiber ligament consisting of 32 tows with 1,000 fibers per tow braided at an angle of 43° (LAFIL). Reference (1) Claes, The elasticity of various carbon fibre ligament prostheses. 2nd Meeting of the European Society of Biomechanics, Strasbourg 1979.

TISSUE REGENERATION ASSOCIATED WITH LACTIDE CONTAINING IMPLANTS

T.N. Salthouse and B.P. Matlaga*

Clemson University, Clemson, South Carolina

INTRODUCTION: Polylactide (and polyglycolide) polymers have been implanted as temporary support and suture materials for more than a decade. They are known to hydrolyse at varying rates in aqueous environments with production of acidic substances including lactate. Polyglactin 910 (copolymer of lactide and glycolide) mesh was applied as a patch graft over aortic defects by Bowald who observed endothelialized arterial tissue ingrowth by 20 days (1). Rapid wound healing of severe abdominal disruption with similar grafts has been reported by French surgeons (2). Recently a polylactide-polyurethane absorbable vascular graft showed excellent regeneration of vascular components including elastin (3). Hollinger has quantitated a positive osteogenic response with polylactide-polyglycolide tibial implants (4). These are but a few examples of the apparent enhancement of tissue regeneration associated with lactide implants reported in the literature.

Recent studies have shown that lactates and lactate dehydrogenase play a pivotal role in wound healing progress (5, 6).

EXPERIMENTAL: Polyglactin 910 (Vicryl) and Dacron® (as control) suture and mesh were implanted in various tissue sites in rats and rabbits and examined at weekly intervals during absorption (10 weeks). Sections stained for collagen, lactate dehydrogenase enzyme activity (LDH) and for the presence and release of acidic components (basic dye binding at pH 2.5) (7) were evaluated.

HISTOLOGIC EVALUATION: Polyglactin 910 implant sites at 1 week revealed a cellular infiltrate surrounding the fibers. Macrophages and fibroblasts (5:2) predominated. Dacron sites were similar. At 2 weeks there was an increase in collagen fibers at polyglactin sites and a lesser increase with Dacron. A substantial addition to the fibrous tissue content of polyglactin mesh sites was seen at 4 weeks in comparison to Dacron. Fibroblastic activity was higher from 2-5 weeks. Methylene blue binding indicated a maximum of acidic release from the polyglactin sites at 3, 4 and 5 weeks. LDH activity was significantly higher with polyglactin implants, peaking at 4 weeks and then declined rapidly during final absorption.

DISCUSSION AND CONCLUSIONS: Evidence from published reports and this study strongly supports the hypothesis that the

presence of hydrolysing polylactide implants in vivo can modify and enhance the tissue regenerative process. The release of lactate and acidic material at lactide implant sites can modulate adjacent cellular activity. The increased LDH enzyme activity in macrophages at polyglactin and polylactide sites is the key to understanding the enhanced collagen regeneration. It has been firmly established that lactate and LDH are essential for the activation of fibroblasts, tissue regeneration and vascular repair. Hunt and others found the highest activity at 2 weeks (5, 6). The release of lactate and acidic material from lactide implants reaching a peak with polyglactin at 4 weeks, can thus supplement and extend the presence of lactate and LDH prolonging the activation of macrophages, fibroblasts and other cells associated with tissue regeneration.

Enhanced wound healing and tissue regeneration has been observed at polylactide and polyglactin implant sites (1-4). There is persuasive evidence that this effect is initiated by the release of lactate and acidic components of implant hydrolysis. This stimulation occurs when the natural release of lactate by macrophages is declining. Thus tissue regeneration may be prolonged beyond the normal expected time span.

REFERENCES:

1. Bowald, S et al: Surg. 86, 722, 1979.
2. Levasseur, JC et al: J. Chir. (Paris) 116, 737, 1979.
3. Gogolewski, S et al: Makromol. Chem. (Rap. C.), 4, 213, 1983.
4. Hollinger, JO: J. Biomed. Mat. Res., 17, 71, 1983.
5. Hunt, TK et al: Am. J. Surg., 135, 328, 1978.
6. Revis, NW et al: Cardiovasc. Res., 12, 249, 1978.
7. Salthouse, TN et al: Surg. Gyn. Obs., 142, 544, 1976.

ACKNOWLEDGEMENT: This study was supported by Ethicon, Inc.

Department of Interdisciplinary Studies,
301 Rhodes Bldg., Clemson University,
Clemson, SC 29631.

*Cell Biology Group, Ethicon Research
Foundation, Somerville, NJ 08876.

RESPONSE TO PARTICULATE POLYSULFONE AND POLYETHYLENE IN AN
ANIMAL MODEL FOR TUMORIGENICITY TESTING

M. Spector, N. Reese and K. Hewan-Lowe

Emory University School of Medicine
Atlanta, Georgia

Since the early 1940's investigators have employed the subcutaneous tissue in the rat abdomen as a site for detecting the tumorigenicity of biomaterials. While it has been recognized for many years that the form of the test material plays a unique role in the "foreign body tumorigenesis" revealed in this animal model, this model has continued to be used to assess the "biocompatibility" of materials. The objective of the present study was to evaluate the response to particulate polysulfone and ultra high molecular weight polyethylene implanted in the subcutaneous tissue of six-week old rats for the period of their lifetime. This investigation was undertaken to reveal the biological response to these specific materials and to better characterize this particular animal model for biocompatibility testing.

One hundred eighty-two (92 males, 90 females) F344 rats, four weeks of age, were obtained from Charles River Co. At sixteen weeks of age the animals were given identifying numbers using a coded system of ear punches and were grouped as follows:

- Group 1, Sham Operated Controls
25 males, 24 females
- Group 2, Polyethylene Particles
34 males, 32 females
- Group 3, Polysulfone Particles
33 males, 33 females

Test materials were particles of medical grade polysulfone* and surgical grade ultra-high molecular weight polyethylene** with a size range of 425-600 μ m (-30 + 40 mesh). The particles were ultrasonically washed in Haem-Sol solution and rinsed in six changes of distilled water. The material was placed into glass tubes and autoclaved. Sixty-five milligrams of the particles were inserted into a pocket made in the subcutaneous layer of the animals. The material was dispersed with 0.5 cc sterile saline. Sham operations were performed in the same manner, the only difference being the absence of the material.

The weight of the rats was recorded at surgery and at monthly intervals. The animals were palpated for signs of tumors at two-week intervals. Rats were killed at the first sign of a tumor at the implant site. Half of the animals surviving 27 months after implantation were sacrificed at that time. The remainder were sacrificed at 28 months of implantation. Necropsy was performed on each animal as soon after death as possible. Specimens taken for histology included the implant site, spleen, liver, kidney, mesenteric lymph node, lung, and any tumor, mass or abnormal organ or tissue.

No tumors formed at the sites of the polysulfone and polyethylene particles, and the sham operated sites. The survival distribution for the animals in each group was similar. Animals not surviving to term a) died of several different causes unrelated to the implants, or b) were sacrificed because of significant tumor or morbidity. There was no significant difference in the weights of the males in the three different groups at selected time periods, postoperatively. The same observation was made for the females, which weighed less than the males. Most of the animals displayed a decrease in weight from the 18th postoperative month to 24 months. This was attributed to their increasing morbidity and age-related changes. Many different types of tumors were found in the animals. There was a high incidence of interstitial cell carcinoma of the testes and many benign skin and salivary gland tumors. No meaningful difference in the incidence of the various types of tumors were recorded for the three groups of animals. The incidences of different tumors in the F344 rats in this study were less than those reported in other studies using the same breed.

Histologically, the tissue responses to the polysulfone and polyethylene particles were comparable. In all instances the particles elicited a foreign body giant cell reaction. Giant cells were apposed to the particles. Cytoplasmic extensions and cells were insinuated between individual particles. Fibrosis occurred around aggregates of particles. It was not possible to identify the presence of particles in macrophages in the spleen or lymph nodes.

The present study demonstrates that polysulfone and ultra-high molecular weight polyethylene in particulate form are not tumorigenic in an animal model often employed to detect tumorigenesis. The foreign body giant cell reaction to the two polymers was similar.

* Union Carbide Corp., Bound Brook, NJ
** Howmedica Corp., Rutherford, NJ

Department of Orthopaedics
Emory University School of Medicine
69 Butler Street
Atlanta, GA 30303

EVALUATION OF POROUS ACRYLIC CEMENT FOR APPLICATION IN RECONSTRUCTIVE SURGERY. ANIMAL EXPERIMENTS AND CLINICAL TRIALS

P.J. van Mullem, J.R. de Wijn¹, J.M. Vaandrager² and M. Ramse-laar³

Dept. of Oral Histology, Dental School, University of Nijmegen, Nijmegen, The Netherlands

Solid acrylic resin was applied for reconstructive treatment of deformities as early as 1940 and still is applied. This long period of use can be understood by its good biocompatibility and easy processability. However, solid acrylic implants become surrounded by a connective tissue capsule. Therefore, implant fixation can be poor and dislocation may result. The development of an in situ curing porous acrylic resin (1) has led to animal experiments in which the material was placed in or against bone. This paper reports on these results (2), on long term experiments and on tissue reactions to porous implants in soft tissues. Moreover, these results are compared to those using solid cement. In addition, the results of clinical trials (2) in which the porous material was used for reconstruction of craniofacial deformities and for soft tissue reconstructions can now be extended to periods of 5 and 4 years resp.

MATERIALS AND METHODS. Cement dough was prepared by mixing polymer powder of a commercial bone cement, purified carboxymethylcellulose (CMC) powder, commercial monomer and water in suitable proportions. After curing, this material contains interconnected pores in which CMC-gel is present. The pore volume was 50%, pore diameter ranged from 300-1000 μ m. In the soft tissue reaction study the dough or solid cement was injected subcutaneously in the back of guinea pigs. Experimental periods were 3 and 8 months and 2 years. In addition, a biopsy from a pectus excavatum correction was obtained. It consisted of in situ cured porous PMMA and surrounding tissue. The implant had served well for 1 year but had to be augmented for esthetical reasons. There were three hard tissue reaction studies. 1) Porous or solid dough was introduced into cavities in the forehead of swine. Experimental periods varied from 2 days to 1 year. 2) Porous material was introduced into extraction cavities in mandibles of beagle dogs. Experimental periods varied from 6 hours to 1 year. 3) Porous or solid cement as augmentation material was applied to monkey skull bone for periods of 3 weeks to 1 year. With some augmentations the tabula externa was removed by chiseling. The implant together with the surrounding bone were fixed, decalcified and processed for embedding in JB4 (Polysciences). This embedding technique permits microscopical observation of hard and soft tissues with the PMMA implant in situ. Seven μ m thick sections were haematoxylin-toluidin blue-acid fuchsin stained. The implants surrounded by subcutaneous tissue were processed for embedding in Paraplast. A step of chloroform was included to dissolve the PMMA. Seven μ m thick sections were haematoxylin-eosin stained.

RESULTS. Animal experiments. Soft tissue reactions. With solid and porous implants giant cells and a low degree of inflammatory reaction were observed. Solid implants were surrounded by a dense connective capsule and appeared to be mobile. In 50% of the cases ectopic hard tissue formation was observed. With porous implants a capsule was less

distinct and collagenous connective tissue entered the pores, thus anchoring the implant to the surrounding tissue. The porous material was well-tolerated by the body over the period of 2 years. **Hard tissue reactions.** Short term reactions (6 hours - 3 weeks) include removal of traumatic necrotic soft tissue and hard tissue resorption with both solid and porous implants. After 3 weeks bone deposition is going to prevail. At 6 weeks bone ingrowth into the pores took place, thus anchoring the implant to the skeletal system. After longer periods both solid and porous implants in the forehead of the pigs were surrounded by a less spongy layer of bone, resembling a lamina dura. After 1 year bone ingrowth appreciable amounts of bone could be observed in the implants. In the augmentations it was observed over a distance of up to 3000 μ m. Otherwise well-vascularised healthy connective tissue was found in the pores. Scattered inflammatory cells and foci were found occasionally with porous and solid implants. Parts of the inner and outer surface were lined with multinucleated giant cells. The implant material is in direct contact with the bone or a thin layer of connective tissue is separating.

Clinical work. Craniofacial reconstructions were performed in 17 patients. In five of these, skull defects were reconstructed by applying the dough directly to the dura. The maximum follow-up is 5 years. After one year one implant became infected and was removed. The others are still in function. Implantation of porous acrylic into soft tissue was performed in 25 cases of the thoracic deformity called pectus excavatum. In 3 patients a sterile seroma developed and the prosthesis was removed. The others, with a maximum follow-up of 4 years, function well. The histology of a 1-year human biopsy did not differ from the 8-month and 2-year porous implants in the guinea pig subcutaneous tissue.

CONCLUSIONS.

The in situ curing porous acrylic cement demonstrated 1) better anchoring to surrounding tissues than solid implants, 2) to be well-tolerated over periods of 1 and 2 years in animals and the human (biopsy) 3) a high degree of clinical success.

REFERENCES.

1. de Wijn, J.R.: J. Biomed. Mat. Res. Symp. 7, 625, 1976.
2. Vaandrager, J.M., van Mullem, P.J. and de Wijn, J.R.: Biomaterials, 4, 128, 1983.

University Depts. of 1) Dental Materials, Nijmegen, 2) Plastic Surgery, Rotterdam and 3) Prosthodontics, Nijmegen, Netherlands.

ADSORPTION CONTROL OF PROTEINS ON COLLAGEN DERIVATIVES

T.Akaike*, Y.Itoh*, T.Miyata**

* Department Material systems Engineering, Tokyo University of Agriculture and Technology Koganei-shi, Tokyo 184 Japan

** Japan Biomedical Material Research Center Meguro, Tokyo 152

It is very important to control the activity of immobilized proteins, such as enzymes, antibody and so on for biomedical applications with the aid of material design. It is necessary to analyze the interaction between polymer support and proteins. Chemically modified collagen (e.g. succinylated collagen, methylated collagen and untreated collagen) were selected as polymer supports. In the first egg white lysozyme which has enzymatic activity for hydrolysis of mucopolysaccharide cell wall structure of such microorganisms as *Micrococcus lysodeikticus* (M.l.) was selected as companion enzyme. Immobilization of egg white lysozyme onto various collagen surfaces coated on glass beads was performed by physical adsorption method and the interaction between the collagen surfaces and egg white lysozyme was analyzed by modified microsphere column method. After immobilization, the enzymatic activity of adsorbed lysozyme for bacteriolysis of *Micrococcus lysodeikticus*. Then the possibility of adsorption control and activity control by designing the chemical structure of collagen was examined.

The results were as follows. (1) The electric charge balance can be varied by chemical modifications of amino groups or carboxyl groups of collagen. (2) The interaction between various collagen membranes and egg white lysozyme is mainly electrostatic, and the amount of adsorbed lysozyme onto the collagen can be controlled by changing the electric charge balance. (Fig.1) (3) High affinity of adsorbed lysozyme to the substrate, M.l. does not necessarily mean high activity of adsorbed lysozyme. (4) The less egg white lysozyme adsorbes onto various collagen membranes, the higher the activity of adsorbed lysozyme is.

The interaction of cytochrome C, -globulin and fibronectin with various modified collagens was examined by the same way as in the case of lysozyme. The amount of adsorbed proteins and the content of ionically adsorbed proteins were also estimated. (Fig. 2) In the adsorption of cytochrome C, which has positive net charge (pI=10.1) succinylated collagen surface attracts much more cyt.C than untreated collagen and methylated collagen. On the other hand, in the case of γ -globulin and fibronectin remarkable difference was not found among three kinds of collagens. The results indicate that the adsorption of γ -globulin is otherwise affected strongly by such nonionic interaction as hydrophobic force. The degree of electrostatic interaction in protein adsorption increases in the order of fibronectin γ -globulin, cytochrome C and lysozyme.

All the results suggest that such a material design of polymer support as chemical modification of collagen is very important in order that both adsorption behavior and function of proteins can be controlled.

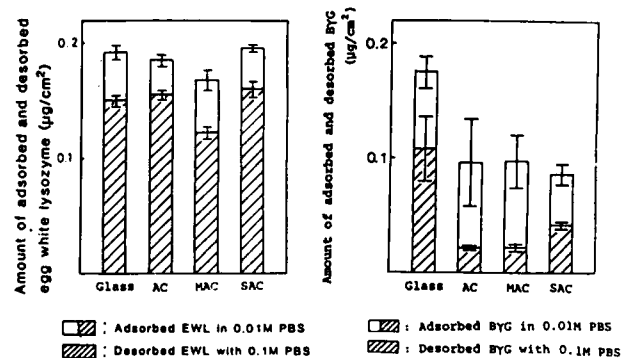


Fig.1
Amount of EWL adsorbed in 0.01M PBS and desorbed with 0.1M PBS

Fig.2
Amount of BYG adsorbed in 0.01M PBS and desorbed with 0.1M PBS

PROBING PROTEIN ADSORPTION: INTERFACIAL FLUORESCENCE AND GAMMA PHOTON DETECTION

D.R. Reinecke, R.A. Van Wagenen, J.D. Andrade, and L.M. Smith

Department of Bioengineering, University of Utah, Salt Lake City, Utah 84112

Total internal reflection interfacial fluorescence (TIRF) measurements are valuable for in situ probing of the quantity, activity, and conformation of protein adsorption at solid-liquid interfaces. Previous attempts to accurately determine with TIRF the quantity of adsorbed protein have relied on several assumptions; most significant is the insensitivity of fluorescence quantum yield to the adsorption process. We have developed a gamma photon counting system to measure protein adsorption in parallel with the TIRF system.

In TIRF, the excitation of the sample is accomplished by the evanescent wave of the internally reflected beam of the monochromatic, polarized light source. The intensity of the evanescent wave falls rapidly with distance t , $I_t = I_0 e^{-2t/\alpha}$ where I_0 is the intensity of the evanescent surface and α is a constant, with the resulting assumption that only a finite layer of sample ("interfacial") is contributing the majority of signal.

Following the development of Van Wagenen, et al. [1], the fluorescence quantum yield of the adsorbed protein, Q_A , can be related to that of the bulk solution, Q_B , as follows:

$$\frac{Q_A}{Q_B} = \frac{[FIU^2]_T}{[FIU^2]_I} \cdot \frac{N_A}{N_B} \cdot \frac{125_{N_B}}{125_{N_A}}$$

Fluorescence counts for bulk and surface adsorbed protein are N_B and N_A , respectively; similarly, 125_{N_A} and 125_{N_B} are the counted γ -emissions of the ^{125}I radiolabelled protein. Evanescent wave intensity integrated across the sample volume is represented by $[FIU^2]_T$ while $[FIU^2]_I$ is that integrated over the adsorbed layer thickness. Clearly, after appropriate sampling geometry and efficiency corrections are applied to the detected gamma emission, the change in quantum yield upon adsorption can be determined.

The protein under study was human γ -globulin (Miles Laboratory) and low activity ^{125}I labelling was achieved by the relatively mild and easy lactoperoxidase-mediated procedure. Tryptophan residues of γ -globulin fluoresce at a wavelength of 335 nm when excited by UV light at 285 nm; this is termed intrinsic fluorescence as no labelling with a fluor is required.

The intrinsic TIRF instrumentation is configured identically to that described by Rockhold, et al. [2]. The flow cell was constructed of an elliptical Silastic^R gasket (.75 mm thick) sandwiched between two hydrophilic quartz slides; cell volume was 0.8 ml and surface area was 22.0 cm². The prism-emission monochromator-photomultiplier tube (Hamamatsu) assembly was placed upon the prism side of the flow field, and the Bicron NaI(Tl) scintillator tube was placed on the other side of the flow cell. A template of 1.3 cm thick aluminum limited the Bicron sensing window to approximately

2.9 cm². Outputs of both detection systems were multiplexed to an Ortec photon counting system, and the data were transferred to an Apple II computer for manipulation and storage.

Experiments were performed with non-adsorptive Na ^{125}I to establish the overall efficiency at about 15%. Minimum detectability (defined as signal/ $\sqrt{\text{background}} \geq 4$) was found to be activity of .008 $\mu Ci/ml$. This sensitivity indicated that for an approximate surface adsorption concentration of .01 $\mu g/cm^2$ an initial labelling specific activity of 100 $\mu Ci/mg$ was required. Concentration effects were negligible as the efficiency remained nearly constant from samples of 5 $\mu Ci/ml$ to .008 $\mu Ci/ml$. There was some concern that the radioisotope labelling procedure might quench the fluorescence of the γ -globulin, but studies with the protein cold-labelled with nonradioactive I^- showed no significant change in the fluorescence spectrum. Additionally, the bound I^- was very stable with little dissociation for periods up to one week.

An essential criterion for these experiments is that radiolabelling does not alter the adsorption properties of the γ -globulin. A previous study has shown that labelling of this protein should indeed not affect its adsorption [3]. Experiments now in progress will verify this for our system; varying the fraction of labelled and unlabelled bulk γ -globulin is predicted to equivalently alter the quantity of detected gamma emission.

If the quantum yield remains constant, the relationship between gamma emission and fluorescence counts for both bulk and adsorbed protein is predicted to be the constant ratio of the field intensities. Preliminary experiments with γ -globulin labelled to an undetermined specific activity show a good linearity with protein concentrations < .1 mg/ml. This suggests that even if there is a change in quantum yield it should be constant and, therefore, easily determined by using γ -globulin of well-characterized specific activity. These investigations are now underway. Some light should also be shed on possible mechanisms of quenching such as adsorbed concentration, temperature, pH, and type of buffer.

1. Van Wagenen, R.A., et al., *Biomaterials*, Cooper, S.L. and Peppas, N.A., Eds., ACS Adv. Chem. Series, 1981.
2. Rockhold, S.A., et al., *J. Electroanal. Chem.*, 150, (1983) 261.
3. Crandall, R.E., et al., *Prep. Biochem.*, 11, (1981) 113.

This work was partially supported by NIH grant NLI8519 and a University of Utah Faculty Grant. We thank Mr. J. Geisler for technical assistance.

Surface Characterization of Protein-Coated Polymer Surfaces by means of Sedimentation Volume

D.R. Absolom, A.W. Neumann, Z. Policova and W. Zingg

Hospital for Sick Children and University of Toronto, Canada

The conformation of protein molecules adsorbed onto cardiovascular implant materials is believed to play a major role in determining the extent of subsequent platelet adhesion and thrombus formation on those surfaces. It is expected that different surfaces will induce different degrees of conformational change for one and the same protein adsorbed onto those materials. For this reason it is of considerable interest to be able to document the extent of conformational change induced in the protein molecules through adsorption onto the various surfaces. These changes will be reflected by differences in the surface properties of the protein-coated materials. This information is, at best, difficult to obtain as the currently available analytical techniques require the pretreatment of the sample in some fashion, or exposure of the protein-coated surface to an air interface, resulting in the introduction of possible artifacts.

We report here on the development of a new technique for determining the surface characteristics of protein-coated materials under non-denaturing experimental conditions. The technique, described below, has been successfully employed to document the varying extent of adsorption induced conformational change of one and the same protein adsorbed onto different polymer surfaces. It also has been used to reveal differences in the surface properties of a single substrate material when coated, under identical conditions, with one type of protein, eg. albumin, obtained from different animal species. These observations have a direct bearing on the use of various animal models for the human situation. The implications of our findings in this regard will be discussed.

Method: The sedimentation volume, V_{sed} , is determined for the protein-coated polymer particles. Monodisperse particles are used as they sediment with a sharp boundary. The V_{sed} measurements were performed as follows: A fixed mass of monodisperse particles of the various polymers were coated under standard conditions of temperature and incubation time with:

a/. varying bulk concentrations of one type of protein;

b/. with the same concentration of one protein obtained from different animal species. After the incubation period the particles were rinsed by a dilution/displacement technique to remove non-adsorbed protein molecules. The protein-coated particles were then resuspended in a standard volume of liquid mixtures of different compositions. The composition was varied by incorporating into the Hanks Balance Salt Solution, small volumes of n-propanol. The n-propanol concentrations ranged from 0.1 to 0.4 % (vol/vol) and gave rise to mixtures with a range of surface tensions from 70.4 to 66.9 ergs/cm². A constant pH was maintained in all cases. At no time were the protein-coated particles allowed to come into contact with an air interface. The particles were then allowed to settle under the influence of gravity for 24hrs after which no further change in V_{sed} occurred. The height of V_{sed} was then measured and plotted as a function of the surface tension of the suspending liquid, γ_{LV} . Maximum V_{sed} occurs when γ_{LV} is equal to the surface tension γ_p of the suspended

protein-coated particle. Under these conditions the Hamaker coefficient for the interaction between the particles becomes equal to zero, i.e. the van der Waals attraction between particles becomes equal to zero implying least close packing of the sediment and hence a maximum of V_{sed} .

Results and Discussion: Table 1 indicates the influence of the bulk concentration of the albumin solution on the resultant surface properties of the coated polymer, in this case nylon 6,6 and Teflon. At the lower bulk concentrations maximum V_{sed} occurs at lower liquid surface tensions indicating that the protein coated surface is more hydrophobic implying increased conformational changes under these conditions of low bulk concentration. The data for the other polymers and three other serum proteins - IgG, fibrinogen and transferrin - will also be presented.

Figure 1 indicates the effect of species origin of the animal protein on V_{sed} . In this case nylon 6,6 particles have been coated with a 1% bulk concentration of purified human, bovine or canine serum albumin under identical conditions. V_{sed} was then determined as a function of γ_{LV} for each species. It is clear that the maximum V_{sed} occurs at a different position for human and canine albumin indicating that the surface properties of the same substrate coated by these two albumins are different and are therefore likely to give rise to differences in the extent of their elicited thrombogenicity. On the otherhand the surface tension of nylon 6,6 coated with human or bovine albumin is the same. Similar data for other serum proteins obtained from the same three animal species has been collected and will be presented. The implication of these findings for the use of the various animal models as a comparison for the human situation will be discussed. Table 1:

Human Albumin Concentration (weight/volume)	Maximum V_{sed} occurs at: (liquid surface tensions)	
	Nylon 6,6	Teflon
5%	69.9	69.9
1%	69.5	68.9
0.1%	65.9	54.2

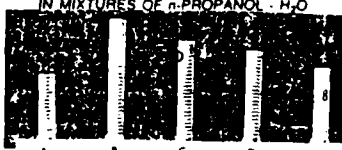
1% BOVINE SERUM ALBUMIN ON NYLON 6,6 IN MIXTURES OF n-PROPANOL - H₂O



1% CANINE SERUM ALBUMIN ON NYLON 6,6 IN MIXTURES OF n-PROPANOL - H₂O



1% HUMAN SERUM ALBUMIN ON NYLON 6,6 IN MIXTURES OF n-PROPANOL - H₂O



The authors acknowledge the support of the Medical and Natural Sciences Research Councils of Canada and the Ontario Heart Foundation. One of us (D.R.A.) acknowledges gratefully the receipt of a OHF Senior Research Fellowship.

TOTALLY BIODEGRADABLE FRACTURE-FIXATION
PLATES FOR USE IN MAXILLOFACIAL SURGERY

R. A. Casper, R. L. Dunn, and B. S. Kelley

Southern Research Institute
Birmingham, Alabama 35255-5305

Introduction:

The need for improved materials for use in the repair and management of maxillofacial injuries is well recognized. Traditionally, metals have been the materials of choice for constructing appliances to aid in fracture fixation. Metals exhibit high values of tensile and compressive modulus and they can be fabricated into fixation hardware by a variety of conventional techniques. However, in maxillofacial repair the need to remove metal implants and the stress-protection effect of rigid metal plates are clear disadvantages. Carbon- or ceramic-fiber reinforced biodegradable aliphatic polyester composites have been fabricated which provide the initial strength and rigidity required for fracture immobilization and the promotion of primary osseous union and gradually decline in strength and rigidity, circumventing the problem of stress-protection atrophy. But these composites are not totally degradable. In this study we have examined the use of an absorbable glass for the preparation of fibers and their use in the reinforcement of poly(DL-lactide) and poly(L-lactide) plates to produce totally absorbable fracture fixation appliances with initially high strength and stiffness.

Materials and Methods:

Films of poly(DL-lactide) and poly(L-lactide) were prepared by centrifugal spin casting from solutions of the polymers in *p*-dioxane. Spin cups were lined with a sheet of Mylar film to prevent the polymer from sticking to the interior of the cups. After the solvent evaporated, the films were removed from the cups and dried at 60 °C in vacuo to remove all traces of solvents. Films were then placed in a hydraulic press under heat and pressure to remove bubbles caused by solvent evaporation.

Glass fibers were prepared by extruding calcium metaphosphate glass from the melt maintained at 1150 °C. Fiber diameter was controlled by controlling extrusion rate. The fiber was then cut into 3 in. lengths for use in plate reinforcement.

Composites were prepared by sandwiching alternating layers of polymer film and glass fiber under heat and pressure to achieve composites with a total thickness of 1/8 in. Glass fiber content of the composites ranged from 30-70% by volume. For all composites the glass fibers were oriented parallel to the long axis of the appliance.

Results and Discussion:

The breaking strength of the biodegradable glass fibers averaged 51,000 psi and Youngs

modulus values exceeded 4×10^6 psi, respectively. Composites fabricated with these fibers and poly(DL-lactide) were found to have flexural strengths and moduli of 13,000 psi and 1.2×10^6 psi, respectively.

Work is currently under way to optimize the strength and stiffness of the composites and to determine the decline in composite properties in vitro. Further work is directed toward a complete evaluation of the biocompatibility of the composites in an animal model.

Acknowledgments:

This study was supported by the US Army Institute of Dental Research under Contract DAMD17-78-C8059.

SOUTHERN RESEARCH INSTITUTE
2000 9th Ave., South
P. O. Box 55305
Birmingham, AL 35255-5305

CHRISTEL P.⁺, CHABOT F.⁺⁺, VERT M.⁺⁺

LABORATOIRE DE RECHERCHES ORTHOPEDIQUES - Faculté de Médecine Lariboisière-Saint-Louis - Paris, FRANCE.

INTRODUCTION

Biodegradable devices for internal fixation of bone require material which maintains suitable initial mechanical properties for at least 4 months post-operatively to allow adequate mineralization of bone callus.

Though the use of bone plates, screws, etc... made of poly (lactic acid) had been suggested several years ago (1), the degradation rates quoted in the literature (2) were, for many years, too high to fulfil the 4-month stability prerequisite.

We have recently found (2) that poly (L-lactic acid), properly synthesized and processed implants up to the time for use can have half-life time of over one year as far as shape and molecular weights are concerned (3).

In order to investigate the fate of these long-lasting implants after implantation, six-hole bone plates elaborated from highly isotactic poly (L-lactic acid) have been fixed on tibiae of sheep for periods of time up to four years.

In this paper, we wish to report some features of the degradation of these plates as monitored by histological examination of implant sites, and by gel permeation chromatography of residual polymeric materials.

MATERIALS AND METHODS

Six-hole bone plates (90 x 14 x 4 mm) were processed by compression moulding of poly (L-lactic acid) obtained by ring-opening polymerization of L-lactide ($M_p = 96^\circ\text{C}$, $[\alpha]_D^{25} = -306^\circ$

for $c = 1,25 \text{ g.100 cm}^{-3}$ in Senzene) at 150°C for three weeks using Zn powder as the initiator. Low molecular weight by-products present in the crude polymer were separated by dissolution in chloroform and further precipitation with methanol. The purified polymer was then compression moulded ($T = 210^\circ\text{C}$, $P = 200 \text{ kg.cm}^{-2}$) to bone plates. These plates were then sterilized using ethylene-oxide and allowed to stand under vacuum for a week.

The plates thus obtained were implanted on sheep tibiae for 5, 13, 24, 36 and 48 months, with metal screws. After retrieval, samples were taken from the plates and conditioned as usual for histologic examination and GPC measurements in dioxane. For GPC, data are given with regard to polystyrene standards.

RESULTS AND DISCUSSION

HISTOLOGY : From 1 to 4 years histology showed a fibrous capsule surrounding the plates with increasing thickness (100μ at 1 year, 800μ at 3 years) and moderate chronic inflammation. Fibrous tissue was always interposed between cortical bone and plate. Giant cells and macrophages were found in direct contact with polymer containing PLA debris. The capsule showed a high degree of vascularization at one year, decreasing later on.

By one year plates exhibited cracks with fibrous invasion that became ossified later on. Plates started to exhibit histological features of degradation by 3 years only at their periphery, the core being fragmented at 4 years. Microradiograms showed a thin remodeled bony layer beneath the

plate only at 1 year. Aortic lymph nodes, spleen, liver, lungs and kidneys were examined at 2 years and did not show any abnormalities or polymer debris.

MOLECULAR WEIGHT CHANGES : Fig. 1 shows GPC chromatograms for various implantation times. Initially, M_{gpc} was 210000 daltons. No more than a 10 to 15 % decrease was observed at 13 months. However, after 24 months, the GPC chromatogram showed a typical bimodal shape similar to those already observed for PGA (4). This bimodal shape agrees with degradation occurring preferentially in the amorphous phase as already suggested from in vitro experiments (4) and alkaline hydrolysis (5). Highly crystalline low molecular weight residues thus formed may explain the well-defined GPC peaks and the slower decrease of M_{gpc} observed in the 36-48 months range. It is note worthy that in this 36-48 month range, the shape of the plate is dramatically affected as the plate turned towards powder and invaded by bony tissue at 48 months.

CONCLUSION

The degradation of long-lasting PLA 100 bone plates show characteristics similar to those of other poly (α -hydroxy-acids) but in an extended time-scale which seems to be suitable for bone surgery.

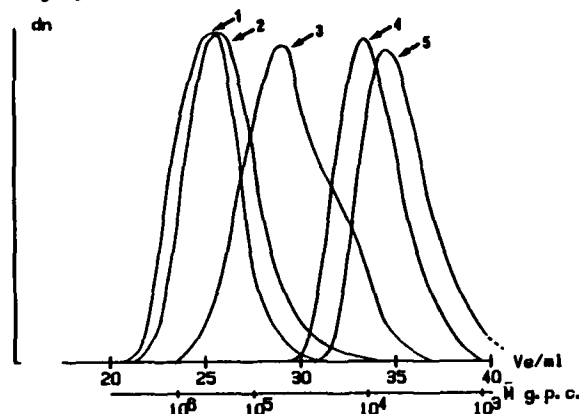


Figure 1 : GPC chromatogram of PLA 100 bone plate residues after various implantation times : 1) 0 and 5 months ($M_{gpc} : 200,000$); 2) 13 months ($M_{gpc} : 160,000$); 3) 24 months ($M_{gpc} : 55,000$); 4) 36 months ($M_{gpc} : 13,000$); 5) 48 months ($M_{gpc} : 7,000$).

REFERENCES

1. R.K. KULKARNI et al., Arch. Surg., 93, 839 (1966).
 2. M. VERT et al., Makromol. Chem., Suppl. 5, 30, (1981).
 3. L. SEDEL et al., Rev. Chir. Orthop., Suppl. II, 64, 92 (1978).
 4. A.M. REED, Ph. D. Thesis, University of Liverpool, 1978.
 5. E.W. FISHER et al., Polym., 252, 980 (1973).
- * Laboratoire de Recherches Orthopédiques
10, avenue de Verdun - 75010 PARIS, France.
** LSM, INSCI Rouen, B.P 8, 76130 Mont-Saint-Aignan, France.

AN ISOELASTIC FIBER COMPOSITE PLATE FOR FRACTURE FIXATION

L. Nicolais, R. Gimigliano°, G. Guida°, C. Migliaresi, S. Pagliuso°, V. Renta°°

Polymer Engineering Laboratory, University of Naples, Naples, Italy

The metal plates actually used in orthopedics for fracture fixation present an elastic modulus much higher than the bones to which they are connected. This difference of rigidity between plates and bones prevents the healing by proliferation of primary callus and results in lower strength of the repaired bone due to excessive stress protection.

Recently a few papers have been published on the preparation and characterization of carbon fiber composite plastic materials to be used as plates for fracture fixation. However, while this composite structure could be designed to fit the mechanical requirements, due to the electrical conductivity of the carbon fibers, corrosion problems cannot be avoided.

In this paper the micromechanics and the lamination theory have been used to design a composite laminate of desired mechanical properties. In particular, assuming that the tensile and torsional rigidity of the bone and the plate are equal, one can write:

$$E_b A_b = E_p A_p = E_p l t$$

$$E_b I_b = E_p I_p = E_p \frac{l t^3}{12}$$

where E is the Young modulus, A the area, I the inertia moment relative to a mass center longitudinal plane, the subscripts b and p refer to the bone and the plate respectively, and l and t are the width and the thickness of the plate.

From the solution of the previous equations, a value of the requested elastic modulus of the prosthesis is calculated once one geometric parameter is opportunely fixed.

In particular for a Kevlar/Epoxy system one can calculate the numbers of laminae at 0, 90 and $\pm 45^\circ$ to achieve the required characteristics.

The experimental results are shown in Figure 1 where a photograph of such plate is reported.

These prostheses have been implanted in animals where it has been possible to follow very clearly the bone healing due to their slight radiopacity of the plate.

Clinical evaluation and histological results are presented.

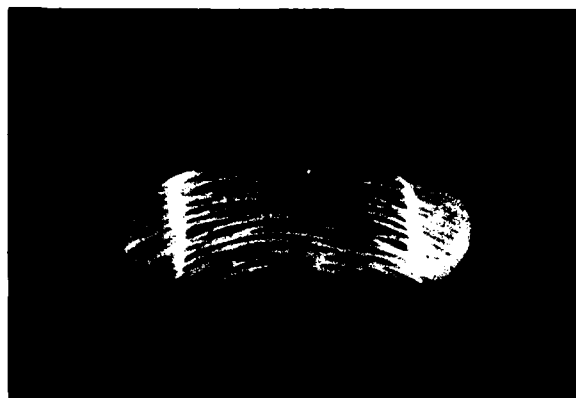


Fig. 1. Longitudinal and cross views of the Kevlar/Epoxy resin fracture fixation plate.

Polymer Engineering Laboratory, University of Naples
Piazzale Tecchio, 80125 Naples, Italy

°II Clinica Ortopedica, I Facoltà di Medicina e Chirurgia, University of Naples, Naples, Italy

°°Aeritalia S.p.A., Pomigliano D'Arco, Italy

FRACTURE FIXATION USING POLYMERIC RODS AND TRANSVERSE SCREWS

Gillett, N.A.*; Brown, S.A.*; Sharkey, N.A.*

Department of Pathology, School of Veterinary Medicine
University of California, Davis, Davis, California 95616

Intramedullary pins are a major method of internal fixation of fractures. Their primary disadvantage is the inability to control rotation. A potential advantage of plastic intramedullary implants is that they can be drilled intraoperatively, allowing the placement of screws distal and proximal to the fracture site to control rotation. Further application of this concept is the fixation of segmental defects; the transverse screws would prevent shortening, yet also provide screw fixation for comminuted fragments. In addition, the implant would not cause stress protection and thus would not require removal. The purpose of this investigation was to evaluate healing of femoral fractures using flexible intramedullary pins with two transverse screws.

Two polymers, a polyacetal (Delrin) and a 30% random short carbon fiber reinforced (CFR) nylon, were used in these experiments. In three point bending, Delrin has a modulus of elasticity of 3.0 GPa, ultimate strength of 70 MPa, and elongation of 75%; the respective values for the CFR nylon are 8.5 GPa, 251 MPa, and 5.4%. Delrin was obtained as a cylinder and turned to rods with diameters of 4mm to 10mm with lengths of 8.5 cm and 11 cm. CFR-nylon was obtained as pre-molded rods with a diameter of 11 mm and length of 11.2 cm. Three groups of animals were used: Group 1 was composed of four adult cats fixed with Delrin pins; Group 2 consisted of two adult mongrel dogs, 25 - 30 Kg, which received Delrin pins; Group 3 was composed of four adult dogs repaired with the CFR-nylon. Two of the animals in Group 3 had the same procedure performed on the opposite femur six weeks prior to sacrifice. The experimental protocol was the same for all of the animals. Under general anesthesia, using sterile technique, a lateral approach to the femur was made. The femur was prestressed in three point bending, notched on the lateral cortex with an osteotome, and then additional stress was applied, producing a transverse fracture. Following reaming of the medullary canal, a metal intramedullary pin with a trocar point was hand drilled through the trochanteric fossa, providing the path for the plastic nail. The plastic pin was then driven retrograde across the reduced fracture using a rod driver and mallet. A transverse metal screw (1.5mm for cats, 2.7 to 3.2mm for dogs) was placed both proximal and distal to the fracture site following predrilling. Routine closure was performed.

Serial radiographs were performed both pre and post operatively, and at 4, 8, and 16 weeks. Fluorochrome labeling of Group 3 was also done at 4, 8, and 16 weeks. The animals were sacrificed at sixteen weeks post surgery. The explanted femurs were cut isolating the screw and fracture sites and then embedded in ethyl methacrylate. Thick sections (200 - 500 microns) were cut on the diamond saw and then hand ground to produce 100 micron sections for

microradiography and fluorochrome analysis. Thin sections (5-7 microns) were cut on a Jung microtome for histologic examination.

All four of the cats in Group 1 had a non-union at sacrifice; one rod broke at 6 weeks post surgery, requiring a second surgery for replacement of the rod. Radiographically all showed a hypertrophic periosteal callus with moderate cortical resorption and some rounding of the callus edges. In Group 2, one dog showed moderate callus formation and bridging at 5 weeks postoperatively. At sacrifice the animal was walking normally and showed good remodeling of the fracture site on xray. The Delrin rod broke in the second dog at 2 weeks post surgery; the animal was deleted from the remainder of the study. In Group 3, at 16 weeks post surgery, two femoral fractures were completely healed and undergoing remodeling with moderate callus formation; two animals had a hypertrophic non union based on gross and radiographic analysis. The contralateral femoral fracture which was six weeks postoperative in two dogs showed moderate callus formation and fragment resorption; bridging was not evident at the time of sacrifice.

Microradiographs and histological examination confirmed the radiographic and gross findings. In addition, an intense inflammatory cell response consisting predominantly of macrophages and eosinophils was present in the popliteal and inguinal lymph nodes of the animals receiving the CFR-nylon rods.

In analyzing the results rods of both polymers appear to have insufficient axial and torsional stiffness. This results in excessive motion at the fracture site producing the hypertrophic non unions seen in the study. The transverse screws aid in controlling rotational instability, however they also prevent axial compression at the fracture site. The improved results obtained with the CFR-nylon rod indicate that a material with greater axial and torsional stiffness might provide sufficient stability at the fracture site to control bending and allow bony union. The fact that both types of materials have been used successfully as plates for fixation of canine femoral fractures would indicate that structural as well as material properties must be considered. Presently, in vitro mechanical testing is being done to measure the torsional and axial strength and stiffness of the pin and screw device to clarify the material and structural properties.

*Department of Pathology, School of Veterinary Med.
University of California, Davis
+Orthopaedic Research Laboratories TB 139
University of California, Davis
Davis, California 95616

BIOCOMPATIBILITY STUDIES OF SILVER-COATED FIXATION PINS

J.A. Spadaro, D.A. Webster, J. Kovach, and S.E. Chase

Department of Orthopedic Surgery, State University of New York (Upstate),
Syracuse, New York.

Previous experiments have demonstrated the inhibition of bacterial growth by electrically activated metallic silver *in vitro* and *in vivo*. This property should be useful in preventing infection near bone fixation pins. We report here early results on the biocompatibility of silver coated pins in rabbit long bones.

METHODS: Ag coated and plain 0.045" smooth Kirschner wires (316L stainless steel) were inserted as half-pins into the tibiae of 2-3 kg NZW rabbits. In Series A (14 rabbits) each animal received *in situ* activated or pre-activated silver plated pins (2) in one side, and plain stainless steel or unactivated silvered pins as controls (2) in the opposite tibia. The pins were drilled slowly and left percutaneous. The animals were sacrificed after 6 weeks. (Fig 1.). In Series B (6 animals) each received 2 *in situ* activated Ag sputtered pins in one tibia, and 2 plain stainless (control) pins in the opposite tibia. These pins were cut short and the skin closed over them (ie., transosseous / buried). This series was sacrificed at 2,4, and 6 weeks. Electrical activation *in situ* was performed by application of 20 μ A direct current (+) to the silvered pins for 15 min. After sacrifice, the pins were studied by: 1) sterile subcutaneous bacterial cultures; 2) peak pull-out force (Instron); and 3) by histological study of the wire tracts.

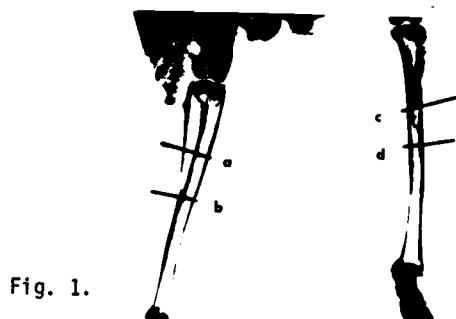
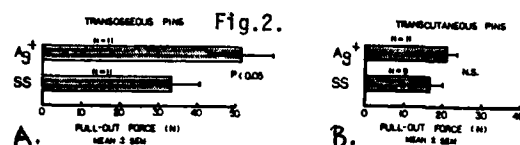


Fig. 1.

POSITIVE PRINT OF X-RAY OF PINS IN RABBIT TIBIAE AT 6 WEEKS. IN SERIES A, a & b WERE ACTIVATED, SILVER COATED PINS AND c & d WERE NON-ACTIVATED SILVER COATED. e & f WERE A STAINLESS STEEL CONTROL PIN. IN SERIES B, a & b WERE ACTIVATED, SILVER COATED PINS AND c & d WERE STAINLESS STEEL CONTROLS.

RESULTS: 1) Bacterial cultures were available from 21 activated silver pin tracts and 13 stainless tracts in Series A. 6/21(28.6%) of the silver and 4/13 (30.8%) of the stainless tracts showed positive cultures, which were identified as *Pasteurella multocida*. 3/7 (42%) of unactivated silver control pins had positive cultures. Active drainage and obvious infection was not observed in any case. Large subcutaneous bulges suggested irritative processes in many cases (all pin types). Series B (buried) implants were uniformly sterile in all cases.

2) Pull out force (Fig 2) for the percutaneous pins (Series A) were about half of that for the transosseous (buried) pins in Series B. For the latter, the activated Ag pins had a statistically significantly higher pull out force than the control stainless pins, although this could have been due to their slightly rougher surface finish.



3) Histological indications of tissue reaction (bone death, resorption, fibrosis, inflammation) and medullary and periosteal bone formation, were graded on a five point scale (0,1,2,3,4) and averaged for each reaction over the implant types. Using equal weighting, the types were compared for overall reactivity. Results (Table I) showed non-significant differences between active silver and stainless controls, although the Series B (buried) implants showed about 40% lower reactivity than the percutaneous rods. Bone growth was not significantly different for silver or stainless, percutaneous or buried rods. Metallic debris particles were observed in the tissue near the silver coated rods and probably indicated flaking of the latter (no pre-drill used).

TABLE I:	MEAN SCORE	
	Active Ag	Stainless
SERIES A:	(n=25)	(n=14)
Reactivity	1.85 \pm 0.69	1.80 \pm 0.59
Bone	2.08	2.18
SERIES B:	(n=14)	(n=11)
Reactivity	1.48 \pm 0.46	1.36 \pm 0.36
Bone	2.14	1.86

CONCLUSIONS: These preliminary studies indicate adequate biocompatibility of electrically activated silver coated antibacterial pins, as compared to control 316L stainless pins *in vivo*. Mechanical fixation was at least equivalent and may have been better for the silver. Percutaneous pins were generally less well fixed and more reactive than buried, transosseous pins. Spontaneous bacterial colonization was the same throughout and may suggest the need for more aggressive activation regimes.

Supported in part by NIH Grant # Am 28203.

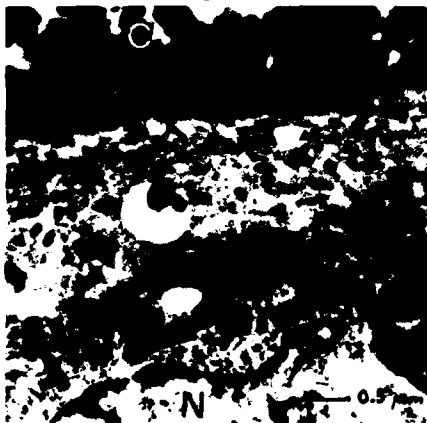
Department of Orthopedic Surgery, State Univ. of New York, 750 E. Adams St., Syracuse, N.Y. USA. 13210.

In recent years research for dental implants has mainly been directed to the bone-implant interaction. Close apposition of bone at the interface of metallic and inert non-metallic materials and bone-bonding mechanisms at the interface of bioglass and glass-ceramics were demonstrated to provide load bearing ankylosis. The mechanisms for epithelial attachment to the neck of an implant, however, are not yet fully understood. Gingival epithelia can form a basal lamina and hemidesmosomes to natural teeth, to vitallium (1), epoxy-resin (2) or titanium (3). Therefore the epithelial attachment to glass-ceramics was investigated.

A new implantation technique was developed to set primary open implants in Sprague-Dawley rats. After the extraction of a lower molar the socket was widened by a twist burr, and a square shaped or cylindrical implant of glass-ceramic KG S (4) or Ceravital^R was inserted. The 44 animals were sacrificed 14 or 30 days post-operatively during glutaraldehyde perfusion. The implants were removed with the surrounding tissue, dehydrated, embedded in acrylate and sliced on a sawing microtome. After staining with Giemsa solution (5), specimens were analysed in the light microscope. Interesting regions of the interface were excised for additional transmission electron microscopy (TEM).

The common findings were food debris or wood-chaff between the glass-ceramic and the bone undergoing resorption or sequestration by a putrid and granulating inflammation. In these cases the epithelium migrates on the inflamed connective tissue without contact to the implant which is often lost.

A few implants were found without foreign bodies or infection. As early as 14 days post-operatively the gingival epithelium in these specimens shows intimate contact to the glass-ceramic (C) in a zone



more than 0.5 mm long. TEM reveals (Fig.1) along the border of the epithelial cells dense structures, which are interpreted to be hemidesmosomes (▲). Between the cell and the ceramic there is an electron-lucent granular seam 100 nm wide, which is probably the basal lamina (BL).

In spite of this attachment, we found an epithelial downgrowth along the implant surface. The apical epithelium consists of 1 to 3 cell-layers, which is in agreement with other observations (1,2). It may be concluded that the formation of an epithelial attachment and the epithelial downgrowth are independent phenomena. In natural teeth such a downgrowth normally does not occur: apical to the epithelium, firmly anchored collagen fibers close the gap between the root surface and the bone. A capsula-like connective tissue does not prevent epithelial downgrowth around an "open" implant. Therefore we think it best to create a structure at the neck of dental implants which permits the tensile anchoring of collagen fibers. For their mechanical interlocking, Squier and Collins(6) found the suitable pore size of implants to be 3 μm or more.

In a limited area of one implant, we found another possibility for functional anchoring of collagen fibers (F) to glass-ceramic material (C) (Fig.2).



The adhesion is mediated by a mineralized interlayer which corresponds morphologically acellular-fibrillar cementum (afC) of roots. The reaction is slightly different from that described for bone bonding of glass-ceramic in a bony implantation bed (6). This implant was situated close to the rats incisor, which is a continuously growing tooth. It is assumed that proliferating periodontal cells migrated from the incisor to the nearby implant surface.

References:

1. James, R., Schultz, R.: Oral Implantology, 4, 294-302 (1973)
2. Listgarten, M., Lai, C.: Journal de Biologie Buccale, 3, 13-28 (1975)
3. Hansson et al.: J.prosth.dent. (in press)
4. Gross, U., Brandes, J., Strunz, V., Bab, I., Sela, J.: J.Biomed.Mater.Res. 15, 291-305 (1981)
5. Gross, U., Strunz, V.: Stain Techn. 52, 217-219, (1977)
6. Squier, C., Collins, P.: J. periodontal.Res. 16, 434-440 (1981)

Prof.Dr.U.Gross, Institut für Pathologie, Klinikum Steglitz der Freien Universität Berlin, Hindenburgdamm 30, D 1000 Berlin 45, Germany

Comparison of Homograft and BioglassTM Implants in a Mouse Ear Model

Merwin, G.E.,*Wilson, J.,*Hench, L.L.

College of Medicine
University of Florida, Gainesville, Florida

Described here are the results of the comparison of homograft incus implantation versus BioglassTM incus replacement, preliminary results of which were presented to this society last year.

The standard against which all materials for use in middle ear ossicular reconstruction are measured is auto or homograft bone or ossicles. Such problems as availability, contouring, storing, etc., have led to research in the development of alternative materials.

In this research we are comparing homograft and BioglassTM incus replacements in the two ears of the same animal. The mouse ear incus replacement model has been previously described. (Merwin et al, 1982) In twenty-three Swiss Webster mice the incus was removed and a previously harvested homograft incus was placed between malleus and stapes in a reversed position. Homograft incuses were stored in 70% alcohol and washed for one-half hour in saline prior to implantation in the left ear. The opposite ear received a BioglassTM rod as an incus replacement. Animals were divided into three groups studied at 1 month, 3 months, and 6 months post implantation. Implants were assessed for position, stability and general appearance of the middle ear and tympanic membrane. Serial sections were done on selected animals from each group.

RESULTS:

Position-Trends in the data indicate that the larger homograft was found on malleus and stapes articular surfaces more frequently than the BioglassTM rod. However, over 50% of both implants were in position at all time intervals.

Stability-Little difference in stability was found between homograft and BioglassTM implants. Again over 50% of implants were stable in both ears at all time periods.

Gross Appearance-A striking difference was seen in the extent of adhesions in the middle ear associated with the homograft implants. Over 80% of homograft ears had marked adhesions at 1 month and 3 months, increasing to 100% at 6 months. BioglassTM implanted ears had minimal adhesions in only 30% of ears at 1 month and 6 months and 56% at 3 months.

Histology-A marked difference was seen between homograft and BioglassTM ears in the nature and extent of the adhesions. Those associated with the homograft were thicker and more cellular. In many cases there was associated mucosal congestion and thickening of the tympanic membrane which did not occur with BioglassTM implants. The capsule around the BioglassTM implant was again found to consist of one or two collagen fibers at all time periods. The homograft incuses showed remodeling with later partial osteoneogenesis by 6 months. Neither type of implant was associated with abnormal tissue fluid or cells of the middle ear.

We can conclude that BioglassTM implants compare well with a standard for ossicular replacement the homograft ossicle.

The apparent difference in maintaining position may relate more to the comparatively larger size and shape of the homograft implant in this model. The appearance of adhesions with the homograft implant while few adhesions occur with the BioglassTM implant in the same animal, and the thin stable capsule associated with the BioglassTM implant suggests an advantage for this biomaterial.

Gerald E. Merwin
Box J-264, JHMHC
University of Florida
College of Medicine
Gainesville, FL 32610

June Wilson
Biomedical Engineering
217 Materials Building
College of Engineering
University of Florida
Gainesville, FL 32610

L. L. Hench
Biomedical Engineering
217 Materials Building
College of Engineering
University of Florida
Gainesville, FL 32610

BIO-PHYSICO CHEMICAL PROBLEMS CONNECTED WITH THE METALLIC
PROSTHESES COATED WITH BIOGLASSES

A.RAVAGLIOLI, A. KRAJEWSKI

INSTITUTE FOR TECHNOLOGY AND RESEARCH ON CERAMICS OF C.N.R. -
FAENZA (ITALY)

INTRODUCTION

The requirement to coat metallic prostheses with bioglass arises from the well-known problems linked to the direct contact between tissue and metal (1). For the adhesion glass-metal studies, the Authors addressed to Dietzel's studies and recent advanced theoretical investigations (2). Not much is known about the strength linking the molecules of the glass to the metal ones. Besides, there is a disagreement between the hypothesis supporting a bond of chemical nature and the physico-mechanical trend. The studies carried out by the Authors (3) let one think of the concurrence of the two theses, with a key role played by the chemical side. The composition shows a great influence on the macroscopic properties involved in the intricate phenomenon of the adhesion for which one must take into account many parameters as linear expansion coefficient, contact angle for a good wettability; structure of glassy network, etc. (4). Actually, the Authors analyzed the behaviour of the doping agents, substances added in small percentages, to demonstrate their influence as a chemical participation to the overall correlations involved in the glass-metal adhesion. At first, the Authors thought of influencing only the expansion coefficient, according to Winkelman and Scotch theory. A great influence was displayed, e.g. on the tearing test (measured as tensile uniaxial traction) given by different combinations among doping substances. Particularly, they ascertained the opportunity to have in the same ratio the moles of the ions of the atomic species constituting the alloy which were added as doping agents into the glass (5). In fact, one has to reach, among the different variables, the electrochemical equilibrium at the interface between the systems: glass and metal.

STATE OF EXPERIMENTALS

More recent investigations (still unpublished) show that the ionic diffusion from the metal to the glass enriches the glass with chromium. This is obvious since in the metallic alloys the chromium atoms show, generally, a higher specific diffusion rate. At the best equilibrium conditions, the Authors observed the adhesion degree to be correspondent to the coated area of the su-

perfacial metallic grains. It was also ascertained that the presence of microcrystalline phases corresponds to coating systems not well linked to the metal. Since the bioglass suffers, in vivo, a transformation in HAP, the Authors consider the modification of the reciprocal ratios among the ionic components and the consequence for the bioglass-metal adhesion.

DISCUSS AND CONCLUSIONS

To stabilize the adhesion properties at the interface glass-metal, besides the ions useful to reach the electrochemical equilibrium, also ions suitable to favour the glass-metal bonding, empirically known and reported in literature, are added. Moreover to avoid an excessive interaction bioglass-tissue, other ions may be added for a bioglass activity control, with a possible diffusion of them towards the tissue, above all during the first phase of quick interaction. Thanks to the experiences in vivo it was observed that some systems, very good from the view point of the adhesion glass-metal, are much weakened because of a prolonged permanence within the living tissue of rabbits. Other vitreous systems, on the contrary, continued to remain in the state they were introduced in vivo. Particularly, some systems show a detaching of the bioglass from the interface and a lifting too. In order to explain the difference of behaviour a hypothesis was made: a depolarizing effect of the physiological liquids takes place. They penetrate into the interface probably through the local adhesion defects.

REFERENCES

- 1-L.L.HENCH, H.A. PASCHALL, J.Biom.Mat. Res.Symp., "Prostheses and Tissue: the interface problem", S.Hulbert, editor.
- 2-S.NIR; R.AVEYARD and B.VINCENT; M.BRODSKIY and M.I.URBAKH; in "Progress in surfaces science vol.8, ed. by S.G.DAVISON, Pergamon Press, Ltd (1979).
- 3-A.KRAJEWSKY, A.RAVAGLIOLI, R.VISANI; Riv. Staz. Sper.Vetro, vol.1 (1983)3-11.
- 4-A.KRAJEWSKI, A.RAVAGLIOLI, G.PERUGINI; Science of Ceramics, vol.11 (1981)85-90.
- 5-A.RAVAGLIOLI, A.KRAJEWSKI; A lesson at 23th Course of the "Inter. School of Medical Sciences: Orthopedics and Traumatology in Erice (TP).

T. Fujiu and M. Ogino

Glass Division, Nippon Kogaku K.K.
Sagamihara, Kanagawa, Japan.

Three types of surface active glasses and two types of sintered apatites were implanted in femurs of rabbits for eight and sixteen weeks and subjected to an improved push out test to measure the bonding strength with bone. The apatite surface layers of these materials, which were formed under in vitro treatment, were studied using IR, NMR and AES. The difference in the bonding strength among these materials was certified statistically. The results of in vitro experiments explained the differences. It was concluded that the microstructure and formation rate of the surface apatite layer significantly influenced the bonding strength.

Surface active glasses such as Bioglass® are known as materials which make a direct bond with living bone. The bonding ability of the glasses have been confirmed in several ways and Hench et al. introduced the push out test to measure the bonding strength. Sintered apatite and some special glass-ceramics containing large amounts of calcium and phosphate ions were also found to have a similar bonding ability. However, exact values of the bonding strength measured by the push out test have not yet been reported for these materials.

In the present research, an improved push out test was first developed, which provided accurate measurement of the bonding strength. Then the microstructure and formation rate of the surface apatite layer were examined using IR, NMR and Auger Electron Spectroscopy (AES). The purpose of this study is to discuss the influence of these two factors on the bonding strength.

Materials used in this experiment were Bioglasses® 45S5, 45S5F1/2 (1/2 amount of calcium oxide was substituted by calcium fluoride), 52S4.6 and sintered hydroxyapatite and fluorapatite. The animal used for push out tests were rabbits of more than 3 Kg. Two specimens were implanted one centimeter apart in each femur of the rabbit. The period of implantation in this experiment was 8 or 16 weeks. After this period the rabbits were killed and femurs removed to measure the bonding strength. Animal implantations, care and autopsies were done at the Dental School of Kagoshima University.

Specimens of each material were soaked in a trisaminomethane buffer solution which had pH value of 7.3. The microstructures of surface apatite layers were investigated using IR and NMR. Formation rates of the layers were investigated only for the surface active glasses using AES.

The results of push out test are listed in Table 1. Student's t-test was applied to confirm the superiority of 45S5. After 8 week implantation the differences in the bonding strength between 45S5 and other materials were assessed at a 20 % level of significance (which means that the possibility of error was less than 20 %). At 16 week implantation the superiority of 45S5 was significant (at 2 % level) to 52S4.6 and to 45S5F1/2 (at 10 % level).

Since there was no significant difference in

Table 1. The measured bonding strength (in MPa) for the different materials.

	45S5	45S5 F1/2	52S4.6	HAP	FAP
8 weeks	46 34 30 25 23	28 28 23 22 20	32 24 31 21 28 20 26 25	33 11 30 26 19 16	26 23 19 12 11
mean value	32	24	26	23	18
16 weeks	36 35 34 33 31	36 31 24 23 14	35 22 35 20 31 20 30 20 25 19		
mean value	34	26	26		

the bonding strength between 8 and 16 weeks in each material, the data were combined to examine the differences between materials. In this case, the superiority of 45S5 to other materials was confirmed at 1 % level of significance.

In vitro experiment showed that the hydroxyl ion on the symmetry axis of apatite structure was substituted by other ions. These ions were found to be carbonate ion (45S5 and 52S4.6), fluorine ion (45S5F1/2 and fluorapatite) and oxygenic ion (hydroxyapatite). From the AES measurement, it was revealed that surface apatite formation rates were significantly different among the glasses. The time for 52S4.6 to form an apatite layer on the surface under the treatment condition was about 240 minutes. On the other hand, for 45S5 and 45S5F1/2, the time was 15 minutes.

The results of push out test can be explained based on the microstructure and formation rate of surface apatite layer. Apatite which contains carbonate ion and hydroxyl ion has good affinity with bone which has been found to have these two ions. If the ions are substituted by other ions, the affinity is reduced. For the surface active glasses, it is desirable to form apatite layer on the surface as fast as possible. Therefore, 45S5 has the highest value of the bonding strength.

Nippon Kogaku K.K., Glass Division,
1773 Asamizodai, Sagamihara-shi, Kanagawa-ken,
228 Japan.

In Vivo and In Vitro Investigations Into Bioglasses™ Which Contain Fluoride

D. B. Spilman, June Wilson, and L. L. Hench

University of Florida, Gainesville, Florida

Introduction: The inclusion of calcium fluoride in Bioglass™ implant formulations produces a material which may have certain advantages in dental applications (1). Studies by Clark and Hench (2,3) showed that the apatite layer essential to tissue bonding formed more quickly in glasses with fluoride than without it.

In contrast, a recent study (4) reports that the time for formation of apatite on surface active glasses is unchanged with fluoride addition even though F^- was substituted for OH^- on the symmetry axis of the surface apatite crystals.

However, we show in this work that the presence of fluoride in surface active glasses affects not only the rate of apatite film formation, but also the composition of the film, the rate of crystallization of the film, and the films' resistance to demineralization. These factors are a function of the relative proportion of CaF_2/CaO in the glass.

Materials and Methods: The control material for the study was 45S5 Bioglass™ samples. Compositions designated F, F/2, and F/4 correspond respectively to substitution of 100%, 50%, and 25% CaO by CaF_2 . All glasses were melted at 1350°C in covered Pt crucibles.

Bone bonding and toxicology tests were done on the control and F/2 glass by the standard methods already described (5).

In vitro surface analysis was done with Fourier Transform Infrared Reflection Spectroscopy after 14 days, 37°C reaction in tris buffer and after 7 days, 25°C reaction in the decalcifying fluid used to process the implants and tissues from the in vivo studies. The resistance of the samples to demineralization was determined by measuring weight change and change in dimensions and/or particle size remaining after decalcification. X-ray diffraction, SEM-EDS, XPS, and AES were used to determine extent of crystallinity and film composition.

Results: Subcutaneous implantation of bulk 45S5 and F/2 Bioglass™ implants in rats and intratibial implantations in rats showed no toxicological effects at 6 and 8 weeks. Thirty day bone-bonding tests using the minipushout test (4) showed no difference in bonding ability between the control and the F/2 Bioglass™ implant. Previous histological studies of 6 mo. and 2 year baboon implants of the F/2 composition also showed bonding and absence of toxicity.

In vitro tests show, by FTIRRS peak area ratios, that the extent of apatite in the surface film decreases with fluoride addition, but only up to the F/2 level. In contrast, the resistance to demineralization progressively increases as the fluoride content increases. However, spectral

analysis of the material left after the decalcification treatment shows considerable difference between the F and F/2 formulas indicating important chemical and structural differences between the two. Surface analysis also indicates that there is less crystalline apatite on the reacted surfaces of the high fluoride glasses than on those with low fluoride. Combining these film formation characteristics leads to a surface performance index which defines an optional glass composition.

We have compared these characteristics with natural and commercial hydroxyl and fluorapatites and discuss possible effects on long term implant performance.

References

1. H. R. Stanley, L. L. Hench, R. Going, C. Bennett, S. J. Chellemi, C. King, N. Ingersoll, E. Ethridge and K. Kreutziger, "The Implantation of Natural Tooth Form Bioglasses in Baboons," *Oral Surg., Oral Med., Oral Pathology*, **42**, No. 5 (1976) 339-356.
2. A. E. Clark, Jr., "Solubility and Biocompatibility of Glasses," Ph.D. Dissertation, University of Florida, 1974.
3. L. L. Hench, "Stability of Ceramics in the Physiological Environment," in *Fundamental Aspects of Biocompatibility*, D. F. Williams, ed., CRC Press, Boca Raton, Florida, Vol. I, 1981, pp. 67-68.
4. T. Fujii and M. Ogino, "Differences in Bonding Behavior with Bone Among Surface Active Glasses and Sintered Apatite," submitted to *J.B.M.R.*, 1983.
5. J. Wilson, G. H. Pigott, F. J. Schoen and L. L. Hench, "Toxicology and Biocompatibility of Bioglass," *J. Biomed. Mater. Res.*, **15** (1981) 805-817.

Department of Materials Science and Engineering
University of Florida, Gainesville, FL 32611

EVALUATION OF THE ANTITHROMBIC ACTIVITY OF HEPARIN-LIKE SURFACES
THROUGH A NEW IN-VITRO TEST PERFORMED UNDER CIRCULATION

MIGONNEY, V., JOZEFOWICZ, M., and FOUIGNOT, C.

Laboratoire de Recherches sur les Macromolécules,
Université PARIS-NORD, 93430 VILLETANEUSE, FRANCE.

Several years ago, we described that the binding of sulfonate and amino acid sulfamide groups to crosslinked polystyrene endows these materials with heparin-like activity. More recently, we evidenced that these insoluble polymers are able to catalyse the thrombin-antithrombin reaction as does soluble heparin. The chemical procedure used to prepare these materials has also been adapted to modify the inner surface of polyethylene tubings radiochemically grafted with polystyrene. We now report a new in-vitro test which measures the ability of the inner surface of these tubings to catalyse the thrombin-antithrombin reaction under circulating conditions.

Materials: Polyethylene tubing (medical grade, 2.9 x 4 mm) is radiochemically grafted with polystyrene (about 2 mg/cm²) on the inner surface. The chemical treatment is performed under circulating conditions: swelling for 2 hrs in CH₂Cl₂; reaction with chlorosulfonic acid in CH₂Cl₂ for 20 min.; extensive washings with CH₂Cl₂; reaction with aspartic acid dimethyl ester in CH₂Cl₂ for 24 hrs; washings with ethanol and hydrolysis of the ester groups with NaOH in water.

The conditioning of the tubings has been found to be an essential step. The series of washings is the following: water solutions of NaCl 1.5 M and sodium citrate M, Michaelis buffer (pH 7.3) and distilled water. The duration of each step has been progressively increased up to 4 days in order to make the surface as active as possible. Finally, just before use, the tubings are rinsed again during several hours with Michaelis buffer under circulation.

In-vitro test: The tubing to be tested (96cm) is connected to a PVC tubing (same diameter, 24 cm) suitable for the chromatography pump used for the circulation. The tubing is first filled up (total volume about 8 ml) with diluted platelet poor plasma previously defibrinated by contact with bentonite. After 30 min. of incubation at room temperature, 250 units of thrombin are injected into the system. After 1, 4, 8, 12, 16 and 20 minutes of reaction, small aliquots (0.1 ml) are taken out at the end of the treated tubing by injection of the equivalent volume of buffer at the beginning of it. The level of residual thrombin is determined in each aliquot through a standard clotting time.

The non-catalysed reaction between thrombin and antithrombin has been evaluated under the same experimental conditions using non-treated polyethylene-polystyrene tubings.

Finally, the direct inactivation of thrombin by adsorption on the surface of the tubing has also been examined using buffer instead of diluted defibrinated plasma.

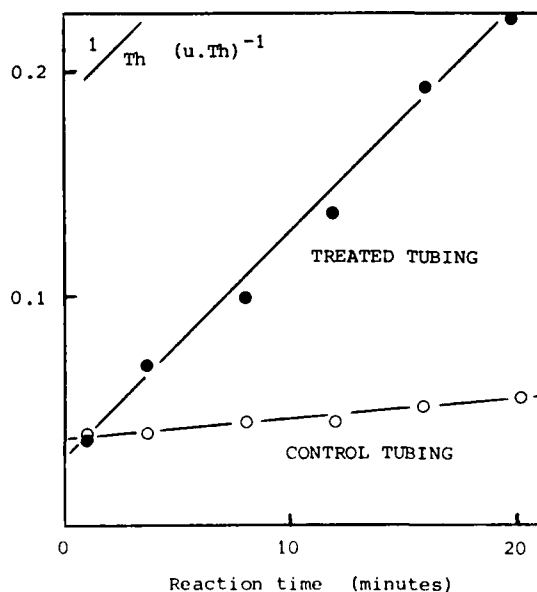
Results: The comparison of the inactivation of thrombin in the non-treated and treated tubings shows that the modified surface is able to inhibit a much larger amount of protease than the initial one. In both cases, the reciprocal of residual

thrombin concentration seems to be a linear function of the reaction time as shown in the figure below. In contrast, the direct inactivation of thrombin by adsorption on the surface is negligible on the polyethylene-polystyrene tubing and reaches a plateau on the treated one. However, this adsorption remains constant after 10 to 15 min. and is never large enough to explain the inhibition observed when thrombin and antithrombin are simultaneously present at the modified surface which evidences a catalytic effect of the surface on the thrombin-antithrombin reaction.

Similar results have been already observed under quasi-static conditions with the polystyrene beads substituted by the same chemical groups but the thrombin inactivated by surface unit is much higher under the circulating conditions than under the static ones.

This test of evaluation of the catalytic potency of the surface on the thrombin-antithrombin reaction has already been used in order to find the best treatment for the tubing. For instance, the performance of the sample has been found to strongly depend on how long the conditioning was. The figure reports the best results obtained until now for a treated tubing; in this case, the constant of initial velocity was about 10⁻² min./unit instead of 10⁻³ for the unmodified tubing.

Studies are now in progress to know more about this catalysis as for instance the effect of flow rate, proteins concentrations....



Acknowledgments: This work is supported by the Commissariat à l'Energie Atomique - Office des Rayonnements Ionisants - Saclay, FRANCE and by the C.N.R.S. GRECO n°48 "Polymères Hémostocompatibles"

IN VITRO CHARACTERIZATION OF HEPARINIZED POLYLACTIDE SURFACE

T.C. Lin, J.H. Joist*, R.E. Sparks**

Hexcel Corporation
Dublin, California

The objective of this study was to investigate blood compatibility on the heparinized poly dl-lactide (PLA) using Chandler rotating loop technique (1) by measuring formation of thrombus in recalcified human blood and adhesion of platelets suspended in buffered Tyrode-albumin solution. Effect of acetylsalicylic acid (ASA) and red blood cells (RBC) on the adhesion of platelets were also studied.

MATERIALS AND METHODS

In vitro thrombus formation: Flexible vinyl tubings (0.3cm I.D., 26cm long) were coated with PLA containing 0, 1.08, 2.00 and 4.20 wt% of micron-sized heparin particles, uniformly distributed in the thin coatings (40-80 μ m). Human blood was citrated with 3.8% trisodium citrate of pH 7.3 in a volume ratio of 0.11 ml citrate to 1.0 ml whole blood and stored at 37°C. 0.8 ml of blood was slowly injected into the loop of vinyl tubing and recalcified with 0.09 ml of 0.155M CaCl_2 solution. The loop (R=8.36cm) semi-immersed in a 37°C water bath, was rotated at 15rpm. Thrombus was soon formed at the forward blood-air interface and caused the interface to shift. The first degree of angular shift of the interface was defined as the characteristic thrombus formation time (CTFT) (2). After 30 minute rotation, blood was filtered and dry-weight of thrombus was obtained. To examine thromboresistance of the heparinized surface after long exposure to blood, deionized water at 37°C was used to wash continuously the surface over 200 hours. Formation of thrombus was then studied.

In Vitro Platelet Adhesion: Platelets were isolated from about 100 ml ACD-human blood, washed 3 times in Tyrode solution and then suspended in the HEPES buffered Tyrode-albumin solution at pH 7.35 (3). 100 μ Ci of Indium-111 was added to the platelet suspension which was incubated for 15 minutes at 37°C (4). Platelet suspension was adjusted to have 300,000 counts per mm^3 solution and kept at 37°C. The remaining RBC were washed twice in a Calcium-free modified Tyrode solution and suspended in the Tyrode-albumin solution at pH 7.3 (5). Just before the platelet adhesion test the RBC suspension was centrifuged at 1000g for 5 minutes. The RBC were then added to the platelet suspension to obtain about 30% hematocrit. 50 μ g of ASA also was added to 1 ml platelet suspension with and without the presence of RBC. 1 ml of platelet suspension was added into the fresh loop of coated vinyl tubing. After 30 minutes rotation at 15rpm and 37°C, the suspension was removed. The tubing was carefully rinsed with 10 ml of modified Tyrode solution, containing 10 mM EDTA at pH 7.35, to remove platelets and platelets aggregates not adherent to surfaces of the tubings (5). The platelets adhered firmly to the surface was completely removed by washing the tubing with 3ml of 0.5% Hemosol. The adhesion of platelets was expressed percentage of the total radioactivity in 1 ml of intact labeled platelet suspension.

RESULTS AND DISCUSSION

PLA surface was found to have no thromboresistance. The CTFT in the PLA coated loop was 6 minutes at time after venipuncture (TAV) of 30 minutes, it decreased gradually to 1.2 minutes at TAV of 250 minutes and maintained at this constant value over several hours. The in vitro thrombus was in the range of 9.6 to 12.8 mg over a period of 330 minutes TAV. No CTFT was detected in the fresh loop coated with PLA containing 1.08 wt % of heparin because of high initial release rate of heparin. After 230 hours exposure to deionized water, the PLA surface was no longer thromboresistant. About 10 mg of thrombus was measured. Apparently, the rate of release of heparin from the surface was not high enough to prohibit formation of thrombus. However, the PLA containing 2.00 and 4.80 wt% of heparin were still highly thromboresistant. No statistically significant amount of thrombus was found. The rate of release of heparin from the PLA containing 2.00 wt% of heparin has been reported to be 0.26 units/ml-hr (or 62 Ng/cm²-hr) (6). Heparin released at such rate seemed to be high enough to inhibit coagulation mechanism. The adhesion of platelets on PLA and PLA-heparin surfaces was same, about 7-8%. When ASA was added, it showed inhibitory effect on platelet aggregation, but did not exhibit any effect on adhesion of platelets. It has been reported that RBC enhanced the adhesion of platelets, and ASA inhibited the adhesion of platelets at low hematocrit, e.g. 20%, and lost its inhibitory effect at high hematocrit, e.g. 40% (5). No significant difference in the adhesion of platelets on the heparinized and non-heparinized surfaces was found when ASA alone or ASA and RBC both were present.

REFERENCES

1. Chandler, A.B., Lab. Investigation 7:(2)110-114 (1958)
2. Gardener, R.A., J. of Lab. and Clin. Med. 184:(4) 494-508 (1974)
3. Thakar, M.L., et al., Thrombosis Research, 9:345 (1976)
4. Joist, J.H. et al., J. of Lab. and Clin. Med. 92: (5) 829 (1978)
5. Cazenave, J.P. et al., J. of Lab. and Clin. Med. 93: 60 (1979)
6. Lin, T.C. "Controlled Release of Heparin from Poly (Lactic Acid)", D.Sc. Thesis, Washington University, St. Louis, MO. (1981)

T.C. Lin, Hexcel Corp. 11711 Dublin Blvd.
Dublin, Ca. 94568

* Department of Oncology and Hematology
St. Louis, University, St. Louis, Mo.

** Biological Transport Lab, Washington
University, St. Louis Mo.

S. Winters, D. E. Gregonis, D. Buerger, and J. D. Andrade

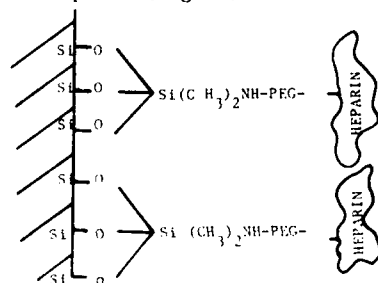
Departments of Pharmaceutics and Materials Science, University of Utah
Salt Lake City, Utah 84112

Protein adsorption is important in the interaction of materials with biological systems. Hydrophilic surfaces induce less total protein adsorption which has been proposed to be a critical factor in eventual thrombus formation. A large number of modifications to the surfaces have been attempted to prevent thrombosis. One method has been to heparinize the polymeric materials to provide antithrombotic activity at the implant-blood interface (1). Heparin is by far the most commonly used anticoagulant. However, due to the complex nature of this mucopolysaccharide and its many interactions (i.e. platelet factors, antithrombins, lipoproteins, etc.) its mechanism of action is not well understood. Here, we combine the advantages of a hydrophilic surface with those of heparin and study the specific interaction of immobilized heparin with antithrombin III (ATIII).

Total internal reflection intrinsic fluorescence spectroscopy (TIRF) provides a sensitive technique for studying interfacial phenomena between the immobilized heparin and blood protein (2). The intrinsic fluorescence of tryptophan residues in ATIII provides information on the molecular level events occurring when this blood clotting protein interacts with heparin. It has been suggested that heparin binds to lysine residues on the ATIII molecule, thereby inducing a conformational change and making its active site more accessible to thrombin (3).

Intrinsic TIRF has a number of advantages for this type of application, including quantitation of adsorbed protein, use of low surface area substrates, real time sensing, and it requires no extrinsic labels which could alter the activities of materials used (2).

Hydrophilic surfaces used for the covalent attachment of heparin have been developed using four different derivatives of polyethylene glycol (PEG-MW3400) (4). These include PEG-bis(2-chloroethyl) ether, PEG-diisocyanate, and PEG-diisothiocyanate by reaction of the PEG with phosgene and thiophosgene. The derivatives are coupled to quartz slides via a urethane linkage using the amino group of aminopropyltriethoxysilane (APS) coupling agent. Heparin is then covalently bound to the PEG derivatives to form a hydrophilic substrate with active heparin (Figure).



FIGURE

The Heparin is probably several angstroms from the surface and therefore relatively free to interact with proteins flowing past the surface. The tritiated or C^{14} heparin is quantitated using a surface planchet counter. A flow cell used for the TIRF studies was developed to provide constant laminar flow with a well characterized flow profile. The volume of the cell is 100 μ l. The hydrophilic surfaces are stable under aqueous conditions as determined by X-ray photoelectron spectroscopy, Wilhelmy plate contact angle measurements, and TIRF using a fluoresceinamine label.

The adsorption of ATIII is monitored in real time on the TIRF system. Excitation energy at 280 nm is used to follow the fluorescence emission at 334 nm by optically coupling the quartz slide to a quartz prism. The kinetics of ATIII adsorption onto clean hydrophilic quartz is relatively slow, taking approximately 20 minutes before a plateau is reached. This surface retains greater than 90% of the adsorbed protein after a buffer flush. Adsorption onto clean quartz, APS treated quartz and PEG/quartz without heparin are used as controls. The interaction of ATIII and PEG surfaces with the immobilized heparin can be seen in the emission spectra and can be correlated with reported fluorescence emission of buried tryptophan residues resulting from a conformational change in the ATIII molecule upon binding (5).

Evidence from TIRF data suggests that immobilizing heparin onto hydrophilic PEG surfaces provides an effective method for improving the blood compatibility of implantable devices.

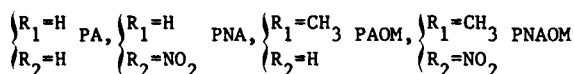
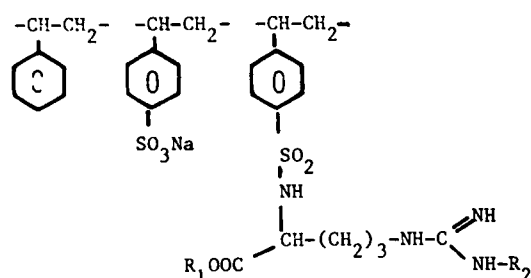
References:

1. C. D. Ebert, Ph.D. Thesis, Univ. of Utah, 1981
 2. R. A. VanWagenen, et al in S. L. Cooper and N. A. Peppas, eds., *Biomaterials*, Adv Chem Series 199, 1982.
 3. R. Rosenberg, P. S. Damus J. Bio Chem 248: 6490-6505 (1973).
 4. D. E. Gregonis, et al., in these Abstracts.
 5. S. T. Olson, J. D. Shore, J. Biol. Chem. 256: 11065-11072, (1981).
- S. Winters has been supported by NIH training Grant HL-07520. Partial support has been provided by Grants HL-18519 and HL-26469. We thank M. Helle, S. W. Kim, H. Chuang and R. A. VanWagenen for their valuable help and advice.

D. GULINO, C. BOISSON and J. JOZEFONVICZ

 Université PARIS-NORD - Laboratoire de Recherches sur les Macromolécules
 Avenue J.B. Clément - 93430 VILLETANEUSE - FRANCE.

Antithrombin III (AT III) inhibits thrombin by the binding of one of its arginyl residues to the serine of the active site of this protease. To try to obtain non thrombogenic materials, mimicking this AT III effect, insoluble polystyrenes substituted by different arginyl derivatives were synthesized :



When suspended on platelet poor plasma (PPP), the polymers increase the thrombin clotting time (TT) (Fig. 1) :

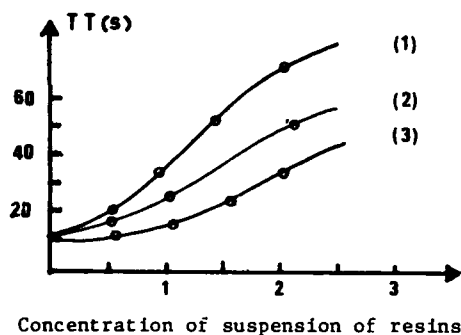


Fig. 1 : Variation of the thrombin clotting time (TT) versus the concentration of the resins :

1) = PAOM, 2) = PNAOM, 3) = PA.
 0.2 ml of PPP + 0.05 ml of polymer suspension ;
 incubation : 10 minutes, then addition of 0.05 ml of thrombin.

However, reptilase clotting time remains normal. So the effect on the thrombin clotting time cannot be due to an alteration of fibrin polymerization. These results were observed both with PPP and fibrinogen solutions and suggest that the anticoagulant effect of the different resins does not require the presence of natural thrombin inhibitors, such as AT III. In fact, the antithrombic property is induced by a strong adsorption of thrombin on the polymer surfaces.

Adsorption measures performed using human thrombin (1094 NIH U/mg) and crude resins (whose the average diameter varies between 60 and 100 μ) show this process is not instantaneous but requires twelve minutes of contact to be sure that the system has gained equilibrium. Isotherms were deter-

minated at 37°C (Fig. 2).

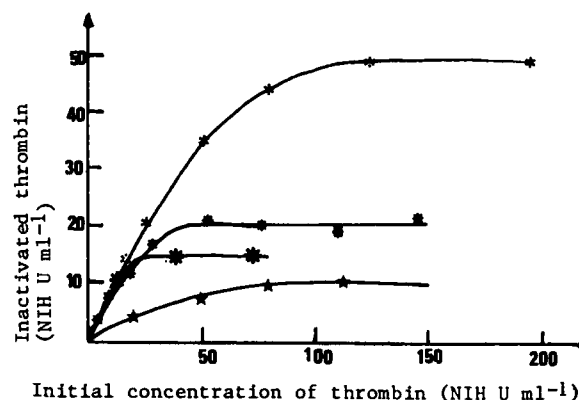


Fig. 2 : Adsorption isotherms of thrombin on resins.
 Clotting system : 0.2 ml of resin suspension was incubated with 0.2 ml of thrombin at various concentrations during twelve minutes at 37°C. Then 0.1 ml of supernatant was prelevé and mixed with 0.2 ml of fibrinogen.

* PNA : concentration of suspension of resin $C_R = 12,5 \text{ mg.ml}^{-1}$; * PNAOM : $C_R = 2 \text{ mg.ml}^{-1}$; * PAOM : $C_R = 5 \text{ mg.ml}^{-1}$; * PA : $C_R = 2 \text{ mg.ml}^{-1}$

So, using a Langmuir isotherm hypothesis, affinity constants between the different resins and the thrombin can be estimated (for a fraction of surface covered by thrombin equal to 0.5) as shown on Table 1 :

Tab 1 : Variation of the affinity constant with the nature of the resins

R_1	R_2	k 1 mole ⁻¹
H	H	0,4.10 ⁶
H	NO ₂	5.10 ⁶
CH ₃	NO ₂	8.10 ⁶
CH ₃	H	45.10 ⁶

It is difficult to compare directly the different resins to each other. In fact, affinity constants vary abnormally with the content of arginyl derivatives. Nevertheless, it appears that the presence of ester groups on the resins involves an affinity constant increasing (Table 1).

Moreover, using a high ionic strength solution, thrombin can be desorbed and after desorption, exhibits normal coagulant properties. This probably means that adsorption on the resins implies no irreversible conformational change on the structure of the enzyme.

A PARALLEL FLOW ARTERIOVENOUS SHUNT TEST SYSTEM FOR THE EVALUATION OF BLOOD COMPATIBLE MATERIALS

W.F. Ip, M.V. Sefton and W. Zingg*

Department of Chemical Engineering and Applied Chemistry
University of Toronto, Toronto, Ontario, M5S 1A4

A parallel flow arteriovenous shunt has been used to test the effectiveness of surface bound heparin in preventing thrombogenesis at low flow rates and in the absence of the surgical artifacts that cause a large sample-to-sample variation in conventional acute A-V shunts. A standard SILASTIC chronic hemodialysis shunt (3.18 mm ID) is inserted between the iliac artery and vein of a dog with anticoagulant therapy to aid in maintaining shunt patency. Experiments are begun after anticoagulant therapy has been stopped and the hemostatic parameters have returned to normal. For an experiment, a smaller diameter heparinized or control tube (1.14 mm ID) is inserted in parallel with the exteriorized portion of the SILASTIC shunt through a pair of SILASTIC Y-connectors, to divert ~ 2.4% of the flow into the test tubing. After an occluding thrombus has developed, the small diameter tube is removed and the chronic shunt reconnected until the next experiment. In this way the heparinized tubes are tested at low blood flowrates (~ 3-5 mL/min) without surgery and so without its associated artifacts but in a test system that can be reused many times as long as the chronic SILASTIC shunt remains patent. Chronic shunts have remained patent for 6-8 months, with this cannulation procedure (1). A not insignificant advantage is that the same animal can be used many times, reducing both the interanimal variability in the results and the cost of experimentation.

The patency of heparin-PVA coated polyethylene tubing (PE, 1.14 mm ID; prepared by chromic acid etching of the PE) is compared with that of control PVA coated tubes without heparin in Table 1.

Table 1
Parallel flow shunt patency

Main shunt flowrate (mL/min)	PVA (min \pm SD)	HEP-PVA (min \pm SD)	HEP-PVA (fraction patent at 2 hours)
130	20 \pm 7 (n=2)	73 \pm 40 (n=6)	0.17
150	30 \pm 22 (n=6)	84 \pm 30 (n=12)	0.25
160	39 \pm 7 (n=7)	116 \pm 55 (n=4)	0.25 (~ 180 min)
170	60 (n=2)	170 \pm 17 (n=3)	1.0 (> 150 min)

No PVA tubes remained patent at 2 hours.

The prolonged patency observed at all flow rates was attributed to the biological effectiveness of the immobilized heparin since heparin release from heparin-PVA is 1/1000 that needed to create a heparin microenvironment (2) and heparin activity has been observed in various clotting or thrombin inactivation tests (e.g., 2,3). The effect of main shunt flowrate was presumed to be the consequence of thromboembolic processes occurring in the Y-connector. Although the Y-connector is an important locus of thrombus initiation, it is not the dominant site for

thrombogenesis, enabling us to use this model to distinguish heparinized from nonheparinized tubing. Modified Y-connectors are currently under evaluation to reduce their impact even further.

Scanning electron microscopy of the tubes after occlusion showed the presence of significantly less platelet and particularly less fibrin deposition in the middle of the heparinized tubing relative to the nonheparinized control. This suggested that the surface bound heparin was effective in preventing fibrin formation and local platelet adhesion. However, it may not be able to prevent platelet deposition initiated by activation proximal to the heparinized tube (i.e., in the Y-connector). Of the hematological parameters measured, the presence of the heparin-PVA coated tubing caused a barely significant decrease only in platelet count. Further experimentation is necessary to determine whether these platelets were involved in the occluding thrombus or had formed aggregates which were sequestered elsewhere in the circulation.

The advantages of this test system enhance its value for assessing other potentially blood compatible materials, regardless of whether they contain heparin or not. The complications and variations induced by surgery are avoided, materials can be compared at lower flow rates and more reasonable shear rates, the animal need not be anaesthetized during the test and the animal may be reused many times over a 6-8 months interval. Despite the presence of the Y-connectors, significant differences in the behaviour of materials can be noted, to guide the biomaterials designer in the selection of materials for clinical application.

References

1. A. Bahoric, R.M. Filler, K. Perlman, W.S. Jackman, A.M. Albisser, *Diabetes Care*, **3**, 338-344 (1980).
2. M.F.A. Goosen, M.V. Sefton, J. Biomed. Mater. Res., **17**, 359-373 (1983).
3. M.F.A. Goosen, M.V. Sefton, M.W.C. Hatton, *Throm. Res.*, **20**, 543-554 (1980).

The authors acknowledge the financial support of the Ontario Heart Foundation.

*Hospital for Sick Children, Toronto, Ontario.

A.D. Callow

New England Medical Center
Boston, Massachusetts

The development of arterial prostheses, of which an estimated 350,000 synthetics were implanted in patients in the U.S. in 1980, has been largely based on intuitive attempts by innovative surgeons to develop crude tubular conduits and not on scientific study and application of arterial biology.(1) Such intuitively designed synthetic conduits, satisfactory in large caliber, high flow reconstructions, fail in small caliber, low flow, high resistance locations such as below the inguinal ligament where the five year patency rate is less than 30%. Because of this high failure rate of small caliber grafts, current interest is increasingly focusing on the cellular and molecular events which characterize blood-biomaterials interactions and the inherent thrombogenicity of the synthetic luminal surface. Because all synthetics lack an endothelial lining, they all activate platelets and the extrinsic clotting cascade to some degree. All currently used synthetic grafts are foreign bodies when implanted and remain foreign bodies forever. Platelet uptake on Dacron grafts continues for at least 9-12 months after implantation (2) and lack of their complete healing is manifested by persistent platelet consumption and failure to develop endothelialization in the human even years after implantation.(3) A possible additional flaw is that of compliance (4) mismatch between host vessel and graft resulting in disturbance of laminar flow, and the possible derivatives of local arterial wall damage and perianastomotic smooth muscle hyperplasia.

Current biologic approaches to the improvement of small vessel prostheses include attempts to decrease the thrombogenicity of the graft surface either by providing a non-thrombogenic synthetic lining or by attempting to induce normal endothelial cells to grow to confluence over the surface, pharmacologic manipulations of the blood-materials' interface, and, additionally, control of the healing response of the arterial wall.(5-8) Vascular endothelial cells will adhere to and thrive on a foreign surface enmeshed in a fibrin and platelet coagulum on a synthetic matrix and eventually grow to the surface of this coagulum and confluent cover its surface, at least in the canine model.(9,10) Attempts to develop similar technology are underway utilizing human vascular endothelial cells. An extension of these observations is the inoculation of vascular endothelial cells from a portion of cephalic or other vein into the clot filled interstices of presently available synthetics at the time of the reconstructive arterial procedure. The development and application of these concepts and techniques are progressing in several laboratories within the United States. Our laboratory efforts, in addition, include studies on platelet-biomaterial interactions, modification of the platelet reaction upon various types of grafts by means of administration of prostacyclin (PGI₂) and aspirin, plus a study of the variations in platelet response to a variety of biomaterials: Dacron, PTFE, glutaraldehyde, stabilized human umbilical vein,

low density polyethylene and polydimethylsiloxane. These substances are being studied in terms of platelet response, thrombosis, and other parameters at varying rates of flow through an *ex vivo* shunt model in the baboon. A major item of concern in our laboratory is the creation of a viable biologic vascular prosthesis utilizing co-cultures of vascular endothelial and vascular smooth muscle cells upon a collagen gel matrix. Multiple and major problems must be solved: the growth to confluence of vascular endothelial cells upon a co-culture of vascular smooth muscle cells with the formation of a basement membrane (11,12), the provision of a synthetic or semi-synthetic biodegradable matrix such as glycosaminoglycan or one that may be provided by the vascular smooth muscle cell (13,14), the development of appropriate tensile strength necessary for a graft to endure in a pulsatile flow system at human blood pressure levels, and control of the immune rejection phenomenon should the source of the endothelial and smooth muscle cells not be the graft recipient.

1. Szilagyi DE, Matas Memorial Lecture, 1981.
2. Goldman M, et al, Surgery 92:947-952, 1982.
3. Berger K, et al, Ann Surg 175:118-127, 1972.
4. Abbott WM, et al, in, "Biologic and Synthetic Vascular Prostheses" (Stanley JC, ed), Grune & Stratton, New York, 1982, pp 189-220.
5. Callow AD, et al, Ann Surg 191:326-366, 1980.
6. Mackey WC, et al, (Subm. Ann Surg, 1983)
7. Callow AD, et al, Arch Surg 117:1447-1455, 1982
8. Libby P, O'Brien KV, J Cell Physiol, In press, 1983.
9. Herring MB, et al, Ann Surg 190:84-90, 1979.
10. Clagett GP, et al, Surg Forum 33:471-2, 1982.
11. Delvos U, et al, Lab Invest 46:61-72, 1982.
12. Jones PA, Cell Biol 76:1882-1896, 1979.
13. Yannas IV, et al, NIH Progress Report, 1978.
14. Yannas IV, et al, Science 215:174-176, 1982.

Supported by NIH RHL 24447-04 & RHL 28855-02, and New England Medical Center Posner, Ziskind and General Research Support Funds.

Allan D. Callow, M.D., Ph.D.
New England Medical Center
171 Harrison Avenue, Box 285
Boston, MA 02111

THE CHARACTER OF THE INITIAL STAGES OF BLOOD INTERACTION WITH BIOMATERIALS AND THEIR HEMOCOMPATIBILITY

V.I. Sevastianov, E.A. Tseytlina, A.V. Volkov

Biomaterials Laboratory, Research Institute of Transplantology and Artificial Organs, Moscow, USSR

We suppose that biomaterials hemocompatibility can be estimated, with high probability, according to the character of the initial stages interaction. The goal of this work was the detection and quantitative analysis of the parameters of two related aspects of hemocompatibility-processes of protein adsorption and activation of complement system.

The methods used were: the method of radioactive indicators (protein adsorption) and detection of hemolytical activity of complement. In both cases the kinetics of the adsorption and activation processes with mathematical analysis of registered phenomenon was studied.

The study of the initial stages of serum albumin (SA) and fibrinogen (FG) adsorption on the polymer surfaces proved the degree of irreversible adsorption β of SA to be the criterion of polymer hemocompatibility (1). The higher the value β , the higher is the probability of given polymers hemocompatibility in vivo.

The protein nature of the complement determines the fact that the interaction of surface with blood causes adsorption processes, inevitably inducing the structural alterations of the macromolecules, resulting in the possible activation of complement components. The performed experimental and theoretical analysis make it possible to suggest the value of relative rate constant of the induced complement activation k_{ind} as the criterion of polymer activating properties on the complement system (2). The study of wide range of biomaterials revealed the evident dependence of β and k_{ind} on the surfaces physico-chemical properties, Table 1.

Table 1. Quantitative characteristics of polymers hemocompatible properties

Material	k_{ind}	RIPA	β
Pellethane	0,07	0,5	3,95
Biomer	0,25	0,5	5,28
Polyethylene (USSR)	0,65	1,0	1,05
Polyethylene (Abimed)	0,97	1,7	1,60
Cuprophane	1,00	0,8	1,49
Vlaccfan	1,20	1,8	0,44
Silurem	1,38	0,6	2,03
OB-2-7	1,60	2,2	0,54
Vitur-T	1,96	1,8	0,35
Polydimethylsiloxane	1,13	2,3	0,30

S.D. were 2,5% for k_{ind} , 15% for RIPA, and 10% for β .

This table also contains the results of the evaluation of hemocompatibility of given polymers in vitro by RIPA (relative index of platelet adhesion) (3). The Spearman rang correlation coefficients (P)

were calculated for pairs RIPA and k_{ind} , k_{ind} and β , RIPA and β . They are equal to 0,71 ($p < 0,025$), -0,88 ($p < 0,001$), -0,96 ($p < 0,001$), respectively. The registered value of k_{ind} reflects the complement consumption by adsorption/desorption processes on the blood/polymer interface, and so the negative correlation between the degree of irreversible adsorption of SA (β) and k_{ind} is quite explainable. The more the tendency of the polymer surface to the irreversible protein adsorption, the lower is the desorption rate of the conformational altered molecules in the volume solution, in particular causing the bulk complement activation.

The results of study of SA and FG adsorption on grafted surfaces can additionally prove the involvement of protein conformational alterations in the adsorption processes. It was demonstrated that the value β decreases for SA and FG with the increase of the degree of hydrophilic grafting (Table 2).

Table 2. Characteristic kinetic parameters of SA and FG adsorption on grafted surfaces

Surface	β_{SA}	β_{FG}
Polyethylene (PE)	1,05	2,25
PE-metacrylic acid (PE-MAC), $\alpha = 2,5\%$	1,00	1,92
PE-MAC, $\alpha = 5,0\%$	0,43	2,32
PE-MAC, $\alpha = 10\%$	0,17	1,46
PE-cetyl alcohol (Cet)	1,43	0,83
PE-polyacrylic acid (PAC)	1,19	1,58
PE-PAC-Cet	2,74	1,82

This can be explained by conformational alterations due to H-binding with -COOH groups of grafted acid. The maximal value of irreversible adsorption in the case of PE-PAC-Cet proves the supposition that conformational alterations of the adsorbed protein positively effects on their desorption rate. This high degree of irreversible adsorption can be explained by the formation of hydrophobic complexes of high association constant with SA. The latter causes the reduced conformational alterations of the adsorbed molecules, as compared with hydrophilic surface. Really, the decrease of the hydrophobic interaction in the system PE-Cet causes the reduction of the value of β .

- 1). V.I. Sevastianov et al, Artif. Organs 7(1) 126-133, (1983)
 - 2). V.I. Sevastianov, E.A. Tseytlina, J. Biomed. Mater. Res. (in press)
 - 3). V.I. Sevastianov et al, Vysokomolek. soed. 23, 1864, (1981)
- Institute of Transplantology and Artificial Organs, Pechotnaya 2/3, Moscow 123436, USSR

Courtney, J.M., Travers, M., Lowe, G.D.O., Forbes, C.D., Bowry, S.K., Wolf, H.

University of Strathclyde, Bioengineering Unit, 106 Rottenrow, Glasgow G4 0NW, UK

Platelet adhesion and the onset of platelet aggregates are regarded as important events in the interaction of blood with an artificial surface. Therefore, in an assessment of platelet changes induced by material contact, it is advantageous to include a measurement of circulating platelet aggregates in blood exposed to the test material. This measurement has been included in this investigation, which has studied platelet adhesion and aggregation with a series of polyamides differing in porosity and surface charge.

Platelet adhesion and aggregation have been determined by a procedure involving the addition of blood to EDTA-formalin, which fixes aggregates, or to EDTA, which disperses them. Platelet counts are determined for blood added to EDTA and to EDTA-formalin and the procedure is repeated following contact of blood with the test material. Therefore, 4 counts are obtained

- E_N - platelet count in normal blood not exposed to test system and added to EDTA
- E_{FN} - platelet count in normal blood not exposed to test system and added to EDTA/formalin
- E_T - platelet count in blood exposed to test material and added to EDTA
- E_{FT} - platelet count in blood exposed to test material and added to EDTA/formalin.

Percentage platelet adhesion (PAR) is given by $100(1 - E_T/E_N)$. Platelet aggregate ratio for blood not exposed to test material is given by E_{FN}/E_N and should be 1.0. PAR for blood exposed to the test material is E_{FT}/E_N and is expected to be 1.0. In material assessment, it is convenient to express platelet aggregation in terms of the Aggregation Number (AGN), the unit complement of the platelet aggregation, with AGN increasing with the extent of aggregation. A feature of this procedure is that platelet adhesion and aggregation can be measured separately.

In this investigation, platelets were counted on the Clay Adams Ultra-Flow 100 whole blood platelet counter, which avoids centrifugation and reduces contact with materials other than that being tested. The PAR value of normal blood was 0.97 ± 0.06 .

Flat sheet polyamide membranes obtained from Pall Process Filtration Ltd. were tested by oscillation in contact with human blood containing no anticoagulant. Table 1 contains the results obtained with 3 membranes with the same polymer structure but different porosity, while Table 2 gives results for membranes with the same porosity but different electronegativity. The results demonstrate a clear dependence of AGN on porosity and electronegativity, while the dependence of platelet adhesion is less marked. AGN increased with increasing porosity and decreased with increased electronegativity. Support for the results was obtained from measurements of the release of β -thromboglobulin (BTG) in that the dependence of BTG release on porosity and electronegativity followed a similar pattern to that for AGN.

The investigation has confirmed the relevance of introducing an estimation of platelet aggregation into in vitro blood compatibility assessment and has demonstrated the limitation of basing an assessment exclusively on platelet adhesion.

Table 1: Platelet adhesion and aggregation on polyamide membranes differing only in porosity. Mean \pm standard deviation, $n = 7$.

Membrane Pore Size (μm)	Aggregation Number (AGN)	Platelet Adhesion (%)
0.2	0.29 ± 0.12	15.2 ± 4.6
0.45	0.42 ± 0.07	19.9 ± 4.8
0.8	0.80 ± 0.12	28.8 ± 5.6

Table 2: Platelet adhesion and aggregation on polyamide membranes of similar porosity ($0.2 \mu m$) differing in electronegativity. Mean \pm standard deviation, $n = 7$.

Zeta Potential (mv)	Aggregation Number (AGN)	Platelet Adhesion (%)
-17	0.71 ± 0.24	21.2 ± 3.4
-28.6	0.29 ± 0.12	13.2 ± 4.6

Dr. J. M. Courtney, Bioengineering Unit, University of Strathclyde, Wolfson Centre, 106 Rottenrow, Glasgow G4 0NW, UK

Department of Medicine, Royal Infirmary, Glasgow, UK
Biomaterials Unit, Humboldt University, Berlin, GDR

Hemoperfusion with Activated Charcoal Coated by Glow Discharge Technique

N. Hasirci and G. Akovali

Middle East Technical University, Department of Chemistry,
Ankara - Turkey

A large number of techniques have been developed in an attempt to remove certain chemicals from the body when natural kidney function fails. Among these techniques are dialysis, ultrafiltration and hemoperfusion. Each technique has its advantages and disadvantages over the other techniques. Dialysis and ultrafiltration become economically unattractive due to the high cost of the membranes and their frequent replacement. Hemoperfusion with activated charcoal granules is better in this aspect but release of fine particles and damage to blood cells render this inapplicable unless these problems are solved. In order to avoid these complications charcoal granules are microencapsulated within artificial cells [1] or coated with biocompatible polymers [2,3].

Glow discharge polymerization technique is a new method which makes it possible to use nonmonomeric chemicals as well as monomeric ones as coating material. Also the products are purer because of the absence of initiator, solvent, etc. that are essential for polymeric coatings obtained with other techniques.

In this study activated charcoal was coated with hexamethyldisiloxane (HMDS) by using the glow discharge technique in order to obtain a hemocompatible adsorbent for use in hemoperfusion. The effect of various parameters on glow discharge polymerization (e.g., discharge power, discharge duration, gas flow rate) were examined and optimum values for these parameters were determined.

SEM examinations of the resultant HMDS coat showed mostly a "snowing" type deposition and this coat was compared with the commercial products prepared by solution coating with acrylic hydrogel. The results indicated that the coat obtained by glow discharge technique is highly crosslinked and strongly adhered to the charcoal surface and it is more uniform and thinner than the commercial sample.

The adsorption capacities of coated and uncoated charcoal were determined by measuring the adsorption of creatinine (MW 113) and vitamin B12 (MW 1355). Solutions of these chemicals were passed through a charcoal column and concentrations were spectrophotometrically measured at certain intervals.

Hemocompatibility of the coated product was assessed by in vitro techniques and compared with that of untreated activated charcoal. The effect on blood cells - erythrocytes, leucocytes, and thrombocytes - was examined and it was observed that while the uncoated samples had caused up to 30% reduction in thrombocytes, 10% reduction in erythrocytes and 7% reduction in leucocytes; the coated samples lead to almost no reduction.

1. T.M.S. Chang, Science, 146, 524 (1964).
2. J.D. Andrade, R. van Wagenen, M. Ghavamian, J. Volder, R. Kirkham and W.J. Kolff, Trans. Am. Soc. Artif. Intern. Organs, 18, 235 (1972).
3. J.F. Winchester, J.M. MacKay, C.D. Forbes, J.M. Courtney, T. Gilchrist and C.R.M. Prentice, Artif. Organs, 2(3), 293 (1978).

THE EFFECT OF BIOMATERIAL-TREATED MACROPHAGES ON FIBROBLAST REPLICATION

A. Pizzoferrato, S. Stea, G. Ciapetti

Istituto Ortopedico Rizzoli
Bologna, Italy.

The development of chronic inflammatory reactions is followed by an involvement of the connective tissue that, under normal conditions, ceases when adequate repair has been achieved.

The macrophages are cells capable of regulating the duration and the extent of fibrogenetic and proliferative activity of fibroblast by means of a soluble factor, macrophage-dependent fibroblast stimulating activity (MFSA) (1).

In this paper we analyze the variations of "in vitro" fibroblast proliferation caused by macrophages stimulated "in vivo" with alloplastic materials.

Briefly the method is the following:

- Mice are intraperitoneally injected with powdered biomaterials (Alumina-Titanium composite, Titanium, Stainless-Steel, Copper) 24 hours prior to harvesting the cell population.
- Macrophages are maintained in culture for 48 hours. Afterwards their conditioned medium is dialyzed overnight against non-conditioned medium.
- The dialyzed medium is then assayed for the presence of MFSA on "in vitro" cultured fibroblasts.
- Fibroblast replication is quantified using ^3H Thymidine uptake test. The optimal uptake has been obtained using a 1 μCi pulse for 24 hours on a fixed number of cells. The most suitable time and the best cell concentration have been previously established by drawing the graph of fibroblast replication (Fig. 1).

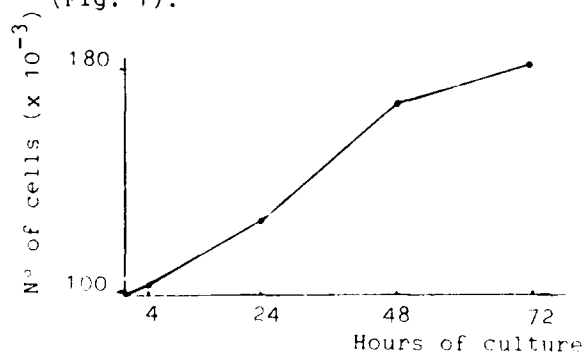


Fig. 1 Fibroblast growth rate. The curve shows the behaviour of fibroblast in a representative experiment.

Our results permitted us to evidence a macrophagic activity on fibroblast replication that differs depending on the employed material.

In addition to this, the factor inhibits fibroblast DNA synthesis when present in high concentrations, whereas stimulation was observed at lower concentrations (2).

Findings to date are consistent with the hypothesis that macrophages contribute to the regulation of fibroplasia during the repair process.

So we suggest a feasible relationship between wear particles of the implanted prostheses and the extent of the fibrosis that develops around them.

- 1 De Lusto F., Le Roy C.; J. Reticuloendothel. Soc. 31, 295-305, 1982.
- 2 Diegelman R. F., Cohen I.K., Kaplan A.M.; Proc. Soc. Exp. Biol. Med. 169, 445-451, 1982.

This work has been supported by National Research Council (CNR).

Prof. Arturo Pizzoferrato
Center for Biocompatibility Research of
Implant Materials
Istituto Ortopedico Rizzoli
Via Codivilla 9
40136 Bologna, Italy.

J. Ricci, H. Alexander*, J.R. Parsons* and A.G. Gona

Section of Orthopaedic Surgery, UMDNJ-New Jersey Medical School,
100 Bergen Street, Newark, NJ 07103.

INTRODUCTION - A composite material consisting of filamentous carbon and polylactic acid (PLA) polymer has been used to repair tendon and ligament injuries¹. The filamentous carbon acts as a scaffold for the formation of new tissue. This scaffold strongly influences the orientation of new tissue. Thus, the growth characteristics of connective tissue cells on filamentous carbon and other types of fibers are of interest. These experiments are part of a series of in-vitro studies to characterize rat tendon fibroblast (RTF) cell response to carbon and other types of synthetic filaments. Preliminary results of these experiments have been presented². This study examined RTF cell response to filamentous carbon, Dacron[®], polyethylene, and Nylon[®] and was specifically designed to examine the effects of fiber composition, geometric configuration, and surface characteristics.

MATERIALS AND METHODS - Morphology and outgrowth rate studies were conducted by culturing tendon explants from 14-day old male Sprague-Dawley rats on single fibers of each material. Culture conditions have been reported previously². Surface striations in the micron and submicron range have been shown to influence cell alignment^{2,4}. Longitudinal surface striations were formed on some of the fibers with size 400 polishing grit. Thus, these series of fibers represented a range of compositions, surface characteristics, and diameters (9 μ m to 102 μ m).

Outgrowth rates were measured by light microscopy on live cultures at 24-hour intervals over 9 days. This is a measure of RTF cell colony formation on these fibers and represents a combination of cell migration and growth rates.

Morphological studies were conducted on preserved cultures using an AMR 1200B scanning electron microscope.

RESULTS OF MORPHOLOGY STUDIES - Single cell orientation on these fibers was influenced by a combination of fiber diameter and surface striations. Striated, small diameter fibers exhibited the strongest influence on single cell orientation while smooth, large diameter fibers exhibited the weakest influence. However, in confluent cultures, cells aligned parallel to the fibers and to nearby cells regardless of surface characteristics or diameters. Fiber composition had no noticeable effect on cell morphology.

RESULTS OF OUTGROWTH RATE STUDIES - The outgrowth rates of RTF cells were linear on all fibers throughout the experiments. Briefly, this indicated that the advancing edges of the growing colonies of cells progressed down the fibers, away from the explants, in a linear fashion. Outgrowth rates were not significantly different on any of the fibers regardless of composition, surface characteristics, or diameter.

DISCUSSION - Fiber composition had no significant effect on cell morphology or outgrowth rates because of (1) the lack of inflammatory response in an in-vitro system and (2) the use of serum in the culture media. Synthetic materials adsorb a protein coating when exposed to serum allowing cell attachment to materials with widely different surface energies³.

Surface striations and fiber diameter had a clear influence on the orientation of single cells. This effect has been observed on both machined and collagen substrates^{4,5}. Dense cell colonies oriented parallel to the fibers regardless of diameter or surface striations. This was probably due to cell orientation influenced by fiber direction and by the proximity of other closely packed cells. Surface characteristic effects on isolated cell orientation may be significant for in-vivo connective tissue regrowth since this tissue is not highly cellular. Also, the orientation of these cells may effect the orientation of new collagen matrix.

The outgrowth rate studies indicated that cell growth rates on these fibers were linear. These growth rates were different from the growth rates of RTF cells grown on culture dishes. These cells exhibited a rapid growth phase, while on fiber substrates they grew in a slower, linear manner. This confirms the results of our previously reported studies². In this study, these linear growth rates were independent of fiber compositions, surface characteristics, and diameters. This may not be true for fibers larger than the 102 μ m Nylon sutures. This effect of substrate geometric configuration on cell growth rate is related to the density dependent growth of these cells and the limited amount of available surface area on the individual fibers. These findings may partially explain studies of cell growth on collagen fiber⁶. The studies reported here demonstrate the profound effect of substrate surface characteristics and geometric configuration on cell growth characteristics.

REFERENCES

1. Weiss, AB et al: Proc. Soc. for Biomat., 6:54, 1983.
2. Ricci, J et al: Proc. Soc. for Biomat., 6:52, 1983.
3. van der Valk, P et al: J. Biomed. Mat. Res., 17:807-817, 1983.
4. Ohara, PT and Buck, RC: Exp. Cell Res., 121:235-249, 1979.
5. Overton, J: Tissue Cell 11(1):89-98, 1979.
6. Sarber, R et al: Mech. Ageing Dev., 17:107-117, 1981.

ACKNOWLEDGEMENT - This research was supported by Veterans Administration Grant V561P-1933. [®]Dupont Corporation, Delaware. Anatomy and Orthopaedic Surgery^{*}, UMDNJ-NJMS, 100 Bergen St. Newark, NJ 07103

AUTO-ALLOPLASTIC TRACHEAL REPLACEMENT PROSTHESIS.BASIC
AND EXPERIMENTAL INVESTIGATIONS.

BERGHAUS , Alexander MD

ENT-Clinic,Klinikum Steglitz,Freie Universität Berlin
Berlin, WEST GERMANY

For the last three years we have inquired into the use of porous synthetics for reconstructive Head and Neck Surgery. For replacement of the trachea, a stable prosthesis out of Porous Polyethylene can be shaped, which becomes an auto-allograft by preoperative implantation in soft tissue like muscle.

Prior to clinical use, we undertook basic investigations on biomechanics of the normal human trachea to which the implant should be assimilated as well as possible concerning form and strength. Therefore - in collaboration with the Federal German Institute for Material Research - the properties of 20 human tracheae were measured immediately post mortem with regard to straining, compression and torsion. The results were related to age, sex, length and diameter of the trachea and evaluated.

On the basis of these findings different types of tracheal frameworks were analysed concerning their mechanical properties; for this Porous Polyethylene with and without reinforcement by Silicone rubber, and Silicone rubber alone were selected. The ingrowth of soft tissue in Porous Polyethylene was taken into consideration.

The various types of prosthesis were finally implanted experimentally in Minipigs by different procedures. Macroscopic and histological evaluation took place in defined intervals.

The reinforcement of Porous Polyethylene by Silicone rubber combines certain advantages, as will be presented.

Alexander Berghaus ,MD
HNO-Klinik , Klinikum Steglitz der FU
Hindenburgdamm 30
D1000 Berlin 45
West Germany

THE INTERACTIONS OF CALCIUMPHOSPHATE CRYSTALS AND POLYMORPHONUCLEAR LEUCOCYTES MONITORED BY LUMINOL DEPENDENT CHEMILUMINESCENCE

C.P.A.T.KLEIN, K.DE GROOT AND F.NAMAVAR*

Depts.of Biomaterials and Medical Microbiology*, Schools of Dentistry and Medicine, Free University, P.O.Box 7161, 1007 MC Amsterdam, The Netherlands

The biodegradation behaviour of various calcium-phosphate materials was studied in *in vivo* experiments. The conclusion was drawn that depending on their porosities β -whitlockite materials (Ca/P ratio 1.50) are more or less biodegradable, in contrast to sintered hydroxylapatite (Ca/P ratio 1.67) (Klein et al. 1983).

It is reasonable to assume that the biodegradation of sintered calciumphosphate ceramics occurs by both solution-mediated processes and cell-mediated processes (Signs et al. 1979, Ferraro 1979). Partially dissolved materials could slough off fine particles which could be removed by phagocytosing macrophages.

Phagocytosis is a highly selective process requiring specific interactions between the surface of the particle to be ingested and the plasmamembrane of the phagocytic cell. The cellular response to the calciumphosphate ceramics may be partly result from interface phenomena such as protein adsorption on the ceramic surface which occurs after implantation (McNamara and Williams 1981). Especially tissue fluid proteins such as α_2 HS-glycoprotein and immunoglobulin (IgG) may be considered to modulate the activities of macrophages and other free cells reacting to the presence of artificial substances or particles. Differences in the adsorption behaviour induced by chemical-physical differences in the surfaces of the materials may result in differences of 1) reactivity and accessibility of the proteins in the adsorbed layer to the cells and 2) biodegradation behaviour of the calciumphosphate materials.

The present study deals with the *in vitro* interaction between different calciumphosphate powders and phagocytosis.

When polymorphonuclear leucocytes phagocytose bacteria or yeast, light is released as a chemiluminescence reaction related to the production of superoxide radicals. This reaction can be amplified chemically by the use of the chemical luminol. We have taken this technique and applied it to the study of leucocytes and crystals.

Assuming the production of chemiluminescence to correlate with phagocytic activity of the cells, we studied the interaction of proteins adsorbed on the crystals and the phagocytic cells.

The chemiluminescence reaction of uncoated β -whitlockite crystals was a factor 2 higher than hydroxylapatite crystals. The response to serum-coated, albumin or α_2 HS-glycoprotein coated β -whitlockite crystals was significant reduced, whereas the response to γ -globulin coated β -whitlockite crystals was similar to uncoated crystals. Coating of hydroxylapatite crystals gave a similar pattern of chemiluminescence response.

References:

1. C.P.A.T.Klein, A.A.Driessen, K.de Groot and A.van den Hooff. J.Biomed.Mater.Res., 17, pg 769 (1983).
2. S.A.Signs, P.K.Bajpai and C.G.Pantano. Biomat.Med.Dev.Art.Org., 7, 183 (1979).
3. J.W.Ferraro. Plast.Reconstruct.Surg. 63, 634 (1979).
4. A.McNamara and D.F.Williams. Biomaterials 2, 33 (1981).

**PROTEIN ADSORPTION ON POLYCARBONATE - CHANGES WITH
L-ASCORBIC ACID AND BLOOD CELLS**

CHANDRA P. SHARMA AND THOMAS CHANDY

BIOSURFACE TECHNOLOGY DIVISION, BIOMEDICAL TECHNOLOGY WING
SREE CHITRA TIRUNAL INSTITUTE FOR MEDICAL SCIENCES AND
TECHNOLOGY, POOJAPURA, TRIVANDRUM - 12, INDIA.

SUMMARY

Adsorption of proteins is the primary event upon contact of blood with foreign surfaces, and subsequent cellular interactions leads to thrombus formation. Much of the early work on the study of adsorption was done in buffered solutions of single proteins, relatively simple mixtures or plasma. However, studies of protein adsorption in presence of blood cells like red cells, platelets and white blood cells are still lacking. The effect of red cells on platelet sticking has been noted widely, causing an augmentation of the rate of adhesion, probably by a combination of physical and biochemical mechanisms (1) Brash et al (2) indicated that the addition of red blood cells to buffered solutions of plasma proteins caused a decrease in the quantity of protein adsorbed from these solutions to a polyethylene surface.

In a previous study we have shown that (3) Vitamin C does have some effect on the polymer surfaces by getting adsorbed on to it which would probably affect the protein adsorption and platelet adhesion. The present work demonstrates the observations of the interaction of RBC, platelets and W.B.C. from the protein mixture (Albumin-25mg%, globulin-15mg% & Fibrinogen-5mg%) on polycarbonate substrate as a function of time using a trace labeling method in presence and absence of Vitamin C.

Table-I show some of the few surface concentration data studied, which indicate that for a period of 15 mts. and 3 hrs., in presence of RBC and WBC, albumin surface conc. is not significant, however platelets cause a decrease in the amount adsorbed. The amount of albumin adsorbed to PC in presence of blood cells and Vitamin C has been considerably decreased, while an increased albumin conc. has been observed with bare PC. This reduction in albumin concentration is maximum with Vit.C in presence of RBC. On the other hand fibrinogen adsorption pattern from Table I, has suggested that in presence of blood cells the surface conc. is enhanced compared to PC surface at 15 mts. interaction where as 3 hrs. of exposure does not change significantly with RBC and platelets. Further with Vitamin C, fibrinogen adsorption has decreased considerably with blood cells, comparing with the effect on polymer substrate.

T A B L E - I

Adsorption of Albumin and Fibrinogen to polycarbonate (PC) substrate with blood cells and Vitamin C at 15 mts. and 3 hrs. exposure.

PC surface exposed to	Protein surface conc. (μgcm^{-2}) without Vit.C		Protein Surface conc. (μgcm^{-2}) with Vit.C	
	15 mts.	3 Hrs.	15 mts.	3 Hrs.
Buffer	0.021	0.038	0.036	0.048
ALB- ⁺ RBC	0.022	0.036	0.014	0.019
UMIN- ⁺ Platelets	0.016	0.022	0.015	0.021
⁺ WBC	0.021	0.037	0.021	0.035
Buffer	0.22	0.40	0.39	0.50
FIB- ⁺ RBC	0.32	0.39	0.18	0.25
RIN- ⁺ Platelets	0.30	0.37	0.35	0.42
OGEN- ⁺ WBC	0.40	0.62	0.38	0.47

Conditions: buffer -0.1M phosphate buffer pH 7.4, protein mixture of 25mg% Alb, 15mg% γ -globulin & 7.5mg% Fibrinogen containing 0.5 μ curie per ml of ^{125}I labeled albumin or fibrinogen, at 37°C. Red cells & white blood cells were washed with phosphate buffered saline and platelets with tyrode solution for the studies. Values are the average of at least three experiments.

The above results will be further discussed with an emphasis of kinetic studies by taking in to account, (a) the interaction of Vit.C with the polymer surface (b) interaction of Vitamin C with the proteins and cellular membrane. (c) interaction of proteins & cells with the polymer itself. It appears that Vitamin C increases the interfacial tension between polymer surface & proteins (3) causing increased protein adsorption. The effect of various blood components also seems to be important, however no significant differences in the adsorption of proteins were observed in presence of urea, creatinine, bilirubin, Fe^{+++} ion and Zinc at normal blood level.

References:

1. Turitto, V.T., Weiss, H.J. Science 1980, 207, 541.
2. Brash, J.L., Uniyal, S. Trans. Am. Soc. Artif. Intern. Organs. 1976, 22, 253.
3. Sharma, C.P. and Paul, L. J. Colloid and Inter Sci. 1982, 87, 436-441.

PLASMA PROTEIN INTERACTION WITH BIOMATERIALS AS
DETERMINED BY ISO-DALT ELECTROPHORETIC ANALYSIS

Connie M. Chen and Donald R. Owen
Materials Science and Bioengineering
University of New Orleans
Lakefront Campus, New Orleans, LA

The interaction with artificial surfaces of plasma proteins in general and specifically of the immunoproteins has been difficult to ascertain. This laboratory has been employing a modified ISO-DALT two dimensional electrophoresis technique as outlined by Anderson and Anderson specifically for the analysis of plasma protein-biomaterial interactions.

The ISO-DALT sample preparation techniques result in the reduction of the plasma proteins to their appropriate subunits via disulfide bond cleavage.

Therefore, the technique does not amend itself to identification of normal dissociation of a plasma protein via a synthetic surface, rather to only fragmentation at other than disulfide linkages, depletion of a component by direct absorption or increases in concentration of a component due to a activation mechanism elicited by the surface. ELISA techniques are being adopted to monitor direct complement activation by determination of circulating C3_a and C1_q levels.

The first phase of this study has been the use of ISO-DALT to monitor alterations in circulating plasma proteins including complement (i.e., C3_a and C4_a) and immunoglobulin (i.e., IgG, light and heavy chains) components as a function of clinical extra-corporeal membrane oxygenation. Several membrane oxygenators of similar design yet containing different oxygenating polymer surfaces are to be contrasted.

The in vivo ISO-DALT results for a particular ECMO polymer type are then subsequently compared with in vitro ISO-DALT results from analysis of the eluted fraction after passing plasma over a fixed particular bed composed of the same polymer type as the oxygenator.

The first series of ISO-DALT experiments were conducted on polypropylene oxygenators. Distinct lowering of IgG light and heavy chain concentrations as a function of oxygenation time was observed. An initial decrease in fibrinogen β -chain concentration was observed 30 minutes to 1 hour after by-pass began followed by a rebounding effect observed after 1 hour.

Also a large number of additional plasma protein fractions between 80,000 and 50,000 daltons in size and 4.5 - 3.0 pI were observed in oxygenations lasting longer than 1 hour. The in vitro studies are presently underway.

L. King-Breeding, M. S. Munro and R. C. Eberhart

Department of Surgery, University of Texas Health Science Center at Dallas,
Dallas, Texas 75235

We have shown that C₁₈ alkylation of polyurethane sheets and tubes selectively increases the affinities of these materials for albumin, *in vitro* and *in vivo* (1,2). We have also demonstrated a correlation between the enhancement of albumin affinity by this process and improved thromboresistance (2,3). In this study we extend the alkylation technique to open cell polyurethane foams of high porosity and pore size, such as are used in blood filtration devices. We report the enhancement of the albumin affinity of these materials by this technique, both with and without Antifoam A pretreatment.

Polyurethane foams (30 PPI, Bard Cardiopulmonary) were obtained either with or without Antifoam A (Dow Corning) surface pretreatment. Alkyl derivatization was accomplished by the reaction of a C₁₈ alkyl isocyanate at the urethane secondary amide group in the presence of a zinc catalyst, utilizing mild solvent swelling with trimethylpentane to access the binding sites (1). A 15 mg% albumin solution was prepared from crystalline bovine albumin (Fr V, Miles, BSA) in degassed phosphate buffered saline (dPBS). BSA was labeled with ¹²⁵I by Iodogen (1,3,4,6 tetrachloro-3,6 diphenyl glycoluril, Pierce) mediated oxidation of iodine with subsequent incorporation of generated iodine radicals in albumin tyrosine residues (2). Samples were hydrated 1 hr in 1.5 ml flow chambers filled with dPBS. Two ml of ¹²⁵I-spiked BSA solution were injected into the chamber, incubated 1 min, then flushed with dPBS. One min exposures were selected to improve the measurement of the rapidly bound albumin at the high affinity alkyl binding site.

Results (Table 1) indicate C₁₈ alkylation significantly increases the albumin affinity of the Antifoam A-treated polyurethane foam material. Alkylation of the polyurethane without Antifoam A treatment yielded a nonsignificant tendency to enhance albumin affinity. Entrapment of air bubbles was observed in the foam mesh of several samples in this latter group. Albumin accumulations were substantially larger for these samples, for both derivatized and control categories. These samples were excluded from subsequent statistical analysis.

Inspection of the results suggests that, as with solid materials, C₁₈ alkylation enhances the albumin affinity of the porous polyurethane. Such enhancements for polyurethanes with uninterrupted surfaces have inhibited fibrinogen adsorption and platelet adhesion *in vivo* (2). Pretreatment of the polymer with Antifoam A, a hydrophobic, silicone oil-based material, does not diminish the property of C₁₈ alkylation to improve the albumin affinity of the polyurethane. The mild solvent swelling technique employed in this procedure appears to allow penetration of the reactants to the urethane secondary amide groups. The rapid and massive albumin uptake for samples with entrapped air bubbles may be linked to the denaturation of the protein at the air-liquid-solid interface (4). Loss of tertiary structure can

have a potent albumin aggregating effect, which apparently overshadows the increase in the affinity for nondenatured albumin of the C₁₈ alkyl group. The role, if any, of air denatured aggregated proteins, including albumin, in modifying the thromboresistance of blood contacting materials has not been adequately investigated. However, it is unlikely that such material accumulations improve thromboresistance; furthermore, such aggregates can, themselves, embolize. Thus, C₁₈ alkylation of porous polyurethane networks used as defoamers in bubble oxygenators probably will not improve the blood compatibility of such devices. In applications where air is not introduced into the porous network, as in other blood filters, or in devices in which the air interface is sequestered from the blood stream (microporous membrane oxygenators), C₁₈ alkylation may improve the albumin affinity of the filtration matrix. This may improve the intrinsic thromboresistance of the filters without adversely affecting their embolus filtration or mass transfer capacities.

TABLE 1.
¹²⁵I ALBUMIN UPTAKE (CPM) IN POLYURETHANE FOAM

	No Antifoam A Pretreatment		Antifoam A Pretreatment	
	Control	Derivatized	Control	Derivatized
1	2225	25159*	3012	3138
2	33414*	6339	20702*	5156
3	3056	71147*	2453	3591
4	2443	3111	2339	3462
5	1694	3084	2807	3770
\bar{x}	2354.5	4179.0	2652.8	3823.4
S_x	563.6	1871.5	311.6	779.9

p < 0.10

p < 0.025

*Bubbles observed in polyurethane mesh.

References:

1. Munro, M.S., et al. Alkyl substituted polymers with enhanced albumin affinity. *Trans ASAIO* 27:499-503, 1981.
2. Munro, M.S., et al. Thromboresistant alkyl derivatized polyurethanes. *asaio J.* 6:65-75, 1983.
3. Eberhart, R.C., et al. Albumin retention on C₁₈ alkylated Biomer® grafts. Second World Congress on Biomaterials, 1984 (submitted).
4. Lee, W.H., Jr., et al. Denaturation of plasma proteins and morbidity and death after intracardiac operations. *Surgery* 50:29-39, 1961.

Supported by USPHS Grant HL28690-02.

Linda King-Breeding, Department of Surgery,
Rm G8.248, University of Texas Health Science
Center at Dallas, 5323 Harry Hines Blvd., Dallas
Texas 75235

SOME SPECIAL FEATURES IN PROTEIN ADSORPTION ON THE SURFACE OF ACTIVATED CARBON FIBERS

V.G. Nikolac., E.V. Eretskaya and V.P. Sergeev

Kavetsky Institute of Onkology Problems
Academy of Sciences of the Ukrainian SSR
Kiev, USSR

The composition of the adsorbed protein layer, its surface concentration and structure, as well as the strength of binding of protein molecules and their conformation state, appear to be of major importance in assessment of foreign surface properties and particularly of its biocompatibility and biological activity.

This publication presents results obtained in the study of interaction of the plasma proteins (albumin, γ -globulin, fibrinogen) and proteolytic enzymes (trypsin, protease *Acremonium-specius*), with the surface of activated carbon fibrillar material AUVM "Dnepr," characterized by the developed microporosity (pore diameter 10-50 Å), as well as by the high specific and geometrical surface (respectively, 1500-3000 and $2m^2 \cdot g^{-1}$).

The kinetic investigations of protein adsorption and desorption were carried out under the static conditions by employing the technique of solution depletion, where protein concentration was estimated according to Lowry, whereas the proteolytic activity was determined after Hagihara. It has been demonstrated, that with the increase of the protein level in the solution the balanced quantity of adsorbed protein rises in the area of the explored concentrations (Table 1), while the length of time required to achieve this balance decreases.

Table 1. Dependence of balanced amount of adsorbed protein on its concentration in initial solution

Protein concentration mg/ml	Adsorbed protein amount, mg/g adsorbent				
	albu- min	γ - glob- ulin	fibrin- ogen	tryp- sin	protease Acr. spec.
0.25	16.5	14.5	11.0	25.0	30.0
0.50	18.0	18.0	11.5	75.0	65.0
1.0	21.0	24.8	16.7	155.0	112.5
2.5	28.5	28.9	39.4	261.0	223.0
5.0	35.0	29.5	-	358.0	340.0
7.5	39.0	30.0	-	450.0	400.0
10.0	-	-	-	580.0	-

The surface concentration of plasma proteins practically is not influenced by their molecular mass and equals for albumin $1.95 g \cdot cm^{-2}$, γ -globulin $1.50 g \cdot cm^{-2}$, fibrinogen $1.97 g \cdot cm^{-2}$. These values of surface concentrations are 3-5 times higher than those for glass, polystyrene, Teflon and other hydrophobic and hydrophilic materials (J.L. Brash, D.J. Lyman, 1971).

On the AUVM the sorption balance can be reached several times faster than on the granulated activated charcoals, the latter exhibiting the same specific surface - though with considerably smaller geometrical surface, that is, the interface surface.

The proteolytic enzymes, such as for instance, trypsin and protease *Acrem. specius*, manifest still higher surface concentrations, amounting to 29 and

$20 g \cdot cm^{-2}$ respectively. So significant absorption of enzymatic proteins with their molecular mass of about 20-30 thos. daltons can be attributed not only to their adsorption on the geometrical surface of tissues but also to adsorption in the pores of the appropriated diameter. It seems to be likely, that on the surface of activated carbon fibers there occurs the autolysis of enzymes and part of them is being absorbed in the form of products degradation. The adsorbed enzymes preserve, at least partially, their specific activity in respect to the high-molecular substrates, and it is noted to enhance with increase in amount of the bound protein (Table 2).

Table 2. Dependence of protease *Acremonium specius* specific activity on quantity of protein adsorbed on AUVM surface

Amount of bound protease, mg/g	7.4	14.4	34.8	67.6	144.4
Specific activity PE/mg protein $\times 10^5$	0.4	0.8	8	15	19

Evidently, conformation changes accompanying the protein adsorption on the AUVM appear to be the less pronounced the higher surface concentration. The study of desorption of plasma proteins and enzymes from the AUVM revealed that none of the solutions employed (0.067 M phosphate buffer, 1 M NaCl, 6 M urea) could eluate the adsorbed proteins from the surface of carbon fibers, i.e., the adsorption seems to be practically irreversible. It is maintained that such strong binding of the proteins explored on the AUVM surface can be due to peculiarities in its structure, along with high adsorption potential resulting from the developed microporosity, and to presence of the ionized groups ($-OH$, $>CO$, $-COOH$, etc.). One cannot also rule out the possibility that on the adsorbent surface there can be established covalent bonds between protein amino groups and carbonyl groups.

Kavetsky Institute of Oncology Problems
Academy of Sciences of the Ukrainian SSR
KIEV
USSR

EFFECTS OF MODEL POLYMERS ON FACTOR V ACTIVITY

M.C. BOFFA*, J. BONBLED*, N. AUBERT**, N. MAUZAC**, C. FOUGNIOT**, J. JOZEFOWICZ**, and M. JOZEFOWICZ**.

Centre National de Transfusion Sanguine
Paris, France.

It has already been demonstrated that negatively-charged (sulfonate) polyelectrolytes induce a loss of factor V activity (1).

In this work different negatively-charged polymers were studied. Negative charges were either sulfonate or carboxyl groups. The activity of factor V has been investigated in the plasma which has either been in contact with insoluble polymers or in the presence of soluble dextran derivatives.

Two series of insoluble polymers were studied:

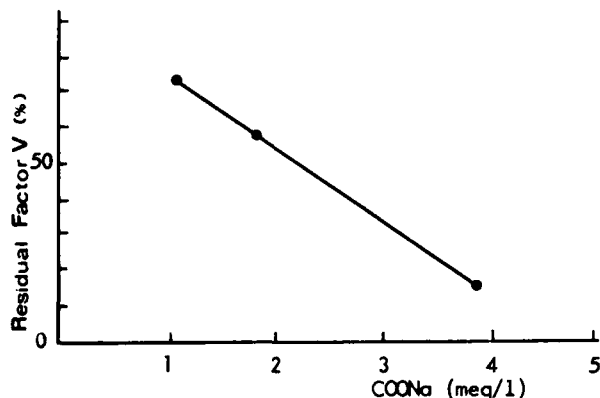
- Sephadex® substituted with methylcarboxyl groups (SCM) and the same partially substituted with benzylamine sulfonate groups (SCMBSO₃) on the one part,

- polystyrene substituted with sulfonate and amino-acid sulfamide groups on the other part (3).

The effect of dextran derivatives was also analysed. Dextrans were substituted at different ratios with methylcarboxyl and benzylsulfonate ± amino-acid groups. At different degrees they all display antithrombin activity.

Factor V was measured by one stage assay in centrifuged plasma after an incubation of 30 min. at 37°C with the washed insoluble polymers, previously allowed to swell in pH 7.3 buffer overnight. Dextrans were directly dissolved in plasma. Usually 100 mg of polymer or 5 to 10 mg of dextran derivatives were used per ml of plasma.

The decrease of factor V by SCM at different substitution ratios of methylcarboxyl groups varied according to the percentage of these groups.



FACTOR V ACTIVITY IN PLASMA IN CONTACT WITH METHYL-CARBOXYLATED SEPHADEX

The curve of factor V activity obtained with PSSO₃ at different ratios of SO₃ varied according to the sulfonate content. However, the swelling of the polymer in water gives a similar curve. Factor V activity seems to depend on the availability of sulfonate groups of the polymer.

In PSSO₃ the sulfonate substituents repre-

sented 82 % of the aromatic groups. In PSO₂AA they represent about 30-40 % and the amino-acid sulfamide groups about 45 to 60 %. The following amino-acids were grafted: glutamic, aspartic, amino-caproic, amino-glutamic acids, glycine, phenyl-alanine, threonine, proline, hydroxyproline. Factor V activity decreased between 65 and 75 % with PSSO₃, between 55 and 93 % according to the amino-acid sulfamide studied. The observed differences might rather be relevant to the physical state (granulometry, porosity) of the polymer than to the amino-acid specificity.

When the carboxyl groups of the amino-acid were blocked by either a methyl or an amide group, the negative charges decreased to 30 % and the factor V was little or not altered.

Whether sulfonate groups were added or not to benzylamine methylcarboxylated Sephadex, factor V activity decreased similarly.

The effect of sulfonate, carboxyl and benzylamine ± amino-acid group on factor V activity was also examined using differently substituted dextrans. It was observed that the decrease of factor V was not directly related to the sulfonate content. It was independent of the antithrombin effect and the inhibitory activity on C3 convertase of the dextrans. It was not related to the presence of the amino groups.

In conclusion factor V activity seems to depend on the total negative charges (COONa and SO₃Na) and also on the benzylamine content of the polymer.

The study of the mechanism of action responsible for the decrease of factor V activity is in progress by means of factor V immunological determination and by measurement of protein C activation.

1- M.C. BOFFA, J.P. FARGES, B. DREYER, B. CONCHE, C. PUSINERI and G. VANTARD: Striking differences observed in the effect of amphipathic polyelectrolytes on contact and other clotting factors. In Biomaterials 1980, ed. G.D. Winter, D.F. Gibbons and H. Plenck. 1982, p. 399-408.

2- M. MAUZAC, N. AUBERT and J. JOZEFOWICZ: Antithrombin activity of some polysaccharide resins. Biomaterials 1982, 3, 221-224.

3- C. FOUGNIOT, J. JOZEFOWICZ, M. SAMAMA and L. BARA: New heparin-like materials part I. Ann. Biomed. Eng. 1979, 7, 429-439.

This work was supported by contrat CNRS - GRECO 180048.

*Laboratoire de Recherche en Hémostase et Thrombose - C.N.T.S. 6 rue A. Cabanel - 75015 Paris-France

**Laboratoire de Recherche sur les Macromolécules Université Paris Nord, Villetaneuse, France

CELL CULTURE METHODS FOR DETECTING IMMUNOTOXICITY OF SYNTHETIC POLYMERS

J.M. Simpson, J.T. Sarley, H.J. Johnson, S.J. Northup

Travenol Laboratories, Inc.
Morton Grove, IL 60053

Methods to assess immunotoxicity of leachables from synthetic polymers have been evaluated. Assays were selected to examine immunological functions of mouse splenic lymphocytes exposed to polymer extracts. Generic classes of polymers included polyvinyl chloride, polyurethane, polyethylene, polypropylene, silicone rubber, polyamide, ethylene vinyl acetate, and acrylonitrile butadiene styrene. Polymers were extracted with serum-supplemented cell culture medium at 37°C to simulate physiological conditions.

Lymphoproliferative responses were evaluated by determining the incorporation of ^3H -thymidine into mitogen-stimulated murine cell culture populations of T- and B-lymphocytes. Mean counts per minute (CPM) were determined for all replicate cultures and compared to control values. In vitro effects of polymer extracts on the induction and expression of direct IgM anti-sheep red blood cell (SRBC) antibody formation by mouse splenic lymphocytes were monitored with the Mishell-Dutton and Jerne assays, respectively. Antibody formation following in vitro or in vivo immunization was quantitated using the hemolytic plaque assay. Mean plaque-forming cell (PFC) responses were determined for all replicate cultures and compared to control values. The statistical significance of the percent change of lymphoproliferative and PFC responses was determined by analysis of variance. Cell culture viability was determined by trypan blue dye exclusion.

Viability determinations were compared with immunological function responses. These results indicated that impairment of lymphocyte function observed may be attributed to immunotoxicity of the polymer extracts rather than to non-specific cytotoxicity. Alterations in immunological function responses were observed in the presence of various polymer extracts. In vitro effects were usually suppressive. Results indicated that B-lymphocyte proliferation was generally more susceptible than T-lymphocyte proliferation to polymer extracts. Polymer extracts also interfered with the induction more often than with the expression of anti-SRBC PFC responses. These assays appear to offer convenient and sensitive methods for preliminary screening of polymers for immunotoxicity.

Janney Simpson
Travenol Laboratories, Inc.
6301 Lincoln Avenue
Morton Grove, IL 60053

IN VITRO MYELOID SUSPENSION CULTURES FOR SHORT-TERM TOXICITY STUDIES

S.L. Hilbert

F.D.A., National Center for Devices and Radiological Health
Rockville, Maryland

The intramural evaluation of a variety of in vitro bone marrow suspension culture techniques are currently being undertaken in order to determine the feasibility of utilizing this tissue for short-term (e.g., seven days) and ultimately long-term (e.g., two to four months) toxicity screening of both biomaterials and low molecular weight compounds associated with these materials. The selection of bone marrow as a target tissue for toxicology screening studies centers about the critical nature of this tissue in vivo and the demonstrated sensitivity of bone marrow to injury as a result of both exposure to physical (e.g., ionizing radiation) and chemical (e.g., benzene, chloramphenicol) insults. Ideally, a primary goal of this project is to provide an in vitro method which will support differentiation and allow the assessment of mechanisms of cellular injury resulting from exposure to test compounds and materials.

A modification of the method of Dexter *et. al.*, 1977 (1) was used in which bone marrow was removed from each femur by both lavage and scraping of the marrow cavity. A cell suspension was prepared and adjusted to a final concentration of 4×10^6 nucleated cells/ml using culture media (RPMI 1640 supplemented with 20 percent fetal calf serum, 1000 units penicillin, 10 mg streptomycin). Cultures consisting of 5 ml cell suspension per 25 cm² plastic flask were initiated and maintained at 35-37°C in 5 percent CO₂ and humidity for a period of one to seven days. Four groups were established; namely, a control and three dose levels of the chemical compound to be tested.

The contents of each flask (adherent layer; suspension phase) were fixed (4% formaldehyde - 1% glutaraldehyde in 0.2M phosphate buffer) for both transmission (TEM) and scanning (SEM) electron microscopy. To ensure a random sampling of the cell population three depths or levels within each TEM block were selected (i.e., top, middle, bottom). Ten random micrographs (2900X) were taken using the top left corner of a section supported on four sides by grid bars as a reference point (2). As a result of this sampling method, the data base consisted of 1440 low magnification micrographs for each chemical tested (e.g., 120/trial x 3 trials x 4 sampling times/trial). These micrographs were then analyzed in the following manner: (A) cells classified as to morphologic type (3); (B) cytotoxicity (numerical ranking); and, (C) extent and type of cellular injury (numerical ranking and organelles affected).

The data was statistically evaluated using a two way analysis of variance (dose*time; probability level, 0.05), general linear model procedure and mean comparisons made utilizing the least significant difference test.

The results of the morphologic characterization of primary non-human (African Green Monkey) bone marrow suspension cultures exposed to benzidine (carcinogen) and diaminobenzidine (suspected carcinogen) will be reported. Briefly, the short-term (seven days) in vitro exposure of bone marrow to this class of chemical compound resulted in quantitative and reproducible changes in the myeloid cell population. In addition, the concurrent ultrastructural evaluation of the cellular response to these test compounds was performed, thus providing a stereologic data base for the initial elucidation of compound specific mechanisms of cellular injury.

The initial results provide support for the feasibility of using this approach to assess chemical sensitivity in a heterogeneous cell population composed of both immature, as well as differentiated cells. Studies are currently in progress to determine the sensitivity of this method for detecting differences in chemical structure between closely related compounds.

References:

1. T.M. Dexter, T.D. Allen and L.G. Lajtha, J. Cell Physiol. 91 (1977) pp. 297-311.
2. E.R. Weibel, W. Stanbli, H.R. Gnagi and F. Hess, J. Cell Biol., 42 (1969) pp. 68-91.
3. D. Zucker-Franklin, M.F. Greaves, L.E. Grossi and A.M. Marmont, Atlas of Blood Cells, Lea-Febiger Philadelphia, (1981) pp. 149-161, 321-336.

Mailing Address: Food and Drug Administration
National Center for Devices
and Radiological Health
5600 Fishers Lane
Rockville, Maryland 20857
HFK-220

An Organ Culture Model for Screening of Bone Implant Materials

Eric E. Sabelman

Rehabilitation R&D Center, Palo Alto VA Medical Center,
3801 Miranda Avenue, Palo Alto, California, 94304

Simple, repeatable model systems are needed to evaluate relative cytotoxicity and rates of cell migration, proliferation and synthesis in contact with bone implant materials [1].

Background: Ray & Holloway [2] introduced the rat parietal defect as an *in vivo* test system; it has recently been used to detect osteoinduction by implanted demineralized bone powder (DBP) [3,4].

Tissue culture has advantages for cytotoxicity, cell attachment and growth inhibition assays [1]. Ainsworth, *et al* [5], tested responses of rat muscle fibroblasts to human DBP compared to Urist's [6] technique of muscle explants in a demineralized bone hemicylinder.

Organ cultures of rat or mouse calvaria have been used to study hormonal effects [7], matrix synthesis [8] and bone resorption [9]. Since the rodent calvarium *in vitro* is well-documented, it was felt to be suitable as a bone defect model.

Method: Hemispherical calvaria of 19-day S-D rat fetuses were aseptically excised, placed on sterile filter paper and 3 mm diameter defects were punched centered on the fontanelle. Each explant was placed on a dialysis membrane disc in a Sykes-Moore chamber [10]. Test materials were: (1) bovine DBP made by a modification of the method of Glowacki [3] gamma sterilized at 1.3 megarads, (2) Calcitite [11] hydroxyapatite periodontal implant and (3) Zyderm Collagen Implant [12], 35 mg/ml. Some defects were left unfilled as controls.

The chambers were sealed, filled with medium (F-12 + 10% FCS + 100 ug/ml ascorbic acid + antibiotics) and incubated at 37 C. Medium was changed at 2 day intervals. After 8 days, neutral red (0.5 ml of 1 mg/ml BSS stock per 4 ml chamber) was added a vital stain for lysosome-bearing cells [13]. The final medium change included 9 ug/ml lead acetate to label sites of mineralization [14]. Cultures were fixed on the 15th day in 10% buffered formalin, then processed for histology using H&E or Gomori's trichrome.

Results: The circular defects were distorted by flattening of the explants; empty defects were most affected. If not compressed, dense Calcitite particles easily fell out of place. Overfilling of the defect occurred with DBP and Zyderm, and underfilling with Calcitite.

Microscopy during culture revealed bridging of the narrowed control defects after 6 days. Calcitite particles lying on top of the explant were rapidly covered by fibroblasts; strands of cells extended into the defect, but never completely covered the particles. DBP supported more uniform colonization by cells within the

defect. Interconnected stained cell masses at varying depths in the collagen suspension could not be seen until after vital labelling.

Outgrowth of cells onto the membrane and glass cover slip was less with DBP implants. All specimens had outgrowths in differing proportions of: unstained stellate cells (presumed osteoblasts), lightly stained spindle-shaped cells (fibroblasts) and darkly stained round cells (small osteoclasts or mast cells).

Histologically, most DBP and Calcitite was detached in mid-defect, implying poor cohesion; remaining particles were covered by at most a single layer of cells. Each explant had more cartilage than was ascribable to chondrocranial remnants.

Discussion: Empty defects were poor controls, since distortion permitted rapid filling similar to that seen by Bucher [15] in fractured embryonic chick long bones. Orientation of migrating cells by DBP described by Bellows, *et al* [16], was evident by comparison with Calcitite, but not widespread. Apparent overgrowth of cartilage at the expense of bone may be due to oxygen depletion [17].

In future experiments it may be possible to improve osteocyte survival, stabilize the implant and simulate functional stresses by replacing the static Sykes-Moore chambers with Isolated Perfusion Chambers [18].

Acknowledgements: This work was performed at Collagen Corporation, Palo Alto, CA. The author is grateful to R. Armstrong, S. Chu and E. de Leon for histology and to K. Piez and B. Weiss for reviewing the text.

References:

- [1] Homsy, C.A., *et al*, *J Am Dent Assoc* 86:817 (1973).
- [2] Ray, R.D. & Holloway, J.A. *J Bone Joint Surg* 39-A:119 (1957).
- [3] Mulliken, J.B. & Glowacki, J. *Plas Recon Surg* 65:553 (1980).
- [4] Urist, M.R., *et al*, *Proc 29th Annual ORS*, p. 266 (1983).
- [5] Ainsworth, T., *et al*, *J Lab Clin Med* 89:781 (1977).
- [6] Urist, M.R. *Calcif Tiss Res* 4(suppl):98 (1970).
- [7] Dietrich, J.W., *et al*, *Endocrinol* 98:943 (1976).
- [8] Lewis, E.A. & Irving, J.T. *Archs Oral Biol* 15:769 (1970).
- [9] Gray, D.H., *et al*, *J Bone Joint Surg* 60-B: 575 (1978).
- [10] Sykes, J.A. & Moore, E.B. *Proc Soc Exp Biol Med* 100:125 (1959).
- [11] TM Calcitek, Inc. [12] TM Collagen Corp. [13] Puchtler, H., *et al*, *Beitr Pathol* 150:174 (1973).
- [14] Schneider, B.J. *Am J Phys Anthropol* 29:197 (1968).
- [15] Bucher, O. *Acta Anat* 14:98 (1952).
- [16] Bellows, C.G., *et al*, *J Cell Sci* 44:59 (1980).
- [17] Rifas, L., *et al*, *J Cell Biol*, 92:493 (1982).
- [18] Sabelman, E.E., *et al*, *Proc 29th ACCEMB*, pg. 112 (1976).

J. R. Dylewski and C. L. Beatty

Dept. of Materials Science & Engineering
University of Florida, MAE 217
Gainesville, Florida 32611

Introduction

The bleeding effect of low molecular weight polydimethylsiloxane (PDMS) material from the bag-gel mammary prosthesis may pose a serious problem related to spherical contracture that occurs after surgical breast implantation (1,2). Other studies indicate that PDMS bleed from the PDMS implants may not cause the same problem (3,4). However, the advent and use of "leak-proof" breast implants indicate that PDMS bleed is still considered by many to be a significant problem. Much of previous work on PDMS bleed has concentrated on in-vivo and rather subjective tests. The goal of our research is to devise a diffusion in-vitro test on new, "as received" implants and used implants to yield a more quantitative and objective evaluation of the PDMS bleed phenomena.

Experimental

All breast prostheses were obtained from Dow Corning Corp (Cat. #541-S). PDMS breasts were implanted in dogs for six months prior to our diffusion studies designated henceforth as "used". A Blue M circulating air oven and a Scientech Model 3300 electronic balance were used for the diffusion studies.

Results and Discussion

The weight loss data obtained for the new and used implants at 310K (body temp.) is plotted in Fig. 1. The used prostheses show an insignificant weight change ($\sim 0.053\%$) over a period of about 1.2 months whereas the new implants indicate a much greater change in weight $\sim .93\%$. At the end of this time interval it was assumed that all the low molecular weight species of PDMS had diffused from the implant so the temperature was raised to 320K in an attempt to confirm this. As shown in Figure 2, it was observed that an additional relatively rapid loss of weight occurred initially followed by a nearly constant rate of weight loss up to about 650,500 minutes (1.2 years). The weight loss ($\sim .28\%$) for the two used prostheses studied was reproducible even for long times (Figure 2). In addition, the weight loss of the two new implants held at 310K, continued to increase from .93% at 0.1 years to about 1.4% after 1.2 years. Most of the difference in weight loss occurs at 310K over a 1.2 month period suggesting that a thermal conditioning cycle prior to implantation may be a useful procedure for eliminating the major portion of silicone bleed that occurs in new prostheses. Increasing the temperature to 320K for the used implants may be considered as an accelerated test of PDMS bleed at long times.

Summary

Simple diffusion experiments have shown that implantation of bag-gel implants significantly reduces the exudation of the PDMS contents. Thus, a simple thermal pretreatment prior to

implantation may minimize the loss of PDMS from these implants. Diffusion measurements at elevated temperatures when utilized as an accelerated aging test suggests that a slow, continual release of PDMS from the bag-gel PDMS prosthesis may occur after implantation.

Acknowledgements

The authors would like to acknowledge the partial financial support of this work by the Microstructure of Materials Center of Excellence, University of Florida.

References

1. Baker, J.L., LeVier, R.R., Spielvogel, D.E., *Plast. Reconstr. Surg.* 69(1), 56 (1982).
2. Barker, D.E., Retsky, M.I., Schultz, S., *Plast. Reconstr. Surg.*, 61(6), 836 (1978).
3. Gayon, R.M., *Plast. Reconstr. Surg.*, 63(5), 700 (1979).
4. Ksander, G.A., Vistnes, L.M., Kosesk, J., *Ann. Plast. Surg.* 6(3), 182 (1981).

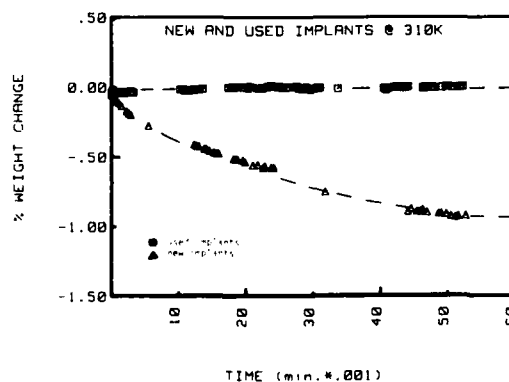


Figure 1. Weight loss experienced for new and previously implanted PDMS gel/PDMS bag breast prostheses.

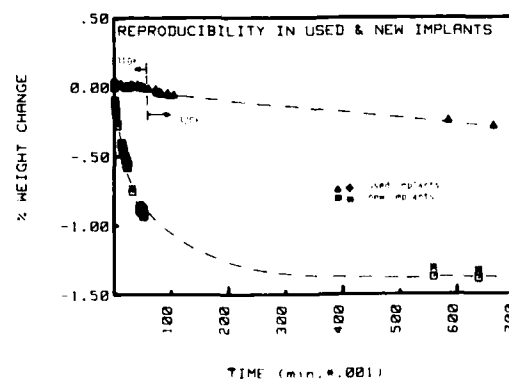


Figure 2. Effects of temperature and time on the weight loss of new and used implants.

Paul Y. Wang and Janet Ditchfield

Laboratory of Chemical Biology, Inst. of Biomed. Eng.
Faculty of Medicine, University of Toronto, Canada M5S 1A8

INTRODUCTION

Inert biomaterials such as silicone, polyethylene, poly(methylmethacrylate), etc., used in the fabrication of implants are insoluble and their biocompatibility can be assessed by cell culture on the surface of these solid polymers. Recent interest in controlled delivery of drugs by bioerodible polymer matrix calls for studies on the effect of the dispersed polymer component in the body. This is often the major part of such drug releasing devices, which may be used by a large population in the treatment of allergy, arthritic pain, or birth control. Bioerosion may be achieved by hydrolysis to give oligomers of various sizes which may be difficult to predict. Therefore, for simplicity in this preliminary study, we selected 3 soluble polymers of m. wt. $\sim 2.5 \times 10^5$ daltons to evaluate the response of the spleen to these macromolecules. A typical response of this organ is the release of antibody into the circulation that can be detected by the highly sensitive solid-phase radioimmunoassay method.

MATERIALS AND METHODS

Polyvinyl alcohol, polyacrylic acid, and polyacrylamide were individually dissolved in saline or emulsified in Freund's complete adjuvant, and injected i.p. at a concentration of 10 μ g in 0.1 ml into groups of five C57BL/6 adult mice. At weekly intervals, serum was obtained by bleeding from the retro orbital plexus. For the detection of antibody (Ab), polyvinyl chloride microtitre plates were first coated with the specific polymer, washed, and then incubated with serum sample at 37°C for 4 hr. After 3 cycles of additional washings with a buffer, the presence of any specific polymer-Ab complex was determined by interaction with an 125 I-labelled anti-mouse immunoglobulin raised in rabbit. For the spleen cell transfer experiment, adult C57BL/6 mice were irradiated with 800R to abolish their natural Ab-producing capacity. Spleens from non-irradiated C57BL/6 mice were disintegrated in sterile Hank's balanced salt solution, centrifuged at low speed, and the free spleen cells were washed several times. Monoclonal rabbit anti-thy-1,2 antiserum was added at 1:20 dilution to the spleen cell suspension at 10^7 cells/ml, incubated, and the treated cells were resuspended. Rabbit complement at 1:12 dilution was added to lyse the small amount of lymphocytes derived from the thymus. One ml of this treated spleen cell resuspended at 10^8 cells/ml was injected into the tail veins of the irradiated mice, and 1 wk later they were injected with 10 μ g of one of the soluble polymers already described. At weekly intervals, blood was collected to test for the presence of specific Ab released by the injected spleen cells.

RESULTS

The level of specific Ab released by the spleen cells was expressed as $1/2^n$, where n = the first serum dilution to exhibit no complexing

activity (i.e., high n generally indicates Ab abundance). These Ab levels were: polyvinyl alcohol (1/64), polyacrylic acid (1/1024), and polyacrylamide (1/512). These values represent the maximum response observed, and the period of time required to reach the maximum value may vary depending on the polymer and the amount injected. Doses of polymer much higher than 10 μ g do not necessarily produce higher responses, possibly because of tolerance due to overdose. Another injection of 10 μ g or less of the same polymer may result in a higher and quicker response, but the duration of this response may not always be longer than that following the first injection. To demonstrate that spleen cells interact with the injected polymer and respond by releasing specific Ab, levels of Ab similar to those given above were detected by the assay only when the irradiated mice were reconstituted with thymus cell-depleted spleen cells from adult, non-irradiated C57BL/6 mice, because the irradiation killed the spleen cells in the irradiated mice and, therefore, their function.

DISCUSSION

Polymer matrix in bioerodible drug releasing devices may be designed to disperse gradually with the release of monomeric, oligo- or polymeric components along with the active drug. Low m. wt. fragments released, even at a very low rate, may result in immediate local or systemic signs of toxicity. Slowly released polymeric components would require additional steps, such as complexing with Ab, for elimination. It is not known whether the polymer-Ab complex will affect the bioerosion rate of the implant, or the release rate of the drug. The pathological consequences of such macromolecular complexes on the function of organs such as the liver and kidneys are also unknown. Our results indicate that simple homopolymers with a hydrocarbon backbone can induce the spleen to respond by producing specific Ab. Furthermore, as such responses can be effected without the co-operation of the thymus, there would be no influence exerted by the genetic background of the host. Thus, responses against polymers would be similar to those against bacterial infections, in that every host would respond, albeit to varying degrees. It is felt that this area of biomaterials research should not be overlooked in the design and testing of erodible implants.

We thank the Medical Research Council of Canada for support: Grant No. MA-8039.

Paul Y. Wang, PhD, Laboratory of Chemical Biology, Inst. of Biomed. Eng., Faculty of Medicine, University of Toronto, Canada M5S 1A8.

Chinese Hamster Ovary Cells (CHO) Clonal Growth Assay for the Evaluation of Cytotoxic Effects of Biomaterials

R. Sernau, T. Cortina, B. H. Keech, N. E. McCarroll, M. G. Farrow

Hazleton Laboratories America, Inc., 9200 Leesburg Turnpike, Vienna, Virginia 22180

The ability of Chinese Hamster Ovary Cells (CHO) to phagocytize particulate matter was exploited in the development of a new testing approach for the cytotoxic evaluation of biomaterials. Actively growing cultures of CHO cells were exposed for five hours to graded doses (125-500 ug/flask) of pulverized fiberglass particles and asbestos powder.

Following treatment approximately 100 cells were plated in triplicate, incubated at 37°C for eight days, fixed, and stained with crystal violet. Transmission electromicrographs prepared from cells treated with 5000 ug of each test material confirmed the phagocytic activity of CHO cells. Results of clonal growth assays indicated that diminished growth accompanied exposure of cells to increasing doses of asbestos; by contrast, fiberglass was not cytotoxic.

The overall results suggest that the use of a cell system with demonstrated phagocytic activity in conjunction with the ability to quantitate cytotoxic effect may provide an excellent alternative to the semi-quantitative tests currently employed to assess in vitro cytotoxicity of insoluble materials.

We selected CHO cells for the development of our Clonal Growth Assay based on our past experience with this mammalian cell system as a multi-purpose target cell for investigation of genotoxic events. We feel that with slight modifications in our in vitro cytotoxicity test, we will be able to assess the potential of insoluble materials to cause gene mutations, chromosomal aberrations and DNA damage. The feasibility of this approach is currently under investigation.

Barbara H. Keech
Genetic Toxicology Department
Hazleton Laboratories America, Inc.
9200 Leesburg Turnpike
Vienna, Virginia 22180

PRODUCTION OF LAF (LYMPHOCYTE-ACTIVATING-FACTOR) BY MONONUCLEAR
PHAGOCYTES ACTIVATED WITH POWDERED BIOMATERIALS

A. Pizzoferrato, G. Ciapetti, S. Stea

Istituto Ortopedico Rizzoli
Bologna, Italy.

Mononuclear phagocytes have been shown to produce a monokine termed LAF (Lymphocyte-Activating-Factor) or Interleukin 1, when stimulated by several agents (e.g. Ab-Ag complexes, bacterial endotoxin).

This soluble factor acts both directly stimulating lymphocyte-DNA-synthesis and, more clearly, increasing the proliferative response of thymocytes to lectins.

In this paper we investigate the possibility that the wear particles from biomaterials, used in constructing artificial prostheses for orthopedic surgery, can influence mononuclear phagocyte production of LAF effective on mouse thymocytes.

Briefly the method used consists of:

- Collection of mononuclear phagocytes from various sources and "in vitro" cultivation of that population in presence of a powdered biomaterial for 24 hours. Controls do not contain any powders in the culture medium.
- After 24 hours of cultivation the supernatant from cultures is collected and dialyzed for 48 hours against physiological saline at 4°C.
- Assay of the LAF activity, if present in the supernate, is performed on mouse thymocytes cultured for 3 days with phytohemagglutinin-P (PHA-P). The optimal concentration of PHA for stimulating thymocytes was assessed after a series of trials. It resulted to be 0.2 µg/ml, which corresponds to a suboptimal dose in comparison to the peripheral blood lymphocyte PHA-dose currently used.
- The proliferation of such cells, triggered by PHA and potentiated by LAF, is measured by means of ^3H Thymidine uptake by thymocytes and subsequent counting of the CPM in a β counter.
- Several materials were tested : alumina-titania composite, titanium, stainless steel and copper (the last one represents the maximum of toxicity). Bacterial endotoxin was used as a LAF-promoting agent.

The results obtained show quite clearly that alumina-titania composite, a biomaterial largely known as non-toxic, may cause an appreciable, even if slight, variation in LAF release by mononuclear phagocytes that have been treated with the alumina powder if compared to the untreated cells (Controls)(Fig. 1).

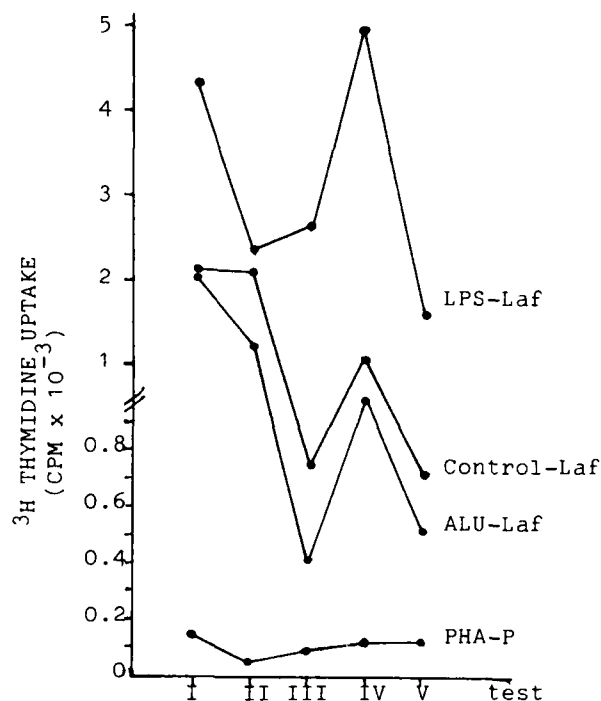


Fig. 1. Effect of alumina-induced LAF on mouse thymocyte proliferation. Each point is the mean of six values. LPS=bacterial endotoxin; ALU=alumina-titania composite.

The effect of the other biomaterials tested are not so clearly reproducible as in the case of alumina.

The possibility that a biomaterial would influence the production or release of a soluble mediator modulating the lymphocyte response, can be regarded as a new aspect of the interaction biomaterial-cell.

It is quite clear that patients who receive artificial prostheses may develop cell-mediated immune responses to the various compounds contained in them.

Conceivably, the modulating effect the mononuclear phagocytes exert on cell-mediated immunity through lymphokine production, could assume importance in the phenomenon of the body tolerance to a prosthetic implant.

Supported by National Research Council(CNR).

Prof. Arturo Pizzoferrato
Center for Biocompatibility Research of
Implant Materials-Istituto Ortopedico Rizzoli
via Codivilla 9 -40136 Bologna, Italy.

POLYETHYLENE WEAR AGAINST TITANIUM ALLOY COMPARED TO STAINLESS STEEL AND COBALT-CHROMIUM ALLOYS

H. McKellop, A. Hosseini, K. Burgoyne, I. Clarke

Orthopaedic Biomechanics Laboratory,
Bone and Connective Tissue Research Program,
Orthopaedic Hospital-U.S.C., Los Angeles, CA 90007

A ten station hip-joint simulator was used to compare the wear rates of UHMW polyethylene acetabular cups bearing against titanium alloy femoral heads from three manufacturers. Control prostheses from the same manufacturers were either 316 stainless steel or cobalt chromium molybdenum alloy. Three prostheses of each type were run in the joint simulator for one million cycles at 68 cycles per minute, under a physiological hip load curve with 2030 N peak, and bovine serum lubrication. Wear of the acetabular cups was determined by removing, cleaning, drying and weighing the cups at approx. 200,000 cycle intervals. Pre-soaking and control cups were used to correct for fluid sorption effects(1). The cups had been sterilized by the manufacturers with approx. 2.5 MRad gamma radiation. Cups from a single batch from each manufacturer were used, such that the alloy type was the only systematic variable within each group of six prostheses. The stainless steel and cobalt chrome femoral heads were passivated by the manufacturers using hot nitric acid (ASTM F86-76). The STH and Anitomic titanium alloy components also had been passivated with hot nitric acid to produce titanium oxide surface layers. In contrast, the Bard-Link titanium alloy components had been passivated in a cyanide-based molten salt bath at 800°C for two hours, which produced a carbon-bearing titanium nitride surface layer.

RESULTS: Wear rates (Figure 1) were taken as the slope of least-squares linear regression fit to the weight-loss measurements (plotted as volumetric wear). The T-28, STH and Anitomic prostheses were tested with random ball-socket pairings. However, during the test we found that some of the Anitomic prostheses had very low or even negative ball-socket clearances. This induced very high frictional torque and specimen heating and probably contributed to the higher wear and greater scatter with the Anitomic prostheses ($\pm 50\%$). For the Bard-Link tests the specimens were paired largest-ball-in-largest-cup, etc. to give a nearly uniform clearance (about 0.3 mm). There was much less scatter in the wear rates with these prostheses ($\pm 12\%$).

The mean wear rates, in cubic millimeters per million cycles, were higher for the STH compared to the T-28 (67 ± 4 vs 42 ± 34 , respectively) and for the Anitomic titanium alloy compared to Anitomic cobalt-chrome (102 ± 49 vs 79 ± 39 , respectively). However, the overlap in results (Fig. 1) was such that these differences were not statistically certain (t-test, $p > 0.1$). The mean wear rates for the Bard-Link titanium alloy and cobalt-chrome were very similar (34 ± 4 and 38 ± 2 mm³ per million cycles, respectively). On visual examination, the STH and Anitomic titanium alloy components showed more extensive surface scratching than was apparent on their stainless steel and cobalt-chrome controls. The Bard-Link nitrided titanium alloy showed the least surface scratching of any of the alloys, possibly a result of the surface hardening.

POLYETHYLENE WEAR AGAINST VARIOUS FEMORAL COMPONENTS

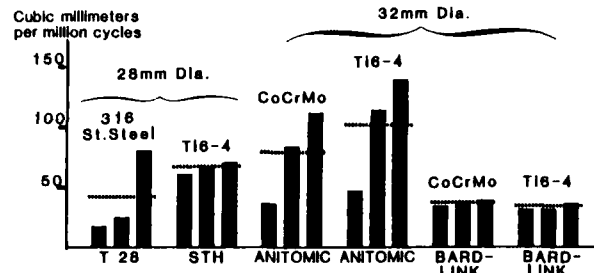


Fig. 1 Polyethylene wear rates (volumetric) for each of the 18 prostheses. The horizontal dashed lines indicate the mean wear rate for three identical tests. The difference in mean values within each group of six is not statistically significant ($p > 0.1$), i.e. T-28 vs. STH, Anitomic vs Anitomic and Bard-Link vs. Bard Link. Repeatability of the results improved considerably for the six tests where the balls and cups were matched to give uniform 0.3 mm diametral clearance (Bard-Link).

The polyethylene wear rates measured in this study span the range reported by Griffith et al.(2) for 493 Charnley prostheses after 8.3 years clinical use. Unfortunately, the upper safe limit clinically for the polymer wear rate is not known. The surface scratching on these joint simulator tested femoral components is much more extensive than that observed on components removed from patients. Thus, the joint simulator test appears to be more aggressive than clinical use (and is therefore a conservative test). Additional studies are planned to compare the resistance of these alloys to abrasion by entrapped acrylic cement particles, representing a more severe clinical situation.

The excellent reproducibility of the wear rates with identical prostheses obtained in the most recent test, where clearance was controlled, demonstrates that the joint simulator and wear measurement protocol now provide a reliable method for evaluating the effect on wear of subtle changes in prosthesis design, such as polymer processing variables and sterilization dose or metal surface finish and passivation.

This research was supported by the Orthopaedic Foundation of Los Angeles and by the Zimmer, Hexcel and Bard corporations.

- (1) McKellop, H., Clarke, I.C., in Functional Behavior of Orthopaedic Biomaterials, Vol. II, CRC Press, Boca Raton (in press).
- (2) Griffith et al., Clin. Orthop., **137** (1978).

Biomechanics Research Laboratory
Orthopaedic Hospital-USC
2400 S. Flower, Los Angeles, CA 90007

IMPROVEMENT OF CREEP AND WEAR PROPERTIES OF POLYETHYLENES.

GAUSSENS G- BERTHET J. CORNET L. - NICAISE M.

COMMISSARIAT A L'ENERGIE ATOMIQUE - C.E.N.-SACLAY
OFFICE DES RAYONNEMENTS IONISANTS - L.A.B.R.A.

INTRODUCTION -

Polyethylene is widely used in orthopedic applications for the construction of articular prostheses. Improvement is dependent on physical properties, which are linked to the network, structure and molecular weight of the polymers. The lifetime of cotyles can be extended by improving resistant wear and creep. This can be achieved by taking action in the following two areas :

- 1) polyethylene forming process (compression or injection)
- 2) controlled reticulation through ionising radiation.

INSTRUMENTATION AND PROCEDURES -

Physical measurements, visual examination and performance tests were made before and after irradiation on a type of polyethylene (ertalene hd 1.000) formed by compression and machined.

The material was subjected to the following comparative test :

- undissolved fraction after dissolving in boiling xylene
- viscosity measurement to 135°, using a 0.03 % solution in the decahydronaphtaline (ISO/R 1191)
- density measurement in butanol
- microscopic examination of sections
- compression testing of specimens with 12 mm diameter and 18 mm length
- compression speed : 5.4 mm/min. n 5 mm maximum deformation (ISO/R 604)
- measurement of creep in the compression mode, using cylindrical specimens (7 mm diameter, 10.5 mm length, stress : 28.3 mpa) as per ASTM - D - 695/80
- surface roughness test
- assessment of deformation of cotyle part placed on test bench (applied load = 100 d.a.n. ; repetition rates : 25 cycles/minute, number of cycles : 500.000).

Fraction synthetis surfaces were then examined using an electron scan microscope.

Dimensions were checked using a SOLEX type spherometer, and a surface roughness test was made.

TEST DATA AND COMMENTS -

Test data show an improvement in creep resistance, as illustrated by the deformation curves of figure 1, obtained from specimens subjected to standard testing.

Compression testing, however, shows no significant differences between irradiated and non-irradiated test specimens. These results were conformed by the decrease in deformation caused by the combined effect of creep and wear on cotyles subjected to bench testing.

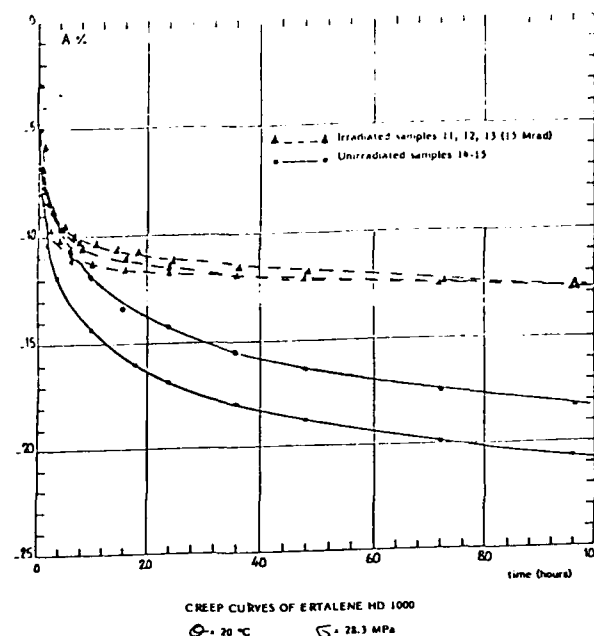


Figure 1

It is difficult to correlate the performance of cotyles under bench testing and involved conditions (1) (2) (3).

Relative performance level, however, can be evaluated on the basis of cotyle bench tests.

Injection moulding under appropriate conditions permits an improvement in fraction surface quality (roughness factor) and limits the immediate wear due to superficial irregularities.

CONCLUSION -

Differences of opinion on the effect of ionising radiation on polyethylen are based on the diversity of test results, which are negative in some cases.

An improvement in the resistance of ultra-high molecular weight polyethylen to creep and wear can be obtained through an appropriate selection of irradiation parameters (oxygen content, dose, dose-rate).

- (1) R.J. ROE, J. of Biomed. Mat. Res. Vol 15 209-230 (1981)
- (2) W.R. JONES, Wear, 70 77-92 (1981)
- (3) S.K. BHATEJA, Polymer, 24, 160-166, (1983)

C.E.A. - OFFICE DES RAYONNEMENTS IONISANTS
Laboratoire des Applications Biologiques des Rayonnement - B.P. 21 - 91190 - GIF-SUR-YVETTE
FRANCE.

BIOMECHANICS OF PEDIATRIC HIP FIXATION FOLLOWING PROXIMAL FEMORAL VARUS OSTEOTOMY

G.G. GLEIS, S.T. WHITE AND J.A. von FRAUNHOFER

DIVISION OF ORTHOPEDIC SURGERY, DEPARTMENT OF SURGERY, UNIVERSITY OF
LOUISVILLE SCHOOL OF MEDICINE, LOUISVILLE, KENTUCKY 40292

The proximal femoral osteotomy is commonly used in the treatment of hip dysplasia and similar disorders. Following surgery, the hip is stabilized with screw and plate fixation devices. The trend has been to shorten or omit plaster cast immobilization in these patients. Because apparent rotations at the osteotomy have been observed, this mechanical study was undertaken to determine the stability in vitro of three devices commonly used in practice. Biomechanical analysis of the hip in the sagittal plane indicates that the muscular forces present can displace the proximal segment unless the fixation device adequately prevents rotation about the axis of the lag screw relative to the distal segment.

The stability achieved with three different pediatric fixation devices following opening and closing osteotomies performed on large dog femurs was studied in the laboratory.

The fixation devices used in this study were the Richards pediatric hip screw, the Howse-Coventry hip screw and plate and the Howmedica hip screw and plate. The Richards system is a 3-hole 110° side plate with a barrel at the proximal end and a lag screw. The barrel engages the lag screw to allow for subsequent sliding of the screw and compression of the osteotomy site. The Howse-Coventry system consists of a 3-hole side plate and a compression screw, the end of the plate being curled to engage the hexagonal head of the lag screw to prevent rotation. The Howmedica system comprises a 3-hole side plate with screw holes that allow for compression of the osteotomy site. The lag screw has a hexagonal hole in the plate to prevent rotation. These fixation devices were inserted into freshly harvested large dog femurs following opening and closing type osteotomies. Both Howse-Coventry and Howmedica plates were bent to 110° before insertion. Fifty-one dog femurs were used in the study, roughly divided equally between the three fixation devices and four torque application modes.

The test regimen involved subjecting the proximal segment to rotation about axis of the lag by means of forces applied in the sagittal plane with the distal segment being held immobile. A special jig was constructed that allowed the femur, following osteotomy and fixation, to be mounted with the proximal segment at right angles to the direction of force application. A Steinman pin was inserted through the femoral head and a torquing force was applied by a plunger attached to the cross-head of a Unite-O-Matic universal testing machine, the rate of force application being 5mm/min. The force applied and associated segment displacement was recorded by the internal chart recorder of the tester. The force to failure, i.e. maximum torque applied before displacement of the proximal segment, and the work done in producing failure were determined for the different test regimens.

The torque application system permitted study of fixation device stability for the

following parameters: (i) opening and closing wedge osteotomy (ii) torque application producing tightening (screwing) or loosening (unscrewing) of the lag screw (iii) torque application producing compression of the anterior or posterior cortex (iv) torque application to the right or left side of the femur.

Overall summary data showed:

	Maximum torque (Nm)	Work done (J)
Richards screw:	4.04 ± 1.97	1.45 ± 1.10*
Howse-Coventry:	3.91 ± 1.25	1.59 ± 0.91
Howmedica:	5.82 ± 2.13	2.43 ± 1.41

*mean value ± standard deviation

the Howmedica system gave the greatest value of maximum torque ($p < 0.01$) and work done ($p < 0.05$) compared to the Richards and Howse-Coventry systems.

Overall comparison of opening and closing wedge osteotomies showed no difference in stability between the two surgical procedures. However, some differences in stability became apparent when the data was subdivided on the basis of the torque application mode. For the Richards hip screw, the closing wedge was more stable than the opening wedge in both maximum torque and work done ($p < 0.05$) when torque was applied to the right side of the femur. Under posterior loading, the work done for the Richards screw with the opening wedge was greater than for the closing wedge ($p < 0.05$) but the work done for the Howse-Coventry system was greater with the closing wedge osteotomy ($p < 0.01$). The Howse-Coventry system also showed greater stability, greater work done ($p < 0.05$), for the closing wedge under the "screw" mode of torque application. The Howmedica system showed greater stability for the opening wedge osteotomy with respect to maximum torque under left side loading ($p < 0.05$) while the closing wedge osteotomy was more stable, i.e. greater work done, ($p < 0.05$), under the unscrew torque application mode.

Conclusions

Overall, there was little difference in the stabilities of opening and closing wedge osteotomies except in a few specific instances arising from different torque application modes. In general no statistically significant ($p > 0.05$) differences were found between the Richards hip screw and the Howse-Coventry hip plate and screw. In most instances, however, the Howmedica hip plate and screw showed the greatest stability, as demonstrated by the maximum torque and work done to failure.

This study was undertaken by one of the authors (S.T.W.) as partial fulfillment of the requirements of the Orthopedic Surgery Residency Programme of the University of Louisville School of Medicine.

The Effect of Surface Treatments on the Interface Mechanics of LTI Pyrolytic Carbon Implants

K.A. Thomas, S.D. Cook, E.A. Renz, R.C. Anderson,
R.J. Haddad, Jr., A.D. Haubold* and R. Yapp*

Tulane University Medical School, Department of Orthopaedic
Surgery, New Orleans, LA and *CarboMedics, Inc., Austin, TX

Previous investigations have demonstrated the promise of low-temperature isotropic (LTI) pyrolytic carbon for use in biomedical implant applications. The ability to manufacture final products from this material may limit its potential applications in the medical device industry, particularly in the orthopaedic area. Manufacturing of the 'as-deposited' surface involves the machining of a substrate followed by deposition of the LTI carbon in a fluidized bed. Alternately products can be fashioned by machining LTI carbon deposited in near-final form. Thus, a mechanical and histological comparison of implants manufactured 'as-deposited' in final shape with implants made by machining LTI carbon has been undertaken. Surface treatments were chosen in an attempt to emulate the original 'as-deposited' carbon surface.

Five LTI carbon implant surface conditions have been investigated, including as-deposited, ground, fine grit-blasted, and coarse grit-blasted surfaces. Also a plasma oxygenated fine grit-blasted surface was investigated. This treatment in an oxygen rich environment depletes the carbon content at the surface, leaving a relatively silicon-rich layer. Attachment strength for each type of implant was evaluated by ultimate interface shear strength in a push-out test. The interface stiffness and the histologic response of each type of implant were also determined. The responses of the implants were compared following implantation periods of 12 weeks and 24 weeks.

Cylindrical implants were fabricated having the nominal dimensions of 18 mm in length by 6 mm in diameter. The implants were surgically placed transcortically in the mid-diaphyseal region of the femora of adult mongrel dogs. The sites were prepared slightly undersized so that gentle tapping of the implants was required for insertion. This insured an interference fit and minimized any initial micromovements of the implants. One of each type of implant was placed randomly in each femur; the animals received two of each implant type. Eight implants of each type were inserted, for a total of 40 implants.

Following sacrifice the implants were isolated by serially sectioning the femora, and each implant was then cut perpendicular to its long axis producing two push-out specimens. A dental handpiece fitted with a carbide burr and a special reamer were used to prepare the endosteal surface of the specimens facilitating proper alignment and seating in the push-out fixture. The specimens were selectively subjected to a push-out test on closed-loop hydraulic test machine operated in stroke control at a displacement rate of 1.27 mm/minute. All samples were tested fresh and sprayed with physiologic saline during the testing procedure. Displacement of the implants and the load generated were recorded from the test machine. After testing, the specimens were prepared for undecalcified histologic evaluation. Interfacial areas were determined directly from the methacrylate embedded sections, and in conjunction with the load-displacement curves interface strength and stiffness values were determined.

The results from the specimens mechanically tested at 12 weeks and at 24 weeks are shown in Table 1. Analyzing the 12 week strength data, the mean strength for the as-deposited implants was significantly greater than each of the other types, except for the fine grit-blasted implants. No other significant differences were noted. For the 24 week strengths, there was no significant difference among the strength values. It is interesting to note that the strength increased in each case, from 12 to 24 weeks, except for the as-deposited implants. The slight decrease in strength for the as-deposited implants was not statistically significant.

For interface stiffnesses tested after 12 weeks, the as-deposited implants were stiffer than the remaining types, and significantly stiffer than each except for the fine grit-blasted implants. For the 24 week data, there was no significant difference among the five stiffness values. All stiffnesses increased from 12 to 24 weeks; for the fine grit-blasted and ground implants these increases were statistically significant.

Histologic evaluation included examination of undecalcified ground sections and corresponding microradiographs in transmitted, polarized, and fluorescent light. The response of all implants was similar at both implantation periods. After 12 weeks the presence of an immature woven bone interface and the presence of extensive osteoid tissue was noted. By 24 weeks a more stable interface with mature, well-organized bone was seen. The as-deposited implants exhibited the greatest amount of direct implant-bone apposition, while the other types exhibited this response to lesser amounts. There was no apparent adverse response to the plasma oxygenated surface.

The results of the mechanical testing indicate that after 24 weeks implantation, the ability to duplicate the as-deposited strengths is possible. Additionally, since the histologic response of the implants was similar, it appears possible to reproduce the behavior of the as-deposited implants by one or more of the surface treatments investigated.

IMPLANT TYPE	TABLE 1	
	STRENGTH, MPa	STIFFNESS, GPa/m
12 WEEK IMPLANTATION		
AS-DEPOSITED	2.66 ± 0.56	35.82 ± 7.63
OXYGENATED	1.17 ± 0.46	26.98 ± 7.07
COARSE GRIT-BLASTED	1.51 ± 0.57	27.42 ± 7.44
FINE GRIT-BLASTED	1.81 ± 1.03	30.71 ± 12.00
GROUND	1.34 ± 0.71	19.76 ± 9.05
24 WEEK IMPLANTATION		
AS-DEPOSITED	2.56 ± 0.70	40.56 ± 9.98
OXYGENATED	2.29 ± 0.86	29.63 ± 16.20
COARSE GRIT-BLASTED	2.23 ± 1.18	32.52 ± 15.28
FINE GRIT-BLASTED	3.40 ± 1.92	49.28 ± 21.04
GROUND	2.99 ± 1.06	44.03 ± 18.25

Supported by CarboMedics, Inc., Austin, Texas.

Biomaterials Laboratory
Department of Orthopaedic Surgery
Tulane University School of Medicine
1430 Tulane Avenue, New Orleans, LA 70112

Sagittal Plane Strain-Gage Analysis of the Femur Before and After Prosthetic Hip Implantation

J.P. Collier, T. Orr, M. Mayor,* F. Kennedy

Thayer School of Engineering, Dartmouth College, Hanover, NH 03755

Introduction

Coronal plane stress analysis has proven useful in determining the effect of femoral prosthesis geometry on the resulting stress distribution the lateral and medial femoral cortices. The test permits the determination of the highest coronal plane stresses, i.e. those present during one-legged stance, but cannot produce the stresses generated by rising from a chair or while ascending or descending stairs. Sagittal plane stress analysis is more difficult to study because the experimental apparatus must be designed to handle out of plane loads and rotation but it is a prerequisite for determining the three-dimensional stresses which prostheses must be designed to resist.

Methods

Five cadaver femurs were strain gaged on their anterior and posterior cortices as well as their lateral and medial cortices. Small expansion bolts were inserted in the areas of attachment of the abductors, the external rotators and the extensors and cables were affixed to the bolts through swivels. The femur was then inserted into the testing apparatus which consists of a pelvis with plastic acetabular cup and attachments for the three cables representing the muscle forces. A lower limb including a knee with a femoral socket was designed to accept and mechanically fasten onto the distal end of the strain gaged femur. The pelvis is mounted on the load cell of an MTS machine, the lower limb pivots on a bearing attached to the hydraulic ram through which the load is applied. Weights are attached to the cables through pulleys to provide the muscle forces to balance the loads from the ram which provides the floor reaction. A computerized data acquisition system is used to monitor all of the strain gages as the femur is loaded at angles of 7 to 11° in the coronal plane and 0 to 40° of flexion in the sagittal plane. Following the initial testing a femoral prosthesis of either the surface replacement type (TARA) or the horizontal platform configuration (HPS) was implanted and the testing repeated.

Results:

With the knee locked at full extension the variation of coronal plane angle from 7 to 11° of abduction caused little change in stress in either implant. Increasing the angle of flexion from 0 to 20° increased the sagittal plane stresses while decreasing the coronal plane stresses. At 40° of

flexion the sagittal plane stress was twice the maximum coronal plane stress determined from the one-legged stance.

The implantation of the surface replacement reduced the stress in the proximal femur slightly in both planes. The stemmed femoral component caused a greater reduction in stress in both planes than the surface replacement and repeated testing at high angles of flexion caused loosening of uncemented stems due to torsion.

Conclusion

The three-dimensional testing indicates that rotational forces and high sagittal plane stresses due to the daily activities of stair climbing and rising from a chair could be contributing causes of femoral prosthesis loosening.

This research was supported by DePuy of Warsaw, Indiana.

* Dartmouth Hitchcock Medical Center
Hanover, NH

A MULTIFACETED APPROACH TO THE ANALYSIS OF THE THR IMPLANTS IN A CANINE MODEL

P. Campbell, R.D. Bloebaum, T.A. Gruen, and A. Sarmiento

Orthopaedic Biomechanics Laboratory, Bone & Connective Tissue Research
Program, Orthopaedic Hospital-USC, 2400 S. Flower St. Los Angeles, CA 90007

INTRODUCTION

A multitude of biomaterials have been used for joint replacement with varying results. Cobalt chrome alloy (CoCr), stainless steel (SS) and titanium alloy (Ti) are commonly used today for total hip replacement (THR), but other metals, ceramics, polymers, and composites are currently being developed to find the optimum material. It is difficult to assess the suitability of a new biomaterial for THR as the majority of data comes from isolated clinical failures or longterm patient follow-up. Experimental data in a functional model is limited and the biological factors determining implant success or failure remain unclear.

Three biomaterials (CoCr, Ti and carbon fibre polysulfone CFPS), are currently being compared in a canine THR model. Radiography, microangiography, ground histology, polariscopy and light microscopy with special staining have been employed to extract the maximum information from each bone specimen.

This paper reports the results from the carbon fibre implant series of the study and illustrates the efficacy of pursuing a multifaceted approach to the problem of implant analysis.

MATERIALS AND METHODS

CFPS femoral stems and polyethylene acetabular components were implanted in 6 dogs with cement fixation. Two dogs were sacrificed at 12, 26 and 52 weeks post-operatively, perfused with Karnovsky's fixative containing micropaque. Both femurs and acetabulae were harvested, X-rayed and photographed. The implanted femur was marked at 1cm intervals from the collar of the implant to 1cm distal to the tip. Three transverse sections (2mm, 2mm and 6mm), were cut from each interval and marked to indicate anatomical alignment. A microangiogram was taken from the first 2mm section following decalcification. The second was embedded undecalcified in Spurr's low viscosity medium, ground to 1mm, microradiographed, then mounted and further ground to approximately 50 microns. The third section was divided as shown (Fig. 1) for interface analysis using celloidin, paraffin and plastic embedding following decalcification and removal of the cement with acetones. Standard processing techniques for celloidin, paraffin and epon-araldite embedding were followed.

GROSS RESULTS

The dogs recovered quickly from the surgery with no post-operative infections. At autopsy, tissues surrounding the implants appeared normal.

The operated femurs were noted to be slightly thicker in diameter than the controls. This correlated on X-Ray to increased cortical thickness. No radiologic signs of loosening of the prostheses were noted.

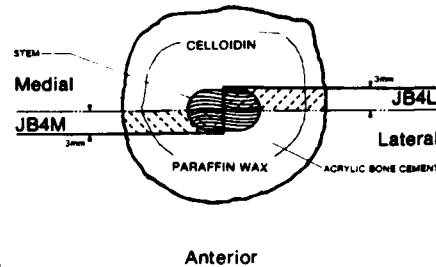


FIG 1

MICROSCOPIC RESULTS

Microangiograms and microradiographs showed a marked vascular response to the implant at 12 weeks. Vessels were seen throughout the cortex with many fine branches near the cement-bone interface particularly in the sections from the trochanteric region. By 52 weeks, this response has decreased. Similarly, paraffin sections showed a reaction to the initial surgical insult with invasion of blood vessels, lymphocytes, macrophages and giant cells near the interface region. There was no evidence of a prolonged foreign body reaction. Necrotic bone was noted in the interface region and early signs of remodelling were seen by light microscopy of plastic and paraffin sections and by polariscopy of large celloidin and ground sections. Remodelling of the cortical bone was apparent by microradiographic and histologic techniques and was characterised by periosteal new bone apposition and osteoblastic activity in the inner third of the cortex.

Evidence of a cellular, laminar, fibrous tissue membrane between the bone and cement was seen in the majority of sections from each time frame. This membrane varied in thickness and regularity, but appeared to be most dense in the earlier sections. Thin plastic sections showed an outer layer of flattened, elongated cells and dense connective tissue fibres, an underlying layer of fusiform fibroblast-like cells and lastly an intermediary zone adjacent to remodelling bone where several different cell types were seen, including fibroblast-like cells and osteoblast-like cells. Celloidin and paraffin sections stained with Goldner's and Masson's trichrome showed collagen production in this interface region which was most marked at 26 weeks.

CONCLUSION

Based on the above multifaceted analysis a favorable short term biological response to the CFPS implant was seen. Comparisons of these results with those from identically designed CoCr and Ti implants presently being conducted in our laboratory, will elucidate the material factor of the present response.

ACKNOWLEDGEMENTS

We wish to acknowledge the financial assistance of Hexcel Medical and University of Southern California School of Medicine.

LOAD TRANSMISSION AT THE IMPLANT-BONE INTERFACE A THEORETICAL, MECHANICAL AND PHOTOELASTIC STUDY

Hobkirk, J.A. and Wolfe, L.W.

Institute of Dental Surgery
London, England

One of the great merits of fibre-reinforced materials is that they can have directional properties which may be related to functional criteria. They are thus becoming popular for implant construction, however, it is important to know the extent and direction of stresses within the implant if optimum use is to be made of this property. This is particularly true of dental implants where design criteria can be difficult to meet, and steep stress gradients occur.

A study has been conducted into the optimum surface contours for a dental implant to be made from a new fibre-reinforced material. Its aims were to determine these theoretically, by mechanical testing, and by two-dimensional photoelastic stress analysis.

For the purpose of the mathematical and photoelastic studies it was assumed that the implants were totally surrounded by, and in intimate contact with, homogenous alveolar bone, and, on the basis of the chemistry of the composite, that there would be no chemical bond between implant and host. The material, as presently formulated, has a modulus of elasticity approximately $2\frac{1}{2}$ times that of bone.

The theoretical analysis of retention grooves was based on screw-thread formulae, and was employed to determine the implant profile providing optimum retention, with ultimate failure occurring in the bone, a clinically more desirable situation. Calculations were based on the formula (MacKenzie 1962):

$$S_t = S_h \cdot \Pi \cdot L_e \left[\frac{K_n}{4} + \tan^2 \theta \cdot K_n (E_g - K_n) \right]$$

where: S_t = Stripping strength of device
 S_h = Shear strength of implant material/bone
 L_e = Axial length of embedded component
 K_n = Minor screw diameter
 θ = Included groove angle
 E_g = Major screw diameter
 P = Pitch of thread

It was concluded on the basis of these calculations that:-

1. The implant should have as long an axial engagement in bone as possible.
2. The diameter of the implant should be as great as possible.
3. Any grooves in the implant should be as deep as possible.
4. The grooves should be as numerous as possible.
5. Preferential failure of bone could be achieved by appropriate groove dimensions and spacing.

Mechanical Tests

Mechanical tests were carried out using rods of the implant material, with various surface profiles ground into them. These were coated with a silicone separating-agent, and placed in PTFE moulds whilst bone substitute was cured around them. This had been developed specially for the study, and was based on Araldite CY219 (Ciba-Geigy); it has similar physical properties to bone.

Push out tests were carried out using an Instron Tester at load rates of 150-200 N/s, similar to those in the molar region during mastication. The specimens were subsequently examined optically to determine failure modes. Failure was predominantly in the 'bone', and there appeared to be advantages in multiple grooving. These results are being correlated with animal studies using miniature swine.

Photoelastic Studies

Whilst several workers have used photoelastic techniques to study stresses around implants, most have been qualitative, rather than quantitative, due to failure to use materials which were stress-free and provided the appropriate modulus ratio.

Custom formulated stress analysis plastics (Stress Engineering Services Ltd) designed to produce a modulus of elasticity ratio of $2\frac{1}{2}:1$ were used to prepare two-dimensional cut-outs of the bone and implant. Twice life-size implant profiles were prepared to be an accurate sliding fit in the plastic sheet representing the bone. They were mounted between stress-free flat glass plates, and loaded at various angles with a calibrated pneumatic ram. At the same time they were trans-illuminated with polarised light to reveal internal strains, and stress gradients were measured by means of a polariscope.

Results

There was a broad measure of agreement between the theoretical and mechanical tests, with multiple grooves providing superior retention and a clinical safety margin due to different failure levels from groove to groove. Wide channels behaved less satisfactorily in all tests.

Acknowledgements

The authors wish to thank the Technology Division of Dunlop Ltd. for their assistance in the development and supply of test materials.

References

MacKenzie, R.V. 1962. Screw Threads, Design, Selection and Specification. The Industrial Press, N. York.

STEM MODULUS IN TOTAL HIP DESIGN

D.W. Burke, J.P. Davies, D.O. O'Connor, and W.H. Harris

Orthopaedic Research Laboratories, Massachusetts General Hospital and
Harvard Medical School, Boston, MA 02114.

There are multiple complex design variables in total hip prosthetic components whose optimization are desirable for long-term servcability in vitro. Issues such as stem geometry, collar vs. no collar, head size and material composition may be important in the prevention or delay of aseptc loosening - the most troublesome long-term complication in total hip replacement.

Central to any femoral prosthetic component design is material selection and how it may offset the biomechanics and biology of the bone-cement-metal composites. Although many different materials are used in manufacturing of total hip stems, in general, for biomechanical purposes these can be divided into two groups. Titanium alloy components exemplifying the so-called "low" modulus group while the stiffer chrome cobalt alloy stems represent the "high" modulus types.

Each type has its potential advantages and disadvantages and claims of superiority have been made by proponents of each.

"Low" modulus advocates point to the potential enhancement of proximal femoral stress transfer because of increased load sharing by these devices. Experimental studies have conflicting conclusions as to the efficacy of this. "High" modulus proponents are quick to warn of the increased proximal cement strains predicted by finite element analysis.

An experimental evaluation of geometrically identical chrome cobalt and Titanium alloy femoral total hip stems was undertaken to help answer the following questions. 1) Can more flexible femoral stems significantly enhance proximal femoral stress transfer? 2) Will this adversely effect cement strains?

Methods and Materials: Four matched pairs of cadaver femurs were studied. Strain gauges were placed at multiple locations on the femurs. Each femur was loaded in an MTS machine under conditions simulating single leg stance including the simulated abductor muscle force. After strain recordings were performed for the intact femurs, they were prepared for insertion of the femoral component of a total hip replacement in the standard fashion. Using our specially devised technique, triaxially oriented strain gauges were placed within the cement inside the femur at multiple locations. Resultant loads of three times body weight were applied.

Results: Longitudinally directed bone strain along the medial femoral cortex are drastically altered after total hip replacement. Very proximal stress transfer was only marginally improved in the Tivanium stemmed femurs compared to the chrome cobalt group, and overall stress patterns shared no difference between the two groups.

Maximum axially, circumferentially, and radial directed cement strains for locations along the medial and lateral cement mantle are shown in Figures 1 and 2.

While on the average, cement strains were slightly higher in the Titanium alloy group, no consistent pattern of strain elevation was found when data from each individual material femoral set was evaluated.

Conclusions: While theoretical advantages and disadvantages exist for the use of "low" and "high" modulus materials in total hip femoral stems no clear difference could be found between the groups in terms of restoration of proximal bone stress and transfer of strain to the acrylic cement mantle.

Figure 1

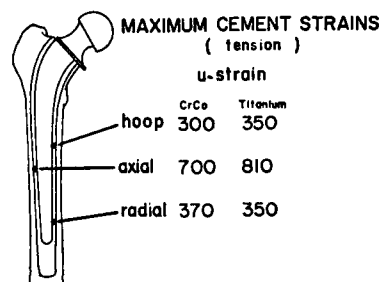
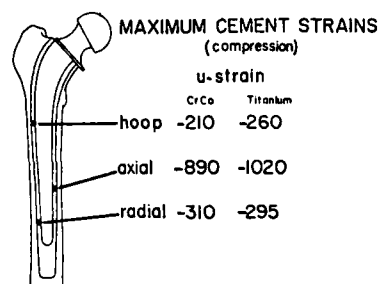


Figure 2



Examination Of The Oral Tissue Interface With The Single Crystal Sapphire
Endosteal Dental Implant: Conventional and Alternative Ultrastructure

Steflik, D.E., McKinney, R.V., Jr. and Koth, D.L.*

School of Dentistry
Medical College of Georgia
Augusta, Georgia

This paper describes the protocol our laboratory has been utilizing to investigate the tissue interface with the single crystal sapphire endosteal dental implant. Our investigation has included clinical, histological and electron microscopic studies of the implants in dog jaws, with the ultrastructural protocols using both conventional and alternative modalities. Implants were placed bilaterally in dog mandibles for periods ranging from 6 to 24 months. Specimens were obtained upon random sacrifice by block resection of the mandible with the implant in situ and fixed by immersion in either 10% neutral buffered formalin or 3% phosphate buffered glutaraldehyde. Alternatively, some dog heads were perfused by employing a carotid artery cutdown procedure. The implant specimens were then removed by block resection after 45 minutes of perfusion fixation, trimmed and immersed into new fixative. Histological (LM) specimens were dehydrated and embedded in polymethyl methacrylate (PMMA); scanning electron microscopy (SEM) specimens were dehydrated to absolute ethanol and critical point dried with CO₂; and, transmission electron microscopy (TEM) specimens were routinely embedded in epoxy resins, either EPON 812 or EMBED 812. The SEM specimens were processed in toto or hemisectioned, while still contained within the jaw, then resected and processed. Following photomicroscopy, the LM sections were retrieved, as well as the TEM orientation sections, for alternative ultrastructural investigation. The specimens were surface etched utilizing oxygen plasma created from oxygen gas by radiofrequency. This exposed the surface topography permitting SEM analysis. The alternative TEM protocol was a modification of the method of James and Schultz (J. Oral Implantology 4(3), 1974). Various PMMA LM sections that ranged in thickness from 120 micrometers to 2 millimeters were cryofractured creating a fracture plane between the implant and the associated tissues. We reembedded the tissue fragment into fresh PMMA for subsequent TEM analysis. Orientation was not a problem since the retrieved gingival fragment was previously stained for histology.

RESULTS: Histology: The gingival sulcular epithelium appeared similar to controls, was closely apposed to the implant, and few inflammatory cells were observed. Bone was either tightly juxtaposed to the implant or separated from the implant by a narrow zone of connective tissue. Anatomical structures such as the alveolar nerve and artery were observed.

SEM: A normal gingival crevicular epithelium was observed by examining block implant specimens in toto. The keratinization pattern of the gingiva varied with the progression of the epithelial cells from the gingival crest to the depth of the sulcus. However, observations of the sulcus base was precluded by the narrow width of the sulcus. This problem was surmounted by hemisecting the implant specimens in situ. This technique demonstrated a transition of the keratinized free gingiva to a nonkeratinized flattened crevicular

epithelia. At the base of the sulcus direct contact of the epithelial cells to the implant was observed.

Surface Etched SEM: This technique revealed a normal gingival maturation pattern adjacent to the implant and direct juxtapositioning of the lower crevicular cells to the implant. Mandibular bone was directly associated with the implant, or in some cases separated from the implant by a narrow band of connective tissue. The alveolar nerve showed the presence of myelin ensheathed neurons, encased within the endoneurium. This technique made possible direct correlation of SEM to LM observations since identical specimens were used.

TEM: Conventional TEM of microdissected crevicular epithelium demonstrated the presence of secretory vesicles, some with a double unit membrane enclosing the granular contents, filamentous material, and structures morphologically similar to hemidesmosomes in the surface cells facing the implant.

Alternative TEM: These methods displayed retention of cellular integrity next to the implant, even though the specimens were formalin fixed. An internal basal lamina with distinct hemidesmosomes was displayed with anchoring fibrils extending to the interstitia. Crevicular cells contained a mixed population of membrane bound secretory vesicles. At the lowest crevicular epithelial level, hemidesmosomes and an external basal lamina were observed on the external cells.

CONCLUSIONS: These correlative results demonstrated a non-toxic tissue response to the sapphire implant. Adjoining tissue appeared viable and similar to that interfacing normal dentition. Observations of the lower crevicular epithelial cells suggest organelles adjacent to the implant which may be responsible for an attachment-like structure. The conventional and alternative procedures used demonstrate that histological prepared tissue can be retrieved for ultrastructural study and true correlative microscopic examination can be carried out using LM, SEM and TEM modalities.

Study supported by Grant No. 7834-0001 from
Kyocera International, Inc.

Department of Oral Pathology
School of Dentistry
Medical College of Georgia
Augusta, Georgia 30912

*Department of Fixed Prosthetics
School of Dentistry
University of North Carolina at Chapel Hill
Chapel Hill, N.C. 27514

HTR™ (HARD TISSUE REPLACEMENT) FOR EDENTULOUS RIDGE AUGMENTATION

Arthur Ashman,*D.D.S, F.A.G.D. and Paul Bruins, Ph.D **

President, Academy of Implant Dentistry, Northeast District;
Former Head, Dental Research, Mount Sinai Hospital, NYC; Private Pract.

The atrophied jaw with its resorbed edentulous ridges has been a rehabilitative "sore spot" for decades. Ill fitting, non-retentive dentures caused by alveolar atrophy has been the source of many patient problems.

For years, dentistry has sought to remedy this problem. Some solutions, such as: sub-periosteal implants, autogeneous bone grafts, and injectable grafting materials, have met with limited success. The problems continue to recur.

A biocompatible plastic composite material --- HTR™ (Hard Tissue Replacement), which has been in limited clinical use until recently, has been successful in restoring atrophied jawbone. This material is unique because it can be customized and molded in the practitioner's office in four minutes to fit a patient's specific jawbone and surgically placed within a half hour. HTR™ in molded form can restore alveolar bone which had resorbed after years of disuse atrophy (post-extraction), from the sequella of trauma, or from cancer surgery.

In this paper, two cases of ridge augmentation will be presented utilizing HTR™ molded. The first one is a partial graft five years post-operative to cancer surgery. The second is a three-year full mandibular augmentation on a severely atrophied mandible. The achieved results have been extremely gratifying in that the HTR™ ridges have been in place for 5 and 3-1/2 years respectively.

Similar results have been obtained in an additional 55 ridge augmentation procedures. This success can be attributed to HTR™'s unique properties which include: its hydrophilic nature, ease of handling, extreme strength, microporous nature, and biocompatibility. It is also inexpensive, lending itself to applications in the mouth, in addition to the treatment of atrophied jawbones, including bone damage or loss resulting from cysts or granulomas, for periodontal lesions, and bone maintenance after extractions (filling the post-extraction opening with granular HTR™). This versatile plastic has the capability of being used in hard tissue and bone replacement capacities in other parts of the body. However, those uses await further study and development.

* 200 Central Park South
New York, NY 10019

** Professor Emeritus, Polytechnical Institute,
New York City.

AN EVALUATION OF DURAPATITE SUBMERGED-ROOT IMPLANTS FOR ALVEOLAR BONE PRESERVATION

P. Kangvonkit, V. J. Matukas* and D. J. Castleberry**

Department of Oral & Maxillofacial Surgery, University of Alabama in Birmingham
Birmingham, Alabama 35294

One of the problems that has plagued dentistry for many years is the post extraction resorption of alveolar bone. The factors involved in this complex mechanism are not clearly understood, but the initiating factor appears to be the loss of teeth. The hypothesis of this study is that the presence of an implant in the socket of an extracted tooth would simulate a tooth root to preserve the alveolar bone. Animal models using Durapatite cones (synthetic dense polycrystalline hydroxylapatite) as the immediate submerged-root implants in dogs and monkeys has been done with success.

The purpose of this study is to evaluate the safety and efficacy of solid cones of Durapatite implanted into extraction sites in humans immediately after extraction as a means of preservation of alveolar bone when compared with no implant.

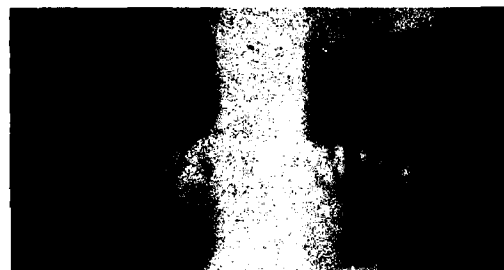
Thirty patients were selected; fifteen to receive the implants; another fifteen for controls. All patients were healthy and at least 14 years of age. Each patient had to have at least six teeth in the mandibular symphysis between teeth #21-28 with at least three teeth on each side of the midline indicated for extraction. All patients were premedicated before surgery with oral penicillin or erythromycin. All teeth were extracted under local anesthesia with or without IV sedation. In the implanted patients, Durapatite cones were shaped with a high speed diamond bur and placed into the socket wound at least 1 mm below the alveolar crest. All extraction sites were sutured. Immediate complete dentures were inserted without impinging on the implanted site. A postoperative panoramic radiograph was taken immediately to determine the position of the implants. The patients returned to clinic at intervals of 24 hours, 1 week, 1 month, 3 months, 6 months and every 6 months for 2 years for clinical and radiographic evaluation by panoramic and lateral cephalograph.

Ninety-six Durapatite root implants were evaluated over a six-month period. Thirteen implants showed dehiscence and were treated successfully by reducing the implant to the level of the surrounding bone and five implants were lost. The clinical presentation of alveolar ridges containing root implants was healthy. The implants maintained the bulk of the alveolar ridge and provided a firm foundation for a denture. Panoramic radiographs revealed the alveolar bone directly in contact with the implants. There was no resorption of alveolar bone in the peri-implant area and no migration or resorption of implant. The mean vertical bone loss of the anterior part of the mandible from the lateral cephalographs in the implant group was 1.1 mm compared with 3.6 mm in the control group. Another significant finding was less contour changes of the anterior part of the mandible in the implant group than in the control group.

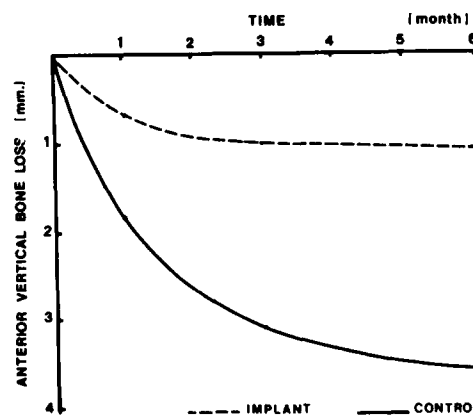
Durapatite is an acceptable biocompatible and biostable material when submerged in human jaw bone. The dehiscence incidence can be eliminated by adequate reduction of the height of the implant at least 1.5-2 mm below the alveolar crest, coupled with well-rounded cervical shape and periodic denture adjustment. Dehiscence of the root implant does not necessitate removal. Surgical reduction of the implant to the level of the residual alveolar bone can be done with success. An important finding was that most of the dehiscent implants were strongly attached to the bone without sign of inflammation or rejection. The gingival tissues surrounding the exposed implants were firm and healthy.

This study presents preliminary evidence that solid cones of Durapatite are an acceptable material for the submerged-root implant system.

A 6-MONTH POSTOPERATIVE PANORAMIC RADIOGRAPH



A COMPARISON OF ANTERIOR VERTICAL BONE LOSS OF MANDIBLES IN IMPLANT AND CONTROL GROUPS



This project was supported by Sterling-Winthrop Research Institute Rensselaer, New York

*Department of Oral & Maxillofacial Surgery, UAB

**Department of Prosthodontics, UAB

HUMAN MANDIBULAR ALVEOLAR RIDGE AUGMENTATION WITH HYDROXYLAPATITE: FINAL REPORT OF A FIVE YEAR INVESTIGATION

Cranin, A.N. and Satler, N.M.

The Brookdale Implant Group The Brookdale Hospital Medical Center
Brooklyn, New York

INTRODUCTION: Previous reports by this group and by other investigators have indicated that dense, polycrystalline hydroxylapatite* is non-toxic and lacks both inflammatory and immune responses. After prolonged contact with host site, fibrous or osseous implant consolidation takes place with the new tissue found around the lattice-like structure of the hydroxylapatite particles.

Our original clinical trial evaluated 50 patients with varying degrees of mandibular atrophy. Patients' mandibles were augmented with hydroxylapatite and have been followed for five years.

METHODS: Patients were divided into two groups depending on the severity of their mandibular atrophy. The first group and majority of patients required only augmentation to fill in minor continuity defects and undercut ridges. The second group, presenting with severe mandibular atrophy, required that hydroxylapatite be combined with autogenous iliac crest bone grafts.

Surgical correction procedures for minor defects utilized a blood-slurry of particulate hydroxylapatite delivered to the implant site via a subperiosteal tunnel along the lateral aspect of the deficient ridge. In the more extensive augmentation procedures, iliac crest grafts mixed with hydroxylapatite were inserted in the host site via a wider incision and retained with splints. All signs suggestive of implant migration, inflammation, infection and rejection were carefully scrutinized during the past surgical management phase. Several instances of implant migration were noted and biopsies were taken from their areas. Post-operative evaluation was determined by extensive clinical observations, utilizing photographs and serial panoramic radiographs. Dentures are fabricated for each patient pre-operatively and post-operatively by the same member of the research group.

RESULTS: Though 50 patients received hydroxylapatite, a total of 67 patients had pre-operative dentures made. 17 patients developed sufficient preoperative denture acceptance and therefore did not require surgery. Clinical performance of all prostheses, pre-and post-operatively, were measured with the Cornell Medical Index. The overall clinical acceptance of hydroxylapatite is extremely encouraging. No instances of implant rejection were detected. Ridge morphology was significantly altered in 47 patients to affect a change in denture stability and retention. Serial radiographs

have demonstrated varying degrees of consolidation of the implant device with its adjacent host site. Postoperative denture acceptance, as measured by the Cornell Medical Index rated significantly better when compared to preoperative denture acceptance. Correlation between the patient's denture acceptance and an empirical radiographic rating coincided except in those cases of the severest mandibular atrophy. After five years, 48 patients retained their implants without alteration. Two patients required corrective procedures to revise their implants mainly due to migrated H/A particles.

DISCUSSION AND CONCLUSIONS: The major problem in analyzing this study is the lack of an effective method of evaluating denture success on an objective basis. Subjectively, 94% of the patients reported improvement. (This was corroborated by our radiographic findings only 65% of the time). However, 25% of the patients of the originally enrolled group (or 17 of 67) felt sufficiently improved simply by the construction of new dentures - to have dropped out of the program prior to augmentation surgery.

The Brookdale Hospital Medical Center
Linden Boulevard at Brookdale Plaza
Brooklyn, New York 11212

HYDROXYLAPATITE (HA) CONE IMPLANTS FOR ALVEOLAR RIDGE
MAINTENANCE-ONE YEAR FOLLOW-UP.

Cranin, A.N., Shpuntoff, R.

Brookdale Implant Dental Group, The Brookdale Hospital Medical Center
Brooklyn, New York

Introduction: The objective of this investigation was to evaluate dense HA root implants to preserve alveolar ridges when implanted immediately after tooth extraction. HA is a synthetic polycrystalline, non-resorbable ceramic bone substitute which when placed in contact with multi-potential mesenchymal cells has demonstrated a lack of inflammatory and immune responses. The HA/bone interface as demonstrated by SEM appears to be indicative of the ability of the root implants to serve as buttresses in the role of alveolar bone maintenance.

Methods: Ten patients were selected after a thorough screening process. All required the extraction of 8 or more teeth. Radiographic evidence of adequate alveolar support to retain an HA cone was required. All patients had x-rays and study models. The protocol called for a variety of surgeons with disparate skills to perform the extractions and implantations without the use of a flap procedure. All patients were treated on an ambulatory basis. Four sizes of dense HA cone were available: 3x10, 4x10, 5x10, 6x12 mm. Immediately after the extraction of each tooth, the cone most closely approximating the root size was selected. If required, the cone was shaped with a diamond bur. The cone was considered properly placed when its cervical plane was at least 1 mm below the most superior aspect of the alveolar crest and secured snugly into the socket by light tapping. All patients returned for follow-up exams at 24 hours, 1 week, 1 month, 3 months and 1 year. Preliminary impressions for dentures were taken no sooner than 8 weeks post-op.

Results: Ten patients: 5 male, 5 female, 62 maxillary, 38 mandibular cones placed, 32 maxillary cones lost, 23 mandibular cones lost at the first year; 45% of the cones were retained, all sites where cones were lost healed well.

Discussion: The objective of this study was to evaluate the feasibility of the use of HA cones as an immediate implant material for the preservation of the residual ridge. The lack of retention was due, in part, to the fact that

the surgery was performed by 10 different residents. The accuracy of implant placement and precision of fit played an important role in the level of success. The placement of a protective gingival flap might have improved the disappointing results. Little difference was noted between maxillary and mandibular results. In no instance were there complications at the host site.

The Brookdale Hospital
Medical Center
Linden Boulevard at Brookdale
Plaza
Brooklyn, New York 11212

PARTICULATE HYDROXYLAPATITE (HA) AS AN IMPLANTABLE
DEVICE TO SALVAGE FAILING ENDOSTEAL IMPLANTS IN DOGS.

Cranin, N., Shpuntoff, R. & Satler, N.

Brookdale Implant Dental Group. The Brookdale Hospital Medical
Center, Brooklyn, New York

Introduction: The endosteal metallic blade implant from the day of insertion, enters a long range mode of failure. In most instances, the prodromal lesion heralding incipient host site degradation is the radiographic symptom of saucerization. This pathologic entity becomes enlarged, engulfing the more nether portions of the infrastructure. A 6 week method of artificially inducing such defects about the cervical areas of dog implants was used by placing them into function within 24 hours of their insertion. The function of HA as a retardant to this catabolic process was to be tested.

Methods: Four mongrel dogs each weighing 25 kg or more had standard dog anchors inserted. Within 24 hours a Brookdale canine prosthesis was cemented spanning the space between the implant and the first molar. Radiographs were taken and pockets probed at that time and at weekly intervals. At the 6 week level, the pockets were found to be 3+ mm and the radiographs showed saucerized defects. Commensurate with the probing measurements, a repair with HA was performed on one side, randomly selected. The contralateral side served as a control. Periodic measurements and radiographs were made weekly. Two of the dogs were sacrificed at the end of 12 weeks and the other two after 6 months.

Results: The (HA) operated sides offered 1 mm or less of passivity to the periodontal probe each week for the entire study period. The control sides showed continuing vertical pocket formation up to 6 mm. Radiographs upheld the clinical charting on operated and control sides. X-rays offered evidence of a radiopaque consolidation at the cervical areas which did not appear to change throughout the test period. After sacrifice, the specimens were examined by hard tissue grinding and staining with H&E modified Masson's trichrome. There appeared to be a dense fibrous envelopment of the HA crystals, clinging intimately to the alveolar bone, closely aligned to the implant cervices

and serving as a retardant to epithelial migration.

Conclusions: HA particles, when implanted into biological environment, create a dense matrix system that serves as a physiological obtundant. During this brief time frame, it appeared to retard or reverse the extremely significant primary pathologic symptoms of permucosal implants: saucerization. Sufficient promise was offered by this preliminary study to encourage a more ambitious long term experiment.

The Brookdale Hospital Medical Center
Linden Boulevard at Brookdale Plaza
Brooklyn, New York 11212

CAPSULES FORMED FROM FIBROBLASTS AID INCORPORATION OF HYDROXYLAPATITE IMPLANT PARTICLES IN MANDIBULAR REPAIR

J.S. Hanker*, J.P. Rausch**, B.C. Terry*, W.W. Ambrose*, S. Li*,
E.J. Burkes, Jr.* and B.L. Giammara***

*Dental Research Center, School of Dentistry, University of North Carolina,
Chapel Hill, NC 27514

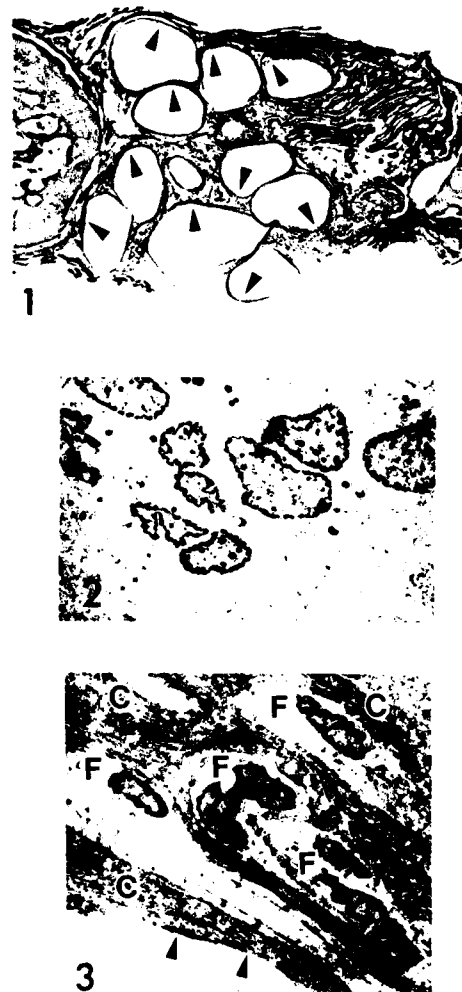
Wounds are closed primarily by a randomly oriented mass of collagen fibers known as a scar. If a "nearly inert" foreign body is present in the wound space, it becomes enclosed in a capsule of fibers that are regularly aligned parallel to the face of the implant. Cells and fibers constituting these granulomatous capsules in chronic inflammation are tightly apposed to each other and usually sharply delineated from the surrounding tissues.

The types of capsular cells present may depend upon the nature of the granuloma and its stage of development. Immunologic granulomas have a high turnover of cells; these hypersensitivity granulomas are due to an infectious agent or allergen. Nonimmunologic, low turnover granulomas are usually due to a foreign body (Warren, 1976; Boros, 1978). Capsular reparative granuloma may also result from trauma independent of any allergenic, infectious or foreign body vector. Indeed, Bagnall postulated in 1980 that the fibrous capsule may aid toleration of the implant and prevent its rejection by the host.

Multinucleate giant cells, fibroblasts and collagen fibers appear to be the principal constituents of these capsules. It has been popular in the medical literature (cf. Adams, 1976) to attribute the derivation of giant cells (Langhans cells with nuclei spread around the cell periphery, or the foreign body type with randomly dispersed nuclei) to fusion of monocytes or macrophages. It has only been since 1969 that fibroblasts have been implicated as precursors.

Hydroxylapatite (Calcite 20-40), a calcium phosphate hard tissue prosthetic, is used for mandibular ridge augmentation in humans. There has been disagreement as to whether or not it elicits a foreign body reaction at its interface with tissue. Biopsy specimens were obtained during vestibuloplasty subsequent to mandibular ridge augmentation with Calcite 20-40 in saline. From rats, necropsy specimens were obtained two or four weeks after filling mandibular defects with Calcite 20-40. The specimens were fixed, decalcified, and stained by the PATS reaction, a variation of the PAS procedure. Adjacent sections were stained with a Papanicolaou trichrome stain. The PATS reaction showed that a connective tissue capsule had formed around each Calcite particle in both humans and rats and suggested that multinucleate giant cells were present in the capsules. This was confirmed by the trichrome stained sections which showed Langhans, as well as foreign body type, multinucleate giant cells. Electron microscopy with the PATS stain showed the close relationship of fibroblasts, collagen fibers, and giant cells in the capsule. Both stains showed that inflammatory cells, especially neutrophils, lymphocytes, macrophages and epithelioid cells, were absent or rare.

These findings support a derivation of foreign body capsular giant cells from fibroblasts.



Figs. 1-3. Micrographs of sections of a defect in the ramus of a rat mandible filled with Calcite particles. After fixation and demineralization, the tissues were stained by the PATS reaction. Fig. 1, light micrograph, shows the capsules (arrows) formed around each particle. Figs. 2 & 3, electron micrographs. Fig. 2 shows a multinucleate giant cell and Fig. 3 shows fibroblasts (F) and collagen fibers (C) from different areas of the same capsule.

Division of Biology, Alfred University, Alfred, N.Y. and *Microelectronics Center of North Carolina, Research Triangle Park, NC.

Supported by ONR Contract N00014-82-K-0305 and USPHS grant RR 05333.

DEVELOPMENT OF A SYSTEM FOR SIMULTANEOUS MEASUREMENT OF THREE FORCE COMPONENTS ON DENTAL IMPLANTS

J.B. Brunski, M. El-Wakad, and J.A. Hipp

Rensselaer Polytechnic Institute, Troy, NY 12181

INTRODUCTION: Numerous trials of dental implants have been conducted in humans and in animal models, including dogs, pigs, baboons, and rhesus monkeys. One of the difficulties in making meaningful evaluation of results from these trials is the paucity of data on forces that implants actually experience when tested *in vivo*. Without force data, it has also been difficult to relate implant-tissue reactions with biomechanical parameters of the implantations, such as interfacial stresses and strains. We have therefore been developing methods enabling *in vivo* measurements of forces and moments on dental implants, particularly when tested in animal models such as dogs. So far, we have only measured axial force components.(1)

The objective of this poster is to describe the components of a system designed to enable simultaneous measurements of three force components on a dental implant. While no bite force data have been collected with it yet, this system should be of interest to those doing dental implant experiments.

MEASUREMENT SYSTEM: The general scheme of measurement can be broken down into four major functions: (1) the bite-force transducer; (2) excitation, calibration, zeroing and balancing of the transducer; (3) signal processing and A/D conversion; and (4) data acquisition, analysis and display by microcomputer.

FORCE TRANSDUCER: Any resultant force on a dental implant can always be resolved into its components along three perpendicular directions of interest, say axial, buccolingual and mesiodistal, i.e., F_x , F_y , and F_z (Fig. 1). Our previous uniaxial transducer (1) measured F_z only while cancelling F_x and F_y components. The new triaxial transducer uses the same arrangement of four strain gauges on the faces of a 3 mm x 3 mm x 6 mm titanium column, but the strains measured by each gauge are now recorded separately as ϵ_1 , ϵ_2 , ϵ_3 and ϵ_4 . When the xyz coordinate system is oriented with respect to the gauges as shown in Fig. 1, it can be shown that each strain signal is simply related to axial and bending force components plus a temperature-induced strain ϵ_T via:

$$\epsilon_1 = a_{1z}F_z + a_{1x}F_x + \epsilon_T$$

$$\epsilon_2 = a_{2z}F_z + a_{2y}F_y + \epsilon_T$$

$$\epsilon_3 = a_{3z}F_z + a_{3x}F_x + \epsilon_T$$

$$\epsilon_4 = a_{4z}F_z + a_{4y}F_y + \epsilon_T$$

where the coefficients a_{1z} , a_{1x} , etc., are known from the column geometry and material properties. These equations are solved to yield the unknown F_x , F_y , and F_z components. For example, it can be shown that

$$F_z = \frac{[(\epsilon_1 + \epsilon_3) - (\epsilon_2 + \epsilon_4)]AE}{2(1 + \nu)}$$

where A = column cross-sectional area, E = Young's modulus of Ti, and ν = Poisson's ratio. Studies with trial strain-gauged beams have confirmed this theory of transducer operation, and evaluations are now underway with miniature titanium sensors instrumented with four semiconductor gauges.

TRANSDUCER EXCITATION: Each of the four gauges per transducer is wired as a 1/4 bridge and excited together with bridge-balancing and zeroing functions using a commercial data acquisition system having 20 available strain-gauge channels (OPTILOG, Optim Electronics). Transducers are calibrated by applying known force resultants and checking measured vs. applied force components.

SIGNAL PROCESSING, A/D CONVERSION: Each of the four strain gauge channels per transducer is signal processed and A-to-D converted under computer control (IBM PC) so that digital input data are available for computer storage, analysis, and display of F_x , F_y and F_z force components. Appropriate information to be gained from the data include the number of bite force components in various size intervals (bite-force histograms), loading rates, duration of loading events, and related analyses of bite-force waveforms.

DATA ACQUISITION: The microcomputer (IBM PC) and OPTILOG enable real-time data collection and reduction. For each transducer, the four strain gauge channels constitute the raw data that must be simultaneously collected and computer-processed to extract the components F_x , F_y and F_z and related data at a particular instant of time. If an experiment required the use of two force transducers in an animal's mouth, a total of 8 strain gauge data channels would have to be handled in this way. The system scans from channel to channel at a speed of about 40 channels/sec.

SUMMARY: The components of a system for measuring three bite-force components on dental implants have been outlined. The system is currently being prepared for *in vivo* trials with dental implants in dog mandibles.

REFERENCES: J. Prost. Dent. (In Press, 1984).

ACKNOWLEDGEMENTS: NIDR Grant #2 R01 DE 5418-04A1

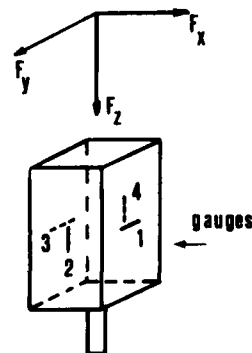


Figure 1

Orientation of strain gauges on the Ti column of the transducer: gauges 1, 3 are transverse; gauges 2, 4 are axial.

Room 7040, Dept. of Biomedical Engineering,
RPI, Troy, NY 12181

Hill T.R., Hobkirk J.A.

Eastman Dental Hospital & Institute of Dental Surgery, London WC1 UK

The Göttingen miniature pig is a useful animal for dental implant research, as the jaws are sufficiently large to house prototype implants, and the animals have a similar physiology to humans, (1). Unfortunately, they are generally considered difficult to intubate and anaesthetise, (2). This paper outlines a safe approach to the problem which has proved reliable in the hands of two dental surgeons with limited veterinary and anaesthetic experience.

Restraining and Immobilisation

The procedure employed is to restrain and weigh the animal, anaesthetise it with an intramuscular injection of Ketamine Hydrochloride at 20 mg/kg, (Vetalar, Parke Davis) deepen the anaesthetic using Halothane (ICI) delivered in a face mask, and then intubate, and maintain a closed circuit of Halothane and oxygen.

Restraining a pig requires a quiet, unflustered, and determined approach. A pig board is used to encourage the animal into a mobile weighing cage, and the dosage of Ketamine Hydrochloride calculated. The pig is then firmly grasped by the tail by one operator whilst the other administers the drug into a gluteal muscle via an 18 gauge 1½ inch needle. The cage is then left in a quiet ante-room until the dissociative anaesthetic has taken effect. After about ten minutes 20-25 kg pigs are safely handleable.

Main Anaesthesia and Intubation

The pigs are carried into the operating theatre and laid on the table. Halothane at 7%-8% in oxygen run at 2-2.5 L/min in a open circuit is administered via a suitable canine-type face mask. The aim of this procedure is to quickly gain deep anaesthesia and suppress the cough reflex to enable an endotracheal tube to be passed. At this depth breathing should be slow and even the pupils of the eyes begin to centre after rolling upwards. The animal is then turned on to its front with the trotters and head over the edge of the table, with two strips of 2" ribbon gauze being used as handles to hold the mouth open during intubation. The strips are positioned distal to the canine teeth taking care not to entrap the tongue. It is unnecessary to force the jaws apart too widely or flex the head backwards, but it is important to keep the head, neck and spine in a straight line. Whilst one operator steadies the head, the second introduces a straight-bladed laryngoscope (Penlon Soper size 8, 185 mm) depressing the tongue slightly and lifting the soft palate dorsally. The use of this instrument itself is not usually enough to free the epiglottis from the free edge of the soft palate. Both of these structures are very long and a further custom-made instrument is therefore required to unravel them. This is a flat, blunt, metal blade about 30 cm long and 1 cm wide with a transverse slit at one end 7 mm by 3 mm to engage the tip of the epiglottis. This has been found essential to quickly, and more importantly, atraumatically, demonstrate the laryngeal opening and arytenoid

cartilages. Having passed the laryngoscope blade as far as possible the tip of the custom-made instrument is gently used to lift the free edge of the soft palate in the centre line, which brings the cartilagenous dorsal edge of the epiglottis into view. The slit in the end of the blade is then engaged on the free edge of the epiglottis, which is gently pulled forward below the soft palate to lie on the dorsum of the tongue where it is retained with the tip of the laryngoscope. Light ventral pressure with the laryngoscope blade over its whole length will now expose the characteristic arytenoid cartilages and laryngeal opening. Miniature swine have small, short tracheas and a 7.0 mm cuffed tube (Portex) (3) is adequate for 20-25 kg pigs. The tube, without a stylet, is gently introduced into the laryngeal opening and passed into the trachea with a twisting motion of 90°-180°. Care must be taken in placing the tube and inflating the cuff, it is inserted too far it is easily obstructed by the bronchial bifurcation, whilst over-inflation of the cuff frequently produces apnoea, which requires mechanical ventilation until spontaneous breathing occurs.

When the breathing has returned to a full, even, rate anaesthesia may be maintained using Halothane and oxygen, concentrations of 4% Halothane have been found adequate, and should be gradually reduced to 0% towards the end of the surgery. The tube should not be removed until the cough reflex has returned, when the animal may be safely transferred to an individual pen, where recovery is usually uneventful within 30-40 minutes.

Conclusion

The miniature pig has not been widely used as a research animal due to difficulties with the anaesthetic routine. This paper shows that with mainly standard apparatus, and readily available drugs, a simple, safe anaesthetic procedure may be readily perfected.

1. Warren, R.G., Scheller, C.E., and Daly, B.D.T. Ketamine-Halothane anaesthesia in miniature swine. *Clinical Research* 27: 3 (September 1979)
2. Lees, P., and Meredith, M.J. Clinical Pharmacology of ketamine in the pig. *Proceedings of the E.A.V.P.T.* 1983
3. Ragan, H.A. and Gillis, M.F. Restraint, venipuncture, endotracheal intubation, and anaesthesia of miniature swine. *Laboratory Clinical Science* 25: 4 (1975)

BIOMATERIALS '84. TRANSACTIONS WORLD CONGRESS ON
BIOMATERIALS (2ND) ANNUA (U) SOCIETY FOR BIOMATERIALS
SAN ANTONIO TX S F HULBERT ET AL JUN 84
DAMD17-84-G-4005 F/G 6/12

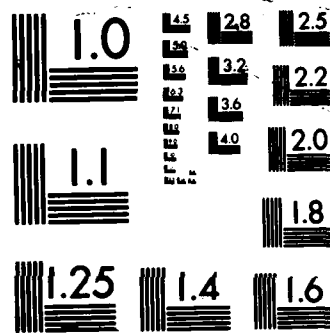


UNCLASSIFIED

F/G 6/12

MI

1000
1000
1000



PHOTOCOPY RESOLUTION TEST CHART

STUDIES ON IMPLANT-TISSUE INTERFACES USING A SCANNING
ULTRASONIC TRANSMISSION IMAGING SYSTEM (SUTIS)*

A. Meunier,[†] H. S. Yoon, J. L. Katz
P. Das,[#] L. Biro[#]

Department of Biomedical Engineering
Rensselaer Polytechnic Institute, Troy, New York 12181

INTRODUCTION

Analyses of the biomaterials-natural tissue interface are limited by the lack of material properties data across the interface. Similarly finite element analyses of implants at present use global, isotropic properties rather than local microscopic anisotropic properties which would be more appropriate.

In order to provide a complete evaluation of the elastic properties continuously from implant through the interface into the tissue system a Scanning Ultrasonic Transmission Imaging System (SUTIS) has been developed at Rensselaer. Prior to the development of this type of system, there was no way of mapping the entire implant-interface-tissue region using traditional mechanical or ultrasonic testing. The SUTIS can yield over 64,000 distinct points of elastic property data in an area as small as 1 mm on a side.

ULTRASONIC IMAGING SYSTEM

The RPI SUTIS consists of two parts: firstly is the data acquisition system containing the basic hardware required to measure sonic attenuation and phase shift information at one location of a sample. Secondly is the motor controller system which governs the scanning motion in order to provide a two-dimensional image.

The basic components of the data acquisition system consist of two spherically focused immersion transducers which are aligned colinearly in a water tank. After transmission through the fluid-immersed specimen the acoustic signal is first amplified and then either amplitude detected or phase detected. The former provides a mapping of the sonic attenuation of the sample while the latter maps the variation of sonic velocity.

The present system samples and stores 256 points of data along a horizontal line; each horizontal scanning in turn is performed 256 times at different vertical positions. This requires approximately 65K of memory to store each image. For Figures 1 and 2 the data retrieval time is about 15 minutes. Pseudocolor can be used in representing the data in order to highlight particular areas by segmented color variations. Software also exists to: expand important areas for improved data analysis; deconvolute in order to sharpen images at high resolution; zoom, which allows an increase in the displayed image's size by a factor up to 64.

EXPERIMENTAL RESULTS

Although the originals of Figures 1 and 2 have been obtained using pseudocoloring techniques, the views presented here are in black and white due to printing limitations.

Figure 1 is of a calcite implant in a rat tibial model. Close apposition of tissue to the implant is observed in the elastic velocity mapping, corresponding to the contiguity observed on the histological preparation. In addition a similar mapping of the attenuation (amplitude) is available in order to complete the descriptive analysis of the implant-tissue system.

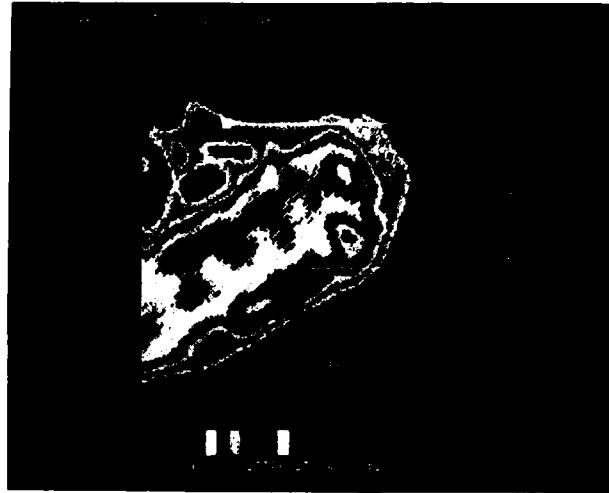


Fig. 1. Calcite implant in rat tibia.

Figure 2 is a velocity (phase) map of a titanium alloy implant in a canine jaw model. In this case, large resorption areas are seen adjacent to the flat sides of the implant, again corresponding to the histological observations. As before, a map of the attenuation is also available for quantitative analysis. In addition a direct representation of both phase and amplitude along a single line scan across the specimen is also available.

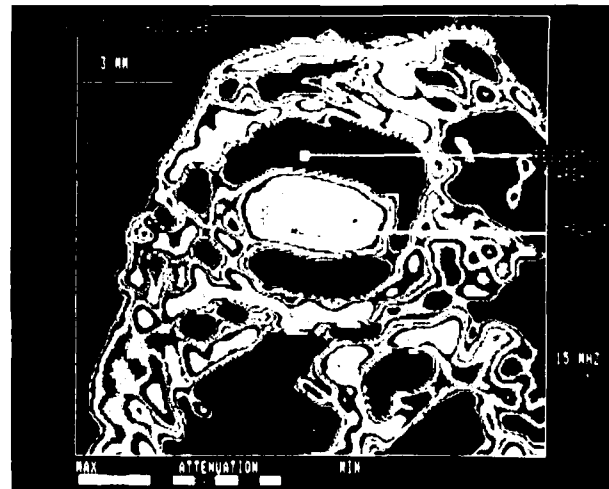


Fig. 2. Ti alloy implant in canine jaw.

*Supported in part by USPHS through NIDR Grant No. 2-T32-DE7054-06.

[†]Laboratoire de Recherches Orthopediques, Faculte Lariboisiere-St. Louis, Paris, France.

[#]Department of Electrical, Computer, and Systems Engineering, RPI.

COMPUTERIZED AXIAL TOMOGRAPHY AS A NEW ADJUNCT METHOD
FOR EVALUATION OF POST-MORTEM CEMENTED
TOTAL HIP REPLACEMENTS IN SITU

T. Gruen, B. Orisek, P. Campbell, S. Chew, W. Boswell,
D. Hillman, and A. Sarmiento

Departments of Orthopaedics and Radiology
University of Southern California
Bone and Connective Tissue Research Program
Orthopaedic Hospital-U.S.C.

The in-vivo performance of cemented total hip replacements (THR) has been evaluated clinically and radiographically. However, there are few studies on the long-term response existing in 'successful' THRs. This can only be obtained from histological evaluation of specimens from hips bequeathed for scientific study. Such published histological studies have been limited to the cement-bone interface.

The objective of the present study was to develop a systematic approach in evaluating post-mortem specimens with cemented components in-situ using computerized axial tomography as a new method to supplement hard-plastic ground histology and microradiography.

Case Report: Bilateral hip joints were obtained post-mortem from a eighty-nine year old white female who, at the age of eighty, had had bilateral Charnley THRs for primary osteoarthritis. The only major clinical complication was a traumatic dislocation of the left hip 5 years after surgery. No other problems were noted until her death almost nine years after initial total hip surgery. The body was embalmed and subsequently both innominate bones and femora with the THR components in situ were removed en bloc.

Materials and Methods: The hip joints were disarticulated and the femora were dissected of all external soft tissues. The superior-lateral portions of the cement encasement was carefully removed, which then permitted extraction of both femoral components. The cavity previously occupied by the stem was then filled with self-curing dental acrylic; this provided support for the membrane noticed at the stem-cement interface as well as the original cement encasement during subsequent sectioning and grinding.

The femora were scanned at 2mm increments from the neck to the lesser trochanter and then at 5mm increments distally. The femora were then sectioned at 10mm increments with a diamond wire saw; with a 2mm section for microradiography and ground hard plastic histology and the remaining 8mm section for paraffin histology.

Results: Detailed serial radiography indicated a proximal-lateral stem-cement radiolucency (less than 1mm) in both hips, one due to surgical technique and the other appearing at five years postop. The last films taken two months prior to death revealed a small and narrow cement-bone radiolucency extending about 15% of the interface with no other evidences of progressive loosening.

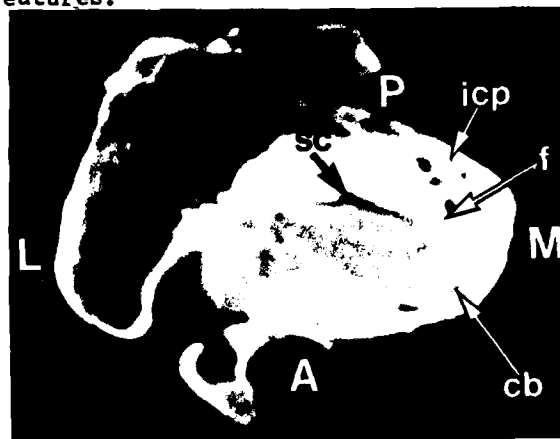
Subtle osteopenia in both proximal-medial femoral neck cortices was the only bone remodeling changes observed.

The CAT scans clearly demonstrated the presence of gaps at the stem-cement (sc) and cement-bone (cb) interfaces, longitudinal cement fractures (f), and extensive intracortical porosity (icp) within the proximal femoral neck (Figure 1).

The longitudinal cracks in the medial cement column were noted to extend from the neck distally toward the level of the lesser trochanter; these cracks as well as the stem-cement gaps were verified in the corresponding microradiographs and histological sections.

The correlated histological sections demonstrated fibrous membrane within the stem-cement and cement fracture gaps and occasionally at the cement-bone interface. Other sections demonstrated extensive intracortical porosity, which may explain the "calcar" osteopenia.

The images from the CAT scans provided significant information regarding the cemented femoral component, which would obviate the need for many tedious histological sections. Its potential together with selective sections for correlated microradiography and histology adds a new dimension in the analysis of post-mortem specimen. This will enhance understanding the in-vivo response of total hip replacements with respect to the integrity of the cement encasement, the interfaces, and bone remodelling, which may be attributed to the load carrying characteristics of the femoral component's structural design features.



Address: Orthopaedic Biomechanics
Orthopaedic Hospital-U.S.C.
2400 S. Flower Street
Los Angeles, CA 90007

THE EFFECT OF A POROUS COATING ON THE FATIGUE RESISTANCE OF Ti-6Al-4V ALLOY.

S. YUE; R.M. PILLIAR; G. C. WEATHERLY.

DEPT. OF METALLURGY AND MATERIALS SCIENCE,
UNIVERSITY OF TORONTO, TORONTO, CANADA M5S 1A4

Implant surfaces are porous coated in order to achieve good implant/tissue fixation characteristics by tissue ingrowth into the porous surface. Numerous papers have been published concerning the viability of the tissue/porous surface interface strength. There are, however, few papers which describe the effect of such a coating on the implant mechanical properties. Fatigue strength is known to be very sensitive to specimen surface finish and thus porous coatings are expected to significantly influence the fatigue properties. In the case of Ti-6Al-4V the sintering technique that is used to produce a porous coating can transform the microstructure from the mill annealed equiaxed structure to a coarse structure of colonies of alpha plates. The effect of both the porous surface and the plate structure on the fatigue strength of Ti-6Al-4V is the subject of this paper.

The alloys used for the substrate and porous surface in this experiment had very similar chemical analyses, both being medically approved Ti-6Al-4V extra low interstitial grades. The powder used for the porous surface was in the particle size range of 44 to 150 microns. All sintering heat treatments were performed in a high vacuum furnace at vacuum better than 10^{-5} Torr, the sintering heat treatment being 1250°C for 3hrs followed by a furnace cool. Fatigue testing was performed on hourglass (waisted) specimens using rotating bend loading. Since the porous coating treatment used here resulted in several surface changes and a bulk microstructural transformation, the relative effect of each of these variations was observed by testing specimens in the following conditions :-

1) the as received condition(A-R)

Specimens were machined from the as received, mill annealed rod stock. The surface of the waisted section of the specimens was prepared by grinding through successive silicon carbide papers such that the final polishing direction was parallel to the specimen longitudinal axis, thus minimising surface effects due to machining and polishing.

2)The sinter annealed and machined condition (SA-M)

The as received material was subjected to the heat treatment used in the sintering stage of porous coating (1250°C for 3hrs etc.). The heat treated alloy was then machined into fatigue specimens and the surface was finished as for the A-R specimens. Thus these specimens would show the effect of the change in microstructure on fatigue strength.

3) The sinter annealed condition (S-A)

Fatigue specimens were machined from the as received alloy and the surface of the waisted sections was prepared as for the A-R specimens. These specimens were then subjected to the sintering heat treatment but no porous surface was applied during this anneal. This series of specimens thus allowed a study of the effect of the heat treatment on the substrate surface and any consequent effects on the fatigue strength without the additional complication of the porous surface.

4) Porous surfaced condition (P-S)

Fatigue specimens were machined and the surface of the waisted sections was prepared as for the A-R specimens. These were then porous surfaced by sintering Ti-6Al-4V powder onto the waisted sections. For these specimens it was assumed that crack initiation in the outer porous region was not effective in causing crack growth in the solid substrate because of the crack blunting effect of voids within the porous layer. Hence the effective maximum stress amplitude was assumed to be that at the solid substrate surface.

The results can be summarised as follows:-

All conditions resulted in decreased high cycle fatigue resistance (endurance limit) with respect to the A-R specimens (Fig 1).

-The sinter annealed and machined condition (SA-M)

Surface condition:-as for the A-R specimens
Endurance limit:-100MPa lower than the A-R specimens.
Bulk microstructure:-coarse alpha plates.

-The sinter annealed condition (S-A)

Surface condition:- extensive grooving i.e. thermal etching due to the sinter anneal. The depth of this grooving was found to be particularly severe at prior beta and plate colony boundaries.

Endurance limit:- 250MPa lower than the A-R specimens.

Bulk microstructure:- coarse alpha plates.

-The porous surfaced condition (P-S)

Surface condition:- porous surfaced

Endurance limit:- 400MPa below the A-R specimens

Bulk microstructure:- coarse alpha plates.

Examination of the substrate of the P-S specimens in the vicinity of the fracture surface revealed cracks close to the particle/substrate interface region (fig 2). The average distance of such cracks from the particle/substrate interface region was found to be approximately 5 microns. Since the average distance between particle/substrate interface regions is about 125 microns it appears that these regions exert a significant influence on the crack initiation behaviour which will affect the fatigue resistance. Chemical analysis and microhardness profiles revealed evidence of high interstitial contents in the surface layer of the substrate of the P-S specimens. This interstitial contamination occurred during the sinter heat treatment, but the degree of contamination was thought unlikely to reduce the endurance limit.

Thus it may be concluded that the porous surfacing of Ti-6Al-4V leads to poor high cycle fatigue resistance due to bulk microstructural changes and stress raising effects of the particle/substrate interface configuration. These stress raising effects may also be compounded by the extensive grooving occurring on the substrate as revealed in the S-A specimens. Interstitial contamination of the surface occurs when the porous surface is sintered onto the substrate surface. However the extent of contamination is such that the endurance limit is probably not adversely affected.

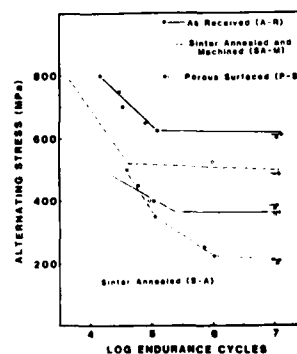


fig 1



fig 2

Financial support from NSERC and Canadian Oxygen(CANOX) Ltd.

Dept. of Metallurgy and Materials Science,
University of Toronto, Toronto, Canada M5S 1A4

Load Carrying and Fatigue Properties of the Stem-Cement Interface
with Smooth and Porous Coated Femoral Components

M.T. Manley, L.S. Stern, R. Averill*, P. Serekian*

State University of New York at Stony Brook, Stony Brook, New York

Failure of the PMMA bone cement mantle has been implicated in loosening of the femoral component after total hip replacement. Subsidence of the stem within the mantle has been shown to produce high levels of tensile hoop strain which leads to longitudinal cracking of the mantle and component loosening (1). Static mechanical tests in vitro have shown that proximal cement mantle stress can be reduced if the prosthesis-cement bond is improved by precoating the stem with PMMA (2) or if surface contours are incorporated in the stem design (3). Little is yet known about the effects of porous coating on the stability of a cemented stem or of the effects of fatigue loading on cement mantle performance. This study was designed to determine the load carrying and fatigue properties of the stem-cement interface when both smooth and porous coated femoral components of the same overall geometry were tested under the same experimental conditions.

MATERIALS

Two sets of Osteonics cast cobalt chromium alloy 300 series medium stems without collar were prepared for the study. The first set consisted of three standard smooth stems while the second set were similar stems, normalized and porous coated with sintered cobalt/chromium beads over the proximal 36mm of the stem length. Each stem was cemented with Cinton bone cement into a 48mm diameter PVC tube; the tubing being used in preference to cadaveric bone to ensure consistency of mechanical properties. Only the porous coated portion of the microstructured stems and the same length of the plain stems were supported by cement, so that the performance of the microstructured and smooth surfaces could be compared directly. Axial and circumferential strain gauges were bonded to the medial aspect of each bone model prior to testing.

METHODS

Specimens from each set of stems were subjected to either axial incremental static loading or axial dynamic loading in a software controlled MTS load frame. Axial loading was chosen so that comparison of cement mantle performance could be based on subsidence properties and hoop strain generation alone.

Specimens from each set of stems were subjected to incremental static loading at the rate of 2,000kN per minute until specimen failure or MTS capacity load (50kN). Hoop strain and axial strain in the medial bone model were measured throughout.

Fatigue testing of both types of specimens was run in compressed time for 10⁷ loading cycles at 40Hz. The dynamic loading range employed was 350N (preload) to 12.5kN (40% of

static failure load of the smooth interface). Load, subsidence and strain data were collected once every minute throughout the test.

RESULTS

The incremental static loading tests of smooth stems showed a random, stepwise increase in stem subsidence, with concomitant stepwise increase in tensile hoop strain as load was increased. Failure of the composite structure was by longitudinal cracking at a load of about 30kN and subsidence of 1.23mm. By comparison, stepwise increases in subsidence or hoop strain were never observed with the porous coated stems. Stem subsidence at machine capacity of 50kN was less than 0.05mm, and cement mantle failure did not occur.

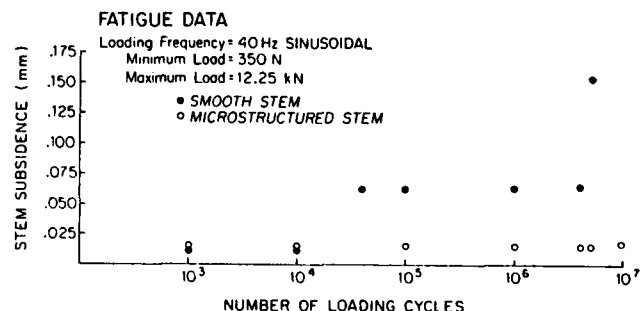
Fatigue testing data from both porous coated and smooth specimens is shown in the figure. Again the smooth stem showed stepwise increases in stem subsidence as the fatigue test progressed. The porous coated specimens only showed a gradual increase in subsidence. It is noticeable that the smooth stem underwent some six times more subsidence over the loading period than its microstructured counterpart.

DISCUSSION

This study has shown that the load carrying capacity of a femoral component-cement-bone model composite can be greatly enhanced if an interlocked interface exists at the stem-cement surface. In addition, the fatigue properties of the interlocked interface is markedly superior to that surrounding a smooth stem. It can be postulated that if stem-cement interlocking is achieved in vivo, stem subsidence will be prevented or delayed and an increase in longevity of the joint replacement will result.

References

1. Manley, M.T., Gurtowski, J., Stern, L., Dee, R. Trans 20 Orthop. Res. Soc. 8:238, 1983
 2. Crowninshield, Toblert, J. J. Biomed. Mat. Res. 17:819-828, 1983
 3. Pugh, J., Averill, R., Pachtman, N., Bartel, D. Trans 27 Orthop. Res. Soc. 6:189, 1981
- *Osteonics, Inc., Allendale, NJ



Analysis of Uncemented LTI Carbon and Porous Titanium Hip Hemiarthroplasties

R.C. Anderson, S.D. Cook and R.J. Haddad, Jr.

Tulane University School of Medicine
New Orleans, Louisiana 70112

The objective of this investigation was to characterize the stress distribution and remodeling changes associated with porous coated titanium and pyrolytic carbon hip hemiarthroplasties, with particular attention given to the implant-bone interface.

The implant design was a polished, hemispherical head, with a straight stabilizing stem. Two material systems were examined, porous commercially pure titanium (pore size 200 μ m) coated Ti-6Al-4V alloy, and low temperature isotropic (LTI) pyrolytic carbon (pore size 5-10 μ m). The experimental model was the adult mongrel dog. Reamers were designed to assure the precise machining of bone in order to achieve an interference fit upon seating the device. Monthly radiographic evaluation and periodic gait analysis were used to monitor the implant status. The animals were sacrificed at periods of 2, 4.5, 9, 12 and 18 months.

A two-dimensional finite element model (FEM) was constructed to represent four cases corresponding to full bone ingrowth into the porous titanium coating, complete bone apposition to LTI carbon, and each device with an interposed fibrous tissue layer.

The FEM results of the alteration in calcar strain energy associated with each device and interface condition are shown in Figure 1. In general, the LTI carbon devices produced strain energy levels 15 - 20% closer to those of the natural femur than did the higher modulus titanium devices. The models of the osseously attached devices calculated a pronounced strain energy decrease in the distal calcar area, while those of the devices with fibrous interfaces calculated a pronounced increase in proximal calcar strain energy. Similar trends were calculated in the cancellous regions, the most prominent trend being a significant decrease in proximal trabecular strain energy for osseously attached devices, while the same region of the models with interposed fibrous tissue presented greatly increased strain energy levels.

Radiographic observations of post sacrifice bone density changes correlated well with FEM results. Implants shown histologically to have extensive ingrowth, appeared radiographically to have calcar and proximal trabecular thinning, with distal cancellous bone density increases. Similarly, LTI carbon devices with areas of direct bone apposition radiographically demonstrated calcar thinning with no proximal trabecular density increase. However, LTI carbon devices with complete fibrous interfaces displayed radiographically prominent increases in proximal calcar and trabecular bone density.

Histologic sections of the titanium implants showed progressive resorption of bone, most notably in the proximal femoral neck. At two months, bone ingrowth was extensive, though proximal trabeculae were thinned with active resorption sites. At one year, the proximal bone remained atrophied, though distal trabecular bone had densified in and around the porous coat.

Thin sections of the LTI carbon implants at 2 months, as well as those at one year, showed a varied response. The first response is exemplified in Figure 2a. An interposed fibrocartilage/fibrous tissue layer approximately 500 μ m thick had formed at all implant-bone interfaces. Proximal trabecular bone had densified significantly. The second response (Figure 2b) was characterized by regional bone apposition under the cap and along the stem. In this case the proximal trabecular bone did not appear hypertrophied. In both cases, the bone adjacent to the fibrous layer gave positive indications of remaining stable, including good organization, good vascularity, little osteoclastic activity and interfacial osteoblastic activity.

The results of FEM, radiography, and histology suggest that the difference between osseously attached devices and those with an interposed fibrous layer was far more significant than the difference due to elastic moduli. Thus, favorable interface stress transfer could be exploited in order to correct the modulus mismatch problem. The two remodeling responses to the LTI carbon devices suggest that *in situ* shear stress levels at the bone-carbon interface approach the strength of the appositional bond.

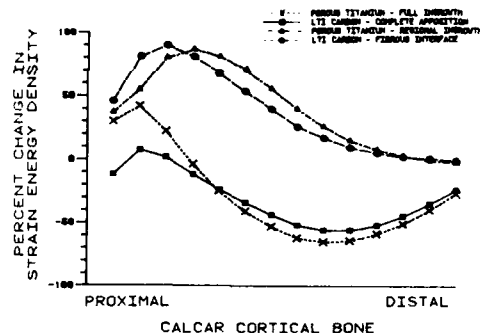


Figure 1

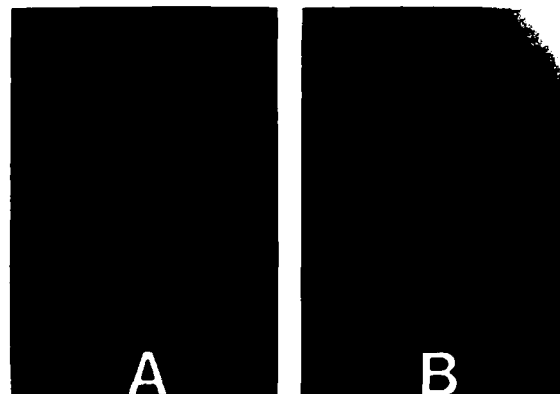


Figure 2

Department of Orthopaedic Surgery
Tulane University Medical School
New Orleans, Louisiana 70112

The In-Vivo Strength of Filler Stabilized Porous Implants

S.I. Reger, PhD., R.E. McLaughlin, M.D., H.C. Eschenroeder, Jr., M.D.

Department of Orthopaedics and Rehabilitation, University of Virginia
Charlottesville, Virginia 22908
Medical Center

The use of porous implants in total joint replacement requires extended immobilization of the prosthesis until bone ingrowth has occurred. Rapid immobilization can be obtained by precision reaming of the bone and press-fit between cortex and the implant. Often, this can not be achieved because of the variable size and shape of the bone and the lack of matching-size prosthesis. When only loose fit is possible, the use of a filler substance could help to provide temporary immobilization of the prosthesis.

The objective of this research was to test filler and bone growth stimulating materials for their stabilizing effect on porous-coated implants in canine femurs. Autogenous ground bone paste, inorganic tricalcium phosphate (TCP) crystals and organic decalcified bone paste ("biologic cement") have been tested for their effects in enhancing the pullout strength of porous implants six weeks after implantation.

METHODS: Identical porous-coated rods were inserted in each femur of 32 mongrel dogs. The cobalt band alloy rods, made by the DePuy Co. were porously coated to a diameter of 5.5 mm at the middle 25 mm length. The distal femora were overreamed to a 6.4 mm diameter using medial knee arthrotomy. Between implant and cortex, 1 ml filler material was packed into one femur, and no filler was used on the control side. Similarly shaped, smooth rods without porosity were also used as a second control. The animals were sacrificed at six weeks, the femora excised and radiographs made. The condyles were removed, the distal ends of the rods exposed, and the proximal end of the femur was mounted in an Instron testing machine. The rods were extracted in tension at a constant rate of 50 mm/min, and the pullout force was plotted as a function of extension. The autogenous ground bone paste was prepared from bone removed from both iliac crest and ground to a fine paste in a commercial "bone mill". The TCP filler was 40-60 mesh crystals provided by Orthograft Miter, Inc. The biocement was made by extraction, decalcification and milling to 75-850 μ m size of diaphyseal bone of mongrel dog limbs by the method of Reddi as modified by Oikarinen (1,2). The data was analyzed, and the results and the ratio of pullout strength of the filler-treated side divided by the control femur value shown in Tables 1 and 2. A ratio greater than one shows an improvement in strength on the treated side.

RESULTS: The recorded data between dogs was highly variable, reflecting the variation in animal size and age. In the control series of 5 dogs, the average pullout strength of the porous side was 55.8 ± 44 kg, or 12 times the strength of the smooth non-porous side at 4.4 ± 3 kg. This shows only a minimum ability of the smooth implant to support loads after 6 weeks. In the autogenous milled bone graft series of 10 dogs, half the dogs showed stronger pullout strength on the grafted side than on the ungrafted control side (Table 1). The means, however, were not significantly different by the pooled t-test ($p > 0.05$). Similarly, the TCP filler showed no significant difference,

in this series of 8 dogs, between the treated and the control sides at 6 weeks after implantation. There was a significant increase of fixation strength on the TCP-packed side immediately after implantation. The unpacked side could not support load, but the crystal-packed femurs could carry 5.6 ± 0.7 kg load. The results in Table 2 from 9 dogs with decalcified bone paste (biocement) showed a 44% increase in extraction force above the average control side value. This difference in means was significant by the Wilcoxon signed rank sum test ($p < 0.05$).

CONCLUSION: The pullout tests showed porous implants to be rigidly fixed in the femoral canals of dogs in 6 weeks with clearly defined sharp break at the ultimate load. Autogenous ground bone filler showed high and low interface strength, indicating that ingrowth effects could be masked by some aspect of the bone graft. Inorganic TCP filler could enhance the immediate strength of implants only, without significant effect in the long term. Decalcified bone matrix could significantly promote long-term bony fixation of porous implants in the dog femoral canal.

Table 1			Table 2		
Pull-out strength(kg)			Pull-out strength(kg)		
Control	BoneGraft	Ratio	Control	Biocement	Ratio
78	30	0.38	104	64	0.61
49	30	0.61	100	98	0.98
139	86	0.62	130	130	1.00
110	79	0.72	54	61	1.13
203	192	0.95	23	34	1.48
27	30	1.11	126	205	1.62
115	137	1.19	89	164	1.84
168	220	1.31	12	23	1.92
29	84	2.90	72	173	2.40
52	154	2.96			
x \pm SD 97 \pm 60 104 \pm 69 1.28			x \pm SD 79 \pm 42 106 \pm 65 1.44		

REFERENCES:

1. Reddi, A.; Huggins, C.: Proc. N.A.S. 69:1601, 1972.
2. Oikarinen, J.; Korhonen, L.: Clin. Orthop. 140:208, 1979.

Supported by NIHR Rehabilitation Research and Training Center Grant #G008300043.

BLOOD TOLERABILITY OF CARBON-CARBON BIOMATERIALS. IN VIVO AND IN VITRO INVESTIGATIONS USING RADIOTRACERS.

B. BASSE-CATHALINAT, Ch. BAQUEY, J. CAIX, L. BORDENAVE, J. BRENDÉL, D. DUCASSOU.

INSERM/CEEMASI-SC 31 - Université Bordeaux II, 33076 BORDEAUX Cedex.

INTRODUCTION.

Composite carbon-carbon materials have been proposed for use in biomedical applications and in particular for elaboration of an implantable left ventricular assist device (project CORA) based on the principle of the Maillard-Wenkel rotating compressor. These materials are resistant and liable to transform their surface into a non-thrombogenic one. A stage of the CORA project concerns the study of hemocompatibility of this materials and specially its interaction with flowing blood.

MATERIALS AND METHODS.

Carbon-carbon tubes 4 cm long and 2.5/4 mm in diameter are used. Each tube undergoes special surface treatment concerning the control of the thickness of the final coating of pyrolytic carbon and oxydation level.

The author's novel methods use radiotracers with a dynamic technique which permits the direct observation of interaction between blood and artificial material.

For in vivo investigations the tubes are tested by insertion into the femoral arteries of anaesthetized mongrel dogs. The animal is previously I.V. injected with autologous platelets, red cells and canin fibrinogen respectively labelled with ^{111}In , ^{99}Tc , and ^{125}I . Using a high energy resolution Ge-Diode as detector, measurements of the specific contribution of each of these isotopes to the radioactivity recorded for blood samples collected periodically during the whole experiment are used as reference to interpret the dynamic measurement processed as follows. The vascular segment containing the carbon tube is placed in front of the same detector equipped with a lead shielding designed to prevent the detector from receiving any emission from outside the artificial tube content. Under these conditions sequential measurements and analysis of the radioactivity due to the artificial tube content can be run for a chosen period of time and the evolution interpreted(a).

For in vitro studies the detector used was a gamma-camera equipped with a special collimator (Fig. 1). The acquisition and treatment of data was performed with a device designed to process scintigraphic information. With this device several tubes can be tested simultaneously in the same hemodynamic conditions.

RESULTS.

Fig. 2 shows that the in vivo technique displays thrombogenic phenomena as soon as they appear and provide a general ranking for the thromboresistance of the surface studied.

Using in vitro technics, detailed studies were made of the influence of flow rate or medium composition on platelet adhesion and protein adsorption. These methods allow precise comparison specially between effects of different surface treatments and checking that surfaces which have received the same treatment are identical. Such a screening reduces inter assay variability during

in vivo experimentation.

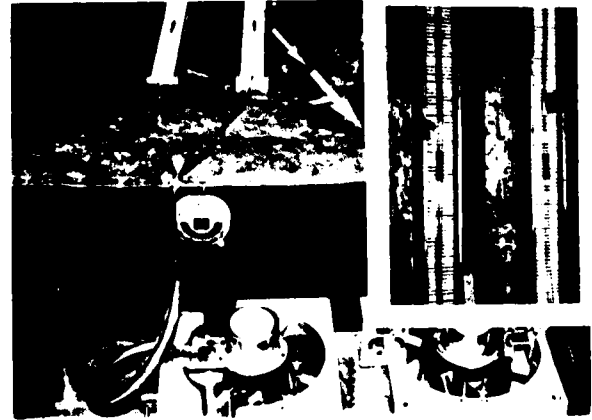


Fig. 1 - Expérimental set-up for in vitro experimentation. The detector used is a gamma-camera connected to a computer. The carbon-carbon tubes are placed on the special collimator (above right) which allows good spatial resolution and high efficiency.

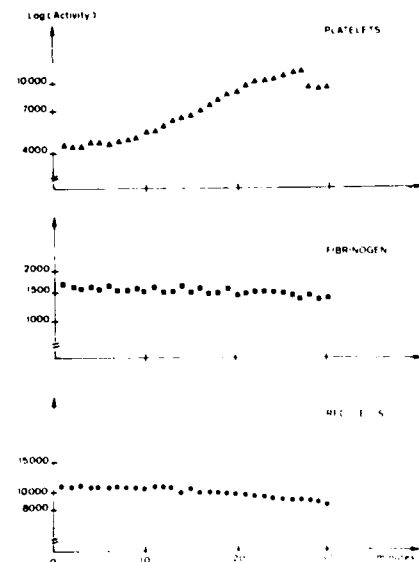


Fig. 2 - In vivo experimentation. Carbon-carbon tube is inserted into the dog femoral veins. Recorded evolution of blood elements concentrations at the blood material interface

Références -

- (a) - Basse-Cathalinat B & al. Int. J. Appl. Rad. Isot., 31 : 747, 1980.

IMPROVED PATENCY IN SMALL DIAMETER DACRON VASCULAR GRAFTS AFTER A TETRAFLUOROETHYLENE GLOW DISCHARGE TREATMENT

A.M. Garfinkle, A.S. Hoffman, B. D. Ratner, and S. R. Hanson*

University of Washington
Seattle, WA 98195, USA

*Scripps Research Institute
La Jolla, CA

The most important clinical challenge for vascular grafts today is the small diameter (≤ 4 mm ID) low blood flow situation. The many factors which may influence the long term patency of such grafts include: host-related variables, graft material composition, the roughness or texture of the luminal surface, the character and magnitude of graft porosity, the graft compliance, the processing during manufacture, the sterilization procedure, and the surgical technique, including preclotting if needed.

We have investigated the effect of graft surface composition on thrombotic occlusion in an *ex vivo* baboon femoral shunt model.¹ Specifically, 4-5mm ID USCI external velour Dacron knit grafts of two porosities, and one low porosity Dacron weave, were selected as controls. A covalently bound, ultrathin fluorocarbon polymer layer was then deposited in a homogeneous and reproducible manner on the luminal surfaces using an inductively coupled TFE glow discharge. The TFE treatment in all cases produced a dramatic reduction in thrombotic occlusion of the grafts.

ESCA was used to characterize treated graft surfaces. These results showed a highly fluorinated, uniformly treated surface.² Untreated Dacron material, which stained evenly when soaked with methylene blue dye, remained totally undyed after glow discharge TFE treatment. SEM observations up to 7000X showed no observable changes in surface morphology. Porosity was remeasured after treatment and did not change. A critical surface tension of about 13 dynes/cm as determined by the Zisman method was measured on similarly treated Mylar surfaces.²

The thrombotic response to changes in graft surface composition was investigated in the baboon model for the different porosity grafts. Graft patency was markedly improved for TFE treated woven and knit grafts when compared with the untreated grafts for all time periods studied (Figs. 1 & 2). Mean relative platelet counts decreased with time for all grafts in the first two hours, with the TFE treated knit grafts showing a significantly smaller decrease than the untreated grafts. Mean relative blood flow also decreased for all untreated grafts during the initial two-hour time period. With further blood exposure, flow continued to decrease in the untreated grafts, while a high flow was maintained throughout in the treated grafts. It is interesting to note in Fig. 2 that an argon glow discharge treatment produced a more thrombogenic surface than the untreated control.

Preliminary *in vitro* data, based on a laser scattering measurement technique using fresh baboon blood, show that the TFE treated graft surfaces are producing significantly fewer microemboli than the untreated control graft surfaces.³ Thus, the improved *ex vivo* patency is probably not due to increased embolization from the treated graft surface.

We are investigating the mechanism for the improved patency exhibited by the glow discharge treated Dacron grafts, and are testing the hypothesis that the mechanism involves modified initial

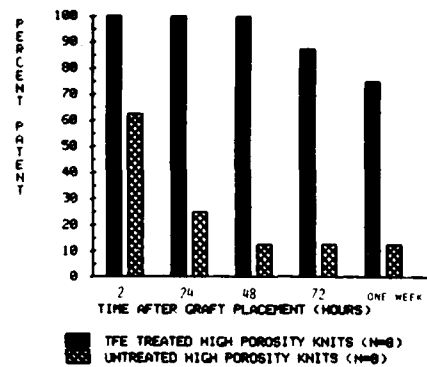


Figure 1. Graft patency for small diameter, high porosity Dacron knit grafts before and after TFE glow discharge treatment. Number of grafts tested is shown in parentheses.

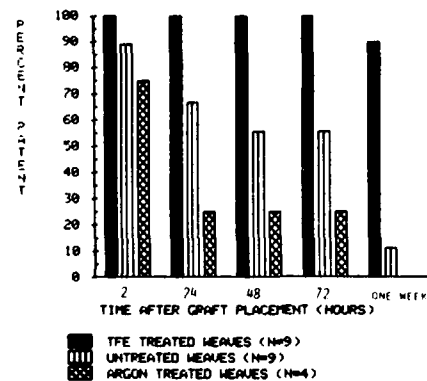


Figure 2. Graft patency for small diameter, low porosity Dacron weave grafts before and after argon and TFE glow discharge treatments. Number of grafts tested is shown in parentheses.

protein adsorption, resulting in differences in the adherent thrombus layer and its subsequent reorganization.

Acknowledgment: The authors would like to acknowledge the support of the NHLBI, Devices and Technology Branch, Grant #HL-22163-03 to -05.

References

- Hoffman, A.S., A.M. Garfinkle and B.D. Ratner, Trans. Soc. for Biomats. Ann. Mtg., Washington, D.C., April 1984.
- Reynolds, L.O., unpublished data, Dept. of Nuclear Eng., Univ. of Wash., Seattle, Wash. (1982, 1983).
- Hanson, S.R., L.A. Harker, B.D. Ratner and A.S. Hoffman, J. Lab. Clin. Med. 95, 289 (1980)

Center for Bioengineering and
Department of Chemical Engineering
University of Washington FL-20
Seattle, WA 98195, USA

Blood Surface Interaction Investigated With Ultrathin Coatings of
Glow Discharge Polymers Applied Onto the Inner Surface of Small Diameter
Silastic Tubing

H. K. Yasuda, Y. Matsuzawa, S. R. Hanson* and L. A. Harker*

Graduate Center for Materials Research, University of Missouri-Rolla,
Rolla, MO 65401, and *Scripps Research Foundation, La Jolla, CA.

Glow discharge polymerization is a unique ultrathin film technology which yields polymers having completely different properties from those of the conventional polymers. Glow discharge polymers have no discernible repeating units and, in many cases, are formed in highly crosslinked and highly branched networks consisting of very short segments, even if a well defined monomer is used as a starting material.

Such an ultrathin film provides a unique opportunity of investigating blood-surface interaction, because 1) the coating can be applied in such a way that chemical nature of a surface can be modified without affecting overall surface topography (thickness of film being less than 500Å), 2) the modification of surface can be achieved without altering the bulk characteristic of substrate material, 3) the coating is an excellent barrier which prevents leaching out of low molecular weight components in the substrate polymer and also imbibition of blood components by the polymer, and 4) the coating offers unperturbable characteristics of surface (in the blood environment).

Although promising blood compatibility of glow discharge polymers have been indicated in previous studies carried out using flat sheets and very short rings (e.g., vena cava rings, of which the length of tube is less than 1 cm and length/diameter ratio is close to 1.0), the more elaborate evaluations of blood surface interaction using longer tubings in in-vivo or ex-vivo experiments was hampered by the difficulty of coating the inside wall of a small tubing of which length/diameter ratio is considerably larger (e.g., over 100). This difficulty stems on problem of creating glow discharge in a small space which has a large surface/volume ratio and of maintaining a uniform supply of monomer along the length of tubing. In this study, a special glow discharge polymerization reactor was constructed so that a sufficiently long (e.g., 10-15 meters) tubing can be coated uniformly with glow discharge polymers in a reproducible manner.

A very thin layer (300-500Å thick) of glow discharge polymers were coated onto the inner surface of Silastic tubings (I.D. 3.3 mm). At this level of thickness, the gross surface topography of tubing did not change. By changing types of monomers and conditions of glow discharge polymerization, the tubings which have nearly identical physical characteristics but considerably different chemical characteristics were prepared. This is a unique advantage of the surface modification of polymers by glow discharge polymerization, since many other chemical methods of surface modification (e.g., surface grafting) tends to alter surface topography as well as bulk properties of the substrate polymer.

The combined effects of imperfection and barrier characteristics of coatings were examined by placing an oil-soluble dye solution inside the tubing. Since the substrate polymer (polydimethylsiloxane) has exceptionally high imbibing characteristics to lipids and lipid-soluble substances, the uncoated tubing can be easily dyed by an oil-soluble dyestuff (e.g., Sudan Red in butanol). The dye tests were performed to insure flawless coating and desired barrier characteristics of the surfaces to be examined in the blood-surface interaction studies.

Thus, prepared tubings with flawless coatings of glow discharge polymers of hydrocarbon (CH₄) and perfluorocarbons were inserted into an A-V shunt in baboon. Clot formation was examined by a γ-camera, and the platelets half-life was compared against that of control experiment according to the previously established standard procedure. Some glow discharge polymers of perfluorocarbons showed excellent athrombogenic characteristics, i.e., no clot formation was observed and platelets half-life was identical to the control value. The details of inside tube coating and results will be presented.

ACKNOWLEDGEMENT: This study is supported by the National Heart, Lung, and Blood Institute, National Institute of Health, under Grant No. 5R01 HL24476-03.

THROMBOGENICITY OF SMALL DIAMETER VASCULAR GRAFTS

J.M. Malone, M.D., R.L. Reinert, B.S., K. Brendel, Ph.D.
and Raymond C. Duhamel, Ph.D.

University of Arizona, Tucson, Arizona

In previous studies, it was demonstrated that vascular grafts consisting of 3-4 mm ID x 4-6 cm segments of dog carotid acellular vascular matrix (AVM) exhibit extensive re-endothelialization and a patency rate of 80% at 90 days after implantation in the carotid position in greyhound dogs. AVM is prepared by extraction of native vessels with detergents, which produces cell-free vascular extracellular matrix that includes an intact sub-endothelial basement membrane and is apparently free of major transplantation antigens.

In the present study, the thrombogenicity of the AVM flow surface was compared in the presence and absence of aspirin (ASA) to that of autogenous vessels and four clinically-available vascular prostheses. Thrombogenicity was evaluated in the thrombus-free surface model of Sauvage and co-workers (Kenney et al. (1980) Ann. Surg. 191:355-361) at flow rates of 25, 50 and 100 ml/min. Preliminary results at the 25 ml/min flow rate were also obtained for two NIH Reference Materials. All grafts were of 4 mm ID x 4 cm and were implanted in the carotid position in adult greyhound dogs using standard microsurgical technique. Flow rates were controlled with an adjustable vessel clamp distal to the graft and continuously monitored with a Stathen-Gould SP2204 Flow Meter via a flow probe positioned proximal to the graft. Flow was maintained at the specified rate for 4 h, after which the graft was recovered and the percentage of thrombus-free luminal surface (TFS) determined. ASA treatment consisted of 300 mg ASA per day for 3 days prior to surgery.

The following grafts were tested:

- Group A: 1. Autogenous Cephalic Vein
2. Autogenous Femoral Artery
- Group B: 3. AVM, Non Cross-Linked
4. AVM, Glutaraldehyde Cross-Linked
5. AVM, Carbodiimide Cross-Linked
- Group C: 6. Polytetrafluoroethylene (Gore-Tex^K)
7. USCI Sauvage Knitted Dacron Velour (pre-clotted)
8. Bard Albumin-Coated Sauvage Knitted Dacron Velour
9. Meadox Dardik Biograft, modified human umbilical vein
- NIH Primary Reference Materials:
10. Polydimethylsiloxane (PDMS)
11. Low Density Polyethylene (LDPE)

Statistical analysis was performed by the Biometry Unit of the University of Arizona Cancer Center. Data were analyzed by one-way ANOVA and pair-wise t-test of individual graft types.

The grafts in groups A, B and C were grouped together in the table because there were no consistent statistically-significant differences among grafts within the respective groups for the categories listed. At the three flow rates, autologous grafts (Group A) and AVM grafts (Group B) were significantly less thrombogenic ($P < 0.01$) than the commercial grafts (Group C) of the NIH Reference Materials.

PERCENT THROMBUS-FREE FLOW SURFACE MEASUREMENTS

Graft Type	ASA Treatment	Flow Rate (ml/min)		
		25	50	100
		% TFS \pm SD		
Group A	-	100 \pm 0	100 \pm 0	100 \pm 0
Group B	-	47 \pm 38	88 \pm 11	94 \pm 6
	+	69 \pm 27	93 \pm 10	98 \pm 5
Group C	-	5 \pm 13	10 \pm 15	31 \pm 28
	+	22 \pm 26	23 \pm 23	46 \pm 23
NIH PDMS	-	11 \pm 22	-	-
	+	30 \pm 34	-	-
NIH LDPE	-	0 \pm 0	-	-
		11 \pm 22	-	-

At 50 and 100 ml/min, the differences between autologous and AVM grafts were not statistically significant, although only the autologous grafts were exclusively thrombus-free. At 25 ml/min, however, the autologous grafts were significantly less thrombogenic than the AVM grafts, which, in turn, were significantly less thrombogenic than either the clinically-available grafts or the NIH reference standards. These data clearly indicate that the AVM flow surface closely approaches the low level of thrombogenicity of autologous grafts and suggests considerable promise for the use of AVM as a small diameter vascular prosthesis.

The data in the table also indicate a significant effect of ASA on thrombus formation, but only at the 25 ml/min flow rate. The ASA effect was statistically significant for both the AVM and commercial grafts at the low flow rate. The autologous grafts exhibited no thrombus formation even without ASA. The lack of ASA effect at the higher flow rates suggests that platelet aggregation may not be the primary mediator of thrombus formation in vascular prostheses under physiological conditions. Further investigations in this area are warranted.

ACKNOWLEDGEMENTS: This work was supported in part by NIH Grant HL29164 to K.B., V.A. Merit Review Grant #008 to J.M.M., and Bard Implants Division of C.R. Bard, Inc.

Department of Surgery, College of Medicine
University of Arizona, Tucson, AZ 85724
and

*Department of Pharmacology, College of Medicine
University of Arizona, Tucson, AZ 85724

Kost, J., Edelman, E., Brown, L., Langer, R.

Massachusetts Institute of Technology, Cambridge, MA 02139

In the past few years, there have been many recent advances in the development of polymeric drug delivery systems. However, nearly all of these systems release drugs at decreasing, or at best, constant rates. There has been no way to increase release rates on demand, nor any way to externally control drug administration once the release process from the implanted polymer matrix has commenced. The necessity of enhanced delivery by demand is manifested in hormonal delivery of substances such as insulin. In diabetes, augmented delivery of insulin is required for short periods associated with meals.

Recent studies in our laboratory suggest the feasibility of delivering insulin and other macromolecules at increased rates on demand(1,2). The polymeric device consists of small magnetic beads embedded in the polymer matrix along with the drug. Release rates can be enhanced when desired by an oscillating external magnetic field. In this study we report the function in vivo of this magnetically modulated system.

The polymeric pellets containing insulin (50% by weight) and a magnetic cylinder (1.4 mm diameter, 1.4 mm height) were implanted subcutaneously in the abdominal area into six rats with streptozotocin-induced diabetes. The control groups were: four healthy rats, six diabetic rats without implants, six diabetic rats with implants containing insulin without the magnet, and six diabetic rats with implants containing magnets, but not insulin.

Over a two-month period, all the rats were exposed to triggering by an oscillating magnetic field at least ten times. The blood glucose levels were followed, one hour before the triggering to 6 hours after. In several cases the glucose levels were followed over a span of 24 hours. It was found that exposure to an oscillating magnetic field for one hour caused a significant decrease in blood glucose levels of rats receiving implants containing insulin and the magnet, compared to all the other groups. For example, a 200 mg % decrease in blood glucose level was observed 15-45 min. after exposure to the magnetic field in the experimental rats. No such lowering of blood glucose was observed in any of the control groups. Histological and electron microscopic evaluation of the implants revealed good biocompatibility and a very little fibrous encapsulation.

References

1. Hsieh, D, Langer, R., Folkman, J., Proc. Natl. Acad. Sci. 78, 3, 1863, 1981.
2. Kost, J., Edelman, E., and Langer, R. 10th International Symposium on Controlled Release of Bioactive Materials, San Francisco, CA July, 1983.

GLUCOSE SENSITIVE MEMBRANES: STABILITY AND BIOCOMPATIBILITY STUDIES

Thomas A. Horbett*, Joseph Kost*, Dennis Coleman, and Buddy D. Ratner*

*University of Washington, Dept. of Chemical Engr., Seattle, WA. 98105

**University of Utah, Department of Pharmaceutics, Salt Lake City, Utah

A membrane which swells in response to glucose is being developed for possible use in the treatment of diabetes. The permeability of the membrane also changes in response to changes in glucose concentrations. The membrane could be used as part of an *in vivo* glucose sensor or as a device for varying insulin delivery rates through the membrane in response to variations in glucose concentrations. Since the stability and biocompatibility of the membrane will partially determine its utility in the treatment of diabetics, a preliminary study of these properties was performed.

The membranes were prepared by ^{60}Co radiation-initiated polymerization of a frozen (-60°C) solution containing hydroxyethyl methacrylate, N,N-dimethylaminoethyl methacrylate, tetraethyleneglycol dimethacrylate, ethylene glycol, water, and glucose oxidase. Enzyme activity was determined by using a pH stat to measure the rate of base uptake needed to maintain pH at 7.4 in a 1 mg/ml glucose solution containing a piece of the membrane. Discs (10 mm diameter, 0.3 mm thick) cut from the membrane were irradiation sterilized and four of the discs were implanted in each of 12 mice. Two discs were placed subcutaneously and two were placed intraperitoneally in each mouse. Implants were removed from each of three mice at 1, 7, 14, and 28 days. One implant from each site was placed in glutaraldehyde solution, and subsequently blocked, cross-sectioned, mounted on microscope slides, stained with hematoxylin/eosin, and examined microscopically. The other specimen from each site was placed in buffer and its enzyme activity determined.

The enzyme activity of unimplanted discs was stable for the duration of the implant period while the enzyme activity of the implanted discs decreased by between 20 and 35%, depending on the implant site (see Figure 1). In separate experiments, membranes kept in blood plasma at 37°C for 60 days retained 45% of the original activity. Membranes stored in buffer for 300 days retained 37% of the initial activity. The irradiation used to sterilize the discs prior to implantation (1.2 Mrad, ^{60}Co) reduced the activity to $74 \pm 16\%$ of its initial value.

The implanted specimens caused only a mild inflammatory reaction. The fibrous capsules formed at 28 days were thin, and neutrophils, giant cells and lymphocytes were few in number. The response was similar to that observed for other materials (e.g. certain silicone rubbers) considered to give mild reactions. Encapsulation was much more pronounced at the subcutaneous sites than at the intraperitoneal sites.

This study shows that these glucose sensitive membranes are relatively stable with respect to enzyme activity. Since they are formulated with great excesses of enzyme over that required to convert all glucose to gluconic acid in a very short time, complete stability is not a requirement. The membranes also appear to be rea-

sonably biocompatible as judged by the mouse implant test. The results therefore encourage the further development of these membranes for eventual use in the treatment of diabetics. Intraperitoneal implantation may be ideal since less enzyme deactivation and encapsulation was observed.

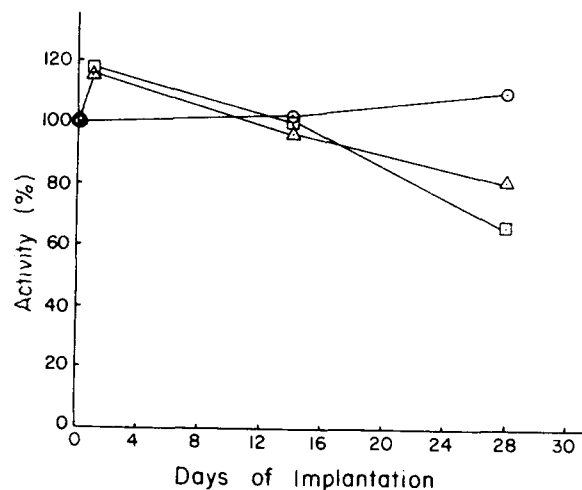


Figure 1. Enzyme activity of glucose sensitive membranes after implantation in mice. Circles: unimplanted controls. Triangles: intraperitoneal implants. Squares: subcutaneous implants.

Acknowledgements: The University of Washington, the California and Washington Affiliates of the American Diabetics Association, and the National Institute of Arthritis, Diabetes, and Digestive and Kidney diseases (grant AM30770) supported this work.

SELF-REGULATING INSULIN DELIVERY SYSTEM

Jeong, S.Y., Sato, S., McRea, J.C. and Kim, S.W.

University of Utah Dept. of Pharmaceutics, College of Pharmacy
Salt Lake City, Utah 84112

A self-regulating insulin delivery system has been designed based on a combination of biological feedback modulation and controlled release of an active compound. In an ideal delivery system, insulin release should be controlled by the amount of blood glucose present at any particular time. This requires a continual feedback between the blood glucose level and insulin release.

The design of our delivery system utilizes the concept of competitive and complementary binding affinity of concanavalin (Con A) with glucose and glycosylated insulin (G-insulin). G-insulin is bound to Con A and its displacement from the Con A is proportional to the amount of glucose present.

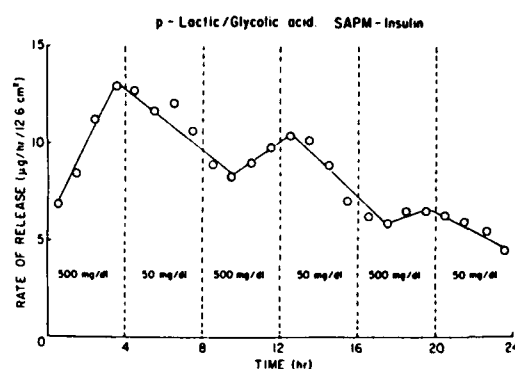
Seven G-insulin derivatives were synthesized: N-succinic glucosamine-insulin (SGAI), N-glutaric glucosamine-insulin (GGAI), p-(succinylamido)-phenyl- α -D-mannopyranoside-insulin (SAPMI), p-(glutaryl-amido)-phenyl- α -D-mannopyranoside-insulin (GAPMI), p-(succinylamido)-phenyl- α -D-glucopyranoside-insulin (SAPGI), p-(glutaryl-amido)-phenyl- α -D-glucopyranoside-insulin (GAPGI) and p-(α -D-glucopyranosyloxy)-phenyl-thiocarbamoyl-insulin (GPTI). The G-insulin derivatives exhibited bioactivity in rats by means of a blood sugar depression test and were more stable than native insulin in aggregation studies (CD and turbidity measurement).

SAPMI was used as a model compound to evaluate the effect of different coupling reaction conditions, such as pH and stoichiometry, on selective glycosylation of insulin. The results showed that monosubstituted SAPMI was the predominant form produced at a low molar concentration of the carbohydrate derivative (SAPM), and that di- and tri- substituted SAPMI were only produced at high molar concentrations of SAPM.

It was estimated that the binding affinities of SAPGI and SAPMI compounds to Con A were 45 and 200 times higher respectively than that of glucose. For this reason, these two compounds were chosen for in vitro release studies in order to avoid G-insulin displacement in the presence of low concentration of glucose (a hypoglycemic condition). The in vitro release study simulated different 'feeding' patterns (continuous glucose challenge and step function challenge) by varying glucose concentrations in a specially designed diffusion cell under sink conditions. The membranes used were a porous biodegradable poly (lactic/glycolic acid) copolymer (50:50) and a porous nonbiodegradable regenerated cellulose ($D=1.40 \times 10^{-7}$ and $D=4.14 \times 10^{-8}$ cm²/sec for insulin, respectively). The results showed that under continuous glucose challenge, release of the G-insulin compounds increased with increasing glucose challenge, where SAPGI showed higher release than SAPMI due to the lower binding affinity to Con A of the SAPGI. Also, both derivatives showed greater release through the poly (lactic/glycolic acid) copolymer membrane than through the regenerated cellulose. Under a step

function glucose challenge through the poly (lactic/glycolic acid) copolymer membrane, the release response of both SAPGI and SAPMI was in phase to the glucose challenge. SAPGI showed a greater response amplitude than SAPMI due to differences in binding affinities discussed above. Both G-insulin derivative showed an out of phase response through the regenerated cellulose membrane to the glucose challenge because of the low diffusion coefficient of the membrane.

In vivo release studies using a polymeric pouch containing a SAPMI-Con A mixture, implanted in peritoneum of diabetic animals, are underway.



Figure

SAPMI release response through poly-(lactic/glycolic acid) copolymer membrane to step function glucose (500 mg/dl and 50 mg/dl) challenge.

Acknowledgement

This work was supported by NIH grant AM-27929-03

POLYACRYLATE COATED ALGinate BEADS FOR MICROENCAPSULATION OF ANIMAL CELLS

F.V. Lamberti and M.V. Sefton

Department of Chemical Engineering and Applied Chemistry
University of Toronto, Toronto, Ontario, M5S 1A4

Microencapsulation of pancreatic islets in a 'tissue-compatible' hydrogel selected to function as an impermeable barrier to high molecular weight antibodies while allowing the free exchange of glucose and insulin has been proposed as a means of developing an implantable self-regulating drug delivery device for insulin-dependent diabetes.

Rather than use water-soluble polymers as microcapsule wall-forming materials (1), we have focussed on the use of water insoluble (non-crosslinked) hydrophilic polyacrylate copolymers, as coatings for previously formed calcium alginate beads containing entrapped cells.

Emulsions of hydrophilic polyacrylate copolymers (Table 1) were prepared by autoclaving ground polymer in distilled water or HEPES buffered calcium chloride (HBC). The copolymers (HEMA/MMA) were synthesized in butanone to a low degree of polymerization (2). Calcium alginate beads were prepared by extrusion (3) and coated by incubation for 60 minutes in each emulsion.

The compression strength of beads was measured by transferring individual beads to the lower platens of an Instron compression cell. The critical compressive force (the ratio between compressive load at failure and bead diameter) measured after coating and rinsing relative to uncoated calcium alginate beads (Table 1), indicated the presence of an adherent coating. Neutral polyacrylate coated capsules yielded a single load maximum unlike the EUDRAGIT RL coated capsules which failed in a nonuniform manner (3).

Table 1: Compressive strength of polyacrylate coated alginate beads.

polymer*	water content (%)	emulsion concentration (%w/w)	critical compressive force (g/mm)
100 HEMA	39.9 ± 0.2	0.3	18 ± 3.2
75 HEMA			
25 MMA	24.4 ± 0.1	0.16	12.8 ± 1.8
HPMA	20.8 ± 0.4	0.21	17.7 ± 1.6
45 HEMA/45 MMA/10 MA	15.9 ± 0.6	4.0	24.1 ± 5.7
EUDRAGIT RL*	15	5.0	33 ± 3
CALCIUM AGLINATE	-	-	13.6 ± 2.2

* Rohm Pharma-Darmstadt FRG

* defined in terms of mole % comonomer in polymerization feed: HEMA-hydroxyethyl methacrylate, MMA-methyl methacrylate, MA-methacrylic acid, HPMA-hydroxy propyl methacrylate.

Relative to hydrophobic polymers, fewer human fibroblasts suspended in protein free Hank's balanced salt solution adhered to hydrophilic copolymer films cast from ethanol (e.g., $52 \pm 24/10^4 \mu m^2$ on 75 HEMA/25 MMA; $108 \pm 65/10^4 \mu m^2$ on teflon). Cell adhesion decreased with increasing hydrophilicity of the polymer surface. Similar

patterns of tissue cell adhesion to xerogel polymer films have been reported by others (4).

Human fibroblasts incubated for 24 hrs on films of water swollen solvent cast polymer films were examined to determine the cytotoxicity of hydrogel films. The majority of cells remained viable and continued to exclude trypan blue, however, cell viability decreased with decreasing equilibrium water contents of the swollen films.

Calcium alginate immobilized fibroblasts remained spherical and excluded trypan blue for up to seven days after immobilization. Since, cell attachment and spreading are expected to be required for prolonged *in vitro* viability and growth, collagen or other cell attachment substrates may need to be added to improve the viability of calcium alginate immobilized fibroblasts (6).

Although the stability and *in vivo* compatibility of the coated beads remains to be determined, the adsorption of non-crosslinked polymers from aqueous systems to animal tissue cells immobilized in calcium alginate beads is expected to lead to a new method for achieving physiological control of diabetes.

References:

1. Lim, F., Sun, A.M., Science, 210, 908-910 (1980).
2. Gilding, P.K., personal communication (1982).
3. Lamberti, F.V., Sefton, M.V., Biochimica Biophysica Acta, 759, 81-91 (1983).
4. Absalom, D.R., van Oss, C.J., Genco, R.J., et al., Cell Biophysics, 2, 113-126 (1980).
5. Jarvis, Jr., A., Grdina, T.A., Biotechniques, 1, 22-27 (1983).

The authors acknowledge the financial support of the Natural Sciences and Engineering Research Council.

S. I. Stupp, G. B. Portelli, H. L. Yau and J. S. Moore

Bioengineering Program and Polymer Group, College of Engineering,
University of Illinois at Urbana-Champaign, Urbana, IL 61801

INTRODUCTION

Over the past three years we have investigated possibilities for the improvement of PMMA bone cements through a molecular level approach. Results from initial efforts were previously reported, for example, higher toughness through the control of stereochemistry (1). The presence of stereoregular macromolecules can change properties in bone cement through crystallization, inter-chain complexation and higher levels of molecular motion at service temperature. Microscopic fracture of bone cement, thermally induced necrosis of bone, and residual monomer are all important factors in the clinical performance of this biomaterial. Thus, through stereostructure control, we seek improvement of properties such as lower polymerization exotherms, higher toughness, fatigue resistance, higher strength, and more complete monomer to polymer conversions in the system.

EXPERIMENTAL

Low temperature ionic polymerizations (-70 - -30)°C were used in our laboratories to synthesize stereoregular PMMA. Fine powders of these polymers are used to prepare bone cements. Temperature rise measurements during setting of mixtures were performed with digital thermometers. The characterization of residual monomer in set cements was carried out by 60Hz proton-NMR. Fatigue tests were carried out in MTS equipment at constant loads at a frequency of 1Hz. Characterization of cement crystallinity involved the use of wide angle X-ray diffraction.

RESULTS AND DISCUSSION

Figure 1 shows a typical temperature-vs.-time curve generated when samples of stereoregular powders (93% isotactic (I), 7% syndiotactic (S)) are mixed with monomer and allowed to set. This temperature-vs.-time curve is compared with that of a control formulation, produced with powders of conventional tacticity (10% I, 39% atactic, 51% S). There is an average difference of approximately 40°C between temperature maxima reached during the setting exotherm.

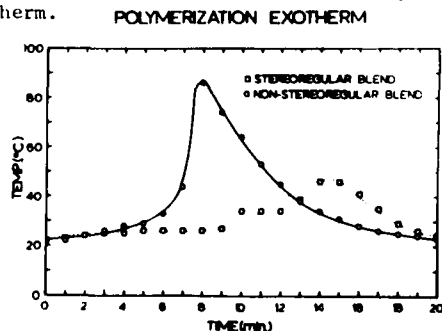


Fig. 1. Temperature as a function of time from the onset of powder/liquid mixing in a stereoregular cement and a control cement of conventional tacticity.

The significant difference in temperature could be partly associated with higher heat capacity in the cement mass due to the solvation of crystals and/or the low glass transition of isotactic

triads (45°C). The semi-crystalline nature of the cement powder was verified by X-ray diffraction scans. In addition to a lower probability of cell damage or necrosis, important consequences of the lower exotherm could include less thermal shrinkage of the cement away from bone surfaces and less infusion of unreacted monomer into surrounding tissues. Analysis of set samples reveals that control cements lose approximately 15.5% by weight of the original monomeric liquid into the environment prior to setting. This compares to 7% for the stereoregular formulation. We also found that an additional 4% by weight of the liquid undergoes polymerization in the stereoregular system. The higher degree of polymerization could be attributed to a catalytic effect by stereoregular molecules.

The bar graph in Fig. 2 shows fatigue data for three different stress amplitudes. The improved fatigue resistance of stereoregular cement might be associated with dispersed crystals, higher toughness of the cement matrix or differences in molecular weight. We believe gradual orientation of the polymer's backbone or that of micro-crystals along the direction of stress can occur in cyclic loading of the stereoregular cements. This would represent an interesting synthetic analog to the enhanced strength of bone along natural stress vectors. This type of phenomenon would not be possible in non-stereoregular PMMA since the polymer with conventional tacticity has a glass transition approximately 70°C above service temperature.

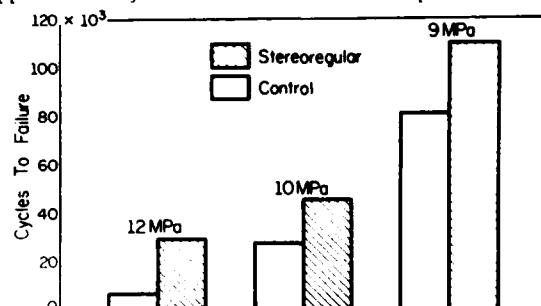


Fig. 2. Number of cycles to failure in specimens of the stereoregular and control cements exposed to stress amplitudes of 12MPa, 10MPa, and 9MPa at a frequency of 1Hz.

(1) G. B. Portelli, H. L. Yau, K. Paulson, A. Zimmerman and S. I. Stupp: Trans. 9th Annual Meeting Soc. for Biomaterials, Vol. VI, 34 (1982).

This work has been supported through a research contract from Zimmer, USA.

College of Engineering, UIUC, 105 S. Goodwin Ave., Urbana, IL 61801

TEMPERATURE AND FREQUENCY DEPENDENT ULTRASONIC ELASTIC PROPERTIES OF BOVINE BONE COMPARED WITH THAT OF PMMA.

R. Maharidge*, H.S. Yoon, J.L. Katz

Rensselaer Polytechnic Institute
Troy, New York 12181

INTRODUCTION

Polymethylmethacrylate (PMMA) is a common bio-compatible material that is often used with orthopaedic implants. Comparison of elastic (visco-elastic) properties of PMMA with that of bone is useful information to materials engineers, especially in light of the fact that stress gradients caused by a mismatch of mechanical or elastic properties between bone and the implant may produce loosening of the prosthesis. An ultrasonic technique is used to measure the elastic stiffnesses of bovine plexiform bone along three orthogonal axes. Temperature and frequency dependent data of the elastic stiffnesses are measured in order to compare the viscoelastic response of bone with that of PMMA and provide a more complete characterization of the rheological behavior of these materials.

METHOD

Bovine plexiform samples were dissected from the anterior quadrant of the mid-diaphysis of the femur of a 1½ year old cow. The samples were prepared in the shape of parallelepipeds using standard metallographic techniques as described by Yoon and Katz (1976). The samples were kept in constant contact with cool water while dissecting them in order to reduce fracturing due to excessive heating. The samples were maintained in saline solution until used in the measurements. Antibiotics were added to the saline solution to eliminate bacteria. The typical dimensions of the samples were 6 mm x 5 mm x 5 mm.

The PMMA samples were machined into circular discs of thickness 12mm (approx.) and a diameter of 25mm (approx.).

Temperature dependent data were collected by submerging the bone and PMMA samples in saline solution between two transducers. The temperature of the saline bath was controlled and monitored by a Haake temperature controller where the temperature was varied from 5 to 44°C. Ultrasonic velocities of the bone and PMMA samples were determined by

measuring the times of transit for longitudinal ultrasonic waves that were propagated through the samples. From the time of flight measurements, density and sample dimensions, the elastic coefficients c_{ij} are then calculated.

A series of aluminum alloy buffer plates were made to which PZT-5A transducers, each pair with a different resonant frequency, were bonded with salol. Thus, by interchanging wear plates using the odd harmonics of the transducers, a wide range of frequencies from 1 to 15 MHz could be used for measuring the dependence of wave velocity on frequency.

Sample densities were measured using a hydrostatic weighing method with purified water as the immersion liquid. Photographs of microstructure of the samples were taken to ensure that plexiform bone was present.

RESULTS AND DISCUSSION

Tables 1 and 2 show the temperature and frequency dependent behavior of the elastic stiffness coefficients of bovine plexiform bone; standard deviations are in (). It should be noted that bovine plexiform bone is anisotropic (9 constants are necessary to fully characterize its elastic properties), while PMMA is isotropic (only 2 constants are necessary). Bone shows a decrease in its stiffness by 5%-10% with increasing temperature ($\Delta T \approx 40^\circ\text{C}$) while PMMA shows a decrease in stiffness of 8.6% over the same temperature range. Bone shows an increase in stiffness of approximately 7%-11% over a frequency range of 1 to 15 MHz while PMMA shows an increase in stiffness of 2% over the same frequency interval.

REFERENCE

Yoon, H.S. and Katz, J.L., Ultrasonic Wave Propagation in Human Cortical Bone II. Measurements of Elastic Properties and Microhardness, *J. Biomech.* 9 459-464, 1976.

This work was supported in part by NIH-NIDR Grant 5T32 DE0 7054-07.

*Standard Oil, 440 Warrensville Rd., Cleveland, OH 44128.

Table 1. Temperature Dependence of Elastic Stiffnesses for Bovine Plexiform Bone and PMMA at 5 MHz

Elastic Stiffness (GN/m ²)		Temperature (°C)				
		5	15	25.5	36.0	44.5
Bone	c_{11}	26.1 (.3)	25.6 (.3)	25.1 (.4)	24.7 (.6)	23.3 (.6)
	c_{22}	30.7 (.6)	30.6 (.6)	29.5 (.6)	29.1 (.6)	28.5 (.6)
	c_{33}	40.2 (.6)	39.9 (.6)	39.4 (.7)	38.4 (.4)	38.2 (.4)
PMMA	c_{11}	9.17 (.02)	9.01 (.02)	8.79 (.02)	8.50 (.02)	[8.38]

Table 2. Frequency Dependence of Elastic Stiffnesses for Bovine Plexiform Bone and PMMA at 23°C

		Frequency (MHz)						
		1	3	4	5	7.3	10	5
Bone	c_{11}	22.3 (.8)	23.2 (.7)	22.6 (.6)	22.9 (.7)	22.6 (.6)	23.4 (.6)	23.9 (.8)
	c_{22}	24.9 (.8)	26.1 (.7)	25.7 (.7)	26.0 (.6)	25.7 (.6)	26.7 (.6)	27.2 (.5)
	c_{33}	33.4 (2.0)	35.8 (2.0)	35.0 (1.7)	35.3 (1.7)	35.3 (1.5)	36.5 (.9)	37.2 (1.3)
PMMA	c_{11}	8.60 (.1)	—	8.63 (.02)	8.71 (.01)	8.67 (.02)	8.72 (.02)	8.73 (.02)

ENHANCING THE MECHANICAL PROPERTIES OF ACRYLIC BONE CEMENT BY POROSITY REDUCTION.

D.W. Burke, E.I. Gates and W.H. Harris

Orthopaedic Research Laboratories, Massachusetts General Hospital and
Harvard Medical School, Boston, MA 02114.

Acrylic bone cement is the keystone of modern total joint arthroplasty. It allows rigid immediate fixation of the prosthesis within the bone cavity. Looseness of the prosthesis is the major long-term problem with joint replacement. There is mounting evidence that mechanical failure of acrylic cement may be a significant contributing factor. Finite element analysis and experimental *in vitro* strain gauges suggest that stresses experienced in the acrylic mantle surrounding total hip replacement approach or exceed the breaking strength of PMMA when considered in a fatigue mode. Clinical studies have demonstrated that the majority of "loose" femoral stems have fractured cement associated with their failure. To address this problem, multiple attempts at improving the strength of PMMA have been made in the past. These have in general consisted of "adding" a reinforced matrix to the cement bulk. Unfortunately, high viscosity, poor rheologic properties and increased cement modulus have made these preparations impractical.

Acrylic bone cement as routinely prepared in the O.R. is many times weaker than its commercial analog "plexiglass". The reason is multifactorial but the major cause is the very porous nature of bone cement due in most part to air entrapped during mixing.

In an attempt to improve strength of bone cement, multiple methods of porosity reduction were evaluated. The most practical method, centrifugation, was evaluated in detail in terms of tensile and fatigue strength of acrylic specimens, setting properties and serum monomer levels.

Methods and Materials: The use of a vacuum during mixing, pressure during mixing, curing, and centrifugation of the cement after mixing were investigated. Centrifugation was carried out at 4,000 rpm.

Control specimens and experimental specimens of surgical Simplex-P were injected into identical Teflon molds three minutes and thirty seconds after the initiation of mixing and the cement was allowed to cure in the molds at 37°C. The polymerized cylinders were then machined into standard waisted contours. All specimens were radiographed prior to testing.

Preliminary data indicated that evacuation during preparation increased the porosity dramatically.

Pressurization of the cement could reduce the porosity, but not as effectively as centrifugation. In order to achieve reduction in porosity equivalent to centrifugation, the pressures required were too high.

Consequently, remaining studies focused on centrifugation.

Control specimens were mixed at 45 seconds stirring at approximately 2 Hz. Centrifugation was carried out for two minutes. Additional specimens were made from cement which had been prepared using monomer which had been chilled. This prolonged the wetting time from 45 seconds to

75 seconds but substantially reduced the viscosity of the preparation.

Tensile tests were carried out on centrifuged and control specimens using an MTS servohydraulic materials testing machine. All specimens were tested at a strain rate of 0.02 per second using extensometer feedback for control. A wet environment at 37°C was maintained. Fully reversed tension-compression tests were carried out on the MTS machine at 1Hz using identical specimens.

To assess the effect of this type of preparation on blood pressure and serum monomer level, serum monomer levels and blood pressure recordings were made in seven dogs in which a canine total hip replacement was cemented in place with conventional surgical simplex on one hip and centrifuged surgical simplex on the other.

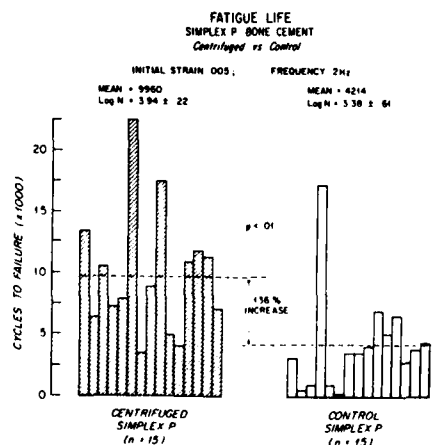
Results: Static testing of machined, waisted specimens show an average improvement of tensile strength of 25% and tensile strain of 50% in the centrifuged as compared to the control group.

Fatigue testing also demonstrated enhanced mechanical properties in the centrifuged group (Figure 1) at a strain level of .005. Centrifuged specimens on the average had more than twice the fatigue life than control specimens. All data was evaluated in terms of probability of survival using Weibull analysis techniques.

No detrimental changes in setting time or peak serum monomer levels were found in the centrifuged cement.

Conclusion: Early fracture of conventionally prepared PMMA bone cement is associated with internal voids. Centrifugation, by decreasing porosity markedly enhances ultimate tensile strain, ultimate tensile strength and fatigue life of acrylic cement. This technique of cement preparation may contribute to enhanced prosthesis servivability.

FIGURE 1



G. M. Brauer, D. R. Steinberger, and J. W. Stansbury

Polymer Science and Standards Division, National Bureau of Standards,
Room A143, Building 224, Washington, DC 20234

Methyl methacrylate monomer polymer slurries have been used as bone cements for over 15 years. Some ingredients of the cement such as the inhibitor and the accelerator are suspect carcinogens and may be replaced by equally efficient inhibitors and by faster acting amines. The BaSO_4 filler added to make the cement radiopaque reduces the mechanical properties of the material. Furthermore, an excessive amount of heat is liberated on polymerization of the large volume of monomer in the slurry. The resulting high temperatures may be injurious to the hard tissues. Any reduction in peak curing temperature, while retaining the otherwise satisfactory properties of bone cement, would be desirable.

The objective of this study was (1) to substitute the more biocompatible di-tert-butyl-p-cresol (BHT) for hydroquinone (HQ) as inhibitor, (2) to examine the reactivity of the biocompatible 4-N,N-dialkylaminophenethanol, dialkylaminophenylacetic acid and esters in the peroxide initiated polymerization of acrylic bone cements, (3) to reduce heat liberated on polymerization by substituting higher M.W. methacrylates for methyl methacrylate or by adding a multifunctional chain transfer agent and (4) to replace BaSO_4 with pentabromophenyl methacrylate as radiopacifier. This monomer should yield a mechanically strong copolymer with methyl methacrylate.

METHODS AND MATERIALS

The methyl methacrylate was distilled under vacuum and BHT was added. Other monomers were used as received. Throughout this study a commercial polymer powder was used. The accelerators except N,N-dimethyl-p-toluidine (DMPT) were synthesized as previously described.

Commercial powders and liquids prepared in this laboratory were mixed using the manufacturers' instructions. Dough time, compressive strength, water sorption, solubility and indentation and recovery of the cured cement were determined using the ASTM specification¹. Setting time (ST) and maximum exotherm were measured as previously described². Dental x-ray film was used to determine radiopacity of the cements.

RESULTS

Substitution of 60 ppm of food grade BHT for the 75 ppm HQ in the commercial liquid resulted in lower ST and an increase in the maximum temp. From the values of the dough and ST of the monomer-polymer slurries, the reactivity of various tertiary aromatic amines, in the benzoyl peroxide initiated polymerization, was obtained. The monomer contained 2.60% DMPT or equimolar conc. of 4-N,N-diethylaminophenylacetic acid (DEAPAA), its ethyl ester (DEAPAA-EE), 4-N,N-dimethylaminophenethanol (DMAPE) or 4-N,N-diethylaminophenethanol (DEAPE), and 60 ppm BHT. The reactivity of the various accelerators was:

DEAPAA < DEAPAA-EE < DEAPE < DMPT < DMAPE
Thus, the shortest ST were obtained with DMAPE containing compositions followed by those having DMPT as accelerator. Reducing the conc. of DMAPE by 50% and 75% resulted, resp. in increases of the

ST by 1 and 4.5 min. and decreases in the maximum temp. of 8°C and 14°C.

Peak temp. and polymerization exotherms were higher for formulations with shorter ST. With the addition of acid, the ST of formulations containing DEAPE is reduced much more than those using DMAPE. Methacrylic acid is slightly more effective than benzoic acid in lowering the ST. Partial replacement of methyl methacrylate monomer by the higher M. W. isobornyl methacrylate or dicyclopentenyl methacrylate yielded mixes that cured only after 25 min. Dicyclopentenylmethacrylate slowed down the polymerization and yielded polymers with slightly lower comp. strength. On addition of small conc. of acid, these formulations hardened in 9 to 10 min. and exhibited considerably lower exotherms and comp. strength similar to the commercial bone cement. Addition of from 1 to 3% pentaerythritol tetra(3-mercaptopropionate) (PETMP) to the monomer resulted in a significant reduction in the peak temp., and increased ST without decreasing the strength of the cement. Addition of 1 to 3% of a dimethacrylate crosslinking agent gave a slight decrease in the comp. strength, but higher percent recovery. Optimum physical properties were obtained with methyl methacrylate monomer containing 3% DMAPE and 1% to 2% PETMP. Mixes hardened in 8 to 9 min with a peak temp. of 62°C compared to a commercial cement with ST of 11 min and a maximum exotherm of 70°C. The comp. strengths for these experimental formulations and the commercial bone cement were 78 and 70 MPa, resp. With 10% pentabromophenyl methacrylate (PBPMA) in the liquid, the monomer-polymer mix had a dough time of 1.75 min., a ST of 9.9 min., and an exotherm of 61.7°C. The comp. strength was 78.3 MPa, i.e. about the same as that of the radiolucent material. Qualitative ranking of selected formulations yielded the following order of increasing radiopacity: Translucent cement (commercial) << cement with 5% PBPMA + 1% PETMP < 5% PBPMA << 10% PBPMA < radiopaque cement with 10% BaSO_4 (commercial).

CONCLUSIONS

Replacement of hydroquinone by the more biocompatible butylated hydroxytoluene as well as substitution by the more reactive 4-N,N-dimethylaminophenethanol for the commonly used N,N-dimethyl-p-toluidine is indicated. Excessive peak temperatures can be reduced by partial substitution of high M.W. methacrylates for methyl methacrylate or by addition of small amounts of pentaerythritol tetra(3-mercaptopropionate). Addition of 10% pentabromophenyl methacrylate to the monomer yield a radiopaque cement without reducing its strength. Composition with short curing times, low exotherms and excellent mechanical properties can be formulated.

REFERENCES

1. Standard Spec. for Acrylic Bone Cement, ASTM Desig. F451-81. Draft 4-7-83-6.
2. Haas, S. S.; Dickson, G. and Brauer, G. M., J. Biomed. Mat. Res. Sym. 6, 105-177, 1975 NBS, Room A143, Bldg. 224, Washington, DC 20234

CEMENT DEFORMATION FROM CYCLIC LOADING OF THE TOTAL HIP FEMORAL COMPONENT

E. Ebrahznadeh, I.C. Clarke, T. Mossessian,
H.A. McKellop, T.A. Gruen and A. Sarmiento

Orthopaedic Biomechanics Laboratory
Bone and Connective Tissue Research Program
Orthopaedic Hospital-USC

In this study, a model femur (Delrin) and cement-embedded strain gages were used to document time dependent change in strains in the cement layer supporting a total hip femoral component. Loosening of the cemented femoral component is a major complication of total hip replacements. The incidence of stem loosening within the acrylic has been documented at 2 to 40% in the 6 months to 6 yrs follow-up period, as indicated by a radiolucent line at the proximal-lateral stem-cement interface visible on radiographs. The appearance of these gaps has been attributed to distal subsidence or medial drift of the femoral component, accompanied by longitudinal cracks within the cement sheath. Our alternative hypothesis is that such stem-cement gaps could result from creep of the proximal-medial cement sheath, without necessary cracking of the cement. The objective of this study was to investigate internal stresses and strains in the cement surrounding a femoral stem, immediately after implantation and following cyclic loading.

A concentric Delrin cylinder was used in place of an actual femur to provide a consistent, reliable, reproducible experimental model. The diameters of the cylinder (20 mm I.D., 40 mm O.D.) were chosen to provide a structural stiffness (330 Nm^2) comparable to a human femur. A titanium alloy femoral stem was cemented in neutral position in the Delrin tube using PMMA. Strain gages were attached to hemi-cylinders of acrylic cement which were then cemented into the PMMA layer around the prosthesis through holes drilled in the lateral and medial walls of the Delrin cylinder. The gages could be precisely oriented to measure radial, circumferential or tangential cement strains. The accuracy of the strain gage modules (SGM's) was determined using PMMA beams placed in three point bending. The gage readings were found to be within 5 to 10% of the values predicted by beam theory.

Static loads were applied to the femoral head in 250 N increments (up to 1500N) and strain measurements were taken at each interval following a 5 minute relaxation period. A sinusoidal load was then applied to the femoral head, cycling at 5Hz from 100N to 500N for 2 million cycles and from 100N to 1000N for the next 2 million. These magnitudes were chosen because they produced a radial strain in the proximal-medial cement typical of published values for hip prostheses (2500 to 3000 microstrain). At intervals, the original static load was reapplied and strain again recorded at 250 N increments.

A 3-D finite element model of the Delrin bone-stem structure was run in order to compare the measured strains with those predicted by a linear elastic FEA model assuming perfect bonding at interfaces, typical of many models used in stress analysis of total hips.

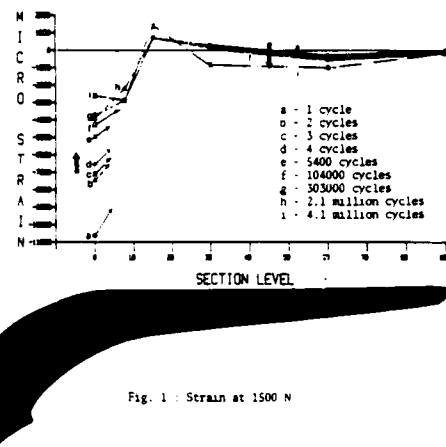
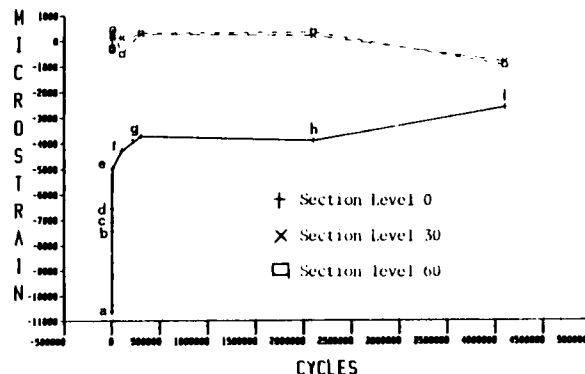


Fig. 1 : Strain at 1500 N

RESULTS: The radial strains within the medial cement were highest in the proximal aspect and rapidly decreased distally along the length of the stem (Fig. 1). The peak (medial) strains under static loading were found to have decreased after each interval of cyclic loading, from an initial 11000 to less than 3000 microstrain (Fig. 2). We suggest that this decrease (73%) represents creep of the proximal-medial cement sheath. Important features of this model were that the SGM's could be precisely oriented with respect to direction and level within the cement and added or replaced when required. In future experiments, strain rosettes will be used to provide principal strain data. The time dependent nature of the cement strain, presumably due to creep, suggests that most of the published data on cement stress and strain is accurate only for the initial few loading cycles when linear analysis applies. The model we have developed will be used to compare cement strains for various stem designs and materials as a function of time, a significant factor in the long-term durability of the stem fixation.



Address: Orthopaedic Biomechanics
Orthopaedic Hospital-USC
2400 S. Flower Street
Los Angeles, CA 90007

William R. Krause and Roger S. Mathis

Clemson University, Clemson, SC 29631

The majority of total joint replacement procedures use acrylic bone cement as the means of anchoring the prosthesis to the bone. In this configuration, loosening occurs as the result of failure at the cement-bone interface or within the cement itself. Because of its inherent weakness in tension, the bone cement often fails mechanically. Although finite element studies predict tensile stress levels well below the ultimate strength of the cement, patient activity can easily produce stresses of sufficient magnitude to cause fatigue failure in a relatively short period of time.

The objective of this project was to determine the response of the currently available acrylic bone cements to a uniaxial sinusoidal stress at 10 Hz. The cements tested were Surgical Simplex, Zimmer Regular (dough type) and Zimmer LVC (Low Viscosity).

Methodology: Tensile test specimens were fabricated in a polyethylene mold according to dimensions specified in ASTM D-638. The cement was mixed according to ASTM F-451 recommendations. At 3 minutes after initiation of mixing, the cement was placed in the mold using a 50 cc syringe. After hardening, the specimen was removed from the mold, trimmed and placed in a 37°C saline bath. The samples were conditioned at 37°C for 24 ± 2 hours and were kept wet with 37°C saline while tested. The specimens were mounted in a servohydraulic Instron machine and uniaxial tension was applied at a frequency of 10 Hz such that a constant stress amplitude resulted. Specimens were subjected to a range of stress levels from stresses which caused failure within a few cycles to levels which did not cause failure at 10⁶ cycles.

Analysis: The resulting stress (σ) vs. number of cycles (N) data was subjected to a non-linear least squares analysis to fit the equation:

$$\sigma = \delta + (\alpha - \delta) / [1 - \frac{N^{\mu}}{\mu}]$$

This equation describes the curve with an upper asymptote (α) and a lower asymptote (δ) where (μ) is the inflection point between the asymptotes and μ is a measure of the slope, Figure 1. The predicted values and standard errors for the three cements are given in Table 1.

In addition, Weibull fracture probability curves for fatigue failure as a function of stress and number of cycles were computed for the data set.

Discussion: The results of the stress vs. number of cycles for each cement showed very little scatter, particularly in comparison to previous reports, even though most specimens broke at some flaw in the specimen. Fractography showed crack initiation at a void in almost all cases. The regression analysis indicates that both an upper and lower stress asymptote exists for all three cements. Students' T-test of the three data sets indicate no significant difference between the upper asymptotes for Simplex and Zimmer Regular while Zimmer LVC was significantly ($p < 0.05$) lower. There was no significant difference between the lower asymptotes of Simplex and Zimmer Regular, Zimmer Regular

and Zimmer LVC. Significant differences in the inflection point and slopes were noted between the cements. Weibull analysis showed an increase ($r^2 = 0.98$) in fracture probability for increasing stress levels or the number of cycles.

Conclusions: This study presents the first fatigue comparison of the three leading acrylic bone cements. The results indicate that Zimmer Regular and Surgical Simplex are not significantly different for the described function. Zimmer LVC did show a significantly lower function than Surgical Simplex and only partial significant difference with Zimmer Regular. This data, along with the fracture probability at any given stress level, as determined from the Weibull analysis, is important in determining the design criteria of total joint replacement.

Figure 1. Fatigue Behavior of Acrylic Bone Cements

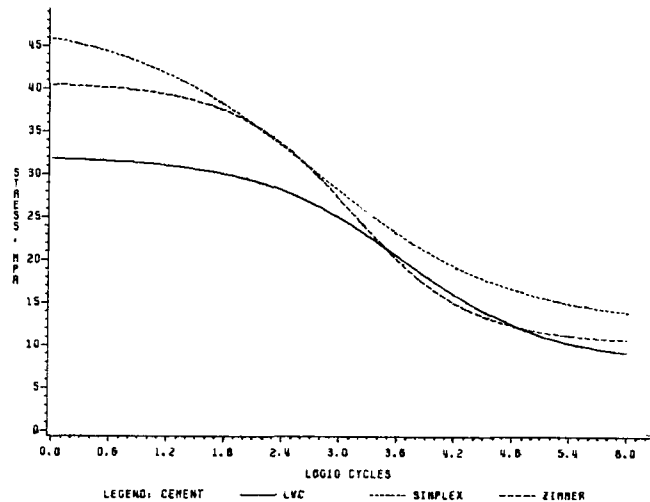


Table 1. Predicted means and standard error for the three bone cements.

	Simplex	Zimmer Regular	Zimmer LVC
δ (MPa)	12.64 2.75	10.45 2.59	8.17 3.09
α (MPa)	47.91 6.60	40.60 2.16	31.97 2.57
μ (cycles)	557.81 429.35	1,346.05 422.53	4,554.00 2,293.87
μ	0.43 0.14	0.70 0.15	0.58 0.17

This work was supported in part by Advanced Biosearch Associates, San Ramon, CA.

William R. Krause, Ph.D., Dept. of Interdisciplinary Studies, 301 Rhodes Engineering Research Bldg., Clemson University, Clemson, SC 29631.

PHYSICAL AND MATERIAL PROPERTIES OF HYDROXYAPATITE COATINGS SINTERED
ON TITANIUM

P. Ducheyne*, W. Van Raemdonck, P. De Meester

University of Pennsylvania, Department of Bioengineering
Philadelphia, Pennsylvania 19104

Calcium phosphate ceramics are appealing materials for clinical use by virtue of their osteophilic nature. Various types of these ceramics such as the tetra calcium phosphates, hydroxyapatite and tricalcium phosphates have been studied. Differences between these materials are related to their chemical stoichiometry and crystallographic structure. In addition, each type of material may come in various physical forms, depending upon size, shape and location of porosity, if any. Both the structural characteristics and the physical properties are largely determined by the method of making. Since these properties control the biological behavior, the manufacturing procedure is a variable of considerable interest in assessing the biomaterial use of calcium phosphates. Accordingly, it is the objective of the present paper to document the physical and material properties of hydroxyapatite (HAp) when applied as sintered coatings on titanium.

Materials and Methods

Two forms of hydroxyapatite were used; one was obtained from a commercial source (Merck, Darmstadt, Germany) (HAp1); one was laboratory made (HAp2). Ti flat sheets 1 mm thick were also commercially obtained (IMI, Birmingham, England). HAp coatings were applied by electrophoretic deposition and subsequent sintering. The parameters of both steps were varied within wide ranges. The characterization methods used were X-ray diffraction (RX), infrared absorption spectroscopy (IRS), scanning electron microscopy (SEM), electron microprobe analysis (EMP) and (AES) Auger electron spectroscopy. The results discussed below represent a selection of the more interesting observations of the study.

Results and Discussion

Sintering of the HAp2 for 6 hours at 850°C in an Ar atmosphere produced the formation of an oxyhydroxyapatite structure: $\text{Ca}_{10}(\text{PO}_4)_6(\text{OH})_{2-2x}$. Controlled experiments indicated that this formation was due to the combined effect of the electrophoretic deposition on one side and the long sintering time on the other side. A reduction of the sintering time to 1 hour, with a concurrent increase of the temperature to 900°C did no longer produce the significant oxyhydroxyapatite formation. The RX measurements indicated differences among the two starting powders, the powders calcined at 900°C and the coating sintered at 900°C, 1 hour. HAp1 was of lesser purity than HAp2. The diffraction pattern of the calcined condition and the sintered coatings were identical, except for the addition of Ti_5P_3 peaks in the sintered condition. SEM and EMP analysis of HAp2 specimens sintered at 900°C, 1 hour

showed a uniform coating with a transition zone between the hydroxyapatite and the Ti. This zone was enriched in P. This observation explains the Ti_5P_3 observed by RX. This finding is further substantiated by the AES data showing different compositional profiles at the surface of the HAp, in the HAp approaching the interface and at the interface. From the coating into the interface there is a steep decrease of the O and Ca content but no substantial change of the P content.

Conclusion

The materials analysis of the coatings applied by electrophoresis and subsequent sintering at 900°C, 1 hour shows that the surface of 15 μm thick coatings is a hydroxyapatite structure. The present method thus allows to obtain osteophilic coatings on titanium.

Acknowledgements

Financial support for part of the present work was obtained from the Foundation for Medical Research, Belgium and Zimmer Inc., Warsaw, USA. The HAp2 was kindly provided by Dr. J.C. Heughebaert and Professor Bonel of the University of Toulouse, France.

* Present address:

Dr. Paul Ducheyne
Associate Professor of Biomedical
Engineering
University of Pennsylvania
Philadelphia, PA 19104

BIOLOGICAL AND MECHANICAL PROPERTIES OF A NEW TYPE OF APATITE-CONTAINING GLASS-CERAMICS

T. KOKUBO, S. ITO, M. SHIGEMATSU, S. SAKKA, T. SHIBUYA*, T. KITSUGI**
T. NAKAMURA** AND T. YAMAMURO**

Institute for Chemical Research, Kyoto University
Uji, Japan

Alumina ceramics have good biocompatibility and high mechanical strength. However, they do not form chemical bond with bone. $\text{Na}_2\text{O}-\text{CaO}-\text{SiO}_2-\text{P}_2\text{O}_5$ glasses, apatite-containing glass-ceramics and hydroxyapatite ceramics can form chemical bond with bone. However, their mechanical strength hitherto reported are not sufficiently high. In this study, for the purpose of obtaining implant materials which can form tight chemical bond with bone and have high mechanical strength, new type of apatite-containing glass-ceramics were prepared, and their biological and mechanical properties were investigated in terms of their microstructure.

Three kinds of apatite-containing glass-ceramics which have different microstructures but the same composition of MgO 4.6, CaO 44.9, SiO_2 34.2, P_2O_5 16.3, CaF_2 0.5 in weight ratio, were prepared; the first one was prepared by heating a glass plate up to 870°C , and the second and the third ones were prepared by heating glass powder compacts up to 1050° and 1200°C , respectively.

The first one, A, contained only oxy- and fluoro-apatite ($\text{Ca}_{10}(\text{PO}_4)_6(\text{O},\text{F})_2$), the second one, A-W, both the apatite and β -wollastonite ($\text{CaO} \cdot \text{SiO}_2$), and the third one, A-W-CP, whitlockite ($8\text{-CaO} \cdot \text{P}_2\text{O}_5$) besides the apatite and the wollastonite. Their approximate contents are shown in Table 1.

Glass-ceramics	Apatite	Wollastonite	Whitlockite
A	35 wt%	0 wt%	0 wt%
A-W	35	40	0
A-W-CP	20	55	15

The porosities of the glass-ceramics A, A-W and A-W-CP were 0, 0.7 and 0.7 %, respectively.

A rectangular specimen $10 \times 15 \times 2$ mm of these glass-ceramics was implanted into a tibia of a rabbit. Ten weeks after the operation, a segment of tibia containing the glass-ceramics was excised. Its thin section was observed with a contact micro-radiograph. The newly formed bone was in direct contact with the glass-ceramics and no foreign body reaction was observed in the cases of all the examined glass-ceramics.

Another segment of tibia containing the glass-ceramics was cut so that the bones on either side of the glass-ceramics were joined only through the intervening glass-ceramics. The bones on either side of the glass-ceramics were pulled perpendicular to the interface in an opposite direction. The fracture occurred in the glass-ceramics in the case of A, whereas in the bones in the cases of A-W and A-W-CP. The load where the fracture occurred is shown in Table 2.

Glass-ceramics	Load (kg)
A	4.30 ± 2.35 (\pm standard deviation)
A-W	7.12 ± 1.37
A-W-CP	7.61 ± 2.05

These results show that all the examined glass-ceramics can form tight chemical bond with the bone and that their mechanical strength increases in the order of $A < A-W < A-W-CP$.

Bars $5 \times 5 \times 20$ mm of the glass-ceramics was abraded with #2000 alumina powders and subjected to

measurement of the bending strengths by three point bending method, at a crosshead speed of 0.5 mm/min in air and N_2 gas at room temperature. Plate $20 \times 50 \times 3$ mm of the glass-ceramics was subjected to measurement of fracture toughness, K_{IC} , by a double torsion method. Cubic specimen $4 \times 4 \times 4$ mm of the glass-ceramics was subjected to measurement of Young's modulus, E, by a resonance method. The results are shown in Table 3.

Glass-ceramics	σ_{air} (MPa)	σ_{N_2} (MPa)	K_{IC} ($\text{MPa} \cdot \text{m}^{1/2}$)	E (GPa)
A	88 ± 12	141 ± 26	1.2 ± 0.1	104
A-W	178 ± 20	193 ± 12	2.0 ± 0.1	117
A-W-CP	213 ± 17	243 ± 18	2.6 ± 0.1	124

\pm standard deviation

The bending strength of the glass-ceramics increased in the order of $A < A-W < A-W-CP$ and those of the glass-ceramics A-W and A-W-CP were almost equal to or larger than that of human bone.

Generally, bending strength σ_{N_2} of ceramics is given by the eq.(1) as a function σ_{N_2} of fracture toughness K_{IC} and flaw size c.

$$\sigma_{\text{N}_2} = K_{IC} / \sqrt{c} \cdot f \quad \text{--- (1)} \quad K_{IC} = \sqrt{2E\gamma} \quad \text{--- (2)}$$

where f is 1.26 for semi-circular surface flaw. Fracture toughness K_{IC} of ceramics is given by the eq.(2) as a function of Young's modulus, E, and fracture surface energy, γ . The c and the γ of the examined glass-ceramics, which calculated from the σ_{N_2} , K_{IC} and E given in Table 3 by using eqs. (1) and (2), are shown in Table 4. It can be seen from Tables 3 and 4 that the higher bending strengths of the glass-ceramics A-W and A-W-CP come from higher fracture toughness but not from smaller flaw size and that the higher fracture toughness of the glass-ceramics A-W and A-W-CP come from higher fracture surface energy rather than from higher Young's modulus.

Glass-ceramics	c (μm)	γ (J/m^2)
A	46	6.9
A-W	68	17.0
A-W-CP	72	27.0

It can be concluded from the results described above that the precipitation of the wollastonite and whitlockite crystals does not give an adverse effect on the ability of apatite-containing glass-ceramics to form chemical bond with bone but considerably increases the mechanical strength of the glass-ceramics by increasing fracture surface energy.

ACKNOWLEDGEMENT

This research was supported by Grant-in-Aid for Special Research, Studies on Design of Multi-Phase Biomedical Materials (No. 58211009), of Ministry of Education, Science and Culture, Japan.

Uji 611 Japan.

* Nippon Electric Glass Company, Otsu 520 Japan.

** Faculty of Medicine, Kyoto University, Kyoto 606 Japan.

Folger, R.L., Kucheria, C.S., Wells, R.E., Gardiner, G.F.

Howmedica Corporate R&D, Groton, Connecticut

In the never ending search for the appropriate implant interface for prosthetic devices, the prospects of Bioglass as an orthopaedic implant interface material have waxed and waned. Our studies indicate that, when Bioglass is used as a coating on other implant materials, the elemental compositions of the base material may effect the reactivity of the Bioglass. We observed a decrease in bone bonding reactivity with increased concentrations of Al_2O_3 in bulk Bioglass and with increased Al_2O_3 in the base material when Bioglass is used as a coating.

Materials tested for their ability to form a mineral matrix continuum between bone and implant in this study were bulk Bioglass rods containing 0.3% (level in raw material) or 1.8% (contamination from a ball mill) Al_2O_3 ; 96% and 99% Al_2O_3 rods coated with Bioglass; and Vitallium® rods. The Vitallium® rods were included as a negative control. The bulk Bioglass rods and the Bioglass coated alumina rods were 3.0-3.1mm in diameter by 7.2mm long. The Vitallium® rods were 2.5mm in diameter by 7.2mm long.

The test system was the tibial crest of White New Zealand rabbits (3.5 kg+). After surgical exposure of the tibial crest, a Dremel® tool with a spade shape excavating bur (3.1 or 2.7mm) was used to drill a hole through the medial to lateral aspect of the tibial crest. The hole was located approximately 4.0mm below the ridge of the crest and 4.0mm proximal to the distal aspect of the crest. The cylindrical implants were placed through the drill hole and fascia and muscles were closed securing the implant in position. At intervals of 15 and 30 days, the tibias were harvested and placed in 0.9% saline for immediate Instron® testing. Some of the tibias were placed in 70% alcohol for subsequent SEM and EDAX analysis.

A measurement of the force required to push out the implants - assessment of bond strength - was performed on an Instron®. The removed tibia was placed in a jig with the implant located vertically between two supports. A cylindrical testing head 1.9mm in diameter was centered over the medial aspect of the implant and a crosshead speed of 0.1 cm/min. was used to determine the required push out force. Loads required to push out the 30 day implants are listed in Table I.

Scanning electron microscopy performed on the bulk Bioglass and Bioglass coated alumina (30 day implants) are illustrated using EDAX analysis for Ca, P and Si in Figures 1 and 2 respectively.

It should be noted from Table I that the mean push-out loads for bulk Bioglass are significantly higher than for the Bioglass coated alumina. And that with increasing amounts of alumina the loads required decrease in both the bulk Bioglass and Bioglass coated alumina systems. The EDAX analysis of the two systems indicates there is also a difference in the elemental profile across the interface. The alumina must in some manner be affecting the reactivity of the Bioglass, thus reducing its apparent bond strength. From further EDAX analysis of the bone-interface-bioglass-Alumina, it was observed that the Al_2O_3 diffuses into the Bioglass layer during firing. This probably accounts for the differences observed between the bulk Bioglass and the Bioglass coated alumina, and the two different alumina grades (96% and 99%).

Table I. Load kq \pm 95% C.I.

Bulk Bioglass 0.3% Al_2O_3	30.33 \pm 4.97
Bulk Bioglass 1.8% Al_2O_3	21.63 \pm 4.36
Bioglass Coated 96% Al_2O_3	10.09 \pm 3.30
Bioglass Coated 99% Al_2O_3	5.79 \pm 3.31
Vitallium Standards	3.13 \pm 2.31
Punch a 2mm diameter hole in the tibial crest	13.9

Figure 1. Bulk Bioglass with 0.3% Al_2O_3

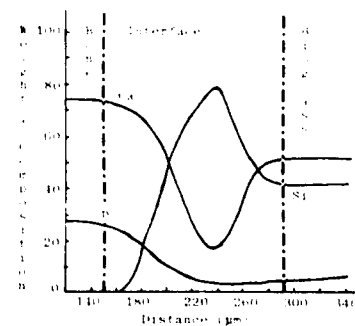
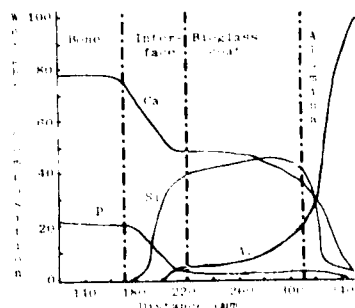


Figure 2. Bioglass Coated 99% Alumina



Howmedica Corporate R&D, Groton, CT 06340

USE OF ALUMINO-CALCIUM-PHOSPHOROUS OXIDE (ALCAP) CERAMICS FOR RECONSTRUCTION OF BONE

D.R. Mattie*, C.J. Ritter**, and P.K. Bajpai**

Pathology Branch, Toxic Hazards Division, AFAMRL,
Wright-Patterson AFB, Ohio 45433

A number of materials, including ceramics, have been implanted into bone in search of ideal bone substitutes. Ceramics composed of aluminum, calcium and phosphorous oxides (ALCAP) were fabricated for correcting defects in bone (1). The effectiveness of ALCAP ceramics as bone substitutes was evaluated by conducting implant analysis (Figure 1), radiography, light microscopy and scanning electron microscopy of ALCAP ceramics implanted for thirty days in rat femurs.

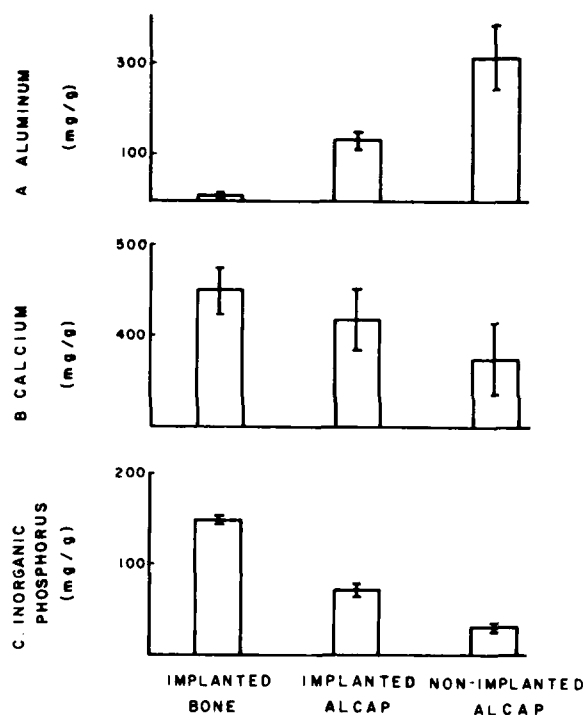


Figure 1. Aluminum, calcium and inorganic phosphorous in non-implanted ALCAP ceramics, bone-autografts (control) and ALCAP ceramics implanted in femurs of rats for 30 days (A. Aluminum B. Calcium C. Inorganic Phosphorous).

ALCAP ceramic plugs (1 X 2 X 3mm) fabricated from 45-60 micrometer calcined particles were implanted bilaterally in femurs of ten male and ten female rats. An equal number of rats were implanted with bone-autografts and served as sham-operated controls. Implantation of ALCAP ceramics had no deleterious effects on body weights, organ/body weight ratios, muscle, bone, blood and kidney functions (2). Alkaline phosphatase activity of excised implant sites indicated greater bone formation in ALCAP ceramic implants than in bone-autografts. A significant amount of aluminum was resorbed from ALCAP ceramic implants without any adverse effect on the host (Figure 1A). Calcium levels in bone-autografts, ceramic implants and non-implanted ceramics were not significantly different (Figure 1B). Inorganic phosphorous was highest in bone-autografts and lowest in non-implanted ALCAP ceramics (Figure 1C). Radiographs, implant histology and scanning electron microscopy demonstrated osseous union of bone and implants as well as ingrowth of new bone into ALCAP ceramic implants. Presence of calcium and inorganic phosphorous at higher than expected levels in ALCAP ceramic implants as well as morphologic observations indicate that new bone grows into ALCAP ceramics implanted in rat femurs.

CONCLUSIONS

Short term implantation in rat femurs indicates that ALCAP ceramics are resorbable and initiate new bone ingrowth. The results of this investigation suggest that ALCAP ceramics are suitable for correcting defects in bone.

REFERENCES

1. P.K. Bajpai, S.N. Khot, G.A. Graves, Jr., and D.E. McCollum, IRCS Med. Sci., 9, 696-697 (1981).
2. D.R. Mattie, Ph.D. dissertation, University of Dayton, 1983.

*Pathology Branch, AFAMRL, Wright-Patterson AFB, OH 45433

**University of Dayton, Dayton, OH 45469

FATE OF RESORBABLE ALUMINO-CALCIUM-PHOSPHOROUS OXIDE (ALCAP) CERAMIC IMPLANTS IN RATS

F.B. McFall* and P.K. Bajpai*

University of Dayton, Dayton, OH 45469

INTRODUCTION

Resorbable ALCAP ceramics have been used successfully for posterior fusion of spine, reconstruction of bone and drug delivery (1, 2). Accumulation of resorbable components of biodegradable ceramics could induce pathogenesis within the host. This investigation was conducted to study the dissolution and accumulation profile of aluminum (Al) calcium (Ca) and inorganic phosphorous (P) resorbed from subcutaneous implants of alumino-calcium-phosphorous oxide (ALCAP) ceramics in rats.

MATERIALS AND METHODS

Resorbable ALCAP ceramic discs were fabricated from 45-60 micrometer particles (3). Ceramic discs, weighing 0.53 gm/each, were implanted subcutaneously on both sides of the spine dorsally in 36 rats. An equal number of rats were sham-operated and served as controls. Urine samples were collected for 24 hours prior to surgery and sacrifice. Six sham-operated and ALCAP implanted rats were sacrificed at one, four, eight and twelve week intervals. Blood was collected from each rat prior to surgery and sacrifice. From each rat after sacrifice bone (femur), brain, heart, implanted ceramic, kidneys, liver, muscle and spleen were harvested and acid-digested in concentrated nitric acid. All acid extracts were analyzed for Al and Ca by atomic absorption spectroscopy and P by a colorimetric procedure. The data collected was analyzed at the $p < 0.05$ level by means of analysis of variance.

RESULTS

Largest amounts of Al, Ca and P were released from ALCAP ceramic implants after one week of implantation. The amounts of Al and Ca resorbed from ALCAP ceramics after one, eight and twelve weeks of implantation did not differ significantly from the amounts of Al and Ca resorbed after one week of implantation. The total amounts of Al, Ca and P resorbed from ALCAP ceramics after 12 weeks of implantation were 93 ± 7 ; 57 ± 7 and 20 ± 3 milligrams respectively.

Aluminum, Ca and P content of bone, brain (Figure 1), heart, liver, and spleen obtained from control and ALCAP implanted rats did not differ significantly. There was no significant difference between the amounts of Ca and P observed in plasma and muscle (surrounding the implant) obtained from control and ALCAP implanted rats. Inorganic phosphorous content of kidneys obtained from control and ALCAP implanted rats also did not differ significantly.

In comparison to the kidneys of control rats the kidneys of ALCAP implanted rats retained significantly higher amounts of Al and Ca. Amounts of Al in the muscle surrounding the ALCAP implant and plasma was significantly higher in ALCAP implanted rats. All ALCAP implanted rats excreted significantly higher amounts of Al and Ca in their urine.

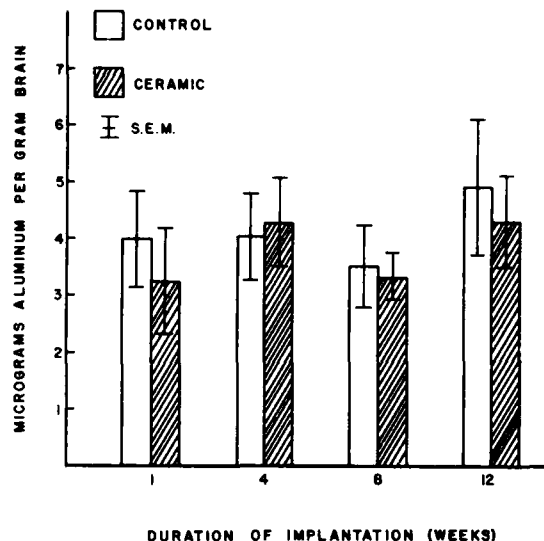


Figure 1. Amounts of aluminum in brain of control rats and rats implanted with ALCAP ceramics.

CONCLUSION

Results of this investigation show that Al, Ca and P resorbed from ALCAP ceramics do not accumulate in toxic amounts in brain, bone, heart, liver and spleen and that the main route of removal from the implant is via the surrounding tissue, plasma, kidney and through excretion in the urine.

REFERENCES

1. D.R. Mattie, Ph.D. dissertation, University of Dayton, Dayton, Ohio, 1983.
2. A. Al-Arabi and P.K. Bajpai, Clin. Res., 30, 294A (1982).
3. P.K. Bajpai, S.N. Khot, G.A. Graves, Jr., and D.E. McCollum, IRCS Med. Sci., 9, 696-697 (1981)

*Biology Department, University of Dayton, Dayton, Ohio 45469

Histological Examination of Beta-Tricalcium Phosphate Ceramic Implanted in the Canine Calvaria

D. Scott Metsger* and James W. Ferraro**

*Miter, Inc., Columbus, OH

**Straumann Research Laboratory, School of Veterinary Medicine, Ohio State University, Columbus, OH

Since 1971 beta-tricalcium phosphate ceramic (β - Ca_3PO_4)₂ has been studied as a resorbable bone grafting substitute¹⁻³. This porous material is vascularized and invaded by bone forming tissue as the ceramic resorbs. Consequently, remodeling bone develops which repairs the original defect. Much of the early animal work involved dental applications. These successful studies, in part, have led to the indication of TPC for repairing some periodontal diseases in humans⁴. Other bone modeling applications have been proposed: Tanski has implanted TPC onlay grafts on the noses of rabbits⁵, Mors and Kaminski have replaced cleft palates in beagle dogs⁶, and Ferraro has repaired orbital rim defects in canines⁷. The results of replacing femoral segments in large dogs have encouraged Goldstrohm, et al. to use a block of porous TPC to lengthen a young girl's femur⁸. This paper describes the use of TPC to regenerate flat bone in the calvaria.

Four bur holes approximately 11 mm in diameter were surgically created in each calvaria of 15 dogs. The average thickness \pm the standard error of the mean of the calvaria in the region of implantation was 3.72 \pm 0.08 mm. Thirty-five defects were filled with TPC, 15 defects were left untreated, and 10 defects were repaired with circular discs of autogenous bone removed from the iliac crest. All grafts were found firmly fixed in 10 dogs sacrificed from 9 to 36 months post-op (median 18.4 months). The remaining five animals will be sacrificed later. No reparative bone formation was noted in untreated control defects; the gaps were filled with connective tissue. Histological evidence to be considered demonstrates that the ceramic implants were vascularized and resorbed radially, being replaced with bone in a slower, but comparable, fashion as the autogenous grafts. In cases where autogenous grafts did not ossify or completely fill with bone there was also limited bony ingrowth into the ceramic plugs. In osteogenically active animals the endosteal surface was repaired first beginning at the bone/implant interface. The amount of bone ingrowth increased with time. No adverse reactions due to TPC were noted.

5. EV Tanski, Tricalcium Phosphate Ceramic As a Bone Onlay, British Association of Plastic Surgeons, Summer Meeting, July 1978, Edinburgh, Scotland.
6. WA Mors and EJ Kaminski, Osteogenic Replacement of Tricalcium Phosphate Ceramic Implants in the Dog Palate, Arch Oral Biol 1975; 20, 365-367.
7. JW Ferraro, Experimental Evaluation of Ceramic Calcium Phosphate as a Substitute for Bone Grafts, Plas Reconstr Surg 1979; 63, 634-640.
8. GL Goldstrohm, et al., Replacement of Canine Segmental Bone Defects with Tricalcium Phosphate Ceramic Implants, 29th Annual Orthopedic Research Society Meeting, Anaheim CA, March 1983.

References

1. SN Bhaskar, et al., Tissue Reaction to Intrabony Ceramic Implants, Oral Surg 1971; 31, 282-289.
2. SN Bhaskar, et al., Biodegradable Ceramic Implants In Bone. Electron and Light Microscopic Analysis, Oral Surg 1971; 32, 336-346.
3. L. Getter, et al., Three Biodegradable Ceramic Phosphate Slurry Implants In Bone, J Oral Surg 1972; 30, 263-268.
4. DS Metsger, et al., Tricalcium Phosphate Ceramic--A Resorbable Bone Implant: Review and Current Status, J Am Dent Assn 1982; 105, 1035-1038.

THE INTERACTION OF BLOOD COMPONENTS WITH PRIMARY REFERENCE MATERIALS IN
A BABOON EX VIVO SHUNT MODEL

E.M. Keough, R. Connolly, W.C. Mackey, K. Ramberg-Laskaris, T. Foxall,
J. McCullough, T. O'Donnell, Jr., and A.D. Callow

Tufts University School of Medicine and New England Medical Center
Boston, Massachusetts

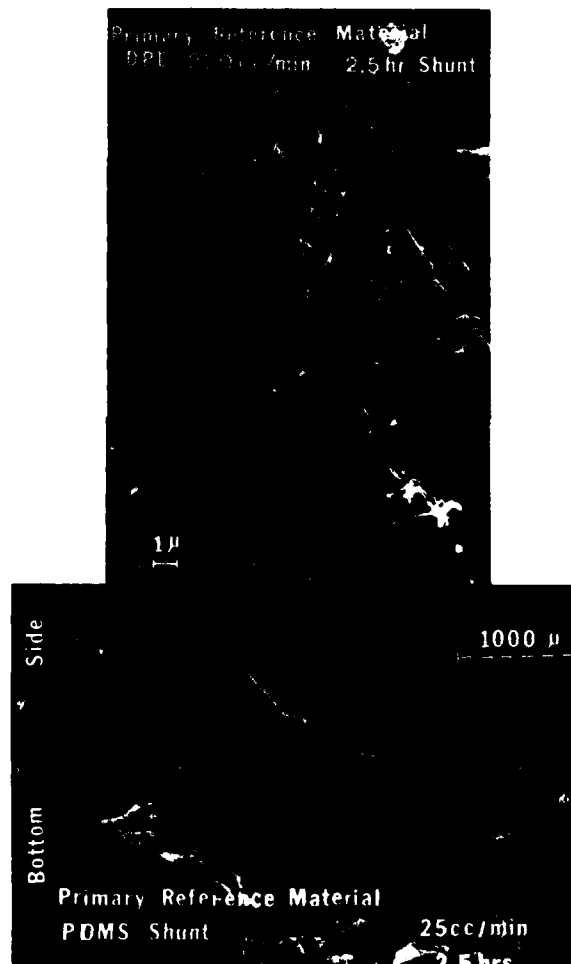
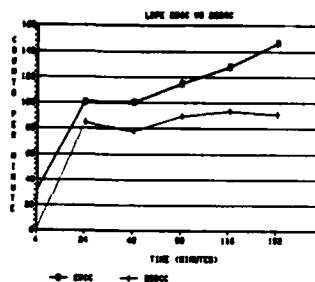
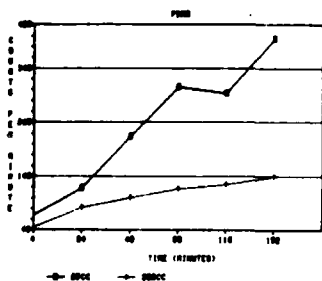
In order to provide standard biomaterials for the evaluation of blood-biomaterial interactions, the NIH has designated low density polyethylene (LDPE) and polydimethylsiloxane (PDMS) as primary reference materials (PRM). In this study the interaction of platelets and other blood components with LDPE and PDMS was evaluated in a baboon ex vivo arterio-venous shunt circuit.

The shunt circuit consisted of test material, a preclotted knitted Dacron graft as a control for animal variability and variations in platelet isolation and labeling, an in-line flowmeter and an adjustable downstream resistance. Platelets were isolated from 450 ml of blood withdrawn from mature male baboons, and labeled with ¹¹¹Indium oxine. Platelet accumulation over a 2.5 hour period at high (200 cc/min) and low (25 cc/min) flow was monitored using gamma camera scans and analyzed. At the end of the 2.5 hours, PRM were processed for scanning electron microscopy (SEM).

Both LDPE and PDMS showed little platelet accumulation when compared to Dacron. PDMS accumulated more platelets at low than at high flow (graph). A saw-tooth pattern of accumulation was seen with PDMS representing periodic loss of platelets. Less flow effect was seen with LDPE (graph).

Under SEM, red and white blood cells could be seen attached to the surface of PRM. White blood cells attached and flattened out much in the manner of cultured cells. Platelets appeared to be confined to patchy areas covered by a fibrin-like meshwork on both PDMS and LDPE.

The low platelet reactivity of LDPE and PDMS suggests their potential use as a coating for the luminal surface of conventional vascular graft materials. The attachment of red and white blood cells to their surface suggests their use as substrates for endothelial cell seeding experiments.



Supported by NIH RHL 24447-04 and RHL 28855-2,
and New England Medical Center Ziskind, Posner
and General Research Support Funds
Ellen M. Keough, Ph.D.
New England Medical Center
Box 37
171 Harrison Avenue
Boston, MA 02111

The Relation of Mechanical Properties of the Hetero-arteriografts for Hemodialysis to their Wall Damage Due to Puncturing with Clinical Needle

A. Toshimitsu Yokobori, Jr., M. Ishizaki,* T. Yokobori,
H. Takahashi,* H. Monma* and H. Sekino*

Department of Mechanical Engineering II, Tohoku University,
Sendai, Japan

1. Objectives: The arteriograf is used as a substitute conduit for blood vessel for hemodialysis where the blood vessel can be no more used due to occlusion, etc. The aim of the study is to characterize the wall damage of arteriograf due to puncturing with clinical needle, and to get the design principle of high performance graft in this respect.

2. Methodologies: The specimen was cut from arteriograf under the same condition of clinical use into the form of rectangular plate of about 10 mm width and 15 mm length and immediately after that, the opposed two ends of the specimen being fixed, the puncturing was made. Materials used are bovine¹⁾ (Johnson & Johnson Company) and swine²⁾³⁾ arteriografs. The swine subjected to enzymatic digestion with chymotrypsin, and the bovine with ficin and tanned with dialdehyde Starch. The swine graft in which enzymatic digestion time is 3 hr is designated as swine²⁾ R, and the one 5 hr x 2 as swine³⁾ S, respectively. 16 G Medicut canula (Argyle Co.) was used as puncturing needle.

The puncturing direction is in accord with actual clinical use, that is, the short axis of the ellipse, which lies on the same plane with edge of needle tip is in the circumferential direction of the graft as shown in Fig. 1.

3. Results: Figs. 2(a) and (b) show typical examples of the observations by SEM of damage pattern left on the inner wall surface for swine graft R and S after the needle tip punctured through the blood vessel wall and then it was taken off, respectively. Fig. 2(c) shows that for bovine graft. For the swine graft R, the remarkable crack type damaged zone extended in the circumferential direction of the blood vessel about 3.3 mm. On the other hand, for the swine graft S, the damaged zone is rather small and healed. For the bovine the damaged zone extended only about 0.8 mm and almost healed, that is, damaged region is very small. In the case of damaged region being large in the graft wall, there may be a possibility of some leakage in the blood flow through near-by damaged region during hemodialysis, and also of leading to the occlusion of the blood vessel canal by the decrease of the blood flow velocity due to the registance of the considerably uneven surface of the damaged zone. Therefore, it may be desirable to minimize damaged region due to puncturing. Fig. 3 shows the stress-strain relation in the circumferential direction of the swines R and S. Fig. 4 is that for bovine graft. It can be seen from Figs. 3 and 4 that the compliance of the bovine graft is much larger than those of swine grafts. The compliance of the swine graft S is larger than that of swine graft R. From Figs. 2~4 it can be seen that the damage region due to puncturing in the circumferential direction becomes much smaller as compliance in the circumferential direction of the graft becomes larger.

4. Conclusions: In design of high performance graft for hemodialysis, it is useful to minimize the damaged region due to puncturing by medicut

canula. For this purpose, it may be desirable to make the compliance high in the circumferential direction of the graft.

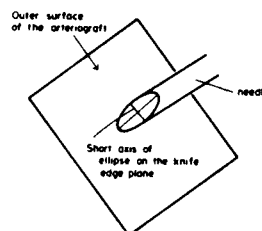


Fig. 1. Schematic illustration of the relative position used of the knife edge to the direction of the arteriograf.

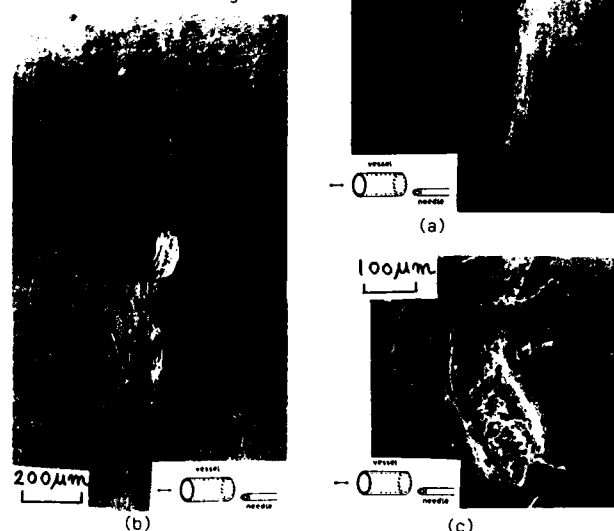


Fig. 2. The damage pattern observed by SEM on the inner wall of the arteriograf left after puncturing by the needle with the sheath in the circumferential direction. (a) swine arteriograf R (b) swine arteriograf S (c) bovine arteriograf.

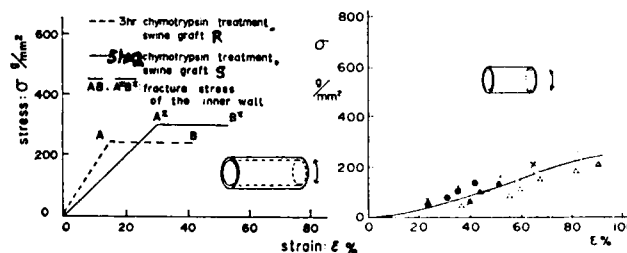


Fig. 3. Stress-strain relation of swine arteriograf (in the circumferential direction)

References: (1) J.H. Merickel, et al., Arch. Surg. 109, (1974) 245, (2) I. Amano and K. Miyata, Zinko Zoki, 4 (1976) 222, (3) I. Amano et al., Zinko Zoki, 7 (1978) 24 *Kidney Center, Sendai Shyakai Hoken Hospital, Tsutsumi 3-chome, Sendai, Japan.

THE EFFECT OF HOLLOW FIBER DIALYZERS ON BLOOD PLATELETS AND PLASMA PROTEINS
DURING EXTRACORPORAL CIRCULATION

H. PELZER, R. MICHALIK*, H. LANGE*, N. HEIMBURGER

Behringwerke AG
D-3550 Marburg, Postfach 1140, West Germany

The passage of blood through dialysis membranes results in interactions between blood components and the foreign surface. Thereby blood platelets are activated and release platelet specific factors. In addition, plasma proteins and blood cells deposit on the surface. The purpose of the present investigation was to study the blood-material interactions during hemodialysis. Therefore the following methods were applied using plasma samples and dialysis tubes: 1. A recently developed highly sensitive enzyme immunoassay to determine the platelet factor 4 (PF 4) concentrations. 2. A modified chromogenic substrate method for the determination of platelet factor 3 (PF 3). 3. Enzyme immunoassays to determine the deposition of fibrinogen, fibronectin, factor VIIIIR:Ag and platelets on blood tubes.

The present study was performed with the consent of fourteen regular dialysis patients. They were treated with the hollow fiber systems cellulose acetate - CORDIS, cuprophane - SMAD, cuprophane - GAMBRO and cuprammonium - ASAHI and received no medication known to influence platelet function. During dialysis all patients were heparinized with an initial dose of 3000 units and then 1000-2000 units per hour of dialysis. Blood samples were collected before and during dialysis, the PVC blood tubes were taken after dialysis and fixed with formaldehyde.

Before dialysis all patients had normal plasma concentrations of platelet factor 4 (mean level: 5 ± 2 ng/ml). A marked increase of PF 4 to 200-300 ng/ml was observed five minutes after the start of dialysis. Within 60 minutes the concentration decreased to 50 ng/ml and remained at this level throughout the procedure. The effect of the artificial kidney on platelets was studied by collecting blood samples from the arterial and venous side of the dialyzer five minutes after initiation of dialysis. Released amounts of PF 4 from 150-250 ng/ml were observed. Plasma PF 4 concentrations in the venous outlet were markedly above those of the arterial side. The determination of platelet factor 3 showed a good correlation with PF 4 release. All patients with high PF 4 concentrations showed significantly increased plasma levels of PF 3.

The platelet activation in four groups of patients was studied; each group was treated with one hollow fiber system (see above). Determination of PF 4 release before and after artificial kidney five minutes after start of dialysis showed PF 4 concentrations between 150 and 250 ng/ml; release of PF 3 occurred likewise.

To determine the intraluminal deposits of plasma proteins different sections of blood tubes were taken. Small amounts of fibrinogen and fibronectin were detectable on the surface of the tube before the blood pump and within it. However, the deposition of fibrinogen and

fibronectin increased significantly within the sections following the blood pump and the artificial kidney. This trend was not observed for factor VIIIIR:Ag and platelets.

Several studies have been undertaken to investigate the interactions of human blood and foreign surface during hemodialysis. The present study demonstrates that the interaction of blood with the artificial kidney results in marked deposition of fibrinogen and fibronectin on the blood tubes. Other blood components, e. g. factor VIIIIR:Ag and platelets were also adsorbed; however, they deposited in nearly constant amounts within all tube sections. The most striking feature observed in this study was the platelet activation which occurred with all patients during hemodialysis. Remarkably, the different hollow fiber systems induced PF 3 and PF 4 release in all patients to nearly the same extent.

Acknowledgement:

This work was sponsored by the German Government (BMFT, MSO 120).

*Zentrum für Innere Medizin
Universitätsklinik Marburg
D-3550 Marburg
West Germany

Behringwerke AG
Postfach 1140
D-3550 Marburg
West Germany

Experimental study of heparinless temporary shunt using TOYOBO-TM3-coated tube

Chisato Nojiri, M.D., Shigeyuki Aomi, M.D., Masahide Yamagishi, M.D.,
Hitoshi Koyanagi, M.D., Kazunori Kataoka, PHD., Teruo Okano, PHD.

Department of Surgery, Heart Institute of Japan, Tokyo Women's Medical
College, Tokyo, Japan.

The temporary shunt in operation of the aneurysm of the descending thoracic aorta has been a very useful and easy method to protect the function of the spinal cord, kidneys, and other vital organs. To avoid the use of anticoagulants associated with fatal bleeding, it is preferable without systemic heparinization. Currently the heparin-coated tube has been employed for this purpose, but its antithrombogenicity was controversial and time-limited, and it has not been so available for clinical use in our country. Then we employed newly designed shunt tube coated with TOYOBO-TM3 (Segmented Polyether Urethane Urea). The mechanism of nonthrombogenicity of TM3 is different from that of heparin-coated materials, i.e., molecular architecture of the surface has nonthrombogenicity by inhibition of platelet aggregations and release reactions. It is the purpose of this report to evaluate the nonthrombogenicity of TM3-coated tube as well as the safety margin of the temporary shunt in experiments in dogs. Smoothly tapered polyvinylchloride (PVC) tube was employed, that was originally designed to prevent the turbulent flow at the orifice of the tube, and obtain a shear rate over 200 sec⁻¹ in the middle of the tube and minimal pressure loss across the shunt. The experimental tube was a PVC tube 70 cm length with a 3.1 mm opening on both ends, widening to a 4.8 mm inner diameter in the midportion, and was coated with TM3 as thin as 15 micrometers. Ten mongrel dogs weighing from 13 to 21 kg (averaging 16.7 kg) were anesthetized with intravenous pentobarbital sodium and mechanically ventilated with a Bird MK8 respirator. Ringer's lactate were given intravenously. Through a left lateral thoracotomy the bypass of the descending thoracic aorta was accomplished by way of aortic arch and left femoral artery cannulations. Initially femoral arterial cannulation was made and flushed saline from another end of the tube into femoral artery to wash out blood from the tube, then clamped femoral artery. Immediately after aortic cannulation was accomplished, declamping femoral artery, the bypass was started. In group A (six dogs), descending aorta was cross-clamped. In group B (four dogs), descending aorta was partially clamped to obtain various shear rates, so as to provide each shunt flow of 50, 70, 100, 200 ml/min. All dogs did not receive systemic heparinization and underwent a five hour period of aorto-femoral bypass. During a bypass, shunt flow, pressures of ascending aorta and abdominal aorta, and urine output were monitored. Blood samples were obtained after thoracotomy was made (control), and after 30, 60, 90, 120, 180, 240, 300 minutes of bypass, drawn for platelet counts and coagulation studies, measuring plasma fibrinogen concentration, FDP, and activated coagulation time using Hemochron. Platelet counts and fibrinogen concentration were corrected for hemodilution using hematocrit values. After five hours of bypass, each dog was sacrificed and a tube was removed, rinsed with saline, and evaluated by gross inspection and scanning electron microscopic (SEM) studies. To

evaluate the effect of bypass to abdominal viscera both kidneys were taken for gross inspection and light microscopic examination to detect embolic materials. In group A, shunt flow was from 350 to 500 ml/min, averaging 450 ml/min. The mean distal pressure was 75 mmHg, and mean pressure gradient across the shunt was 65 mmHg. Urine output exceeded 1 ml/kg/hr. In all six dogs, tubes were clear by gross inspection without detectable emboli. SEM study revealed minimal platelet attachments and they seemed before release reaction and easily detachable from the surface. And there were no platelet aggregations or fibrin strands. Platelet counts did not decrease during a period of bypass and revealed 114% control after five hours. Fibrinogen concentration maintained control value for first three hours, and decreased slightly to 89.9% control after five hours. FDP remained within normal range. ACT was slightly prolonged during bypass, but remained within normal range. The sections of kidneys showed no evidence of thromboembolism by gross inspection, and light microscopic examinations revealed normal renal architecture with no embolic materials, hemoglobin deposits, or tubular casts. In group B, only a tube developed thrombus in the middle of the tube, and its shunt flow was 50 ml/min, and shear rate was only 76 sec⁻¹. In other three cases, results were consistent to those of group A. The originally designed TM3-coated tube demonstrated to have good nonthrombogenicity under low shear rate and excellent performance within five hours of bypass in experimental dogs. It seems that the mechanism of nonthrombogenicity of TM3 is due to biorization of the surface by multilayered protein deposition, so TM3 has potential application to more long-term usages such as left heart bypass and veno-arterial bypass without systemic heparinization. We believe this shunt tube should be employed to clinical use and reveal excellent performance.

Acknowledgement: We would thank Mr. Murayama and Mr. Tanaka for offering TM3, and Mr. Thutui for coating tubes. And also thank Mr. Iwai and Miss Morishima for technical assistance.

10 Kawada-cho, Shinjuku-ku, Tokyo 162, Japan.

Michael D. Lelah, Jeffrey A. Pierce, Teryl S. Madsen, Linda K. Lambrecht
and Stuart L. Cooper

Department of Chemical Engineering, University of Wisconsin-Madison,
Madison, Wisconsin 53706

Introduction: When blood contacts a polymer, initial deposition of proteins, platelets and other formed elements leads to the formation, growth and embolization of thrombi. The extent of surface-induced thromboembolism is determined, in part, by the nature of the polymer surface.

Polyether-urethane polymers have found application in both experimental and clinical blood contacting implants and devices. Polyether-urethanes are segmented elastomers that have a glassy or semicrystalline chain-extended urethane hard phase, dispersed in a viscous or rubbery polyether matrix soft phase. This two phase structure gives rise to exceptional physical and mechanical properties. Polyether-urethanes have also been found to exhibit relatively good thromboresistance, making them interesting and desirable for blood-contacting applications.

In this study, we investigate the blood compatibility of two polyether-urethanes of different hard/soft segment ratios, and a series of polyetherurethane-ionomers, in which the hard segment chain extender has been ionized to form an anionomer, cationomer and zwitterionomer. The purpose was to determine the effects of surface molecular changes on thrombogenesis, in order to understand the mechanisms determining the interaction of blood with polymers.

Blood compatibility was determined using a new canine acute ex-vivo femoral A-V series shunt experiment², which allows for simultaneous testing of the polymers under similar hematological and physiological conditions. A multiprobe approach was used to characterize the surfaces of the laboratory synthesized polyether-urethanes, including contact angle measurement, ESCA (electron spectroscopy for chemical analysis) ATR-IR (attenuated total reflection infrared spectroscopy) and SEM.

Experimental: The synthesis and bulk characterization of the polyether-urethanes and ionomers have been described previously³. The polyether-urethanes examined all had 1000 M.W. polytetramethyleneoxide soft segments. The hard segments were composed of 4,4'-diphenylmethane diisocyanate chain extended with N-methyl diethanolamine at hard segment concentrations of 21.5 wt% (21.5U) and 38 wt% (38U). The 38 wt% material was ionized to produce 100% chain-extender ionized propane sulfone-zwitterionomer (38Z), alkyl halide cationomer (38C) and metal acetate treated-anionomer (38A).

The ex-vivo blood compatibility studies were conducted as described previously². Canine fibrinogen was labeled with ¹²⁵I by an enzymatic technique. Autologous platelets from adult mongrel dogs were labeled with ⁵¹Cr. The femoral artery and vein in one leg was exposed, ligated and cannulated with the series shunt. A cannulated branch artery proximal to the shunt cannulation site was used for flushing the bulk blood out of the shunt at each time point in order to detect the surface radioactivity associated with deposited blood components. A new set of randomized

identical test surfaces was inserted for each time period studied (1/2-60 min). Surface analysis on the elastomers was done prior to implant using the captive bubble technique of Hamilton (contact angle), a PHI 548 ESCA spectrometer, a Nicolet 7299 FTIR and a JEOL 35C SEM.

Results and Discussion: Platelet and fibrinogen results showed a peak at 15-20 minutes of blood contact for all surfaces studied as observed previously on other surfaces². The peak heights were used as a measure of thrombogenicity. Table I shows partial results for the blood contact and surface characterization experiments. The lower hard segment content urethane (21.5U) was more thromboresistant (lower peak) than the higher hard segment content urethane (38U). Surface analysis by ESCA & ATR-IR (hard/soft-ratios) confirm the same trends on the surface. The zwitterionomer (38Z) was more thromboresistant than the anionomer (38A), neutral urethane (38U) and cationomer (38C), within the same series, even though the surface hard segment content as determined by ESCA on the zwitterionomer (38Z) was double that on the neutral urethane (38U). These results indicate that although the hard/soft segmental ratios may be the important surface determinants of blood compatibility in the neutral urethanes, ionization of the hard segment affects both thrombogenicity and surface chemical structure. The relative thrombogenicity of the cationomer (38C) may be expected due to the negative charge on the surface of platelets and other blood components. The surface tension data indicates that the more thromboresistant surfaces, have, in general lower surface-water (γ_{sw}) tensions.

TABLE I	21.5U	38U	38A	38C	38Z
peak platelet deposition (thrombogenicity) (#/1000 μm^2)	43	211	124	1078	62
ESCA hard/soft	.033	.061	.055	.060	.12
γ_{sw} (dynes/cm)	7.2	13.9	16.9	11.7	7.3
ATR-IR hard/soft	.15	.50	.44	.46	.47

Conclusions: The blood compatibility of a series of polyether-urethanes and ionomers was determined using a canine ex-vivo femoral series shunt experiment. The surface properties of these materials were examined using a number of different surface techniques. Higher surface soft segment concentration was correlated with thromboresistance for the neutral urethanes. Ionization altered both thromboresistance and surface morphology. Thromboresistance decreased in the order zwitterionomer, anionomer, neutral urethane and cationomer.

References:

- (1) Lelah, et al., JBMR, 17, 1, 1983.
- (2) Lelah, et al., JBMR, submitted 1983.
- (3) Hwang, et al., Poly. Engr. Sci. 21, 1027, 1981.
- (4) Miller, et al., J. Macromol. Sci-Phys. B(22), 321, 1983.

Thomas A. Horbett, Mark Chopper and Larry O. Reynolds

University of Washington, Dept. of Chemical and Nuclear Engr., Seattle, WA. 98195

PreadSORption of biomaterials with plasma proteins, particularly albumin, has been attempted by many investigators in order to improve blood compatibility (1-3). However, albumin appears to be readily removed from some surfaces (4) and is therefore probably subject to replacement by other proteins from the blood. The use of proteins with higher affinity for surfaces or the optimization of conditions to assure tight binding of the protein has not yet been thoroughly explored. The partial purification of a plasma factor which blocks platelet adhesion (5) and efforts to improve albumin affinity by alkylation of polymers (6) are recent examples of other attempts to improve on this approach. To more fully evaluate this "passivation" approach, we have measured ^{125}I fibrinogen adsorption and thromboembolization rates in blood circulated through preadsorbed Silastic or polyacrylamide/Silastic (pAAM/SR).

Thromboembolization rates (7) were found to increase by a factor of ~ 15 in the following order: Hemoglobin on Silastic < Silastic \approx immunoglobulin G on pAAM/SR \approx hemoglobin on pAAM/SR < lipoprotein cholesterol on pAAM/SR \approx albumin on pAAM/SR < fibronectin on pAAM/SR < pAAM/SR < plasma on pAAM/SR < fibrinogen pAAM/SR (see Table 1). Fibrinogen adsorption from blood to hemoglobin preadsorbed pAAM/SR was reduced (see Figure 1). Thromboembolization from hemoglobin treated pAAM/SR was markedly reduced in some cases (see Figure 2) but considerable variability in this effect was observed (see Table 1).

The wide range in thromboembolization rates demonstrates the strong influence of plasma protein type on baboon blood interactions with pAAM/SR. The inability of hemoglobin to completely block fibrinogen adsorption or reduce thromboembolization from pAAM/SR to zero suggest that further improvements in blood compatibility by the preadsorption method are possible. Manipulation of other parameters in the preadsorption process (e.g. temperature, pH, ionic strength, dehydration) besides protein type is also expected to influence the binding of the preadsorbed protein and may therefore lead to further improvements.

References

- Salzman et al. *J. Biomed. Mater. res.* 3, 69 (1969).
- Lyman et al. *Thromb. Diath. Haem. (Suppl.)* 42: 109 (1971).
- Jenkins et al. *J. Lab Clin. Med.* 81: 280 (1973).
- Brash et al. *Trans. Amer. Soc. Artif. Intern. Org.* 20: 69-76 (1974).
- Sharma et al. *ASAIO Journ.* 3: 43-49 (1980).
- Munro et al. *Trans. Amer. Soc. Artif. Inter. Org.* 27: 499-503 (1981).
- Reynolds et al. *Trans. Soc. Biomat V*, 37 (1982).

Acknowledgments: The work was supported by NHLBI #HL22163.

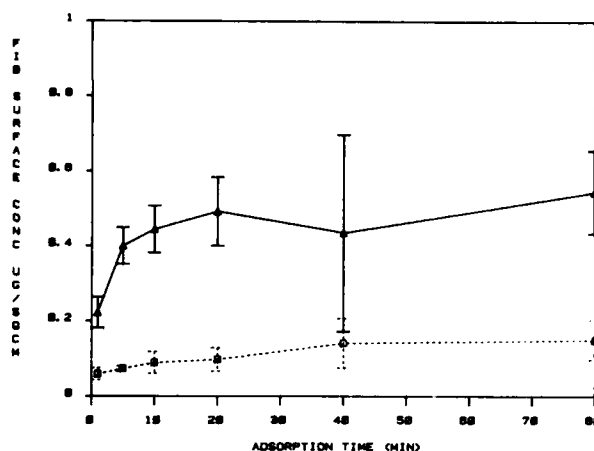


Figure 1. Fibrinogen adsorption from blood to pAAM/SR (Triangles) and hemoglobin pAAM/SR (Squares).

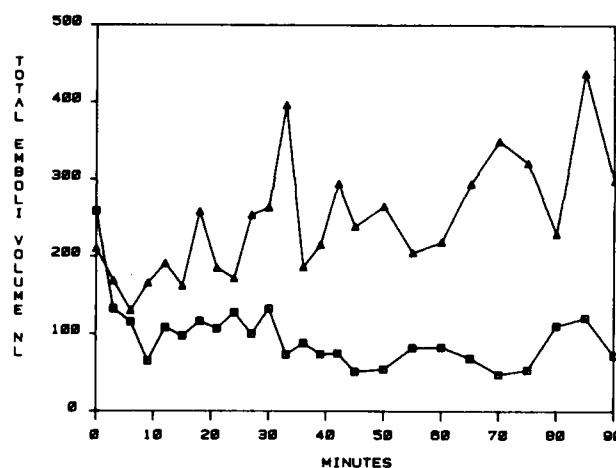


Figure 2. Embolization from pAAM/SR (Triangles) and hemoglobin preadsorbed pAAM/SR (Squares).

TABLE 1 THROMBOEMBOLIZATION FROM SURFACES PREADSORBED WITH PROTEINS

SURFACE	PROTEIN	CONDITIONS	AMOUNT ADSORBED ($\mu\text{g}/\text{cm}^2$)	THROMBOEMBOLIZATION		
				NUMBER OF RUNS	RATE ($10^3/\text{SEC.} \times 10^{-4}$)	AVERAGE
SILASTIC	NONE	---	---	18	0.3	2.6
SILASTIC	HEMOGLOBIN	A	---	5	0.4	0.9
pAAM/SILASTIC	NONE	---	---	18	1.4	7.1
pAAM/SILASTIC	PLASMA	B	---	6	2.4	11
pAAM/SILASTIC	FIBRINOGEN	C	2.1	12	2.0	14
pAAM/SILASTIC	FIBRONECTIN	D	0.067	6	1.2	6.4
pAAM/SILASTIC	ALBUMIN	E	0.61	10	0.6	4.7
pAAM/SILASTIC	LIPOPROTEIN	F	10.57	5	0.5	4.5
pAAM/SILASTIC	IMMUNOGLOBULIN G	G	0.35	6	0.6	3.0
pAAM/SILASTIC	HEMOGLOBIN	H	---	11	1.7	3.5

A BABOON HEMOGLOBIN, 1 MG/ML

B CITRATED BABOON PLASMA

C BABOON FIBRINOGEN, 0.1 MG/ML

D BOVINE FIBRONECTIN, 0.0052 MG/ML

E BABOON ALBUMIN, 0.1 MG/ML

F BOVINE LIPOPROTEIN CHOLESTEROL, 0.23 MG/ML

G BABOON IMMUNOGLOBULIN G, 0.1 MG/ML

H BABOON HEMOGLOBIN, 1 MG/ML

AUTHOR INDEX

Abbas, N.A.	136	Bernard, P - F.	178
Abd El Baset, M.S.	56	Berry, J.L.	255
Abdulla, d.	69, 166	Berthet, J.	314
Abram, J.	77	Bichon, D.	212
Absolom, D.R.	277	Bidez, M.W.	60
Akaike, T.	11, 275	Biro, L.	330
Akovali, G.	296	Black, J.	130
Akutsu, T.	10	Blagoeva, R.	220
Albrektsson, T.	84, 89	Blais, P.	92
Alberts, L.R.	246	Blitterswijk van, C.A.	151
Albright, J.A.	44	Block, M.S.	274, 248
Allen, M.B.	2	Bloebaum, R.D.	82, 83, 318
Alexander, H.	132, 257, 298	Blomberg von, M.	131
Ambrose, W.W.	237	Blumel, G.	203
Ambrosio, L.	258	Blyzniuk, J.W.	200
Anderson, J.M.	25, 33, 90, 140, 211	Bobyn, J.D.	69, 70, 166, 233, 269
Anderson R.C.	179, 316, 334	Boerman, J.W.	261
Andrade, J.D.	263, 265, 266, 276, 290	Boffa, M.C.	305
Antonucci, J.M.	137	Boisson, C.	291
Aomi, S.	359	Bonfield, W.	77
Arlin, N.E.	7	Bonnel, F.	244
Ascherl, R.	203	Bordenave, L.	96, 336
Asgian, C.	145	Borloz, W.	212
Ashman, A.	322	Borovetz, H.S.	105
Askill, I.N.	13	Boss, J.	271
Atsumi, K.	12, 28	Boswell, W.	331
Aubert, N.	305	Bowman, J.	77
Averill, R.	333	Bowry, S.K.	295
Baier, R.	102, 173, 190	Boyne, P.J.	63, 150, 216, 249
Bailey, A.J.	169	Brankov, G.	220
Bajpai, P.K.	170, 194, 217, 353, 354	Branson, D.F.	95
Baldet, P.	244	Brant, A.M.	105
Baquey, C.	96, 336	Brash, J.L.	264
Barbier, D.	305	Braud, C.	171
Bardos, D.I.	144	Brauer, G.M.	347
Barroso, E.G.	14	Brendel, J.	336
Barrows, T.H.	210	Brendel, K.	98, 339
Bartoli, S.	184	Briana, S.	13
Basse-Cathalinat, B.	96, 336	Bridges, G.O.	97
Baswell, I.	144	Brooker, A.	113
Batich, C.	31	Brose, M.D.	7
Batich, S.	31	Brown, K.	219
Beatty, C.L.	309	Brown L.	340
Beck, L.R.	199	Brown S.A.	86, 181, 281
Beguin, S.	206	Bruins, P.	322
Behiri, J.C.	77	Brunet, M.E.	27
Bejuri, J.	270	Brunski, J.B.	229, 328
Bejuri-Thivolet, F.	270	Buchanan, R.A.	128, 168, 182
Bence, J.L.	40	Buerger, D.E.	266, 290
Ben-Slimane, S.	9	Bundy, K.J.	125, 127
Berg, W.S.	255	Bunel, C.	171
Berghaus, A.	299	Burgoyne, K.	313

Burke, D.W.	45, 320, 346	Cook, S.D.	27, 109, 179, 224, 316, 314
Burke, J.F.	35	Cooper, S.L.	360
Burkes, E.J.	327	Cornet, L.	314
Burri, C.	78	Corretge, E.	205
Bushelow, M.	148	Cortina, T.	311
Cadossi, R.	133	Costerton, J.W.	175
Cahalan, P.T.	252	Courtney, J.M.	295
Caix, J.	96, 336	Courtois, B.	241
Callow, A.D.	93, 293, 356	Coury, A.J.	252
Cameron, H.U.	69	Cranin, A.N.	196, 324, 325, 326
Campbell, P.	83, 318, 331	Cross, F.S.	193
Capezza, M.R.	61	Cullom, C.D.	149
Carter, D.R.	164	Cunningham, J.	53
Carter, J.M.	173	Curti, T.	94
Cartledge, S.A.	197	D'Addato, M.	94
Casper, R.A.	199, 232, 278	Dale, P.	182
Castleberry, D.J.	323	Dallant, P.	71
Catron, W.	101	Dal Monte, A.	133
Cavallaro, J.F.	38	Danniels, R.G.	160
Cavedagna, D.	94	Das, P.	330
Cenni, E.	94	Davidovitch, Z.	134
Cerulli, G.	43	Davidson, S.J.	2
Chabot, F.	279	Davies, J.P.	45, 47, 320
Chamoun, E.	222	Deaton, J.B.	237
Chandy, T.	301	Dehl, R.E.	112
Chapman, D.	188	Delpont, P.	185
Charit, Y.	177	De Meester, P.	350
Chase, S.E.	282	Dempsey, D.	24
Chen, C.M.	302	Deasai, V.H.	125, 127
Chen, G.	87	DesPrez, J.	39, 95
Chen, J.	263	Dick, H.M.	230
Cheng, C.	31	Ditchfield, J.	310
Cheung, D.T.	30	Dore, S.	233
Chew, S.	83, 331	Douzon, C.	207
Christel, P.	67, 71, 72, 178, 279	Doyle, C.	77
Christofferson, R.A.	254	Dreher, D.M.	193
Chiu, T.H.	34, 38	Driessen, A.A.	245
Chopper, M.	361	Drouin, G.	233, 269
Chu, C.C.	106, 107, 209	Dryll, A.	67, 72
Ciapetti, G.	279, 312	Ducassou, D.	336
Ciegler, G.W.	135	Ducheyne, P.	185, 350
Claes, L.	78, 223	Dudderar, D.J.	137
Clark, C.C.	130	Duhamel, R.C.	98, 339
Clarke, I.C.	116, 117, 240, 313, 348	Ducan, P.E.	191
Cocharan, G.V.	229	Ducan, R.	197
Cohn, L.S.	80	Dunn, R.L.	199, 278
Coleman, D.L.	187, 341	Dupont, J.A.	180
Colen, W.	185	Durroux, R.	79
Collier, J.P.	113, 317	Dussault, R.	233
Collins, C.L.	109	Duval, J.L.	9
Compton, R.	168	Dylewski, J.R.	309
Comte, P.	129	Eberhart, R.C.	97, 303
Connolly, R.	93, 356	Ebramzadeh, E.	117, 348
Cooke, F.W.	80	Eckstein, E.C.	14

Edelman, E.	340	Gettleman, L.	61
Eitenmuller, J.	201	Giammara, B.L.	327
El-Wakad, M.	328	Giancecchi, F.	133
Enger, C.D.	39	Gianoli, G.	224
Engh, C.A.	70, 113	Gibson, S.J.	210
Engelhardt, A.	218	Gilbertson, L.N.	145, 236, 238
Enomoto, S.	153	Gilding, D.K.	13
Eretskaya, E.V.	304	Gill, Y.	182
Erhardt, W.	203	Gillett, N.A.	281
Eschenroeder, H.C.	335	Gimigliano, R.	280
Eskin, S.G.	142	Gleis, G.G.	315
Estridge, T.	37, 88	Glousman, R.	240
Etter, C.	78	Goggins, J.A.	99
Eyerer, P.	68	Goldberg, E.P.	15, 75
Farrell, E.C.	105	Goldfarb, D.	101
Farrington, G.C.	134	Gona, A.G.	298
Farrow, M.G.	311	Gosselin, C.	92
Feldman, D.	36, 37, 88, 103	Graves, G.A.	217
Ferracane, J.L.	138	Green, R.	234, 235
Ferraro, J.W.	355	Gregonis, D.E.	187, 263, 266, 290
Ficat, J.J.	79	Griffin, D.	182
Ficat, P.	79	Grishkan, A.	271
Fischer, A.M.	206	Gristina, A.G.	175
Folger, R.L.	114, 352	Groot de, K.	131, 151, 158, 159, 245, 261, 300
Fontanesi, G.	133	Gross, U.	283
Forbes, C.D.	295	Grote, J.J.	151
Fornalik, M.	102	Gruen, T.A.	65, 82, 318, 331, 348
Fougnot, C.	96, 207, 288, 305	gucinski, H.	190
Foxall, T.	356	Guida, G.	49, 258, 280
Fraker, A.C.	123, 124, 169	Guidoin, R.G.	9, 92, 104
Francis, M.J.	79	Gulino, D.	291
Fraunhofer von, J.A.	204, 315	Gumaer, K.I.	215
Frazer, W.A.	254	Gunasekera, K.R.	92
Freeman, M.J.	217	Gurny, R.	202
French, G.	239	Gurtowski, J.	256
French H.G.	27	Haddad, R.J.	109, 179, 224, 316, 334
Freud, T.S.	29	Hahn, H.	169
Fry, W.J.	97	Hale, S.	103
Fujimasa, I.	12	Haller, W.	203
Fujiu, T.	286	Hamada, T.	183
Furst, L.	134	Hamaguchi, T.	183
Galletti, P.M.	34, 38	Hamburger, S.	271
Gardiner, G.E.	214, 352	Hanker, J.S.	327
Garfinkle, A.M.	186, 337	Hansson, H - A.	84
Gariepy, R.	233	Hanson, S.R.	337, 338
Garner, S.	144	Haque, Y.	189
Garreau H.	171	Harding, A.	224
Gates, E.I.	346	Harker, L.A.	338
Gatto, S.	49	Harley, D.P.	32, 85
Gaussens, G.	67, 314	Harmand M.F.	52
Gebert, P.H.	61	Harrigan, T.P.	226
Geissdorfer, K.	203	Harris, W.H.	45, 46, 47, 164, 165, 226, 320, 346
Gendler, E.	227	Hartmann, D.	270
Georgette, F.S.	146	Hasirci, V.N.	198, 296

Hassler, C.R.	7	Ives, C.L.	142
Haubold, A.D.	316	Iwase, H.	172
Hawley, M.	195	Iwata, H.	8
Hayashi, K.	10, 253	Jacob, J.T.	23
Hayashi, T.	87	James, R.A.	64, 160
Hayward, J.A.	188	Jansen, J.A.	156, 157
Hegarty, J.M.	38	Jarcho, M.	247
Heimbürger, N.	358	Jasty, M.	46, 165, 226
Hench, L.L.	284, 287	Jensen, N.F.	46, 165
Henson, P.	6, 222	Jeong, S.Y.	342
Hensten-Pettersen, A.	262	Johnson, C.	31
Hering, T.M.	33	Johnson, F.	235
Heriz, R.	90	Johnson, H.J.	306
Hewan-Lowe, K.	273	Johnson, J.D.	210
Hilbert, S.L.	307	Johnston, D.S.	188
Hill, T.R.	329	Joist, J.H.	28j9
Hillberry, B.M.	149	Jones, R.D.	99, 193
Hillman, D.	331	Jozefonvicz, J.	206, 208, 267, 291, 305
Hiltner, A.	25, 211	Jozefowicz, M.	205, 207, 267, 288, 305
Hipp, J.A.	229, 328	Judy, R.W.	237
Hirabayashi, M.	250	Kamel, I.L.	139, 198
Hitmi, N.	52	Kammerer, G.W.	234
Hobkirk, J.A.	319, 329	Kampner, S.L.	228
Hobson, C.E.	192	Kangvonkit, P.	323
Hoffman, A.S.	186, 189, 268, 337	Kanmangne, F.M.	207
Hollinger, J.O.	5	Kasai, S.	11
Hollis, M.	232	Kasemo, B.	231
Holmes, R.E.	154	Kataoka, K.	141, 359
Homerin, M.	67, 72	Kato, M.	12
Homsy, C.A.	110, 243	Katz, J.L.	152, 330, 345
Horbett, T.A.	76, 189, 341, 361	Kawaguchi, A.	118
Hori, M.	108	Kawahara, H.	121, 143, 250
Hori, R.	145	Kazatchkine, M.D.	208
Hosseinian, A.	313	Keech, B.H.	311
Hsu, H.M.	128	Keller, J.C.	161
Hultman, S.	36	Kelley, B.S.	278
Hunt, M.S.	177	Kennedy, F.	317
Hunter, J.	103	Kent, J.N.	247, 248
Hunter, S.K.j.	187, 266	Keough, E.	93, 356
Ibrahim, S.I.	136	Kerlins, V.	191
Idezuki, Y.	213	Kester, M.A.	27
Imachi, K.	12	Kesteren van, P.J.	16
Imai, K.	121	Kettelkamp, D.B.	149
Imam, M.A.	237	Kifune, K.	28, 172
Inoue, Y.	172	Kilpikari, J.	242
Ip, W.F.	292	Kim, S.W.	342
Isenberg, B.P.	60	King, M.W.	92
Ishida, S.	153	King-Breeding, L.	303
Ishizaki, M.	357	Kitamura, Y.	116, 117, 118
Ito, F.	59	Kitsugi, T.	351
Ito, S.	351	Klein, C.P.	300
Itoh, Y.	275	Kleiner, H.	223
Iusim, M.	271	Kline, E.V.	105
Ivarsson, B.	84	Kline, S.A.	211

Knutson, K.	19	Liu, Y.K.	115
Kobayashi, M.	108	Llyod, J.B.	197
Kokolus, K.	102	Louie, M.C.	209
Kokubo, T.	351	Lowe, G.D.	295
Kolarik, J.	258	Lowe, R.E.	263
Konowal, A.M.	130	Lucas, L.	168, 182, 222
Kootwijk, A.	159	Luedemann, R.E.	224
Kopecek, J.	197	Lyberg, T.	262
Korostoff, E.	134	Lyman, D.J.	19
Kost, J.	340, 341	Maarek, J.M.	92
Kotera, S.	250	Mabuchi, K.	12
Koth, D.L.	321	MacEwen, S.R.	111
Kottke-Marchant, K.	90	Machka, K.	203
Kotzur, T.	283	Mackey, W.C.	93, 356
Kovach, J.	282	Macon, N.	34
Kayanagi, H.	359	Madsen, T.S.	360
Krajewski, A.	119, 285	Maeda, T.	143
Kram, H.B.	32, 85	Maharidge, R.	345
Krause, W.R.	349	Maijer, R.	259
Kucheria, C.S.	214, 352	Maillet, F.	208
Kulkarni, P.V.	97	Malkan, S.R.	106
Kullmann, A.	262	Malone, J.M.	98, 339
Kusy, R.P.	26	Mangino, P.D.	204
Kuypers, W.	151	Manley, M.T.	66, 256, 333
Laanemae, W.M.	111	Mann, R.W.	226
Labaree, D.	207	Merchant, R.E.	33, 140
Lacabanne, C.	52, 79	Marois, M.	92
LaFaye de, D.	104, 241	Martens, M.	185
Lakes, R.S.	115	Martin, L.	92
Lamberti, F.V.	343	Maruyama, A.	141
Lambrecht, L.K.	360	Masubuchi, M.	120
Lamure, A.	52	Matlaga, B.F.	272
Lanfranchi, M.	9	Mathis, R.S.	349
Lange, H.	358	Matsuda, T.	8, 10, 253
Lange de, G.L.	158, 159	Matsuzawa, Y.	338
Langer, R.	340	Mattamal, G.J.	124
Langhammer, H.	203	Matthews, R.S.	214
Lausmaa, J.	231	Mattie, D.R.	353
Lautenschlager, E.P.	167	Matukas, V.J.	323
Lautenschlager, J.A.	167	Maurel, E.	52
Lee, H.B.	239	Mauzac, M.	205, 206, 208, 305
Lee, J.M.	166	Mayeda, M.	172
Lefevre, C.	104, 241	Mayor, M.	113, 317
Legendre, J.M.	104	McCarroll, N.E.	311
LeGeros, R.Z.	57	McCoy, L.G.	7
Lelah, M.D.	360	McCullough, J.	93, 356
Lemons, J.	6, 60, 168, 182, 222, 232	McCutcheon, M.	222
Leong, F.L.	74	McFall	354
Levy, J.T.	195	McKellop, H.A.	240, 313, 348
Levy R.J.	195	McKinney, R.V.	321
Li, S.	327	McLaren, A.	83, 176
Li, S.T.	29, 91	McLaughlin, R.E.	335
Lin, T.C.	289	McRea, J.C.	342
Linder, L.	81	Meenaghan, M.	190

Mehlisch, D.R.	215	Nicolas, L.	49, 258, 280
Mehta, D.	239	Niemann, K.	6
Mendes, D.G.	177, 271	Nieuw Amerongen, A.V.	261
Merritt, K.	86	Nigretto, J.M.	205
Merwin, G.E.	284	Nikolaev, V.G.	304
Metsger, D.S.	355	Nimni, M.E.	30
Meuiner, A.	71, 178, 330	Nishizawa, S.	11
Meyer, A.	102, 173	Niwa, S.	108
Meyers, W.E.	4	Noishiki, Y.	87
Michalik, R.	358	Nojiri, C.	359
Micheron, F.	79	Northup, S.J.	306
Migliaresi, C.	49, 258, 280	Nyilas, E.	34, 38
Migonney, V.	96, 288	Obermayer, A.S.	2
Mikanagi, K.	120	O'Connor, D.O.	45, 47, 320
Miller, D.R.	18	Oderkerk, C.H.	261
Miller, K.M.	140	O'Donnell, T.	93, 356
Minns, R.J.	50	Oette, P.	117
Miroux, D.	241	Ogino, M.	286
Miura, I.	121	Oh, I.	146, 148
Miyaga, M.	183	Okabe, N.	183
Miyata, T.	11, 275	Okano, T.	141, 359
Monma, H.	357	Okuno, O.	121
Mooney, V.	154, 219	Olmi, B.	119
Moore, J.S.	344	Ono, M.	108
Mordejovich, D.	271	Ooi, Y.	120
Moroni, A.	119	Oonishi, H.	116, 118, 183
Morris, D.M.	130	Oppenheimer, P.H.	130
Mossessian, T.	348	Orgill, D.	35
Mueller, H.J.	260	Orisek, B.	331
Mullem van, P.J.	156, 157, 274	Orr, T.	317
Munro, M.S.	97, 303	Osborn, D.C.	75
Murakami, M.	213	Oser, Z.	234, 235
Murice, E.A.	114	Otter den, G.	245
Musso, E.	230	Owen, D.R.	23, 302
Nabeshima, T.	183	Pagliuso, S.	280
Nagaoka, K.	59	Pal, S.	44
Nagata, K.	58	Paoletti, G.C.	43
Nagura, H.	153	Paris, D.A.	155
Nair, A.K.	100	Park, H.C.	115
Nakabayashi, N.	54	Park, J.B.	239
Nakajima, A.	87	Parr, J.	66
Nakajima, M.	12, 28	Parsons, J.R.	132, 257, 298
Nakamura, M.	121	Patka, P.	245
Nakamura, T.	10, 253, 351	Pawluk, R.J.	230
Nakatani, T.	10, 253	Pelzer, H.	358
Nakeeb, S.	190	Penugonda, B.	57
Namavar, F.	300	Peppas, N.A.	18, 202
Nasca, R.	232	Pernot, F.	244
Nasu, T.	59	Peters, G.	210
Natiella, J.	173	Petrov, N.	220
Negele, J.	818	Petty, R.W.	174
Neumann, A.W.	277	Pezzoli, F.	43
Nicaise, M.	314	Pham, M.C.	137
Nichols, L.D.	2	Pherson, T.R.	22

Phua, K.	25	Roukema, P.A.	261
Picha, G.J.	39, 40, 95	Rowe, R.H.	169
Pieraggi, M.T.	52	Rudigier, J.	42
Pierce, J.A.	263, 360	Ruse, D.	259
Pilliar, R.M.	69, 111, 162, 166, 332	Sabelman, E.E.	308
Pinchuk, L.	14	Sage, B.E.	150, 155, 215, 216
Pizzoferrato, A.	94, 297, 312	Saha, S.	41, 44, 48, 221, 225
Poandl, T.	132	Saint-Andre, J.M.	244
Pohler, O.E.M.	122	Sakka, S.	351
Poirier, V.L.	24	Sakurai, Y.	141
Poli, G.	133	Salgaller, M.L.	194
Policova, Z.	277	Salsbury, R.L.	215
Pollack, S.R.	220	Salthouse, T.N.	272
Portelli, G.B.	344	Salzstein, R.	220
Pourdeyhimi, B.	106, 107	Sander, T.W.	146, 148
Powers, D.L.	80	Sarley, J.T.	306
Prewitt, J.M.	110, 243	Sarmiento, A.	65, 82, 240, 318, 331, 348
Putter de, C.	158, 159	Sasken, H.	34
Quach, H.	22	Satler, N.M.	324, 326
Quinn, J.H.	247	Sato, H.	87
Rabinovitch, A.	90	Sato, S.	342
Rabischong, P.	244	Schaaf, J.A.	149
Ramberg-Laskaris, K.	93, 356	Scheper, R.J.	131
Ramselaar, M.	274	Schmidt, K.H.	201
Ratner, B.D.	76, 186, 189, 337, 341	Schoen, F.J.	192, 195
Rausch, J.P.	327	Schultz, E.L.	252
Ravaglioli, A.	119, 258	Schwartz, A.	21
Rawe, R.	191	Schwartz, G.L.	139
Rawls, H.R.	61	Schway, M.B.	189
Reed, A.M.	13	Schwinn, C.P.	65
Reese, N.	273	Scott, J.R.	187
Refojo, M.F.	74	Sedel, L.	71
Reger, S.I.	335	Sefton, M.V.	200, 292, 343
Reinecke, D.R.	276	Seidell, C.L.	142
Reinert, R.L.	98, 339	Sekino, H.	357
Rejmanova, P.	197	Seligson, D.	204
Renta, V.	280	Serekian, P.	333
Renz, E.A.	109, 316	Sergeev, V.P.	304
Reynolds, L.O.	361	Sernau, R.	311
Reynvaan, C.	147	Serne, H.	207
Ricci, J.C.	257, 298	Sernka, T.J.	170
Riffle, J.S.	251	Setterstrom, J.A.	3, 4
Rijnhart, P.E.	157	Sevastianov, V.I.	294
Ritter, C.J.	353	Sevick, E.M.	105
Ritter, G.	42	Shafqat, J.P.	63, 249
Rodriguez, V.	31	Shah, J.	255
Roffman, M.	177	Shah, S.	105
Rogers, S.P.	165	Shaker, Y.M.	136
Roldan, M.	74	Sharkey, N.A.	281
Ronca, D.	258	Sharma, C.P.	100, 301
Rosencwaig, A.	191	Shephard, M.S.	229
Rothschild, D.	216	Sherer, A.D.	150, 216
Rothstein, S.S.	150, 155, 216	Shigematsu, M.	351
Rotini, R.	133	Shibuya, T.	351

Shoemaker, W.C.	32, 85	Szycher, M.	24
Shpuntoff, R.	325, 326	Taenaka, Y.	10, 253
Shuster, J.J.	174	Tagai, H.	108
Siew, C.	260	Taira, M.	167
Sigot, M.	9	Takahashi, H.	357
Sigot, M.F.	9	Takahashi, S.	108
Silbermann, M.	271	Takakura, T.	12
Sillevis-Smitt, P.A.	159	Takanok, H.	10, 253
Silva, P.A.	219	Takatani, S.	10
Silverthorne, C.A.	174	Takeuchi, H.	108
Simpson, J.M.	306	Tanaka, T.	10
Sines, G.	116	Tanzawa, H.	213
Singh, S.	221	Tapon-Brethaudiere, J.	206
Skraba, J.S.	255	Tarabushi, C.	94
Skrabut, E.M.	35	Tarr, R.R.	176
Smith, C.W.	65	Tatsumi, M.	1181
Smith, D.C.	259	Tauro, J.C.	257
Smith, J.K.	61	Tencer, A.F.	219
Smith, L.M.	276	Tenney, B.	101
Smith, R.	17	Teramoto, K.	213
Smyth, M.B.	62	Terry, B.C.	327
Snyder, R.	101	Terry, R.N.	199j
Sohmiya, M.	108	Theiss, D.	42
Soltesz, U.	147	Thibodeau, J.A.	264
Sonoda, T.	213	Thomas, K.	316
Sorg, K.	203	Thomas, T.	195
Soudry, M.	271	Tice, T.R.	4
Spadaro, J.A.	282	Tominaga, N.	11
Spanier, S.S.	174	Tormala, P.	242
Sparks, R.E.	289	Townsend, P.R.	180
Spector, M.	273	Toyosaki, T.	8
Spilman, D.B.	287	Traiger, M.	62
Stacholy, J.	75	Tranquilli-Leali, P.	43, 184
Stansbury, J.W.	137, 347	Travers, M.	295
Stea, S.	297, 312	Treharne, R.W.	148
Steflik, D.E.	321	Trekoval, J.	73
Steinberger, D.R.	347	Trudell, L.A.	34, 38
Steinemann, S.G.	129	Truitt, H.P.	64
Stemberger, A.	203	Tseytlina, E.A.	294
Sterling, R.	15	Tsuji, E.	183
Stern, L.S.	66, 256, 333	Tsukagoshi, S.	12
Stevenson, W.T.	200	Tsuruta, T.	141
Stith, W.J.	22, 239	Turnbull, T.	173
Stokes, K.B.	252, 254	Turner, D.T.	21, 58
Stringer, D.E.	62, 249	Tzitzikalakis, G.I.	230
Struntz, V.	283	Umezu, M.	10, 253
Stupp, S.I.	135, 344	Urry, R.L.	187
Sugamori, M.	200j	Vaandrager, J.M.	274
Suka, T.	120	Vacik, J.	73
Sumithra, N.	62	Vaidyanathan, J.	55
Sunwoo, M.H.	29	Vaidyanathan, T.K.	55, 126
Suzuki, K.	59	Valentijn-Benz, M.	261
Suzuki, Y.	183	VanDeMark, M.R.	14
Szota, P.	264	Van Orden, A.C.	123

Van Raemdonck, W.	350	Wigginton, R.	144
Van Wagenen, R.A.	265, 266, 276	Wijn de, J.R.	16, 156, 157, 274
Vasu, R.	164	Wilcox, L.G.	217
Venz, S.	137	Williams, D.F.	53
Vert, M.	171, 279	Williams, R.L.	181
Vignon, E.	270	Wilson, J.	284, 287
Vincent, J.W.	3, 4	Winters, S.	290
Vogelbaum, M.A.	127	Wirth, J.	190
Volkov, A.V.	294	Wolf, H.	295
VonderBrink, J.P.	170	Wolfe, L.W.	319
Vreeburg, K.J.	170	Wolters-Lutgerhorst, J.M.	156, 157
Wagner, W.	218	Yahia, H.	269
Waknine, S.	55, 62	Yalon, M.	75
Walker, M.M.	152	Yamabe, M.	12
Wall, C.	105	Yamagami, A.	250
Wallace, D.G.	51	Yamagishi, M.	359
Wang, P.Y.	310	Yamamuro, T.	1, 351
Ward, R.S.	251	Yamashita, N.	153
Warman, M.L.	41, 48	Yannas, I.V.	35
Watts, D.C.	17	Yapp, R.	316
Weatherly, G.C.	111, 332	Yasuda, H.K.	338
Webster, D.A.	282	Yau, H.L.	344
Weinberg, E.H.	165	Yokobori, A.T.	357
Weinstein, A.M.	180, 228	Yokobori, T.	357
Weiss, A.B.	132, 257	Yoon, H.S.	330, 345
Weiss, B.A.	51	Young, F.A.	161
Wells, R.E.	214, 352	Yue, S.	332
Weltin, R.	201	Zalesky, P.	29, 91
Wenda, K.	42	Zarzycki, J.	244
White, K.A.	251	Zide, M.F.	247
White, R.A.	163	Zimmerman, M.	132
White, S.T.	315	Zingg, W.	227, 292
Whitely, J.Q.	26	Zoephel, G.P.	218
Whittam, M.A.	188	Zoller, J.H.	255
Wichterle, O.	20, 73		

END

2-87

DTIC